Precision Measurement and Calibration

Electricity — Low Frequency

Special Publication 300

Volume 3

United States Department of Commerce

National Bureau of Standards

UNITED STATES DEPARTMENT OF COMMERCE • C. R. Smith, *Secretary*

NATIONAL BUREAU OF STANDARDS • A. V. Astin, *Director*

Precision Measurement and Calibration

Selected NBS Papers on

Electricity — Low Frequency

F. L. Hermach and R. F. Dziuba
Editors

A compilation of previously published papers by the staff of the National Bureau of Standards, including selected abstracts by NBS and non-NBS authors. Issued in several volumes, see page iv.

NBS Special Publication 300 — Volume 3

Issued December 1968

(Supersedes in part Handbook 77—Volume II)

For sale by the Superintendent of Documents U.S. Government Printing Office
Washington, D.C. 20402 - Price $4.50

Abstract

This volume is one of an extended series which brings together some of the previously published papers, monographs, abstracts and bibliographies by NBS authors dealing with the precision measurement of specific physical quantities and the calibration of the related metrology equipment. The contents have been selected as being useful to the standards laboratories of the United States in tracing to NBS standards the accuracies of measurement needed for research work, factory production, or field evaluation.

Volume 3 contains reprints through 1967 on d-c and low-frequency electrical measurements covering the following topics: Electrical Units, Electrical Standards, Standard Cells, Zener Diodes, Resistors, Resistance Apparatus, Capacitors, Inductors, Instruments, AC–DC Transfer Standards, Transformers, Inductive Voltage Dividers, High Voltage Measurements, Dielectric Measurements, and Magnetic Measurements. A selected list of NBS publications on electrical measurements is also included.

Key Words:

Electrical units; electrical standards; electrical measurements; electrical calibrations; standard cells; zener diodes; resistors; resistance apparatus; capacitors; inductors; ac–dc transfer standards; current transformers; voltage transformers; inductive voltage dividers; high voltage measurements; dielectric measurements; magnetic measurements.

Library of Congress Catalog Card Number: 68–60042

Foreword

In the 1950's the tremendous increase in industrial activity, particularly in the missile and satellite fields, led to an unprecedented demand for precision measurement, which, in turn, brought about the establishment of hundreds of new standards laboratories. To aid these laboratories in transmitting the accuracies of the national standards to the shops of industry, NBS in 1959 gathered together and reprinted a number of technical papers by members of its staff describing methods of precision measurement and the design and calibration of standards and instruments. These reprints, representing papers written over a period of several decades, were published as NBS Handbook 77, Precision Measurement and Calibration, in three volumes: Electricity and Electronics; Heat and Mechanics; Optics, Metrology, and Radiation.

Some of the papers in Handbook 77 are still useful, but new theoretical knowledge, improved materials, and increasingly complex experimental techniques have so advanced the art and science of measurement that a new compilation has become necessary. The present volume is part of a new reprint collection, designated NBS Special Publication 300, which has been planned to fill this need. Besides previously published papers by the NBS staff, the collection includes selected abstracts and references by both NBS and non-NBS authors. It is hoped that SP 300 will serve both as a textbook and as a reference source for the many scientists and engineers who fill responsible positions in standards laboratories.

A. V. Astin, *Director.*

Preface

The general plan for this compilation has been reviewed by the Information Committee of the National Conference of Standards Laboratories. The plan calls for Special Publication 300 to be published in 12 volumes having the following titles and editors:

Statistical Concepts and Procedures, H. H. Ku
Frequency and Time, A. H. Morgan
Electricity—Low Frequency, F. L. Hermach and R. F. Dziuba
Electricity—Radio Frequency, A. J. Estin
Heat, D. C. Ginnings
Temperature, J. F. Swindells
Mechanics, R. L. Bloss
Dimensional Metrology—Length and Angle, H. K. Hammond, III
Radiometry and Photometry, H. K. Hammond, III
Colorimetry and Image Optics, H. K. Hammond, III
Spectrochemical Analysis, B. F. Scribner
Ionizing Radiation, E. H. Eisenhower

This division of subject matter has been chosen to assure knowledgeable selection of content rather than to attain uniform size. It is believed, however, that the larger volumes, of approximately 600 pages, will still be small enough for convenient handling in the laboratory.

The compilation consists primarily of original papers by NBS authors which have been reprinted by photoreproduction, with occasional updating of graphs or numerical data when this has appeared desirable. In addition, some important publications by non-NBS authors, as well as publications by NBS authors that are too long to be included, are represented by abstracts or references; the abstracts are signed by the individuals who wrote them, unless written by the author.

Each volume has a subject index and author index, and within each volume, contents are grouped by subtopics to facilitate browsing. Many entries follow the recent Bureau practice of assigning several key words or phrases to each document; these may be collated with titles in the index. Pagination is continuous within the volume, the page numbers in the original publications also being retained and combined with the volume page numbers, for example 100–10. The index notation 3–149 refers to volume 3, page 149 of this volume. A convenient list of SI (Systeme International) physical units and a conversion table are to be found inside the back cover.

The publications listed herein for which a price is indicated are available from the Superintendent of Documents, U S. Government Printing Office, Washington, D.C. 20402 (foreign postage, one-fourth additional). Many documents in the various NBS nonperiodical series are also available from the NBS Clearinghouse for Federal Scientific and Technical Information, Springfield, Va. 22151. Reprints from the NBS Journal of Research or from non-NBS journals may sometimes be obtained directly from an author.

Suggestions as to the selection of papers which should be included in future editions will be welcome. Current developments in measurement technology at NBS are covered in annual seminars held at either the Gaithersburg (Maryland) or the Boulder (Colorado) laboratories. These developments are summarized, along with a running list of publications by NBS authors, in the monthly NBS Technical News Bulletin.

H. L. Mason
Coordinator for Measurement Services
NBS Institute for Basic Standards.

Editors' Note

We have selected from the many papers published by NBS authors on electrical measurements those which we felt best fitted W. R. Tilley's criterion; "References dealing with precision instruments, measurement and calibration procedures, or treatment of measurement data, of value particularly to standards and calibration laboratories or designers of laboratory instruments and equipment." No papers or abstracts by non-NBS authors are included; however, the references listed in these NBS papers can serve as a guide to some of the excellent world-wide literature on the subject of precision measurement of d-c and low-frequency electrical quantities.

Unfortunately, some very useful NBS Technical Notes on calibration procedures could not be included because of space limitations. However, they are listed in the abstracts sections, and are readily available from the Superintendent of Documents, U.S. Government Printing Office, Washington, D.C. 20402.

F. L. Hermach and
R. F. Dziuba, *Editors.*

Contents

Resistors and Resistance Apparatus—Continued

Papers

Abstracts

Capacitors and Inductors

Papers

Abstracts

Instruments and AC–DC Transfer Standards

Papers

Instruments and AC–DC Transfer Standards—Continued

Abstracts

Transformers and Inductive Voltage Dividers

Papers

Abstracts

High Voltage and Surge Measurements

Papers

Abstracts

Dielectric and Magnetic Measurements

Papers

Abstracts

General Papers on Electrical Measurements

Papers

Abstracts

PREPRINT INSTRUMENT SOCIETY of AMERICA
20th Annual ISA Conference and Exhibit • October 4-7, 1965, Los Angeles
Preprint Number 33.3-1-65

International Weights and Measures

by Dr. Chester H. Page
Chief, Electricity Division
National Bureau of Standards
Washington, D. C.

ABSTRACT

A brief survey of the background, organization, and operation of the International Bureau of Weights and Measures and related committees.

The realization of the need for a simple system of weights and measures, based on uniform standards in different states and countries, appears in the early history of our country. In his first annual message to Congress, January 1790, Washington stated that "uniformity in the currency, weights, and measures of the United States is an object of great importance, and will, I am persuaded, be duly attended to." The matter was referred to the Secretary of State, Thomas Jefferson; one of his proposals was "to reduce every branch to the same decimal ratio already established for coin, and thus bring the calculations of the principal affairs of life within the arithmetic of every man who can multiply and divide plain numbers."

In May of the same year, the National Assembly of France requested the French Academy of Sciences to work out a system of units suitable for adoption by the entire world. At that time there was a great confusion of units of weights and measures, not only in France but everywhere. Units in use were poorly defined and varied from one place to the next, and from one guild to another. In 1799, France enacted a law making the metric system compulsory (but later repealed it, allowing the use of both old and new units side by side!).

Meanwhile, in 1792, a committee of the U. S. Senate recommended adoption of Jefferson's proposal of a decimal system, but no definite action was taken.

The metric system, based on the meter as the unit of length, the cubic decimeter as the unit of volume, the mass of a unit volume of water as the unit of mass, and using only decimal multiples and submultiples of these units, gradually won acceptance in Europe. Eventually the U. S. Congress (in 1866) legalized the metric system in this country, that is, made its use permissive, but not compulsory, in all commercial and legal transactions. The metric system has not gained favor with the man on the street, who uses the foot, pound, gallon, and bushel. These customary U. S. units are now defined in terms of the meter and kilogram. Although the original concept of the kilogram was the mass of a cubic decimeter of water, for practical reasons a solid standard was made (of platinum-iridium alloy); this prototype was then defined to be the kilogram.

For international uniformity, the various national metric standards should be consistent; an international conference was held in Paris in August of 1870 to consider the advisability of constructing new metric standards. The work of this conference, and later ones, resulted in the "Treaty of the Meter", or "Convention of the Meter", signed on May 20, 1875, by 17 countries, including the U. S. This treaty provided for a General Conference on Weights and Measures, meeting at least once every six years, an International Committee on Weights and Measures, elected by the General Conference and meeting every two years, and the establishment and maintenance of a permanent International Bureau of Weights and Measures (BIPM). In addition to the original primary work of verifying the new metric standards the International Bureau was charged with various duties, including:

(1) The custody of the international prototype standards

(2) The periodic comparison of the several national standards with the international prototypes

(3) The comparison of metric standards with other standards, such as the British yard and pound.

The French government donated a small historic manor, the Pavillon de Breteuil, located in the Parc de St. Cloud, on a hillside overlooking Paris from across the Seine. This building contains a large meeting room, offices, and the residence of the director of the bureau. Specially designed buildings have been erected on the grounds, to house the metrological laboratories. The bureau has a staff of about 40 persons; it operated on an annual budget of about $300,000 in 1964 but is to be escalated to about $600,000 by 1968 with an increase of staff.

The organization chart for this international operation is shown in Figure 1. The General Conference is a diplomatic operation; our representation is via our Department of State. The International Committee on Weights and Measures (ICWM) is an 18-man technical committee, elected by the General Conference. The ICWM nominates the director and senior staff of the

International Bureau, and also nominates the members of seven Advisory Committees of experts. Most of the committee seats are held by national laboratories, but there are also a few individuals named as members. In these Advisory Committees the work of the national laboratories towards improved standards of measurement can be discussed, and international decisions prepared. The International Committee has the privilege of calling the governments participating in the Convention of the Meter to meet in a General Conference. It submits to the General Conference proposals concerning the program and financing of the International Bureau, and also drafts of resolutions by which the governments agree on physical units and constants, or other matters of metrology, such as research in new directions. Examples of the recent work of this hierarchy of committees are the redefinition of the meter in terms of the wavelength of a particular spectral line of krypton 86; the assignment of the frequency 9 162 631 770 hertz to the cesium oscillator; the establishment of the thermodynamic temperature scale based on the triple point of water; and establishment of the International System of Units, whose electrical subset is the MKSA system incorporating the practical electrical units instead of the confusing statvolts, abamperes, etc., found in the old physics textbooks.

The legal values of units in the United States are those represented by or derived from, national reference standards maintained by the National Bureau of Standards operating under the Treaty of the Meter. The ICWM has resolved that "The values assigned to the national standards of reference will be determined in accordance with the results of comparisons made with the standards of reference of the International Bureau." Thus we have a legal chain of connection from the international actions right down to the working standards used throughout the U. S.

National standards are intercompared at the International Bureau. For example, at approximately three-year intervals, the major nations submit standard cells and standard resistors for massive intercomparisons. Drifts in any nation's standards are thereby spotted, and that nation can take whatever corrective action it sees fit. Precision three-terminal capacitors are now being intercompared by round-robin procedures. The BIPM is planning to acquire equipment allowing it to play a central role, such as it does for resistance and voltage.

At a recent (May 1965) meeting of the Advisory Committee on Electricity, arrangements were made for international round-robin comparisons of high-frequency measurements, such as the measurement of power at 10 GHz. In addition, the Advisory Committee is recommending to the International Committee that the International Bureau be given competent personnel and appropriate equipment for getting into the business of precise measurement of high frequency quantities.

Let me close with this brief sketch of international metrology with a quotation from a recent paper by Dr. Terrien, Director of the International Bureau of Weights and Measures: "Young scientists of to-day are much more aware than formerly of the necessity and interest of metrology, and of the fascinating field of scientific research it offers; they know, or they can learn, that the out-of-date picture of metrology where a patient observer spends weeks to calibrate a divided scale, must be replaced by the picture of a living and modern laboratory. But what is peculiar to metrological work is perhaps the perfection which is aimed at. No aspect of a metrological experiment can be neglected; the endeavour to have complete control and knowledge of what is being done, and to get quantitative proof with one more decimal than was possible yesterday, that is truly science, research for truth. Aiming at perfection is also the concern of the artist. And that is why metrology can be said to be not only science, but art."

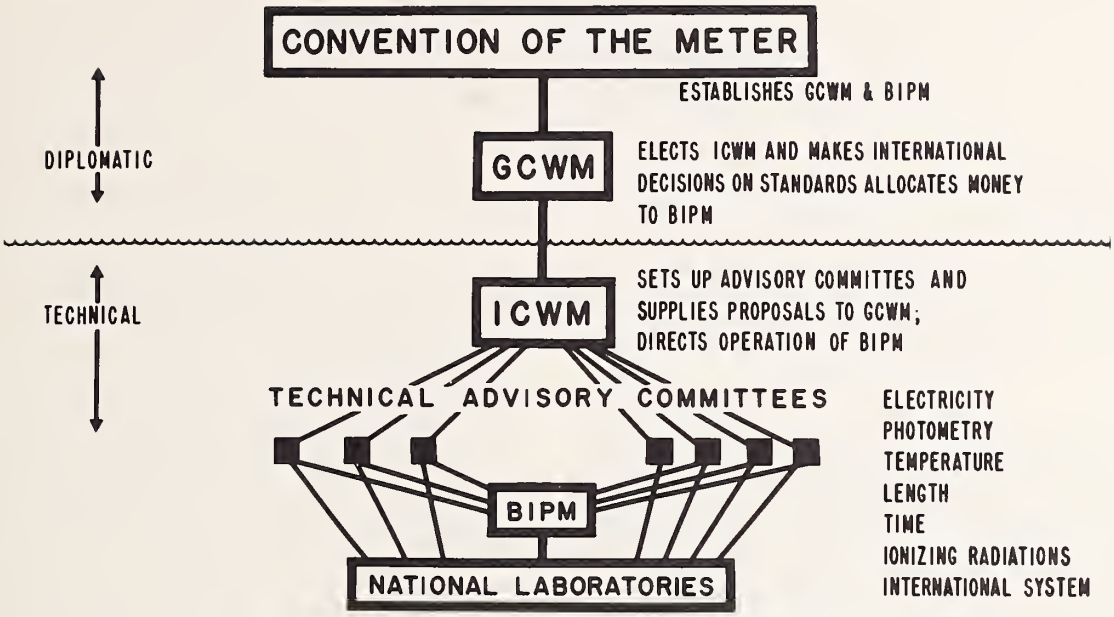

GCWM = GENERAL CONFERENCE ON WEIGHTS AND MEASURES

ICWM = INTERNATIONAL COMMITTEE ON WEIGHTS AND MEASURES

BIPM = INTERNATIONAL BUREAU OF WEIGHTS AND MEASURES

Fig. 1

PREPRINT INSTRUMENT SOCIETY of AMERICA
19th Annual ISA Conference and Exhibit • October 12-15, 1964, New York
Preprint Number 12.1-1-64

ELECTRICAL UNITS

by Dr. Forest K. Harris - Non-member
Physicist
National Bureau of Standards
Washington, D. C.

ABSTRACT

The origin, development and present status of the units of electrical measure are briefly reviewed. The distinction between the defined MKSA units and the "legal" units that form the basis of the practical measuring system in the United States is stated, and the differences between the two systems are examined.

Many systems of electrical units have been used in describing electrical phenomena and the relations between electrical quantities, and in making electrical measurements. Some of these units are of historical interest only. Others have been used by theoreticians; and their continuing fondness for them has elements of tradition as well as convenience. Two systems of units are presently of concern to all of us who must make engineering measurements--the MKSA system of absolute units; and the "legal" units to which any meaningful electrical measurement in the United States must somehow be referred. These we shall examine later, critically and in detail. For the moment, it may be stated simply that the MKSA units are the defined absolute units that form the electrical portion of the Système International d' Unités accepted throughout the world as the common theoretical basis for metric measuring systems; and the legal units are the practical units maintained in the Washington laboratories of the National Bureau of Standards, based on physical standards that represent the defined MKSA units as nearly as the state of measurement art permits.

The only means we have of detecting or measuring any electrical quantity is through a force that it produces or an energy transformation it brings about. Thus it is natural that one should seek to express electrical quantities in terms of the mechanical units that we use to evaluate force and energy (or work); and it is also desirable that the system of electrical units be compatible with the system of mechanical units, i.e., that quantities--such as force, torque, power, work--common to the two systems be expressed in identical units, whatever their origin.

It is on this basis--compatibility between the electrical and mechanical units--that the MKSA system of electrical units was defined in terms of the prototype mechanical units of length, mass, and time--the Meter, Kilogram and Second. Compatible systems of electrical and mechanical units have been in use almost exactly 100 years. It was in 1863 that a committee of the British Association for the Advancement of Science, under the chairmanship of Maxwell, recommended the adoption of an "Absolute-Practical" system based on the centimeter-gram-second system of electromagnetic units suggested by the earlier work of Gauss and Weber. In this context, the term--absolute-practical--meant that the units were defined in terms of relations between electrical and mechanical quantities, and were of such size as to be most useful in practical measurements. The "absolute-practical" units of the BA committee were, in fact, decimal multiples of the cgs electromagnetic units, and were of such size that the product of unit current by unit potential difference was one watt, the practical unit of power in the mechanical system of units. The BA unit of resistance--the Ohm (10^9 cgs electromagnetic units of resistance)--was also conveniently close to a German unit of resistance--the Siemens Einheit*--that had been used to a considerable extent. Similarly, the BA unit of potential difference--the Volt (10^8 cgs electromagnetic units of potential difference)--differed by little more than 20% from the emf of a Daniell cell, which had been used to some extent as a unit of potential difference. The BA units were thus of reasonable size, convenient for measurement purposes, and soon achieved international acceptance in principle. Much later (in 1901) it was pointed out that, if the meter, kilogram and second had been used as the defining mechanical units rather than the centimeter, gram and second, and if the value 10^{-7} were assigned as the permeability of free space rather than the value unity that it has in the cgs electromagnetic system, the MKS Absolute* system so defined would be identical with the Absolute-Practical units of the British Association.

*The Siemens unit was the resistance of a mercury column 100 cm long and 1 mm^2 in section at 0°C, and was about 6% smaller than the Ohm.

*In the MKSA (meter, kilogram, second, ampere) system presently used the ampere is defined in such a way that the value of the permeability of free space is $4\pi \times 10^{-7}$. This system has units that are identical with the "Rationalized MKS System."

The first truly international system was the system of "reproducible" units*, adopted by the International Electrical Congress of 1893, and made the legal units of the United States in 1894 by a Congressional Act (Public Law 105). These "International Reproducible" units* were the best approximation of the British Association's "Absolute-Practical" units possible in the state of the art at that time. There was need for units which were reproducible in the sense that they would be set up independently by a careful experimenter in his own laboratory; but the establishment of the units soon became the task of the various National laboratories, established near the turn of the century. These laboratories set up reference standards of resistance and emf in terms of the reproducible units; and in 1910 representatives of the British, French, and German laboratories met with NBS representatives in Washington to resolve certain discrepancies in the units they maintained and to assign their national reference standards on a common basis. At the conclusion of this international meeting at the National Bureau of Standards, each representative returned to his own laboratory with a group of resistance standards and of standard cells which were in agreement and whose values had been assigned on the basis of the reproducible units--the mercury ohm and silver ampere. Following this, each national laboratory maintained the electrical units in terms of these standards.

*In the International-Reproducible system the ohm was represented by the resistance at 0°C of a column of mercury 106.3 cm long and about 1 mm^2 in section; the ampere was defined as the current required to deposit silver from a silver nitrate solution at a rate of 0.001118 g/sec.

*not to be confused with the MKSA units of the present Système International d' Unités.

With the development of calibration and test services at the various national laboratories, the need for reproducible standards diminished, since it was easier and simpler to have a value assigned to a standard by comparing it to a National Reference Standard than by setting up mercury-ohm and silver-ampere apparatus and making the required measurements in one's own laboratory.

In the decade that followed the first World War, as interest revived in international agreement of standards, it became apparent that there were serious discrepancies between the electrical units as maintained by some of the National laboratories, and further that the accuracy with which the defined "mercury-ohm" and "silver-ampere" could be reproduced no longer met the needs of science and technology. Thus a strong movement developed to abandon the International-Reproducible units and return to the Absolute-Practical system. This stimulated studies of absolute measurements and the performance of absolute ohm and ampere determinations in several of the National laboratories.

The movement toward international agreement on the readoption of absolute units and the reassignment of national reference standards on the basis of absolute measurements was interrupted by the second World War, but was taken up again immediately afterward and culminated in the 1948 reassignment of the electrical units. The ohm, as maintained in the United States was decreased in value by 495 ppm (parts per million) and the volt was decreased by 330 ppm. Historically, this is the last change that has been made in our electrical units. Our defined system is now the MKSA system; and the legal units are maintained on the basis of their 1948 assignment.

The Congressional Act that defines the electrical units of the United States, has the following provision:

> "It shall be the duty of the National Bureau of Standards to establish the values of the primary electrical units in absolute measure, and the legal values for these units shall be those represented by, or derived from, national reference standards maintained by the National Bureau of Standards."

How then are values assigned to the "national reference standards;" how are these standards maintained; and how closely do the legal units of the United States--based on these standards--agree with the defined units of the MKSA absolute system?

If our electrical units are to be established in such a way that the electrical and mechanical units of energy shall be identical, it is inevitable that the mechanical quantities force and distance be involved in the physical realization of the electrical units. Physical realization of the units involves the assignment of numerical values to physical standards that represent and embody the units. This is done by means of absolute experiments in which an electrical quantity is measured directly in terms of its relation to the basic mechanical quantities--length, mass and time.

Two types of absolute measurement form the basis of the present assignment of values to our system of electrical units. In one experiment, the ohm is measured as a function of length and time; in another experiment, the mechanical force between current-carrying conductors is used to measure the ampere.

Absolute Ohm experiments have traditionally evaluated the ohm in terms of a calculable inductor and a frequency, the value of the inductor being computed from its measured dimensions. The ohm is thus established in terms of the mechanical units of length and time--the meter and the second. The absolute ohm experiment could be carried out equally well in terms of a capacitive reactance in a network that takes proper account of the phase relation between them. Here the value of the capacitor is computed from its

measured dimensions. Such determinations have, in fact, been made and, while their results have not been incorporated into the value of the "legal" ohm maintained by the Bureau, there is little doubt that any future reassignment of the national reference standard of resistance will rely heavily on the results of ohm experiments that involve a calculable capacitor. The metrology of a calculable capacitor is much simpler and more direct than that of a calculable inductor and--of equal importance--a capacitor can be so shielded that its value is completely independent of anything outside the shield, whereas an inductor cannot be isolated so as to be completely independent of its surroundings.

In the traditional ampere experiment, the force between two current-carrying coils is measured by opposing it to the gravitational force on a known mass. The electrical force involves the rate of change of mutual inductance between the coils with linear or angular displacement; and the ampere is measured in terms of the mechanical units of length, mass and time--the meter, kilogram and second. The current, measured in absolute amperes is passed through a resistor whose value is known in absolute ohms. The resulting voltage drop is opposed to the electromotive force of a standard cell, and its value is assigned in absolute volts. This experiment gives us a second physical standard in terms of which the electrical units can be preserved.

In theory the second of the two absolute measurements required to establish our system of electrical units could be an absolute volt experiment, in which the mechanical force produced by a potential difference between the plates of a capacitor is measured directly and related to the emf of a standard cell without resort to an absolute ampere experiment. At the present time (1964) no such absolute volt determination has been made with sufficient accuracy to justify its consideration in assigning values to the National Reference Standard, but such an experiment is under study.

The National Reference Standards consist of a group of 10 Thomas-type 1-ohm resistors and a group of 44 standard cells. Their values were assigned on January 1, 1948, in terms of absolute ohm and ampere experiments in our own and other National Laboratories. Although additional absolute measurements have since been reported, there have been no reassignments of our National Reference Standards. The legal units of electrical measure for the United States are based on the 1948 values assigned to the National Reference groups, and on the assumption that the average values of these groups have remained unchanged. The members of each group are regularly intercompared; and the values of the ohm and volt as maintained at the National Bureau of Standards are periodically compared with the units maintained by other National laboratories. This comparison is carried out at the International Bureau of Weights and Measures at Sevres (near Paris); and it insures that the electrical standards used throughout the world remain in substantial agreement. In the fifteen years that have elapsed since the 1948 assignment, the measured differences between the ohm maintained by the National Bureau of Standards and that maintained by the International Bureau have never been greater than 1 ppm, and in only one comparison was the measured difference greater than 0.4 ppm. In the standard-cell comparisons, the greatest difference between the U. S. volt and that of the International Bureau was 3 ppm (in 1955), and the differences in other comparisons have been less than 2 ppm.

It must be recognized that these comparisons do not constitute complete proof that our National Reference Standards have kept their 1948 values. The most one may conclude is that, if they are changing in value, the drift rate is not significantly different between our reference groups and those of the International Bureau. Some further proof of stability is needed. A means of examining the stability of the National Reference group is a repetition of an absolute experiment.

The results of four absolute-ohm determinations have been reported between 1948 and 1960. The average of these determinations differs by less than 1 ppm from the ohm as maintained by NBS, and there is no evidence of any systematic change of the unit with time. Preliminary results from another ohm determination (as yet unpublished) also indicate that the NBS ohm differs by less than 1 ppm from the defined absolute unit. Taking into account the estimated uncertainties of the various ohm determinations, it may be said that it is very unlikely that the difference between the absolute ohm and the legal unit (as maintained by NBS) is as much as 5 ppm, and there is substantial evidence that this difference does not exceed 1 ppm.

The situation of the legal volt does not appear to be as favorable as that of the legal ohm. The mean of two ampere determinations made since the 1948 assignment indicate that the difference may be about 12 ppm between the absolute ampere and the NBS ampere--the latter being determined as the ratio of the legal volt to ohm. The estimated uncertainty of the most recent ampere determination was 6 ppm. If one accepts the evidence of agreement between the absolute and NBS ohms, it follows that the NBS volt may be 9-13 ppm greater than the absolute volt.

Recently, a new means has become available to maintain surveillance on the constancy of the NBS ampere, and hence on the ratio of the legal volt to ohm. If a measured current is used to set up a magnetic field in a coil of simple geometry and fixed dimensions (a single-layer solenoid wound on a fused-quartz cylinder), the precession frequency of protons in a pure water sample immersed in this field is a measure of the field strength and therefore of the current in the solenoid. A series of such measurements over a 4-year period, using a current whose value was always the same in terms of the NBS volt and ohm,

yielded nearly constant precession frequencies. When the data were reduced to a fixed solenoid temperature, the largest departures from a constant precession frequency amounted to no more than 0.4 ppm over the 4-year interval. Uncertainties in the measured dimensions of the soleniod at the beginning and end of this period amount to about 1 ppm in terms of the calculated magnetic field, and this uncertainty limits any statement concerning the constancy of the NBS ampere. However, in the light of other evidence concerning the constancy of the NBS ohm, it seems likely that the "legal" volt has also remained constant within 1 ppm over the 4-year interval.

A number of questions may properly be asked at this point--1) Apart from the challenge of doing a better job, what need is there for further refining of absolute measurement techniques? 2) Assuming that further refinements can be made in the experimental techniques of absolute measurement, are there other factors that limit their accuracy? 3) Are any changes to be expected in the National Reference Standards or in the way they are maintained? These questions will be considered in turn.

1) The stability of a reference standard is its most important characteristic, and an absolute measurement is the only direct and certain test of the stability of the National Reference Standards. Clearly then, absolute measurements must be repeated occasionally. Such absolute determinations as have been reported in the recent past had estimated uncertainties that ranged from 2-6ppm or more. Obviously, the smaller the uncertainty of such a determination, the more informative it is about the stability of the "legal" unit, maintained by the National Reference Standard; and an immediate goal of not more than 1 ppm uncertainty in absolute determinations seems appropriate. In the field of science, the accuracy with which many of the atomic constants can be assinged is now beginning to be limited by how well we know the ampere and the volt; better assignment of these electrical quantities can only come from better absolute determinations. Finally, as the measurement demands of space-age technology grow more severe, it is reasonable to suppose that more nearly exact compatibility will be required between mechanical and electrical units of measure.

2) Future ohm determinations will probably be based on a calculable capacitor, and its computed value is a function of the permittivity of free space. In the MKSA system, it is the permeability of space that is assigned through the definition of the ampere ($4\pi \times 10^{-7}$). Therefore the permittivity of space must be computed from this assigned constant and the speed of light. Thus the value of permittivity used in assigning a value to the calculable capacitor can be no more certain than the accuracy with which the speed of light is known. In an ampere or volt determination, force is measured in terms of the gravitational force on a known mass, and its accuracy is limited by how well the acceleration of gravity is known at the place where the experiment is performed. In a volt determination, dependent on the measured force between capacitor plates, the speed-of-light uncertainty would also have to be taken into account. The accuracy with which the prototype mechanical units can be reproduced and subdivided does not impose any significant limits on absolute electrical measurements at the present time, but uncertainty in the speed of light and in the acceleration of gravity are presently (1964) such limiting factors.

3) Both the National Reference Standard of resistance and of emf appear to be stable within the uncertainty limits of the pertinent experimental information as, indeed, they should be from structural considerations. The 1-ohm resistors of the National Reference Standard are thoroughly annealed, are mounted to be free from strain, and are sealed against contact with air and moisture. It would appear that only the hazards of misuse or abuse (i.e., overload or mechanical shock) would be likely to affect their stability; and in either instance one would expect a sudden change in value (easily detected) followed by a period of drift and finally stabilization about a new value. The saturated cells of the National Reference Standard are inherently stable, being sealed and isolated chemical systems that are in equilibrium when maintained at a constant temperature. Changes of temperature and even very small temperature gradients across the cell limbs must be avoided, as this would upset the equilibrium with a consequent slow recovery period. Another reason for avoiding temperature gradients is the rather high thermal emf (8 μv/°C) that would develop across the junctions between the platinum conductors used in sealing through the glass envelope of the cell and the copper leads going to the measuring circuit. If proper precautions are taken with temperature, it would appear that only the hazards of misuse or abuse remain, and most of these are more likely to render the cell completely inoperative rather than to exert a minor effect on its stability. One hears occasionally the suggestion that Zener elements with appropriate circuitry might replace standard cells as voltage reference standards. Certainly such a device has many attractive features including ruggedness and ability to withstand abuse without injury. Thus Zener reference devices may eventually replace standard cells in many laboratory operations and in most field operations, but in their present state of development they do not compare at all favorably with saturated standard cells either from the viewpoint of stability or freedom from electrical noise. Even if their development were to continue at its present rate, it would take many years to establish a history of stability and reliability comparable to that of saturated standard cells. Thus there is nothing in sight at present that suggests either a change in the National Reference Standards of electrical measure or in their maintenance.

315-411 O - 68 - 2

Definition of "Ampere" and "Magnetic Constant"

There appears to be some confusion about the definition of the electrical units in the MKSA system. Some engineers believe that the *ampere* is arbitrarily defined, with the result that the numerical value of μ_0 is $4\pi 10^{-7}$, while others hold the view that μ_0 has an arbitrarily *assigned* value. In view of the current IEC (International Electrotechnical Commission) proposal to assign the name "magnetic constant" to the quantity (μ_0) commonly called "permeability of space," it seems desirable to clarify the definitional basis of the electrical units.

Part of the confusion arises from two different concepts, both called "ampere." One meaning of ampere is the *measurement unit* of current, which is a physical entity realizable in the laboratory; the other meaning refers to the *abstract*, or *symbolic*, *unit* in the mathematical representation of current.[1] It is in this second meaning that the ampere is chosen, *for purposes of dimensional analysis*, to be independent of length, mass, and time. This is the origin of the A in the name MKSA system. Mathematical representation of physical relations is always influenced by individual taste; dimensional analysis and interpretation vary widely, and all this plays a role in the "ampere" as an *abstract unit*. The *measurement unit*, on the other hand, must be the same for all laboratories, so I shall take the measurement unit problem as basic, and the abstraction as secondary.

There are several experimental situations that can be used to define the numerical measure of a current. After one of these is chosen, it can be used in an operational procedure for realizing the unit of current (ampere). One could use an experiment which determines current in terms of a natural quantum of charge, as was done in the old international silver coulometer definition, or one could use magnetic effects, such as the interaction force between two currents. The latter is the one that has been adopted for all "absolute" unit systems.

The electromagnetically produced force between conductors is known to satisfy a certain proportionality; the *magnetic* constant $(\Gamma_m)^2$ is the name given to the proportionality constant when the relation is written in the form

$$dF = \Gamma_m I_1 I_2 \frac{ds_2 x (ds_1 x r)}{4\pi r^3}$$

expressing the force between two current elements in vacuo. If the ampere were defined *independently* of this relation, then the measure $\{\Gamma_m\}$ would be subject to *experimental* determination.[3] If, on the other hand $\{\Gamma_m\}$ is arbitrarily chosen, the ampere is thereby defined because we anc deduce a recipe (operational description) for realizing a current of specified measure, *e.g.*, a current such that $\{I\}=1$. This current is then defined to be the ampere. Superficially, it would appear that we could choose this recipe as the definition of the ampere, and thus define the ampere without assigning a value to $\{\Gamma_m\}$. The change is purely psychological, not logical; it corresponds to a change of word order in the definition of $\{\Gamma_m\}$, since $\{\Gamma_m\}$ can be *computed* from such a definition of the ampere and no experiment need be performed.

The old international ampere based on the silver nitrate coulometer was independent of Γ_m. In the Système International d'Unités, however, the ampere is actually defined by assigning the number $4\pi 10^{-7}$ as the measure of Γ_m in the interaction-force equation.

Choosing $\{\Gamma_m\}$ and specifying the equation in which Γ_m appears, *implicitly* defines the ampere. The corresponding *explicit* definition is the familiar "legal" form relating the ampere to a force of 2.10^{-7} newton per meter between infinitely long parallel wires in empty space.

The above viewpoint is not only logically correct but also historically accurate. In 1938, the IEC Subcommittee EMMU (now TC 24) followed the 1935 actions of the International Committee on Weight and Measures, and its Advisory Committee on Electricity, by adopting the *assignment* of $4\pi 10^{-7}$ as the connecting link between electrical and mechanical units.

Symbolic Unit

The quantity equation representation of the facts of physics are based on a representation of physical entities as mathematical elements in a many-dimensional vector space.[1,4] Such an abstraction is much more sophisticated than a quantitative description of physics by measure equations alone. It is not a consequence of experimental physics, but a useful intellectual tool invented by man. Like any other tool, its design is affected by individual esthetic preferences; in fact, many people object to the abstraction *per se*.

Among practitioners of abstraction, there is universal agreement on the choice of mass, length, and time as orthogonal axes in the vector space of quantity calculus. The addition of electrical entities to this mechanical subspace requires an additional dimension. Various tastes prefer Γ_e,[5] Γ_m, I, or Q as the fourth axis. Some physicists even prefer to ignore this fourth axis and interpret all electrical quantities as being dimensionally only mechanical quantities.

In 1938, when TC 24 chose the measure $4\pi 10^{-7}$ as the defining link between mechanical units and the Giorgi System of electrical units, it made no decision on matters of taste. In 1950, however, this committee decided that the ampere could be taken as the "fourth principal unit," and accepted as the *definition* of the ampere, the *measurement unit* definition applicable to infinitely long parallel conductors, deducible from the force relation by assigning $\{\Gamma_m\}=4\pi 10^{-7}$.

Thus the ampere, as a *measurement unit*, is defined by the IEC both implicitly and explicitly; as a *symbolic unit*, it has not been "defined" but has been "accepted" as a "principal unit" on which to "base" the Giorgi system.

It is difficult to define symbolic units. We can define symbolic or abstract quantities as mathematical elements that "correspond" (in some unspecifiable manner) to observable physical quantities, or as mathematical entities that "represent" the corresponding physical entities. The symbolic units then "correspond" to the measurement units in the same unspecifiable manner. If the quantity equations are to be formally the same as the measure equations, there are compatibility relations on products of symbolic quantities and units, but there is an independent ("basic," "principal," "fundamental") set of symbolic units that can be arbitrarily chosen. This set is customarily chosen to comprise three mechanical units and one electrical unit. The remaining symbolic units of electromagnetism are defined mathematically in terms of these four. These basic four are in principle *undefinable*, they are postulated units in terms of which the remainder are defined. Thus the choice of the ampere as the "fourth principal unit" is tantamount to stating that the ampere is the *only* symbolic electromagnetic unit which *cannot* be defined.

In summary, the symbol Γ_m has been defined as the proportionality constant in a particular equation; its measure has been arbitrarily assigned; the consequent explicit form of the definition of the ampere (measurement unit) has been adopted, and the abstract mathematical element (symbolic ampere) representing a physical ampere has been chosen as the undefinable "intuitive" element of the electrical set.

Chester H. Page
Electricity Div.
U. S. Dept. of Commerce
National Bureau of Standards
Washington, D. C.

Manuscript received September 1, 1964.

[1] C. H. Page, "Physical entities and mathematical representation," *J. Res. Nat. Bur. St.*, vol. 65B, pp. 227–235; October–December, 1961.

[2] The symbol μ_0 is traditionally employed but is gradually being replaced by Γ_m by reason of the misleading implications of a "permeability" symbol.

[3] The notation $\{x\}$ indicates the numerical value of x, without statement of its unit or dimension. See Page.[1]

[4] Wilhelm Quade, Über die algebraische Struktur des Grössenkalküls der Physik, Abhandlungen der Braunschweigischen Wissenschaftlichen Gesellschaft, Band XIII, 1961.

[5] The electric constant, also represented by ϵ_0.

Reprinted from the PROCEEDINGS OF THE IEEE
VOL. 53, NO. 1, JANUARY, 1965

ELECTRICAL STANDARDS AND MEASUREMENTS*

I. L. Cooter, B. L. Dunfee, F. K. Harris, W. P. Harris, F. L. Hermach, C. Peterson
National Bureau of Standards

Introduction - Many millions of measurements of electrical quantities made every year throughout the United States are based on a consistent system of reference standards established and maintained by the National Bureau of Standards in cooperation with the National Laboratories of other countries. Our National Measurement System derives from the International System in terms of which the legal units of measure of 38 countries are defined. Among the duties of the Bureau of Standards are included the establishment of electrical units that are consistent with the International System and the assignment of values to reference standards which will preserve the legal units and serve as the starting point of all the measurement chains whose final links are the myriads of electrical measurements made daily throughout the nation. It is only by using a consistent system that scientists in different laboratories can talk in the same terms, or that one can expect proper functioning of devices assembled from components made in different places at different times, or that competing sources of energy can be fairly compared, or that complex industrial processes can be made to yield a product of constant and acceptable quality. We shall here review briefly the means by which the Bureau has established the legal units of electrical measure and shall discuss the experimental procedures by which the values of the basic reference standards are made available as initial links in all the measurement chains that form the National Measurement System.

Fundamentals - By international agreement, the official basis for electrical measurements throughout the world is the International System of Units--based on the meter, kilogram, and second--together with a value of the unit of electric current (the ampere) defined in such a way that the permeability of free space has the value $4\pi \times 10^{-7}$. One constraint on the system--essential to its compatibility with the corresponding system of mechanical units--is that the electrical unit of energy be identical with the mechanical unit of work. A second constraint is that the physical laws which state the basic relations between the units be expressed in the simplest possible terms, without the need (in most cases) of numerical proportionality constants other than unity. The first of these constraints leads inevitably to the experimental realization of the tie between the electrical and mechanical units in terms of units of force and length--the components of work. The second constraint simplifies the derivation of all the remaining electrical units, once we have fixed two of them by "absolute" experiments in terms of the mechanical units. In the present context, an absolute experiment is one in which the value of an electrical quantity is established directly in terms of mechanical units.

The most recent assignment of our basic reference standards was made in 1948--consequent to an international agreement--and was based largely on the results of absolute ohm and ampere determinations made at the National Bureau of Standards and at the National Physical Laboratory of Great Britain. Absolute measurements of the quality needed for assignment of basic reference standards require access to the fundamental mechanical reference standards and, thus, can be carried out effectively only at the larger national laboratories of the world; and, while a number of the other national laboratories have programs of absolute measurements, none of their results were available in final form at the time of the 1948 revision. A number of additional results have since been reported from various national laboratories (including our own), and there is substantial evidence that the ampere determinations on which the 1948 assignments were based were in error by about 10 to 12 parts in a million. Thus, it is reasonable to suppose that when further evidence has been accumulated, the assignments of the basic reference standards may be modified to bring them more closely into agreement with the defined units of the International System.

Over the past century--since reference standards of resistance were first assigned by Maxwell and his colleagues of the British Association for the Advancement of Science--the classical ohm experiment has involved the construction of a self- or mutual-inductor whose value could be computed from its measured dimensions and the assigned value of space permeability--unity in the cgs electromagnetic system or $4\pi \times 10^{-7}$ in the MKSA System of Units. The reactance of this calculable inductor at a known frequency was then compared to a resistance in a suitable network, and the value of the resistor was thus assigned in terms of the units of length and time. Since the relative positions of all the conductor turns in the inductor must be determined, the dimensional metrology required for an absolute ohm experiment has been very elaborate, time-consuming, and tedious.

Within the past decade, a new type of ohm determination of appropriate accuracy has become feasible, based on a calculable capacitor. A new theorem in electrostatics, published by Thompson and Lampard of the Australian National Standards Laboratory, has led to a capacitor construction whose configuration is such that only a single length determination is critical to the calculation of its capacitance. One can compare a capacitive reactance and resistance at a known frequency and determine the resistance in units of length and time and the permittivity of space. The dimensional metrology is very much simpler than for the calculable inductor, and the experiment appears capable of a precision at least an order of magnitude better. In fact, the element of greatest uncertainty in this procedure at the present time is the speed of light--it is from this experimental constant and the assigned value of space permeability that the value of space permittivity must be obtained for the calculation of capacitance. An

*Expanded version, with corrections, of "Electrical Standards and Measurements," by I. L. Cooter, B. L. Dunfee, F. K. Harris, W. P. Harris, F. L. Hermach, and C. Peterson, Electro-Technology 79, 53 (Jan. 1967).

absolute ohm determination based on a calculable capacitor has been reported which checks the present assignment of the National Reference Standard within a part in a million, and other determinations are under way that have not yet been reported.

The second absolute experiment required to assign the electrical reference standards in terms of mechanical units has been classically the absolute ampere determination. In this experiment, the value of a current in two coils is measured in terms of the force between them, using a balance in which this force is opposed to the gravitational force on a known mass. Thus--from the balancing mass and the local acceleration of gravity--the ampere is expressed in units of length, mass, and time. In this experiment, a resistance standard is connected in series with the coil system, and the potential drop produced in it by the measured current is compared to the electromotive force of a standard cell. By this means, the emf of the cell is assigned in absolute volts, and the cell preserves the result of the experiment. A variety of coil shapes and arrangements have been used in current balances at the Bureau and in several of the other national laboratories. In any arrangement, dimensional measurements are required to determine relative coil size and positions, since the statement of force between the coils requires that the change of mutual inductance with moving-coil displacement be evaluated.

The units realized by these absolute measurements are preserved at the Bureau by a group of 10 stable 1-ohm resistance standards and a group of 44 saturated cadmium-mercury standard cells. To maintain the legal units, the assumption is made that the mean of each reference group does not change with time. To guard against drift of individuals, they are intercompared regularly; to guard against group drift relative to the legal units of other countries, triennial intercomparisons are made at the International Bureau of Weights and Measures at Sevres, France. Further assurance that there is no important group drift is obtained by the occasional repetition of absolute ampere and ohm determinations, and by proton precession frequency measurements which will be discussed below.

The relations between the electrical and mechanical units, and the steps involved in assigning values to basic reference standards are shown in the block diagram of Figure 1. It will be noted that this diagram indicates the units and steps currently in use (1966) rather than those which served in the absolute measurements on which the 1948 reference-standard assignments were based.

Reference Standards for Electrical Quantities - The many electric and magnetic quantities used in science, engineering, and industry--current, voltage, inductance, capacitance, resistance, magnetic flux, etc.--are connected to each other and to the various mechanical quantities by exact mathematical relations. Similarly, the various units--ampere, volt, henry, farad, ohm, weber, etc.--in terms of which these quantities are measured, are linked by a parallel structure of exact definitions. Starting with any group of independent units, designated as "base" units, it is possible to derive definitions of all the others by successively applying appropriate mathematical relations. Both the choice of "base" units and the particular order in which the "derived" units are successively defined may be made

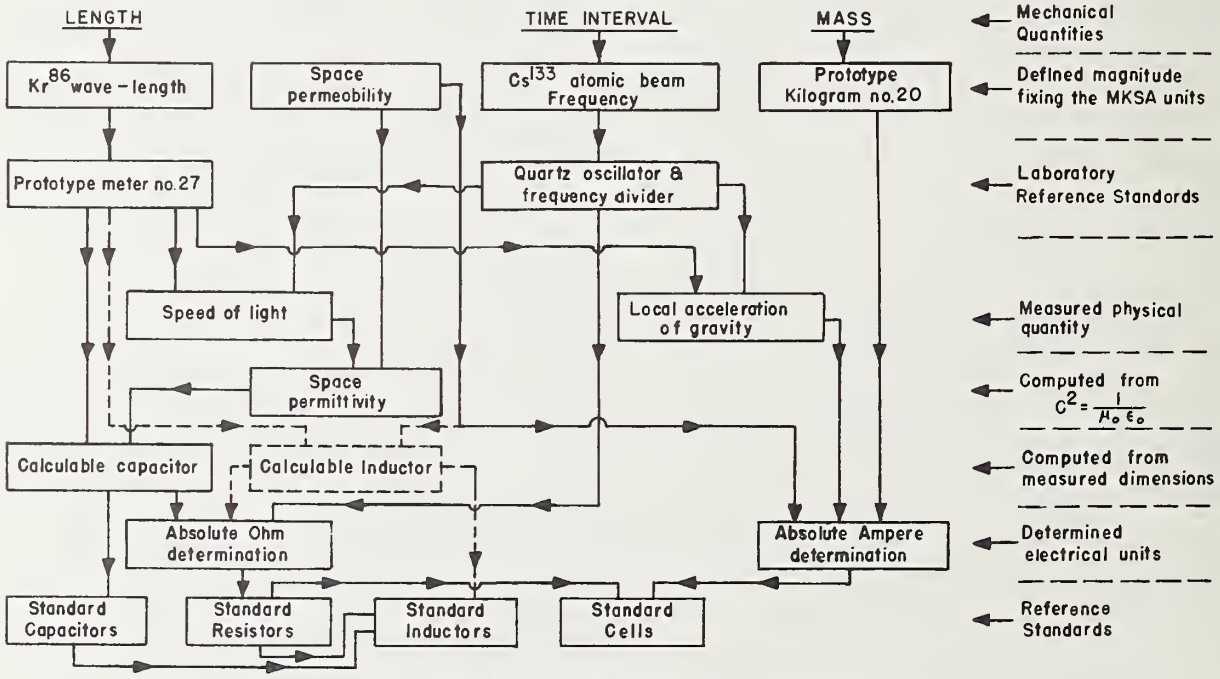

Figure 1. The Derivation of the Electrical Units.

It should be noted that the terms "magnetic constant" and "electric constant" are preferred by IEC to the terms "space permeability" and "space permittivity" used in this chart.

Figure 2. Calculable Cross Capacitor assembled from gage rods.

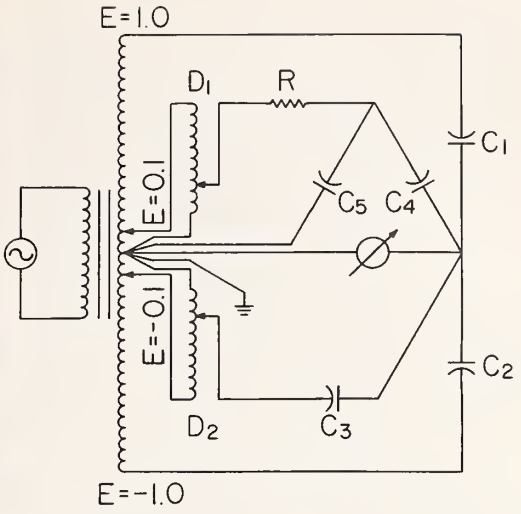

Figure 3.

Schematic diagram of a transformer-ratio-arm bridge for comparing capacitors.

C_1 and C_2 are capacitors being compared. C_3 is capacitor used to balance difference between C_1 and C_2, by varying tap point on inductive divider D_2 connected to 0.1 tap of ratio transformer. R is resistor used to balance phase difference between C_1 and C_2 by varying tap point of divider D_1 and current divider ratio $C_4/(C_4 + C_5)$.

arbitrarily, as taste, convenience, or practical experience suggests. In the discussion which follows, we shall examine in some detail the steps by which the Bureau arrives at reference standards for the measurement of various electrical quantities. Whether these steps appear straight forward or devious in particular cases depends solely on the exigencies of laboratory practice.

Capacitance - For many years, the unit of capacitance was derived from the ohm and second by means of a Maxwell commutator bridge. Within the past decade, the capacitance theorem of Thompson and Lampard has led to the construction of calculable capacitors whose values can be assigned from length and space permittivity with an uncertainty no more than a part in a million. During the same interval, the techniques of transformer ratio-arm bridges have been developed to an extent that permits comparison of equal capacitors to parts in 10^8 and extension of the unit upward through several decades at the part per million level. Finally, a stable capacitor design has been developed at the 10 pF level whose drift rate appears to be less than 1×10^{-7} per year. Thus, the unit of capacitance can now be established by absolute measure as a part of the ohm determination and values assigned directly from the calculable capacitor to stable reference standards which can effectively preserve the unit.

The theorem of Thompson and Lampard may be stated as follows: "If four infinite cylindrical conductors of arbitrary sections are assembled with their generators parallel, to form a completely enclosed hollow cylinder in such a way that the internal cross-capacitances per unit length are equal, then in vacuum these cross-capacitances are each $\ln 2/(\mu_0 \pi V^2)$." In the International System, where μ_0 has the assigned value $4\pi \times 10^{-7}$ and V is the speed of light in meters per second, the cross-capacitances are expressed in farads per meter. For small inequalities of cross-capacitance between pairs of opposite electrodes, it can be shown that the departure of their mean from the theoretical value is approximately $0.087\ (\Delta/C)^2$, where Δ is their difference and C their mean. Thus, if the inequality is no more than a part in 10^3, the error in the computed value is less than 1 in 10^7. A practical realization of such a capacitor consists of four equal closely-spaced cylindrical rods with their axes parallel and at the corners of a square. Arranged as a 3-terminal capacitor, the internal cross-capacitance amounts to 1 pF for a length about a half meter, and, if end effects are eliminated, this capacitance can be computed nearly as accurately as the length can be measured. Figure 2 shows the calculable capacitor, constructed of gage rods of known length, which is at present the basis of the Bureau's capacitance unit. Another calculable capacitor is now under construction whose active length will be measured interferometrically; it is expected that its use will improve the accuracy of the length measurement by at least an order of magnitude. Figure 3 is a schematic diagram of a transformer ratio-arm bridge such as is used for comparing 3-terminal capacitors and in extending the measurement range upward from the calculable capacitor. The ratio-arm transformer used in this bridge is of special design, and can provide a bridge ratio which is known and stable to a part in 10^8.

Figure 4 shows the construction of the 10 pF capacitors used to preserve the unit. The capacitor is a fused silica disc with fired-on silver electrodes. The measured direct capacitance is between the plane faces of the disc, and the cylindrical surface forms a guard electrode. The

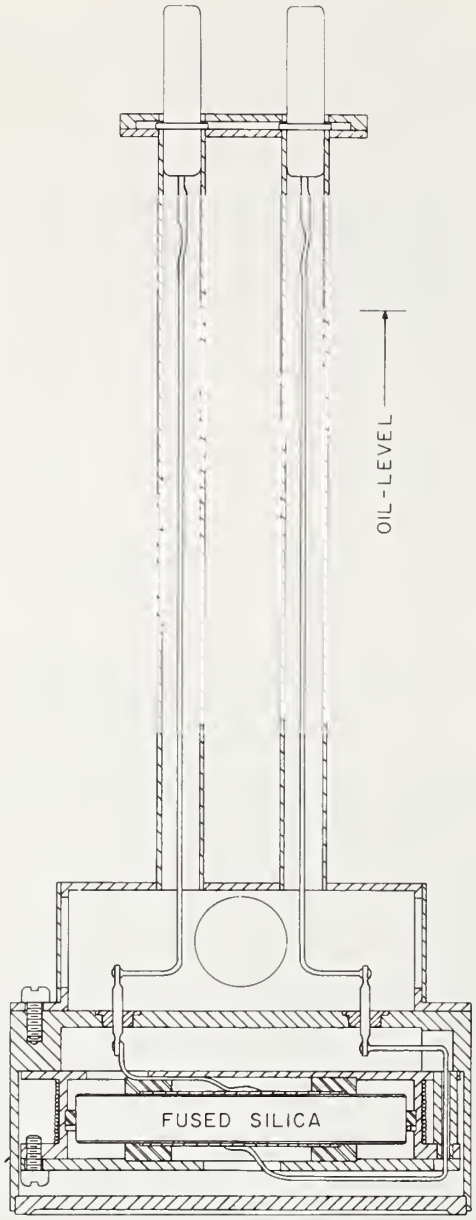

Figure 4. Cross-section of stable 10 pF capacitance standard with fused silica dielectric.

mounting protects the disc from mechanical shock, and the housing contains a resistance thermometer in addition to the capacitor so that proper allowance can be made for the temperature coefficient of capacitance.

The Capacitance Scale - The Bureau uses three types of capacitance bridges in the calibration of capacitance standards and high-quality decade capacitance boxes in the audio-frequency range--55 Hz to 30 kHz. Details of one of these bridges--a transformer ratio-arm bridge of NBS design and construction--are shown schematically in Figure 5. The bridge has eight built-in fixed 3-terminal capacitors ranging in value from 100 pF to 10^{-5} pF. Each of these capacitors can be connected to accurate decimal fractions (0.0, 0.1, 0.2 --- 1.0) of the transformer secondary voltage, the adjustment being provided by lever switches having contacts connected to taps on the transformer. Thus, eight decades of capacitance balancing adjustment are available. Means are also provided for balancing the loss component of capacitors being calibrated. The maximum direct-reading range of the bridge is 1111.1111 pF. Small 3-terminal capacitors having a value of 10^{-3} pF can be measured in this bridge with a total uncertainty of 0.3%. While this bridge was designed for the measurement of direct capacitance in 3-terminal capacitors, the use of auxiliary fixtures make it possible to perform measurements on certain 2-terminal capacitors. The design of the transformer incorporated in this bridge limits its operation--for best measurements--to the frequency range from 100 Hz to 2 kHz. Other transformers could be built to accommodate higher frequencies.

The second transformer ratio-arm bridge is a commercial version of the first, but with only six decades of capacitance balancing adjustment. Its chief advantage lies in the fact that 2-terminal measurements can be made conveniently and directly to a maximum of 10 μF. Indeed, with appropriate external build-up techniques, low-frequency measurements can be extended to 10 x 10 μF, using the bridge as a "tare" and relying upon a previously calibrated 10 μF capacitor as a substitution standard connected close to the terminals of the large capacitor being calibrated.

The third bridge has resistance ratio arms. It covers a wide frequency range--from 50 Hz to 100 kHz and is used for the routine calibration of capacitors having values up to 1.10 μF.

Each of these bridges can be calibrated by means of working standards of capacitance evaluated in terms of the unit of capacitance preserved with the group of 10 pF standards already described. For the most accurate calibration of standards adjusted close to the decimal scale of values, no reliance need be placed upon the bridge calibration. In fact, the best calibration of any physical standard is made by comparing it with a similar standard of known value, using a simple substitution technique. For capacitance measurements then, the bridge is used at unity ratio merely to measure the small difference between the two standards, and no bridge errors of significance are introduced if the upper dial settings of the bridge are not changed during the comparison.

Dielectric Constant - (or relative permittivity) is a property of materials that is closely related to capacitance measurements. It is generally determined as the ratio of the capacitance of a pair of electrodes in a cell with the material occupying all space in which there is appreciable electric field, to the capacitance of the same electrode configuration in vacuum. A typical cell for dielectric-constant measurements consists of a pair of flat parallel electrodes, a means of maintaining and measuring their positions, and provisions for inserting and removing a specimen: if one electrode is guarded (a 3-terminal capaci-

tor), the field can be more easily confined to the volume occupied by the specimen.

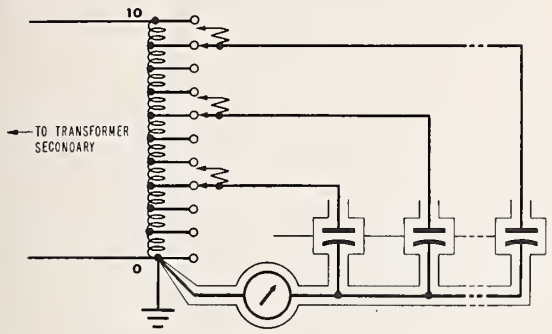

a. Schematic of low-range decade capacitor

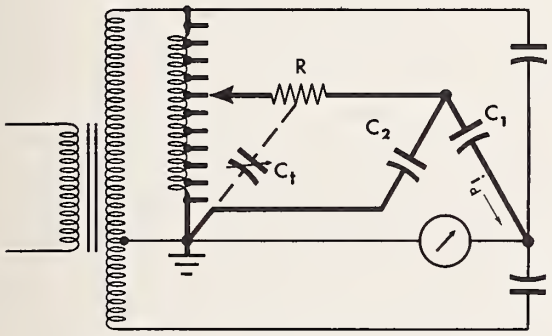

b. Basic conductance balance control circuit

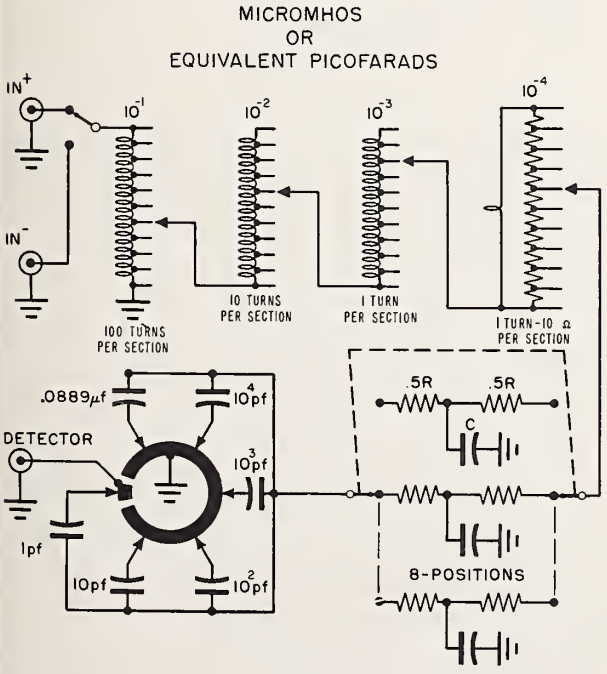

c. Details of conductance balance control circuit

Figure 5. Details of NBS capacitance bridge.

The practical frequency range for 3-terminal measurements is 10^{-3} to 10^{6} Hz, the lower limit being determined by the time required to achieve a bridge balance and the upper limit resulting from difficulties in maintaining the guard and guarded electrode at the same potential. The accuracy of 3-terminal measurements falls off from a part in 10^{6} or 10^{7} at 1 kHz to about a part in 10^{3} at the lower and upper frequency limits. Two-terminal measurements can be made up to 1 GHz with an accuracy of about 5 parts in 10^{3}.

The dielectric constant of a fluid can be determined to an accuracy limited only by the mechanical stability of the cell and the accuracy with which the cell capacitance can be measured. Very accurate measurements can be made on fluids by using a Thompson-Lampard capacitor in a constant temperature enclosure into which the fluid can be introduced and removed. In the measurement of solid specimens, additional errors result from practical difficulties in insuring that the specimen fills all the space between the electrodes and in determining the specimen dimensions which enter into the calculation of the dielectric constant. Typical solid disc specimens are 1-5 mm thick. Discs of hard mechanically stable materials such as ceramics can be machined very flat and their thickness measured to better than 0.1 micron. Uniform discs of less stable materials, such as plastics, are difficult to prepare and uncertainties in thickness measurement limit the accuracy of dielectric constant determination to about 0.1%.

For thin films, the accuracy of dielectric constant determination is severely limited by uncertainty in thickness measurements. This sensitivity to thickness error can be reduced by immersing the solid specimen in a fluid of similar dielectric constant during the measurement, and completely eliminated if the dielectric constants are equal. A 2-fluid immersion technique involving four capacitance measurements makes possible the calculation of the dielectric constant of solid disc specimens independent of area and thickness measurements. This technique is valuable for very accurate measurements on reference specimens that will be used for checking measuring apparatus in industrial and other laboratories.

Resistance - The unit of resistance is preserved by a National Reference Group of ten 1-ohm resistors hermetically sealed against air and moisture in double-walled enclosures after being fully annealed in an inert atmosphere at 400°C. Periodic intercomparisons show that their individual values do not vary with respect to the group mean by as much as 1 part in 10^{7} per year, and recent absolute-ohm determinations indicate that the group mean is within 1 part in 10^{6} of the defined absolute ohm.

The Resistance Scale - The primary instrument used at the Bureau for the measurement of resistance is a precision bridge built in the Bureau shops in 1918, which incorporates many features developed as a result of earlier experience in the field of precise measurement. The more critical resistance sections consist of hermetically sealed coils; the dial-adjustment resistances are of the Waidner-

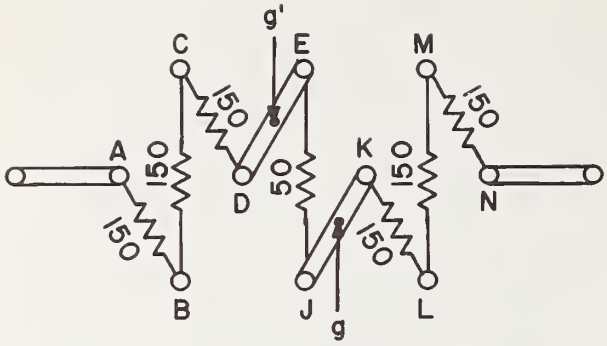

Figure 6. Circuit for establishing 10/1 resistance ratio.

Wolff type, made by changing the shunting around fixed resistors so that the effects of contact resistances and thermal emfs generated in the decade switches are greatly reduced; all resistors and contacts operate in oil in a temperature-controlled bath; and the circuit is shielded from stray currents. The bridge may be used either as a Wheatstone or a Kelvin bridge and is commonly used with a ratio that is nominally either 1/1 or 10/1. This ratio can be adjusted over a limited range (±0.5%) in the vicinity of the nominal value. The adjustment is made by means of four decade dials, one step on the lowest dial corresponding to a shift of one part in 10^6 in ratio. The detector sensitivity is such that parts in 10^7 can be interpolated.

The step that is fundamental to extending the resistance scale is the establishment of an accurate 10/1 ratio between the ratio arms of the bridge. This is done with a special assemblage of resistors, shown schematically in Figure 6. Six of these resistors are nominally 150 ohms each, and the seventh is 50 ohms. By successive substitution in the precision bridge, the relative values of the six resistors can be measured. Also by substitution the values of the resistances of nominally 50 ohms each, formed by connecting in parallel each of the two sets of three 150-ohm units, is determined relative to the 50-ohm resistor with high accuracy. The three 150-ohm units of one set are then connected in series with each other and with the 50-ohm unit to form a 500-ohm group. The three 150-ohm units of the other set are connected in parallel to form a 50-ohm group. These two groups, having a ratio close to 10/1, are connected to form two arms of the precision bridge, the remaining two arms being the adjustable ratio described above. The bridge is then balanced and the setting N_1 of the adjustable ratio is noted. The paralleling links are then shifted so that the 150-ohm coils of the first set are connected in parallel to form a 50-ohm group, and those of the second set are in series so that, with the 50-ohm unit, they form a 500-ohm group. The groups are turned end for end and again connected in the bridge, and a second balance setting N_2 is noted. The mean of N_1 and N_2 is adjusted by applying a small correction derived from the observed differences between the 50-ohm coil and the mean of the groups of three in parallel. A further correction for the paralleling links is applied and, with these corrections taken into account, the setting of the bridge ratio dials for a 10/1 ratio is then known to about 3 parts in 10^7. Other procedures are available for establishing an accurate 10/1 ratio, and are sometimes used to check the result of the regularly used procedure described above--agreement within a few parts in 10^7 is usually achieved.

The bridge, thus calibrated, is used to measure in successive steps the values of standard resistors of 10, 100, 1000, or 10,000 ohms, and similarly to step down to 0.1, 0.01, 0.001, and 0.0001 ohm standards. Resistances of intermediate value are occasionally measured by using analogous series or parallel combinations of nominally equal resistors to evaluate other bridge ratios that involve small integers.

When making precise measurements with resistors of 1 ohm or less, it is essential to use resistors of the 4-terminal type to eliminate the effects of contact resistance. The Kelvin bridge or some equivalent circuit has proved to be generally the most suitable for the comparison of such resistors. Of the various procedures that can be used to balance out the effects of the resistance of potential leads, that which involves applying a short-circuit across the main ratio arms is commonly used.

At the other extreme, the measurement of high resistance merges into measurement of the resistivity of insulating materials. High-grade wire-wound elements are available up to 10 megohms. Units of higher individual value are either thin deposited films of conducting material on an insulating substrate or a filamentary mixture of conducting and insulating particles. Either type is likely to show large changes of resistance with temperature, voltage, and (unless very carefully protected) ambient humidity. Also, their values are much less stable with time than wire-wound resistors. Thus, measurement methods of high precision would be inappropriate.

A series of standards, suitable for the upward extension of the resistance scale by substitution techniques is made in the following way. Starting with a group of ten 0.1-megohm units which can be connected in parallel for comparison with a 10,000-ohm standard, they can then be connected in series and used, with the same correction in proportional parts, to establish a 1-megohm standard. The error involved in this step up is a tenth of the sum of squares of the departures of the individual values from the group mean, so that the step-up error becomes negligible for a group of well-matched units. For example, if the spread of the individual units is 0.1%, the step-up error in a parallel-to-series reconnection is less than a part in 10^6. Similarly, groups of 1- and 10-megohm resistors are used to extend the range in a similar manner to 10^{11} ohms. Up to the latter value, comparisons are made in a nominally 1/1 megohm bridge, using a substitution technique, with restrictions on the applied voltage in the upper range because of the rather large voltage coefficients of the film type of resistors, ranging from 1.3×10^{-6} V^2 for the 10^7-10^9 group to 2.6×10^{-6} V^2 for the 10^9-10^{11} group. These approximations are valid only for relatively low voltages--at 40 volts, a neglected term involving V^4 may amount to 20-30 parts in 10^6.

For yet higher resistances, the charge carried by the current in the resistor under test is ac-

cumulated on an adjustable air-dielectric capacitor. The rate of accumulation may be measured by changing the capacitance at a rate which maintains a null indication on an electrometer used as a detector. An accuracy of 0.2% can be achieved up to 10^{13} ohms with this method at 1.5 V.

Voltage - The unit of voltage is preserved by a National Reference Group of saturated cadmium cells, whose values were assigned in 1948 in terms of the absolute ampere and ohm determinations available at that time. This reference group--which at present consists of 44 cells--has been selected from a much larger stock of cells that have been made in the Bureau laboratories at various times, using very carefully purified materials. The cells of the reference group are intercompared regularly about once a month; and every three years, a small group is taken to the International Bureau at Sevres, France, for comparison with the International Reference Group maintained there, and also with the groups of cells carried there from the other national laboratories.

In addition to the above comparisons--in which differences between the cells are measured with a microvolt potentiometer--a further indirect check is made on the stability of the reference group by periodic measurements of proton precession frequency in the field produced by the NBS ampere--defined as the ratio of the NBS volt to ohm--in a solenoid of fixed dimensions. In view of other available evidence that the NBS reference ohm is stable, the constancy of this measured frequency becomes a measure of the stability of the NBS reference volt. Over the past six years, since this measurement technique became available, the NBS volt--as maintained by the mean of the National Reference Group of cells--appears to be stable within a part in 10^6.

Proton Gyromagnetic Ratio - It has been demonstrated that if a substance whose nuclei have non-zero spin is placed in a steady magnetic field of flux density B, on which is superposed a weak radio-frequency field, the material will show a resonance absorption at a frequency ν, given by $\nu = \gamma B/2\pi$, where γ is the gyromagnetic ratio of the atomic nuclei of the substance used. In a converse--free precession--experiment the protons of a water sample are first polarized in a strong magnetic field and the sample is then moved to a field of much lower intensity where the precession frequency is measured, using the alternating voltage induced in a pick-up coil by the precessing protons in the time (3-4 seconds) before their alignments again become random. As in the absorption experiment, the precession frequency is a measure of the magnetic field, since the gyromagnetic ratio for a nucleus is an atomic constant that is unaffected by the field strength. From the free precession experiment, a value--$\gamma/2\pi = 4.25759 \times 10^7$ hertz/tesla, uncorrected for diamagnetism--has been determined for the proton gyromagnetic ratio. The absorption experiment is appropriate for the measurement of fields greater than about 0.02 tesla, and the free precession experiment is appropriate for moderately low intensity fields. In the free precession experiment described above as a means for periodically monitoring the stability of the NBS ampere, the field of the solenoid is about 0.0012 tesla (12 gauss).

The Direct Voltage Scale - The value of a voltage other than that of a standard cell, may be determined with a ratio device, and thus referred to the assigned emf of the reference cell. In the general range from 1.5 V down to a microvolt or less, the ratio device used for this purpose is a potentiometer. Since potentiometers measure, in effect, merely the ratio of the unknown emf to that of the standard cell, their calibration need not involve any direct measurement of resistance, but merely the determination of ratios of resistance. Hence, for the testing of potentiometers, it has been found convenient to use a universal ratio set (a precision voltage divider) which is equivalent to a slide wire having a total resistance of 2111.1 ohms, with a tap adjustable in steps of 0.01 to 0.0001 ohm, depending on model available and resolution required. In the very low voltage range, from a few microvolts downward to a nanovolt, extreme care must be taken in the design and operation of the special-purpose potentiometers used, to avoid the inclusion of parasitic emfs in the measuring circuit. The limited sensitivity available in the usual types of d'Arsonval galvanometers precludes their use at levels much below a microvolt, and other detectors are used, either a moving-coil galvanometer equipped with a photovoltaic or photoresistive network to amplify the unbalance signal or a dc-to-ac conversion device followed by a low-level a-c amplifier, and finally an ac-to-dc conversion for the signal read-out. In such detector systems, also, extreme precautions must be observed to avoid parasitic emfs or electrical noise that would mask signals at a level higher than the resolution limit imposed by the Brownian motion of the moving-coil galvanometer or the Johnson noise of the measuring circuit.

The extension of the direct voltage scale to values higher than 1.5 volts, while still using the potentiometer, is achieved through special resistive voltage dividers (commonly, but inappropriately, called "volt boxes") having a limited number of discrete ratios for operation at convenient voltage levels. In their simplest form, these dividers comprise a group of resistors connected in series. Taps are brought out at the ends and from appropriate intermediate points to binding posts to accommodate the input voltages; at the zero end a section is brought out as the "low-side" which operates through a detector into a potentiometer. Twin binding posts are provided at the ground or zero end so that the divider is used as a 4-terminal device (i.e., separate "input" and "potentiometer" terminal pairs). If the input resistance is $(R_a + R_b)$, where R_b is the low-side and R_a the high-side resistance exclusive of R_b, the true ratio of input to output voltage is

$$N_T = \frac{V_{in}}{V_{pot}} = \frac{R_a + R_b}{R_b}$$

since no current is drawn through the output leads at balance. It might be supposed that this ratio could be determined conveniently from separate measurements of R_a and R_b; but this is not desir-

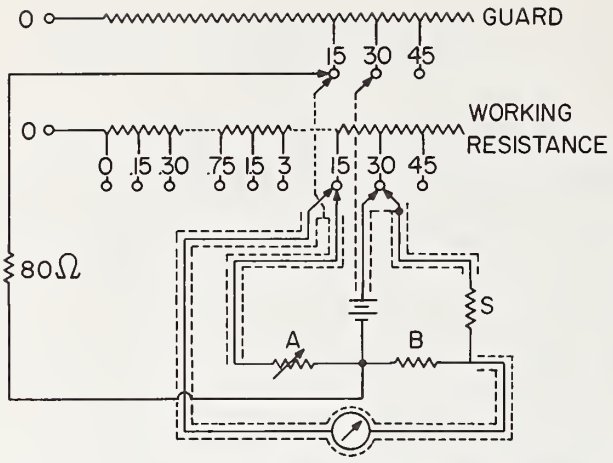

Figure 7. Circuit for self-calibration of voltage-ratio standard.

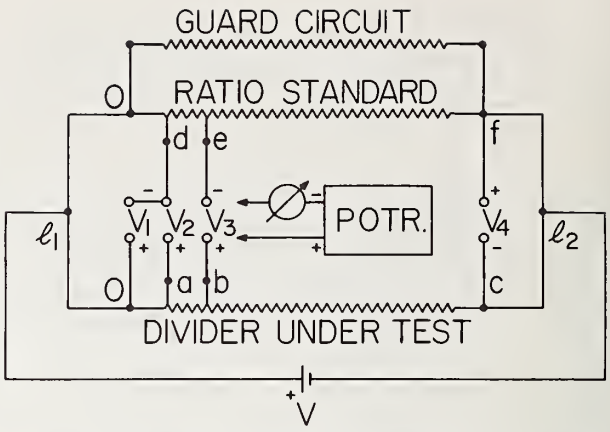

Figure 8. Test circuit for calibration of voltage divider in terms of voltage-ratio standard.

able. Not only would two separate resistance measurements be required but the problems of self-heating and of leakage current would be ignored.

The voltage ratio standard used at the Bureau to calibrate high-grade commercial dividers incorporates a number of special features to minimize self-heating and leakage errors, to insure ratio stability, and to provide capability of self-calibration. As a result, this divider can be operated at rated voltage (1500 V) on its top range with a change in correction that amounts to no more than 3 parts in 10^6 from its correction determined at 20% of rated voltage. To reduce leakage-current errors to negligible amounts, a guard resistor (333 1/3 ohms/volt) operating in parallel with the working resistor maintains, through internal connections, proper potentials on metal sleeves that surround the binding posts bushings and on metal plates that support the resistance coils. By this arrangement, voltage across working insulation sections is never more than 75 volts and is zero across the bushings. The guard resistance is also equipped with binding posts corresponding to those on the working circuit, permitting continuation of the guarding feature to the shielding of external measuring circuits.

The self-calibration technique for measuring the errors of the Bureau's ratio standard to better than 5 parts in 10^6 is made possible by arranging the resistance sections in a particular sequence. The first five sections have the same nominal resistance (50 ohms) and the sixth section has the same nominal resistance as their sum (250 ohms). With these six sections, totaling 500 ohms, considered as a group (M_1) and also as the first section of the next group (M_2), the sequence is repeated by making each of the next four sections 500 ohms each, followed by a 2500-ohm section. This process is repeated twice more to form a total of four groups, with group M_n always considered as the first section of group M_{n+1}. Thus, each group is characterized by five nominally equal resistors, and a sixth nominally equal to their sum.

In the calibration of this arrangement, a "Direct Reading Ratio Set" with a range of 1/1 ± 0.05% and a resolution of 1 part in 10^7 forms two arms of a bridge. One or more resistance standards, always chosen to have the same nominal resistance as the section (or summation of sections) being measured, forms the third bridge arm. Each successive divider section occupies the fourth arm in turn. Corresponding guard sections maintain proper potentials on the guard sleeves and plates of the standard, and connection to the bridge shielding prevents leakage currents from entering or leaving the measuring network. Starting with the first section, differences between each of the successive sections and the first section of the group are measured, followed by a difference measurement between the sixth section and the sum of the first five in the group. The correction to any ratio can then be computed by summing the measured differences. The first section of group M_1 is taken as the reference, and all measured differences are normalized to this base. The bridge arrangement for measuring the higher resistance sections is shown schematically in Figure 7.

The method used in calibrating other fixed-ratio dividers by comparison with the Bureau's standard is indicated in Figure 8. It also takes advantage of the accuracy gain afforded by a "difference" technique wherein the difference between nearly equal quantities need be measured with only moderate accuracy to realize high accuracy in the measurement of the quantity itself, when it is established in terms of a known reference standard. The ratio standard and the divider under test are connected in parallel for the same nominal ratio and supplied as indicated from the same regulated d-c source, at the required test voltage (rated voltage or some known fraction of it). The junction points ℓ_1 and ℓ_2 are located so that V_1 and V_4 are nearly zero. The small potential differences V_1 to V_4 that exist between corresponding points on the two dividers are measured in turn by introducing an opposing voltage across the gaps and adjusting for a detector null. A low-range potentiometer supplies the opposing voltage and permits measurements to 0.1 μV. These measured voltages, together with the correction to the standard permit computation of the ratio correction. A timed sequence of measurements of V_3 permit establishing warm-up error in the divider under test. Evidence indicates that measurement

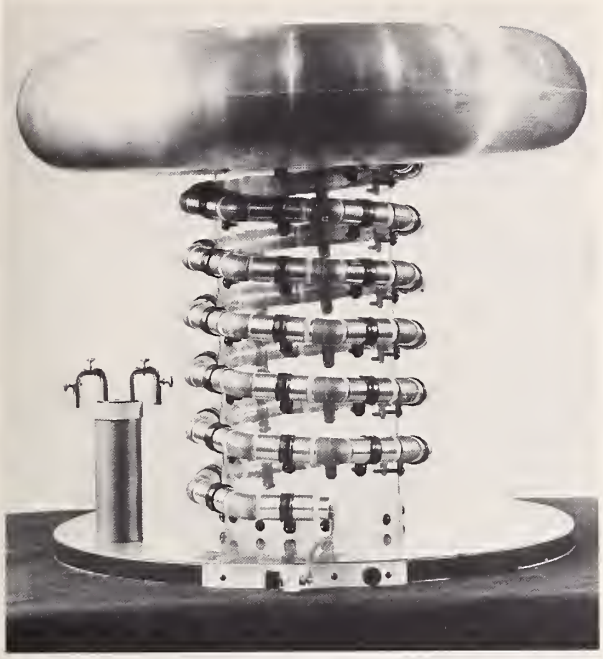

Figure 9. 100-megohm helical resistance unit for 100 kV operation.

accuracy can be 1 part in 10^5 or better.

Other voltage ratio networks and methods of measurement are being examined by the Bureau in an effort to improve both the standard and measurement accuracy. Of several experimental designs studied, the most promising and versatile appears to be one that will operate on a series-parallel principle, lend itself to several methods of calibration, including the self-calibration technique described earlier, and will be suitable for low frequency as well as d-c operation. In addition, a proposed two-stage transformer network looks promising as a corollary a-c ratio standard. This could serve to further evaluate the a-c performance of the above ac-dc model and be useful in other experimental work involving the measurement of voltage ratios.

For the measurement of very high direct voltages, a new problem--loss of current through corona discharges at intermediate points of the resistor string--becomes important, in addition to the problem already discussed--self-heating and leakage across the insulation of supporting structures. Figure 9 shows the construction of a resistor, appropriate for use to 100 kV, in which these problems have all been adequately met. It is made up of a large number of individually shielded 1-megohm wire-wound resistors connected in series and arranged to form a vertical helix (supported on a lucite cylinder) between a ground plate and a high-voltage electrode. The individual shields completely enclose each 1-megohm resistor and prevent corona formation at the resistor face, whatever the potential of the shield above ground; the pitch of the helix is such that the gradient between turns is below what would give rise to corona; and the configuration of the helix together with the large high-voltage electrode on top serves to prevent field concentration and consequent corona formation at the high-voltage end of the resistor string. An experimental check

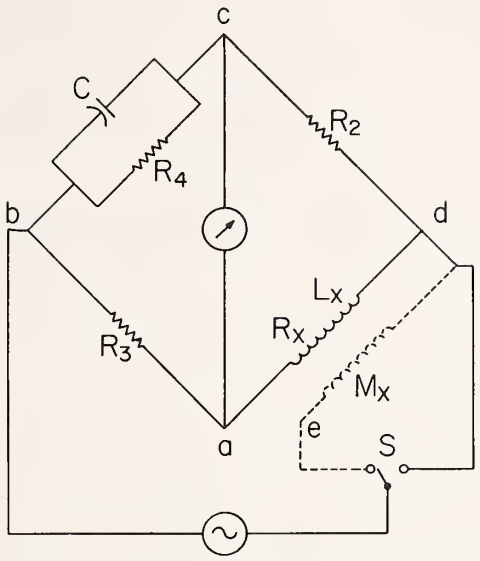

Figure 10. Maxwell-Wien bridge for measurement of self and mutual inductance.

at high voltage for corona or leakage errors consisted of accurately comparing the current "in" at the high-voltage end of the resistor string with the current "out" at the ground end. Corona and leakage errors were found to be less than 1 part in 10^5 at 50 kV and less than 2 parts in 10^5 at 100 kV for humidities up to 50% RH. All the resistors had temperature coefficients less than 2 parts in 10^6; some coefficients were positive and some negative so that they could be selected in matched parts for an overall coefficient less than 4 parts in 10^7 per °C. The equilibrium temperature rise of the unit is large at rated voltage, but if it is excited less than 30 minutes, the maximum error caused by heating was estimated to be less than 4 parts in 10^5.

Inductance - While in theory the NBS unit of inductance could be preserved by the calculable inductors constructed for the Bureau's ohm determinations, it has been generally more expedient in the practical work of inductance measurement to derive the henry from the ohm and farad through the reference standards of resistance and capacitance. The calculable inductors are quite bulky and, hence, have relatively large capacitance to ground and considerable coupling to other circuits. Also, they are wound with thick wire whose skin effect would be appreciable even at moderately high frequencies.

The Inductance Scale - The circuit regularly used to measure inductance is that of the Maxwell-Wien bridge shown in Figure 10. The adjustable capacitor is a 3-dial mica capacitor having minimum steps of 0.001 μF. A precision variable air capacitor with a range of 1000 pF is used for interpolating between the lowest steps of the mica capacitor. The bridge is well suited for the measurement of inductances in the range 1 μH to 10 H at frequencies in the range 100 Hz to 10 kHz. The mica capacitor must be calibrated at each frequency used--100, 400, 1000, and 10,000 Hz.

Over the middle range of inductance values, and at a frequency of 1 kHz, the total uncertainty in the measurement is no more than ±0.01%. Wagner arms (not shown in the diagram) must be used generally to eliminate the effect of admittances to ground from the bridge corners. The bridge must also be carefully shielded and its temperature closely controlled if measurement uncertainties are to be kept within the stated limit.

Mutual inductances up to 50 mH for a-c use are regularly measured with the circuit shown, including the dotted lines of Figure 10. With switch S closed to the right, capacitor C is adjusted to a balance value C_L, which is a measure of L_x. Switch S is then closed to the left and C is readjusted to a new balance at C_M. The mutual inductance is then computed from the relation $M = (C_L - C_M) R_2R_3R_4/(R_3 + R_4)$, with further correction terms involving the residual inductances of the resistance arms. For inductors of larger value, or at higher frequencies where the effects of distributed capacitance are larger, this method becomes impractical. In such cases, the primary and secondary windings of the mutual inductor are connected in series, first aiding and then opposing, and the self-inductance of each combination is measured with the Maxwell-Wien bridge. If the observed values are L_a and L_o respectively, and if L_p and L_s are the inductances of the primary and secondary windings measured separately,

$$M = \frac{L_a - L_o}{4} = \frac{L_a - L_p - L_s}{2} = \frac{L_p + L_s - L_o}{2} .$$

Any inconsistencies among these equations give a valuable indication of the order of magnitude of the effects of stray capacitance between the coils.

At low values of inductance, errors from the residual phase defects of the bridge arms may become appreciable. Hence, for the measurement of the residual inductances of nominally "non-inductive" 2-terminal resistors, it becomes essential to use a substitution method. In this, a standard whose inductance can be computed and whose resistance is nominally equal to that of the impedance under test, is substituted for the unknown in the X-arm of the bridge. Computable standards are available for 10,000 and 1000 ohms. Each consists of a fine wire stretched down the axis of a brass tube about 5 cm in diameter. For 100- and 10-ohm standards, parallel wires are used. The time constants (L/R) of these standards can be computed to 1 x 10^{-8} second. For still lower resistances, 4-terminal standards are used--either parallel wire, reflex-strip, or coaxial-tube types. Some of the coaxial-tube type have their potential leads inside the inner tube, whereas others have them outside the outer tube. These 4-terminal standards range in resistance from 0.1 to 0.0002 ohm and in current rating from 5 to 2500 amperes.

Magnetic Quantities - The unit of magnetic flux, the weber is derived from the henry and the ampere, the latter being derived, in turn, from the volt and ohm. A change in flux-linkages in a "search-coil"--produced either by a change in the flux or a motion of the coil--is proportional to the time integral of the voltage induced in the coil and is measured usually by the resulting ballistic deflection of a galvanometer. The galvanometer may be calibrated by connecting it to the secondary winding of a mutual inductor and observing its ballistic response when a known current is produced in the primary winding of the inductor. The change in flux linkages, $N\triangle\Phi$, with N turns of the secondary winding, resulting from a change $\triangle I$ in the primary current is $N\triangle\Phi = M\triangle I$.

For convenience, the primary current is reversed so that $\triangle I = 2I$. If I is in amperes and the mutual inductance, M, is in henrys, $N\triangle\Phi$ is in webers. The ballistic response of the galvanometer to changes in flux-linkages is strongly dependent on the resistance of the circuit connected to its terminals; and, normally, the resistance of this circuit, including search coils. is adjusted to make the galvanometer scale direct reading in convenient decimal fractions of a weber. The value in henries of the mutual inductor used in the calibration is obtained by comparing it directly with the computable mutual inductance standard that was constructed initially for an absolute ohm determination.

The weber, as thus established, is used to measure the flux in test specimens in various types of permeameter. The test specimen in the permeameter is surrounded by a coil of a known number of turns connected to the calibrated galvanometer. A measured change in magnetizing current in the permeameter produces a change in the flux linking the coil, and the resulting galvanometer deflection measures the flux change. A measurement of the cross-section, A, of the test specimen then permits computation of the change in magnetic induction $\triangle B = \triangle\Phi/A$. If A is in square meters, $\triangle B$ is in webers/meter^2 or teslas. The area of the specimen and the number of turns in the coil may be lumped with other factors in the galvanometer calibration, so that the induction is read directly from the deflection.

Magnetizing force may be computed directly from the current turns per unit length for a uniform ring specimen or for a magnetic circuit in which the magnetomotive force is distributed around the circuit in proportion to the reluctance of the various portions so that all portions carry the same flux. Under these conditions, the tangential component of the magnetizing force is the same inside the metal as outside at the surface of the specimen, and the computed value applies to the interior of the specimen if its magnetic properties are uniform. A second method of measuring magnetizing force is to measure the tangential component of flux density in the air closely adjacent to the test specimen. This measured flux density in teslas divided by the magnetic constant μ_m (the assigned permeability of free space, $4\pi \times 10^{-7}$) yields the value of magnetizing force in amperes/meter.

The principal object of testing ferromagnetic materials by d-c (ballistic) methods is to obtain data from which normal induction curves and hysteresis loops can be plotted. This is done either by using suitably shaped specimens, such as rings, which constitute the entire magnetic circuit, or by means of permeameters. When permeameters are used, the test specimens are bars submitted for test by the laboratories of steel companies and other organizations. The circulation of calibrated bars insures uniformity and accuracy through-

out the industry.

A related service is the calibration of search coils to determine their effective area-turns. This is done by placing the search coil near the center of a long uniformly wound, single-layer solenoid so that the axes of the search coil and solenoid are aligned. Their mutual inductance is measured ballistically by comparison with a standard; and the area turns, AN, of the search coil are computed by the equation AN = MI/B. The ratio of the solenoid current I to the central flux density B is a constant that is computed from the measured dimensions and winding pitch of the solenoid.

Another calibration service of importance is the measurement of flux density in the air gaps of permanent magnets that are to be used as standards. The calibration procedure is based on the accurate measurement of flux density in the gap of an electromagnet, using the nuclear magnetic resonance technique. This accurately known flux density is compared with the flux density in the gap of the permanent magnet standard through the use of a suitable transfer instrument, such as a Hall effect magnetometer or a rotating-coil magnetometer. By using the established value of proton gyromagnetic ratio ($\gamma/2\pi = 4.25759 \times 10^7$ hertz/tesla) and a suitable resonance probe, the induction in an unknown magnetic field can be measured by a simple determination of the resonance frequency. Such a resonance detector is also used to study flux distribution in a magnetic field and, with suitable circuitry, as a monitor to hold the induction constant at a given place in the field.

Direct Current, Power, and Energy Measurements - The block diagram of Figure 11 shows the derivation of the units of current, power, and energy from those of resistance, voltage, and time. It also shows the ac-dc transfer instruments on which all a-c measurements are based.

An electric current (if one excepts the persistent current in a superconducting circuit and the α or β emission from a radioactive isotope) is in the nature of things a transitory affair, and a "standard ampere" cannot be preserved in the laboratory as can a standard ohm. For the accurate measurement of direct current, the normal procedure is to insert a known resistance in the circuit and to compare the voltage drop produced in this resistance by the unknown current, with the emf of a standard cell. This comparison is usually made with a potentiometer. With this technique, measurements to perhaps 10 parts in 10^6 are now possible. In rare cases where extreme accuracy is needed, special resistors are used of such value that the IR drop at the desired current is very closely equal to the emf of one or more standard cells connected in series. Thus, the circuit becomes very simple and errors from contacts, thermal emfs, and drift in the potentiometer circuit are minimized or eliminated.

The extension of measurement to several hundred amperes depends on 4-terminal resistors properly designed to carry the large currents without excessive heating and without abnormalities of current distribution. A Kelvin double bridge used with a substitution technique permits

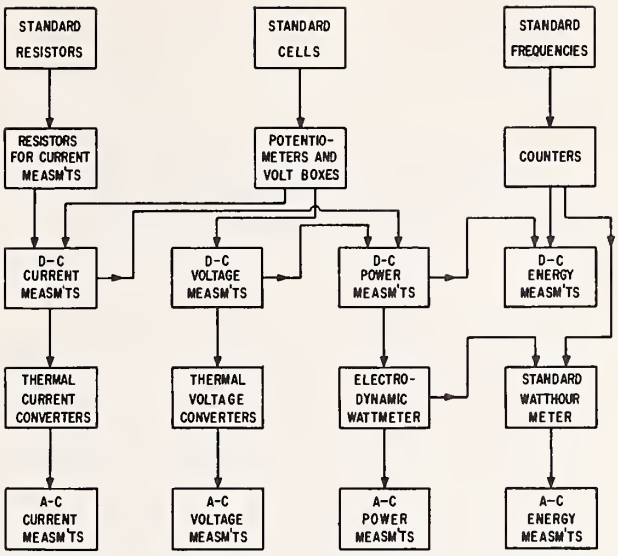

Figure 11. Measurement of current, voltage, power, and energy.

measurements to 0.01% accuracy up to a maximum current of 1000 A. This 6-arm bridge circuit is of the conventional type in which auxiliary balances minimize the effects of contact and lead resistances which could otherwise mask the value of the resistor. The substitution technique involves two bridge balances, the first being made with a calibrated standard in the "unknown" arm of the bridge and the second with the resistor under test substituted for it. In this way, only the measurement of small differences between nearly equal quantities is required. Oil-cooled standards of 0.0001 and 0.00001 ohm nominal resistance are used at the 1000 ampere level.

Recent current comparator developments at the Canadian National Laboratory constitute a breakthrough in current ratio measurements, and a d-c comparator permits the measurement of current ratios over a wide range to an accuracy approaching a part in 10^6. Extending the direct current scale to 20 kA should soon be possible, and the application of the direct-current comparator to comparisons of 4-terminal resistances is expected to increase the accuracy of that measurement by an order of magnitude or more.

The measurement of power in a d-c circuit as, for instance, in calibrating a calorimeter can be made most accurately by using a potentiometer with an accessory shunt and a voltage divider ("volt box") to measure the current and the voltage of the circuit separately, and by then taking their product. Electric energy is, of course, the integral of power with respect to time, and if the power is constant, can be measured by using the potentiometer, voltage divider, and shunt to obtain a known and constant power for a measured time. Accuracies of perhaps 20 ppm in power measurements and 50 ppm in energy measurements are possible. Of course, if the applied power varies with time, some sort of integrating meter must be used. The d-c watthour meter of either the commutator or mercury-motor type is a relatively inaccurate device with errors of 0.1 percent or more. More accurate measurements can be made with digital watthour meters incorporating feed-back wattmeters as explained below.

Transfer from D-C to A-C Measurements - The standard cell and the units of voltage and of current realized from it directly or in conjunction with a standard resistor are applicable to the measurement of d-c quantities only. On the other hand, by far the more frequent and important measurements in the power and communication fields involve alternating currents. The procedure used to transfer from the d-c standards to a-c measuring apparatus, as indicated in Figure 11, therefore, constitutes an essential link in the chain of electrical measurements.

There are at least eight quantities that may be determined for an unmodulated periodic a-c wave. These are: 1) the rms or effective value; 2) and 3) positive and negative average values, i.e., the average of all of the positive or all of the negative values during one cycle; 4) the rectified or full-wave average; 5) and 6) the positive and negative crest (peak) values; 7) the crest-to-crest (peak-to-peak) value; and 8) the fundamental component only. Instruments for measuring each of these values are commercially available (with widely varying accuracies). Ordinarily, however, only one of these values is really required in a measurement. Unfortunately, it is impossible to deduce one value accurately from the measurement of another except for certain known wave forms. In most cases, the rms value is the one desired, since the rate of transformation of electrical to other forms of energy (which is governed by the heating produced by a current and by the electromagnetic force produced by currents acting on each other) is a function of the square of this value. For these reasons, the transfer from d-c to a-c measurements at the Bureau has traditionally been made in terms of the rms value. However, peak ac-to-dc measurements can also be made over a restricted range of voltages and frequencies.

There are three general types of ac-dc transfer instruments which are at present suitable for rms measurements of high accuracy. They are dependent upon these same laws of the interchange of energy and are: 1) electrodynamic instruments, which depend upon the force between current-carrying conductors; 2) electrostatic instruments, which depend upon the force between charged conductors; and 3) electrothermic instruments, which depend upon some effect produced by the heating of a current-carrying conductor. The first and third respond essentially to current and the second to voltage, but series or shunt resistors make all three types suitable for both measurements, while other circuit arrangements also make power measurements feasible.

The differential equation governing the angular deflection of an electrodynamic instrument in which two sets of coils carrying the same current, one fixed and one rotatable about an axis, is: $P\theta'' + A\theta' + U\theta = Bi^2$, where P, A, and U are the inertial, damping, and spring constants, respectively, and B is a parameter which depends upon the rate of change of the mutual inductance between the coils with respect to the angular deflection. If the mechanical inertia of the movable system is sufficiently great with alternating current applied, the periodic fluctuations of θ are negligible compared with the average (steady-state) value. Then by integrating each term over one cycle and dividing by T, we have simply

$$U\theta_f = \frac{B}{T}\int_0^T i^2 dt = BI^2.$$

Thus, if U and B each have the same dc-to-ac value on direct and alternating currents, the instrument may be used for the dc-to-ac transfer.

Similar equations can be developed for the electrostatic instrument, with V replacing I, or for an electrothermic instrument with the temperature difference replacing the angular deflection θ. (The parameter B is, of course, also different.) In each instrument, the basic equation holds even if the parameters U and B are dependent upon the response θ. This important advantage arises because each instrument combines in a single measuring element a function proportional to the square of the instantaneous current or voltage, a restraining function, and an inertial function which enables it to integrate so that the time-average value of the response is proportional to the square of the rms current or voltage. For this very fundamental reason, high accuracy may be more easily attained with such instruments than with other squaring devices or circuits which must synthesize exact and equal square-law responses in two quadrants (or in one quadrant with an accurate rectifier) and provide a separate accurate integrator.

At the Bureau, thermal converters are used as rms ac-to-dc comparators for current and voltage. Each of these electrothermic ac-dc transfer standards contains a thermoelement consisting of a heater and thermocouple. In its usual form, the heater is a short, straight wire suspended by the two supporting lead-in wires in an evacuated glass bulb. Its temperature rise is dependent on the current through it. The hot junction of a thermocouple is fastened to the midpoint of the heater and is electrically insulated from it with a small bead. Thus, the thermocouple emf (about 5 to 10 mV for a conventional thermoelement at rated current) is a measure of the heater current.

Sets of thermal voltage converters are used for voltage measurements. Each consists of one or more cylindrical metal-film resistors in a coaxial metal cylinder, connected in series with one of two 5 mA thermoelements mounted in a separate cylinder, so that the output emf is then a measure of the input voltage. A thermal current converter consists of a coaxial a-c shunt with a low-range thermoelement connected to its potential terminals. Alternatively, thermoelements of higher ranges (up to 20 A) can be used directly without shunts.

The ac-dc difference of a transfer standard may be defined as $\delta = (X_a - X_d)/X_d$, where X_a and X_d are the magnitudes of a-c and d-c quantities that are required to give the same response (such as deflection or output emf) of the standard. (Normally, the average for the two directions of the d-c quantity given the best measure of the d-c reference.) This is a useful definition, for the a-c quantity corresponding to a given response is then simply $X_a = X_d (1 + \delta)$. The instrument may be used as an ac-dc transfer standard for a-c measurements simply by observing the response with the a-c quantity applied and then measuring (with

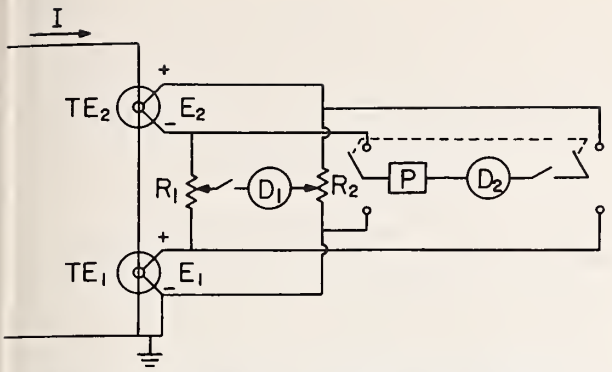

Figure 12. Circuit of determining differences in ac-dc performance of thermoelements.

a potentiometer, d-c shunt, and voltage divider as needed) the average for the two d-c quantities required to obtain the same response, thus avoiding many of the limitations of an ordinary instrument.

Pairs of thermoelements (or converters) are evaluated with the emf comparator shown in Figure 12 to determine the differences in their ac-dc performance, i.e., $\delta_1 - \delta_2$ as defined above. With the desired voltage applied, R_1 and R_2 are adjusted in a preliminary balance to obtain a near null on detector D_1. Then, in regular succession, a-c, d-c, reversed d-c, and a-c currents are applied to the thermoelements at nearly equal time intervals without changing R_1 or R_2. In each case, the current is adjusted to obtain the same output emf, E_1, of TE_1 as indicated by an auxiliary Lindeck potentiometer (P with its detector D_2), and the resulting deflections of D_1 are observed. The relative ac-dc difference is simply $\delta_1 - \delta_2 = S(D_a - D_d)$, where D_a and D_d are the averages of D_1 with the a-c and d-c currents applied, respectively. The sensitivity factor (S) is easily determined. With this circuit, small fluctuations in the supply current or voltage do not appreciably change the balance point, and the sequence of readings greatly reduces the effects of drift in either thermoelement. In this way, a precision approaching a few parts in 10^6 is attainable.

Fourteen thermoelements, each of which theoretically should have negligible (less than 2 parts in 10^6) ac-dc error at audio frequencies form the Bureau's present ac-dc reference group. They are of different manufacture, range, and type. Two of them are of a new design by F. J. Wilkins of the National Physical Laboratory in England, having many junctions fastened along the length of a bifilar heater. The ac-dc differences of this type should be very different than those of the more conventional kind. The ac-dc differences of all of them agree to a few parts in 10^6 providing the necessary concordance of theory and experiment. The extension to higher voltages and currents is made by step-wise intercomparisons of adjacent ranges of the thermal voltage converters and the thermal current converters (or high range thermoelements). In this way, the ac-dc differences of any range can be determined in terms of any one.

The same circuit and the same techniques are used with the same standards to determine the ac-dc differences of various kinds of commercially available thermal ac-dc transfer standards that are sent to the Bureau for calibration. Measurements are normally made to 1 part in 10^4, with 5 parts in 10^5 projected at audio frequencies for the near future.

An electrodynamic wattmeter is used as the basic ac-dc transfer standard for power and energy measurements at NBS. Its movable coils carry a current proportional to and in phase with the applied voltage, and its fixed coils carry the load current. The torque is then a function of the applied power.

The Bueau's standard ac-dc transfer wattmeter was carefully designed to be as free as practicable from sources of a-c error such as eddy currents, capacitance, and inductance. In addition, a great many checks were made on its performance by comparing it with a hot-wire instrument and a quadrant electrometer, and using it to measure the loss in capacitors which previously had been measured in an a-c bridge. Based on these tests it is believed that the errors are known to at least 0.005 percent of the applied volt-amperes at any power factor at power frequencies, and that the instrument can still be used with reasonable accuracies at frequencies up to perhaps 1 or 2 kHz.

This wattmeter is used principally to determine the ac-dc differences of electrodynamic wattmeters of high accuracy, which, in turn, are used as the reference instruments in other laboratories for calibrating watthour meters with alternating current. The sequence of ac-dc tests is similar to that already described with the thermal converters, and the ac-dc difference of the instrument to be calibrated is determined in terms of the deflections of the standard wattmeter and a sensitivity factor, with a correction for the ac-dc difference of the standard. "Phanton loading" with separate sources to energize the voltage and current circuits of the standard wattmeter and the instrument under test, make it easy to obtain any desired fictitious power and to insure that both wattmeters "see" the same value of power.

The standard wattmeter is used with counting relays which are closed for periods of an integral number of seconds to provide a measured power for a known time interval, in order to calibrate a bank of five high-grade standard watthour meters. These meters are maintained under carefully controlled temperature conditions and are used only at rated voltage and current on their 5 ampere, 120 volt ranges to serve as a standard of a-c energy. Periodic calibrations with the wattmeter several times a year have shown a repeatability better than 0.03 percent for the average of the registration of the five watthour meters. One of the five serves as a working standard between calibrations to determine the registration of standard watthour meters that are sent for calibration. In this way, the watthour is literally carried from Washington to the power companies' laboratories with an accuracy approaching 0.05 percent, if the average of at least three meters is used.

A number of wattmeters have been developed with a second instrument (usually a d-c milliammeter) connected to the same shaft as the electrodynamic wattmeter element and arranged so that the adjustable current through it produces

a torque opposing that of the wattmeter. This current is, thus, directly proportional to the measured power when the pointer is at zero. As an extension of this principle, the out-of-balance position can be detected electronically or otherwise to generate this counter-current automatically in a feed-back circuit. The integral of this current with respect to time is thus proportional to energy. This energy can be measured by passing the current through a fixed resistor and integrating the voltage drop with a voltage-to-frequency converter and a counter. Such "digital watthour meters," which may be used over a wide range of frequencies including direct current, are available commercially and are under study at the Bureau in the hope of providing a better reference standard for the calibration of standard watthour meters.

The Alternating Voltage Scale - The set of thermal voltage converters offers a convenient means for measuring alternating voltages from about 0.2 V to 500 V with high accuracy over a wide frequency range. Lower voltages may be generated by measuring the voltage applied to the input of an inductive voltage divider, using the thermal voltage converter and appropriate d-c equipment (potentiometer and resistive voltage divider). The output of the voltage divider can be applied directly to digital voltmeters, for example, to calibrate their low ranges.

Inductive voltage dividers, consisting of a group of cascaded multi-tap transformers with special windings on high-permeability toroidal cores, are available with six or seven decades of voltage division. Some are capable of accurately dividing their input voltage to about a part in 10^7 at their design frequency. The accuracy of voltage division may be determined with reference to a divider made up of known 3-terminal capacitors, or may be measured against a master inductive voltage divider that has been so calibrated. The Bureau now has the capability of making such calibrations over the frequency range from 50 Hz to 10 kHz.

For the measurement of higher alternating voltage, at 60 Hz, instrument voltage transformers are used universally by the power industry. The ratio corrections and phase angles of voltage transformers that will be used as reference standards in other laboratories are determined at the Bureau either directly by means of capacitive voltage dividers or indirectly by comparison with standard transformers whose corrections have been determined by this means. In the latter case, the primary windings of the standard and test transformer are connected in parallel to a suitable high-voltage source, and the difference between their secondary voltages is measured with a comparator. The comparator now used at the Bureau shown schematically in Figure 13, employs an inductive voltage divider for comparing the magnitudes of the two secondary voltages and a resistance-capacitance network to evaluate their phase difference. Uncertainties in the inductive comparator have been estimated at 2 parts in 10^6 in ratio correction factor and 10 μ radians. The Bureau's group of standard transformers covers the voltage range to 250 kV, and the capacitive-divider technique has been used for calibrations to 350 kV. The direct determination of the ratio corrections and phase angles of voltage transformers, using a capacitive voltage divider, depends essentially on the stability of the 3-terminal capacitors and the accuracy with which their values can be measured. In a recent international calibration comparison that covered the range 50-350 kV, agreement was generally within 2 parts in 10^5.

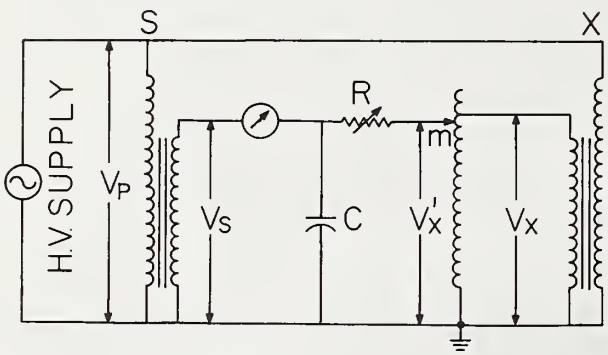

Figure 13. Circuit of voltage-transformer comparator.

There is no significant degradation of accuracy for either method at higher frequencies, at least up to 400 Hz. Calibration tests of voltage transformers have been made at this frequency over a voltage range up to 9 kV.

The Alternating Current Scale - The transfer principle and its embodiment in a set of thermal current converters provide a convenient and accurate means for measuring alternating currents from 1 mA to 20 A at frequencies to at least 20 kHz while preserving a direct tie with their d-c equivalents. Extension of the current scale to several thousand amperes with high accuracy is accomplished by use of instrument current transformers and, more recently, current comparators.

In its simple form, a current transformer comprises two windings (primary and secondary), electrically insulated but coupled magnetically through a high-permeability core. Operating under nearly short-circuit conditions, it reproduces in the secondary circuit a reduced replica of the primary current. For a perfect transformer, the relation between these currents would be

$$\frac{I_p}{I_s} = \frac{N_s}{N_p}$$

where N_s and N_p are the number of turns in the respective windings, zero phase displacement between the currents being inferred. But transformer operation requires that a finite flux be established in the core, and power for the secondary circuit must be supplied through the windings and core from the primary circuit, so that both ratio and phase angle will depart from their ideal values. Furthermore, these departures from the ideal relations are functions of frequency, current, and secondary burden; and, for multi-ratio units, the errors may differ for the several ratios. Thus, a current transformer must be calibrated under the conditions in which it will be used.

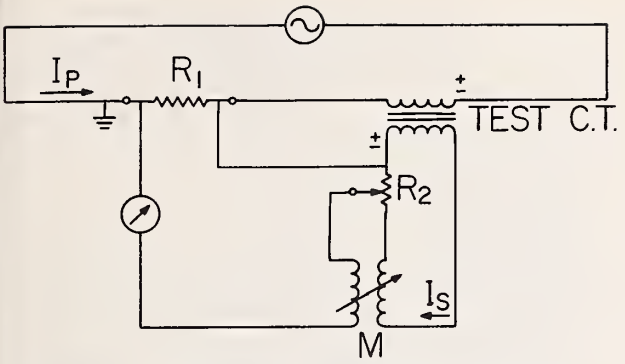

Figure 14. Circuit for direct calibration of current transformers.

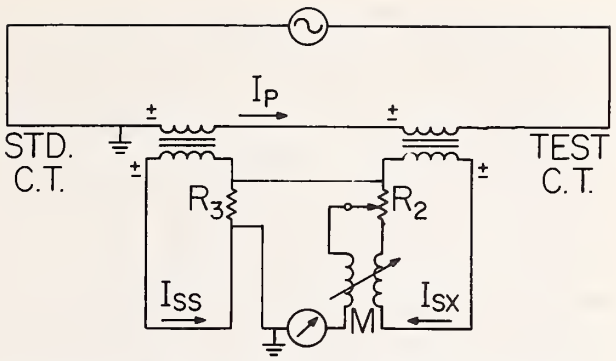

Figure 15. Circuit for calibration of current transformers in terms of a standard transformer.

The method used for many years at the Bureau for calibrating current transformers up to 2500/5 A is shown schematically in Figure 14. Resistor R_1, in series with the transformer primary, is a 4-terminal astatic network which, based on theoretical considerations, has negligible skin effect and a very small known phase angle; resistor R_2, in series with the transformer secondary, has the same features and, in addition, permits step changes of 0.01 ohm in its 4-terminal resistance over a range from 0.01 to 0.1 ohm, with a continuously adjustable section having a span of ±6%, and a resolution of 10 parts in 10^6; the mutual inductance M is characterized by its broad range with continuous adjustment and by its astatic configuration. With the ratio R_2/R_1 chosen to equal the nominal current ratio, balance is obtained by adjusting R_2 and M for a detector null. With zero voltage around the detector loop, the transformer errors can be computed from the known circuit parameters.

For primary currents greater than 2500 A and up to 12000 A, the comparison method of Figure 15 is used. A standard transformer and secondary resistance R_3 replace R_1 of the previous method. Comparisons are made from the secondary circuits, but the balancing procedure is unchanged. The error of the standard transformer must be taken into account in the balance equation and must be known. Its measurement rests on the principle that the error of a current transformer, properly designed, remains unaltered if the change-of-range is effected by changing the numbers but not the symmetrical distribution of the primary turns, while the secondary turns remain the same. This principle is realized in the Bureau's standard transformer by dividing the primary winding into n equal sections and arranging them so that k sections can be connected in series to form n/k groups connected in parallel. Deviations from the principle arise only from the product of two factors: 1) relative differences in current distribution among the primary groups in parallel; and 2) relative difference in the coupling (mutual inductance) between the primary sections and the secondary winding. The primary winding has 24 sections of one turn each, whose symmetrically disposed series and parallel combinations provide 8 ratios for a given secondary; added ratios are available by changing the number of secondary turns through a series-parallel arrangement. When the standard is used in calibrating high-ratio transformers, a 1 or 2 turn arrangement of the primary turns is used. Its errors are measured periodically by reconnecting it for a lower ratio and using the resistance method described above. Commercial transformers of the highest quality can be calibrated by either method to an accuracy of 200 ppm and when time and effort are justified (e.g., an international comparison) an accuracy of 100 ppm or better is possible.

The demand for increased accuracy in measurements at power frequencies has been felt in current-ratio measurements; and needs have developed for current-ratio measurements over a frequency range extending to 10 kHz or more. These requirements have led to a reconsideration of the entire problem of current-ratio determination. In recent years, a ratio standard, operating on a principle quite different from the current transformer and with potential accuracy better than 1 part in 10^6, has been developed by Kusters and his co-workers in the National Research Council of Canada (NRC) in cooperation with Professor Miljanic of the University of Belgrade and the Nicola Tesla Institute. The essential components of the latest version--the compensated current comparator--are indicated in Figure 16, and its application as a ratio standard for calibrating current transformers is shown in Figure 17.

Ampere's circuital law states that the line integral of magnetizing force around a closed path equals the sum of the enclosed currents, i.e. $\oint Hdl = \Sigma I$. In a current transformer, this integral has a value not zero, and this accounts for its magnetic or low-frequency error; in the current comparator, however, this integral is zero at balance, and the ratio of currents is the inverse of the turn ratio. Referring to Figure 16, a high-permeability toroidal core carries a single-layer detection winding (d) of many turns which senses the condition of zero flux in the core as indicated by the detector; a compensation winding (c) having the same number of turns as the secondary (S) encloses both the core and the magnetic shield (Sh_2) and provides a path for the magnetizing current of what may be considered a "transformer," comprised of the primary (P) and secondary (S) windings and the shield (Sh_1).

A necessary and sufficient condition for proper functioning of the comparator is that the core

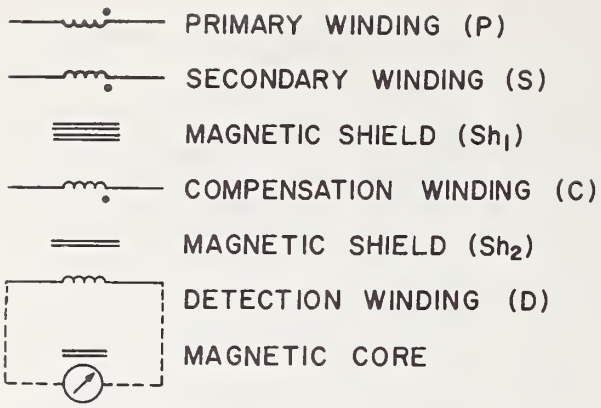

Figure 16. Components of a compensated current comparator.

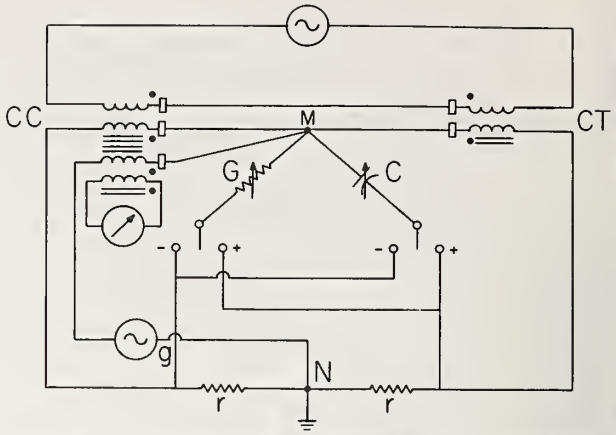

Figure 17. Comparison circuit used in calibrating a current transformer.

flux, as sampled by the detection winding, must truly reflect $\oint Hdl$ when it encompasses only those currents pertinent to the measurement. Thus, extraneous magnetic fields, such as those associated with leakage inductance or arising from sources external to the comparator, must not be permitted access to the core. More insidious, but no less important, is the effect of non-uniform permeability around the magnetic path of the core. This results in an abnormal distribution of the flux produced by the primary and secondary currents when these windings are separated in space. The result is that the detection winding may sense flux even though the line integral of magnetizing force is zero; the converse is equally possible. The magnetic shield (Sh_1), of material whose saturation level is high, prevents extraneous flux from reaching the core, and essentially nullifies the effect of the physical separation of primary and secondary turns; the inner, high-permeability shield (Sh_2), performs a similar function with respect to the compensation winding. The shield (Sh_1) also enables the comparator to support its burden without imposing any of it on the current transformer under test.

The operation of a compensated current comparator used as a ratio standard to calibrate a current transformer may be explained with the aid of Figure 17 and an initial oversimplification. At first, we shall assume that the current transformer (CT) is free from error (i.e., its primary and secondary ampere turns are exactly equal) and that the adjustable balancing elements (G-C) are disconnected from junction M. The primary and secondary windings of the current comparator (CC) together with its outer shield (Sh_1 of Figure 16) form, in effect, a current transformer whose ampere turns are not equal. The compensating winding has the same number of turns as the secondary winding. Now from Figure 17, the sum of currents through compensation and secondary windings must equal the secondary current of the assumed perfect current transformer. Thus, the total ampere turns in the comparator must be zero, and detector D will indicate a null. The current in the compensation winding is thus associated with the ampere turn difference between the primary and secondary of the comparator as a result of its current transformer action with shield Sh_1. Injection of a small voltage at g to compensate the impedance drop in the compensation winding of the comparator can be used to bring the point M to the same potential as N. For this condition, no burden is imposed on the current transformer (CT) by the comparator. If the resistance of the compensation winding is very low, M is sufficiently close to ground potential without any voltage being injected at g.

Now the current transformer (CT) is not error free, but it is made to appear so to the current comparator (CC) by injecting appropriate in-phase and quadrature currents through the G-C balancing network. At balance, indicated by null on the detector, the error of the current transformer is given by the equation $\epsilon = r\,(G + j\omega C)$, where the real component is the error in ratio and the imaginary is the quadrature error. To this must be added any error of the current comparator. With minor modifications in the G-C loop, the resistance r in the transformer secondary circuit can be eliminated, making it possible to test the transformer with nearly zero burden.

A compensated comparator has been built at the Bureau, providing the most common ratios encountered from 5/5 to 600/5. Designed primarily for 60 Hz operation, its errors remain less than a part in 10^6 at 1 kHz. This unit will be used in the calibration circuit just described and in development work directed toward extension of the comparator principle to higher ratios. The current-comparator systems are intended to replace the existing transformer calibration methods and to improve calibration accuracy by an order of magnitude. A current-comparator-current-transformer test set, comprising the essential features of the test circuit described above, is now commercially available for transformer testing up to a 1200/5 ratio.

The above discussion has been concerned with low-frequency operation, since additional parameters become increasingly important when the frequency increases to 10-20 kHz. The one most profound effect is that of the distributed capacitance which shunts current around portions of a given winding or from one winding to another. Although the distribution of capacitance currents depends on design, their effects are present in both types of ratio standards, and the marked low-frequency advantage of the current comparator over the current transformer diminishes with increasing

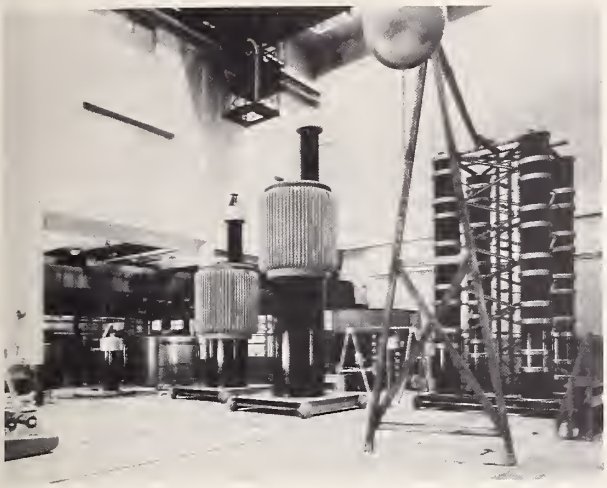

Figure 18. High Voltage Laboratory at National Bureau of Standards.

The 2 MV, 33 kJ surge-voltage generator is at the extreme right. In the center is the 1 MV 60 Hz cascaded transformer set.

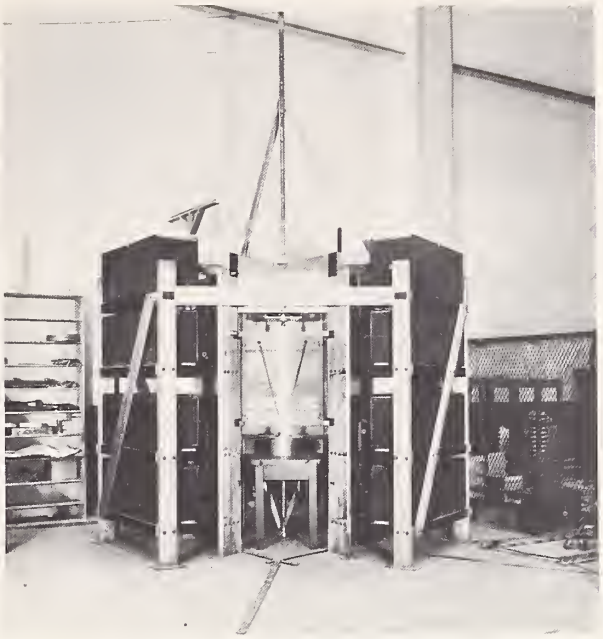

Figure 19. 200 kA, 50 kJ surge-current generator.

frequency. An important new concept regarding the definition of ratio must be introduced at the higher frequencies. A primary or secondary current, as such, can no longer be assigned to the respective windings, since the current entering a given winding may not be the same as that which leaves it. Thus, the ratio of currents being measured must be identified with a specific pair of terminals and with a given voltage distribution along the windings. With proper attention given to capacitance distributions, both the comparator and the transformer can be designed for broad frequency range of operation with small errors.

At the Bureau, two nearly identical standard current transformers with consecutive ratios 1/1 to 6/1 have been designed and evaluated over the frequency range 400 Hz to 16 kHz. Their changes in complex error with range, frequency, and secondary current are relatively small. The ratio error for any combination of these variables is no more than 25 ppm and the quadrature error no more than 50 ppm (μ radians). If only the frequency decade 1 - 10 kHz is considered, the ratio error is never more than 7 ppm and the quadrature error 22 μ radians. NRC has pursued a corresponding development program for current comparators.

Measurement of Crest and Surge Voltages - In the range of very high alternating voltages, engineers are frequently concerned with crest rather than rms values. This is because the breakdown of insulation is to a large extent dependent on the crest value of the voltage to which it is subjected. A technique which has been much used in this field is to note the sparkover voltage between metal spheres of known diameter and spacing in air under standard test conditions. The value of crest voltage is then determined within 2-5% by reference to standard sphere-gap tables. The Bureau has 1-meter and 2-meter sphere pairs which can be used for this purpose.

A closely related field is the measurement of surge voltages and currents. Transient voltage surges are much used in the proof-testing of electrical apparatus, since the duration and distribution of electric stress can, in this way, be made to approximate the extreme conditions to which the equipment will be exposed in service as a result of lightning and switching transients. The Bureau has a 2 MV, 33 kJ surge-voltage generator, shown in Figure 18, and a 200 kA, 50 kJ surge-current generator, Figure 19, which are used for studying methods of surge measurement. A 3 MV, 250 kJ surge-voltage generator is being planned for the extension of this work.

The complications that arise from inductance and skin effect in measuring transient currents are closely related to those encountered in the precise measurement of phase angle of current transformers. By applying similar procedures, standard forms of shunts and inductors have been developed for measuring surge currents and the rates of rise of such currents.

The design of voltage dividers that will be accurate for rapidly changing voltages, especially during the first microsecond of the surge, is a difficult problem. Thin ribbon resistors have been constructed at the Bureau, suitable for high-voltage surges and having a very low time constant, 2×10^{-9} second. They have been used in making voltage dividers for measuring linearly rising chopped impulses with peak voltages to 300 kV and time to sparkover from 30 nanoseconds to 50 microseconds. Divider ratio errors due to residual inductance are computed to be less than 1%. Stray capacitance errors are kept low by making the total divider resistance 1000 ohms or less. By a combination of computation and experiments, capacitance errors have been deduced to be less than 1% for time to sparkover down to 0.1 microsecond. Using this divider, data have been derived giving relations between rate of rise and flashover vol-

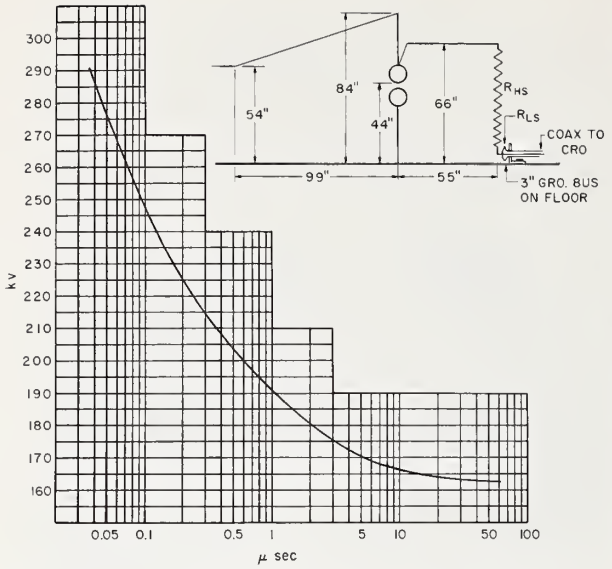

Figure 20. Volt-Time curve for 250 mm spheres at 60 mm spacing.

tages for various gaps. The relation is shown in Figure 20 for 250 mm spheres spaced 60 mm apart. It has been suggested that this curve be used as a reference standard for interlaboratory comparisons of measurement techniques in the field of steeply rising voltage surges. This suggestion has received international consideration and is being studied further in a number of high-voltage laboratories.

Dissemination of the Electrical Units - In addition to the Bureau's statutory responsibilities to develop, maintain, and have custody of the national standards of measurement, it has the further responsibility of making these standards available through appropriate calibration services. Thus, a great number of laboratories--operated by manufacturers, universities, public utilities, Federal agencies, or private individuals--send their reference standards to the Bureau for comparison with the national reference standards and for assignment in terms of the latter. The Bureau's Electricity Division receives for calibration standards of resistance, inductance, and capacitance, standard cells, ac-dc transfer standards, ratio standards, standard watthour meters, and other instruments which are intended to serve as reference standards in the laboratory that sends them. Some must be recalibrated at intervals which are determined by the stability and the type of use proposed for the standard. The conditions of test and the fees charged for calibration services are listed in Miscellaneous Publications 250--"Calibration and Test Services of the National Bureau of Standards,"--together with listings of items which are appropriate for calibration and other relevant information.

Bibliography

General

31 Stat., ch. 872, p. 1449 (1901), Establishment of the National Bureau of Standards.

Public Law 617, 81st Congress (ch. 484--2nd Session). An act to redefine the units and establish the standards of electrical and photometric measurements.

F. B. Silsbee, Establishment and maintenance of the electrical units, NBS Circular 475 (1949).

NBS Handbook 77, Vol. 1, Precision Measurement and Calibration; selected papers on electricity and electronics--a compilation of previously published technical papers by NBS staff members (1961).

NBS Technical Note 262, Accuracy in Measurements and Calibrations (1965).

NBS Miscellaneous Publication 250, Calibration and Test Services.

Absolute Measurements

R. L. Driscoll, Measurement of Current with a Pellat-Type Electrodynamometer, NBS J. Res. 60, p. 287-296 (1958).

R. L. Driscoll, and R. D. Cutkosky, Measurement of Current with the NBS Current Balance, NBS J. of Res. 60, p. 297-305 (1958).

J. L. Thomas et al, An Absolute Measurement of Resistance by the Wenner Method, NBS J. Res. 43, p. 291 (1949).

R. D. Cutkosky, Evaluation of the NBS Unit of Resistance based on a Computable Capacitor, NBS J. Res. 65A, p. 147-158 (1961).

Capacitance

W. D. Volker, An Improved Capacitance Bridge for Precision Measurements, Bell Lab Record 20, 133, 1942.

A. M. Thompson, D. G. Lampard, A New Theorem in Electrostatics and Its Application to Calculable Standards of Capacitance, Nature 177, p. 888 (1956).

A. M. Thompson, The Cylindrical Cross Capacitor as a Calculable Standard, Proc. IEE 106B, May (1959).

A. M. Thompson, The Precise Measurement of Small Capacitances, Trans. IRE Instrumentation I-7, December (1958).

M. C. McGregor, et al, New Apparatus at NBS for Absolute Capacitance Measurement, Trans. IRE Instrumentation I-7, December (1958).

R. D. Cutkosky, Active and Passive Direct-Reading Ratio Sets for the Comparison of Audio-Frequency Admittances, NBS J. Res. 68C, October (1964).

R. D. Cutkosky, L. H. Lee, Improved 10 pF Fused Silica Dielectric Capacitor, NBS J. Res. 69C, July (1965).

J. Q. Shields - Voltage Dependence of Precision Air Capacitors, NBS J. Res. 69C, October (1965).

Resistance

F. Wenner, Methods, Apparatus, and Procedures for the Comparison of Precision Standard Resistors, NBS J. Res. 25, August (1940).

J. L. Thomas, Stability of Double-Walled Manganin Resistors, NBS J. Res. 36, p. 107 (1946).

J. L. Thomas, Precision Resistors and Their Measurement, NBS Circular 470 (1948).

A. H. Scott, Measurement of Multimegohm Resistors, NBS J. Res. 50, March (1953).

Voltage

W. J. Hamer, Standard Cells, Their Construction, Maintenance, and Characteristics, NBS Monograph 84 (1965).

F. K. Harris, Electrical Measurements (Chapter 6, Potentiometers), a book published by J. Wiley (1952).

F. B. Silsbee, F. J. Gross, Testing and Performance of Volt Boxes, NBS J. Res. 27, p. 269 (1941).

B. L. Dunfee, Method for Calibrating a Standard Volt Box, NBS J. Res. 67C, January (1963).

J. H. Park, Special Shielded Resistor for High-Voltage d-c Measurements, NBS J. Res. 66C, January (1962).

Inductance

B. Hague, Alternating Current Bridge Methods (Pitmen, 5th Edition, Revised 1957).

F. K. Harris, Electrical Measurements (Chapter 15, a-c bridges), ibid.

F. B. Silsbee, Notes on the Design of 4-Terminal Resistance Standards for Alternating Currents, NBS J. Res. 4, 73, (1930).

B. L. Dunfee, An A-C Kelvin Bridge for the Audio Frequency Range, IEEE Trans. (Communications and Electronics), May (1956).

Magnetic Quantities

R. L. Sanford, I. L. Cooter, Basic Magnetic Quantities and the Measurement of the Magnetic Properties of Materials, NBS Monograph 47 (1962).

R. L. Sanford, E. G. Bennett, An Apparatus for Magnetic Testing at Magnetizing Forces up to 5000 oersteds, NBS J. Res. 23, p. 415 (1939).

R. L. Sanford, P. H. Winter, A Permeameter for Magnetic Testing at Magnetizing Forces up to 300 oersteds, NBS J. Res. 45, p. 17 (1950).

R. L. Sanford, E. G. Bennett, Determination of Magnetic Hysteresis with the Fahy Simplex Permeameter, NBS J. Res. 15, p. 517 (1935).

I. L. Cooter, The Calibration of Permanent Magnet Standards, Reprint 14, 1-3-65, Proceedings of the 20th Annual ISA Conference, Los Angeles (1965).

E. M. Purcell, et al, Resonance Absorption by Nuclear Magnetic Moments in a Solid, Phys. Rev. 69, p. 37 (1946).

P. L. Bender, R. L. Driscoll, A Free Precession Determination of the Proton Gyromagnetic Ratio, Trans. IRE, I-7, December (1958).

AC-DC Transfer

F. L. Hermach, E. S. Williams, Thermal Converters for Audio-Frequency Voltage Measurements, IEEE Trans. Instrumentation, 15I, December (1966).

F. L. Hermach, et al, A System for Direct and Alternating Voltage Measurements, Trans. IEEE, I-14, December (1965).

J. H. Park, A. B. Lewis, Standard Electrodynamic Wattmeter and ac-dc Transfer Instrument, NBS J. Res. 25, p. 545 (1940).

A. W. Spinks, T. L. Zapf, Precise Comparison Method of Testing a-c Watthour Meters, NBS J. Res. 53, p. 95 (1954).

R. F. Estoppey, Watthour Meter Calibration Referred to d-c Volts and Amperes, Electrical World, December 1963.

Transformers and Comparators

B. Hague, Instrument Transformers, Pitman (1936).

F. B. Silsbee, Equipment for Testing Current Transformers, NBS J. Res. 11, p. 93 (1933).

N. L. Kusters, W. J. M. Moore, The Current Comparator and Its Application to the Absolute Calibration of Current Transformers, Trans. AIEE, 80-III, April (1961).

P. N. Miljanic, et al, The Development of the Current Comparator, a High-Accuracy a-c Ratio Measuring Device, Trans. AIEE, 81-I, Nov. (1962).

N. L. Kusters, W. J. M. Moore, The Development and Performance of Current Comparators for Audio Frequencies, Trans. IEEE, 14I, Dec. (1965).

B. L. Dunfee, The Design and Performance of Multi-Range Current Transformer Standards for Audio Frequencies, IEEE, 14-I, Dec. (1965).

B. L. Dunfee, W. J. M. Moore, An International Comparison of Current-Ratio Standards at Audio Frequencies, Trans. IEEE, 14-I, Dec. (1965).

W. K. Clothier, L. Medina, The Absolute Calibration of Voltage Transformers, Proc. IEEE, 104A, June (1957).

F. K. Harris, et al, An International Comparison of Voltage-Transformer Calibrations to 350 kV, Trans. IEEE (Communications and Electronics), January (1964).

W. C. Sze, Comparators for Voltage Transformer Calibrations at NBS, NBS J. Res. 69C, October (1965).

J. J. Hill, A. P. Miller, A 7-Decade Adjustable Ratio Inductively Coupled Voltage Divider with 0.1 Part per Million Accuracy, IEEE, 109B, March (1962).

W. C. Sze, et al, An International Comparison of Inductive Voltage Divider Calibrations at 400 and 1000 Hz, Trans. IEEE 14-I, p. 124 (1965).

R. D. Cutkosky, J. Q. Shields, The Precision Measurement of Transformer Ratios, Trans. IRE, 9-I, p. 243 (1960).

Surge Measurements

J. H. Park, Shunts and Inductors for Surge-Current Measurements, NBS J. Res. 39, p. 191 (1947).

J. H. Park, H. N. Cones, Spark-Gap Flashover Measurements for Steeply Rising Voltage Impulses, NBS J. Res. 66C, July (1962).

Electrical Calibration Accuracies at NBS

Normal and best capabilities

INSTRUMENTATION TECHNOLOGY
November 1967

F. L. HERMACH, National Bureau of Standards

The National Bureau of Standards concentrates on calibration of electrical standards of high stability and accuracy. This review presents data on the present ranges and accuracies of basic electrical measurements, from direct current to 50 kHz. Those interested in NBS capabilities and services can examine charts which show accuracies normally available and also the best attainable.

CALIBRATION, as used in this review, is *the process of making appropriate measurements to determine the correct value of a standard.* NBS calibrates standards of resistance, capacitance, inductance, voltage, and current over many decades of both magnitude and frequency. The charts contain the latest data on these variables.

Figure 1 shows the major calibration standards used by NBS. Directional lines indicate the major relationships. For clarity, some minor relationships and the kinds of calibrations are not shown. The diagram has prototype standards in the top row. The meter, a unit of *length,* is defined as a certain number of wavelengths of the orange-red line of Krypton-86. The meter bar is a reference standard, rather than a prototype (Ref. 1). A specified transistion of cesium-133 defines *time* — the atomic second, and stable oscillators serve as working standards of frequency (Ref. 2). The kilogram is still defined as the *mass* of the prototype Pt-Ir standard.

Two experiments at NBS determine the basic electrical units in terms of the three prototype standards and two measured constants, the speed of light in vacuo *c* and the acceleration of gravity *g*. The experiments are simple in principle but extremely difficult and involved in practice because of the required accuracy.

One experiment—to establish the standard ohm—consists of constructing a capacitor from gage bars and computing the capacitance in electromagnetic units (about 1 picofarad) from the length of the bars and the speed of light. With suitable bridges, the step-up is made at 1,592 Hz to two 10,000 pF capacitors, across to two 10,000 ohm resistors of known ac-dc difference, and down to 1-ohm resistors (Ref. 3). The final step is taken because 1-ohm Thomas-type resistors are still the most stable impedance standards known. The average resistance of a group of such resistors serves to maintain the ohm at NBS between absolute determinations.

The other experiment—to establish the standard volt—consists in "weighing the ampere" with a current balance, and is based directly on the definition of the ampere in terms of the force between current-carrying conductors (Ref. 4). One conductor (coil) is suspended from one arm of a balance, and the change in force when its current is reversed is measured in terms of the acceleration of gravity on a known mass. The voltage drop in a 1-ohm standard resistor carrying this measured direct current is then used to determine the emf of a group of saturated standard cells, which in turn maintain the volt at NBS.

Direct-reading ratio-sets were developed at NBS to calibrate resistors by the substitution method, and to step up and down on the resistance scale (Ref. 5). No line leads to the ratio-sets in Figure 1 because their accuracy depends on ratios of resistors, not on the unit of resistance. Standard cells are calibrated by connecting the known and unknown cells in opposition and measuring the small voltage difference with a low-range thermofree potentiometer. Potentiometers and volt boxes are calibrated with universal and direct-reading ratio-sets (Ref. 5 and 6). With these the user can then extend the dc voltage scale very accurately.

AC-DC transfer instruments are comparators for determining the equality of ac and dc currents, ac and dc voltages, and ac and dc powers (Ref. 7 and 8). At NBS they serve chiefly to check other ac-dc comparators. Since such comparators are very stable, the user can made accurate ac measurements based on his known dc standards.

AC bridges extend the scale of capacitance and inductance measurements, but NBS calibrates only the more stable capacitors and inductors, with which bridges can be checked. AC voltage dividers or ac potentiometric networks are used to determine the ratios (expressed as complex numbers) of the phasor voltages and currents of the NBS standard transformers and inductive voltage dividers which in turn are used to calibrate other standards. In principle the ratios of these networks are also independent of units; however in practice some of the component impedors are measured with the dc ratio-sets and ac bridges. Build-up or "boot-strap" techniques are used for the newer current comparators and audio-frequency current transformers (Ref. 9 and 10).

The standard watthour meters and standards for magnetic measurements depend on the other standards as shown in Figure 1 (Ref. 11 and 12).

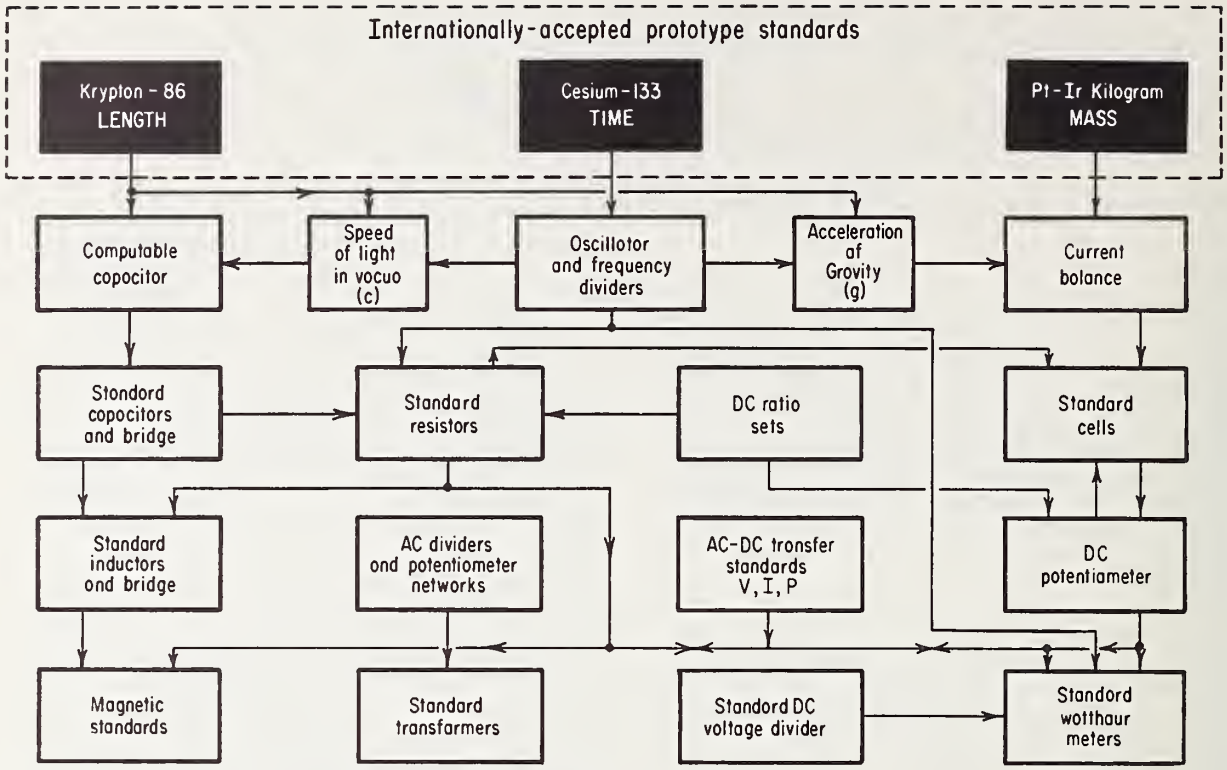

Figure 1. Major electrical standards used by NBS.

Accuracy at NBS

Figures 2 to 6 show the *uncertainty* (accuracy) in the calibrations of standards at NBS. Because of the wide ranges, logarithmic scales are used. In each figure the uncertainty is the "limit of error" which should be exceeded only very rarely. Uncertainty data includes the calculated imprecision (at least three times the standard deviation of the average) plus the estimated limits of the systematic errors of the NBS working standards and the calibration process. Uncertainty data does not include the differences between the absolute units and the legal units maintained at NBS (Ref. 3 and 4).

The solid lines and circles in the figures show the accuracies normally available in the calibration of commercially available standards of the highest grade, by established techniques, and for the fees given in the published NBS fee schedules. These accuracies include allowances for short-time variations in the standards under test under the controlled conditions at NBS, but not for possible larger variations in other environments nor for long-time drifts or other changes. The dotted lines and open circles show the best accuracies that might be attainable by special techniques, and with repeated tests made with great care and effort in the calibration of "ideal standards" which are perfectly stable and free from environmental influences.

Resistance—Figure 2 shows the familiar *accuracy triangle* with the peak at the value of the 1-ohm basic standard. Note that only decimal multiples and submultiples of 1-ohm are shown. NBS does not usually offer calibrations of other values, nor does it maintain an accurate resistance-measuring facility as such. However, stable standards of any nominal value can be calibrated at greater cost and lesser accuracy than standards of neighboring values on the decimal scale. Thomas-type 1-ohm resistors are normally calibrated to 1 ppm in terms of the ohm maintained at NBS.

High-quality direct-reading and universal ratio-sets (not shown in Figure 2) can be calibrated with an uncertainty not exceeding 1 ppm of input resistance. Using relatively simple equipment and established calibration procedures, many users of these ratio devices could perform these calibrations with comparable uncertainties. This is also true for many types of range-extending ratio standards. In many cases the equipment and techniques are quite involved, so it may be very desirable to verify the results by "round-robin tests" on a traveling standard in several laboratories, or by a direct calibration of a few ranges at NBS.

Capacitance—The chart for capacitance measurements, Figure 3, should be three-dimensional, with frequency as another independent variable. One would

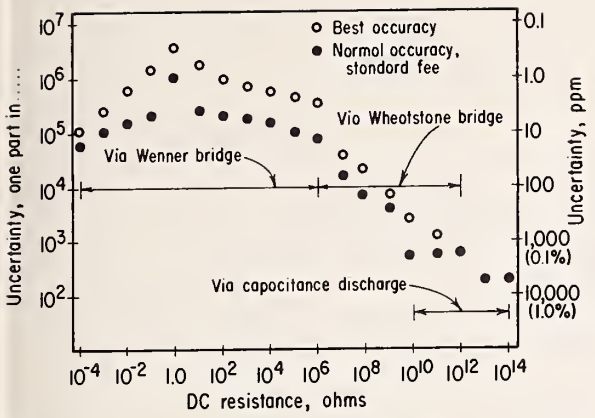

Figure 2. NBS measures dc resistance.

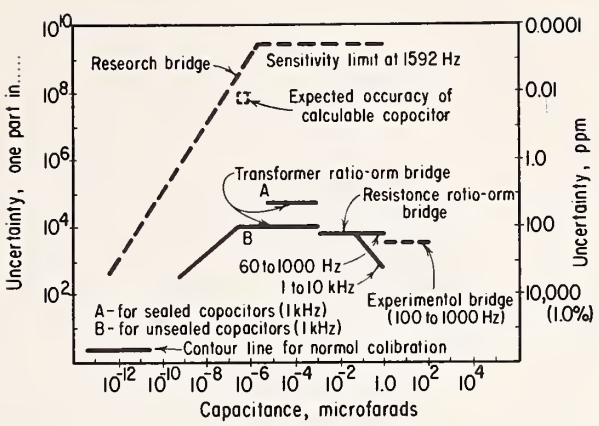

Figure 3. NBS measures capacitance.

expect, in a rough way, an "accuracy cone" with the peak at 1 picofarad and 1,592 Hz, where the best measurements with the computable capacitor have been made.

The dotted line in Figure 3 shows the sensitivity limit at 1,592 Hz of a new research bridge which is developed in conjunction with a new calculable capacitor. The estimated accuracy of the capacitor is also shown. The accuracy of the research bridge for stepping up and down from its value of 0.5 picofarad will be somewhat poorer than the sensitivity limit indicated. Some of the normal calibrations of the best available commercial capacitors are shown. Note the extremely wide ranges in magnitude of 10^{-9} to 10^{2} μF and in frequency of 60 to 10,000 Hz.

Some sealed three-terminal air capacitors from 10 to 1,000 pF have shown unusual stabilities. Projected improvements in the NBS ratio arm bridge should make it possible to measure such capacitors to at least 10 ppm. Even better accuracy may be required to calibrate 10 pF sealed capacitors of fused silica with silvered electrodes, which are apparently stable to better than 1 ppm/year (Ref. 13).

Inductance—Standard inductors are calibrated with standard capacitors in a Maxwell Wien bridge. Some of the contours in the accuracy cone are shown in Figure 4. The available accuracy is generally limited by the environmental conditions affecting the bridge and the standards being calibrated.

Voltage—The graphs of voltage measurements, Figures 5 and 6, are complicated not only because of applied frequency but also because NBS does not offer a voltage calibration service as such. Only the dc voltage of a standard cell is available directly, and is determined to 1 ppm in terms of the volt maintained at NBS. The scale is extended in voltage and frequency by the calibrations of ratio standards and ac-dc transfer standards. The user makes accurate dc and ac mea-

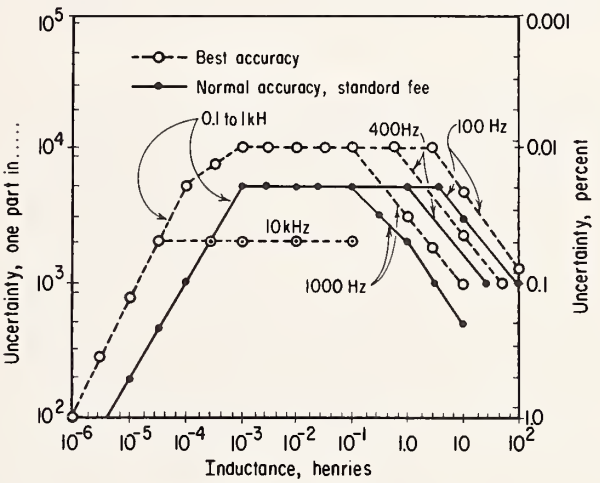

Figure 4. NBS measures inductance.

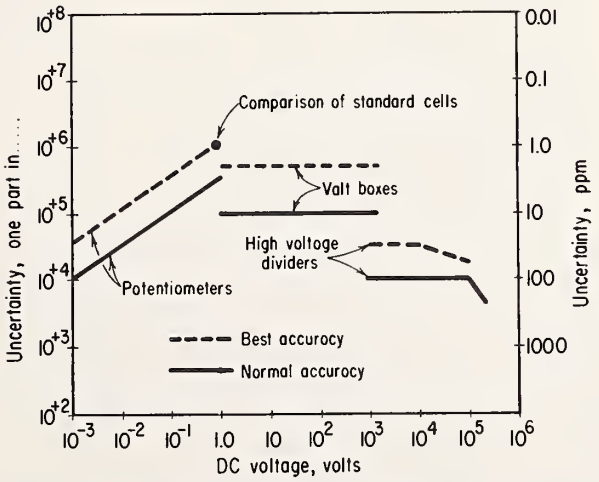

Figure 5. NBS measures dc voltage. Accuracy of V/V_r is shown for ratio standards, $V_r = 1$ v.

Figures 2, 3, and 4 were contributed by Chester Peterson, Chief of the N.B.S. Resistance and Reactance Section.

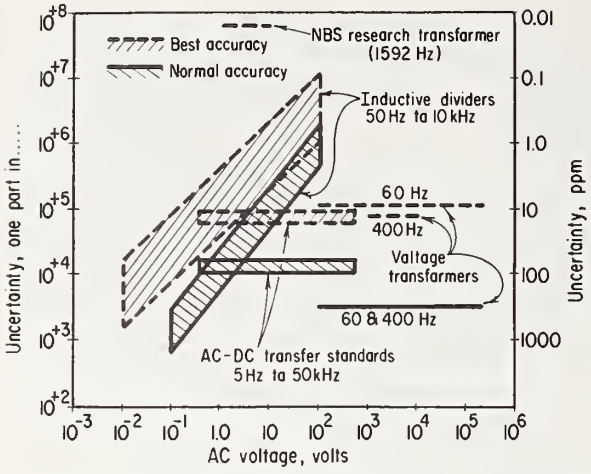

Figure 6. NBS measures ac voltage. Accuracy of V/V_r is for ratio standards, $V_r = 100$ v.

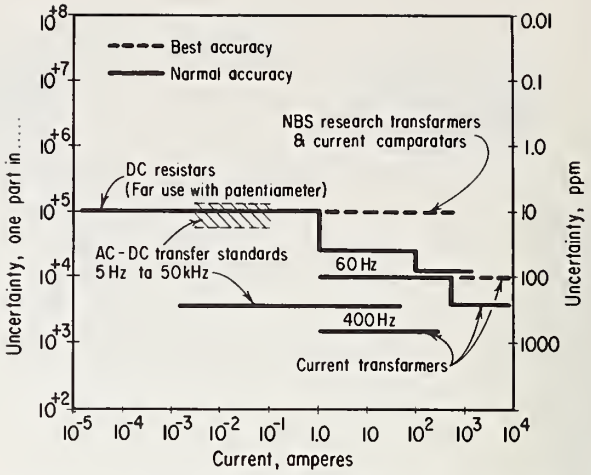

Figure 7. NBS measures current. Accuracy of I/I_r is shown for ratio standards, $I_r = 5$ amp.

surements with these standards and a standard cell. Potentiometers, fixed resistance dividers, and transformers are ratio standards which are generally used with some reference voltage. The emf of a standard cell would be used with dc ratio standards, and approximately 100 volts for ac standards. The ratio standards have upper and lower voltage limits. The charts therefore show the accuracy of the ratio V/V_r, where V is given along the abscissa, and V_r is this reference. Note that this is the accuracy of the indicated ratio, not of a fraction of the applied voltage. A 1,000/1 volt box certified to 0.001 percent of ratio has one hundredth the uncertainty of a 1-ppm-of-input voltage divider at this same ratio. Dotted lines show the "attainable" accuracies. Normal calibrations are as follows:

- potentiometers of the highest grade—
  to 3 ppm at 1 volt
- volt boxes—
  to 10 ppm of ratio
- decade transformers—
  to 0.5 ppm of input voltage at 1 kHz
- voltage transformers—
  to 0.03 percent of ratio at 60 Hz
- ac-dc transfer instruments for voltage—
  to 50 ppm from 20 Hz to 20 kHz,
  and 100 ppm at 5 Hz to 50 kHz.

Current—The chart for current measurements, Figure 7, is similar. NBS offers only calibrations of dc shunts (for use with a potentiometer), ac ratio standards, and ac-dc transfer standards. A chart for power and energy measurements would be based on the NBS standard transfer wattmeter, accurate to better than 50 ppm of the applied volt-amperes at 60 Hz and 0.1 percent at 2 kHz. The five NBS standard watthour meters are calibrated periodically in terms of the dc standards through this wattmeter, and are in turn used to calibrate standard watthour meters to 0.05 percent at 60 Hz.

References

1. "Actions of 11th Conference on Weights and Measures," *NBS Technical News Bulletin, 44, 199*, Dec. 1960.
2. "World Sets Atomic Definition of Time," *NBS Technical News Bulletin, 48, 209*, Dec. 1964.
3. Cutkosky, R. D., "Evaluation of the NBS Unit of Resistance Based on a Computable Capacitor," *Journal of Research NBS, 65A, 147*, 1961.
4. Driscoll, R. L., and Cutkosky, R. D., "Measurement of Current with the NBS Current Balance," *Journal of Research NBS, 60 297*, 1958.
5. Thomas, J. L., "Precision Resistors and Their Measurements," *NBS Circular, 470*, 1948.
6. Dunfee, B. L., "Method for Calibrating a Standard Volt Box," *Journal of Research NBS, 67C*, 1963.
7. Hermach, F. L., and Williams, E. S., "Thermal Converters for Audio-Frequency Voltage Measurements of High Accuracy," *IEEE Transactions on Instrumentation and Measurement, Vol. IM-15, No. 4*, Dec. 1966.
8. Park, J. H., and Lewis, A. B., "Standard Electrodynamic Wattmeter and AC-DC Transfer Instrument," *Journal of Research NBS. Vol. 25, p 545*, 1940.
9. Kusters, N. L., "The Precise Measurement of Current Ratios," *IEEE Transactions on Instrumentation and Measurement, Vol. IM-13, No. 4*, Dec. 1964.
10. Dunfee, B. L., "The Design and Performance of Multirange Current Transformer Standards for Audio Frequencies," *IEEE Transactions on Instrumentation and Measurement, Vol. IM-14, No. 4*, Dec. 1965.
11. Spinks, A. W., and Zapf, T. L., "Precise Comparison Method of Testing AC Watthour Meters," *Journal of Research NBS, 53, 95*, 1954.
12. Sanford, R. L., and Cooter, I. L., "Basic Magnetic Quantities and the Measurements of Magnetic Properties of Materials," *NBS Monograph 47*, 1962.
13. Cutkosky, R. D., and Lee, L. H., "Improved 10-Picofarad Fused Silica Dielectric Capacitor," *Journal of Research NBS, Sec. C., Vol. 69C, No. 3*, July-Sept. 1965.

Francis L. Hermach is Chief of the Electrical Instruments Section at the National Bureau of Standards, Washington, D. C. Article is based on Paper M5-1-MESTIND-67 presented at the 22nd ISA Conference & Exhibit, Chicago, Ill., Sept. 11-14. 1967.

UNITED STATES DEPARTMENT OF COMMERCE • Sinclair Weeks, *Secretary*
NATIONAL BUREAU OF STANDARDS • A. V. Astin, *Director*

Suggested Practices for Electrical Standardizing Laboratories

Francis B. Silsbee

National Bureau of Standards Circular 578

Issued August 30, 1956

33-I

Preface

Since World War II there has been a very marked increase in the number and scope of private standardizing laboratories throughout the United States. The function of each such laboratory is to maintain the accuracy and uniformity of the measuring instruments and apparatus used by the organization or organizations that the laboratory serves. A basic phase in this process is necessarily to correlate the reference standards of the laboratory with those of the National Bureau of Standards. This Circular has been prepared to suggest techniques and principles that experience has shown to be useful in such operations. Although this Circular covers explicitly only the field of electrical measurements, many of the principles involved are equally applicable in other kinds of measurement.

A. V. Astin, *Director.*

Contents

Suggested Practices for Electrical Standardizing Laboratories

Francis B. Silsbee

A number of basic principles are given that experience has shown to be important in the operation of private standardizing laboratories. Types of standard apparatus are classified and schedules appropriate for their intercomparison and for their checking at the National Bureau of Standards are suggested.

1. Introduction

The purpose of this Circular is to indicate recommended procedures and schedules for the calibration testing of electrical instruments and measuring apparatus used in the range of frequency from 0 to 30 kilocycles per second.

For many years the electric-power companies have maintained large and efficient laboratories [1, 2] [1] suited to their particular needs, and certain universities have similarly supplied services [3] to their teaching and research staffs. More recently, laboratories are being established in many newly founded manufacturing plants, in firms concerned with research and development, and in Government agencies (particularly in the military services). Although the particular problems that confront the various agencies may differ greatly, their standardizing laboratories have a great many common functions in their work of maintaining and disseminating the units of measurement.

The process of measurement always involves a succession of steps in which the units in terms of which the measurement of any quantity is expressed are transmitted by using measuring apparatus that has been standardized, by comparison with standards of a higher level, to calibrate other measuring apparatus which is to serve as a standard at a lower level. At the source is the National Bureau of Standards, authorized by Congress to establish and maintain the basic standards of the nation [4, 5]. Next, in any organization, may come a primary group of laboratory workers, which maintains its basic reference standards and in turn calibrates the working standard apparatus used by the next lower, or secondary, group, which in turn calibrates the instruments used in making measurements in the plant or shop. In some cases these latter two operations are merged in a single group, while, at the other extreme, a single primary group may serve many secondary groups located in different cities.

It is the rest of the organization that uses the shop instruments standardized by the working-standards group, and carries on the day-to-day work in the power systems, manufacturing operations, research studies, or acceptance tests. This use insures proper billing, adequate quality, and valid criteria for the acceptance of manufactured articles. In this Circular the terms "laboratory" or "standardizing laboratory" will be used to indicate the segregated part of the complete organization that is charged with the duty of supplying calibration services, at either the reference or the working-standard level, to the measuring apparatus used by the rest of the organization, which will here be designated as "plant" or "shop," even though it may actually be more correctly described as a research or testing laboratory.

For clarity in the rest of this Circular, the measuring instruments and apparatus used in an industrial organization will be referred to under the following categories:

(a) Reference standards, which embody fixed electrical quantities and serve to maintain their respective units during the intervals between checks with a laboratory at a higher echelon.

(b) Working standards, calibrated in terms of the reference standards and reserved for use in the calibration of shop instruments and apparatus. Working standards should never be used directly for measurements in the plant or shop.

(c) Comparison equipment such as bridges, potentiometers, etc., and consoles used in comparing shop instruments with working standards.

(d) Interlaboratory standards, often similar in construction to reference standards, used for transport to NBS and return in the periodic checking of the local reference standards.

(e) Shop instruments and measuring apparatus calibrated in the standardizing laboratory and used in the day-to-day operation of the plant.

[1] Figures in brackets indicate the literature references at the end of this Circular.

390925°—56

2. General Principles

The following general principles have been found by experience to be applicable to many of the problems involved in the maintenance of accuracy in laboratory work and any program of calibration service testing should conform to them so far as possible.

2.1. Competence of Personnel

The person in direct charge of any standardizing laboratory must be thoroughly familiar with the fundamentals of electricity and magnetism and with the principles of operation of all types of electrical measuring apparatus [8, 9]. To be competent to carry on within the laboratory the various sequences of calibration testing outlined below, he must have taken a college-level course in electrical measurements or have had laboratory experience equivalent thereto. It is very desirable that he be a graduate in physics or electrical engineering from an accredited college. He must be mentally alert to detect discrepancies and inconsistencies in internal check tests and to recognize abnormal behavior of any part of the apparatus or circuits. Unless persons of this type are available in a standardizing laboratory, both its calibration service and the measurement work that depends upon it throughout the plant is certain to become unsatisfactory, regardless of how often particular pieces of apparatus may be tested by other persons in some higher echelon or at NBS.

2.2. Position in Organization

Experience through the years has shown that the most satisfactory results are obtained by maintaining a definite separation of the standardizing laboratory from the rest of the organization. Responsibilities for accuracy are thereby made definite, and team spirit can be developed in the staff of the standardizing laboratory that keeps them interested in their work, which might otherwise seem routine and unimportant. This separation protects them from pressures that demand improper haste and sloppy workmanship, and gives them authority directly delegated from a high level in management.

Closely related to the foregoing is the valuable principle that team spirit can be developed and maintained by recognizing that the quality of the reference standards of a laboratory are to a considerable extent a measure of the competence of its staff ("a worker is known by the sharpness of his tools"). Hence, in cases where a given large organization maintains a plurality of standardizing laboratories in its plants in different cities, it is very desirable that each reference and interlaboratory standard should be assigned permanently to an individual standardizing laboratory, and returned to it following periodic checks at any laboratory of a higher echelon. If this is not done, it becomes difficult to fix responsibility for errors that may be discovered subsequently, and the laboratory workers lose the basis for much of their pride in workmanship.

2.3. Appropriate Scope and Accuracy

The nature and accuracy of the work done in a standardizing laboratory may vary considerably with the size of the plant it serves and the nature of the output of the plant. However, there are very few modern activities in which some phases do not require measurements of rather high accuracy. A standardizing laboratory must, of course, be equipped for calibration measurements of a higher accuracy than any used elsewhere in the plant, because the accuracy of measurement can never rise above that of its source.

Many such local standardizing laboratories provide service in many scientific fields, e. g., mechanics, heat, optics, and chemistry, in addition to their standardizing work in electricity and magnetism, which alone is the subject of this Circular. The direction and extent of such activities, as well as the degree of specialization in particular branches of electrical science, may greatly affect the types and ranges of the electrical standards required.

2.4. Laboratory Atmosphere

Atmospheric conditions are of considerable importance in an electrical standardizing laboratory. If the relative humidity exceeds 65 percent, a conducting film of moisture is adsorbed on the surface of many types of insulating material. Leakage over such surfaces, particularly to the circuit of a sensitive galvanometer, may introduce serious errors.

Certain types of apparatus, for example some wire-wound resistors of high value, show changes of several parts per 10^4 with prolonged changes in humidity. Such variations can be detected by comparing calibrations made near the middle of the winter heating season, during which indoor humidities are normally very low, with those made near the middle of the summer when the ambient humidity is high.

Most electrical apparatus is compensated for temperature to some extent. However, if the ambient temperature is subject to changes, the response of the various components may not be equally prompt. In such circumstances the compensation may be temporarily ineffective. It is therefore important that the laboratory temperature be held fairly constant (± 2 deg F) at all times. Such room control also makes easier the task of the thermostats that control the baths in which more temperature-sensitive apparatus, such as standard cells or standard conductivity samples, are kept. The particular temperature chosen is of less importance. The conditions specified by the American Society for Testing Materials for its

"Standard Laboratory Atmosphere" are a relative humidity of 50 ±2 percent and a temperature of 23° ±1.1 deg C (73.4° ±2 deg F). This combination is widely used in tests of dielectrics and other materials, and, in addition, is very close to the maximum of comfort for the workers. Hence it is a good target to aim at in designing a new laboratory.

Freedom from vibration and dust are also important. A shop in which electrical instruments may be opened for repair should be scrupulously clean and dust free. Magnetic particles are attracted to the air gaps of permanent magnet instruments and must be constantly guarded against. Effective air filtering or electrostatic precipitation are very desirable.

2.5. Care of Standards

In many categories, a good standard piece of apparatus improves with age but deteriorates with handling and shipping. The shipping of primary and working standards and of comparison equipment can be minimized and the transfer of the units be achieved best by the use of interlaboratory standards of particular types that are as rugged as practicable.

The adjustment of a piece of measuring equipment to be close to its nominal value is very often desirable in the shop instruments used in the plant, because of the great saving in time and reduction in possible erroneous applications of corrections that result. On the other hand, the exact opposite is usually true of working and reference standards. In general, such standards should not be readjusted, even if their values have gradually drifted materially away from their nominal values. Any standardizing laboratory naturally maintains records of the values of its reference standards [10]. These are preferably kept on an individual card or record sheet for each standard, so that its history is apparent at a glance. Each such record provides a valuable indication of the quality of the standard, and gives warning of deterioration and the need for replacement toward the end of its useful life. Frequent adjustments tend to interfere with such records and increase the probability of improper corrections, as the proper corrections before and after a slight readjustment may not be conspicuously different. Even more important is the risk that the adjustment may initiate a progressive drift in value of the standard as a result of introducing mechanical strain, or local heating.

2.6. Timing of Calibrations

The most desirable sequence of steps and the frequency with which comparisons of measuring apparatus should be made depend, of course, upon a great number of circumstances, such as the volume of equipment to be tested, the delicacy of the apparatus, and particularly the type of personnel by which it is to be handled. (For measurements made by inexperienced students or by military recruits, the likelihood of damage is much greater than when a laboratory is staffed by experts.) In every laboratory a real possibility is always present that an abrupt change may occur in some standard as a result of an unrecognized accident or abuse. Fairly frequent checks made locally are therefore an indispensable supplement to any program of calibrations to a higher echelon.

Cooperative arrangements with a similar laboratory in the same city may allow frequent checks to be made against an independently maintained group of standards. This may permit a much less frequent checking schedule between either laboratory and one of higher echelon.

In any laboratory, the accuracy needed in measurement may differ widely on different projects. Hence the frequency with which the working instruments should be checked may vary considerably from project to project, even though instruments of the same accuracy class are used [2, 6, 7]. The time intervals suggested elsewhere in this Circular for check tests represent in most cases the considered opinion of persons who have had long experience with standard apparatus of the types now commonly used. Similar test intervals are listed in the American Standards Association Code for Electricity Meters [2]. When a new type comes into use, it must be appraised by being checked at frequent intervals during its first few years of service. After its good stability has thus been demonstrated, the interval between tests may safely be made longer. Several types of standard capacitors and inductors are currently in this probational stage.

A procedure that is often of value, particularly for the checking of consoles and complex equipment such as a-c bridges, is to use an interlaboratory standard that is measured in one laboratory and shipped to a laboratory of lower echelon for a repeat measurement, the lower laboratory not initially being aware of the value obtained at the higher. This procedure can detect significant defects in the wiring or insulation of the test console, improper procedure and careless operations at the lower-level laboratory, as well as changes or deterioration in the reference or working standards of the lower laboratory.

When systematic local intercomparisons indicate changes or abnormal performance in primary or working standards, checks with a higher echelon are in order regardless of whether any formal scheduled time for such a check has been reached. If the local periodic checks uncover unsteadiness of operation, large sudden changes in value, or other indication of a constructional defect in the reference or working standard, this standard should be sent to its manufacturer for repair before it is submitted to NBS for calibration.

3. Reference Standards

The function of the reference standards of a laboratory is to maintain locally a continuity of value in the units of measurement that they embody. Successive comparisons with the higher-echelon standards of NBS by means of interlaboratory standards shipped back and forth will give an indication of any slow drift of the reference standard. When this cumulative drift exceeds the confidence interval of the values derived by the comparisons with the interlaboratory standards, the value assigned to the reference standard is corrected accordingly. The reference standards are used primarily to calibrate periodically the working standards of a lower echelon, such as indicating instruments. Also, on occasion they may be used as working standards themselves.

It is evident that both reference standards and working standards should be as permanent and reliable in construction as possible. Definiteness and repeatability are of major importance, whereas sensitivity, low losses, and freedom from extraneous influences are relatively much less important. Closeness of adjustment to nominal value is of decidedly minor importance. An undetected change in a reference standard may easily initiate a chain of error that will propagate throughout the plant and cause losses in time and material exceeding manyfold the original cost of the standard. Hence, these reference standards should be purchased only on very strict specifications, and from manufacturers of high reputation and of long experience in producing shop instruments and apparatus of demonstrated permanence.

3.1. Standard Cells

A large and important laboratory, which is expected to need a standard of voltage with an accuracy of 0.002 percent and to certify the emf of unsaturated standard cells used in its plant or by its subcontractors, normally maintains as a reference standard a group of 5 or 6 cadmium standard cells of the saturated type. These cells are relatively permanent but have a temperature coefficient of about 0.005 percent per degree Celsius (centigrade) at room temperature. They must therefore be kept in a bath thermostatted to ± 0.01 deg C [11, 12]. A highly refined, water-white, acid-free mineral oil, having a viscosity of about 0.25 poise at 25° C and a flash point of 170° C, has been found suitable for baths for standard cells and for resistors. Such a group of saturated cells should preferably be checked initially at NBS and its value reassigned annually for the first 3 years and biennially thereafter, by using a second group of 2 or 3 saturated cells as an interlaboratory standard. The individual cells of the reference group can be intercompared monthly. The reference group is used to check the laboratory's working-standard cells of the unsaturated type and, on occasion, shop-standard cells also.

For laboratories requiring an accuracy of not over 0.01 percent in their standard of voltage, the reference standard often consists of a group of three cadmium standard cells of the unsaturated type. The individual cells are intercompared weekly by connecting them by pairs in series opposition and measuring the differential emf. These cells have a very small temperature coefficient and can be shipped safely by parcel post (if carefully packed). However, they are less constant than saturated cells and their emf usually decreases at a rate ranging from 40 to 120 microvolts per year. Therefore, their values should be reappraised at least annually on the basis of a periodic check from a higher echelon. A second group of 2 or 3 unsaturated cells can be used as an interlaboratory standard for such checks. When the emf of an unsaturated standard cell has fallen below 1.0183 volts, it is approaching the end of its useful life and can no longer be used as a reference or an interlaboratory standard. Following a moderate change in temperature, many cells tend to show a very considerable change in emf, which may persist for several days. This thermal "hysteresis" must be guarded against by allowing cells to stand for some time after shipment before taking readings. Temperature troubles with unsaturated standard cells can be minimized by keeping them in a thermally lagged copper-lined box. This reduces temperature fluctuations and differences in temperature between the two electrodes. It is important that the leads be brought out through very high grade insulation to an external terminal board. [13,14].

3.2. Resistors

If the laboratory possesses at least two standard resistors of each decimal value covering the range over which it expects to make accurate measurements, one of these can be submitted to NBS every 2 years as an interlaboratory standard, while the other resistor of each pair remains undisturbed as a reference standard in its laboratory.

3.3. Inductors

Many laboratories find it useful to possess two fixed standard inductors of each decimal value over the range it expects to cover with accurate measurements. In recent years the quality of standard inductors has been greatly improved, and this Bureau does not yet have sufficient data on the stability of the newer types to make a definite estimate of their expected stability. It is suggested therefore that one inductance standard of each denomination be submitted annually to the NBS, until a sufficient history is obtained to predict its performance.

3.4. Capacitors

Reference standards of capacitance include small fixed air-dielectric units, precision-variable air capacitors, and solid-dielectric capacitors using mica or an equivalent dielectric. Fixed standards 1,000 picofarads (micromicrofarads) or less in

value must be of three-terminal construction in order to avoid uncertainties due to stray capacitances. Precision-variable air capacitors are preferably hand carried, although shipment of the capacitor in its wooden container within a padded carton is usually satisfactory. Variable capacitors with noticeable backlash must be adjusted or repaired before submission to NBS for calibration. Capacitors with worm reduction gear are calibrated at the cardinal points corresponding to each whole revolution of the worm wheel. If the worm is eccentric, capacitance increments between cardinal points will depart from linearity, but it is usually not necessary to calibrate the vernier dial for every turn.

Each laboratory should possess two capacitance standards of each decimal value and type needed to cover the range of concern. After its initial check at NBS, one standard of each value can be kept as a reference standard while the other is submitted to NBS at regular intervals as an interlaboratory standard. This interval should initially be 1 year for any one pair of standards. After the first 3 or 4 calibrations, an examination of the record will indicate the appropriate future frequency of calibration, taking into account the actual accuracy demands made on particular standards. On variable air capacitors the eccentricity correction ordinarily will be determined only during the initial calibration; thereafter, calibration at a few cardinal points is usually sufficient.

3.5. Volt Boxes

Each laboratory should have one volt box with a plurality of ratios, which can serve as a reference standard. This can be checked initially at NBS. Unless the laboratory is rather large, this same volt box may be rechecked at NBS at intervals of 2 years, and thus serve as an interlaboratory standard also.

3.6. Time Standards

Although time is not an electrical quantity, many electrical laboratories require reference standards of time or of frequency. A high-grade seconds pendulum clock with photoelectric pickup or a standard crystal-controlled oscillator may form the reference standard. Either can be calibrated by reference to the standard-frequency radio signals emitted by NBS stations WWV or WWVH.[2] By the use of a multivibrator in combination with the reference-standard oscillator, the frequency of working-standard oscillators can be calibrated over a wide range. Such an oscillator can be used to control a standard frequency circuit to which, in turn, synchronous timers can be connected to serve as working standards for measuring time intervals. The use of the frequency of local electric-power circuits as a time standard, while very convenient, may be subject to errors approaching 1 percent for short periods of time, even though the average frequency over a longer time as shown by a clock is very high. These short-time fluctuations in frequency are materially less if the supply is tied in synchronism with a large power system.

[2] For information on this service, consult Radio Standards Division, National Bureau of Standards, Boulder Laboratories, Boulder, Colo.

4. Working Standards

The working standards constitute the principal tools of the standardizing laboratory. They are calibrated at intervals by comparison with the reference standards, and used in the daily work of checking shop instruments. The number needed of any one kind and range will depend upon the volume of testing service demanded in that range. If the volume is very small, and also in special cases where extreme accuracy is needed, a reference standard can be used as a working standard also.

4.1. Standard Cells

Most laboratories will need a number of unsaturated cadmium standard cells to serve as working standards and relieve their reference cells of excessive use and of the hazard of accidental abuse. Such working-standard cells should be checked against a reference standard at intervals of 1 or 2 weeks.

4.2. Resistors

Depending upon the nature of the work in the laboratory, there will probably be required, in addition to sets of fixed standard resistors, a number of dial-type resistance boxes, perhaps including resistors in the megohm and multimegohm ranges, and also resistors or shunts capable of carrying larger currents than are appropriate to the reference standards. These working standards may initially be tested at NBS to determine the effects, if significant, of current and temperature on their resistance. Thereafter these working standards need to be checked, using a moderate current, at intervals of about 6 months by comparison with the reference standards of resistance, using a direct reading ratio set, Wheatstone bridge, or double ratio set [15], or the potentiometer method. If it is believed that a resistor has been overloaded, it should be checked against the appropriate reference standard without delay, and if a significant change in value has occurred since the last regular check, the overloaded resistor should be checked at frequent intervals until its resistance again becomes steady.

Most standard resistors are made of manganin. This alloy has the valuable property of showing low thermal electromotive force to copper and of changing relatively little in resistance with change in temperature. The resistance, R_t, at a temperature $t°$ C is related to that, R_{25}, at 25° C by the formula

$$R_t = R_{25}\{1+\alpha(t-25)+\beta(t-25)^2\}.$$

Here the coefficient α is usually less than 10×10^{-6} and β usually lies between -3×10^{-7} and -6×10^{-7}.

4.3. Capacitors and Inductors

Each laboratory should compare all of its working standards with its reference standards once a year, and also immediately after an interlaboratory group has been calibrated at NBS. Working standards that are used frequently, or upon which great dependence is placed, may be compared with the laboratory reference standards whenever an important series of plant calibrations is undertaken.

4.4. Volt Boxes

A small laboratory may find it sufficient to use its reference volt box as a working standard also. This can be checked initially and at intervals of 2 years at NBS. It is well to measure and record the resistance of each section of each volt box initially, and monthly thereafter, as a means for detecting possible changes such as might be caused by inadvertently overloading one of the lower-voltage ranges. More often other working-standard volt boxes will be used as auxiliaries to potentiometers for the calibration of both working-standard indicating instruments and shop instruments. These can be compared monthly with the reference-standard volt box by a null method [16].

4.5. Indicating Instruments

Direct-current and alternating-current ammeters, voltmeters, and wattmeters of either the 0.1-percent or the 0.25-percent class [17] will be needed for the range of current, voltage, and power over which the shop instruments used in the plant are to be checked. The a-c instruments must be of the electrodynamic, electrostatic, or electrothermal (thermocouple) types, which can be used on direct as well as on alternating current [6, 8, 18]. The usual a-c instrument of the moving-iron type is not suitable as a transfer standard. The working-standard indicating instruments can be submitted to NBS for an initial test, and the a-c instruments for the additional determination, on appropriate ranges, of the ac-dc difference by comparison with a transfer instrument. This ac-dc difference test should cover the full range of frequency over which the instrument is likely to be used. After this initial test, they can be retained in the laboratory and checked in terms of a standard cell and standard resistor, using a potentiomenter. Preferably, the frequency of these checks ranges from 2 weeks to 2 months, depending upon the frequency of use of the working standards and their reliability as indicated by earlier check tests. Direct-current working-standard indicating instruments, when built into a console, usually have terminals so arranged that the instrument and its range-extending resistors can be checked by using a potentiometer and a bridge. Alternating-current instruments may have to be checked by comparison with interlaboratory standard instruments of a multirange type.

4.6. Watthour Meters

Laboratories that have occasion to test large numbers of watthour meters, as do those of power companies, are best guided by the Electrical Metermen's Handbook [1]. This book was prepared by a committee of experienced meter engineers for the instruction of meter-laboratory personnel.

If the laboratory has occasion to test watthour meters only rarely, it is sufficient to have available an electrodynamic wattmeter of suitable range and a standard of time accurate to the degree needed in the energy measurement. The wattmeter can be calibrated by using direct current and a potentiometer, and then used to hold a known constant power while the revolutions of the watthour meter are timed.

In intermediate cases it may be desirable to install a group of three working-standard watthour meters. These can be calibrated as indicated in the preceding paragraph, and each can be used to check a number of other meters. To minimize friction they should be used without register mechanisms but with photoelectric pickups. The complete but time-consuming calibration against the wattmeter need be made only at intervals of a month or so, provided quick intercomparisons among the three working-standard meters shows no relative change in their rates. Provision can be made by means of suitable precision current transformers so that the standard meter can be operated always at about its full-load speed, even when the meter under test is at light load.

4.7. Instrument Transformers

Many laboratories will need a set of multirange current and voltage transformers covering the range of current and voltage over which other shop transformers are to be calibrated. An initial calibration at NBS, using the burden of the standard circuit of the transformer testing set (plus ammeter or voltmeter), can be made at 60 cycles per second. The errors of current transformers in general are smaller at higher frequencies, but the initial tests should include tests at 400 or 800 cycles per second if the transformer is to be used at such frequencies. Subsequent tests at NBS need be made only at intervals of 5, or even 10, years.

5. Comparison Apparatus

The term "comparison apparatus" includes equipment by means of which the calibration of a shop instrument or standard is checked by comparing it with an appropriate working standard of the laboratory. In many cases the working standard is substituted for the device under test in the same circuit of the comparison equipment, and the change in its indication is taken as the measure of their difference. Such substitution methods are in general capable of very high accuracy, and should be used wherever practicable.

In other cases a working standard is in effect built in as part of the comparison equipment. Examples of the latter are (1) the working standard indicating instrument built into an instrument testing console and (2) the rheostat arm of a Wheatstone bridge when used directly (as contrasted with its use by substitution).

5.1. Consoles

These devices, containing appropriate sources, adjusting transformers and rheostats, and panel instruments for approximate adjustment, will provide the circuits for the comparison of shop indicating and recording instruments with working-standard instruments [19, 20]. In some types of console the working-standard instruments and their auxiliary range-extending apparatus also are permanently built into the equipment [20]. If suitable special terminals are available, these working standards can be calibrated like portable standards. If not, some secondary procedure must be set up by which the console in effect tests other working standards that have previously been checked over the full range. The console can be shipped direct from the manufacturer to the laboratory. The person in charge of calibration work at the laboratory can then satisfy himself, by appropriate measurements of insulation resistance and of circuit resistance, that the connections are correct and that the leakage and lead resistance are not such as to introduce errors. In general, these particular hazards are less if the leads can be run directly in the open between the working standard and the instrument under test.

The working-standard indicating instruments are sometimes mounted at an angle of 45° for greater convenience in reading. This arrangement, however, tends to introduce additional pivot friction. Care must also be taken to insure that no ferromagnetic material is located near enough to either the instrument under test or the standard instrument to affect its calibration. Even nonmagnetic metal supports can cause trouble by providing eddy-current circuits which can affect unshielded a-c instruments. Stray magnetic fields from supply transformers and rheostats (particularly those wound on enameled steel tubes) must be eliminated. The familiarity that the supervisor will obtain by carrying on this acceptance test forms an essential part of his training for the job. His success in it can be verified adequately by the use of a group of indicating instruments as interlaboratory standards in annual tests. The local checks of insulation and of lead resistance should be repeated every 6 months.

5.2. Direct-Current Bridges, Direct-Reading Ratio Sets, Universal Ratio Sets, Direct-Current Potentiometers

These can be tested initially at NBS and in most cases need only to be resubmitted at intervals of 3 years. During the interim, local checks can be made at intervals of 6 months by using the bridge or ratio set to measure or compare interlaboratory-standard resistors. A potentiometer can be given a rough check at least annually at one point by using it to measure a standard cell of known emf or, alternatively, by using a single cell first as the standard by which to adjust the potentiometer current and then as the unknown to be measured.

5.3. Lindeck Potentiometer

Any laboratory will find very useful a combination of a standard resistor and milliammeter (of the 0.25% class) to use as a low-range Lindeck potentiometer for the purpose of intercomparing the various standard cells in the laboratory by measuring the differences between them in pairs. The resistor and milliammeter can then be checked on the same schedule as the working-standard resistors and the working-standard instruments, respectively [12, 21, 22]. Care must be taken to minimize thermal emf in such a circuit.

5.4. Voltage-Calibrating Transformers

The ratios of the voltages of the various tapped sections of the secondary winding to the voltage of the tertiary winding to which the standard voltmeter is connected can be determined initially at each operating frequency. This should be done with no load and with rated load on the secondary while the standard voltmeter, or an impedance duplicating it, is connected to the tertiary. Subsequent tests need be made only at intervals of 5 or even 10 years.

5.5. Instrument-Transformer Test Sets

The instrument-transformer test sets can easily be checked annually at the 100-percent point and also at one other point.[3] These checks can be supplemented by using the test set and working-standard instrument transformer to measure once a year the ratio and phase angle of an interlaboratory-standard instrument transformer of the same range, which is checked at NBS every 5 years. These test sets are currently available for use at 60 and 25 cycles per second only. Radical modifications in procedure or in component values are required if they are to be used at other frequencies.

6. Interlaboratory Standards

Interlaboratory standards in general are similar in nature and inherent accuracy to reference standards and working standards. The smaller laboratories may well use some of their reference standards to serve as interlaboratory standards also. These should, so far as possible, be of rugged construction to minimize damage and change of value in shipment. On this account they usually are standards of fixed value rather than continuously adjustable devices.

[3] Simple methods for such one-point checks on instrument-transformer test sets are now being developed at the National Bureau of Standards.

The function of an interlaboratory standard is to transmit some one of the electrical units of measurement from a laboratory of higher echelon, such as the NBS, to the local laboratory. It is sent systematically to NBS for a calibration and is compared before and after this operation with the appropriate reference standard of the local laboratory. In those cases in which a large organization maintains a plurality of separate standardizing laboratories under its authority, a single set of interlaboratory standards may profitably be circulated to give a "round-robin test" by being sent to 3 or 4 of the company's laboratories in succession between trips to NBS. Such a program provides a check both on the comparison apparatus and on the operating competence of the personnel at the various laboratories. It also performs the function of maintaining the assigned values of the reference standards of each laboratory in concordance with NBS standards.

6.1. Shipment

Electrical measuring instruments such as ammeters, voltmeters, wattmeters, and watthour meters contain extremely delicate jewels and pivots, upon which the operation of each instrument depends. These delicate parts must be carefully protected from mechanical shocks and jars during shipment. Sensitive instruments will not arrive in satisfactory operating condition unless great care is taken in packing. Every effort is made to handle and to repack these instruments carefully at the Bureau, and whenever possible the return shipment is made in the original container.

Before each instrument is packed, all binding posts should be tightened, and any externally operated clamping device for the moving system should be switched to the "clamp" or "transit" position. Plugs and other small accessories should be enclosed in a small separate container tied to the instrument. Glass windows of instruments lacking protective cases should be protected by pieces of thin wood or heavy cardboard before wrapping. Each instrument should then be wrapped in heavy manila paper or similar covering and sealed with gummed tape to exclude dust and excelsior.

Boxes in which instruments are packed should be strong, preferably of wood, with screwed-on tops to avoid damage to pivots or jewels, which may be caused by a hammer or nail puller.

Clean, fresh excelsior or its equivalent in special packaging material should be used as the shock-absorbing material. A layer of excelsior at least 3 to 4 inches deep, pressed down firmly, should surround each wrapped instrument. Instruments having pivoted components should be packed upside down.

High-grade pivoted instruments of the laboratory-standard type, which have comparatively heavy moving systems without clamping devices, should be packed with special care and should always be individually shipped in wooden boxes with 4 to 6 inches of excelsior around the wrapped instrument. Portable standard watthour meters (rotating standards) should also be individually packed.

Certain heavy accessories used with instruments, such as ammeter shunts, current transformers, and voltage (potential) transformers, should be packed in separate boxes to avoid possible damage to the instruments. Heavy pieces should always be shipped in wooden boxes and held in place, if necessary, by checks or cleats. Large transformers, especially those having oil-filled iron cases, should be crated singly, and arranged whenever possible so that the terminals can be made accessible for tests without removing the entire crate.

The tops of boxes and crates must be marked "This Side Up." Boxes containing delicate instruments should be marked "Fragile, Handle With Care." Those containing any glass parts should be marked "Glass." Failure to use such markings precludes recourse in the event of loss or damage in shipping.

6.2. Standard Cells

A laboratory having reference-standard cells of the saturated type would logically provide itself with a group of about three saturated standard cells which can be sent to the NBS annually, while the reference cells are new, but biennially thereafter. Cells of this type must be kept upright at all times and protected as far as possible from shock and temperature changes. This necessitates hand carrying and arrangements at each end for installing them in a thermostatted bath [11, 12]. Smaller laboratories having unsaturated reference standards may use 2 or 3 unsaturated cadmium standard cells as interlaboratory standards. These can be shipped by parcel post. Shipments in extremely cold or hot weather should be avoided. If each interlaboratory cell is compared with the cells of the laboratory reference group before and after their transport to NBS, a very desirable check is obtained on any changes that may have occurred during transport. If any one cell shows the same value relative to the local group, before and after its travels, it is highly probable that its emf did not change and recover by an equal amount. If all cells are unchanged, the probability of the comparison being valid is greatly increased.

6.3. Resistors, Capacitors, and Inductors

Fixed standard resistors, capacitors, and inductors, whether of the fixed-unit type or groups of these combined in dial-type boxes, are satisfactory as interlaboratory standards and can be used at intervals of 1 to 2 years for comparison with NBS, depending on the stability of the reference standards that they serve. Intercomparison between the laboratories of a single organization at intervals of 1 year may prove useful in cases where the volume of testing at the individual laboratories is large and the working standards at these laboratories are therefore un-

usually liable to deterioration or accidental damage. The values of the interlaboratory standards of this group should be such as to cover the range of measurements with which the laboratory is concerned.

6.4. Instrument Transformers

Standard multirange current and voltage transformers can be obtained which are of quite rugged construction and give reliable performance for long periods of time. For a small laboratory, a single set of such transformers covering the complete range may be tested initially at NBS and resubmitted at intervals of 5 or even 10 years for verification. A larger laboratory in which the program of transformer testing cannot be interrupted will need a duplicate set of standard-instrument transformers, one set being used as interlaboratory standards at intervals of 5 years, while it and the other set both serve as working standards the rest of the time.

6.5. Indicating Instruments

The use of indicating instruments as interlaboratory standards is often of great value as an over-all check on the comparison equipment and on personnel and procedures. On the other hand, in general, the actual transport of the units of measurement from a higher to a lower echelon is done more accurately by standard cells and resistors. The transfer of the electrical units from d-c to a-c standards is based on the initial tests at NBS [23] of suitable 0.1-percent or 0.25-percent wattmeters, ammeters, and voltmeters. It may be found desirable, as a guard against accidental changes, to verify the performance of the transfer standards by comparing them with similar interlaboratory standards at 5-year intervals. A group of multirange a-c instruments may be used as interlaboratory standards to check the over-all accuracy of the a-c working standards built permanently into some types of consoles.

7. Summary

In the foregoing sections, some of the basic principles on which the operations of an electrical standardizing laboratory should be based have been listed; the types of standard equipment needed have been classified; and the intervals at which these pieces of equipment should be intercompared locally and checked by comparison with a laboratory of higher echelon have been suggested.

The most important considerations in such an enterprise are:

(1) The leader must have a high degree of technical knowledge and competence in the specialized field of electrical measurements;

(2) The measuring apparatus must be adequate and chosen specifically to fit the kinds of measurement and level of accuracy demanded;

(3) The checking procedures must be definite and followed carefully, but should be flexible enough to meet emergencies;

(4) The laboratory must accept responsibility for the internal consistency of its measurements, and should look to a higher echelon (such as NBS) only for its initial calibration and for periodic checks to detect drifts in the values of its reference standards.

8. References

[1] The meter laboratory, Electrical metermen's handbook, 6th ed., chap. 12 (Edison Electric Inst., New York, N. Y., 1950).

[2] American standard code for electricity meters, Am. Standards Assoc. C12–1941 (Edison Electric Inst., New York, N. Y.)

[3] H. N. Hayward, The calibration, checking and testing of electrical instruments in an education laboratory, Eighth Natl. Conf. Instr. Soc. Amer., paper 53–2–2 (1953).

[4] F. B. Silsbee, Establishment and maintenance of the electrical units, NBS Circ. 475 (1949).

[5] F. B. Silsbee, Extension and dissemination of the electrical and magnetic units, NBS Circ. 531 (1952).

[6] F. L. Hermach, The testing of electrical instruments, Eighth Natl. Conf. Instr. Soc. Amer., paper 53–2–3 (1953).

[7] F. D. Weaver, Notes on the care and use of electrical instruments, Instruments **23,** 1236–1239 (1950).

[8] F. K. Harris, Electrical measurements (John Wiley & Sons, Inc., New York, N. Y., 1952).

[9] F. A. Laws, Electrical measurements (McGraw-Hill Book Co., Inc., New York, N. Y., 1938).

[10] J. B. Dowden, Organizing an electrical instrument standardizing laboratory, Weston Engineering Notes **2,** 6 (June 1947); **4,** 3 (Feb. 1949).

[11] E. F. Mueller and H. F. Stimson, A temperature-control box for saturated standard cells, J. Research NBS **13,** 699 (1934) RP739.

[12] A. W. Spinks and F. L. Hermach, Portable potentiometer and thermostatted container for standard cells, Rev. Sci. Instr. **26,** 770 (1955).

[13] J. H. Park, Effect of service temperature conditions on the electromotive force of unsaturated portable standard cells, BS J. Research **10,** 89 (1933) RP518.

[14] G. W. Vinal, Primary batteries, chap. 6, Standard cells (John Wiley & Sons, Inc., New York, N. Y., 1950).

[15] J. L. Thomas, Precision resistors and their measurement, NBS Circ. 470 (1948).

[16] F. B. Silsbee and F. J. Gross, Testing and performance of volt boxes, J. Research NBS **27,** 269 (1941) RP1419.

[17] American standard, Electrical indicating instruments, ASA C39.1–1955 (American Standards Association, New York, N. Y.).

[18] F. L. Hermach and E. S. Williams, Multirange audio-frequency thermocouple instruments of high accuracy, J. Research NBS **52,** 227 (1954) RP2494.

[19] F. D. Weaver, An easily assembled console for rapid testing of electrical indicating instruments, Instruments **22,** 396–399 (1949).

[20] E. A. Gilbert, Equipment for instrument calibration, Elec. Eng. **68,** 1065 (1949).

[21] H. B. Brooks, The standard cell comparator, a specialized potentiometer, BS J. Research **11,** 211 (1933) RP586.

[22] J. H. Miller, Simplified standard cell comparator, Weston Engineering Notes **9,** 1 (Dec. 1954); Trans. Am. Inst. Elec. Engrs. **73,** (Pt. 1), 413 (1954).

[23] J. H. Park and A. B. Lewis, Standard electrodynamic wattmeter and ac-dc transfer instrument, J. Research NBS **25,** 545 (1940) RP1344.

[24] S. C. Richardson and F. A. Ludewig, A solution to the problem of electrical instrument standardization service, First Intern. Conf. Instr. Soc. Amer., paper 54–21–2 (1954).

Washington, May 10, 1956.

FRANK D. WEAVER
Low Frequency Calibration Services
National Bureau of Standards
Boulder Laboratories

ACHIEVEMENT OF MEASUREMENT AGREEMENT AMONG ELECTRICAL STANDARDS LABORATORIES

Trained measurement personnel with a determination and a planned program, good equipment, and good laboratories can achieve near measurement agreement with the National Bureau of Standards over a period of years. Details are given whereby the NBS Electronic Calibration Center, Boulder, Colorado, established and maintains the low-frequency units and achieves measurement agreement with NBS, Washington. Other laboratories can follow this precedent.

A STANDARD is a suitable device (physical embodiment) for accurately maintaining a unit of measurement and for transferring a unit of resistance, capacitance, inductance, current or emf, or a measurement of ratio, from one laboratory to another.

A number of standards and measuring equipments, such as resistors, saturated cells, capacitors, inductors, and bridges, must be obtained when setting up facilities for a low-frequency calibration program. An important consideration in the selection of such equipment is the specification of characteristics that one would like embodied in a good standard suitable for transferring a unit from one laboratory to another.

Some of the characteristics are:

1. Ruggedness
2. Simplicity in construction and use
3. Stability (short term and long term repeatability)
4. Accuracy (close to nominal value)
5. Portability
6. Insensitiveness to changes in environmental conditions, temperature, pressure, humidity, sunlight, vibration, position, capacitance, magnetic material, etc.
7. Readability
8. Low voltage or current coefficient
9. Reasonable price.

There are likely no standards that fulfill all these requirements. The Thomas-type resistor probably comes most nearly to approaching the ideal. On the other hand, the emf of the saturated cell is affected by nearly all environmental conditions and, therefore, the cells must be kept under carefully-controlled ambient conditions.

A number of things can be done to improve the quality of standards. Recently, manufacturers have taken some steps in this direction. For example, one manufacturer builds a capacitor enclosed in a temperature-controlled air bath. Another places the resistors in his Wheatstone bridge in a temperature-controlled oil bath, and in so doing raises his quoted accuracy by a factor of two. Other manufacturers build resistors of improved resistance material having low temperature coefficients, long-term stability, and actual values within a few ppm of nominal.

The accuracy to which a standard may be calibrated depends on the quality of the standard. There is no point in attempting to calibrate a resistor having an accuracy rating of 0.1% to an accuracy of 0.0001% because a measurement 10 minutes later may show an entirely different value. In order to improve accuracy, laboratories must be provided with better standards—for example, resistors having an accuracy rating of 0.01% rather than an accuracy rating of 0.05%. In addition, they must have more accurate bridges for comparison and must be provided with better-trained measurement personnel. There is no object in hiring an inexperienced and untrained person for a laboratory and placing a Thomas-type resistor and a Wenner Bridge at his disposal. Such a person would not know what to do with either piece of equipment. Yet, with the same type of resistor and bridge in the hands of

trained personnel in a good laboratory, comparison measurements to one part in ten million can be obtained.

Traceability Concept

Efforts to improve the accuracy of standards and measurements have lead to the concept of *traceability*. This concept implies knowledge of the value of a standard through either direct or indirect measurements, with reference to the unit maintained as a National Standard by the Bureau. It should also imply the capability of making accurate measurements. As a result of the misuse of the idea of traceability, NBS is called upon to calibrate and issue Certificates on an unnecessarily large number of standards. In many instances it is believed that the corrections reported on the Certificate are not applied by the user to the nominal value of the standard. The Certificate too often is hidden in a file to be made available upon request to prove traceability. Certificates issued on this basis result in a waste of NBS time and effort, and a waste of the user's money.

Methods of Achieving Equality

The procedure whereby the Electronic Calibration Center (ECC) of the Radio Standards Laboratory of NBS, Boulder, achieved equality with NBS, Washington, has an important lesson for all standards labs.

The Electronic Calibration Center began operation in late 1957. The establishment of this facility grew out of the needs of the Department of Defense and of industry for additional calibration service covering the frequency spectrum from dc through microwaves, at a convenient location. In the Low-Frequency (dc-30kc) Unit of the Center, services are provided for the calibration of electrical standards and instruments such as standard cells, standard resistors and resistance apparatus, standard inductors and capacitors, volt boxes and other d-c ratio devices, standard resistors for current measurements, electrical instruments, inductive voltage dividers, and instrument transformers.

The Electronic Calibration Center started issuing Certificates on low-frequency standards in 1958. Last year about 3000 low-frequency standards were calibrated and certificates issued. The measurements on which Certificates are issued are determined from intercomparison with high-quality working standards. Periodically the working groups at both Boulder and Washington are calibrated by comparison with the National Reference Group. The main purpose of the reference group of resistors and cells is for maintaining the units of resistance and voltage.

The *ohm* is maintained at NBS Washington by a group of Thomas-Type resistors. These are referred to as *national reference standards of resistance*. The *volt* is maintained by a number of saturated standard cells. These are referred to as *national reference standards of voltage*. The Center has, at the present time, working standards of resistance and voltage

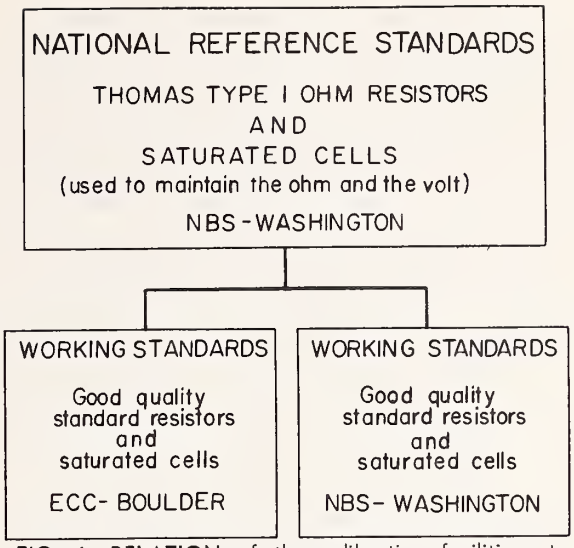

FIG. 1. RELATION of the calibration facilities at NBS-Washington and ECC-Boulder.

that have been assigned values by comparison with the national reference standards. Fig. 1 shows the relation of the calibration facilities at the two laboratories, for resistance and voltage, to the national reference standards.

Laboratory standards sent to either location for calibration are compared with working standards, and are not ordinarily directly compared with the national reference standards. The working standards are of equal quality and reliability whether they are across the hall from the reference standards in Washington, D. C., or seventeen hundred miles away in Boulder, Colorado.

In 1957 it was believed that within a few years it would be possible to establish the ohm and the volt at the Electronic Calibration Center with the highest precision and that the units would, if a carefully planned inter-comparison program was followed, approach closely the value of the volt and the ohm maintained at Washington. There were no plans for establishing the units at the Center by the long and tedious process involved in the absolute determination of the volt and the ohm. Instead, by using the best of standards and techniques with many intercomparisons over a period, possibly five years, the same goal could be achieved. Evidence indicates that this objective has been approached closely, and that practically identical calibration accuracies have been achieved at the two locations.

The laboratory wishing to obtain the best possible calibrations on its electrical standards, resistors, capacitors, inductors, bridges, etc., may have these standards calibrated in either Washington or Boulder on the basis of convenience.

Resistance Standards

Several methods are used to be sure that the measurement accuracies in the two laboratories, Boulder and Washington, are equivalent. The present working group for resistance measurements includes five Thomas-type resistors. Each year three of these, after being measured in Boulder, are hand-carried to NBS Washington, for comparison with the nation-

Abstracts from paper presented at ISA Conference, Los Angeles, September, 1961.

al reference standards. To date there has been little change in the value of the Boulder Thomas-type resistors. As indicated in Table 1, the maximum change over four years in any one resistor is 1.2 ppm, and the minimum about 0.4 ppm. In the most recent intercomparison (April 1961) two of the three resistors showed no change from a year ago in parts in ten million; the other showed a change of 1 part in ten million.

TABLE 1—ECC THOMAS-TYPE RESISTORS

Resistor No.	Corrections (ppm)				
	Febr 1957	June 1958	April 1959	April 1960	April 1961
149	+3.1	+2.8*	+2.4*	+1.9*	+2.3*
148	+8.1	+7.7	+7.3	+7.3	+7.3
147	+7.1	+7.0	+6.6	+6.7	+6.8
146	+5.1	+5.2*	+4.8*	+4.7*	+5.0*
145	+2.1	+2.4*	+2.1	+2.1	+2.1

*Indicates Boulder calibrations

TABLE 2—COMPARISON OF WASHINGTON AND BOULDER CALIBRATIONS—

(Step-Up and Step-Down from the Thomas 1-Ohm Resistors).

Nominal Resistance ohms	Corrections (ppm)	
	Washington April 1961	Boulder June 1961
100000	− 7	− 10
100000	+ 16	+ 14
10000	− 22	− 21
10000	− 25	− 24
1000	− 25	− 26
1000	+ 40	+ 40
100	− 6	− 6
100	− 29	− 29
10	− 7	− 7
10	− 3	− 3
0.1	− 9	− 10
0.1	− 24	− 26
0.01	+ 8	+ 5
0.01	+ 11	+ 10
0.001	+ 11	+ 11
0.001	0	0
0.0001	+145	+145
0.0001	+ 8	+ 9

In addition to the Thomas-type resistors, the Center also sends yearly to Washington two of each other nominal values from 0.0001 ohm to 100,000 ohms. This enables ECC personnel to check all working standards by two methods with the Wenner bridge, by (1) the direct comparison method and by (2) step-up or step-down procedures from the one ohm. Table 2 shows close agreement in this step-up and step-down procedure.

When the resistors are returned to the Center after intercomparison in NBS Washington, the new values of resistance for the three Thomas-type resistors are used to calibrate the other one-ohm resistors by direct comparison. Two of the Thomas-type resistors then are used to step-up to the two 10-ohm resistors for which recent Washington values are available. If the values (Washington value and ECC step-up value) for these 10-ohm resistors agree within 1 ppm, then they are used to calibrate the other 10-ohm resistors and also to step-up to the two recently calibrated 100-ohm resistors.

If differences between the Washington value and the Boulder step-up value exceed about 1 to 2 ppm, depending on nominal value, additional comparisons are made with other resistors in an effort to resolve the disagreement. Sometimes values for past measurements are useful in resolving such differences. This procedure continues up through the 100,000-ohm value and down to the 0.0001-ohm resistors.

The records show that the expected differences between the Washington values and the ECC values at the 1-ohm level should be less than 1 ppm. At nominal values other than one ohm, the uncertainty may amount to N ppm; where N is the number of decades removed from the one-ohm level. At a value of 100,000 ohms we would be concerned if the difference exceeded about 4 ppm.

The Center frequently receives resistors from other laboratories that were previously calibrated in Washington. The Washington data on resistors have been made available to ECC personnel. This has provided an opportunity to make a large number of intercomparisons with good quality resistors over the past three years. Table 3 indicates close agreement. Large differences probably indicate a change in the resistor itself rather than imprecision in the measurements. The table indicates, in general, that the resistance of a good resistor changes very little (a few ppm) from one year to another. With all this information, considerable confidence has been built up in the ECC ohm to the point where it is believed to be within a few parts per ten million of the ohm maintained in Washington.

TABLE 3—CORRECTIONS FOR SOME RESISTORS CALIBRATED IN WASHINGTON AND CALIBRATED IN BOULDER APPROXIMATELY A YEAR LATER.

Nominal Resistance (ohms)	Date of Calibration		Corrections (ppm)	
	Washington	Boulder	Washington	Boulder
100000	Jan 60	Mar 61	+33	+27
10000	Jan 60	Mar 61	−25	−24
10000	Jan 58	Sep 59	−29	−28
10000	Jul 57	Jul 58	+52	+54
1000	Jun 59	Jul 60	+22	+23
1000	Jan 58	Sep 59	− 2	+ 1
1000	Jul 57	Jul 58	+12	+12
100	Nov 59	Jun 60	−10	−15
100	Nov 59	Nov 60	+22	+ 9
100	Jan 58	Sep 59	+ 6	+ 6
100	Jul 57	Jul 58	−15	−17
10	Sep 59	Sep 60	−89	−91
10	Jan 58	Sep 59	+ 4	+ 2
10	Jul 57	Jul 58	−74	−77
1	Apr 58	Jul 59	−58	−59
1	Feb 58	Apr 59	−64	−67
1	Sep 59	Sep 60	−80	−80
1*	Oct 58	Nov 59	+24.9	+26
1*	Oct 58	Jan 60	+22	+23
1*	Jun 59	Aug 60	− 3	− 3.4
1*	Jun 59	Sep 60	− 5	− 5.3
1*	Mar 58	Nov. 59	+12.1	+13.0
0.1	Jul 57	Aug 58	+367	+359
0.1	Nov 57	Apr 58	− 18	− 33
0.1	Mar 58	Mar 59	− 6	− 12
0.01	Jul 58	Jul 59	− 24	− 18
0.01	Feb 58	Mar 59	− 2	− 2
0.01	Jul 57	Jul 58	+550	+549
0.001	May 57	Jul 58	+508	+507
0.0001	Dec 59	Jul 60	−137	−149

*Denotes Thomas-type 1-ohm resistors.

Voltage Standards

To establish the volt in Boulder the low-frequency unit started with eighteen saturated cells, three groups of six each, with each group in an air bath. It was evident in 1958 that the Center would be called upon to calibrate saturated cells. This meant increased accuracy and the need for placing ECC cells in an oil bath for better temperature control. Two oil baths were designed and constructed; one to regulate at 28°C and the other to regulate at 35°C. Of the original eighteen cells only nine turned out to be stable enough to use as a working group. Later, additional cells were obtained. The Center has a group of six that now appear stable enough to add to the working group, making a total of fifteen. This group is never moved. Six cells are used as a traveling group and hand-carried to Washington and returned for intercomparison purposes. It now appears that the volt, as maintained at the ECC, is within about 0.6 microvolt of the volt maintained at NBS Washington, as shown in Table 4. This gap will be closed to possibly 0.2 microvolt with a little more history on ECC cells. An additional period of a year or so may be required to achieve this goal.

TABLE 4—COMPARISON OF CALIBRATIONS ON SIX SATURATED CELLS

Position Number	Washington Value Jan 1961 (volts)	Boulder Value Mar 1961 (volts)	Difference microvolt
1	1.0182250	1.0182259	+0.9
2	1.0182222	1.0182229	+0.7
3	1.0182492	1.0182494	+0.2
4	1.0182501	1.0182507	+0.6
5	1.0182462	1.0182467	+0.5
6	1.0182478	1.0182485	+0.7
Mean	1.0182401	1.0182407	+0.6

In helping to establish a volt, some laboratories have been thoughtful enough to have their cells delivered to the Center after calibration in Washington and prior to their return to their own laboratory. This enables additional intercomparisons to be made.

Volt boxes have been used as an intercomparison device by the Electronic Calibration Center and Washington to assure measurement agreement. Table 5 shows the results of a number of intercomparisons on a volt box.

TABLE 5—RATIO COMPARISONS (CORRECTIONS, PPM) FOR A VOLT BOX.

Voltage Range	Washington Aug 58	Boulder Aug 58	Washington Jun 60	Boulder Jul 60
3	+ 4	+ 6	0	+ 6
7.5	+ 19	+ 25	+ 21	+ 26
15	+ 34	+ 38	+ 32	+ 38
30	+ 20	+ 24	+ 23	+ 32
75	− 85	− 79	− 78	− 74
150	−120	−112	−114	−118
300	−175	−152	−158	−161
750	− 96	− 86	− 82	− 86

The data, in ppm, show close measurement agreement in d-v ratio as determined at NBS Washington and Boulder.

Capacitance and Inductance

In the area of *capacitance* and *inductance* the Center has three standards of each nominal value that manufacturers ordinarily make. One standard of each of the nominal values is sent to Washington each year for intercomparison purposes.

Other interlaboratory standards such as inductive voltage dividers, current and potential transformers, standard resistors for current measurement, voltmeters and a-c transfer standards are periodically shipped between the two laboratories and calibrated for intercomparison purposes. In addition to giving information about the stability of standards that have been transported by the usual means of public transportation, repeatability of measured values on these items gives us additional assurance of measurement agreement.

Conclusion

With the system of intercomparison described above it appears that close measurement agreement has been achieved between the two laboratories. The achievement of the Electronic Calibration Center in this area can be closely approached by another laboratory. Some laboratories already have long history of comparisons on their standards by NBS. It would seem that another laboratory, in a period of a few years, could establish a volt and ohm that closely approaches the value of the volt and ohm maintained at NBS.

Another standards laboratory with well-trained personnel having a determination to make the best measurements and working with high quality standards and facilities can achieve near measurement equality with the National Bureau of Standards. To do this their Thomas-type resistors should have annual comparisons with the national working standards, and their saturated cells should be intercompared by a traveling group annually with the national working standard cells. The time can be foreseen when a number of laboratories will reach this objective.

What Is the Best Calibration Interval?

Some items may require NBS certification once per year; and others at less-frequent intervals. The calibration by NBS each year of every standard in a laboratory generally is not necessary. The calibration interval for a given type of standard depends upon a number of factors, but experience indicates the recommended period for some items to be as much as 5 years. Furthermore, NBS should not be called upon to calibrate standards that the laboratory can do with sufficient accuracy. With only a few selected calibrated standards as a nucleus, it is sometimes possible to calibrate a wide range of other standards by step-up and intercomparison techniques.

It may be advisable to consider the use of the service of a commercial organization. A number of commercial testing laboratories have adequate facilities for calibrating many of the standards associated with the usual standards laboratory.

Minimum requirements should be established by some national organization to guide laboratories seeking to establish traceability.

(Pre-Printed from *Instruments & Control Systems*, 1962)

August
1966

U. S. DEPARTMENT OF COMMERCE
NATIONAL BUREAU OF STANDARDS
Washington, D. C.

List of
Publications
LP 38

ELECTRICAL UNITS, INSTRUMENTS, AND MEASUREMENTS

Publications by the Members of the Staff of
The National Bureau of Standards

CONTENTS

1. Introduction

This list of publications is a selection which describes the methods and equipment used in the establishment and maintenance of the electrical units and the standards that have been developed at the National Bureau of Standards for the calibration of measuring apparatus. It includes references to older publications of the Bureau which describe basic principles and methods and are therefore still useful. References to articles on electrical measurements at radio and higher frequencies are not included.

Many inquiries sent to this Bureau can best be answered by reference to a recognized national standard, or by reference to a particular textbook or handbook. Accordingly a few such standards and books are listed that include the information on instruments and measurements most frequently requested.

This Bureau makes no tests on motors, generators, or transformers used for power or lighting service, and has no current publications on their design or performance. It cannot undertake to answer questions concerning the design, construction, repair, or rewinding of such apparatus. A number of pertinent references are listed in a folder, "Electric Motors and Generators, Basic Information Sources," available on request from the Office of Publications, Department of Commerce, Washington, D. C. 20230.

Some of the publications by Bureau authors have appeared in the regular series of publications of this Bureau, and others in various scientific and technical journals. Reprints of some of the more recent papers may be available upon request from the authors. Where the price is stated Government publications can be purchased from the Superintendent of Documents, U. S. Government Printing Office, Washington, D. C., 20402. Remittances should be made either by coupons (obtainable from the Superintendent of Documents in sets of 20 for $1.00 and good until used), or by check or money order payable to the "Superintendent of Documents, U. S. Government Printing Office" and sent with the order. Publications may be consulted in leading libraries.

2. Library of Congress Photoduplication Service

The Photoduplication Service, Library of Congress, Washington, D. C. 20540, makes photoduplicates of material in its collections for research use. National Bureau of Standards publications are on file at the Library, so that a copy of any Bureau document that is out of print can usually be obtained. Full information concerning this service may be secured by writing to the Library of Congress at the address noted above. In making such inquiry, it is important to give an accurate and complete identification (author, title, place of publication, name of the series and number, if known) of the document desired.

3. General Information

3.1 Periodicals of the National Bureau of Standards

Journal of Research

The Journal of Research reports National Bureau of Standards research and development in physics, mathematics, chemistry, and engineering. Comprehensive scientific papers give complete details of the work, including laboratory data, experimental procedures, and theoretical and mathematical analyses. Illustrated with photographs, drawings, and charts.

All NBS nonperiodical publications and articles by the Bureau staff in professional journals will be abstracted in the appropriate section of the Journal. In addition, each section will carry a complete listing of all Bureau publications that are not abstracted in that section.

Three sections . . . . . .

A. PHYSICS AND CHEMISTRY

Papers of interest primarily to scientists working in these fields. This section will cover a broad range of physical and chemical research, with major emphasis on standards of physical measurement, fundamental constants, and properties of matter. Issued six times a year. Annual subscription: Domestic, $5.00; Foreign, $6.00

B. MATHEMATICAL SCIENCES

Studies and compilations designed mainly for the mathematician and theoretical physicist. Topics in mathematical statistics, theory of experiment design, numerical analysis, theoretical physics and chemistry, logical design and programming of computers and computer systems. Short numerical tables. Issued quarterly. Annual

subscription: Domestic, $2.75; Foreign, $3.50.

C. ENGINEERING AND INSTRUMENTATION

Reporting results of interest chiefly to the engineer and the applied scientist. This section will include many of the new developments in instrumentation resulting from the Bureau's work in physical measurement, data processing, and development of test methods. It will also cover some of the work in acoustics, applied mechanics, building research, and cryogenic engineering. Issued quarterly. Annual subscription: Domestic, $2.75; Foreign, $3.50.

Technical News Bulletin

Summaries of current research at the National Bureau of Standards are published each month in the Technical News Bulletin. The articles are brief, with emphasis on the results of research, chosen on the basis of their scientific or technologic importance. Lists of all Bureau publications during the preceding month are given, including Research Papers, Handbooks, Applied Mathematics Series, Building Materials and Structures Reports, Miscellaneous Publications, and Circulars. Each issue contains 12 or more two-column pages; illustrated. Annual subscription: Domestic, $1.50; Foreign, $2.25.

All NBS periodicals issued by the Bureau may be obtained by purchase on an annual subscription basis from the Superintendent of Documents, U. S. Government Printing Office, Washington, D. C. 20402.

3.2 Catalogs of National Bureau of Standards Publications

National Bureau of Standards Circular 460 and its supplement list all Bureau publications issued from 1901 through June 30, 1957. Brief abstracts for the publications issued after January 1, 1942 are included. Copies of these catalogs may be obtained from the Superintendent of Documents, U. S. Government Printing Office, Washington, D. C. 20402, as follows:

Circular 460, publications issued 1901 through June 30, 1947, (375 pages), ($1.25).

Supplement I to Circular 460, publications issued July 1, 1947 through June 30, 1957 (373 pages), ($1.50).

Miscellaneous Publication 240, publications issued July 1, 1957 through June 30, 1960, (391 pages), ($2.25).

Supplement to Miscellaneous Publication 240, publications issued July 1, 1960 through February 26, 1965.

3.3 Field Offices of the U. S. Department of Commerce

Department of Commerce Field Offices are maintained in the cities listed below. Their purpose is to provide ready access, at the local level, to the Department's reports, publications, statistical statements, surveys, as well as to the specialized and experienced staff in charge. Each Field Office serves as an official sales agent of the Superintendent of Documents, U. S. Government Printing Office, making available for purchase locally a wide range of Government publications. The reference library maintained by each Field Office contains many Government and private publications, periodicals, directories, reports, and other reference material.

For additional information concerning available publications consult the Field Office in your area.

LIST OF FIELD OFFICES

Albuquerque, New Mexico 87101
U. S. Courthouse
William E. Dwyer, Director
Area Code 505 Tel. 247-0311

Anchorage, Alaska 99501
306 Loussac-Sogn Building
Clyde S. Courtnage, Director
Area Code 907 Tel. 272-6331

Atlanta, Georgia 30303
4th Floor, Home Savings Building
75 Forsyth Street, N. W.
Daniel M. Paul, Director
Area Code 404 Tel. 526-6000

Baltimore, Maryland 21202
305 U. S. Customhouse
Gay and Lombard Streets
Carroll F. Hopkins, Director
Area Code 301 Tel. Plaza 2-8460

Birmingham, Alabama 35203
505 Title Building, 2030 Third Avenue, North
Gayle C. Shelton, Jr., Director
Area Code 205 Tel. 325-3131

Boston, Massachusetts 02110
Room 230, 80 Federal Street
Paul G. Carney, Director
Area Code 617 Tel. CA 3-2312

Buffalo, New York 14203
504 Federal Building
117 Ellicott Street
Robert F. Magee, Director
Area Code 716 Tel. 842-3208

Charleston, South Carolina 29403
Federal Building - Suite 631
334 Meeting Street
Paul Quattlebaum, Jr., Director
Area Code 803 Tel. 747-4171

Charleston, West Virginia 25301
3002 New Federal Office Building
500 Quarrier Street
J. Raymond DePaulo, Director
Area Code 304 Tel. 343-6196

Cheyenne, Wyoming 82001
6022 Federal Building
2120 Capitol Avenue
Albert B. Kahn, Director
Area Code 307 Tel. 634-5920

Chicago, Illinois 60604
1486 New Federal Building
219 South Dearborn Street
Anthony J. Buchar, Director
Area Code 312 Tel. 828-4400

Cincinnati, Ohio 45202
8028 Federal Office Building
550 Main Street
Robert M. Luckey, Director
Area Code 513 Tel. 684-2944

Cleveland, Ohio 44101
4th Floor, Federal Reserve Bank Building
East 6th Street and Superior Avenue
Charles B. Stebbins, Director
Area Code 216 Tel. 241-7900

Dallas, Texas 75202
Room 1200, 1114 Commerce Street
Harry C. Meyers, Director
Area Code 214 Tel. RIverside 9-3287

Denver, Colorado 80202
16407 Federal Building
20th and Stout Streets
Charles E. Brokaw, Director
Area Code 303 Tel. 297-3246

Des Moines, Iowa 50309
1216 Paramount Building
509 Grand Avenue
Raymond E. Eveland, Director
Area Code 515 Tel. 284-4222

Detroit, Michigan 48226
445 Federal Building
Frank A. Alter, Director
Area Code 313 Tel. 226-6088

Greensboro, North Carolina 27402
412 U. S. Post Office Building
Joel B. New, Director
Area Code 919 Tel. 275-9111

Hartford, Connecticut 06103
18 Asylum Street
James E. Kelley, Director
Area Code 203 Tel. 244-3530

Honolulu, Hawaii 96813
202 International Savings Building
1022 Bethel Street
H. Tucker Gratz, Director
Tel. 588977

Houston, Texas 77002
5102 Federal Building
515 Rusk Avenue
Edward T. Fecteau, Jr., Director
Area Code 713 Tel. 228-0611

Jacksonville, Florida 32202
512 Greenleaf Building
208 Laura Street
William B. Curry, Director
Area Code 305 Tel. 354-7111

Kansas City, Missouri 64106
Room 2011, 911 Walnut Street
Nathan L. Stein, Director
Area Code 816 Tel. BA 1-7000

Los Angeles, California 90015
Room 450, Western Pacific Building
1031 South Broadway
Stanley K. Crook, Director
Area Code 213 Tel. 688-2833

Memphis, Tennessee 38103
345 Federal Office Building
167 North Main Street
John M. Fowler, Director
Area Code 901 Tel. 534-3214

Miami, Florida 33130
928 Federal Office Building
51 S. W. First Avenue
Marion A. Leonard, Director
Area Code 305 Tel. 350-5267

Milwaukee, Wisconsin 53203
Straus Building
238 West Wisconsin Avenue
David F. Howe, Director
Area Code 414 Tel. BR 2-8600

Minneapolis, Minnesota 55401
306 Federal Building
110 South Fourth Street
Ernest G. Booth, Director
Area Code 612 Tel. 334-2133

New Orleans, Louisiana 70130
909 Federal Office Building, South
610 South Street
Edwin A. Leland, Jr., Director
Area Code 504 Tel. 527-6546

New York, New York 10001
61st Floor, Empire State Building
350 Fifth Avenue
Arthur C. Rutzen, Director
Area Code 212 Tel. Longacre 3-3377

Philadelphia, Pennsylvania 19107
Jefferson Building
1015 Chestnut Street
David Jamieson, Director
Area Code 215 Tel. 597-2850

Phoenix, Arizona 85025
5413 New Federal Building
230 North First Avenue
Donald W. Fry, Director
Area Code 602 Tel. 261-3285

Pittsburgh, Pennsylvania 15222
2201 Federal Building
1000 Liberty Avenue
John A. Donely, Director
Area Code 412 Tel. 644-2850

Portland, Oregon 97204
217 Old U. S. Courthouse
520 S. W. Morrison Street
James W. Goodsell, Director
Area Code 503 Tel. 226-3361

Reno, Nevada 89502
2028 Federal Building
300 Booth Street
Jack M. Howell, Director
Area Code 702 Tel. 784-5203

Richmond, Virginia 23240
2105 Federal Building
400 North 8th Street
William S. Parker, Director
Area Code 703 Tel. 649-3611

St. Louis, Missouri 63103
2511 Federal Building
1520 Market Street
Alfred L. Rascher, Jr., Director
Area Code 314 Tel. MA 2-4243

Salt Lake City, Utah 84111
3235 Federal Building
125 South State Street
Stephen P. Smoot, Director
Area Code 801 Tel. 524-5116

San Francisco, California 94102
Federal Building, Box 36013
450 Golden Gate Avenue
Philip M. Creighton, Director
Area Code 415 Tel. 556-5864

Santurce, Puerto Rico 0097
Room 628, 605 Condado Avenue
John H. Shoaf, Director
Phone: 723-4640

Savannah, Georgia 31402
235 U. S. Courthouse and
Post Office Building
125-29 Bull Street
Joseph G. Stovall, Director
Area Code 912 Tel. 232-4321

Seattle, Washington 98104
809 Federal Office Building
909 First Avenue
William H. Flood, Director
Area Code 206 Tel. 583-5615

4. Units and Absolute Electrical Measurements

1. A Determination of the Absolute Ohm, Using an Improved Self Inductor, H. L. Curtis, C. Moon, and C. M. Sparks, J. Research NBS 21, 375, (1938), RP 1137.

2. An Absolute Determination of the Ampere, Using Helical and Spiral Coils, R. W. Curtis, R. L. Driscoll, and C. L. Critchfield, J. Research NBS 28, 133, (1942), RP 1449.

3. Review of Recent Absolute Determinations of the Ohm and the Ampere, H. L. Curtis, J. Research NBS 33, 235, (1944), RP 1606.

4. An Absolute Measurement of Resistance by the Wenner Method, J. L. Thomas, C. Peterson, I. L. Cooter, and F. R. Kotter, J. Research NBS 43, 291, (1949), RP 2029.

5. Establishment and Maintenance of the Electrical Units, F. B. Silsbee, NBS Circular 475, 38 p., (1949), 35 cents.

6. Measurement of the Proton Moment in Absolute Units, H. A. Thomas, R. L. Driscoll, and J. A. Hipple, J. Research NBS 44, 569, (1950), RP 2104.

7. A New Method for Determining the Value of the Faraday, D. N. Craig and J. I. Hoffman, Phys. Rev. 80, No. 3, 487, (1950).

8. Standards for Electrical Measurement, F. B. Silsbee, Physics Today 4, 19, (1951).

9. Measure for Measure: Some Problems and Paradoxes of Precision, F. B. Silsbee, J. Washington Academy of Sciences 41, No. 7, 213, (1951).

10. Fundamental Units and Standards, F. B. Silsbee, Instruments 26, 1520 (1953).

11. Extension and Dissemination of the Electrical and Magnetic Units by the National Bureau of Standards, F. B. Silsbee, NBS Circular 531, 33 p., (1952).

12. Electrochemical Constant, NBS Circular 524 (1953), $2.00
    This circular includes:
    a) Standard Cells and the Unit of Electromotive Force, W. J. Hamer and L. H. Brickwedde, P. R. Robb, pp. 103 - 118.
    b) Determination of the Faraday Constant by the Electrolytic Oxidation of Oxalate Ions, D. N. Craig, and J. I. Hoffman, pp. 13 - 20.
    c) The Faraday and the Omegatron, H. Sommer and J. A. Hiple, pp. 21 - 26.

13. Nuclear Magnetic Resonance and the Measurement of Magnetic Fields, R. L. Driscoll, Natl. Phys. Lab. Symp. of Precision Electrical Measurements, (1955).

14. Measurement of Current with a Pellat-Type Electrodynamometer, R. L. Driscoll, J. Research NBS 60, 287, (1958), RP 2845.

15. Measurement of Current with the National Bureau of Standards Current Balance, R. L. Driscoll and R. D. Cutkosky, J. Research NBS 60 297, (1958) RP 2846.

16. New Apparatus at the National Bureau of Standards for Absolute Capacitance Measurement, M. C. McGregor, J. F. Hersh, R. D. Cutkosky, F. K. Harris, and F. R. Kotter, IRE Trans. Instrumentation, I-7, No. 3-4, 253, (Dec. 1958).

17. A Free Precession Determination of the Proton Gyromagnetic Ratio, P. L. Bender and R. L. Driscoll, IRE Trans. Instrumentation, I-7, No. 3-4, 176 (Dec. 1958).

18. The Ampere, F. B. Silsbee, Proc. IRE 47, No. 5, 643, (May, 1959).

19. Simplification of Systems of Units, F. B. Silsbee, AAAS Symposium, 1959.

20. Some Results on the Cross Capacitances Per Unit Length of Cylindrical Three-Terminal Capacitors With Thin Dielectric Films on Their Electrodes, D. G. Lampard and R. D. Cutkosky, Inst. Elec. Engs. (London) Mono. No. 351M, January 1960.

21. Determination of the Value of the Faraday With a Silver-Perchloric Acid Coulometer, D. Norman Craig, C. A. Law, J. I. Hoffman, and W. J. Hamer, J. Research NBS 64A5, 381, (1960).

22. Refining Measurements by Capacitance Techniques, F. K. Harris, R. D. Cutkosky, ISA Journal, (1961).

23. An Evaluation of the NBS Unit of Resistance Based on a Computable Capacitor, R. D. Cutkosky, J. Research NBS 65A, No. 3, 97, (1961).

24. The Systems of Electrical Units, F. B. Silsbee, J. Research NBS 66C, No. 2, 137, (1962).

25. Four Terminal Pair Networks as Precision Admittance and Impedance Standards, R. D. Cutkosky, IEEE Trans. Paper 63-928, (1963).

26. A New Type of Computable Inductor, Chester H. Page, J. Research NBS 67B, No. 1, (1963).

27. Definition of "Ampere" and "Magnetic Constant", Chester H. Page, Proc. of the IEEE, Vol. 53, No. 1, 1965.

28. The Value of the Faraday, W. J. Hamer and D. N. Craig, J. Electrochem. Soc., III, No. 12, (Dec. 1964).

5. Standard Cells
(see Section 9 also)

1. Effect of Service Temperature Conditions on the Electromotive Force of Unsaturated Portable Standard Cells, J. H. Park, J. Research NBS 10 89, (1933), RP 518.

2. Standard Cells and the Unit of Electromotive Force, W. J. Hamer, L. H. Brickwedde, and P. R. Robb, NBS Circular 524, p. 103 - 118, (1953).

3. A Temperature-Control Box for Saturated Standard Cells, E. F. Mueller and H. F. Stimson, J. Research NBS 13, 699, (1934), RP 739.

4. Standards of Electromotive Force, G. W. Vinal, D. N. Craig, and L. H. Brickwedde, Trans. Electrochem. Soc. 68, 139, (1935).

5. Metastability of Cadmium Sulfate and its Effect on Electromotive Force of Saturated Standard Cells, G. W. Vinal and L. H. Brickwedde, J. Research NBS 26, 455 (1941), RP 1389.

6. Standard Cells and the Change From International to Absolute Electrical Units, G. W. Vinal, J. Electrochem. Soc. 93, 95, (1948).

7. New Quartz Container for Standard Cells at the National Bureau of Standards, G. W. Vinal, L. H. Brickwedde, and W. J. Hamer, Compt. Rendu., Sept. 5 - 10, 92, (1949).

8. Controlled Temperature Oil Baths for Saturated Standard Cells, Patrick H. Lowrie, Jr., NBS Tech. Note 141, (1962).

9. Effect of Vibration and Shock on Unsaturated Standard Cells, R. J. Brodd, W. G. Eicke, J. Research NBS 66C, No. 2, 85, (1962).

10. Comments on Zener Diodes as Voltage Standards, W. G. Eicke, Jr., Comite Consultatif, D'Electricite Aupres, Du "Comite Internationale Des Poids et Mesures," 10th Session 'les, (1963).

11. Making Precision Voltage Measurements on Zener Diodes, W. G. Eicke, Jr., IEEE Trans. Paper CP 63-416, (1963).

12. The Operating Characteristics of Zener Reference Diodes and Their Measurements, W. G. Eicke, Jr., ISA Trans., 3, No. 2 (April 1964).

13. Standards of Electromotive Force, W. J. Hamer, J. Washington Academy of Sciences, 54, (Oct. 1964).

14. Standard Cells, Their Construction, Maintenance, and Characteristics, W. J. Hamer, NBS Mono. 84, (Jan. 1965), 35 cents.

15. On the Long-Term Stability of Zener Reference Diodes, W. G. Eicke, Jr. and H. H. Ellis, Proc. of the 11th Session, Comite Consultatif D'Electricite, (May 1965).

16. The "Volt Standard" Moves to Gaithersburg, Maryland, W. J. Hamer, J. Washington Academy of Sciences, 56, pp. 101 - 108, (1966).

6. Resistors

1. The Four-Terminal Conductor and the Thomson Bridge, F. Wenner, Bul. BS 8, 559, (1912), S181.

2. Adjustments of the Thomson Bridge in the Measurement of Very Low Resistances, F. Wenner and E. Weibel, Bul. BS 11, 65, (1915) S22.

3. A Study of the Inductance of Four-Terminal Resistance Standards, F. B. Silsbee, Bul. BS 13, 375, (1916-17), S281.

4. Notes on the Design of Four-Terminal Resistance Standards for Alternating Currents, F. B. Silsbee, BS J. Research 4, 73, (1930), RP 133.

5. A Method of Adjusting the Temperature Coefficient and Resistance of Low-Valued Resistance Standards, F. Wenner and J. L. Thomas, J. Research 12, 147, (1934), RP 639.

6. Methods, Apparatus, and Procedures for the Comparison of Precision Standard Resistors, F. Wenner, J. Research NBS 25, 229, (1940), RP 1323.

7. Stability of Double-Walled Manganin Resistors, J. L. Thomas, J. Research NBS 36, 107, (1946), RP 1692.

8. Precision Resistors and Their Measurement, J. L. Thomas, NBS Circular 470, 32 p. (1948), 30 cents.

9. Best Arrangement of Resistors in a Series Group, H. B. Brooks, Rev. Sci. Instr. 21, No. 5, 491, (1950).

10. Measurement of Multimegohm Resistors, A. H. Scott, J. Research NBS 50, 147, (1953), RP 2402.

11. Alloys For Precision Resistors, C. Peterson, Natl. Phys. Lab. Symp. of Precision Electrical Measurements, (1955).

12. Rack for Standard Resistors, P. H. Lowrie, Jr., Rev. Sci. Instr. 30, 291 - 292, (April 1959).

13. A Method of Controlling the Effects of Resistance in the Link Circuit of the Thomson or Kelvin Double Bridge, D. Ramaley, J. Research NBS 64 C4, 267, (1960).

14. Calibration Procedures for D-C Resistance Apparatus, P. B. Brooks, NBS Mono. 39, (1962), 40 cents.

315-411 O - 68 - 5

15. Errors in the Series-Parallel Buildup of Four-Terminal Resistors, Chester H. Page, J. of Research, Vol. 69C, No. 3, July-Sept. 1965.

7. Inductors
(See Section 4 also)

1. Design of Standards of Inductance, and the Proposed Use of Models in the Design of Air-Core and Iron-Core Reactors, H. B. Brooks, J. Research NBS 7, 289, (1931), RP 342.

2. Improved Continuously Variable Self and Mutual Inductor, H. B. Brooks and A. B. Lewis, J. Research NBS 19, 493, (1937), RP 1040.

3. Formulas for Computing Capacitance and Inductance, C. Snow, NBS Circular 544, 64 p. (1954).

4. A Study of Absolute Standards of Mutual Inductance and in Particular the Three-Section National Bureau of Standards Type, F. W. Grover, J. Research NBS 53, 297, (1954), RP 2548.

5. Methods for Measuring the Q of Large Reactors, C. Peterson, B. L. Dunfee, and F. L. Hermach, Am. Inst. Elec. Engrs. Trans. Paper 56-87, (1956).

6. Inductive Efficiency of Reactive Coils, H. B. Brooks, Elec. Engr., (1956).

7. Calibration of Inductance Standards in the Maxwell-Wien Bridge Circuit, T. L. Zapf, J. Research NBS 65C No. 3, 183, (1961).

8. Capacitors
(See Section 4 also)

1. Measurement of Relative and True Power Factors of Air Capacitors, A. V. Astin, J. Research NBS 21, 425, (1938), RP 1138.

2. Nature of Energy Losses in Air Capacitors at Low Frequencies, A. V. Astin, J. Research NBS 22, 673, (1939), RP 1212.

3. Standards for Low Values of Direct Capacitance, C. Moon and C. M. Sparks, J. Research NBS 41, 497, (1948), RP 1935.

4. A Standard of Small Capacitance, C. Snow, J. Research NBS 42, 287, (1949), RP 1970.

5. Formulas for Computing Capacitance and Inductance, C. Snow, NBS Circular 544, 69 p., (1954).

6. Variable Capacitor Calibration with an Inductive Voltage Divider Bridge, T. L. Zapf, NBS Tech. Note 57 (PB 161558) $1.60. (Available only by purchase from the Office of Technical Services, Department of Commerce, Washington, D. C. 20230).

7. Capacitor Calibration by Step-Up Methods, T. L. Zapf, J. Research NBS 64C, 75, (1960).

8. New Apparatus at the National Bureau of Standards for Absolute Capacitance Measurement, M. C. McGregor, J. F. Hersh, R. D. Cutkosky, F. K. Harris, and F. R. Kotter, IRE Trans. Instrumentation, I-7, No. 3-4, 253, (Dec. 1958).

9. The Construction and Behavior of a Transportable Ten Picofarad Capacitor, R. D. Cutkosky, L. H. Lee, Comite Consultatif, D'Electricity Aupres, Du "Comite Internationale Des Poids et Mesures," 10th Session 'les (1963).

9. Potentiometers, Volt Boxes, and Bridges

1. Deflection Potentiometers for Current and Voltage Measurements, H. B. Brooks, Bul. BS 8, 395, (1912), S172.

2. A Multi-Range Potentiometer and its Application to the Measurement of Small Temperature Differences, H. B. Brooks and A. W. Spinks, BS J. Research 9, 781, (1932), RP 506.

3. The Standard-Cell Comparator, A Specialized Potentiometer, H. B. Brooks, J. Research 11, 211, (1933), RP 586.

4. The Waidner-Wolff and Other Adjustable Electrical-Resistance Elements, E. F. Mueller and F. Wenner, J. Research NBS 15, 477, (1935) RP 842.

5. Les Potentiometres, H. B. Brooks, Cong. Ind. d'Elec. (Paris), 3, 275, (1932).

6. Testing and Performance of Volt Boxes, F. B. Silsbee and F. J. Gross, J. Research NBS 27, 269, (1941), RP 1419.

7. Portable Potentiometer and Thermostatted Container for Standard Cells, A. W. Spinks and F. L. Hermach, Rev. Sci. Instr. 26, No. 8, 770, (1955).

8. Lindeck Potentiometer, D. W. Oliver, Rev. Sci. Instr. 26, No. 11, 1078, (1955).

9. An A-C Kelvin Bridge for the Audio Frequency Range, B. L. Dunfee, Am. Inst. Elec. Engrs. Trans. Paper 56-25, (1956).

10. The Use of an A-C Bridge to Measure Core Loss at High Inductions, I. L. Cooter and W. P. Harris, Am. Inst. Elec. Engrs. Trans. Paper 56-26, (1956).

11. A Low-Cost Microvolt Potentiometer, W. H. Wood, Rev. Sci. Instr. 28, No. 3, 202, (1957).

12. Method for Calibrating a Standard Volt Box, Bernadine L. Dunfee, J. Research 67C. No. 1, (1963).

13. Practical Methods for Calibration of Potentiometers, D. Ramaley, NBS Tech. Note 172, (1963), 30 cents.

14. A Method for Comparing Two Nearly Equal Potentials Directly in Parts Per Million, C. J. Saunders, Rev. Sci. Instr. 34, (12), 1452, (1963).

15. A Method for Calibrating Volt Boxes, With an Analysis of Volt-Box Self-Heating Characteristics, R. F. Dziuba and T. M. Souders, IEEE Conv. Record, March 1966.

Calibration Procedures
(Copies available at NBS, Resistance and Reactance Section)

1. Notes on the Calibration of the Direct Reading Ratio Set.
2. Calibration of the Wenner Low Range Potentiometer.
3. Calibration of the Mueller Thermometer Bridge.
4. Calibration of the Universal Ratio Set.
5. The Six-Dial Thermofree Potentiometer.

10. Instruments, Meters, and AC-DC Transfer Standards

1. Accuracy of Commercial Electrical Measurements, H. B. Brooks, Trans. Am. Inst. Elec. Engrs. 39, 495, (1920).

2. A Suppressed-Zero Electrodynamic Voltmeter, F. K. Harris, J. Research NBS 3, 445, (1929), RP 105.

3. Composite-Coil Electrodynamic Instruments, F. B. Silsbee, J. Research NBS 8, 217, (1932), RP 411.

4. Temperature Compensation of Millivoltmeters, H. B. Brooks, J. Research NBS 17, (1936), RP 926.

5. Standard Electrodynamic Wattmeter and AC-DC Transfer Instrument, J. H. Park and A. B. Lewis, J. Research 25, 545, (1940), RP 1344.

6. Performance of Portable Electrical Instruments in Magnetic Fields, A. E. Peterson, Trans. Am. Inst. Elec. Engrs. 67, 1228, (1948).

7. An Easily Assembled Console for Rapid Testing of Electrical Indicating Instruments, F. D. Weaver, Instruments 22, 396, (1949).

8. Notes on the Care and Use of Electrical Instruments, F. D. Weaver, Instruments 23, No. 12, 1236, (1950).

9. Thermal Converters as AC-DC Transfer Standards for Current and Voltage Measurements at Audio Frequencies, F. L. Hermach, J. Research NBS 48, 121, (1952), RP 2296.

10. A-C Measurements to 10,000 cps, F. D. Weaver, Instruments 25, No. 6, 757, (1952).

11. The Testing of Electrical Instruments, F. L. Hermach, Proc. Instr. Soc. Am. 8, 18, (1953).

12. Testing Electrical Instruments, F. D. Weaver, Instruments 26, No. 9, 1362, (1953).

13. Lead Resistance Errors in Watthour Meter Tests, F. L. Hermach and T. L. Zapf, Elec. World 141, No. 16, 113 (1954).

14. Multirange, Audiofrequency Thermocouple Instruments of High Accuracy, F. L. Hermach and E. S. Williams, J. Research NBS 52, 227, (1954), RP 2494.

15. Precise Comparison Method of Testing Alternating-Current Watthour Meters, A. W. Spinks, and T. L. Zapf, J. Research NBS 53, 95, (1954), RP 2521.

16. Scale and Reading Errors of Electrical Indicators, F. D. Weaver, Instr. and Automation 27, No. 11, (Nov. 1954).

17. Power Supplies for 60-Cycle Tests of Electrical Instruments and Meters, F. L. Hermach, Proc. Instr. Soc. Am. 11, Paper No. 56-21-3, (1956).

18. AC-DC Transfer Instruments for Current and Voltage Measurements, F. L. Hermach, IRE Trans. Instrumentation, I-8, 235, (1958).

19. The Definition and Measurement of the Time Constant and Response Time of Thermal Converters, F. L. Hermach, Trans. Am. Inst. Elec. Engrs. 77, 277, (1958).

20. A Wide Range Volt-Ampere Converter for Current and Voltage Measurements, F. L. Hermach and E. S. Williams, Communications and Electronics, Trans. Am. Inst. Elec. Engrs. Paper 59-161, (1959).

21. Thermal Voltage Converters for Accurate Voltage Measurements to 30 Megacycles, F. L. Hermach and E. S. Williams, Trans. Am. Inst. Elec. Engrs. Paper 60-135, (1960).

22. An Analysis of Errors in the Calibration of Electrical Instruments, F. L. Hermach, AIEE Trans. Paper 61-63, (1960).

23. A Differential Thermocouple Voltmeter, F. L. Hermach and J. E. Griffin, AIEE Trans. Paper 62-819, (1962).

24. The Calibration of Volt-Ampere Converters, E. S. Williams, NBS Tech. Note 188, (1963), 20 cents.

25. Practical Aspects of the Use of AC-DC Transfer Instruments, E. S. Williams, NBS Tech. Note 257,(March 9, 1965), 15 cents.

26. A System for Accurate Direct and Alternating Voltage Measurements, F. L. Hermach, J. E. Griffin, E. S. Williams, IEEE Transactions on Instrumentation and Measurements, Vol. IM-14, No. 4, Dec. 1965.

27. Calibration of Peak A-C to D-C Comparators, Donald Flach and L. A. Marzetta, ISA Preprint No. 14.2, March 1965.

28. Thermal Converters as AC-DC Transfer Standards for the Measurement of Alternating Current and Voltage, F. L. Hermach, Proc. of the 11th Session of the International Committee of Weights and Measures - Advisory Committee on Electricity, May 1965.

29. Thermal Converters for Audio Frequency Voltage Measurements, F. L. Hermach and E. S. Williams, IEEE Trans. on Instrumentation Measurements, 1966.

30. A Comparator for Thermal AC-DC Transfer Standards, R. S. Turgel, ISA Convention Record, Fall 1966.

11. Transformers and Inductive Voltage Dividers

1. A Method for Testing Current Transformers, F. B. Silsbee, Bul. BS 14, 317, (1918-19), S309.

2. Lead Resistance for Current Transformers, F. B. Silsbee, Elec. World, 81, 1082, (1923).

3. Methods for Testing Current Transformers, F. B. Silsbee, Trans. Am. Inst. Elec. Engrs., 43, 282, (1924).

4. A Shielded Resistor for Voltage Transformer Testing, F. B. Silsbee, BS Sci. Paper 20, 489, (1924-26), S516.

5. Equipment for Testing Current Transformers, F. B. Silsbee, R. L. Smith, N. L. Forman, and J. H. Park, BS J. Research 11, 93, (1933), RP 580.

6. Accuracy of High-Range Current Transformers, J. H. Park, NBS J. Research 14, 367, (1935), RP 775.

7. Information for the Amateur Designer of Transformer for 25- to 60-Cycle Circuits, H. B. Brooks, NBS Circular 408, 25 pages, (1935).

8. Effect of Wave Form Upon the Performance of Current Transformers, J. H. Park, NBS J. Research 19, 517, (1937), RP 1041.

9. Measurement of Voltage Ratio at Audio Frequencies, W. C. Sze, Trans. Am. Inst. Elec. Engrs., Paper 57-648, (1957).

10. A Standard Transformer and Calibration Method - A Basis for Establishing Ratios of Currents at Audio Frequencies, B. L. Dunfee, IRE Trans. Instrumentation I-9, (1960).

11. The Precision Measurement of Transformer Ratios, R. D. Cutkosky and J. Q. Shields, IRE Trans. Instrrumentation I-9, (1960).

12. Voltage Ratio Measurements With A Transformer Capacitance Bridge, T. L. Zapf, J. Research NBS 66C, No. 1, 25, (1962).

13. The Calibration of Inductive Voltage Dividers and Analysis of their Operational Characteristics, T. L. Zapf, ISA Trans. 2, No. 3, (1963).

14. An International Comparison of Inductive Voltage Divider Calibrations at 400 and 1000 Hz, W. C. Sze, A. F. Dunn and T. L. Zapf, IEEE Trans. on Instr. and Meas., Vol. IM-14, No. 3, Sept. 1965.

15. Comparators for Voltage Transformer Calibrations at NBS, W. C. Sze, J. Research NBS, Vol. 69C, No. 4, Oct. - Dec. 1965.

16. An International Comparison of Current Ratio Standards at Audio Frequencies, B. L. Dunfee and W. J. M. Moore, IEEE Trans. on Inst. and Meas., Vol. IM-14, No. 4, Dec. 1965.

17. The Design and Performance of Multirange Current Transformer Standards for Audio Frequencies, B. L. Dunfee, IEEE Trans. on Inst. and Meas., Vol. IM-14, No. 4, Dec. 1965.

12. Galvanometers

1. General Design of Critically Damped Galvanometers, F. Wenner, Bul. BS 13, 211, (1916-17), S273.

2. A New Form of Vibration Galvanometer, P. G. Agnew, BS Sci. Paper 16, 37, (1920), S370.

3. Sensitivity of a Galvanometer as a Function of its Resistance, H. B. Brooks, J. Research NBS 4, 297, (1930), RP 150.

4. Galvanometer Efficiency as a Design Parameter, F. K. Harris, Trans. Am. Inst. Elec. Engrs. 56-60, (1956).

13. High-Voltage and Surge Measurements

1. An Experimental Study of the Corona Voltmeter, H. B. Brooks and F. M. Defandorf, J. Research NBS 1, 589, (1928), RP 21.

2. Calculations of Electrical Surge-Generator Circuits, A. B. Lewis, J. Research NBS 17, 585, (1936), RP 929.

3. An Absolute Electrometer for the Measurement of High Alternating Voltages, H. B. Brooks, F. M. Defandorf, and F. B. Silsbee, J. Research NBS 20, 253, (1938), RP 1078.

4. A Transformer Method for Measuring High Alternating Voltages and its Comparison with an Absolute Electrometer, F. B. Silsbee and F. M. Defandorf, J. Research NBS 20, 317, (1938), RP 1079.

5. Shunts and Inductors for Surge-Current Measurements, J. H. Park, J. Research NBS 39, 191, (1947), RP 1823.

6. The Measurement of High Voltage, F. M. Defandorf, J. Wash. Acad. Sci. 38, No. 2, 33, (1948).

7. A Fifty-Fold Momentary Beam Intensification for a High Voltage Cold-Cathode Oscillograph, J. H. Park, J. Research NBS 47, 87, (1951), RP 2231.

8. Puncture Tests on Porcelain Distribution Insulators Using Steep-Front Voltage Surges, J. H. Park and H. N. Cones, AIEE Paper 53-257, June 1953.

9. Surge Voltage Breakdown of Air in a Non-Uniform Field, J. H. Park and H. N. Cones, J. Research NBS 56, 201, (1956), RP 2669.

10. High Voltage Pulse Generator and Tests on an Improved Deflecting System of a Cold-Cathode Oscillograph, H. N. Cones, J. Research NBS 57, 143, (1956), RP 2704.

11. Surge Measurement Errors Introduced by Coaxial Cables, J. H. Park, AIEE Paper 58-110, February 1958.

12. Special Shielded Resistor for High-Voltage D-C Measurements, J. H. Park, J. Research NBS Paper 66C1-83; page 19, (1962).

13. Spark-Gap Flashover Measurements for Steeply Rising Voltage Impulses, J. H. Park, H. N. Cones, J. Research NBS Paper 66C3-96, page 197, (1962).

14. An Experimental 350 kv, 1 Picofarad Air Capacitor, Alvin Peterson, IEEE Trans. Paper No. 63-926, (1963).

15. Some Impulse Sparkover Voltages for a 200 cm Sphere Gap, H. N. Cones, IEEE Conf. Paper No. 63-929, (1963).

16. An International Comparison of Voltage Transformer Calibration to 350 kv, Wilbur Sze, Forest K. Harris, N. L. Kuster, O. I. Petersons, W. J. M. Moore, IEEE Trans. Paper No. 63-992, (1963).

14. Dielectric Measurements
(see also Section 8)

1. Edge Correction in the Determination of Dielectric Constant, A. H. Scott and H. L. Curtis, J. Research NBS 22, 747, (1939), RP 1217.

2. Dielectric Constant, Power Factor and Conductivity of the System Rubber-Calcium Carbonate, A. H. Scott and A. T. McPherson, J. Research NBS 28, 279, (1942), RP 1457. (Describes measurements by a three-terminal bridge.)

3. Measurements of Dielectric Properties at Temperature up to 500°C, A. H. Scott, P. Ehrlich, and J. F. Richardson, Symp. on Temperature Stability of Electrical Insulating Materials, Am. Soc. Testing Materials Spec. Tech. Publ. No. 161, (1954).

4. Precise Measurements of Dielectric Constant over a Wide Range of Frequencies, and Temperatures, A. H. Scott, Proc. Instr. Soc. Am. 11, Paper No. 56-8-2, (1956).

5. An Ultra Low Frequency Bridge for Dielectric Measurements, D. J. Scheiber, J. Research NBS 65C, 23, (1961).

6. Residual Losses in a Guard-Ring Micrometer-Electrode Holder for Solid-Disk Dielectric Specimens, A. H. Scott and W. P. Harris, J. Research NBS 65C, 101, (1961).

7. Precise Measurement of Dielectric Constant by the Two-Fluid Technique, W. P. Harris and A. H. Scott, CEI Report NRC-NAS, 51, (1962).

8. Standards for Plastics - Standard Tests for Electrical Properties, A. H. Scott, S. P. E. Journal, 1375, (1962).

9. Dielectric Properties of Semicrystalline Polychlorotrifluorethylene, A. H. Scott, D. J. Scheiber, A. J. Curtis, J. I. Lauritzen, Jr., J. D. Hoffman, J. Research 66A, No. 4, 269, (1962).

10. Insulation Resistance Measurements, A. H. Scott, Fourth E. I. Conf., AIEE Paper No. P-137-52, (1962).

15. Magnetic Measurements

1. An Apparatus for Magnetic Testing at Magnetizing Forces Up to 5000 Oersteds, R. L. Sanford and E. G. Bennett, J. Research NBS 23, 415, (1939), RP 1242.

2. Permanent Magnets, R. L. Sanford, NBS Circular 448, 39 p., (1944).

3. A Permeameter for Magnetic Testing at Magnetizing Forces up to 300 Oersteds, R. L. Sanford and P. H. Winter, J. Research NBS 45, 17, (1950), RP 2109.

4. The Use of an AC Bridge to Measure Core Loss at High Inductance, I. L. Cooter and W. P. Harris, Trans. Am. Inst. Elec. Engrs., (1956).

5. Investigation of an Alternating Current Bridge for the Measurement of Core Losses in Ferromagnetic Materials at High Flux Densities, I. L. Cooter and W. P. Harris, J. Research NBS 57,103, (1956), RP 2699.

6. Improved Bridge Method for the Measurement of Core Losses on Ferromagnetic Materials at High Flux Density, W. P. Harris and I. L. Cooter, IRE Natl. Conv. Record, Pt. 5, 217, (1958).

7. A Feedback Amplifier with Negative Output Resistance for Magnetic Measurements, I. L. Cooter and W. P. Harris, IRE Natl. Conv. Record, Pt. 5, 217, (1958).

8. Basic Magnetic Quantities and the Measurement of the Magnetic Properties of Materials, R. L. Sanford, I. L. Cooter, NBS Mono. 47, (1962), 30 cents.

9. Absolute Magnetic Susceptibilities by the Gouy and the Thorpe-Senftle Methods, George A. Candela, IRE Trans. on Instrumentation, I-11, Nos. 3 and 4, (1962).

10. Absolute Magnetic Susceptibilities by the Thorpe-Senftle Method, G. A. Candela and R. E. Mundy, Rev. of Sci. Inst., Vol 32, No. 9, pp. 1056-1057, Sept. 1961.

11. A New Absolute Null Method for the Measurement of Magnetic Susceptibilities in Weak Low-Frequency Fields, Charles T. Zahn, Rev. Sci. Inst. 34, No. 3, 285 - 291 (1963).

12. The Calibration of Permanent Magnet Standards, Irvin L. Cooter, Reprint No. 14.1-3-65, Proc. 20th Annual ISA Conf., Oct. 1965.

16. Miscellaneous

1. Accuracy Tests for Meggers, H. B. Brooks, Elec. World 85, 973, (1925).

2. Precautions Against Stray Magnetic Fields in Measurements with Large Alternating Currents, F. B. Silsbee, Trans. Am. Inst. Elec. Engrs. 48, 1301, (1929).

3. Suggested Practices for Electrical Standardizing Laboratories, F. B. Silsbee, NBS Circular 578, 9 p., (1956), 15 cents.

4. Copper Wire Tables, NBS Handbook 100, February 1966, 50 cents.

5. Measurement of the Resistance-Strain Relation and Poisson's Ratio for Copper Wires, T. E. Wells, Proc. Instr. Soc. Am. 11, (1956).

6. Electrical Measurement in the Core Curriculum, F. R. Kotter, Proc. Am. Inst. Elec. Engrs., Analog & Digital Instrument Conf., (April 1959).

7. Phase Angle Master Standard for 400 cycles per second, J. H. Park and H. N. Cones, J. Research NBS 64C3, 229, (1960).

8. Shielded Coaxial Leads for Low Temperature Electrical Measurements, N. L. Brown and R. N. Barfield, Rev. Sci. Inst. 31, (5), 517, (1960).

9. Achievement of Measurement Agreement Among Electrical Standards Laboratories, F. D. Weaver, Instruments and Control Systems, 36, No. 7, 128, (1963).

10. Method for Comparing Two Nearly Equal Potentials Directly in Parts Per Million, C. J. Saunders, Review of Scientific Instruments, Vol. 34, No. 12, 1452 - 1453, Dec. 1963.

11. Low Frequency Electrical Calibrations at NBS, F. L. Hermach, National Conf. of Standards Laboratories, NBS Misc. Publ. 248, (1962), $1.75.

17. References to Books and Standards on Electrical Instruments and Measurements

The National Bureau of Standards receives frequent inquiries for information on electrical instruments and measurements which is not specifically covered in its publications. To meet the needs of such inquiries a list of books and standards is given below.

17.1 Textbooks (Arranged alphabetically by author's name)

1. Electrical Measurements and Instrumentation, D. Bartholemew, (Allyn & Bacon, Boston, 1963).

2. Principles of Electrical Measurements, H. Buckingham and E. M. Price, (Philosophical Library, New York, New York, 1957).

3. Electrical Measurements, H. L. Curtis, (McGraw-Hill Book Company, New York, New York, 1937).

4. Electrical Measuring Instruments, Drysadle and Jolley - revised by Tagg (John Wiley and Sons, New York, New York, 1952).

5. Industrial Instrumentation, D. P. Eckman, (John Wiley and Sons, New York, New York, 1950).

6. Electrical Measurements and Their Application, E. Frank, (McGraw-Hill Book Company, New York, New York, 1959).

7. Electrical Measurements and Measuring Instruments, E. W. Golding, (Pitman Publishing Company, New York, New York, 1955).

8. Inductance Calculations, F. W. Grover, (D. Van Nostrand & Co., Princeton, New Jersey, 1946).

9. Alternating-Current Bridge Methods, B. Hague, (Pitman Publishing Co., New York, New York, 1957).

10. Instrument Transformers, B. Hague, (Pitman Publishing Co., New York, N. Y., 1936).

11. Structure of Electrolytic Solutions, Edited by W. J. Hamer, Published by John Wiley and Sons, New York, New York, (1959).

12. Electrical Measurements, F. K. Harris, (John Wiley & Sons, New York, N. Y., 1952).

13. Applied Electrical Measurements, I. F. Kinnard, (John Wiley & Sons, New York, New York, 1956).

14. Electrical Measurements, F. A. Laws, (McGraw-Hill Book Company, New York, N. Y., 1938).

15. Electrical Measurements and Their Applications, W. C. Michels, (D. Van Nostrand and Company, Princeton, New Jersey, 1957).

16. Elektrische Messgerate und Einrichtungen, A. Palm (Springer, Berlin, Germany, 1948).

17. Principles of Electronic Instruments, G. R. Partridge, (Prentice Hall, Englewood Cliffs, New Jersey, 1958).

18. Electronic Measurements, F. E. Terman & J. M. Pettit, (McGraw-Hill Book Company, New York, New York, 1952).

19. Elektrische Messgerate und Messverfahren, P. M. Pflier (Springer, Berlin, Germany,1957).

20. Basic Electrical Measurements, M. B. Stout, (Prentice Hall, Englewood Cliffs, New Jersey, 1960).

21. Storage Batteries, 4th Edition, George W. Vinal (John Wiley & Sons, New York, New York, 1955).

17.2 Standards and Handbooks

Standards and Handbooks are frequently revised, and the current edition should always be consulted.

1. American Standard for Electrical Indicating Instruments, (Am. Standards Association, 10 East 40th Street, New York, New York, C39.1) (Supersedes AIEE Standard No. 33).

2. American Standard for Instrument Transformers, (American Standards Association, 10 East 40th Street, New York, New York, C56.13).

3. Code for Electricity Meters, (Edison Electric Institute, New York, New York).

4. Standard Handbook for Electrical Engineers, (McGraw-Hill Book Company, New York, New York).

5. Electrical Metermen's Handbook, (Edison Electric Institute, New York, New York).

6. Master Test Code for Resistance Measurements, (Institute of Electrical & Electronic Engineers, IEEE Publication 118, Supersedes AIEE Publication No. 550).

7. Automatic Digital Voltmeters and Ratio Meters, Part 1 - Direct Current Instruments, (American Standards Association, C39.6).

ADDENDUM

September 1967

Units and Absolute Electrical Measurements

1. Physical entities and mathematical representation, C. H. Page, J. Research NBS 65B, No. 4, 227 (1961).

2. Electrical units, F. K. Harris, ISA 19th Ann. Conf., Preprint 12.1.1.64 (1964).

3. International weights and measures, C. H. Page, ISA 20th Ann. Conf., Preprint 33.3-1-65 (1965).

4. Electrical standards and measurements, I. L. Cooter, B. L. Dunfee, F. K. Harris, W. P. Harris, F. L. Hermach, and C. Peterson, Electro-Technology 79, No. 1, 53 (1967).

Standard Cells

1. Oil baths for saturated standard cells, P. H. Lowrie, Jr., ISA J. 9, No. 12, 47 (1962).

2. The establishment and maintenance of the unit of voltage at the NBS Boulder Laboratories, B. A. Wickoff, ISA 18th Ann. Conf., Preprint 28.2.63 (1963).

3. Designs for surveillance of the volt maintained by a small group of saturated standard cells, W. G. Eicke and J. M. Cameron, NBS TN 430 (1967).

Inductors

1. Some techniques for measuring small mutual inductances, D. N. Homan, J. Research NBS 70C, No. 4, 221 (1966).

Capacitors

1. Active and passive direct-reading ratio sets for the comparison of audio-frequency admittances, R. D. Cutkosky, J. Research NBS 68C, No. 4, 227 (1964).

2. Improved ten-picofarad fused silica dielectric capacitor, R. D. Cutkosky and L. H. Lee, J. Research NBS 69C, No. 3, 173 (1965).

3. Voltage dependence of precision air capacitors, J. Q. Shields, J. Research NBS 69C, No. 4, 265 (1965).

Potentiometers, Volt Boxes, and Bridges

1. Calibration of potentiometers by resistance bridge methods, D. Ramaley, Instr. Control Syst. 37, 106 (1964).

2. Some modifications in methods of calibration of universal ratio sets, D. Ramaley, NBS TN 220 (1964).

3. Human engineering in the design of a console for the comparison of volt boxes, P. H. Lowrie, Jr., ISA J. 12, No. 7, 67 (1965).

4. Console for the rapid and precise comparison of volt boxes, P. H. Lowrie, Jr., J. Research NBS 70C, No. 3, 173 (1966).

5. A versatile ratio instrument for the high ratio comparison of voltage or resistance, A. E. Hess, J. Research NBS 70C, No. 3, 169 (1966).

6. Direct ratio readings from a URS, D. Ramaley and J. F. Shafer, Instr. Control Syst. 39, No. 1, 73 (1966).

Instruments, Meters, and AC-DC Transfer Standards

1. DC differential current meter, E. Niesen, Rev. Sci. Instr. 32, No. 12, 1407 (1961).

2. Voltage ratio detector for millivolt signals, J. R. Houghton, NBS TN 266 (1965).

Transformers and Inductive Voltage Dividers

1. Inductive voltage dividers with calculable relative corrections, T. L. Zapf, C. H. Chinburg, and H. K. Wolf, IEEE Trans. IM-12, No. 2, 80 (1963).

2. Comparison calibration of inductive voltage dividers, R. V. Lisle and T. L. Zapf, ISA Trans. 3, No. 3, 238 (1964).

3. The accurate measurement of voltage ratios of inductive voltage dividers, T. L. Zapf, ACTA IMEKO 3, 317 (1964).

4. Comparator for calibration of inductive voltage dividers from 1 to 10 kHz, W. C. Sze, ISA 21st Ann. Conf., Preprint 12.3.2.66 (1966).

High Voltage and Surge Measurements

1. The design and operation of a high voltage calibration facility, W. W. Scott, Jr., NBS TN 349 (1966).

Dielectric Measurements

1. Two-terminal dielectric measurements up to 6×10^8 Hz, M. G. Broadhurst and A. J. Bur, J. Research NBS 69C, No. 3, 165 (1965).

2. Electrical testing, A. H. Scott, Ency. Chem. Tech. 7, 716 (1965).

3. Low frequency dielectric behavior, W. P. Harris, Proc. Electrical Insulation Conf., IEEE-NEMA (1967).

Miscellaneous

1. A standard for accurate phase-angle measurements at audio frequencies, W. W. Scott, Jr., NBS TN 347 (1966).

2. Low-frequency electrical calibrations at the National Bureau of Standards, F. L. Hermach, ISA 22nd Ann. Conf. (1967).

JOURNAL OF RESEARCH of the National Bureau of Standards—B. Mathematics and Mathematical Physics
Vol. 65B, No. 4, October–December 1961

Physical Entities and Mathematical Representation

Chester H. Page

(August 22, 1961)

Certain basic postulates about physical observables yield the structure of their mathematical representation. Measure equations are contrasted with quantity equations, and measurement units with abstract units. The abstract vector spaces in which observables are represented comprise the core of dimensional analysis.

Systems of equations, units, and dimensions are discussed, along with comments on rationalization. The problem of assigning a dimension to angle is discussed, and a new proposal offered.

NBS Monograph 56
September 1962

Systems of Electrical Units

Francis B. Silsbee

(January 19, 1962)

The various systems of measurement, with their respective sets of units, used in the literature on electricity and magnetism are described in detail. Their historical development is summarized. The manner in which each is derived from either of the two alternative points of view of the experimentalist and the theoretician is compared and contrasted. The desirability of recognizing both points of view in international standardization, particularly when discussing rationalization, is pointed out. The present status of the absolute measurements on which all electrical units are based is reported, and tables are included for the conversion of equations and numerical values from one system to another.

NBS Circular 475
June 1949

Establishment and Maintenance of the Electrical Units

By F. B. Silsbee

Abstract

A history is given of the establishment of the "international" system of electrical units, its operation during the interval 1911 to 1947, inclusive, and of the developments that caused it to be superseded. It includes a record of the international comparisons, which indicated that the units of some countries have at times drifted nearly 0.01 percent from the mean, an account of the maintenance procedures used at the National Bureau of Standards, and brief descriptions of the methods currently available for the absolute measurement of resistance and of current, which will be used in the future as a check on the maintenance of the units.

NBS Circular 531
July 1952

Extension and Dissemination of the Electrical and Magnetic Units by the National Bureau of Standards

By Francis B. Silsbee

Starting with the ohm and the volt as maintained by groups of standard resistors and cells, this paper describes the experimental processes by which the other electric and magnetic units, e. g., farad, henry, ampere, watt, joule, gauss, and oersted are derived. It also describes the series of steps by which the scales of measurement of resistance, direct and alternating current, and voltage are derived experimentally. Brief mention is made of the procedures for the dissemination of these standards of measurement throughout the world by the calibration of standard electrical measuring apparatus. An extensive bibliography lists papers describing the measurement procedures in greater detail and serves as a historical report of the work of the National Bureau of Standards in the field of electrical measurements during its first 50 years.

Journal of Research of the National Bureau of Standards Vol. 60, No. 4, April 1958 Research Paper 2845

Measurement of Current with a Pellat-Type Electrodynamometer

R. L. Driscoll

The value of an electric current has been determined in absolute measure by means of an electrodynamometer, and simultaneously by standard cells and standard resistors as currently maintained. The electrodynamometer used was of the Pellat type, and featured a fused silica balance beam and single layer helical coils.

The relation of the NBS ampere to the absolute ampere, from this determination, may be expressed as

1 NBS ampere = 1.000013 absolute amperes. *

The uncertainty in this result from all known sources is estimated to be eight parts per million.

Journal of Research of the National Bureau of Standards Vol. 60, No. 4, April 1958 Research Paper 2846

Measurement of Current with the National Bureau of Standards Current Balance

R. L. Driscoll and R. D. Cutkosky

Prior to the adjustment of the electrical units in 1948, the value of a current had been determined in absolute units by means of a current balance and simultaneously measured in NBS amperes by comparison with standard resistors and standard cells. This work was reported in RP1449. Similar measurements made recently with an electrodynamometer indicate a possible change in the values of the standards. The present paper reports a repetition of the work described in RP1449. The purpose of this remeasurement was to determine whether or not the standards had changed. Only minor changes were made in the equipment in order that factors which might have introduced small systematic errors in the results would remain unchanged.

According to the work described in this paper, 1 NBS ampere = 1.000008 absolute amperes. Recent work with the Pellat electrodynamometer gave the result 1 NBS ampere = 1.000013 absolute amperes. The weighted mean of these two values is

1 NBS ampere-1.000010 ± 0.000005 absolute amperes *

The results given above for the current balance differ by 6 ppm from those obtained in 1942. This indicates, in view of the uncertainties of measurement, that any change in the ampere as maintained by standard resistors and standard cells does not exceed a few parts in a million.

*The above values for the NBS ampere are based on the Dryden reduction value of the acceleration of gravity, g. In light of new determinations of g, the NBS ampere is

1 NBS ampere = 1.000012 ± 0.000005 absolute amperes.

This value is the weighted mean of the results obtained with the NBS current balance and the Pellat electrodynamometer.

R. L. Driscoll
November 1967

JOURNAL OF RESEARCH of the National Bureau of Standards—A. Physics and Chemistry
Vol. 65A, No. 3, May–June 1961

Evaluation of the NBS Unit of Resistance Based on a Computable Capacitor

Robert D. Cutkosky

(January 16, 1961)

An evaluation of the unit of resistance maintained at the National Bureau of Standards, based on the prototype standards of length and time, is described. The evaluation is based on a nominally one-picofarad capacitor whose value may be calculated from its mechanical dimensions to high accuracy. This capacitor is used to calibrate an 0.01-microfarad capacitor. A frequency-dependent bridge involving this capacitor establishes the value of a 10^4-ohm resistor. Comparison of that resistor with the bank of one-ohm resistors maintaining the NBS unit of resistance establishes that this unit is

$$\Omega_{EU} = 1.000002_3 \text{ ohms} \pm 2.1 \text{ ppm.}^*$$

The indicated uncertainty is an estimated 50 percent error of the reported value based on the statistical uncertainty of the measurements and allowing for known sources of possible systematic errors other than in the speed of light, assuming that the speed of light $c = 2.997925 \times 10^{10}$cm/sec.

*Since the publication of this paper, it was discovered that the small correction resulting from the ac-dc differences of the 10^4-ohm resistors was misapplied. The corrected value for the NBS unit of resistance is

$$\Omega_{EU} = 1.000000_6 \text{ ohms} \pm 2.1 \text{ ppm.}$$

R. D. Cutkosky
November 1967

Standard Cells and Zener Diodes

Papers

Abstracts

315-411 O - 68 - 6

UNITED STATES DEPARTMENT OF COMMERCE • Luther H. Hodges, *Secretary*

NATIONAL BUREAU OF STANDARDS • A. V. Astin, *Director*

Standard Cells

Their Construction, Maintenance, and Characteristics

Walter J. Hamer

National Bureau of Standards Monograph 84

Issued January 15, 1965

73-I

Foreword

Accurate measurement of electromotive force is important in many areas of science and technology. Physical standards for such measurement are provided by standard cells, which are long-lived electrochemical systems of highly stable electromotive force.

This publication gives the origin and derivation of the unit of electromotive force and outlines the procedures by which the National Bureau of Standards maintains and disseminates this unit by means of standard cells. Information is also given on the construction, maintenance, and characteristics of standard cells as well as a history of their development. Emphasis is placed on the precision and accuracy of electromotive force measurements; the stability of standard cells, especially those of the National Reference Group; and efforts made to construct standard cells of high quality.

A. V. Astin, *Director*

Library of Congress Catalog Card Number: 64–60065

Contents

Standard Cells

Their Construction, Maintenance, and Characteristics

Walter J. Hamer

This Monograph contains information on the construction, maintenance, and characteristics of standard cells. The effects of temperature, pressure, electric current, light, shock, and vibration on standard cells are discussed. A history of the realization and maintenance of the unit of electromotive force is also included. A record of international comparisons of the unit of electromotive force is presented as well as information on the constancy of the National Reference Group of Standard Cells.

1. Introduction

Standard cells are physical representations of the unit of electromotive force (emf), serve in the maintenance of the unit, and are used as standards with which the emf of other cells and systems and IR drops are compared. Together with standards of resistance (R) they are also used in the measurement of current, I. When measurements of electric power, P, are made in terms of standards for emf (E) and resistance, the expression for power, $P=E^2/R$, shows the necessity of knowing E accurately, since a small error in the standard for E would produce a percentage error twice as great in the value for the power, P.

Standard cells are electrochemical systems composed of two dissimilar electrodes immersed in an electrolytic solution. They are not intended to supply electric current and, therefore, are of different design from those electrochemical systems which are intended for such purpose. Owing to their special use, standard cells are required to meet certain performance criteria and, for precise measurements, to have certain inherent characteristics. They must be reasonably reproducible, exhibit good permanency, possess low emf-temperature coefficients, have a low or moderately low internal resistance, be relatively insensitive to current drains of low magnitude, and, if possible, have an emf of convenient magnitude. Since a standard cell is a physical representation of a unit it is obvious why permanency is of prime importance in a standard cell. The precision with which the emf of standard cells is measured, accordingly, exceeds that normally required for other types of galvanic cells.

2. The Unit of Electromotive Force

2.1. Realization

The practical unit of emf, the volt, is not an arbitrary one but like the other electrical units is derived from the basic mechanical units of length, mass, and time using the principles of electromagnetism with the value of the magnetic constant (the so-called permeability of free space) taken as $4\pi/10^7$ in the rationalized mksa (meter-kilogram-second-ampere) system of units.[1] It has been customary, following the first use of the term by Gauss [9],[2] to refer to electrical units based on the basic units of length, mass, and time as absolute electrical units.[3] The transition from arbitrary to absolute units began with the work of Gauss [9] in 1833 and of Weber [2] in 1851, who showed that it was possible to measure electrical quantities in terms of mechanical units. Weber pointed out the desirability of making the electrical units consistent with those used in other branches of science and engineering.

The electrical units determined in the cgs electromagnetic (em) system are of inconvenient size for practical use. For example, Sir William Thomson (Lord Kelvin) [10] in 1851 showed that the emf of a Daniell cell was about 1×10^8 cgs em units. Even so, a Committee of the British Association for the Advancement of Science in 1873 [6] recommended the cgs em system for use both in basic science and practical engineering. However, the practitioners, although they agreed with the desirability of relating electrical units to mechanical ones, objected to the use of the cgs em system of units in practice both because of the magnitudes involved and because they had been using such terms as ohms and volts for their units. Their views prevailed and in 1881 the International Congress of Electricians [11] meeting in Paris adopted the cgs em system of units as the fundamental system and the volt-ohm-ampere system for practical use, with the practical units being made larger or smaller than the corresponding cgs em units by an appropriate power of 10.

[1] This is the Giorgi system [1], which is a part of the *Système International d'Unités* (SI), adopted in a resolution, 11th General Conference on Weights and Measures, Paris, October 1960. Other systems for the basic units of length, mass, and time have been used. These include the millimeter-milligram-second system of Weber [2], the meter-gram-second system recommended by the first committee of the British Association for the Advancement of Science appointed to consider electrical units [3], the quadrant-(eleventh-gram)-second or Q.E.S. system of Maxwell [4], the foot-grain-second system used in England for a time [5], and the cgs (centimeter-gram-second system [6] (see *Appendix 1*). Heaviside also proposed a rationalized system wherein the cgs unit of emf was increased by a factor $\sqrt{4\pi}$ (unit of resistance increased by a factor 4π and the unit of current decreased by the factor $\sqrt{4\pi}$ [7]). In all of these, the Giorgi system excepted, the magnetic constant (the permeability of free space) is taken as unity. Regardless of which system is chosen the practical system remains unaffected. Additional information on electrical units is given in reference [8].

[2] Figures in brackets indicate the literature references on page 31.

[3] It is unfortunate that the name "absolute" has persisted. It is sometimes wrongly interpreted to imply that there are no errors involved in the measurements or that perfection has been attained.

The factors chosen for emf, resistance, and current were:

1 volt (practical unit) $= 10^8$ cgs electromagnetic units of emf

1 ohm (practical unit) $= 10^9$ cgs electromagnetic units of resistance

1 ampere (practical unit) $= 10^{-1}$ cgs electromagnetic unit of current.

The factor 10^8 was chosen for emf since then the emf of a Daniell cell, widely used at that time as a rough standard of emf, became approximately 1 volt. The factor 10^9 was chosen for resistance, for in this way the value of the Siemens mercury column, already used as a resistance standard, especially on the European continent, became approximately 1 ohm (actually about 0.94 ohm). The factor for the ampere was then fixed as 10^{-1} by the requirement of Ohm's law.

The unit of emf, although a most important unit, is obtained from the ohm and the ampere. To date, no direct absolute measurement of emf in the em system of units has been found feasible. Instead its value is established experimentally in em units through Ohm's law and the measurement of the fall of potential produced in a resistance by a current, each of these being capable of determination in absolute measure.[4]

The *ohm in absolute measure* is usually obtained in terms of length and time by means of inductance and frequency. In the Wenner [15] method, a mutual inductor of known dimensions, and thus of calculable inductance, is placed in a suitable circuit containing the resistor the value of which is to be determined, a battery, a galvanometer, and two rotary reversing switches. The primary of the mutual inductor is placed in series with the battery and resistor, and with one rotary reversing switch so arranged as to reverse the connections to the primary. The secondary of the mutual inductor is connected to the potential terminals of the resistor through a galvanometer and a rotary reversing switch for reversing the connections to the secondary terminals. The galvanometer detects the balance between the induced emf in the secondary and the I_rR drop across the resistor. When balance is obtained, i.e., when the galvanometer shows no deflection, $I_rR = 4nI_pM$ where I_r is the current in the resistor, I_p the current in the primary, M is the computable mutual inductance, and n is the frequency of commutation in cycles per second ($2n$ = a number of reversals per second of the rotary reversing switch in the secondary). The circuit is so arranged that during that portion of the cycle when the primary of the mutual inductor is in series with the resistor, $I_r = I_p$; thus

$$R = 4nM. \tag{1}$$

Since M is calculated from dimensions with reference to length standards and from the permeability of the medium, and n is measured indirectly in terms of the unit of time, R is given in terms of the basic units of length and time and of the permeability of the space surrounding the windings of the inductor. The overall precision (repeatability) of the method is ± 5 parts per million (ppm). For more details, reference [16] should be consulted. The ohm in absolute measure may also be obtained with similar accuracy using a self inductor [17], or with lesser accuracy by measuring the relative rotation of a coil and a magnet or the motion of a coil in the earth's magnetic field. Although the latter methods are now obsolete they are mentioned here because of their historical importance in the evolution of the electrical units.

The *ohm in absolute measure* may also be obtained using a computable capacitor [18]. In this method the evaluation of resistance is based on a nominally 1-pf capacitor whose value in es units may be calculated with high accuracy from its dimensions and thence in em units using the speed of light. This capacitor is then used to calibrate 0.01-μf capacitors, the admittances of which are then compared with that of a 10^4-ohm shielded a-c resistor using a special bridge network. A conventional d-c step-down is then used to provide "absolute" calibration of d-c resistors of lower magnitude, specifically 1 ohm. For more details, reference [18] should be consulted. The overall precision (repeatability) of the method is about ± 2 ppm. Operationally, this method is less involved than the inductance methods and may be used on an annual basis to check on the constancy of the resistance standard.

The *ampere in absolute measure* is obtained in terms of length, mass, and time with a current balance [19]. In the current balance the electrodynamic force of attraction or repulsion, in the x (vertical) direction, between two coils (one movable and one stationary) through which a current is flowing is balanced against the force of gravity, mg, acting on a known mass, m, at a location where g is the acceleration due to gravity. From this force and the measured dimensions of the coils (from which the rate of increase, dM/dx, of the mutual inductance between the stationary and movable coils may be calculated) together with the permeability of space in which the coils act, the current is expressed in terms of units of length, mass, and time, where time enters into the calculations through the acceleration of gravity. The overall precision (repeatability) of this method is about ± 6 ppm. The ampere may also be obtained

[4] The unit of emf may also be determined in cgs *electrostatic* (*es*) *units*, with the electric constant (the so-called permitivity of free space) taken as unity, using absolute electrometers. The accuracy of the methods, however, is much lower than the em approach, the order of magnitude being 1 part in 10,000. The unit of emf in es units is, therefore, arrived at indirectly by converting em values to es values using the experimental factor, $(2.997925 \pm 0.000003) \times 10^{10}$ cm sec^{-1}, the speed of propagation of an electrical disturbance (within experimental error, the speed of light in free space). As an example, Sir William Thomson (Lord Kelvin) [12] found the emf of a Daniell cell to be 0.00374 cgs es unit from the attraction between two parallel disks connected to the opposite poles of a Daniell cell. This value of Thomson is equivalent to 1.121×10^8 cgs em units or 1.121 volts.

An atomic standard for the volt, although most desirable, has not been forthcoming to date. The Stark effect has been proposed [13] but can be used only to measure relative voltage and is of insufficient accuracy, with the limiting factor residing in the measurement of the electric dipole moment [14].

with an uncertainty of about ±8 ppm by an electrodynamometer in which a torque rather than a force is measured [20]. The combined precision (repeatability) in determining the ampere in absolute measure is about ±5 ppm. For more details references [19] and [20] should be consulted. The ampere in absolute measure may be obtained qualitatively by using a tangent or sine galvanometer where the current is measured in terms of the deflection of a magnetic needle, the radius of the galvanometer coil, and the horizontal component of intensity of the earth's magnetic field. Although these measurements are now obsolete they are of historical importance; see later. The current balance methods are involved and accordingly are used only about once every five or ten years. However, in recent years, following the discovery of nuclear resonance, a new method, although not an "absolute" one, has been developed to check on the constancy of the ampere as maintained at NBS in terms of the physical standards of resistance and emf. This method [21] is based on the determination of the gyromagnetic ratio of the proton in which the precession frequency of the proton is measured in a magnetic field known in terms of the "absolute" ampere and the constant of an accurately made solenoid. By this method drifts in the national ampere of about ±1 ppm over a period of years can now be detected; also the method may be used annually to check the constancy of the ratio of the national standards of emf and resistance (see sec. 2.3). For more details on this method, reference [21] should be consulted.

The *volt in absolute measure* is obtained at the same time a measurement of the absolute ampere is made. The usual procedure is to connect in series with the coils of the current balance a resistor having a value, R, previously obtained in absolute measure. The voltage drop, IR, in this resistor is opposed to the emf, E, of a standard cell. When the current, I, is held at such a value that IR balances E and at the same time the mass, m, of the weight has been adjusted to balance the electrodynamic force, the relation

$$E = R[mg/(dM/dx)]^{1/2} = RI \qquad (2)$$

follows and gives the emf of the standard cell in absolute measure. The experimental uncertainty in the balance between the emf of the standard cell and the IR drop in the standard resistor is less than 0.1 microvolt. Considering the experimental precisions of the absolute determinations of R and I, the precision in the determination of the volt in absolute measure is about ±7 ppm (rms).

The volt, as now maintained in the United States, may exceed the absolute volt by as much as 18 ppm or as little as 2 ppm. Driscoll and Cutkosky [19] in 1958, as a result of measurements with a current balance and a Pellat electrodynamometer reported that

1 NBS ampere = 1.000010 ± 0.000005 absolute amperes.

In these measurements they used a value for gravity 17 ppm lower than that derived from Potsdam. Recent studies have shown that −13 ppm is a better correction of the value derived from Potsdam. Using this correction,

1 NBS ampere = 1.000012 ± 0.000005 absolute amperes.

Cutkosky [18] in 1961, as a result of studies with precision computable capacitors, found that [5]

1 NBS ohm = 1.0000006 ± 0.0000021 absolute ohms.

He also, by recalculating the results of Thomas, Peterson, Cooter, and Kotter [16] obtained with a Wenner mutual inductor, gave

1 NBS ohm = 0.999997 absolute ohm.

(J. L. Thomas has estimated the uncertainty in this value to be ±0.000005). From these relations for the ohm and using the second relation for the ampere,

1 NBS volt = 1.000013 ± 0.000005 absolute volts,

or

1 NBS volt = 1.000009 ± 0.000007 absolute volts.

The NBS volt, as now maintained by standard cells at the National Bureau of Standards, is the one disseminated. When additional data on the above relations are obtained in the United States and other countries, the International Committee of the Bureau International des Poids et Mesures, Sèvres, France, which, by international treaty, has authority to coordinate the standards of measurements in the field of electricity as well as of length and mass, may recommend adjustment in the electrical units. Until then, the units as maintained and disseminated by NBS serve to place laboratories in the United States on the same standard basis, accepted by all nations cooperating in the Treaty of the Meter.

The emf of any or all standard cells could be determined in like fashion. Obviously, such a procedure would be cumbersome and time consuming and if required would be unfortunate, indeed. Absolute measurements are involved, require painstaking work and, therefore, are unsuitable for frequent or routine measurements of emf. To circumvent the necessity for frequent absolute measurements, standard cells [6] are constructed, their emfs are determined in relation to current and resistance in absolute measure, and these cells are then used to maintain the volt; these

[5] This value differs by 1.7 ppm from that (1.000002_3) published by Cutkosky [18]. He has since uncovered an error of this magnitude in the published value.

[6] Standard resistors, usually hermetically sealed coils of annealed manganin wire [22], are used similarly to maintain the unit of resistance. Owing to the transitory nature of an electric current no physical standards for an ampere have been, to date, possible. Instead the standard ampere is given by the ratio of the values for the standard cell and the standard resistor.

cells are also used to assign emfs to other cells that may be constructed. In other words, the results of absolute measurements are preserved in a physical object, the standard cell.[6] The validity and realization of this approach depends on the possibility of constructing standard cells, the emfs of which are independent (or nearly so) of time; otherwise, the unit of emf would be lost or drift in value in the interim and a repetition of absolute measurements would be imperative at frequent intervals. It is obvious that this matter was and is of critical importance. Over the years extensive work has been conducted to find that electrochemical system which would exhibit constant emfs for long periods of time, say decades. Fortunately, such an electrochemical system (see below under the Weston Cell) has been found. The manner in which the unit of emf is maintained by a group of standard cells is discussed below under maintenance.

2.2. History

In 1893 the International Electrical Congress meeting in Chicago chose the Clark cell, a cell devised by Latimer Clark in 1872 [23], as the standard of emf to which they assigned a value of 1.434 international volts at 15 °C in terms of the then accepted standards for the ohm and the ampere. The Clark cell and this value for it were legalized as the standard of emf in the United States by an act of Congress, July 12, 1894 (see Appendix 1). The value, 1.434 international volts at 15 °C, followed from the determinations made by Rayleigh and Sidgwick [24], Carhart [25], Kahle [26], and Glazebrook and Skinner [27] who used current balances or silver coulometers (the electrochemical equivalent of silver having been determined by absolute methods) to determine current and B.A. coils[7] or Siemens mercury columns (or British legal ohms)[7] (known in cgs em units) as standards of resistance. Their results are summarized in table 1. In each case, the results were converted to a common international basis (see Appendix 1 for the defined international units). The emf-temperature formula of Lord Rayleigh [24, 29] which was then available was used to convert all the values to a temperature of 15 °C. The values were referred to as "international" because international agreement had been attained; it was also realized at the time that additional work would be needed to place the values on a basis truly representative of the theoretical cgs em units.

In the years immediately following 1893 most countries adopted 1.434 V for the emf of the Clark cell at 15 °C. Later work showed that cells made with specially purified mercurous sulfate (see below for a description of the Clark cell) had an emf 0.0003 V lower than 1.434 V obtained for cells made prior to the meeting of the Chicago International Electrical Congress. Germany, however, in 1898 recommended and adopted 1.4328 V at 15 °C for the Clark cell based on the German values for the ohm and ampere. Although the German value was not universally accepted, it was a more nearly correct value as later experiments showed. Also during the years 1893 to 1905 the standard cell devised by Edward Weston [30] was found to have many advantages over the Clark cell and at an informal international conference called by the Physikalisch-Technische Reichsanstalt at Charlottenburg in October 1905, the Weston Normal Cell (see later for description) was first proposed as a standard to be used for maintaining the volt and was officially adopted in 1908 at the London International Conference on Electrical Units and Standards [31].

This London Conference went further and adopted provisionally 1.0184 V as the emf of the Weston Normal Cell at 20 °C and recommended for the emf-temperature coefficient of the Weston Normal Cell the formula based on the measurements of Wolff [32]. The London Conference still felt, however, that further work was needed and recommended that additional experiments be made.

[7] B.A. coil refers to British Association for Advancement of Science coil of silver-platinum alloy (66.6 percent Ag, 33.4 percent Pt); the B.A. ohm = 0.9866 international ohm. The Siemens ohm standard consisted of a column of chemically pure mercury 1 meter long and 1 square millimeter in cross-section at a temperature of 0 °C. Carhart and Kahle used Siemens units and then converted their results to British legal ohms. The British legal ohm was represented by B.A. coils, the resistances of which were related to the 1884 "legal ohm," the resistance at 0 °C of a column of mercury 106 centimeters long and one square millimeter in cross-section; one British legal ohm = 0.9976 international ohm; one British legal ohm = 1.06 Siemens ohm.

TABLE 1. *Absolute measurements of the electromotive force of the Clark cell*

Experimenters	Temperature	Resistance unit	Current method	Experimenters' value (prior to reduction)	International values	
					at observed temperature	at 15 °C
	Celsius			*volts*	*volts*	*volts*
Rayleigh and Sidgwick	15.0	B.A. ohm [b]	current balance	1.4539 [e]	1.4344	1.4344
Carhart	18.0 [a]	Siemens ohm [c]	silver coulometer [d]	1.434 [f,g]	1.431	1.434
Kahle	15.0	Siemens ohm [c]	silver coulometer [d]	1.4377 [f,g]	1.4342	1.4342
Glazebrook and Skinner	15.0	B.A. ohm [b]	silver coulometer [d]	1.4537 [e]	1.4342	1.4342
					average	1.4342
					rounded value	1.434

[a] — Carhart [28] later stated that the value 1.434 V was for a mean of two experiments, one at 18 °C and one at 17 °C; a correction for this does not alter the rounded value of 1.434 V given above for the absolute emf of the Clark cell.
[b] — 1 B.A. ohm = 0.9866 international ohm.
[c] — Carhart and Kahle converted their values from Siemens units to British legal units, using the relation 1 British legal ohm = 1.06 Siemens ohm.
[d] — 1.118 mg silver deposited per second per ampere (international value of electrochemical equivalent of silver).
[e] — B.A. volt.
[f] — British legal volt.
[g] — 1 British legal ohm = 0.9976 international ohm.

Accordingly, scientists from England, France, and Germany met with United States scientists at the National Bureau of Standards in 1910, and as a result of their experiments with a large number of Weston normal cells and silver-coulometer determinations adopted 1.0183 V as the emf of the Weston Normal Cell at 20 °C. Values derived from this were later assumed to be significant to the fifth, sixth, or seventh decimal as a basis of measurement [33, 34]. This value (1.0183 V) was still characterized in "international" units since the basis on which the new measurements (1910) were made was the same as it was in 1893; the precision of the measurements was higher, however.

Values assigned to the reference groups of each cooperating nation served as the fundamental basis of all emf measurements from 1911 to 1948. By 1948, after interruptions caused by the two World Wars and after improvements in techniques, an accurate determination of the electrical quantities in cgs em units was achieved, and on January 1, 1948, changes from international to absolute units were officially made internationally.[8] The legal status of these new units in the United States is exactly the same as that of the older ones because the law of 1894 (see Appendix 1) mentions both sets of units on an equivalent basis. However, in order to remove the ambiguities of the old act, new legislation was passed by the Congress in 1950 (see Appendix 2). The changes [35] for the United States were:

1 international volt (US) = 1.000330 absolute volts
1 international ohm (US) = 1.000495 absolute ohms
1 international ampere (US) = 0.999835 absolute ampere
1 international coulomb (US) = 0.999835 absolute coulomb
1 international henry (US) = 1.000495 absolute henries
1 international farad (US) = 0.999505 absolute farad
1 international watt (US) = 1.000165 absolute watts
1 international joule (US) = 1.000165 absolute joules

The conversion factors in other countries were nearly the same as these. The emf of the Weston Normal Cell at 20 °C on the new basis then became 1.01864 V. This value is now of historical interest only.

The relation of the fundamental units to the measurement of power and energy in both the new and former systems of units is shown diagrammatically in figure 1. The left half represents the fundamental units and standards maintained by the National Bureau of Standards, the right half the units and standards used by the public.

2.3. Maintenance

The unit of electromotive force in the United States was originally maintained (1897–1906) by seven Clark cells, the mean emf of which was assigned a value of 1.4337 V (this value was 0.0003 V lower than the value recommended in 1893 by the

[8] Although "international" and "absolute" are frequently used in referring to the units it is now best to consider these terms of historical interest only. There is only one kind of volt in the em system of units, and the above terms had significance only during the period during which efforts were being made to achieve the theoretical unit. It is deemed advisable to speak, therefore, of only one kind of volt; when the term "volt" is used, "absolute volt" is implied, i.e., the volt has a direct relation to the theoretical unit.

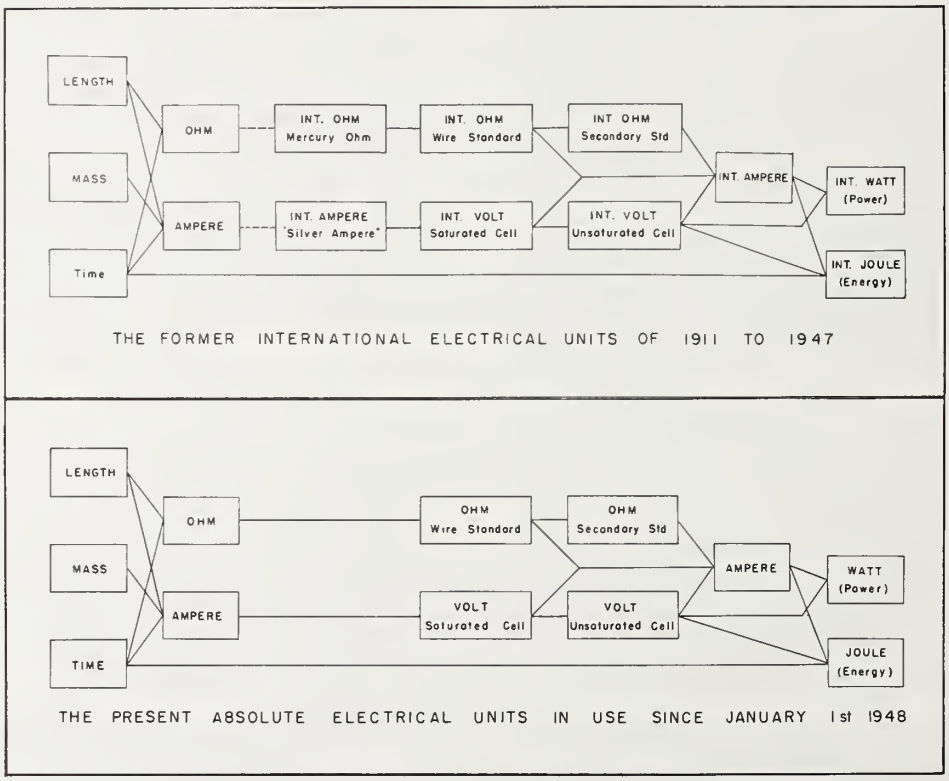

FIGURE 1. *Diagram showing the relation of the present and former systems of electrical units to the basic mechanical units of length, mass, and time.*

Chicago International Electrical Congress because specially purified mercurous sulfate had been used in the preparation of the cells; it was 0.0009 V higher, however, than the value then recommended by Germany). In 1906 the standard consisted of both Clark and Weston Normal cells and after 1908 of Weston cells only; an emf of 1.019126 V was assigned to the mean of the Weston cells at 20 °C based on a direct comparison with the Clark cells (on the German basis the emf of the Weston cells was 1.018226 V which was only slightly lower than 1.0183 V found in 1910 by the International Committee which met at the National Bureau of Standards). After 1911, this latter unit was maintained in each country until 1948 when "absolute" units were adopted. The number of cells constituting the national standard has varied from time to time; when a cell shows a steady change from its previously steady value it is removed from the group (see later for criterion and procedure).

Today, the National Reference Group of Standard cells consists of 44 saturated Weston (or cadmium sulfate) cells, all of which have been made at the National Bureau of Standards from highly purified materials and assembled under controlled conditions (see later for details). The National Standard is based on the mean emf of these 44 cells. The emf of any one cell in the group is equal to the mean emf, less the average deviation in emf of all 44 cells from the emf of a selected reference cell in the group, plus the deviation in emf of the individual cell from that of the selected reference cell, or

$$E_c \text{ (in volts)} = E_m - \frac{\Sigma\Delta}{44} + (E_c - E_r) \qquad (3)$$

where E_c = the emf of an individual cell, E_m = the mean emf of the 44 cells, $\Sigma\Delta$ = the algebraic summation of the differences between the emf of a selected reference cell, E_r, and the emfs of all of the other cells in the group. This reference group (of cells) consists of three parts, of 11 "neutral" cells made in 1906, 7 "acid" (0.05N) cells made in 1933, and 26 "acid" (0.026N) cells made in 1948. The last two groups of cells were added to the reference group in 1937 and 1955, respectively. The meaning of the terms "neutral" and "acid" appears later. This National Reference Group of cells is also supplemented by a group of cadmium sulfate cells made with 98 percent deuterium oxide (heavy water) [36], the emf of which is about 380 μV lower than that of cadmium sulfate cells made with normal water. These cells are discussed in Appendix 3, but suffice it to say here that a study of the ratio of the emfs of cells made with normal and heavy water offers an auxiliary check on the stability of the national unit of emf.

Obviously, all of a group of "identical" cells may increase or decrease in emf with time without departures from the original assigned mean becoming evident. Therefore, an alternative type of standard cell of approximately the same emf as the Weston cell[9] but of different composition would be most valuable, for if changes in emf with time in two different systems occurred, they would not be likely to follow the same pattern. Thus, studies of the ratio of emfs of two different systems over a period of years would give valuable insight into the stability of the standard. It is for this reason that the National Standard or Reference Group was eventually designed to include "neutral" and "acid" cells [10] and to be supplemented by cadmium sulfate cells made with heavy water. The ratio of or the difference between the emfs of "neutral" and "acid" cells is followed in the course of maintaining the unit of emf.

A cell is removed from the reference group when its emf has drifted by more than 1.0 μV from its previously steady value. When a cell is removed, the mean emf of the group is "recaptured" by reverting in the records to the time the cell had been added to the reference group, calculating a new mean for the reduced group (less the cell removed) at that time, and finally carrying the new mean forward. In some cases it has entailed going back as much as 20 years. Since the cells have closely agreeing emfs the removal of one cell has only a minor effect on the mean emf of the group; this effect has generally been below 1 μV. The effect on the emf of the mean of removing one cell obviously is smaller the larger is the number of cells in the group (for practical reasons there is a limit to this number; if too high a number, it might not be possible to measure the emfs of all the cells within any one day—this would then increase the problems associated with maintenance).

It is difficult to provide incontrovertible evidence regarding the long-term stability of the volt maintained with saturated standard cells. A considerable body of evidence indicates, however, that it is very unlikely that the unit of emf preserved with the National Reference Group of Standard Cells has changed by any significant amount in the last 53 years. This evidence follows:

(1) *In terms of measurements with silver coulometers (or voltameters) and standard resistors* —prior to 1948 silver coulometers were used in defining the international ampere (see Appendix 1). To date, however, there are no international specifications that enable the coulometer to be used unambiguously as a means of reproducing the international ampere. Even so, experiments repeated with *a given type* of coulometer under the same conditions after a lapse of a number of years can serve to establish the same current to high accuracy. From 1910 to 1912, inclusive, [37] a series of experiments were made at the National Bureau of Standards with a Smith form of coulometer and the results were expressed in terms of the emf of the saturated Weston cell at 20 °C; the average of 55 experiments gave 1.018274 V for the Weston cell at 20 °C. In

[9] Measurements of large emf differences of the order of magnitude of 0.3 V to 0.5 V with the precision required imposes a problem, though not an insurmountable one.

[10] Cells that differ much more in their chemical composition than "neutral" and "acid" cells or "normal water" and "heavy water" cadmium sulfate cells would be even more desirable for this purpose. However, to date, the prime requirement of constancy in emf has not been as well realized in other systems as it has been in cells of the cadmium sulfate type.

1931 a series of coulometer experiments were conducted at the Physikalisch-Technische Reichsanstalt by representatives from Germany, Great Britain, and the United States [34, 38, 39]; the results obtained by the United States with the Smith form of coulometer gave 1.018273 V for the Weston cell at 20 °C.[11] Assuming that the unit of resistance had not changed during this interval of time the results indicate that the drift in the unit of emf was not over 0.05 μV per year.

(2) *In terms of measurements with current balances and standard resistors*—in 1934 Curtis and Curtis [40] using a current balance originally used by Rosa, Dorsey, and Miller [41] found that 1 NBS international ampere (given by ratio of NBS units of emf and resistance) was equal to 0.999928 absolute ampere, whereas the results of Rosa et al. in 1911 gave 0.999926 absolute ampere. Accordingly, assuming that the unit of resistance had not changed, these results indicate that any apparent drift in the unit of emf could not have exceeded 0.1 μV per year. Also, since 1938 all checks of the NBS unit of emf have agreed within the precision ($\pm$7 ppm) of absolute measurements made with current balances or electrodynamometers and self or mutual inductors; these checks indicate that the unit of emf is constant to $\pm$0.2 to $\pm$0.3 μV per year if the unit of resistance has remained unchanged.

(3) *In terms of the gyromagnetic ratio of the proton*—in these experiments the precession frequency, as stated above, is measured in a magnetic field known in terms of the absolute ampere and the constant of an accurately made solenoid. The solenoid current, when compared with that given by the ratio of the NBS standards of emf and resistance, has been found to have the same value to better than 0.1 μA during the interval from January 1960 to March 1963.[12] If the unit of resistance remained constant during this period, the unit of emf has also remained constant to better than 0.1 μV per year. The construction and properties of standard resistors and standard cells are radically different; the possibility that the two systems should drift in such a manner as to maintain a constant ratio seems remote. The accuracy of absolute resistance measurements has increased significantly in recent times. Modern absolute resistance measurements coupled with reference to atomic constants should, in the foreseeable future, supply convincing evidence regarding the stability of both resistors and cells.

(4) *In terms of "neutral" and "acid" cells*—the difference between the average emfs of the "neutral" and "acid" cells in the National Reference Group of Standard Cells has increased by 8.5 μV in 26 years, with the increase being only 1.0 μV during the last 10 years [42]. This comparison was made for 7 "neutral" and 11 "acid" cells, or for cells of this type in the National Reference Group since 1937. Since the emfs of "neutral" and "acid" cells have remained relatively constant during the last 10 years the earlier drift in their difference may be attributed to an aging effect exhibited by the "acid" cells (the "neutral" cells were 26 years old at the start of the comparison between the "neutral" and "acid" cells). For the last 10 years the average annual change has been 0.10 μV.

(5) *In terms of international comparisons*—in 1948 the units of emf of the United States (USA) and the Bureau International des Poids et Mesures (BIPM) agreed whereas in 1960 the USA unit was 1.9 μV smaller than the BIPM unit. Assuming that the BIPM unit had remained constant during this time the USA unit has changed at a rate of -0.16 μV per year. Assuming that the BIPM and USA units changed at the same rates but in opposite directions the USA unit then changed at a rate of -0.08 μV per year. Additional data on international comparisons are given in section 2.5.

(6) *In terms of customers' cells*—customers' saturated cells, checked in terms of the National Standard of emf, show, on the average, an annual variation of $\pm$1.2 μV per year, but no drifts in emf in one direction or the other. This relative stability refers only to cells that are about 3 or more years of age; saturated standard cells usually exhibit an aging effect of several microvolts during the first 3 years after their construction.

(7) *In terms of newly prepared cells*—saturated standard cells freshly made from new materials usually agree with old or aged cells within 5 μV. Of course, in this type of comparison the cells must be made with amalgams of the same percentage of cadmium and with cadmium sulfate solutions of the same acidity with respect to sulfuric acid. The point here is that saturated cadmium cells, made at different times to essentially the same specification, are highly reproducible. Cells made in the past cannot have drifted seriously in emf if similar cells of recent construction agree closely in emf with them.

(8) *In terms of the relative emfs of cells within a group of cells*—the differences in emf between the cells in the National Reference Group of Standard Cells have remained remarkably constant for decades. Although, as stated above, all "identical" cells may increase or decrease in emf without evident departures from their mean emf, constancy in the difference between the emf of individual cells in a group of cells with time nevertheless, in combination with items (1), (2), and (3) above, increases confidence in the constancy of the mean emf of a group of cells.

Although the above remarks apply to the stability of standard cells in the National Reference Group of Standard Cells they should also apply to any standard cell of the saturated type providing it is a quality cell properly maintained. Cells made with impure materials or poorly assembled will invariably show much less stability in emf. In section 2.5 the need for adjustments in the assigned values to

[11] These results published by Vinal [34] were reported to the fifth decimal and Vinal said "The value for Washington in terms of B.S. unit is, however, exactly the same as the result of the bureau's own experiments on the voltameter [37] published in 1913" (actually 1914). These data have been recalculated, retaining the sixth decimal, and are given in Appendix 4.

[12] The author is indebted to Forest K. Harris and Raymond L. Driscoll for this information.

standard cells, although infrequent, is discussed. The need for these adjustments is not clear. It may be that the cells were of poor quality, were affected by transport, or had not come to equilibrium after temperature changes which are involved in international comparisons.

The standard cells of the National Reference Group are housed in slowly stirred oil baths maintained at 28 °C under diffuse light in an air-conditioned room maintained at 25 °C ± 1 °C; the relative humidity automatically remains below 50 percent. The temperature of the baths is maintained at 28 °C within 0.01 °C on a long-term basis and within 0.001 °C during measurements using a Gouy controller [43]. In a Gouy controller, a steel piano wire extending into the mercury of the mercury-toluene regulator is connected to a wheel which revolves at a slow rate whereby the wire is made to periodically make and break contact with the mercury. The design of the bath and its temperature control are described in Appendix 5. A special mineral oil, having the characteristics listed in Appendix 6, is used as fluid in the constant-temperature baths. Tests made to determine the temperature of the oil at various locations within the baths indicated a uniform temperature within 0.001 °C, i.e., no hot or cold spots prevail within the bath or in the vicinity of the standard cells. This design follows closely that described many years ago by Wolff and Waters [44]. A bath for use with saturated standard cells has also been described recently by P. H. Lowrie, Jr. [45].

The cells are supported about 2 in. below the surface of the oil on seasoned mahogany strips about 16 mm wide (slightly smaller than the distance between the limbs of NBS H-shaped cells) and about 10 mm thick and either 24 or 48 cm long, with grooves into which the cross-arms of the cells fit snugly. Some racks carry 18 cells equally spaced, except for a somewhat wider space at the middle of the rack where the rack is supported; others carry 9 cells. Hard rubber, bakelite, or lucite strips (widened U-shaped), about 40 mm long, 10 mm wide, and 10 mm thick in the center and 13 mm at each end, are mounted between cells across the underedge of the mahogany strip. In the top of each strip, at each end, is inserted a short copper rod provided with a pair of holes, one 1 mm and the other 2 mm in diameter and both about 9 mm in depth; these holes serve as mercury cups, one for a cell terminal and the other for external connections. These two copper cups are spaced at the same distance apart on each strip, so that any cell can be put in the electric circuit by a stabber consisting of a pair of stiff copper wires mounted in a lucite block (copper wires are amalgamated on the tips). This is a copper-copper connection through the mercury and under the oil. From this point on all contacts are copper-copper to avoid thermal emfs. The other end of the stabber connection goes to a post position. There are two post positions, one for the Reference Cell and one for the Unknown Cell. The leads of the cells go from the posts through conduits to another post at the emf-measuring instrument (see later), where the two cells are placed in series opposition by joining the negatives and the difference is measured.

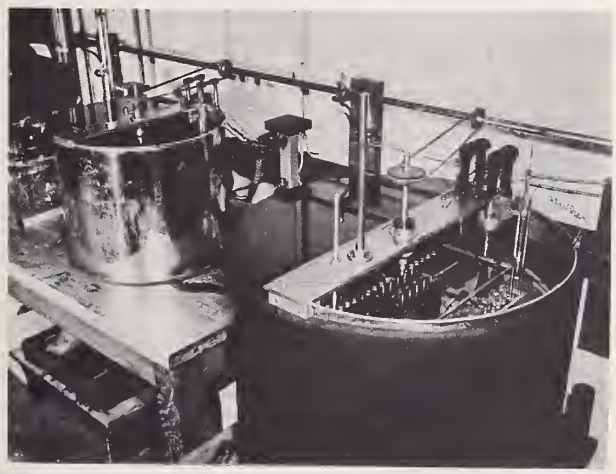

FIGURE 2. *Oil baths used to house the National Reference Group of Standard Cells.*

A photograph showing the oil baths that house the National Reference Group of Cells is shown in figure 2. Other baths of intermediate size are also available for housing cells on test. The temperature of the baths is measured with a platinum-resistance thermometer and a Mueller bridge, having a sensitivity of 0.0001 ohm, corresponding to 0.001 °C.

2.4. Dissemination

Comparisons of the emf of standard cells, such as may be required in the dissemination of the unit of emf, i.e., the transfer of the unit from a standardizing laboratory, must or should be carried out by procedures of the highest precision involving a minimum of uncertainty. In this case, comparisons are made between standard cells, the emf of which have been determined in absolute units and other standard cells, the emf of which have not been so determined. The former may be called *reference cells* and the latter *unknown cells*. These intercomparisons may be made with high accuracy with potentiometers by the *opposition* method (preferably called the *difference* method). In this method the two cells (reference and unknown) are connected in series with their emfs in opposition and the difference in emf between the two is measured with a potentiometer using a galvanometer of high sensitivity. Because the difference in emf between the two cells is small, only a moderate percentage accuracy in its determination is required to give the emf of the unknown cell accurately in terms of the known reference cell. If the difference between the two cells were 100 μV the accuracy of the measurements need be only 1 percent to give the difference to 1 μV or only 0.1 percent to give an accuracy of 0.1 μV.

This method is not direct reading, however, and

the operator must determine which of the two cells has the higher emf. The greatest source of error in measurements by the difference method is the presence in the circuit of spurious emfs, such as those from thermoelectric action. At the National Bureau of Standards a special comparator, designed by Brooks [46], is used. This comparator is direct reading and compensates for parasitic thermal emfs. The reference and unknown cells are connected in series-opposition in series with a galvanometer and an auxiliary source of a few microvolts and adjustments are made in the auxiliary source until the galvanometer indicates a null balance. The D'Arsonval galvanometer (see G_1, figure 3) used with the comparator has a free period of 8 sec, an external damping resistance of 1200 ohms, and a sensitivity of 5 mm per microvolt at one meter lamp and scale distance when operated slightly underdamped.

With the Brooks comparator, differences in emf as large as 2100 μV may be read with a precision of 0.1 μV. The Brooks comparator contains an opposing circuit for the detection and compensation of thermal emfs in the galvanometer circuit, contains no sliding parts in the main circuit, and has a "read-out" device by which the measured difference in the emf is added algebraically to the emf of the reference cell thereby giving directly the entire emf of the unknown cell.

A circuit illustrating the principle of the Brooks comparator is shown diagrammatically in figure 3 and the exterior and interior of the comparator are shown in figures 4 and 5, respectively. The uppermost of the three sections shown in figure 3 relates to the adjustment of the current in the comparator to the proper value. A current I_1 from battery B_1 (No. 6 dry cell) is regulated by the rheostat R_1 to a definite value in the usual manner by reference to an auxiliary standard cell. All parts with exception of the battery are housed in the comparator. In the middle section, the substitution resistances connected to tap points numbered 3 to 16 are selected by the central dial as needed. Each step is 100 μV. It is necessary to interpolate between successive steps to complete the process of measuring the emf of the unknown cell, X (lower section). This is done automatically by the circuits attached to points 17 and 18. B_2 and B_3 are No. 6 dry cells, also. The milliammeter A_3 measures the current I_3 when an exact balance is indicated by the galvanometer G_1 as a result of varying the resistance R_3. The milliammeter A_3 is calibrated to make its scale read directly in microvolts. A similar circuit attached at 1 and 2 performs a like function for the reference cell N (lower section) whose emf value must be set exactly if the readings for the unknown cell X are to be correctly determined. The lowest section of figure 3 shows the circuit wherein the unknown, X, and the reference cell, N, are connected in series opposition. This circuit also contains the galvanometer, G_1, of sensitivity, given above.

Thermal emf compensation is achieved by a simple copper slide wire connected in series with the main galvanometer, G_1. About 15 μA from a No. 6 dry cell (not shown in the figure) enters this slide wire at its central point and leaves by a slider. If the slider is set at the central point of the copper wire there is no current in the copper wire and, therefore, no potential drop. By setting the slider away from the central point, a small adjustable potential drop may be introduced into the galva-

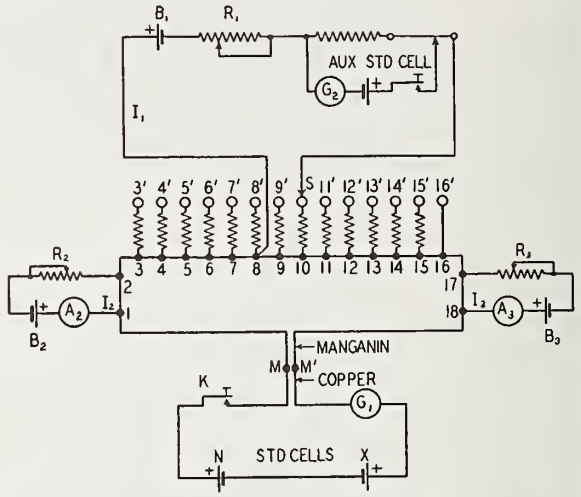

FIGURE 3. *Diagrammatic plan of circuits illustrating the principle of the potentiometric part of a Brooks standard-cell comparator.*

FIGURE 4. *Photograph of a Brooks comparator (top view).*

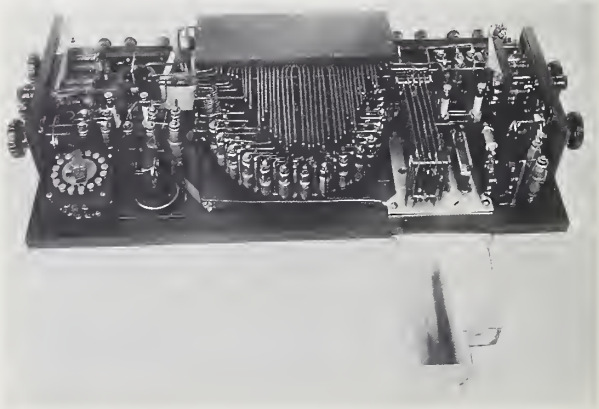

FIGURE 5. *Photograph of the interior of a Brooks comparator.*

nometer circuit to neutralize any parasitic emf in the galvanometer and the wires connecting it to the comparator. By depressing a "shunt" key any appreciable parasitic emf can be detected; if present it will maintain a corresponding deflection of the galvanometer and when the "shunt" key is depressed the galvanometer coil will assume its open-circuit zero position. To neutralize this undesired emf the slider is manipulated until no motion of the galvanometer coil ensues when the "shunt" key is depressed. For additional details the original paper by Brooks [46] should be consulted.

Although compensation for thermal effects is provided in the instrument, thermal effects may also arise at the cell terminals. These are eliminated by making connections to the cells through mercury cups immersed two inches below the surface of oil maintained at the same temperature as the cells, as was mentioned above under *maintenance* (section 2.3). In those cases (for example, unsaturated cells or saturated cells in air boxes; see later) where the terminals of the unknown cell cannot be immersed in oil, thermal effects are kept at a minimum by using like metal connections in a constant-temperature room. Other types of standard cell comparators have been described by Miller [47], Vincent [48], and by Spinks and Hermach [49]. The comparator (portable potentiometer) of Spinks and Hermach also includes two saturated and two unsaturated standard cells in a temperature-controlled enclosure.

In the dissemination of the unit of emf, i.e., the comparison of unknown and reference cells, working groups of standard cells are used instead of the National Reference Group of Standard Cells. Of course, the emfs of the cells within these working groups are known in terms of the National Reference Group. These comparisons are made with a precision of 0.6 μV. One working group is maintained in the Standard Cell Laboratory in Washington, D.C., the other at the NBS Boulder Laboratories in Boulder, Colo. [50]. A total of 10 comparisons of the emf of the unknown (customer) cells with the working groups is made, one per day, over a period of ten days, at a specified temperature for saturated cells and at an ambient temperature of 25 °C (at Washington) and of 23 °C (at Boulder) for unsaturated cells.[13] The best saturated cells are calibrated with an uncertainty of 0.0001 percent; the best unsaturated cells with an uncertainty of 0.005 percent. The results are transmitted to customers in Reports of Calibration.

2.5. International Comparisons

Since 1932 the units of emf of various nations have been intercompared at specified intervals at the Bureau International des Poids et Mesures (BIPM), Sèvres, France. At the present time this interval is 3 years. For many years the comparisons were rather sporadic, and they were interrupted by the two World Wars (see fig. 6). Prior to 1948 the intercomparisons were made in "international volts" and since 1948 in "absolute volts" (see figs. 6 and 7). These intercomparisons are effected by standard cells maintained by the participating countries and by the International Bureau and are conducted at 20 °C. As a rule each country submits 4 to 10 cells to BIPM for the intercomparisons; at the present time the cells are carried to BIPM by messenger.

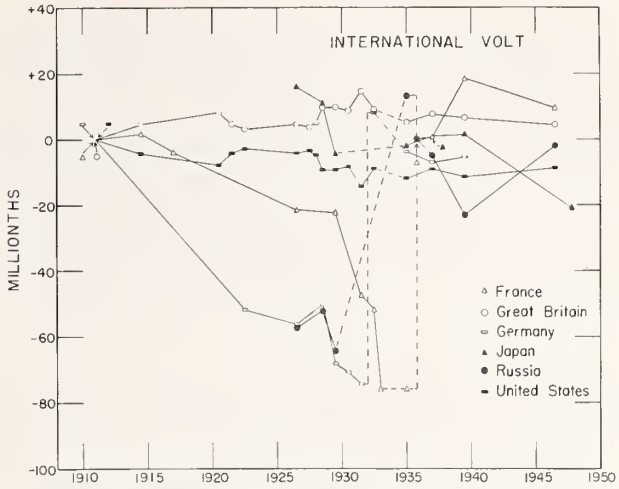

FIGURE 6. *International comparisons of the unit of electromotive force in international volts prior to 1948.*

The first comparison involved the measurements at the National Bureau of Standards in 1910, at which time the units of the participating countries, France, Germany, Great Britain, and the United States were identical (see fig. 6). From 1911 to 1932 the major intercomparisons were between the units as maintained in the United States and in Great Britain. In preparing figure 6 it was assumed that the mean value for these two nations remained constant and this mean is made the axis of abscissas. A few comparisons were also made of the United States unit with those of France, Germany, Japan, and Russia and are shown in figure 6 in terms of the mean unit of the United States and Great Britain. In 1931 it was apparent that there was an increasing discrepancy between the unit as maintained in Germany at the Physikalisch-Technische Reichsanstalt (or PTR) in Charlottenburg and those maintained in the United States at the National Bureau of Standards (or NBS) in Washington, D.C., and in Great Britain at the National Physical Laboratory (or NPL) in Teddington. Consequently, at the invitation of the PTR arrangements were made to have an international committee carry out experiments with the silver coulometer at PTR and thus reestablish the international volt. Accordingly, P. Vigoureux of NPL and G. W. Vinal of NBS took silver coulometers to the PTR together with standard cells and standard resistors, the values of which had been carefully determined at their respective laboratories. At the PTR, these standards were compared with those of the PTR and an extensive series of experiments with different types

[13] The National Bureau of Standards provides emf calibrations of unsaturated standard cells only for public utilities and others having operations of such a nature as to require calibrations by the National Bureau of Standards.

of silver coulometers were made. As a result of these measurements, subsequently published [34, 38, 39], Germany increased its unit by 82 ppm (see Appendix 4 for United States data).

As a result of extensive work on silver coulometers by Kolossov [51], Russia changed its unit in 1934 by 87 ppm.

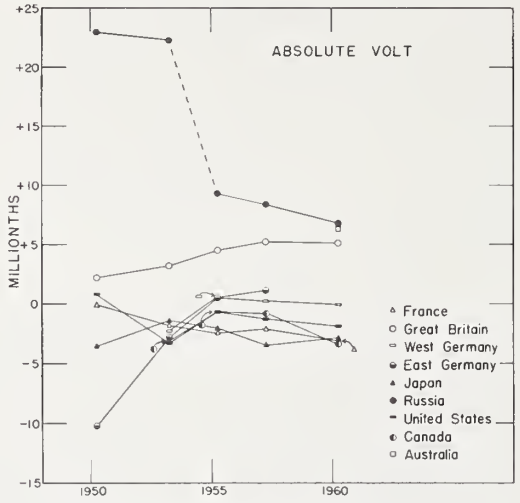

FIGURE 7. *International comparisons of the unit of electromotive force in absolute volts since 1948.*

International comparisons at BIPM began in 1932 [52] and after 1934 the data in figure 6 are plotted on the assumption that the "Mean International Volt" as defined in 1935 by the Consultative Committee on Electricity [53] has remained constant. In December 1934 the six countries listed in figure 6 submitted cells to BIPM. France, on finding its unit out of line from the others, increased its unit by 76 ppm in 1935. The Consultative Committee on Electricity suggested that the mean unit of the five remaining countries be adopted by all thus assuring immediate unification. However, only Russia accepted this suggestion and reduced its unit by 13 ppm. In 1937, 1939, and 1945–48, BIPM carried forward its mean value obtained in 1935 for the six countries after correcting for the Russian adjustment; this adjustment made the BIPM unit 2.2 ppm lower than its 1935 unit; the data in figure 6 are so reported. For the last comparison in international volts the National Physical Laboratory submitted cells in 1945 and the comparison with BIPM was completed in 1946; the other countries submitted cells in 1948 and the comparisons with BIPM were done the same year. Russia reported its values in absolute units using the international relation: 1 mean international volt = 1.00034 absolute volts. In 1939 the Russian unit had been 23.1 μV below the mean international unit. For comparisons with other countries and assuming that this difference still applied, BIPM converted the Russian absolute values to international values using a conversion factor of 1.000317.

On January 1, 1948, "absolute" units were adopted but international comparisons on this basis were not made until 1950. Intercomparisons in the "absolute" units, obtained since 1950, are given in figure 7 (note that the scale in figure 7 is much larger than in figure 6); Australia and Canada were new additions. In 1950 the German value was from East Germany while in 1953, 1955, and 1957 both East and West Germany took part in the international comparisons; since 1957 the German value is for West Germany. The data shown in figure 7 are the deviations from the BIPM mean value. In 1950 Russia had apparently corrected their "absolute" values of 1948 by the average deviations of the various countries, Russia excepted, from the BIPM unit, thus, ignoring the fact that their unit had been 23.1 μV below the mean international unit in 1939; this procedure, then placed their unit in 1950 above the BIPM unit by approximately this magnitude. In 1955 Russia made an adjustment in its unit of about 13 μV. In 1960 the spread between the 8 countries was 10.2 μV with the units of Australia, Great Britain, and Russia being high. The spread between the other 5 countries was 3.3 μV. In 1960, values for Italian cells were included with the values listed with the French cells; France had first made a direct comparison of the Italian cells with their cells at the Laboratoire Central d'Electricité, Fontenay-aux-Roses, France.

3. Early Standard Cells

Many types of galvanic cells have been proposed as standards of emf and some of these have appeared in a variety of forms. Although Faraday and others of his time used various galvanic cells, such as Grove and Bunsen cells, in their investigations, the Daniell cell [54] represented by

$$(-)\,Zn(s)\,|\,ZnSO_4, H_2SO_4(aq)\,\|\,CuSO_4(aq)\,|\,Cu(s)\,(+)$$

was the first cell seriously used as a standard of emf, as it exhibited less gassing than its predecessors. Here a single vertical line is used to indicate the interface of two distinct phases, a double vertical line to indicate a liquid-liquid junction, s = solid, and aq = aqueous solution. However, this type of cell did not exhibit a long-term stability in emf. Being a two-fluid cell, the solutions diffused into each other causing local action at the electrodes and a steady decrease in emf. Somewhat better results were obtained when saturated solutions, no acid, and amalgamated zinc were used, but, even so, the cells did not exhibit the permanency required in a standard. Nevertheless, for over 35 years, Daniell cells were used as a standard of emf. Absolute electrical measurements gave 1.07 to 1.14 V for the emf of freshly prepared cells; the actual value depended on the concentration and acidity of the solutions used. Absolute measurements were not needed to show the lack of constancy in the emf of the cells; this

behavior was evident from comparing new cells with old ones. The cell reaction is

$$Zn(s) + CuSO_4(aq) \rightarrow ZnSO_4(aq) + Cu(s). \quad (4)$$

The Daniell cell has an emf-temperature coefficient of about +34 μV/deg C at room temperature (18 to 30 °C).

Daniell cells were made in various forms. The original form consisted of a glass jar containing a porous pot of unglazed earthenware in which a zinc plate or rod was placed. Outside and around the pot a cylindrical sheet of copper was placed. The outer jar was filled with a concentrated solution of copper sulfate and the porous pot with dilute sulfuric acid, or zinc sulfate, or zinc sulfate acidified with sulfuric acid [55]. Important modifications were the gravity [56] and Fleming-Thomson cells [57]. In the gravity cell the less dense solution of zinc sulfate was placed over the more dense solution of copper sulfate so that the porous cup was eliminated. Zinc in circular or crow-foot form and copper in leaf form were used as electrodes in their respective salt solutions. In practice the cell was kept on closed circuit to curtail the mixing of the two solutions. In the Fleming-Thomson cell a U-tube was used containing a solution of copper sulfate in one arm and a solution of zinc sulfate of the same density in the other arm. Rods of copper and zinc were supported in their respective salt solutions.

In 1872 Latimer Clark [23] proposed a cell which had a profound effect on work pertaining to the electrical units. His cell, represented by

$$(-)Zn(s) \mid ZnSO_4 \cdot 7H_2O(c) \mid ZnSO_4(\text{sat aq}) \mid ZnSO_4 \cdot 7H_2O(c) \mid Hg_2SO_4(s) \mid Hg(l)(+)$$

where c = crystals, s = solid, l = liquid, and sat aq = saturated aqueous solution, was a one-fluid cell free of a liquid-liquid junction and exhibited relatively good stability in emf. Because of the historical importance of the Clark cell (see sec. 2) it is discussed in more detail in section 4. Owing to the success that was obtained with the Clark cell several other one-fluid cells were proposed as standards, the more important being those suggested by De la Rue [58], Helmholtz [59], Gouy [60], and Weston [30]. Of these four the first three exhibited larger drifts in emf and had higher internal resistances than Clark cells, while the last one had many advantages over the Clark cell. As a result, Weston cells are now used almost exclusively as standards of emf. Weston cells had an emf-temperature coefficient about 1/30th of that of the Clark cell, better emf stability, and an emf closer to unity than the Clark cell.

Early types of standard cells are listed in abbreviated form in table 2 together with their nominal emf and emf-temperature coefficient. As is evident from the table the Weston cell is similar to the Clark cell except that Cd replaces Zn. In all of these cells, the original Clark cell excepted, amalgamated anodes were generally recommended and H-shaped containers (see below) were frequently used. In general, saturated solutions were used and excess crystals of the stable salt added to the cells at the electrode surfaces. Weston [61] and Carhart [62] proposed the use of an unsaturated solution of zinc sulfate in the Clark cell in order to decrease its emf-temperature coefficient. The original Weston patents also covered the unsaturated form of Weston cell.

TABLE 2. *Early types of standard cells*

(represented in abbreviated form)

Name	Date	System	Approximate emf, volts	Approximate dE/dt, volt per deg C
Daniell	1836	$Zn\|ZnSO_4\|\|CuSO_4\|Cu$	1.04–1.14 (n) [1]	+0.000034 (n)
Clark	1872	$Zn\|ZnSO_4\|Hg_2SO_4\|Hg$	1.433 (15 °C)	−0.0012 (15 °C)
De la Rue	1878	$Zn\|ZnCl_2\|AgCl\|Ag$	1.03 (n)	−0.001 (n)
Helmholtz	1882	$Zn\|ZnCl_2\|HgCl\|Hg$	1.000 (15 °C)	+0.000087 (n)
Gouy	1888	$Zn\|ZnSO_4\|HgO\|Hg$	1.390 (12 °C)	−0.0014 (n)
Weston	1892	$Cd\|CdSO_4\|Hg_2SO_4\|Hg$	1.01864 (20 °C)	−0.000041 (20 °C)

[1] — n represents nominal value at room temperature (about 18 to 30 °C).

Somewhat later Brönsted [63] proposed the cell:

$$(-)Pb, Hg(l) \mid K_2SO_4 \cdot PbSO_4(c) \mid K_2SO_4(\text{sat aq}) \mid Hg_2SO_4(s) \mid Hg(l)(+)$$

as a standard, stating that at 22 °C it had an average emf of 1.0481 V and an emf-temperature coefficient of −0.0001 V/deg C. Henderson and Stegeman [64], however, stated that the Brönsted cell did not exhibit steady emfs with time and that better results were obtained when Na_2SO_4 was used as the electrolyte. However, their cell at 25 °C had a lower emf of 0.96463 V and a higher emf-temperature coefficient of + 0.000174 V/deg C. These cells have not been used probably because of their high emf-temperature coefficients. Vosburgh, Guagenty, and Clayton [65] proposed the cell:

$$(-)Cd, Bi, Hg(3p) \left| \begin{array}{l} CdSO_4 \cdot 8/3\, H_2O(c), \\ CdSO_4 \cdot Na_2SO_4 \cdot 2H_2O(c) \end{array} \right| \begin{array}{l} \text{sat aq sol of the} \\ \text{two salts in 0.1 M} \\ \text{acetic acid or in} \\ 0.01\ M\ H_2SO_4 \end{array} \left| Hg_2SO_4(s) \right| Hg(l)(+)$$

which is a modified Weston cell in which a 3-phase (3p) amalgam (8.9 percent Cd, 11.1 percent Bi, 80 percent Hg) and a 0.1 M acetic acid or 0.01 M H_2SO_4 solution saturated with the two salts, as indicated, are used. The cells were sealed with a nitrogen atmosphere inside. At 25 °C they reported an average emf of 1.0184 V and an emf-temperature coefficient of +0.000013 V/deg C which is about 2 to 10 times that of unsaturated Weston cells but less than one-third of that of the saturated Weston cell at 20 to 30 °C but of opposite sign. Data available on this cell indicate that it does not have the long-term stability exhibited by saturated Weston cells, but compares most favorably with the unsaturated type [66].

4. The Clark Cell

As stated above, the original Clark cells consisted of a zinc anode and a mercury-mercurous sulfate cathode in a saturated solution of zinc sulfate containing crystals of $ZnSO_4 \cdot 7H_2O$. Clark used a very simple construction as shown by (a) in figure 8. Various modifications of this general construction were used in commercial cells; one such modification being the British Board of Trade cell illustrated by (b) in figure 8. In all of these the zinc anode was in contact with the paste consisting of mercurous sulfate, a saturated solution of zinc sulfate, and crystals of $ZnSO_4 \cdot 7H_2O$.

Clark determined the emf of his cell in absolute units with (a) a sine galvanometer and (b) an electrodynamometer and a B. A. resistor (see footnote 7, p. 4). With these he obtained 1.45735 V and 1.45761 V, respectively, at 15.5 °C, the mean of which he rounded to 1.457 V as the absolute emf of his cell. Clark's cell, although much better as a standard than the two-fluid cells, did not show the permanency in emf hoped for. The cell tended to gas at the zinc anode and the emf showed large variations owing mainly to concentration gradients that developed, during slight changes in ambient temperatures, within the compact paste.

In 1884 Rayleigh and Sidgwick [24] introduced two modifications in the Clark cell that resulted in substantial improvements. They substituted zinc amalgam (percentage not stated) [14] for zinc and used an H-shaped container in which the zinc anode could be kept entirely under solution and out of contact with the mercurous sulfate paste. Their design is illustrated by (c) in figure 8. The zinc amalgam reduced the rate of gassing at the anode and by being under solution and out of contact with the mercurous sulfate paste the zinc anode exhibited more nearly constant potentials. Rayleigh and Sidgwick obtained 1.453 V for the absolute emf of their cells at 15 °C using a current balance (now known as a Rayleigh balance) and a B.A. resistor.

[14] Rayleigh and Sidgwick presented their paper in June 1884; in the paper published in Dec. 1884 they added the note "Some H-cells have been set up Mr. Threlfall, with amalgams of known composition, varying from 1/32 zinc to 1/5 zinc by weight. The duration of the test has as yet been scarcely adequate, but it appears that the smaller quantity of zinc is sufficient." In general, Clark cells were made, at a later date, with 7 to 10 percent amalgams.

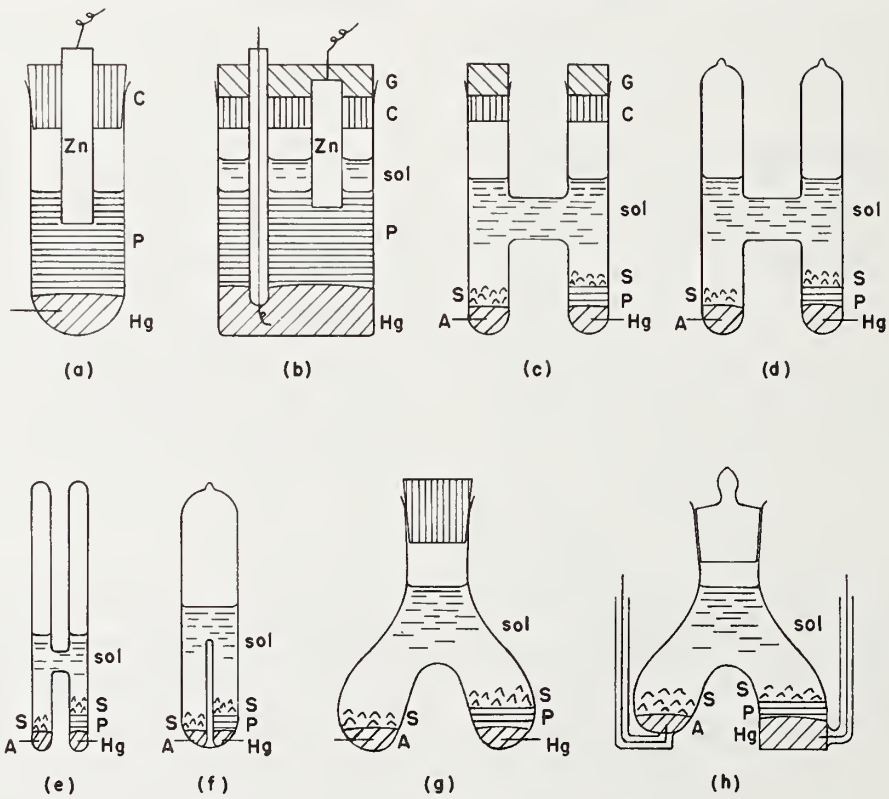

FIGURE 8. *Various forms of standard cell containers.*

(a) Original Clark cell
(b) Board of Trade (British) Clark cell
(c) Rayleigh-Sidgwick H-shaped Weston cell
(d) Sealed H-shaped cell
(e) Hulett H-shaped cell
(f) Modified Hulett container
(g) Wright-Thompson container
(h) Cooper container

Zn—zinc
Hg—mercury
P—mercurous sulfate paste
C—cork
G—glue
sol—solution
A—amalgam
S—salt crystals

These cells tended to leak in time, and Callendar and Barnes [67] recommended their hermetic sealing, (d) in figure 8. Other types of cell containers, also used for Weston cells, have been proposed and are illustrated in figure 8. Hulett [68] proposed a shorter crossarm (e) and today some cells are made with no crossarm but with a partition at the base of a single tube (f). Wright and Thompson [69] proposed the inverted-Y form, hermetically sealed, and Kahle [70] the same form but with a cork or ground-glass stopper (g); these are more difficult to fill. Cooper [71] proposed a modified Kahle type (h) which required no support in a thermostatically-controlled bath; his form could rest on a flat surface without support. The Cooper cell could also be used in water as well as in non-conducting oil because the cell terminals were not exposed but protruded above the bath fluid. Today, the H-shaped container, hermetically sealed, is used most widely; some single-tube types, either like (f) or in a modified form of the original design (a) are also made.

The reaction in the saturated Clark cell made with amalgamated anodes is:

$$x\mathrm{Zn},(y\mathrm{Hg})(2p)+\mathrm{Hg_2SO_4}(s)+\frac{7}{m-7}(\mathrm{ZnSO_4}\cdot m\mathrm{H_2O})(\mathrm{sat\ aq})$$

$$=\frac{m}{m-7}(\mathrm{ZnSO_4}\cdot 7\mathrm{H_2O})(c)+2\mathrm{Hg}(l)+(x-1)\mathrm{Zn},\ y\mathrm{Hg}(2p) \quad (5)$$

where x = moles of Zn associated with y moles of Hg in the amalgam, $2p$ = 2-phase, and m is the number of moles of water associated with 1 mole of $ZnSO_4$ in the saturated solution. Ten-percent amalgams are most commonly used; they are of two phases, solid and liquid, with the solid phase being pure zinc (see fig. 9) [72]. The composition of the liquid phase of a 10 percent zinc amalgam at various temperatures is given in column 2 of table 3.

The solubility of zinc sulfate in water changes considerably with temperature. Above 39 °C the stable sulfate is $ZnSO_4 \cdot 6H_2O$; below 39 °C it is $ZnSO_4 \cdot 7H_2O$. The solubility of $ZnSO_4 \cdot 7H_2O$ in water from 0 to 39 °C is given in table 4. In saturated solution zinc sulfate hydrolyzes to give a solution containing 0.004 N sulfuric acid and having a pH of 3.35 at 25 °C [73]. This concentration of acid is sufficient to prevent the hydrolysis of the mercurous sulfate used in the positive electrode (see later).

The emf of the Clark cell decreases as the temperature is increased; the decrease is about 0.1 percent per degree C. For the range 0 to 28 °C Callendar and Barnes [67] gave, in volts:

$$E_t = E_{15^\circ} - 0.0012(t-15\ ^\circ) - 0.0000062(t-15\ ^\circ)^2 \quad (6)$$

for the dependence of the emf on temperature. At 15 °C and 25 °C this relation gives −0.00120 V/deg C and −0.001076 V/deg C, respectively, for dE/dt. Kahle [74] and Jaeger and Kahle [75] who also studied the temperature dependence of Clark cells obtained results in substantial agreement with eq (6).

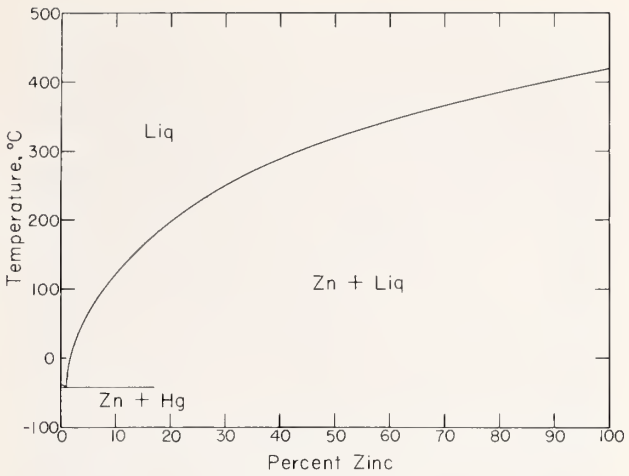

FIGURE 9. *Phase diagram for the zinc-mercury system.*

TABLE 3. *Composition of the liquid phases of 10 percent zinc and cadmium amalgams*

Temperature, °C	Percentage of zinc	Percentage of cadmium
0	1.35	2.50
10	1.60	3.70
20	1.99	5.00
30	2.40	6.40
40	2.90	7.80

TABLE 4. *Solubility of* $ZnSO_4 \cdot 7H_2O$ *in water*

Temperature °C	$ZnSO_4$ in 1000g H_2O,
	grams
0	419
5	446
10	477
15	509
20	542
25	579
30	620
35	663
39[a]	701

[a]—transition temperature, $ZnSO_4 \cdot 7H_2O = ZnSO_4 \cdot 6H_2O$.

The Clark cell has three advantages over the Weston cell, namely, (1) zinc sulfate hydrolyzes to produce sufficient sulfuric acid to prevent the hydrolysis of the mercurous sulfate paste; it, thereby supplies its own buffering action, (2) the solid phase of the amalgam is a single component (zinc) whereas in the Weston cell the solid phase is a solid solution of cadmium and mercury; the emf of the Clark cell is less dependent, therefore, on the composition of the amalgam than is the Weston cell, and (3) the Clark cell shows less emf-temperature hysteresis than the Weston cell. However, the disadvantages of the Clark cell over the Weston cell well outweigh its advantages. These are: (1) The Clark cell tends to gas at the amalgam electrode. This gas, as it forms slowly over the surface of the amalgam, may dislodge crystals of $ZnSO_4 \cdot 7H_2O$ with adhering solution from over the amalgam, and may eventually cause an open-circuit in the electric circuit unless a

constriction, as discussed later, is used in the container at the level of the crystals. (2) Zinc amalgam slowly alloys with the platinum lead at the base of the amalgam electrode. Since this alloy occupies more space than the platinum, strains are produced, and breakage of the glass container follows. (3) The Clark cell has an emf-temperature coefficient which is about 30 times that of the Weston cell. (4) Owing to the relatively large change in the solubility of zinc sulfate with changes in temperature crystals of $ZnSO_4 \cdot 7H_2O$ tend to pass from the positive to the negative limb of the cell. During a temperature rise the volume of electrolyte over the positive electrode becomes saturated more quickly because it is usually a smaller volume than that over the negative electrode. As a result a concentration difference between the limbs results and diffusion of electrolyte to the negative limb takes place until the concentration difference is dissipated. This phenomenon can be prevented by making the volume above the negative and positive electrodes equal. A similar phenomenon does not occur in Weston cells because the change in solubility of cadmium sulfate with temperature is much less than that of zinc sulfate. (5) The Clark cell has an emf which is considerably higher than unity which, although not necessarily a disadvantage, makes its use as a standard less convenient than a Weston cell.

The emfs of saturated Clark cells are decreased by addition of sulfuric acid to the electrolyte. Some data based on measurements of Hulett [76] are given in table 5.

TABLE 5. *Effect of sulfuric acid on the emf of Clark cells at 25 °C*

Normality of sulfuric acid[a]		Change in emf.
Before saturation with $ZnSO_4 \cdot 7H_2O$	After saturation with $ZnSO_4 \cdot 7H_2O$	
		volt
0.2024	0.1074	−0.00028
1.012	0.5400	−0.00233
2.024	1.1488	−0.00448

[a]—normality of acid in a saturated solution of pure zinc chloride at 25 °C is 0.004 *N* [73].

5. The Weston (or Cadmium Sulfate) Cell

5.1. General

The Weston (or cadmium sulfate) cell is, for all intents and purposes, the only electrochemical system used today as a standard cell. Accordingly, the words "standard cell" when used today invariably mean cadmium sulfate cells, and the remainder of this Monograph, appendices excepted, relates to this type of cell. The cell is made in two general types, saturated and unsaturated where these terms refer to the state of the electrolyte. The saturated type is the precision cell used in the maintenance of the unit of emf. It may be made in a highly reproducible form and exhibits a constant emf for long periods of time. However, for high precision it must be maintained at a constant temperature owing to its relatively high emf-temperature coefficient. Most saturated cells must be hand carried, although some recent types have been made shippable by locking the electrodes in place with inert and porous septa. The unsaturated cell is less stable than the saturated type in that its emf decreases slowly with time and is regarded as a reference of d-c voltage known within ±0.005 percent. It is usually made in a shippable form with a septum over each electrode. It has a low emf-temperature coefficient and accordingly is used widely in ambient temperatures as an emf reference where 0.005 percent (0.05 mV) accuracy suffices.

The saturated cell is also known as the Weston Normal Cell (or Element). It consists of a cadmium amalgam anode and a mercury-mercurous sulfate cathode in a saturated solution of cadmium sulfate with crystals of $CdSO_4 \cdot 8/3H_2O$ over the surface of both electrodes. This cell may be represented by:

$$(-)\text{Cd, Hg}(2p)|\text{CdSO}_4\cdot 8/3|\text{H}_2\text{O}(c)|\text{CdSO}_4(\text{sat aq})|$$
$$\text{CdSO}_4\cdot 8/3\ \text{H}_2\text{O}(c)|\text{Hg}_2\text{SO}_4(s)|\text{Hg}(l)(+)$$

where the symbols have the same significance as given above. The cell reaction is:

$$x\text{Cd}, y\text{Hg}(2p) + \text{Hg}_2\text{SO}_4(s) + \frac{8/3}{m-8/3}(\text{CdSO}_4 \cdot m\text{H}_2\text{O})(\text{sat aq})$$
$$= \frac{m}{m-8/3}(\text{CdSO}_4 \cdot 8/3\text{H}_2\text{O}(c) + 2\text{Hg}(l) + (x-1)\text{Cd}, y\text{Hg}(2p). \quad (7)$$

where x moles of Cd are associated with y moles of Hg in the amalgam and m is the number of moles of water associated with 1 mole of $CdSO_4$ in the saturated solution. At the end of the reaction the amalgam may be two phases (liquid and solid) or may be a liquid phase only, depending on the extent of the reaction and the relative amounts of amalgam and mercurous sulfate used in preparing the cell. When not discharged, as is normal when the cell is used as an emf standard, the amalgam remains in two phases. Cells are usually made with 10 or 12½ percent amalgams (see later).

The unsaturated cell differs from the saturated type only in that an unsaturated solution of cadmium sulfate and no crystals of $CdSO_4 \cdot 8/3H_2O$ are used. It is customary to use a solution that is saturated at 3 or 4 °C, the temperature range at which the salt exhibits a minimum solubility; the solution is then unsaturated at higher temperatures. The emf of the unsaturated cell at ambient room temperature is about 0.05 percent higher than that of the saturated type. The cell reaction is simply:

$$x\text{Cd}, y\text{Hg}(2p) + \text{Hg}_2\text{SO}_4(s) = \text{CdSO}_4(\text{aq}) + 2\text{Hg}(l) + (x-1)\text{Cd}, y\text{Hg}(2p) \quad (8)$$

unless the reaction is continued until crystals of $CdSO_4 \cdot 8/3H_2O$ are formed; then the reaction is the same as in the saturated cell. Again, when the cell is not discharged, as is normal when the cell is used as an emf standard, the solution remains unsaturated and the amalgam in two phases.

Both saturated and unsaturated standard cells have been made as "neutral" or as "acid" cells; the saturated "neutral" type is also known as the Weston Normal Cell. These terms refer to the degree of acidity of the electrolyte with respect to sulfuric acid in the cell. If an aqueous solution of pure cadmium sulfate, to which no sulfuric acid is added, is used in the preparation of the cell, the cell is called a "neutral" type, even though the *p*H of a saturated aqueous solution of cadmium sulfate, owing to hydrolysis, is 4.00 at 25 °C [73]. If sulfuric acid is added in sufficient amount to make the acidity 0.03 *N* to 0.1 *N*, the cell is called an "acid" type. The purpose of adding the acid to the electrolyte is to prevent hydrolysis of the mercurous sulfate used in the cell; more details are given later. Today, most, if not all, cells are made of the "acid" type.

5.2. Preparation and Properties of Materials

The procedures employed at the National Bureau of Standards for the preparation and purification of materials for use in the construction of standard cells are described in the next few sections. In addition some properties of the materials, as they relate to standard cells, are given. Only four materials are required. These are mercury, cadmium, sulfuric acid, and water, all of which may be purified by distillation. To these four materials may be added a fifth, $CdSO_4 \cdot 8/3\ H_2O$, to avoid preparing it from cadmium and sulfuric acid; it may be purified by repeated crystallizations from conductivity water.

Mercury of good grade, after washing in dilute nitric acid, then in distilled water, is dried and then distilled in a Hulett [77] still in a stream of dry air. In this method, the mercury is distilled near 200 °C in a partial vacuum, air being drawn through the condenser at a rate to maintain the air pressure at 25 mm, corresponding to an oxygen partial pressure of 5 mm. Any metallic vapor, except mercury, is oxidized and collects as a scum on the distillate which is removed by filtering through a fine pinhole in filter paper. Metals more noble than mercury remain in the boiler of the still. Finally, the mercury is redistilled in a vacuum still. Procedures for purification of mercury of various grades are outlined in reference [78].

Cadmium of electrolytic grade is sublimed under reduced pressure. The sublimation is done at about 350 to 400 °C in an evacuated Pyrex glass tube with an external electrical heating jacket. The distilled cadmium crystallizes out on the cooler parts of the tube but frequently adheres tightly to the glass walls. It is usually necessary to break the glass walls to remove the distilled cadmium adhering to the walls.

Sulfuric acid of reagent grade is twice distilled in an all-Pyrex still at a temperature of 270 to 290 °C with the middle fraction being retained. Glass beads are placed in the boiler to reduce bumping and the distillation is carried out in a hood.

Water is repeatedly distilled in a Barnstead or comparable still until the conductivity of the water becomes as low or lower than 1×10^{-6} ohm^{-1} cm^{-1}. This water is frequently called "conductivity water."

Cadmium sulfate ($CdSO_4 \cdot 8/3\ H_2O$) of high grade is obtained by several recrystallizations of the C.P. salt. These recrystallizations are carried out from aqueous solutions below 43.6 °C [79] since above this temperature the stable salt is the monohydrate, $CdSO_4 \cdot H_2O$. Cadmium sulfate of high grade may also be prepared from pure cadmium and redistilled sulfuric acid solutions or from pure cadmium nitrate and redistilled sulfuric acid solutions, followed by recrystallizations of the salt from aqueous solutions in each case. The latter method is preferred rather than the use of very impure cadmium sulfate as starting material.

Both hydrates, $CdSO_4 \cdot 8/3\ H_2O$ and $CdSO_4 \cdot H_2O$, are highly soluble in water; the solubility of the former increases with temperature while that of the latter decreases. The solubilities of each as a function of temperature are given in table 6 [79, 80, 81]. The solubilities are expressed as the number of grams of the anhydrous salt in 1000 g of water.

Saturated solutions of $CdSO_4 \cdot 8/3\ H_2O$ begin to freeze at −17 °C and become completely frozen at −24 °C; these temperatures, then, represent the lower limit for the use of cadmium sulfate cells (see later). It has been reported [82] that $CdSO_4 \cdot 8/3\ H_2O$ shows a transition to $CdSO_4 \cdot 7H_2O$ at 4 °C. However, cells tested in this temperature range do not exhibit an abrupt inflection in emf at 4 °C indicative of a phase change but a smooth maximum in the range of 3 to 4 °C indicative of a minimum solubility in cadmium sulfate (see table 6).

The amalgam may be prepared either electrolytically by depositing cadmium in mercury or by heating the two metals together. In the former, crystals of purified $CdSO_4 \cdot 8/3H_2O$ are placed on the surface of mercury (contained on the bottom of a beaker) and covered with distilled water acidified with a few drops of sulfuric acid. Mercury is made

TABLE 6. *Solubility of* $CdSO_4 \cdot 8/3H_2O$ *and* $CdSO_4 \cdot H_2O$ *in aqueous solution*

(given as grams of $CdSO_4$ in 1000 grams of water)

Temperature, °C	$CdSO_4 \cdot 8/3\ H_2O$ (as $CdSO_4$)	$CdSO_4 \cdot H_2O$ (as $CdSO_4$)
−18	767.6	.....
−15	765.3	.....
−10	762.1	.....
− 5	759.2	.....
0	757.5	.....
3	757.2	.....
5	757.5	.....
10	759.4	.....
15	761.4	.....
20	763.7	.....
25	766.9	.....
30	771.0	.....
35	776.5	.....
40	783.8	.....
42	787.2	.....
43.6 [a]	790.5	.....
45	793.5	786.5
50	806.1	770.6
55	.....	754.7
60	.....	738.9
65	.....	722.0
70	.....	707.0
72	.....	700.0

[a]—transition temperature.

the cathode and a platinum foil suspended in the acidified solution at the top serves as anode. Usually only the amount of $CdSO_4 \cdot 8/3\ H_2O$ needed to prepare an amalgam with the desired percentage of cadmium is used. Since the crystals dissolve slowly, a current of low magnitude is used initially until nearly all the cadmium is deposited. The current is then increased to about 5 times the initial value for 30 minutes, and then, with the current still flowing, washing with distilled water is started. Water is successively added and decanted until the current decreases to less than 0.01 A for an impressed voltage of 110 V. The remaining water is then siphoned off and the last drops of water removed from the surface of the amalgam by filter paper. A cadmium rod may be used as anode in an alternative procedure; the amount of cadmium deposited in the mercury is determined from the current and time by Faraday's law.

The method in which the two metals are heated together is more convenient. The proper weights of the two metals are heated together in a covered porcelain casserole, in a hood, until completely melted and homogeneous. A slight scum may form on the surface. This is brushed aside and the liquid amalgam immediately transferred to an electrically heated covered buret and introduced directly to the cell through an electrically heated delivery tube. Any small amount of scum on the surface of the amalgam will disappear as soon as acidified cadmium sulfate is added to the cell. This is the method now used at the National Bureau of Standards.

No difference in the properties of standard cells containing amalgams prepared by these methods has been observed.

Amalgams exhibit less erratic behavior and corrode less rapidly, if at all, than pure unamalgamated metals when in contact with aqueous solutions of their salts. Amalgamation raises the hydrogen overvoltage of metals and reduces stresses within the metal. It is for these reasons that amalgams make better anodes for standard cells than the pure metals. A 10 or 12½ percent amalgam is generally used commercially in constructing cadmium sulfate cells. A 10 percent amalgam is now used by the National Bureau of Standards. These are weight percentages. At normal temperatures amalgams of these precentages consist of two phases, a liquid and a solid phase. The solid phase is a solid solution of cadmium and mercury. The phase diagram [83] for the cadmium-mercury system is given in figure 10. The composition of the liquid phase of a 10 percent amalgam is listed for various temperatures in column 3 of table 3.

Mercurous sulfate may be prepared in a number of ways. Shortly after Weston patented his cell much research was devoted to methods of preparing and storing mercurous sulfate and cells made with various preparations were extensively studied. Some samples were white, i.e., devoid of free mercury while others were gray in appearance owing to the presence of finely dispersed mercury. Some samples were thoroughly washed with absolute alcohol and anhydrous ether and dried *in vacuo* while other samples were kept moist with either dilute sulfuric acid or saturated solutions of cadmium sulfate acidified slightly with sulfuric acid.

Mercurous sulfate may be prepared in a number of ways as follows:

(1) By the reaction between sulfuric acid and mercurous nitrate [84].
(2) By the action of fuming sulfuric acid on mercury [84].
(3) By the action of dilute nitric acid in sulfuric acid on mercury [44, 84].
(4) By the reduction of mercuric sulfate by mercury [44].
(5) By the reduction of mercuric sulfate by sulfurous acid [44].
(6) By the reduction of mercuric sulfate by formaldehyde [85].
(7) By the recrystallization of commerical mercurous sulfate from sulfuric acid [84].
(8) By a-c electrolysis [86].
(9) By d-c electrolysis [44, 68].

Of these methods standardization has been on the last one which is now used by the National Bureau of Standards. By d-c electrolysis uniform samples of mercurous sulfate of high purity and reproducible grain size are obtained. Such samples are free of all foreign materials except sulfuric acid, water, and mercury, all of which are used in standard cells, and especially in the mercurous sulfate paste. In this method [44, 68] mercury anodes, platinum cathodes, and a 1:6 sulfuric acid-water solution are used and electrolysis is carried out in a darkened room (see sec. 7.7). Mercury is placed on the bottom of one or two shallow glass vessels. These vessels are then placed on a glass stand one above the other, as shown in figure 11, in a deeper and larger dish ⅔ filled with the sulfuric acid solution; the acid solution extends over the shallow vessels. The upper dish contains a central glass tube through which passes the shaft for the stirrer for the lower dish; obviously this is unnecessary if only one shallow dish were used. A platinum-foil cathode is placed near the top of the solution. The solution is vigorously stirred at 70 to 200 rpm and

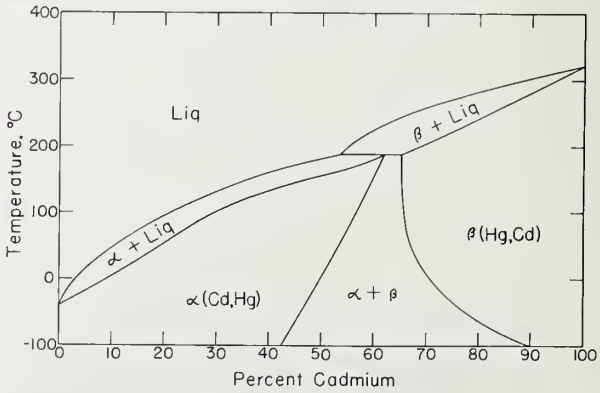

FIGURE 10. *Phase diagram for the cadmium-mercury system.*

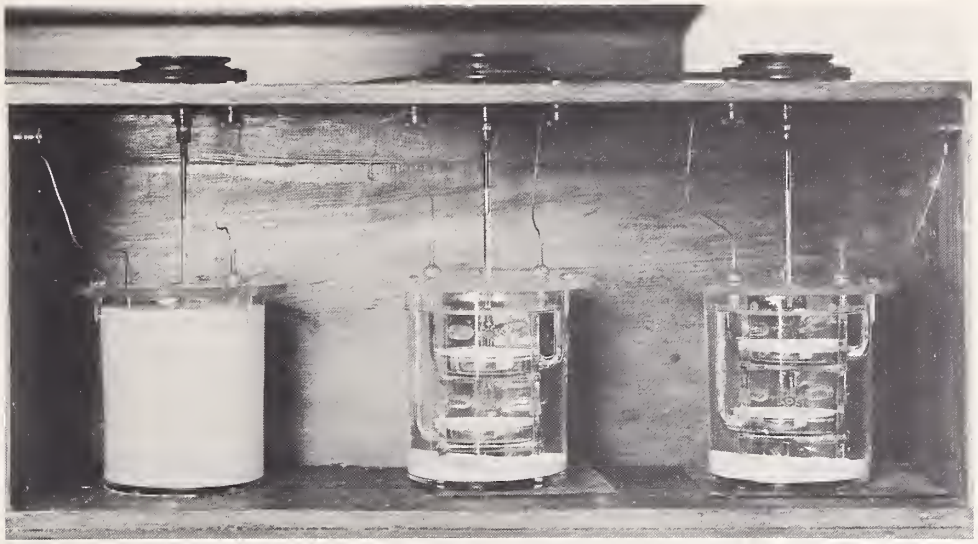

FIGURE 11. *Views of the electrolytic preparation of mercurous sulfate.*
Left vessel—stirrer in operation, cloudiness due to mercurous sulfate suspended in solution. Center and right vessels—stirring stopped, mercurous sulfate at bottom of vessels and on surface of mercury in dishes.

the current density at the mercury surface is maintained at 1 to 2 A per 100 cm ^{2}. When the electrolyte becomes saturated with mercurous sulfate the solid salt appears on the surface of the mercury and must be swept off into the outer dish by stirring in order to keep the surface of the mercury anode clean. In this stirring finely divided mercury becomes mixed with the mercurous sulfate to give a gray product. Electrolysis is continued until the desired amount of gray mercurous sulfate has been prepared; the current is then cut off but stirring is continued for several hours. Photographs of the electrolytic production of mercurous sulfate are shown in figure 11.

For "neutral" cells the mercurous sulfate is then washed repeatedly with a saturated solution of cadmium sulfate and then stored under such a solution until used. For "acid" cells the mercurous sulfate is stored under the electrolysis solution until needed at which time it is washed thoroughly with the solution of the type to be used in the cells.

Mercurous sulfate is the oxidizing agent or the "depolarizer" used in Weston cells. It is highly insoluble in water and in dilute solutions of sulfuric acid. The solubility of mercurous sulfate, expressed in terms of mercury, in various concentrations of sulfuric acid is listed in table 7 at 0 and 28 °C [87]. In aqueous solutions mercurous sulfate hydrolyzes according to the reaction:

$$2Hg_2SO_4(s) + H_2O(l) = Hg_2O \cdot Hg_2SO_4(s) + H_2SO_4(aq) \quad (9)$$

to form a basic salt, $Hg_2O \cdot Hg_2SO_4$, and an equilibrium amount of sulfuric acid. Gouy [88] and Hager and Hulett [89] found this concentration to be 0.002 N while Craig, Vinal, and Vinal [87] showed that it did not change appreciably with temperature, being 0.00198 N at 0 °C and 0.00216 N at 28 °C. Although, theoretically, a concentration slightly exceeding the equilibrium concentration could be used to prevent the hydrolysis of mercurous sulfate, a higher concentration is recommended. In initial studies [90], solutions 0.03 N to 0.06 N with respect to sulfuric acid were used, in part because mercurous sulfate exhibits a minimum solubility in the range from 0.04 to 0.08 N. (Hulett [91] and Sir Frank Smith [92] found the minimum solubility of mercurous sulfate to be at approximately 0.04 N, while Craig, Vinal, and Vinal found it to be at 0.06 N at 28 °C and 0.08 N at 0 °C.) Now, the lower acidity value is preferred since cells with the lower acidity have shown the greater stability in emf. Cells with 0.10 N acid, for example, tend to gas as a result of the action of the acid with the cadmium amalgam.

Concentrations of sulfuric acid somewhat higher than the equilibrium value are chosen, not only because of the decrease in the solubility of mer-

TABLE 7. *Solubility of mercurous sulfate in aqueous solutions of sulfuric acid*

Molarity of H_2SO_4	Grams of Hg per 100 ml		Molarity of H_2SO_4	Grams of Hg per 100 ml	
	t = 0 °C	t = 28 °C		t = 0 °C	t = 28 °C
0.002	0.0290	0.0463	0.100	0.0183	0.0344
.004	.0239	.0395	.200	.0198	.0379
.006	.0215	.0360	.300	.0212	.0403
.008	.0203	.0346	.400	.0224	.0423
.010	.0197	.0338	.500	.0233	.0438
.020	.0182	.0318	.600	.0239	.0451
.030	.0179	.0313	.700	.0244	.0461
.040	.0178	.0317	.800	.0247	.0467
.050	.0178	.0322	.900	.0248	.0470
.060	.0178	.0327	1.000	.0249	.0470
.070	.0179	.0332	2.000	.0240	.0409
.080	.0180	.0337	3.000	.0139	.0294
.090	.0181	.0341	4.000	.0078	.....

curous sulfate but because the acid decreases the rate of solubility of the glass container by the electrolyte. It is well known that glasses are more soluble in neutral salt or alkaline solutions than in acidic ones [93, 94]. The final solution is titrated against sodium hydroxide using methyl purple as an indicator, which has a pH transformation interval of 4.8 to 5.4 [95].

5.3. Containers for Standard Cells

Saturated standard cells as made at the National Bureau of Standards are of the H-form shown in figure 12. Photographs of a cell container and a completed cell constitute figure 13. The container is made of Kimble Standard Flint glass, a chemically resistant soda-lime glass, having an average linear thermal expansion coefficient of 92×10^{-7} per degree C. (The coefficient of linear thermal expansion is the increase in length per unit length, measured at 0 °C, per degree Celsius.) Since this linear thermal expansion coefficient approximates that of platinum, 89×10^{-7} per degree C, vacuum-tight seals are obtained at the platinum leads. No lead-containing sealing-in glass is used in sealing in the platinum leads at the bottom of each limb as the solution may extract the lead leading to cell deterioration. On the average the height of the cell is about 92 mm, the diameter of the vertical limbs about 16 mm, the diameter of the cross-arm about 11 mm, and the distance between limbs about 22 mm. A constriction is made near the base of both limbs, as shown, to lock in part of the crystals of $CdSO_4 \cdot 8/3H_2O$. The constriction may be a complete circumferential indentation or may consist of several knobs directed inward. The constrictions are so placed that crystals of $CdSO_4 \cdot 8/3H_2O$ are both below and above them. These locked crystals prevent the displacement of the materials in the cell limbs, and those at the anode help prevent an opening of the circuit within the cell by any gas that might form on the amalgam. The platinum leads are secured by cotton thread to the side of each limb at the constrictions and cemented in place by collodion; platinum leads have a tendency to break mechanically at the glass seal if not securely held in place. For permanent records a number is etched on each cell on the outside wall of the container with hydrofluoric acid. Prior to filling with cell constituents the container is thoroughly cleaned with nitric acid, rinsed with distilled water, steamed, and then dried at 110 °C.

At various times attempts have been made to use Pyrex for cell containers. However, since Pyrex has an average linear thermal expansion coefficient of 32×10^{-7} per degree C tungsten which has a linear thermal expansion coefficient of 43×10^{-7} per degree C must be used for external electrical connections to assure vacuum-tight seals. Tungsten, however, is more brittle than platinum and a number of cells have had to be discarded because of breaks at the tungsten-Pyrex seal.

Fused silica, owing to its extreme inertness, has frequently been suggested for standard-cell containers. Fused silica, however, has two major drawbacks. It has such a low linear thermal expansion coefficient (5×10^{-7} per degree C) that the electrical leads have to be brought into the cell in a special way. Also, a very high temperature must be employed to seal the cell; the chemicals within the cell may thereby be affected. These two drawbacks have been solved by the cell design [96] shown in figure 14. The main features of this design are (1) the use of two seals at each arm and (2) a graded seal between the fused silica and Pyrex at the top of each limb of the container. The use of the graded seals makes possible the sealing of the cell at a low temperature after filling. Transparent silica is used to facilitate the filling of the cells. The two seals at each arm are spaced about 7 cm

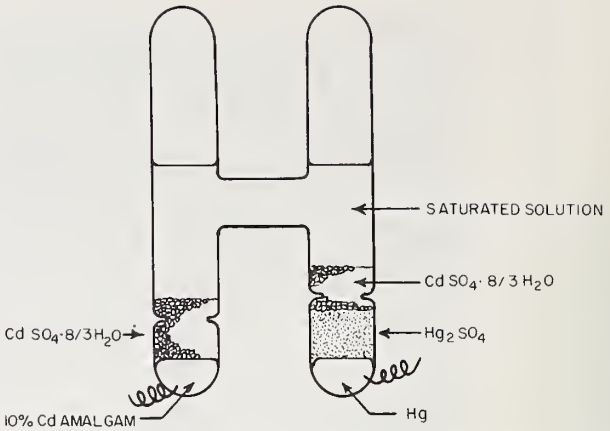

FIGURE 12. *Sketch of a saturated standard cell of the cadmium sulfate type (National Bureau of Standards type).*

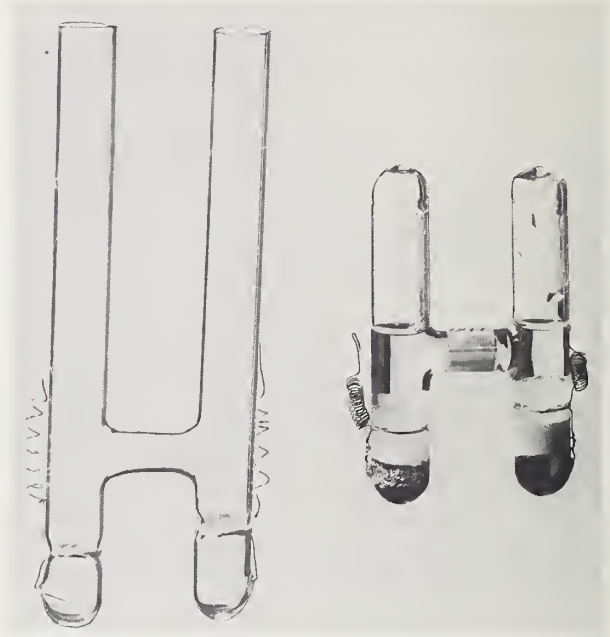

FIGURE 13. *Photograph of container and completed saturated standard cell of cadmium sulfate type (National Bureau of Standards types).*

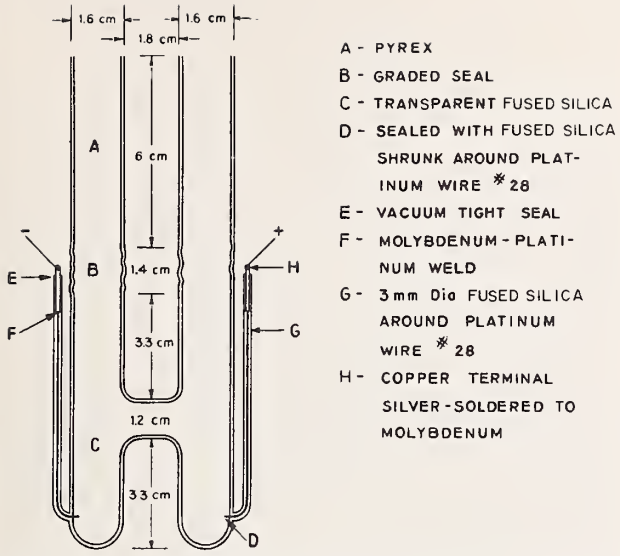

FIGURE 14. *Cross-sectional sketch of standard-cell container made of fused silica.*

apart. The lower seal consists of platinum wire No. 28 sealed in silica, and although this seal is not vacuum-tight it is sufficiently tight to retain the cell constituents. The upper vacuum-tight seal is a Houskeeper [97] type and consists of molybdenum ribbon sealed in silica (this type of seal cannot be used as the lower seal since molybdenum is chemically attacked by the cell constituents). The molybdenum ribbon and platinum wire are welded at a point about 2 cm below the upper seal. Silica is shrunk around the weld, the molybdenum ribbon, and platinum wire. Copper terminals are used and are silver-soldered to the molybdenum ribbon. Errors that might arise from thermoelectric effects are prevented by completely immersing the cells in oil at a constant temperature. Dimensions of the cell are included with the figure.

Although it has been generally thought that interactions between the glass container and the cell electrolyte cause "aging" or drifts in the emf of standard cells, available data have not shown significant differences between cells made in soft glass, Pyrex, or fused silica on a long-term basis. Plastic containers have also been proposed [98]. These must prevent vapor transport or a drying out of the cells may occur.

5.4. Assembly and Mounting of Standard Cells

Two long-stemmed funnels, one sliding through the other, are employed at the National Bureau of Standards for introducing materials into the container. The inner funnel carries the material and the outer one serves to prevent the material from coming into contact and "mussing up" the walls of the container. After introducing the material the stem of the inner funnel is drawn up into the stem of the outer funnel; both funnels may then be withdrawn from the cell without any of the material touching the container walls.

Mercury is first placed in the bottom of one limb and the amalgam in the bottom of the other limb, each to a depth of about 6 mm. The amalgam is added while warm and in a single liquid phase; on cooling the amalgam becomes two-phased, solid and liquid. The mercurous sulfate is then placed in a Gooch or similar crucible, washed free of the solution under which it was stored with dilute sulfuric acid and then washed with solution of the type to be used in the cell, and then while moist introduced over the mercury to a depth of about 13 mm. The mercurous sulfate should be mixed with a small amount of mercury (partially done during the electrolytic preparation of mercurous sulfate) and finely divided crystals (fineness of granulated sugar) of $CdSO_4 \cdot 8/3H_2O$ prior to introduction to the cell; this mixing may be done prior to the washing procedure. The mixing and washing of the mercurous sulfate paste hastens the attainment of chemical equilibrium within the cell after its assembly.

Crystals of $CdSO_4 \cdot 8/3H_2O$, of a size that will pass through a tube of 4-mm bore, are then added to both limbs of the cell to a depth of about 10 mm at the negative electrode and about 8 mm at the positive electrode. Finally, a saturated solution of $CdSO_4 \cdot 8/3H_2O$ is added to a level slightly above the crossarm, and the cell is then hermetically sealed.

In some cells, especially of larger size, large crystals (about 10 to 15 mm in diameter) of $CdSO_4 \cdot 8/3H_2O$ are used. Larger crystals have an advantage over smaller crystals in that any gas that may form at the electrode surface (especially the negative one) will not become entrapped by the crystals whereby an open circuit might be produced. However, cells with large crystals tend to come to equilibrium, after a temperature change, more slowly than those made with small crystals.

Unsaturated cells are made similarly except that no crystals of $CdSO_4 \cdot 8/3H_2O$ are used and they are made portable (shippable) by inserting cork or plastic rings, covered with linen, over the electrode surfaces. In some cells ceramic discs, either locked in place or supported by ceramic rod which protrudes through stoppers in each limb, are used [99,100]. The unsaturated cell is the commercial type used widely in the United States for work requiring no greater accuracy than ± 0.005 percent; it is not made at the National Bureau of Standards. It is used for pyrometer work, in pH meters, recording instruments, etc., and is usually housed in nontransparent copper-shielded cases for general laboratory work. A copper-shielded case is employed to assure a uniform temperature at both limbs of the cell (see later). Saturated cells are not mounted in cases since they are intended for immersion in temperature-controlled oil or air baths. Commercial saturated cells are usually mounted in groups of 3, 4, or 6 on special racks

for convenience in use. NBS saturated cells are mounted in oil as described above in section 2.3.

In practice, saturated standard cells are maintained at a constant temperature in thermostatically controlled oil baths or in portable thermostatically controlled air boxes. The latter are generally made after a design first proposed by Mueller and Stimson [101]. The cells are housed in a thin-walled aluminum box which rests in a larger thick-walled aluminum box, the temperature of which is controlled by a mercury-in-glass thermoregulator. The aluminum boxes are thermally insulated and are enclosed in a wooden box which also contains an a-c relay, a transformer, and a pilot light. The box is operated on 110 V 60-cycle a-c line. The leads from the individual cells are brought to binding posts on the outside of the box. These boxes are designed to operate at temperatures above room temperature; the choice of temperature depends on the location where the boxes will be used or on the size of the box. As a rule these boxes operate at some temperature between 28 and 37 °C. The temperature of the cells in the air box is measured by a mercury-in-glass thermometer provided with the box. In some boxes, a well is added to provide for a platinum-resistance thermometer in which case the temperature is so measured. A detailed description of a Mueller-Stimson box is given in Appendix 7.

5.5. Electromotive Forces of Newly Made Cells

Cells when first made will, except in the most rare cases, exhibit emfs that will differ considerably from the final steady values. Values steady to 0.01 mV or 10 μV are usually obtained within a few days but one to three years may be required before values steady to 0.1 μV are attained. In some cases the emfs decline in their approach to equilibrium, in other cases they increase. There are two main reasons for this "aging" process, namely, (1) equalization of acid throughout the cell and especially within the mercurous sulfate paste, and (2) attainment of solution saturation. Although attempts are made to take care of both of these during cell assembly, inequalities in acid concentration may readily occur during the filling process owing to evaporation; and since the preparation of solutions of cadmium sulfate which are truly saturated is an extremely slow process unsaturated solutions may inevitably be used in preparing cells. Cells that "age" with a decrease in emf probably have been made with unsaturated solutions, even though crystals of $CdSO_4 \cdot 8/3H_2O$ are present, or have too much acid in the negative limb while those that increase in emf during "aging" probably have excess acid in the positive limb. Also, the reaction between the electrolyte and the glass container probably contributes to "aging" since as the glass neutralizes some of the acid in the cell the emf will increase. However, this reaction eventually ceases as is shown by the emf stability of cells which have been "aged" (see later). If reproducibility of 0.01 mV in emf is considered adequate, all of these factors are inconsequential.

Cells within any one group, although made at the same time of the same materials, may have emfs that differ by as much as 0.005 mV (or 5 μV). These differences may not only be present initially but may persist for years; i.e., individual cells, although differing in emf may show high stability in emf. Although diffusion is a slow process, acid or solution concentration inequalities within any one cell cannot explain these differences. Instead they must arise (1) from slight differences in the composition of the amalgam between cells (see fig. 15, especially the horizontal sections; this figure is discussed in sec. 6.3) even though precautions are taken to keep the amalgam homogeneous during the filling process, (2) from slight differences in the acidity of the solutions between cells produced during the filling process or in interactions with the glass containers, and/or (3) to slight differences between cells in the grain size of the mercurous sulfate used in the positive electrodes.

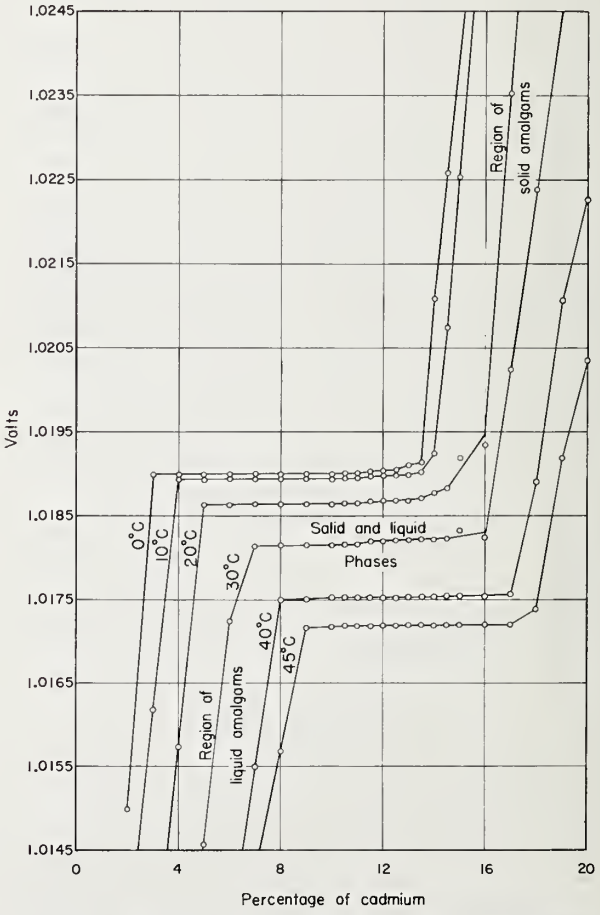

FIGURE 15. *Relation of the electromotive force of the cadmium sulfate standard cell to the percentage of cadmium in the amalgam and the temperature.*

6. Effect of Variations in Components on the Electromotive Force of Standard Cells

6.1. Concentration of Solution

The emf of cadmium sulfate cells depends on the concentration of the cadmium sulfate solution. Over a limited range of concentration near saturation the emf increases about 0.0017 V for a one percent decrease in cadmium sulfate content. For more dilute solutions the change is somewhat greater. In table 8 the emfs at 25 °C corresponding to various concentrations of cadmium sulfate, near saturation, are given. These data are based on results of Vosburgh and Eppley [102] for cells containing 12½ percent amalgams and 0.023 N H_2SO_4; their data reported in international volts have been converted to absolute volts here. For neutral solutions the emfs listed here would be 18 μV higher.

TABLE 8. *Electromotive forces of cadmium sulfate cells at 25 °C as a function of electrolyte concentration*

$CdSO_4$	Emf	$CdSO_4$	Emf
percent	*V*	*percent*	*V*
41.84	1.021289	42.98	1.018990
42.39	1.020019	43.06	1.018883
42.63	1.019673	43.12	1.018704
42.77	1.019315	43.22	1.018603
42.90	1.019121	43.402 [a]	1.018392 [a]
42.94	1.019043		

[a] — saturated solution.

6.2. Acidity of Solution

The addition of sulfuric acid slightly decreases the emf of a cadmium sulfate cell. For the saturated cell several equations have been proposed relating the change in emf to acid concentration. For acid concentrations up to 4 N Sir Frank Smith [103] gave:

$$\Delta E(\text{volts}) = -(0.00060x + 0.00005x^2) \qquad (10)$$

where ΔE is the difference in emf of acid cells from neutral ones and x is the normality of the sulfuric acid solution before it is saturated with $CdSO_4 \cdot 8/3\ H_2O$. For acid concentrations up to 0.4 N only, the National Physical Laboratory [104] gave the linear relation

$$\Delta E(\text{microvolts}) = -615x. \qquad (11)$$

Obata [105] and Ishibashi and Ishizaki [106] also gave linear relations with the coefficients being, respectively, −855 and −833; Vosburgh [107] found Obata's equation to be valid to 1.49 N. In these last two, x refers to the normality of the acid in a saturated solution of $CdSO_4 \cdot 8/3\ H_2O$. All of these formulas agree closely if applied properly. For low acidities, the acidity of a solution of sulfuric acid after saturation with $CdSO_4 \cdot 8/3\ H_2O$ is 0.767 of that before saturation.

Differences between the emf of "neutral" and "acid" cells according to the Smith formula are listed in table 9. Sir Frank Smith [103] also investigated the effect on the emf of cadmium sulfate cells if the acid were confined to one or the other of the electrode compartments. For these effects, valid to 4 N, he gave:

$$\Delta E_{\text{negative}}(\text{volts}) = 0.01090x - 0.00125x^2 \qquad (12)$$

$$\Delta E_{\text{positive}}(\text{volts}) = -0.01150x + 0.00120x^2 \qquad (13)$$

the summation of which gives the Smith equation above for the effect of acid on the emf of the cell as a whole. These differences for various normalities of acid are given in table 10. These relations show that more acid at the negative electrode increases the emf while more acid at the positive electrode produces a decrease in emf. It is necessary, then, for high reproducibility and stability in emf that the acidity be the same and remain the same at the two electrodes.

TABLE 9. *Differences of emf of "acid" cells from the standard value of Weston "neutral" cells*

Normality of H_2SO_4	Difference of emf	Normality of H_2SO_4	Difference of emf
	μV		μV
0.01	−6	0.30	−185
.02	−12	.40	−248
.03	−18	.50	−312
.04	−24	.60	−378
.05	−30	.70	−444
.06	−36	.80	−512
.07	−42	.90	−580
.08	−48	1.00	−650
.09	−54	2.00	−1400
.10	−60	3.00	−2250
.20	−122	4.00	−3200

TABLE 10. *Differences of emf of cells from the standard value of Weston "neutral" cells if the acid is confined to the negative or positive limb of cell*

Normality of H_2SO_4	Differences of emf, microvolts	
	Negative limb	Positive limb
0.01	+109	−115
.02	+218	−230
.03	+326	−344
.04	+434	−458
.05	+542	−572
.06	+650	−686
.07	+757	−799
.08	+864	−912
.09	+971	−1025
.10	+1078	−1138
.20	+2130	−2252
.30	+3157	−3342
.40	+4160	−4408
.50	+5138	−5450
.60	+6090	−6468
.70	+7018	−7462
.80	+7920	−8432
.90	+8798	−9378
1.00	+9650	−10300
2.00	+16800	−18200
3.00	+21450	−23700
4.00	+23600	−26800

6.3. Composition of the Amalgam

The emf of cadmium sulfate cells depends on the composition of the amalgam as may be seen by the data (converted to absolute volts) of Sir Frank Smith [108] and shown plotted in figure 15. This figure clearly shows that the useful range of amalgam composition is from about 8 to 14 percent cadmium for normal temperatures. The useful range of amalgam composition for standard cells is limited to the horizontal part of the curves; here the emf is very insensitive to or not critically dependent on the exact percentage of cadmium in the amalgam. In this range the amalgam consists of two phases, solid and liquid, with the solid phase being a solid solution of mercury and cadmium. For low and high percentages of cadmium the emf is very sensitive to the exact amount of cadmium in the amalgam; this sensitivity is more marked at lower temperatures. In figure 16 is shown the range over which amalgams of various cadmium content may be safely used. The range for use for a 12½ percent amalgam is about 12 to 62 °C while for a 10 percent amalgam the range is from about −8 to 51 °C. It is for this reason that a 10 percent amalgam is used in cells made at the National Bureau of Standards. The significances of the lower dotted lines *A* and *B* appearing in figure 16 were discussed under the section on cadmium sulfate; the significance of the upper dotted line is discussed in the next section.

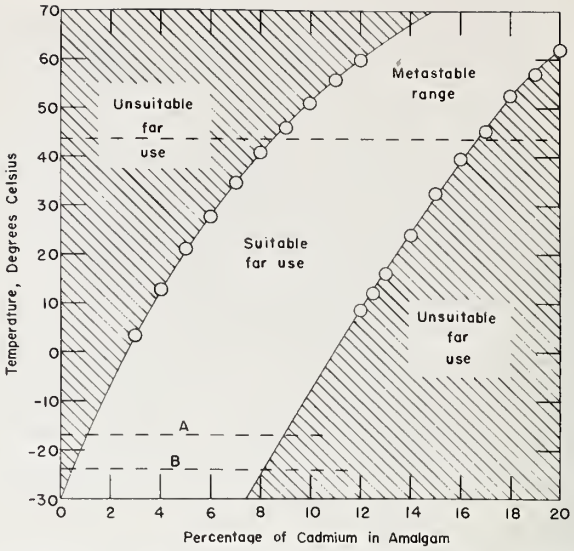

FIGURE 16. *Range of temperature over which cadmium amalgams of various cadmium content may be used in standard cells.*

6.4. Crystal Phases of Cadmium Sulfate

As was stated above, cadmium sulfate over a normal temperature range exists in two different hydrates, $CdSO_4 \cdot 8/3H_2O$ and $CdSO_4 \cdot H_2O$ with the transition temperature being 43.6 °C, below which the former hydrate is the stable form. The emfs of saturated standard cells made with these two different hydrates differ except at the transition point where the emfs are the same. Cells can be used in the metastable range for short periods of time. In either case, at a particular temperature, cells made with the more stable hydrate have the higher emf. These facts are illustrated by the data [109] given in table 11. These cells were "neutral" cells made with 10 percent amalgams. When a cell made with a particular hydrate is carried over into the metastable range its emf will correspond at first to that for a supersaturated solution of the metastable hydrate and then slowly rise in value as the hydrate is converted to the more stable form. This transition in phase is slow unless the two hydrates are present; then the transition is relatively fast. Accordingly, overheating of normal cells may have only transient adverse effects if the overheating is only momentary; otherwise the adverse effects may persist for long periods of time. In any case normal type saturated cells made with crystals of $CdSO_4 \cdot 8/3\ H_2O$ should not be heated above 43.6 °C; the upper dotted line in figure 16 corresponds to this upper temperature limit.

TABLE 11. *The emfs of Weston Normal Cells made with crystals of* $CdSO_4 \cdot 8/3\ H_2O$ *or crystals of* $CdSO_4 \cdot H_2O$*

Temperature	$CdSO_4 \cdot 8/3\ H_2O$ cells	$CdSO_4 \cdot H_2O$ cells
°C	*volts*	*volts*
20	1.01866	1.01333
25	1.01844	1.01417
30	1.01817	1.01501
35	1.01785	1.01587
40	1.01752	1.01672
43.4**	1.01729	1.01729
45	1.01716	1.01757
50	1.01682	1.01842

*Original data of ref. [109] were in international volts; are converted here to absolute volts.

**A better value for the transition temperature is 43.6 °C [79].

7. Characteristics of Standard Cells

7.1. Emf-Temperature Coefficient

Unsaturated standard cells have a very low emf-temperature coefficient. Although it is frequently stated that unsaturated standard cells have a dE/dt of −0.00001 V/deg C, the emf-temperature coefficient is a function of temperature, is dependent on the concentration of the electrolyte, and increases as the cell ages. In table 12, values of dE/dt are given for temperatures from 15 °C to 45 °C for various weight percents of $CdSO_4$. The emf values corresponding to cells made with the various concentrations of $CdSO_4$ are given at 25 °C as an aid to users in determining the emf-temperature coefficient of a particular cell. For example, if a cell had at 25 °C an emf of 1.019043 V its dE/dt would be

TABLE 12. *Emf-temperature coefficients of unsaturated standard cells*
(In microvolts per degree Celsius)

$CdSO_4$	Emf, 25 °C	dE/dt						
		15 °C	20 °C	25 °C	30 °C	35 °C	40 °C	45 °C
wt %	*volts*							
41.84	1.021289	−12.0	−13.2	−13.5	−12.9	−11.5	−9.2	−6.1
42.39	1.020019	−3.7	−5.3	−6.0	−5.7	−4.4	−2.2	+1.0
42.63	1.019673	−1.2	−3.0	−3.8	−3.6	−2.5	−0.4	+2.7
42.77	1.019315	+0.2	−1.3	−2.0	−1.6	−0.2	+2.2	+5.6
42.90	1.019121	+1.6	−0.1	−0.7	−0.4	+1.0	+3.5	+6.9
42.94	1.019043	+1.9	+0.3	−0.4	0	+1.3	+3.8	+7.3
[a] 42.98	1.018990	+2.3	+0.6	0	+0.1	+1.7	+4.2	+7.6
43.06	1.018883	+3.2	+1.5	+0.8	+0.9	+2.5	+4.9	+8.4
43.12	1.018704	[b] +3.8	+2.0	+1.3	+1.6	+3.0	+5.5	+8.9
43.22	1.018603	[b] +4.8	+2.9	+2.2	+2.5	+3.9	+6.4	+9.9
[c] 43.402	[d] 1.018392	−30.4	−40.6	−49.4	−56.6	−62.4	−66.6	−69.4

[a] —this composition corresponds to a solution saturated at 4 °C and gives a cell with a dE/dt of zero at 25 °C.
[b] —supersaturated.
[c] —percentage of $CdSO_4$ in a saturated solution at 25 °C; dE/dt values given are for solutions saturated with $CdSO_4 \cdot 8/3\,H_2O$ at the respective temperatures.
[d] —contains 0.03 N H_2SO_4.

-0.4 μV/deg C at 25 °C, while if it had an emf of 1.018704 V its dE/dt would be $+1.3$ μV/deg C. Inspection of the data of table 12 also shows that a cell made with a solution containing 42.98 wt percent of $CdSO_4$ has a zero emf-temperature coefficient at 25 °C. Vosburgh and Eppley [102] showed that this percentage corresponds closely to a solution saturated at 4 °C (the solutions of Vosburgh and Eppley also contained 0.023 N H_2SO_4). Since a solution saturated in the range from 3 °C to 4 °C leads to cells with negligible emf-temperature coefficients such solutions are frequently used in the construction of unsaturated standard cells.

Saturated standard cells exhibit a much larger emf-temperature coefficient than unsaturated standare cells owing to the change in solubility of $CdSO_4 \cdot 8/3H_2O$ with temperature. They exhibit a maximum emf at 3 to 4 °C, the temperature range of the minimum solubility of $CdSO_4 \cdot 8/3H_2O$ (see table 6). Two formulas relating the emf to temperature have been proposed. Wolff [32] working with 12½ percent amalgams obtained:

$$E_t = E_{20°} - 0.00004060(t-20) - 0.000000950(t-20)^2 + 0.000000010(t-20)^3 \qquad (14)$$

in international volts where E_t is the emf at temperature t and $E_{20°}$ is the emf at 20 °C. This equation is known as the International Temperature Formula. It is valid from 12 to 40 °C but may be used to 0 °C as long as the liquid and solid phases of the amalgam are present. Vigoureux and Watts [110] using 6 and 10 percent amalgams, to extend the temperature range, obtained:

$$E_t = E_{20°} - 0.00003939(t-20) - 0.000000903(t-20)^2 + 0.00000000660(t-20)^3 - 0.000000000150(t-20)^4 \qquad (15)$$

in international volts. These two equations are also applicable in absolute volts. This later equation is valid from −20 to 40 °C; Vigoureux and Watts used the 6 percent amalgam for the lower temperatures but the 10 percent amalgam gives the same results as long as the amalgam contains liquid and solid phases; thereafter the emf decreases below that given by eq (15). The cell becomes completely frozen at −24 °C; eq (15) gives −1139.5 μV for $E_{-24\,°C} - E_{20\,°C}$. However, when the cell becomes completely frozen the emf is approximately 1.007 V.

The emf of "neutral" saturated standard cells, as a function of temperature, based on the above formulas, is given in figure 17. Both formulas reproduce the maximum in emf at 3 °C to 4 °C, the temperature range of the minimum solubility of $CdSO_4 \cdot 8/3H_2O$. Since the acidity of the electrolyte does not appreciably affect dE/dt, the emfs of "acid" cells would parallel the curve shown. The displacements in the curves would depend on the acidity employed (see sec. 6.2). In this figure the value at 20 °C, the temperature at which international comparisons are made, is labeled Emf standard.

The differences between eq (14) and (15) are not large. In table 13 the differences in emf at various temperatures from the emf at 20 °C as given by these two formulas, are given. Since 10 percent amalgams are now used widely in preparing saturated standard cells eq (15) (or 18 below) should be used to calculate the change in their emf with temperature.

Above 43.6 °C where $CdSO_4 \cdot 8/3H_2O$ transforms to $CdSO_4 \cdot H_2O$ the emf-temperature relation is given by [109]:

$$E_t(\text{volts}) = E_{43.6°} + 0.000173(t-43.6) \qquad (16)$$

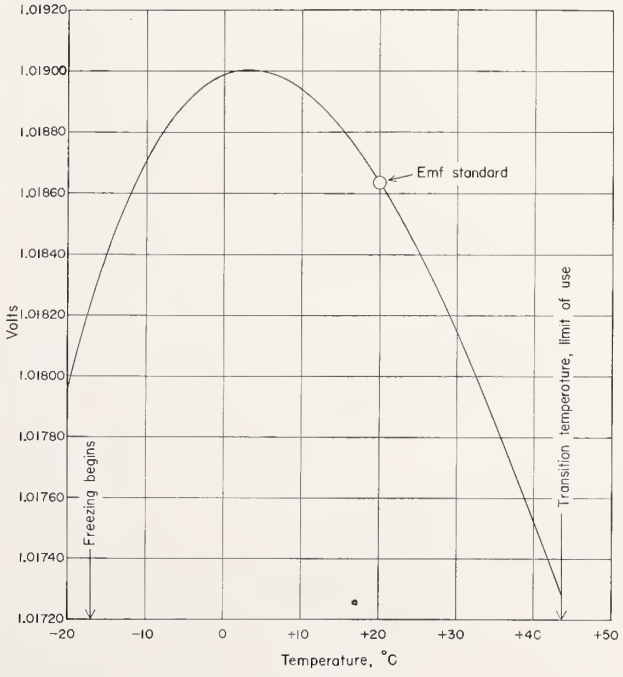

FIGURE 17. *Relation of the electromotive force of the cadmium sulfate standard cell to the temperature.*

TABLE 13. *Differences in emf of saturated standard cells from the value at 20 °C*

Temperature	Vigoureux and Watts formula	International formula	Temperature	Vigoureux and Watts formula	International formula
°C	*microvolts*	*microvolts*	°C	*microvolts*	*microvolts*
−20	−675.6[a,b]	.....	13	229.0	234.3
−19	−575.8[a,b]	.....	14	202.3	207.4
−18	−482.0[a,b]	.....	15	173.5	178.1
−17	−394.2[a,b]	.....	16	142.7	146.7
−16	−312.1[b]	.....	17	109.9	113.1
−15	−235.6[b]	.....	18	75.2	77.4
−14	−164.5[b]	.....	19	38.5	39.7
−13	−98.6[b]	.....	20	0.0	0.0
−12	−37.8[b]	.....	21	−40.3	−41.5
−11	+18.2[b]	.....	22	−82.2	−84.9
−10	69.3[b]	.....	23	−126.1	−130.1
−9	115.8[b]	.....	24	−171.6	−177.0
−8	157.9[b]	.....	25	−218.8	−225.5
−7	195.6	.....	26	−267.7	−275.7
−6	229.2	.....	27	−318.1	−327.4
−5	258.7	.....	28	−370.2	−380.6
−4	284.3	.....	29	−423.9	−435.2
−3	306.0	.....	30	−479.2	−491.1
−2	324.1	.....	31	−536.1	−548.4
−1	338.7	.....	32	−594.6	−606.9
0	350.0	352.2	33	−654.6	−666.6
+1	357.8	360.0	34	−716.3	−727.4
2	362.4	364.8	35	−779.6	−789.3
3	363.9	366.7	36	−844.4	−852.1
4	362.4	365.6	37	−911.0	−915.9
5	358.0	361.7	38	−979.1	−980.6
6	350.8	354.9	39	−1049.0	−1046.1
7	340.8	345.4	40	−1120.6	−1112.4
8	328.3	333.3	41	(−1193.8)	(−1179.3)
9	313.2	318.5	42	(−1268.9)	(−1246.9)
10	295.6	301.1	43	(−1345.7)	(−1315.1)
11	275.7	281.3	43.6	(−1392.3)	(−1355.8)
12	253.5	259.0			

[a]—for first few hours after a change from a higher temperature; electrolyte starts to freeze at −17 °C.
[b]—6 percent amalgam.
[c]—values in parenthesis were obtained by extrapolation.

and unlike the cells made with $CdSO_4 \cdot 8/3\ H_2O$ the emf-temperature coefficient is positive. The equation also applies for the metastable monohydrate down to 20 °C. Vinal and Brickwedde used 43.4° in eq (16) but later results [79] showed 43.6° to be a better value and is used here.

Since 28 °C is frequently used as a maintenance temperature for saturated standard cells, it is convenient in such instances to have the emf-temperature relation expressed in terms of this temperature. Equations corresponding, respectively, to eq (14) and (15) but with 28 °C as the reference temperature are:

$$E_t = E_{28°} - 0.00005390(t-28) - 0.00000071035(t-28)^2 + 0.000000010(t-28)^3 \qquad (17)$$

and

$$E_t = E_{28°} - 0.000052899(t-28) - 0.00000080265(t-28)^2 + 0.000000001813(t-28)^3 - 0.0000000001497(t-28)^4 \qquad (18)$$

in volts.

TABLE 14. *Nominal emfs of saturated standard cells at some common temperatures*
(Cells made with 10% cadmium amalgam)

Temperature	Acidity (H_2SO_4) of solution in cell			
	neutral[a]	0.03*N*	0.05*N*	0.10*N*
°C	*volts*	*volts*	*volts*	*volts*
20	1.018636	1.018612	1.018596	1.018556
25	1.018417	1.018393	1.018377	1.018337
28	1.018266	1.018242	1.018226	1.018186
30	1.018157	1.018133	1.018117	1.018077
32	1.018041	1.018017	1.018001	1.017961
35	1.017856	1.017832	1.017816	1.017776
37	1.017725	1.017701	1.017685	1.017645

[a]—Actually 0.00092*N*; cadmium sulfate hydrolyzes to produce H_2SO_4 of this acidity at 25 °C [73].

In table 14 the nominal values of the emf of "neutral" and "acid" saturated cells are given at a series of temperatures at which cells are most frequently calibrated at the National Bureau of Standards. Exact agreement with these nominal values cannot be expected since the emfs of saturated cells are very sensitive to the acidity of the electrolyte, to the amalgam composition, and to the extent of the solubility of the glass container in the cell electrolyte; even so they have high emf stability.

Frequently, the question arises as to the effect of small changes in temperature on the emf of saturated standard cells. Table 15 lists the changes in emf that are produced by changes in temperature of only ±0.001 or ±0.01 °C. The + sign for the emf refers to changes in emf produced by a decrease in temperature while the − sign for the emf refers to changes in emf produced by an increase in temperature. These data show that temperature must be controlled more accurately at the higher temperatures for comparable control of emf. They also show that for precisions of 0.5 μV the temperature must be controlled to slightly better than ±0.01 °C; for 0.05 μV to better than ±0.001 °C.

The emf-temperature formulas given above refer to the saturated cell as a whole, assuming that all parts of the cell are at the same temperature. The separate limbs of the cell have much larger coefficients, the negative limb having a negative coefficient and the positive limb a positive coefficient. The emf-temperature coefficient of the whole cell is the summation of those of the two limbs. The emf-temperature coefficients for each limb from 0° to 37 °C are given in table 16; those given in parenthesis were obtained by interpolation or extrapolation of the data of Sir Frank Smith [103]. The summation of those for the two limbs are given in column 4; these agree well with those calculated by International Temperature Formula. It is obvious, in view of these data, that saturated standard cells must be kept at a uniform temperature for high accuracy and precision. In table 17, are given the errors that would arise in the emf of a cell if the positive limb were at a slightly higher or slightly lower temperature than the negative limb. Also given are data for the case in which the temperature of the negative limb were slightly higher or lower temperature than the negative limb. It is for

TABLE 15. *Effect of small changes in temperature on the emf of saturated standard cells at various temperatures*

Temperature	±0.001 °C	±0.01 °C
°C	*microvolt*	*microvolt*
20	∓0.04	∓0.4
25	∓0.05	∓0.5
28	∓0.05	∓0.5
30	∓0.06	∓0.6
32	∓0.06	∓0.6
35	∓0.06	∓0.6
37	∓0.07	∓0.7

+ sign for the emf refers to a decrease in temperature.
− sign for the emf refers to an increase in temperature.

TABLE 16. *Temperature coefficient of positive and negative limbs of saturated standard cells and of complete cells at various temperatures*

Temperature	Negative limb	Positive limb	Complete cell		
			Observed	International temperature formula	Vigoureux and Watts formula
°C	*volt/deg*	*volt/deg*	*volt/deg*	*volt/deg*	*volt/deg*
0	−0.000288	+0.000290	+0.000002	+0.000009	+0.000009
5	−0.000297	+0.000291	−0.000006	−0.000005	−0.000006
10	−0.000315	+0.000295	−0.000020	−0.000019	−0.000019
15	−0.000333	+0.000302	−0.000031	−0.000031	−0.000030
20	−0.000350	+0.000310	−0.000040	−0.000041	−0.000039
25	−0.000366	+0.000314	−0.000052	−0.000050	−0.000048
28	(−0.000372)[a]	(+0.000314)	(−0.000058)	−0.000054	−0.000053
30	−0.000374	+0.000314	−0.000060	−0.000057	−0.000056
32	(−0.000376)	(+0.000314)	(−0.000062)	−0.000059	−0.000059
35	(−0.000380)	(+0.000314)	(−0.000066)	−0.000062	−0.000064
37	(−0.000382)	(+0.000314)	(−0.000068)	−0.000064	−0.000067

[a]—Values in parenthesis obtained by interpolation or extrapolation.

this reason that copper shields are used around the portable unsaturated cells (see sec. 5.4). Park [111] and Eppley [112] investigated the effect of service temperature conditions on the emf of unsaturated standard cells and Park showed that errors in emf arising from thermal inequalities could be reduced to a minimum by enclosing the cell in a copper shield.

7.2. Emf-Temperature Hysteresis

In general, if saturated or unsaturated standard cells are subjected to slowly changing temperatures their emf will follow closely the relations given above. If, on the other hand, the cells are subjected to abrupt temperature changes, deviations from the true emf will occur. These deviations are generally referred to as hysteresis. On cooling, the cells show first too high an emf and then a slow decrease in emf to the equilibrium value. On heating, the cells show first too low an emf and then a slow rise in emf to the equilibrium values. The magnitude of the hysteresis is given by the percentage deviation from the equilibrium value and is usually greater when the temperature is decreased than when it is increased. These general relations are illustrated in figure 18 for abrupt heating of new cells from 25 to 30 °C and for abrupt cooling from 30 to 25 °C for unsaturated standard cells having a dE/dt of −5 μV/deg C in this temperature range. The magnitude of the hysteresis in each case is given by the distance marked by an "*h*" divided by the emf of the cell at the starting temperature (this emf may be taken as unity). This figure clearly shows that the magnitude and duration of hysteresis obtained on cooling is nearly double that found on heating; in either case the magnitude of the hysteresis is less than 0.01 percent.

TABLE 17. *Errors produced in emf of saturated standard cells if the temperature of the positive limb (or negative limb) differed from that of the negative limb (or positive limb), by small amounts, at various temperatures*

Temperature difference	Temperature							
	0 °C	20 °C	25 °C	28 °C	30 °C	32 °C	35 °C	37 °C
	Positive limb							
	μV	μV	μV	μV	μV	μV	μV	μV
+0.01	+2.9	+3.1	+3.1	+3.1	+3.1	+3.1	+3.1	+3.1
+0.005	+1.5	+1.6	+1.6	+1.6	+1.6	+1.6	+1.6	+1.6
+0.001	+0.3	+0.3	+0.3	+0.3	+0.3	+0.3	+0.3	+0.3
−0.001	−0.3	−0.3	−0.3	−0.3	−0.3	−0.3	−0.3	−0.3
−0.005	−1.5	−1.6	−1.6	−1.6	−1.6	−1.6	−1.6	−1.6
−0.01	−2.9	−3.1	−3.1	−3.1	−3.1	−3.1	−3.1	−3.1
	Negative limb							
+0.01	−2.9	−3.5	−3.7	−3.7	−3.7	−3.8	−3.8	−3.8
+0.005	−1.5	−1.8	−1.9	−1.9	−1.9	−1.9	−1.9	−1.9
+0.001	−0.3	−0.4	−0.4	−0.4	−0.4	−0.4	−0.4	−0.4
−0.001	+0.3	+0.4	+0.4	+0.4	+0.4	+0.4	+0.4	+0.4
−0.005	+1.5	+1.8	+1.9	+1.9	+1.9	+1.9	+1.9	+1.9
−0.01	+2.9	+3.5	+3.7	+3.7	+3.7	+3.8	+3.8	+3.8

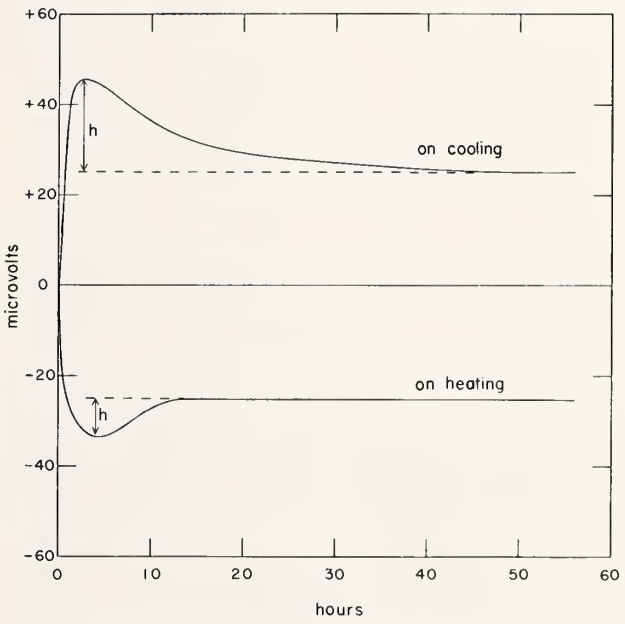

FIGURE 18. *Relations showing the emf-temperature hysteresis of unsaturated standards when abruptly heated or cooled 5 °C.*

For unsaturated cells the magnitude and duration of hysteresis depend on the type of construction, age, acidity and concentration of the electrolyte, on the purity of the materials, and on the rate and magnitude of the temperature change. To these must be added the size and change of solubility with temperature of the crystals of $CdSO_4 \cdot 8/3\ H_2O$ for the saturated cell. Therefore, it is not possible to give quantitative data that may be applied as

corrections to the emf of cells under diversified conditions involving abrupt temperature changes. Furthermore, the magnitude of hysteresis for unsaturated cells increases with age; a cell 10 years old exhibits about 10 times the hysteresis of a new cell. In general, for a 5 °C abrupt change in temperature the hysteresis of new unsaturated cells ranges from 0.01 to 0.02 percent (0.0001 to 0.0002 V) on cooling and from 0.005 to 0.01 percent (0.00005 to 0.0001 V) on heating. The cells usually recover their original emf within 1 to 2 days after cooling and within 10 to 12 hours after heating. For older cells, hysteresis may persist for days or even months. Proportionate hysteresis is to be expected for larger or smaller temperature intervals than 5 °C. In general, saturated cells show less hysteresis than unsaturated ones. In some cases, saturated standard cells do not exhibit the "overshoot" typical of hysteresis. Instead they approach steady emfs at a new temperature at an exceedingly slow rate. This phenomenon here called "lag" is sometimes referred to as "negative hysteresis" and is attributed to the slowness in the precipitation of $CdSO_4 \cdot 8/3\ H_2O$ on cooling or to the slowness of dissolution of $CdSO_4 \cdot 8/3\ H_2O$ on heating.

Many explanations have been given for hysteresis but no single factor is alone responsible. The difference between the heat capacities of the two limbs of the cell, changes in solubility of $CdSO_4 \cdot 8/3\ H_2O$ (for the saturated cell) with temperature, septa (in the unsaturated cell), and the disturbances of equilibrium conditions within the cell during temperature changes must all contribute to hysteresis. In any case standard cells should be maintained at constant temperature if at all possible. Temperature fluctuations may be kept at a minimum for portable unsaturated cells by placing them in temperature-lagged boxes or in Dewar flasks. A view of a temperature-lagged box used at the National Bureau of Standards in the testing of unsaturated cells is shown in figure 19.

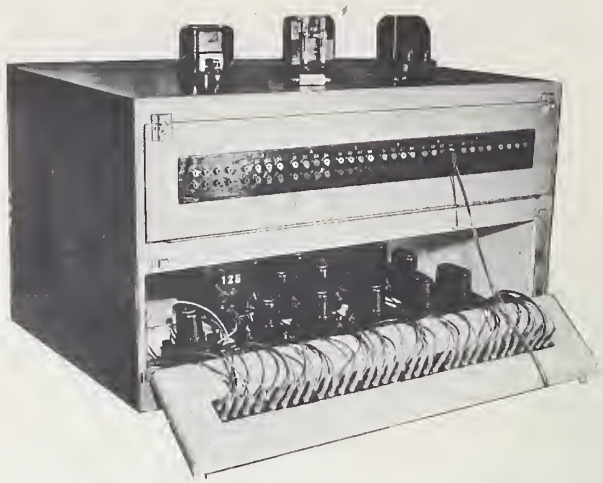

FIGURE 19. *Temperature-lagged box used at the National Bureau of Standards in the testing of unsaturated standard cells.*

7.3. Temperature Range

The range of temperature over which standard cells may be used is dictated by the composition of the amalgam, the transition temperature of the cadmium sulfate hydrates, and the freezing point of the electrolyte. The range over which amalgams of various cadmium contents may be safely used was shown above in figure 16. For 12½ percent amalgams this range is 12 to 62 °C; for 10 percent amalgams it is −8 to 51 °C. Both of these amalgams may be used for a short time (2 to 3 hr) below these temperatures (12½ percent amalgam to 0 °C; 10 percent amalgam to −20 °C) or as long as the amalgams consist of two phases, solid and liquid. However, for work of the highest precision the cells should be confined to the temperature ranges shown in figure 16.

A 6 percent amalgam should be chosen for lower temperatures; its useful range is −24 to 28 °C. For high temperatures amalgams of high cadmium content should be used, viz, a 14 percent amalgam will give cells that could be used, from 24 to 67 °C. It may be possible to use unsaturated standard cells to temperatures of the boiling point of the electrolyte (slightly above 100 °C) by using amalgams of high cadmium content (above 20 percent) but these cells would not be suitable for precision work much below 80 °C.

At temperatures above 43.6 °C, even though the higher-percentage amalgams are satisfactory, saturated cells must be made with crystals of $CdSO_4 \cdot H_2O$ since this is the stable form of solid cadmium sulfate above 43.6 °C. For unsaturated standard cells no such problem exists and attention need be given only to the composition of the amalgam.

The lower limit of use is −24 °C where the cell becomes completely frozen. Freezing begins at −17 °C. Cells completely frozen at −24 °C will behave normally after thawing if freezing has not caused a fracture in the cell. The time required for the cell to recover its normal emf may be long, however. The internal resistance of standard cells at −10 °C is about 6 times that at 25 °C and this increase in internal resistance may limit the use of the cell.

Significant temperatures in the use of standard cells are summarized in table 18. In practice, cells should probably be subjected to a somewhat lesser range of temperatures than shown; −16 to 40 °C is a good range for saturated cells and 4 to 40 °C for unsaturated ones.

7.4. Emf-Pressure Coefficient

The effect of pressure on the emf of a galvanic cell at constant temperature is given by

$$\left(\frac{dE}{dP}\right)_T = \frac{-(\Delta V)k}{nF} \text{ volt atm}^{-1} \qquad (19)$$

where ΔV is the volume change in cubic centimeters at atmospheric pressure per faraday, n is

TABLE 18. *Significant temperatures in the use of standard cells (also temperature limits for use of standard cells)*

Temperature		Remarks
°C	°F	
67	152.6	Upper limit for 14 percent amalgam, unsaturated cell
62	143.6	Upper limit for 12½ percent amalgam, unsaturated cell
51	123.8	Upper limit for 10 percent amalgam, unsaturated cell
43.6	110.5	Transition temperature for $CdSO_4 \cdot 8/3\ H_2O = CdSO_4 \cdot H_2O$
40	104	Upper practical limit recommended for standard cells
28–37	82.4–98.6	Suitable range for thermostated air boxes
28	82.4	Temperature at which primary standard of United States is maintained; also upper limit for 6 percent amalgam
24	75.2	Lower limit for 14 percent amalgam
20	68	Weston Normal Cell has a nominal emf of 1.0186360 absolute volts
12.1	53.8	Lower limit for 12½ percent amalgam
4	39.2	Lower practical limit for unsaturated cells
3–4	37.4–39.2	Emf of Weston Normal Cell is at a maximum; solubility of $CdSO_4 \cdot 8/3\ H_2O$ is a minimum
−8	17.6	Lower limit for 10 percent amalgam
−17	1.4	Freezing begins
−24	−11.2	Cell completely frozen; will recover normal emf in about a week after thawing, if not cracked

the number of equivalents involved in the reaction, F is the faraday, and k is a conversion factor, 0.101325, which converts cubic centimeter-atmospheres into joules, i.e., volt coulombs. The volume change may be calculated from the atomic or molecular weights and the densities of the reactants and products of the reaction; for saturated standard cells this reaction is given by eq (7). At 20 °C, the accepted densities of Cd, Hg_2SO_4, $CdSO_4 \cdot 8/3\ H_2O$, Hg, and a saturated solution of $CdSO_4$ are, respectively, 8.648, 7.56, and 3.090 g cm^{-3} and 13.5463 and 1.6119 g ml^{-1} [113]. Using these data, accepted atomic weights on the C^{12} scale [114] and 96,487 coulombs/gram-equivalent [115] [15] for the faraday equation 19 gives 6.4 μV/atm for $(dE/dP)_T$. This value agrees excellently with 6.1 μV/atm found experimently by Ramsey [116] (this value is an interpolated value, Ramsey found 6.02 μV/atm at 20.4 °C and 7.6 μV/atm at 19 °C).

The effect of pressure on an unsaturated cell would be nearly the same, since unsaturated cells are made with solutions that are nearly saturated.

A priori no effect on the emf of sealed cells would be expected providing the pressure was insufficient to fracture the cell. Recent experiments by Catherine Law and D. N. Craig of this Bureau, in which the external pressure on the cell was increased to approximately 5 atm, has confirmed this. Standard cells have an air space above the electrolyte which would act as a cushion to absorb pressure change even if the elasticity of the glass container were such as to transmit pressure change to the cell components.

[15] In the original paper [115] values based on the physical and chemical scales of atomic weights were given. The value given here is based on an atomic weight of silver relative to the C^{12} scale of atomic weights, namely, 107.870.

7.5. Internal Resistance

The internal resistance in the vicinity of 25 °C ranges from 100 to 500 Ω for unsaturated cells and from 500 to 1000 Ω for saturated cells manufactured in the United States. The internal resistance increases at the rate of about 2 percent for a decrease in temperature of one degree C; this fact should be taken into account in calculating the *IR* drop in a cell (see table 19). The resistances of the positive and negative limbs of symmetrical H-shaped cells are approximately equal. As a cell ages its internal resistance increases slightly. The internal resistance of a standard cell may be estimated by momentarily placing a 10-MΩ resistor across the cell terminals and reading the emf, E_R. The value of the internal resistance is then given by

$$R = 10^7(E_0 - E_R)/E_R \text{ ohms}, \qquad (20)$$

where E_0 is the open-circuit emf. The cell recovers its initial emf within a few minutes after the 10-MΩ resistor is removed. If a cell exhibits high internal resistance or insensitivity it may contain a gas bubble at the anode which may be frequently removed by tapping the cell when inclined 45°. If this treatment is ineffective a new cell is recommended.

7.6. Effect of Current

Standard cells are not intended to serve as sources of electric current. Even so, the question frequently arises about the effect of current on standard cells, especially the unsaturated type. When standard cells are charged or discharged the

TABLE 19. *Effect of current on the emf of unsaturated standard cells at 25 °C*

Current, ampere	Internal resistance (initial change)	
	100 ohms	500 ohms
	μV	μV
10^{-10}	0.01	0.05
10^{-9}	0.1	0.5
10^{-8}	1.0	5.0
10^{-7}	10.0	50.0
10^{-6}	100.0	500.0
10^{-5}	1000.0	5000.0

Changes owing to changes in amalgam (V_a) and electrolyte (V_e) composition (after one year)

	V_a	V_e	V_a	V_e
	μV	μV	μV	μV
10^{-10}	---[a]	---	---	---
10^{-9}	---	---	---	---
10^{-8}	---	---	---	0.03
10^{-7}	---	0.05	---	0.26
10^{-6}		0.5	0.02	2.6
10^{-5}	0.05	5.3	0.17	26.3

Changes arising from electrode polarization (after one year)

	μV	μV
10^{-10}	0.1	0.3
10^{-9}	0.7	2.0
10^{-8}	4.3	12.5
10^{-7}	26.	76.
10^{-6}	159.	466.
10^{-5}	970.	2844.

[a]—dash means that the change is less than 0.01 μV.

rise or drop in emf is initially dictated by the IR drop and subsequently by a voltage change, V_c, associated with the chemical changes in the cell, and by electrode polarization and changes in internal resistance. For the unsaturated cell V_c is made up of two parts: V_a, the change in emf associated with the change in the composition of the amalgam during charge or discharge and V_e, the change in emf associated with the change in electrolyte content of the solution during charge or discharge. When unsaturated cells have been discharged until their solutions are saturated the latter no longer applies. For saturated cell, V_c consists of V_a only.

The magnitude of V_a obtained on discharge at 25 °C is given by

$$V_a \text{ (in volts)} = \frac{-0.001067It}{FW} = -1.106 \times 10^{-8} \frac{It}{W} \tag{21}$$

where I is the current in amperes, t is time in seconds, W is the total weight of the amalgam in grams, and F is the faraday (96487.0 coulombs). For NBS saturated cells the total weight of amalgam is generally about 10 g. In this case eq (21) reduces to

$$V_a \text{ (in volts)} = -1.106 \times 10^{-9}\, It. \tag{22}$$

For unsaturated cells having internal resistances of 100 and 500 Ω the weight of the amalgam is approximately 67 and 20 g, respectively.

The magnitude of V_e obtained on discharge at 25 °C is given by

$$V_e \text{ (in volts)} = \frac{-0.161\, It}{FW} = -1.67 \times 10^{-6} \frac{It}{W} \tag{23}$$

where W is now the weight of the electrolytic solution in grams and the other symbols have the meaning given above. For unsaturated cells the weight of solution is about 100 and 20 g, respectively, for cells having internal resistances of 100 and 500 Ω. Equation (23) then becomes

$$V_e \text{ (in volts)} = -1.67 \times 10^{-8}\, It \tag{24}$$

for the 100-Ω cell and

$$V_e \text{ (in volts)} = -8.35 \times 10^{-8}\, It \tag{25}$$

for the 500-Ω cell.

The magnitudes of electrode polarization [16] during discharge may be calculated, within a few microvolts, by the equation

$$\log \Delta E \text{ (in microvolts)} = 1.6048 + 0.786 \log \left(\frac{C}{A}\right) \tag{26}$$

where ΔE is the change in emf, in microvolts, arising from electrode polarization and changes in internal resistance, C is quantity of electricity in coulombs (ampere seconds) and A is apparent (geometric) electrode area in square centimeters [117]. For unsaturated cells having internal resistances of 100 and 500 Ω, A is about 5.5 cm² and 1.4 cm², respectively. Some miniature types having internal resistances of about 1000 Ω and apparent surface areas of less than 1 cm² are also available. The length of time standard cells will sustain a discharge depends on the amount of material in the cells; most unsaturated cells of United States manufacture contain sufficient material to yield from 700 to 5000 coulombs if the current is kept below about 2×10^{-5} A per cm² of electrode area.

When an external load is removed, the cells recover their initial emf, provided the discharge has not been a prolonged one. The time required for recovery depends on the severity of the discharge. For example, if an unsaturated cell (internal resistance ≅ 100 Ω) is discharged for 5 min at 6×10^{-6} A cm^{-2} it will recover its original emf within 5 μV in 30 min and will completely recover after 6 hr. At a higher current density of 6×10^{-4} A cm^{-2} the emf will be about 180 μV below its original value after 30 min, 5 μV after 6 hr, and several days will be required for complete recovery. If the cell were discharged at a current density of 6×10^{-4} A cm^{-2} to a low cutoff voltage of 0.001 V, recovery will be exceedingly slow requiring several months and

[16] Includes any change in internal resistance that may occur as a cell is discharged.

full recovery will not be attained after this prolonged period because the normal emf will have declined (see below). The time of recovery, therefore, is seen to depend on the rate and extent of the discharge.

In table 19 changes in emf caused by various currents of low magnitude are illustrated for cells having electrode cross-sectional areas of 5.5 cm^2 and 1.4 cm^2 and internal resistances of 100 and 500 Ω. The changes arising from internal resistance are initial changes whereas those arising from changes in amalgam composition, V_a, electrolyte composition, V_e, and electrode polarization (see footnote 16), ΔE, are functions of time of discharge (for illustration, a period of 1 year is chosen for these). The total changes in emf during a discharge is the sum of the four effects. On a current density basis it should be noted the changes for the 100-Ω and 500-Ω cells are nearly identical since the electrode area for the former cell is approximately five times that of the latter.

Standard cells may be *short-circuited* momentarily without permanent damage to the cells. The cells will recover their original emf within a few minutes after taken off short circuit. If kept on short circuit they will be completely discharged within ½ to 2 days depending on the size and internal resistance of the cell, and will not recover their initial emf. The short circuit current is given by the ratio of the open-circuit emf and the internal resistance of the cell. For cells having internal resistances of 100 Ω and 500 Ω, the short-circuit (flash) current will, therefore, be 1×10^{-2} and 2×10^{-3} A, respectively.

7.7. Effect of Light

Mercurous sulfate is sensitive to light and changes in color at a slow rate through tan, to gray-brown, to dark brown, and finally to black. Although standard cells having discolored mercurous sulfate may have normal emfs [118] they exhibit slower approach to equilibrium values after temperature or other changes. Standard cells should, therefore, be mounted in nontransparent cases or kept in the dark and used only for short periods at a time under diffuse light.

7.8. Effect of Shock

Mechanical shocks insufficient to fracture or break or scramble the components of unsaturated standard cells have no lasting effects on the cells. Unsaturated standard cells packaged in excelsior and shipped by common carrier to the National Bureau of Standards have been observed to perform satisfactorily. When subjected to shocks of 10 to 40 g for durations of 6 to 18 msec unsaturated cells exhibit large transient changes in emf ranging from 4,200 to 31,000 μV [119]. After the shock the cells immediately recover their original emf within 2 μV. The transient emfs observed during shock probably arise from a disturbance of the mercury and amalgam surfaces during the period of shock.

On the other hand, the usual types of saturated cells of United States manufacture should not be subjected to sudden shock, should not be shipped by common carrier, should be transferred by messenger, and should not be tilted more than 45°. Some new saturated standard cells of novel design are stated to be portable, i.e., may be shipped by common carrier. However, studies over a period of time will be required to ascertain the long-term stability of their emf.

7.9. Effect of Vibration

Vibrations at frequencies from 10 to 1,000 Hz (c/s) with accelerations of 1 to 10 g have no lasting effects on the emf of unsaturated standard cells [119]. During the vibration, however, rather large a-c voltages of the same frequency are generated. For an unsaturated cell having an internal resistance of 500 Ω this a-c voltage ranges from about 25 μV at 1 g and 1000 Hz to 9900 μV at 10 g and 50 Hz. Furthermore, there is a decrease in the d-c emf ranging from 3 μV at 1 g and 1000 Hz to about 200 μV at 10 g and 100 Hz. In general at frequencies above 100 Hz the waveform of the a-c voltage is sinusoidal whereas below 100 Hz it is nonsinusoidal owing to the resonance of the various components of the cell. In most cases the a-c and d-c effects of the vibration appear and disappear instantaneously when vibration is started or stopped. In some instances the d-c change may be rapid in the initial moments of vibration and then build up slightly in an exponential manner for 2 or 3 min. In these instances when the vibration is stopped the d-c emf decays in the same fashion as it was built up.

8. Life of Standard Cells

Saturated standard cells have an exceedingly long life. Some cells at the National Bureau of Standards have been in use for nearly 60 years, and they have retained their emfs within a few microvolts; see section 2.3. On the other hand, unsaturated cells at room temperature (about 25 °C) decrease in emf at a rate of about 20 to 40 μV per year [48]. This decrease in emf is equivalent to a corrosion rate for the amalgam of about $(6.8 \text{ to } 13.6) \times 10^{-7}$ A cm^{-2}. Since the emf of new unsaturated standard cells generally range from 1.01900 to 1.01940 V, depending on the concentration and acidity of the electrolyte, these cells on the average reach an emf of 1.01830 V within 23 to 37 years, providing they are maintained at 25 °C or thereabouts, and are not subjected to abuse, such as discharging or charging current; a practical life time for these cells is probably 12 to 18 years. When unsaturated standard cells reach an emf of 1.01830 V or lower the cells generally behave erratically (largely because the electrolyte may become supersaturated on cooling), have large emf-temperature coefficients, and show excessive emf-temperature hysteresis. The life of the cell is considerably reduced

if the cell is stored at higher temperatures. The rate of decrease in emf is approximately doubled for every 12 °C increase in temperature [120]; thus at 37 °C the life of an unsaturated cell would be one half that given above. Cells of the miniature type with short diffusion path between electrodes will have a shorter life.

Earlier unsaturated standard cells decreased in emf at room temperature at a rate of 70 to 85 μV per year [121, 122, 123] and, therefore, had an average theoretical life of 10 to 15 years or a practical life of 8 to 12 years. The improvement in life noted in modern cells has resulted mainly, if not entirely, from the use of improved septa in the cells.

9. References

[1] Giovanni Giorgi, Unità razionali di electtromagnetisimo, Atti dell' Assoc. Elettr. Ital. **5,** 402 (1901); Proposal concerning electrical and physical units, Trans. Intern. Electrical Congr. **1,** 136 (St. Louis, Mo., 1904).

[2] Wilhelm (E.) Weber, Messungen galvanische Leitungswiderstände nach einem absoluten Maasse, Ann. Physik. (Pogg. Ann.) 2, **82,** 337 (1851); see also ref. [4].

[3] Reports of the Comm. on Electrical Standards of the Brit. Assoc. Adv. of Science (reprinted by Cambridge Univ. Press., 1913), Second Report, p. 60, Newcastle-on-Tyne, 1863.

[4] J. C. Maxwell, A treatise on electricity and magnetism, 3d ed., Vol. 2, Ch. 10, p. 263, Clarendon Press (Oxford, 1892).

[5] Ref. [3], First Report, p. 9, Cambridge, 1862.

[6] Report of the 43d meeting of the British Association for the Advancement of Science, Bradford, First report of the Committee for the Selection and Nomenclature of Dynamical and Electrical Units, Brit. Assoc. Report, p. 222, 1873.

[7] Oliver Heaviside, The relations between magnetic force and electric current.—I., The Electrician (London) **10,** 6 (1882).

[8] F. B. Silsbee, Establishment and maintenance of the electrical units, NBS Cir. 475 (1949); Systems of electrical units, NBS Mono. 56, (1962); J. Res. NBS **66C,** (Eng. & Instr.), 137 (1962).

[9] C. F. Gauss, "Intensitas vis magneticae terrestris ad mensuram absolutam revocata," read before Royal Society of Göttingen on December 15, 1832, Commentationes Societatis regiae Scientarum Gottingensis recentiores, VIII, pp. 3–44 (1832–1837), Göttingen, 1841; reprinted in Carl Friedrich Gauss Werke, V, pp. 79–118, (Göttingen, 1867; 2nd printing, Göttingen, 1877), German translation in Poggendorff's Ann. Physik., **XXVIII,** 241–273, 591–615 (1833); second German translation by E. Dorn, Ostwald's Klassiker der exakten Wissenschaften No. 53, Leipzig, 1894.

[10] Sir William Thomson (Lord Kelvin), On the mechanical theory of electrolysis, Phil. Mag. (4) **2,** 429 (1851); Practical electricity by W. E. Ayrton and T. Mather, p. 205, Cassell and Co., Ltd., London (1911); Brit. Assoc. reports on electrical standards, p. 137, Cambridge Univ. Press, 1911.

[11] A. E. Kennelly, Historical outline of the electrical units, J. Eng. Education **19,** 229 (1928) reviews these developments.

[12] Sir William Thomson (Lord Kelvin), Papers on electrostatics and magnetism, Macmillan and Co., Ltd., London, p. 246, 1884.

[13] J. W. Trischka, U.S. Patent No. 2,959,683, Electric resonance voltage standards, Nov. 8, 1960; for theory see C. H. Townes and A. L. Schawlow, Microwave spectroscopy, Ch. 10, McGraw-Hill Book Co., Inc., New York, 1955.

[14] Y. Beers and G. L. Strine, The measurement of voltage by the use of the Stark effect, IRE Trans. Instrumentation **I–II,** Nos. 3 and 4, 171 (1962).

[15] F. Wenner, A proposed modification of the Kirchhoff method for the absolute measurement of resistance, by title only, Science **29,** 475 (1909); see ref. [16] for details.

[16] J. L. Thomas, C. Peterson, I. L. Cooter, and F. R. Kotter, An absolute measurement of resistance by the Wenner method, J. Res. NBS **43,** 291 (1949) RP2029.

[17] H. L. Curtis, C. Moon, and C. M. Sparks, A determination of the absolute ohm using an improved self-inductor, J. Res. NBS **21,** 375 (1938) RP1137.

[18] R. D. Cutkosky, Evaluation of the NBS unit of resistance based on a computable capacitor, J. Res. NBS **65A** (Phys. and Chem.) 147 (1961).

[19] R. L. Driscoll and R. D. Cutkosky, Measurement of current with the National Bureau of Standards current balance, J. Res. NBS **60,** 297 (1958) RP2846; R. W. Curtis, R. L. Driscoll, and C. L. Critchfield, An absolute determination of the ampere, using helical and spiral coils, J. Res. NBS **22,** 485 (1939) RP1200; see also H. L. Curtis, Electrical measurements, Ch. XIX, McGraw-Hill Book Co., Inc., New York, 1937.

[20] R. L. Driscoll, Measurement of current with a Pellat-type electrodynamometer, J. Res. NBS **60,** 287 (1958) RP2845.

[21] P. L. Bender and R. L. Driscoll, A free precession determination of the proton gyromagnetic ratio, IRE Trans. Instr. **I–7,** Nos. 3 and 4, 176 (1958).

[22] J. L. Thomas, Precision resistors and their measurement NBS Circ. 470 (1948).

[23] Latimer Clark, On a voltaic standard of electromotive force, Proc. Royal Soc. (London) **20,** 444 (1872); On a standard voltaic battery, Phil. Trans. Royal Soc. I, **164,** 1 (1874).

[24] Lord Rayleigh and Mrs. H. Sidgwick, On the electrochemical equivalent of silver, and on the absolute electromotive force of Clark cells, Phil. Trans. II, **175,** 411 (1884).

[25] H. S. Carhart, Relation between the electromotive force of a Daniell cell with the strength of the zinc sulfate solution, Am. J. Sci. (3) **28,** 374 (1884); Ref. [3], nineteenth report, Edinburgh, 1892.

[26] K. Kahle, Beiträge zur Kenntniss der elektromotorischen Kraft des Clark'schen Normalelementes, Z. Instrumentenkunde **12,** 117 (1892).

[27] R. T. Glazebrook and S. Skinner, On the Clark cell as a standard of electromotive force, Proc. Royal Soc. (London) **51,** 60 (1892).

[28] H. S. Carhart, The various determinations of the e.m.f. of the Clark cell, Phys. Rev. **12,** No. 3, 129 (1900).

[29] Lord Rayleigh, On the Clark cell as a standard of electromotive force, Phil. Trans. II, **176,** 781 (1885).

[30] Edward Weston, Normalelement, German Patent 75,194 (Jan. 5, 1892); Improvements in voltaic cells, British Patent 22,482 (Feb. 6, 1892); Voltaic cell, U.S. Patent 494,827 (Apr. 4, 1893).

[31] Report of International Conference on electrical units and standards, Oct. 12, 1908; given as Appendix 2 in ref. [8].

[32] F. A. Wolff, The temperature formula of the Weston standard cell, Bull. BS **5,** 309 (1908); data were submitted in October 1908 to the London International Conference on electrical units and standards.

[33] Announcement of a change in the value of the International Volt, NBS Circ. 29, p. 9, footnote 1, Dec. 31, 1910; records of NBS carried results of emf of saturated standard cells to 6 decimals from 1911 until 1934 and to 7 decimals since then.

[34] G. W. Vinal, International comparison of electrical standards, BS J. Res. **8,** 729 (1932) RP448.

[35] Announcement of changes in electrical and photometric units, NBS Circ. 459, 1947.

[36] L. H. Brickwedde and G. W. Vinal, Electromotive force of saturated Weston standard cells containing deuterium oxide, J. Res. NBS **20,** 599 (1938) RP1094; Relation of electromotive force to the concentration of deuterium

oxide in saturated standard cells, J. Res. NBS **27,** 479 (1941) RP1435.
[37] E. B. Rosa, G. W. Vinal, and A. S. McDaniel, The silver voltameter—Part IV, Third series of quantitative experiments and special investigations, BS Bull. **10,** 475 (1914), Table 3 (experiments made from 1910 to 1912, inclusive).
[38] P. Vigoureux, International determination of the electromotive force of the Normal Weston Cell in International Volts, Coll. Res. Nat. Phys. Lab. **24,** 79 (1932).
[39] H. von Steinwehr and A. Schulze, Neubestimmung der EMK des Internationalen Westonelements, Z. Instrumenk. **52,** 249 (1932).
[40] H. L. Curtis and R. W. Curtis, An absolute determination of the ampere, BS J. Res. **12,** 665 (1934) RP685.
[41] E. B. Rosa, N. E. Dorsey, and J. M. Miller, A determination of the International Ampere in absolute measure, BS Bull. **8,** 269 (1911).
[42] W. J. Hamer, L. H. Brickwedde, and P. R. Robb, Standard cells and the unit of electromotive force, NBS Circ. 524, Electrochemical constants, Ch. 12, 1953; results obtained since 1953 extend and modify the data given in fig. 12.2 of this ref.
[43] M. Gouy, Sur une étuve à température constante, J. Physique (3) **6,** 479 (1897).
[44] F. A. Wolff and C. E. Waters, Clark and Weston standard cells, BS Bull. **4,** 1 (1907).
[45] P. H. Lowrie, Jr., Controlled temperature oil baths for saturated standard cells, NBS Tech. Note 141, 1962.
[46] H. B. Brooks, The standard-cell comparator, a specialized potentiometer, BS J. Res. **11,** 211 (1933) RP586.
[47] J. H. Miller, A simplified standard cell comparator, AIEE Communications and Electronics, No. 14, 413 (Sept. 1954).
[48] G. D. Vincent, The construction and characteristics of standard cells, IRE Trans. Instr. **I-7,** Nos. 3 and 4, 221 (1958).
[49] A. W. Spinks and F. L. Hermach, Portable potentiometer and thermostatted container for standard cells, Rev. Sci. Instr. **26,** No. 8, 770 (1955).
[50] Barbara A. Wickoff, The establishment and maintenance of the unit of voltage at the National Bureau of Standards—Boulder, ISA Preprint No. 28.2.63, 18th Annual Conference and Exhibit, Chicago, Sept., 1963.
[51] A. C. Kolossov, Determination by the method of the silver voltameter of the electromotive force of the International Weston Normal Cell, Procès Verbaux, Comité international des Poids et Mesures **16,** 150 (1933) Annexe No. 19.
[52] Appendix 3 of ref. [8] and p. 16 of ref. [8].
[53] Procès Verbaux, Comité International des Poids et Mesures **17,** 94 (Resolution 4), 1935.
[54] J. F. Daniell, On voltaic combinations, Phil. Mag. III, **8,** 421 (1836).
[55] W. R. Cooper, Primary batteries: their theory, construction and use, 2d ed., Ch. IX, D. Van Nostrand Com. Ltd., London, 1916.
[56] G. W. Vinal, Primary batteries, pp. 32, 232, 233, John Wiley & Sons, New York, 1950.
[57] Normal-Daniell-Element der Edison and Swan United Electric Light Company (Fleming and W. Thomson), Dingler's polytechnisches J. **258,** 319 (1885); also Reports of Paris International Electrical Congress, 1882.
[58] W. De la Rue and H. W. Müller, On a new form of constant battery, J. Chem. Soc. **21,** 488 (1868); Experimental researches on the electric discharge with the chloride of silver battery, Phil. Trans. Royal Soc. I, **169,** 55 (1878); this second paper deals with the cell as a standard and compares the cell with a Clark standard cell.
[59] H. Helmholtz, Die thermodynamik chemischer Vorgänge, Sitzungsber. der Königlich Preussischen Akad. der wissenschaften zu Berlin, p. 27, 1882; see also ref. [75], p. 11, 74; W. Ostwald, Das kompensations-elektrometer, Z. phys. Chem. **1,** 403, 1887.
[60] M. Gouy, Sur une pile étalon, Compt. Rendu. **104,** 781 (1887), J. de phys. (2) **7,** 532 (1888); Über ein Normalelement, Z. physik. Chem. **2,** 978 (1888).
[61] Edward Weston, Galvanic battery, U.S. Patent 310,004 (Dec. 30, 1884).
[62] H. S. Carhart, An improved standard Clark cell with low temperature coefficient, Phil. Mag. **28,** 420 (1889), Am. J. Sci. (3) **38,** 402 (1889); Relation between the electromotive force of a Clark cell and the density of the zinc sulphate solutions, (Proc.) Am. Ind. Elect. Eng. **9,** 615 (1892).
[63] J. N. Brönsted, Studien zur chemischen affinität. V. Die bildung des kaliumbleisulfats, Z. physik. Chem. **77,** 315 (1911).
[64] W. E. Henderson and G. Stegeman, A lead standard cell and a determination of the potential of the lead electrode, J. Am. Chem. Soc. **40,** 84 (1918).
[65] W. C. Vosburgh, M. Guagenty, and W. J. Clayton, Saturated standard cells with small temperature coefficients. II, J. Am. Chem. Soc. **59,** 1256 (1937).
[66] W. C. Vosburgh and R. G. Bates, Constancy of modified Weston standard cell over long periods, J. Electrochem. Soc. **111,** 997 (1964).
[67] H. L. Callendar and H. T. Barnes, On the variation of the electromotive force of different forms of the Clark standard cell with temperature and strength of solution, Proc. Royal Soc. (London) **62,** 117 (1897).
[68] G. A. Hulett, The constancy of standard cells and a constant temperature bath, Phys. Rev. **32,** 257 (1911); The construction of standard cells and a constant temperature bath, The Electrician **67,** 129 (1911), see also ref. [91].
[69] C. R. A. Wright and C. Thompson, On the determination of chemical affinity in terms of electromotive force. Part VII. On the electromotive force of Clark's mercurous-sulphate cell; on the work done during electrolysis. On the e.m.f. of Clark's cell, Phil. Mag. V, **16,** 25 (1883).
[70] K. Kahle, Instructions for preparing Clark standard cells, The Electrician **31,** 265 (1893).
[71] Ref. [55], p. 336.
[72] International Critical Tables, Vol. 2, p. 436, 1927.
[73] W. J. Hamer, Hydrolysis of aqueous solutions of cadmium and zinc sulfates at 25 °C, unpublished, NBS.
[74] K. Kahle, Zur behandlung des silvervoltameters und seine verwendung zur bestimmung von Normalelementen, Ann Physik. (or Wied. Ann.) (3) **67,** 1 (1899), Z. Instrk. **18,** 230 (1898).
[75] W. Jaeger, Die Normalelement und ihre anwendung in der elektrischen messtechnick, Wilhelm Knapp, Halle a.S., 1902.
[76] G. A. Hulett, Equilibria in standard cells, Phys. Rev. **27,** 337 (1908).
[77] G. A. Hulett, Die destillation von amalgamen und die reinigung des quecksilbers, Z. physik. Chem. **33,** 611 (1900); see also G. A. Hulett and H. D. Minchin, Distillation of amalgams and purification of mercury, Phys. Rev. **21,** 388 (1905).
[78] C. L. Gordon and E. Wichers, Purification of mercury and its physical properties, Ann. N.Y. Acad. Sci. **65,** 369 (1957).
[79] L. H. Brickwedde, Solubility of cadmium sulfate in H_2O–D_2O mixtures, J. Res. NBS **36,** 377 (1946) RP1707.
[80] F. Mylius and R. Funk, Über die hydrate des cadmiumsulfats, Ber. deut. chem. Ges. **30,** 824 (1897).
[81] Ph. Kohnstamm and E. Cohen, Physikalisch-chemische studien am Normalelement von Weston, Ann. Physik. (or Wied. Ann.) (3) **65,** 344 (1898).
[82] International Critical Tables, Vol. 1, p. 120, 1926.
[83] International Critical Tables, Vol. 2, p. 429, 1927.
[84] F. E. Smith (Sir Frank), On the preparation of a cadmium cell, The Electrician **55,** 857 (1905).
[85] G. Deniges, Sur de nouvelles classes de combinaisons mercurico-organiques et sur leurs applications, Ann. chim. phys. [7] **18,** 382 (specifically 397) 1899, see also ref. 102.
[86] F. Laporte, Report to the International Committee on electrical units and standards, p. 111, Washington, D. C., Jan. 1, 1912.
[87] D. N. Craig, G. W. Vinal, and F. E. Vinal, Solubility of

mercurous sulphate in sulphuric-acid solutions, J. Res. NBS **17,** 709 (1936) RP939.
[88] M. Gouy, Action de l'eau sur le sulfate mercureux, Compt. rendu. **130,** 1399 (1900).
[89] O. B. Hager and G. A. Hulett, The hydrolysis of mercurous sulphate, J. Phys. Chem. **36,** 2095 (1932).
[90] L. H. Brickwedde, Method of making saturated cells at the National Bureau of Standards, Compt. rendu. de la Quatorzième Conference, Int. Union Pure and Applied Chem. p. 105, July 1947.
[91] G. A. Hulett, A study of the materials used in standard cells and their preparation, Part 1. Mercurous sulphate and standard cells, Trans. Am. Electrochem. Soc. **6,** 109 (1904), Trans. Int. Elec. Cong., St. Louis **2,** 109 (1904).
[92] F. E. Smith (Sir Frank), A dictionary of applied physics, p. 267, ed. Sir Richard Glazebrook, Macmillan and Co., Ltd., London, 1911.
[93] P. H. Walker and F. W. Smither, Comparative tests of chemical glassware, J. Ind. Eng. Chem. **9,** 1090 (1917). Tech. Pap. BS **10** (1918) T107.
[94] E. Wichers, A. N. Finn, and W. S. Claybaugh, Comparative tests of chemical glassware, J. Res. NBS **26,** 537 (1941) RP1394.
[95] H. Fleischer, Chemical indicator, U.S. Patent 2,416,619 (Feb. 25, 1957); Sensitive indicator for volumetric determination of boiler feedwater alkalinity, Ind. Eng. Chem., Anal. Ed. **15,** 742 (1943); the author did not specifically call his indicator "methyl purple" but the indicator he suggested later became to be known by this name; see also, Water Works Manual, 1947–48 Ed.
[96] G. W. Vinal, L. H. Brickwedde, and W. J. Hamer, New quartz containers for standard cells at the National Bureau of Standards, Compt. rendu. de la Quinizième Conference, Int. Union Pure and Applied Chem., p. 92, Amsterdam, Sept. 1949.
[97] W. G. Houskeeper, The art of sealing base metals through glass, J. Am. Inst. Elec. Eng. **42,** 954 (1923).
[98] C. A. Dyer, Primary electrolytic cell or group of cells (to Minneapolis-Honeywell Regulator Co.), U.S. Patent 2,647,155 (July 28, 1953).
[99] R. O. Heinrich, Standard voltaic cell, U.S. Patent 631,044 (Aug. 15, 1899).
[100] H. Eicke and A. Kessner, Eine stabförmige Bauart des Weston-Normalelementes, Electrotech. Z. (A) **74,** 623 (1953).
[101] E. F. Mueller and H. F. Stimson, A temperature-control box for saturated standard cells, J. Res. NBS **13,** 699 (1933) RP739.
[102] W. C. Vosburgh and M. Eppley, The temperature coefficients of unsaturated Weston cells, J. Am. Chem. Soc. **45,** 2268 (1923).
[103] Ref. [92], p. 268.
[104] Report of Natl. Phys. Lab., Electrician **75,** 463 (1915).
[105] J. Obata, Cadmium standard cells containing acid electrolyte, Proc. Math. Phys. Soc. (Japan), (3), **2,** 232 (1920).
[106] V. Ishibashi and T. Ishizaki, Further studies on acid standard cells, Researches Electrotechnical Lab., No. 318, 1931.
[107] W. C. Vosburgh, Conditions affecting the reproducibility and constancy of Weston standard cells, J. Am. Chem. Soc. **47,** 1255 (1925).
[108] F. E. Smith (Sir Frank), On cadmium amalgams and the Weston Normal Cell, Proc. Phys. Soc. (London) **22,** 11 (1910); Phil. Mag. **19,** 250 (1910); Natl. Phys. Lab. Coll. Res. **6,** 137 (1910).
[109] G. W. Vinal and L. H. Brickwedde, Metastability of cadmium sulfate and its effect on electromotive force of saturated standard cells, J. Res. NBS **26,** 455 (1941) RP1389.
[110] P. Vigoureux and S. Watts, Temperature coefficient of Weston cells, Proc. Phys. Soc. (London) **45,** 172 (1933).
[111] J. H. Park, Effect of service temperature conditions on the electromotive force of unsaturated portable standard cells, BS J. Res. **10,** 89 (1933) RP518.
[112] M. Eppley, International standard of electromotive force and its low-temperature-coefficient form, Trans. AIEE **50,** No. 4 1923 (1931).
[113] International Critical Tables, Vol. 1, $CdSO_4 \cdot 8/3\ H_2O$ (p. 120), Hg_2SO_4 (p. 121); Vol. 2, Cd (p. 456), Hg (p. 458); Vol. 3, sat. sol. $CdSO_4$, interpolated (p. 66).
[114] Table of atomic weights, 1961 (Based on carbon-12), Chem. and Eng. News., p. 43, Nov. 20, 1961.
[115] D. N. Craig, J. I. Hoffman, C. A. Law, and W. J. Hamer, Determination of the value of the faraday with a silver-perchloric acid coulometer, J. Res. NBS **64A** (Phys. and Chem.) 381 (1960).
[116] R. R. Ramsey, The change of volume in Clark and cadmium cells and its relation to change of electromotive force due to pressure, Phys. Rev. **XVI,** No. 2, 105 (1902).
[117] Based on measurements made at Natl. Bur. Standards by Phyllis R. Robb and W. J. Hamer, 1950–52; see also ref. [120].
[118] G. A. Hulett, Mercurous sulphate and the standard cell, Phys. Rev. **22,** 321 (specially 336, footnote 1) 1906.
[119] R. J. Brodd and W. G. Eicke, Jr., Effect of vibration and shock on unsaturated standard cells, J. Res. NBS **66C** (Eng. and Instr.) 85 (1962).
[120] G. D. Vincent, Effect of current drains on cadmium standard cells, J. Electrochem. Soc. **104,** 712 (1957).
[121] G. W. Vinal, D. N. Craig, and L. H. Brickwedde, Standards of electromotive force, Trans. Electrochem. Soc. **68,** 139 (1935).
[122] Ref. [56], p. 211.
[123] F. X. Lamb. Aging of standard cells, NBS Circ. 524, Electrochemical constants, Ch. 11, 1953.

10. Appendix 1

U.S. Law of 1894, 53d Congress, 28 Stat., Ch. 131, p. 102 (Public—No. 105)

An Act To define and establish the units of electrical measure

Be it enacted by the Senate and House of Representatives of the United States of America in Congress assembled, That from and after the passage of this Act the legal units of electrical measure in the United States shall be as follows:

First. The unit of resistance shall be what is known as the international ohm, which is substantially equal to one thousand million units of resistance of the centimeter-gram-second system of electro-magnetic units, and is represented by the resistance offered to an unvarying electric current by a column of mercury at the temperature of melting ice fourteen and four thousand five hundred and twenty-one ten-thousandths grams in mass, of a constant cross-sectional area, and of the length of one hundred and six and three tenths centimeters.

Second. The unit of current shall be what is known as the international ampere, which is one-tenth of the unit of current of the centimeter-gram-second system of electro-magnetic units, and is the practical equivalent of the unvarying current, which, when passed through a solution of nitrate of silver in water in accordance with standard specifications, deposits silver at the rate of one thousand one hundred and eighteen millionths of a gram per second.

Third. The unit of electro-motive force shall be what is known as the international volt, which is the electro-motive force that, steadily applied to a

conductor whose resistance is one international ohm, will produce a current of an international ampere, and is practically equivalent to one thousand fourteen hundred and thirty-fourths of the electro-motive force between the poles or electrodes of the voltaic cell known as Clark's cell, at a temperature of fifteen degrees centigrade, and prepared in the manner described in the standard specifications.

Fourth. The unit of quantity shall be what is known as the international coulomb, which is the quantity of electricity transferred by a current of one international ampere in one second.

Fifth. The unit of capacity shall be what is known as the international farad, which is the capacity of a condenser charged to a potential of one international volt by one international coulomb of electricity.

Sixth. The unit of work shall be the Joule, which is equal to ten million units of work in the centimeter-gram-second system, and which is practically equivalent to the energy expended in one second by an international ampere in an international ohm.

Seventh. The unit of power shall be the Watt, which is equal to ten million units of power in the centimeter-gram-second system, and which is practically equivalent to the work done at the rate of one Joule per second.

Eighth. The unit of induction shall be the Henry, which is the induction in a circuit when the electromotive force induced in this circuit is one international volt while the inducing current varies at the rate of one Ampere per second.

Sec. 2. That it shall be the duty of the National Academy of Sciences to prescribe and publish, as soon as possible after the passage of this Act, such specifications of details as shall be necessary for the practical application of the definitions of the ampere and volt hereinbefore given, and such specifications shall be the standard specifications herein mentioned.

11. Appendix 2

Public Law 617—81st Congress
(Chapter 484—2d Session)
(S. 441)

AN ACT

To redefine the units and establish the standards of electrical and photometric measurements.

Be it enacted by the Senate and House of Representatives of the United States of America in Congress assembled, That from and after the date this Act is approved, the legal units of electrical and photometric measurements in the United States of America shall be those defined and established as provided in the following sections.

SEC. 2. The unit of electrical resistance shall be the ohm, which is equal to one thousand million units of resistance of the centimeter-gram-second system of electromagnetic units.

SEC. 3. The unit of electric current shall be the ampere, which is one-tenth of the unit of current of the centimeter-gram-second system of electromagnetic units.

SEC. 4. The unit of electromotive force and of electric potential shall be the volt, which is the electromotive force that, steadily applied to a conductor whose resistance is one ohm, will produce a current of one ampere.

SEC. 5. The unit of electric quantity shall be the coulomb, which is the quantity of electricity transferred by a current of one ampere in one second.

SEC. 6. The unit of electrical capacitance shall be the farad, which is the capacitance of a capacitor that is charged to a potential of one volt by one coulomb of electricity.

SEC. 7. The unit of electrical inductance shall be the henry, which is the inductance in a circuit such that an electromotive force of one volt is induced in the circuit by variation of an inducing current at the rate of one ampere per second.

SEC. 8. The unit of power shall be the watt, which is equal to ten million units of power in the centimeter-gram-second system, and which is the power required to cause an unvarying current of one ampere to flow between points differing in potential by one volt.

SEC. 9. The units of energy shall be (a) the joule, which is equivalent to the energy supplied by a power of one watt operating for one second, and (b) the kilowatt-hour, which is equivalent to the energy supplied by a power of one thousand watts operating for one hour.

SEC. 10. The unit of intensity of light shall be the candle, which is one-sixtieth of the intensity of one square centimeter of a perfect radiator, known as a "black body", when operated at the temperature of freezing platinum.

SEC. 11. The unit of flux of light shall be the lumen, which is the flux in a unit of solid angle from a source of which the intensity is one candle.

SEC. 12. It shall be the duty of the Secretary of Commerce to establish the values of the primary electric and photometric units in absolute measure, and the legal values for these units shall be those represented by, or derived from, national reference standards maintained by the Department of Commerce.

SEC. 13. The Act of July 12, 1894 (Public Law Numbered 105, Fifty-third Congress), entitled "An Act to define and establish the units of electrical measure", is hereby repealed.

APPROVED July 21, 1950.

12. Appendix 3

Standard Cells with Deuterium Oxide

The electromotive forces of saturated standard cells, made with deuterium oxide and normal water follow:

Percentage of D_2O in the water	Emf at 20 °C,[b] volts
0.02 [a]	1.018603
10	1.018567
20	1.018531
30	1.018495
40	1.018459
50	1.018423
60	1.018384
70	1.018344
80	1.018301
90	1.018255
100 (extrapolated from 98 percent)	1.018204

[a]—Normal water contains 0.02 percent deuterium oxide.
[b]—Original data were reported in international volts and have here been converted to absolute volts.

These cells were made with crystals of cadmium sulfate in equilibrium with the respective solutions. This was accomplished by saturating each solution with anhydrous cadmium sulfate; the crystals that separated from the solution were then in equilibrium with the saturated solution. The solutions were then made 0.035 to 0.042 *N* with respect to sulfuric acid; the above emfs are reported on a uniform basis of 0.04 *N*.

Cadmium sulfate is about 8 percent less soluble in heavy water than in normal water in the temperature range of 0 to 60 °C. This comparison follows:

	Temperature °C	Moles $CdSO_4$ per mole water	
		normal water [b]	heavy water
$CdSO_4 \cdot 8/3$ aq [a]	0	0.06546	0.06026
	5	.06555	.06033
	10	.06566	.06042
	15	.06580	.06055
	20	.06600	.06073
	25	.06627	.06097
	30	.06663	.06130
	35	.06710	.06174
	40	.06773	.06232
	45	.06857	.06311
	50	.06955	.06415
$CdSO_4 \cdot aq$ [a]	45	.06797	.06326
	50	.06659	.06181
	55	.06522	.06037
	60	.06385	.05893

[a]—here aq means either H_2O or D_2O.
[b]—contains 0.02 percent heavy water.

Studies of the changes in the difference between the emf of cells made with normal and heavy water with time have given supplemental evidence on the stability of the National Reference Group of Standard Cells. These studies have shown that this difference is within the spread, namely, 0.05 μV/year, discussed under item (1) on maintenance in section 2.3. However, cells made with heavy water have not, to date, shown the same internal consistency as those made with normal water, i.e., individual cells show greater day-to-day variations in emf than normal water cells.

13. Appendix 4

Coulometer (Smith form) measurements* by the United States in the Physikalisch-Technische Reichsanstalt at Charlottenburg, 1931

Item	Experiment Number**									
	1	2	3	4	5	7	8	9	10	
A	4.09189	4.09328	4.09600	4.08556	4.08615	4.10120	4.09495	4.09105	4.16814	
B	4.09172	4.09317	4.09591	4.08543	4.08621	4.10123	4.09507	4.09110	4.16824	
C	7230.00	7199.85	7200.06	7199.84	7200.01	7200.16	7200.06	7199.84	7320.05	
D	1.999989	1.999973	1.999973	1.999975	1.999973	1.999971	1.999975	1.999981	1.999985	
E	0.000005	0.000005	0.000005	0.000005	0.000005	0.000005	0.000005	0.000005	0.000005	
F	1.018301	1.018429	1.018411	1.018336	1.018334	1.018331	1.018328	1.018332	1.018334	
G	1.018301	1.018430	1.018402	1.018336	1.018334	1.018330	1.018328	1.018330	1.018332	
H	1.012582	1.017114	1.018145	1.015176	1.015326	1.019020	1.017458	1.016712	1.018796	
J	1.018259	1.018390	1.018694	1.018296	1.018293	1.018288	1.018283	1.018283	1.018286	
K	0.000011	0.000011	0.000014	0.000014	0.000013	0.000015	0.000013	0.000013	0.000012	
L	1.018116	1.018299	1.018234	1.018229	1.018220	1.018238	1.018266	1.018070	1.018144	ave = 1.018202
M	1.018187	1.018370	1.018305	1.018300	1.018291	1.018309	1.018337	1.018141	1.018215	ave = 1.018273

*Electrical measurements made in PTR units; (USA − PTR) ohm = 9 ppm; (USA − PTR) volts = − 61 ppm.
**Experiment Number 6 was conducted with a porous-cup coulometer, therefore, not included.
A—weight of silver deposit in one coulometer, grams.
B—weight of silver deposit in second coulometer in series with A, grams.
C—time of electrolysis, seconds.
D—resistance *R* of standard resistor, ohms.
E—correction for resistance owing to leads, etc., ohm.
F—average emf of control cell at 20 °C, volts.
G—emf of control cell at 20 °C at end of run, volts.
H—*IR* in standard resistor, volts; *I* is current in amperes.
J—emf of German reference cell at 20 °C, volts.
K—correction to *J* to give mean value of Kleiner Stamm (primary volt standard of Germany), volt.
L—German value of selected cell at 20 °C; given by

$$E_s = \left[\left(\frac{A+B}{2}\right)\left(\frac{D}{0.001118C}\right)\frac{FJ}{GH}\right] + (E+K) \text{ volts}$$

M—USA (USA units) value of selected cell at 20 °C; given by

$$M = 1.000070L \text{ volts, since (USA} - \text{PTR) ohm} = 9 \text{ ppm and (USA} - \text{PTR) volts} = -61 \text{ ppm}$$

14. Appendix 5

Constant-Temperature Oil Baths

Constant-temperature oil baths of the type used to maintain the National Reference Group of Standard Cells at a constant temperature were shown in figure 2. In this appendix a general description of a typical bath is presented. A circular bath of stainless steel or nickel-plated copper, about 75 cm in diameter and 45 cm deep, may be used (all other metal parts are also of steel or nickel-plated copper to prevent the possibility of galvanic corrosion). It is filled with oil (see Appendix 6) to a depth of about 35–40 cm. The oil is stirred by a centrally located two-blade agitator which produces an upward and rotary circulation. The agitator (9) is about 48 cm in length, 5 cm wide, 0.3 cm thick, has a pitch of 20° and rotates at about 45 rpm. It is supported on a shaft (1) which is supported in ball bearing housings at the bottom and top of the bath (the one at the top is supported in a metal slab (3), about 10 cm wide and 0.3 cm thick, which rests on the central top edges of the bath. A drip cup (4) is placed on the shaft at the position shown to collect any grease that may flow down the shaft from the ball bearing housing. To guide the direction of oil circulation a metal baffle (5), 25 cm in height, is placed in the bath in the position shown in figure A1. This baffle extends to 10 cm of the bottom of the bath and slightly above the agitator. This baffle serves also to protect the cells from direct influence of the heating element and the cooling coils.

Heating is supplied by a heating coil (8) of bare manganin wire wound on a Pyrex rod having a diameter of 1 cm. This rod is supported about 5 cm above the bottom of the bath by glass supports and circles the bath; its position is clearly shown in figure A1. The heating coil has a resistance of 90 ohms and operates on 110-V d-c supply. A bank of four incandescent lamps in parallel is included in the heating circuit; two lamps operate intermittently during control while two operate continuously, i.e., some heating is provided continuously and some intermittently. Cooling coils (7), (11), as shown, are also provided. Through these coils flow oil of the same type as used in the bath. These coils are connected to similar coils in the freezing compartment of a refrigerator and the required cooling is attained by controlling the rate of oil flow. Cooling by this means is required only in emergencies or when tests of standard cells are made at temperatures below room temperature. The temperature of the bath is determined by a platinum resistance thermometer and a Mueller bridge; the thermometer is supported at the position (2) shown in the figure. The lamps in the circuit also aid an operator in determining when the bath has attained a peak temperature (one reading on Pt resistance thermometer) and a

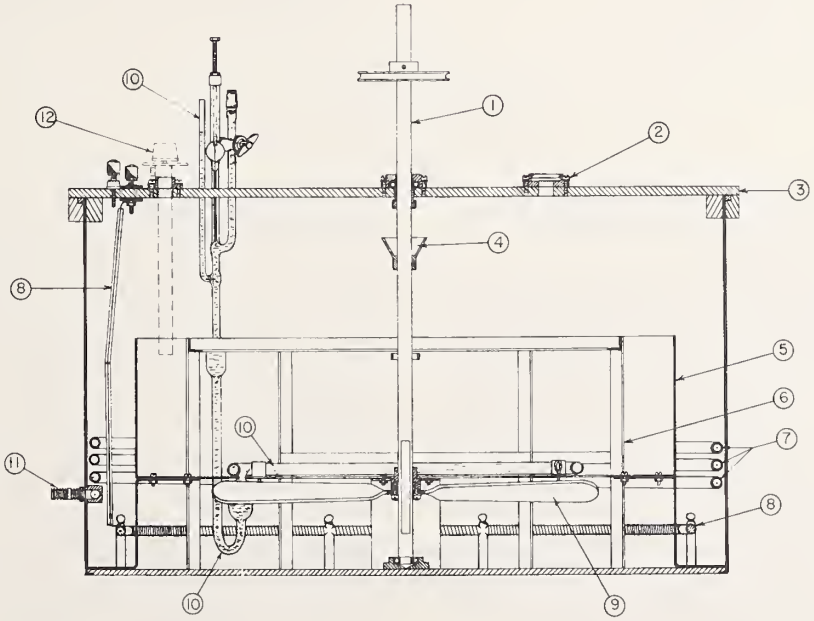

FIGURE A1. *Cross-sectional sketch of a constant-temperature oil bath used at the National Bureau of Standards.*

1—Agitator shaft
2—Thermometer mount
3—Center plate
4—Drip cup
5—Baffle
6—Cell rack
7—Cooling coils
8—Heater
9—Agitator
10—Mercury-toluene regulator
11—Cooling coil connector
12—Fenwall thermoswitch

lower temperature (second reading on Pt resistance thermometer) and thereby determine the mean temperature of the bath (the period between peak and low temperatures is about 15 sec).

A mercury-toluene regulator (10) is used as the temperature-control element. It consists of a reservoir in the form of a rectangle, 40 cm on an edge, made of thin-walled Pyrex tubing, 1.5 cm in diameter, containing the thermometric substance (toluene), the volume changes being transmitted by a U-shaped connecting tube filled with mercury to a vertical capillary as shown in the figure. The U-shaped connecting tube is provided with a downward extension from the toluene reservoir to allow for expansion and contraction of the toluene thereby preventing the tolucne from reaching the capillary. The capillary is about 1 mm in diameter and 8 cm long and the adjustable electrical contact to the mercury is made with a steel piano wire. The permanent electrical terminal to the mercury is made through a seal about 4 cm below the capillary tube. This terminal is connected to the electromagnet of a sensitive 150-Ω relay, whereas the adjustable terminal is connected to one terminal of a long-life Lalande battery of 2.5 volts; the other terminal of this battery is connected to the electromagnet. The secondary of the relay is in the 110-volt d-c heater circuit. The regulator is supported on the baffle about 10 cm from the bottom of the bath. The capillary extends above the oil and is therefore, exposed to the air; this exposure, however, does not cause a significant error in regulation. A Fenwall thermoswitch (12) is included in the heating circuit as a precaution in case the regulator does not function; this thermoswitch opens the heating circuit at a preset value, usually 1 °C, above the temperature at which the bath is controlled. The standard cells are mounted in the bath on the metal rack (6) in the manner described in the text (sec. 2.3). Other details on the bath are shown in figure A1.

15. Appendix 6

Oil for Constant-Temperature Baths

The quality of the oil in which standard cells are submerged is of considerable importance, and for this purpose a white mineral oil with the following specifications is used:
Colorless, odorless, tasteless;
Viscosity, in poises at 25 °C, 0.245*;
Specific gravity, 25 °C, 0.846;
Flashpoint, 171 °C (340 °F);
Burning point, 207 °C (405 °F);
Acidity (mg KOH/gm oil), none;
Sulfur, none;
Oxidation number, 0;
Gum, on heating in oxygen, none;
Discoloration, on heating in oxygen, slight orange.
*Sufficiently low as to make the stirring effective.

In addition this oil, when new, has a resistivity of about 3×10^{14} ohm-cm or higher.

16. Appendix 7

Constant-Temperature Enclosure for Saturated Standard Cells

The Mueller-Stimson temperature-control box for saturated standard cells was described in general terms in section 5.4. In this appendix more details are given. In this control box, the temperature of an outer aluminum case is automatically controlled by a conventional mercury-in-glass thermoregulator. A second aluminum case, inside the first and thermally well insulated from it, contains five saturated standard cells. The inner case assumes a temperature very nearly the time average of that of the outer case. The inner case is 3⅝ in. long, 2¾ in. wide, and 4 in. deep inside. This case is a casting with ¼-in. walls and ⅜-in. bottom. A ¼-in.-thick cover is secured to the casting by numerous screws to improve thermal contact. The inner case is spaced within the outer one with ½ in. balsa wood on all six sides. The outer case is also a casting, with ⅜ in. sidewalls and ½ in. bottom. A cover of sheet ⅜-in. aluminum is secured to the top by screws. The endwalls of the casting are plane on the inside and cylindrical on the outside, the thickness at the edges being ⅜ in. and ¾ in. at the middle; this extra thickness at the middle provides space for a vertical hole, 15/32 in. in diameter and 6 in. deep, to accommodate the thermoregulator at one end and a smaller hole to accommodate a thermometer at the other end.

The outer case is insulated with a layer of balsa wood 1 in. thick on the sides and bottom and 2 in. thick on the top. The pieces of balsa wood fit neatly into an outer wooden box. This box is of sufficient size to provide a compartment at one end to house a transformer, relay, and binding posts for the necessary connections. These accessories are mounted on a wooden panel which slides in vertical grooves in the sides of the box. The outside dimensions of the box are 8 by 13 in., by 10 in. deep, and its weight, complete, is 22 lb. A horizontal section of the control box is shown in figure A2.

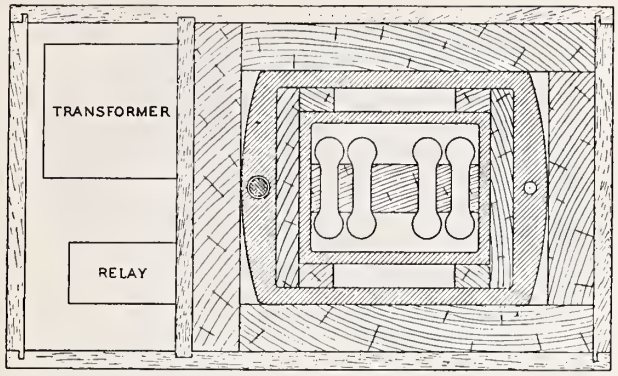

FIGURE A2. *Horizontal sketch of Mueller-Stimson temperature-controlled box.*

The standard cells are mounted on balsa wood of appropriate size. No. 28 (0.013 in.) insulated copper wire, 4 ft. in length, is used for connections to the cell terminals. About one-third of this length is formed in a helix which is kept inside the inner case and another one-third is placed between the inner and outer cases. The wires are brought through the cases in smoothed saw cuts in the upper edges of the sides and insulated additionally with silk and glyptal whereby good thermal contact with the metal cases is assured. These thermal tiedowns and lengths of wire reduce heat conduction to a negligible amount. Sheets of mica are placed on the surfaces of the aluminum cases, adjacent to the connecting wires, to protect them against accidental electrical grounding. Outside the outer case the wires are brought to binding posts supported on a hard-rubber strip; the positive terminal is placed on one side of the box, the negative on the other.

The thermoregulator is an adjustable mercury-in-glass type with a bulb 4 in. long about $^{15}/_{32}$ in. in diameter, and 8 in. long. It is covered with grease to assure good thermal contact to the reservoir into which it fits.

The heating resistor, No. 38 (0.004 in.) constantan wire, has a resistance of about 70 Ω and is wound in four turns on the sides and ends of the outer aluminum case on silk fabric. One turn is placed near the top edge and another near the bottom edge of the case. It operates on 20 V. A small, quick-acting 12-V a-c relay operating on about 0.05 A is used. Power for the heater and relay is supplied by a bell-ringing transformer rated at 50 W.

ISA JOURNAL
INSTRUMENTATION ■ SYSTEMS ■ AUTOMATIC CONTROL

Oil Baths for Saturated Standard Cells*

Patrick H. Lowrie, Jr.
National Bureau of Standards
Boulder, Colorado

Limiting bath temperature variations to less than 0.002°C per day, a modified on-off control system helps achieve the inherent accuracies attributable to standard cells.

INDUSTRY today is faced with the need for continually increasing accuracy of measurement. One result: the increasing use of saturated standard cells in industrial standards laboratories. Because of their rather large temperature coefficient of emf, these saturated cells[1] must be contained in a temperature-controlled environment to realize their inherent accuracy. In answer to the growing demand for temperature-controlled baths, several companies are now manufacturing baths appropriate for use with these cells. Frequently, however, the user prefers to build his own bath to include special features. In the design of any enclosure of this type the two most important requirements are close temperature control and the control of gradients. No matter how elaborate the design, if these two requirements are not met, the bath will be inadequate.

The oil bath has many advantages over the air bath. In oil the temperature gradients may be controlled with a much lower fluid velocity than that required in air. Thus, larger oil baths may be built without requiring fluid velocities that might adversely affect the cells. As a result, more groups of cells may be contained in a single bath when using oil as the medium. In addition, provided the proper precautions are taken, cells or groups of cells may be introduced into or removed from the oil without disturbing the other groups in the same bath. This is because there is no heat loss due to convection when the lid of the bath is opened. Furthermore, better temperature control can be achieved in an oil bath than can be achieved in an air bath of equivalent size.

Much experience with oil baths has been gained in the many years during which they have been in use at NBS. (However, with the exception of very early papers,[2,3] the published information has been rather sparse.) When it became necessary to establish and maintain an accurate standard of voltage at the NBS Boulder Laboratories, this experience was drawn upon. Additional features were incorporated to obtain the desired temperature control and allow a large calibration workload to be handled conveniently. The accuracy desired in the measurement of cells dictated a short-time temperature variation of no greater than ± 0.001°C, with day-to-day variations held to no greater than 0.005°C. It was desired that temperature gradients be unmeasurably small because of the extreme sensitivity of emf to temperature differences between the two legs of the saturated cells.[4] Moreover, the baths had to exhibit a flexibility of design such that they could accept any type of normally used cell rack.

*An abbreviated version of NBS Technical Note 141.

Reprinted from ISA Journal, December, 1962

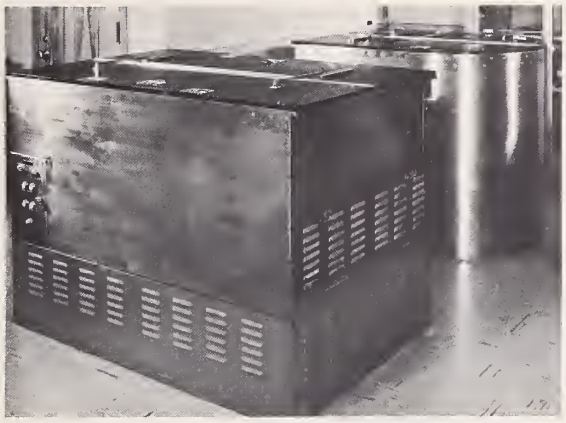

Figure 1. Standard cell oil baths at NBS, Boulder, Colo.

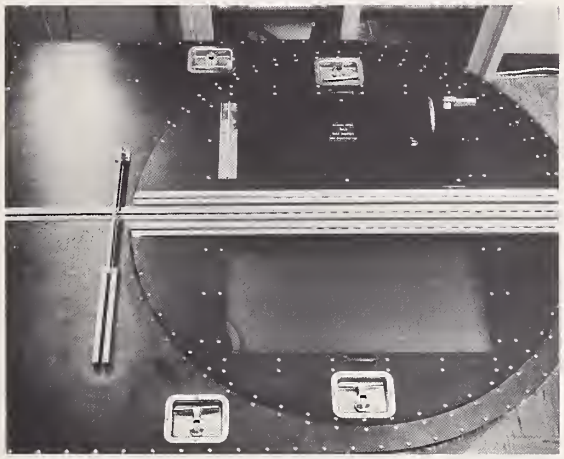

Figure 2. Top view of 28°C oil bath.

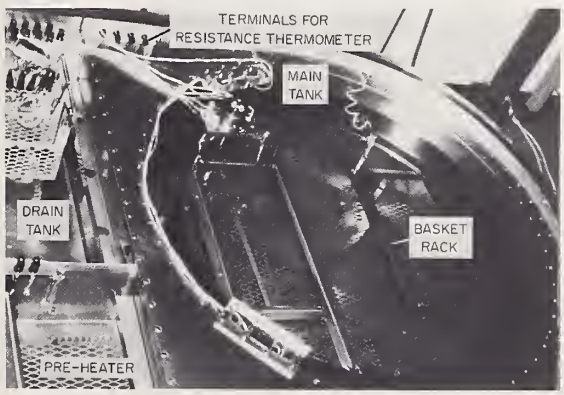

Figure 3. View of bath with cover removed.

General Description

The oil baths discussed here were designed as free-standing self-contained units. At present two baths are in use (Figure 1). The rectangular bath is used for measurements of 35°C; and the D-shaped bath, containing the reference group of standard cells, is used for measurements at 28°C. Each bath consists of three tanks: a main tank, in which the cells are contained during measurement (and usually for 3 to 5 weeks before measurement), a drain tank, and a pre-heater tank. The pre-heater is used to bring a group of cells and its container, basket, etc., to the approximate temperature of the oil in the main tank. This is done to prevent temperature gradients in the oil of the main tank, which otherwise would be caused by the introduction of new groups of cells, and would degrade the accuracy of measurements for periods of one to two hours. The space between the main tank and the outer wall of the bath is filled with crushed cork. The bath time constant is long enough to eliminate nearly all effects of changes in room temperature over an eight-hour period. Approximately four hours after a room temperature change of 2°C, the oil temperature will have changed only by about 0.001°C. Each bath is covered with a compound lid (Figure 2), designed so that only a small section need be opened for measurement of the cells. When cells are transferred from pre-heater to main tank, or from main tank to drain tank, one whole side is opened. The entire cover may be quickly removed if the need arises. One-inch thick, and fabricated of aluminum channel faced with sheet aluminum, the cover is filled with rigid polystyrene foam. Figure 3 shows the D-shaped bath with the cover removed. Toward the rear of the main tank may be seen part of the temperature-regulating apparatus. In the left rear corner of the basket rack is the guard regulator which serves to prevent a malfunction in the main circuit from damaging the cells. The small glass tube at the right rear corner of the basket rack is the upper end of the main thermoregulator. The temperature of the oil is measured with a platinum resistance thermometer, the terminals for which can be seen at the rear of the bath.

In general, the cell groups are contained in baskets hung from the framework in the main tank. As a protection against tipping, the baskets are designed to have the center of gravity of the cell group below the point of suspension. The baskets are provided with handles to facilitate their transfer to and from the oil.

Temperature Control

The control of temperature within very close tolerances requires careful coordination of both sensing and heating elements. To allow for overshoot, the sensing element must detect a somewhat smaller change in temperature than the maximum permissible temperature variation, and the heater must be designed to minimize overshoot. The sensing element is a Pyrex thermoregulator (Figure 4). It consists of a large sensing tube filled with toluene, to which is attached a second mercury-filled tube in the form of a "J". In operation, the toluene (which has a temperature coefficient of expansion approximately six times that of mercury) expands with increasing temperature and forces the mercury upward in the capillary section, causing it to make electrical contact between the sealed platinum electrode and a piece of platinum wire inserted in the capillary tube. The

contact closes a relay, which causes the heater voltage to be reduced.

Though simple in principle, the regulator poses many problems in practice, most of which can be overcome by the methods described. One inherent problem, of course, is its fragility; the J-tube is more than 13 inches long and only ¼ inch in diameter. For this reason extensive experimental work was done with thermoregulators of stainless steel (Figure 5), but these proved to be inconsistent in control. The cause of the inconsistency was not determined with certainty, but is believed to be the dimensional instability of the steel. Stainless steel regulators are in use in less critical applications and appear to be satisfactory for these purposes.

The first problem encountered after the regulator has been fabricated is that of filling it. Since the presence of air in the regulator would cause erratic operation and temperature fluctuation with changes in atmospheric pressure, it is necessary that the toluene be boiled to liberate all dissolved air before it is introduced into the sensing tube. (Toluene should be treated with care as it is highly flammable, and the fumes are toxic.) After the toluene has been boiled, it is carefully poured into a flask connected to the regulator through a three-way valve. The third port of the valve is connected to a vacuum pump. After the pump has evacuated the regulator, the valve is turned, allowing the toluene to flow into the regulator without contaminating the pump. Even though all connections are tight and sealed with vacuum grease, an air bubble probably will remain after the regulator has been filled. The bubble can be removed in the following manner. The regulator is cooled in an ice bath and additional toluene is allowed to flow into it. It is then carefully inverted to position the bubble at the junction of the sensing tube and the J-tube, and the sensing tube is gently warmed by holding it with bare hands until the expanding toluene has forced the bubble out. The easiest way to introduce mercury is to heat the regulator to about one degree higher than the highest temperature at which it will ever be used, and then pour as much mercury as possible into the J-tube. The regulator is then allowed to cool to room temperature; meanwhile mercury is added as needed.

In order to achieve a cyclic control of $\pm 0.001°C$, use was made of a principle discussed by T. Deighton.[5] The circuit using this principle is called an anticipator since it causes the regulator to act as though it anticipated the increase in temperature that would result in temperature overshoot, and to reduce the heater current before this effect can occur. Such anticipating action is controlled by a heater wire wound directly on the sensing tube of the regulator. This heater, being of much lower wattage than the main heater, introduces very little heat into the oil. It is supplied with current during the heating cycle, but is completely disconnected during the cooling cycle. The main heater is supplied continuously with current, adjusted to produce on the heating cycle slightly more heat than would be required to maintain temperature, and on the cooling cycle slightly less than would be required. Thus, while every effort is made to minimize the temperature change in the main heater (and still retain control), the temperature of the anticipator heater is allowed to change significantly during the cycle. As a result, the regulator senses a larger, faster temperature change than actually exists, and overshoot is minimized.

The regulator operates a sensitive relay which in turn controls two power relays. One of these changes the voltage applied to the main heater; the other operates the anticipator. The relay contacts are protected by zener diode spark suppressors. In order to eliminate relay chattering, an R-C delay (about a half second) circuit was added between the regulator and the sensitive relay.

The heater is of an open-grid design to minimize its heat capacity and obtain a short reaction time in order to prevent overshoot. The heater, wound on linen-base phenolic tubes reinforced with stainless steel, can be seen below the cylindrical baffle in Figure 5.

Control of Gradients

Originally considered was the possibility of using a high-speed centrifugal-type impeller to circulate the oil. This method, however, has two disadvantages: it tends to promote the existence of gradients in a large tank, and the impeller introduces considerable heat into the oil because of friction. Since gradients could not be tolerated, and since it was desired to operate one of the baths only 5°C above ambient (without cooling coils if possible), the design was

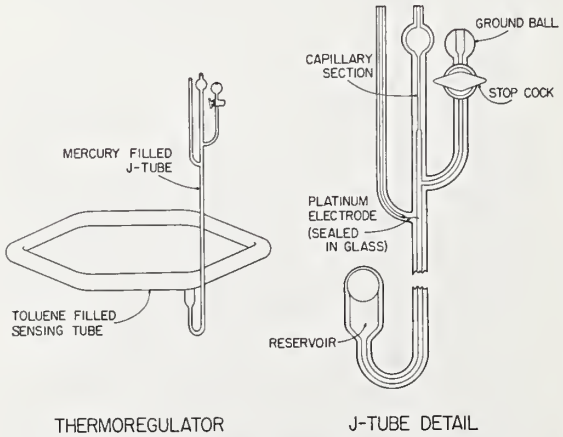

Figure 4. Oil bath temperature sensing element is a Pyrex thermoregulator.

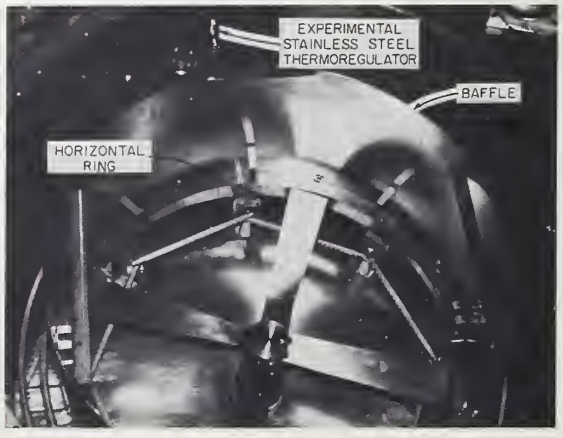

Figure 5. Internal view of 35°C oil bath.

changed to incorporate a large, low-speed, propeller-type stirrer. The present circulation system is shown in Figure 5. The four-bladed stirrer may be seen in the center of the figure.

In operation, the rotation of the stirrer draws the oil down through the center area of the tank. The oil then moves outward through the heater grid and up outside the cylindrical baffle. The horizontal ring, at the level of the blades, was added to prevent the oil from re-circulating without passing through the heater. Another problem was a volume of still oil at the center of the tank below the stirrer that caused some uncontrolled recirculation. This was solved by the addition of vertical blades (not visible in photo) welded to the underside of two horizontal blades to thrust the oil outward after it had been drawn through the horizontal blades. The stirrer is rotated at 50 rpm by a shaft inserted through the bottom of the tank. Leakage through the shaft hole is prevented by a mercury seal.

The temperature gradients were determined by establishing the minimum distance between two points in the oil, which, when probed with a platinum resistance thermometer, exhibited a temperature difference of 0.001°C. This distance was found to exceed 10 inches in all horizontal directions throughout the area in which the cells are contained.

EMF Connections

Electrical connection to the cells presented another problem: the system had to be flexible enough to accommodate any possible terminal configuration. To accomplish this, the various connectors are equipped with leads terminated in polarized copper plugs which are inserted in copper sockets provided at strategic points within the bath. The most common terminal with which cell racks are fitted is a ⅛-inch diameter copper post to which each platinum lead is soldered. Since these posts occasionally carry beads of solder, and since the diameter of the posts as well as their spacing may differ from rack to rack, a unique connector had to be designed. This contact clamp (Figure 6) accommodates any copper post configuration, clean or solder-covered, that has been encountered to date.

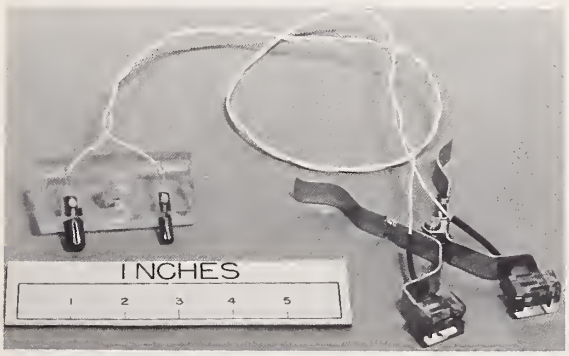

Figure 6. Specially designed contact clamp for making electrical connection to cells.

All leads that come in contact with the oil are insulated with Teflon, since cloth insulation acts as a wick, and vinyl becomes stiff after prolonged contact with the oil.

Protective Devices

If a standard cell of the type commonly in use today is allowed to reach a temperature of about 43.6°C, it may become unstable because of a transition of the cadmium sulfate crystals at this temperature.[6] Therefore a protective circuit must be included in the bath to prevent possible circuit malfunctions from causing the temperature to increase above, say, 40°C. Also, it was felt that the cells should be protected against an excessive decrease in temperature, since a temperature shock in either direction can cause the cells to become unstable for an extended period. The guard circuit in each bath consists of a bimetal regulator that is set to take control if the temperature of the oil either increases or decreases by about ½°C. In the event of a line power failure, the power to the baths is supplied through a transfer panel that automatically connects the baths to a small engine-generator fueled by natural gas.

Conclusion

The baths have been in use for more than two years. The temperature at the peak of the heating cycle does not exceed 0.001°C above the mean temperature, and that at the lowest point in the cooling cycle is less than 0.001°C below the mean. While the temperature of the room in which the baths are located may vary by as much as 2°C during the day, the mean temperature of the oil will not change more than 0.002°C per day. The mean temperature increases somewhat from month to month due to the contamination of the platinum wire electrode by the oxidized mercury. When the temperature has increased by 0.01°C, it is readjusted to within about 0.005°C of nominal. Such readjustment is required three or four times a year, during which times the platinum wire and capillary tube are cleaned.

Because of recent advances in solid-state and magnetic devices, equally close and reliable control may be achieved by completely electronic means. These new devices should be explored with the goal of replacing the fragile mercury-toluene regulator—a device that requires a steady hand to prevent breakage.

References

1. "The Construction and Characteristics of Standard Cells," by G. D. Vincent, *IRE Transactions on Instrumentation*, Vol. 1-7, Nos. 3 and 4, Dec. 1958, pp. 221-234.
2. "Clark and Weston Standard Cells," by D. A. Wolff and C. E. Waters, *Bulletin of the Bureau of Standards*, Vol. 4, No. 1, 1907-08, pp. 33-39.
3. "The Construction of Standard Cells and a Constant Temperature Bath," by G. A. Hulett, *The Physical Review*, Vol. 32, No. 3, Mar. 1911, p. 257.
4. "Primary Batteries," by G. W. Vinal, *John Wiley and Sons, Inc.*, New York, 1950, p. 193.
5. "A Precision Thermostat for the Temperature Regulation of a Room," by T. Deighton, *Journal of Scientific Instruments*, Vol. 13, Sept. 1936, pp. 298-300.
6. "Metastability of Cadmium Sulfate and Its Effects on Electromotive Force of Saturated Standard Cells," by G. W. Vinal and L. H. Brickwedde, *Journal of Research*, NBS, Vol. 26, May 1941, pp. 455-465.

Acknowledgments

The author is indebted to Mr. Frank D. Weaver for his inspiration and guidance throughout the period of design and experimentation with the baths, and also to Dr. Walter J. Hamer and Miss Catherine Law of the Electrochemistry Section at NBS, Washington, for assistance and suggestions that contributed materially to the success of the project. The preheater resulted from a suggestion by Mr. David Ramaley and Mr. John F. Shafer of NBS, Boulder.

The Operating Characteristics of Zener Reference Diodes and Their Measurements*

WOODWARD G. EICKE, JR.
Electrochemistry Section
National Bureau of Standards
Washington, D. C.

▶ Described is a measurement technique with an accuracy in terms of the saturated standard cell of 20 ppm and capable of 2 to 4 ppm accuracy for making stability studies. Typical stability data are presented on several diodes. Results of a study of the effect of current and temperature on the output voltage are given, including an equation relating the three variables. The effect of AC components on the DC output is discussed and a cause for this effect is suggested. Also discussed is the electrical noise generated by the diode.

INTRODUCTION

RECENT TECHNOLOGICAL ADVANCES in the field of semiconductors have resulted in significant improvements in Zener reference diodes. As a result they are finding wider application as a precise standard of electromotive force. It has been reported that temperature-compensated reference diodes having a long-term stability of 20 ppm are now commercially available.[1] At this accuracy level the operating characteristics of the diodes become increasingly important since they can have a significant effect on the observed stability. Although there are data on some characteristics for single-junction diodes,[2–4] very little has been published on the temperature-compensated ones. In the subsequent sections the electrical characteristics of temperature-compensated diodes will be discussed in terms of their use as a standard of electromotive force. Methods for measuring operating parameters, typical data, and equations relating the variables will be given. Because a detailed discussion would make this paper extremely lengthy, only the major aspects of each area covered will be presented, and the reader should consult the appropriate references cited for more specific information.

*Presented at the 18th Annual ISA Conference & Exhibit, Chicago, Illinois, September 9–12, 1963.

STABILITY AND STABILITY MEASUREMENT

The stability of a Zener diode may be defined as the constancy of its output voltage with time when all other operating parameters are constant. Unfortunately, there has been a tendency to confuse stability with regulation. The latter refers to the ability of a diode or complete reference source to maintain a constant output voltage under varying operating conditions. The stability is the most important factor in the use of Zener diodes as a voltage reference source, and at present it must be determined experimentally for each diode. This determination involves not only the diode but the measuring system and current source as well. Therefore, as stability requirements become more stringent, greater attention must also be given to the measurement system and power supply in order to minimize the errors which they contribute to the final results. There are a number of methods that can be

employed, the basic principles of which have been previously described by the author.[5] However, the one to be described in some detail is to be recommended since it combines both simplicity and potentially high accuracy.

Diode Measurement

The technique employed to measure Zener diodes is based on the opposition principle and has been used by other investigators[2,6,7] in a variety of ways. The method consists of opposing the unknown voltage to be determined with a known voltage of approximately the same magnitude and measuring the resulting small difference.

In Figure 1 is shown a complete circuit for investigating Zener diodes. This circuit is designed to measure, one at a time, five or less diodes connected in series. A detailed description and analysis of the circuit will be given elsewhere.[8] The circuit consists of three major sections, the diode, the power or current source, and the measuring circuit.

The diodes under test are mounted in a stirred oil bath. During the voltage measurements, the oil temperature is controlled to within ± 0.01 C. Potential leads are soldered to each device in order to minimize the errors arising from connecting the diode to the measuring circuit.

The power supply is an 80-V lead–acid battery isolated from ground. During use the battery current is kept constant to improve the regulation of the supply. The current through the diodes is adjusted by varying R_1 and it can be set to within ± 0.3 μa of the desired value. The current is determined by measuring the voltage drop across a calibrated 10-Ω NBS type resistor.

The measuring circuit consists of a bank of unsaturated standard cells, mounted in a stirred oil bath maintained at 28.00 ± 0.01 C, and a potentiometer. The cells are compared to a group of saturated standard cells just prior to and immediately after measuring the Zener voltage. The cells are measured singly, and the sum of the individual emf's is taken as the value of E_s. The standard deviation of a single determination of E_s is approximately 0.4 ppm. The potentiometer is a 0.01% instrument and can be used to determine the voltage of a Zener diode with an accuracy ranging from 6 to 20 ppm, depending on the voltage being measured, whether or not the instrument has been calibrated, and other factors. Independent tests indicate that stability measurements can be made to about 3 to 4 ppm.[8]

The actual measurement of the Zener voltage is quite simple. The current is first set to the desired value by means of R_1 and the magnitude determined by connecting the potentiometer to the standard resistor as

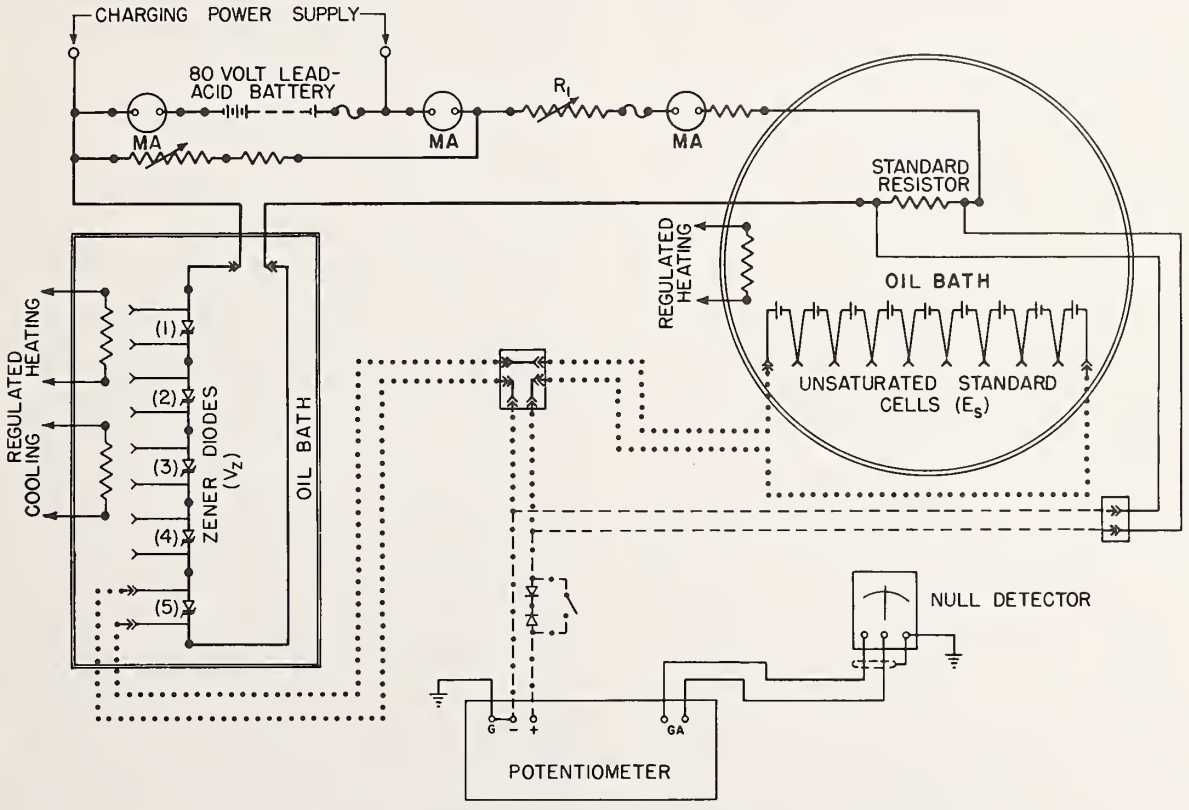

Figure 1. Experimental circuit for studying Zener diodes.

shown by the dashed lines in Figure 1. The voltage of the diode is then measured by connecting E_s, the potentiometer, and the diode as shown by the dotted lines. Finally the current is measured again after the voltage measurement. The mean of the two current readings is taken as the current at the time of the voltage measurement. The voltage is given simply by the equation,

$$V_z = E_s + \Delta E \tag{1}$$

where ΔE is the voltage measured by the potentiometer.

Diode Stability

The stability of a number of different diodes was studied using the measuring technique just described and an auxiliary power supply to maintain a current through the diodes at all times. This stand-by supply current (not shown in Figure 1) was adjusted to keep the current within 3% of the nominal diode current. The regulation was approximately 1.5%. Except for the period of the temperature–current–voltage study, the diode temperature was 25.2 ± 0.2 C. Diode voltages were measured at intervals and the data corrected to give the diode voltage at nominal operating current and 25.2 C. The stability curves were prepared from these data (expressed in ppm) by plotting the reading at a particular time minus the initial reading, as a function of time.

Typical stability curves are shown in Figure 2 for various diodes. None of these diodes had been preconditioned or aged, as is now frequently done with diodes for reference use. There are large differences between the types of curves obtained. These curves have two sections, the first in which the slope (rate of change of voltage with time) is varying, and the second in which the slope is approximately constant. This first part will be referred to as the stabilization time, the second part the useful period. The first part of the curve represents the time required for the diode to stabilize or come to a steady-state condition. Diode 1 stabilized in about 1 week and then began to show a nearly linear drift with time for approximately 400 days. From 400 to 600 days it remained quite steady. The rate of drift was somewhat less than 75 ppm/year. Diode 2 stabilized in about 5 days and showed no tendency to drift with time. It did, however, show a sensitivity to changes in operating condition. Diode 3 required about 100 days to stabilize after which it drifted linearly with time. For the diodes studied, stabilization periods, ranged from a few days to as long as 12 months, with the mean of 25 diodes being 3+ months. The stability of the diodes for the balance of the time (periods ranging from 6 to 20 months) averaged 40 ppm. For simplicity, the stability is simply taken as the maximum voltage less the minimum voltage during the period in question. Their distribution was approximately normal and the standard deviation was approximately 20 ppm. It should be emphasized that these data are based on the maximum changes in voltage during the period in question and therefore include (1) random normal variations, (2) drifts with time, (3) the effect of temperature cycling (shaded area of Figure 2), and (4) the effect of not being under electrical power for a short period (two points connected by the line). Note that if the last two effects were eliminated there would be a substantial improvement in the stability. These effects have been included in the overall picture because a reference unit could be subjected to such conditions in normal operation. Diode 2 in Figure 2 shows a remarkable stability except for the effects of temperature and power. When maintained at nearly a constant operating condition this diode showed a total variation in voltage of 7 ppm. These data indicate that it should be possible to obtain a usable yield of diodes having stability of better than 10 ppm.

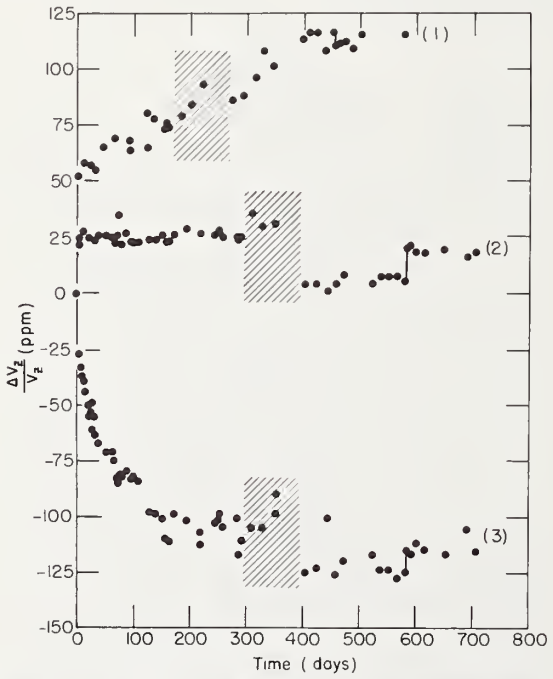

Figure 2. Stability curves for three typical temperature-compensated Zener reference diodes.

There is no ready explanation for the effect of temperature cycling or the effect of removing the power from the diode for a substantial time interval. Analysis of the data indicated that some diodes were affected by only one condition or the other, some by both, and others by neither condition. It was noted, however, that all diodes affected by temperature cycling showed a drop in voltage, and that when the power was removed some time later, most diodes showed an increase in voltage when put back on power. These data are still being analyzed in an effort to ascertain the causes for the observed phenomena, if possible. It is also worthy of note that those diodes showing the poorest stability and requiring the longest stabilization times were usually the most adversely affected by the changes in

operating conditions. These effects of temperature and power change, may well arise from causes suggested by Banga.[9] He proposed that drifts and other phenomena associated with stability might be due to surface effects on the silicon die and to Al_2O_3 that might be present if aluminum is used as a doping agent. In light of these data and recently published information[1] it seems reasonable to anticipate highly stable diodes that may be more or less immune to operational changes.

VOLTAGE–TEMPERATURE–CURRENT RELATIONSHIP

In order to make a meaningful statement about the voltage of a Zener diode, it is necessary to specify the current and temperature at which the measurement is made. Therefore, it is necessary to know the manner in which the voltage is affected by these parameters. Generally, only the approximate dynamic resistance at the nominal bias current and the maximum temperature coefficient are given for a diode. However, for precise applications these data must be known to higher accuracy than given; hence it is frequently necessary to measure these parameters for each diode. Temperature-coefficient measurements are usually made by measuring the voltage at a particular current (usually the nominal bias current) at several temperatures. The temperature coefficient is assumed to be linear between the intervals used.[10] Two methods may be employed to measure the voltage–current relationship. In the first and most widely used method the dynamic impedance is actually determined. A small alternating current is superimposed on the direct-current bias and the alternating voltage drop measured; the resistance is calculated from Ohm's law. The other method involves the measurement of the voltage at various currents. This method is a direct one and can be combined with measurements of the effect of temperature variations on diodes to give a complete picture of diode characteristics. The resistance can then be calculated from the voltage–current data. Where precise information is desired, the latter method should be employed. However, the first or AC method is extremely useful when only an estimate of R_z is required. There is no assurance, however, that this method will give the same value for the resistance as would be obtained by the DC technique. Of a small group of diodes investigated by both methods at their normal bias current, it was found that the average ratio of R_{AC}/R_{DC} was 0.88 where R_{AC} and R_{DC} are the dynamic resistances measured by the AC and DC methods.

To make a detailed study of the effect of current and temperature on diodes, a group of diodes was studied over a temperature range of 10 to 60 C and at bias currents of -30 to $+50\%$ of the nominal. Typical sets of curves obtained in this investigation are shown in Figures 3 and 4. These curves are of two general types: one in which the voltage varies linearly with temperature over the entire temperature range, the other in which the data are not linear. The nonlinear case can

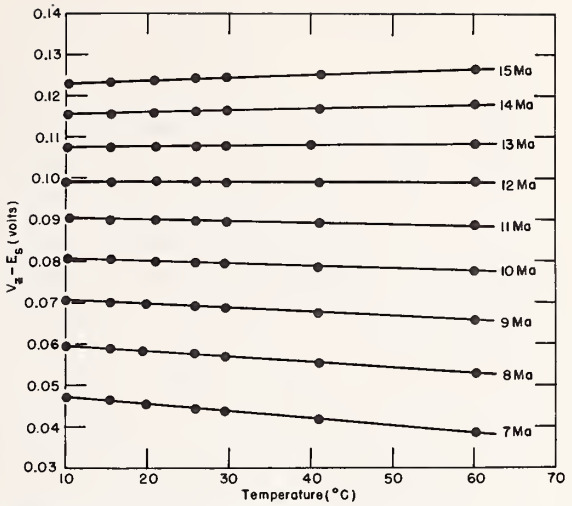

Figure 3. Variation of voltage with temperature of a typical Zener reference diode (linear case).

be represented approximately by two straight lines. It was found that for all diodes showing this nonlinear behavior, the point of intersection of the two lines was approximately 30 C. The data of Figure 4 were further analyzed by making a least-squares fit to the equation

$$V = V_{25} + \alpha(T - 25) + \beta(T - 25)^2 \qquad (2)$$

where V is the voltage at a current I, and T is the temperature. It was found that, although V_{25} and α were functions of the current as expected; β was a constant over the current range studied. For the linear case the simple relationship $V = V_{25} + \alpha(T - 25)$ can be used. When α is plotted as a function of the log of the current,

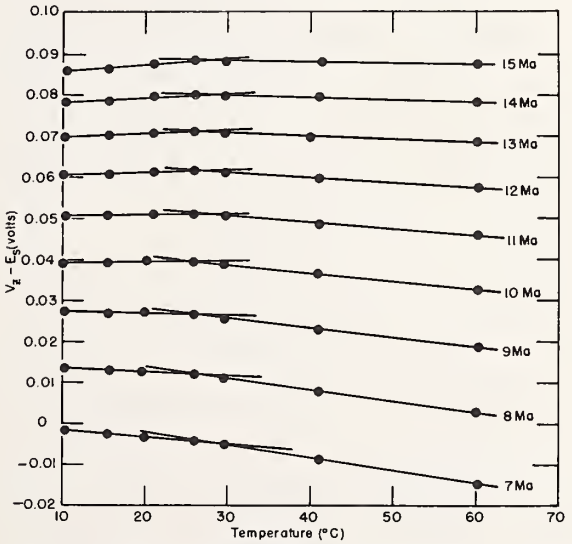

Figure 4. Variation of voltage with temperature of a typical Zener reference diode (nonlinear case).

a linear relationship results and may be expressed as

$$\alpha = k \log (I/I_0) \tag{3}$$

where I_0 is the current required to make $\alpha = 0$. This is true whether α is found from either the linear or the quadratic case. The variation of voltage with current was also studied and the relationship

$$V = A + B \log I + CI \tag{4}$$

was found to be satisfactory when T was a constant. Equations (2), (3), and (4) can be combined to give a single equation relating voltage, temperature, and current as follows:

$$V = V_0 + [B + k(T - 25)] \log (I/I_0) + C(I - I_0) + \beta(T - 25)^2 \tag{5}$$

where V_0 is now the voltage at I_0. For the case where the voltages of the diodes are linear over the entire temperature range, $\beta = 0$. The quality of the fit of the above equations depends, as expected, on the span of the data being fitted. Equation (2) gave a good fit over the temperature intervals studied; equation (3) shows evidence that a second-order term is necessary. Equation (4) was not fitted by itself; however, equation (5) was; a study of the deviation showed that other terms would be required to improve the fit. The standard deviation of the fit of equation (5) was approximately 100 ppm over the whole range covered. There is evidence that k, α, β, B, and C may be functions of the diode voltage and the diode construction.

ALTERNATING-CURRENT EFFECTS

In most applications of Zener reference diodes an AC component will exist through the diode in addition to the normal DC bias, unless special precautions are taken. Because of the relative complexity of the device, it is reasonable to expect that the alternating current will have some effect on the measured output voltage of the diode. To ascertain the magnitude of rectification and other effects, if any, an alternating current

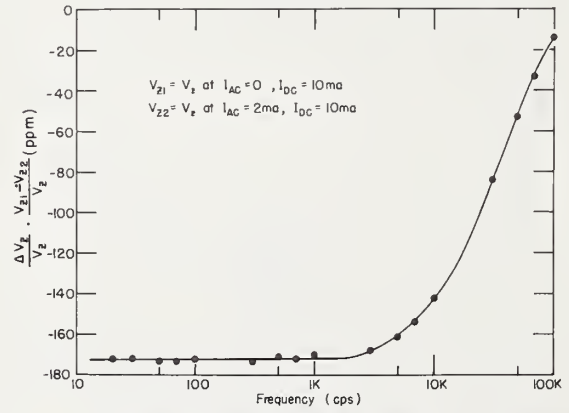

Figure 5. Variation of the DC shift in V_z due to AC as a function of frequency.

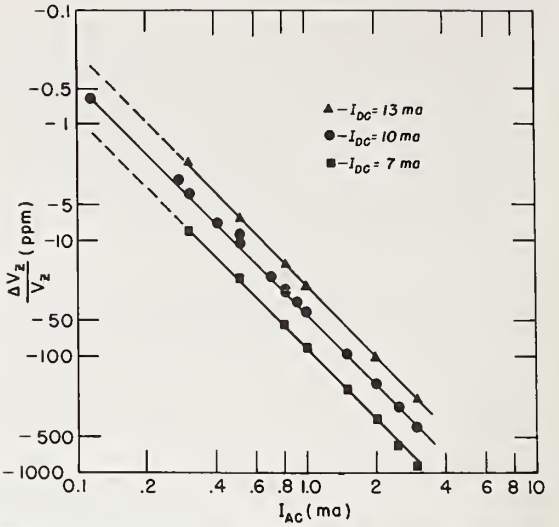

Figure 6. The DC voltage shift due to an AC component superimposed on the DC bias.

was introduced into the current circuit of the diode. The AC component was determined by measuring the voltage drop across a known resistance, and the shift in DC was determined using the measuring circuit of Figure 1 and a permanent-magnet-moving-coil galvanometer because it is an excellent filter. Tests were conducted in the current range of 100 μa to 3 ma AC and in the frequency range of 20 cps to 100 Kcps. The effects of varying these parameters are shown in Figures 5 and 6.

The effect of frequency was determined at an alternating current of 2 ma. Below 1 Kcps varying the frequency had virtually no effect on the voltage shift, while at the higher frequencies there was a marked continual decrease in the effect of alternating current.

When the change in DC is plotted as a function of current as shown in Figure 6, a straight line having a slope of very nearly 2 results. The center curve is made up from data obtained at various frequencies, while the other two curves were obtained from data obtained at 1 Kcps. When the abscissa is converted from I_{AC} to I_{AC}/I_{DC}, all three curves coincide. Hence, the shift in DC ΔV, owing to the AC component, can be represented by the equation

$$-\Delta V = K(I_{AC}/I_{DC})^2 \tag{6}$$

where K is a constant characteristic of the diode.

NOISE

Baker and Nagy[6] reported a relationship between the measured noise and the stability of single-junction alloy-type Zener diodes. Their findings indicated that diodes having a noise voltage, as measured by the procedure they described, of more than 5 μV would not be stable and that diodes with a noise voltage of less than

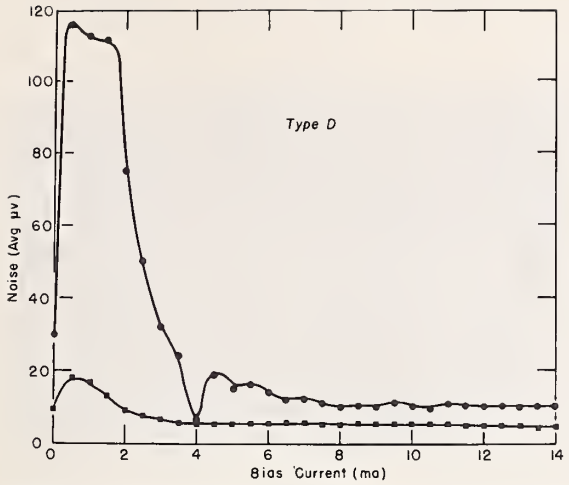

Figure 7. Noise voltage of two alloy-type Zener reference diodes.

5 μV *may* be stable. Measurements by the author qualitatively support their findings for alloy-type temperature-compensated diodes. However, no such correlation was found for diffused-junction diodes.

In Figure 7 are shown typical plots of noise voltage as a function of bias current for two 1N430 reference diodes. These measurements were made using the same circuit as used by Baker and Nagy except the amplifier pass band was 80 cps to 40 Kcps instead of 80 cps to 10 Kcps. The upper curve is for a diode that was not stable; the lower curve for a stable diode. These curves are typical of those of this type measured. It was found that the noise is accentuated at the lower currents and that at currents greater than 5 ma there was little change in noise voltage as the current was increased. This suggests that lower currents be used if noise measurements are to be used to select diodes. In Figure 8 are shown typical curves obtained for diffused-junction temperature-compensated reference diodes. The separate curves are for diodes of three different manufacturers. The three different diodes were relatively stable; however, their noise–current curves were quite different. Diodes A and B showed a certain amount of fluctuation whereas diode C did not. It is thought that these fluctuations arise from microplasms in the diode structure[11] which result from nonuniformity within the diode.

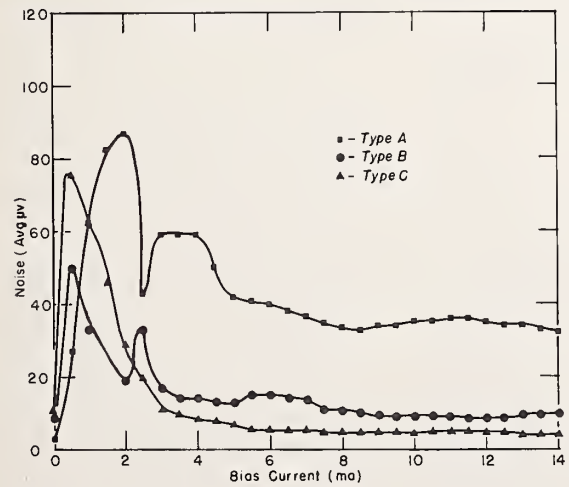

Figure 8. Noise voltage of representative diffused-junction Zener reference diodes.

Table I gives the average noise voltage for the diode types shown in the two figures. These values are for the normal bias current recommended by the manufacturer. There is wide variation in noise voltage between the different types of diffused-junction diodes as to both magnitude and standard deviation. No analysis of the noise spectrum was made; however, such an analysis would be of interest as it might give a clue as to the origin of the noise, which may reside in bulk or surface effects.

In addition to the noise just discussed, noise in the very low-frequency region is also of considerable interest since it affects the DC voltage measurement. If this type of noise were present, it may make the voltage measurement quite difficult. Unlike the higher-frequency noise which arises primarily from the electrical properties of the diode, this low pass-band noise arises from both electrical and thermal effects. The latter come about because of the variation in velocity of the oil over the surface of the diode package. As a result there is a change in the temperature of the junctions in the package. If the temperature changes are not the same for all junctions, a relatively large variation in output voltage will result. This low pass-band component was estimated by observing the variation in voltage on an oscilloscope. The oscilloscope was driven by the output of the electronic galvanometer (see Figure 1). In Figure 9 are shown photographs of this type of noise. The total time for each trace is 50 sec; the voltage scales are about 10 μV/cm for all but the photograph in the upper left, which is about 50 μV/cm. Diode A shows a very large sensitivity to stirring while B does not. Note, however, that A shows less noise than B when unstirred. Although these observations indicate that thermal effects can be minimized by operating the

TABLE I

Average Noise Voltage of Various Types of Diodes

Type	Av. noise μV*	Standard deviation μV*	Type of junction
A	33	8.4	Diffused
B	16	11.4	Diffused
C	4	1 (approx.)	Diffused
D	5.5	0.7	Alloyed

*As measured with an averaging type voltmeter.

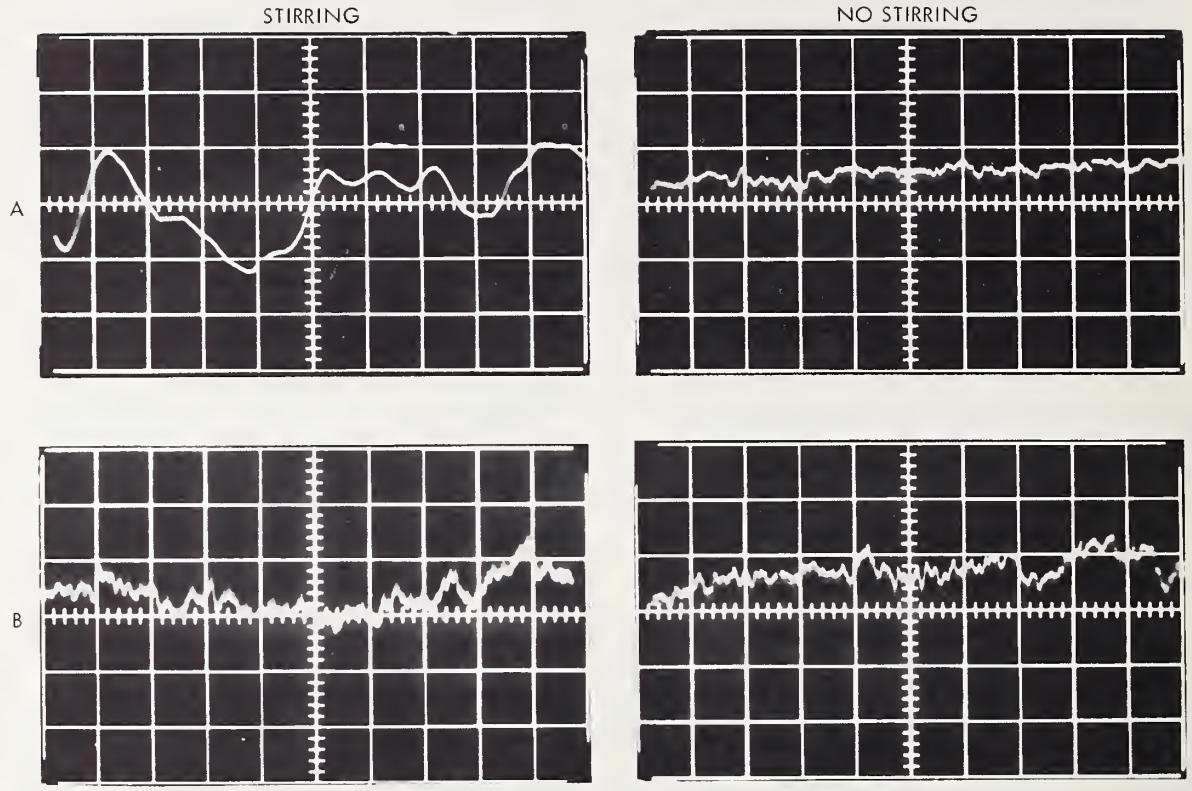

Figure 9. Low pass-band noise of two Zener reference diodes. Time scale: 1 cm (large div.) = 5 sec. Voltage scale 1 cm approx. = 10 μV except upper left photograph which is approximately 50 μV/cm.

diode in an unstirred oil bath, it is not a complete solution to the problem. What is not shown in the photograph is the difference in voltage between the stirred and unstirred conditions. For diode A it is about 800 μV and for B less than 10 μV. Therefore, very careful consideration must be given each diode, if thermal effects are to be evaluated and minimized. The low pass-band noise can also be estimated by making successive voltage measurements at intervals of 10 to 20 sec and comparing the results between diodes.

REFERENCES

1. Anonymous, "Ultrastable Reference Elements," *Electronic Ind.* **22**, 84–88, Feb. 1963.
2. Enslein, K., "Characteristics of Silicon Junction Diodes as Precision Reference Voltage Devices," *IRE Trans. on Instrumentation* **I-6**, 106–118, June 1957.
3. Chandler, J. A., "The Characteristics and Application of Zener (Voltage Reference) Diodes," *Electronic Eng.* **32**, 384, 78–86, Feb. 1960.
4. Stohr, H. J., "Bemerkungen zum Stabilisierungsverhalten von Zenerdioden," *Electron. Rundschau* **16**, 7, 297–301, July 1962.
5. Eicke, W. G., "Making Precision Measurements of Zener Diode Voltages," *Conference Paper CP63-416*, Presented at the Winter Meeting of the IEEE, Jan. 28.–Feb. 1, 1963, NYC.
6. Baker, R. P., and J. Nagy, Jr., "An Investigation of Long-Term Stability of Zener Voltage References," *IRE Trans. on Instrumentation* **I-9**, 2, 226–231, Sept. 1960.
7. Arnett, W., "Automatic DC Data Logging System," *IRE Trans. on Instrumentation* **I-11**, 3 and 4, 148–152, Dec. 1962.
8. Eicke, W. G., and H. H. Ellis, "A Study of Zener Diodes as a Standard of Electromotive Force," manuscript in preparation.
9. Banga, J., "Zener Diodes and their Application in Reference Units," *Brit. Communications and Electronics* **8**, 10, 760–764, Oct. 1961.
10. Morganstern, L. I., "Temperature-Compensated Zener Diodes," *Semiconductor Products* **5**, 4, 25–29, April 1962.
11. Batdorf, R. L., A. G. Chynoweth, G. C. Dacy, and P. W. Foy, "Uniform Silicon *p-n* Junctions. I. Broad Area Breakdown," *J. Appl. Phys.* **31**, 7, 1153–1161, July 1960.

Making Precision Measurements of Zener Diode Voltages

W. G. EICKE, JR.
MEMBER IEEE

ZENER DIODES have come into wide use in the last few years as working standards of electromotive force (emf) for many applications. They have been used to replace standard cells in recording and controlling equipment and are, in some cases, being used as a standard at the 0.01% level. Interest is also being shown in their use as a reference standard of emf at the 0.001 and 0.0001% levels.

Unlike the standard cell, which has an emf in the range of approximately 1.018 to 1.019 volts, zener diodes presently being considered as standards have operating voltages that range from 5 to 12 volts. At these voltages simple and accurate comparison with existing standards is somewhat difficult because, in general, no current should be drawn from the diode circuit by the measurement circuit.

In the subsequent paragraphs the requirements for making precise measurements will be considered, methods currently in use will be described, and several proposed methods will be presented. The methods to be described, in so far as possible, are based on equipment that should be available in standards laboratories.

Since stability studies are by far the most important aspect of any study of zener diodes, most experimental methods are designed primarily for this purpose. To assess the stability of zener diodes in a reasonable period of time the method must be far more precise than the desired final accuracy of the standard. Some feel that in order to evaluate diodes to be used as a 0.01% standard, the measurement process must be capable of resolving precisely a few parts per million (ppm) if meaningful stability data are to be obtained in a period of 3 to 4 months. The method must also be stable with respect to time.

In the discussion to follow, equations for computing the zener voltage V_Z and small variations in the zener voltage δV_Z of a single measurement will be given where applicable. The variation equations are useful in studying the effect of small variations in circuit elements and operating parameters on V_Z. The equations for δV_Z have been derived assuming that the variations are small; therefore certain approximations can be made. Although the variation equations apply specifically to a single measurement they can be extended to estimating errors in the measurement process. However, it is necessary to know whether the variation in question is caused by random errors, systematic errors, or a combination of both. Once this determination has been made, appropriate statistical techniques may be applied to estimate the error of a group of measurements. In some studies, such as stability investigations, systematic errors, as long as they are constant with time, do not affect the results since only changes in voltage are of importance. If, on the other hand, one is calibrating zener diodes, both random and systematic errors, are important. It will be assumed that in making measurements on zener diodes the reader will apply statistical technique where necessary and is familiar with making precision electrical measurements. For further information in the latter area it is suggested that texts on this subject be consulted.[1-3]

Paper 63-1445, recommended by the IEEE Recording and Controlling Instrumentation Committee and approved by the IEEE Technical Operations Committee for presentation at the IEEE–Illinois Institute of Technology–Northwestern University–University of Illinois National Electronics Conference, Chicago, Ill., October 28-30, 1963. Manuscript submitted April 25, 1963; made available for printing August 7, 1963.

W. G. Eicke, Jr., is with the National Bureau of Standards, Washington, D. C.

General Considerations

Current Source

Zener diodes are passive circuit elements requiring a source of operating current. Most reference diodes in use at the present time require a current ranging from 5 to 15 ma (milliamperes). Because the current source may interact with both the zener and the measuring circuit it must be considered in any discussion of the measurement process. This interaction may take several forms: (1) the effect of random supply fluctuations on the zener output voltage, (2) the effect of a-c components on the diode voltage, and (3) the effect of leakage between the supply and other parts of the circuit. Current for the diodes may be supplied by a regulated a-c operated d-c supply or by a battery. If the former is used, it may be either of the constant-voltage or constant-current type.

In all power supplied there will be some fluctuations of output with time and this variation must be considered as it will affect the voltage measurements. For a constant voltage supply having a small variation of $K_V\%$ the expected variation of the zener voltage δV_Z due to the supply voltage is given by equation 1.

$$\delta V_Z = \frac{K_V I R_Z}{100(1 - V_Z/V_S)} \tag{1}$$

where I is the current, R_Z the dynamic resistance of the zener, V_S the supply voltage, and V_Z the zener voltage. For a particular diode at a specified current, IR_Z will be constant, hence the error caused by the power supply depends on K and V_Z/V_S.

For a constant-current power supply the variation in the zener voltage as a result of supply fluctuations of $K_I\%$ is

$$\delta V_Z = \frac{K_I I R_Z}{100} \tag{2}$$

Note that equation 2 is the limiting case for equation 1 where $(V_Z/V_S) = 0$. In practice V_Z/V_S can usually be made small so that the constant voltage supply acts as though it were a constant current supply.

In addition to regulation requirements, the power supplies must have low leakage to ground (power lines) and low ripple (a-c supplies). The first requirement is essential in ungrounded systems or those in which the ground is at some point other than the power supply.

For the most accurate work a battery supply is recommended because it can be easily isolated from ground and affords excellent regulation. If the battery is partially discharged and the load kept constant, and a correction is made for the slight downward drift in current during voltage measurements on the zener, the resultant small variation in the current will have a negligible effect on the voltage measurement.

The effect of supply variations can be further reduced by using a bridge circuit in which the diode under study is one arm of the bridge. This circuit is discussed in detail elsewhere.[4] If stable resistors are used and care is exercised in constructing the bridge, the effect of small variations in the supply voltage on the output voltage of the circuit will be almost nonexistent.

Current Measurements

At some time during the measurement of a zener voltage the diode current must

be determined. Two general techniques may be employed:

1. The use of a stable power supply and a stable current-limiting resistor.

2. The measurement of the current at the time of the voltage measurement by determining the voltage drop across a standard resistor.

In the first method a highly regulated power supply is used to power a group of diodes. The voltage and regulation of the supply must be selected in light of equation 1. From a knowledge of the supply voltage, diode voltage, and optimum diode current, the current-limiting resistor R_L is selected. Assuming that the supply voltage, the zener voltage, and the limiting resistor are accurately known, the diode current is equal to $(V_S - V_Z)/R_L$. The limiting resistor is the total resistance of the circuit, excluding the diode, between the terminals of the power supply. Thus not only must the basic resistor be stable, but contact and lead resistances must also be constant. The variation in zener voltage caused by variations in the measurement of the supply voltage δV_{SM} and the limiting resistor δR_L is

$$\delta V_Z = \frac{IR_Z(\delta V_{SM} - I\delta R_L)}{V_S(1 - V_Z/V_S)} \qquad (3)$$

where δV_{SM} is the variation of measured value of V_S, and can be thought of as the measured value minus the true value. This variation in V_Z differs from that of the previous two equations in that it refers to the variation associated with the measurement process alone and it must be added to the former in computing the total variation of a single measurement.

The second method requires a variable resistance for current adjustment and a calibrated standard resistor across which a voltage drop V_I is measured. By measuring V_I, knowing the resistance of the standard resistor R_S, and applying Ohm's Law, the current is determined. The variation in V_Z due to the variations in V_I and R_S is

$$\delta V_Z = \frac{R_Z}{R_S}(\delta V_1 - I\delta R_S) \qquad (4)$$

Using a high-grade calibrated 4-terminal standard resistor maintained at a constant temperature and a calibrated potentiometer for measuring V_I, the total error as a result of the current measurement can be made small. If the standard resistor is 10 ohms or less, precautions must be taken to minimize thermal emf's. The precision of this method can be further improved by measuring V_I immediately before and after the diode voltage measurement. The mean is assumed to be the current at the time of the voltage measurement. When used in conjunction with the appropriate statistical techniques, this method gives an experimental estimation of the error calculated by equations 1 or 2.

Grounding

It has been found that grounding is frequently required to minimize electrostatic effects and pick-up. However, the point at which the ground should be made must be determined experimentally. When grounds are used precautions must be taken to avoid "ground loops."

The actual leakage resistance between any part of the circuit and ground must be determined from a careful analysis of the whole circuit in light of the desired precision. Where a-c operated equipment is to be used extreme care must be exercised particularly when more than one instrument is being used in the same circuit. Such an analysis must take into account the potential differences that exist between circuit elements, and the effect of leakage currents through or around certain elements as they affect the voltage measurements. Furthermore, the effect of humidity on the leakage resistance must also be ascertained.

When grounding is used leakage resistance of sensitive parts of the circuit to ground must be checked. Leakage resistance can be measured by several methods. One that is quite simple and effective is based on the use of an electrostatic voltmeter. In Fig. 1 is shown the equivalent circuit that exists between the various parts of the circuit and ground.

To measure resistance using this arrangement, the total capacitance (C_T) between the circuit and ground is measured. A potential V_1 is then applied between ground and the circuit and the time (t) required for the voltage to fall from V_1 to V_2 is measured.

The total leakage resistance is given by

$$R = \frac{t}{C_T}[\ln(V_1/V_2)]^{-1} \qquad (5)$$

where $C_T = C + C_V$.

For a good electrostatic voltmeter the leakage resistance will be high and R can be assumed to be the leakage resistance R_L of the circuit to ground. When low resistances are encountered or the time to fall from V_1 to V_2 is too small, the overall circuit capacitance may be increased by placing a high-quality-capacitor in parallel with the electrostatic voltmeter. The initial voltage V_1 should be approximately 150 volts.

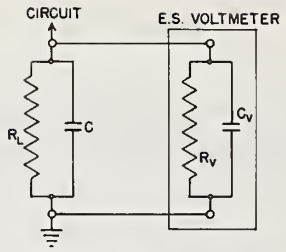

Fig. 1. Equivalent circuit for measuring leakage resistance to ground

This method is primarily for the current source and diode; when applied to the measuring circuit extreme care is necessary since instruments such as galvanometers may be damaged by the applied voltage. For this reason it is well to consider grounding at some point in the measuring circuit to avoid excessive potentials between the measuring circuit and ground.

Shielding

Very little is known about the effect of alternating current on the d-c output voltage of zener diodes. However, it is reasonable to expect alternating current to cause a shift in the d-c zener voltage in multijunction units because of the two diodes used in the forward direction for temperature compensation. Therefore, pick-up by leads should be minimized by shielding as a precautionary measure. If an a-c operated power supply is used checks should be made to determine the effect of ripple on the zener voltage.

The Zener Diode

Although the diodes used as reference voltage sources are either temperature-compensated or have been selected to have a low temperature coefficient, stabilization of the junction temperature is required. The degree of temperature control required for a particular diode depends on its construction and temperature coefficient. Both oil and air baths are used to study individual diodes.

In a private communication K. E. Miller of the Fluke Company told of finding some diodes extremely sensitive to stirring when operated in an oil bath. He found that the problem could be eliminated by using an unstirred air bath. Robinson[5] reported that some diodes were position-sensitive. He attributed this to the effect of diode orientation on the rate of heat transfer from the junction to the environment. The author has also observed the sensitivity of certain diodes to stirring. Although air baths or unstirred oil baths and careful mounting overcome these prob-

lems it is difficult to be able to define precisely the temperature of the diode because of its own heat generation and the heat generated by adjacent diodes. For extremely precise work a well-stirred oil bath is recommended and the diodes that are sensitive to stirring should be avoided unless they can be mounted in such a manner as to eliminate this problem.

In addition to temperature control the connection of the diode to the measuring circuit is of importance. Leads used in manufacturing diodes are usually of iron–nickel or iron–nickel–cobalt alloys. These alloys have a high resistivity compared with copper [40×10^6 ohm-cm (ohm-centimeters) to 1.7×10^6 ohm-cm]. Furthermore, the lead wires are quite small; hence there is an appreciable resistance associated with the leads. For example, a No. *24* Awg(American wire gage) lead wire of one of the mentioned materials would have a voltage gradient of about 200 μv/cm (microvolts/cm) at 10 ma. Even copper leads would have a gradient of of about 20 μv/cm.

This means, therefore that the points on the leads at which the potential is measured must be permanent for very precise studies. This can best be accomplished by attaching potential leads to the diode leads, thereby making it a 4-terminal device. Some zener reference diodes such as the *1N430* do not have leads, but terminals. Even so, it is recommended that the device be made into a 4-terminal one. For less accurate work voltage measurements can be made using a jig that has a fixed distance between clips. Such a device will introduce a lead error into the measurement of 20 to 50 μv from one time to the next (for noncopper leads).

Measuring Systems

Numerous systems may be used to measure the voltage of a zener diode. They may be classified under one of the following types of method.

1. Opposition.
2. Direct comparison.
3. Precision voltage divider.

Although the last two are both of the ratio type they differ sufficiently, when applied to the problem at hand, to warrant separate consideration.

The opposition method is probably the most widely used and it has been previously reported in the literature.[6,7] Essentially it consists of measuring the small difference between the zener voltage and a known constant voltage of approximately the same magnitude. The direct comparison method is the direct measurement of the zener voltage in terms of a suitable standard, while no current is being drawn by the measuring circuit. The precision divider method consists of placing either a fixed or adjustable divider across the diode and measuring an accurately known fraction of the zener voltage. This latter method differs from the other two because the measuring circuit draws some current from the diode circuit.

In addition to the variation in zener voltage to be discussed in this section the variations resulting from the current measurement and power supply must also be taken into account when considering the over-all measurement.

Opposition Methods

As was stated before, this method requires a known voltage E_S to oppose most of the zener voltage. Since E_S represents most of the zener voltage being measured, it will, to a great extent, determine the precision and/or accuracy of the over-all measurement. There are several ways in which E_S can be constructed; however, the one using a group of unsaturated standard cells connected in series is recommended. If the cells are carefully thermostated and calibrated frequently against calibrated saturated standard cells, it is possible to set up a 5- to 10-volt standard with an accuracy of 1 to 2 ppm. At the National Bureau of Standards two such working standards have been set up using 500-ohm unmounted unsaturated cells. Taps are provided so that the emf of individual cells may be measured. It has been found that by measuring the emf's twice daily, prior to and after measuring the zener diodes, the differences between the two measurements are less than 1 to 2 ppm. Where less accuracy is required, less frequent calibrations are needed. A 10-ppm standard can readily be made using encased cells in a lag box and calibrating them at 1- to 2-week intervals. In this case it will be necessary to make a small correction for the cell temperature. [For small changes in temperature, the temperature coefficient can be taken as -5 μv/C (degree centigrade).] It will be assumed for the balance of the discussion that a group of unsaturated cells having the appropriate accuracy is being used for E_S.

In Figs. 2, 3, and 4 are shown three circuits making use of the opposition principle. These vary in equipment and serve to illustrate ways in which the measurements can be made.

The first and most precise of the three is shown in Fig. 2. It is essentially

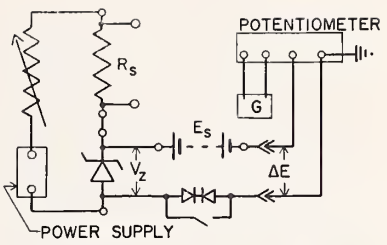

Fig. 2. Opposition method using a potentiometer

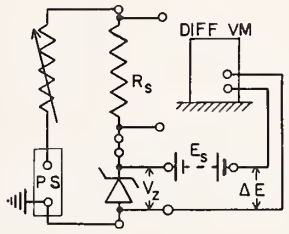

Fig. 3. Opposition method using a differential voltmeter

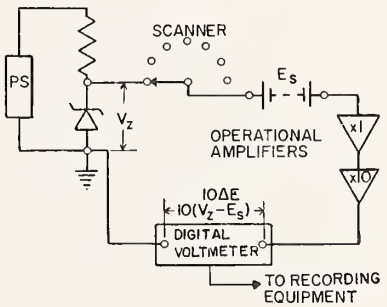

Fig. 4. Opposition method for automatic data logging (programming equipment omitted)

the same as the circuits used by Enslein[6] and Baker and Nagy.[7] Only the essential parts of the circuit are shown in the figure. The voltage of the zener is given by

$$V_Z = E_S + \Delta E \tag{6}$$

and the effect of variation of E_S and ΔE on the measured value of V_Z is

$$\delta V_Z = E_S + \delta(\Delta E) \tag{7}$$

Equations 6 and 7 apply to all three circuits that will be discussed in this section. Equation 7 shows that there is a simple dependence of δV_Z on the variations of E_S and ΔE. In general

$\delta(\Delta E)$ will depend primarily on the potentiometer. Since E_S is picked to be near the voltage of the zener being measured the resulting difference will not usually exceed 0.5 volt. Hence the accuracy of the potentiometer need not be as great as the accuracy requirement for knowing E_S. For example, using 0.01% class potentiometer, measurements accurate to better than 10 ppm can be made. If the potentiometer is calibrated, its standard cell calibrated at frequent intervals, and the instrument is in a reasonably constant temperature environment, then its accuracy will be somewhat better than 0.01%.

The preceding statements apply to accuracy in terms of the saturated standard cells used as the laboratory standard. If only the stability of diodes or relative measurements are to be made, the same equipment can be used and the relative accuracy of a group of measurements will be greatly improved. In an experiment conducted by the author it was found that a 0.01% potentiometer, when used in the circuit of Fig. 2, would repeat within 15 μv over a 1-month span. This means that under these conditions the relative value of V_Z can be determined to 1 to 3 ppm depending on the nominal voltage of the diode being studied.

The use of standard cells brings up two problems not previously mentioned. The first is the danger of excessive currents affecting E_S. This is solved by placing two low-leakage diodes back to back as shown in Fig. 2 to limit the current to less than 10 microamperes. The use of these diodes is also recommended in any circuit in which it is necessary to limit the current. They will not be shown in subsequent figures but should be used to protect galvanometers and standard cells. For the final balance the diodes must be short-circuited. The second problem is caused by the relatively high resistance of the standard cells. Because the resistance of the total circuit ranges from 2,500 to 5,000 ohms, the galvanometer must have sufficient sensitivity so that the null can readily be detected. The particular null detector that must be used should be determined from an analysis of the circuit. It has been found that a galvanometer sensitivity somewhat greater than 10^{-9} amperes per millimeter is required to detect 1 μv under the conditions mentioned previously.

In Fig. 3 is shown the circuit used by Miller for measuring the voltage of zener diodes. This circuit is interesting because it makes use of two electronic instruments: a regulated power supply (PS) and a differential voltmeter (DIFF VM). Extreme care must be taken to see that there are no leakage paths between the two instruments. One lead of the power supply is grounded and the differential voltmeter is isolated from ground. In such a circuit various circuit configurations must be thoroughly investigated to insure that leakage currents will have a negligible effect on the measurement. Miller states that by frequently checking the differential voltmeter, a precision of 5 to 7 ppm can be attained. This circuit has two advantages: first, it is very useful where the voltage of a large number of diodes must be measured by relatively unskilled personnel; and second, the differential voltmeter can be used to drive a recorder for making continuous records.

In Fig. 4 is shown a circuit for automatically recording zener voltages. This is the circuit described by Arnett.[8] The source of known voltage has been modified to include a 0.1-volt step in addition to the 1.019-volt steps afforded by standard cells. In this case the current is determined by a constant voltage supply and a known fixed resistor. With this type of equipment the data are punched on cards and the system is capable of measuring 100 diodes in 6 minutes. In addition to recording $10\Delta E$ the equipment also records other data essential to the measurement process. As described, the voltage of a group of 100 diodes is automatically recorded once an hour so that data on both short- and long-term stability are obtained. Arnett also discussed the method of calibrating the overall systems. As a result of careful studies he estimated the precision of a single measurement to be about 6 ppm. The use of active elements in the measuring circuit is unique. Two operational amplifiers are used. The *X1* is simply an isolation amplifier and serves to protect the standard cell from damage. The other is an *X10* amplifier and it is used to increase the voltage ΔE to a level that can be readily measured on the digital voltmeter. Further study of the use of such active elements should show other areas in which they might be useful. A discussion of this subject is given by Hall and Fulks.[9]

Direct Comparison Method

To the author's knowledge there are no direct comparison methods in use for measuring the voltage of zener diodes although such a technique is quite feasible. Recently McKnight[10] described a direct-reading voltage divider which could be adapted to measure zener voltages directly with an over-all accuracy of 100 ppm. In addition to this, two other methods, using conventional equipment have been devised by the author. Neither has been tried, but both show promise of yielding high-quality results.

The first is shown in Fig. 5. It makes use of a precision voltage divider (volt box) and a potentiometer. In this circuit the voltage drop IR_2 across the divider is adjusted to give a null on galvanometer G. The drop E_0 is then measured by means of the potentiometer. Two methods are given: in one a potentiometer is used alone; in the second, E_0 is opposed by a standard cell and the difference measured by using the potentiometer. The latter gives better resolution. Defining $S=(R_1/R_2)$, the

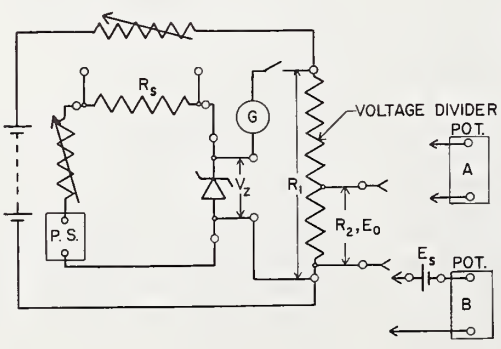

Fig. 5 (left). Direct comparison method using a voltage divider

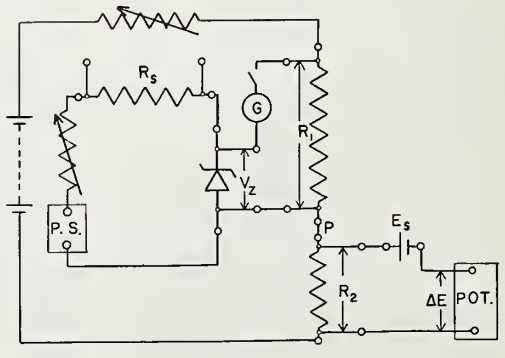

Fig. 6 (right). Direct comparison method using two standard resistors R_1 and R_2

voltage of the zener in terms of the measurement variables is

$$V_Z = SE_0 \qquad \text{for } A \quad (8)$$

and

$$V_Z = S(E_S + \Delta E) \qquad \text{for } B \quad (9)$$

for the two circuit configurations shown in Fig. 5. The variation of V_Z with respect to the variables in equation 9 is

$$\delta V_Z = E_0 \delta S + S \delta E_0 \qquad \text{for } A \quad (10)$$

and

$$\delta V_Z = S(\delta E_S + \delta \Delta E) + (E_S + \Delta E)\delta S \quad \text{for } B \quad (11)$$

The ratio (R_1/R_2) is obtained by calibrating the voltage divider against appropriate standards.* The only difficulty is the problem of two balances. However, this can be readily overcome by the proper layout of the equipment.

Fig. 6 shows the same basic circuit except that it is somewhat more sophisticated. Instead of a volt box this circuit uses standard resistors. They can be calibrated more readily than a volt box and a ratio more nearly equal to V_Z/E_S can be established. Since the four terminal values of both R_1 and R_2 can be readily determined, the problem of error arising from interconnecting the two is eliminated by use of the arrangement as shown. Care must be taken, however, to be certain that the point P, where the interconnection is made, is isolated so that no leakage occurs between this point and other parts of the circuit. The zener voltage and its variation are given by equations 9 and 11, respectively. In this case, however, R_1 and R_2 are determined separately by calibrating the individual resistors. This circuit is, in theory, capable of both high accuracy and precision. This circuit and that of Fig. 5 can both be of relatively low resistance as far as the potentiometer measurement is concerned.

A method using a precision variable voltage divider instead of a fixed ratio divider is shown in Fig. 7. In this technique two balances are made, one with the switch in the S-position, the other with it in the X-position. Although desirable, the power supply for the divider need not be adjustable, but it must have excellent short-term stability. Referring to Fig. 7, the voltage of the zener is given by the following:

$$V_Z = \frac{S_S}{S_X} E_S \qquad (12)$$

where S_X and S_S are the ratios (R_1/R_2) with the switch in the X- and S-positions respectively. The variation of V_Z is given approximately by

$$\delta V_Z = \frac{S_S E_S}{S_X}\left[\frac{\delta S_S}{S_S} - \frac{\delta S_X}{S_S} + \frac{\delta E_S}{E_S}\right] \qquad (13)$$

Since the error of the adjustable dividers is frequently a function of the setting, δS_X and δS_S will not necessarily be the same. As in the previous situation care must be taken to maintain proper isolation between the various parts of the circuit.

Precision Voltage Divider Methods

In this method the measuring circuit draws current from the diode. This method in its simplest form is shown in Fig. 8. In this arrangement a stable calibrated voltage divider has been permanently placed across the diode and the output is measured using a potentiometer. The divider must be stable both with respect to its ratio and its total resistance. This technique is suitable only for relative measurements such as stability studies because of the difficulty of constructing a divider with a precisely known ratio (across the diode).

An improvement can be obtained by using a precision voltage divider as shown in Fig. 9. In this circuit the voltage divider must be of high resistance. Furthermore, the total resistance (R_1+R_3), where R_1 is the total resistance of the voltage divider and R_3 is the total lead resistance, must be known with sufficient accuracy so that a correction for the measuring-circuit current can be made. The voltage of the zener is given by the equation

$$V_Z = SE_S\left(1 + \frac{R_3}{R_1}\right) \qquad (14)$$

where $(R_1/R_2) = S$ is determined by the setting of the divider. In addition, a correction is required for the current because the current determined using R_S is $(I_Z + I_D)$ where I_Z is the current through the zener and I_D the current through the divider. If the effects of lead resistance R_3 are small compared to R_1, then δV_Z is given approximately by

$$\delta V_Z = E_S \delta S + S \delta E_S + S E_S \delta\left(\frac{R_3}{R_1}\right) \qquad (15)$$

Thus, if appropriate corrections are made for the current lead, resistance, and (R_3/R_1), V_Z will depend only on the quality of the divider and E_S. The lead resistance R_3 can be estimated by determining

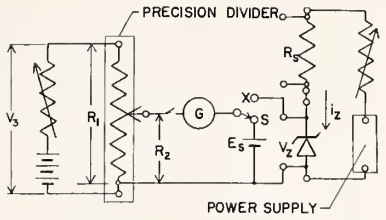

Fig. 7. Direct comparison using a precision divider

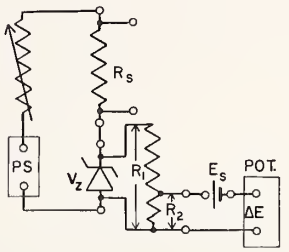

Fig. 8. Precision voltage divider method I

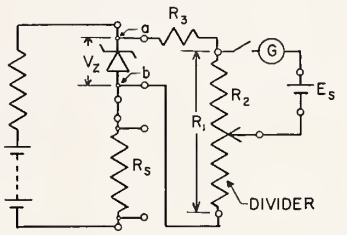

Fig. 9. Precision voltage divider method II

the total resistance between points a and b excluding the divider. To minimize the effects of R_3 and of loading of the diode circuit, R_1 should be as large as possible. However, there is a limit to this because of difficulties in making, calibrating, and using high-resistance dividers. At present the highest resistance unit normally has an over-all resistance of 100,000 ohms.

An alternate method is shown in Fig. 10. In this arrangement the voltage divider measures the complete drop from a to b, thereby eliminating the error resulting from the current drawn by the divider. This technique, however, introduces a new correction, the correction for R_{cb} which is the resistance of the circuit from a to b excluding the diode. The zener voltage for this circuit is

$$V_Z = E_S S\left(1 + \frac{R_3}{R_1}\right) - I_Z R_{cb} \qquad (16)$$

* Voltage dividers, including adjustable ones, are calibrated by measuring the ratio R_1/R_2 and not R_1 and R_2 separately. To take into account the possibility of leakage between portions of the dividers when in use, voltages approximating those found under operating conditions are usually employed during calibration (see reference 3, pp. 211–29).

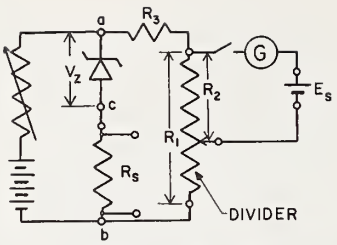

Fig. 10. Precision voltage divider method III

As before, the variation in V_Z is given by

$$\delta V_Z = E_S\delta S + S\delta E_S + E_S S\delta\left(\frac{R_3}{R_1}\right) - R_{cb}\delta I_Z - I_Z\delta R_{cb} \quad (17)$$

The three circuits discussed are more useful in making stability studies because of the difficulty of assessing sources of error. Nevertheless, great care must be exercised to see that critical resistances remain constant with time.

References

1. Basic Electrical Measurements (book), **M. B. Stout.** Prentice-Hall, Englewood Cliffs, N. J., 1960.

2. Electrical Measurements (book), **F. K. Harris.** John Wiley & Sons, New York, N. Y., 1952.

3. Precision Measurement and Calibration, Electricity and Electronics Handbook 77—Vol. I. National Bureau of Standards, Washington D. C., 1961.

4. Silicon Zener Diode Handbook. Motorola, Inc., 1959.

5. A Precision, Continuous Voltage Reference for Industrial Recorders, **P. B. Robinson.** *AIEE Transactions*, pt. I (*Communication and Electronics*), vol. 79, July 1960, pp. 197–200.

6. Characteristics of Silicon Junction Diodes as a Precision Voltage Reference Device, **K. Enslein.** *Transactions on Instrumentation*, Institute of Radio Engineers, New York, N. Y., vol. I–6, June 1957, pp. 105–18.

7. An Investigation of Long-Term Stability of Zener Voltage References, **R. P. Baker, J. Nagy, Jr.** *Ibid.*, vol. I–9, no. 2, Sept. 1960, pp. 226–31.

8. Automatic D-C Data Logging System, **W. Arnett.** *Ibid.*, vol. I-11, nos. 3 and 4, Dec. 1962, pp. 148–52.

9. The Use of Active Devices in Precision Bridges, **H. P. Hall, R. G. Fulks.** *Electrical Engineering*, vol. 81, May 1962, pp. 362–72.

10. A Direct Reading Voltage Divider with Standard Cell Reference, **R. P. McKnight.** *Transactions on Instrumentation*, Institute of Radio Engineers, vol. I-11, nos. 3 and 4, Dec. 1962, pp. 128–32.

Discussion

John C. Garrigus (The Bristol Company, Waterbury, Conn.): Mr. Eicke has described several useful methods for measuring the voltage and long-term stability of the zener diode element.

It would seem that these techniques can also be used to check the complete reference package provided some precautions are observed.

A complete reference source is normally powered from the a-c power line and consists of an isolation transformer, a demodulation and preregulation stage which produces relatively high output impedance (a current source), final zener reference stage, and output circuitry which may be simply a voltage divider or which may employ feedback techniques to obtain the desired output reference voltage.

The following points should be noted when testing this type of reference source.

1. A specified stable load resistance should be connected across the output terminals.

2. Care must be taken to minimize the effects of electrical coupling or leakage which is inherent in line-powered sources. If one side of the output is grounded for initial testing the common mode voltage is reduced practically to zero; however, when this unit is then used as a reference in some application, such as recording and controlling instrumentation, the output normally cannot be grounded. Then, leakage from the a-c line through the reference and measuring circuitry can cause errors in the reading.

3. Not only must the leakage from the supply be low but the impedance between the output terminals and ground must be very high. As mentioned previously, some circuit applications require the output to be floated, as in null-balance potentiometric recorders, and any ground loops through the reference can cause voltage drops which then, show up as errors in the measurement.

W. G. Eicke: The points made by Mr. Garrigus are extremely important and must be given careful consideration when measuring a complete reference package. In my paper it should be noted that when measuring single diodes it is possible to select a power supply that will be satisfactory. On the other hand, when measuring a complete zener reference unit the power supply and the diode now form an integral unit, hence the measuring procedure employed must be compatible with the unit under study. For a particular technique for measuring a zener reference unit, either the opposition or the direct comparison method may be employed. Unless the precision divider is built into the reference unit the voltage divider method would not be particularly satisfactory. If there is one generalization that can be made it is that the voltage as measured under test conditions must be identical to that which the unit will be able to deliver under normal operating conditions.

A reprint from **COMMUNICATION AND ELECTRONICS**, published by The Institute of Electrical and Electronics Engineers, Inc.

September 1964 issue

NBS Technical Note 430
October 1967

Designs for Surveillance of the Volt Maintained by a Small Group of Saturated Standard Cells

W. G. Eicke
Electricity Division
Electrochemistry Section

and

J. M. Cameron
Applied Mathematics Division
Statistical Engineering Laboratory

This technical note describes a procedure for maintaining surveillance over a small group of saturated standard cells. The measurement process is briefly discussed and the principle of left-right balance as a means of eliminating certain systematic errors is developed. Specific designs and their analysis for intercomparing 3, 4, 5 and 6 cells in a single temperature controlled environment are given. Procedures for setting up control charts on the appropriate parameters are given, and a technique is described for detecting certain types of systematic errors.

Key words: Control charts, experiment design, saturated standard cells, standard cells calibration, statistics, voltage standard.

Resistors and Resistance Apparatus

Papers

Abstracts

U. S. Department of Commerce National Bureau of Standards

RESEARCH PAPER RP1692

Part of Journal of Research of the National Bureau of Standards, Volume 36, January 1946

STABILITY OF DOUBLE-WALLED MANGANIN RESISTORS

By James L. Thomas

ABSTRACT

The international ohm is now maintained at the National Bureau of Standards by means of double-walled manganin resistors. It is assumed that the average resistance of a group of 10 standards, selected from a group of 24 constructed in 1933, remains constant with time. No one of the 10 standards has changed in resistance with reference to their average by more than 1 part in a million in 12 years.

CONTENTS

I. INTRODUCTION

Although the international ohm is defined in terms of the resistance of a column of mercury, wire-wound standards are used at national standardizing laboratories for maintenance of the unit of resistance. At the National Bureau of Standards the international ohm is maintained by means of a group of 1-ohm resistors. From this group 10 standards have been selected, and the assumption is made that the average of their resistances remains constant with time. If there is a relatively large change in the resistance of one standard with reference to the average, it is replaced with one that has remained constant. In this way standards are eliminated from the reference group when they become defective.

Values of resistance were originally assigned to standards of the reference group in terms of mercury-ohm determinations made in England and in Germany before 1910. Mercury-ohm determinations were made at this Bureau in 1911 and 1912, and the results were consistent with the English and German results to 15 or 20 parts in a million.[1] In 1910 the reference group consisted of 1-ohm standards of the type developed by Rosa,[2] and resistors of that group were used for over 25 years. Starting in 1931 the standards of the Rosa type were gradually replaced by standards of the double-walled type.[3] Since 1939, maintenance of the international ohm has been entirely by means of a new group of double-walled resistors constructed in 1933. Resistors of the later group have been far superior to any others made at this Bureau, and, judged on the basis of relative stability, are about one order better than well-aged standards of the Rosa type. It is the purpose of this paper to describe the new standards and give a report of their performance to date.

[1] F. A. Wolff, M. P. Shoemaker, and C. A. Briggs, Construction of primary mercurial resistance standards, BS Sci. Pap. 12, 375 (1915) S256.
[2] E. B. Rosa, A new form of standard resistance, BS Sci. Pap. 5, 413 (1908-9) S107.
[3] J. L. Thomas, A new design of precision resistance standard, BS J. Research 5, 295 (1930) RP201.

315-411 O - 68 - 10

II. DESCRIPTION OF NEW RESISTORS

The standards constructed in 1933 consisted of a group of 24 of the double-walled type, and the same technic was used for annealing and mounting as that described in Research Paper RP201. The containers, however, were larger than those of the original double-walled group, and were similar in size and general appearance to O. Wolff's model IV.

The increase in the size of the containers made possible the use of larger resistance wire, thus decreasing the ratio of area to volume and thereby reducing possible changes in resistance from surface changes. The resistance coils were made of 28 turns of No. 12 AWG manganin wire (2.05 mm=0.081 in.) from two lots of specially selected wire,[4] wound on 8-cm mandrils and spaced with copper wire. Before the wire was annealed, it had a slightly negative temperature coefficient of resistance at 25° C, and after being annealed, the coefficients were very small, averaging 1 part in a million per degree centigrade for the 24 standards, the maximum coefficient being 3.05 ppm per degree centigrade.

For annealing the resistance coils, a special furnace was constructed, using a fuzed-quartz tube about 10 cm in diameter and 75 cm in length. This tube was sealed at one end, and the other end was covered with a ground-glass plate through which were sealed thermocouple leads and an exhaust tube. Several parallel aluminum plates were placed in front of the glass cover plate to protect it from radiant heat from inside the furnace. The heating coil around the tube was nowhere nearer than 6 inches to the cover plate, and a good seal was maintained by the use of ordinary stopcock grease.

The resistance coils mounted on the steel mandrils were annealed in the quartz furnace. An oil-sealed pump was used to evacuate the furnace, maintaining a pressure of the order of 0.001 mm of mercury. About an hour was required to bring the furnace to the annealing temperature of 550° C, at which it was maintained for half an hour, after which the power supply was disconnected and the furnace allowed to cool fairly rapidly.

After the annealed resistance coils had been adjusted to the correct lengths, manganin terminal plates were silver-soldered to the ends. Manganin rather than copper plates were used in order to keep the temperature coefficient of resistance as low as possible.

The mounted resistance coils were spaced with many turns of linen thread wound between the turns of wire. All but two of the coils were then impregnated with shellac varnish and baked at 120° C before sealing them in dry air in the containers. In the 2 months immediately after sealing, each resistor, except the two which were not shellacked, decreased in resistance by from 1 to 5 parts in a million, after which the resistance appeared to be stabilized. No change was obtained even during the initial period for the coils that were not shellacked, which suggests that the initial change was from dimensional changes in the shellac.

One of the completed standards is shown in figure 1. The outside diameter of the container is 9 cm and its length 13 cm. The series of holes near the top are just above the double-walled part and are intended to increase the facilities for cooling, and the containers are

[4] Chemical analysis of one lot: Cu 82.2, Mn 13.2, Ni 4.2, Fe 0.3; of second lot, Cu 82.7, Mn 12.1, Ni 4.6, Fe 0.5.

left open at the bottom for the same purpose. The terminal posts are entirely of nickel-plated copper, mounted on a hard-rubber top; the distance between the amalgamated current terminals being 16 cm.

III. STABILITY OF RESISTANCE

In the fall of 1933, after all standards had been on hand for at least 2 months, the group of 24 was intercompared, resistance measurements being made to parts in 10 million. Three of the standards were then sent to the International Bureau of Weights and Measures, and since that time four more have been sent to other national laboratories. The remaining 17 standards have been intercompared to parts in 10 million nearly every year since their completion. Two of the standards have changed in resistance by 4 and 8 parts in a million, in the 12 years since their construction and are considered to be of inferior quality. The remaining 15 resistors comprise the group now used for maintenance of the international ohm. The average value of 10 standards is assumed to remain constant with time, and 5 are kept in reserve to replace standards in the group of 10 if any of them should become defective and change in resistance by an unusual amount.

TABLE 1.—*Stability of double-walled resistors in maintenance group*

Standard No.	Change in resistance, in microhms, from 1933 until—										
	1933	1934	1936	1937	1938	1939	1940	1941	1943	1944	1945
68	0	0.1	0.8	0.6	0.7	0.6	0.1	0.2	0.0	0.0	0.1
70	0	.0	−.1	−.7	−.2	−.2	−.4	−.4	−.6	+.2	.3
74	0	−.2	−.1	.0	−.2	−.4	−.6	−.6	.0	−.4	−.7
77	0	−.6	−.8	−1.2	−.8	−1.0	−.9	−1.0	−.7	−1.1	−1.0
78	0	.0	.2	0.1	.4	0.6	.9	0.8	.9	1.0	1.0
81	0	.0	−.4	−.9	−1.0	−1.2	−.9	−.9	−.9	−1.0	−0.9
82	0	−.1	−.1	.0	−0.1	−0.2	−.1	+.0	−.2	−0.2	−.4
84	0	.5	.0	.3	.0	.8	.8	.8	.5	.8	.6
89	0	.0	.5	.0	.1	.1	.0	.0	.1	−.3	+.1
90	0	−.2	−.3	1.3	.8	.8	.6	.7	.7	.5	.5
Average of numerical values without regard to sign											0.56

Table 1 shows how exactly standards in the maintenance group of 10 have kept their relative values during the last 12 years. This table shows the total change, in parts per million, since 1933, calculated on the assumption that their average value has remained constant. Table 2 gives similar data for the 5 reserve standards, measured in terms of the average of the group of 10. Data for the 5 are somewhat incomplete.

TABLE 2.—*Stability of double-walled resistors in reserve group*

Standard No.	Change in resistance, in microhms, from 1933 until—										
	1933	1934	1936	1937	1938	1939	1940	1941	1943	1944	1945
67	0	1.1	0.6	−0.1	−0.2	−0.4	−0.5	−0.6		−0.9	−1.5
69	0	−0.1	.1	.1	.7	1.0	1.2	1.5	1.9	2.0	1.9
72	0	.2								0.6	0.4
73	0	.0	.3	.0						−.8	−.9
83	0	.2	.4	.2	−.2			−1.0	−1.5	−1.9	−2.1

For the 10 resistors now being used in maintaining the international ohm, the maximum net change in 12 years has been 1.0 part per million. The average net change without regard to sign has been 0.56 part per million in 12 years, or at the average yearly rate of about 5 parts in 100 million.

The bridge which has been used for the intercomparison of these resistors has dials that can be set to parts in a million, the next place being obtained from galvanometer deflections. The method of measurement is such that the bridge is relied upon to measure differences in resistance only. The facilities for cooling and the low-temperature coefficients of resistance make possible measurements to 1 or 2 parts in 10 million, when the standards are measured in a well-stirred, thermostatically controlled, oil bath.

With double-walled containers having the resistance coils mounted tightly in contact with one wall, variations in atmospheric pressure tend to expand or compress the walls and thus apply stresses to the coils. To test the change in resistance so produced, three of the double-walled resistors were placed in a closed chamber and measured at about normal and half-normal pressures. The decrease in resistance as the pressure changed from normal to half-normal was found to be from 2 to 4 parts in a million. Assuming the change to be linear, changes in barometric pressure can therefore be expected to produce uncertainties in the resistances of the standards of only 1 or 2 parts in 10 million, which is about the limit of measurement.

On the basis of relative values, standards of this group are about one order better than well-aged standards of the Rosa type. It does not necessarily follow that their average value is more stable. Unfortunately, there has been no satisfactory method of judging the quality of resistors used in maintaining the unit except their ability to maintain relative values. A group that keeps the same relative values could all be changing, but at the same rate.

Before the war, some preliminary results had been obtained from a commutating method of measuring resistance in terms of inductance, which in turn could be calculated from the measured dimensions of a mutual inductor. By this method it was found possible to duplicate measurements of a 1-ohm resistor to 1 part in a million in terms of the calculated mutual inductance. It is expected that such measurement will in the future give data on the stability of groups of resistors over long periods of time. The stability of the inductor can be checked from time to time from its measured dimensions, and it is believed that this can be done to 1 part in a million. Measurements of the resistors in terms of the inductance would then disclose changes as large as 1 or 2 parts in a million in the resistance of the group being used to maintain the unit. It is not expected that resistance can be measured in absolute units to 1 part in a million by this method. It does appear, however, that systematic errors will be sufficiently constant to permit checks of the stability of the unit of resistance to 1 or 2 parts in a million.

Washington, September 24, 1945.

FIGURE 1.—*Double-walled standard resistor.*

Since the original publication of this paper these resistors have been measured at approximately yearly intervals. The changes in resistance between the yearly measurements are about the same as the changes shown in tables I and II, indicating that there has been no deterioration in the stability of the resistors.

Thomas E. Wells
August 17, 1967

JOURNAL OF RESEARCH of the National Bureau of Standards—C. Engineering and Instrumentation
Vol. 69C, No. 3, July–September 1965

Errors in the Series-Parallel Buildup of Four-Terminal Resistors

Chester H. Page

(April 20, 1965)

The use of n equal resistors (a) in series and (b) in parallel provides an n^2:1 ratio of potentially high accuracy. Such devices are important for extending the use of the national one-ohm standard to the hundred-ohm, and thence to the 10 000-ohm, level.

Formulas are derived for the error in the ratio, expressed (a) in terms of design tolerance, and (b) in terms of first-order residual misadjustments which combine to yield the second-order error of the ratio.

It seems feasible to construct a 1:100 ohm buildup device with a ratio uncertainty of less than 1 in 10^8.

The use of n equal resistors (a) in series and (b) in parallel provides an n^2:1 ratio of potentially high accuracy. Such devices are important for extending the use of the national 1-Ω standard to the 100-Ω, and thence to the 10 000-Ω level.

The first stage of this step-up involves the use of ten 10-ohm resistors, which must be four-terminal resistors to avoid large errors due to the connecting networks.

Hamon [1] has described an arrangement of four-terminal resistors permanently connected in series, and convertible to a parallel connection by adding jumpers. In that paper, he shows the use of compensating resistors in the potential leads to eliminate errors introduced by the added connections.

Compensated lead "fans" may be used for the potential terminals of the paralleled resistors, for the current terminals, or for *both*. The aim of the present paper is to present a complete analysis of the general case, and formulas for the errors introduced by imperfectly compensated fans.

[1] B. V. Hamon, A 100Ω build-up resistor for the calibration of standard resistors, J. Sci. Instr. **31**, 450-453 (Dec. 1954).

We consider four-terminal resistors connected in series by means of "tetrahedral" junctions, having the equivalent circuit shown in figure 1. Each junction supplies current and potential leads. This array can be converted to a parallel connection by adding four "terminal fans," as in figure 2. For analysis, the junction resistances can be considered as absorbed in the fan-conductor resistances. The problem is to make the four-terminal resistance of the combination precisely equal to R/n. If the resistances of the various arms of the current fan are adjusted to make each main resistor (R) carry identical current, the corresponding voltage drops will be identical and there will be no circulating current in the potential fans, and the potential across V_1-V_2 will be independent of the resistances of the potential fans, and equal to IR/n. This requires that each arm of the current fan on the left have the same resistance, say r, except for the top and bottom arms, each of which feeds only one main resistor. These end arms must have the resistance $2r$. For the right-hand current fan, each arm must have the same resistance, say r'. The reciprocity theorem leads to the conclusion that if we use these compensated fans as potential fans, the four-terminal

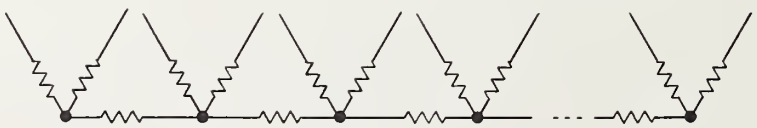

FIGURE 1

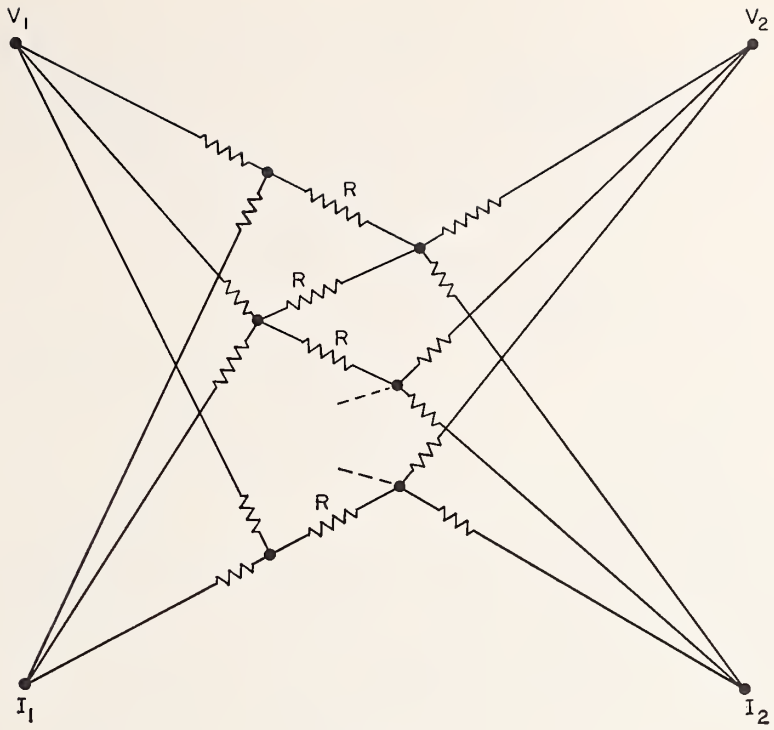

FIGURE 2

resistance would be R/n, independent of the current-fan resistances. Since the potential fans can tolerate larger resistance than can the current fans, the compensation is usually made in the potential fans; resistances of several tenths of an ohm can be added to the arms, allowing adjustment to reasonable accuracy.

Making either set of fans perfect yields zero error. This suggests that the overall error is in the nature of a product of fan errors, and suggests the possibility of reducing the effect of residual potential fan errors by making at least a rough adjustment of the current fan. For analysis, we consider four perfectly compensated fans as a nominal condition, with arbitrary maladjustments allowed in each arm. In addition each main resistor is allowed a departure from nominal.

The complete circuit to be analyzed is shown in figure 3, where the labels indicate *conductance* rather than resistance. Capital letters indicate "average" values, i.e.,

$$\sum a_i=\sum b_i=\sum c_i=\sum d_i=\sum g_i=0.$$

Considering terminal G as the "ground" terminal, we have a network possessing three external nodes, and $(n+1)$ internal nodes. A complete description of the network requires $3+(n+1)$ simultaneous equations, and we must eliminate the last $n+1$.

If we impress currents I_{I}, I_{II}, I_{III} into the external nodes, and I_1, I_2 . . . I_{n+1} into the internal nodes, the voltages on these nodes are implied by the simultaneous equations:

$$\begin{aligned}
I_{\mathrm{I}}&=Y_{\mathrm{I\,I}}V_{\mathrm{I}}+Y_{\mathrm{I\,II}}V_{\mathrm{II}}+\quad+Y_{\mathrm{II}}V_{\mathrm{I}}+\quad+Y_{\mathrm{I}\,n+1}V_{n+1}\\
I_{\mathrm{II}}&=Y_{\mathrm{II\,I}}V_{\mathrm{I}}+\qquad\qquad+Y_{\mathrm{II}\,n+1}V_{n+1}\\
&\vdots\\
I_{n+1}&=Y_{n+1\,\mathrm{I}}V_{\mathrm{I}}+\qquad\qquad+Y_{n+1\,n+1}V_{n+1}
\end{aligned}\tag{1}$$

These equations are conveniently symbolized by the matric equation

$$I=YV \tag{2}$$

where I and V are column vectors (each having $n+4$ components), and Y is an $(n+4)\times(n+4)$ square matrix.

Consider I_{I}, I_{II}, and I_{III} as components of an "external" current vector, I_e, and I_1 . . . I_{n+1} as components of an "internal" current vector, I_i; similarly consider "external" and "internal" unknown voltage vectors, V_e and V_i. Grouping the terms appropriately:

$$\begin{aligned}
I_e&=\alpha V_e+\beta V_i\\
I_i&=\tilde{\beta}V_e+\gamma V_i
\end{aligned}\tag{3}$$

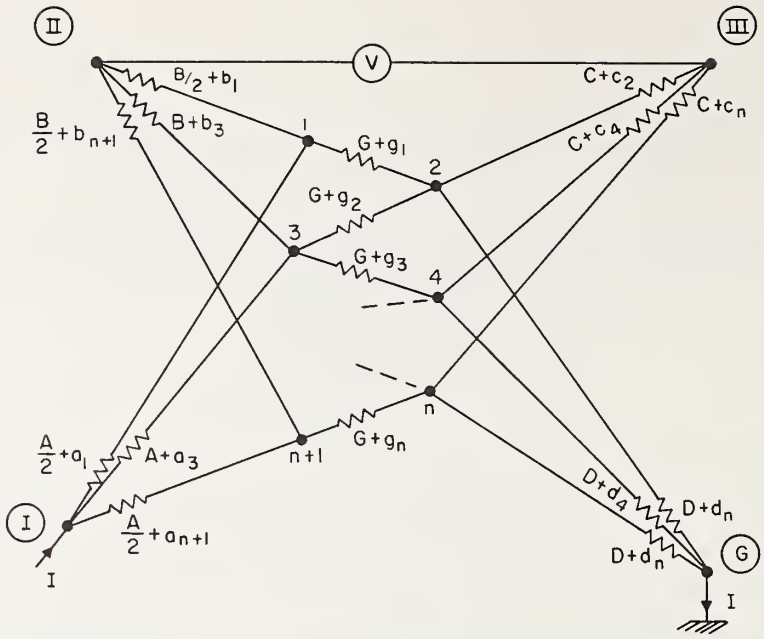

FIGURE 3

where α is a 3×3 matrix, β is a $3\times(n+1)$ matrix, $\tilde{\beta}$ is its transpose, and γ is an $(n+1)\times(n+1)$ matrix. In other words, the matrix is partitioned:

$$I=\begin{pmatrix}\alpha & \beta\\ \tilde{\beta} & \gamma\end{pmatrix} V. \tag{4}$$

Since we are interested in knowing the external voltage with *no* impressed internal current, we must eliminate V_i from

$$\begin{aligned} I_e&=\alpha V_e+\beta V_i\\ 0&=\tilde{\beta}V_e+\gamma V_i \end{aligned} \tag{5}$$

finding

$$\begin{aligned} I_e&=(\alpha-\beta\gamma^{-1}\tilde{\beta})V_e\\ V_e&=(\alpha-\beta\gamma^{-1}\tilde{\beta})^{-1}I_e. \end{aligned} \tag{6}$$

This last equation can be written as

$$\begin{pmatrix}V_{\mathrm{I}}\\ V_{\mathrm{II}}\\ V_{\mathrm{III}}\end{pmatrix}=\begin{pmatrix}z_{11} & z_{12} & z_{13}\\ z_{21} & z_{22} & z_{23}\\ z_{31} & z_{32} & z_{33}\end{pmatrix}\begin{pmatrix}I_{\mathrm{I}}\\ I_{\mathrm{II}}\\ I_{\mathrm{III}}\end{pmatrix}. \tag{7}$$

The required four-terminal resistance is the transfer resistance $(V_{\mathrm{II}}-V_{\mathrm{III}})/I_{\mathrm{I}}$ under the condition $I_{\mathrm{II}}=I_{\mathrm{III}}=0$, hence

$$R=(z_{21}-z_{31})\equiv(0,\,1,-1)z\begin{pmatrix}1\\ 0\\ 0\end{pmatrix}. \tag{8}$$

The problem is to carry out all the indicated algebraic manipulations, with all resistors subject to arbitrary tolerances. This will be done in an appendix, using the following strategy.

First, we carry out the manipulations required for $(\alpha-\beta\gamma^{-1}\tilde{\beta})^{-1}$ assuming the nominal values of the network elements; then, assuming that the departures from nominal are small, find the resulting correction to the nominal $R_0\left(=\frac{1}{nG}\right)$ as a series in powers of the perturbations. This yields a formula for the fractional error as a sum of terms of the type g_ig_j; g_ia_i, g_ib_i, etc.; a_ib_i, c_id_i. The terms involving the g_i (tolerances in the resistors of the series-parallel set) are ordinarily negligible compared with the pure measurement-network errors. These latter give (from eq (A38)):

$$\begin{aligned}\text{Error}=&\frac{4}{n}\frac{G}{A+B}\left(2\frac{a_1}{A}\frac{b_1}{B}+\frac{a_3}{A}\frac{b_3}{B}\right.\\ &\left.+\frac{a_5}{A}\frac{b_5}{B}+\ldots+2\frac{a_{n+1}}{A}\frac{b_{n+1}}{B}\right)\\ &+\frac{4}{n}\frac{G}{C+D}\left(\frac{c_2}{C}\frac{d_2}{D}+\frac{c_4}{C}\frac{d_4}{D}+\ldots+\frac{c_n}{C}\frac{d_n}{D}\right). \end{aligned} \tag{9}$$

Since $\Sigma a_i=0$, etc., this error arises from accidental correlation between errors of fan connections to common points. The worst case is where half the a_i have maximum positive error, the other half having maximum negative error—and where these pair up with the same situation among the b_i. Normal design would have $D=A$, $B=C$, and $A>>B$. Now let the maximum fractional error in the voltage fans be ϵ_v; in the current fans, ϵ_i. The resulting extreme error is $4\frac{G}{A}\epsilon_v\epsilon_i$. Reasonable estimates are $\frac{1}{G}=10\ \Omega$, $\frac{1}{A}=1\ \text{m}\Omega$, $\epsilon_i=10^{-1}$, $\epsilon_v=10^{-3}$, yielding a maximum error in the series-parallel ratio of 4×10^{-8}. Fractional errors of 10^{-5} in the main resistors make the g_i contributions completely negligible.

The above computation is for *maximum* error. Random pairing of the fan errors gives a much smaller expected error.

The next problem is to adjust the device after it has been constructed, and to evaluate the residual error. We note that if the current fans are perfect, there will be no voltage across any arm of the potential fans, hence any voltage across an arm of a potential fan is a measure of current-fan errors.

The potential fans have relatively high resistance, so are conveniently "trimmed" on a resistance bridge. To adjust the current fans, we can connect a microvoltmeter across each potential fan resistor in turn. This essentially measures the deviation of the potentials on the internal nodes, from their average. The current-fan arms can be filed to reduce these voltages to approximately zero.

In the analysis, we have treated the tetrahedral junctions as though their centers were available terminals. Any adjustment procedure must take cognizance of the fact that these terminals are fictitious; any physical connection is separated from the tetrahedron center by a low resistance. This could cause errors in direct measurement of current-fan resistance. The proposed scheme of measuring potential-fan resistances and voltage drops avoids this difficulty, since the potential fans are loaded with additional resistance.

In appendix A, we evaluate these residual adjustment errors quantitatively. We find to first order that the voltage across the arm $B+b_3$ is given by

$$IX_3=\frac{2}{n(A+B)}\frac{a_3}{A}I \tag{10}$$

and similarly the voltage across $A+a_3$, for current I into terminal (II) and out of terminal (III), is

$$IW_3=\frac{2}{n(A+B)}\frac{b_3}{B}I. \tag{11}$$

Comparison with eq (9) yields

$$\text{Error}=nG\Big\{(A+B)\left(\frac{X_1W_1}{4}+X_3W_3+X_5W_5+\ldots+\frac{X_{n+1}W_{n+1}}{4}\right)+(C+D)(X_2W_2+X_4W_4+\ldots+X_nW_n)\Big\}. \tag{12}$$

For a test current of 1 A, the fan tolerances assumed before yield voltages of the order

$$IX\sim2\times10^{-5}\text{V}$$
$$IW\sim2\times10^{-7}\text{V}$$

with

$$nGA\sim10^3.$$

Note that the larger voltage is generated by the current-fan error (under the assumed construction tolerances); this should make it feasible to adjust the current fan to the next order of magnitude.

The most sensitive set of measurements for evaluating the residual error is probably the set of residual adjustment errors; i.e., the residual potential-fan resistance differences and voltage drops. The appropriate formula is (from eq (A34)):

$$\text{Residual error}=2G\{X_1b_1/B+X_3b_3/B\ldots+X_{n+1}b_{n+1}/B-X_2c_2/C-X_4c_4/C-\ldots-X_nc_n/C\} \tag{13}$$

where positive X_i is associated with node i positive with respect to the appropriate potential terminal.

Note that the *measured* error quantities are first-order effects in the network tolerances; the computed residual error is a second-order product of these terms, so can be reasonably accurately evaluated by this procedure.

There are, of course, additional errors not attributable to the current and potential fans. The first of these arises from the fact that the *series* resistance is not n/G, but is

$$R_s=\sum\frac{1}{G+g_i}\doteq\frac{n}{G}\left(1+\frac{1}{n}\sum g_i^2/G^2\right)$$

yielding a fractional error of only 10^{-10} for $g_i/G\sim10^{-5}$. Another source of error lies in the imperfections of the tetrahedral junctions. Under conditions of suitable design and proper adjustment procedure, these junctions can be balanced to transfer resistances of less than $10^{-8}\ \Omega$. In a string of 10-Ω resistors, this is then a potential source of error of the order of 10^{-9}.

It seems feasible, therefore, to construct a 1:100 Ω buildup device with a ratio uncertainty of less than 1 in 10^8.

Appendix A

The submatrices of equation (4) are

$$\alpha=\begin{pmatrix} \frac{A}{2}+a_1+A+a_3+\ldots & 0 & 0 \\ 0 & \frac{B}{2}+b_1+B+b_3+\ldots & 0 \\ 0 & 0 & C+c_2+C+c_4+\ldots \end{pmatrix}$$

$$=\begin{pmatrix} \frac{nA}{2} & 0 & 0 \\ 0 & \frac{nB}{2} & 0 \\ 0 & 0 & \frac{nC}{2} \end{pmatrix}=\frac{n}{2}\begin{pmatrix} A & 0 & 0 \\ 0 & B & 0 \\ 0 & 0 & C \end{pmatrix} \qquad \text{(A1)}$$

$$\beta=\begin{pmatrix} -\left(\frac{A}{2}+a_1\right) & 0 & -(A+a_3) & 0 & -(A+a_5)\ldots \\ -\left(\frac{B}{2}+b_1\right) & 0 & -(B+b_3) & 0 & -(B+b_5)\ldots \\ 0 & -(C+c_2) & 0 & -(C+c_4) & 0\ldots \end{pmatrix}. \qquad \text{(A2)}$$

$$\gamma=\begin{pmatrix} G+g_1+\frac{A}{2}+a_1+\frac{B}{2}+b_1 & -(G+g_1) & 0\ldots \\ -(G+g_1) & 2G+g_1+g_2+C+c_2+D+d_2 & -(G+g_2)\ldots \\ 0 & -(G+g_2) & 2G+g_2+g_3+A+a_3+B+b_3\ldots \\ \vdots & \vdots & \vdots \end{pmatrix}. \qquad \text{(A3)}$$

It is convenient to decompose these matrices into sums of nominal values and perturbations:

Let

$$\beta\equiv\beta_0+\beta_1$$

$$\gamma\equiv\Gamma+\gamma_0+\gamma_1+\gamma_2 \qquad \text{(A4)}$$

where

$$\beta_0=\begin{pmatrix} -A/2 & 0 & -A & 0 & -A & \ldots \\ -B/2 & 0 & -B & 0 & -B & \ldots \\ 0 & -C & 0 & -C & 0 & \ldots \end{pmatrix} \qquad \text{(A5)}$$

$$\beta_1=\begin{pmatrix} -a_1 & 0 & -a_3 & 0 & \ldots \\ -b_1 & 0 & -b_3 & 0 & \ldots \\ 0 & -c_2 & 0 & -c_4 & \ldots \end{pmatrix} \qquad \text{(A6)}$$

$$\Gamma=\begin{pmatrix} \frac{A+B}{2} & 0 & 0 & \ldots & 0 \\ 0 & C+D & 0 & \ldots & 0 \\ 0 & 0 & A+B & \ldots & 0 \\ \cdot & & & & \cdot \\ \cdot & & & & \cdot \\ \cdot & & & & \cdot \\ 0 & \ldots & & & \frac{A+B}{2} \end{pmatrix} \qquad \text{(A7)}$$

$$\gamma_0\equiv GS$$

$$S=\begin{pmatrix} 1 & -1 & 0 & 0 & \ldots & 0 \\ -1 & 2 & -1 & 0 & \ldots & 0 \\ 0 & -1 & 2 & -1 & \ldots & 0 \\ \cdot & & & & & \cdot \\ \cdot & & & & & \cdot \\ \cdot & & & & & \cdot \\ & & & -1 & 2 & -1 \\ 0 & \ldots & & & -1 & 1 \end{pmatrix} \qquad \text{(A8)}$$

$$\gamma_1=\begin{pmatrix} a_1+b_1 & 0 & 0 & \dots & 0 \\ 0 & c_2+d_2 & 0 & \dots & 0 \\ 0 & 0 & a_3+b_3 & \dots & 0 \\ \cdot & & & & \cdot \\ \cdot & & & & \cdot \\ \cdot & & & & \cdot \\ 0 & \dots & & & a_{n+1}+b_{n+1} \end{pmatrix} \tag{A9}$$

$$\gamma_2=\begin{pmatrix} g_1 & -g_1 & 0 & 0 & \dots & 0 \\ -g_1 & g_1+g_2 & -g_2 & 0 & \dots & 0 \\ 0 & -g_2 & g_2+g_3 & -g_3 & \dots & 0 \\ \cdot & & & & & \cdot \\ \cdot & & & & & \cdot \\ \cdot & & & & & \cdot \\ & & & & g_{n-1}+g_n & -g_n \\ 0 & \dots & & & -g_n & g_n \end{pmatrix} \tag{A10}$$

We write the admittance matrix as the sum of a nominal value and a perturbation:

$$Y=\begin{pmatrix} \alpha & \beta_0 \\ \tilde{\beta}_0 & \Gamma+\gamma_0 \end{pmatrix}+\begin{pmatrix} 0 & \beta_1 \\ \tilde{\beta} & \gamma_1+\gamma_2 \end{pmatrix}$$

$$\equiv Y_0\begin{pmatrix} 0 & \beta_1 \\ \tilde{\beta}_1 & \epsilon \end{pmatrix}. \tag{A11}$$

Let

$$Y_0^{-1}\equiv\begin{pmatrix} Z_0 & Z_1 \\ \tilde{Z}_1 & Z_2 \end{pmatrix} \tag{A12}$$

where

$$Z_0=(\alpha-\beta_0(\Gamma+\gamma_0)^{-1}\tilde{\beta}_0)^{-1} \tag{A12a}$$

$$Z_1=-Z_0\beta_0(\Gamma+\gamma_0)^{-1} \tag{A12b}$$

$$Z_2=(\Gamma+\gamma_0)^{-1}-(\Gamma+\gamma_0)^{-1}\tilde{\beta}_0 Z_1. \tag{A12c}$$

Now $(\Gamma+\gamma_0)^{-1}$ is not readily found, but the combination $\beta_0(\Gamma+\gamma_0)^{-1}$ is, from appendix B:

$$\beta_0(\Gamma+\gamma_0)^{-1}=-[1+2G(E+F)]^{-1}$$
$$\left\{2GEF\begin{pmatrix} A & A & A \dots \\ B & B & B \dots \\ C & C & C \dots \end{pmatrix}\right.$$
$$\left.+\begin{pmatrix} AE & 0 & AE & 0 & \dots \\ BE & 0 & BE & 0 & \dots \\ 0 & CF & 0 & CF & \dots \end{pmatrix}\right\} \tag{A13}$$

where

$$E\equiv\frac{1}{A+B},\ F\equiv\frac{1}{C+D}.$$

This yields

$$Z_0=\frac{1}{n}\begin{pmatrix} \frac{2}{A}+\frac{1}{G}+\frac{2}{D} & \frac{1}{G}+\frac{2}{D} & \frac{2}{D} \\ \frac{1}{G}+\frac{2}{D} & \frac{2}{B}+\frac{1}{G}+\frac{2}{D} & \frac{2}{D} \\ \frac{2}{D} & \frac{2}{D} & \frac{2}{C}+\frac{2}{D} \end{pmatrix} \tag{A14}$$

$$Z_1=\frac{1}{n}\begin{pmatrix} \frac{1}{G}+\frac{2}{D} & \frac{2}{D} & \frac{1}{G}+\frac{2}{D}\dots \\ \frac{1}{G}+\frac{2}{D} & \frac{2}{D} & \frac{1}{G}+\frac{2}{D}\dots \\ \frac{2}{D} & \frac{2}{D} & \frac{2}{D}\ \dots \end{pmatrix}. \tag{A15}$$

These matrices are readily verified by inspection of the circuit when the elements have their nominal values.

The matrix Z_2 involves the term $(\Gamma+\gamma_0)^{-1}$ standing by itself; we shall eventually need this term and shall use a series expansion for it.

The four-terminal resistance of interest is the transfer resistance expressed as $V_{II}-V_{III}$ for $I_I=1$, all other input currents being zero:

$$R=[(0\quad 1-1)(0\quad 0\dots 0]Y^{-1}\begin{bmatrix}\begin{pmatrix}1\\0\\0\end{pmatrix}\\ \begin{pmatrix}0\\0\\\cdot\\\cdot\\\cdot\\0\end{pmatrix}\end{bmatrix}. \tag{A16}$$

In (A16), we have partitioned the vectors into "external" and "internal" vectors, corresponding to the partitioning of Y. For the nominal case we find

$$R_0=(0\quad 1-1)Z_0\begin{pmatrix}1\\0\\0\end{pmatrix}=\frac{1}{nG}. \tag{A17}$$

We are also interested in the transfer resistances that are measured as voltage drops across the potential-fan arms:

$$X_1=[(0-1\quad 0)(1\quad 0\quad 0\dots 0)]Y^{-1}\begin{bmatrix}\begin{pmatrix}1\\0\\0\end{pmatrix}\\ \begin{pmatrix}0\\\cdot\\\cdot\\\cdot\\0\end{pmatrix}\end{bmatrix}$$

$$X_2=[(0\quad 0-1)(0\quad 1\quad 0\ldots 0)]\,\Upsilon^{-1}\begin{bmatrix}\begin{pmatrix}1\\0\\0\end{pmatrix}\\ \begin{pmatrix}0\\\cdot\\\cdot\\\cdot\\0\end{pmatrix}\end{bmatrix}$$

$$X_3=[(0-1\quad 0)(0\quad 0\quad 1\quad 0\ldots 0)]\,\Upsilon^{-1}\begin{bmatrix}\begin{pmatrix}1\\0\\0\end{pmatrix}\\ \begin{pmatrix}0\\\cdot\\\cdot\\\cdot\\0\end{pmatrix}\end{bmatrix} \tag{A18}$$

All $X_i=0$ for the nominal case.

The perturbation from nominal is found by expanding Υ^{-1} in a series (as shown in appendix B for $(\Gamma+\gamma_0)^{-1}$):

$$\Upsilon^{-1}=\Upsilon_0^{-1}-\Upsilon_0^{-1}\begin{pmatrix}0 & \beta_1\\ \tilde{\beta}_1 & \epsilon\end{pmatrix}\Upsilon_0^{-1}$$

$$+\Upsilon_0^{-1}\begin{pmatrix}0 & \beta_1\\ \tilde{\beta}_1 & \epsilon\end{pmatrix}\Upsilon_0^{-1}\begin{pmatrix}0 & \beta_1\\ \tilde{\beta}_1 & \epsilon\end{pmatrix}\Upsilon_0^{-1}+\ldots \tag{A19}$$

to second order in the perturbation.

The algebra will be alleviated by noting some special properties of the matrices β_1, γ_1, and γ_2:

$$\begin{aligned}(1\quad 0\quad 1\quad 0\ldots)\tilde{\beta}_1&=(0\quad 0\quad 0)\\ (0\quad 1\quad 0\quad 1\ldots)\tilde{\beta}_1&=(0\quad 0\quad 0)\end{aligned} \tag{A20}$$

since $\Sigma a_i=\Sigma b_i=\Sigma c_i=0$

$$\begin{aligned}(1\quad 0\quad 1\quad 0\ldots)\gamma_1&=(a_1+b_1\quad 0\quad a_3+b_3\quad 0\quad \ldots)\\ (0\quad 1\quad 0\quad 1\ldots)\gamma_1&=(0\quad c_2+d_2\quad 0\quad c_4+d_4\quad \ldots)\\ (1\quad 0\quad 1\quad 0\ldots)\gamma_2&=(g_1\quad -(g_1+g_2)\quad (g_2+g_3)\quad \ldots)\\ (0\quad 1\quad 0\quad 1\ldots)\gamma_2&=(-g_1\quad (g_1+g_2)\quad -(g_2+g_3)\quad \ldots).\end{aligned} \tag{A21}$$

Note that premultiplication of either γ_1 or γ_2 by either $(1\quad 0\quad 1\quad 0\ldots)$ or $(0\quad 1\quad 0\quad 1\ldots)$, followed by postmultiplication by either

$$\begin{pmatrix}1\\0\\1\\0\\\cdot\\\cdot\end{pmatrix}\text{ or }\begin{pmatrix}0\\1\\0\\1\\\cdot\\\cdot\end{pmatrix}$$ results in a null vector.

Thus from (A12b) and (A13) in conjunction with (A20) and (A21), we have the very useful relations:

$$\begin{aligned}Z_1\tilde{\beta}_1&=\mathbf{0}\\ Z_1\gamma_1\tilde{Z}_1&=\mathbf{0}\\ Z_1\gamma_2\tilde{Z}_1&=\mathbf{0}.\end{aligned} \tag{A22}$$

These simplify the multiplications required by eq (A19):

$$\Upsilon_0^{-1}\begin{pmatrix}0 & \beta_1\\ \tilde{\beta}_1 & \epsilon\end{pmatrix}=\begin{pmatrix}Z_0 & Z_1\\ \tilde{Z}_1 & Z_2\end{pmatrix}\begin{pmatrix}0 & \beta_1\\ \tilde{\beta}_1 & \epsilon\end{pmatrix}=\begin{pmatrix}0 & Z_0\beta_1+Z_1\epsilon\\ Z_2\tilde{\beta}_1 & \tilde{Z}_1\beta_1+Z_2\epsilon\end{pmatrix}$$

$$\equiv\begin{pmatrix}0 & M\\ Z_2\tilde{\beta}_1 & \tilde{Z}_1\beta_1+Z_2\epsilon\end{pmatrix} \tag{A23}$$

Note that

$$M\tilde{Z}_1=Z_0\beta_1\tilde{Z}_1+Z_1\epsilon\tilde{Z}_1=\mathbf{0},\qquad Z_1\tilde{M}=\mathbf{0} \tag{A24}$$

so that

$$\Upsilon_0^{-1}\begin{pmatrix}0 & \beta_1\\ \tilde{\beta}_1 & \epsilon\end{pmatrix}\Upsilon_0^{-1}=\begin{pmatrix}0 & MZ_2\\ Z_2\tilde{M} & Z_2\tilde{\beta}_1Z_1+\tilde{Z}_1\beta_1Z_2+Z_2\epsilon Z_2\end{pmatrix} \tag{A25}$$

and finally

$$\Upsilon_0^{-1}\begin{pmatrix}0 & \beta_1\\ \tilde{\beta}_1 & \epsilon\end{pmatrix}\Upsilon_0^{-1}\begin{pmatrix}0 & \beta_1\\ \tilde{\beta}_1 & \epsilon\end{pmatrix}\Upsilon_0^{-1}$$

$$=\begin{pmatrix} MZ_2\tilde{M} & Mz_2(\tilde{\beta}_1 z_1+\epsilon z_2) \\ (z_2\epsilon+\tilde{z}_1\beta_1)z_2\tilde{M} & \text{etc.} \end{pmatrix} \quad \text{(A26)}$$

Using these expressions in (A19) yields

$$R=\frac{1}{nG}+(0 \quad 1-1)MZ_2\tilde{M}\begin{pmatrix}1\\0\\0\end{pmatrix} \quad \text{(A27)}$$

with no first order correction.

The X_i have first order terms:

$$X_1=-(1 \quad 0 \quad 0\ldots)Z_2\tilde{M}\begin{pmatrix}1\\0\\0\end{pmatrix}$$

$$X_2=-(0 \quad 1 \quad 0\ldots)Z_2\tilde{M}\begin{pmatrix}1\\0\\0\end{pmatrix}$$

$$X_3=-(0 \quad 0 \quad 1 \quad 0\ldots)Z_2\tilde{M}\begin{pmatrix}1\\0\\0\end{pmatrix} \quad \text{(A28)}$$

etc.

These can be interpreted as the components of a vector, X:

$$X=-Z_2\tilde{M}\begin{pmatrix}1\\0\\0\end{pmatrix}. \quad \text{(A29)}$$

We can now write

$$R=\frac{1}{nG}-(0 \quad 1-1)MX \quad \text{(A30)}$$

as an alternate expression.

From (A12c) and (A24) we have

$$Z_2\tilde{M}=(\Gamma+\gamma_0)^{-1}\tilde{M} \quad \text{(A31)}$$

so that

$$R=\frac{1}{nG}+(0 \quad 1-1)M(\Gamma+\gamma_0)^{-1}\tilde{M}\begin{pmatrix}1\\0\\0\end{pmatrix}. \quad \text{(A32)}$$

Now

$$(0 \quad 1-1)M\equiv(0 \quad 1-1)Z_0\beta_1+(0 \quad 1-1)Z_1\epsilon$$

$$=\frac{1}{n}\left(\frac{1}{G},\ \frac{2}{B}+\frac{1}{G},\ -\frac{2}{C}\right)\beta_1$$

$$+\frac{1}{nG}(1 \quad 0 \quad 1 \quad 0\ldots)(\gamma_1+\gamma_2)$$

$$=\frac{1}{n}\left(\frac{g_1}{G}-\frac{2b_1}{B},\ -\frac{g_1+g_2}{G}+\frac{2c_2}{C},\right.$$

$$\left.\frac{g_2+g_3}{G}-\frac{2b_3}{B},\ldots\right). \quad \text{(A33)}$$

Neglecting g/G relative to b/B and c/C, we have

$$R\doteq\frac{1}{nG}+\frac{2}{n}\sum X_{2i+1}b_{2i+1}/B-\frac{2}{n}\sum X_{2i}c_{2i}/C \quad \text{(A34)}$$

for evaluation of error in terms of measured residuals.

To express R in terms of circuit element tolerances, we need to express X:

$$\tilde{X}=-(1 \quad 0 \quad 0)M(\Gamma+\gamma_0)^{-1}$$

$$=-(1 \quad 0 \quad 0)\{Z_0\beta_1+Z_1(\gamma_1+\gamma_2)\}(\Gamma+\gamma_0)^{-1}$$

which becomes

$$\tilde{X}=\frac{1}{n}\left(\frac{2a_1}{A}-\frac{g_1}{G},\ -\frac{2d_2}{D}+\frac{g_1+g_1}{G},\right.$$

$$\left.\frac{2a_3}{A}-\frac{g_2+g_3}{G},\ldots\right)(\Gamma+\gamma_0)^{-1}. \quad \text{(A35)}$$

We need $(\Gamma+\gamma_0)^{-1}$; we have

$$(\Gamma+\gamma_0)^{-1}\equiv(\Gamma+GS)^{-1}=\Gamma^{-1}-G\Gamma^{-1}S\Gamma^{-1}$$

$$+G^2\Gamma^{-1}S\Gamma^{-1}S\Gamma^{-1}-\ldots. \quad \text{(A36)}$$

Now

$$\Gamma^{-1}=\begin{pmatrix} 2E & 0 & 0 & \ldots & 0 \\ 0 & F & 0 & & . \\ 0 & 0 & E & & . \\ & & & & . \\ . & & & & \\ . & & & & \\ . & & & & \\ 0 & \ldots & & & 2E \end{pmatrix}$$

and the successive terms of (A36) diminish as powers of GE and GF, which are small compared to unity. Hence the first term of (A36) is sufficient for our purposes, for use in (A35):

$$X\doteq\frac{E}{n}\left(\frac{4a_1}{A}-\frac{2g_1}{G},\ 0,\ \frac{2a_3}{A}-\frac{g_2+g_3}{G},\ 0\ldots\right)$$

$$-\frac{F}{n}\left(0,\ \frac{2d_2}{D}-\frac{g_1+g_2}{G},\ 0,\ \frac{2d_4}{D}-\frac{g_3+g_4}{G},\ 0\ldots\right) \quad \text{(A37)}$$

and

$$R\doteq\frac{1}{nG}+\frac{E}{n^2}\left\{2\left(\frac{2a_1}{A}-\frac{g_1}{G}\right)\left(\frac{2b_1}{B}-\frac{g_1}{G}\right)\right.$$

$$\left.+\left(\frac{2a_3}{A}-\frac{g_2+g_3}{G}\right)\left(\frac{2b_3}{B}-\frac{g_2+g_3}{G}\right)+\ldots\right\}$$

$$+\frac{F}{n^2}\left\{\left(\frac{2c_2}{C}-\frac{g_1+g_2}{G}\right)\left(\frac{2d_2}{D}-\frac{g_1+g_2}{G}\right)\right.$$

$$\left.+\left(\frac{2c_4}{C}-\frac{g_3+g_4}{G}\right)\left(\frac{2d_4}{D}-\frac{g_3+g_4}{G}\right)+\ldots\right\}. \quad \text{(A38)}$$

Appendix B

A power series expansion yields

$$(\Gamma+\gamma_0)^{-1}\equiv(\Gamma+GS)^{-1}=\Gamma^{-1}(I+GS\Gamma^{-1})^{-1}$$
$$=\Gamma^{-1}(I-GS\Gamma^{-1}+G^2S\Gamma^{-1}S\Gamma^{-1}-\ldots)$$
$$=\Gamma^{-1}-G\Gamma^{-1}S\Gamma^{-1}+G^2\Gamma^{-1}S\Gamma^{-1}S\Gamma^{-1}-\ldots. \quad \text{(B1)}$$

The series converges if the norm of $S\Gamma^{-1}$ is less than $1/G$. A sufficient condition is

$$G<\min\left(\frac{\sqrt{2}}{4}(A+B),\frac{C+D}{2}\right). \quad \text{(B2)}$$

Premultiplication of the series by β_0 yields:

$$\beta_0(\Gamma+\gamma_0)^{-1}=\beta_0\Gamma^{-1}-G\beta_0\Gamma^{-1}(S\Gamma^{-1})$$
$$+G^2\beta_0\Gamma^{-1}(S\Gamma^{-1})^2-\ldots. \quad \text{(B3)}$$

For convenience, let

$$E\equiv\frac{1}{A+B},\ F\equiv\frac{1}{C+D} \quad \text{(B4)}$$

then

$$\Gamma^{-1}=\begin{pmatrix}2E & 0 & 0 & \ldots & 0\\ 0 & F & 0 & & \vdots\\ 0 & 0 & E & & \\ \vdots & & & & \\ 0 & \ldots & & & 2E\end{pmatrix} \quad \text{(B5)}$$

$$\beta_0\Gamma^{-1}=\begin{pmatrix}-AE & 0 & -AE & 0 & \ldots\\ -BE & 0 & -BE & 0 & \ldots\\ 0 & -CF & 0 & -CF & \ldots\end{pmatrix} \quad \text{(B6)}$$

$$S\Gamma^{-1}=\begin{pmatrix}2E & -F & 0 & 0 & \ldots & 0\\ -2E & 2F & -E & 0 & & \vdots\\ 0 & -F & 2E & -F & & \\ 0 & 0 & -E & 2F & & \\ \vdots & \vdots & & & & \\ 0 & \ldots & & & & 2E\end{pmatrix} \quad \text{(B7)}$$

We compute

$$\beta_0\Gamma^{-1}(S\Gamma^{-1})=\begin{pmatrix}-2AE^2 & 2AEF & -2AE^2 & \ldots\\ -2BE^2 & 2BEF & -2BE^2 & \ldots\\ 2CEF & -2CF^2 & 2CEF & \ldots\end{pmatrix} \quad \text{(B8)}$$

and

$$\beta_0\Gamma^{-1}(S\Gamma^{-1})^2=\begin{pmatrix}-4AE^2(E+F) & 4AEF(E+F) & -4AE^2(E+F) & \ldots\\ -4BE^2(E+F) & 4BEF(E+F) & -4BE^2(E+F) & \ldots\\ 4CEF(E+F) & -4CF^2(E+F) & 4CEF(E+F) & \ldots\end{pmatrix} \quad \text{(B9)}$$

Comparison of (B9) with (B8) shows that

$$\beta_0\Gamma^{-1}(S\Gamma^{-1})^2=2(E+F)\beta_0\Gamma^{-1}(S\Gamma^{-1}) \quad \text{(B10)}$$

so that

$$\beta_0\Gamma^{-1}(S\Gamma^{-1})^{k+1}=2^k(E+F)^k\beta_0\Gamma^{-1}S\Gamma^{-1} \quad \text{(B11)}$$

allowing (B3) to be evaluated as

$$\beta_0(\Gamma+\gamma_0)^{-1}=\beta_0\Gamma^{-1}-G\beta_0\Gamma^{-1}S\Gamma^{-1}$$
$$\{1-2G(E+F)+4G^2(E+F)^2-\ldots\}$$
$$=\beta_0\Gamma^{-1}-\frac{G}{1+2G(E+F)}\beta_0\Gamma^{-1}S\Gamma^{-1} \quad \text{(B12)}$$

We note that the result (B12) is valid (by analytic continuation) without restriction on the size of G. Substituting (B6) and (B8) into (B12) yields

$$\beta_0(\Gamma+\gamma_0)^{-1}=-[1+2G(E+F)]^{-1}$$
$$\left\{2GEF\begin{pmatrix}A & A & A\ldots\\ B & B & B\ldots\\ C & C & C\ldots\end{pmatrix}\right.$$
$$\left.+\begin{pmatrix}AE & 0 & AE & 0\ldots\\ BE & 0 & BE & 0\ldots\\ 0 & CF & 0 & CF\ldots\end{pmatrix}\right\}. \quad \text{(B13)}$$

(Paper 69C3-197)

UNITED STATES DEPARTMENT OF COMMERCE • Charles Sawyer, *Secretary*
NATIONAL BUREAU OF STANDARDS • E. U. Condon, *Director*

Precision Resistors and Their Measurement

by James L. Thomas

National Bureau of Standards Circular 470
Issued October 8, 1948

149-I

Preface

There are few fields of scientific investigation in which accurate measurements of electrical resistance are not required. For this purpose the Wheatstone bridge, in one of its several forms, is almost universally used. This instrument is comparatively simple to use and at the same time has a very high sensitivity. Unfortunately, however, sensitivity and accuracy are not synonomous, and some knowledge of the practical limitations of resistance-measuring bridges is needed by all users. This circular is intended to supply such information. Although the presentation is essentially nontechnical, it is believed that the subject matter will be of value to any one interested in the accurate measurement of resistance

In addition to information about the use of resistance bridges, this circular presents methods for their calibration. The subject matter is limited to direct-current calibrations, and the methods discussed are those regularly used at this Bureau when an accuracy of 0.01 percent or better is required. No attempt is made to present a complete discussion of methods of resistance measurement or to consider the relative merits of various methods. Those presented are comparatively simple, being based largely on substitution procedures, yet they are capable of yielding results of high accuracy.

E. U. Condon, *Director.*

Contents

315-411 O - 68 - 11

Precision Resistors and Their Measurement

By James L. Thomas

Abstract

This circular contains information on the construction and characteristics of wire-wound resistors of the precision type. There are also included descriptions of the methods used at this Bureau for the test of precision resistors and the calibration of precision resistance measuring apparatus. Although the presentation is nontechnical, there is a considerable amount of information on the characteristics and limitations of apparatus of this type that should be of interest to any one making accurate measurements of electrical resistance.

I. Introduction

1. Definition of Resistance

The modern concept of electrical resistance is based largely on the work of G. S. Ohm, who in 1826 published an equation that was formulated on the basis of his experiments with direct-current circuits. In modern terminology this equation is

$$I=\gamma\frac{A}{l}E, \tag{1}$$

where E is the potential difference across a conductor of length l and cross-sectional area A when a current, I, flows. The factor γ depends upon the material of the conductor and is now called conductivity (see sec. VI). The above equation was abbreviated by Ohm as

$$I=\frac{E}{\mathscr{L}}, \tag{2}$$

where $\mathscr{L}$ is the length of a hypothetical wire having unit conductivity and cross-sectional area. $\mathscr{L}$ was then the length of a wire across which unit current would produce a unit of potential difference, that is, $\mathscr{L}$ was Ohm's unit of resistance and his experimental equation can be abbreviated as

$$E=RI. \tag{3}$$

This equation is almost universally referred to as Ohm's Law, although some writers contend that the longer form should be so designated. Although experimentally determined for individual conductors, Ohm's Law was soon applied to the entire circuit if E designates the net electromotive force in the circuit.

2. Importance of Resistance Measurements

Although Ohm found that the ratio of potential difference across a conductor to the current flowing in it is dependent on the material and dimensions of the conductor, more precise experiments showed it to depend upon temperature and even upon the presence of stress in the conductor. Instead of incorporating such quantities in our equation for the current, we say that the resistance is a function of temperature and stress, and for a given conductor we must state the values of temperature and stress for which a value of resistance is given.

The fact that resistance is a function of temperature is made use of in temperature measurements, the resistance of a wire being measured at known temperatures or fixed points and then at the unknown temperatures. Also, changes in resistance with dimensions are utilized for measuring small displacements, and change in resistance with stress is utilized for the measurement of liquid pressures. In addition to such phenomena, a large number of physical and chemical phenomena are investigated by means of measurements of electromotive forces, and the measurement of electromotive force is customarily carried out by measurements of resistance ratios. Electric current is readily measured in terms of the potential difference across a known resistor. In fact, a large proportion of electrical quantities is measured by methods that involve the measurement of resistance.

In some cases the resistance of a conductor depends upon the magnitude of the current flowing through it. That is to say, Ohm's law is not applicable, and the resistance must be determined under the conditions of use. Also, the resistance of all conductors is to some extent a function of frequency, and the resistance must often be determined in such a way as to allow for the effect of frequency. However, the content of this circular is limited largely to direct-current measurements of resistors which follow Ohm's law, with special emphasis on precision measurements, i. e., measurements to 0.01 percent or better.

3. Types of Resistors

Resistors are used for many purposes with a correspondingly large range of types and accuracies of adjustment. They are used as electric heaters, as current-limiting devices such as motor starters, for component parts of radio, telephonic and similar equipment, and in electrical instruments of greater or less precision. For some applications adjustments must be made to perhaps 10 to 20 percent, whereas in others the resistors must be within 0.01 percent or less of their nominal values.

For use as heaters, resistors are usually made of special alloy wire that will withstand high temperatures for long periods of heating. The most used alloy for this purpose is of nickel and chromium, with or without the addition of a considerable amount of iron. These alloys can be kept at a "red heat" in air for long periods of time without damage from oxidation. High-resistance units for radio circuits are often made from a nonconducting binder, such as clay, with which is mixed sufficient powdered graphite to make the material slightly conducting; or from a nonconducting rod on the surface of which is deposited a conducting film. For resistors to be used in precision instruments the important quality desired is stability with time and temperature, and special alloys have been developed, which are discussed in section II. Stability with time and temperature are also the important characteristics required for resistors that are to be used as reference standards for the calibration of other resistors.

Standard resistors are usually commercially available only in decimal multiples or fractions of the unit, usually from 0.0001 ohm to 10,000 ohms. These are of two general types of construction, either two-terminal or four-terminal types. For values of resistance where the resistance of the contacts, made in connecting to the resistor, is not negligible, it is customary to use four-terminal resistors. Whether or not the contact resistances are negligible depends upon the accuracy desired, but in general standard resistors of 1-ohm and less are of the four-terminal type, higher valued resistors needing only two terminals. Special standard resistors are required if an accuracy of better than 0.01 percent is required. These are usually sealed to protect the resistors from the effects of oxygen and moisture in the atmosphere, whereas resistors for an accuracy of 0.1 percent do not require such protection. Although precision resistors are ordinarily adjusted to their nominal values to 0.01 percent or better, they gradually change in resistance with time. For work to this accuracy it is desirable to have standards recalibrated occasionally, applying if necessary corrections corresponding to their departure from nominal values.

II. Resistance Materials and Construction Methods

1. Resistance Alloys

Manganin. Since their introduction in about 1890, alloys of copper, manganese, and nickel have come into almost universal use as resistance materials for precision resistors and for resistance measuring apparatus. The most common of these alloys is "manganin" which has the nominal proportions of 84 percent of copper, 12 percent of manganese and 4 percent of nickel. This material has a resistivity of 45 to 50 microhm-cm, a thermoelectromotive force against copper of 2 or 3 μv/° C., and, when properly heat treated, is very stable in resistance with time.

The electrical properties of alloys of copper, manganese, and nickel over a large range of proportions were investigated in 1925 by Pilling [1] [1] and later for alloys made of high-purity ingredients by Dean and Anderson [2]. Both of these investigations showed that an alloy having a temperature coefficient that averaged zero over the interval 0 to 100° C. would be obtained with approximately 10 percent each of manganese and nickel, the remainder being copper. A series of alloys also having zero temperature coefficients could be obtained by increasing separately either the manganese or the nickel up to as much as 20 or 30 percent, with a corresponding reduction in copper.

On the basis of small temperature coefficients there would appear to be a wide choice of compositions for alloys of the manganin type. However, in order to keep the thermoelectric power against copper as low as possible it is necessary to keep the nickel content low, as the thermoelectric power increases rapidly in proportion to the amount of nickel above 2 or 3 percent. Also, if the nickel is kept constant and the percentage of manganese is increased the curvature of the resistance-temperature curve increases. This means that although the resistance might have the same value at 0° and 100° C., the departure from this value at intermediate temperatures increases with the manganese content. It is therefore desirable for general use to have an alloy that is as low as possible in both nickel and manganese.

The published data on copper-manganese-nickel alloys give average temperature coefficients over a temperature interval of some 80 to 100° C. These data do not show the best compositions for use at ordinary laboratory temperatures. If it is desired to keep the thermoelectric power against copper as small as possible, the alloy should have a content of about 2 percent of nickel and 14 percent of manganese in order to obtain at the

[1] Figures in brackets indicate the literature references at the end of this paper.

same time a small temperature coefficient of resistance at ordinary room temperatures. On the other hand, if the thermoelectric power is of no importance the resistance of an alloy of about 20 percent of nickel and 10 percent of manganese would be most constant with temperature in the ordinary range of laboratory temperatures. The accepted composition of manganin, 84 percent of copper, 12 percent of manganese and 4 percent of nickel is reasonably close to the optimum for a general purpose resistance alloy. Fortunately the proportions need not be exact, as the melting losses make the composition somewhat difficult to control.

If the resistance of a sample of manganin is plotted against temperature, the curve will be found to be of the general shape of that shown in figure 1.

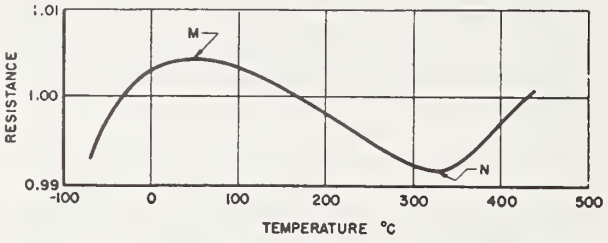

FIGURE 1. *Resistance-temperature curve for manganin.*

The maximum, M, of this curve is in the neighborhood of room temperature, being generally between 20° and 50° C, while the minimum, N, is at about 350° C. Somerville [3] found the difference in resistance between the maximum and the minimum to be about 1½ percent of the value at the maximum.

For an interval at least 15° to 20° C on each side of the maximum, the resistance-temperature curve for manganin is symmetrical with respect to a vertical axis. Its equation can be accurately represented by

$$R_t = R_{25}[1+\alpha(t-25)+\beta(t-25)^2], \qquad (4)$$

where R_t is the resistance at t°C and R_{25} is the resistance at 25° C. The coefficient α is the slope of the resistance-temperature curve at 25° C, and for manganin of good quality α has a value of 10×10^{-6} or less. The value of β, which determines the curvature at any point in the interval, is usually between -3×10^{-7} and -6×10^{-7}. This means that 10° C either side of the maximum the resistance is less than at the maximum by from 30 to 60 parts per million (ppm).

The temperature at which the maximum of resistance occurs is a function of the thermal and mechanical treatment of the manganin as well as of its composition. Different size wires drawn from the same melt will have maxima at different temperatures, that is, at any given temperature their coefficients of resistance will not be the same. From the ingot, manganin is usually worked cold with an occasional softening by heating to a "red heat." If this annealing is done in air there is a selective oxidation of the surface that breaks down the alloy and leaves a coating with a relatively high conductivity. This surface layer may be removed by "pickling" in an acid, but again the action of the acid is somewhat selective, and the surface layer is left with a slightly different composition from that of the interior. These complications add to the difficulty of the control of the quality of manganin wire. In addition, the completed resistance coils are usually baked at about 150° C for 24 to 48 hours in order to stabilize the resistance. This baking also affects the temperature coefficient of the wire by amounts depending upon the size of the wire and the length of time of the baking. All of these factors make it difficult to produce resistors with the maximum at the best temperature, usually between 20° and 25° C. However, precision resistors of good quality usually can be obtained with temperature coefficients in that interval of not more than 10 ppm/° C.

Temperature coefficients of resistance change little with time, and if changes do occur in their values there is very probably an accompanying large change in resistance. Standards that are stable in resistance need not have redeterminations of their temperature coefficients. Although the data are meager and only the order of magnitude is known, it appears that for manganin resistors a change in resistance of one part in a thousand will be required to change the slope of the temperature-resistance curve at room temperature by one or two parts in a million per degree centigrade.

Constantan.—A series of alloys of nickel and copper containing 40 to 60 percent nickel, with a small amount of manganese to improve their mechanical properties, all have practically the same electrical properties. These alloys are sold as "constantan," or under various trade names, for use as thermocouple materials, and have thermoelectric powers against copper of about 40 μv/° C. However, except for their large thermoelectric powers the electrical properties of these alloys are remarkably similar to those of manganin.

The resistance-temperature curve for constantan is similar to that for manganin shown in figure 1. Its maximum is at or near room temperature with the minimum around 500° C. The difference in resistance between the maximum and minimum is somewhat less than for manganin, and the curvature in the neighborhood of the maximum is also less. As a consequence, constantan changes somewhat less in resistance over the ordinary range of atmospheric temperatures than does manganin. Its stability with time is about the same as that of manganin. At room temperature the resistivity

of constantan is 45 to 50 microhm-cm as it is for manganin.

Resistance coils of constantan are sometimes used instead of manganin in values of 1,000 ohms and above. They may also be used in smaller denominations in cases where no difficulty will arise from the large thermal emf's, as for example in alternating current circuits.

Therlo.—When manganin was first developed a small amount of nickel was added to the copper and manganese in an attempt to reduce the thermoelectric power of the alloy against copper. With the proportion of nickel now used the thermoelectric power against copper at room temperature is almost the same, although of opposite sign, as when the nickel is omitted. However, the nickel improves the mechanical properties of the alloy and probably reduces the surface action during forging and annealing.

The development of therlo was another attempt to reduce the thermoelectric power of copper-manganese alloys against copper. Instead of nickel, an equal percentage by weight of aluminum was added to the copper and manganese. As its name implies, the resulting alloy had a very small thermoelectric power against copper at room temperatures, less than 1μv/°C. Its other electrical properties are almost identical with those of manganin. However, as the thermoelectric power of manganin against copper is only of the order of 2 or 3μv/°C, the improvement was of little significance.

At the National Bureau of Standards [4] an investigation has been made of copper manganese-aluminum alloys of the therlo type. There it was found that for a resistance alloy the best composition is 85 percent of copper, 9.5 percent of manganese, and 5.5 percent of aluminum. This alloy has nearly the same resistivity as manganin, its temperature coefficient at 25° C can be brought to zero by a suitable heat treatment, and the change in the temperature coefficient with temperature is about half that of manganin, at least in the ordinary range of room temperatures. Its thermoelectric power against copper at 25° C is only about 10 percent of that of manganin, and this thermoelectric power may be further reduced by the addition of a very small percentage of iron, without materially affecting the other properties of the alloy. The stability of such alloys with time was found to be equal to that of manganin. Except for unusual applications, the difference between manganin and therlo is of little importance and the alloys may be used interchangeably.

Gold-chromium.—An alloy of recent introduction, which appears to be very promising for some applications, is gold with slightly over 2 percent of chromium [5]. This alloy has a resistivity at room temperatures of about 20 times that of copper. By baking at fairly low temperatures the temperature coefficient can be made extremely small. Resistors of this material have been produced such that the total change in resistance in the interval 20° to 30° C did not exceed a few parts in ten million. The thermoelectric power of this gold-chromium alloy against copper is several times that of manganin, being 7 or 8 μv/° C at 25° C. The stability of this alloy with time has not been thoroughly tested but preliminary results were promising.

For many applications the extremely small temperature coefficient of gold-chromium alloy makes its use desirable. However, the temperature coefficient must be adjusted for each coil by baking, and the cost of this adjustment limits the use of the material. Although the temperature coefficient may be made small at room temperature, the interval over which the coefficient is small is not more than 20° or 30° C. The temperature-resistance curve is similar to that for manganin, as shown in figure 1, but with M and N much closer together in temperature and in resistance.

Other Alloys.—It is probable that all resistance alloys that have small temperature coefficients at room temperature have temperature-resistance curves that are cubics, similar to that of manganin shown in figure 1. These curves are nearly straight in the neighborhood of the inflection points between the maxima and minima. The ideal resistance alloy for use in instruments would have this inflection point at room temperature with a zero slope. Moreover, the maximum and minimum should be at widely separated temperatures so that the zero slope would be obtained over the usual range of atmospheric temperatures. Of the alloys already discussed, only gold-chromium has the inflection point in the neighborhood of ordinary room temperatures, the others having small slopes because of use near the point of maximum resistance. None of these have small coefficients over a very large temperature interval.

Alloys of nickel and chromium are commercially available that have practically linear temperature-resistance curves over an interval of several hundred degrees centigrade, which interval includes ordinary atmospheric temperatures. Although the temperature coefficient is constant, it is too large for use in apparatus where the highest accuracy is required. Recent attempts to reduce the coefficients of these alloys by the addition of comparatively small amounts of other materials, such as copper and aluminum, appear very promising. It is quite possible that an alloy and heat treatment will be developed such that no correction for temperature will need be made, at least throughout the range of laboratory temperatures.

2. Spools, Winding and Adjustment

In the beginning of the electrical instrument industry, wire coils were wound on wooden spools

like those that are still used for thread. However, because of the demand for increased accuracy, these wooden spools have been entirely replaced by metal spools for resistors of high quality. The reason for the change to metal has been twofold. In the first place, the wooden spools absorb moisture in amounts dependent upon the humidity in the air, and expand or contract therefrom. This results in varying stresses applied to the wire, with accompanying changes in resistance.

A more important reason for the use of metal spools is the fact that they more readily dissipate the heat produced in a coil by the passage of the current. The wire is wound in rather intimate thermal contact with the metal spools, and the heat is readily transferred to the spools. The entire surface of the spools, both inside and outside, is effective in dissipating heat to the surrounding air. However, for wooden spools the area that is effective in dissipating heat is largely the exposed outer surface of the resistance wires. When metal spools are used, the temperature rise for a given heat dissipation depends primarily upon the size of the spool and only to a minor extent upon the size of the wire. However, the wire size should be selected so as to cover the spool as completely as possible, and if necessary the turns should be spaced to prevent bunching of the coil at one end of the spool.

For many alternating-current applications, the use of metal spools is undesirable or even out of the question. For such applications, when wire-wound coils are required, wooden spools may be used, although for these purposes ceramic spools have come into rather general use. The objections to ceramic spools for resistors of high precision are their poor heat conductivity and the fact that their temperature coefficients of linear expansion are very much smaller than for the resistance wire.

Metal spools are ordinarily of brass, which has a coefficient of thermal expansion nearly the same as that of the resistance alloys. This avoids large changes in stress in the coils because of temperature changes. The spools are ordinarily mounted with their axes vertical, and both ends should be left at least partially open in order to allow a ready flow of convection currents of air through the spools. Before being wound, the spools are enameled or covered with a single layer of silk, which is impregnated with shellac varnish and allowed to air dry.

The resistance wire is generally double-silk or silk and cotton covered, and often the wire is enameled before these coatings are applied. The correct length of resistance wire is cut, doubled at its center, and the center is attached by means of a thread near one end of the insulated metal spool. The two halves are then wound side-by-side (bifilarly) after which the free ends are tied down with silk thread.

High-quality resistors are wound with only one layer of wire. Although this requires the use of smaller wire than for multilayer coils, there are several advantages. In the first place, the heat dissipation is more satisfactory for a single-layer coil, since a considerable temperature rise may be obtained in the center of a multilayer coil as a result of the passage of the current through the coil, and the load coefficients are usually large. Moreover, multilayer coils are more subject to change in resistance because of changes in atmospheric humidity (see section II, 6), and are usually found to be less stable in resistance with time.

After being wound, the coils are artificially aged by baking in air at about 150° C for 48 hours, after which they are kept for a considerable period of time before final adjustment. Some manufacturers impregnate coils before baking with a shellac varnish, while others impregnate them after baking with special waxes. The final adjustment is usually accomplished in two steps. The excess wire is cut off in order to make the resistance just slightly less than the nominal value. Copper lead-wires, which are usually somewhat larger in diameter than the resistance wire, are then silver-soldered to the ends of the coil. Final adjustment is made by filing or scraping the resistance wire near the end, care being taken to see that the metal cuttings are not forced into the insulation. Any filed part is finally painted with shellac varnish, which is allowed to air dry. For coils of the highest precision the interval between baking and final adjustment should be as long as practicable, an entire year being desirable.

3. Sheet-Metal Resistors

Precision resistors having values of 0.1 ohm or below are usually made of sheet manganin brazed or silver-soldered to heavy copper terminal posts.

Potential leads are attached as shown in figure 2. Here C and C are copper rods, with binding posts at the top, attached to the sheet of resistance material, S. The resistance material may be a single sheet of manganin or several sheets in parallel. The sheets are often not straight but are bent in an S-shape in order that greater lengths can be used. Additional binding posts P, P are used as potential terminals and are connected by copper wires soldered at some point on the copper terminal bars. For a resistor of this type the resistance is measured between the two branch points. This is to say, the resistance is equal to the ratio of the potential difference between the potential terminals P, P to the current flowing in and out the current terminals C, C. For standards, sheet-metal resistors are mounted in perforated containers with hard rubber or bakelite tops. These are often used in oil baths in order to facilitate the dissipation of the heat

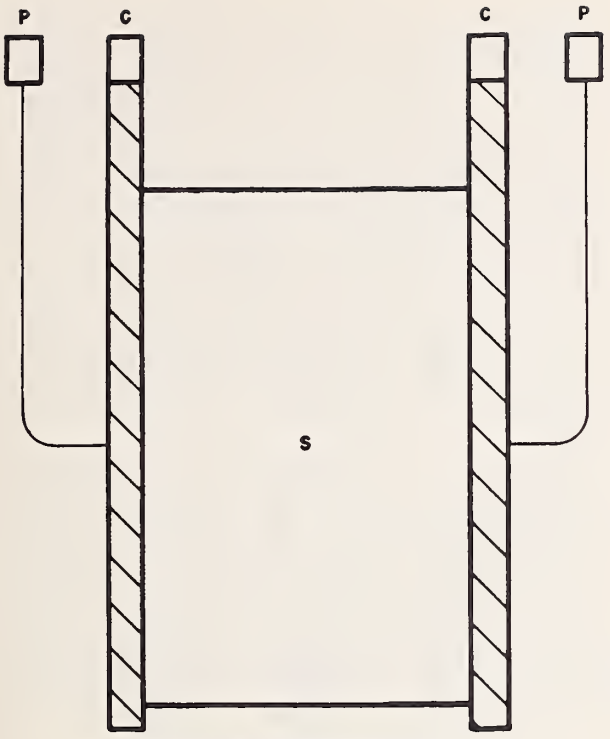

FIGURE 2. *Sheet-metal resistor.*

caused by the flow of current through the resistance element.

An accelerated aging of these resistors is obtained by heating in air at 150° C for 48 hours, as is done for wire-wound resistors. Final adjustment of the resistance may be accomplished by changing the points of attachment of the potential leads, the resistance decreasing as the points of attachment are lowered. Increases in resistance may be obtained by scraping or by drilling holes in the resistance material. Small changes can be obtained by filing the copper current posts, but the direction of the change is dependent upon the location of the potential leads.

Adjustment of sheet metal resistors is often accomplished by making U-shaped saw cuts in the sheet, with the open ends of the U's pointing in the direction of flow of the current. The U-shaped tabs so formed are bent outward and to them are attached the potential leads. Adjustment is made by increasing the length of the U cut. Lengthening one cut will increase the four-terminal resistance, whereas lengthening the other cut will decrease the resistance.

Not only may the resistance of a four-terminal resistor of the type shown be altered by changes in the points of attachment of the potential leads, but it is possible to change the temperature coefficient of resistance in the same way. In fact, the temperature coefficient is lowered at the same time as the resistance if the points of attachment are lowered on the current posts [6]. This effect is large when the resistance of the copper terminal posts is high in proportion to that of the resistance element. For standards of very low resistance, large temperature coefficients may result unless the potential branch points are carefully located.

4. Accelerated Aging

After being wound, resistance coils are impregnated with a shellac varnish and given an accelerated aging by baking. The temperature for baking is limited by the silk insulation, which should not be heated above about 150° C, and the coils are usually baked at this temperature for 48 hours. As a result of the baking the resistance of a coil may decrease, sometimes as much as 1 or 2 percent, and a sufficient length of wire must be used to compensate for this change. After being baked, the resistance of the coils is much more stable with time than is that of unbaked coils. This aging process is often called "annealing", but it is doubtful that the improvement in stability results from the relieving of internal stresses in the wire, as happens during true annealing. In the two or three months immediately following their baking, resistance coils will ordinarily increase in resistance by an amount that is usually of the order of 0.01 percent. They then are ready for final adjustment.

Sheet-metal resistors are usually painted with a lacquer or shellac varnish as a protection of the surface. This coating limits the temperature to which these resistors can be raised during aging, and they are usually treated in the same way as insulated wire-wound coils, being baked at 150° C for 48 hours. Sheet resistors may be heated at high temperatures before being lacquered, but such treatment is apparently no improvement over baking at 150° C, as far as subsequent stability is concerned.

5. Annealed Resistors

As has already been stated, the usual baking of wire-wound and sheet-metal resistors is not done at a sufficiently high temperature to anneal the resistance material. As baking at 150° C improves the stability with time, it would be logical to expect greater stability if the heating were carried on at a sufficiently high temperature to obtain actual annealing. In the case of manganin this takes place between 500° and 600° C.

The annealing of metal is a complicated process, but the first step is probably a reforming of the metallic crystals to the shape they had before being cold-worked. This results in the relieving of many of the internal stresses that resulted from the distortions of the crystals. The amount of this restoration of the metal to its preworked condition depends upon both the annealing tem-

perature and the time. In general, the higher the temperature the shorter the time required for a given annealing. If the annealing is continued after crystals have been restored to their original condition, there may result an actual uniting of adjacent crystals, with an accompanying decrease in the mechanical strength of the material.

For base-metal alloys, annealing should take place in a vacuum or in an inert atmosphere to avoid a reaction between the metal and the surrounding air. Such reaction might take place inside the metal at the intercrystalline boundaries as well as at the surface of the metal. These reactions do not necessarily decrease the stability of resistance with time if the products are stable. There may, however, be a selective reaction that makes the material inhomogeneous, and this might have a considerable effect on the resistivity and temperature coefficients.

When a resistor is made by winding wire on a spool, the wire usually will not straighten if it is removed from the spool. This means that parts of the wire have been stressed past their elastic limit and a permanent deformation has taken place. For such a bent wire the portions farthest from the center of the spool have been elongated past their elastic limit, while the filaments nearest the center of the spool have been compressed beyond the elastic limit. Intermediate filaments are subjected to stresses that depend upon the changes in their length, which resulted from the bending. The stress distribution is from a maximum in tension to zero and then to a maximum in compression. These stresses are superimposed upon the stresses that were produced in the wire as it was being fabricated.

These internal stresses in a wire result in a slight change in the shape of its cross section. In addition to this change there is a change in resistivity, which results from the presence of the stress [7]. The resistivity is therefore not uniform across the wire, and the difference between parts of the wire may amount to nearly 1 percent in the case of manganin, and perhaps more for other alloys. Although the resistivity changes considerably when a wire is bent, there is not necessarily much change in resistance, as the change in resistance of the parts under compression may compensate for the change in the parts under tension.

The effect of annealing of a coil of wire is to reduce the internal stresses, thus making the resistivity more nearly uniform in the wire. It is probable that a slow annealing takes place at room temperatures, and the accompanying reduction in the internal stresses may be one reason for the change with time of the resistance of a coil of wire. Another cause for change might well be some reaction between the wire and the surrounding atmosphere. Both of these sources of instability would be avoided or reduced if a coil were annealed and mounted in a vacuum.

Annealed resistors mounted in vacuo have been tested at the National Bureau of Standards and found to be very stable. It is difficult, however, to seal the coils in suitable containers for high evacuation. Equally good results have been obtained with annealed coils mounted in sealed metal containers filled with dry air. Whatever the effect of the air, an equilibrium condition is soon obtained when the supply of air is limited. Probably the most stable resistors that have been made are a group of annealed 1-ohm manganin resistors mounted in double-walled air-filled containers, now being used at the National Bureau of Standards [8] for maintenance of the unit of resistance.

Although good annealing improves the stability of sealed resistors, it is apparently of no special value for unsealed coils. When mounted in open containers, annealed resistors cannot be expected to be any better than, if as good as, those baked at 150° C. This is true even if the resistors are varnished or enameled after the annealing. None of these coatings is impervious to the atmosphere, and they merely retard any reaction between the air and the resistance material.

6. Effects of Humidity

It has long been known that wire-wound resistors undergo seasonal variations in resistance, being higher in resistance in summer and lower in winter. This effect is most noticeable in high resistance coils of small wire, and even in high-grade resistors may amount to several hundredths of a percent of the resistance. The effect is to a large extent a result of changes in average humidity, and is greatest in climates where there is a large difference in humidity between winter and summer. This seasonal change was first observed in the case of manganin resistors made with silk-covered wire. The accepted explanation was that the resistance changes resulted from dimensional changes of the shellac with which the coils were impregnated, as the shellac absorbed or gave off water vapor.

The effect of moisture on resistors has been thoroughly investigated by Dike [9], who came to the conclusion that the effect of changes in humidity is to change the tension in the silk with which the wire is customarily insulated. This change in tension changes the pressure transmitted to the wire by the insulation and hence changes the resistance. He also found that the effect of humidity on cotton insulation is opposite to that on silk, and by using a mixture of cotton and silk fibres for insulating the wire he was able to eliminate most of the seasonal changes in resistance that result from changes in humidity.

For standard resistors the effect of humidity

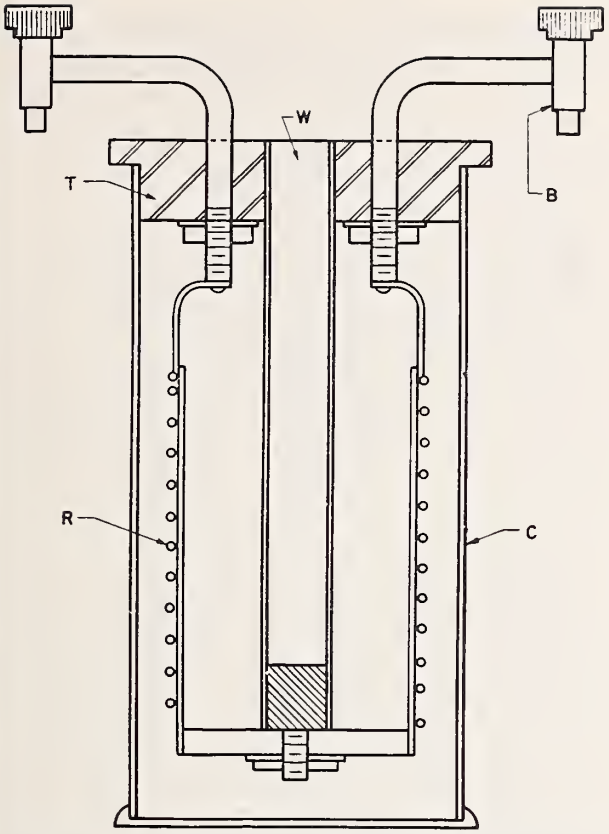

FIGURE 3. *National Bureau of Standards standard resistor.*

may be also eliminated by mounting the coils in sealed containers. This procedure was first advocated by Rosa [10] who designed the resistor shown in figure 3, known as the NBS type of standard resistor. In this figure, R represents the manganin coil mounted on a silk-insulated brass spool and baked as described in section II, 4. This coil is supported from the hard-rubber top, T, by means of the thermometer tube, W, which is so arranged that a thermometer can be inserted from the outside. The copper lead wires, which are silver-soldered to the ends of the resistance coil, are in turn soft-soldered to the copper binding posts, B. The hard-rubber top is screwed into the metal container, C, which is filled with a good quality light mineral oil. The binding posts, thermometer well and the threads by which the hard-rubber top is connected to the container are all sealed with shellac, which is not soluble in oil.

The purpose of the oil is to give good thermal contact between the resistor and the case and to facilitate the dissipation of the heat developed in the resistor by the current through it. In addition, the oil in effect increases the heat capacity of the resistor, thus increasing the current that it can carry temporarily without overheating. The objection to the oil is the fact that it may in time become somewhat acid, and the acid may corrode the resistance wire or injure the insulation.

The advantage of ready dissipation of heat combined with the advantage of hermetic sealing is found in the double-walled type of standard resistor [8] developed at the Bureau. In this type the container is made of coaxial cylinders only slightly different in diameter with the space between the cylinders sealed. The resistance element is mounted in this sealed space in good thermal contact with the smaller cylinder, which serves as the inside wall of the container. One of these resistors is shown in figure 4. The outside diameter of the container is 9 cm and its length 13 cm. The series of holes near the top are just above the double-walled part and are intended to increase the facilities for cooling, and the containers are left open at the bottom for the same purpose. These double-walled resistors readily give up heat to an oil bath yet are not affected by humidity changes. The sealed space in which the coil is mounted is filled with dry air, and no oil comes in contact with the resistance material.

The seasonal changes in resistance of standard resistors that arise from changes in humidity are readily eliminated, as has just been discussed, by sealing in metal containers. This arrangement is not satisfactory for large instruments and measuring apparatus, which are not readily sealed. If the cases of such equipment are reasonably tight a drier, such as calcium chloride, may be kept inside the case. This procedure is somewhat hazardous, since if not replaced with a sufficient frequency the drier may become dissolved in

FIGURE 4. *Double-walled standard resistor.*

adsorbed water and be spilled on the coils. The use of silica gel avoids this danger. A more satisfactory method is to mount a heater in the apparatus and, by means of a thermostat, maintain the temperature of a metal box containing important resistors at a constant value, above that of the laboratory. In this way the relative humidity is kept always low and seasonal variations may be reduced. Additional advantages are that no temperature corrections need be applied when calibration is made under conditions of use, and that resistors will usually be more stable in resistance if kept at a constant temperature instead of being allowed to follow variations in laboratory temperatures.

7. Load Coefficients

The load coefficient of a resistor is defined as the proportional change in resistance caused by the production of heat in the resistor at the rate of one watt. This change, however, is a function of time. When a current starts flowing in a wire-wound resistor the wire very quickly takes up a temperature above that of the spool on which the wire is mounted. The amount of this change depends upon the thermal contact between the wire and the spool. If the current continues to flow, this initial difference in temperature is maintained, but the coil and spool continue to rise in temperature together. The maximum temperature that will then be attained depends upon the facilities for dissipation of heat by the spool, and often upon the facilities for cooling the material to which heat from the spool flows.

Suppose we have a standard resistor of the NBS type resting on a table and we send through it a sufficient current to liberate one watt in the coil. Within about 30 seconds the temperature of the coil will rise to a steady value about 1° C above that of its spool. Spool and coil will then continue to rise in temperature at the rate of about 10° or 15° C per hour, and if allowed to continue will in about 2 hours reach a steady temperature of some 10° to 20° C above that of the room. This may cause a permanent change in resistance, which, however, ordinarily amounts to only a few parts in a million. If, instead of being mounted in an oil-filled container, the same resistor had been left open in the air of the room, its final rise in temperature would probably have been less by some 50 percent and would have been reached in 15 to 20 minutes.

The rise in temperature of the resistance coil will be accompanied by a change in resistance, whose amount depends upon the temperature coefficient of resistance of the wire and also upon changes in stress in the wire because of dimensional changes of the coil and its support. For single-layer manganin coils mounted on brass spools the relative changes in dimensions are small, and the change in resistance results primarily from temperature changes of resistivity. For such resistors the effect of the heating may usually be taken into account by measuring the temperature change and calculating the change in resistance from the temperature coefficients of the resistor. For sheet-metal resistors the effect of stress changes may be important and the calculated change cannot be relied upon.

It should be evident from the above discussion that the load coefficient of a resistor is a rather indefinite quantity, varying with time of flow of the current and with the environment of the resistor. To be of value it should be measured under conditions of use. Measurement is usually made by passing the desired current through the resistor and a second resistor connected in series, measuring the ratio of resistance both with negligible and with the required heating. This ratio may be measured by means of a bridge or a potentiometer, and the comparison resistor should be one that is not appreciably affected by the test current. A resistor of one-tenth or less the resistance of that under test should be used, and its load will be one-tenth or less than for the resistor under test. For the reference lower-valued resistor one that is known to have a small load coefficient should be chosen. If such a resistor is not available one with a low temperature coefficient should be selected, on the assumption that its load coefficient is correspondingly low, and its load coefficient should be roughly determined to make sure that it is small. This can be done by balancing the resistor in any bridge using a small test current. From an external source a large current is then sent through the resistor under test for several minutes, after which the extra circuit is disconnected and the bridge circuit is again balanced. This last balance must be made quickly before the heat from the large current is dissipated.

If a resistor is being used under conditions where the load changes its resistance, the amount of the change may often be determined experimentally. To do this the heating may be doubled, by increasing the current by 40 percent, and the resulting change noted. To a first approximation this doubling of the heating doubles the change in resistance, and twice the change should be subtracted algebraically from the final value. Such a procedure is especially satisfactory in the case of Wheatstone bridges, as the procedure will correct back to zero test current, whichever branch or branches are being changed by the current.

8. Stability of Resistors With Time

In applications where stability with time is of importance, as for instance for standard resistors or precision measuring apparatus, manganin is used almost exclusively. In such applications low temperature coefficients of resistance and small thermal emf's against copper are usually also required,

and few alloys other than manganin are suitable. Consequently, a discussion of the stability of resistors is largely a discussion of the stability of manganin.

Most national standardizing laboratories keep a selected group of manganin resistors, which are regularly intercompared and used for maintenance of the unit of resistance. The relative values of such standards are remarkably constant, the individual resistances not changing by more than one or two parts in a million per year with reference to one another and for some groups very much less. It is supposed that the average of a group remains constant to a high degree, but such stability can be only assumed. No method of measurement has been used that would detect with certainty changes of less than 10 or 20 parts in a million in the group as a whole. The international ohm was defined as the resistance of a mercury column of specified dimensions at the temperature of melting ice. However, such resistors have not been constructed with sufficient accuracy to demonstrate the performance of manganin resistors used to maintain the unit. Likewise, absolute ohm determinations have not been sufficiently reproducible to give such information. If the unit as maintained by means of manganin resistors were tested every ten years by comparing against mercury ohm or absolute ohm determinations, the apparent change would probably not exceed 10 or 20 parts per million. This could be just as well attributed to errors in realizing the unit experimentally as to changes in the unit as maintained by the manganin resistors.

The average user of standard resistors is interested in the stability that may be expected from standards available commercially. In this connection, an analysis made in 1941 at this Bureau is relevant. Of nearly 600 standard resistors that had been submitted more than once to this Bureau for test, the average yearly change in resistance, without regard to sign, was found to be 8 ppm. Of the total only 2 percent averaged greater than 60 ppm per year, and for nearly 90 percent of all standards tested the annual change was 10 ppm or less. If signs were neglected there was no significant difference between the average yearly change of sealed and unsealed resistors. This would appear to mean that sealing merely reduces seasonal variations without improving the long-time stability. However, if regard is taken of sign, the performance of sealed and unsealed resistors was quite different. In this case the average yearly change was about $-.3$ ppm for sealed and about $+5$ ppm for unsealed standards. That is to say, sealed standards about as often decrease as increase in resistance with time, whereas the change in unsealed standard resistors is predominantly upward. In connection with the sealed resistors it is interesting to note that practically the same result would have been obtained if the unit of resistance had been maintained by supposing the average value of the 400 sealed resistors had remained constant, as was obtained by assuming the average of a group of 10 selected resistors of special construction to be constant.

III. Methods of Comparison of Resistors

1. Ammeter-Voltmeter Methods

Precise measurements of electrical resistance are made with comparative ease with bridge methods, an accuracy of a few parts in a million being readily obtained in the comparison of nominally equal resistances of say 10 or 100 ohms. Although the actual measurements are rather simple, special apparatus is required. For many types of resistors high accuracy is not desired and the measurements may be made with deflecting instruments, which are usually available in electrical laboratories. The most common method, where an accuracy of 1 or 2 percent is sufficient, is the ammeter-voltmeter method. In this method a measured current is passed through the resistor under test, and the potential difference across its terminals is also measured. The current is measured with an ammeter and the potential difference by means of a voltmeter, the resistance in ohms being the ratio of the voltmeter reading in volts to the ammeter reading in amperes, in accordance with Ohm's Law.

The accuracy that may be attained by the ammeter-voltmeter method depends upon the accuracy of the two instruments. However, there are a few precautions that must be observed. Referring to figure 5, if the voltmeter, V, is connected as shown across the resistor, R, the current read by the ammeter, A, is the sum of the current through R and the current through the voltmeter. If the resistance of the voltmeter is large as compared with R, the current through the voltmeter

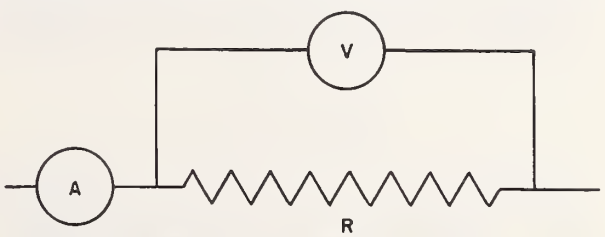

FIGURE 5. *Connection for ammeter-voltmeter measurement of resistance.*

may be neglected and R may be calculated as the ratio of the instrument readings. If the resistance of the voltmeter is not large as compared with R, the latter may be calculated from the equation

$$R=\frac{E}{I(1-E/IR_v)} \tag{5}$$

where R_v is the resistance of the voltmeter, its reading being E volts, and the ammeter reading I amperes. If the resistance of the ammeter is known or if it is negligible as compared with the unknown resistance, the voltmeter may be connected across both the resistance and the ammeter, as shown in figure 6. In this case the ratio of

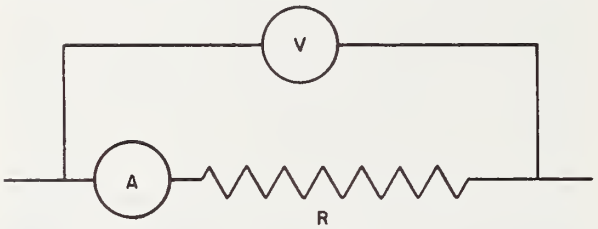

FIGURE 6. *Alternate connection for ammeter-voltmeter measurement of resistance.*

voltmeter to ammeter readings gives the total resistance between the points of attachment of the voltmeter, that is, the resistance of the ammeter and of the connecting leads is included. That is

$$R=\frac{E}{I}-R_A, \tag{6}$$

where R_A is the resistance of the ammeter and of all lead wires between the points of attachment of the voltmeter leads.

With suitably calibrated instruments it is possible to measure resistance to 0.1 or 0.2 percent provided the instruments are of such ranges that large deflections are obtained. For this accuracy it is usually necessary to calibrate the voltmeter with the same leads as those that are to be used in the resistance measurements.

2. Ohmmeters

Ohmmeters are instruments for indicating directly on a scale, with a minimum of manipulation or computation, the resistance of the circuit connected across their terminals. They are available in a wide range from milliohmmeters reading to 0.001 ohm to megohmmeters reading to 50,000 megohms. Their accuracy is limited both by the calibration and reading of the indicating instrument and in the simple ohmmeter by their dependence upon a fixed value of voltage. They are, therefore, in general, not suited for applications requiring high precision such as the determination of temperature rise or of the conductivity of line conductors. When used with circuits that are highly inductive or capacitive, the precautions appropriate for such resistance measurements should be observed.

Ohmmeters may be classified according to either their principles of operation, their source of energy, or their range.

The principles commonly used are: Simple ohmmeter, ratio ohmmeter, Wheatstone bridge.

In the simple ohmmeter a source, the voltage of which is assumed to be definite and to correspond to the calibration of the instrument, is applied to the unknown resistor and the resulting current causes an indicating instrument to deflect over a scale. This scale is so graduated that the pointer indicates directly the resistance in ohms (or megohms). In many cases provision is made by a magnetic or electric shunt to adjust the instrument at one point, usually at zero resistance, to fit the existing value of the voltage. In some of these instruments the final indication is by a vacuum-tube voltmeter, which measures the drop produced in a very high resistance by the current through the specimen.

In the ratio meter or "crossed-coil" type of ohmmeter, the current through the unknown resistor flows in one of the coils, while the other carries a current that is proportional to the voltage. The current is led to the coils by ligaments, which exert a negligible torque so that the moving system takes up a position that depends on the relative magnitude of the currents in the two coils. The scale can therefore be laid off to indicate resistance directly, and the indication will be independent of the voltage used, provided that the resistor under test obeys Ohm's Law.

The designation "ohmmeter" is also applied (though perhaps incorrectly) to certain forms of the Wheatstone bridge in which the dial that adjusts the balance is calibrated to read directly the value of the unknown resistance.

3. Potentiometer Method

It was pointed out in section III,1 that the ammeter-voltmeter method for measuring resistance is complicated by the current drawn by the voltmeter. Such complications may be avoided by using a voltmeter of some type that requires no current from the circuit being measured, i. e., electrostatic or vacuum tube voltmeters.

Potentiometers are also suitable for the measurement of potential difference when it is desired to avoid drawing a current from the source of potential difference. They are especially good in cases where an accuracy of 0.1 percent or better is required, as such accuracy is difficult to attain with deflecting instruments. Where a potentiometer is available, the ammeter-voltmeter method may

be modified so as to use the potentiometer to measure the current through the unknown resistor as well as the potential difference across it. This requires the replacement of the ammeter with a standard resistor, and the measurement of the potential difference across the standard resistor yields the value of the current if this potential difference is divided by the value of the resistance of the standard.

Actually, if a suitable standard resistor is available, it is unnecessary to calculate the current through the unknown resistor. If the same current flows through the known and the unknown resistor, the ratio of the potential differences across the two is the same as the ratio of the resistances. Hence

$$X = S\frac{V_x}{V_s}, \tag{7}$$

where X and S are the values of the unknown and standard resistances, V_x and V_s are the measured potential differences across X and S respectively. Care must be exercised in using this method to insure that the current through X and S remains constant during measurement. This may be verified by measuring the potential differences alternately several times.

High accuracy in the measurement of resistance can be attained with the potentiometer method if a good potentiometer and good standard resistors are used. It has an advantage over the ordinary Wheatstone bridge in that the resistance in terms of which the unknown is measured may be that of an actual standard resistor instead of one of the coils of the bridge. Standard resistors are so mounted that they are ordinarily more constant in resistance and hence more accurately known than are unsealed coils usually used in bridges. The potentiometer method, however, is more difficult to use as the currents through the potentiometer and in the measuring circuit must both be kept constant, whereas the balance of a Wheatstone bridge is independent of the current flowing through it. In comparing resistors, the accuracy of a potentiometer is not dependent upon the accuracy of calibration of the standard cell used with the instrument.

A type of measurement for which the potentiometer method is especially well suited is for the measurement of four-terminal resistors, which are parts of complicated networks, where connections to the resistors must be made through other resistors. The resistances in the potential leads, which connect to the potentiometer, have no effect upon the balance of the potentiometer. There may be, however, a reduction in sensitivity unless the damping resistor for the galvanometer may be changed to allow for these extra resistances.

4. Differential-Galvanometer Method

The differential galvanometer was formerly used rather extensively for the comparison of equal resistances. Such a galvanometer has two separate windings made as nearly the same as possible, so that when equal emf's are applied to the terminals of the windings, equal and opposite torques are produced on the deflecting element. The windings are constructed with two wires side-by-side, wound at the same time and as nearly as possible symmetrically with respect to the magnetic circuit.

For the moving-magnet galvanometer the field coils are wound in duplicate, and a small movable coil is usually connected in series with one winding. This moving coil is adjusted in position to compensate for any lack of equality of the fields produced by the two windings. Unfortunately this adjustment is different for different conditions of use. Moreover the differential galvanometer of the moving-magnet type has the same handicaps as others of the moving-magnet type. That is to say, the damping is difficult to control and elaborate precautions must be taken to avoid magnetic disturbances from external sources.

Many of the troubles of the moving-magnet galvanometer are avoided in the D'Arsonval, or moving-coil galvanometer, and this coil may be made in duplicate for differential use. However, this requires two sets of leads from the moving element, which are difficult to arrange, and which also in effect stiffen the suspensions and lower the sensitivity. With the need for greater and greater precision, the differential galvanometer has been gradually discarded, but it still is very satisfactory for some types of measurements.

In theory, the use of the differential galvanometer is very simple. A current, I, is passed through the standard, S, and the unknown, X, connected in series, and one winding, G, of the galvanometer is connected to the terminals of each resistor, as shown in figure 7. If the galvanometer circuits were exactly alike in resistance and opposite in their magnetic effects there would be no deflection if X and S were equal. These conditions on resistance and magnetic effect are difficult to

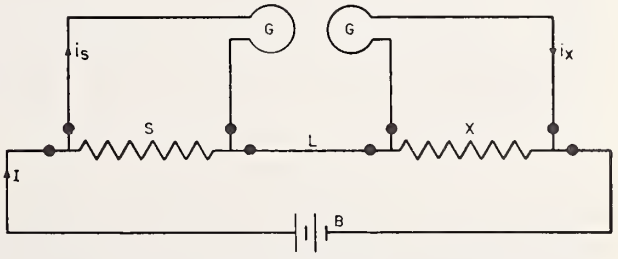

FIGURE 7. *Connections of differential galvanometer.*

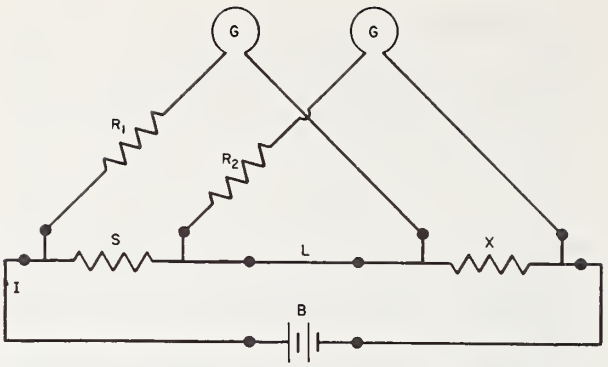

FIGURE 8. *Kohlrausch's connection of differential galvanometer.*

meet, and it is necessary to devise methods of use for which the conditions need be only approximately met, if high accuracy is to be attained. Such is that due to Kohlrausch [11], and known as his method of overlapping shunts.

For Kohlrausch's method the circuit is as shown in figure 8. The two galvanometer windings, G, are connected respectively across X and S, and in addition each shunt bridges the resistance, L, which is used to connect X and S in series. The resistance of L is usually small as compared with the other resistances. In series with the galvanometer windings are connected the resistors, R_1 and R_2, one or both of which are adjustable. In addition, a special switch not shown must be used, which will interchange the battery B and the lead resistance L. This must be done without materially changing the current furnished by the battery. The effect of the interchange is to reverse the current through both galvanometer windings. The values of the adjustable standard, S, and the rheostat, R_1 or R_2, are adjusted until there is no deflection of the galvanometer for either position of the battery, or until the deflection is the same in magnitude and direction for both battery positions. Under either condition of adjustment, S and X are equal.

In actual practice, where S and X are standard resistors under comparison, the larger is made adjustable by a precision rheostat connected in parallel, and the amount of the shunt required to make X and S equal allows an easy calculation of the difference in resistance between the two. The balance is exact even if the two circuits of the galvanometer are not exactly alike electrically or magnetically.

5. Bridge Methods

By far the largest proportion of measurements of electrical resistance are made by means of bridge methods. For resistors above 1 ohm the simple Wheatstone bridge is used, whereas for 1-ohm resistors and below the Kelvin double-bridge is more suitable. The choice between the simple and the double bridge is usually made on the basis of the required accuracy.

It is difficult to attach a copper lead wire to a resistor by means of binding posts or other clamped connections without introducing an unknown contact resistance of the order of 0.0001 ohm. For resistors above 1 ohm such an uncertainty is usually negligible, whereas for a resistor of say 0.01 ohm the uncertainty is 1 percent. For standard resistors the contact resistance is often reduced by amalgamating the contact surfaces. For clean well-fitted contacts the resistance then amounts to only a few microhms, but the resistance of such contacts will rise with time as the copper combines with the mercury to form a granular material. This material should be removed every few months by scraping and wiping the surfaces.

Where accuracy is required, low-valued resistors are usually of the four-terminal type. For these, two leads are soldered or brazed to each end of the resistance material, as shown in figure 9. The

FIGURE 9. *Four-terminal resistor.*

resistance in question is that between the branch points at the two ends. That is to say, the resistance is the ratio of the potential difference between the terminals P, P to the current flowing in and out the current terminals, C, C. Methods of measurement are used such that any effect from the lead resistances is avoided or reduced to a negligible amount. For such a purpose the potentiometer method is suitable as no appreciable current is drawn through the potential leads, and the potential drop between branch points is independent of the magnitude of the lead resistances in the current circuit. Double-bridge methods balance out the lead resistances or connect them in high-resistance branches where they are negligible.

Simple Wheatstone bridge.—The simple Wheatstone bridge is primarily a group of four resistors connected in series-parallel as shown in figure 10. A current, I, is passed through the two parallel branches, and G is a detector connected to the junctions of the resistors as shown. It may be readily shown that if there is no potential difference across the detector, G, the relation between the resistances of the four arms is as follows:

$$\frac{X}{S}=\frac{A}{B} \tag{8}$$

or

$$X=S\frac{A}{B} \tag{9}$$

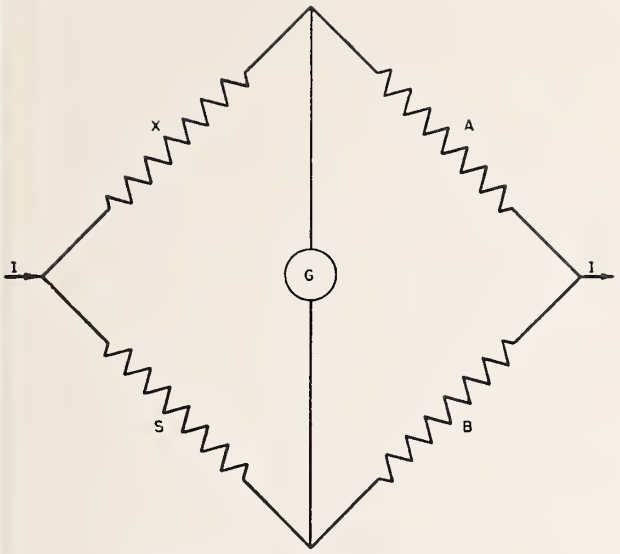

FIGURE 10. *Wheatstone bridge.*

The detector, G, is usually a galvanometer, and the lack of a potential difference across it is evidenced by a lack of motion of the galvanometer coil if a switch or key in series with G is opened or closed, or better, if the battery circuit is opened or closed. Opening or closing of the battery circuit should be avoided, however, if there is inductance or capacitance in the circuit of the unknown resistance or in any arm of the Wheatstone bridge. In measuring the resistance of a field winding of an electric motor, for example, the galvanometer may be damaged if its circuit is left closed and the battery circuit of the bridge is opened. In this case the current should be left on until a steady state is reached before testing the bridge balance by opening and closing the galvanometer circuit.

From the above equation it is evident that the resistance of any one of the four arms, say X, can be calculated if the resistances of the other three are known, or if one of the three and the ratio of the other two are known. The usual general purpose Wheatstone bridge is made in such a way that any one of several known resistors may be selected for use as either A or B and hence their ratio may have any one of a number of values. S is then a known resistor whose value may be adjusted in small steps over a wide range of resistance.

In commercial instruments the ratio arms A and B are usually coils that are connected into the bridge by inserting suitable plugs. As there are resistances in these plug contacts, which may be rather variable, it is desirable to use relatively high values of resistance for A and B in order to reduce the uncertainty in the resistance of the ratio arms. On the other hand, high-resistance coils are more affected by humidity and are less stable in resistance with time and therefore retain their calibration for a shorter time. Other things being equal, ratio coils of from 10 to 100 ohms are therefore about the best compromise.

The choice of resistance for the adjustable arm of a Wheatstone bridge is influenced by the same factors as the choice of resistances for the ratio arms. That is to say, the lower the value the greater the stability in resistance but the more troublesome the contact resistances become, and in the adjustable arm several contact resistances are required. Steps smaller than 0.1 ohm, which allow readings of the adjustable arm to about 0.01 ohm by interpolation from galvanometer deflections, are seldom used as it is not wise to rely upon the combined effect of the several contacts of the arm to be definite to much better than 0.01 ohm.

Wheatstone bridges for the measurement of resistance to 0.1 percent are available commercially at moderate prices. To this accuracy these can usually be relied upon without the application of corrections to the readings. However, for measurements to 0.01 percent, corrections to the readings of the ratio arms and of the rheostat arm must usually be applied, and the bridge must be maintained at the temperature of calibration within a few degrees. Primarily because of the effects of changes in humidity, calibrations of a Wheatstone bridge must be made rather frequently if an accuracy of 0.01 percent is to be attained. This is especially true where there is a marked change in ambient conditions. For example, between winter and summer the ratio coils and the rheostat arm may each change by 0.01 percent or more, and the errors may be additive rather than compensating. The use of air-conditioned laboratories improves the performance markedly, but even then it is advisable to make occasional spot checks by measuring standard resistors. Whenever possible, ratio arms below 10 ohms or above 1,000 ohms should be avoided, as should rheostat readings in excess of 1,000 ohms. This means that the Wheatstone bridge is best suited for the measurement of resistance in the range 10 to 10,000 ohms.

When an accuracy greater than 0.01 percent is required, special bridges are required or special techniques are used. One of the best of the special methods is that of substitution, in which the unknown resistor is replaced with a standard resistor or resistors having the same nominal resistance as that of the unknown. The bridge that is being used is then relied upon to determine only the difference between the standard and the unknown, and this difference need not be accurately measured. If the unknown and standard differ by 0.1 percent, the difference need be determined to only 1 percent to give the unknown to 10 parts in a million in terms of the standard. Nearly any good bridge can be so used without calibration, provided contact resistances are sufficiently constant that readings can be repeated to the desired precision. It is evident that the calibration of the measuring

bridge is of least importance when the standard and unknown resistances are nearest equal. Standard resistors are usually available only in decimal multiples or submultiples of an ohm and for many resistance measurements the lack of a suitable standard prevents the use of the substitution method.

Mueller bridge.—For the accurate measurement of odd-sized resistances, one of the best bridges is that designed by E. F. Mueller [12] of the National Bureau of Standards for use in resistance thermometry. This is a special bridge intended for the accurate measurement of resistances up to about 110 ohms. The effects of humidity changes are greatly reduced by mounting the resistors in a compartment that is electrically heated and whose temperature is maintained at 35° C by means of a thermostat. As this is a temperature to which the laboratory temperature seldom rises, the relative humidity in the compartment housing the resistors is kept low and variations in the low humidities have little effect on the resistances of the coils.

For the Mueller bridge the ratio arms are equal, and the arms can be interchanged to test the equality. A small slide wire is connected between the ratio coils, and the sliding contact is used as the branch point for the bridge as shown in figure 11. The operator can set the ratio arms to equality by properly proportioning the resistance of the slide wire between the two ratio arms by changing

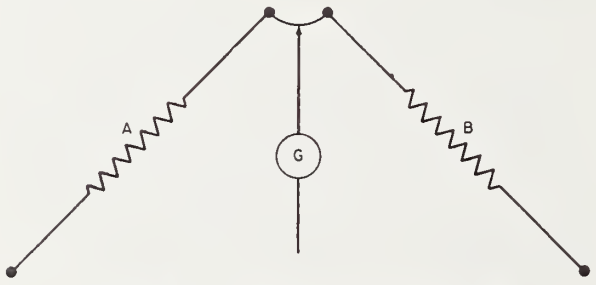

FIGURE 11. *Ratio arms of Mueller bridge.*

the setting of the slide contact. This setting is correct if no change in the bridge results when the arms A and B are interchanged. The remaining two arms are the adjustable rheostat and the unknown resistor, which must be of the four-terminal type. Resistance thermometers are usually of the four-lead type, and other resistors should be provided with four leads when they are to be measured on a bridge of this type. The method of connection of the unknown resistance is as shown in figure 12. R is the adjustable rheostat arm that will be discussed in detail later. X is a four-terminal resistor with lead wires L_1, L_2, L_3, and L_4 connected to the binding posts 1, 2, 3, and 4, respectively. If the galvanometer is connected to binding post 2,

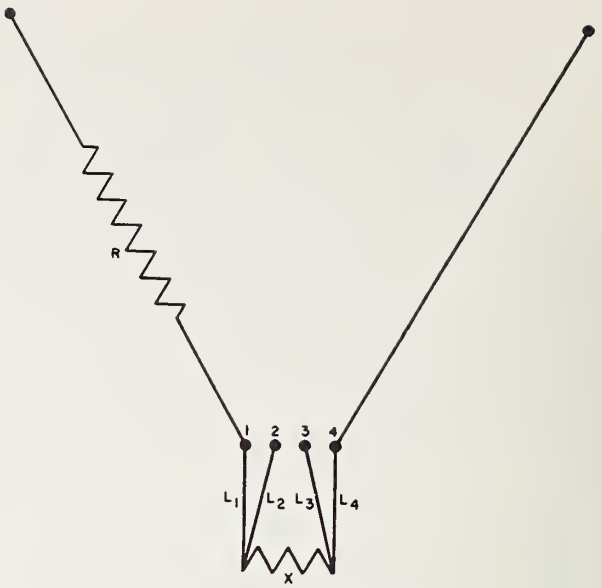

FIGURE 12. *Connection of bridge to 4-lead thermometer.*

the resistor X and the lead resistor L_4 are connected into the right-hand arm, and the lead resistor L_1 is in the adjustable arm, R. With equal ratio arms, R and X would be equal for a balance of the bridge only if L_1 and L_4 are equal. Instead of adjusting L_1 and L_4 to exact equality, their connections are interchanged and a second bridge balance is obtained, the average of the two balances being that which would be obtained with L_1 and L_4 equal. When L_1 and L_4 are interchanged, it is necessary to shift the branch point from lead 2 to lead 3 in order to keep X in the right-hand arm. In actual use, instead of the lead wires being interchanged, the internal connections of the bridge arms to the binding posts 1 and 4 are interchanged to obtain the same result. This interchange is effected by means of an amalgamated switch for which the uncertainty in contact resistance is only a few microhms.

The rheostat arm of the Mueller bridge is adjustable in steps as small as 0.0001 ohm. In order that such steps should not be masked by changes in contact resistance, special types [13] of decades are used. The 0.0001-ohm-per-step decade is approximately as shown in figure 13. With the

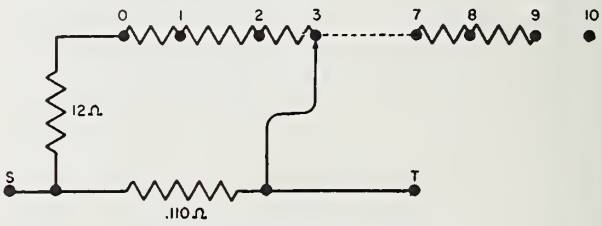

FIGURE 13. *Shunt-type decade.*

switch contact on the 0 stud, the resistances of 12 ohms and 0.110 ohm are connected in parallel, and the resistance between the terminals S and T is about 0.1090 ohm. When the switch contact is moved to stud 1, the 12-ohm branch is increased sufficiently to increase the parallel resistance from 0.1090 to 0.1091 ohm, an increase of 0.0001 ohm. Likewise when the switch is moved to 2 the parallel resistance increases to 0.1092 ohm, etc. Thus the resistance between the terminals S and T may be increased in steps of 0.0001 ohm, although the value is not zero when the switch is set to read zero.

The 0.001- and 0.01-ohm-per-step decades are made in the same way as the 0.0001-ohm decade. When these three decades are connected in series and all set to zero, there is a series resistance of about 1.6 ohms. However, since the bridge has equal ratio arms an equal resistance of 1.6 ohms may be included in the X-arm, and the value of X is measured by observing the increase in the resistance of the rheostat arm when X is inserted in its arm. A short-circuiting plug is provided with the bridge that connects together the terminals 1 and 4 of figure 12. The bridge is then balanced with and without this shorting plug, and the difference in the readings of the rheostat arm gives the resistance of X, and leads.

The purpose of the shunted type of decade that was described above is to reduce the effect of variations in contact resistances and transient emf's in the switch. Referring again to figure 13, it is seen that the switch contact is in the high resistance branch. The ratio of resistance for the two branches is about 100 to 1, and it may be readily shown by differentiation that the effect of a variation of switch contact resistance is reduced by the square of this ratio. Thus a contact variation as high as 0.01 ohm would vary the resistance from S to T by only 1 microhm, which is negligible in the rheostat arm where the minimum steps are 100 microhms. For the 0.001 and 0.01 decades, the ratio of currents in the branches is less than 100 to 1, and less variation in the switch-contact resistance can be tolerated.

The 1-ohm and 0.1-ohm steps of the rheostat arm are not made of the shunt type, as the resistance with the dial set on zero would be rather large. The contact resistances for the 1-ohm dial are thrown into the ratio arm A, as shown in figure 14. The bridge current is introduced through the 10 1-ohm coils of this decade, and the switch merely changes the point of connection of the ratio arm, without opening the circuit of the 1-ohm decade. In this case a variation of the switch contact resistance changes the resistance of ratio arm A. This effect is reduced by using high resistance ratio arms, A and B each being 1,000 ohms. The 0.1-ohm-per-step dial is arranged in the same way as the 1-ohm-per-step dial, with the switch contact in series with the B ratio arm. With the 0.1-ohm dial set at zero, all 10 of the

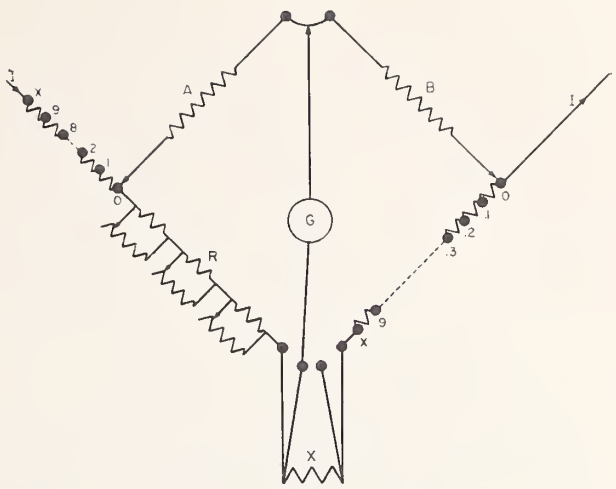

FIGURE 14. *Switch connections for Mueller bridge.*

0.1-ohm resistors are in series in the X-arm. When the dial reading is increased, the resistance is removed from the X-arm, the effect being the same as if equal resistance were added to the rheostat arm, R, since the bridge has equal arms. This may be seen from the following consideration. Assume that the bridge is balanced with the unknown resistor and the 10 steps of the 0.1-ohm dial all connected in the X-arm. If now X is increased by 0.1 ohm, the X- and R-arms may be brought again to equality by either increasing R by 0.1 ohm or by decreasing the resistance in series with X by 0.1 ohm. The readings of the dial in the X-arm are such that increases in readings of the dial correspond to decreases in the resistance in the X-arm.

The 10-ohm-per-step decade of the rheostat, not shown, is the only one that has contact resistances directly in series with the arm. A special type of dial that has amalgamated contacts is used for this purpose. Such contacts are uncertain by only a few microhms, which may be tolerated in the rheostat arm where the minimum steps are 100 microhms. For Mueller bridges available commercially, the galvanometer and battery are interchanged from the positions assumed in the above discussion. This in no way affects the validity of the conclusions.

Adjustable-ratio bridges. As has already been stated, the Wheatstone bridge shown in figure 10 is balanced if

$$X=S\frac{A}{B}, \tag{10}$$

and this balance may be realized by keeping A and B fixed and adjusting S, or by keeping S fixed and adjusting the ratio A/B. In most commercial Wheatstone bridges the balance is obtained with S. However, for comparing nominally equal resistances, bridges are sometimes constructed in which the ratio is adjustable.

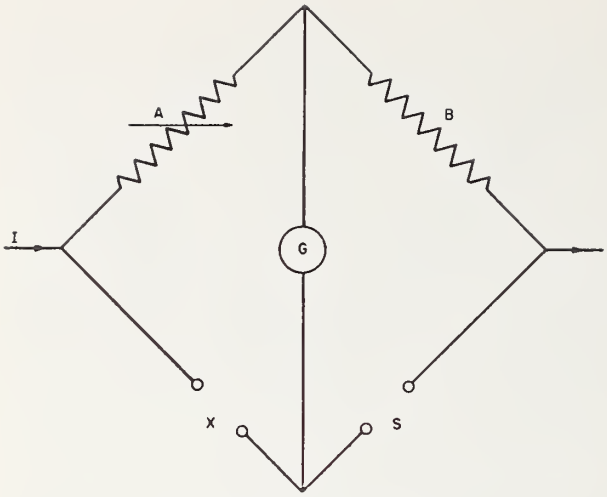

FIGURE 15. *Limit bridge.*

An adjustable-ratio bridge is very convenient for use in sorting large numbers of resistors that must be equal within given tolerances. Such a bridge may be constructed as shown in figure 15, where A and B are the two arms of a resistance ratio that is adjusted by changing A. A resistor is connected to the binding posts S, and the resistors that are to be compared with it are connected in turn to the X terminals. If the resistors are to be the same to, say, 0.1 percent, the arm A is made to have either of two values, which give ratios, A/B, of 0.999 or 1.001. This could be realized by making B 100 ohms and A either 99.9 ohms or 100.1 ohms, the latter accomplished, for instance, by making A equal to 100.1 ohms and having a plug to short-circuit 0.2 ohm of this total. The procedure is then to observe the direction of deflection of the galvanometer with either ratio setting and then change to the other ratio. If this causes a reversal of the direction of deflection of the galvanometer, the correct balance of the bridge is between the two ratio settings. In other words the ratio of X/S is between the two ratios 0.999 and 1.001, i. e., the two are equal within ± 0.1 percent.

Besides this use in limit bridges, adjustable ratio bridges may be used for precise measurements of resistors in terms of nominally equal standards. Such bridges when used in conjunction with the substitution method permit very accurate measurements of resistance. Such an adjustable ratio is the "direct-reading ratio set" described in section IV, 1, where the appropriate techniques are also discussed.

Kelvin double-bridge.—As has been already stated, four-terminal resistors are used in order to avoid uncertainties arising from variations in contact resistances. For precision work, resistors of 1 ohm or below are usually of the four-terminal type.

For measurement, a four-terminal resistor is usually connected in series with a four-terminal standard. The ratio of the potential differences across the two resistors is then determined when a current flows through the two. This ratio may be determined by means of a potentiometer or in terms of a resistance ratio by means of the Kelvin double-bridge.

The circuit of the Kelvin double bridge is shown in figure 16, where X and S denote the unknown and standard resistors, each with both current and potential terminals. The two are connected by means of a conductor L, preferably of low resistance as compared with X or S. The resistors A and B and also a and b provide resistance ratios that must be known, as must also be the value of S. This bridge is balanced if there is no change in the deflection of the galvanometer when the current circuit is opened or closed. When balanced the following relation holds between the values of the resistance:

$$X=S\frac{A}{B}+\frac{b\left(\frac{A}{B}-\frac{a}{b}\right)}{a+b+L}L. \qquad (11)$$

This equation would be exactly the same as that for a simple Wheatstone bridge if the last term on the right side were zero or negligibly small as compared with the term $S\,A/B$. That last term can be made zero by making $a/b=A/B$, irrespective of the value of the link resistance, L. However, the smaller the value of L, the less important is any lack of equality between the ratios A/B and a/b.

In actual use two methods are employed for balancing the double-bridge. The resistors A and B, and also a and b may be fixed ratio coils so chosen that $A/B=a/b$ and the bridge balanced by varying S, which is an appropriate adjustable standard; or S may be a fixed standard resistor and the bridge balanced by adjusting the ratios A/B and a/b, keeping these ratios at all times equal.

When a double-bridge is to be balanced by means

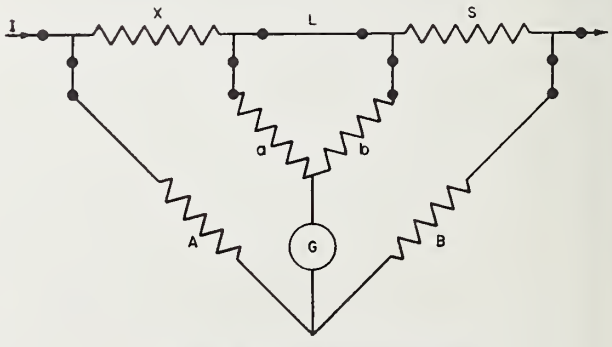

FIGURE 16. *Kelvin double-bridge.*

of an adjustable standard, care should be taken in connecting up such a standard in order to keep the resistance small between it and the unknown. Adjustable standards are usually made such that the position of one or both of the potential terminals is adjustable. As a result, varying amounts of resistance are left at the ends in series with the used part of the resistor. The adjustable standard should be connected in the circuit in the way that connects the larger part of unused resistance in the external circuit rather than between resistors so as to form part of the link resistance, L.

When a fixed standard is used for S, and the bridge is balanced by adjusting the ratios A/B and a/b, the most convenient arrangement is to have the ratios adjustable together. This is accomplished by having the same dial handle operate two dials together so that both ratios are changed simultaneously. This arrangement requires special apparatus, but such double-ratio sets are commercially available.

If not "ganged" together, the two ratios are changed separately but always by the same amount. Actually, however, it is not necessary to be able to adjust the auxiliary ratio, a/b, in known steps, and any convenient adjustable ratio, such as a slide wire, may be used. In this case the balance of the double bridge is by successive approximation. It is first balanced by adjusting the main ratio, A/B, after which the circuit is opened at the link, L, and a balance now obtained by varying the auxiliary ratio a/b. The link circuit is again closed and a new balance obtained with the main ratio. The procedure is repeated until the same balance is obtained with or without the link circuit's being open. Ordinarily the final balance is obtained after only a few sets of adjustments, and accurate results may be so attained. Since only one ratio need be known any apparatus having such a ratio, as for example a simple Wheatstone bridge, may be used in conjunction with a slide wire and a fixed standard resistor to make good measurements by the double-bridge method.

In work of the highest accuracy, account must be taken of the resistance of the leads that are used to connect the ratio arms to the unknown and standard resistors. There is also lead resistance in these resistors, between the branch points and the terminal binding posts, which is not necessarily negligible. One way of taking these lead resistances into account is to use such high resistances in the ratio arms that the connecting leads have a negligible effect. Usually, however, this reduces the sensitivity of balance of the bridge. A better arrangement is to make the lead resistances adjustable and select their ratio in such a way as to balance out their effects. A convenient method of adjusting the lead resistances is as follows: Referring to figure 17, the

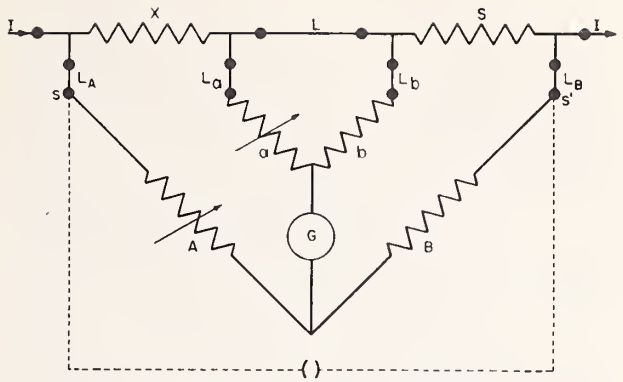

FIGURE 17. *Kelvin double-bridge.*

ratio A and B are such that their ratio is known only for the resistance between the two binding posts s and s'. The lead resistors L_A and L_B and the internal leads in X and S add to the resistance of A and B. This ordinarily prevents the ratio of the bridge arms from being the same as the known ratio of A to B. In other words

$$\frac{A+L_A}{B+L_B} \neq \frac{A}{B}, \tag{12}$$

except under the condition that L_A and L_B are respectively negligible as compared with A and B, or under the condition that the ratio of the leads is the same as the ratio of A to B. That is

$$\frac{A+L_A}{B+L_B} = \frac{A}{B}, \tag{13}$$

if

$$\frac{L_A}{L_B} = \frac{A}{B}. \tag{14}$$

If the lead resistances are small as compared with A and B, the second equation need be only approximately satisfied.

The same considerations apply to the lead resistance L_a and L_b in the auxiliary ratio arms. Their effect may be made negligible by making their ratio the same as the ratio a/b.

The following procedure for balancing the bridge and eliminating the effects of the leads by adjusting their ratio may be followed. Arrangement is made for readily opening and closing the circuit at L and for short-circuiting the main ratio arms by connecting together s and s'. Shorting s to s' is the equivalent of reducing A and B both to zero, leaving only the lead resistances in the arms. If the ratios are ganged and nominally equal, the bridge is balanced in the following steps:

1. With the circuit as shown, the ratios A/B and a/b are adjusted until the galvanometer indicates a balance. This gives

$$\frac{A+L_A}{B+L_B} = \frac{X}{S} \text{ approximately.} \tag{15}$$

2. The main ratio A/B is now short-circuited

and the bridge is again balanced, by changing the ratio of the lead resistances. This may be done by adjusting the length of one lead wire, or a small rheostat may be used in series with one of the leads. This step makes the ratio of the lead resistances the same as X/S and hence to a first approximation also to A/B.

3. The short is removed from the main ratio and the link opened. The bridge then becomes the simple Wheatstone bridge shown in figure 18. To a first approximation

$$X/S=A/B=a/b=L_A/L_B, \tag{16}$$

and the simple bridge is unbalanced only if the resistances of the leads L_a and L_b are not in this same ratio. They are made in this ratio by adjusting L_a or L_b until the simple bridge shows a balance.

4. The link, L, is restored, giving again the double-bridge, and a second balance is obtained by varying the ratios A/B and a/b. This balance is more nearly correct than the first, as the leads have been approximately adjusted to their proper ratio.

5. The entire procedure is repeated until no further change is required in the settings of the main ratio, under which condition

$$X/S=A/B=a/b, \tag{17}$$

or

$$X=SA/B=Sa/b. \tag{18}$$

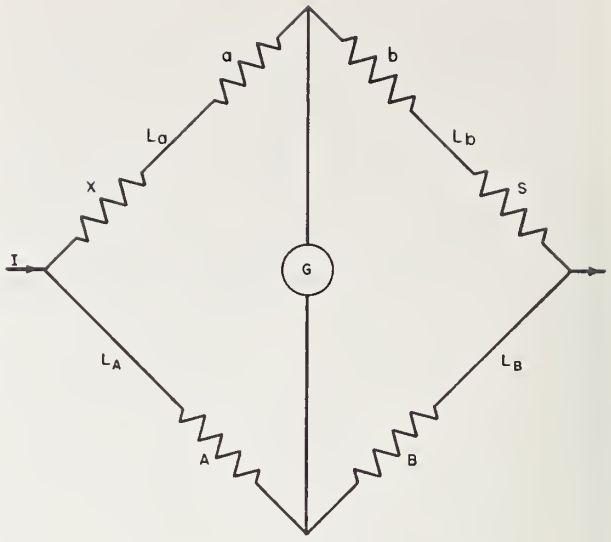

FIGURE 18. *Equivalent Wheatstone bridge.*

In case a/b is obtained from a slide wire, or a ratio that is adjustable but not known, the same procedure is followed as that outlined above. In this case, however, the balance for step 3 is obtained by varying the ratio a/b, if necessary making a fine adjustment of the ratio by varying the lead resistances L_a and L_b.

IV. Special Apparatus for Precision Measurements

1. Direct-Reading Ratio Set

The problem of calibrating precision resistance apparatus usually involves the comparison of resistors in the instrument with standard resistors of the same nominal value. This is most readily done by some substitution method, which is usually a method for determining differences between the resistances of the unknowns and of the standards. For well-adjusted instruments, the differences are small and need to be determined only approximately. For example, if the difference between the standard and unknown is 0.01 percent, the difference need be determined to only 1 percent to give the value of the unknown to one part in a million in terms of the standard.

One of the most convenient instruments for the measurement of such differences in ratio is the "direct-reading ratio set." With this comparatively inexpensive instrument and a group of standard resistors, it is possible to calibrate accurately most types of resistance apparatus such as Wheatstone bridges, potentiometers, resistance boxes, etc.

The direct-reading ratio set is merely an adjustable resistance ratio with which bridges may be assembled, the remainder of the bridges being ordinary laboratory equipment. In its simplest form the ratio set is as shown in figure 19. The resistor B is a 100-ohm coil, which constitutes the fixed arm of the ratio. The adjustable arm consists of a fixed resistor of 99.445 ohms and three dials, D_1, D_2, and D_3. The dial D_1 consists of ten steps of 0.1 ohm each, and D_2 and D_3 have

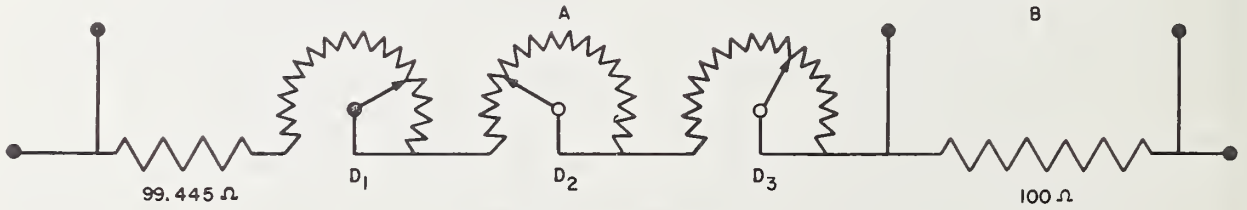

FIGURE 19. *Direct-reading ratio set.*

ten steps each of 0.01 and 0.001 ohm respectively. When at their center positions, the resistance of the three dials is 0.555 ohm, and with the fixed coil of 99.445 ohms the total of the arm is 100 ohms. Starting from these center positions, a step on D_1 will either raise or lower the A-arm by 0.1 ohm. The ratio of A to B is then changed from 100/100 to 100.1/100 or to 99.9/100, that is to say, it is raised or lowered by 0.1 percent. Likewise, steps on D_2 and D_3 change the ratio by steps of 0.01 and 0.001 percent respectively. By interpolation of the steps on the lowest dial, changes of 0.0001 percent may be determined.

Although the ratio set described above is correct in theory, variations in the resistances of the contacts of the dial switches would make the readings uncertain by several steps on the lowest dial when ordinary dial switches are used. The use of mercury switches will reduce the variations to a few microhms, but such switches are somewhat difficult to operate and keep in condition.

To avoid difficulties from variations in switch-contact resistances the design is usually modified so as to reduce their effect. This is done by placing the switches in high-resistance shunt circuits that require comparatively large changes in resistance to obtain small changes in the parallel resistance, as was done in the rheostat of the Mueller bridge (see section III, 5). The shunt circuits may be made sufficiently high that switch contact variations are negligible even when switches of moderate quality are used. An example of a shunted dial for obtaining steps of 0.1 ohm is shown in figure 20. With the dial set at 0 the resistance of the shunt arm totals 133.636 ohms, and this in parallel with the 30-ohm branch gives a total resistance of 24.5 ohms. When the dial is moved to stud 1, the resistance of the parallel combination increases by 0.1 ohm to 24.6 ohms, which requires that the shunt arm be 136.666 ohms. That is to say, between studs 0 and 1 there is a resistance of 3.030 ohms. Likewise between studs 1 and 2 there is a resistance of 3.145 ohms so that when the dial is at 2, the shunt arm totals 139.811 ohms and the parallel combination is 24.7 ohms. The successive steps of the dial are not of equal magnitude, but the parallel resistance may be changed by 0.1-ohm steps from 24.5 to 25.5 ohms. For this the steps on the dial average about 3.6 ohms each.

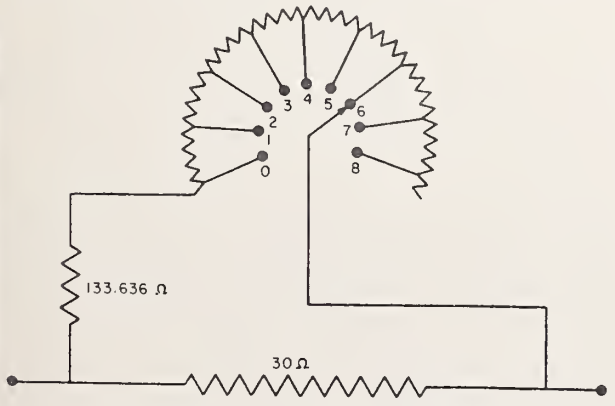

FIGURE 20. *Shunt-type decade.*

Since a change in the high-resistance arm of about 3.6 ohms is required to change the parallel resistance by 0.1 ohm, it is obvious that switch contact variations in the high resistance arm will have their effect reduced by a factor of about 36 to 1. Their effect could be still further reduced by increasing the resistance of the shunt, the effect being reduced as the square of the ratio of the current in the high resistance branch to the total current.

In the same way, it is possible to make a decade for changing in 0.01-ohm or 0.001-ohm steps by means of a 150-ohm shunt in parallel with a 30-ohm resistor, the 150-ohm shunt to be changed in steps that average about 0.36 or 0.036 ohm respectively. Three decades with appropriate shunts and a 25-ohm series resistor could be used to obtain the equivalent of the A-arm of figure 19, but with the ratio not appreciably affected by normal variations in switch contact variations. An equivalent instrument is available commercially and, together with a group of standard resistors, is one of the most useful pieces of apparatus for the measurement of electrical resistance, especially for the calibration of resistance apparatus. Some of the procedures will now be described.

Comparison of two-terminal resistance standards, substitution methods.—In nearly all measurements where the highest possible accuracy is desired, a substitution method is used. That is, the change required to restore balance after replacing a standard with an unknown is measured. In comparing two-terminal standard resistors by substitution, the direct-reading ratio set is very rapid and convenient, and accurate results may be obtained. For this comparison a Wheatstone bridge is set up as shown in figure 21. A and B are the two arms of the ratio set, and Y is an auxiliary resistance of the same nominal value as the standard resistors under comparison. The two resistors are in turn placed in the mercury cups Q, and the bridge balanced by varying the ratio A/B. The difference in the ratio for the two balances gives the percentage difference between the two standard resistors. Thus, if the difference in the ratio for the two balances is one step on the 0.001 dial, one resistor is 0.001 percent higher than the other. If we are comparing 1,000-ohm coils, for example, the difference is 0.001 percent of 1,000 ohms, i. e., 0.01 ohm. Which coil is the larger is determined by observing whether the ratio is increased or decreased when the standard resistor is replaced by the unknown resistance. Actually the dif-

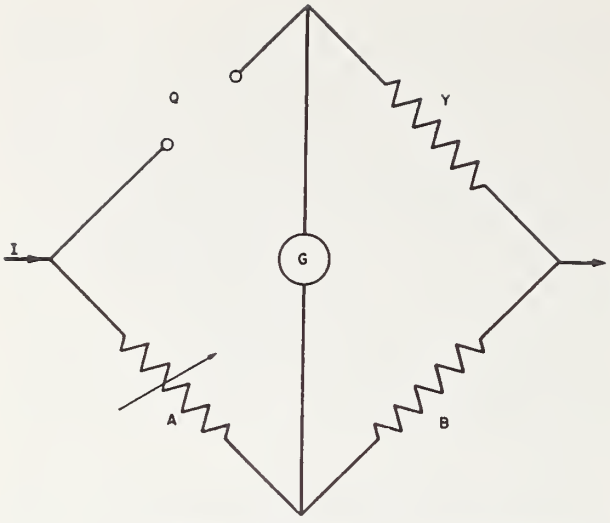

FIGURE 21. *Wheatstone bridge for substitution method.*

ference is determined in percentage of the arm Y, but for small differences any departure of Y from its nominal value is of no consequence.

Although the dials of a direct-reading ratio set change the ratios in decimal parts of a percent, it is desirable to mark the dials in parts per million. Thus the steps on the 0.001-percent dial would be marked, 0, 10, 20, etc., and the 0.01-percent dial would be 0, 100, 200, etc. Readings of the instrument and data taken from it are then whole numbers of moderate sizes rather than decimals. In the discussion that follows, it is assumed that the ratio set is marked in parts per million, and that corrections to resistors are also expressed in parts per million. Bridge readings and corrections to standards are then readily added and subtracted and calculations are greatly simplified.

In comparing nearly equal resistances by substitution, the lack of correct adjustment of the coils of a well-made ratio set will cause errors of much less than 1 part in a million. The variation in the contact resistance of the dial switches may be appreciable unless they are kept clean. The switches should be frequently cleaned and lubricated with a little good-quality light oil. When kept in good condition, the resistance of the three switch contacts should not vary as much as a thousandth of an ohm. From the values of the coils on the 0.001 percent dial, we see that a variation of a thousandth of an ohm will cause variations in the ratio of 1/3.6 of a part in a million.

In comparing resistances by the substitution method, the two balances of the ratio set should be made quickly so that temperature changes will not cause variations in the ratio set between readings. It is best to have all coils of the ratio set made from the same lot of resistance material. If this is done and manganin coils are used, a change in temperature of 1 deg C should not change the ratio more than 2 or 3 parts in a million.

In spite of these sources of error, it is probably possible to compare standard resistors ranging from about 10 ohms to 1,000 ohms to within 1 or 2 parts in a million by the use of this ratio set. This, of course, requires that the set be well constructed, that a fairly sensitive galvanometer be used and that the resistances differ by not more than about a tenth of a percent. With resistances less than 10 ohms, the resistance of the mercury cup contacts may cause trouble. For this reason standard resistors smaller than 10 ohms are now almost always four-terminal resistors. Methods of comparing such resistors will be discussed later.

Another method for comparing nominally equal two-terminal standard resistors, which is practically equivalent to the preceding substitution method, is what might be called a double substitution method. In this latter arrangement, the two resistors under comparison are used to form two arms of a Wheatstone bridge, the ratio set forming the other two arms. The resistors are both mounted in mercury cups so that they may be interchanged without affecting lead resistances in series with them. After a balance is obtained by adjusting the ratio set, the resistors are interchanged, and a new balance is obtained. The percentage difference between the two resistors is half the difference between the two readings of the ratio set. This method is used for the same range of resistances as those measured by the simple substitution method, and about the same accuracy may be attained.

Comparison of four-terminal resistances with two-terminal resistance.—The direct-reading ratio set is convenient for the comparison of two-terminal with four-terminal resistances. Although the occasion seldom arises for the comparison of two-terminal with four-terminal standard resistors, it is often necessary to compare a standard resistor of one type with a resistance coil of the other type. Thus, in measuring the coils of many pieces of electrical apparatus it is impossible to make connection with the coils except through comparatively large connecting resistances. However, it is generally possible to make potential connections to the two ends of the coils and measure them as four-terminal conductors. In doing so, it is often convenient to compare them with two-terminal standard resistors.

In figure 22, X is a four-terminal resistor to be measured, having the current terminals T_1 and T_2, and potential terminals P_1 and P_2. The potential leads may contain considerable resistance in addition to that of the leads. A and B are the two arms of the direct-reading ratio set, and M_1 and M_2 are mercury cups into which either a two-terminal standard resistor or a short circuiting link may be placed.

Suppose we start with the galvanometer con-

nected at P_1, a standard resistor nominally equal to X inserted in M_1, and with M_2 shorted. We then have a simple Wheatstone bridge, which is balanced by varying the setting of the ratio set. After this balance is obtained, the galvanometer connection is shifted to P_2, and the standard resistor is placed in M_2, M_1 being shorted with the link. We again have a Wheatstone bridge but with the standard resistor and unknown interchanged. This interchange has been obtained without making any change in the resistance of the leads of the measuring circuit, except for possible variations in the resistances of the mercury cup contacts, which will be small if the mercury contacts are clean. The bridge is now again balanced by means of the ratio set. The percentage difference between the unknown and the standard resistor is half the difference in reading of the ratio set for the two balances. Unless the resistances under comparison are fairly large, it will be necessary to take into account the resistance of the short-circuiting link. This is done by subtracting the link resistance from the resistance of the standard resistor and considering that the resistor has this new value and is being interchanged with a link of zero resistance.

The resistance of the link can be measured as follows: Connect the link between two 1-ohm resistors to form two arms of a Wheatstone bridge, using the direct-reading ratio set for the other two arms, as shown in figure 23. L is the link, and A and B are the arms of the ratio set. Two balance readings are taken, first with the galvanometer connected at one end of L and then at the other. Half the difference in the readings is the value of the link resistance in percentage of the 1-ohm arms. If the link resistance is large, it may be necessary to use larger resistances in place of the 1-ohm coils. This method is very convenient for the measurement of small resistances such as links, connecting wires, switch contact resistances, etc. It is not a precision method but usually is sufficiently accurate for the measurement of resistances such as those just mentioned, which are to be used in series with larger resistances.

Substitution method for decades.—In the calibration of precision rheostats the occasion often arises for the measurement of a series of resistors of the same nominal value. This is readily done by the substitution method, using a standard resistor of the same value as the steps of the rheostat, reading differences on a direct-reading ratio set. The procedure is illustrated in figure 24. In this figure PR is the precision rheostat to be calibrated, and let us assume that the 10-ohm-per-step dial is to be checked. PB is then a plug box or any decade with 10-ohm steps, and M is a pair of mercury cups in which is placed a standard 10-ohm resistor. The arm Y is a 100-ohm resistor whose value need not be accurately

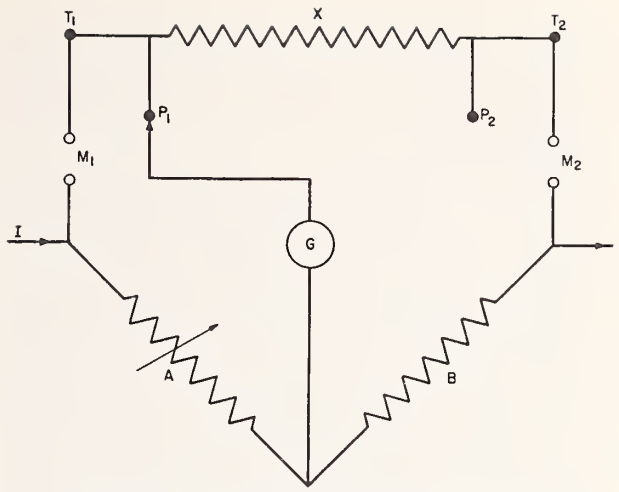

FIGURE 22. *Measurement of 4-terminal resistor.*

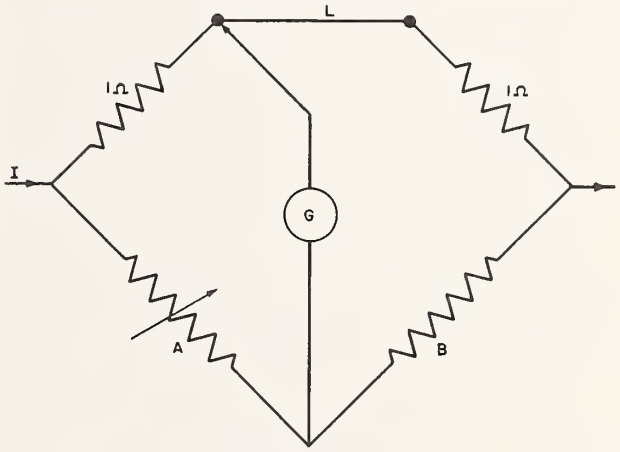

FIGURE 23. *Measurement of lead resistance.*

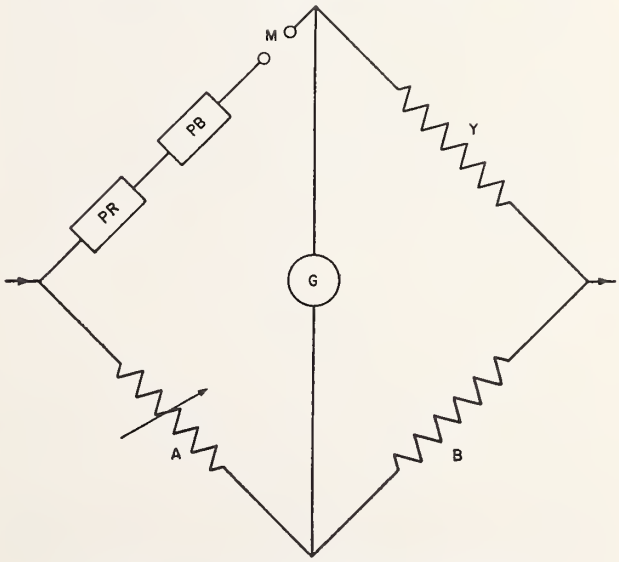

FIGURE 24. *Test of decades by substitution.*

known, and A and B are the two arms of a direct reading ratio set. The reading of the rheostat under calibration is set at zero, the plug box is set at 90 and the 10-ohm resistor is placed in M, making the total nominal resistance of the arm 100 ohms.

After the bridge has been balanced by changing the setting of A, the standard resistor is removed and the mercury cups shorted with an amalgamated copper link, and also the reading of PR is changed from 0 to 10 ohms. This has in effect substituted a 10-ohm step of PR for the 10-ohm standard resistor. The change in the reading of A required to again obtain a balance of the bridge is a measure of the difference between the step on the rheostat and the standard resistor, such difference being a percentage of 100 ohms. The second 10-ohm step on the rheostat is obtained by leaving PR at its 10-ohm reading, again placing the standard resistor in M and reducing the PB resistance to 80 ohms. These three resistors still total 100 ohms, nominally. The standard is now again replaced by a short-circuiting link, and PR is set to read 20 ohms, the resulting change being read from A. The change was produced by the substitution of the second 10-ohm step of the precision rheostat for the 10-ohm standard.

The procedure is continued, the steps of PR being successively substituted for the standard resistor. It should be noted that the steps of the auxiliary plug box, PB, are also being replaced by the standard resistor as PR is being increased and PB decreased in reading, the standard being cut in and out of the circuit. Data are therefore obtained for calibration of both PR and PB in terms of the standard resistor. Hence by this method, two precision rheostats may be calibrated simultaneously.

When 10-ohm steps are calibrated in a 100-ohm arm, the accuracy is reduced by one order. That is to say, differences in readings of the ratio set must be obtained to 0.0001 percent if the 10-ohm steps are to be determined to 0.001 percent. The method has the advantage that changes in the over-all resistance of the rheostat are determined under the conditions of use, which is often not the

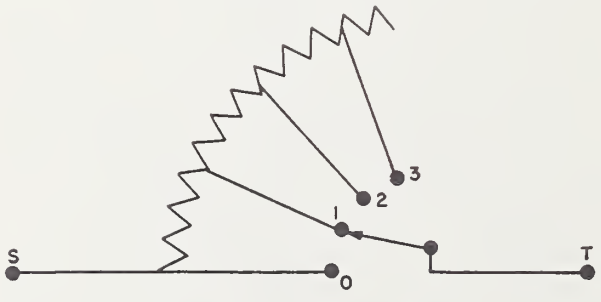

FIGURE 25. *Dial connections.*

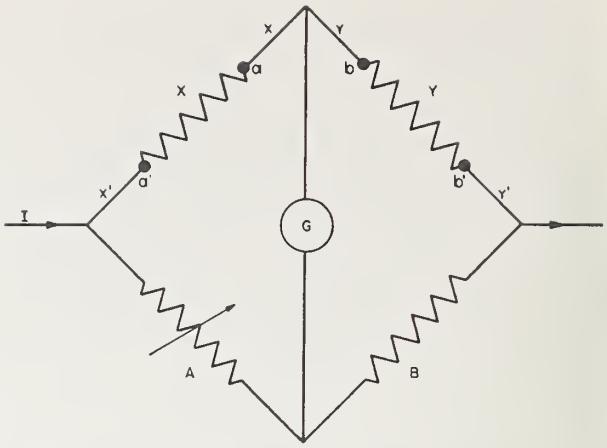

FIGURE 26. *Lead resistances in Wheatstone bridge.*

case when the individual resistors are measured directly. This may be seen by reference to figure 25, which represents the connections to one dial of the rheostat. The switch contact may be set on the contact studs marked 0, 1, 2, 3, etc., thus connecting 0, 1, 2 or more resistors between the dial terminals S and T. It should be noted that the resistors are usually connected in series and lead wires are connected from the junctions of the resistors to the switch contact studs. If the resistors are calibrated by measuring between studs 0 and 1 ,1 and 2, 2 and 3, etc., two of these leads are included with each resistor. In actual use all the leads to the coils in use are not in the circuit, but only one lead is used for any setting of the dial. The above method of calibration determines the step as in actual use, the only additional data required being the resistance between terminals with the dial set at zero. This is readily measured by the method just described for the determination of link resistances. For any setting, this "zero resistance" must be added to the sum of the steps as determined by substitutions.

Comparison of four-terminal resistance standards.—Before taking up the question of the comparison of four-terminal standard resistors, let us consider briefly the effect of the lead wires of a simple Wheatstone bridge. In figure 26, X and Y are nominally equal resistances, and A and B are the two arms of a direct-reading ratio set. The conductors x, y, x', and y' are used to connect up the bridge, and we will also denote their resistances by x, y, x', and y', respectively. The ratio of the resistances of the two arms containing X and Y is not in general the same as the ratio of X to Y because of the resistance of these connecting leads. If we could select leads such that the ratios x/y and x'/y' were the same as X/Y, the ratio of the two arms would be independent of the actual values of the lead resistances. That is, the balance would be the same as if the resistances of

the leads were negligibly small. It is possible to make the leads adjustable and make the ratios x/y and x'/y' the same as X/Y. In fact, such an arrangement is used at the National Bureau of Standards to reduce the effect of the leads when using the Kelvin double bridge. Instead of adjusting the leads, it is possible to balance the bridge with fixed leads, and then find what this balance would have been with the proper ratio of lead resistances, or with negligibly small lead resistances.

X and Y were assumed to have practically equal resistances. Instead of connecting the galvanometer as shown, suppose we balance the bridge with the upper galvanometer connection first at a and then at b. The average of the two readings is the value that would have been obtained had the conductors x and y been equal or negligibly small in resistance. Thus, by taking two readings we can take into account the effect of these two connecting resistances. This average balance reading is not the correct reading, however, unless also $x'=y'$, which is probably not true. We must now find what this balance would have been with $x'=y'$. To do this suppose we shift the current connections from the points shown to the points a' and b'. In doing so we remove the lead resistances x' and y' from the X and Y arms and connect them in series with the ratio arms A and B. If x' and y' are not equal, we will change the balance of the bridge by removing them from the arms X and Y. We will have still further changed this balance by adding them to the ratio arms A and B. Which of these changes is the greater depends upon the relative sizes of the two pairs of arms. If A and B are equal to X and Y, the changes will be equal. That is, with all arms nominally equal the balance would be changed a certain amount if the battery connections were shifted to a' and b'. This change is twice that which would have been obtained had we only removed x' and y' from the X and Y arms. The average of the readings before and after changing the battery connections is then the reading that would have been obtained with $x'=y'$ or both negligibly small.

Suppose, however, that A and B are ten times as large as X and Y. Then connecting x' and y' in series with A and B produces only a tenth as large a change as is caused by their removal from X and Y. Then ten-elevenths of the change in balance when the battery connections are shifted is due to the removal of x' and y' from the X and Y arms, and the remaining one-eleventh is due to the connection of the leads in the ratio arms. This enables us to calculate what the balance would be with x' and y' equal or negligibly small. As an example, suppose X and Y are each 10 ohms, and the arms of the direct-reading ratio set are 100 ohms. Assume that with the battery connected as shown in figure 26 and the galvanometer at a, the reading of the ratio set with the bridge balanced is 5497 millionths, and with the galvanometer connection changed to b, the reading is 5613. Let us further assume that when we change the battery leads to a' b', leaving the galvanometer connected at b, the balance reading changes to 5835. Then with leads of the proper ratio, or leads with negligibly small resistances, the balance would have been at $(5{,}613+5{,}497)/2+10/11(5{,}835-5{,}613)$; i. e., at 5,757.

As a matter of fact, this scheme for taking into account the connecting leads is practically never used in comparing two-terminal resistors. As the substitution method requires no consideration of the lead resistances, except to see that they are reasonably small, it is generally used. However, in comparing four-terminal resistances with a simple Wheatstone bridge we follow exactly the steps outlined above. Figure 27 shows a bridge set up for this purpose. A and B are the two arms of the direct-reading ratio set. X and Y are the four-terminal resistors under comparison, with current terminals T_1, T_2, T_1', and T_2', and potential terminals P_1, P_2, P_1', and P_2'. The bridge is balanced when connected as shown, and a second balance is obtained after shifting the galvanometer connection to P_2'. The third balance is obtained after now changing the current connections from T_1 and T_1' to P_1 and P_1', and calculations are made as above. The two arms X and Y are now interchanged and the three readings again obtained. From these two sets of readings, we get two balance points on the ratio set. Half the difference between these two balance readings is the percentage difference between the two four-terminal resistors.

Although the direct-reading ratio set was developed for use in the comparison of nominally equal resistances, it can be readily adapted for the comparison of resistances of any ratio provided some independent means is available for accurately

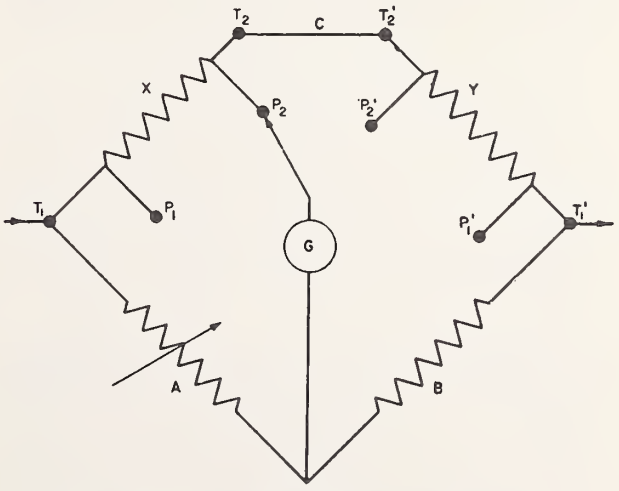

FIGURE 27. *Comparison of 4-terminal resistors.*

realizing the same resistance ratio. As an example of such a use let us consider the calibration of a 25-ohm resistor by comparison with a 100-ohm standard.

As has been described above, the direct-reading ratio set consists of the arm A, which is adjustable in small steps from values slightly below to slightly above 100 ohms. The B-arm is ordinarily a fixed 100-ohm arm. Suppose we change the B-arm by connecting an additional 300 ohms in series. The ratio A/B then becomes 100:400, which is adjustable in the same percentage steps as was the 100:100 ratio. Using two sets of mercury cups, let us set up the bridge shown in figure 28. The 25-ohm resistor is placed at X and the 100-ohm standard at S, and the bridge is balanced by adjusting A, and let us call this reading A. Also let A_0 be the reading A would have had if the X and S arms had been exactly in the ratio 25:100. If c_x and c_s designate the proportional corrections of X and S, the actual balance A, of the bridge, will be

$$A=A_0+c_x-c_s. \tag{19}$$

Since A is obtained experimentally and c_s is known, this equation could be solved for c_x if A_0 were also known. To obtain A_0, the arms X and S must be replaced by a resistance ratio of exactly 1:4.

To realize a 1:4 ratio it is necessary merely to have five resistors that are reasonably nearly equal. If one of these five is connected in place of X and the other four in series in place of S, the ratio will be only approximately 1:4. However, if the five resistors are placed one after the other in X, the remaining four each time being connected in S, the average of the five ratios will be 1:4 to a very high accuracy. In other words, the average of the five readings of A with the five resistors in turn at X, the remaining four in series in the S-arm, will be A_0, the reading of A for an exact 1:4 ratio. This value of A_0 can be substituted in eq 19 to allow the calculation of c_x, the proportional correction to the unknown 25-ohm resistor.

Another method of obtaining A_0 would be to balance the ratio set with one resistor at X and the other four at S, thus obtaining A of eq 19. The five resistors could then be substituted in any bridge and their differences determined. The terms c_x and c_s are then the amounts in proportional parts that the resistor in X and those in S differ respectively from the average value of the five.

To get an accurate value of the 1:4 ratio, the five resistors should have large enough resistances that the lead resistances of the X and S arms are negligible, or the lead resistances should be in the ratio 1:4. They may usually be so set with a sufficient accuracy by shorting X and S and adjusting the bridge circuit so obtained to a balance by changing the length of the lead wires. The five

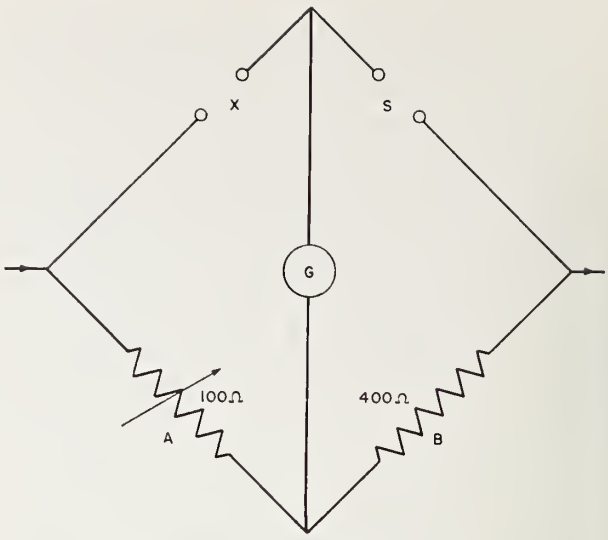

FIGURE 28. *Bridge with 1:4 ratio.*

resistors do not need to be equal to a very high precision. However, they must not differ by more than 0.1 percent if the average of the five ratios is to be correct to one part in a million.

A procedure analogous to this method of obtaining a ratio of 1:4 may be followed to determine any ratio $1:n$, where n is an integer, by taking the average of $n+1$ ratios. It may also be used to determine any ratio $r:n$, where both r and n are integers. Starting with $r+n$ equal resistors, r in one arm and n in the other, the resistors are rotated in a cyclic order until each resistor occupies each position once. The average of the $r+n$ readings is the reading that would be obtained if all resistors were equal. Moreover, the resistors in either arm may be in parallel rather than in series.

In the calibration of high resistances, use may be made of the fact that the proportional correction to a group of nominally equal resistors is the same when they are connected in parallel as when connected in series. For example the ten 100,000-ohm sections of a megohm box may be connected in parallel and measured against a 10,000-ohm standard resistor. If the parallel group is high in resistance by 0.01 percent, the series resistance of 1 megohm will also be high by 0.01 percent. Here it is assumed that the ten sections are sufficiently near to equality that in the expansion

$$\frac{1}{1+c}=1-c+c^2-c^3, \text{ etc.} \tag{20}$$

the second and higher powers of c are negligible, where c is the proportional amount by which the resistance of any section differs from the average of all. If this condition is satisfied, the ratio of

the resistance of n resistors in parallel to their resistance in series is exactly $1:n^2$.

The methods that have just been presented assume the use of a direct-reading ratio set. These methods, however, are entirely satisfactory when use is made of any ratio set that has small and definite steps. Such a set may be assembled from ordinary laboratory apparatus. For example, the adjustable 100-ohm arm might be made of a 105-ohm coil with a parallel decade box reading about 2,500 ohms. A change in reading of the decade box by 0.1 ohm would change the 100-ohm arm by about 1 ppm. The changes in the parallel resistance are not directly proportional to the change in the high resistance arm, but they may be readily calculated. This adjustable 100-ohm arm, together with a fixed 100-ohm resistor, constitutes an adjustable ratio set.

2. Universal Ratio Set

Precision standard resistors are usually made only in integral multiples or submultiples of an ohm. Consequently odd-valued resistors usually cannot be measured by a substitution method, except in a few cases where standard resistors can be combined to give a resistance nearly that of the unknown. The comparison of odd-valued resistors with standards is then not possible with a direct-reading ratio set, but a ratio set is required that is accurately adjustable over a wide range, at least from a 1:1 to a 5:1, or preferably to a 10:1 ratio.

A very convenient wide-range ratio set is one used at the National Bureau of Standards and called a "universal ratio set" [14]. This instrument is one having a constant resistance, between two external terminals, of about 2,111 ohms. An arrangement of dials is such that in effect a potential connection may be made at any point of the 2,111 ohms to the nearest 0.01 ohm. The ratio of the resistance between the potential point and one terminal of the set to the resistance between the potential point and the other terminal is therefore adjustable in small steps over a very large range. The device is the equivalent of a long slide wire with a movable contact, and its uses are analagous.

Suppose it were desired to measure a resistance of say 6.8 ohms by comparing it with a 10-ohm standard resistor. The two resistors could be connected in series and the combination connected across a slide wire as shown in figure 29, X being the unknown, S the standard, and W a slide wire. If a galvanometer, G, is connected to terminal a of the unknown and to the slide wire, a Wheatstone bridge is obtained that will balance with the slide wire at some point, 1, near the end. If now the galvanometer connection is changed successively to b, c, and d, successive balances will be obtained with the slide wire at 2, 3, and 4, respectively. The ratio X/S is then the same as

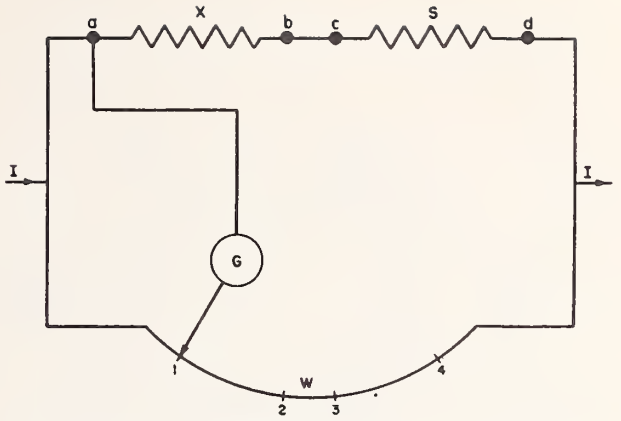

FIGURE 29. *Comparison of resistors with slide wire.*

$R_{1,2}/R_{3,4}$ where $R_{1,2}$ and $R_{3,4}$ are the resistances of the slide wire between the points 1 and 2, and 3 and 4, respectively.

It is very difficult to make a wire of sufficient length and uniformity that the ratio $R_{1,2}/R_{3,4}$ can be accurately determined. Instead of a slide wire, the universal ratio set makes use of a group of wire wound resistors so that the resistances between the balance points 1, 2, 3, and 4 can be accurately known. The arrangement of its dials is as follows. The highest dial consists of twenty 100-ohm resistors in series, with the dial contact acting as the potential connection to the instrument, as shown in figure 30. As the dial is rotated in a clockwise direction, the 100-ohm resistors are successively changed from the right to the left side of the contact. To change resistance from the right to left side in 10-ohm steps, two more dials are used, each having ten 10-ohm steps as seen in figure 31. These two dials are operated by the same handle but with one dial increasing as the other decreases in resistance. The total resistance between S and T remains constant for any setting of the 10-ohm decades,

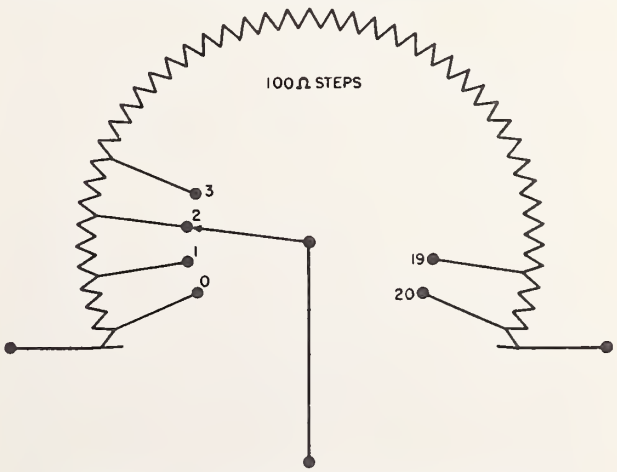

FIGURE 30. *100-ohm dial of universal ratio set.*

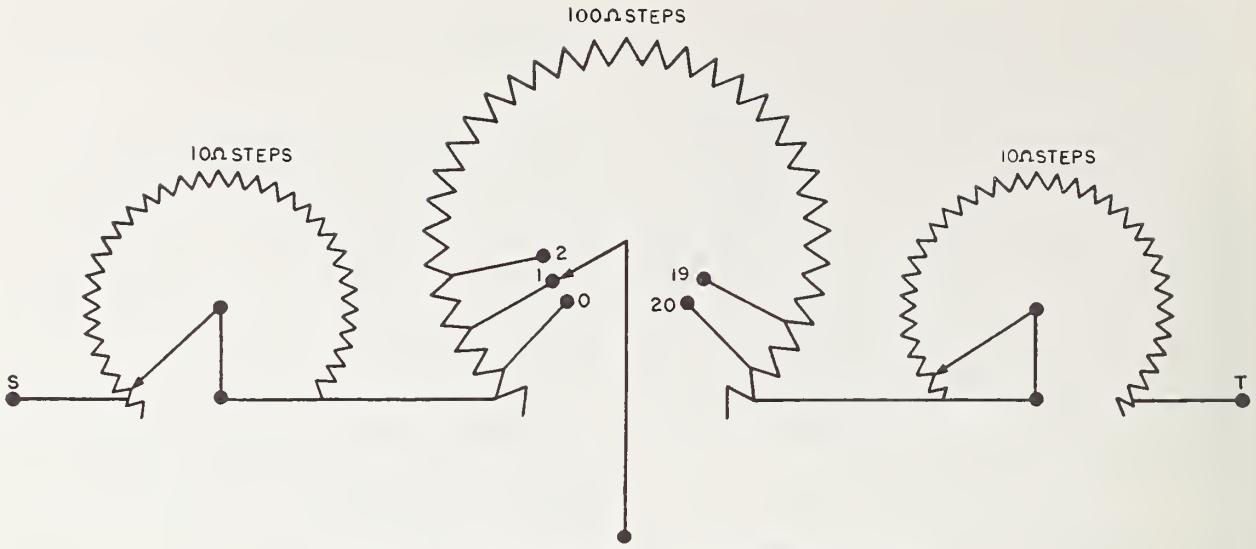

FIGURE 31. *100- and 10-ohm dials of universal ratio set.*

and of course it is unaffected by the position of the 100-ohm dial switch that is merely a potential contact.

Steps of 1, 0.1, and 0.01 ohm-per-step are obtained in the same way as the 10-ohm steps, that is with two decades of each denomination operating together, one on each side of the 100-ohm dial. This scheme for the change of the potential point along a fixed resistance is essentially the same as that of the Feussner type potentiometer. The large number of contacts in series limits its use for precision work to circuits having a rather high resistance.

The universal ratio set is used only for the determination of resistance ratios and hence may be calibrated in terms of any unit. It is most conveniently calibrated in terms of an average step on the highest or lowest dial. This is done by comparing each step of a decade with the ten steps of the preceding dial starting with the smallest dials. Only the steps on one side of the 100-ohm dial need be tested, as the function of the other group is to keep the total resistance constant. A check of the constancy of the over-all resistance needs to be made for all readings of the double dials.

The use of a universal ratio set is the same as that of a slide wire as described in conjunction with figure 29, for the measurement of odd-sized resistances. It may be used in the measurement of four-terminal resistors and is especially convenient for the tests of potentiometers. The test of a potentiometer consists in the measurement of the ratio of the emf-dial resistance to the standard-cell resistance for all settings of the emf and standard-cell dials. These resistors are of the four-terminal type with potential connections brought out to emf and standard-cell binding posts. The method is satisfactory even when some resistance is common to both the standard-cell and main-dial resistance. The arrangement for such a test is shown in figure 32. The ratio set, URS, which is shown as a slide wire, is connected in parallel with the potentiometer, the connection to the latter being made to the battery binding posts, *BA*+ and *BA*—. Readings on URS are made with the galvanometer connected successively to the *SC* and emf binding posts, for all settings of the emf dials. It should be noted that changes in the emf dials are merely changes in potential points and do not affect the readings obtained for the *SC* dial.

Potentiometers are provided with rheostats in the battery circuit for adjusting the potentiometer current. A change in this battery rheostat will change the differences in readings obtained on the universal ratio set but not the ratio of the differences. It is possible to make the ratio set direct-reading by adjusting the battery rheostat until the difference on the ratio set for the standard-cell posts is a decimal multiple, preferably 1,000, of the reading of the standard-cell dial. Corrections for the emf dials may then be read directly from differences across the emf terminals.

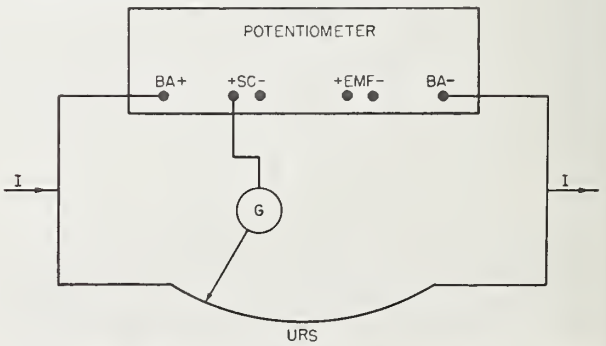

FIGURE 32. *Check of potentiometer with universal ratio set.*

V. Calibration of Precision Bridges

1. Calibration of Wheatstone Bridges

The circuit of a commercial precision Wheatstone bridge is usually as shown in figure 33. The two ratio arms A and B may have any one of several values, the choice being made by inserting a plug in series with the desired resistor. The rheostat arm, R, consists of four to six decades of not less than 0.1 ohm nor more than 10,000-ohm steps. The unknown resistor is connected to heavy binding posts, X, and a battery and galvanometer are connected to the external binding posts BA and GA. The switches S_B and S_G open and close the battery and galvanometer circuits.

In calibrating a bridge of this type, it is necessary to determine the resistance of the ratio arms between the branch points 2 and 3 or 3 and 4 rather than between the external binding posts, as the resistances from the branch points to the binding posts are usually not negligible. Also it is necessary to find the resistance between 1 and 4 with the rheostat dial, R, set at zero, as well as the corrections to the readings of the rheostat dials themselves. It is also necessary to measure the lead resistances between the branch points 1 and 2, as these are in series with the unknown resistance connected at X. The bridge balance determines the entire resistance of the X-arm, and the leads must be subtracted in order to obtain X itself. These four types of resistance measurements are made by application of some of the general principles previously discussed.

To measure the ratio arm B, for example, it is necessary to determine the four-terminal resistor having branch points 3 and 4. This is easily done by comparing it with a two-terminal standard of the same nominal value, making application of the method outlined in section IV, 1 and using the circuit shown in figure 34. The resistors a and b are the arms of a direct-reading ratio set, or any two ratio arms that may be adjusted in small known steps. As shown, one side of the galvanometer is in effect connected to the branch point 4, through the rheostat arm, R, which may be set at zero. The standard resistor is placed in the mercury cups, M_1, and a short-circuiting link is placed across the other mercury cups, M_2. After a balance is obtained by adjusting arm a, the standard and shorting link are interchanged and the galvanometer connection is shifted in effect to point 3 by connecting to the other X binding post. Half the change in the ratio that results gives the difference between the B-arm and the standard resistor.

The resistance of the A ratio arm may be measured in exactly the same way as for the B arm by making connection to the other GA terminal instead of the one shown. Some difficulty may arise from variations of the contact

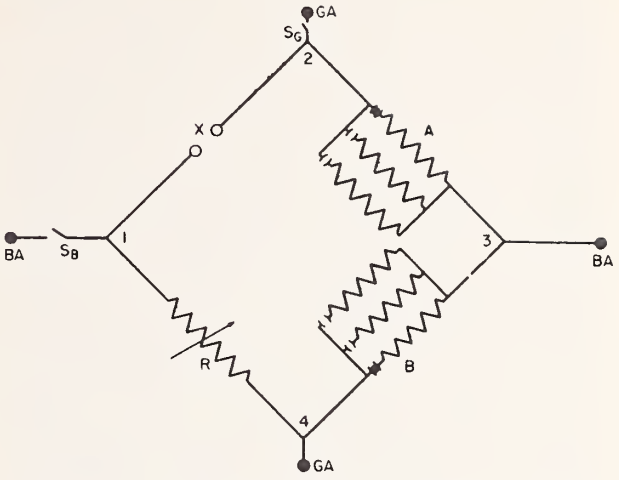

FIGURE 33. *Wiring arrangement of Wheatstone bridge.*

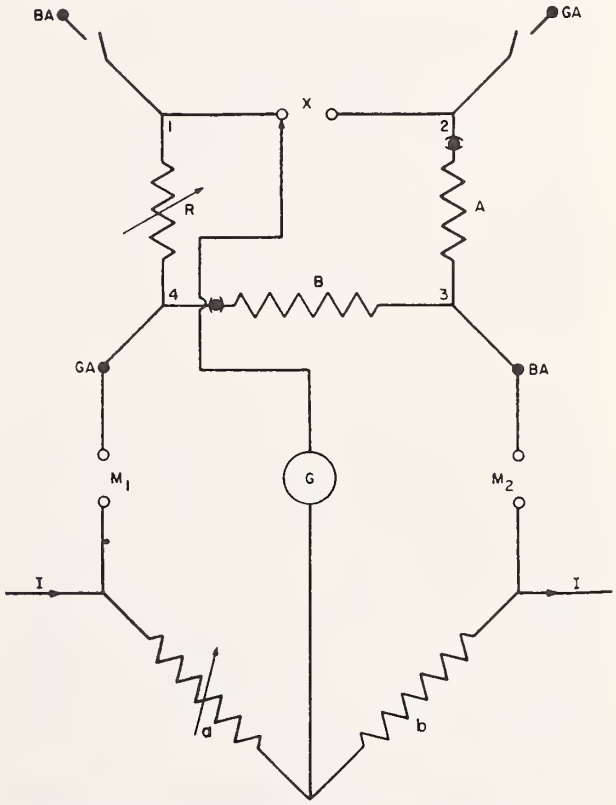

FIGURE 34. *Check of ratio arm of Wheatstone bridge.*

resistance of the galvanometer key, which will now be in the measuring circuit. This may be avoided by interchanging the adjacent X terminal and the GA terminal. The galvanometer would then be shifted from one X binding post to the GA binding post instead of from one X binding

post to the other. That is to say, the current and potential connections at point 2 may be interchanged. This will place the variable galvanometer switch resistance in series with the galvanometer where it will not affect the bridge balance.

The rheostat arm, R, may be calibrated like any other precision rheostat as described in section IV, 1. Connection should be made through the appropriate X and GA terminals. The resistance of the rheostat arm with all dials set at zero may be measured by connecting the arm between two equal resistors, using a direct-reading ratio set to connect up a Wheatstone bridge. The change in the reading of the ratio set is determined when the galvanometer connection is changed from one branch point of the rheostat arm to the other. This is the same as the method given in section IV, 1 for the measurement of lead resistances. In a similar way, the lead resistances in the X arm may be determined, taking readings with the galvanometer connection to branch points 1 and 2 and to the external X binding posts, with the latter connected by a shorting wire. The calculation must be made in two parts in order to exclude the resistance of the shorting wire.

For calculating X from the calibration data, it is convenient to express the corrections to the readings of the rheostat arm in ohms and to express the corrections to the ratio arms in proportional parts. The calculation in proportional parts involves merely a division of the correction in ohms by the nominal value in ohms. The value of X for a given balance is calculated from the equation

$$X=\frac{A}{B}(1+a-b)(R+r+r_0)-X_0. \qquad (21)$$

In this equation a and b are the proportional corrections to the ratio arms A and B respectively, $R+r$ is the sum of the dial readings and corrections, and r_0 is the resistance of the rheostat arm with all dials at zero. The term X_0 is the resistance in ohms of the lead wires in the X-arm of the bridge. The factor $(1+a-b)$ is an approximation for $(1+a)/(1+b)$ and is accurate if a and b are small as compared with unity. If neither a nor b exceeds 0.001, the error from neglecting the second-order terms does not exceed two parts in a million.

2. Calibration of Thermometer Bridges

Because of the space limitations and structural difficulties, platinum resistance thermometers usually have resistances of less than 100 ohms. The common values are about 2.5 or 25 ohms, the actual values being so chosen that the change in resistance is very close to 0.01 or 0.1 ohm per degree centigrade change in temperature. In order to read to 0.001° C, it is necessary to read these thermometers respectively to 0.00001 or 0.0001 ohm. For such measurements, bridges of special design are usually used.

In this country thermometer bridges for precision work are usually made with equal ratio arms. These arms are interchangeable, so that the use of an average value eliminates errors from lack of equality of the ratio arms, or the ratio arms may be interchangeable and adjustable so that they may be made equal at any time. With such interchangeable ratio arms, actual calibrations of them are unnecessary. The calibration of a thermometer bridge requires only a calibration of the rheostat arm.

In order to measure platinum resistance thermometers, which as stated above are usually not very high in resistance, with a bridge having equal ratio arms, it is necessary to have the rheostat arm adjustable in small steps. In fact, steps as low as 0.0001 or 0.00001 ohm are needed for work of the highest precision. In order to obtain such small steps, contact resistances cannot be used directly in the rheostat arm. Hence recourse is had to decades of the Waidner-Wolff type described above in section III, 5, in which the changes in resistance result from changes in the values of high-resistance shunts on comparatively small resistances. Switches are placed in the high-resistance shunts, where variations in their resistance will have a negligible effect. Decades of the Waidner-Wolff type cannot be set to have zero resistance, but the small changes start from an appreciable minimum value. However, for equal-arm bridges, compensating resistance may be placed in the X-arm. The value of the unknown is then measured by the increase in reading of the rheostat arm when the unknown is connected into the circuit.

The use of a resistance thermometer to measure temperature involves merely the determination of resistance ratios. Hence in calibrating thermometer bridges it is necessary to determine only relative values of resistance, which does not require the use of standard resistors. This calibration is readily made by the user, especially for bridges having equal ratio arms.

The calibration of such thermometer bridges requires as auxiliary equipment only an adjustable resistor that has the same range as that of the bridge rheostat. This resistor needs to be accurately adjustable, although the resistance need not be known for any position. Such an adjustable resistor may be assembled, for example, from a decade box with minimum steps of 0.1 ohm in series with an 0.1- or 1-ohm resistor, which is in turn shunted by a slide wire or a rheostat of fairly high resistance. This adjustable resistor is connected across the X-terminals of the bridge and is used to balance the bridge after the rheostat arm is set to certain required readings. The shunted 0.1- or 1-ohm should be attached to the X-termi-

nals so as to be adjacent to the rheostat arm. If a slide wire is used for the shunt, the sliding connection should be used as the galvanometer branch point so that its variable resistance will be in the galvanometer branch where it will not affect the balance. This, in effect, throws the shunted resistance partly in the X and partly in the rheostat arm. We then have the equivalent of the bridge shown in figure 35, the ratio arms A and B being

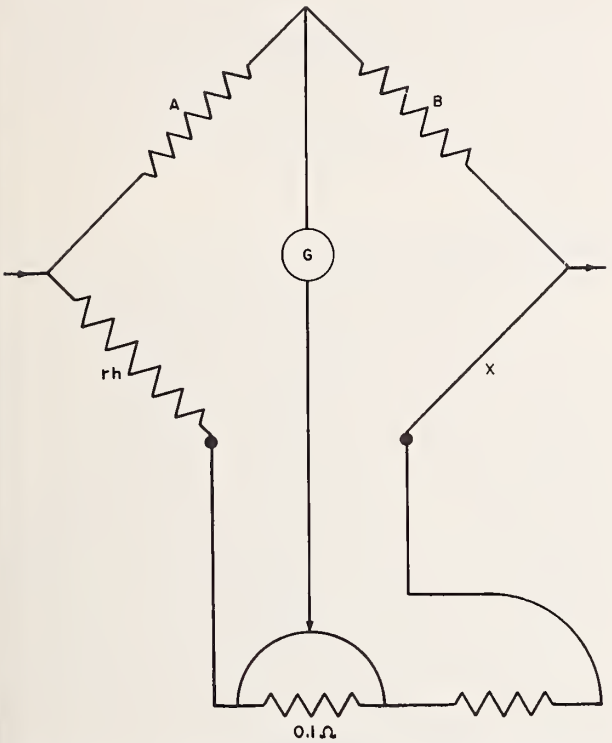

FIGURE 35. *Calibration of rheostat arm of thermometer bridge.*

accurately adjusted to equality. For a balance the rheostat arm, *rh*, and the X-arm must be also equal. If then X is changed by any amount, as by the insertion of a resistance thermometer in series, the rheostat would have to be changed by an equal amount to again balance the bridge. Thus, actual values of the rheostat arm need not be known if changes in the arm are accurately determined.

The procedure for checking the rheostat arm is usually as follows. The resistances of all steps in the arm are determined in terms of an average step on the smallest dial. The steps of the smallest dial are first intercompared to see that they are equal within 0.1 step, which is as accurately as the steps may be readily read by interpolation from galvanometer deflections. An easy way to intercompare the steps on the lowest dial is to set it at 0, the other dials being at any convenient setting, and balance the bridge by adjusting X. The galvanometer deflection is now read when the lowest dial reading is changed from 0 to 1. Leaving this dial on 1, the bridge is again balanced with the X-rheostat, and the galvanometer deflection then again read for a shift of the lowest rheostat dial from 1 to 2. These alternate balances with *rh* and X are continued until the value of all the steps on the smallest dial of *rh* are determined in terms of galvanometer deflections. Unless one of the steps is defective, these should be the same to the nearest 0.1 step.

The steps on the second dial of *rh* should each equal the 10 steps of the lowest dial. They are measured in terms of the lowest dial by setting the lowest dial at 10 and the second dial at 0, the other dials being at any convenient value, usually small in order to obtain good sensitivity. With the lowest dial at 10 and the next larger dial at 0, the bridge is balanced by adjusting the value of X, after which the smallest dial is turned to 0 and the other dial shifted from 0 to 1. If there is now any galvanometer deflection, it is because the first step on the second dial is not the same as 10 steps on the smallest. The amount that they differ, in terms of steps of the lowest dial, is determined by reading the galvanometer deflection and evaluating this deflection by reading the additional change in deflection resulting from a change of the smallest dial setting from 0 to 1.

To measure the second step on the second dial its reading is left at 1 and the lowest dial now set at 10, a balance being obtained with X. The lowest dial is now set back to 0 and the other increased to 2, thus substituting the second step of the higher dial for 10 steps on the lower. The lack of balance is again translated into fractions of a step on the lowest dial by interpolation, using galvanometer deflections. This procedure is continued, each step of the second dial being compared in turn with the 10 steps of the lowest dial. A table is now made showing the value, in terms of steps of the lowest dial, of the first step of the second dial, the sum of the first two steps, sum of the first three steps, etc. This table will give the resistance corresponding to any reading of this dial in terms of steps on the smallest dial, which we might call "bridge units".

The values of the steps on the next higher dial are now determined in the same way but in terms of the 10 steps on the second dial, the unit again being a step on the smallest dial. The continuation of this process gives the resistance of each step of each dial in terms of the 10 steps on the preceding dial, from which finally is calculated the resistance for each setting of each dial in terms of bridge units.

The resistances as determined may be used with any resistance thermometer without converting their values to ohms. It is sufficient to standardize the resistance thermometer on this

same bridge, by measuring its resistance at known temperatures. However, it is often desirable to convert the values to ohms in order that the bridge may be used for the measurement of resistance other than that of thermometers. This is done by measuring the resistance of a standard by balancing the bridge with the standard resistor connected to the X-terminals. All readings of the rheostat should then be multiplied by the ratio of the resistance of the standard in ohms (rather, the difference between its resistance and that of the shorting connector) to its resistance in bridge units in order to convert the rheostat calibration to ohms.

The above procedure may be used for the calibration of the rheostat arm of any Wheatstone bridge, in terms of steps of the lowest decade and then in ohms, by comparison with a standard resistor. When used with equal ratio arms, the "zero" resistance of the rheostat need not be determined, if two bridge balances are obtained, the first with the unknown connected to the X-terminals and the second with the unknown resistance short-circuited.

Many precision thermometer bridges provide a shorting plug for short-circuiting the resistor connected to the X-terminals. The galvanometer connects to the center of the shorting connector so that equal amounts of its resistance are inserted in the X and rheostat arms thus giving the same balance as if the shorting connector had a negligible resistance. With this method it is unnecessary to know the resistance of the shorting connector, although such resistance may usually be estimated with sufficient accuracy from its length and gauge size.

VI. Resistivity of Solid Conductors

1. Resistivity, Definition and Units

In the experimental work that led to the formulation of his law, Ohm found that the resistance, R, of a conductor is directly proportional to its length, l, and inversely proportional to its cross-sectional area, A. These experimental facts may be written in the form of an equation as

$$R=\rho\frac{l}{A}, \tag{22}$$

where ρ is a constant of proportionality whose value depends upon the material of the conductor and upon the units used in measuring l and A. This constant of proportionality is called resistivity.

The above equation, which defines resistivity may be written

$$\rho=R\frac{A}{l}. \tag{23}$$

No name has been assigned to the unit of resistivity, and consequently the unit is specified by stating the units used in measuring R, A, and l. This has resulted in the use of a large number of units, as each of R, A, and l may be expressed in more than one unit or subunit. From the above equation for ρ, it is seen that the value of ρ is numerically equal to that of R for a conductor having unit length and unit cross-sectional area. A cube is such a conductor, and this has led to the rather common expressions for the unit of resistivity "ohms per cubic inch" or "microhms per cubic centimeter". These expressions are undesirable, because they imply that resistivity is the ratio of resistance to volume. It is logically better to say "ohms times square inches per inch", "microhms times square centimeters per centimeter" or more briefly "ohm-inches" and "microhm-centimeters".

2. Measurement of Resistivity

For a uniform conductor, it is merely necessary to measure the resistance of a known length of the conductor and then measure its cross-sectional area in order to determine its resistivity. For conductors of small cross section, it is usually possible to use a sufficient length that the resistance may be accurately measured with a simple Wheatstone bridge. For conductors of large cross section, it is customary to measure the resistance with a Kelvin double bridge in order to avoid errors from contact resistances. Wherever possible, the cross-sectional area is calculated from micrometer measurements. For conductors of small or irregular cross section, micrometer measurements are not sufficiently accurate, and the average area is determined from mass and density measurements.

For a uniform conductor the cross section, A, is

$$A=\frac{V}{l}, \tag{24}$$

where V is the volume and l the length of the conductor. But since, from the definition of density, D,

$$V=\frac{m}{D} \tag{25}$$

where m is the mass, the preceding equation may be written

$$A=\frac{m}{lD}. \tag{26}$$

For many purposes it is sufficient to assume the density as that given in tables. If this is not sufficiently accurate, the specific gravity is determined from weighings in air and in water, and from these data and the density of the water, the

density of the conductor is determined by the equation

$$D=\frac{w_a}{w_a-w_w}D_w, \tag{27}$$

where w_a and w_w are the weights of the specimens in air and water, respectively, and D_w is the density of the water. At a temperature of 21° C, the density of water is 0.998 gm/cm³ and this value decreases uniformly to 0.997 gm/cm³ at about 25° C.

Instead of calculating A separately, the value of A from eq 26 may be substituted into eq 23, giving

$$\rho=\frac{R}{l}\times\frac{m}{l}\times\frac{1}{D}. \tag{28}$$

From this equation it is seen that the resistivity, ρ, equals the product of resistance per unit length and mass per unit length, divided by density. The length need not be the same for the resistance and mass measurements if the material is uniform. For two conductors having the same density, the ratio of their resistivities is the same as the ratio of their values for the product $R/l\times m/l$. This product is called "mass resistivity", and is a constant that is characteristic of the material of a conductor, being D times as large as the ordinary, or volume, resistivity. The mass resistivity is often specified in the purchase of conductors for electrical uses, and it is sometimes more readily measured than is volume resistivity. However, it is doubtful that this advantage is sufficient to compensate for the confusion that arises from the use of two types of resistivity.

It is usual commercial practice to specify percentage conductivity rather than resistivity, especially in the purchase of copper conductors. Conductivity is the reciprocal of resistivity, and percentage conductivity is obtained by dividing the resistivity of the given sample into that of the standard and multiplying by 100.

By international agreement, the resistivity of annealed copper is taken as 1.7241 microhm-cm at 20° C [15]. This value was selected from measurements of the resistivity of a large number of samples of high-purity commercial copper wire from both American and European refiners. The value was agreed upon as a standard for reference and was not intended to be the value for absolutely pure material. Copper has been produced with a conductivity of several percent greater than 100, which probably indicates a material of higher purity than that of the standard.

Some effort has been made to secure international agreement for a standard for the resistivity of aluminum, but so far copper is the only metal for which such a value has been adopted.

The measurement of the resistivity of a liquid may often be made by comparison with another liquid of known resistivity. In this case measurements of dimensions may be avoided, as the known and unknown are given the same dimensions by placing them in turn in the same container or "conductivity cell." The ratio of their resistivities is then the same as the ratio of their resistances. Mercury is often used as the liquid of known resistivity, since its value is accurately known.

Although the resistivity of mercury is known to a high accuracy, its use as a liquid of known resistivity may lead to errors of considerable magnitude. In comparing the resistivity of liquids by placing them in turn in the same cell and measuring their resistance, it is tacitly assumed that the current distribution through the cell is the same for both liquids. This may be incorrect unless the liquids have very nearly the same resistivity, as the distribution of current in the cell depends to some extent upon the resistance of the metal electrodes. For high-resistivity liquids the resistance of the electrodes may play a negligible part in determining the current distribution, but in the case of mercury, which is a relatively good conductor, the current distribution may depend to a considerable degree upon the dimensions of the electrodes and upon the resistivity of the metal of which they are made.

In determining the resistance of a liquid, it is necessary to use an alternating-current bridge. When a direct current is used, the ions in the liquid will drift towards the electrodes thus making the density nonuniform. Moreover, polarization will often be produced by the liberation of gases at the electrodes. When measured with alternating current a conductivity cell is found to be electrically the equivalent of a resistor and a capacitor in parallel. This requires a balance of reactance as well as of resistance when the cell is measured in an alternating current Wheatstone bridge.

VII. References

[1] N. B. Pilling, Trans. Am. Electrochem. Soc. **48,** 171 (1925).
[2] R. S. Dean and C. T. Anderson, Trans. Am. Soc. Metals **29,** 899 (1941).
[3] A. A. Somerville, Phys. Rev. **31,** 261 (1910).
[4] J. L. Thomas, J. Research NBS **16,** 149 (1936) RP863.
[5] J. L. Thomas, J. Research NBS **13,** 681 (1934) RP737.
[6] F. Wenner and J. L. Thomas, BS J. Research **12,** 147 (1934) RP639.
[7] P. H. Bridgman, Proc. Am. Acad. Arts Sci. **52,** 573 (1917).
[8] J. L. Thomas, J. Research NBS **36,** 107 (1946) RP1692.
[9] P. H. Dike, Rev. Sci. Inst. **7,** 278 (1936).
[10] E. B. Rosa, BS Bul. **5,** 413 (1908–09) S107.
[11] F. Kohlrausch, Wied. Ann. **20,** 76 (1883).
[12] E. F. Mueller, BS Bul. **13,** 547 (1916) S288.
[13] E. F. Mueller and F. Wenner, J. Research NBS **15,** 485 (1935) RP842.
[14] F. Wenner and E. Weibel, BS Bul. **11,** 27 (1914) S223.
[15] BS Circular C31 (1914).

Washington, March 30, 1948.

315-411 O - 68 - 13

Calibration of Potentiometers by Resistance Bridge Methods

DAVID RAMALEY
National Bureau of Standards
Boulder Laboratories

Convenience and ease in calibration of general-purpose potentiometers is provided by a Universal Ratio Set. Any moderate-sized electrical standards laboratory should consider the procurement of a URS for potentiometer calibrations, especially if other resistance measurements also are required.

Instruments & Control Systems—Vol. 37

It might seem that the simplest way to calibrate a potentiometer would be to set up the instrument under test to furnish potential differences which can be measured by a potentiometer of similar range which previously has been calibrated. This method does have the advantage of calibration under actual operating conditions and can be used advantageously on instruments of moderate accuracy. The method requires that currents in both potentiometers be held as nearly constant as possible for optimum calibration accuracy. Also, thermal electromotive forces constitute a possible source of calibration errors.

If the appropriate resistance portions of a potentiometer are composed of resistance bridge circuits, then the precision of measurement is not limited by the extent to which currents can be maintained constant. The resistance ratio data can be converted rapidly into potential corrections for switch settings and dials on the potentiometer under calibration.

The resistance bridge method requires step changes in resistance as small or smaller than one part per million (Fig. 1). The total resistance between terminals A and B must be constant, and independent of the positioning of the contactor terminal C. The ratio of resistance between terminals A and C to the resistance between terminals C and B is thus variable in small increments. Such a tapped-resistor function is provided by ratio sets or dividers.

The Universal Ratio Set (URS)

A conventional six-dial URS provides the equivalent of a resistor of 2111.11 ohms, having 2,111,110 separate taps, providing step changes of 0.001 ohm. It contains twenty 100-ohm steps (right in Fig. 2), and five dial switches of the Fuessner or double-action ganged type. Decades have resistance elements of 10, 1, 0.1, 0.01, and 0.001 ohms, respectively. The total resistance between terminals A and B is independent of the positions of the ganged dials. Turning any dial adds as much resistance on one side of contact C as it removes from the other side of contact C. The resistance from C to A (or from C to B) can be varied over the entire range in increments of 0.001 ohm. The URS is calibrated and corrections applied to its readings when using the instrument.

A Kelvin-Varley type of resistive voltage divider with six dials could be used as the tapped resistor. 1,000,000 equal-valued steps are available, but even more steps are desirable for calibrating potentiometers in bridge circuits.

Comparison of Resistances

The resistances to be compared are connected in a series circuit, which in turn is connected to the A and B terminals of a URS. The parallel circuit thus formed is shown in Fig. 3. A battery or other source of direct current is applied across this parallel circuit. A Wheatstone bridge can be formed by connecting a galvanometer between terminal C of the URS and any desired point along the resistances to be compared, such as P_1, P_2, etc. A simple analysis[1,4] indicates that resistors, a, b, and c can be compared by means of readings taken on the URS for balanced-bridge conditions when the galvanometer is connected

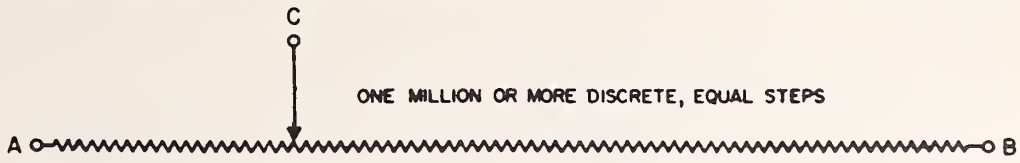

FIG. 1. SCHEMATIC CIRCUIT diagram of a resistor suitable for bridge circuit calibration of potentiometers.

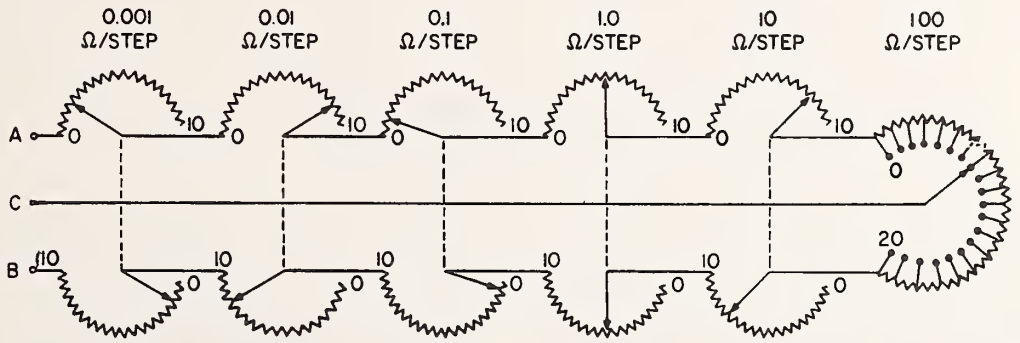

FIG. 2. SCHEMATIC DIAGRAM of six-dial universal ratio set (URS).

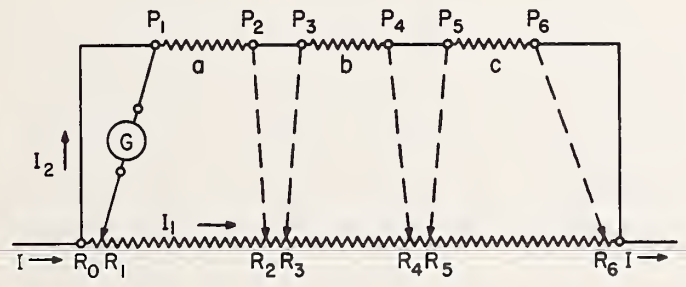

FIG. 3. ARRANGEMENT for comparing resistances by means of a URS, a slidewire, or a resistive divider.

in turn to resistor terminal points P_1, P_2, P_3, P_4, etc. The relationships can be expressed as follows:

$$\frac{R_3 - R_1}{R_4 - R_2} = \frac{a}{b} \qquad (1)$$

$$\frac{R_3 - R_1}{R_6 - R_2} = \frac{a}{c} \qquad (2)$$

R_1, R_2, R_3, R_4, etc. are the URS readings, and a, b, and c are the resistances of resistors, a, b, and c.

Because these are truly Wheatstone bridge arrangements, the power source and the galvanometer can be, and commonly are, interchanged in the circuit.

Potentiometer Calibration

This same type of Wheatstone bridge can be arranged by connecting the appropriate portions of the potentiometer circuit to a URS. Usually the resistance comparisons required in calibrating a potentiometer include (1) intercomparison of all step resistors in the "measuring" or "EMF" circuit, (2) determination of the uniformity or linearity of the standard-cell (SC) circuit (if it is adjustable), and (3) determination of the ratio of resistance of the EMF circuit to that of the SC circuit for all ranges of the instrument. In case the potentiometer is of the Lindeck type, certain resistances usually will have to be measured directly in terms of a known standard actually inserted in series with the potentiometer.

Fig. 4 is a schematic diagram of a simple potentiometer connected for calibration. The URS forms two arms of a Wheatstone bridge, and the potentiometer circuit forms the other two arms, thus completing the bridge. Bridge balance readings are taken at all desired potentiometer settings of the EMF and SC dials by connecting the power source in turn to

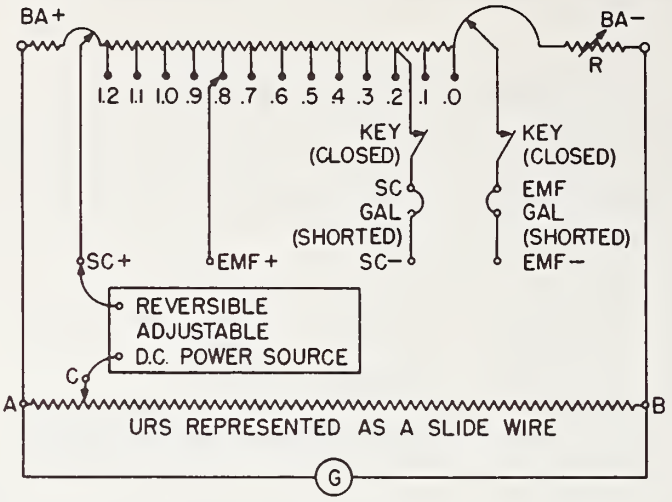

FIG. 4. ARRANGEMENT of universal ratio set (URS) for calibrating a potentiometer.

the SC+, SC−, EMF+, and EMF− binding posts of the instrument. Connections to all circuit resistors requiring calibration can be made through these four terminals. The required resistance comparisons are obtained from the URS readings by means of equations similar to equations (1) and (2).

The computation of resistances and the ease of making the balances with the URS can be simplified by making the URS direct reading in terms of a desired portion of the circuit under calibration. Usually, the choice corresponds to the voltage expected from a typical standard cell, such as a voltage of 1.0190 volts. To make the ratio set direct reading for this selected voltage setting on the standard-cell dial, the difference in readings of the URS when the power source is connected to SC+ and SC− terminals, respectively, should be 1019.000 ohms, if the ratio set is calibrated in ohms. This is achieved by adjusting R by trial and error, usually with the help of previously calculated data.

Assume that the URS has been made direct reading for the SC circuit and that the readings for the circuit of Fig. 4 are those shown in Table 1. The uniformity of the standard cell circuit has thus been determined for points 1.01800, 1.01850 and 1.01950.

TABLE 1—Calibration Data for Standard Cell Dial Circuit of Fig. 4.

POWER TO TERMINAL	POTENTIOMETER SETTING (VOLTS)	URS READING (OHMS)	READING DIFFERENCE
SC−	1.0190	1023.363	1019.000
SC+	1.0190	4.363	
SC+	1.01800	5.369	1017.994
SC+	1.01850	4.866	1018.497
SC+	1.01900	4.363	1019.000
SC+	1.01950	3.832	1019.531

The resistance of the circuit for setting 1.01800 is lower than it should be by about 6 parts in a million. For a setting of 1.01850 the circuit resistance is low by 3 ppm and for 1.01950 the circuit resistance is high by about 30 ppm. If we wish to achieve maximum accuracy when using this potentiometer with a standard cell of 1.01950 volts, we should set the standard cell dial at 1.019469 instead of 1.019500.

The EMF circuit is calibrated in like manner. If this has been accomplished and the results tabulated, it becomes simple to compute corrections to the EMF dial positions if the URS is direct reading.

Ranges or factors for multirange instruments are obtained by taking readings on the URS for bridge balances with the potentiometer factor switch set on the available ranges. The exact procedure differs with different makes and models of instruments. One feature of importance in determining procedure is the standardizing circuit. Some instruments standardize on all ranges and some only on one range[1,4,6]

Special-purpose potentiometers and potentiometers containing Lindeck-type circuits usually can be calibrated by the URS and appropriate resistors inserted into the circuit. The procedure in each case depends on a circuit analysis of the instrument under consideration. Usually it is necessary to measure the resistance of the Lindeck element resistors and also to obtain a calibration of the indicating meter.[1]

References

1. D. Ramaley, "Practical Methods for Calibration of Potentiometers," NBS Technical Note 172.
2. J. L. Thomas, "Precision Resistors and Their Measurement," NBS, Cir. 470 (1948).
3. F. K. Harris, *Electrical Measurements*, John Wiley and Sons, Inc., New York, New York, 1952.
4. P. P. Brooks, "Calibration Procedures for D. C. Resistance Apparatus," NBS Monograph No. 39.
5. F. Wenner and E. Weibel, The Testing of Potentiometers, BS Bul. 11, 27 (1914) S223.
6. "Procedure for Certification of 7553 Type K-3 Universal Guarded Potentiometers," Leeds and Northrup Company, Directions Booklets Nos. 177151 and 177189.

NOTES ON THE CALIBRATION OF THE DIRECT READING RATIO SET

by

Paul P. B. Brooks

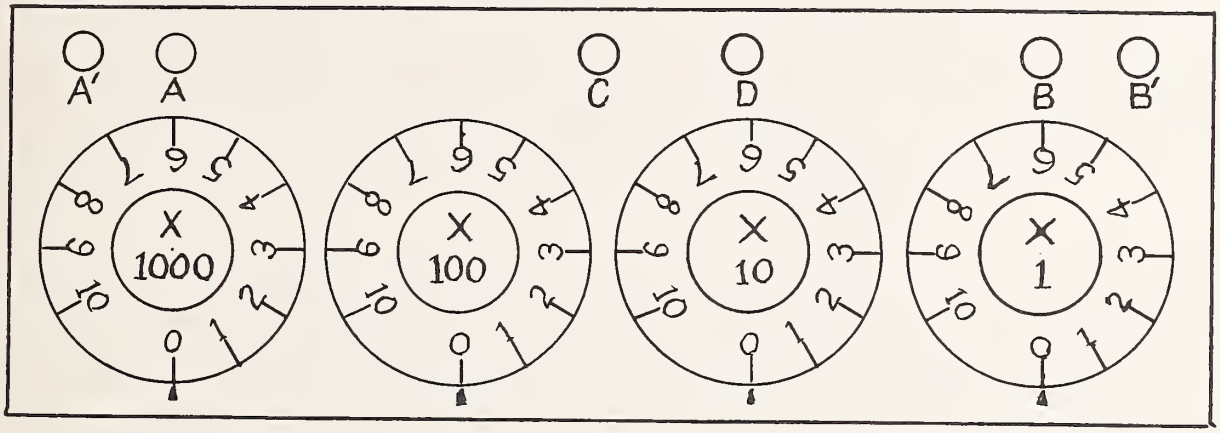

FIGURE 1. - Panel of Direct Reading Ratio Set

Figure 1 shows the essential features of the panel of a typical Direct Reading Ratio Set. The ratio arms of the set are represented schematically in figure 2. The arm CA is variable from 99.4445 ohms to 100.5555 ohms. Adjustment of the resistance is made by the four dials on the panel. The arm CB, with a resistance of 100 ohms, is used for an approximate 1:1 ratio. Use of the binding post D, instead of B, provides a 10-ohm arm, DC, for a 10:1 ratio. A' and B' are extra binding posts at the ends of the respective arms to provide for additional lead connections.

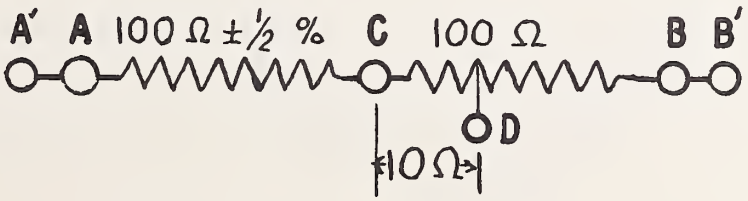

FIGURE 2. - Schematic diagram of ratio arms

The dials for adjustment of the variable arm will be designated from left to right as -

dial I, 0.1 ohm/step equivalent to 0.1% or 1000 ppm;
dial II, 0.01 ohm/step equivalent to 0.01% or 100 ppm;
dial III, 0.001 ohm/step equivalent to 0.001% or 10 ppm;
dial IV, 0.0001 ohm/step equivalent to 0.0001% or 1 ppm;

It is required to test each step on each dial to find the correction for each dial setting to the nearest part per million. If a calibrated Mueller thermometer bridge is available it may be used to check both the fixed and adjustable arms. Another method is to set up another resistance ratio that can be changed in accurately known steps. For example, two 1000-ohm resistance standards may be connected in series and, of course, their ratio is $\frac{1000}{1000}$, that is, $\frac{1}{1}$. If now a 1-ohm standard is connected in series with one arm, the ratio is changed to $\frac{1001}{1000}$, i.e., 1.001. Thus the ratio is increased by 0.1% (1000 parts per million). If this ratio is connected in parallel with the Direct Reading Ratio Set a Wheatstone bridge can be formed. When the ratio formed with the standards is increased by 0.1% the setting of the DRRS must be also increased by 0.1% to keep the two ratios equal, that is, to keep the Wheatstone bridge balanced. Any departure of this change from 0.1% is a measure of the correction to the DRRS reading. This, in brief, is the method of producing known changes in ratio to calibrate a DRRS.

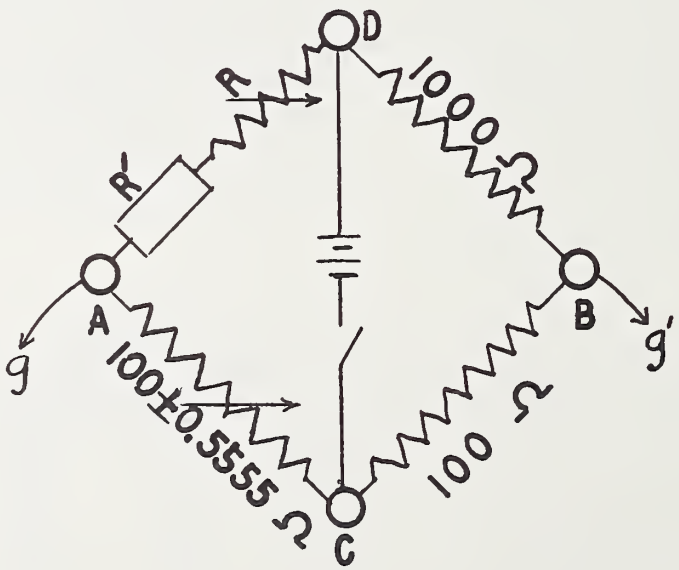

FIGURE 3. - Bridge circuit for dial tests

A Wheatstone bridge circuit (fig. 3) is set up using the arms AC and BC of the Direct Reading Ratio Set as the lower arms of the bridge. A 1000-ohm resistance standard forms the right upper arm of the bridge. R in the left upper arm is a decade resistance box in series with a finely adjustable resistance which will permit adjustment of resistance to about 0.0001 ohm. R is used to balance the circuit. R' is a link and a resistor or a combination of resistors used to change the resistance of the arm in increments accurately proportional to the nominal values of the dial steps on the DRRS. A change of 1 ppm in the upper arm corresponds to a change of 1 ppm in the lower arm. Since the ratio of the respective arms is 10:1, a change of 1 ohm in the upper arm corresponds to a change of 0.1 ohm in the lower arm. Hence, the increments in R' corresponding to steps on the different dials, left to right, are 1 ohm, 0.1 ohm, 0.01 ohm, and 0.001 ohm, respectively, and they should be accurate to better than 0.0001 ohm. The method for obtaining the desired increments will be explained with the detailed procedure for each dial.

The dial being tested is initially on zero. Since corrections will be taken from dial IV, dial IV is set near its middle position. The settings of the other dials are immaterial provided they are not changed during the test of the selected dial. The circuit is balanced by adjusting R. Then R' is used to increase the resistance of the upper arm by the appropriate increment (1 ohm for dial I, 0.1 ohm for dial II, etc.) and the DRRS dial is advanced one step. If the step resistor is sufficiently accurate, and the circuit is still balanced the correction for the step is zero. If it is necessary to advance dial IV to balance the circuit, the dial step in question is too small and its correction is negative by the number of steps that dial IV is advanced. If dial IV was advanced one step, the correction is -1 ppm. If dial IV has to be set back one step, the correction is +1 ppm.

After the correction to each step has been found, a step-by-step summation is made to supply the total correction applicable to each dial setting.

The fixed arms, CB and CD of the DRRS can be measured with standard resistors and another DRRS. Their values are not critical.

Resistance boxes do not supply the fine adjustment required of the balancing resistor, R, so a fine adjustment in series with the resistance box is required. The variable arm of another DRRS will supply steps of 0.0001 ohm. If a standard resistor (100 ohms for example) is connected in parallel with the variable arm of the second DRRS, the parallel resistance can be adjusted in very small increments. Likewise, a decade box adjustable in 0.1-ohm steps in parallel with a 1-ohm standard is usually satisfactory. With 30 ohms in the box an increase of 0.1 ohm increases the parallel resistance 0.0001 ohm.

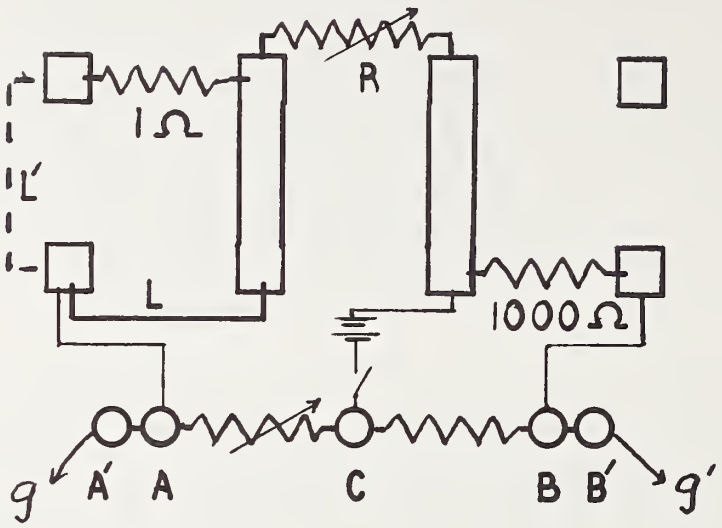

FIGURE 4. - Test circuit for dial I

Figure 4 shows the connections of the DRRS and accessories to a mercury stand to form the Wheatstone bridge circuit shown schematically in figure 3. Corresponding to R' in figure 3 is a 1-ohm standard and a link arranged so that when the link is in position L the standard is out of the circuit, but when the link is switched to position L' the resistance of the left upper arm is increased S ohms, that is, the 2-terminal resistance of the standard.

An alternate method is to remove the link from the stand and to replace it at L with the standard. The resistance of the arm is increased S-L ohms, that is the 2-terminal resistance of the standard minus the resistance of the link. The resistance of the link in most common use at the National Bureau of Standards is about 40 microhms or 40 ppm of 1 ohm (NBS Monograph 39, Sec. 5.1). It is approximately the same as the difference between the 4-terminal resistance and the 2-terminal resistance of most 1-ohm standards of recent manufacture. Hence, if the 2-terminal correction to the standard is small or the 4-terminal correction is negative, it is preferable to use the link as a switch. If the 4-terminal correction is positive, it is preferable to make the change by substitution. Any inaccuracy in the 1-ohm increment should not exceed 50 or 60 microhms.

The test of the dial proceeds as follows:

1. Set dial I on 0, dial IV on some step in advance of 0. The setting of the other dials is immaterial provided they are not changed during the test of dial I.
2. Place the link at L, to remove the standard resistor from the circuit.
3. Balance the circuit with the balancing resistor, R.
4. Transfer the link to L (or substitute S for L) increasing the resistance of the upper arm 1 ohm.
5. Advance dial I to step 1. If the circuit is still balanced, the correction for step 1 is zero.
6. If the correction is not zero, adjust dial IV to obtain balance (nearest balanced setting).
7. Find the correction from the number of steps that dial IV was changed and the direction of rotation. For example, if the initial setting of dial IV was 5 and it was set back to 4 to balance the circuit the correction was +1 ppm. If dial IV was moved to 7 to obtain balance, the correction was -2 ppm.
8. For the next step, leave dial 1 on step 1 and return dial IV to its initial setting.
9. Proceed as above for the test of step 2. Note that to rebalance the circuit with the link at L, R must be increased about 1 ohm.
10. After each step has been tested, make a step-by-step summation of the step corrections to show the total correction applicable to each dial setting.
11. With the 1-ohm standard on the stand, test the total of the ten steps of dial II by the same procedure. The result will serve as a check on the total correction found in the next test.
12. A check on the total correction for dial I can be made by comparing the ten steps on the dial with a 10-ohm resistor on the stand in place of the 1-ohm standard.

Table I illustrates the above procedure with data for a few steps taken from laboratory notes. In the first column, the plus sign denotes the unknown resistance of the fine adjustment. Since R serves only to balance the circuit its numerical value is not important.

TABLE I. - Sample data from a test of dial I

R	DRRS Rdgs		Correction	Σ
	S out	S in	ppm	ppm
1000.6+	0003	1002	+1	+1
1001.6+	1003	2002	+1	+2
1002.6+	2003	3002	+1	+3
-------	----	----	--	--
-------	----	----	--	--
1009.6+	9003	X002	+1	+8
	Ten Steps on dial II			
1000.6+	0003	0X04	-1	
Ten steps on dial I with 10-ohm Standard				
1000.6+	000X	X002	+8	

Test of Dial II, 0.01 Ohm per Step

This dial may be tested by the procedure used for dial I if a 0.1-ohm standard of the NBS type is available. This would be used on the stand in place of the 1-ohm standard.

Otherwise an accurate 0.1-ohm reference resistance may be set up from the usual laboratory equipment as shown in figure 5.

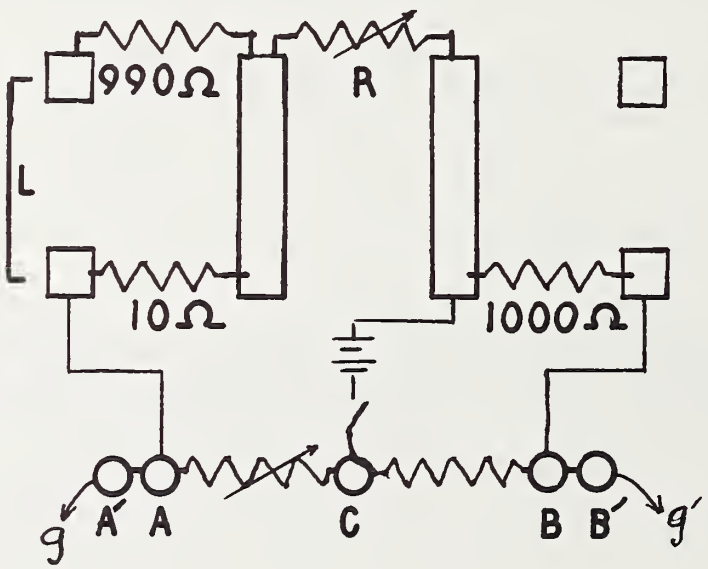

FIGURE 5. - Test circuit for dial II

The circuit is the Wheatstone bridge circuit described above with a 1000-ohm standard resistor in the right upper arm and the balancing resistor, R in the left upper arm. Also in the left arm, there is a 10-ohm standard resistor which can be placed in parallel with 990 ohms by the link. With the link in circuit the parallel resistance of 990 ohms and 10 ohms is 9.9 ohms. Removal of the link increases the resistance of the arm 0.1 ohm, which is the reference resistance required for testing dial II. The reference resistance is accurate provided the 990 ohms in a resistance box is not in error by more than 1 ohm.

To obtain an accurate resistance of 990 ohms, if a calibrated plug box is not available, a 1000-ohm standard resistor can be used in the left upper arm of the bridge, maintaining a ratio of 1000:1000. After the circuit has been balanced by adjusting the DRRS, the standard is replaced by a 10-ohm standard and a plug box in series. The bridge is rebalanced by adjusting the plug box in 0.1-ohm steps. The resistance of the plug box plus 10 ohms **equals** 1000 ohms, that is, the resistance in the plug box is 990 ohms.

The following adaptation of the above procedure permits calibration of the plug box without changing the test circuit.

a. Disconnect the plug-box from the stand (fig. 5).
b. Replace the plug-box by a 1000-ohm resistance standard on the stand.
c. Place the link on the stand to connect the 1000-ohm standard and the 10-ohm standard in parallel.
d. Balance the circuit with the DRRS, or R, or both.
e. Remove the 1000-ohm standard, reconnect the plug-box, and replace the link on the stand with an extra 10-ohm standard.
f. With 10-ohms plus the plug-box in place of the 1000-ohm standard, 990 ohms are required in the plug-box to rebalance the circuit. Adjust the plug-box in 0.1-ohm steps until balance is restored.
g. Remove the extra 10-ohm standard and proceed with the test.

Test Procedure

1. Place the link on the stand, set dial II on zero, dial IV on some step in advance of zero.
2. Balance the circuit with R.
3. Remove the link which increases the resistance of the arm 0.1 ohm.
4. Advance dial II to step 1. If the circuit is still balanced, the correction for the first step is zero.
5. If the correction is not zero, balance the circuit with dial IV, and find the correction from the setting of dial IV as explained for dial I.
6. Test each step of the dial in the same way and make a step-by-step summation of the corrections.
7. By the same procedure, find the correction for ten steps of dial III.

TABLE II. - Data from a test of dial II

STEP	DRRS L in	DRRS L out	Cor. ppm	Σ ppm
1	0003	0103	0	0
2	0103	0203	0	0
3	0203	0303	0	0
4	0303	0404	-1	-1
-	----	----	-	-
X	0903	0X03	0	-1
Ten Steps on Dial III				
	0003	00X4	-1	

Test of Dial III, 0.001 Ohm Per Step

This dial may be tested by the procedure outlined for dial II by replacing the 990 ohms in the left arm with 9990 ohms. Since this value is not critical, it may be replaced by a 10000-ohm standard.

The following method reduces the number of readings one half. No link is used and the resistance of the upper arm is increased step by step by increments of 0.01 ohm, corresponding to the 0.001 ohm steps on the dial.

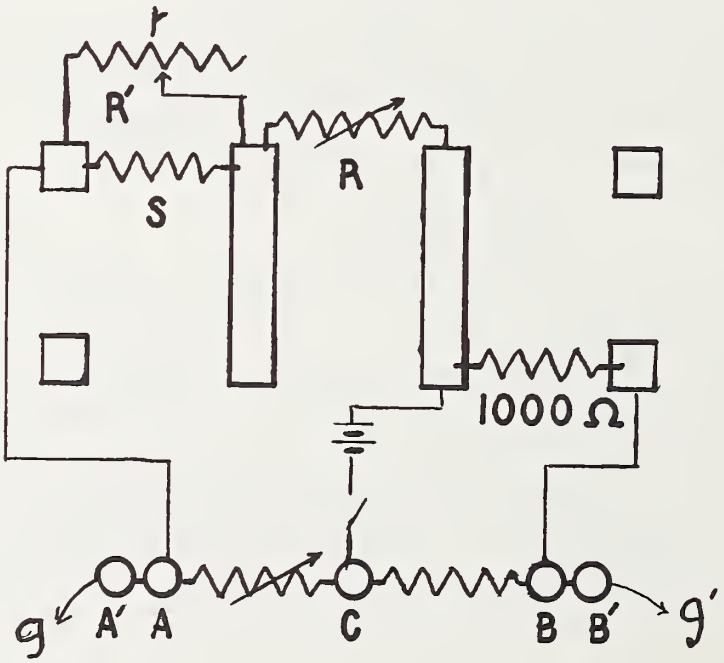

FIGURE 6. - Test circuit for dials III and IV

The test circuit is modified as shown in figure 6 by using a standard resistor, S, in parallel with a decade box, r, to produce a variable resistance, R', which can be increased in accurately-known increments approximately proportional to the steps on the DRRS dial. The decade box, r, is adjustable in steps of 0.1 ohm, accurate to 0.001 ohm. Values of S and r have been determined so that an increase of 0.1 ohm on the decade box will increase the parallel resistance, R', 0.01 ohm each step within the range of the dial with sufficient accuracy. For dial III, the value of S is 1000 ohms and the values of r range, in 0.1 ohm steps, from 2162.0 ohms for step 0 on the DRRS dial to 2163.0 ohms for step 10. R' will be about 684 ohms, so about 316 ohms will be required on R to balance the circuit.

Procedure:

Step 0 - Set dial III on 0, dial IV in advance of 0. Adjust r to 2162.0 ohms. Balance the circuit with R.

Step 1 - Increase r 0.1 ohm (2162.1). Advance dial III to step 1. If the circuit is still balanced (or nearly balanced) the correction to step 1 is zero. If a better balance is obtained with a different setting of dial IV take the correction from dial IV as for the preceding dials.

Step 2 - Return dial IV to its initial setting. Rebalance the circuit with R. Increase r 0.1 ohm (2162.2). Advance dial III to step 2. If the circuit is still balanced, the correction is zero. Otherwise, find the correction from the change in dial IV.

Follow the above procedure for each step. Make a step-by-step summation of corrections.

The following table includes data from a test of dial III. Column D_0 shows the initial setting of the dials for the test of the step. After the circuit was balanced with the balancing resistor, R, the decade resistance, r, was increased 0.1 ohm to the value shown in column r, dial III was advanced one step, and dial IV was adjusted, if necessary, to restore balance, giving the dial setting shown in column D_1.

TABLE III. - Data from a test of dial III

STEP	r	D_0	D_1	Cor. ppm	Σ ppm
0	2162.0	0003	----	--	--
1	2162.1	0003	0013	0	0
2	2162.2	0013	0024	-1	-1
3	2162.3	0023	0033	0	-1
-	------	----	----	--	--
X	2163.0	0093	00X3	0	-1

If an error of one or two parts per million is not objectionable, the same procedure may be used for dial II. For S use a 1000-ohm standard resistor and advance the decade resistance, r, in 1-ohm steps from 2157 ohms for step 0 to 2167 ohms for step 10.

Dial IV, 0.0001 Ohm Per Step

The procedure is the same as for dial III. Use a 100-ohm standard resistor on the stand in parallel with the decade box, r. Increase r in 0.1-ohm steps from 899.5 ohms for step 0 on the DRRS dial to 900.5 ohms for step 10.

Dial IV can be tested by the procedure outlined for dial II. The required resistances are 1 ohm in a standard resistor and 999 ohms. A 1000-ohm standard resistor instead of 999 ohms in a plug box is quite satisfactory. The resistance of the two standards in parallel is 0.999 ohm. When the link is removed from the stand to disconnect the 1000-ohm standard the resistance of the arm is increased 0.001 ohm.

Summary

As explained above, the Direct Reading Ratio Set forms the lower arms of a Wheatstone bridge. The ratio of the 1000-ohm upper arms can be varied to correspond to any change in the ratio of the DRRS arms. This is done by resistance increments in the left upper arm which are proportional to the nominal values of the dial steps on the DRRS. Resistance elements which provide accurately known increments for each dial are as follows:

Dial I. - A 1-ohm standard resistor in combination with a link to introduce the required increment into the arm.

Dial II. - A 10-ohm standard resistor in the arm. A resistance of 990 ohms in a plug box which can be connected in parallel with the standard by a link. Removal of the link increases the resistance of the arm 0.1 ohm.

Dial III. - A 1000-ohm standard resistor in parallel with a plug box. The plug-box resistance is increased in 0.1-ohm steps from 2162.0 ohms for step 0 to 2163.0 ohms for step 10.

Dial IV. - A 100-ohm standard resistor is parallel with a plug-box. The plug-box resistance is increased from 899.5 ohms for step 0 to 900.5 ohms for step 10.

Alternate Methods

Dial II. - A 0.1-ohm NBS type standard resistor (if available) to be used as the 1-ohm standard was used for dial I.

Dial III. - A 10-ohm standard in the arm as used for dial II. A resistance of 9990 ohms in a plug box (or a 10000 ohm standard resistor) which can be connected in parallel with the standard by a link. Removal of the link increases the resistance 0.01 ohm.

Dial IV. - A 1-ohm standard resistor in the arm. Instead of 999 ohms in a plug box, a 1000-ohm standard resistor can be connected in parallel with the 1-ohm standard by a link. Removal of the link increases the resistance 0.001 ohm.

Instead of the above procedures the fixed arms and the dial steps of a DRRS can be measured with a calibrated Mueller bridge if one is available.

USCOMM-NBS-DC

Text corrected November 1967.

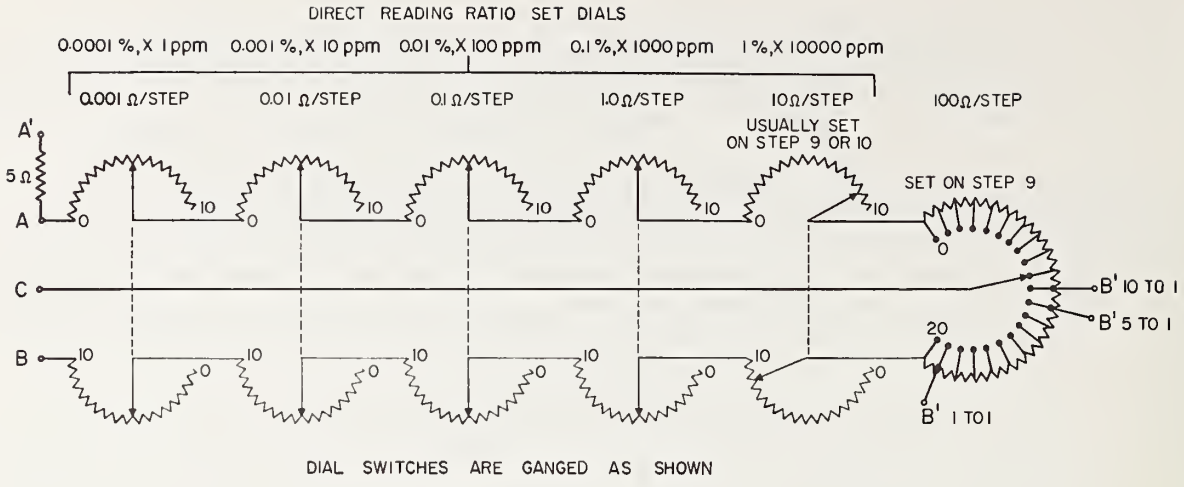

FIG. 1. SIX-DIAL Universal Ratio Set (URS) with provisions for converting URS to a Direct Reading Ratio Set with ratios of 1 to 1, 10 to 1, and 5 to 1.

DIRECT RATIO READINGS FROM A URS

DAVID RAMALEY and JOHN F. SHAFER
National Bureau of Standards

A SIX-DIAL Universal Ratio Set (URS) can be quickly and easily modified for use as either a four- or five-dial Direct-Reading Ratio Set (DRRS) without altering its functioning as a Universal Ratio Set. Such a modification may be a convenience for those who have a limited use for both a Universal Ratio Set and a Direct-Reading Ratio Set, and who now have a Universal Ratio Set but cannot justify the expense of an additional instrument. (It is assumed that the reader is acquainted with the discussion on ratio sets to be found in Section IV of NBS Circular 470. An abstract of this article is presented in *NBS Technical News Bulletin*, Vol. 47, No. 9, September, 1963.)

Using a simple modification, the resulting Direct-Reading Ratio Set has a variable ratio arm of one-thousand ohms, adjustable in steps of 0.001 ohm (one part per million). The conventional four-dial Direct-Reading Ratio Set or Wenner Ratio Set, described in NBS Circular 470 (Ref. 1) and NBS Monograph 39 (Ref. 2) contains a 100-ohm ratio arm adjustable in steps of 0.0001 ohm (likewise one part per million).

The Direct-Reading Ratio Set obtained by modifying a Universal Ratio Set is suitable for measuring re-

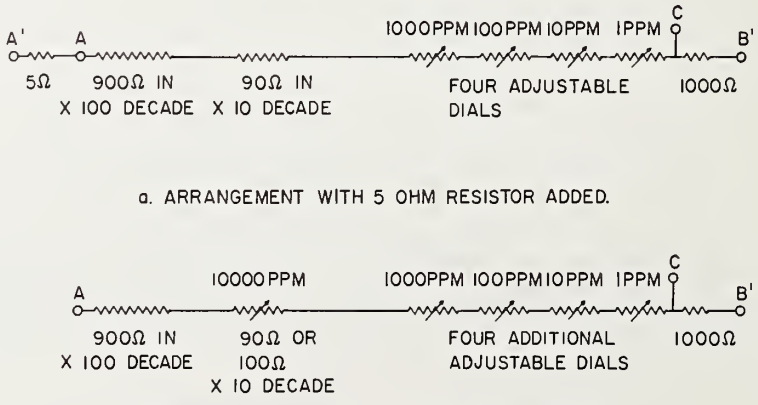

FIG. 2. SCHEMATIC of Direct-Reading Ratio Sets resulting from Modifications of Universal Ratio Set.

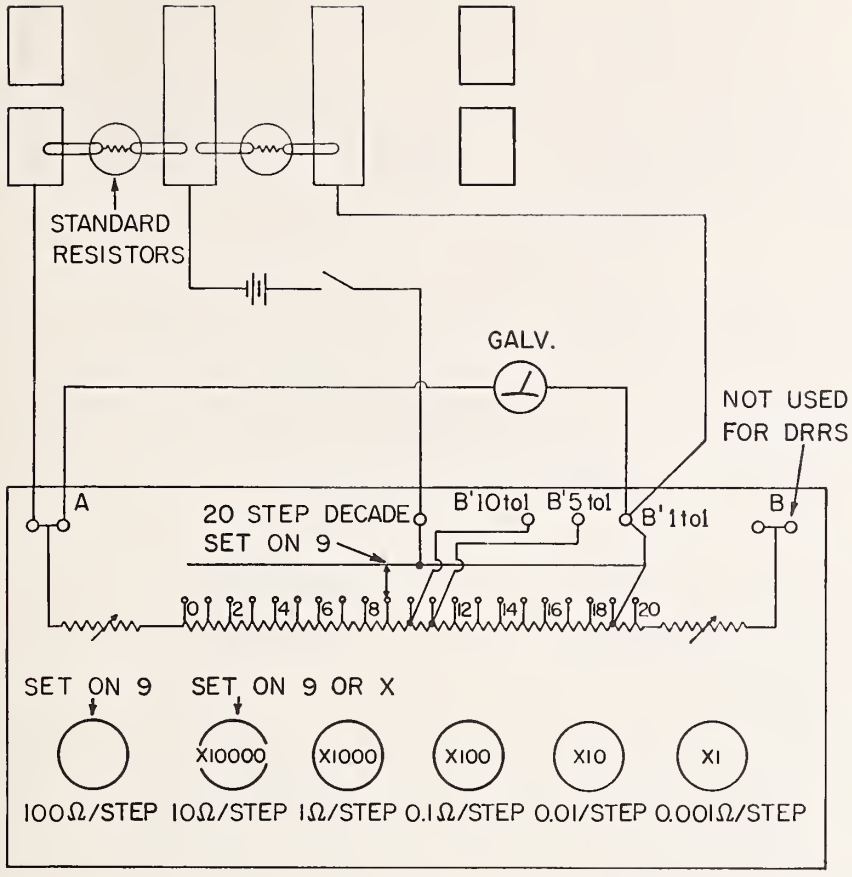

FIG. 3. TYPICAL MEASUREMENT setup using Universal Ratio Set as Direct-Reading Ratio Set.

sistors ranging from about 1 ohm to about 1 megohm. To obtain a precision of a few parts per million, the switch contacts in the adjustable arm should be repeatable within about 0.001 ohm. The ten-step decade dial-switches of most Universal Ratio Sets meet this requirement. The switch contact resistance is not critical in the 20-step (100 ohms per step) decade dial because this resistance is either in the battery branch or galvanometer branch when the instrument is in use.

The modification required to make the adaptation consists of a lead soldered to step 19 on the 20-step dial decade, and terminated in an external binding post $B'_{1\ to\ 1}$ as shown in Fig. 1. A 5-ohm precision quality resistor (or two 10-ohm resistors in parallel) is connected to binding-post A and terminated in a separate binding post, A'. With these additions, the instrument is usable for a 1-to-1 ratio, 4-dial Direct-Reading Ratio Set when the 100-ohm-per-step and the 10-ohm-per-step dials are both set on step 9 for all measurements.

Fig. 2a is the schematic diagram of the resulting Direct-Reading Ratio Set. A fixed resistance of 995 ohms is obtained by the use of the steps of each of the first two decades and the added five-ohm resistor. The four lowest URS decades constitute the adjustable DRRS dials. These dials become the X1000, X100, X10, and X1 part-per-million step dials, respectively.

This modification can be simplified even more by omitting the 5-ohm resistor, if the user is willing to read five dials instead of four. When the 5-ohm resistor is omitted (as shown in Fig. 2b), some of the readings for the Direct-Reading Ratio Set will necessitate setting the 10-ohm-per-step dial on step 9, and others will necessitate setting this dial on step 10.

This modified Universal Ratio Set will actually cover a larger ratio range when step changes in the 10-ohm-per-step dial are made. Therefore, when making computations of reading differences, it will be necessary to record the readings of the 10-ohm-per-step dial, as well as the four lowest dials. (We are considering a ratio range of 0.995 to 1.005, such as is covered by most conventional Direct-Reading Ratio Sets.)

A Direct-Reading Ratio Set capable of measuring ratios of 10-to-1 or 5-to-1 can be arranged by soldering additional leads into other steps of the Universal Ratio Set. For a 10-to-1 ratio, a lead should be soldered into step 10 on the twenty-step dial and, for a 5-to-1 ratio, a lead is soldered to step 11. These additional ratio connections are shown to the added $B'_{10\ to\ 1}$ and $B'_{5\ to\ 1}$ binding posts in Fig. 1.

Fig. 3 is a schematic diagram of a URS modified to a DRRS, and arranged to compare standard resistors in a Wheatstone Bridge circuit using a 1-to-1 ratio.

References

1. J. L. Thomas, *Precision Resistors and Their Measurement*, NBS Circular 470.

2. P. P. B. Brooks, *Calibration Procedures for Direct Current Resistance Apparatus*, NBS Monograph 39.

Reprinted from the January 1966 issue of—*Instruments & Control Systems*

JOURNAL OF RESEARCH of the National Bureau of Standards—C. Engineering and Instrumentation
Vol. 64C, No. 4, October–December 1960

A Method of Controlling the Effect of Resistance in the Link Circuit of the Thomson or Kelvin Double Bridge*

David Ramaley

(May 12, 1960)

Circuitry of the double bridge is reviewed to emphasize the significance of the link circuit as a part of the bridge network. A simple analysis demonstrates the need of some equivalent or substitute for low link circuit resistance in situations where adequately low link circuit resistance cannot be achieved physically. An appropriate method of controlling the potential difference in the link circuit is shown to accomplish the same effect as an actual reduction of resistance in the link circuit. The simple circuit modifications required to utilize this method are explained. A step-by-step procedure is outlined for making measurements with bridges incorporating these modifications, and some typical examples are discussed illustrating the advantages realized.

1. Introduction

Double bridges of the Kelvin type are convenient not only for the measurement of low-resistance standards, conductivity samples, and components, but also for calibrating resistors incorporated as intrinsic parts of circuits. When using the double bridge for calibrating resistors permanently connected in circuits, it is sometimes not feasible to achieve an arrangement with a link circuit of sufficiently low resistance. For such situations the precision of measurement will be diminished if the usual procedure is followed in balancing the bridge.

The method outlined in this paper utilizes a supplementary power source and an auxiliary galvanometer to minimize the potential difference in the link circuit.[1] The application of this method has been found to reduce substantially the effect of excessive link resistance, and its practicability has been demonstrated in several different situations.

Descriptions and uses of double bridges are given in references listed at the end of this paper.

2. Review of Double-Bridge Fundamentals

Figure 1 is a circuit commonly used in double bridges. X and S are four-terminal resistors; X is the unknown and S is a reference standard of known resistance. The link circuit is designated as L and includes the resistance of the link itself and also the additional resistance in the circuit between the resistor branch points m and n. A and B are the main ratio arms, and a and b are the auxiliary ratio arms. These same symbols are used also to refer to resistance values. The ratio arms are connected to the potential terminals of X and S by leads designated as L_A, L_B, L_a, and L_b. When these notations are used to indicate lead resistances, they include not only the resistances of the external connectors but all resistances between the ratio arms and the resistor branch points m, n, etc. Leads L_A and L_a are constructed to be conveniently varied in resistance by means of built-in adjustable rheostats. P is a direct current power source such as a battery, R is a reversing switch, and G is a suitable galvanometer.

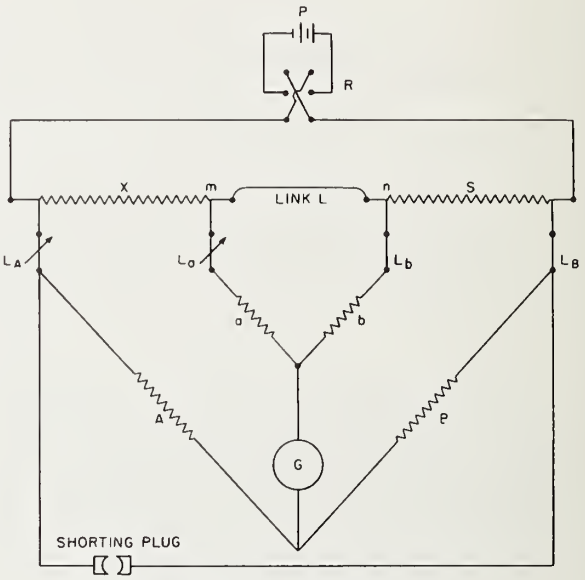

FIGURE 1. *Double bridge.*

The delta network consisting of the two auxiliary ratio arms and the link circuit can be transformed readily into the equivalent Y network. The resistance of that branch of the Y between the Y junction point and m, adjacent to the resistor, X, is $L(a+L_a)/(a+L_a+b+L_b+L)$. The resistance of that Y branch, between the Y junction and n, adjacent to the resistor, S, is $L(b+L_b)/(a+L_a+b+L_b+L)$. The third Y branch is in series with the

* Contribution from the Radio Standards Laboratory, National Bureau of Standards, Boulder, Colo.

[1] This method was suggested by the late Dr. Frank Wenner of the National Bureau of Standards in 1940.

galvanometer and need not be considered in the present discussion because it does not affect the position of bridge balance.

This transformation enables one to treat the double bridge as a simple Wheatstone arrangement, from which one obtains the equation of balance:

$$\frac{A+L_A}{B+L_B}=\frac{X+\dfrac{L(a+L_a)}{(a+L_a+b+L_b+L)}}{S+\dfrac{L(b+L_b)}{(a+L_a+b+L_b+L)}}. \tag{1}$$

When rearranged this equation becomes

$$X=\frac{(A+L_A)S}{(B+L_B)}+\frac{L(A+L_A)(b+L_b)}{(B+L_B)(a+L_a+b+L_b+L)} -\frac{L(a+L_a)}{(a+L_a+b+L_b+L)}. \tag{2}$$

If the substitions:

$$\frac{A+L_A}{B+L_B}=\frac{A(1+g)}{B}, \tag{3}$$

$$\frac{a+L_a}{b+L_b}=\frac{A(1+h)}{B}, \tag{4}$$

and

$$\frac{L(b+L_b)}{S(a+L_a+b+L_b+L)}=D \tag{5}$$

are made, eq (2) becomes

$$X=\frac{SA[1+g+D(g-h)]}{B}. \tag{6}$$

This can be considered a fundamental equation of the double bridge and can be reduced to the simple Wheatstone equation, $X=SA/B$, provided the terms g and $D(g-h)$ can be made negligible. This is achieved in practice as follows: With A and B shorted out and with the bridge essentially balanced, the term, g, commonly is made very small by adjusting L_A so that the leads L_A and L_B have nearly the same ratio as X to S or A to B. The term, h, is made closely equal to g by making a/b as nearly as possible the same as A/B, not only by using a common set of controls for the main and auxiliary ratio arms but also by removing the link and then making a balance by adjusting the ratio L_a/L_b to nearly X/S or A/B. The term D usually is much smaller than one and normally is minimized by using a link circuit of low resistance.

In some situations it is impractical to arrange a link circuit with suitably low resistance. Then the balancing procedure employed in minimizing the term $(g-h)$ must be accomplished with much higher precision to avoid deterioration in accuracy. This necessity is evident from the term $D(g-h)$ in eq (6). If L is large, D also is proportionately large, and the term $(g-h)$ must be made extremely small. However, this requires extremely fine adjustment of the leads, and some double bridges are not provided with means of making sufficiently precise lead adjustments, so that the accuracy of measurement is definitely limited. A reduction in accuracy under conditions of excessive link circuit resistance therefore may be unavoidable unless one makes some modification of the usual double bridge. Such a modification is described below. It minimizes the effect of link resistance even though the actual resistance of the link is abnormally high.

With the bridge in balance and power applied, the ratio of the potential difference E_L, developed across the link circuit, to the sum of the potential differences E_X+E_S, developed across the resistors X and S, is given by

$$\frac{E_L}{E_X+E_S}=\frac{L(a+L_a+b+L_b)}{(a+L_a+b+L_b+L)}\cdot\frac{}{X+S}. \tag{7}$$

When all circuits of the bridge have been properly adjusted, the ratio of S to X is almost identical to the ratio of $B+L_B$ to $A+L_A$ and also to the ratio of the corresponding auxiliary branch arms. It may be assumed with sufficient accuracy that

$$\frac{S}{X+S}=\frac{b+L_b}{a+L_a+b+L_b}. \tag{8}$$

Combining eqs (7) and (8) gives

$$\frac{E_L}{E_X+E_S}=\frac{L(b+L_b)}{S(a+L_a+b+L_b+L)} \tag{9}$$

which from eq (5) is the term D. For practical use, then, the double bridge eq (6) may be written as

$$X=\frac{SA}{B}\left[1+g+\frac{E_L(g-h)}{E_X+E_S}\right]. \tag{10}$$

Consequently, reduction of the potential difference E_L across the link circuit would produce the same effect as reduction of the link resistance and would eliminate the necessity of adjusting the ratios L_a to L_b and L_A to L_B with higher precision than ordinarily used when the link resistance is small. This can be accomplished by introducing into the link circuit a potential difference of such magnitude and polarity that the potentials at the branch points m and n are brought to practically the same value. This applied potential difference is introduced across an auxiliary resistor of appropriate magnitude which has been inserted into the link circuit.

3. Double Bridge Modification for Abnormal Link Circuit Resistance

Figure 2 is the circuit of the modified double bridge. P' is the auxiliary power supply. Z is the resistor inserted into the link circuit across which the auxiliary potential difference is applied. R and R' are reversing switches which can be operated simultaneously. G' is an auxiliary galvanometer

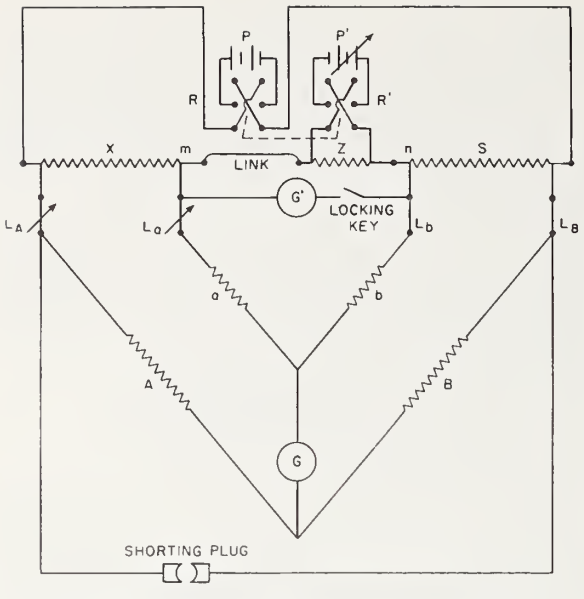

FIGURE 2. *Double bridge with modified link circuit.*

used in detecting potential differences in the link circuit. The auxiliary galvanometer is connected as shown rather than to m and n because of physical difficulties sometimes encountered in connecting directly to the branch points. By varying the potential difference applied to Z from the auxiliary power source, the potentials at the branch points can be adjusted to practically the same value.

The modified double bridge can be balanced by the following steps:

(1) With both battery circuits closed, the potential difference indicated by the auxiliary galvanometer is minimized by varying P'.

(2) A preliminary balance of the bridge is made by adjusting in unison the main and auxiliary ratio arms while operating the two reversing switches simultaneously until a balance is indicated by the main galvanometer.

(3) The leads in series with the main ratio arms are adjusted to the proper ratio by shorting out the main arms and adjusting one of these leads. Both power sources are used simultaneously, and the balance is indicated by the main galvanometer.

(4) With the main power supply disconnected, the lead resistances in series with the auxiliary ratio arms are adjusted to the proper ratio by varying one of the leads until balance is indicated by the main galvanometer. Current is supplied by the auxiliary power supply. An alternate method of adjustment, commonly followed for double bridge operation, is to open the link circuit and use only the main power supply while adjusting the leads to the auxiliary ratio arms.

(5) Final balance is achieved by repeating step 2. If the bridge is too far out of balance at the outset, a repetition of steps 3, 4, and 2 may be required.

The readings of the bridge ratio arms A and B corresponding to the final balance are used to compute the value of the resistor X.

Except for step 1, involving the auxiliary galvanometer, the above procedure is that commonly used in balancing a double bridge. The selection of circuit components as well as the precision necessary in making the adjustments in steps 1 to 5 will be governed by the particular case under consideration and the desired accuracy of measurement. Ordinarily step 1 is not unduly critical. However, good stable power supplies and switches are required, since variations in either power source adversely affect the accuracy obtainable with the modified double bridge.

This modification was developed in connection with the calibration of a special microvolt potentiometer. The measuring circuit of this potentiometer utilizes low-resistance elements connected in series within a thermally shielded enclosure. In the measurement of one of these resistors using a double bridge, current lead connections were found to be feasible only by incorporating the adjacent, permanently connected, circuit resistors. This arrangement produced an abnormally high link circuit resistance, and the resulting ratio of the link circuit resistance to the sum of the resistances of X and S was approximately 10. With the modified double bridge, however, it was feasible to measure the low-resistance element to the desired accuracy.

4. Examples

The improvement in accuracy achieved by use of this modification can be evaluated for each individual case. It depends upon the resistors under comparison and upon the bridge parameters. Both the main and auxiliary ratio arms commonly have resistances of 50 to 500 ohms. Lead resistances commonly range in magnitude from 0.01 to possibly 2 ohms. Resistors suitable for comparison in a double bridge may range in magnitude from a few microhms to about an ohm.

An arrangement that will serve as an example for this ordinary range of measurements will now be considered. Let us assume that four-terminal 0.001 ohm resistors X and S are to be compared in a bridge with ratio arms of approximately 100 ohms and lead resistances of about 1 ohm, and that the ratio of A to B can be adjusted to or estimated to about one part in a million. The accuracy of adjustment of the resistor S and the ratio of A to B will be considered to be known adequately. The uncertainty associated with these terms outside of the bracket in eq (6) is a systematic error inherent in the measurement regardless of the arrangement of the link circuit or lead connections and is not relevant to the present consideration. We are concerned primarily with the effect of link resistance and the precision of lead balances upon the correction terms g and $D(g-h)$ in eq (6). Let us assume that a precision of ± 30 ppm is desired and that the expression SA/B can be treated as a constant during the adjust-

ments. The sum of the correction terms g and $D(g-h)$ in eq (6) can differ with each successive measurement depending upon how consistently balances are executed but in no case should exceed ± 0.00003 at the time of reading if the desired precision is to be maintained. Ordinarily a very low-resistance shorting link can be used and the term D in eq (5) or its equivalent $E_L/(E_X+E_S)$ or $L/(X+S)$ is less than or equal to one. To maintain the desired precision for this situation, g and h each can be as large as ± 0.00001 without giving $g+D(g-h)$ a value larger than ± 0.00003. The ratio arms including the leads need not be balanced more precisely than ± 10 parts in a million or ± 0.001 ohm. This implies that the leads must be adjusted to one part in a thousand because they are 1 ohm in magnitude. If this is accomplished, each of the terms g and h in eqs (3) and (4), will be not larger than ± 0.00001 and the sum of g and $D(g-h)$ will be not larger than ± 0.00003.

Next consider the situation in which it is impossible to arrange a link circuit so low in resistance that D can be held to a value of one or less. The expression $D(g-h)$ can be held within the prescribed limit only by adjusting the leads more closely than ± 0.001 ohm because $(g-h)$ must be decreased to the same extent that D is increased. Contact resistance variations in adjustable lead circuits commonly exceed 0.0001 ohm and thus may limit the fineness of lead adjustment. Furthermore, some rheostats used for the adjustable leads may not be variable in steps finer than 0.001 ohm. If we assume such excellent conditions that variations in contact resistances of ± 0.0001 ohm constitute the factor limiting the fineness of adjustment of leads, g and h in eqs (3) and (4), can be reduced to ± 0.000001 and $(g-h)$ to a maximum of ± 0.000002. For these values D must be smaller than 15 if diminished precision is to be avoided. For $D=15$, $g+D(g-h)$ could be a maximum of $\pm 0.000001 \pm 15(\pm 0.000001 \pm 0.000001)$ or ± 0.000031 which is slightly larger than the permissible ± 0.00003.

If in the comparison of the above 0.001-ohm resistors, the value of L cannot be physically reduced below 0.05 ohm, D will be about 25, as computed from eq (5). The terms $g+D(g-h)$ will be equal to ± 0.000051 if the leads can be adjusted to ± 0.0001 ohm and to ± 0.00051 if the leads can be adjusted to ± 0.001 ohm. If the link potential difference is reduced by a factor of 25, then for making a measurement, the conditions are the same as if D were actually no greater than one. In considering again the favorable condition in which the leads can be adjusted to 0.0001 ohm, the improvement in precision obtained by reducing the link potential will be in the ratio of 0.000051 to 0.000031 or a factor of about two. In the case of the bridge in the less favorable condition, the precision gained will be about 0.00051 to 0.00003 or about 17. These same factors likewise can be regarded as representing an unavoidable loss in precision if this modification is not employed. Other examples with different circuit values and requirements can be treated in like manner.

5. References

[1] F. Wenner, The four-terminal conductor and the Thomson Bridge, Bul. BS 8, 559 (1912) S181.

[2] F. Wenner, Methods, apparatus, and procedures for the comparison of precision standard resistors, J. Research NBS **25,** 229 (1940) RP1323.

[3] J. L. Thomas, Precision resistors and their measurement, NBS Circ. 470 (1948).

[4] F. K. Harris, Electrical measurements, p. 282–288 (John Wiley & Sons, Inc., New York, N.Y., 1952).

(Paper 64C4–44)

JOURNAL OF RESEARCH of the National Bureau of Standards—C. Engineering and Instrumentation
Vol. 67C, No. 1, January–March 1963

Method for Calibrating a Standard Volt Box

Bernadine L. Dunfee

(August 22, 1962)

A volt box provides several diserete ratios and permits the accurate measurement of direct voltages (maximum about 1,500 volts) through their reduction by suitable factors to values within the measuring capability of a potentiometer. The ratios of a volt box are measured against those of a standard using a "difference" technique. The standard volt box used at the National Bureau of Standards possesses those design features required for a ratio standard and lends itself to a "self-calibration" technique. This paper describes a method for measuring its ratios at rated and above rated voltage to an accuracy of 10 parts per million or better using a Direct Reading Ratio Set and a group of resistance standards. Although the method is described in its particular application to the NBS standard it can be used equally well in the measurement of other ratio networks. Errors that might appear in the measurements and procedures for evaluating their magnitudes are outlined and the derivation of a general expression that defines all ratios in terms of measured quantities is presented in an appendix. Comments and further details regarding the standard and its use are included.

1. Introduction

The value of a measured voltage, either direct or alternating, is derived from the national standard of emf. At the National Bureau of Standards the unit of voltage is maintained in terms of the mean value of emf of 48 saturated cells. This emf is only slightly larger than one volt so that the accurate measurement of larger voltages of any frequency usually requires the design of special ratio networks that can serve as voltage ratio standards, because of their stability and high accuracy. The volt box and the potentiometer with which it is used are classic examples in the measurement of moderately high direct voltages.

The volt box referred to here, as differentiated from other types of d-c ratio devices (or voltage dividers), provides several discrete ratios so that the voltage to be measured (maximum about 1,500 v) is reduced by a suitable factor to a value within the measuring capability of a potentiometer. Insertion of a volt box in a measuring circuit introduces an error in the measurement unless the volt box divides perfectly or the corrections to its nominal ratios are known and applied. In any event, each ratio must be measured, preferably at rated voltage and at a reduced voltage to evaluate the effects of self heating and leakage resistance.

The method of calibration employed at NBS utilizes a difference technique in which the potential at each binding post of a volt box under test is measured with respect to that at the corresponding binding post of the standard volt box, with both instruments connected in parallel and for the same nominal ratio. Special features must therefore be incorporated in the standard volt box to assure long term stability and the resistance sections must be arranged in a proper sequence with respect to magnitude so that a "self-calibration" procedure is possible and accurate to better than 10 parts per million (ppm). The standard volt box used at NBS, as well as a method developed for its calibration, have been described by Silsbee and Gross [1].[1]

A second method for calibrating the standard volt box was recently developed and has been under observation for more than a year. The associated circuitry and components have been incorporated in a semiportable test console and the only connections that need be made at the time of test are those to the d-c supply and to the volt box. The present paper describes this method and uses the NBS standard volt box to illustrate the technique. Additional comments are included on the use of the standard volt box in calibrating other volt boxes.

2. Comments on the Calibration of a Volt Box Against the Standard

A volt box consists, in general, of a large number of resistance coils connected in series. At both the low- and high-potential ends and at appropriate junctions along the resistor, taps are brought out to binding posts to form the high voltage side. The maximum voltage that can be applied between the zero post and any of the others is governed by the design of the resistance coils and is so marked at each binding post. In addition, the resistance of the lowest section is tapped at an appropriate point and

[1] Figures in brackets indicate the literature references at the end of this paper.

leads are brought out from the zero potential end and this tap point to binding posts, forming the low voltage side for connection to a potentiometer. Any given voltage ratio is defined as the ratio of the voltage applied to the high side to that appearing across the low side. These ratios are integers and a given volt box, for example, may cover values from 1,500/1.5 to 3/1.5 if it is to be used with a 1.5-v potentiometer or values from 1,500/0.15 to 3/0.15 for a 150-mv potentiometer.

The test instrument is calibrated with reference to the standard in the circuit shown schematically in figure 1. The two volt boxes, having the same nominal ratio, are connected in parallel through leads l_1 and l_2 across a suitable d-c source. The measuring branch, consisting of a detector, a low range potentiometer, and a reversing switch (not shown), is inserted, in voltage opposition, into gaps identified at positions v_1, v_2, v_3, and v_4. For each position the output of the potentiometer is adjusted for a null on the detector so that at balance the potential difference between corresponding points on the two volt boxes is equal to that of the potentiometer. The potential differences v_1 and v_4 are small since they are essentially the potential drops in leads l_1 and l_2; similarly, if the volt box under test is of high quality, potential differences v_2 and v_3 will be small. Thus only moderate accuracy is required in the measurement of the potential differences in order to realize an extremely high accuracy for the values of ratio.

The equation that defines the ratio of the volt box under test in terms of the ratio of the standard and the measured potential differences may be derived as follows. Let the respective polarities be as shown in figure 1. By definition, the true ratio of the volt box under test is

$$N_{xt}=N_{xn}[1+\mu_x]=\frac{V}{V_{ab}} \tag{1}$$

where μ_x is the correction in proportional parts and N_{xn} is the nominal ratio.

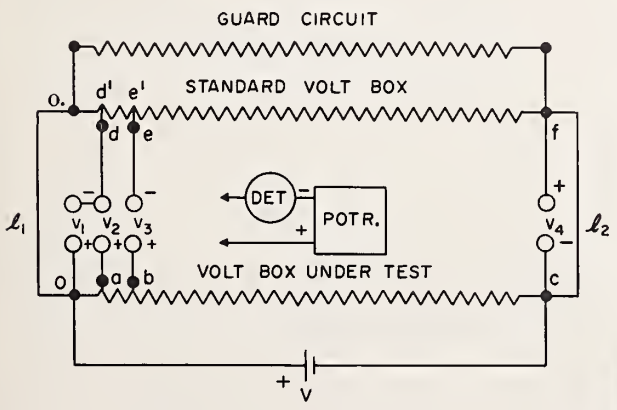

FIGURE 1. *Circuit for calibrating a volt box.*

Summing the potential drops around loop "badeb" gives

$$V_{ab}-v_2-V_{de}+v_3=0$$

or

$$V_{ab}=V_{de}+(v_2-v_3). \tag{2}$$

By definition, the true ratio of the standard volt box is

$$N_{st}=N_{sn}[1+\mu_s]=\frac{V_{df}}{V_{de}}$$

or

$$V_{de}=\frac{V_{df}}{N_{sn}[1+\mu_s]}$$

where N_{sn} is the nominal ratio of the standard and μ_s is the correction in proportional parts. Substituting this value in eq (2) gives

$$V_{ab}=\frac{V_{df}}{N_{sn}[1+\mu_s]}+(v_2-v_3). \tag{3}$$

Summing the potential drops around loop "defcod" we have

$$-V_{df}-v_4+V-v_1=0$$

or

$$V_{df}=V-(v_1+v_4).$$

When this expression is substituted in eq (3) V_{ab} becomes

$$V_{ab}=\frac{V-(v_1+v_4)}{N_{sn}[1+\mu_s]}+(v_2-v_3)$$

and if substituted in eq (1) the true ratio of the volt box under test becomes

$$N_{xn}[1+\mu_x]=\frac{VN_{sn}[1+\mu_s]}{V-(v_1+v_4)+N_{sn}[1+\mu_s](v_2-v_3)}.$$

On rearranging terms and remembering that $N_{xn}=N_{sn}\approx N_{sn}[1+\mu_s]$ the above expression becomes

$$[1+\mu_x]=\frac{[1+\mu_s]}{1-\frac{(v_1+v_4)}{V}+N_{sn}\frac{(v_2-v_3)}{V}}$$

so that

$$\mu_x=\mu_s+\frac{(v_1+v_4)}{V}-\frac{(v_2-v_3)}{V/N_{sn}} \text{ plus higher order terms.} \tag{4}$$

If v_1, v_2, v_3, v_4, and V are expressed in volts then, neglecting higher order terms, the correction to the nominal ratio is

$$\mu_x=\mu_s+\frac{(v_1+v_4)}{V}+\frac{(v_3-v_2)}{V/N_{sn}} \text{ in proportional parts.} \tag{5}$$

If v_1, v_2, v_3, and v_4 are expressed in microvolts and μ_s in ppm the correction is given in ppm. It should be noted that if the relative polarities of the supply voltage (V) and the potentiometer differ from those assumed in figure 1, the appropriate sign must be given to the recorded values of the measured quantities.

As will be seen later in the discussion on the calibration of the standard volt box, the measured resistances of all sections and their summations are referred to the resistance of the first section which is chosen to lie between junctions $d'-e'$. Thus the true ratio of the standard volt box, given as $\frac{V_{af}}{V_{de}}$ in the above derivation, is consistent with the measured ratio. (The effects of rod resistances,[2] such as o.d.′, on the measured ratios are discussed in the section on errors.)

It is advisable that the potential drops in leads l_1 and l_2 be small in order to achieve the highest accuracy in the measured ratios without placing undue demands on the accuracy required in the measurement of the potential differences. A slight modification made in the test circuit would eliminate the lead effect and at the same time simplify the computation of test data. Referring to figure 2, let small resistances R_1 and R_2 be connected in the l_1 and l_2 branches with the d-c supply connected between their sliding contacts. The potential drops in the two sections of branch l_1, as well as those in branch l_2, are in opposition so that it is only necessary to adjust the respective sliders to achieve cancellation, which is indicated by a null on the detector connected at the v_1 and v_4 positions, respectively (see fig. 1). For this condition, the second term on the right of eq (5) becomes zero.

3. Standard Volt Box

A volt box must have several special features incorporated in its design if it is to serve as a standard in making ratio measurements to an accuracy of a few ppm. (1) Some provision must be made for reducing the effects from leakage paths to negligible amounts; (2) the selection and arrangement of the resistance wire must guarantee freedom from the effects of relative humidity as well as those arising from self-heating; (3) the corrections to the ratios should be small and the resistances of the tapped sections proportioned so that a "self-calibration" procedure of sufficient accuracy is applicable.

3.1. Leakage

The volt box is a high resistance network operating at rather high voltages so that careful consideration must be given to minimizing leakage paths into which a portion of the current may be diverted from points along the working resistance. Effects from such parallel paths may be reduced sufficiently by keeping the insulation resistance high. For example, if the total resistance of the high side is 250,000 ohms, the resistance of a leakage path bridging this section must be 2.5×10^9 ohms for an uncertainty no greater than 0.01 percent, and 2.5×10^{11} ohms if an error no greater than 1 ppm is required. This protection

[2] The rod resistances mentioned throughout the text refer to the leads which extend from the resistance sections to the binding posts where connections are made to the external circuit.

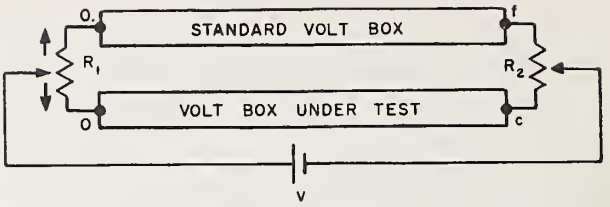

FIGURE 2. *Branches for compensating lead drops.*

may not be adequate in maintaining long-time stability because of possible accumulation of moisture and contamination across the insulating surface or possible deterioration of the insulation over long use. Additional protection must be provided by a guard network which, in effect, maintains the shields surrounding the resistance sections at the same potential as that of the resistance section within.

The standard volt box discussed here is equipped with a guarding resistance whose corresponding sections can be connected in parallel with the working circuit when the 15-v and higher ranges are used. Metal guard rings surrounding each binding post of the working resistance and connected to the corresponding binding post of the guarding resistance prevent leakage across and through the top panel. The working resistance is divided into sections of not more than 25,000 ohms with the resistance coils of each section mounted on separate insulating panels. Each of these insulating panels is fastened to the top panel through a metal block that is connected to the guard resistance and maintained at the appropriate potential to prevent leakage from one insulating panel to another. In use, leads that connect the standard volt box to the volt box under test and to the other parts of the measuring circuit carry their own shields which are maintained at their appropriate potentials through connections to the binding posts of the guard circuit.

3.2. Humidity and Self-Heating

Any effect from relative humidity on a properly guarded volt box originates at the resistance coils. It has long been known that certain insulating materials used for wire covering and for protective coatings of resistance coils are susceptible to changes in relative humidity and produce changes in the resistance of the coils. Although the effect might be expected to be negligible in materials available today or, if not, to be sufficiently suppressed in ratio devices, the matter must be considered if accuracies of a few ppm are desired. The particular standard volt box referred to in the original paper was found to have seasonal variations as large as 30 ppm as a result of changing humidity, so that provision was made for continuously supplying dry air at a pressure slightly higher than atmospheric. In 1960 a new unit was purchased in which the individual resistance coils are hermetically sealed. To date, no measurable seasonal variations because of changing humidity have been observed.

In theory, the effects from self-heating could be measured and the appropriate correction applied; but these effects can be avoided by designing the unit for lower rated current, by selecting the proper kind of resistance material and by providing the coils with sufficient cooling surface within an adequate exchange volume. Both the original standard and the one recently acquired have a working resistance of 333 ⅓ ohms/v and each coil is wound with a single layer of manganin wire taken from the same spool. There is sufficient freedom from self-heating that, with double rated voltage applied, the correction differs from that at reduced voltage by less than 5 ppm.

3.3. Self-Calibration Feature

The most difficult and critical problem encountered with any standard is the determination of its corrections to an accuracy considerably better than that required for the test instrument. The method should not only satisfy the immediate requirements in accuracy but should be capable of providing still better accuracy in the anticipation of future demands.

One of the most powerful measuring techniques available and one capable of the highest accuracy is that in which small differences are measured between like and nearly equal quantities. The circuit suggested by Silsbee and used in the designs of both standard volt boxes lends itself to this "difference" technique. Its arrangement and adaptation to difference measurements can be best understood by referring to figure 3. The circuit has 21 tapped sections beginning with the "0 to 0.15" section of 50 ohms and continuing to the "750 to 1500" section of 250,000 ohms.[3] This resistance chain can be considered as being formed of four groups M_1, M_2, M_3, and M_4 in which group M_1 serves as the first section of group M_2, M_2 as the first section of group M_3, and M_3 as the first section of group M_4. Being so considered the following pattern is observed. Each group contains six sections. The first five sections of any group have nominally equal resistances while the sixth section has a value nominally equal to the sum of the first five. It is possible, therefore, to measure the small differences between the first 50-ohm section and each of the remaining four sections of group M_1, and follow this by measuring the difference between the 250-ohm section and the sum of the first five sections. Since M_{n-1} forms the first section of M_n this measuring sequence can be repeated for each group in turn. Because of the continuity within a group and from one group to the next, the resistance of any portion summed from the zero end, compared with that of the first 50-ohm section can be computed from the nominal value of their ratio and the sum of the measured differences.

4. Direct Reading Ratio Set Test Method

With the rapid growth of standards laboratories evident in recent years, voltage ratio standards of the type discussed here are no longer the exclusive property of the National standardizing laboratory. The method recently adopted at NBS for calibrating the standard volt box and described herein makes use of equipment that is readily available in many of these laboratories. Thus, from the information that is given on both the theoretical and practical aspects of the method, the standards laboratory can perform the calibration without recourse to NBS. The method is not limited solely to those volt boxes having the particular sequence of sections indicated in figure 3 but can be used for any network in which the resistance of each section is nominally equal to the resistance of some combination of lower-valued sections. The only change lies in the defining equation and its derivation.

4.1. General Comments

A Wheatstone bridge network is used in which the successive difference measurements, referred to in the previous section, are made by inserting in turn each section or summation of sections in the unknown arm of the bridge. Aside from a d-c supply and detector, the only equipment required is a Direct

[3] The last section of 250,000 ohms is not present in the standard volt boxes at NBS. It is included here for completeness.

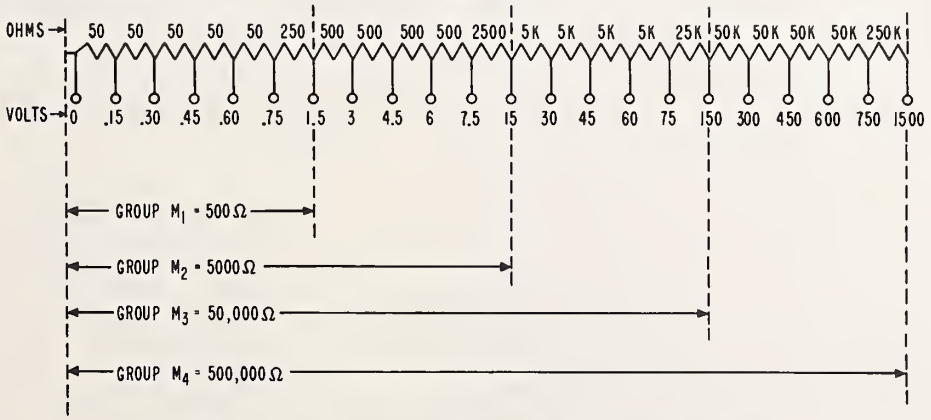

FIGURE 3. *"Self-calibrating" network of a standard volt box.*

Reading Ratio Set (DRRS) and a group of seven resistance standards: one each having the values 50, 200, 500, 2,000, and 5,000 ohms, and two having a value of 50,000 ohms. (Other types of resistors or resistance assemblies could be substituted for the standard resistors if they remain stable during the sequence of measurements.) The execution of the test is quite rapid and with the circuit incorporated in a suitable console a complete calibration including computation can be made in an hour by experienced personnel.

In the original method the test voltage was limited to some extent because of possible heating of the components. For example, measurements on the 50,000-ohm sections, if made at their rated voltage of 150 v, required a power dissipation of 2.25 w in one of the standard resistors. Since it is advisable to keep the power dissipation appreciably less than this amount, periodic calibrations were made at reduced voltage after it was initially established that changes arising from self-heating were negligible. The DRRS method has the advantage that all sections can be measured at their rated voltage. Under this condition the maximum power dissipation required of the standard resistor is 0.45 w. With some of the resistor assemblies now available the method can be extended to measurements at 200 percent rated voltage so that the overload capability of the standard volt box can be easily determined.

The method has a further advantage in that the positions of the supply and galvanometer (detector) relative to the circuit are such that the change in circuit resistance as seen by the galvanometer is quite small. Thus the damping and galvanometer response are little affected throughout the measurements.

4.2. Calibration Procedure

The measuring circuits are indicated schematically in figures 4a and 4b; the reversing switch for the supply is omitted to preserve simplicity. Resistances A and B represent the two arms of a DRRS (including leads) each having a nominal value of 100 ohms and S is a standard resistor always serving as a "Dummy" resistance and having a nominal value equal to that of the volt box section being measured. The guard branch that appears in figure 4b includes a resistance of about 80 ohms [4] in series with the appropriate guard section of the volt box; and the leads of the measuring circuit are of such length and size that at balance the DRRS reads near midscale.

Measurements on the first five sections are made with the circuit of figure 4a. The d-c supply is connected to the 1.5 binding post and the detector to the zero dot (0.) so that rod resistances l_1, l_2 . . . l_{n-1} appear in the A- and S-arms of the bridge rather than as part of the resistance being measured. Inequalities among the rod resistances can introduce errors in the measured ratios and are of greater significance when the low-valued sections are measured. There are three alternatives for locating the rod resistances: (1) both rods may be connected as part of the section being measured, (2) one rod may be so connected and the other located in the S-arm, and (3) they may be arranged as shown in figure 4a. The relative magnitudes of the rod resistances in the NBS standard volt box indicate figure 4a as the preferred connection.[5]

The remaining sections whose resistances are 250 ohms or more are measured in the network of figure 4b. (The rod resistances are expected to be negligible compared with the resistance of the section to which they are assigned.) The guard circuit of the particular standard volt box under discussion is not equipped with taps below the 15-v range so that it is used only on the ranges of 15 v and higher. Thus, for all successive resistances measured after the first five and to, but not including, the "15 to 30" section, the guard branch of figure 4b is not used. For all remaining measurements the guard branch is connected as shown in the figure.

The appropriate bridge network is balanced by adjusting the dials of the DRRS for a null on the detector as each section, or summation of sections, beginning with $R_{1,1}$ is inserted in succession in the "unknown" arm of the bridge. The procedure is as follows. With $S=S_{a1}=50$ ohms, the bridge of figure 4a is balanced with the first 50-ohm section

[4] The resistance per section of the guard of the volt box is 0.8 that of the working resistance.

[5] The influence of these rod resistances can be completely avoided by modifying the circuit so that the 50-ohm sections are measured as 4-terminal resistors. This technique is described in reference [2].

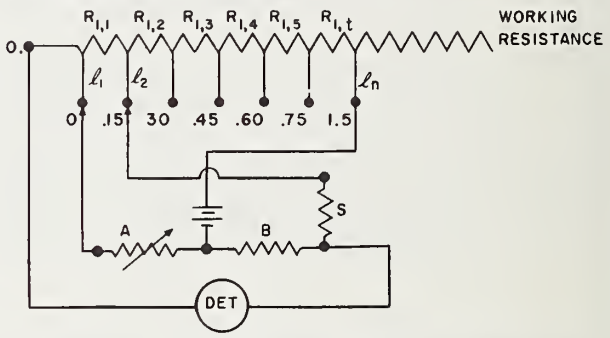

FIGURE 4a. *Circuit for measuring the lower-valued ratios.*

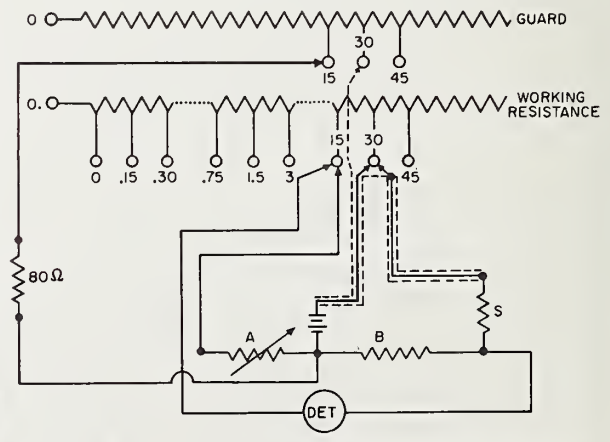

FIGURE 4b. *Circuit for measuring the higher-valued ratios.*

($R_{1,1}$) inserted in the unknown arm. In rapid sequence, each of the remaining four 50-ohm sections is inserted in turn and the bridge rebalanced in each instance. The resistance of each 50-ohm section can now be stated in terms of the resistance of $R_{1,1}$ and the measured difference, and the group can be summed to give $\sum_{k=1}^{k=5} R_{1,k}$ (computed). The next set of balances completes the series of measurements required for group M_1. It consists of two measurements using the appropriate circuit of figure 4b and with $S=S_{b1}=250$ ohms. The reference balance is made with the sum of the 50-ohm sections $\sum_{k=1}^{k=5} R_{1,k}$, having a nominal value of 250 ohms, connected into the unknown arm through the zero and 0.75 binding posts and is immediately followed by a measurement of $R_{1,t}$. This set of measurements provides a value of $R_{1,t}$ (sixth section) in terms of $\sum_{k=1}^{k=5} R_{1,k}$ and the measured difference. Since the value of $\sum_{k=1}^{k=5} R_{1,k}$ is obtained by summing the values from the first five measurements, straightforward substitution gives the value of $R_{1,t}$ in terms of $R_{1,1}$ and the sum of the measured differences. Adding this value of $R_{1,t}$ to the value of $\sum_{k=1}^{k=5} R_{1,k}$ (computed) gives the total resistance of group M_1 referred to the reference section $R_{1,1}$. These two sets of measurements expressed mathematically are as follows:

$$R_{1,1}=S_{a1}[1+(D_{1,1}-D_0)]$$
$$R_{1,2}=S_{a1}[1+(D_{1,2}-D_0)]$$
$$R_{1,3}=S_{a1}[1+(D_{1,3}-D_0)]$$
$$R_{1,4}=S_{a1}[1+(D_{1,4}-D_0)]$$
$$R_{1,5}=S_{a1}[1+(D_{1,5}-D_0)]$$

where $(D_{1,1}-D_0)$, $(D_{1,2}-D_0)$, etc., are the differences in proportional parts [6] as deduced from the readings of the DRRS; D_0 is the reading of the DRRS for an exact 1:1 ratio. (The significance of D_0 is explained in appendix A.)

Subtracting the first equation from each succeeding equation and from itself, gives

$$R_{1,1}=R_{1,1}$$
$$R_{1,2}=R_{1,1}+S_{a1}d_{1,2}$$
$$R_{1,3}=R_{1,1}+S_{a1}d_{1,3}$$
$$R_{1,4}=R_{1,1}+S_{a1}d_{1,4}$$
$$R_{1,5}=R_{1,1}+S_{a1}d_{1,5}$$
$$\sum_{k=1}^{k=5} R_{1,k}=5R_{1,1}+S_{a1}\sum_{k=1}^{k=5} d_{1,k}$$

[6] See appendix A.

where $d_{1,2}=(D_{1,2}-D_{1,1})$; $d_{1,3}=(D_{1,3}-D_{1,1})$ etc.

Since $S_{a1}=R_{1,1}$ closel y enough,

$$\sum_{k=1}^{k=5} R_{1,k}=5R_{1,1}\left[1+\sum_{k=1}^{k=5}\frac{d_{1,k}}{5}\right]. \tag{6}$$

The second set of measurements stated in similar fashion is

$$\sum_{k=1}^{k=5} R_{1,k}=S_{b1}[1+(D_{1,s}-D_0)]$$
$$R_{1,t}=S_{b1}[1+(D_{1,t}-D_0)].$$

On subtracting, this gives

$$R_{1,t}=\sum_{k=1}^{k=5} R_{1,k}+S_{b1}d_{1,t} \text{ where } d_{1,t}=(D_{1,t}-D_{1,s}).$$

Substituting eq (6) in the above expression and remembering that

$S_{b1}=5R_{1,1}$ closely enough, $R_{1,t}$ becomes

$$R_{1,t}=5R_{1,1}\left[1+\sum_{k=1}^{k=5}\frac{d_{1,k}}{5}+d_{1,t}\right]. \tag{7}$$

Adding eqs (6) and (7) and arranging terms gives

$$\sum_{k=1}^{k=5} R_{1,k}+R_{1,t}=10R_{1,1}\left[1+\sum_{k=1}^{k=5}\frac{d_{1,k}}{5}+\frac{d_{1,t}}{2}\right] \tag{8}$$

which states the total resistance of group M_1 in terms of $R_{1,1}$ and the measured differences.

Group M_1, having a nominal value of 500 ohms and a true value given by eq (8), serves as the first section of group M_2 which, as in the case of group M_1, consists of five nominally equal sections plus a sixth section having a value nominally equal to the sum of the five sections (see fig. 3). The sequence of seven balances is now obtained for group M_2. In the first set of this sequence, with $S=S_{a2}=500$ ohms, each of the 500 ohm sections, beginning with group M_1 as the reference section, is inserted in the bridge to obtain five measurements. In the second set two balances are obtained, first with all 10 sections (2,500 ohms) in the unknown arm and then with the eleventh section (2,500 ohms) inserted; for this set, $S=S_{b2}=2{,}500$ ohms. Since group M_1 has a computed value given by eq (8), the summation procedure can be extended through group M_2 which contains all sections up to the 15 v tap and becomes the first section of M_3.

The same procedure is carried forward through groups M_3 and M_4 with resistance S always having a value nominally equal to that of the section being measured.

The mathematical treatment presented in this section attempts to clarify the significance of the computation process associated with the step-up procedure (sometimes called a bootstrap technique), which may be masked in the more formal approach given in appendix B.

4.3. Computations

The readings of the DRRS having been recorded, the summation of their differences can be computed according to the following equation (developed in appendix B) to give the correction to the nominal ratios of the standard volt box

$$N_{m,k}=N'_{m,k}\left[1+\frac{\sum_{k=1}^{k=5} d_{1,k}+\sum_{k=1}^{k=5} d_{2,k}\ldots+\sum_{k=1}^{k=5} d_{m-1,k}}{5}+\frac{d_{1,t}+d_{2,t}\ldots+d_{m-1,t}}{2}+\frac{\sum_{k'=1}^{k'=k} d_{m,k'}}{k}\right]. \quad (9)$$

Where $N_{m,k}$=true value of the ratios,
$N'_{m,k}$=nominal values of the ratios;
$d's$=measured differences in proportional parts.

The schedule of computation given in table 1 was derived, in effect, by applying eq (9) to successively increasing values of k and m. Its arrangement permits the computation of all corrections in a single process without having to apply the equation directly each time a ratio is determined. The summation of the differences within a set (five-set or two-set) are kept separate until the final manipulation. This is indicated by columns 4, 5, and 6. The d's are the differences within each set; the q's are the corresponding summations; and the r's refer to the separate quantities appearing in the final terms of eq (9). Column 7 is the summation of the sets for each successive ratio.

5. Test Console

After the test method was investigated for more than a year with the circuit assembled in "breadboard" fashion, a small test console was designed and built so that the set-up time for a test would be reduced to a minimum. The console, shown in the photograph and indicated in figure 5, houses the DRRS, the galvanometer with its damping resistance, a mercury stand to accommodate the standard resistors, the 80-ohm guard resistor and the battery reversing switch. The DRRS, located in the lower portion of the console, is connected to the circuit by short leads brought to three binding posts located on the vertical panel immediately above the terminals of the DRRS. (With this arrangement the DRRS can be easily removed and made available for other work.) The detector is a portable galvanometer mounted on a platform within the enclosure immediately above and to the left of the DRRS. The galvanometer scale is observed through an opening in the front panel and the damping resistance, permanently mounted on the inside, is adjustable in steps by a knob accessible to the operator. The mercury stand, located within the console on a platform adjacent to the detector and above the DRRS, can accommodate either a single resistor or several arranged in either series or parallel combination. A removable top permits ready access to all components and wiring.

As shown in the wiring diagram of figure 5, the battery reversing switch, accessible on the front panel, carries a two-conductor shielded cable that terminates at a fitting located on the side panel.

TABLE 1. *Schedule for computing corrections for the standard volt box*

1	2	3	4	5	6	7	8
Section in bridge arm	Resistor S	Reading of DRRS	$d's$	$\frac{q's}{=\Sigma d's}$	$\frac{r's}{\frac{=\Sigma d's}{k}}$	Correction referred to 0–0.15 section	Range
	Ohms					*ppm*	
0–0.15	50	$D_{1,1}$	$d_{1,1}=D_{1,1}-D_{1,1}=0$			$\mu_{1,1}=0$	0–0.15
0.15–0.30	50	$D_{1,2}$	$d_{1,2}=D_{1,2}-D_{1,1}$	$q_{1,2}=d_{1,2}$	$r_{1,2}=\frac{1}{2}q_{1,2}$	$\mu_{1,2}=r_{1,2}$	0–0.30
.30–0.45	50	$D_{1,3}$	$d_{1,3}=D_{1,3}-D_{1,1}$	$q_{1,3}=q_{1,2}+d_{1,3}$	$r_{1,3}=\frac{1}{3}q_{1,3}$	$\mu_{1,3}=r_{1,3}$	0–0.45
.45–0.60	50	$D_{1,4}$	$d_{1,4}=D_{1,4}-D_{1,1}$	$q_{1,4}=q_{1,3}+d_{1,4}$	$r_{1,4}=\frac{1}{4}q_{1,4}$	$\mu_{1,4}=r_{1,4}$	0–0.60
.60–0.75	50	$D_{1,5}$	$d_{1,5}=D_{1,5}-D_{1,1}$	$q_{1,5}=q_{1,4}+d_{1,5}$	$r_{1,5}=\frac{1}{5}q_{1,5}$	$\mu_{1,5}=r_{1,5}$	0–0.75
0–0.75	250	$D_{1,s}$	$d_{1,s}=D_{1,s}-D_{1,s}=0$				
0.75–1.5	250	$D_{1,t}$	$d_{1,t}=D_{1,t}-D_{1,s}$	$q_{1,t}=d_{1,t}$	$r_{1,t}=\frac{1}{2}q_{1,t}$	$\mu_{2,1}=\mu_{1,5}+r_{1,t}$	0–1.5
0–1.5	500	$D_{2,1}$	$d_{2,1}=D_{2,1}-D_{2,1}=0$				
1.5–3.0	500	$D_{2,2}$	$d_{2,2}=D_{2,2}-D_{2,1}$	$q_{2,2}=d_{2,2}$	$r_{2,2}=\frac{1}{2}q_{2,2}$	$\mu_{2,2}=\mu_{2,1}+r_{2,2}$	0–3.0
3.0–4.5	500	$D_{2,3}$	$d_{2,3}=D_{2,3}-D_{2,1}$	$q_{2,3}=q_{2,2}+d_{2,3}$	$r_{2,3}=\frac{1}{3}q_{2,3}$	$\mu_{2,3}=\mu_{2,1}+r_{2,3}$	0–4.5
4.5–6.0	500	$D_{2,4}$	$d_{2,4}=D_{2,4}-D_{2,1}$	$q_{2,4}=q_{2,3}+d_{2,4}$	$r_{2,4}=\frac{1}{4}q_{2,4}$	$\mu_{2,4}=\mu_{2,1}+r_{2,4}$	0–6.0
6.0–7.5	500	$D_{2,5}$	$d_{2,5}=D_{2,5}-D_{2,1}$	$q_{2,5}=q_{2,4}+d_{2,5}$	$r_{2,5}=\frac{1}{5}q_{2,5}$	$\mu_{2,5}=\mu_{2,1}+r_{2,5}$	0–7.5
0–7.5	2,500	$D_{2,s}$	$d_{2,s}=D_{2,s}-D_{2,s}=0$				
7.5–15	2,500	$D_{2,t}$	$d_{2,t}=D_{2,t}-D_{2,s}$	$q_{2,t}=d_{2,t}$	$r_{2,t}=\frac{1}{2}q_{2,t}$	$\mu_{3,1}=\mu_{2,5}+r_{2,t}$	0–15
0–15	5,000	$D_{3,1}$	$d_{3,1}=D_{3,1}-D_{3,1}=0$				
15–30	5,000	$D_{3,2}$	$d_{3,2}=D_{3,2}-D_{3,1}$	$q_{3,2}=d_{3,2}$	$r_{3,2}=\frac{1}{2}q_{3,2}$	$\mu_{3,2}=\mu_{3,1}+r_{3,2}$	0–30
30–45	5,000	$D_{3,3}$	$d_{3,3}=D_{3,3}-D_{3,1}$	$q_{3,3}=q_{3,2}+d_{3,3}$	$r_{3,3}=\frac{1}{3}q_{3,3}$	$\mu_{3,3}=\mu_{3,1}+r_{3,3}$	0–45
45–60	5,000	$D_{3,4}$	$d_{3,4}=D_{3,4}-D_{3,1}$	$q_{3,4}=q_{3,3}+d_{3,4}$	$r_{3,4}=\frac{1}{4}q_{3,4}$	$\mu_{3,4}=\mu_{3,1}+r_{3,4}$	0–60
60–75	5,000	$D_{3,5}$	$d_{3,5}=D_{3,5}-D_{3,1}$	$q_{3,5}=q_{3,4}+d_{3,5}$	$r_{3,5}=\frac{1}{5}q_{3,5}$	$\mu_{3,5}=\mu_{3,1}+r_{3,5}$	0–75
0–75	25,000	$D_{3,s}$	$d_{3,s}=D_{3,s}-D_{3,s}=0$				
75–150	25,000	$D_{3,t}$	$d_{3,t}=D_{3,t}-D_{3,s}$	$q_{3,t}=d_{3,t}$	$r_{3,t}=\frac{1}{2}q_{3,t}$	$\mu_{4,1}=\mu_{3,5}+r_{3,t}$	0–150
0–150	50,000	$D_{4,1}$	$d_{4,1}=D_{4,1}-D_{4,1}=0$				
150–300	50,000	$D_{4,2}$	$d_{4,2}=D_{4,2}-D_{4,1}$	$q_{4,2}=d_{4,2}$	$r_{4,2}=\frac{1}{2}q_{4,2}$	$\mu_{4,2}=\mu_{4,1}+r_{4,2}$	0–300
300–450	50,000	$D_{4,3}$	$d_{4,3}=D_{4,3}-D_{4,1}$	$q_{4,3}=q_{4,2}+d_{4,3}$	$r_{4,3}=\frac{1}{3}q_{4,3}$	$\mu_{4,3}=\mu_{4,1}+r_{4,3}$	0–450
450–600	50,000	$D_{4,4}$	$d_{4,4}=D_{4,4}-D_{4,1}$	$q_{4,4}=q_{4,3}+d_{4,4}$	$r_{4,4}=\frac{1}{4}q_{4,4}$	$\mu_{4,4}=\mu_{4,1}+r_{4,4}$	0–600
600–750	50,000	$D_{4,5}$	$d_{4,5}=D_{4,5}-D_{4,1}$	$q_{4,5}=q_{4,4}+d_{4,5}$	$r_{4,5}=\frac{1}{5}q_{4,5}$	$\mu_{4,5}=\mu_{4,1}+r_{4,5}$	0–750

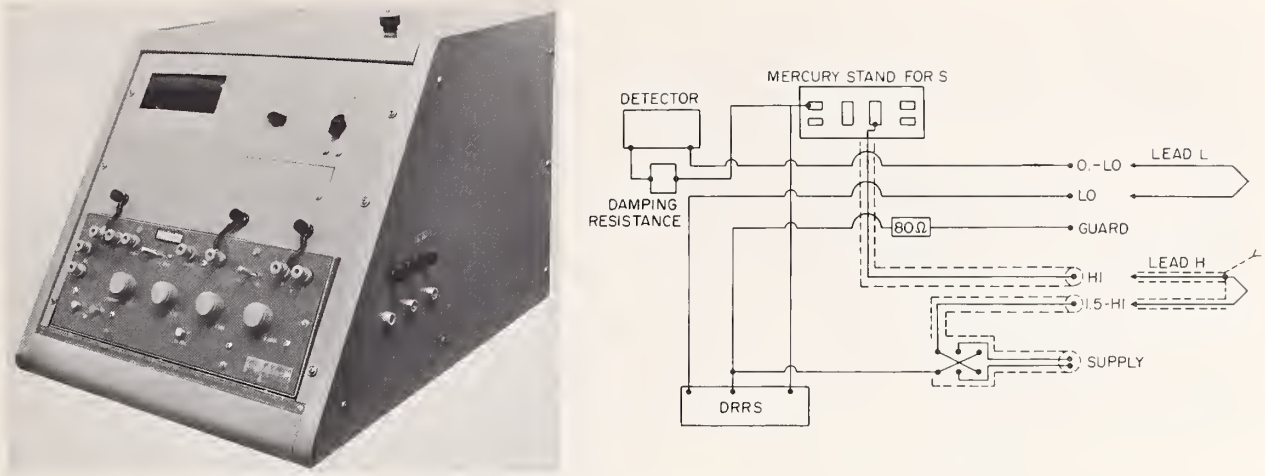

FIGURE 5. *Test console and layout.*

An external d-c supply is connected to this fitting with a pair of shielded leads equipped with a mating connector. The side panel also carries two single-conductor coax fittings, identified as "1.5-Hi" and "Hi," and three binding posts, identified as "0.-Lo," "Lo,", and "Guard."

When the first five sections of the standard volt box are measured separate unshielded leads are used to connect the terminals of the volt box (1.5 post, high-potential post of the section being measured, 0. post, and low-potential post of the section being measured) to the respective terminals of the console (1.5-Hi, Hi, 0.-Lo, and Lo). For all other measurements special leads H and L are used to connect the section under test as indicated in figure 5. When the guard of the volt box is used, the pigtail of lead H is connected to the high-potential terminal of the guard section and a connection is made from the "Guard" binding post to the low-potential terminal of the guard section. Otherwise, these last two connections are omitted.

6. Consideration of Errors

An examination of errors requires a careful study of all known effects that could render a measured value different from the true value within the specified accuracy. An appraisal of all components of the measuring circuit as well as a justification of approximations must be included, even though in this instance one would expect the associated errors to be negligible.

The first possible source of error to consider is the DRRS. As in the usual case, this type of error can be avoided by calibrating the instrument and applying corrections. Apart from this procedure, however, it should be emphasized that an error in the measured value is diluted when the values of the *ratios* are considered. For example, if each scale reading were in error by $\epsilon=1$ ppm and all errors were in such a direction as to add when computing each difference their contribution to the error of a given ratio, when summed within any one of the five-sets, would be

$$\frac{(k-1)2\epsilon}{k}=\frac{2(k-1)}{k}$$

where k is the number of summed sections. For $k=5$ the error would be $8/5=1.6$ ppm. Similarly, the error introduced in the measurements of the two-sets would be

$$\frac{2\epsilon}{2}=1 \text{ ppm.}$$

The maximum error would occur for the highest range since it contains all the sets. This would amount to only 9.4 ppm under these adverse conditions. Since the corrections to the DRRS used at NBS are less than 0.3 ppm and their signs and magnitudes have a random distribution, the errors in the ratio measurements are almost certain to be less than 1 ppm with no corrections applied to the dial readings.

A source of error is concealed in the base (or balance) equation used in appendix B to develop the general expression for the volt box ratios. Referring to appendix A, the exact base equation is given as

$$R_{m,k}=S\left[1+\frac{1}{1+\frac{l_2}{B_m}}(D_{m,k}-D_0)\right]$$

whereas, the approximate value used in the mathematical development in appendix B is

$$R_{m,k}=S[1+(D_{m,k}-D_0)].$$

The latter departs from exactness by an amount $\frac{l_2}{B_m}(D_{m,k}-D_0)$ but is of second order. For example, if $\frac{l_2}{B_m}$ were as large as 0.1 percent and $(D_{m,k}-D_0)$ rep-

resented a change of 500 ppm in the A-arm, the value for $R_{m,k}$ would be in error by only 0.5 ppm.

Another error is concealed through approximation in developing the general expression that defines the volt box ratios (appendix B) when it is assumed that the value of the "Dummy" resistor, including leads, is exactly equal to that of the section being measured. The error introduced through this assumption is second order since it is the product of two small terms. For example, consider the summation of the first five sections (refer to eq (6)).

$$\sum_{k=1}^{k=5} R_{1,k}=5R_{1,1}+S_{a1}\sum_{k=1}^{k=5} d_{1,k}.$$

If S_{a1} differs from $R_{1,1}$ and is given by $S_{a1}=R_{1,1}[1+\mu_1]$ the summation becomes

$$\sum_{k=1}^{k=5} R_{1,k}=5R_{1,1}\left[1+\sum_{k=1}^{k=5}\frac{d_{1,k}}{5}+\mu_1\sum_{k=1}^{k=5}\frac{d_{1,k}}{5}\right]$$

where the magnitude of the error is $\mu_1\sum_{k=1}^{k=5}\frac{d_{1,k}}{5}$.

If both μ_1 and the summation were as large as 500 ppm, the error would be only 0.05 ppm.

Another possible source of error arises if the resistance in any one arm changes during the measurements of a given set. This change could occur in the leads and contacts, for example, and its effect would be greatest when measuring the 50-ohm sections. A change of this nature can be considered as a change in D_0 and an estimate of the error it introduces in a measured ratio can be obtained by considering the measurements of the first set. Assume an extreme case in which the resistance of a given arm increases in equal increments after the first measurement so that for subsequent balances D_0 takes on new values. The measured values for the set become

$$\begin{aligned}
R_{1,1}&=S_{a1}[1+(D_{1,1}-D_0)]\\
R_{1,2}&=S_{a1}[1+D_{1,2}-(D_0+\epsilon)]\\
R_{1,3}&=S_{a1}[1+D_{1,3}-(D_0+2\epsilon)]\\
R_{1,4}&=S_{a1}[1+D_{1,4}-(D_0+3\epsilon)]\\
R_{1,5}&=S_{a1}[1+D_{1,5}-(D_0+4\epsilon)]
\end{aligned}$$

where ϵ is the change in D_0 between successive balances. After taking differences, any given sum within the set can be written as

$$\sum_{k'=1}^{k'=k} R_{1,k'}=kR_{1,1}\left[1+\sum_{k'=1}^{k'=k}\frac{d_{1,k'}}{k}-\sum_{k'=1}^{k'=k}\frac{(k'-1)\epsilon}{k}\right].$$

Thus an error in any ratio formed within the set is $\sum_{k'=1}^{k'=k}\frac{(k'-1)\epsilon}{k}$. For example, if a lead resistance increased in increments of 0.0001 ohm in the S-arm (50 ohms) the magnitude of the error introduced in the ratio $\frac{\sum_{k=1}^{k=5} R_{1,k}}{R_{1,1}}$ would be 4 ppm. If the usual precautions are taken, the probability of this kind of an occurrence is quite remote and could be easily observed from the detector response. A single, abrupt change would be more difficult to detect but an error from this cause can be avoided by taking a repeat set of measurements.

The final consideration involves those errors that arise from the unavoidable presence of the rod resistances. This source of error could be the most critical of any because of its insidious nature. Two errors must be examined when considering the rod resistances. If the rod resistances are equal they can introduce an error if, when the standard volt box is used, the connections differ from those made during the process of calibration. The second error occurs if the rod resistances differ in magnitude.

Consider the cause of the first error. When in use, the connections to the standard volt box are as shown in figure 6. There are no currents in rods l_1 and l_2; rod l_n, however, carries current by virtue of its connection to the supply. Thus the ratio of the standard in use is

$$N_s=\frac{\sum_{1}^{n} R_{n'}+l_n}{R_{1,1}}. \tag{10}$$

When the first five sections are measured (refer to fig. 4a) the rods are in the A- and S-arms. Thus, if the ratio under consideration were one confined solely to these sections, the measured ratio would be

$$N'_s=\frac{\sum_{1}^{n} R_{n'}}{R_{1,1}} \tag{11}$$

and eq (10) can be written as

$$N_s=N'_s+\frac{l_n}{R_{1,1}}=N'_s\left[1+\frac{l_n}{N'_sR_{1,1}}\right] \tag{12}$$

In the measurement and summing process through the higher ranges, the rod resistances form part of the section being measured. (See fig. 4b.) However, if the rod resistances are equal, their effects

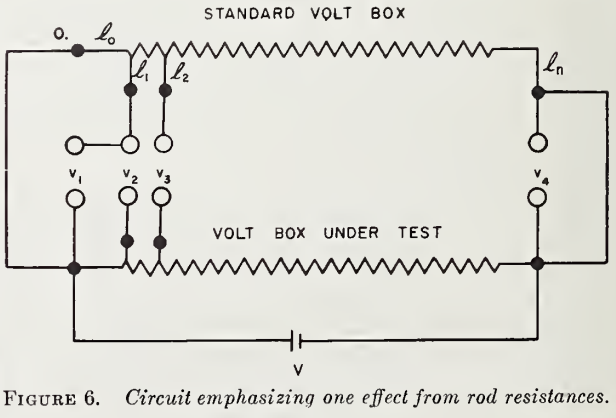

FIGURE 6. *Circuit emphasizing one effect from rod resistances.*

cancel and the difference between the ratio in use and the one measured is the same as that given in eq (12). It is apparent then that the ratio in use differs from the measured ratio by an amount equal to the rod resistance divided by the total resistance of the range used and occurs even though the rod resistances are equal. If the standard volt box were used as a 4-terminal voltage divider the above correction to the ratio in use would be $\frac{l_n+l_0}{N'_s R_{1,1}}$ since l_0 becomes part of the high voltage side.

The magnitude of an error arising from inequalities in the rod resistances depends on where the rods are located in the bridge network. As stated in section 4.2, there are three alternatives for connecting the rods and the choice of orientation is not as clearly indicated when measuring the 50-ohm sections as when measuring the higher-valued sections. For the purpose of analysis, consider the measurement of the low-valued sections and the particular connection shown in figure 4a.

For this condition, differences among the rod resistances may be considered as producing changes in D_0 so that, if the respective rod resistances are identified as l_1, l_2, etc., the measured resistances are

$$R_{1,1}=S_{a1}[1+D_{1,1}-D_0]$$

$$R_{1,2}=S_{a1}\left[1+D_{1,2}-D_0+\frac{l_2-l_1}{A}+\frac{l_3-l_2}{S_{a1}}\right]$$

$$R_{1,3}=S_{a1}\left[1+D_{1,3}-D_0+\frac{l_3-l_1}{A}+\frac{l_4-l_2}{S_{a1}}\right]$$

$$R_{1,4}=S_{a1}\left[1+D_{1,4}-D_0+\frac{l_4-l_1}{A}+\frac{l_5-l_2}{S_{a1}}\right]$$

$$R_{1,5}=S_{a1}\left[1+D_{1,5}-D_0+\frac{l_5-l_1}{A}+\frac{l_6-l_2}{S_{a1}}\right].$$

If the rod resistances are measured, their contribution to the error of any ratio can be evaluated. Comparable sets of equations can be formed for the other two cases and corresponding errors evaluated. If the successive values of rod resistances neither increase nor decrease, it cannot be stated categorically that one connection is preferred to another. Thus a comparison of the resulting errors for the three possible connections must be made and the connection chosen which yields the smallest errors. Such a comparison applied to the NBS standard volt box indicated that the circuit of figure 4a is preferred. As measurements are continued through the higher ranges, the rods are connected as part of the large resistance being measured so that their effects are further reduced.

In the NBS standard volt box recently acquired, rod resistances from zero through the 6-v range are about 5×10^{-4} ohm and their differences are sufficiently small and random in sign that the maximum error they produce in a ratio measurement is less than 0.3 ppm.

7. Summary

A particular type of voltage ratio standard and a method for its calibration are discussed. Although the method is described in its particular application to the NBS standard it can be used equally well in other networks. Errors that might appear in the measurement of its ratios and procedures for evaluating their magnitudes are outlined. With a standard volt box of proper design, the calibration method as set forth should yield results that are good to an accuracy of 10 ppm or better. This estimate of accuracy is based on the theoretical considerations of the circuit and its parameters, on the continued good agreement with those values of ratio obtained by the older method, and on other self-consistent tests.

The author appreciates the assistance of Rita McAuliff and Ronald Dziuba who made most of the measurements and constructed the test console.

8. Appendix A

8.1. Comments on the DRRS

Complete discussions on the DRRS and its use in the accurate measurement of d-c resistance are contained in references [2], [3], and [4] so that an elaborate treatment is not warranted. However, certain aspects are emphasized here in order to clarify the meaning of particular equations, as well as justify their use.

The DRRS is used principally in comparing two nearly equal resistances and under these conditions has an accuracy of about 1 ppm. It comprises two resistance arms of about equal magnitudes with one arm B' having a single-valued resistance (in most cases 100 or 1,000 ohms) and the other consisting of a fixed resistance in series with an adjustable section. The adjustable branch contains, in most cases, four resistance groups, each provided with a selector to vary the resistance and register the change on suitably marked dials. The resistance of the A'-arm can be varied by about 0.5 percent on either side of the B'-arm value to a least count of 1 ppm. The dials register in increasing numbers as resistance is added to the fixed portion of the A'-arm. Since the DRRS is used to measure differences between two nearly equal quantities, the dial readings can be translated to ppm or, as is often the case, the dials may be marked in ppm.

The reader should note carefully the form in which small corrections are recorded or used in derivations and computations. As usually constructed, a *change* of one step on the lowest dial of a four-dial DRRS corresponds to a change of 1 ppm in the ratio. At one particular balance of a measuring circuit the reading of the DRRS should be thought of simply as a four-digit number, such as 5472. If a second balance of the same circuit yields a DRRS reading of 5459 the measured ratio change is −13 ppm, this

being the first point at which the abbreviation "ppm" should be introduced. In recording data and computations (see table 1) it is convenient and space saving to enter DRRS readings as four-digit numbers, and ratio changes in ppm. In deriving equations, however, (and corrections based thereon) ratio changes should be expressed in proportional parts. A ratio change in proportional parts is one millionth of the change expressed in ppm. In the above illustration the ratio change is -0.000013 proportional parts. See reference [2] for further discussion of these terms.

8.2. Bridge Balance Equation

Figure 7 indicates a bridge network in which the adjustable arm of the DRRS is represented as a section of fixed resistance in series with a uniform slide wire of high resolution. Let B_m indicate the resistance of the B-arm of the DRRS, A_m the resistance of its A-arm for which $A_m=B_m$, l_2 and l_1 the respective lead resistances with $l_2 \neq l_1$, and S the resistance of a standard serving as the "Dummy" resistor. For convenience, let the DRRS be without error as previously determined from calibration.

Assume first that a standard resistor S_1, having a resistance equal to S, is inserted in the unknown arm and the bridge balances at some point for which the A- and B-arms of the DRRS are not equal. Let the resistance of the A-arm of the DRRS be A_0 for this balance condition. The equation of balance is given by

$$S=S\left[\frac{(A_0+l_1)}{(B_m+l_2)}\right]. \tag{13}$$

Thus A_0 is the resistance of the A-arm of the DRRS when the ratio arms (A- and B-) of the *bridge* are in a 1:1 ratio. Next, let S_1 be replaced by a resistance whose value is R and let A_R be the resistance of the A-arm of the DRRS under the new balance condition. The equation of balance is

$$R=S\left[\frac{(A_R+l_1)}{(B_m+l_2)}\right]. \tag{14}$$

Subtracting (13) from (14) and rearranging terms gives the value of R as

$$R=S+S\left[\frac{(A_R+l_1)}{(B_m+l_2)}-\frac{(A_0+l_1)}{(B_m+l_2)}\right]$$

$$=S\left[1+\frac{(A_R-A_0)}{(B_m+l_2)}\right]. \tag{15}$$

Since A_m and B_m equal the respective resistances of the A- and B-arms of the DRRS when $A_m=B_m$, let

$$A_R=A_m+\Delta_R$$

$$A_0=A_m+\Delta_0$$

where Δ_R and Δ_0 are small changes in the resistance of the slide wire. Equation (15) becomes

$$R=S\left[1+\frac{(A_m+\Delta_R)-(A_m+\Delta_0)}{B_m+l_2}\right]$$

which can be written as

$$R=S\left[1+\frac{\left(1+\frac{\Delta_R}{A_m}\right)-\left(1+\frac{\Delta_0}{A_m}\right)}{\left(1+\frac{l_2}{B_m}\right)}\right] \tag{16}$$

since $\frac{A_m}{B_m}=1$. Now the dials of the DRRS (assumed to be without error) indicate, in effect, that in going from a position corresponding to the resistance A_m to that of A_R, the resistance of the A-arm of the DRRS has changed by $\frac{\Delta_R}{A_m}$ in proportional parts; and similarly, in going from A_m to A_0 the resistance has changed by $\frac{\Delta_0}{A_m}$. Hence,

$$\frac{\Delta_R}{A_m}=(D_R-D_m) \text{ and } \frac{\Delta_0}{A_m}=(D_0-D_m)$$

where D_R, D_0 and D_m refer to the respective readings of the DRRS translated into proportional parts. Substituting these values in (16) gives

$$R=S\left[1+\frac{1}{1+\frac{l_2}{B_m}}(D_R-D_0)\right] \tag{17}$$

or, if $\frac{l_2}{B_m}$ is sufficiently small

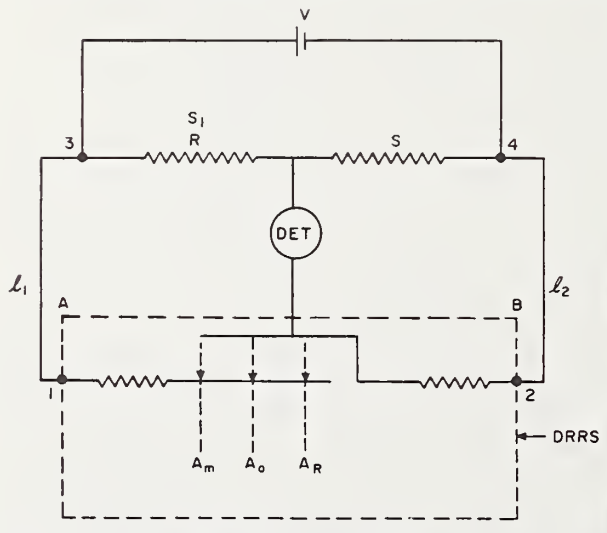

FIGURE 7. *Circuit indicating the DRRS with respect to the balance equation.*

$$R \approx S[1+(D_R-D_0)]. \quad (18)$$

In the notation used in developing the general expression given in appendix B, this corresponds to

$$R_{m,k}=S_{am}[1+(D_{m,k}-D_0)].$$

It should be noted that the concept of D_0 has been generalized for the purpose of this paper to indicate that setting on the DRRS for which the ratio arms between terminals 3 and 4 have a 1:1 ratio. In most uses of the DRRS, particularly in the comparison of resistance standards, arms A and B contain only the DRRS and D_0 is a constant, defined as the setting for which the A- and B-arms of the *DRRS* have a 1:1 ratio.

9. Appendix B

Referring to the text and to figure 3, the working resistance is considered as made up of four groups, with each group containing six sections. The first five sections of any one group have nominally equal resistances and the sixth section has a resistance nominally equal to five times this value (sum of the five sections). Counting from the low-potential end, the first section of each group (after the first) is formed by all the preceding sections connected in series. Any section, therefore, can be identified by two integers; the first, m, specifying the group to which the section belongs, and the second, k, specifying the position of the section within its group.

If the Wheatstone bridge of figure 4 is balanced as each of the first five sections of group m is inserted in succession in the unknown arm, then the resistance of the first section and of the kth section can be written as,

$$R_{m,1}=S_{am}[1+(D_{m,1}-D_0)] \quad (19)$$

and

$$R_{m,k}=S_{am}[1+(D_{m,k}-D_0)] \quad (20)$$

where

S_{am} is the resistance of S and has a nominal value equal to that of the volt box section being measured;

$D_{m,1}$ and $D_{m,k}$ are the readings of the DRRS in proportional parts [7] when the first and kth sections, respectively, of group m are inserted in the unknown arm;

D_0 is the reading that would be indicated on the DRRS if the Wheatstone bridge were in exact 1:1 ratio.

Subtracting (19) from (20) gives

$$R_{m,k}-R_{m,1}=S_{am}[D_{m,k}-D_{m,1}]$$

or

$$R_{m,k}=R_{m,1}+S_{am}d_{m,k} \quad (21)$$

where

$$d_{m,k}=[D_{m,k}-D_{m,1}]$$

The sum of the first five sections of group m is

$$\sum_{k=1}^{k=5} R_{m,k}=5R_{m,1}+S_{am}\sum_{k=1}^{k=5} d_{m,k} \quad (22)$$

since each section has the same nominal value and S_{am} is used throughout the set of measurements.

If now the resistor S_{am} is replaced by S_{bm} and the bridge is balanced first, with the five sections (connected in series) and then with the sixth section inserted in the unknown arm, we have

$$\sum_{k=1}^{k=5} R_{m,k}=S_{bm}[1+(D_{m,s}-D_0)] \quad (23)$$

and

$$R_{m,t}=S_{bm}[1+(D_{m,t}-D_0)] \quad (24)$$

where

$D_{m,s}$ is the reading of the DRRS when the sum of the five sections is inserted;

$D_{m,t}$ is the reading when the sixth section is inserted.

Subtracting (23) from (24) gives

$$R_{m,t}-\sum_{k=1}^{k=5} R_{m,k}=S_{bm}[D_{m,t}-D_{m,s}]$$

or

$$_{m,t}=\sum_{k=1}^{k=5} R_{m,k}+S_{bm}d_{m,t} \quad (25)$$

where

$$_{m,t}=[D_{m,t}-D_{m,s}].$$

Substituting (22) into (25) gives

$$R_{m,t}=5R_{m,1}+S_{am}\sum_{k=1}^{k=5} d_{m,k}+S_{bm}d_{m,t} \quad (26)$$

which defines the resistance of the sixth section of the group m in terms of the sum of the first five sections and the measured differences.

The total resistance of group m is the sum of the resistances of the six sections that comprise the group. Its value is found by adding (22) and (26) so that

$$R_m \equiv \sum_{k=1}^{k=5} R_{m,k}+R_{m,t}=10R_{m,1}+2S_{am}\sum_{k=1}^{k=5} d_{m,k}+S_{bm}d_{m,t} \quad (27)$$

Remembering that the total resistance of group m is also the first section of group $(m+1)$ and noting that

$$S_{am}=10^{m-1}R_{1,1}$$

and

$$S_{bm}=5\times 10^{m-1}R_{1,1}$$

[7] Strictly speaking, as emphasized elsewhere in the paper, $(D_{m,1}-D_0)$ and $(D_{m,k}-D_0)$ are the *differences* in proportional parts as deduced from the readings of the DRRS.

we have from (27)

$$R_{m+1,1}=10R_{m,1}+(2\times10^{m-1}R_{1,1})\sum_{k=1}^{k=5}d_{m,k}+(5\times10^{m-1}R_{1,1})d_{m,t}. \quad (28)$$

Equation (28) serves as the connecting link between one group and the next. If it is applied successively to increasing values of m, beginning with $m=1$, one finds that the resistance of the first section of any group m can be expressed in terms of the resistance of the first section of the first group and the measured differences by the general equation

$$R_{m,1}=10^{m-1}R_{1,1}+(2\times10^{m-2}R_{1,1})\left[\sum_{k=1}^{k=5}d_{1,k}+\sum_{k=1}^{k=5}d_{2,k}\ldots+\sum_{k=1}^{k=5}d_{m-1,k}\right]+(5\times10^{m-2}R_{1,1})[d_{1,t}+d_{2,t}\ldots+d_{m-1,t}]. \quad (29)$$

Equation (21) states that the resistance of the kth section of group m is

$$R_{m,k}=R_{m,1}+S_{am}d_{m,k}=R_{m,1}+(10^{m-1}R_{1,1})d_{m,k}$$

so that the sum of all resistances up to and including the kth section of group m is

$$\sum_{k'=1}^{k'=k}R_{m,k'}\equiv S_{m,k}=kR_{m,1}+(10^{m-1}R_{1,1})\sum_{k'=1}^{k'=k}d_{m,k'}. \quad (30)$$

Substituting (29) in (30) and factoring out $k\times10^{m-1}R_{1,1}$ gives

$$S_{m,k}=k\times10^{m-1}R_{1,1}\left[1+\frac{\sum_{k=1}^{k=5}d_{1,k}+\sum_{k=1}^{k=5}d_{2,k}\ldots+\sum_{k=1}^{k=5}d_{m-1,k}}{5}+\frac{d_{1,t}+d_{2,t}\ldots+d_{m-1,t}}{2}+\frac{\sum_{k'=1}^{k'=k}d_{m,k'}}{k}\right]. \quad (31)$$

Any given ratio of the volt box is defined as the ratio of the sum of all resistances up to the kth tap of group m to the resistance of the first section of the first group. Thus, by definition, any ratio of the volt box is $\frac{S_{m,k}}{R_{1,1}}$ so that, since $(k\times10^{m-1})$ is the nominal ratio, eq (31) can be written in the form

$$N_{m,k}=\frac{S_{m,k}}{R_{1,1}}=N'_{m,k}[1+\mu_{m,k}]$$

where $N'_{m,k}$ are the nominal ratios and $\mu_{m,k}$ are the corresponding corrections in proportional parts, computed from the difference terms that appear in eq (31). The corrections can be stated in ppm by multiplying by 10^6.

10. References

[1] Francis B. Silsbee and Francis J. Gross, Testing and performance of volt boxes, J. Research NBS **27,** 269 (1941) RP1419.

[2] Paul P. B. Brooks, Calibration procedures for direct-current resistance apparatus, NBS Mono. 39 (1962).

[3] James L. Thomas, Precision resistors and their measurement, NBS Circ. 470 (1948).

[4] Forest K. Harris, Electrical measurements (John Wiley & Sons, Inc., New York, N.Y., 1952).

(Paper 67C1-114)

Human Engineering A Console for The Comparison of Volt Boxes

P. H. Lowrie, Jr.
NBS Boulder Laboratories
Boulder, Colo.

The principles of humon engineering ore os opplicoble to moking precise meosurements os they ore to the production line. Too often the human element is not given adequate considerotion in the design of precise measuring equipment and as a result, accuracy declines. To reduce this source of error, a calibration console was designed in which the human engineering foctors were given the some considerotion os the technicol requirements. In this system the console operator is considered to be a decision moker, and those functions not requiring judgment are automaticolly processed by the console. Most of the calculations are performed automatically by internol circuits, ond the results ore displayed digitolly upon commond.

OFTEN, in the zeal to produce a measurement device that is technically superior, the designer does not place enough emphasis on the fact that the device must be operated by a human. As the goal of technical perfection comes closer to attainment, the role of the operator as an uncertainty factor becomes more and more apparent. Certainly a technically perfect device that is incompatible with the operator is less than desirable.

Prior to the design of a new console for the measurement of volt boxes at the NBS Boulder Laboratories, the relationship between the operator and the equipment was studied. The conclusions resulting from this study led to the extensive use of the principles of human engineering in the design of the console. At no point, however, were the technical requirements subordinated to the human-engineering requirements. The result is a man-machine system that introduces measurement uncertainties of less than 10 parts per million (ppm) while allowing measurements to be made with greater efficiency than was previously possible and allowing a more extensive study to be made of each measured volt box.

Method of Measurement

The design is based on the method first described by Silsbee and Gross[1] in 1941. In this method, the input terminals of unknown and standard volt boxes are connected in parallel, and the difference between the voltages at the corresponding output terminals are measured. This measurement is usually made with a Lindeck-Rothe potentiometer.[2] The circuit is as shown in Fig. 1.

To correct for voltage drop in the leads between the corresponding input terminals, these voltages are also measured. The resulting equation for the corrected ratio, X_c, can be readily derived by the application of Kirchhoff's Voltage Law to the circuit of Fig. 1. A derivation of this equation has been published by Dunfee.[3] If the voltages v_1, v_2, and v_3, are defined as positive when of the same polarity as v_4, the correction equation is

$$X_c = X_n \left[1 + \left(\mu_s + \frac{v_4}{V} - \frac{v_1}{V} + \frac{S_n v_2}{V} - \frac{S_n v_3}{V} \right) 10^{-6} \right] \quad (1)$$

In equation 1

X_n is the nominal ratio of the unknown volt box.
μ_s is the previously determined correction to the ratio of the standard volt box, in ppm.
v_2 and v_3 are the voltages between corresponding output terminals in microvolts.
v_1 and v_4 are the voltages between corresponding input terminals, in microvolts.
S_n is the nominal ratio of the standard volt box and is equal to X_n.
V is the applied voltage, in volts.

Human Factors Influencing the Design

Before starting the design, it was necessary to determine what the design should promote and what it should prevent, with regard to its effect on the operator. A short study into the matter resulted in the following conclusions:

- When an operator becomes tired or bored, he unconsciously becomes less careful.
- He is much less likely to misread a digital display than he is an analog display.
- He is less reliable than a machine in the performance of repetitive calculations. As Sinaiko and Buckley put it, he "is not very effective in performing routine calculations. He is rather slow and likely to make errors."[4]

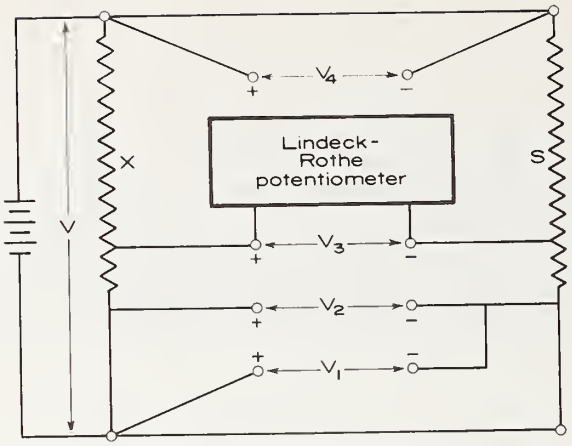

Figure 1. Basic voltbox measurement circuit.

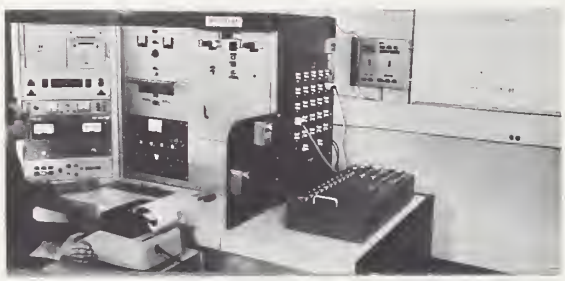

Figure 2. Console at the NBS Boulder Laboratories

Figure 3. Main control panel

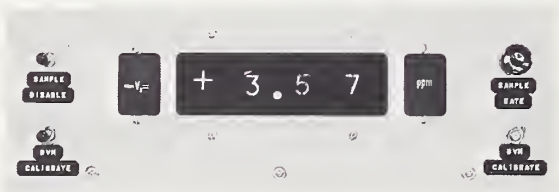

Figure 4. Output display panel

• Irritating situations, such as the necessity of fitting many leads under one terminal post, produce a state of mind that is not conducive to highest accuracy.

Design Requirements

In the design of the console, human engineering aspects were subordinated only in those instances in which they would jeopardize the technical quality of the console. The design objectives included the following:

1. The operator should be able to change ranges on the standard volt box quickly and easily. This not only increases efficiency and reduces irritation, but also minimizes the time during which the boxes are cooling. This is important since the boxes are measured under temperature equilibrium conditions.

2. Controls should be centralized. Operations that must be done simultaneously should be performed by the movement of a single control.

3. Digital presentation should be used both for controls and displays.

4. As much of the computing as practicable should be done automatically. This is important in the measurement of volt boxes, since corrections may have to be calculated by means of Equation 1 as many as 32 times for an ordinary volt box and as many as 96 times for a master volt box. Though the mathematics is simple, the repetition is tedious. At best, it will lower the morale of the calculator and at worst it will result in the increasing occurrence of errors toward the end of the calculations.

5. Recopying of data should be reduced to a minimum.

6. An automatic record should be kept of control settings and displayed values to provide a check against gross error.

7. Adequate safety measures must be provided because d-c voltages as high as 1,500 volts may be present during a measurement.

Additionally, there was the overlying technical requirement that the measurement uncertainty introduced by the console should be held to a few ppm. Among other things, this necessitated that guarded circuitry be used throughout to minimize leakage currents, and that a reversing technique be used to minimize the effects of thermoelectromotive forces.

Features

In the console shown in Fig. 2, most of the design objectives were realized. The design features of the console include:

1. A specially designed plug-panel which allows the operator to change ratios on the standard quickly and easily. The panel is completely guarded and uses heavily gold-plated connectors.

2. All controls used during a measurement are grouped in front, or slightly to the side, of the operator. No control is more than eighteen inches away. Those operations that must be done at the same time are performed by the movement of a single control. This was accomplished by the extensive use of relays. The operator thus needs to move very little during the measurement of any range. However, he must get up and move around the end of the console to change ranges. This change of pace helps to reduce fatigue.

3. Wherever possible displays and controls are in digital form. Some examples are shown in Fig. 3.

4. Console circuits reduce the measured voltages to parts per million of the ratio of the unknown

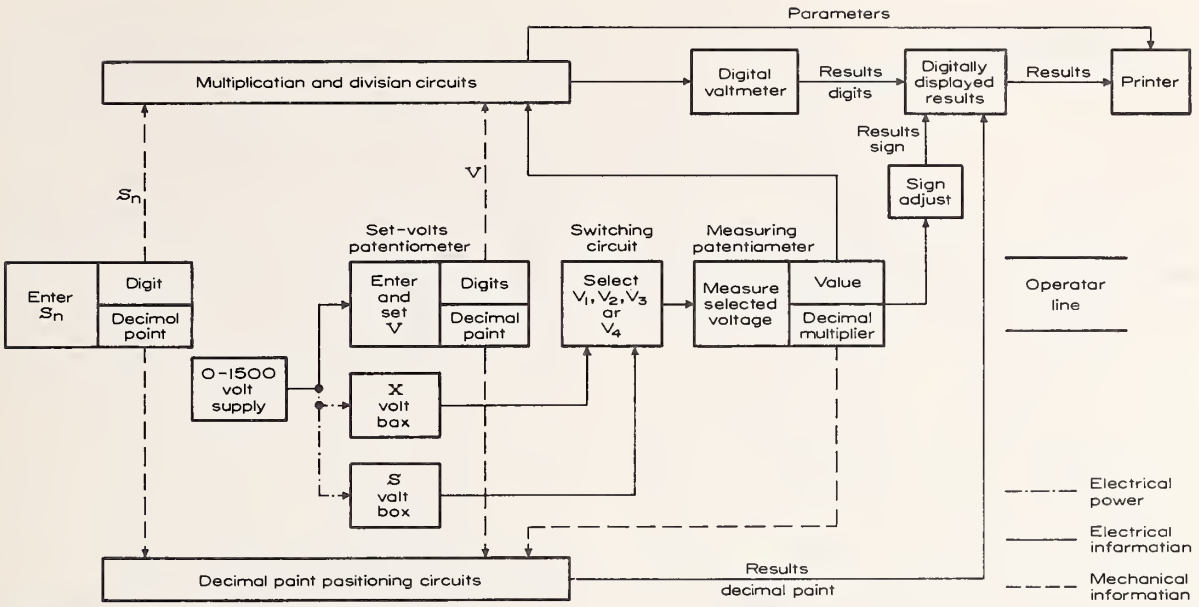

Figure 5. Block diagram of measurement system.

volt box and display them as shown in Fig. 4.

5. The operator records the data on an adding machine, adding or subtracting as indicated on the display. At the completion of the measurement, he then enters correction to the standard, μ_s, in the machine and depresses the totaling key. The adding machine sums the values, and thereby completes the calculations. When the calibration of a volt box is complete, the tape from the calculator is reproduced photographically on 8 x 10½ sheets which become the permanent records. Recopying of the data is thus reduced.

6. A digital printer monitors the controls on the main control panel and the digital display. A comparison of this tape with that from the adding machine detects operator error and shows up equipment malfunctions.

7. Safety measures include a photoelectric fence that disconnects the high voltage whenever the high voltage area is entered, an illuminated sign that is energized whenever the high voltage is applied, and neon lights connected across the high-voltage circuit to provide a warning even if all other safety circuits fail.

The Measurement

The objective of the measurement is, of course, to determine the parameters and variables of Equation 1 and then to use them to determine the correction. Equation 1 may be rewritten in the form

$$X_c = X_n\,[1 + (\mu_s + V_1 + V_2 + V_3 + V_4)10^{-6}] \quad (2)$$

where V_1, V_2, V_3, and V_4 are the equivalents of the terms in v_1, v_2, v_3, and v_4 respectively. If v_1, v_2, v_3, and v_4 are in microvolts, and V is in volts, then V_1, V_2, V_3, and V_4 will be in ppm of ratio of the unknown box. X_c, X_n, and μ_s have the same meaning as in Equation 1. In order for Equation 2 to hold, the signs of the values of V_1, V_2, V_3 and V_4 must be appropriately adjusted.

From Equation 2 it can be seen that, provided the values of the difference voltages can be automatically reduced to ppm of ratio as they are measured, the calculations involve only addition and subtraction and thus lend themselves ideally to performance on an adding machine.

To assist the operator in making the measurement, the main function switch indicates what the operator should do, or what the console is doing, at each position. This switch, which can be seen in the lower center of Fig. 3, controls the measurement sequence and hence is the program control for both console and operator.

In the performance of a measurement, the operator first enters the value of S_n, the nominal ratio of the standard voltage box, into the console by means of the S_n switches shown at the upper right of Fig. 3. These switches are connected to the computing circuits shown in Figure 5. He then selects the desired value of V, applied voltage, by adjusting the four "V=" dials shown in Fig. 3 to display that value. In so doing he also enters the value into the computing circuits. When the 0-1500 volt supply has been adjusted to the selected voltage, the "set V" galvanometer will be at null. This type of indicator was chosen because, though the eye, in general, does not notice small changes in the angle of a needle, it readily detects such changes when they are from the vertical.

Since the galvanometer indicator is within the operator's field of vision while he is concentrating on the measuring circuit galvanometer, shown immediately above the main control panel in Fig. 2, he is able to continuously monitor the supply voltage during the measurement.

After having entered S_n and V into the console, the operator rotates the main function switch to select one of the four difference voltages. He then adjusts the measuring potentiometer to obtain a null on the measuring circuit galvanometer. While he is making this adjustment, the output from the measuring potentiometer is continuously being reduced to ppm of ratio by the computing circuits. See Fig. 5. Note that he may select any one of a number of

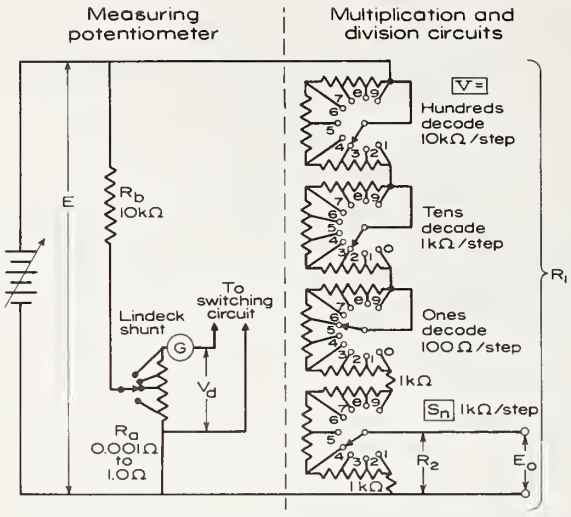

Figure 6. The computing potentiometer

measurement ranges by rotation of the Lindeck Shunt switch (Fig. 3). The position of this switch is fed to the decimal point positioning circuit as a decimal multiplier (Fig. 5). As shown in Fig. 5, the circuits in the console perform the required multiplication and division, position the decimal point, and adjust the sign of the value so that the digitally displayed result can be directly recorded on an adding machine by the operator.

Computer Principle

Human-engineering considerations suggested the use of digital controls and displays. However, analog circuits were preferrable for computing because of their simplicity in this application. Hence, the computing circuits were designed to allow digital entry of the parameters, and digital display of the results. The calculations, however, are performed by electrical analogs of the v_1, v_2, v_3, and v_4 terms in Equation 1. As an illustration of how such an analog was developed, consider the v_3 term in Equation 1. When this term is compared with the equivalent term in Equation 2, the result is

$$V_3 = \frac{S_n v_3}{V} \tag{3}$$

An electrical analog of Equation 3 is the common voltage divider circuit:

$$E_o = E\,\frac{R_2}{R_1} \tag{4}$$

where R_2 is the portion of R_1 across which E_o appears. The only requirements for the analogy to hold are that:

E is proportional to v_3,
R_1 is proportional to V,
R_2 is proportional to S_n, and
R_1 and R_2 can be varied independently.

Computing Potentiometer

Fig. 6 shows the computing potentiometer. The difference voltage, v_d, at galvanometer null, is developed across the Lindeck element, R_a. At this point the resemblance to a Lindeck potentiometer ends however, because the current is converted to a voltage by R_b rather than being displayed on a milliameter. The voltage across $R_b + R_a$ is applied also to the multiplier-and-divisor resistor chain. This resistor chain corresponds to the R_1 and R_2 of Equation 4. The "hundreds," "tens," and "ones" decades shown in Fig. 6 are automatically adjusted to be proportional to V as the set-volts potentiometer is adjusted to measure V. Consider for example, the adjustment to the value $V = 325$. The adjustment of the hundreds decade to 3 introduces 20 kilohms into the series resistance circuit. The adjustment of the tens decade to 2 introduces 2 kilohms, and the adjustment of the ones decade to 5 introduces 500 ohms. Note that there always is a minimum resistance of 10 kilohms in the circuit. With the adjustments as described, the current through R_2 is

$$I_{R2} = \frac{E}{10{,}000 \quad +20{,}000 \quad +2{,}000 \quad +500}$$
$$= \frac{E}{32{,}500} \tag{5}$$

which, considering only significant figures, corresponds to dividing by the voltage $V = 325$.

The voltage E_o (Fig. 6) is proportional to $I_{R2} \times R_2$, hence the result will satisfy Equation 4. It is seen from Fig. 6 that either R_1 or R_2 can be varied without affecting the value of the other. Thus the requirements previously stated are satisfied. Since at balance v_d is equal to either v_1, v_2, v_3, or v_4, whichever is being measured, the relationship between E_o and v_d is

$$E_o = \frac{R_2}{R_1}\; M v_d \tag{6}$$

where M is a multiplier, determined by the ratio R_b/R_a, and is equal to some integral power of ten. A complete analysis of the circuit will be published shortly.

Decimal Point Positioning Circuit

The use of a digital display reduces the problem of positioning the decimal point to one of simple switching. The circuit is shown in Fig. 7. From the figure it can be seen that switching to a larger Lindeck element, R_a, or to a larger ratio, S_n, will move the display decimal point to the right, but moving the "$V=$" decimal point (Fig. 3) to select a

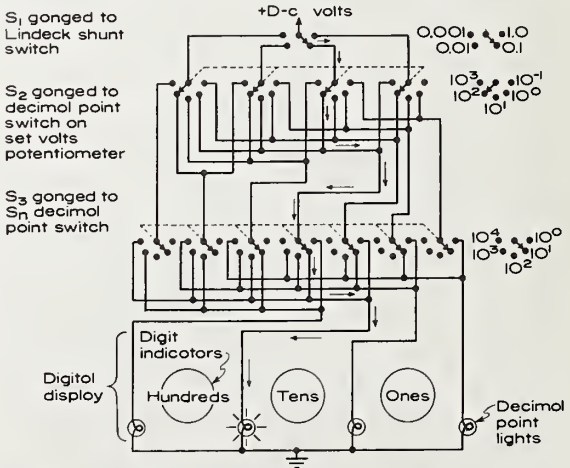

Figure 7. Decimal point positioning (simplified).

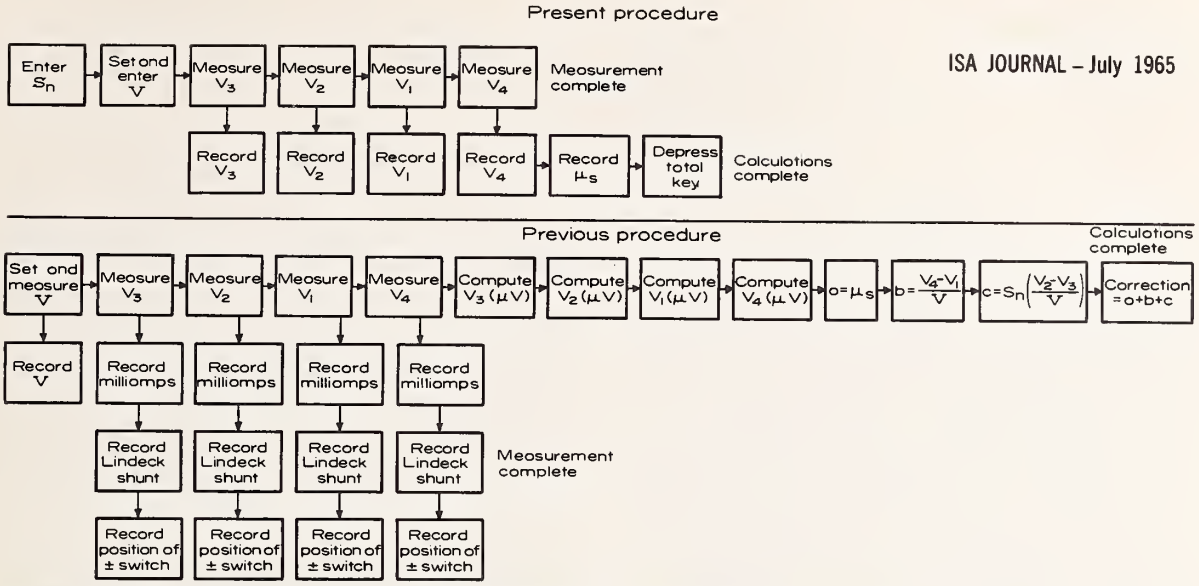

Figure 8. The procedure used with the console contrasted with the previous procedure.

larger value will move the display decimal point to the left. Thus the effect of adjusting the Lindeck element or S_n switches is to multiply by powers of ten, and the effect of adjusting the set-volts, "$V=$" switch is to divide by powers of ten. The result is automatic placement of the decimal point. In the actual circuit, provision is included for the fact that v_1 and v_4 are not multiplied by S_n.

The Guard Circuit

The console is completely guarded, and the measurement circuit is guarded at ground potential. This allows the guard to act as a shield also. A relay grounds the side of the power supply connected to v_1 (Fig. 1) to ground when v_1, v_2, or v_3 is being measured, and grounds the side connected to v_4 when v_4 is being measured. This arrangement allows the cabinet to be grounded without the need for extensive high-voltage insulation.

Problems Encountered

Before active electronic equipment could be added to the measurement circuit, it was necessary to determine its effect on that circuit. The digital voltmeter was found to disturb the circuit when sampling. To remedy this problem, sampling is disabled during the actual measurement. At the completion of the measurement, on command of the operator, the voltage, E_o, is sampled by the digital voltmeter. However, the interaction of the digital recorder was found to be even more severe, and it had to be extensively modified before it was usable.

During the experiments with the console, it was established that the insulation resistance between the working and guard circuits must be kept high. If difference voltages between the two circuits are only as high as 1.5 volts, resistance values below about 100 megohms can result in excessive leakage currents.

It was found that extremely high transient voltages existed under some conditions of reversing the supply voltage. The use of capacitive-resistance spark suppression circuits solved this problem. Of course, the fact that the full supply voltage, 1500 volts, can be used, makes high voltage wiring techniques necessary in some of the circuits.

The 1500-volt supply is not adequately stable for use below about 50 volts, and a chopper-stabilized supply is therefore included for use up to 100 volts. The voltage adjusting circuits of this supply were replaced by a decade resistor of the type found in the standards laboratory, thereby making the supply satisfactory for use down to voltages of less than one volt.

Conclusion

The new console has been in use for more than a year. Through the use of the console, measurement uncertainties have been reduced from approximately ±25 ppm to less than ±10 ppm.* The reduction in the amount of time and effort required in the calibration of a volt box is diagrammed in Fig. 8. Not only has the number of steps been significantly reduced, but the complexity of the steps is also much less. From information gained during the past months of console use, we conclude that the judicious application of the principles of human engineering can be of significant value in the design of precise measuring equipment.

---

*This uncertainty figure, which is consistent with experiment, is the result of the simple addition of the errors that would be introduced in the worst case if all components differed from nominal value by the full amount of the manufacturers' stated tolerance limit and is considered to be the pessimistic limit. It does not include the uncertainty in the correction to the ratio of the standard volt box, nor does it include uncertainties resulting from the effects of ambient conditions on the volt box undergoing measurement.

References

1. Silsbee, F. B., and Gross, F. J., "Testing and Performance of Volt Boxes," RP1419, *J Research NBS*, Vol. 27, Sept. 1941, pp 269-287.

2. Harris, F. K., *Electrical Measurements*, John Wiley and Sons, Inc., New York, 1952, pp 176-177.

3. Dunfee, B. L., "Method for Calibrating a Standard Volt Box," *J. Research NBS*, Vol. 67C, No. 1, Jan.-Mar. 1963, pp 1-3.

4. Sinaiko, H. W., and Buckley, E. P., "Human Factors in the Design of Systems," *NRL Report 4996*, Naval Research Laboratory, Washington, D.C., Aug. 29, 1957.

A METHOD FOR CALIBRATING VOLT BOXES, WITH ANALYSIS OF VOLT-BOX SELF-HEATING CHARACTERISTICS

Ronald F. Dziuba and T. Michael Souders
Electrical Instruments Section
Electricity Division
National Bureau of Standards
Washington, D. C.

Summary

The direct comparison of a "working" volt box with a standard volt box of the same nominal ratio is well known and widely used, since the Guarded Standard Volt Box has recently become commercially available to measurements laboratories.[1] An alternate technique, the Julie ratiometric method,[2] has been recently described, which permits calibration of volt boxes without the need for this standard. The method described herein, suggested by F. L. Hermach, is a modification of the Julie method that has been under study at NBS for well over a year. It proves to be a useful calibration method, featuring speed of operation and high accuracy while requiring only an inexpensive and versatile "ratio standard."* The method is limited to the calibration of volt boxes whose self-heating errors are within the desired accuracy range. However, with the production of volt boxes designed to decrease the self-heating errors by decreasing the rated current (higher "ohms per volt" characteristic) and by using resistance materials having lower temperature coefficients, the method could be increasingly useful for calibrating working volt boxes quickly and easily, to an accuracy within 10 ppm.

Test Method

The Julie method uses a calibrated Kelvin Varley voltage divider in a bridge network to measure successive "step-down ratios"** of a volt box. (An s-d ratio is defined as a ratio of any volt box range to its immediate lower range; for example, 3/1.5, 7.5/3, 15/7.5, . . . 1500/750.) Bridge balance is achieved by adjusting the divider for a null on the detector; the s-d ratio of the volt box is then computed from the corrected divider setting, applying its corrections as measured in a separate test. Any volt box ratio, referred to its lowest section, is obtained by multiplying all the s-d ratios up to and including the first one containing the desired voltage range. If the s-d ratio corrections are small, the correction for the volt box ratio is simply the algebraic sum of the individual s-d ratio corrections.

*Not to be confused with a Guarded Standard Volt Box. Standard in the sense that it is used to calibrate a test instrument.

**Step-down ratio is the inverse of step ratio, the notation used by Julie. The "step-down" ratio lends itself better to the derivation of voltage ratios.

The modification introduced at NBS simplifies the measurement procedure, preserves the precision needed for the s-d ratio measurements, and permits measurements at rated voltage. A guarded ratio standard, see figure 1, comprised of a string of thirteen nominally equal, fixed resistors and a three-dial resistance box, is used directly to measure the s-d ratio of a volt box. Suitable combinations of the thirteen 100 kΩ resistors provide the ratios required to measure s-d ratios from 2/1 to 20/1.* The ratio resistors in the NBS assembly are connected to guarded binding posts mounted on the top panel. The decade resistor, which includes the 10-, 1-, and 0.1-ohm dials of a resistance box, provides the means for balancing the bridge circuit when performing either a self-calibration of the ratio standard or a calibration of a working volt box. A resolution of 1 ppm is possible when performing either test. This is not always feasible when a Kelvin Varley divider is used to measure large s-d ratios.

Calibration Procedure

Ratio Standard

The NBS ratio standard is evaluated, following Julie's method, by using three resistors as fixed arms of a square bridge to measure the remaining ten in succession (see figure 2). By using a different set of three resistors for the fixed arms, the deviations of all thirteen resistors can be referred to one reference resistor. The resistance decade is used to balance the bridge, and is located either in the unknown arm or one fixed arm as necessary, depending on the individual corrections of the resistors. A high resistance detector is necessary, but its impedance does not limit the accuracy, as it might if it were used as a deviation indicator rather than a null device. The guard resistors eliminate errors from leakage resistance of the d-c source to ground, and enable the detector to be at ground potential. The decade dial setting becomes direct reading in ppm when multiplied by 10. From the data, ratios of the standard can be computed. A ratio of the standard is defined as the resistance of a series-connected string of k resistors (high side) divided by the resistance from the low voltage end to any tap point along the string consisting of n resistors (low side). As shown in Appendix A, if Δ_i is the deviation in ppm of the i^{th} resistor in the string from a reference resistor, the expression for computing ratios of the standard is:

*The 20/1 ratio is needed to calibrate a "s-d ratio" of 3/0.15, the largest "s-d ratio" encountered at NBS. All thirteen resistors are needed to provide this ratio.

$$S = S'(1 + s) \approx \frac{k}{n}\left[1 + \frac{\sum_{i=1}^{k}\Delta_i}{10^6 k} - \frac{\sum_{i=1}^{n}\Delta_i}{10^6 n}\right], \quad (1)$$

where s is the correction to the nominal ratio, S', of the standard. Higher order terms are neglected. It should be noted that $k \geq n$ and the n resistors in the low-side are a part of the k resistors in the high-side.

Volt Box

A calibrated ratio of the ratio standard is then compared to an s-d ratio of a volt box (see figure 3). If d_k is the decade resistance reading expressed in ppm of 100 kΩ when the detector is located at position a in figure 3 and d_n is the decade reading in ppm when the detector is located at position b, then, as shown in Appendix A, the expression for computing an s-d ratio of a volt box is:

$$M = M'(1 + m) \approx S'\left[1 + \frac{d_k + d_n}{10^6 k} - \frac{d_n}{10^6 n} + s\right], \quad (2)$$

where m is the correction to the nominal s-d ratio, M'. Higher order terms are neglected. (Note that either $d_k \equiv 0$ or $d_n \equiv 0$, depending on the connection to the decade resistor.) Generally only three different ratios of the ratio standard are required to calibrate a working volt box.

A voltage ratio of the volt box is obtained by multiplying all the s-d ratios up to and including the first one containing the desired voltage range. The expression for computing the voltage ratio is:

$$N_j = N_\rho'(1+\mu_\rho) \approx [M_2' \cdot M_3' \cdot M_4' \cdot \cdots \cdot M_{\rho-1}' \cdot M_\rho'][1 + \sum_{i=2}^{\rho} m_i], \quad (3)$$

where μ_λ is the correction to the nominal voltage ratio, N_λ'. Higher order terms and the limitations of detector sensitivity are considered in Appendices A and B.

Evaluation of the Ratio Standard

When the resistors of the standard are connected in a ratio configuration to measure a volt box s-d ratio, they experience different conditions than when measured individually in the intercomparison circuit. They are subject to ratio errors caused by self-heating, leakage, ambient conditions and high voltage effects.

The resistors used in constructing the ratio standard are hermetically sealed, Evanohm resistors, each having a temperature coefficient not exceeding 5 ppm/°C and a self-heating coefficient not exceeding 10 ppm/watt. The worst case encountered at NBS was in measuring the 1500/750 ratio at rated voltage, where each ratio resistor was required to dissipate nearly 0.3 watt. At this power level, tests indicate that the maximum ratio error caused by self-heating is within 3 ppm, if the standard is calibrated at low voltages. If each resistor is calibrated at the same power level used in the test of a volt box, the uncertainty of ratio caused by self-heating is within 1 ppm.

The guard circuit increases the effective leakage resistance that shunts each 100 kΩ coil to greater than 10^{14} ohms. Consequently, the ratio error caused by leakage is much less than 1 ppm.

Ratio errors, resulting from the effects of high voltage applied to the ratio standard, were determined by a method similar to the one recommended by Julie.[3] Leakage currents were measured when a d-c voltage of 1000 volts in series with a vacuum tube electrometer was applied between the metal case and the series-connected resistors of the ratio standard with the guard resistors not connected. The leakage currents from the resistors to the case of the standard were thus measured by the electrometer which had an input resistance greater than $10^{13}\Omega$. The measured currents were less than 10^{-12} A. The resulting ratio error due to high voltage effects would be negligible.

Rod and Lead Resistance Errors

A volt box is either a three or four-terminal network depending on the number of connecting posts it has at its low end. Julie has considered the effects of rod* resistances on ratio error for the three-terminal type.[4] It is a calibration error inherent in the "bootstrap" procedure of the method. Each s-d ratio measurement necessarily includes the effect of the rod resistance at its high voltage tap. The s-d ratios along with their rod resistance terms are multiplied to give a voltage ratio. However, the voltage ratio of a volt box includes only the rod resistance at its highest voltage tap, not those associated with the intermediate, unused taps. Thus, the calibration error caused by the rod resistances can become accumulative, increasing for higher voltage ratios. This error can be reduced by a proper connection procedure and can be evaluated as discussed by Julie.[5]

The calibration error of a four-terminal volt box includes not only the effects of rod resistances at the high voltage taps, but also the rod resistances at the low input and output terminals. An analysis of these errors and a test procedure for determining their magnitude is given in Appendix C. The error term is the ratio of rod resistance to low-side resistance. The worst case encountered at NBS is the 3/1.5 ratio of a 200 "ohms per volt" volt box. For this situation the error was within 3 ppm.

*Rod resistance is the resistance between the external binding post and the internal tap-point at the resistance string of the volt box. In a standard volt box it is a rod, but in a working volt box it is usually a wire lead.

The leads connecting the test volt box with the ratio standard are in the standard circuit (see figure 3). The maximum error occurs for the 2/1 ratio measurement. Since all lead resistances are less than 0.01 ohm, the resulting error is within 0.1 ppm.

Results

The validity of this method was verified by comparing the results with those obtained by direct comparison with a calibrated guarded standard volt box. At low voltages (negligible self-heating), the agreement was within 10 ppm. This also held true for rated voltage calibrations with volt boxes having negligible self-heating errors. However, rated voltage calibrations differed more than the inherent accuracy of the method with volt boxes having self-heating errors greater than 10 ppm (see Table I). A further investigation indicated that the method did not simulate the manner in which a volt box is normally operated, as did the direct comparison method. To resolve these differences, a study of volt box self-heating, then in progress, was accelerated.

Volt Box Self-Heating

The self-heating errors of over fifty working volt boxes have been observed at NBS during the past two years. Their characteristic curves resemble those shown in figure 4. The magnitude of ratio change and the time required for a state of "ratio equilibrium"* to be established varies with volt box construction and on operating and ambient conditions. Representative values for various volt boxes are given in Table II. Over 80 percent of the volt boxes tested were of manganin construction and had self-heating curves on the higher voltage ranges represented by c in figure 4.

To determine why some heating curves went through a maximum value; resistance and temperature measurements were performed on the high and low sections of several volt boxes. Results of some typical measurements are given in figures 5 and 6. The curves indicate that the heating of the high section is significant, with temperature changes approaching 12°C. The major portion of this resistance heating and the major changes in ratio occur within 10 minutes after the volt box is energized. In contrast, the resistance heating of the low section is small. Eventually, the low side temperature increases by external heating caused by the transfer of heat from the high side. This effect, called "proximity heating," has a long time constant because of poor air circulation within the box. When ratio equilibrium is established, the high side, low side, and box temperatures are constant.

*Some volt boxes, which have large self-heating errors, do not come to a true state of equilibrium after a reasonable warm-up period. When the ratio changes less than 2 ppm/15 minutes, a state of "ratio equilibrium" is said to exist.

A peak can occur as a result of these two heating effects and as a consequence of the resistance-temperature (R-T) properties of manganin wire. Figure 7 depicts a typical R-T curve for manganin, divided into several zones. The maximum, zone B, of this curve is in the neighborhood of room temperature, being generally between 20° and 50°C, while the minimum, zone D, is at 350°C.[6] The majority of the commercial volt boxes calibrated at NBS were constructed of manganin wire whose maximum was specified to occur around 28°C. Figure 5 indicates that the resistance of the high side, initially in zone A on the R-T curve, passes through zone B into zone C. The low side resistance, which increases slightly is always in zone A. Since the voltage ratio is directly proportional to a resistance increase in the high side and inversely proportional to a resistance increase in the low side, curve c in figure 4 is the resultant. The temperature measurements, shown graphically in figure 6, further substantiate the existence of this peak value.

The other self-heating curves of working volt boxes constructed of manganin can be explained in a similar fashion. Curve a in figure 4 results when the resistance material is initially in zone A and never leaves this zone. Curve d, the mirror image of a, is observed when the resistance material is initially in zones B or C and never leaves zone C during a heat run. In any practical construction the manganin will not heat sufficiently to pass into zone D. Curve b has been observed for one volt box and the reason for its shape is not certain. A reasonable explanation is that initially its resistance material is located in zones B or C. During the heat run, the high side reaches temperature equilibrium quickly, then follows the proximity heating effect of the low side causing the reversal of the volt box ratio.

Working volt boxes constructed of Evanohm or of a similar alloy have self-heating curves represented by a or d in figure 4. This results from the linear temperature coefficient of Evanohm. Generally, the magnitude of the self-heating error is less than that for manganin volt boxes of the same ohms-per-volt characteristics.

The general procedure for calibrating a working volt box at NBS by the direct comparison method is to observe the ratio at rated voltage on the highest voltage range as a function of time and then proceed to the lower ranges in descending order. A moderate amount of time is spent waiting for ratio equilibrium at these lower ranges, approximately five to fifteen minutes. Tests performed in the reverse order (ascending) could differ significantly from the decending order tests on ranges where self-heating is a problem. This is observed with working volt boxes having no ventilating ports. The slow rate of heat transfer in these boxes accounts for these differences. To limit this uncertainty, calibration procedures should be specified.

A further complication to the self-heating problem is the effect of ambient conditions. Temperature, humidity, and air circulation, modulate

the magnitude of the error and the time for ratio equilibrium to be established. For high accuracies in volt box measurements, these conditions should be known during calibration and duplicated during use.

The above analysis pertains to working volt boxes but can also be applied to Guarded Standard Volt Boxes. Some standards can have significant self-heating errors as large as 30 ppm. Some of the heating effect within a standard can be attributed to the self-heating of the guard resistors. Their curves usually resemble a or d in figure 4.

Conclusion

The accuracy of a volt box calibration is limited by the uncertainty of the self-heating error of the volt box. To reduce this uncertainty test conditions and procedures should be strictly specified and then duplicated by the user. This is not always practical or desirable. As a result, the tendency on the part of the manufacturer has been to decrease the rated power dissipation of a volt box to decrease this self-heating error.

Consequently, working volt boxes having negligible heating errors can be calibrated by methods that do not necessarily duplicate the conditions of use. The technique described herein serves as such a useful calibration method. Working volt boxes can be calibrated to accuracies within 10 ppm of ratio by this method, which requires only an inexpensive and versatile standard.

References

1. Dunfee, Bernadine, "Method for Calibrating a Standard Volt Box," Journal of Research, National Bureau of Standards, C, Engineering and Instruments, Vol. 67C, No. 1, Jan.-Mar., 1963.

2. Julie, Loebe, "A Ratiometric Method for Precise Calibration of Volt Boxes," Julie Research Laboratories, Inc., 1964. A similar technique has been used for several years in the Standards Laboratory of the Scintilla Division of the Bendix Corporation.

3. Julie, op. cit.

4. Ibid.

5. Ibid.

6. Harris, Forest K., Electrical Measurements, John Wiley & Sons, Inc., New York, New York, 1952.

7. Julie, op. cit.

Appendix A

Derivation and Evaluation of Calibration Equations

As mentioned in the text, a ratio of the standard is defined as a series-connected string of k resistors (high-side) to any tap point along the string consisting of n resistors (low-side). The ratio equals:

$$S = S'(1+s) = \frac{\sum_{i=1}^{k} R_i}{\sum_{i=1}^{n} R_i}, \quad \text{where } k>n. \tag{4}$$

The R_i's can be expressed in terms of a reference resistor, R_1, and ppm deviations from R_1, Δ_i's, as:

$$R_i = R_1 \left(1 + \frac{\Delta_i}{10^6}\right) \tag{5}$$

Therefore, the ratio S becomes:

$$S'(1+s) = \frac{\sum_{i=1}^{k} R_1\left(1+\frac{\Delta_i}{10^6}\right)}{\sum_{i=1}^{n} R_1\left(1+\frac{\Delta_i}{10^6}\right)} = \frac{kR_1\left(1+\frac{\sum_{i=1}^{k}\Delta_i}{10^6 k}\right)}{nR_1\left(1+\frac{\sum_{i=1}^{n}\Delta_i}{10^6 n}\right)} \tag{6}$$

Expanding the denominator by the binomial theorem, S becomes:

$$S'(1+s) \approx \frac{k}{n}\left[1+\frac{\sum_{i=1}^{k}\Delta_i}{10^6 k} - \frac{\sum_{i=1}^{n}\Delta_i}{10^6 n} + \ldots\right] \tag{7}$$

The resistor deviations, Δ_i's, are less than 10 ppm. The error introduced when neglecting higher order terms is less than 10^{-10}.

An s-d ratio of a volt box is compared to a standard ratio S. To balance the bridge network, a decade resistor is inserted at point a or point b of the standard (see figure 3). If this decade resistance is expressed as r_k when the detector is at point a in figure 3, and r_n when the detector is at point b, then the equation of an s-d ratio is:

$$M = M'(1+m) = \frac{\sum_{i=1}^{k} R_i + r_k + r_n}{\sum_{i=1}^{n} R_i + r_n} \tag{8}$$

Substituting in equation 5 gives:

$$M'(1+m) = \frac{kR_1 + R_1\frac{\sum_{i=1}^{k}\Delta_i}{10^6} + r_k + r_n}{nR_1 + R_1\frac{\sum_{i=1}^{n}\Delta_i}{10^6} + r_n} \tag{9}$$

Factoring out kR_1 and nR_1, expanding by the binomial theorem and using equation 7, M becomes:

$$M'(1+m) \approx S'\left[1 + \frac{r_k+r_n}{kR_1} - \frac{r_n}{nR_1} + s + \ldots .\right] \qquad (10)$$

where $S' = k/n$. If r_k and r_n are expressed in ppm of R_1 (100 kΩ) as d_k and d_n respectively, M then becomes:

$$M'(1+m) \approx S'\left[1 + \frac{d_k+d_n}{10^6 k} - \frac{d_n}{10^6 n} + s\right] \qquad (11)$$

where, as mentioned in the text, $d_k \equiv 0$ or $d_n \equiv 0$, depending on the connection of the decade resistor.

The s-d ratio corrections for a volt box are usually within 100 ppm. An error less than 10^{-8} is introduced when nelgecting higher order terms of this equation.

The s-d ratios can also be expressed in terms of the resistance sections of a volt box. If ℓ refers to the number of sections, the general term for M would be:

$$M_\ell = M'_\ell(1+m_\ell) = \frac{\sum_{i=1}^{\ell} R_i}{\sum_{i=1}^{\ell-1} R_i}, \qquad (12)$$

where $\ell \geq 2$.

The voltage ratio of a volt box is obtained by multiplying all the M_ℓ's up to and including the first one containing the desired voltage range. The expressions for computing this ratio are:

$$N_\ell = N'_\ell(1+\mu_\ell) = M_2 \cdot M_3 \cdot \cdots M_{\ell-1} \cdot M_\ell , \qquad (13)$$

$$N'_\ell(1+\mu_\ell) = M'_2(1+m_2) \cdot M'_3(1+m_3) \cdot \cdots \cdot M'_\ell(1+m_\ell) \qquad (14)$$

$$N'_\ell(1+\mu_\ell) \approx \left[M'_2 \cdot M'_3 \cdot \cdots \cdot M'_{\ell-1} \cdot M'_\ell\right]\left[1 + \sum_{i=2}^{\ell} m_i + \ldots .\right] \qquad (15)$$

Equation 15 is identical to equation 3 in the text. To analyze the higher order terms, assume a maximum s-d ratio correction δ_m, in equation 14. Therefore equation 15 becomes:

$$N'_\ell(1+\mu_\ell) = \left[M'_2 \cdot M'_3 \cdot \cdots \cdot M'_{\ell-1} \cdot M'_\ell\right]\left[1+\delta_m\right]^{\ell-1} \qquad (16)$$

Expanding the correction term by using the binomial theorem, N_ℓ becomes:

$$N_\ell \approx \left[M'_2 \cdot M'_3 \cdot \cdots \cdot M'_\ell\right]\left[1 + (\ell-1)\delta_m + \frac{(\ell-1)(\ell-2)\delta_m^2}{2!} + \ldots .\right] \qquad (17)$$

The worst case would be for the highest ratio, where ℓ might be as large as 10. For this case, even if δ_m = 100 ppm the error introduced by neglecting higher order terms is less than 0.5 ppm.

Appendix B

Evaluation of Errors Associated with Sensitivity Limit

The accumulation of errors in the voltage ratio equation that are due to the limit of sensitivity of the detector in the determination of each s-d ratio can be significant. If each step-down ratio has an error of α as a result of the sensitivity limit, the voltage ratio equation can be expressed as:

$$N'_\ell(1+\mu_\ell) \approx \left[M'_2 \cdot M'_3 \cdot \cdots \cdot M'_{\ell-1} \cdot M'_\ell\right]\left[1 + \sum_{i=2}^{\ell} \alpha_i\right] \qquad (18)$$

The total error could apprximate $(\ell-1)\alpha_m$, where α_m is the maximum resolution error for a s-d ratio measurement. However, a more realistic evaluation of the total error would be to combine the independent errors by the square root of the sum of the squares, as they are as likely to compensate for one another as to add. The total error would be:

$$\epsilon = \sqrt{(\ell-1)} \cdot \alpha_m \qquad (19)$$

Assuming a α_m of 1 ppm, the total error when ℓ = 10 would be 3 ppm.

Appendix C

Evaluation of Errors Associated with Rod Resistors

A four-terminal volt box in an operational setup is shown in figure 8. Rod resistance r'_o is part of the high side resistance only. Rod resistance r_o and r_1 are in the potentiometer circuit and consequently are not significant in the voltage ratio of the volt box. The voltage ratio is expressed as:

$$N_{i\ell} = \frac{r'_o + \sum_{i=1}^{\ell} R_i + r_\ell}{R_1}, \qquad (20)$$

where $\ell \geq 2$.

There are four possible ways to connect leads to the low end of a four-terminal volt box when calibrating an s-d ratio. The lead connection employed at NBS is shown in figure 3 and is the best arrangement for supressing the ratio error caused by rod resistances r'_o and r_o, if the resistance of each unit of the ratio standard is greater than that of the lowest section of the volt box. The s-d ratio for this circuit arrangement is:

$$M_\ell = \frac{\sum_{i=1}^{\ell} R_i + r_\ell}{\sum_{i=1}^{\ell-1} R_i} \qquad (21)$$

A voltage ratio expressed in terms of the s-d ratios is:

$$N_\ell = M_2 \cdot M_3 \cdot \cdots \cdot M_{\ell-1} \cdot M_\ell \qquad (22)$$

After substituting, rearranging and then dividing by equation 20, the voltage ratio for the connections of figure 8 can be expressed as:

$$N_\ell = N_{\ell u} \left[1 - \frac{r_o'}{\sum_{i=1}^{\ell} R_i} + \sum_{k=2}^{\ell-1} \frac{r_k}{\sum_{i=1}^{k} R_i} \right], \qquad (23)$$

where $\ell \geq 2$.

The error term,

$$\frac{r_o'}{\sum_{i=1}^{\ell} R_i} \qquad (24)$$

is maximum for i=1; and is greatest for the lowest "ohms per volt" volt boxes. The error was measured by using the bridge circuit shown in figure 9, where d is the three-dial resistance decade reading and R a 100 kΩ resistor. The error term can be computed from the following expression:

$$\frac{r_o'}{R_1} = \frac{d}{R} \qquad (25)$$

Lead resistance L, which is located in the decade arm, must be sufficiently small or known so as not to introduce an added error.

The term,

$$\sum_{k=2}^{i-1} \frac{r_k}{\sum_{i=1}^{k} R_i}, \qquad (26)$$

is the accumulative error caused by the rod resistances at the high end. It is identical with the calibration error associated with a three-terminal volt box as discussed and evaluated by Julie.[7] It can be suppressed by placing the rod resistances in the ratio standard circuit. Since rod resistances are usually less than 0.01 ohm, the error introduced by this term is negligible.

Table I

A. 200 "ohms per volt" volt box

Voltage Range	Voltage Ratio Correction in ppm: At 20% Rated Voltage, Direct Comparison Method	At 20% Rated Voltage, S-D Ratio Method	At 100% Rated Voltage, Direct Comparison Method	At 100% Rated Voltage, S-D Ratio Method
750	- 65	- 58	-140	- 99
300	+ 11	+ 2	- 42	- 12
150	+ 30	+ 22	- 10	+ 15
75	- 3	- 13	- 28	- 19
30	+100	+ 98	+110	+118
15	+141	+143	+144	+148
7.5	+100	+ 99	+ 98	+ 98
3	+ 9	+ 7	+ 9	+ 8

B. 1000 "ohms per volt" volt box

500	- 2	- 5
300	- 3	- 6
200	- 3	- 5
100	- 4	- 5
50	- 10	- 13
30	- 23	- 25
20	- 22	- 24
10	- 18	- 19
5	- 7	- 8
3	+ 1	+ 1
2	+ 2	+ 2

Table II

Volt Box: ohms/volt	Volt Box: Voltage Range	Ratio Correction in ppm Referred to 20% Rated Voltage Value: At Peak	At Equilibrium
200	750	+45	-190
	750	+48	-104
	750*	+59	- 67
	300*	+44	+ 12
750	1500**	+57	+ 8
	750**	+50	+ 18
	750	+18	- 8

* Same Volt Box
** Same Volt Box

Two hour heat run for 200 ohms/volt volt boxes
One hour heat run for 750 ohms/volt volt boxes

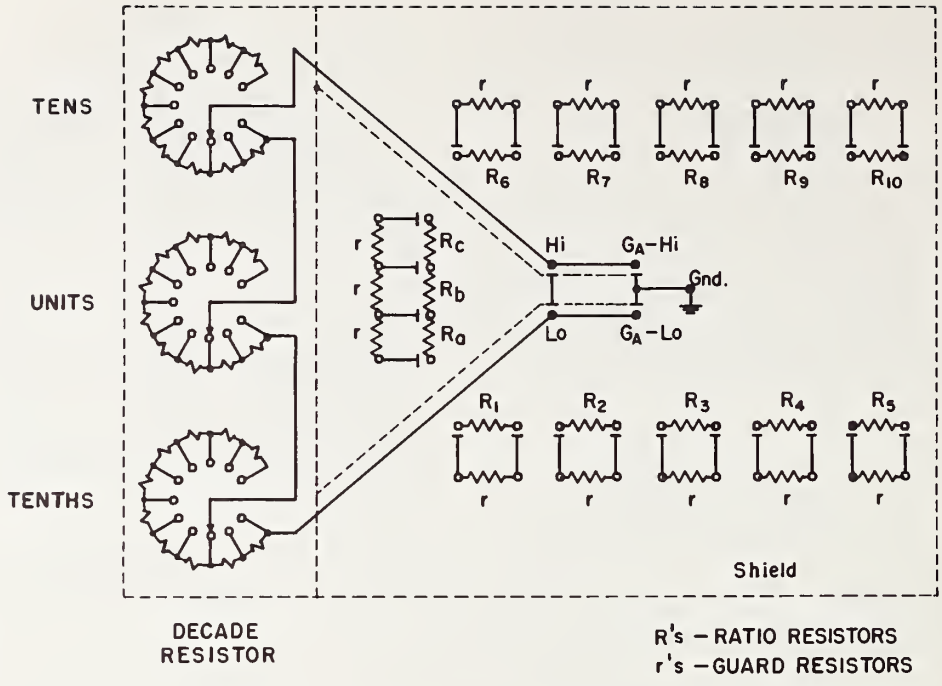

Figure 1 Layout Diagram of Ratio Standard

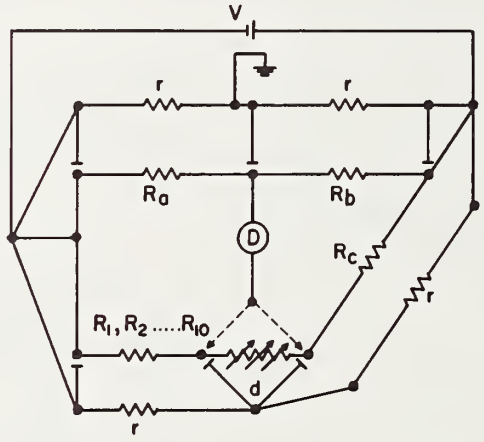

R_a, R_b, R_c – Fixed Bridge Arms
$R_1, R_2 \ldots R_{10}$ – Ratio Resistors
r's – Guard Resistors
d – Decade Resistor

Figure 2 Intercomparison of Ratio Resistors

$$\text{Standard Ratio} = S'(1+s) \approx \frac{k}{n}\left[1 + \frac{\sum_{i=1}^{k} \Delta_i}{10^6 k} - \frac{\sum_{i=1}^{n} \Delta_i}{10^6 n}\right]$$

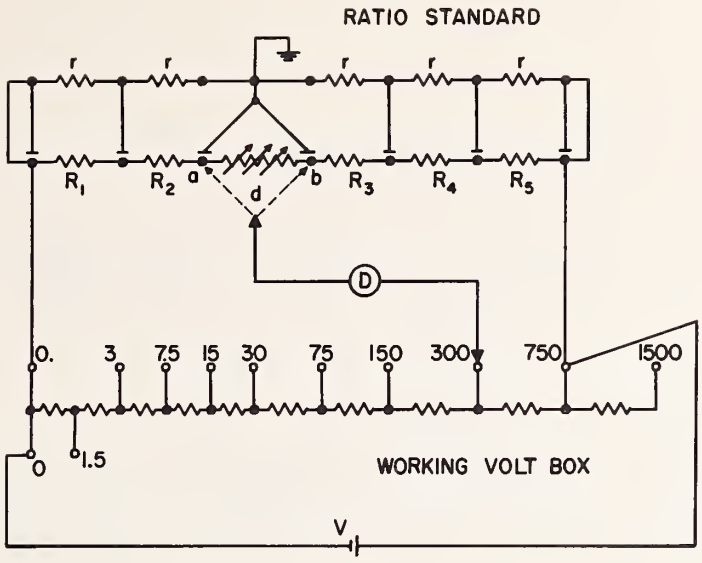

Figure 3

S-D Ratio Measurement

$$\text{S-D Ratio} = M'(1+m) \approx S'\left[1 + \frac{d_k + d_n}{10^6 k} - \frac{d_n}{10^6 n} + s\right]$$

$$\text{Voltage Ratio} = N_l'(1+\mu_l) \approx \left[M_2' \cdot M_3' \cdot \cdots \cdot M_{l-1}' \cdot M_l'\right]\left[1 + \sum_{i=2}^{l} m_i\right]$$

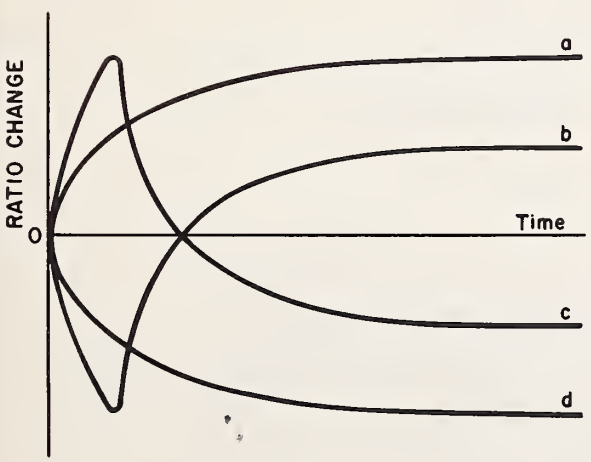

Figure 4 Self-Heating Curves

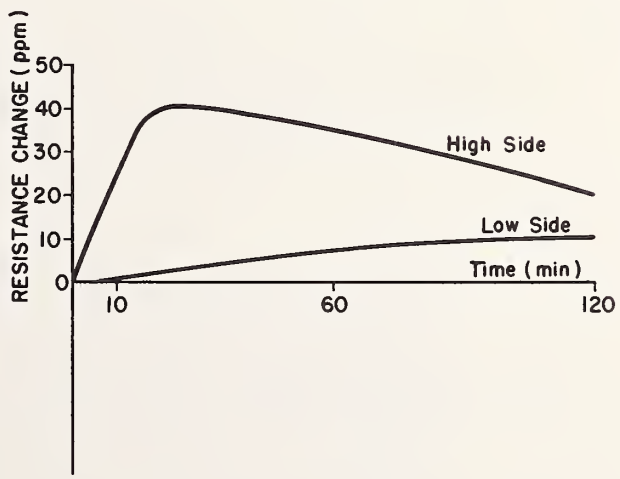

Figure 5 Resistance-Time Curve of a Volt Box

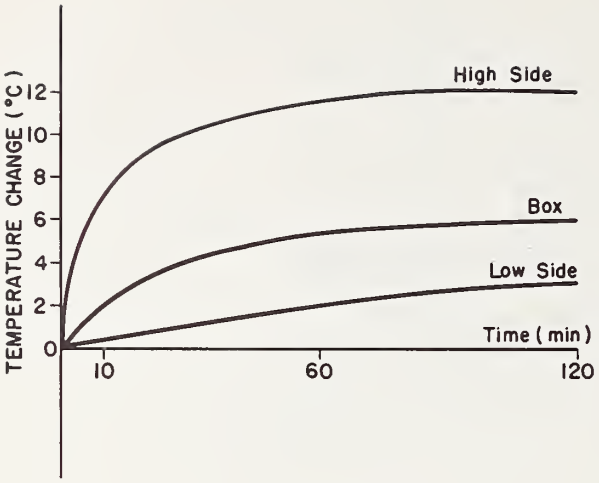

Figure 6
Temperature-Time Curve of a Volt Box

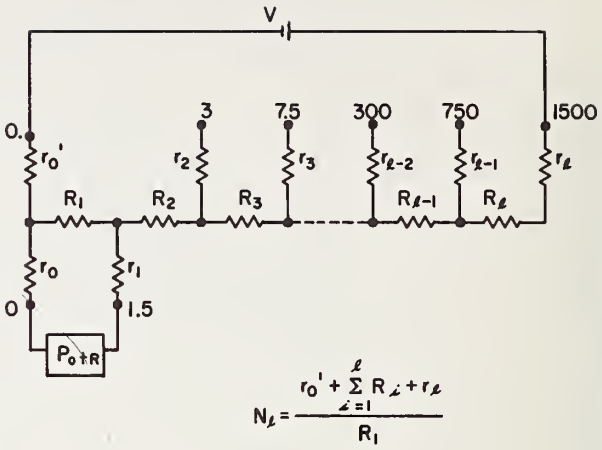

Figure 8
Volt Box Operating as a Four-Terminal Network

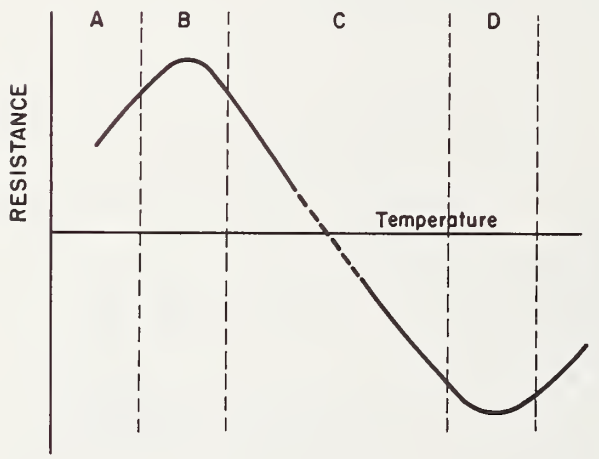

Figure 7
Resistance-Temperature Curve for Manganin

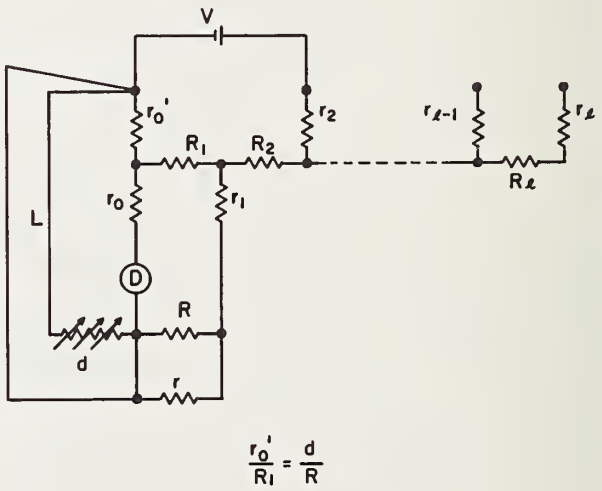

Figure 9
Method for Measuring Rod Resistance

Reprinted from:
1966 IEEE INTERNATIONAL CONVENTION RECORD
Part 10

U. S. Department of Commerce National Bureau of Standards

RESEARCH PAPER RP1323

Part of Journal of Research of the National Bureau of Standards, Volume 25, August 1940

METHODS, APPARATUS, AND PROCEDURES FOR THE COMPARISON OF PRECISION STANDARD RESISTORS

By Frank Wenner

ABSTRACT

Reference is made to some of the more important contributions that have been made to the subject of precise measurements of electrical resistance. The sensitivity of bridges when used with the modern high-sensitivity moving-coil galvanometer is discussed rather fully. Special consideration is given to the methods and apparatus used and to the procedures followed in the National Bureau of Standards in those comparisons in which the precision desired is of the order of 1 part in a million.

The more important factors limiting the precision of the comparisons, such as load coefficients, terminals, and contacts, thermoelectromotive forces, insulation, and the optical system of the galvanometer, are discussed rather fully. A method of analysis of networks containing both linear and nonlinear four-terminal conductors is given, and the theoretical basis for the experimental procedure used in determining the effect of slight defects in the insulation is pointed out. This is followed by a brief discussion of Ohm's law from the standpoint of precise resistance measurements and by a brief discussion of units of resistance. Finally, reference is made to more than 100 publications having a more or less direct bearing on the subject of resistance comparisons.

Research Paper 133
NBS Journal of Research
Volume 4, January 1930

NOTES ON THE DESIGN OF 4-TERMINAL RESISTANCE STANDARDS FOR ALTERNATING CURRENTS

By Francis B. Silsbee

ABSTRACT

The design of a resistance standard for use with alternating current involves not only the consideration of the value, definiteness, and permanence of the resistance and the adequate cooling of the metal parts, which are encountered in direct-current standards as well, but also the consideration of the inductance and of the possible change in the resistance of the standard with the frequency of the current flowing in it. These notes give the theoretical basis for the computation of the inductance of resistance standards which consist of a system of straight conductors long in comparison to their diameters. Most standards used in the measurement of large currents are of this type. Formulas are given for the skin effect in various combinations of flat strips and coaxial tubes. Methods of attaching and locating the potential leads so as to minimize the possibility of error from stray magnetic fields and yet permit of convenient adjustment of the resistance are discussed. As examples of the principles here set forth, detailed descriptions are given of two groups of resistance standards which have been constructed at the Bureau of Standards for testing current transformers. These standards range in resistance from 0.05 to 0.0002 ohm and in current capacity from 10 to 2,500 amperes.

315-411 O - 68 - 16

Journal of Research of the National Bureau of Standards Vol. 50, No. 3, March 1953 Research Paper 2402

Measurement of Multimegohm Resistors

Arnold H. Scott

The method by which multimegohm resistors are measured at the National Bureau of Standards is a null method using an electrometer as the null detector. The charge flowing through the resistor during the time of measurement is obtained from a variable air capacitor maintained at a fixed potential. The potentials across the variable air capacitor and thus across the specimen are maintained constant as indicated by the null reading of the electrometer by decreasing the capacitance of the air capacitor at just the right rate. The capacitance of the capacitor is varied by a small direct-current motor geared to the shaft of the capacitor and whose speed can be controlled. Several multimegohm resistors of two different makes have been studied over a period of about three years. Although these are the most stable multimegohm resistors available, it was found that they had erratic fluctuations of 0.5 to 1 percent and were generally voltage sensitive. With the impressed voltage varied from 1.5 to 180 volts, various resistors showed resistance changes ranging from 0.4 to 26.9 percent.

NBS Monograph 39
March 1962

Calibration Procedures for Direct-Current Resistance Apparatus
Paul P. B. Brooks

This monograph was written in response to a demand for information on methods used at the National Bureau of Standards for the calibration of d-c resistance apparatus. The paper was written primarily for use by laboratory technicians and therefore contains much detail that is unnecessary for those with scientific training. However, the techniques described have been found helpful by physicists and engineers concerned with accurate electrical metrology.

The monograph is divided into three parts. Part 1 entitled "General Outline of Equipment and Procedures" discusses errors, corrections, tolerances, standard resistors, galvanometers, the algebra of small quantities, the Direct Reading Ratio Set, and the Universal Ratio Set. Practical examples of the use of these ratio devices are given. Part 2 given detailed information on the calibration of a Wheatstone Bridge using the DRRS and techniques described in Part 1. Part 3 discusses the calibration of general purpose potentiometers using the URS and gives detailed instructions regarding the calibration of a specific type of potentiometer.

Chester Peterson
August 24, 1967

NBS Technical Note 172
March 1963

Practical Methods for Calibration of Potentiometers

David Ramaley

Potentiometer circuitry, particularly as related to calibration, is discussed with the primary consideration given to the required circuit measurements. The more feasible means of calibrating potentiometers are described in considerable detail. Emphasis is placed upon the use of the Universal Ratio Set as the basic implement for accomplishing the major portion of potentiometer calibrations.

NBS Technical Note 220
August 1964

SOME MODIFICATIONS IN METHODS OF CALIBRATION OF UNIVERSAL RATIO SETS

David Ramaley

Universal Ratio Sets can be calibrated by a number of different methods. The well established methods are very briefly outlined and emphasis is placed on some more recent developments. The choice of methods will depend upon available laboratory equipment and other considerations.

JOURNAL OF RESEARCH of the National Bureau of Standards—C. Engineering and Instrumentation
Vol. 70C, No. 3, July–September 1966

A Versatile Ratio Instrument for the High Ratio Comparison of Voltage or Resistance

Alfred E. Hess*

Institute for Basic Standards, National Bureau of Standards, Boulder, Colo.

(April 12, 1966)

A 9-dial resistance ratio instrument capable of precise high ratio comparison of voltage or resistance (from 1/1 to 10^7/1) is described. Also described is the modification of a 6-dial universal ratio set to permit its additional use as a versatile ratio instrument. Paramount to the accuracy of these high ratio instruments is the carefully adjusted "common point" junction which is briefly discussed.

Key Words: DRRS (direct reading ratio set); junction; precision measurements; ratio, resistor, four-terminal; resistance decade; transresistance; URS (universal ratio set); VERI (versatile ratio instrument).

Capacitors and Inductors

Papers

Abstracts

JOURNAL OF RESEARCH of the National Bureau of Standards—C. Engineering and Instrumentation
Vol. 69C, No. 3, July–September 1965

Improved Ten-Picofarad Fused Silica Dielectric Capacitor[1]

R. D. Cutkosky and L. H. Lee

(March 8, 1965)

Some defects in a set of fused silica dielectric capacitors constructed in 1961 are listed, and methods for their reduction or elimination are described. The construction of a new set of capacitors completed in 1964 is described in detail. Preliminary stability data presented indicate that the typical drift of the 1964 capacitors with respect to their mean was less than two parts in 10^7 in five months.

1. Introduction

Capacitors utilizing fused silica as the dielectric have been under investigation at NBS and elsewhere [1][2] for many years. Early indications were that suitably constructed capacitors of this type would be at least as stable as air capacitors, and additionally would be sufficiently rugged to withstand shipment between laboratories.

A set of four fused silica dielectric 10-pF capacitors was constructed at NBS in 1961 [2]. The capacitance elements of these capacitors consisted of fused silica disks 7 cm in diameter and 1 cm thick. Silver electrodes were fired on the two faces of the disks and a third electrode was fired on the cylindrical surface. The cell in which the element was mounted shielded the face electrodes from each other in the region external to the fused silica element, and was connected electrically to the cylindrical electrode of the element. The housing contained a four-terminal resistance thermometer for temperature measurement and was hermetically sealed.

One of the 1961 capacitors was successfully hand-carried to several distant laboratories and returned. These laboratories included NRC (Canada), NPL (England), and NBS Boulder. The largest change in capacitance observed upon completion of the round trip was 0.2 parts in 10^6 (ppm). A shipment of this capacitor by commercial carrier was not successful and resulted in a change in its capacitance of 36 ppm. This change was traced to a sensitivity to severe mechanical shock.

The 1961 capacitors had a number of undesirable features, the shock sensitivity being by far the most important. Further investigation indicated that all of the capacitors in the set suffered from this flaw, and that the change in capacitance was caused by motion of the fused silica element in its cell. The element was supported in the cell by means of phosphor bronze springs which permitted motion of the element along the cell axis. The element could not return to its equilibrium position after displacement because of frictional forces between the cylindrical surface of the element and the spring contacts attached to the cell. This mechanism could not have caused a capacitance change if the direct electrical field between the face electrodes had been entirely within the fused silica. Unfortunately, the direct capacitance included a small contribution due to fields from the back of a face electrode which entered the fused silica element at the insulation gap between this face electrode and the cylindrical shield electrode, and terminated at the opposite face electrode. Motion of the element within its cell altered the leakage field and consequently changed the total direct capacitance.

A second flaw in the 1961 capacitors was a pronounced dependence of capacitance upon voltage. It was necessary to restrict the voltage applied to these capacitors to 10 V rms to reduce the measurement uncertainty from this cause below 0.1 ppm. Since sufficient sensitivity is available at this voltage to see one part in 10^7, the voltage dependence did not seriously limit measurement accuracy. An investigation into the mechanism of the voltage dependence was made, and it was found that the dependence could be almost eliminated by increasing the thickness of the fired silver electrodes. The evidence indicates that the existence of islands of silver on the dielectric surface which are not in good electrical contact with the body of the electrode is in some way responsible for the large voltage dependence. A similar effect has been observed in mica capacitors with fired or deposited silver electrodes [3].

Measurements of capacitance and dissipation factor as a function of frequency indicated a capacitance difference from 50 Hz to 20 kHz of about 25 ppm, with a maximum slope and a maximum dissipation factor at about 1600 Hz. The shape of the curve suggested a relaxation mechanism involving polar impurities in the fused silica. An investigation of several optical grades of fused silica disclosed that the use of a grade possessing exceptionally good ultraviolet transmission characteristics resulted in capacitors with very much smaller frequency dependencies and with dissipation factors not greater than 3×10^{-6} throughout the audio-frequency region.

Examination of the published optical characteristics for the various grades tested disclosed no correla-

[1] This work was supported in part by the Metrology Engineering Center, Bureau of Naval Weapons, Pomona, Calif.
[2] Figures in brackets indicate the literature references at the end of this paper.

tion between optical absorption and audio-frequency behavior. It is felt that the presence or absence of the audio-frequency relaxation phenomenon is an accidental result of the technique for producing fused silica. It is possible that changes in manufacturing technique which have no effect on the optical properties of the fused silica may greatly affect the audio-frequency characteristics.

The temperature coefficients of the 1961 capacitors were about 14 ppm/°C. The large values were believed to be the result of a large temperature coefficient of dielectric constant in fused silica. Resistance thermometers were built into the capacitor housings to eliminate the measurement uncertainties caused by unknown temperatures.

A set of twelve 10-pF fused silica dielectric capacitors was built in 1964. Care was taken to reduce greatly all of the flaws listed above. The capacitance elements were constructed of type II Suprasil,[3] and were supported in their cells by means of tightly fitting polytetrafluoroethylene (PTFE) rings. Care was taken to keep the gaps between the face electrodes and the cylindrical shield electrode as small as seemed consistent with operation up to 200 V rms. The voltage dependence of each capacitor was measured before final sealing, and the electrodes were replated when necessary. The 1964 capacitors are physically smaller and much lighter than the 1961 capacitors, but were not designed with this as a principal objective.

The construction of these new capacitors is described in some detail to allow their reproduction elsewhere. Some characteristics of the completed set are then presented.

2. Construction

2.1. Housing

A cross section of the capacitance standard is shown in figure 1. The exterior of the assembly is constructed entirely of stainless steel. The hermetically sealed region at the bottom containing the fused silica element is welded shut upon completion, and after baking, the container is filled with dry N_2 through a copper sealoff tube. Electrical connections are made to the capacitor element and to the four-terminal resistance thermometer by means of glass-Kovar seals soft soldered to the sealed compartment.

Electrostatic shields not shown in figure 1 isolate the two face electrode leads from each other and from the resistance thermometer leads. The face electrode leads pass through stainless steel tubes as shown to a pair of coaxial connectors located above the liquid level of a constant-temperature oil bath. The resistance thermometer leads are attached to four binding posts located below the liquid level. Details of the construction can be seen in figure 2.

[3] Available from Amersil Quartz Company.

FIGURE 1. *Cross section of the capacitance standard.*

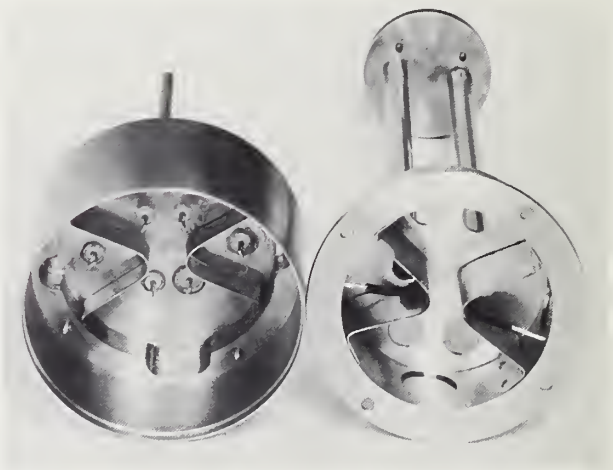

FIGURE 2. *Details of the capacitor housing and superstructure.*

The dimensions of the fused silica element and its mounting are shown in figure 3. The PTFE radial support is inserted into the slot of the brass cell before the inside diameter of the PTFE is finish machined. Each fused silica element is individually fitted to its cell by machining this radial support so

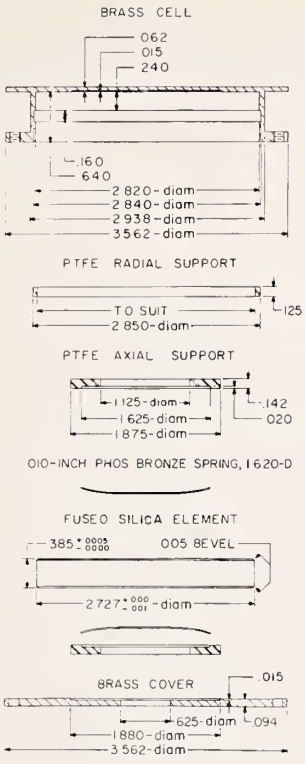

FIGURE 3. *Fused silica capacitance element and cell dimensions*

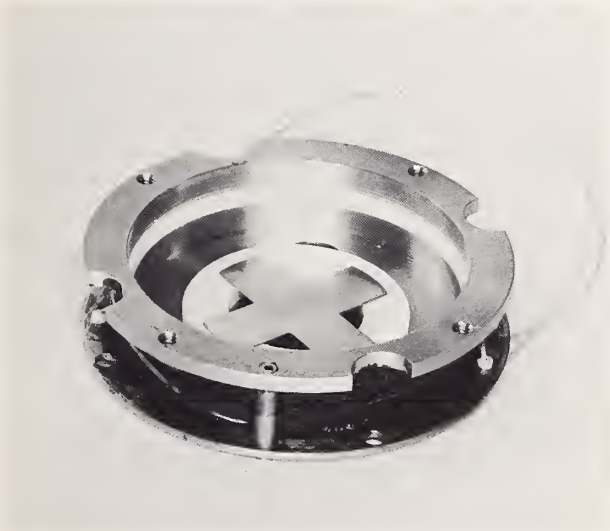

FIGURE 4. *Partially assembled capacitance element cell.*

that the element with its silver electrodes in place can just be removed from the cell with a rubber suction cup. The axial (vertical) constraint on the element is controlled by the use of shims or by machining, so that an axial interference of about 0.001 in. is obtained. This results in a slight compression of the PTFE axial supports.

Electrical connections to the face electrodes on the fused silica element are made by means of wires soldered to the phosphor bronze disk springs shown in figure 3. The disks are cut to the shape of an X and bent as shown in figure 4. Electrical connection between the cylindrical electrode and the cell is made by inserting three 0.030-in. diam phosphor bronze wires about 2 in. long into the circular gap between the cell and the element. The ends of these wires lie in the slot at the sides of the cell with the PTFE radial support. The three wires are positioned uniformly around the circumference of the cell and provide three points of electrical contact.

2.2. Resistance Thermometer

The four-terminal thermometer is located on the outside of the cell containing the fused silica element, as shown in figures 1 and 4. The cell is prepared by cementing a layer of linen cloth over it with shellac and baking at 100 °C. A length of B & S No. 36 Formvar insulated copper wire with a resistance of 25 Ω is doubled over and wound bifilarly over the linen. More shellac is then applied and baked. Leads to the current and potential terminals are connected to the resistance wire with soft solder. The junctions are tied down securely and shellac is applied. The completed thermometer is baked for 24 hr at 75 °C.

2.3. Fused Silica Element

The fused silica element is ground to the dimensions shown in figure 3 with conventional toolroom grinding equipment. Some care is necessary to prevent chipping of the edges. After inspection for chips, the element is cleaned with alcohol, and then with soap and water. It is next immersed in an ultrasonic cleaning bath containing a wetting agent, and rinsed with water. Finally, it is immersed in an ultrasonic cleaning water bath and rinsed with distilled water. After drying at 100 °C, Dupont Silver Paint #4666 is sprayed onto one face and the cylindrical surface, and allowed to air dry. The other face is then sprayed and dried, and the silver is fired onto the element at 480 °C. It is found that single silver deposits thicker than 0.0005 in. are often defective, and that a single application is not sufficient to prevent a dependence of capacitance upon voltage. A satisfactory remedy is to buff the electrode surface with fine steel wool and apply two additional coats of paint to the electrodes. The preferred final electrode thickness is between 0.0010 and 0.0015 in. If the electrode thickness is increased to 0.002 in., the large thermal expansion coefficient of the silver often causes the fused silica element to chip when it is

cooled from the firing temperature. No noticeable chipping occurs when the silver thickness is less than 0.0015 in.

After the third electrode coat has been fired, the edges of the element are very lightly beveled to separate the cylindrical electrode from the face electrodes. This is done by hand with a diamond wheel and a special jig, using water as a lubricant. Care must be taken at this point to avoid making the gap excessively wide and to remove all traces of silver from the beveled portions of the fused silica. If the diamond wheel is allowed to become contaminated with silver, a thin layer of silver will remain on the fused silica, and a large dependence of capacitance upon voltage will result.

The element is next fitted to its cell by machining the PTFE radial support. The element is then baked 24 hr in vacuum at 175 °C to eliminate adsorbed water, placed in its cell, and the cell is evacuated. The baking and evacuation are essential to produce a small dissipation factor and a stable capacitance.

After the capacitor has reached room temperature, it is measured and the adjustment necessary to produce exactly 10 pF at 25 °C is estimated. Using the element and cell dimensions shown in figure 3, the capacitance will probably not depart from 10 pF by more than ± 0.05 percent. An adjustment as small as this can be made quite easily by cutting a cavity into either a face or the cylindrical surface of the element with a small diamond wheel. The cavity is then sprayed with silver paint and refired. The adjustment sensitivity depends upon the diamond wheel diameter and thickness, the depth of cut, and the position of the cavity on the element. A jig may be readily set up to regulate depth of cut, and a calibration of capacitance change versus depth of cut measured with a trial element. Usually two or three successive adjustments suffice to produce a capacitance of 10 pF ± 50 ppm. A typical fused silica element after adjustment is shown in figure 5.

After final adjustment, a test is made for voltage dependence, and if necessary, the entire element is replated. The stainless steel housing is then welded shut, and the system is baked at 65 °C with a vacuum pump attached to the sealoff tube. After cooling, the housing is filled with dry N_2 at atmospheric pressure, and the sealoff tube is pinched off and soldered. A series of temperature cyclings is made between 50 and 0 °C, and the unit is placed into operation. Figure 6 shows a completed capacitor.

FIGURE 5. *Completed fused silica element with an adjustment of minus 50 ppm.*

3. Performance

3.1. Capacitance Stability

All measurements of capacitance stability reported here were made at 1592 Hz using a 10:1 bridge, with all capacitors in an oil bath maintained at 25.0 °C. The measurements seemed to indicate that these capacitors were at least as stable as any other capacitors in our laboratory. Accordingly, the mean of five of these capacitors, numbers 108, 109, 110, 112, and 113 was taken to be the basis for the comparisons. No temperature corrections were applied since the capacitors were at nearly the same temperature and had nearly identical temperature coefficients. The application of individual corrections for temperature slightly reduces the scatter in the measurement series reported below. Initially, all measurements were made with 10 V rms applied to the capacitors to allow ready comparison with the 1961 set of capacitors which had large voltage dependencies. Bridge readings were recorded under these conditions to the

FIGURE 6. *Completed capacitance standard.*

nearest part in 10^7. Beginning November 9, 1964, the new capacitors were intercompared at 100 V rms. This allowed considerably greater precision, but prevented simple comparison with the 1961 fused silica capacitors.

Capacitance differences between each capacitor in the set and the mean of the select five are listed in table 1. The table demonstrates that most of the capacitors are stable with respect to each other, but they could possibly all be drifting at the same rate. Comparisons of the 1964 set of capacitors with the 1961 set indicate no appreciable relative drifts, but conclusive proof of stability must await the completion of a new calculable capacitor.

TABLE 1. *Relative stability of eleven fused silica capacitors*

Decimal points indicate parts in 10^6.

Date	Capacitor										
	108	109	110	111	112	113	114	115	116	117	118
8/4/64	−2.5	+1.6	−28.3	+5.0	+18.2	+10.8					
8/4	−2.5	+1.6	−28.3	+5.0	+18.2	+10.9					
8/17	−2.5	+1.5	−28.3	+5.0	+18.3	+10.9	+31.5				
8/26	−2.5	+1.5	−28.3	+4.9	+18.2	+10.9	+31.5				
9/8	−2.6	+1.6	−28.2	+5.0	+18.2	+10.9	+31.5	+21.6	+15.6	−23.2	
9/11	−2.6	+1.5	−28.2		+18.2	+10.9	+31.6	+21.4	+15.5	−23.1	
9/22	−2.6	+1.5	−28.2		+18.2	+10.9	+31.5	+21.4	+15.6	−23.1	
10/5	−2.6	+1.5	−28.2		+18.2	+10.9	+31.5	+21.5	+15.6	−23.0	
10/20	−2.5	+1.6	−28.2		+18.2	+11.0	+31.6	+21.6	+15.8	−22.9	+6.1
10/22	−2.5	+1.6	−28.2		+18.2	+11.0	+31.5	+21.6	+15.8	−22.9	+6.1
10/30	−2.5	+1.6	−28.1		+18.2	+11.0	+31.5	+21.6	+15.8	−22.9	+6.1
11/5	−2.5	+1.5	−28.2		+18.2	+10.9	+31.5	+21.5	+15.7	−22.9	+6.1
11/9	−2.57	+1.58	−28.18		+18.19	+10.98	+31.49	+21.59	+15.76	−22.85	+6.23
11/16	−2.53	+1.57	−28.18		+18.18	+10.97	+31.46	+21.59	+15.73	−22.87	+6.20
11/24	−2.53	+1.54	−28.15		+18.10	+11.04	+31.38	+21.60	+15.67	−22.76	+6.22
11/30	−2.58	+1.55	−28.13		+18.11	+11.06	+31.40	+21.62	+15.69	−22.73	+6.26
12/7	−2.59	+1.56	−28.13		+18.12	+11.05	+31.41	+21.60	+15.68	−22.74	+6.24
12/14	−2.62	+1.56	−28.12		+18.12	+11.07	+31.41	+21.59	+15.68	−22.69	+6.27
12/21	−2.52	+1.55	−28.15		+18.08	+11.04	+31.37	+21.60	+15.66		+6.21
12/28	−2.56	+1.55	−28.14		+18.09	+11.06	+31.37	+21.56	+15.64	−22.70	+6.21
1/4/65	−2.51	+1.54	−28.15		+18.08	+11.04	+31.36	+21.54	+15.64	−22.69	+6.20
1/12	−2.50	+1.54	−28.15		+18.07	+11.04	+31.36	+21.56	+15.65	−22.68	+6.21
1/19	−2.50	+1.54	−28.15		+18.06	+11.04	+31.36	+21.56	+15.65	−22.68	+6.19
1/26	−2.50	+1.54	−28.15		+18.07	+11.04	+31.37	+21.56	+15.65	−22.67	+6.21

Capacitor number 117 exhibits a fairly steady increase of capacitance with time. The electrodes of this capacitor were about 0.002 in. thick. This capacitor also has a large voltage dependence of capacitance, as will be seen later. It is believed that the diamond wheel used to bevel the edges of the element was contaminated with silver.

3.2. Resistance Stability

Measurements of each resistance thermometer are plotted in figure 7. The effect of variations in the mean oil bath temperature was eliminated from the data by plotting the differences between each resistance and the mean of the resistances of capacitors 108, 109, 110, 112, and 113.

Figure 7 indicates that the resistance thermometers are quite stable relative to each other, but shows a flaw in our oil bath. Between September 20 and October 10, a blast of air from a fan was directed at the southwest corner of the oil bath, where capacitor number 115 was located. This blast of air introduced a temperature gradient of about 0.02 °C into the bath and is believed responsible for the relative variations observed on September 22 and October 5.

The stabilities of the copper resistance thermometers were determined from a series of measurements made with a Mueller bridge. A calibrated platinum resistance thermometer in conjunction with measured data for the dependence of the copper resistances upon temperature was used to refer all measurements

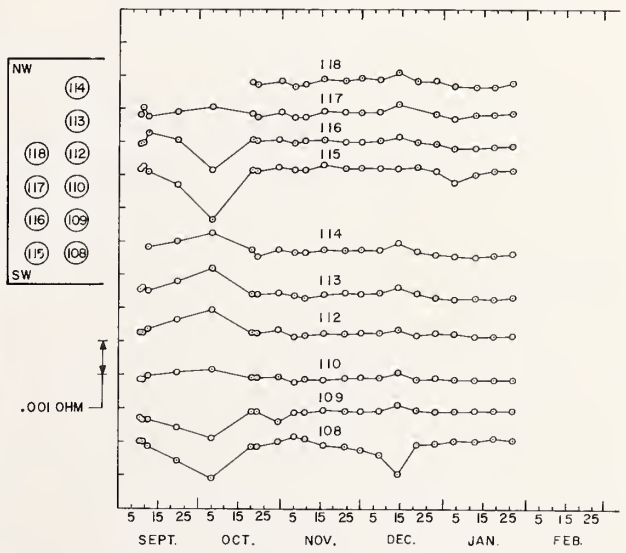

FIGURE 7. *Relative resistance thermometer stability.*

Insert shows relative positions in the oil bath. The southwest corner was abnormally cold between September 20 and October 10. A resistance change of 0.001 Ω corresponds to a temperature change of about 0.01 °C, or a capacitance change of about 0.1 ppm.

to a standard temperature. The limited information currently available indicates that the mean of the five selected resistances at a constant temperature has not changed more than 0.0001 Ω in 2 months. This corresponds to about 0.001 °C; or, referred to a capacitance correction, about 0.01 ppm.

3.3. Temperature Coefficients

The temperatures of the capacitance standards may be measured by means of the internal 25-Ω resistance thermometers. The capacitances at a specific temperature may then be determined if the capacitance temperature coefficients are known.

In practice, the temperature is usually treated as an implicit variable. A report of capacitance calibration then contains values for the capacitance and for the thermometer resistance at a temperature near 25 °C. A later measurement yielding a different thermometer resistance is corrected to the standard resistance thermometer value by reference to a plot of capacitance versus resistance for the standard.

Measurements of the capacitance-resistance function have been made over the temperature range 20 °C to 30 °C. The curves deviate from a straight line by about 2 ppm at the extremes and are all concave upwards. The slopes at 25 °C range from 100.4 ppm/Ω to 110.0 ppm/Ω. The actual capacitance temperature coefficients are about 10 ppm/°C which is substantially smaller than the 14 ppm/°C temperature coefficients of the 1961 fused silica capacitors. No explanation for this difference has been found.

3.4. Hysteresis

The capacitances of most air or solid dielectric standards at a given temperature depend upon the previous temperatures to which the standards have been subjected. Table 2 shows the magnitude of this hysteresis effect in the 1964 set of capacitors. Prior to September 8 all of the capacitors were subjected to a temperature of 50 °C, and then replaced in the oil bath at 25 °C. On September 8, their capacitances were measured with respect to a capacitor maintained at 25 °C throughout the experiment. Following these measurements, the capacitors were cooled to 0 °C, and then placed back into the oil bath. They were measured a second time on September 9. Table 2 shows that the capacitances increased an average of 0.28 ppm following the 0 °C treatment. A second subjection to 50 °C and a return to 25 °C resulted in the September 11 data in table 2. The capacitances returned most of the way to their original September 8 values, but an average capacitance increase of 0.06 ppm remained. Since the data were only recorded to the nearest part in 10^7, this overall change may not be real. The effect illustrated by table 2 represents one of the most serious faults in the capacitors, and one for which the mechanism is not completely understood. It is believed that the large differential expansion coefficient between the fused silica element and the silver electrodes may be partially responsible.

Table 2. *Dependence of capacitance upon prior thermal history*

September 8 and September 11 data were taken at 25 °C after subjection to 50 °C; September 9 data were taken at 25 °C after subjection to 0 °C (see text). Capacitance differences from the September 8 data are given in parts per million.

Capacitor	September 8	September 9	September 11
108	0	+0.15	+0.1
109	0	+.35	.0
110	0	+.45	+.1
112	0	+.35	+.1
113	0	+.25	+.1
114	0	+.25	+.1
115	0	+.35	−.1
116	0	+.35	.0
117	0	+.05	+.1
Mean change		+.28	+.06

3.5. Voltage Dependence

Some techniques and apparatus were developed recently at NBS for measuring the dependence of 100 and 1000 pF capacitors upon voltage, with uncertainties in the order of 1 part in 10^9 [4]. The equipment was used for measuring the voltage dependencies of the 10 pF capacitors with slightly larger uncertainties. Table 3 shows the capacitance differences observed when the voltage was changed from 100 V to 200 V. The computed probable error of the data in table 3 is 6 parts in 10^{10}, and the systematic error is estimated to be less than 2 parts in 10^9. Since the voltage dependence of a standard depends upon which electrode is at ground potential, all of the standards are marked with a "D" near the coaxial connector chosen for the ground potential lead.

Table 3. *Dependence of capacitance and dissipation factor upon voltage*

The increases in capacitance and dissipation factor due to increasing the voltage from 100 V to 200 V rms at 1592 Hz are shown.

Capacitor	$\frac{\Delta C}{C}$	$\frac{\Delta G}{\omega C}$
108	$+1.3\times10^{-9}$	-3.1×10^{-9}
109	−3.6	−2.2
110	−5.2	+1.2
112	−5.0	−4.6
113	−2.6	+0.6
114	−1.0	+1.0
115	+4.8	−0.1
116	−1.8	−.3
117	+12.4	−2.2
118	+9.8	−1.4

3.6. Frequency Dependence and Dissipation Factor

The result of comparing the fused silica capacitors with two 10 pF air capacitors at three frequencies is reported in table 4. Capacitor A was constructed with concentric cylindrical electrodes, and capacitor B with rigid parallel plates. Identical results were obtained at 159 Hz, using the two capacitors, but a significant difference was observed at 15900 Hz. The cause of the discrepancy is not known, but probably involves either mechanical resonances or excessive series inductances in one or both of the

air capacitors. The measurements at 159 Hz were extremely difficult to make due to poor bridge sensitivity. The computed probable error of the 159 Hz data in table 4 is 2×10^{-7}.

Table 4. *Frequency dependence of the fused silica capacitors relative to two air capacitors (see text)*

Capacitor	159 Hz	1592 Hz	15900 Hz A	15900 Hz B
	ppm		*ppm*	*ppm*
108	+1.3	0	−0.6	−1.9
109	+1.0	0	−.2	−1.5
110	+1.8	0	−.8	−2.1
112	+0.2	0	+.2	−1.1
113	+1.9	0	−.9	−2.2
114	+0.1	0	+.2	−2.1
115	+1.2	0	−.8	−3.1
116	+0.3	0	−.3	−2.6
117	+1.6	0	−1.2	−3.5
118	+1.8	0	−0.6	−1.9

Accurate measurements of dissipation factor cannot be made at NBS at this time. Comparisons of the fused silica dielectric capacitors with several types of air capacitors suggest that the dissipation factors of the fused silica capacitors are probably between 0 and $+3\times10^{-6}$ at 1592 Hz.

3.7. Shock Sensitivity

The capacitors were tested upon completion for shock sensitivity by dropping them onto a hardwood table. Various angles of impact and various heights up to 8 in. were tried. The largest capacitance change observed was 1 part in 10^7 which occurred when a capacitor fell about 8 in. in an upright position. Falls through smaller distances usually produced no observable change in capacitance.

3.8. Transportation Experiences

A fused silica dielectric capacitor designated number 107 and which was identical with those described in this paper was shipped to the National Research Council of Canada (NRC) on July 28, 1964, via air parcel post. Prior to shipment, it was compared with capacitor number 108. Number 108 was hand-carried to NRC and returned between August 4 and August 17, 1964, and again between December 8 and December 11, 1964. Comparisons of the two capacitors at NRC indicated no relative change in the two capacitances larger than 0.2 ppm; and as can be seen from table 1, no change in number 108 occurred during either of the two round trips.

4. Conclusion

Much more data is needed to evaluate conclusively the reliability of the 1964 set of fused silica dielectric capacitors. Existing evidence suggests that stabilities in the order of a few parts in 10^7 may be expected, and that the capacitors can probably withstand normal handling during shipment between laboratories.

Some further modifications of the design may result in an improved standard. A study of the mechanism which produces the capacitance hysteresis effect with large temperature changes would be of value, and consideration might be given to improving the support system for the fused silica element.

It is felt that the choice of 10 pF for a fused silica dielectric capacitor results in a design of nearly optimum stability. Other values would be useful as secondary standards and should not be difficult to construct.

5. References

[1] M. Kanno, Researches on standard capacitors, researches of the electrotechnical laboratory (Japan), No. 597, April 1961 (in Japanese).

[2] R. D. Cutkosky and L. H. Lee, The construction and behavior of a transportable ten picofarad capacitor, comite consulatif d'electricite, Aupres Du "Comite International Des Poids et Mesures," 10 Session 1963, p. 44.

[3] Standard capacitors and their accuracy in practice, Notes on Applied Science **13,** (NPL) 1955.

[4] J. Q. Shields, The voltage dependence of precision air capacitors, to be published.

(Paper 69C3–196)

JOURNAL OF RESEARCH of the National Bureau of Standards—C. Engineering and Instrumentation
Vol. 69C, No. 4, October-December 1965

Voltage Dependence of Precision Air Capacitors

J. Q. Shields

(August 1, 1965)

Methods are presented for measuring both the relative and absolute voltage dependence of admittance standards. The practical circuits based on the methods are composed of precision bridges which are described in detail. Measurements with these circuits yield values for the proportional changes in admittance which result from specified changes in voltage. The results of measurements on selected capacitors are presented. Uncertainties are of the order of one part in 10^9.

A general instability in the voltage dependence of precision air capacitors was observed at the higher accuracy levels. Most of the instability is believed to be caused by changes in the electrode surfaces.

Key Words: Bridge, capacitor, coaxial choke, difference transformer, electrode surfaces, thin films, three-terminal, transformer, voltage coefficient, voltage dependence, voltage ratio.

1. Introduction

Several years ago a computable cross capacitor, based on a theorem by A. M. Thompson and D. G. Lampard [1],[1] was constructed at NBS [2]. The value of this capacitor is computable, in esu, within an estimated accuracy of 2 parts per million (ppm). A new cross capacitor of improved design is now being constructed. It is expected that this capacitor will be computable, in esu, within a few parts in 10^8 or better.

The expected increase in accuracy not only requires better bridges and capacitors, but also requires that many sources of error be reevaluated. One such source of error is the voltage dependence of precision air capacitors.

To meet our particular needs, the quantity chosen as a measure of voltage dependence is termed γ and is defined by the equation

$$Y_2 = Y_1(1+\gamma)$$

where Y_1 is the admittance of a given standard at voltage V_1, Y_2 is the admittance of the same standard at voltage V_2, and the condition $V_2 > V_1$ is imposed to restrict the meaning of γ. A given standard may have any number of values of γ, each with a specified voltage change. Since γ represents a proportional change in admittance ($\Delta Y/Y$), this measure of voltage dependence is in the preferred form for corrections to precision measurements.

In the past, most measurements of voltage dependence have been confined to a determination of the ratio, $(1+\gamma_a)/(1+\gamma_b)$, where γ_a and γ_b apply to different capacitors but have the same specified voltage change. One exception to the above is the work of N. L. Kusters and O. Petersons [3]. They developed a method for measuring the voltage dependence of an individual capacitor, provided the voltage dependence results only from electrode deflections.

The accuracy requirements described earlier resulted in the need for a method which would be independent of the mechanisms which cause voltage dependence. Such a method is described in section 2. The method yields values of γ corresponding to a change in voltage from V to $2V$, where V is a variable.

The practical circuits based on the method are described in sections 3 and 4. These circuits were used to measure values of γ for several capacitors corresponding to the following voltage changes: 12.5 to 25, 25 to 50, 50 to 100, and 100 to 200 V, rms, at 1592 Hz. Measurement uncertainties had to be kept small since the above values of γ are used to calculate other values of γ in different voltage ranges such as from zero to 200 V. The latter value is needed for the determination of the absolute unit of capacitance. Small uncertainties also provide the means for quickly detecting instabilities in the voltage dependence of capacitors. It was found that the voltage dependence of precision air capacitors was, in general, unstable at the accuracy level described. This subject is discussed in section 5.

2. Theory

One method for measuring the voltage ratio of a transformer is to connect admittance standards to the transformer so as to form a bridge as shown in figure 1 [4]. In general, if the transformer has a nominally $m:n$ ratio, then $m+n$ nominally equal admittances are used, and $m+n$ detector balances are required corresponding to a cyclic permutation of these admittances. In this sequence of balances each admittance appears with voltage E_1 m times, and with voltage E_2 n times. If $E_1 \neq E_2$, a ratio measurement error results since the admittance of a practical standard changes when the voltage applied to it

[1] Figures in brackets indicate the literature references at the end of this paper.

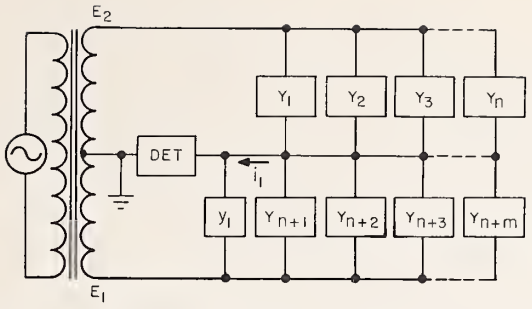

FIGURE 1. *Circuit for measuring the voltage ratio of a transformer* [4].

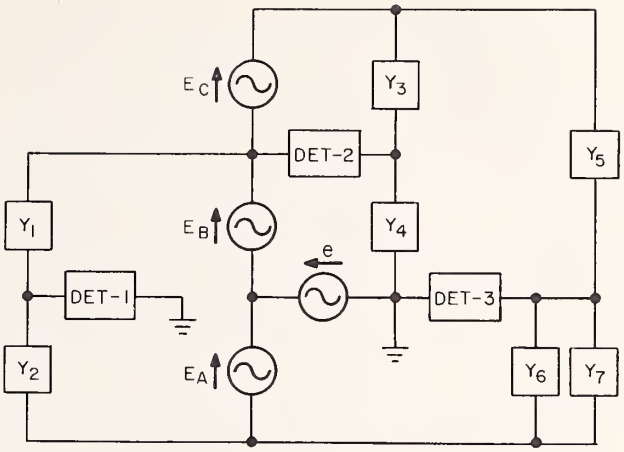

FIGURE 2. *Basic three-bridge-circuit.*

is changed. The difference between the measured ratio and the true ratio is related to the average change in admittance of the standards.

If the transformer ratio can be determined from a second set of measurements which is independent of voltage, the combination of the two sets of measurements will yield a value for the average change in admittance of the $m+n$ standards corresponding to a change in voltage from E_1 to E_2. The change in admittance of each standard can then be determined by measuring the relative changes between various pairs of standards.

The basis of this paper is a method of the type described above in which the second set of measurements consists of determining a group of 1:1 ratios which can be combined to determine the $m:n$ ratio of a transformer. For simplicity, a transformer having a 2:1 ratio was chosen so that only two 1:1 ratios need be determined.

It is assumed that taps are brought out from the secondary winding of a bridge transformer [5] so as to obtain three secondary voltages of approximately equal magnitude. These voltages are represented by E_A, E_B, and E_C in figure 2. The circuit shown in figure 2 consists of three bridges, each of which may be balanced, in turn, by the small, adjustable voltage e. For the case in which the circuit elements are closely matched, $e/E_A \equiv q \ll 1$, and only a low accuracy calibration of q is needed for high accuracy determinations of ratios such as E_B/E_A.

It is assumed that the changes in $Y_1, Y_2, Y_3 \ldots Y_7$ which result from changes in e can be neglected. Following from this, we may consider the voltages applied to Y_5, Y_6, and Y_7 to be either E_A or $2E_A$ and define the values of Y_5, Y_6, and Y_7 to be Y'_5, Y'_6, and Y'_7 at voltage E_A, and $Y'_5(1+\gamma_5)$, $Y'_6(1+\gamma_6)$, and $Y'_7(1+\gamma_7)$ at voltage $2E_A$.

The balance equations for bridge 1 are

$$\frac{Y_1}{Y_2}=\frac{E_A-e_1}{E_B+e_1}=\frac{1-q_1}{1+\delta_B+q_1} \tag{1}$$

$$\frac{Y_2}{Y_1}=\frac{E_A-e_2}{E_B+e_2}=\frac{1-q_2}{1+\delta_B+q_2} \tag{2}$$

where $\frac{E_B}{E_A}\equiv 1+\delta_B$. Eliminating Y_1 and Y_2, we obtain

$$\delta_B=-(q_1+q_2). \tag{3}$$

The balance equations for bridge 2 are

$$\frac{Y_3}{Y_4}=\frac{E_B+e_3}{E_C}=\frac{1+\delta_B+q_3}{1+\delta_C} \tag{4}$$

$$\frac{Y_4}{Y_3}=\frac{E_B+e_4}{E_C}=\frac{1+\delta_B+q_4}{1+\delta_C} \tag{5}$$

where $\frac{E_C}{E_A}\equiv 1+\delta_C$. Eliminating Y_3 and Y_4, we obtain

$$\delta_C=\frac{q_3+q_4+2\delta_B}{2}+\epsilon_1 \tag{6}$$

where ϵ_1 is a small correction term consisting of second and higher order terms in q.

The balance equations for bridge 3 are

$$\frac{Y'_5(1+\gamma_5)}{Y'_6+Y'_7}=\frac{E_A-e_5}{E_B+E_C+e_5}=\frac{1-q_5}{2+\delta_B+\delta_C+q_5} \tag{7}$$

$$\frac{Y'_6(1+\gamma_6)}{Y'_7+Y'_5}=\frac{E_A-e_6}{E_B+E_C+e_6}=\frac{1-q_6}{2+\delta_B+\delta_C+q_6} \tag{8}$$

$$\frac{Y'_7(1+\gamma_7)}{Y'_5+Y'_6}=\frac{E_A-e_7}{E_B+E_C+e_7}=\frac{1-q_7}{2+\delta_B+\delta_C+q_7}. \tag{9}$$

Eliminating Y'_5, Y'_6, and Y'_7, we obtain

$$\bar{\gamma}=-\frac{\delta_B+\delta_C+q_5+q_6+q_7}{2}+\epsilon_2. \tag{10}$$

where

$$\bar{\gamma}\equiv\frac{\gamma_5+\gamma_6+\gamma_7}{3} \tag{11}$$

and ϵ_2 is a small correction term consisting of second and higher order terms in q and γ.

Solving eqs (3), (6), and (10), we obtain

$$\bar{\gamma}=\frac{4q_1+4q_2-q_3-q_4-2q_5-2q_6-2q_7}{4}-\frac{\epsilon_1-2\epsilon_2}{2}. \quad (12)$$

In order to separate real and imaginary parts, let

$$\gamma \equiv \gamma' - j\gamma'' \quad (13)$$

and

$$q \equiv q' - jq'' \quad (14)$$

so that

$$\bar{\gamma}'=\frac{4q_1'+4q_2'-q_3'-q_4'-2q_5'-2q_6'-2q_7'}{4}-\frac{\epsilon_1'-2\epsilon_2'}{2} \quad (15)$$

and

$$\bar{\gamma}''=\frac{4q_1''+4q_2''-q_3''-q_4''-2q_5''-2q_6''-2q_7''}{4}-\frac{\epsilon_1''-2\epsilon_2''}{2} \quad (16)$$

For the capacitors and accuracies described in this paper, γ' is equal to the proportional change in capacitance ($\Delta C/C$), and γ'' is equal to the change in dissipation factor, corresponding to a specified increase in voltage.

The values of γ_5, γ_6, and γ_7 can be separated from the value of $\bar{\gamma}$ by measuring the differences, $\gamma_5-\gamma_6$, $\gamma_6-\gamma_7$, and $\gamma_7-\gamma_5$. Measurements of this type are described in section 4. Combining the differences, we obtain

$$\gamma_5=\bar{\gamma}+(\gamma_5-\gamma_6)/3-(\gamma_7-\gamma_5)/3 \quad (17)$$

$$\gamma_6=\bar{\gamma}+(\gamma_6-\gamma_7)/3-(\gamma_5-\gamma_6)/3 \quad (18)$$

$$\gamma_7=\bar{\gamma}+(\gamma_7-\gamma_5)/3-(\gamma_6-\gamma_7)/3. \quad (19)$$

3. Practical Three-Bridge-Circuit

The method described in the previous section was used to determine the voltage dependence of three 100 picofarad (pF) air capacitors, designated 100A, 100B, and 100C. This section describes the equipment and techniques used to determine the values of

$$\bar{\gamma}_{100} \equiv \frac{\gamma_{100A}+\gamma_{100B}+\gamma_{100C}}{3} \quad (20)$$

corresponding to the following voltage changes: 12.5 to 25, 25 to 50, 50 to 100, and 100 to 200 V, rms, at 1592 Hz.

If small capacitors are to be well defined, they must be shielded. The addition of shielding to the circuit of figure 2 is shown in figures 3a, 3b, and 3c. Each of the admittance standards represented in figures 3a, 3b, and 3c consists of a completely shielded three-terminal air capacitor connected to a pair of coaxial

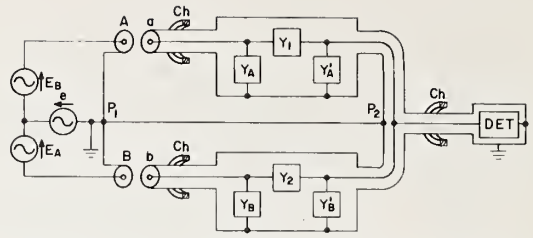

FIGURE 3a. *Bridge 1 of the practical three-bridge-circuit.*

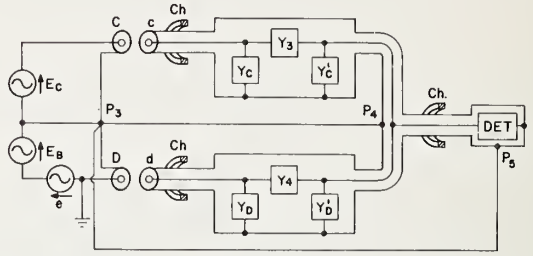

FIGURE 3b. *Bridge 2 of the practical three-bridge-circuit.*

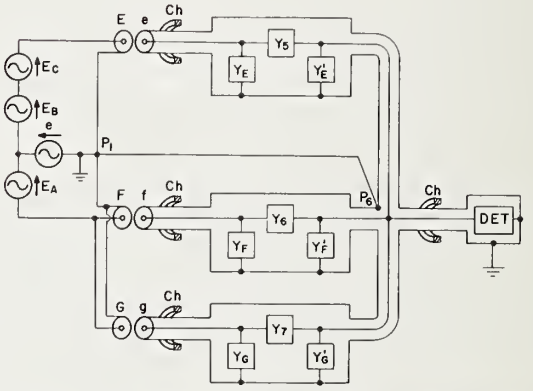

FIGURE 3c. *Bridge 3 of the practical three-bridge-circuit.*

cables. The defining terminals of each standard are located at one of the detector junctions and at one of the coaxial connectors designated a, b, c . . . g.

The required circuits are obtained by joining connectors a, b, c . . . g to connectors, A, B, C . . . G in various configurations. When connector a is joined to connector A and b to B, the balance equation is given by equation (1), section 2. When a is joined to B and b to A, the balance equation is given by eq (2). Similarly, eqs (4) and (5) are applicable to figure 3b and eqs (7), (8), and (9) are applicable to figure 3c. For purposes of evaluating the effects of self and mutual impedances in the leads (not shown in the figures), it will initially be assumed that: (1) net cur-

rents through the "coaxial chokes" [6], designated Ch in the figures, are negligibly small, (2) the voltages at connector A are, to sufficient accuracy, independent of whether A is joined to a or to b, and similarly for the voltages at connectors B, C, D . . . G, (3) only negligible effects result from externally induced emfs and external loading, e.g., capacitance from the bridge shielding to its surroundings.

Subject to the above assumptions, the two values of e corresponding to the two balance conditions for bridge 1 yield a measure of the voltage ratio, V_A/V_B where V_A is the voltage between the inner and outer terminals of connector A with $e=0$ and V_B is the voltage between the inner and outer terminals of connector B with $e=0$. Similarly, a measure of the voltage ratios, V_C/V_D and V_E/V_F are obtained using bridges 2 and 3, respectively. The value of $\overline{\gamma}_{100}$ is calculated from the measured values of V_A/V_B, V_C/V_D, and V_E/V_F. It is assumed that the relationship between voltages V_A, V_B, V_C . . . V_G is known. Ideally, the voltage drops in the leads which precede connectors A, B, C . . . G should be zero, but if the voltage drops are small, eq (12) is sufficiently accurate when the relationship between the voltages is as follows: $V_A=-V_D$, $V_B=V_F=V_G$, $V_E=V_A+V_C$. Since voltage ratios rather than voltages are measured, other satisfactory relationships between the voltages can be described, e.g., V_C and V_D can each be changed if V_C/V_D remains unchanged. Thus, the error in the measurement of $\overline{\gamma}_{100}$ which results from voltage drops in the leads will be small if the impedances in the leads which join various terminals of connectors A, B, C . . . G are small or properly matched. These features are present in the junction box shown within broken lines in figure 4. Parallel lines represent copper strips separated by thin strips of insulation.

The error in the measurement of $\overline{\gamma}_{100}$ resulting from lead impedances within the junction box and resulting from contact impedances between connectors A, B, C . . . G and connectors a, b, c . . . g was found to be approximately 1×10^{-9}. Most of this error was corrected for by changing the currents at the terminals of connectors a, b, c . . . g and observing the change in the measured value of $\overline{\gamma}_{100}$. Since the current at the inner or outer terminal of connector a was nearly proportional to the internal load, Y_1+Y_A, and similarly for the currents at the terminals of b, c, d, . . . g, the following procedure was used: (1) Y_A, Y_B, Y_C . . . Y_G were adjusted so that each of the seven internal loads, Y_1+Y_A, Y_2+Y_B, Y_3+Y_C . . . Y_7+Y_G, were increased by a known factor, (2) the change in the measured value of $\overline{\gamma}_{100}$ was used to calculate a third value of $\overline{\gamma}_{100}$ corresponding to the internal loads being zero. The above procedure amounts to an extrapolation of the effect of internal loads to zero.

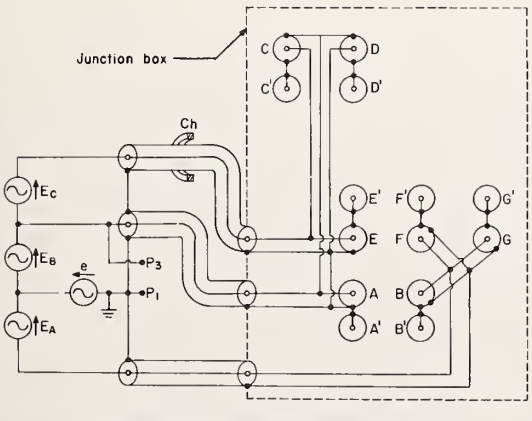

FIGURE 4. *Source of bridge voltages.*
Junction box (within broken lines) connected by coaxial cables to an "active direct-reading ratio set" [7].

The internal loads were measured by disconnecting A, B, C . . . G from a, b, c . . . g, shorting the detectors, and measuring the two-terminal admittances between the inner and outer terminals of connectors a, b, c . . . g. Since the lead impedances within the junction box were small, low accuracy measurements were sufficient for purposes of extrapolating the internal loads to zero. The larger equivalent lead impedances in that portion of the circuit which preceded the junction box (see fig. 4) required that more accurate measurements be made for purposes of adjusting Y_B, Y_D, Y_F, and Y_G so that $Y_1+Y_A=Y_2+Y_B$, $Y_3+Y_C=Y_4+Y_D$, and $Y_5+Y_E=Y_6+Y_F=Y_7+Y_G$. The accuracy of adjustment needed was determined by connecting additional loads between the inner and outer terminals of A, B, C . . . G, each in turn, and noting the changes in e required to rebalance the bridges. It was found that if the internal loads were adjusted within $\pm1\times10^{-9}$ mho, the voltages at connector A were, to sufficient accuracy, independent of whether A was joined to a or to b, and similarly for the voltages at B, C, D . . . G.

The coaxial chokes used consisted of a number of turns of the coaxial cable threaded through a high permeability core. The resulting impedance to net current in the cable was about 400 Ω at 1592 Hz. Since the impedance in the path, $P_1-A-a-P_2$, of figure 3a was about 0.1 Ω, net current through the coaxial choke was of the order of a few parts in 10^4 of the current in the inner or outer conductor of the cable [6]. The impedances in the paths, P_1-A-a and P_1-B-b, differed by less than 2 mΩ. The maximum internal load was about 3000 pF.

Thus far in the discussion the effects of externally induced emfs and external loading have been neglected. Although these effects were small in the practical circuit used, they were not negligible. Appropriate corrections were determined from additional measurements which consisted of recording the unbalance at the detectors when the admittance standards of each bridge, in turn, were joined to the shorting connectors, A', B', C', . . . G', (see fig. 4) while the other standards were joined to A, B, C, . . . G. Since the accuracy of the corrections depended on the size of the unbalance at each detector, it was desirable for the effects of externally induced emfs and external loads to be small. The techniques used to reduce these effects will be considered next.

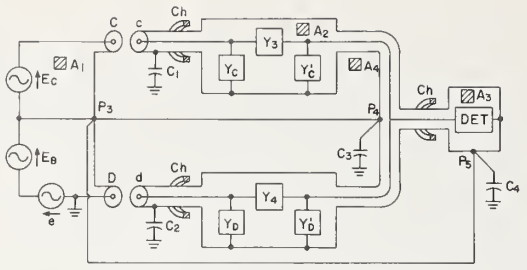

FIGURE 5. *Bridge 2 redrawn to illustrate external loads and sources of induced emf.*

Bridge 2 has been redrawn in figure 5 for purposes of illustrating the different types of induced emf's and external loads. Since the shielding of bridge 2 is not at ground potential, the largest external loads are associated with this bridge. External loads are represented by C_1, C_2, C_3, and C_4 in figure 5. Induced emfs are represented indirectly by showing areas in which a time-varying magnetic flux is assumed to exist. These areas are designated A_1, A_2, A_3, and A_4 in figure 5.

Most of the flux through A_1 existed in the region preceding the junction box and thus had no effect on the measured value of $\overline{Y}_{100}$. Flux through A_2 was reduced by using coaxial cables of sufficient length so that the three-terminal capacitor could be positioned at a distance from sources of appreciable magnetic field. Flux through A_3 was reduced by using coaxial cables and magnetic shielding in that portion of the detector circuit which precedes voltage amplification. The effects of flux through A_4 were reduced by the use of coaxial chokes, e.g., if the high permeability core positioned between connector c and P_4 were removed from the circuit, the current through Y_3 which results from flux through A_4 would be increased by a factor of a few thousand.

The effects of external loads were reduced by the use of coaxial chokes in conjunction with low-impedance leads which bypass the junction box (hereafter termed bypass leads). The lead connecting P_3 to P_4 and the lead connecting P_3 to P_5 are examples of bypass leads in figure 5. These leads, which have impedances of about 0.1 Ω, supply most of the current to C_3 and C_4. Thus, if coaxial chokes and bypass leads are properly positioned, voltage drops will be reduced in critical portions of the circuit such as the junction box leads and the cables of the admittance standards and detector circuit.

The effects of external loads were also reduced by the use of an electrostatic shield which is represented by a broken line in figure 6. This figure represents more closely the actual circuit used. The electrostatic shield, maintained at a potential of approximately E_B with respect to ground, encloses those circuit elements which would otherwise have a large capacitance to the grounded surroundings. Current to the shield is supplied by the bypass lead connected to P_3.

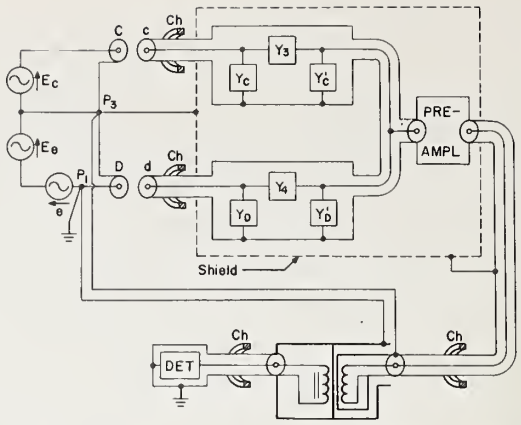

FIGURE 6. *Bridge 2 redrawn to show the difference transformer and additional shielding.*

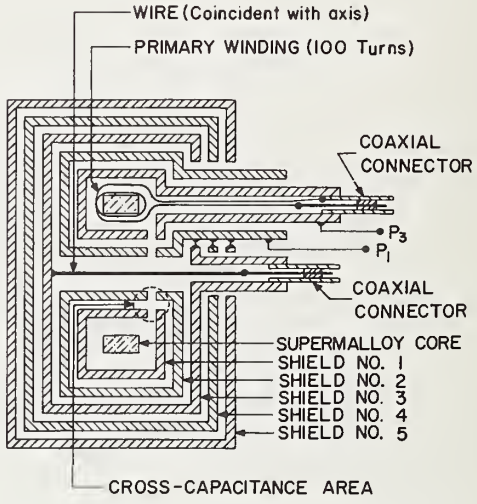

FIGURE 7. *Cross section through the axis of the difference transformer.*

The transformer shown in figure 6 is termed a difference transformer [2] and is used to change the potential of the detector cables with respect to ground from approximately E_B to zero. This was necessary in order that a phase-sensitive detector having a grounded power supply could be used. An adequate signal-to-noise ratio was maintained by using a battery-operated preamplifier having a voltage amplification of approximately 10^3 (see fig. 6). Coaxial chokes assured that the bypass leads in figure 6 supplied most of the current to the large capacitance which existed between the shielding of the difference transformer.

A cross-sectional view of the difference transformer is shown in figure 7. The secondary winding is a

[2] The basic ideas in the transformer are similar to those in a transformer built by A. M. Thompson and termed by him a difference transformer.

single turn consisting of shield No. 3 connected to a wire through the center of the core. With the exception of shield No. 4 which is mu-metal, all shielding is brass.

Most of the current resulting from the capacitance between shield No. 1 and shield No. 2 does not encircle the Supermalloy core. The current which does encircle the core, if not compensated, would induce a voltage in the detector winding. The two capacitances which result in core excitation are associated with the corners of the shield gaps. With reference to the cross-capacitance area shown in figure 7, the two capacitances are (1) from the upper left to the lower right, (2) from the upper right to the lower left. It can be seen that the two currents encircle the core in opposite senses, and hence their effects can be made to cancel by proper adjustment of the gap geometry. The gap was adjusted experimentally by observing the detector voltage with the transformer input open circuited and with the bypass leads connected.

As a result of the techniques described above, the unbalance at the detectors was small when the admittance standards of each bridge, in turn, were joined to the shorting connectors, A', B', C' . . . G', while the other standards were joined to A, B, C . . . G. Thus, accurate corrections were obtained for most of the effects of induced emf's and external loads. Those effects which were not accounted for in the corrections will be considered next.

Since currents were reduced when the standards were connected to the shorting terminals A', B', C', . . . G', induced emf's resulting from currents in that portion of the circuit shown in figure 4 were not entirely accounted for in the above corrections. The use of coaxial cables, parallel-strip leads, and magnetic shielding assured that the resulting errors were negligible. It is interesting to note that if the errors had not been negligible, they would have been accounted for in the extrapolation of the internal loads to zero. The effect of induced emf's resulting from currents within the standards was negligible since the phase of the induced emf's was shifted by 180° when the standards were permuted.

Magnetic fields in the vicinity of the junction box may induce emf's which are selective with respect to connectors A, B, C . . . G, thus causing errors in the measurement of $\overline{Y}_{100}$. Induced emf's of this type were kept small by using closely spaced copper strips in the construction of the junction box (see fig. 4). The following procedure was used to assure that the remaining errors were negligible: (1) A small probe was used to measure the magnetic field in the vicinity of the junction box, including the region where changes in geometry occur due to changes in the connections of the standards to the junction box, (2) the current in a loop of wire was adjusted so as to increase the measured field by a factor of approximately 100, (3) the changes in e required to rebalance the bridges were related to changes in $\overline{Y}_{100}$.

The external loads, C_1 and C_2 in figure 5, represent the capacitances between the grounded surroundings and those cables which are located between the coaxial chokes and connectors c and d. The circuit was designed so that C_1 and C_2 would be small and nearly equal. Measurements of C_1 and C_2 and of the lead impedances in the junction box indicated that the resulting error in the measurement of $\overline{Y}_{100}$ was small. This error is accounted for in item 1, table 1. Also accounted for in item 1, table 1 are errors resulting from capacitance between the copper strips of the junction box and errors resulting from imperfect balancing of the internal loads.

TABLE 1. *Uncertainties in the measurement of* $\overline{Y}_{100} \equiv \overline{Y}'_{100} - j\overline{Y}''_{100}$

Sources of error	Systematic errors in $\overline{Y}'_{100}$	Systematic errors in $\overline{Y}''_{100}$
	Parts in 10^{10}	Parts in 10^{10}
1. Loading	1	1
2. Contact impedances	.....	2
3. Detector zero	1	1
4. Calibration of q	2	1
5. Drift of admittances and transformer ratio	2	1
Sum	6	6

Standard deviation of $\overline{Y}'_{100}$ or $\overline{Y}''_{100}$ is 3×10^{-10}.

Table 1 lists only the significant errors which were not corrected for by extrapolating the internal loads to zero or by using the shorting terminals, A', B', C' . . . G', as described earlier. Item 2, table 1, accounts for small changes in the contact impedances between a, b, c . . . g and A, B, C, . . . G which were found to occur with continued use. Item 3, table 1, accounts for possible systematic errors which result from observer bias in determining the null balance condition.

Item 4, table 1, accounts for errors in the calibration of the instrument used to obtain E_A, E_B, E_C, and e. The essential features of the instrument, termed an "active direct-reading ratio set," are described in reference [7]. The adjustments of $q \equiv \frac{e}{E_A} \equiv q' - jq''$ were made by adjusting two sets of dials, one corresponding to changes in q' and the other to changes in q''. The maximum range of q' or q'' was ± 10 ppm with a minimum adjustment of 2×10^{-10}.

Item 5, table 1, accounts for errors which result from the admittances and transformer ratio having a nonconstant drift rate and from observer bias in timing the bridge balances which were made so as to obtain values of q in the following sequence: q_3, q_4, q_3; q_1, q_2, q_1; q_5, q_6, q_7, q_6, q_5; q_1, q_2, q_1; q_3, q_4, q_3. The above set of values could be obtained in about 12 minutes with $E_A = 100$ V, rms. The standard deviations of $\overline{Y}'_{100}$ and $\overline{Y}''_{100}$, obtained from one such set, were about 6×10^{-10}. Slightly larger standard deviations were obtained at lower voltages. A sufficient number of measurements was made so that the final values of $\overline{Y}'_{100}$ and $\overline{Y}''_{100}$ had standard deviations of about 3×10^{-10}.

4. Difference Measurements

The difference in voltage dependence between two standards whose admittances are approximately equal can be determined from ordinary bridge measurements, e.g., simple substitution combined with a change in bridge voltage. The particular circuit used for this type of difference measurement is described in section 4.1.

When the admittances of the two standards are radically different, additional measurements are required. These measurements are described in section 4.2.

4.1. Difference Measurements Involving Approximately Equal Admittances

The circuit shown in figure 3a is typical of the circuits used for difference measurements. The two general balance equations for this bridge have already been presented, namely eqs (1) and (2). For the case in which the voltage, E_A, has two specific values, E_{AL} and E_{AH}, four specific balance equations may be written:

$$\frac{Y_{1L}}{Y_{2L}}=\frac{E_{AL}-e_{1L}}{E_{BL}+e_{1L}}=\frac{1-q_{1L}}{1+\delta_{BL}+q_{1L}} \tag{21}$$

$$\frac{Y_{2L}}{Y_{1L}}=\frac{E_{AL}-e_{2L}}{E_{BL}+e_{2L}}=\frac{1-q_{2L}}{1+\delta_{BL}+q_{2L}} \tag{22}$$

$$\frac{Y_{1H}}{Y_{2H}}=\frac{E_{AH}-e_{1H}}{E_{BH}+e_{1H}}=\frac{1-q_{1H}}{1+\delta_{BH}+q_{1H}} \tag{23}$$

$$\frac{Y_{2H}}{Y_{1H}}=\frac{E_{AH}-e_{2H}}{E_{BH}+e_{2H}}=\frac{1-q_{2H}}{1+\delta_{BH}+q_{2H}}. \tag{24}$$

If

$$Y_{1H}\equiv Y_{1L}(1+\gamma_1) \tag{25}$$

and

$$Y_{2H}\equiv Y_{2L}(1+\gamma_2) \tag{26}$$

then

$$\gamma_1-\gamma_2=(q_{2H}-q_{2L})-(q_{1H}-q_{1L})+\epsilon_3 \tag{27}$$

where ϵ_3 is a small correction term consisting of second and higher order terms in q and γ.

The method described above was used to measure each of the following differences: $\gamma_{100A}-\gamma_{100B}$, $\gamma_{100B}-\gamma_{100C}$, $\gamma_{100C}-\gamma_{100A}$, $\gamma_{1000A}-\gamma_{1000B}$, $\gamma_{1000B}-\gamma_{1000C}$, and $\gamma_{1000C}-\gamma_{1000A}$, where the subscripts refer to three 100 pF air capacitors and three 1000 pF air capacitors designated 100A, 100B, 100C, and 1000A, 1000B, 1000C, respectively. Four values were obtained for each of the above differences corresponding to the following voltage changes: 12.5 to 25, 25 to 50, 50 to 100, and 100 to 200 V, rms, at 1592 Hz. The discussion of measurement uncertainties which follows is applicable to each of these values.

Since the differences, $q_{2H}-q_{2L}$ and $q_{1H}-q_{1L}$, were small and of opposite sign in eq (27), most errors of the type described in section 3 were negligible. The only exceptions were errors resulting from drift of the admittances and transformer ratio. These errors were partially reduced by the measuring sequence which follows: q_{1L}, q_{1H}, q_{1L}, q_{2L}, q_{2H}, q_{2L}. Rather than attempting to obtain a precise bridge balance at a specified time, each balance in the above sequence was made as quickly as possible. Nonuniform timing was almost inevitable since the detector sensitivity was better at high voltage. The resulting errors were kept small by injecting a small current to compensate the effect of capacitor drift. This was accomplished with an auxiliary circuit, termed a "drifter circuit."

If no adjustments of e are made, the relative changes in capacitance with time result in a time-variation in the amplitude of the current at the detector. The drifter circuit is used to inject a compensating current at the detector. The basic part of the circuit is a three-terminal, variable, air capacitor having a maximum capacitance of 10 pF. The adjusting shaft of the capacitor is connected to a constant-speed motor with speed reducer, thus providing a capacitance which varies linearly with time. Coaxial cables are used to connect the terminals of the capacitor to the detector junction and to an inductive voltage divider whose voltage is supplied by the "active direct-reading ratio-set" used to obtain E_A, E_B, and e.

The amplitude of the current injected at the detector has a first derivative with respect to time which can be adjusted by adjusting the inductive voltage divider and a second derivative which is zero. Since the drift rate of the admittance standards changed only slightly during the time needed for a set of detector balances, the use of the drifter circuit resulted in appreciable reductions in the time rate of change of e required to maintain a detector balance. In addition, the deviations from constant drift rate, which can result in systematic errors, were easily measured.

A sufficient number of measurements was made so that the standard deviation of each of the final values, $\gamma'_{100A}-\gamma'_{100B}$, $\gamma''_{100A}-\gamma''_{100B}$, $\gamma'_{1000A}-\gamma'_{1000B}$, etc., was 3×10^{-10} or less. A systematic error of 2×10^{-10} was assigned to each of the final values to account for incomplete compensation of the admittance and transformer ratio drift.

4.2. Difference Measurements Involving Radically Different Admittances

The circuit shown in figure 8 is used to measure the difference,

$$\overline{\gamma}_a-\overline{\gamma}_b\equiv\frac{\gamma_8+\gamma_9+\gamma_{10}}{3}-\frac{\gamma_5+\gamma_6+\gamma_7}{3}. \tag{28}$$

If connectors Q, R, and S are permuted cyclically with respect to connectors E, F, and G of the junction box (fig. 4), six different bridge balances can be made.

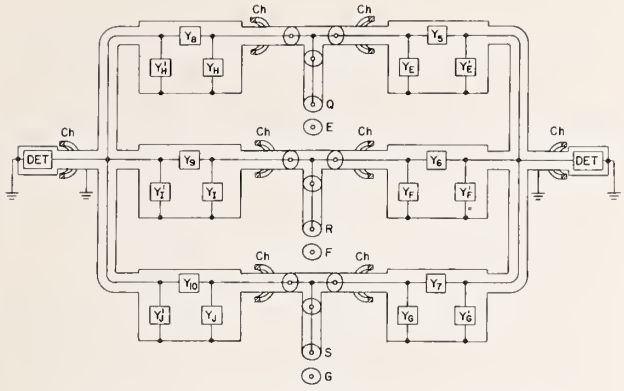

FIGURE 8. *Circuit used for difference measurements with* $Y_5 \approx Y_6 \approx Y_7 \neq Y_8 \approx Y_9 \approx Y_{10}$.

Three of the six balance equations have already been presented, eqs (7), (8), and (9). The other three equations are easily obtained by changing the subscripts of Y', γ, e, and q in eqs (7), (8), and (9). Solving the six equations, we obtain

$$\overline{\gamma}_a - \overline{\gamma}_b = \frac{q_5 + q_6 + q_7 - q_8 - q_9 - q_{10}}{2} + \epsilon_4 \qquad (29)$$

where ϵ_4 is a small correction term consisting of second and higher order terms in γ and q.

The method described above was used to measure the difference,

$$\overline{\gamma}_{1000} - \overline{\gamma}_{100} \equiv \frac{\gamma_{1000A} + \gamma_{1000B} + \gamma_{1000C}}{3} - \frac{\gamma_{100A} + \gamma_{100B} + \gamma_{100C}}{3} \qquad (30)$$

Four different values were obtained for the above difference, corresponding to the following changes in voltage: 12.5 to 25, 25 to 50, 50 to 100, and 100 to 200 V, rms, at 1592 Hz. The discussion of measurement uncertainties which follows is applicable to each of these values.

Corrections were obtained for the effects of induced emf's and external loads (see section 3) by joining connectors Q, R, and S to the shorting connectors, E', F', and G' (fig. 4). It was not necessary for the internal loads to be equal or to extrapolate the internal loads to zero. Errors resulting from admittance and transformer ratio drift were reduced by obtaining values of q in the following sequence: q_5, q_6, q_7, q_6, q_5, q_8, q_9, q_{10}, q_9, q_8, q_5, q_6, q_7, q_6, q_5. A sufficient number of measurements was made so that the standard deviation of each of the differences, $\overline{\gamma}'_{1000} - \overline{\gamma}'_{100}$ and $\overline{\gamma}''_{1000} - \overline{\gamma}''_{100}$, was reduced to about 5×10^{-10}. In addition, an allowance of 5×10^{-10} was assigned to each of the differences to account for systematic errors which may be described as similar to items 3, 4, and 5 in table 1.

5. Results

The values in tables 2, 3, and 4 were calculated from the results of measurements described in sections 3 and 4. Capacitors 100A, 100B, and 100C are of cylindrical construction, whereas capacitors 1000A, 1000B, and 1000C are of parallel-plate construction. Most of the voltage dependence of capacitors 1000A, 1000B, and 1000C is believed to be caused by electrode deflections [3]. Most of the voltage dependence of capacitors 100A, 100B, and 100C is believed to be associated with the electrode surfaces.

The values in table 4 were obtained either immediately after assembly of the capacitors, one month after assembly, or eight months after assembly. The values in table 2 were obtained eight months after assembly. A comparison indicates that the values of γ_{100A}, γ_{100B}, and γ_{100C} were probably smallest immediately after assembly. The changes in γ are believed to have been caused by structural changes on the surfaces of the brass electrodes or by the migration of thin films onto the electrode surfaces from regions of the capacitor which were difficult to clean. A consideration of typical dimensions leads to the conclusion that sizeable effects could result from thin films, e.g., the ratio of molecular diameters to typical electrode separations is considerably larger than the desired accuracy of a few parts in 10^9.

Measurements, similar to those in table 4 and with comparable accuracies, were also made on capacitors 1000A, 1000B, and 1000C. The largest change during the eight month period was 4×10^{-10}. Capacitors 1000A, 1000B, and 1000C had been in use for a number of years prior to the measurements described. The electrodes were gold plated. These capacitors and capacitors 100A, 100B, and 100C were evacuated with an oil sealed mechanical pump trapped with dry ice.

TABLE 2. *Voltage dependence of capacitors 100A, 100B, and 100C*

Values of γ' represent proportional changes in capacitance ($\Delta C/C$). Values of γ'' represent changes in dissipation factor. Standard deviation $= 3 \times 10^{-10}$. Systematic error $< 7 \times 10^{-10}$.

Change in voltage	γ'_{100A}	γ'_{100B}	γ'_{100C}
Volts (rms)	Parts in 10^9	Parts in 10^9	Parts in 10^9
100 to 200	+1.9	+8.0	+0.9
50 to 100	+.9	+2.9	+.6
25 to 50	+.3	+1.4	+.4
12.5 to 25	.0	+0.6	+.1
Change in voltage	γ''_{100A}	γ''_{100B}	γ''_{100C}
Volts (rms)	Parts in 10^9	Parts in 10^9	Parts in 10^9
100 to 200	+0.1	−0.4	0.0
50 to 100	.0	+.2	+.1
25 to 50	−.4	−.5	−.2
12.5 to 25	.0	−.2	−.3

TABLE 3. *Voltage dependence of capacitors 1000A, 1000B, and 1000C*

Standard deviation $= 6 \times 10^{-10}$. Systematic error $< 1.2 \times 10^{-9}$.

Change in voltage	γ'_{1000A}	γ'_{1000B}	γ'_{1000C}
Volts (rms)	Parts in 10^9	Parts in 10^9	Parts in 10^9
100 to 200	+70.8	+55.7	+84.5
50 to 100	+18.2	+14.9	+23.2
25 to 50	+5.0	+4.3	+6.7
12.5 to 25	+2.0	+1.2	+1.9
Change in voltage	γ''_{1000A}	γ''_{1000B}	γ''_{1000C}
Volts (rms)	Parts in 10^9	Parts in 10^9	Parts in 10^9
100 to 200	+0.1	+1.2	+2.3
50 to 100	.0	+1.1	+2.2
25 to 50	+.3	+1.1	+1.6
12.5 to 25	+.6	+0.3	+0.8

TABLE 4. *Instabilities in the voltage dependence of capacitors 100A, 100B, and 100C*

All values correspond to a change in voltage from 100 to 200 V, rms. Standard deviation $= 2 \times 10^{-10}$. Systematic error $< 2 \times 10^{-10}$.

Time	$\gamma'_{100A} - \gamma'_{100B}$	$\gamma'_{100B} - \gamma'_{100C}$	$\gamma'_{100C} - \gamma'_{100A}$
Months	Parts in 10^9	Parts in 10^9	Parts in 10^9
0	−0.5	+0.9	−0.4
1	−.6	+.8	−.2
8	−6.1	+7.1	−1.0
Time	$\gamma''_{100A} - \gamma''_{100B}$	$\gamma''_{100B} - \gamma''_{100C}$	$\gamma''_{100C} - \gamma''_{100A}$
Months	Parts in 10^9	Parts in 10^9	Parts in 10^9
0	−0.2	+0.4	−0.2
1	+.1	.0	−.1
8	+.5	−.4	−.1

The values of γ' in tables 2 and 3 can be used to determine the functions which relate capacitance to voltage. If we assume the function

$$C_V = C_0(1 + kV^m) \tag{31}$$

where C_V is the capacitance at voltage V and C_0 is the capacitance at zero voltage, then the values of γ' in each column of tables 2 and 3 will be in the ratio of $2^{3m}:2^{2m}:2^m:1$. Values of m were calculated from the measured values, γ_{100A}, γ_{100B}, γ_{1000A}, etc., and also from the measured differences, $\gamma_{100A} - \gamma_{100B}$, $\gamma_{1000A} - \gamma_{1000B}$, etc., which had smaller uncertainties of essentially different origin (see sec. 4.1). The results of the two types of calculations differed only slightly. The calculations yielded $m \approx 3/2$ for capacitors 100A, 100B, and 100C and $m \approx 2$ for capacitors 1000A, 1000B, and 1000C.

As a partial check on the overall measuring system, the value of $\bar{\gamma}_{1000} \equiv (\gamma_{1000A} + \gamma_{1000B} + \gamma_{1000C})/3$ from 100 to 200 V was determined by two methods: (1) Indirectly by measuring the difference, $\bar{\gamma}_{1000} - \bar{\gamma}_{100}$, as described in section 4.2, (2) directly by using capacitors 1000A, 1000B, and 1000C in bridge 3 of the three-bridge-circuit (sec. 3). The results differed by less than 3×10^{-10}.

Capacitors were chosen from more than two dozen capacitors on the basis of stability ascertained by difference measurements, similar to those described in section 4.1. The voltage dependence of capacitors 100A, 100B, 100C, 1000A, 1000B, and 1000C was found to be considerably more stable than that of the other capacitors. The measurements were limited to 100 pF capacitors and 1000 pF capacitors. The use of the drifter circuit (sec. 4.1) eliminated the need for special temperature control of the capacitors.

The earliest measurements involved three commercial 100 pF air capacitors of parallel plate design. The values obtained from difference measurements were observed to depend not only on time but also on the voltages which had previously been applied to the capacitors. In addition, a sudden, nonreversible change in capacitance of 14 ppm was observed in one of the capacitors when the applied voltage was increased beyond 50 V rms. The cause of the unusual behavior was found to be metallic whiskers on the tin-plated housing of the capacitor.

Difference measurements were also made on a set of ten 100 pF capacitors of cylindrical design. The construction of these capacitors is described in reference [2]. The values obtained from the difference measurements, corresponding to a change in voltage from 80 to 160 volts, were observed to change by as much as 3×10^{-8} over a period of a few days. Changes as large as 3×10^{-8} were also observed when the temperature of the capacitors was increased by approximately 10 °C.

A different phenomenon was observed when difference measurements were made on a set of three 100 pF capacitors of cylindrical design which were evacuated during measurement. The time rate of change of capacitance was found to be a function of voltage. The phenomenon is believed to be related to outgassing of the epoxy which was used to insulate and support the electrodes. Measurements of the time rate of change of capacitance as a function of voltage were made as follows: (1) The bridge was balanced and the drifter circuit was adjusted so as to obtain a steady bridge balance, (2) the detector was shorted, and the voltage applied to one capacitor was reduced to zero for 30 sec, (3) the original conditions were restored and the change in bridge balance was recorded. With 160 V originally applied to the capacitors, the changes in bridge balance were equivalent to proportional changes in capacitance of about 1×10^{-8}.

Difference measurements, corresponding to a change in voltage from 100 to 200 V, were made on three commercial 1000 pF capacitors of parallel plate construction. The changes in the values obtained from the difference measurements varied from a few parts in 10^9 to 2×10^{-8} over the period of one week.

The basic design of capacitors 100A, 100B, and 100C is shown to approximate scale in figure 9. Critical radii differ by approximately 3.2 mm. Line and detector electrodes are separated from the ground electrodes by four sets of three glass spacers. The force of the compressed springs is about 45 N.

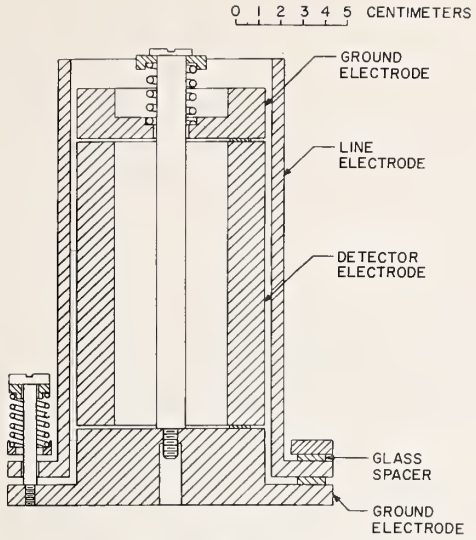

FIGURE 9. *Cross section through the axis of capocitor 100A, 100B, or 100C.*

It was found that after the capacitor was assembled and connected into a measuring circuit, very small radial displacements of the line electrode could be obtained by sharply tapping its base radially. This procedure was used to adjust the capacitance very close to a minimum, thus assuring that the radial components of the electrical forces were small. The design of the capacitor is such that it can easily be disassembled for cleaning or for experimental purposes. A grounded housing (not shown in the figure) is used to evacuate the capacitor.

6. Conclusion

The basic purpose of the present work has been to develop an accurate system for measuring both the relative and absolute voltage dependence of admittance standards. The causes of voltage dependence have been pursued only to the extent necessary to reduce instabilities. Additional measurements will be required to evaluate the instabilities which remain.

Since the mechanisms which cause instabilities in the voltage dependence of capacitors may also result in general instability, the present work has pointed out certain problem areas which should be considered in the construction of precision standards of capacitance. In addition, the present work has served as a proving ground for bridge measurements and voltage ratio measurements at the higher accuracy levels.

The author acknowledges the many suggestions of R. D. Cutkosky and the assistance rendered by D. N. Homan and Lai H. Lee in obtaining the numerical results of this paper.

7. References

[1] A. M. Thompson and D. G. Lampard, A new theorem in electrostatics and its application to calculable standards of capacitance, Nature **177**, 888 (1956).
[2] M. C. McGregor, et al., New apparatus at the National Bureau of Standards for absolute capacitance measurement, IRE Trans. Instru. **I-7**, December 1958.
[3] N. L. Kusters and O. Petersons, The voltage coefficients of precision capacitors, IEEE Trans. Communication and Electronics **82** (1963).
[4] R. D. Cutkosky and J. Q. Shields, The precision measurement of transformer ratios, IRE Trans. Instr., **I-9** (Sept. 1960).
[5] A. M. Thompson, The precise measurement of small capacitances, IRE Trans. Instr. **I-7** (Dec. 1958).
[6] A. M. Thompson, A C bridge methods for the measurement of three-terminal admittances, IEEE Trans. Instr. and Measurement (Dec. 1964).
[7] R. D. Cutkosky, Active and passive direct-reading ratio sets for the comparison of audio-frequency admittances, J. Res. NBS **68C** (Engr. and Instr.), No. 4 (Oct.-Dec. 1964).

(Paper 69D4–207)

JOURNAL OF RESEARCH of the National Bureau of Standards—C. Engineering and Instrumentation
Vol. 64C, No. 1, January–March 1960

Capacitor Calibration by Step-Up Methods

Thomas L. Zapf

(October 8, 1959)

Step-calibration methods are used in many physical laboratories for the extension of measurements to quantities far removed from the magnitude of greatest accuracy at which absolute determinations are made. The excellent precision of repetitive substitution procedures is exploited by step-up or step-down methods to extend measurements to higher or lower magnitudes without serious degradation of accuracy. The application of step-up techniques to the calibration of variable air capacitors is described in this paper as a practical example of the method.

1. Introduction

One of the important statutory functions of the National Bureau of Standards is the calibration of physical standards of measurement used in science and industry. The chain of measurements connecting this calibration service to the national prototype standards of length, mass, and time is complex, and for electrical measurements involves meticulous experiments to assign numerical values to calibration standards and corrections to standard instruments. These devices, designed for excellent stability and definitude, serve as comparison standards basic to the calibration services rendered by the Bureau. Equally important to accurate scientific work is the proper use of these standards to overcome their inherent limitations. Frequently an appropriate choice of method and the employment of suitable techniques are as important as the judicious selection of equipment. The close association between methods, techniques, and equipment is particularly evident when, in the course of calibration activities, it is necessary to obtain accurate measurements at magnitudes far removed from that at which absolute determinations are made. The extension of range of electrical measurements is sometimes accomplished by the establishment of accurately known ratios. For example, ratios very nearly equal to the squares of integers may be obtained through the successive measurement in series and parallel of resistors having nearly equal values [1].[1] Resistance ratios of approximately 10:1 may be realized by the successive measurement of 11 resistors in arbitrary units and the use of these as the 10:1 ratio arms of a bridge. A unique 10:1 ratio apparatus used with a special resistance bridge is described by Wenner [2].

The building-up to ratios larger than 10:1 is particularly well exemplified by the procedure followed in calibrating the standard volt box at the Bureau [3] in which a group of sections of nominally equal resistance is intercompared. These sections, connected in series, form the first section of a group of larger denomination. The buildup to large ratios is rapid and exact. The standard volt box was designed specially for self-calibration by this method.

The calibration of resistance decade boxes and the resistance decades of bridges by the step-substitution or step-up method illustrates yet another technique of obtaining accurate measurements over wide ranges [4]. A similar process is used by the Bureau for the calibration of the capacitance bridges that are used daily to measure standards of capacitance.

In order to obviate the concern over connection errors and avoid the detailed consideration of connectors, it is customary and convenient to use as standards of low grounded capacitance such devices as variable air capacitors and capacitance decade boxes which may be calibrated accurately for capacitance difference from some arbitrary setting. The calibration of such variable capacitors may be accomplished quite effectively by the step-up method employing fixed standards or standards of capacitance difference.

An excellent description of a step-up method applied to the calibration of decade capacitors for both capacitance and dissipation factor has been described by Ford and Astbury of the British National Physical Laboratory [5].

2. Equipment

Very little special equipment is needed to calibrate a variable capacitor by step-up methods. If the variable air capacitor, X, having a range from 100 to 1,100 pf, is to be calibrated at every 100-pf division mark, it is necessary to have a fixed air capacitor, S, of approximately 100 pf that can be connected in parallel with the variable capacitor under test in a precisely repeatable manner. This can be achieved if the mating connectors introduce no significant uncertainties to the capacitance added to the circuit and if the connectors are designed to couple quickly and easily to either the variable capacitor or the

[1] Figures in brackets indicate the literature references at the end of this paper.

bridge that will be used, or if a capacitor can be connected or disconnected by a precise switching arrangement. The 100-pf capacitor should be adjusted close to the nominal value, but it need not be calibrated. It must, however, be free from significant drift over the period of a quarter-hour or so during which the test is being run.

A calibrated 1,000-pf air capacitance standard, S', is needed to relate the results of the step-up test to the national reference standard of capacitance.

The bridge used for this step calibration need not have great accuracy but must be stable, for it is used with a sensitive detector for substitution measurements. A small variable capacitor, V, is required, having a least count (smallest readable increment) one-tenth that of X or smaller. It is advantageous to choose the smallest possible precision variable capacitor, V, consistent with other limitations so that the corrections to V are negligibly small relative to the corrections to X. The total range of V must be at least a little larger than the range of errors in the capacitor to be calibrated. The readable accuracy of this capacitor, if expressed in percent of total range, need not be very great.

The equipment described is assembled as shown in figure 1. It is most important that the cables used to connect components be shielded and rigid, or if flexible cables are used, it should be ascertained that variations in cable capacitance are negligible. The cables must be fixed in position and must not be disturbed during the entire calibration. This precaution is intended to emphasize the importance of particular care to one of those sources of systematic error that could impair good calibration accuracy. The operator must have a good technical appreciation of the apparatus and quantities measured, gained through study and experience.

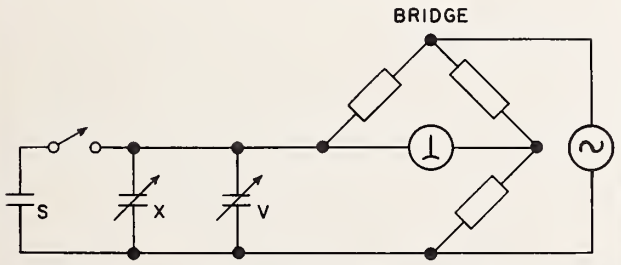

FIGURE 1. *The variable capacitor under test,* X, *is calibrated by a step-up method employing a fixed capacitor,* S, *and a small variable capacitor,* V.

3. Procedure and Computations

The true value of each of the capacitors involved in the calibration may be defined as the nominal value plus a correction; thus, the true capacitance of the uncalibrated 100-pf capacitor is $S=S_n+s$, where $S_n=100$ (exactly) and s is the small correction. Similarly the calibrated 1,000-pf standard has the value $S'=S'_n+s'$, and the variable air capacitor to be calibrated may be represented by $X=X_n+x$, where x is the correction to the reading (or setting) X_n. The calibration will consist of the determination of the relatively small correction, x, to each 100-pf division mark, X_n, and since only capacitance differences are of interest, the observer is free to choose any one of the division marks as a reference point. It is frequently convenient to choose as a reference the first marked point on the dial. In this case the 100-pf mark is considered as a reference and a correction of 0.00 is arbitrarily assigned to it. For this example it will be assumed that the small variable capacitor, V, has corrections that are negligibly small.

The capacitor under test is first carefully set to the 100-pf mark ($X_{n1}=100$ pf) avoiding backlash errors by approaching the mark in the direction of increasing dial readings. The small variable capacitor, V, is set to any convenient mark near the center of its range. The 100-pf capacitor, S, is connected in parallel with X and V. Now the bridge must be balanced using the controls on the bridge itself. If a balance cannot otherwise be obtained, V may be used to attain balance. When the bridge is balanced the reading V_A is recorded. The fixed capacitor, S, is then removed and X set to the 200-pf mark ($X_{n2}=200$ pf), again approaching the mark in the same direction. Without changing any other component the circuit is rebalanced by changing V alone, and the reading V_B recorded as before. In the first balance the external bridge arm consisted of $S+X_1+V_A$, and for the second balance, with the bridge unchanged, the external arm consisted of X_2+V_B. These can be equated to yield

$$S+X_1+V_A=X_2+V_B \tag{1}$$

The cable and connector capacitance, as well as residuals within the bridge, contribute equally to both balances and are therefore deliberately disregarded.

It is convenient to work with small numbers, and eq (1) can be expressed as

$$S_n+s+X_{n1}+x_1+V_A=X_{n2}+x_2+V_B \tag{2}$$

and since

$$S_n=X_{n2}-X_{n1} \text{ and } x_1=0 \tag{3}$$

$$x_2=(V_A-V_B)_2+s \tag{4}$$

where the subscript is appended to the difference (V_A-V_B) to distinguish this set of data from other sets and to appropriately correlate the difference with the setting of X in the second balance of each set.

The quantity x_2 is the desired correction to X_n when $X_n=200$ pf. The difference $(V_A-V_B)_2$ is easily computed from the recorded data.

Without changing X, S is reconnected and the bridge rebalanced using the bridge controls and V, if necessary, to attain exact balance. The reading, V_A, is then recorded. Capacitor S is then removed and X set to the 300-pf mark ($X_n=300$). The bridge is rebalanced using V alone and the reading,

V_B, recorded. When the first balance is equated to the second balance

$$S+X_2+V_A=X_3+V_B \tag{5}$$

or

$$S_n+s+X_{n2}+x_2+V_A=X_{n3}+x_3+V_B \tag{6}$$

and since

$$S_n=X_{n3}-X_{n2} \tag{7}$$

$$x_3=x_2+(V_A-V_B)_3+s. \tag{8}$$

Substituting eq (4) in eq (8)

$$x_3=(V_A-V_B)_2+(V_A-V_B)_3+2s. \tag{9}$$

Continuing this process step-by-step, in general for the mth step

$$x_m=\sum_2^m (V_A-V_B)+(m-1)s \tag{10}$$

and finally

$$x_{11}=\sum_2^{11} (V_A-V_B)+10s \tag{11}$$

A tabulation of the differences and the cumulative sum of the differences is shown in table 1, which shows the data and computations for a typical calibration. It remains to determine the value of s so that the corrections x_2 through x_{11} can be evaluated.

The 1,000-pf standard capacitor, S', accurately calibrated for insertion capacitance, is now connected in parallel with X and V. With X set at 100 pf, the bridge is balanced with the bridge controls and V, if necessary, and the reading, V_A, recorded. S' is removed, X is set to the 1,100-pf mark, the bridge rebalanced using V alone, and the reading, V_B, recorded. Then

$$S'+X_1+V_A=X_{11}+V_B \tag{12}$$

or

$$S'_n+s'+X_{n1}+V_A=X_{n11}+x_{11}+V_B \tag{13}$$

and since

$$S'_n=X_{n11}-X_{n1} \tag{14}$$

$$x_{11}=(V_A-V_B)_T+s' \tag{15}$$

where the subscript T denotes the V difference obtained when the capacitor, S', is used.

In this way x_{11} is determined accurately in terms of a small difference reading of the variable capacitor, V, and the known correction, s', to the standard capacitor, S'. The correction, s, to the fixed capacitor, S, can now be computed from eq (11)

$$10s=x_{11}-\sum_2^{11} (V_A-V_B) \tag{16}$$

or

$$10s=s'+(V_A-V_B)_T-\sum_2^{11} (V_A-V_B) \tag{17}$$

The quantity $10s$ is then added algebraically to the sum of the V differences corresponding to the test of the 1,100-pf mark, the result being the correction to this reading. Similarly $9s$ is added to the sum of the V differences corresponding to the 1,000-pf mark, and so on, until only s is added to the V differences corresponding to the 200-pf mark. These small corrections are listed in table 1 under the heading ns.

The observations can be made rapidly and the computations are simple, since only small differences appear. A second complete calibration, preferably by another observer, enables one to appraise the precision of the measurements including the stability and resetability of the capacitor under test, and serves to reveal measurement and arithmetic errors that might otherwise remain undetected.

In the procedure described above the fixed increment of calibration was 100 pf. It is well to point out that other increments can be accommodated as well. A 50-pf capacitor, if used as a fixed step, would permit calibration at 50-pf intervals. Although the procedure has been described using a fixed capacitor as a step, a continuously variable capacitor or decade capacitor would also be satisfactory if it were used in such a manner as to provide a repeatable difference of capacitance. Care would be necessary to avoid setting errors caused, for example, by backlash in the control mechanism, or by careless setting to the index.

A variable capacitor calibrated for capacitance difference by this method can be used as a standard for extending the method to capacitance calibrations of still lower magnitudes.

TABLE 1. *Observations and calculations*

All values in picofarads

S	X	V	V_A-V_B	$\Sigma(V_A-V_B)$	ns	x
100	100	5.00				
			0.31	0.31	−0.14	0.17
0	200	4.69				
100	200	4.84				
			−.02	.29	−.29	.00
0	300	4.86				
100	300	4.99				
			.06	.35	−.43	−.08
0	400	4.93				
100	400	4.92				
			.41	.76	−.58	.18
0	500	4.51				
100	500	4.65				
			.01	.77	−.72	.05
0	600	4.64				
100	600	4.81				
			.05	.82	−.86	−.04
0	700	4.76				
100	700	4.87				
			.27	1.09	−1.01	.08
0	800	4.60				
100	800	4.73				
			.31	1.40	−1.15	.25
0	900	4.42				
100	900	4.57				
			.04	1.44	−1.30	.14
0	1000	4.53				
100	1000	4.67				
			.55	1.99	−1.44	.55
0	1100	4.12				
1000	100	5.04				
			0.92	----------	----------	----------
0	1100	4.12				

$s'=-0.37$ pf $10s=-1.44$ pf

4. Dual Calibration

Reviewing the calibration described above, it is noticed that for each set of two balances, one balance is obtained with the bridge controls and V, if necessary. The fact that the change in the bridge reading is always an amount approximately equal to S (or S') leads to the consideration of calibrating two variable capacitors having the same range with practically no extra work.

If X and U, the variable capacitors to be calibrated, are connected as shown in figure 2, the procedure is similar to that described above except that the bridge need not be changed after the initial setting. The settings of X and U are listed in table 2. Care must be taken to apply the proper sign to the differences and to cumulatively add the differences for the calibration of U beginning at the bottom of the table rather than the top.

Lower range capacitors can be calibrated similarly, but extreme attention must be paid to good mechanical rigidity in all parts of the circuit.

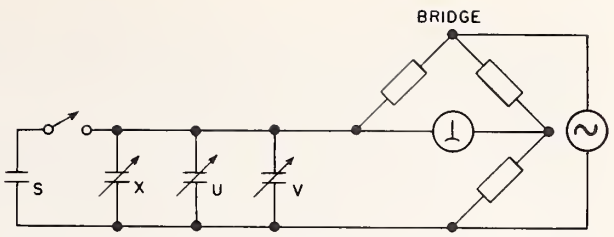

FIGURE 2. *Two variable capacitors, X and U, may be calibrated simultaneously by a step-up method.*

5. Discussion

If attention is confined to the calibration of two-terminal variable air capacitors having a capacitance range from several picofarads to about 1,000 pf, the procedure outlined in this paper demonstrates the ability of step-calibration methods to provide accurate calibrations of capacitors at levels at which good accuracy is otherwise difficult to obtain.

TABLE 2. *Observations and calculations (dual calibration)*

All values in picofarads

S	X	U	V	V_A-V_B	$\Sigma(V_A-V_B)$	ns	x [a]	V_B-V_A	$\Sigma(V_B-V_A)$	ns	u [a]
0	100	1100	5.00								
								0.34	2.05	−1.38	0.67
100	100	1000	5.34								
				0.31	0.31	−0.14	0.17				
0	200	1000	5.03								
								.04	1.71	−1.24	.47
100	200	900	5.07								
				−.03	.28	−.28	.00				
0	300	900	5.10								
								.07	1.67	−1.10	.57
100	300	800	5.17								
				.06	.34	−.41	−.07				
0	400	800	5.11								
								.24	1.60	−0.97	.63
100	400	700	5.35								
				.37	.71	−.55	.16				
0	500	700	4.98								
								.36	1.36	−.83	.53
100	500	600	5.34								
				.02	.73	−.69	.04				
0	600	600	5.32								
								.31	1.00	−.69	.31
100	600	500	5.63								
				.05	.78	−.83	−.05				
0	700	500	5.58								
								.26	0.69	−.55	.14
100	700	400	5.81								
				.26	1.04	−.97	.07				
0	800	400	5.58								
								.29	.43	−.41	.02
100	800	300	5.87								
				.31	1.35	−1.10	.25				
0	900	300	5.56								
								.01	.14	−.28	−.14
100	900	200	5.57								
				.03	1.38	−1.24	.14				
0	1000	200	5.54								
								.13	.13	−.14	−.01
100	1000	100	5.67								
				.54	1.92	−1.38	.54				
0	1100	100	5.13								
1000	100	1100	5.37								
				.91							
0	1100	1100	4.46								
								1.04			
1000	1100	100	5.50								
$s'=-0.37$ pf				$10s=-1.38$ pf				$10s=-1.38$ pf			

[a] The columns x and u are the corrections to the dial readings of the variable capacitors X and U. The good precision of the method is noticeable by comparing the test of X in table 2 with table 1, which represents a test of the same capacitor about an hour earlier.

Standards of grounded capacitance, often called two-terminal capacitors, are characterized by having one of the capacitor electrodes connected to the case, in contrast with standards of direct capacitance (three-terminal capacitors) having both capacitive electrodes insulated from the case. The direct capacitance, C_D, between the two active electrodes, as shown in figure 3, is definite to the extent that the separate terminals and associated leads are shielded from each other. Adequate shielding that does not interfere with the direct capacitance is relatively easily obtained, and excellent accuracy in direct capacitance measurements is possible to a fraction of a micropicofarad (10^{-18} f).

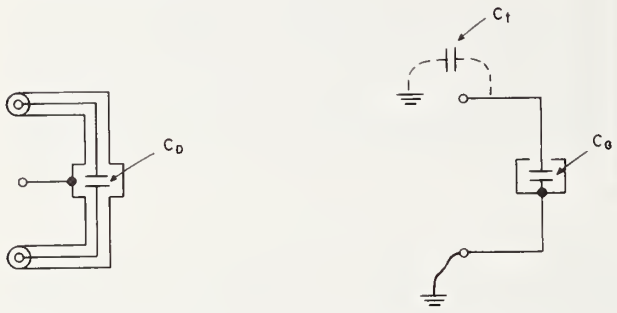

FIGURE 3. *The direct (three-terminal) capacitance,* C_D, *is made definite by complete shielding. The grounded (two-terminal) capacitance,* C_G, *is indefinite because of variations in the stray capacity.*

The grounded capacitance, C_G, shown in figure 3, is more difficult to define in a precise manner, because the capacitance between the ungrounded terminal and all grounded objects, C_t, is indistinguishable from C_G unless a separate "zero-balance" of the measuring apparatus is made with the leads attached but the capacitor disconnected. Even this procedure will not insure good precision unless care is used to connect the capacitor to the measuring apparatus in identically the same way every time. The best precision in practical measurements of grounded capacitance is possible only if the method of connection to the measurement circuit is well defined. An adequately shielded rigid adapter or connector is necessary as an auxiliary part of the capacitor and must be used with it for every measurement. If the capacitor is to be used as a standard for accurate capacitance measurements, the same connector must be used with the capacitor when it is calibrated, and the assembly becomes a standard of, capacitance added to a circuit, or in other words, capacitance difference. Thus, good precision of repeated measurements is simply obtained in any laboratory if the successive measurements are accomplished using rigid wiring and the same connectors every time. The best accuracy in terms of the national reference standards can be obtained only for magnitudes sufficiently large that negligible errors result from differences between the connectors used in the several laboratories involved. Accurate calibration of small fixed capacitors can only be accomplished if mating connectors are submitted.

The accuracy of measurements on fixed standards of grounded capacitance having electrodes terminated in binding posts or unshielded plugs is limited by the variation in the geometrical design of the instrument panels, cables, and connectors to which the standard can be attached. Differences as large as several tenths of a picofarad are possible with present commercially available standards and apparatus with which they may be used. It is understandable that differences of several tenths of a percent are to be expected if a fixed 100-pf standard of this type is measured in several laboratories or on different equipment, while if measurements are performed on 1,000-pf standards the uncertainties at the connectors would be only several hundredths of a percent of the quantity measured. In the step-up procedure described in this paper it is evident that the precision of repeated measurements, the freedom from the effects of residuals in test apparatus obtainable by substitution methods, and the accuracy of measurements at magnitudes closer to optimum, are combined in a manner favorable to the accurate calibration of the capacitance differences of variable capacitors. The method is quite applicable at any frequency although at higher frequencies residuals in components can be troublesome and may require special attention. For example, it may be necessary to apply corrections for errors introduced by residual inductance in the cables connecting the apparatus.

6. Conclusion

Step-calibration methods can be employed for the calibration of variable capacitors. The few necessary items of equipment are generally available in any electrical measurements laboratory. Reference to the national electrical standards is made through the use of a single fixed capacitance standard that can be transported to other standardizing laboratories more easily, and calibrated less expensively than variable capacitors.

7. References

[1] Lord Rayleigh, Phil. Trans. **173,** 661 (1882).
[2] F. Wenner, J. Research NBS **25,** 252 (1940). RP 1323.
[3] F. B. Silsbee and F. J. Gross, J. Research NBS **27,** 269 (1941). RP1419.
[4] J. L. Thomas, NBS Circ. 470 (1948).
[5] L. H. Ford and N. F. Astbury, J. Sci. Instr. **15,** 122 (1938).

BOULDER, COLO. (Paper 64C1–27)

JOURNAL OF RESEARCH of the National Bureau of Standards—C. Engineering and Instrumentation
Vol. 65C, No. 3, July–September 1961

Calibration of Inductance Standards in the Maxwell-Wien Bridge Circuit*

Thomas L. Zapf

(February 28, 1961)

This paper discusses the errors from residuals in the Maxwell-Wien bridge and the effect of these on the measurement of inductors in a bridge not having a Wagner ground. Particular attention is given to the use of substitution methods for accurate measurements and especially to the "equal-substitution" (comparison) method, which can yield excellent precision in the calibration of inductance standards.

1. Introduction

Self inductors and mutual inductors can be constructed to have inductance that is computable from their geometry and dimensions. Although the inductance of certain inductors having measurable mechanical dimensions and simple geometrical form can be computed with excellent accuracy, such inductors are not often used as reference standards for inductance measurements. In practice, inductance measurements are more conveniently made with reference to noncomputable reactances in the form of compact and stable reference standards of inductance or capacitance. Accurate values of inductance can be determined by comparing the reactance of the inductor with the reactance of either standard capacitors or standard inductors by use of appropriate bridge circuits. However, the most precise measurement of an unknown quantity (in this case inductance) is made by comparing it with a standard of like kind and magnitude, the small difference being measured by a corresponding small change in one element of the bridge circuit. When comparison methods are used, it is often possible to reduce the detrimental effects of residuals in the measuring circuit to such an extent that the precision of comparison is much better than the accuracy with which the calibration standard is known.

The Maxwell-Wien bridge circuit has long been used for the accurate measurement of inductance. For measurements of best accuracy with any alternating-current bridge circuit, even for comparison measurements, it is necessary to consider the effects of residuals, the ways of reducing these effects, and the handling of corrections to offset the net errors.

2. Maxwell-Wien Bridge

A bridge circuit originally developed by J. C. Maxwell [1] [1] for use with ballistic detectors was adapted by M. Wien [2] for a-c measurements. For many years the circuit has been used widely by standardizing laboratories for measurements of inductance. Figure 1 shows a schematic of a well-shielded Maxwell-Wien bridge with Wagner arms for elimination of errors resulting from current diverted to ground through leakage impedances. The inductance, L, to be measured is placed in series with a resistance, r_L. If the components of the bridge arms shown in figure 1 were pure, the inductance measured when the bridge is balanced would be

$$L=CR_PR_S, \tag{1}$$

and to obtain the balance it is necessary that

$$\frac{R}{R_S}=\frac{R_P}{r_L}. \tag{2}$$

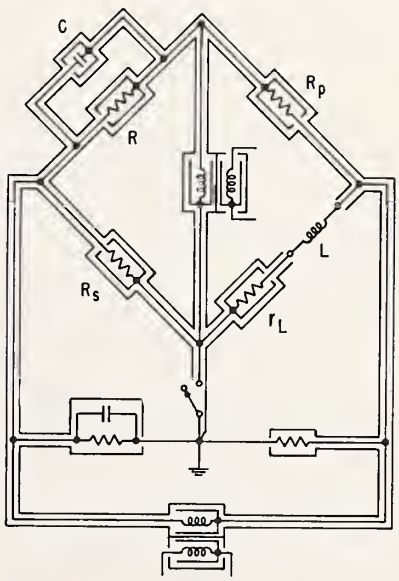

FIGURE 1. *The Maxwell-Wien bridge circuit with complete shielding and a Wagner ground.*

*Contribution from the Radio Standards Laboratory, National Bureau of Standards, Boulder, Colo.

[1] Figures in brackets indicate the literature references at the end of this paper.

In practical situations it is not possible to obtain completely pure components. The residuals in the components contribute to the systematic errors, and it is necessary to analyze the circuit sufficiently to correct for these errors or to determine the maximum uncertainty in the results if the errors are neglected. Figure 2 shows the components of figure 1 with the addition of appropriate residual components, but without the Wagner arms. For example, the series resistor, r_L of figure 1, in the inductance arm is represented in figure 2 by a pure resistance, r_L, in series with an inductance, l_L. The inductance, l_L, is a lumped constant that may be either positive or negative depending upon the relative magnitudes of inductive and capacitive effects. Although lumped constant residuals are not independent of frequency, the lumped constant concept provides a useful equivalent circuit at low frequencies. The other resistive components are similarly represented by a pure resistance and an effective series inductance. The variable capacitance, C, is presumed to contain an effective series resistance, r. The resistance R_L in figure 2 is the equivalent series resistance of the inductor.

3. Equation of Balance

The impedances of the four bridge arms are

$$Z_{RC}=\frac{[(R+j\omega l)(1+\omega^2 r^2 C^2)}{1+\omega^2 r^2 C^2+\omega C(\omega rC+j)(R+j\omega l)}, \tag{3}$$

$$Z_P=R_P+j\omega l_P, \tag{4}$$

$$Z_L=R_L+r_L+j\omega(L+l_L), \tag{5}$$

and

$$Z_S=R_S+j\omega l_S. \tag{6}$$

The derivation of eq (3) is given in the appendix. When the bridge is balanced

$$Z_{RC}Z_L=Z_PZ_S. \tag{7}$$

After the multiplication indicated by eq (7) is performed, the equation of imaginary components can be written

$$\begin{aligned}(1+\omega^2r^2C^2)[R(L+l_L)+(R_L+r_L)l-R_Sl_P-R_Pl_S]\\ =C[RR_PR_S+\omega(RR_Pl_S+RR_Sl_P+R_PR_Sl)\omega rC\\ -\omega^2(Rl_Pl_S+R_Pll_S+R_Sll_P)-\omega^3ll_Pl_S\omega rC].\end{aligned} \tag{8}$$

Considerable simplification of eq (8) is possible if the residuals are expressed as time constants and dissipation factors, as follows. Let

$$\omega rC=D_C, \tag{9}$$

$$\frac{l}{R}=\tau_R, \tag{10}$$

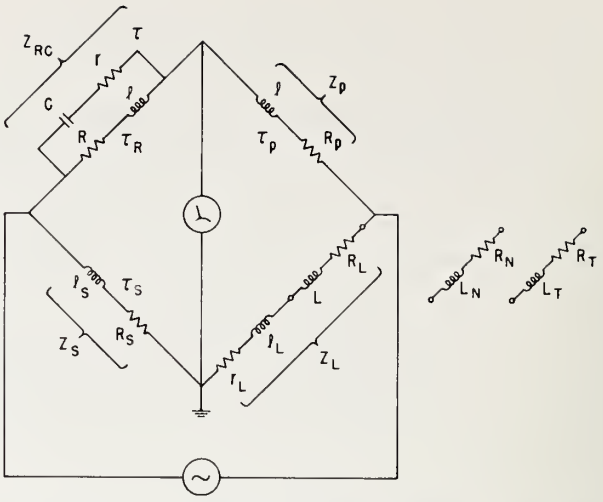

FIGURE 2. *The Maxwell-Wien bridge circuit showing the residuals in the arms as lumped constants.*

$$\frac{l_P}{R_P}=\tau_P, \tag{11}$$

and

$$\frac{l_S}{R_S}=\tau_S. \tag{12}$$

With negligible error it will be found that

$$\begin{aligned}L=CR_PR_S[1-\omega^2(\tau_P\tau_S+\tau_R\tau_P+\tau_R\tau_S)-D_C^2\\ +\omega(\tau_P+\tau_S+\tau_R)D_C-\omega^3\tau_P\tau_S\tau_RD_C]\\ -(R_L+r_L)\tau_R+\frac{R_PR_S}{R}(\tau_P+\tau_S)-l_L,\end{aligned} \tag{13}$$

and a convenient simplification results if the small terms in brackets are replaced by the symbol K. Then the equation of balance becomes

$$L=CR_PR_S(1+K)-(R_L+r_L)\tau_R+\frac{R_PR_S}{R}(\tau_P+\tau_S)-l_L, \tag{14}$$

where

$$\begin{aligned}K=-\omega^2(\tau_P\tau_S+\tau_R\tau_P+\tau_R\tau_S)-D_C^2\\ +\omega(\tau_P+\tau_S+\tau_R)D_C-\omega^3\tau_P\tau_S\tau_RD_C.\end{aligned} \tag{15}$$

4. Effect of Stray Capacitance

Before analyzing this equation in detail it is profitable to consider the effect of stray capacitance across the terminals of the inductor. Such capacitance can be introduced by the leads connecting the inductor to the bridge (see fig. 3). For this analysis, whatever capacitance exists within the case of the inductor is considered not a part of C_S, but rather part of the inductor. It should be understood that this internal shunt capacitance contributes to the

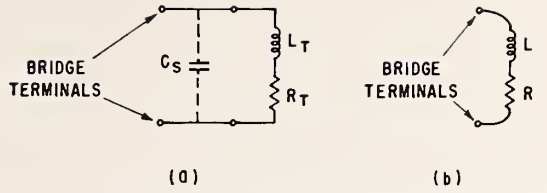

FIGURE 3. *The inductor under test,* L_T, *is connected to bridge terminals with leads having stray capacitance,* C_S, *between them.*

The bridge measures the equivalent inductance, L, which differs from L_T because of the stray capacitance.

effective series inductance measured at the terminals of the inductor, thereby causing the effective series inductance to vary with frequency to some extent.

Figure 3a shows the equivalent series inductance under test, L_T, in series with the internal resistance of the inductor, R_T. The stray capacitance, C_S, external to the inductor is in parallel with L_T and R_T. The bridge measurement does not completely separate these elements but indicates the effective inductance, L, as shown in figure 3b. The effective series inductance, L_T, at the terminals of the inductor is related to the measured value, L, at the ends of the leads by the approximation

$$L_T \approx L\left(1-\omega^2 L_T C_S+\frac{R_T^2 C_S}{L_T}+\omega^2 R_T^2 C_S^2\right). \quad (16)$$

The derivation of eq (16) is given in the appendix. The last three terms in parentheses constitute the small correction terms resulting from stray capacitance. The first and the last of these vary as the square of the frequency. The last term is usually much the smaller of the two in practical situations. The second correction term is not dependent upon frequency and must never be overlooked as a source of error in measurements of the highest accuracy. For example, in the measurement of a 10 h inductor having an internal resistance of 10,000 ohms, at the end of a coaxial cable having a capacitance of 100 pf, the error from neglecting the second correction term is 0.01 h, equivalent to 0.1 percent of the quantity measured. Often the first correction term is significant while the other terms are negligible, and the effective series inductance then can be written

$$L_T \approx L(1-\omega^2 L_T C_S). \quad (17)$$

However, in this paper both the first and second correction terms will be carried in the analysis to follow.

5. Substitution Methods

The existence of the residuals and the consequent correction terms in eqs (14) and (16) are detrimental to good accuracy for residuals are often very difficult to measure or estimate to better than an order of magnitude. To eliminate the effect on measurements of some of these residuals, substitution methods are used. For example, if a standard inductor of equal nominal value is substituted for the test inductor and the difference of inductance is measured by changing C and r_L (or R) slightly, then the residuals in the resistance arms of the bridge have negligible effect on the measurement. Also, the effect of the stray capacitance across the inductor under test or across the standard inductor is much reduced. The standard inductor must be very accurately known, however.

If accurate measurements of large inductors are contemplated and a shorting plug of negligible, or relatively small, inductance is substituted for the test inductor, C_S must be reduced to a negligible value by complete shielding, and a Wagner ground should be used. The effect of the residual, l_L, in the resistor, r_L, is eliminated by this method only if l_L is the same for the two conditions of balance.

The latter method, in which a relatively small inductance replaces the inductor under test, can be designated the "zero-substitution" method to distinguish it from the "equal-substitution" method, in which the test inductor is replaced by a standard of equal nominal inductance.

A general formula for inductance measurements by substitution methods with the Maxwell-Wien bridge may be derived from the two balance equations, the first with the inductor, L_T, in the circuit, and the second with a standard, L_N, in its place. If the small correction terms represented by K in eq (14) are constant for both conditions of balance and if C_S is changed only slightly (to C_{SN}) when the standard inductor or shorting plug is connected, then with certain justifiable approximations

$$L_T = L_N + (C-C_N)R_P R_S[1-\omega^2(L_T+L_N)C_S+K] - \omega^2 L_T L_N(C_S-C_{SN}) + (R_T^2-R_N^2)C_S-(l_L-l_{LN}). \quad (18)$$

The derivation of eq (18) is given in the appendix. This equation is useful in showing the effect of uncertainties in the magnitude of circuit components on the determination of inductance.

If good quality components are used and the bridge is well designed, the time constants that contribute to K will be small. However, K cannot be determined with certainty and is somewhat variable (dependent upon actual circuit constants). The uncertainty in K sets an ultimate practical limit to the accuracy of measurement of inductance by the Maxwell-Wien bridge.

6. Zero-Substitution Method

When the zero-substitution method is employed the small inductance, L_N, need not be accurately known, but the capacitor, C, and the resistance product, $R_P R_S$, must be known with better accuracy than that desired for the inductance, L_T. It is possible to construct very small inductances that are computable from geometry and dimensions. A shorting bar between two terminals has a finite inductance

that can often be calculated or estimated well enough to serve as the "zero-reference", L_N, for bridge measurements of inductors of much larger magnitude. If the measured inductance is defined as the increase in inductance when a shorting-link or switch associated with the inductor is manipulated in a specified manner, then the actual inductance of the short circuit, L_N, is immaterial. The term $(l_L - l_{LN})$ can be minimized if the resistance, r_L, is inductance compensated; i.e., if designed so that the effective series inductance remains constant as the resistance is varied. The uncertainties in this term may limit the accuracy of measurement of small inductors. If C_S is not extremely small, it is evident that the uncertainty in C_S can have a significant effect on the accuracy of measurement by this method. In eq (18) the term in brackets containing C_S can become objectionably large when large values of inductance are being measured. For example, if the inductance being measured is approximately 10 h, if $C_S = 100$ pf ± 10 pf, and if $\omega = 10{,}000$ radians per second, then $\omega^2 L C_S = 0.10 \pm 0.01$. Thus the correction term is 10 percent of the measured inductance, and the measurement uncertainty is 1 percent from this cause alone, disregarding the probable lack of validity of the assumptions (when the correction terms are so large) that were used to derive eq (18). The effect of capacitance C_S thus places a definite limitation on the accuracy which can be obtained by the zero-substitution method with a grounded bridge. In order to obtain better accuracy when $\omega^2 L$ is large it is necessary to use the "equal-substitution method" (described below) or to resort to separate shielding on the inductor leads with an ungrounded bridge using Wagner arms. This latter possibility involves considerations beyond the scope of this paper.

7. Equal-Substitution Method

If an accurately known standard inductance, L_N, is substituted for the test inductor, L_T, the capacitance, C, and the resistance product, $R_P R_S$, need not be so accurately calibrated. Between the two conditions of balance the only circuit components changed are C and r_L, both by small amounts. The residuals D_C and l_L are essentially unchanged in this case, and all the other residuals are identical for both conditions of balance. For the equal-substitution method the general eq (18) can be rewritten with negligible additional error as

$$L_T = L_N + (C - C_N) R_P R_S (1 - 2\omega^2 L_T C_S + K) - \omega^2 L_T^2 (C_S - C_{SN}) + (R_T^2 - R_N^2) C_S - (l_L - l_{LN}). \quad (19)$$

In eqs (18) and (19) the stray capacitances, C_S and C_{SN}, are not considered to be exactly equal; however, it is expected that they will be maintained nearly equal. The importance of this, even in equal-substitution measurements, is evident from eq (19). In the comparison of 10 h inductors at an angular frequency of 10,000 radians per second, if the difference $C_S - C_{SN}$ is only 1 pf, then $\omega^2 L_T^2 (C_S - C_{SN})$ is 0.01 h. This error of 0.1 percent shows the importance of maintaining C_S nearly constant during the substitution.

The term $(l_L - l_{LN})$ can be reduced to a minimum by employing an adjustable resistor, r_L, having inductance compensation. Uncertainties in this term may limit accuracy if the resistances of the test and standard inductors differ greatly, and the inductance compensation of the resistor, r_L, is inadequate. The adjustable resistor is in series with the inductor and is connected to the grounded corner of the bridge as shown in figure 2. If, instead, this resistor were connected to the ungrounded end of the inductance arm of the bridge, the capacitance to ground from the several decades of this resistor would shunt the inductor, and as the resistance is varied to accommodate inductors having different internal resistance the change in stray capacitance would cause an error that would be difficult to correct. If one end of the resistor is grounded, and if care is taken to keep the resistance as low as possible, the capacitance to ground within the resistor merely shunts the resistance, contributing to the effective residual inductance, l_L, which is generally insignificant.

The term $(R_T^2 - R_N^2) C_S$ deserves special attention because it is directly dependent upon the effective series resistances of the inductors. As an example of the effect of this term, consider that, in the measurement of a 10 h inductor, $R_T = 10{,}000$ ohms, $R_N = 8{,}000$ ohms, and $C_S = 100$ pf. Then the term $(R_T^2 - R_N^2) C_S = 0.0036$ h, nearly 0.04 percent of the quantity measured. This correction, being independent of frequency (if skin effect may be neglected) exists even at low frequencies, at which most of the other correction terms are negligible.

If the time constants, τ_P, τ_S, and τ_R, are 1 μsec or less and D_C is 0.001 or less (these are conservative but reasonable estimates for commercially available components), and the angular frequency is 10,000 radians per second, the magnitude of K is less than 0.0003. For a 1 percent difference in inductors, if this term were neglected the resulting error would be only 3 ppm of the measured inductance.

Thus, the equal-substitution method can be employed without the necessity of using a Wagner ground providing care is taken to keep the stray capacitance, C_S, reasonably small and nearly constant and to apply corrections to the measured values to offset errors resulting from the difference in the internal resistances of the inductors.

8. Effect of Frequency Difference

It has been assumed that the frequency of the a-c supply is stable. If the frequency, ω_N, when the standard inductor is in the circuit is not equal to the frequency, ω, when the test inductor is connected, there can be an error resulting from the stray capacitance, C_S. A difference of frequency between the test balance and the standard balance will necessitate the addition of the term

$$-C_S L_T L_N (\omega^2 - \omega_N^2)$$

to the right side of eq (18), and since $\omega \approx \omega_N$ in any practical case, this can be factored to produce

$$-2\omega C_S L_T L_N(\omega - \omega_N).$$

Since $L_T \approx L_N$ for the equal-substitution method, the additional term to be added to eq (19) is

$$-2\omega C_S L_T^2(\omega - \omega_N).$$

If $\omega = 10{,}000$ radians per second, $\omega_N = 10{,}010$ radians per second (a 0.1% difference), and $C_S = 100$ pf, for the measurement of a 10 h inductor by the equal-substitution method the magnitude of the correction term is 0.002 h, an error of 0.02 percent. It is important to realize that this analysis of the effect of frequency variation does not account for the change of effective series inductance with frequency resulting from eddy currents, skin effect, or distributed capacitance within the inductors.

9. Calibration of Inductors

In recent years standard inductors having good stability have become available in a wide range of nominal values. These have made accurate measurements by the equal-substitution method feasible and convenient. Several complete sets of standards are maintained in the laboratories of NBS both at Washington and at Boulder, and are used regularly for calibrating similar standards submitted for certification. The values assigned to NBS working standards ultimately depend upon a computable inductor or capacitor.

The equal-substitution method can be utilized with a variety of a-c bridge circuits. The essential requirements are that the bridge have good short-time stability, adequate resolution, and means for externally equalizing the storage factor (Q) of the inductors being compared. An advantage of the equal-substitution method is the lessened need for accuracy of adjustment of the bridge components because the bridge is used merely to measure small differences. A number of commercially available bridges embody the Maxwell-Wien bridge circuit to which the analysis given in this paper is primarily devoted. It is almost invariably necessary, however, to improve their resolution by adding a calibrated variable capacitor in parallel with those built into the bridge.

The resistor, r_L, is partially inductance compensated and is connected in series with the cable connecting the inductors to the bridge. It has been determined that the existing variations of inductance are negligible relative to the inductance being measured by this method. This resistor may be regarded as serving the purpose of externally equalizing the Q of the standard and test inductors.

It is seldom necessary to apply a correction for the term $(R_T^2 - R_N^2)C_S$ in eq (19). On rare occasions when this term is significant, a crude measurement of R_T and R_N is adequate.

The resistance product (range) in the bridge is set so that the difference between the test and the standard inductors can be accommodated by adjustment of the externally connected variable capacitor and resistor, the other bridge controls being left unchanged.

The analysis of errors in the Maxwell-Wien bridge circuit described in this paper was carried out as part of the investigation of the feasibility of adopting the equal-substitution method for the rapid and convenient measurement of inductance.

The use of the equal-substitution method for the precise comparison of inductors at the Electronic Calibration Center, NBS, Boulder, Colo., was instigated by Chester Peterson, NBS, Washington, D.C. The author is indebted to Mr. Peterson for helpful comments and suggestions pertaining to this paper.

10. Appendix: Derivation of Equations

Equation (3) is derived from the equation of the impedance of Z_C and Z_R in parallel.

$$\frac{1}{Z_{RC}} = \frac{1}{R+j\omega l} + \frac{\omega C}{\omega r C - j}$$

$$= \frac{1}{R+j\omega l} + \frac{\omega C(\omega r C + j)}{\omega^2 r^2 C^2 + 1}$$

$$= \frac{1+\omega^2 r^2 C^2 + \omega C(\omega r C + j)(R+j\omega l)}{(R+j\omega l)(1+\omega^2 r^2 C^2)}.$$

Therefore

$$Z_{RC} = \frac{(R+j\omega l)(1+\omega^2 r^2 C^2)}{1+\omega^2 r^2 C^2 + \omega C(\omega r C + j)(R+j\omega l)}.$$

Equation (8) is obtained by substituting eqs (3), (4), (5), and (6) into eq (7), giving

$$(1+\omega^2 r^2 C^2)(R+j\omega l)[(R_L+r_L)+j\omega(L+l_L)]$$

$$= [1+\omega^2 r^2 C^2 + \omega C(\omega r C + j)(R+j\omega l)]$$

$$(R_P+j\omega l_P)(R_S+j\omega l_S),$$

from which the equation of imaginary components is

$$(1+\omega^2 r^2 C^2)[R(L+l_L)+(R_L+r_L)l - R_S l_P - R_P l_S]$$

$$= C[RR_P R_S + \omega(RR_P l_S + RR_S l_P + R_P R_S l)\omega r C$$

$$-\omega^2(Rl_P l_S + R_P l l_S + R_S l l_P) - \omega^3 l l_P l_S \omega r C].$$

Equation (16) describes the effect of stray capacitance. Figure 3a represents an inductor, L_T, having an internal resistance, R_T, connected to the bridge terminals by a cable having shunt capacitance, C_S.

The impedance of this circuit, Z, is derived as follows

$$\frac{1}{Z}=\frac{1}{R_T+j\omega L_T}+j\omega C_S,$$

$$Z=\frac{(R_T+j\omega L_T)(1-\omega^2 L_T C_S-j\omega R_T C_S)}{(1-\omega^2 L_T C_S+j\omega R_T C_S)(1-\omega^2 L_T C_S-j\omega R_T C_S)},$$

$$Z=\frac{R_T+j\omega[L_T(1-\omega^2 L_T C_S)-R_T^2 C_S]}{(1-\omega^2 L_T C_S)^2+\omega^2 R_T^2 C_S^2}.$$

In the equivalent circuit shown in figure 3b

$$Z=R+j\omega L,$$

and from the two preceding equations it is evident that

$$L=\frac{L_T(1-\omega^2 L_T C_S)-R_T^2 C_S}{(1-\omega^2 L_T C_S)^2+\omega^2 R_T^2 C_S^2}$$

and, with negligible error,

$$L=\frac{L_T\left(1-\omega^2 L_T C_S-\dfrac{R_T^2 C_S}{L_T}\right)}{(1-2\omega^2 L_T C_S+\omega^2 R_T^2 C_S^2)}.$$

It should be noted that the discarded term, $\omega^4 L_T^2 C_S^2$, in the denominator is always much smaller than the term, $2\omega^2 L_T C_S$, which is usually much smaller than 1 in practical inductance measurements at low audiofrequencies. Since the terms in parentheses, other than 1, are small, this equation can be solved for L_T and simplified by neglecting higher order terms.

$$L_T\approx L\left(1-\omega^2 L_T C_S+\frac{R_T^2 C_S}{L_T}+\omega^2 R_T^2 C_S^2\right).$$

Equation (18) is obtained from the following two equations which are derived from eq (14) modified according to eq (16)

$$L_T=CR_P R_S\left(1-\omega^2 L_T C_S+\frac{R_T^2 C_S}{L_T}\right)(1+K)$$
$$-(R_L+r_L)\tau_R+\frac{R_P R_S}{R}(\tau_P+\tau_S)-l_L$$

and

$$L_N=C_N R_P R_S\left(1-\omega^2 L_N C_{SN}+\frac{R_N^2 C_{SN}}{L_N}\right)(1+K)$$
$$-(R_{LN}+r_{LN})\tau_R+\frac{R_P R_S}{R}(\tau_P+\tau_S)-l_{LN}.$$

In eq (15) it will be noted that at the higher frequencies the first term in K is the largest term, and that at lower frequencies all terms in K are small and often negligible. The first term in K is independent of D_C, which may vary slightly between the two conditions of balance; hence, the assumption that K is constant is justifiable. In the above equations since

$$CR_P R_S\approx L_T$$

and

$$C_N R_P R_S\approx L_N$$

and

$$(R_L+r_L)\approx(R_{LN}+r_{LN})$$

$CR_P R_S R_T^2 C_S/L_T\approx R_T^2 C_S$ and

$$C_N R_P R_S R_N^2 C_{SN}/L_N\approx R_N^2 C_{SN}.$$

Therefore,

$$L_T-L_N=[(C-C_N)R_P R_S-R_P R_S\omega^2(CL_T C_S$$
$$-C_N L_N C_{SN})+R_T^2 C_S-R_N^2 C_{SN}](1+K)-(l_L-l_{LN}).$$

The factor $(CL_T C_S-C_N L_N C_{SN})$ can be expanded as follows:

$$(CL_T C_S-C_N L_N C_{SN})=(C-C_N)(L_T C_S+L_N C_{SN})$$
$$+C_N L_T C_S-CL_N C_{SN}.$$

If C_S and C_{SN} can be reduced to zero, this factor becomes zero, and the equation is greatly simplified. However, if C_S is not zero, but if C_S approximately equals C_{SN},

$$CL_T C_S-C_N L_N C_{SN}=(C-C_N)(L_T+L_N)C_S$$
$$+C_N L_T C_S-CL_N C_{SN}$$

and

$$L_T-L_N=\{(C-C_N)R_P R_S[1-\omega^2(L_T+L_N)C_S]$$
$$-R_P R_S\omega^2(C_N L_T C_S-CL_N C_{SN})$$
$$+(R_T^2-R_N^2)C_S\}(1+K)-(l_L-l_{LN}),$$

and with negligible error the substitution $C_N R_P R_S=L_N$ and $CR_P R_S=L_T$ can be made in the small correction terms. The second term in braces can be reduced to $-\omega^2 L_T L_N(C_S-C_{SN})$. If the terms under consideration are not relatively small, the approximations are not valid.

Neglecting second order terms, the above equation can be simplified, giving eq (18):

$$L_T=L_N+(C-C_N)R_P R_S[1-\omega^2(L_T+L_N)C_S+K]$$
$$-\omega^2 L_T L_N(C_S-C_{SN})+(R_T^2-R_N^2)C_S-(l_L-l_{LN}).$$

11. References

[1] J. C. Maxwell, A treatise on electricity and magnetism, 1st ed., **2**, 377–379 (1873), or 3d ed., Art. 778.
[2] Max Wien, Ann. der Phys., **44**, 689–712 (1891).
[3] H. L. Curtis, Electrical Measurements, 113–117, McGraw-Hill Book Co., Inc., New York, N.Y. (1937).

(Paper 65C3–69)

JOURNAL OF RESEARCH of the Notional Bureau of Stondords—C. Engineering and Instrumentation
Vol. 70C, No. 4, October–December 1966

Some Techniques for Measuring Small Mutual Inductances

D. N. Homan*

Institute for Basic Standards, National Bureau of Standards, Washington, D.C. 20234

(July 6, 1966)

A method of measuring small mutual inductances is presented. The smallest inductor measured was 0.1 μH. The circuit is a transformer-ratio-arm bridge with multiple balances and is described in detail. Uncertainties are of the order of one part in 10^7.

Several ideas for the design and construction of suitable mutual inductance standards are presented.

Key Words: Auxiliary generator, bridge, coaxial choke, mutual inductor, stray magnetic field, transformer.

1. Introduction

A recent theoretical study by Page [1][1] suggests the desirability of making accurate measurements of mutual inductance at the 0.1 μH level and of stepping up to larger values. An experimental bridge has been constructed for the purpose of investigating some techniques which seemed appropriate in this range. Some of those techniques which appear to be particularly useful are described in this paper. The bridge is a transformer-ratio-arm bridge, having a ratio of 10 to 1, and has been designed to compare mutual inductors through five orders of magnitude, from 0.1 μH to 1 mH at a frequency of 1592 Hz. Sensitivity of a part in 10^7 is achieved at the 0.1 μH to 1 μH level provided the inductors carry 3A in their primary windings.

2. Bridge Circuit

A simplified version of the bridge is shown in figure 1. Mutual impedances Z_1 and Z_2, which are both mainly inductive, are defined by the equations

$$Z_1 = j\omega M_1 + R_1$$

$$Z_2 = j\omega M_2 + R_2.$$

If both inductors have the same current, i, in their primary windings,[2] the comparison of Z_1 to Z_2 is achieved by measuring the ratio of the induced voltages e_1 and e_2. Since $Z_1 = \frac{e_1}{i}$ and $Z_2 = \frac{e_2}{i}$, then $\frac{Z_1}{Z_2} = \frac{e_1}{e_2}$. The ratio of e_1/e_2 is compared with the 10 to 1 voltage ratio of an inductive voltage divider, which may be calibrated by a modification of the capacitance-ratio method described by Cutkosky and Shields [2]. The bridge balance is accomplished by the adjustment of e_3, which is an adjustable voltage source, small relative to e_1 and e_2.

The detector consists of a tunable amplifier and a tuned high-impedance preamplifier, coupled to the bridge through an impedance matching transformer. The transformer is tuned with a variable capacitor to give maximum output voltage.

Accurate measurement of small inductances requires that all sources of stray magnetic field be well controlled. To that end, inductors and transformers are toroidal, bridge components are enclosed in copper eddy-current shields, components are interconnected by coaxial cables, and shield current of the coaxial leads is restricted to be nearly equal and opposite to current in their inner conductors. Figure 2 illustrates shielding and the use of the technique of threading a coaxial lead through a high permeability core [3] forming a coaxial choke to equalize current in the inner conductor and outer shield of the coaxial cable.

Following construction of the bridge, tests were made to establish the effectiveness of the design in keeping stray magnetic fields small. Such tests were made by using two coils of wire, one connected to a

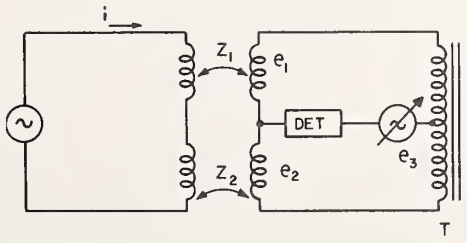

FIGURE 1. *Simplified inductance bridge circuit.*

*Present address: High Frequency Impedance Standards Section, NBS, Boulder, Colo. 80302.

[1] Figures in brackets indicate the literature references at the end of this paper.

[2] Ground capacitance current between the primary windings is negligible; it is discussed in section 4 of this paper.

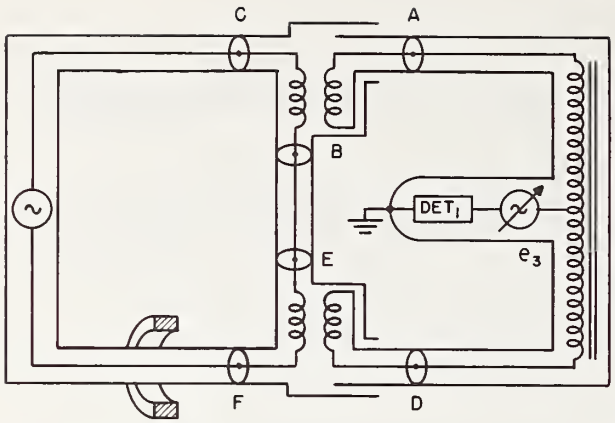

FIGURE 2. *Inductance showing shielding, junction points (A, B, C, D, E, F) of the mutual inductor, and use of high-permeability core to equalize coaxial current.*

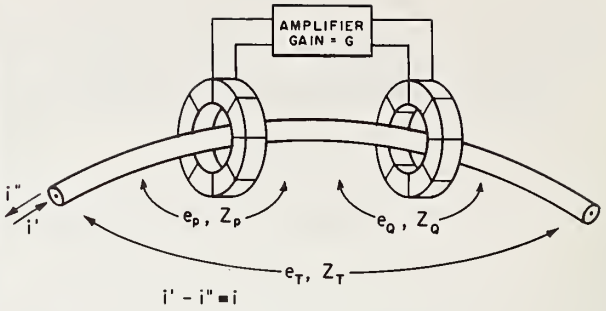

FIGURE 3. *Active coaxial choke.*

detector and used to find sources of stray field, and the other connected to a generator and used to find places in the circuit that were sensitive to stray field. For example, the detector coil was moved around until a source of stray field was found, and the amount of detector off-balance was noted. The coil connected to the generator was driven so that its field gave about the same off-balance at a comparable distance from the detector coil. Then the driven coil was used as a probe to determine the effect of such a field on the main bridge balance when brought near various bridge components.

The largest sources of stray field were the coaxial leads in the loop that includes the inductor primary windings since the current is largest in that part of the circuit. It was determined that the coaxial choke, mentioned above, was not sufficient to equalize current in the inner conductor and outer shield of the coaxial cable. A greatly improved coaxial choke was realized by making it an active device using two cores in a manner described by Gibbings [4]. As it is used in this application, it may be called an "active coaxial choke." The principle is shown in figure 3. If $e_P = Z_P i$, $e_Q = G e_P$, and $e_T = e_P + e_Q$, it can be shown that $Z_T = Z_P(1+G)$. Thus, the active choke reduces net current much more than a coaxial choke composed of a single magnetic core. The gain of the amplifier and the number of turns of cable through the device was adjusted to reduce net current by an amount which made the error negligible.

Small stray magnetic fields due to slight nonsymmetries in the coaxial cables remained. Using the probe technique discussed above, three modifications were made. First, the copper can serving as an eddy-current shield for the inductive divider was found to be unsatisfactory because the lid was electrically attached to the can at only one point. The shield was improved by bolting the lid to the can firmly with screws spaced about 2 in apart around its circumference. Second, an uncertainty in the value of mutual inductance arises from the coupling between the leads connected to the inductor primary windings and the leads connected to the inductor secondary windings, if the leads move relative to each other. Subsequent inductors were designed to have the primary winding terminals on the opposite side of the shield can from the secondary terminals. Third, the smallest inductors (for which the ratio of mutual inductance of the leads to mutual inductance of the inductor is largest) were modified as follows: The eddy-current shield was extended over the secondary leads by passing these leads through a three-inch-long copper cylinder having 1/8-in wall thickness (about two skin depths at the frequency used).

The standards to be compared, as illustrated in figure 2, are defined as follows: Let i'_A be the current into the inner terminal of connector A, i''_A be the current out of the outer terminal, and e_A be the voltage from the inner to the outer terminal. Currents and voltages are similarly defined at connectors B, C, D, E, and F. Then the mutual impedances of interest are defined by $Z_{AB} = \frac{e_A}{i'_B}$ with the conditions $i'_B = i''_B$, $e_B = 0$, and $i'_A = i''_A = 0$; $Z_{DE} = \frac{e_D}{i'_E}$ with the conditions $i'_E = i''_E$, $e_E = 0$, and $i'_D = i''_D = 0$. The above conditions are similar to those used in the theoretical analysis by Cutkosky of four-terminal-pair networks [5].

3. Auxiliary Balances

The techniques used to assure the realization of the conditions defining the inductors involve the use of several auxiliary generators and detectors. Figure 4 shows the complete system. Each of the four auxiliary generators consists of a decade capacitance network in parallel with a decade conductance network, driven by a 40-turn winding on the magnetic core of the bridge supply transformer. Figure 4 shows two such 40-turn windings, the sign of the voltage of one being opposite to that of the other so that each capacitance decade or conductance decade can be switched

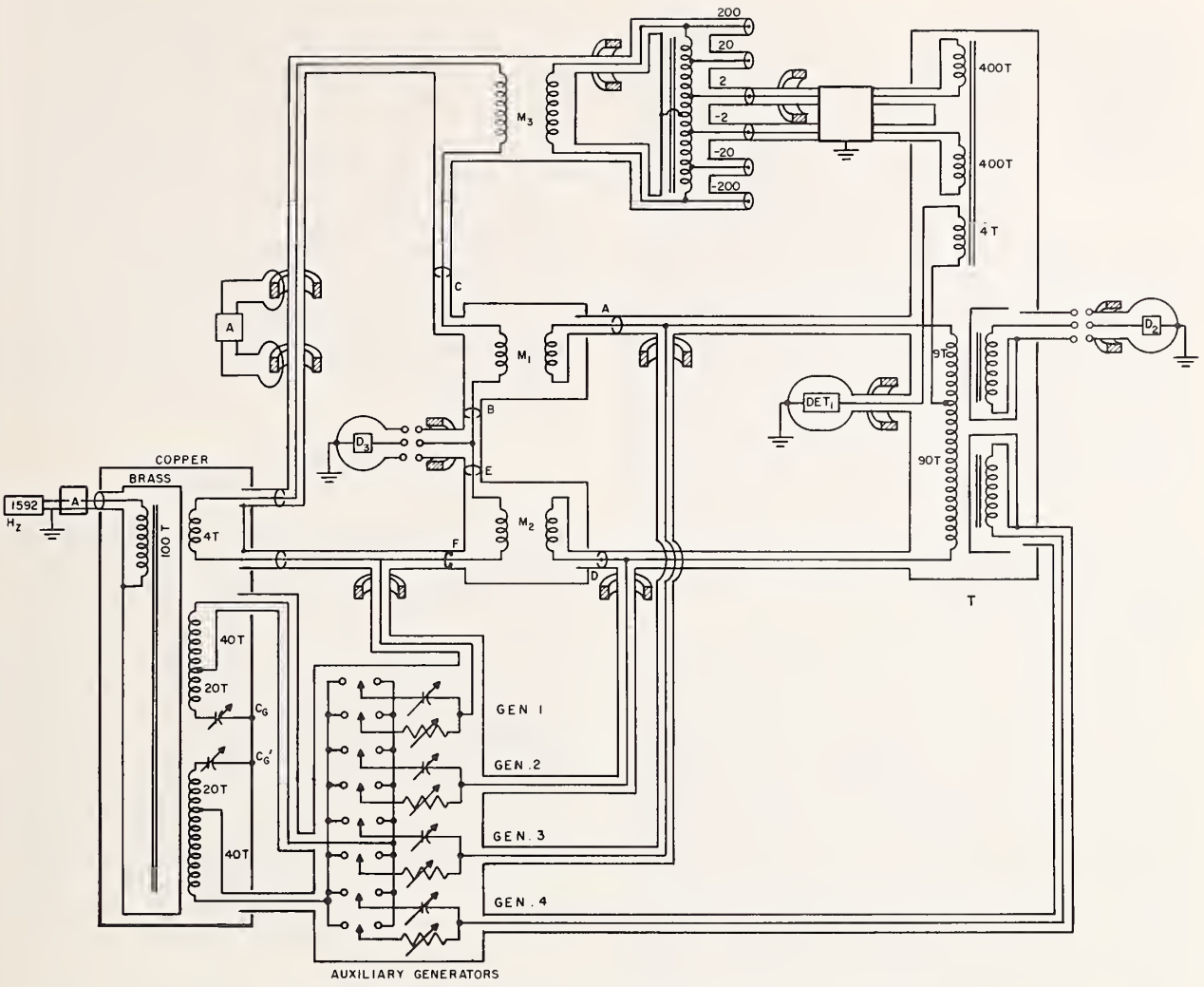

FIGURE 4. *Complete system for measurement of small mutual inductances.*

independently to reverse the sign of the voltage driving it. Stray capacitance from the 40-turn winding to the shield raises the potential of the shield and would result in current in the shield. This difficulty is overcome if an adjustable capacitor, C_G, is attached to the 20-turn winding, the voltage of which is opposite in sign to that of the 40-turn winding. A capacitance bridge is formed by placing a detector between the shield and the bottom of the 40-turn winding, and the bridge can be balanced by adjusting C_G. A similar bridge is formed with C_G' as one component. Permanent adjustments of C_G and C_G' were made following the completion of this component of the system.

The load on the secondary winding of each inductor is supplied by an auxiliary generator. The loading consists of capacitance in the cable connecting the inductors to the inductive voltage divider, T, and capacitance in the inductive voltage divider itself. Each of the auxiliary generators is adjusted until unplugging the inner conductor of the coaxial connection at the inductor secondary shows no change in the null at detector No. 1. Such a condition can be expressed as $i_A'=0$ and $i_D'=0$. The impedances of the auxiliary generators are high relative to the inductor secondary windings so that convergence to balance is more quickly achieved. Without the auxiliary generators, the loading in the circuit is such that the voltage e_A at connector A of a 100 μH inductor was changed by approximately one part in 10^5 when the load was disconnected from the circuit by unplugging the lead to the secondary winding. Thus the auxiliary generators need to be adjusted to one part in 10^3 to obtain accuracy of one part in 10^8.

At the 1 mH level, an error arises from a capacitance change at the secondary terminal when a coaxial cable is connected to the terminal. When such a connection is made, the inner connector of the coaxial cable slips over the inner member of the connector on the inductor, thus changing the capacitance from the inner connector of the inductor to its shield about 0.3 pF. The impedance of the secondary winding of the 1 mH inductor used in this work is about 20 Ω. A calculation shows that one could expect an error of about 6 in 10^8 due to such a capacitance change. This error can be made reproducible by using the same coaxial cable each time the 1 mH inductor is measured.

The inductive voltage divider T is a two-stage device. Two stage devices have been analyzed by Gibbings [4] and by Cutkosky [6]. The auxiliary generator (gen. 4 in fig. 4) incorporated in the transformer supplies the excitation current in the ratio winding. With the bridge balanced, a detector winding on the second core assures that no excitation current is supplied by the inductor secondary windings. Thus this inductive voltage divider behaves like a device having infinite input impedance in that it draws no current. An additional feature of the two-stage design is a highly accurate 10 to 1 ratio [4].

The conditions $e_B = 0$ and $e_E = 0$ are met by adjustment of the auxiliary generator 1 in the part of the circuit containing the primary windings of the mutual inductors such that detector No. 3 indicates null. Shunt admittances in conjunction with the impedance of the coaxial cable from the detector junction to points B or E may cause an error. A calculation based on an assumed equivalent circuit and approximate values for the impedance and admittance indicates that such an error is in the order of 1 in 10^8 or less for typical length of coaxial cable used at this point. An experimental verification of the above calculation was made by observing the difference in the main bridge balance caused by changing the length of coaxial cable between B and E.

Tests of interdependence of the detector balances were made by bringing the bridge to balance, and then changing one auxiliary generator voltage while observing changes in the null conditions at the detector junctions. Such tests and experience in bringing all the detectors to a simultaneous null indicate some dependence of one balance on another. However, the time involved in obtaining convergence of all balances is not unreasonably long.

The condition $i'_A = i''_A$ can be assured by an auxiliary device illustrated in figure 5. One can adjust e_4 (to null D_4) to compensate for net current which can result from capacitance from the primary to the secondary winding of an inductor. However, it is possible to construct inductors in such a way that the change in the main bridge balance (detector 1) when e_4 is switched in and out is small enough so that the corresponding error is less than 1 part in 10^8. The 1 mH mutual inductor was altered by inserting a permanent short between the low-voltage side of the primary winding to the low-voltage side of the secondary. Inductors smaller than 1 mH were not fixed with a short as described above since the error corresponding to the change in the main bridge balance when e_4 is switched in and out in their case was smaller than 1 in 10^8 without the short.

4. Main Bridge Balance

The circuit used to obtain the small adjustable voltage, e_3 is shown in figure 6. That portion of figure 6 shown within dotted lines represents a component part of an "a-c direct-reading-ratio set" which has been described by Cutkosky [6]. This is an active circuit with high input impedance and low output impedance. Hence M_3 is not strongly loaded, and reasonably large loads can be driven by the circuit. The in-phase and quadrature components of e_3 are read directly from dials of two inductive voltage dividers, IVD#1 and #2 in figure 6. The mutual inductor M_3 has nearly the same current in its primary winding as the inductor M_1. The voltage e_3 is related, through current i, to e_1 and e_2. The relationship is controlled by the choice of the value of M_3, which provides a scale factor. The value of M_3 has been calculated such that one step of the last dial is one part in 10^8.

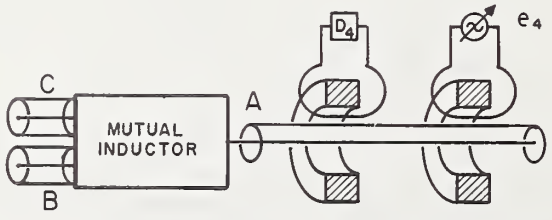

FIGURE 5. *Method of assuring zero net current at inductor secondary terminal.*

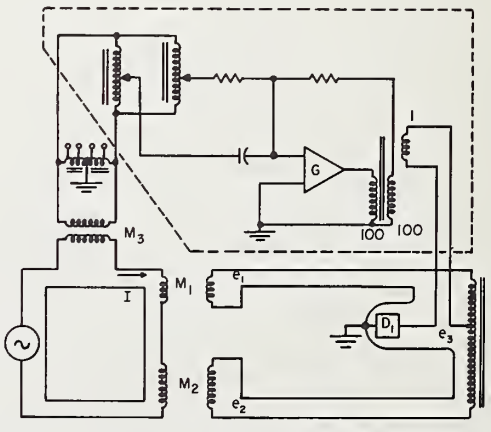

FIGURE 6. *Basic bridge and, in dotted lines, circuit used to obtain balance.*

The range of e_3 is ± 5 in 10^4 and the least count is 1 in 10^8. The current in M_3, therefore, must be no more than 2 in 10^5 different from that in M_1 for accuracy of 1 in 10^8. A calculation shows that ground capacitance between M_1 and M_3 and in M_3 must not exceed 1000 pF for this accuracy. The inductor M_3 is constructed to have ground capacitance well below 1000 pF. Components of the apparatus shown within dotted lines in figure 6 were initially adjusted to an accuracy of a few parts in 10^5. Past experience with the type components used in the apparatus indicates that at the time of these measurements the accuracy of the dial readings was better than 1 part in 10^3 of the dial reading. Thus if the inductors being compared (i.e., M_1 and M_2) are adjusted so that their values differ by less than 1 in 10^5, the measurements can be relied upon to 1 in 10^8.

5. Measurement Procedure

A single detector is used for all balances; it is plugged alternately into positions D_1, D_2, and D_3 (fig. 4). Balancing starts by bringing D_1 to null by the dials IVD#1 and IVD#2 (fig. 6). Next, leaving the detector at D_1, the secondaries of the mutual inductors M_1 and M_2 are unplugged in turn. With the secondary M_1 unplugged, a null at D_1 is obtained by turning the dials of gen. 3 (fig. 4); similarly, the secondary of M_2 is unplugged, and the balance reached with gen. 2. The detector is then plugged into the D_2 position and a null is achieved by turning dials of gen. 4. Finally, the detector is plugged into the D_3 position and brought to null by gen. 1.

All balances described above are then repeated several times until convergence is reached.

6. Inductors

Some of the requirements of the inductors are that they be stable, astatic, have small phase angle, be close to nominal value, and be capable of carrying substantial current in their primary windings.

To make the inductors astatic, both the primary and secondary have toroidal symmetry about the same axis; the primary winding is outside the secondary winding and, therefore, has a larger cross section. The leads, as shown in figure 7, are brought out to the coaxial connectors in such a way as to create a minimum loop. The inductor is mounted in a copper shield of 1/8-in thickness (about two skin depths at 1592 Hz). The coaxial connector of one of the primary leads is connected to the copper shield at one point inside the shield. The primary leads and the secondary leads are brought out on opposite sides of the toroid as shown in figure 7 to keep magnetic coupling to a minimum outside the toroid.

If two windings have toroidal symmetry about a common axis, and if one of these windings is totally within the other, the mutual inductor thus formed has been observed to have the following property: The phase angle of the inductor is practically independent of the thickness of the wire used for the outside winding; the phase angle depends on the thickness of the wire used on the inside winding, a larger phase angle being produced by thicker wire. The outside winding is, therefore, better suited for the primary, since the primary should have low resistance for minimum heat dissipation.

A few inductors have been constructed using toroidal forms of Bakelite; they were potted in epoxy resin and enclosed in 1/8-in thick copper shield cans. These inductors are useful for testing some of the features of the inductance bridge, but have temperature coefficients that are too large to make them useful as standards in this work.

A 0.1 μH inductor was made by painting silver windings onto a toroidal form of fused silica. The silica form, with the silver secondary winding, was baked and then a primary of copper wire was wound around the form but mechanically isolated from it. A critical problem is that of bringing the leads from the secondary out through the primary (see fig. 8). A cylindrical fused-silica rod was fused to the toroidal form as in figure 9 so that the leads could be brought out on a solid mount. An attempt to use silver painted leads was made but abandoned in favor of using #36 copper wire. These lead wires were tightly twisted

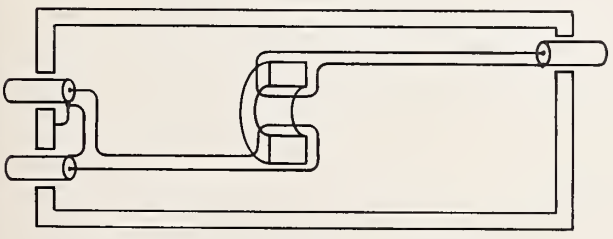

FIGURE 7. *Lead geometry and shielding of mutual inductor.*

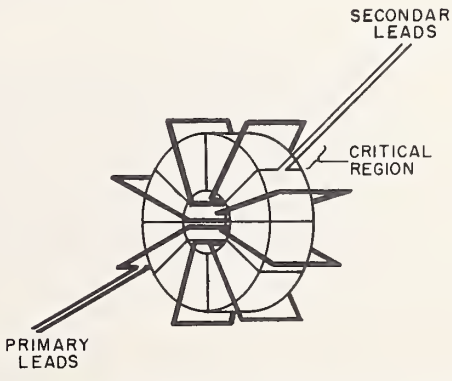

FIGURE 8. *Winding geometry of mutual inductors having fused silica toroidal form.*

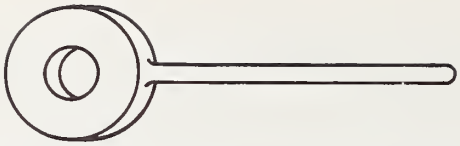

FIGURE 9. *Fused silica toroidal form and lead mount.*

FIGURE 10. *Illustration of painted secondary winding showing skew of turns concentrated in inner toroidal surface.*

and attached to the fused-silica rod with alkyd resin paint, and electrical contact to the secondary was made with silver paint. The gage of the wire was chosen to be as small as possible to keep the loop area small, but large enough such that lead resistance was below the resistance of the painted secondary.

A possible source of uncertainty due to relative motion between primary and secondary is the magnetic coupling from the "single turn" produced by the progression of the turns about the toroid. This is an effective loop around the toroid in which an emf can be induced by a component of magnetic field parallel to the axis of the toroid. To reduce this uncertainty all the skew of the turns was concentrated at the inner surface of the toroid as shown in (fig. 10). After a thin insulating coating of alkyd resin paint was applied, a return loop was painted on top of the skewed wires forming a loop in the opposite direction to the loop formed by the skew.

A nonuniformity of the secondary winding painted on the toroidal form could create a net loop which would cause the inductors in effect to be lopsided. Thus relative motion between the primary and secondary windings could change the inductance. A calculation for the 0.1 μH inductor indicates that such a net loop of 1 mm^2 would dictate that for stability of one part in 10^8, the relative motion of primary to secondary must be 10^{-5} mm.

It appears that improved techniques in painting the secondary winding onto a fused-silica toroidal form would result in inductors of good stability.

(Paper 70C4–233)

7. Conclusion

At the smallest level of inductance measured here, bridge sensitivity is one part in 10^7. Sensitivity improves at larger values of inductance such that 100 μH can be compared with 1 mH with sensitivity of a few parts in 10^8. It appears likely that the bridge techniques described here can be relied on to yield errors that are less than one part in 10^7. An analysis of all errors in such a step-up from 0.1 μH to 1 mH must await the development of a more reliable set of mutual inductance standards.

The author thanks R. D. Cutkosky for suggesting the scheme of measurement used here.

8. References

[1] C. H. Page, A new type of computable inductor, J. Res. NBS **67B** (Math. and Math. Phys.) 1, (Jan.–Mar. 1963).
[2] R. D. Cutkosky and J. Q. Shields, The precision measurement of transformer ratios, IRE Trans. Inst. **1-9**, 2 (1960).
[3] A. M. Thompson, The precise measurement of small capacitances, IRE Trans. Inst. **1-7**, 3 and 4 (1958).
[4] D. L. H. Gibbings, A Circuit for Reducing the Exciting Current of Inductive Devices, The Proceedings of the Institution of Electrical Engineers, London, England, **108**, Part B, 39 (1961).
[5] R. D. Cutkosky, Four-terminal-pair networks as precision admittance and impedance standards, IEEE Trans. Communications and Electronics, pp. 19–22 (Jan. 1964).
[6] R. D. Cutkosky, Active and passive direct reading ratio sets for the comparison of audio frequency admittances, J. Res. NBS **68C** (Engr. and Instr.) (Oct.–Dec. 1964).

IRE Transactions on Instrumentation
Volume I-7, Numbers 3 & 4, December 1958

New Apparatus at the National Bureau of Standards for Absolute Capacitance Measurement

M. C. McGregor, J. F. Hersh, R. D. Cutkosky,
F. K. Harris, and F. R. Kotter

This paper describes a transformer bridge constructed at the National Bureau of Standards for measuring the direct capacitance of 3-terminal capacitors ranging in values up to 1 μF and having a least count of 10^{-6} pF. The transformers and network components were designed specifically for operation at 1 kHz, however, with relatively minor modifications, satisfactory operation should be possible over the audio-frequency range to at least 10 kHz. The construction of a cylindrical cross capacitor as a computable standard is also described.

F. K. Harris
August 28, 1967

JOURNAL OF RESEARCH of the National Bureau of Standards—C. Engineering and Instrumentation
Vol. 68C, No. 4, October–December 1964

Active and Passive Direct-Reading Ratio Sets for the Comparison of Audio-Frequency Admittances

Robert D. Cutkosky

(July 17, 1964)

Design considerations and constructional details for two audio-frequency direct-reading ratio sets are presented. These devices allow the comparison of admittances with accuracies up to one part in 10^7. The first direct-reading ratio set (DRRS) is based upon operational amplifier circuitry, and utilizes a two-stage amplifier system. With this technique, only a moderate voltage amplification per stage is required, and the circuitry is therefore not difficult to stabilize to prevent oscillation. The second DRRS is purely passive and makes use of two-stage voltage transformers to reduce the detrimental effects of transformer excitation current upon the linearity and ratio stability of the device. Equivalent circuits representing the behavior of critical parts of the two direct-reading ratio sets are presented and analyzed. A convenient procedure for calibrating a DRRS is treated mathematically.

IEEE Transactions on Communication and Electronics
Volume CE-70, January 1964

Four-Terminal-Pair Networks as Precision Admittance and Impedance Standards

R. D. Cutkosky

Practical accuracy limitations of four-terminal impedance and three-terminal admittance measurements are discussed. It is shown that there exists a middle impedance range in which neither technique results in good measurement precision. A theoretical analysis of measurement systems using the two techniques simultaneously is made.

NBS Technical Note 57
May 1960

VARIABLE CAPACITOR CALIBRATION WITH AN INDUCTIVE VOLTAGE DIVIDER BRIDGE

Thomas L. Zapf

ABSTRACT

The use of an inductive voltage divider bridge for the calibration of three-terminal and two-terminal variable air capacitors is discussed.

JOURNAL OF RESEARCH of the National Bureau of Standards—B. Mathematics and Mathematical Physics
Vol. 67B, No. 1, January-March 1963

A New Type of Computable Inductor

Chester H. Page

(November 21, 1962)

The mutual inductance analog of the generalized Thompson-Lampard theorem (for cross capacitances) is developed. An infinitely long cage of five parallel wires can yield an absolute inductance of

$$10^{-7} \ln \frac{3+\sqrt{5}}{2}$$

henries per meter. End-effects of order $1/l^2$ occur in a finite cage, but can be reduced to order $1/l^4$ by using eight wires.

The eight-wire cage has the advantage of overdetermined relations among the inductances to be measured, allowing an estimate of experimental error in the calibration of a standard. Errors due to faulty cage geometry are shown to be of the order of 1 in 10^7.

Instruments and AC–DC Transfer Standards

Papers

Abstracts

AC-DC Transfer Instruments for Current and Voltage Measurements*

FRANCIS L. HERMACH†

Introduction

THE basic electrical units are maintained by groups of standard cells and resistors. With these standards and a dc potentiometer, measurements of direct voltage and current are readily made with an accuracy of 0.01 per cent or better. Corresponding measurements of alternating voltage and current at power and audio frequencies depend, at the present time, upon ac-dc transfer instruments which have nearly equal ac and dc response. Such instruments may be calibrated on direct current and then used on alternating current, or alternatively, may be used directly to make ac-dc difference measurements, as in the certification of other instruments.

In addition to the instantaneous values as determined by an oscilloscope or point-by-point methods, there are at least seven other quantities that may be determined for a periodic ac wave in which all values separated by the periodic time, T, are equal. These are: 1) the rms or effective value, I, defined by

$$I^2 = \frac{1}{T}\int_0^T i^2 dt$$

where i is the instantaneous value; 2) and 3) the positive and negative average values, *i.e.*, the average of all the positive or all of the negative values during one cycle, defined by

$$I_{a+} = \frac{1}{2T}\int_0^T (|i| + i)dt \text{ and } I_{a-} = \frac{1}{2T}\int_0^T (|i| - i)dt$$

where $|i|$ is the magnitude of i; 4) the rectified full-wave average, defined by

$$I_{ar} = \frac{1}{T}\int_0^T |i|\, dt;$$

5) and 6) the positive and negative crest or peak values; and 7) the crest-to-crest or peak-to-peak value.

Instruments for measuring each of these values of an ac voltage or current wave are commercially available (with widely varying accuracies). Ordinarily, however, only one of these values is really required in a measurement. Unfortunately, it is difficult to deduce accurately one value from the measurement of another, except for a few waveforms (which, of course, must be known). In most cases the rms value is the one really desired, since the rate of transformation of electrical to other forms of energy (which is governed by the heating produced by a current and by the electromagnetic force produced by currents acting on each other) is a function of the square of this value.

The three general types of ac-dc transfer instruments which are at present suitable for rms measurements of better than 0.1 per cent accuracy are dependent upon these same laws of the interchange of energy. They are: 1) electrodynamic instruments, which depend upon the force between current-carrying conductors; 2) electrostatic instruments, which depend upon the force between charged conductors; and 3) electrothermic instruments, which depend upon some effect produced by the heating of a current-carrying conductor. The first and third respond essentially to current and the second to voltage, but series or shunt resistors make all three types suitable for both measurements, while other circuit arrangements make power measurements almost equally feasible.

Response Equations

The instantaneous torque of an electrodynamic instrument in which two sets of conductors, one fixed and one rotatable about an axis, carry the same current, i, is[1]

$$\tau = i^2 \frac{dM}{d\theta}$$

where M is the mutual inductance and θ some well-defined angle between the two sets of conductors.

In its simplest form such as instrument has an opposing torque, $U\theta$, so that, with direct current applied, the rest position, θ_f, is defined by

$$U\theta_f = B_1 I^2 \quad \text{where} \quad B_1 = \frac{dM}{d\theta}\Big]_{\theta=\theta_f}.$$

The differential equation governing the angular deflection is[1]

$$P\theta'' + A\theta' + U\theta = Bi^2$$

where P and A are the inertial and damping constants, respectively. If the mechanical inertia is sufficiently great that with alternating current applied the periodic fluctuations of θ are negligible compared with the average value, termwise integration over an integral number of cycles gives

* Manuscript received by the PGI, August 14, 1958.
† National Bureau of Standards, Washington, D. C.

[1] F. K. Harris, "Electrical Measurements," John Wiley and Sons, Inc., New York, N. Y., pp. 47 and 413; 1952.

$$U\theta_f = \frac{B_1}{T}\int_0^T i^2 dt = B_1 I^2.$$

Thus if U and B each have the same value on direct as on alternating current, the instrument has the same response, θ_f.

The instantaneous torque of the usual two-element electrostatic instrument with an applied voltage, v, is

$$\tau = \frac{v^2}{2}\frac{dC}{d\theta}$$

where C is the capacitance between the elements. Similar considerations lead again to identical expressions for the rest position with direct or alternating voltage applied, *viz.*,

$$U\theta_f = B_2 V^2 \quad \text{where} \quad B_2 = \frac{1}{2}\frac{dC}{d\theta}\Big]_{\theta=\theta f}.$$

With reasonable restrictions, the temperature rise, θ, of a thin homogeneous conductor carrying a current i in the x direction is governed by the differential equation

$$\frac{\partial^2\theta}{\partial x^2} - \frac{H\theta}{K} + \frac{i^2 R}{K} = \frac{1}{D}\frac{\partial\theta}{dt}$$

where D is the thermal diffusivity and R, K, and H are the electrical resistance, thermal conductance, and rate of surface heat loss per degree rise of a unit length of the material. Again, if the "thermal inertia" is sufficiently great that periodic fluctuations in temperature are negligible, the average temperatures are equal with equal direct and rms alternating currents.

In each instrument the equality holds even if the "constants" such as U, B, R, D, H, and K in the equations are dependent upon the response, θ. This important advantage stems from the property that each instrument combines in a single measuring element a function proportional to the square of the instantaneous current or voltage, a restraining function, and an inertial function or "flywheel effect" to enable it to integrate so that the time-average value of the response is proportional to the square of the rms current or voltage. For this reason high accuracy may be more easily attained with these instruments than with other squaring devices or circuits, which must synthesize exact and equal square-law responses in two quadrants (or in one quadrant with an accurate rectifier) and provide a separate integrator. However, each of these three types of instruments has a lower limit of frequency below which the average value of the response is incorrect if the constants are dependent upon θ.

Transfer Instruments

It is easier in an actual instrument to insure that the constants in the equations are indeed equal on direct and alternating current than it is to measure them separately and compute the response of the instrument. Thus with few exceptions[2] absolute instruments, such as the electrodynamic current balance,[3] are used solely for dc measurements, and most ac instruments of high accuracy are calibrated in terms of dc standards. In the usual instruments, this calibration is preserved on a scale, and the instrument is tested or standardized periodically to guard against changes in the factors which affect the response. However, if the instrument is calibrated at the time of each use, long-time stability, extremely low temperature coefficients, and other normally desirable characteristics become of secondary importance, and the instrument may be designed and constructed to have high resolution and the best possible frequency characteristic. Indeed, in a standardizing laboratory in which the standard is used primarily to test other instruments, a dc calibration may not be necessary because most instruments which are submitted to such laboratories can also be used on direct as well as alternating current. The scale calibration of such instruments may be verified on direct current with a potentiometer (taking the mean of the values required to obtain the same deflection for the two directions of applied current or voltage). The ac-dc difference or frequency influence may then be determined by connecting the instrument under test and the transfer instrument so that they respond to the same quantity (current, voltage, or power) and successively switching both to alternating-, direct-, reversed-direct, and alternating current. In each case the measured quantity is adjusted to obtain the same deflection of the test instrument and the differences in deflection of the standard instrument are observed. From these differences and the scale factor of the standard instrument (per cent change per division) the ac-dc difference of the test instrument may be determined.

This procedure has been used for over 40 years in the certification of instruments at the National Bureau of Standards, because it separates several sources of errors and can be carried out with great accuracy. Since the ac-dc differences of a well-designed instrument are small within its working frequency range and are relatively permanent, they need not ordinarily be redetermined, so that the periodic tests of the instrument need be made only with direct current.

For either a direct ac measurement or an ac-dc difference determination, however, the ac-dc difference of the standard instrument must be known to the full accuracy of the measurement. The determination of this difference has been recognized as a major problem in

[2] H. B. Brooks, F. M. Defandorf, and F. B. Silsbee, "An absolute electrometer for the measurement of high alternating voltages," *J. Res. NBS*, vol. 20, pp. 253–316; 1938.

[3] R. L. Driscoll and R. D. Cutkosky, "Measurement of current with the NBS current balance," *J. Res. NBS*, vol. 60, pp. 297–305; 1958.

most national standardizing laboratories. In general, there are three rather distinct steps in a complete determination. These are: 1) choice of two different types of instruments that are inherently suitable as ac-dc transfer instruments, and a theoretical study of all known effects that can cause ac-dc differences in each type; 2) construction of instruments of each type in such a way that each of these effects by computations and tests can be evaluated over the required ranges; and 3) comparison of the actual transfer performance of the two instruments to guard against unknown sources of error. The tests of step 2) will often take three forms. These are: a) tests of components of the instrument for the effects of known factors (such as magnetic susceptibility, for example; b) intercomparisons of instruments of the same type but of different ranges, in which some of the effects (such as residual reactance) may be expected to be very different; and c) repeated intercomparisons, in which each known source of error in one instrument is accentuated by definite amounts (such as by the deliberate introduction of known reactance). Normally the comparisons of step 3) can be made over only part of the useful ranges of frequency, voltage, etc., and the performance must also be judged by the results of steps 1) and 2). Normally also one of the two instruments will have better-known characteristics, wider or more suitable ranges, or better-behaved ac-dc differences than the other, and thereafter is used as the principal transfer instrument for that laboratory, but both are important.

The accuracy of ac measurements is often limited by the stability of the source rather than the instrument. For the calibration of instruments with a transfer instrument, stabilized sources free from short-time fluctuations are required, but long-time stability and good load regulation are of less importance.[4,5] Repeated sets of readings make it possible to determine the ac-dc difference to a precision considerably better than the fluctuations in the source, and the procedure described tends to eliminate drifts in both the test and standard instruments. If both instruments inherently respond to the same values (rms for example), low-order harmonics up to several per cent ordinarily cause the test to be in error by much less than 0.1 per cent.

Electrodynamic Instruments

The electromagnetic force between two conductors with reasonable geometry and currents is so small that to obtain satisfactory torque the effect is magnified by coiling the conductors. The torque-weight ratios thus obtained are still considerably less than those enjoyed by dc instruments with permanent magnets, but reasonably rugged and portable pointer-and-scale instruments of the 0.1 per cent accuracy class, based on Weston's designs, have been available for a number of decades. For increased resolution and accuracy, recently developed commercial instruments, following Silsbee's composite-coil design,[6] now use a taut-suspension system with the moving coil of a second instrument rigidly fastened to it to provide an electromagnetic restoring torque.[7–9] This torque can be precisely determined by measuring the current through the second instrument with a resistor and dc potentiometer.

As the torque equations indicate, an electrodynamic instrument responds to the square of the current, the scale being marked to indicate current directly. As an unshunted ammeter (limited to about 0.1 ampere because of the springs or ligaments which must carry the current to the moving coil), it will be useful as a transfer instrument over the range of frequencies for which the average torque, $T=f(I)$, is the same as with direct current. The chief factors which affect this in an actual instrument are: 1) capacitances between turns and between coils, which alter the currents; 2) eddy currents in neighboring metals, which alter the field that links with the moving coil; and 3) electrostatic torque, caused by differences in potential between the fixed and moving coils. In general, these set an upper limit of about 1 kc for such instruments. The frequency ranges of ammeters, which use shunts across the moving coils, and voltmeters, which use series resistors to limit the current, are more sharply limited by the inductances of the coils. The manufacturer must insure that the ratio of the impedances of the two parts of the divided circuit of the ammeter is equal to the ratio of resistances, to the full accuracy of the measurement over the frequency range of interest. Similarly he must insure that the magnitude of the impedance of the voltmeter (defined as the ratio of the applied voltage to the current through the coils) is equal to its dc resistance. By connecting resistors in series with the coils of the ammeter and capacitors across portions of the voltmeter, the upper frequency limit for 0.1 per cent error in commercial instruments can be raised from 100 cps to about 1000 cps, and for 0.25 per cent error to about 2500 cps.[10]

Because the mutual inductance between the coils changes with scale position (the operating torque depends upon this) complete compensation cannot be attained at all scale positions. Mutual inductance intro-

[4] A. H. M. Arnold, "Alternating-current instrument testing equipment," *Proc. IEE*, vol. 101, pp. 121–133; 1954.

[5] F. L. Hermach, "Power supplies for 60-cycle tests of instruments and meters," *Proc. ISA*, vol. 11, paper 56-21-3; 1956.

[6] F. B. Silsbee, "Composite coil electrodynamic instruments," *J. Res. NBS*, vol. 8, pp. 217–264; 1932.

[7] G. F. Shotter and H. D. Hawkes, "A precision ac/dc comparator for power and voltage measurements," *Proc. IEE*, vol. 93, pp. 314–324; 1946.

[8] J. Sorge, "A new precision instrument for ac power measurements," *VDE Fachberichte*, vol. 17, pp. 27–30; 1953.

[9] R. F. Estoppey, "Inductronic Electrodynamometer," Conference on Electronic Standards and Measurements, paper 35; August, 1958.

[10] J. H. Miller, "Frequency compensation of ac instruments," *Trans. AIEE*, vol. 70, pp. 217–221; 1951.

duces other errors as well, so that the electrodynamic ac-dc transfer instruments designed and constructed at the U.S. National Bureau of Standards[11] and the National Physical Laboratory of South Africa[12] are normally operated only over a narrow range of deflections about the position of zero mutual inductance, by the use of a continuously adjustable external multiplier for the first instrument and a torsion-head for the second. In the NBS instrument (see Fig. 1), two sets of coils are astatically arranged to eliminate the effect of uniform external fields, and a strip suspension and light-beam pointer with a scale 2 meters from the instrument insure definite readings and permit a scale factor at 0.01 per cent/mm at currents from 0.1 to 20 amperes. The instrument is normally used as a wattmeter or ammeter, and a similar but older companion instrument as a voltmeter (10 to 600 volts).[13] The NPLSA instrument is quite similar, but may be connected as a voltmeter as well (0.05 to 5 amperes and 25 to 500 volts). The ac-dc difference of each of these instruments is believed to be known to better than 0.01 per cent at power frequencies and to perhaps 0.1 per cent up to 3 kc (above 50 volts), verified by careful study and by comparison with electrothermic and electrostatic instruments.

Fig. 1—NBS electrodynamic ac-dc transfer instrument (external multiplier and scale not shown).

Electrostatic Instruments

The electrostatic force between two conductors at reasonable spacings is very low at normal line voltages. The resultant torque can be multiplied, as in the Kelvin electrostatic voltmeter, by interleaving the fixed and moving conductors (plates), but unfortunately only on a one-to-one basis, so that torque-weight ratio remains low. Thus electrostatic instruments, as distinct from electrodynamic instruments where the fixed coil may be designed to have more ampere-turns than the moving coil, seem rather delicate except at voltages above about 1 kv, and are rarely available commercially for precision measurements. However, taut-suspension, light-beam-pointer constructions, using improved optical systems and modern materials, have begun to appear commercially in Europe and may presage a renaissance of this type of instrument.

Electrostatic instruments inherently respond to voltage but may be adapted for current measurements by measuring the voltage across a resistor carrying the current. However, the voltage must be rather high (50 to 100 volts) for adequate accuracy and the shunt must then dissipate considerable power at high currents, or an instrument transformer must be used (either a current transformer with a resistor in its secondary, or a voltage transformer between a resistor and the instrument).

Electrostatic instruments also have a number of sources of ac-dc differences. Among these are: 1) the series impedance of the suspension or springs, 2) surface charges on insulation in the electric field, which can modify the field with direct voltage applied, and 3) imperfectly conducting films on the plates which can cause the field strength between the plates to differ on direct and alternating voltage.[14] None of these limit the frequency range as sharply as does the inductance of electrodynamic instruments, and electrostatic voltmeters may be accurate to perhaps 1 mc. However, when an electrostatic instrument is used as an ammeter the impedance of the 4-terminal resistor must be equal to its dc resistance. (If a transformer is used, it is no longer an ac-dc transfer instrument.) This is difficult to achieve above about 20 kc.

Electrostatic voltmeters with ranges from 50 to 160 volts have been the principal ac instruments for over 40 years at the National Physical Laboratory in England[14] and somewhat modified instruments of the same basic design are similarly used at the National Standards Laboratory in Australia. The ac-dc differences of the NPLE instruments are known to 0.01 per cent at power frequencies and to better than 0.05 per cent up to 100 kc (verified by calculations of the known sources of error and by comparison with electrodynamic and electrothermic instruments and with other electrostatic

[11] J. H. Park and A. B. Lewis, "Standard electrodynamic wattmeter and ac-dc transfer instrument," *J. Res. NBS*, vol. 25, pp. 545–579; 1940.

[12] J. W. Whittaker, "A precision electrodynamometer standard and ac/dc transfer instrument," *Proc. IEE*, vol. 101, pp. 11–20; 1954.

[13] F. K. Harris, "A suppressed zero electrodynamic voltmeter," *J. Res. NBS*, vol. 3, pp. 445–457; 1929.

[14] R. S. J. Spilsbury and A. Felton, "The electrostatic voltmeter as a dc/ac transfer instrument," *J. IEE*, vol. 89, pp. 129–137; 1942.

instruments having noble-metal conductors). Special transformers and resistors have been constructed and tested to permit the measurement of current and of voltage below 20 volts, and resistance voltage dividers have been evaluated for voltage measurements to 1000 volts (at audio frequencies).[4]

Electrothermic Instruments

Easily measurable effects are produced by the heating of short straight metallic conductors or very small beads of semiconductors, having very low electrical time-constants. These effects can thus be independent of frequency up to 100 mc or more. In addition, the effects can be measured electrically, rather than mechanically, with high precision and freedom from mechanical resonances. These are the chief advantages of electrothermic instruments.

Because their output is electrical, and because of their low reactance, thermocouple instruments and bolometer bridges are the only two forms now generally used. In commercial thermocouple instruments the temperature rise of a conductor (heater) is measured with a thermocouple and millivoltmeter. The combination of the heater and thermocouple is called a thermal converter. Many commercial bolometer bridges now contain bead thermistors (temperature-sensitive resistors) and are unbalanced by the temperature rise caused by the heating of the applied current. The unbalance voltage is measured or balance is restored by additional currents of a different frequency, which are measured. Thermocouple instruments of the $\frac{1}{2}$ to 2 per cent class have long been commercially available for current and voltage measurements, while most commercial bolometers are used for power measurements (absorbing all of the measured power). In either case undesired thermal effects, such as high ambient temperature coefficients, accelerated aging of the heater at the elevated temperature, and transfer of heat to other parts of the measuring element have limited the sustained accuracy obtainable. However, by using such instruments solely as ac-dc transfer instruments, calibrating them before and after each reading, these effects can largely be eliminated. Studies at the National Bureau of Standards[15] have shown that properly designed thermal converters may be used as ac-dc transfer instruments at currents from 1 ma to 50 amperes with an accuracy approaching 0.01 per cent at power and audio frequencies and very probably up to 200 kc. Their low reactance also makes possible transfer voltmeters from 0.2 to 600 volts (at 133 ohms per volt) with wire-wound series resistors that have ac-dc differences less than 0.03 per cent at audio frequencies. Voltmeter elements with film resistors in coaxial lines terminated by thermal converters have been constructed and intercompared to 0.05 per cent to 10 mc.[16] The calculated ac-dc differences of the converters and of the voltmeter elements were verified by intercomparisons of different ranges and by comparisons (over limited ranges) with electrodynamic and electrostatic instruments. A Lindeck deflection potentiometer is used at NBS with these converters and voltmeter elements to provide high resolution (0.005 per cent/mm at rated output emf) and rapid reading.

Similarly it has been shown that a properly selected and mounted pair of indirectly heated thermistors may be used in a bridge as an ac-dc transfer instrument for an audio-frequency potentiometer to better than 0.02 per cent at frequencies from 0.2 to 20,000 cps.[17] Thermistors are also used for ac measurements at the Physikalisch-Technische Bundesanstalt in Germany.[18] Their rather long thermal time constants (about 10 seconds) provide good low-frequency response but make highly stable sources necessary.

The small ac-dc differences of thermal converters and thermistor bridges at audio frequencies are caused almost solely by: 1) thermoelectric effects in the heater, which affect the temperature rise on direct current, but because of thermal inertia do not affect it on alternating current; 2) integration errors at low frequencies, which are inversely proportional to the square of the frequency; and 3) small reactance effects in the voltmeter elements, such as capacitance currents between parts of the multiplier, and from the multiplier to its surrounding shield. Fortunately, it is possible to obtain thermal converters with heaters of manganin or other alloys of low thermoelectric effects and of sufficient length to make the ac-dc differences 0.01 per cent or less from 20 cps to 200 kc.

A single 10-ma thermal converter is used with multirange shunts and series resistors for ac measurements in the U.S.S.R., both in a central standardizing laboratory and in convenient consoles at branch laboratories.[19] Series and shunt resistors are also used in the laboratories of the Germany Authority for Weights and Measures, but with two converters in a differential circuit.[20] As a further modification of the transfer principle, the heater of the thermal converter alone (without the shunt or series resistors) can be switched to direct current for the dc calibration.[21] Only a small dc source is

[15] F. L. Hermach, "Thermal converters as ac-dc transfer standards for current and voltage measurements at audio frequencies," *J. Res. NBS*, vol. 48, pp. 121–138; February, 1952.

[16] F. L. Hermach, "Electrothermic instruments for the measurement of alternating current and voltage," *Proc. NPL Symposium on Precision Electrical Measurements*, HMS Stationary Office, London, Eng., paper No. 15; 1955.

[17] F. C. Widdis, "The indirectly heated thermistor as a precise ac-dc transfer device," *Proc. IEE*, vol. 103, pt. B, pp. 693–703; 1956.

[18] H. J. Schrader, "A-C potentiometer measurements with indirectly heated NTC resistors," *Electrotech. Z.*, vol. 73-A, pp. 547–549; 1952.

[19] K. P. Shirokov, "An installation for calibrating ammeters and voltmeters at high frequencies," *Proc. Russ. Inst. Meteorology*, vol. 24, p. 24, 1954.

[20] W. Rump, "On the exact absolute measurement of ac voltages and a potentiometer for testing ac instruments," *Elektrotechnik*, vol 5, pp. 64–67; 1951.

[21] F. L. Hermach and E. S. Williams, "Multirange audio-frequency thermocouple instruments of high accuracy," *J. Res. NBS* vol. 52, pp. 227–234; 1954.

315-411 O - 68 - 19

required, making possible a convenient portable accessory to a dc potentiometer, which, in a recently improved model (see Fig. 2) provides ranges of 7.5 ma to 20 amperes and 0.5 to 600 volts with an accuracy of 0.05 per cent at frequencies from 5 to 50,000 cps.

Other Instruments

A transfer instrument is an essential part of any accurate ac potentiometer. Such potentiometers have been used to some extent in Europe but rarely in the United States, except for special measurements. They require phase as well as magnitude balance, and with the usual tuned detector, measure only the fundamental component rather than the rms value. An electrodynamic milliammeter is most commonly used with a standard cell to standardize the current through the resistance network, but a thermal converter or thermistor bridge could serve equally well and over a wider range of frequencies.[15,17] Recent studies[22] have shown that some converters have excellent long-time stability if they are maintained at a constant ambient temperature.

A method of determining the equality of a dc voltage and the crest-to-crest value of an ac voltage to better than 0.005 per cent has been developed at the National Standards Laboratory of Australia[23] as well as a method of generating an ac voltage wave with no harmonic greater than 0.001 per cent of the fundamental. The equipment has been used to verify the ac-dc performance of the NSL electrostatic voltmeter to better than 0.01 per cent at 50 cps and may be considered to be a crest-value ac-dc transfer instrument.

Fig. 2—Volt-ampere converter for ac current and voltage measurements.

High-gain amplifiers with a rectifier in a feedback loop, and driven rectifiers based on the ring modulator, may be used with a potentiometer to measure the average value of an ac voltage wave to 0.1 per cent or better, provided the galvanometer or other detector properly integrates the rectified output. Their accuracy must also be verified by the procedure outlined for ac-dc transfer instruments. At present this is most easily done by comparison with rms instruments in circuits with voltages of known waveforms.

[22] J. J. Hill, "A precision thermo-electric wattmeter for power and audio frequencies," *Proc. IEE*, vol. 105, pt. B, pp. 61–68; January, 1958.

[23] W. E. Smith and W. K. Clothier, "Determination of the dc/ac transfer error of an electrostatic voltmeter," *Proc. IEE*, vol. 101, pp. 465–469; 1954.

Reprinted from IRE TRANSACTIONS
ON INSTRUMENTATION
Volume I-7, Numbers 3 & 4, December, 1958

Thermal Converters for Audio-Frequency Voltage Measurements of High Accuracy

F. L. HERMACH, FELLOW, IEEE, AND E. S. WILLIAMS

Abstract—**The ac-dc differences of a reference group of thermoelements have been evaluated at audio frequencies to a few parts per million (ppm) at currents from 5 to 20 mA. A technique for comparing the ac-dc differences of two thermoelements with an uncertainty of about 2 ppm has been developed. Two 5 mA thermoelements are used with a plug-in set of resistors of computable reactances to form thermal voltage converters for voltage measurements. With this same technique adjacent ranges of these converters can be compared to step up from 0.5 to 500 V to better than 10 ppm.**

I. Introduction

IN PRINCIPLE, the current balances which have been developed to determine the ampere in absolute measure with direct current could also be used with alternating current. However, the most stable electrical standards are still the dc standard cell, and 1 ohm resistors, which are not usually designed for ac use. Thus, ac measurements of current and voltage have, in practice, been based on rms ac-dc transfer standards or comparators. For many decades these were electrodynamic or electrostatic instruments, designed to have the same torque constant with either alternating or direct current (or voltage) applied, making it easier to obtain a wider frequency range than with instruments like the current balance which must have a computable torque constant. More recently, electrothermic instruments such as thermocouple transfer standards and bolometer or thermistor bridges have been used. All of these instruments have been highly developed in the national laboratories of several countries to make ac measurements at audio frequencies to about 100 ppm in combination with dc standards. The combination possesses a number of advantages over ac potentiometers (which must also include a transfer instrument), and over electronic and other squaring circuits (which must have exact square-law characteristics in two quadrants).

Recent advances in operational amplifiers and inductive voltage dividers have made possible wide-range ac power sources with linearity and day-to-day stability better than 100 ppm. This implies a need for better accuracy in basic ac-dc transfer standards.

At this accuracy, conventional forms of electrodynamic transfer instruments are limited to power frequencies by the effects of inductive and capacitive reactances in their coils, and electrostatic instruments have a serious minimum-voltage limitation because of their low torque-weight ratio. Both would require new means of sensing deflections to obtain precisions of 10 ppm or better. This could be done by measuring the reactance, which is a function of the deflection of the instrument. However, a major difficulty would remain —that of vibrations from external forces or from the cyclic variations of the ac driving torque. Experience has shown that it is often difficult to control spurious torques caused by minor mechanical resonances. It is possible that floating the moving system in a liquid of the same density would minimize these difficulties. However, it has seemed to the authors that improved thermal converters (thermocouple instruments) offer better promise of obtaining an ac-dc transfer accuracy of 10 ppm or better, and considerable effort has been concentrated on them over the past five years. This paper may be considered as a progress report describing the present group of reference thermoelements and coaxial thermal voltage converters, and the techniques and equipment which have been developed to compare them to a few ppm.

II. Thermal Converters

A thermoelement (TE), defined as the simplest type of thermal converter [1], consists of a heater and thermocouple. In its usual form, the heater is a short, straight wire suspended between two supporting lead-in wires in an evacuated glass bulb. The hot junction of a thermocouple is fastened to the midpoint of the heater, and is electrically insulated from it with a small bead. The thermocouple EMF (about 5 to 10 mV for a conventional TE at rated current)[1] is then a measure of the heater current. For voltage measurements, a resistor is connected in series with the heater to form a thermal voltage converter [1].

At the National Bureau of Standards, fourteen TEs form the present reference group for ac-dc difference. Twelve of them (made by four different manufacturers) are of conventional design but with heaters of Evanohm or Karma (modified nickel-chromium alloys), which have low thermoelectric effects.[2] They were chosen from

Manuscript received June 23, 1966. This paper was presented at the 1966 Conference on Precision Electromagnetic Measurements, Boulder, Colo. This work was supported in part by the Army Metrology and Calibration Center, Frankford Arsenal, and the Metrology Engineering Center, Bureau of Naval Weapons, Pomona, Calif.

The authors are with the Electrical Instruments Section, Electricity Division, National Bureau of Standards, Gaithersburg, Md.

[1] The international system (SI) of units with its symbols is used in this paper. Because of their frequent occurrence, the word thermoelement is abbreviated as TE and thermal voltage converter as TVC in this paper.

[2] Evanohm and Karma are registered trademarks of the Wilbur B. Driver Company and the Driver-Harris Company, respectively. (See Acknowledgments.)

larger groups on the basis of low dc reversal differences and high bead resistances, and are all mounted in one aluminum enclosure lined with foamed plastic for thermal insulation. Each is supported by its heater leads, which are soldered directly to binding posts mounted on the low-loss phenolic top plate of the enclosure, and its thermocouple output leads, which are soldered to two-pin connectors. The other two thermal current converters are of a radically different design having many thermocouples (40 or more) attached to a bifilar (doubled-back) heater [2]. They were obtained from their inventor, F. J. Wilkins of the National Physical Laboratory in England.

The fourteen TEs are identified in Table I, along with certain pertinent characteristics, as well as the ac-dc differences assigned to them at audio frequencies as a result of the tests to be described.

TABLE I

Reference Thermoelements

Identification	Rated		Dc reversal† ppm	Approx. heater length mm	Bead resistance‡ GΩ	Ad-dc difference (ppm)	
	Current mA	EMF mV				20 Hz	2 kHz‖
NPL 14*	20	25	<10	—	>1	0	0
NPL 15*	20	25	<10	—	>1	0	0
A20E3	20	5	40	5	>1	0	0
A20E6	20	5	60	5	>1	0	−1
A10E18	10	8	130	5	0.3	+6	+1
A10E19	10	8	160	5	0.5	0	−1
W10E1	10	7	200	8	0.6	+1	+3
W10E2	10	7	<10	8	0.8	−2	0
B10E45	10	8	160	4	>1	−8	−2
A5E8	5	7	10	5	0.7	+1	+1
A5E9	5	6	40	5	0.6	0	−1
F5K9	5	4	20	5	0.5	−3	−2
F5K13	5	4	260	5	0.5	−2	0
B5E77	5	8	110	6	>1	+6	0

* These can be used at much higher currents.
† $\Delta I/I$ for the same EMF.
‡ At 2 kHz and rated I.
‖ Same value assigned at 20 kHz.

III. Thermal Voltage Converters (TVCs)

Each of a new set of TVCs developed at NBS for this work consists of one or more cylindrical metal-film resistors in a coaxial metal cylinder. The resistors can be connected in series with one of two 5 mA TEs mounted in separate cylinders so that the output EMF is then a measure of the input voltage. Like an earlier set developed at NBS [3], the effect of the reactance on the frequency response can be computed at least roughly from the simple geometry. Adjacent ranges of these TVCs may be compared with greater certainty than those of the older design, which had integrally mounted TEs.

As shown in Fig. 1, a single two-watt resistor is used for each range below 200 V. The higher-voltage resistor units have two or more resistors in larger cylinders, with two adjustable inner shields to control capacitance currents, as shown in Fig. 1, and have ports and baffles to permit the controlled flow of cooling air from the laboratory compressed-air supply.

Pertinent data on the TVCs, and the ac-dc differences assigned to each range are given in Table II. The TVCs are shown in Fig. 2.

IV. EMF Comparator

The ac-dc differences of a transfer instrument may be defined as

$$\delta = (X_a - X_d)/X_d$$

where X_a and X_d are the magnitudes of the ac and dc quantities that are required to give the same response (such as deflection or output EMF) of the instrument. (Normally, the average for the two directions of the dc quantity gives the best measure of the dc reference.) This is a useful definition, for the ac quantity for a given response is then simply $X_a = X_d(1+\delta)$. As is well known, the instrument may be used as an ac-dc transfer standard simply by observing the response with the ac quantity applied, then measuring (with external standards) the average for the two dc quantities required to obtain the same response, thus avoiding many of the limitations of an ordinary instrument.

At the National Bureau of Standards, TEs are evaluated in pairs with the EMF comparator shown in Fig. 3, to determine the differences in their ac-dc transfer performance, i.e., $\delta_1 - \delta_2$ as defined previously. TVCs are connected in parallel and evaluated in the same way. With the desired current or voltage applied, R_1 and R_2 are adjusted in a preliminary balance to obtain a near null on the detector D_1. Then, in regular succession, alternating-, direct-, reversed direct-, and alternating-currents are applied to the TEs at nearly equal time intervals and without changing R_1 or R_2. In each case, the current is adjusted to obtain the same output EMF, E_1 of TE_1, as indicated by an auxiliary Lindeck potentiometer (P with its detector D_2), and the resulting deflections of D_1 are observed. Then, as shown in Appendix I, the relative ac-dc difference is

$$\delta_1 - \delta_2 = s(D_a - D_d)$$

where D_a and D_d are the averages of D_1 with alternating and direct currents applied, respectively. The sensitivity factor s can be determined in one of several ways, as indicated in the Appendix, such as by changing the current in the heater of TE_2 by a small known amount and observing the resulting deflection of D_1.

The sequence of readings, nearly equally spaced in time, greatly reduces errors from drifts, temperature changes, etc., in either TE and from either constant or slowly changing thermal EMFs in the comparator. The comparator accommodates any reasonable range of thermocouple EMFs, which need not be equal, and the small currents (up to 20 μA) in the thermocouple circuit do not affect the measured values.

With this circuit, small fluctuations in the supply (heater) current do not appreciably change the deflection if the two TEs have reasonably equal proportional changes in EMF ($\Delta E/E$), with a given change in heater current and reasonably equal time constants. Although

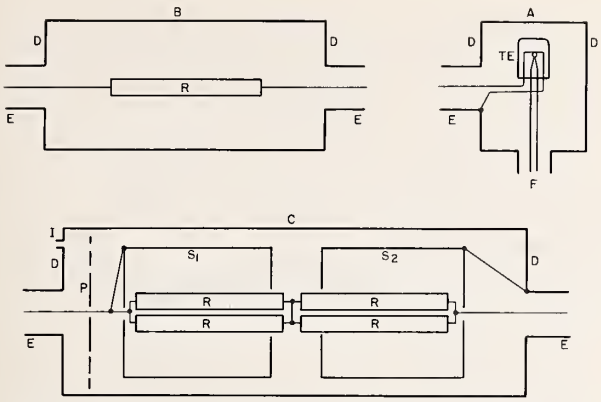

Fig. 1. Essentials of thermal voltage converters (construction details not shown).

A Thermoelement unit, with 5 mA 100 Ω TE, for 0.5 V, in brass cylinder, 4 cm long and 5.1 cm diameter, with brass end plate D.
B Low-voltage resistor unit (1 to 100 V) with one 2-watt metal film resistor R in brass cylinder 11 cm long and 5.1 cm diameter.
C High-voltage resistor unit (200–500 V) with multiple 2-watt metal-film resistors, in brass cylinder 18 cm long and 6.4 cm diameter with brass end plate D. Air inlet at I, outlet holes at other end (not shown).
S_1, S_2 Inner brass shields 5.5 cm long, 5.1 cm diameter, connected as shown, with no end plates. S_2 can be moved parallel to axis and locked in place.
P Non-conducting air-baffle plate with holes.
E Coaxial connector GR874.
F Two-pin output connector AN10SL.

it would be difficult to calculate the resultant "stabilization factor" of the circuit, in practice, fluctuations are much less than those observed when the output EMF of each TE is balanced against a constant voltage source, as in earlier comparators [4]. Thus, with this circuit and technique, TEs may be intercompared with an imprecision which is much less than the fluctuations of the supplies used.

R_1 consists of ten 100 Ω resistors mounted on an enclosed-contact silver-alloy switch whose thermal EMFs are much less than 0.1 μV when the wiper is stationary. R_2 is a 100 Ω, 10-turn helical resistor of manganin, with a manganin wiper to minimize thermal EMFs. Detector D_1 consists of a commercially available primary galvanometer, incorporating photocells in an adjustable negative-feedback circuit, which serves as a current amplifier to a secondary galvanometer. The scale factor of the combination is about 10 pA/mm, and the input resistance (which is dependent on the negative feedback) ranges from 200 to 3000 Ω. The primary galvanometer is liquid filled to reduce disturbances from mechanical shocks and vibrations and, with its period of two seconds, is an excellent mechanical low-pass filter. A similar pair of galvanometers is used for D_2. Both secondary light beams appear on one scale so that the observer may quickly read the deflection of D_1 if it is stationary and if D_2 is in the desired range. (Residual

TABLE II

NBS "Model F" Thermal Voltage Converters

Range V	Resistors No.	Resistors kΩ (each)	Total kΩ†	δ_r (ppm)‡ 2 kHz	20 kHz	50 kHz
0.5-A*	none		0.1	+1	+1	+15
0.5-B*	none		0.1	−4	−2	+11
1	1	0.1	0.2	−2	0	+11
2	1	0.3	0.4	−3	−2	+ 3
3	1	0.5	0.6	−1	0	+ 3
5	1	0.9	1.0	−1	0	− 1
10	1	1.9	2.0	0	+1	− 1
20	1	3.9	4.0	0	+1	− 1
30	1	6	6.1	+1	+1	− 2
50	1	10	10	+1	0	− 4
100	1	20	20	+1	0	− 7
200	4	40	40	+1	0	− 7
300	6	90	60	+1	0	− 3
500	8	200	100	+1	−6	+13

* TEs A and B as TVCs, without series resistors.
† Including 0.5 V TE. Resistors connected in series-parallel for higher ranges.
‡ δ_r is the impedance error only (see text) computed from Table III with either TE of pair #1. A similar table with the #2 pair differs from it by not more than 1 ppm at 2 and 20 kHz except at 0.5 V range.

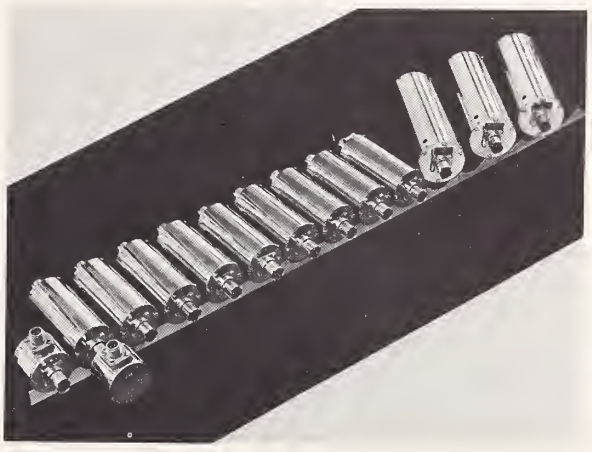

Fig. 2. Thermal voltage converters.

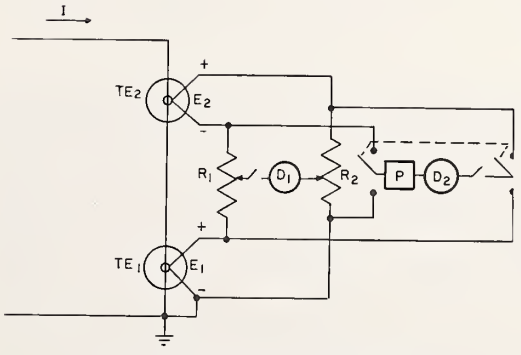

Fig. 3. Essentials of EMF comparator.

deflections of D_2 are less critical if the TEs are well matched.)

All of the components of the comparator except the detectors are mounted in a metal box behind a metal panel to provide electrostatic shielding, and the box is lined with foamed plastic to reduce temperature fluctuations. The metal cases of the primary galvanometers are connected to this box by the shields of two-conductor cables.

With R_1 and R_2 at their midpoints and each of the thermocouple inputs to the EMF comparator short-circuited, peak-to-peak fluctuations in the secondary galvanometer of D_1 in periods of 10 seconds amount to 1 mm at the gain setting normally used. With 7 mV at each thermocouple input, this corresponds to a value of $\delta_1 - \delta_2$ of 2 ppm. This is only about four times the calculated Johnson-noise value for this circuit.

A comparison of two TEs (or TVCs) usually consists of four or more determinations of $\delta_1 - \delta_2$ by the method described. Three times the standard error (standard deviation of the average) computed from a number of typical series of such measurements is about 2 ppm. This is a reasonable measure of the uncertainty in the comparator. Comparisons of various pairs taken from three TEs, with the TEs interchanged in the comparator and with the EMF of first one TE and then the other held constant in each sequence, have disclosed no systematic error as large as 1 ppm.[3] These measurements were made with commercially available dc and ac voltage sources, having peak-to-peak instabilities, observed with a TVC in 10-second intervals, of about 10 and 20 ppm, respectively, at 2 kHz.

A TVC can be used for ac measurements with appropriate dc standards by balancing its output EMF against an adjustable stable voltage source such as the potentiometer P. To reduce errors from drifts, a similar sequence of ac and dc readings can be used, with the setting of P fixed, and the direct voltage V_d preset and accurately known. Then

$$V_a = V_d[1 + \delta + s(D_a - D_d)]$$

where s, the sensitivity factor, is determined as before.

V. Comparisons of TEs

The fourteen reference TEs were compared, using sinusoidal currents at frequencies of 20 Hz, and 2 and 20 kHz. All of these measurements (as well as the comparisons of TVCs) were made in a shielded room to reduce electromagnetic interference, which is particularly troublesome with TEs because of their high sensitivity and very wide frequency range. The step down from one current to the next was made by connecting the heaters of two low-current TEs, a and b, in parallel and their thermocouples in series aiding, and considering the combination as a single TE connected in the TE_1 position of Fig. 3.[4] As shown in Appendix II, if the TEs are reasonably well matched, the ac-dc difference of the parallel combination is simply $\delta_p = (\delta_a + \delta_b)/2$ to better than 1 ppm. From the test, $\delta_p - \delta_2 = K_1$ where δ_2 is the ac-dc difference of the high range TE in position 2, and $K_1 = s(D_a - D_d)$. The two low-current TEs are then connected in series and compared to determine $K_2 = \delta_a - \delta_b$. Thus, $\delta_a = K_1 + \delta_2 + K_2/2$ and $\delta_b = K_1 + \delta_2 - K_2/2$.

The network of comparisons at 2 kHz and the results are shown in Fig. 4. Here the circles identify individual TEs and the rectangles represent a pair in parallel. The arrows indicate comparisons, and the numbers on them are the values of the relative ac-dc differences in ppm; i.e., the ac-dc difference of the TE at the point of the arrow is greater or less than that at the tail by the amount shown. These tests have extended over a period of three years during the development of this project; in many cases, each number is the average of two or more tests, each consisting of four or more sequences of ac-dc readings already described.[5]

As indicated by Wilkins, the ac-dc difference of the two NPL TEs should, theoretically, be less than 1 ppm. In tests at NBS at 20 mA, the two agreed to better than 0.2 ppm with a 3σ imprecision of 0.3 ppm.[6] Thus, it is reasonable as well as convenient to start with an assignment of zero ppm to the ac-dc differences of each. Then, following principles given by Youden [5] in weighting the various paths in a network, it is possible to calculate the ac-dc differences of the other TEs. The resulting values are given to the nearest ppm in each circle and in Table I.

The average for all of the conventional TEs is only -0.3 ppm. Thus, these simple TEs agree with the more complicated multijunction converters very closely, and essentially the same values would have been obtained for each TE on the alternative basis of assigning zero to the average of the entire group.

A complete but less redundant chain of measurements was carried out at 20 Hz to evaluate low-frequency errors of each TE. The precision was less at that frequency because of much larger instability in the ac source. The results of the values assigned on the basis of zero error for the NPL TEs are given in Table I.

Not enough TEs were intercompared at 20 kHz to assign independent values to each, because ac-dc dif-

[3] If the net dc reversal difference of the two TEs is more than 300 ppm, an error is introduced by nonlinearities in D_1. This can be minimized by taking determinations with first one and then the other TE EMF held constant.

[4] To minimize certain aberrations discussed in Section IX, resistors of at least five times the heater resistance were added to each of the heaters before paralleling them.

[5] Because measurements were made over an extended time in a developing program, the network is not symmetrical.

[6] The EMF was higher and a higher detector sensitivity could be used than with other TEs since the two TEs were well matched, so that an extraordinarily high precision was attained.

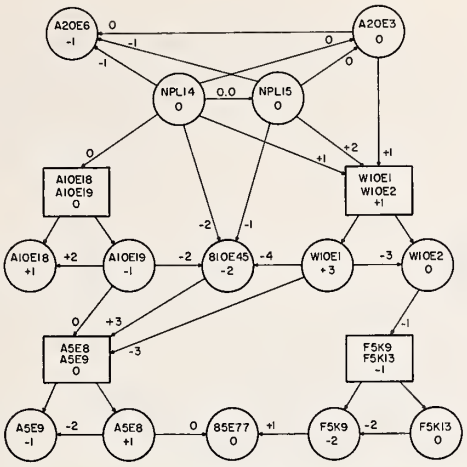

Fig. 4. Intercomparisons of NBS TEs, and assigned ac-dc differences in ppm at 2 kHz.

ferences from all known sources [3] should be the same as at 2 kHz within 1 ppm. No measured values at the two frequencies differed by more than 2 ppm. Thus, the same values were assigned to each TE at the higher frequency.

VI. Comparisons of TVCs

The TVCs were designed so that adjacent ranges could be compared to step up and down the voltage scale. Their nearly identical 5 mA TEs were each first compared with one of the reference group of TEs as current converters, i.e., with the heaters connected in series. They were then paralleled through a "T" connector and compared with each other as voltage converters (basic range 0.5 V). The lowest resistor (see Table 2) was then connected in series with one TE, say TE_a, to make a one-volt TVC. This was connected in parallel with the other, TE_b, and compared at 0.5 volt. A two-volt TVC was then formed with the next resistor and TE_b, and compared with the one-volt TVC at 1 V. This process was continued until the highest range was reached. If the ac-dc difference of each combination is independent of the voltage level, the ac-dc difference of any range may be found in terms of one as a reference. This requirement is easily met if the TEs have no significant errors, for the reactance errors of each resistor unit should be independent of voltage. The validity of this assumption itself can easily be verified by making each comparison at two voltage levels.

If we define $Z_t = V_i/I_o$ for a TVC, where V_i is the magnitude of the applied voltage and I_o is the magnitude of the current through the TE, then, from the definition for ac-dc difference, applied to a TVC,

$$\delta_v = \frac{V_{ia} - V_{id}}{V_{id}} = \frac{I_{oa}Z_t - I_{od}R_t}{I_{od}R_t}$$

where the subscripts a and d refer to alternating and direct current (or voltage). Since I_{oa} and I_{od} produce equal output EMFs, $I_{oa} = I_{od}(1+\delta_c)$. If we let $Z_t = R_t(1+\delta_r)$, we get, if second-order terms are negligible, $\delta_v = \delta_r + \delta_c$. Thus, δ_v can be determined if δ_r can be deduced from the comparisons of adjacent ranges, since δ_c can be evaluated in terms of the reference group of TEs.

Two complete sets of adjacent-range comparisons from 0.5 to 500 V were carried out at frequencies of 2, 20, and 50 kHz, with two different pairs of 5 mA TEs. These TEs had 80Ni20Cr heaters but were otherwise similar to those in the reference group. Measured values of δ as current converters were -1 or -2 ppm, except at 20 Hz where they ranged from -6 to -9 ppm.[7] The results of the adjacent-range tests given in Table III showed excellent precision. In addition, the inter-range differences were less than 2 ppm through 20 kHz, except for the lowest and highest ranges. The differences of a few ppm observed on the lowest ranges were rather puzzling and will be discussed in Section IX. They were essentially independent of frequency through 20 kHz but were negligible above the 1 volt range.

TABLE III

Comparisons of Thermal Voltage Converters

TVC 1	TVC 2	Voltage V	$\delta_1 - \delta_2$ in ppm					
			2 kHz		20 kHz		50 kHz	
			#1*	#2†	#1	#2	#1	#2
A	B	0.5				+2		
B	A	0.5	−3	−3	−4	−3	−4	−4
1-B	A	0.5	+2		0		−2	
1-A	B	0.5	+2		+2	+1	0	+3
2-B	1-A	1	−1		−2	−1	−8	−4
3-A	2-B	2	+2		+2	+1	0	−1
5-B	3-A	3	0		0	0	−4	0
10-A	5-B	5	+1	+1	+1	0	0	−2
20-B	10-A	10	0		0	+1	0	−1
30-A	20-B	20	+1		0	0	−1	0
50-B	30-A	30	0		−1	0	−2	0
100-A	50-B	50	0		0	0	−3	−2
200-B	100-A	100	0	+1	0	−1	0	+4
300-A	200-B	200	0		0	0	+4	+6
500-B	300-A	300	0		−6	−5	+16	+8

* Test #1—With one pair of 5 mA, 100 ohm TEs.
† Test #2—With another pair of 5 mA, 100 ohm TEs. These tests were made three months after those with pair #1.

Except for this, the results of the comparisons are in excellent agreement with computed values (see Section VIII), which show that δ_r should be less than 1 ppm through the 100 V range. It is extremely unlikely that any single source or combination of sources of ac-dc difference should produce the same δ_r in each of these ranges. Thus, the authors believe that, from the concordance of theory and experiment, it is safe to assign zero ppm to the average of the values of δ_r from the 2 V

[7] These TEs, which were the only ones available at the time with the correct heater resistance, will be replaced by others.

through the 100 V ranges in establishing the values given in Table II from the comparisons of Table III.

The comparisons at 50 kHz (which were less precise) were made to verify that ac-dc differences were not sharply dependent on frequency at 20 kHz. They indicate that excellent accuracy should be expected for most ranges at even higher frequencies.

A complete set of measurements at 75 percent of rated voltage was also made at 2 kHz with TE pair #1 in order to investigate voltage coefficients. These results agreed with the rated-voltage measurements to 1 ppm, with no systematic difference.

A completely independent verification of the accuracy of these reference TVCs has come from some careful comparisons by Flach and Marzetta [8] of a "time-gate" peak ac-to-dc voltage comparator (designed by Marzetta) with an rms comparator which incorporated a TVC that had been calibrated with the reference set. In a long series of tests at 400 and 1000 Hz, where the error in the comparison introduced by distortion of the ac source was less than 10 ppm, the two comparators agreed on the average to 4 and 8 ppm, respectively, at the two frequencies.

VII. Thermoelectric Errors

Hermach's treatment of the ac-dc errors arising from Thomson effects in the heater of a conventional TE [4] has been extended by Widdis [6] to include the effects of Peltier heating, and to correct for the heat abstracted by the thermocouple. Widdis' expression for the Thomson ac-dc difference, $\delta_t = \alpha^2\theta/12\rho k$, is the same as that found by Hermach for high-range TEs, where α, ρ, and k are, respectively, the Thomson coefficient, electrical resistivity, and thermal conductivity of the heater alloy, and θ is the midpoint temperature rise (100°C to 150°C in a conventional TE). The error can thus be computed reasonably well if α can be determined. The Thomson heating of copper is reasonably well known [7], and is not much affected by moderate temperature elevations or by the cold working of ordinary handling. Thus, this metal can serve as a practical reference. The authors have calculated the Seebeck and the absolute Thomson coefficients of a number of pertinent alloys from careful measurements of the EMF vs. temperature of thermocouples formed from each of these alloys and copper. The results are shown in Table IV, along with the calculated ac-dc difference δ_t (using Widdis' formula) in a TE having midpoint heater temperature rise of 150°C (giving a 10 mV output with a typical NiCr-constantan thermocouple). With Evanohm or Karma, δ_t should not exceed 1 ppm. At an output of 5 mV it should be less than 1 ppm, since both θ and α are smaller.

Additional measurements indicated that the thermoelectric coefficients may be sensitive to cold working and may be changed by exposure to high temperature. For Evanohm and Karma significant changes were observed at 800°C, but not at 400°C. Thus, care must be taken in controlling the temperature of the wire near welded joints and when out-gassing during the construction of TEs. Here the use of TEs in the reference group by four different manufacturers having differing techniques provided powerful assurance against unknown errors.

TABLE IV

Thermoelectric Data and Errors

Metal or Alloy	α, μV/°C* at 400°K	S μV/°C	Calculated Error in a TE‖	
			Dc reversal** $\Delta I/I$, ppm	Ac-dc difference δ_t, ppm
Copper	−2.0	—	—	—
Evanohm	−1.5	+0.3†	200	−1
Karma	−1.0	+1.8	150	<1
Manganin	−3.0‡	−1.8‡	400	−4
80Ni20Cr	−3.9	+4.4	500	−7
60Ni16Cr24Fe	−2.3	+0.8	300	−2

* α (Thomson coefficient) is proportional to the absolute temperature.
† S is Seebeck coefficient vs. copper.
‡ This was quite dependent on heat treatment.
‖ From Thomson heating, with $\theta = 150$°C and $\rho k = 25 \times 10^{-6}$ V²/°C at 500°K, the weighted average temperature of the heater.
** With the bead off center (see text).

As indicated by Wilkins, the thermoelectric errors are greatly reduced in the NPL TEs because of the bifilar heater and the low temperature rise (about 10°C at 20 mA in the present TEs). The resulting error should be much less than 1 ppm, even with nickel-chromium heaters.

Rather unfortunately, commercial TEs have lead-in wires (see Fig. 1), through the glass bulb to the heater, of a copper-coated nickel alloy to match the thermal expansion coefficient of the glass. The combination has a rather uncertain but fairly large Seebeck coefficient vs. the heater alloys used. With direct current applied, Peltier heating and cooling of the junctions of these lead-in wires and the heater can cause a temperature difference (+ at one junction and − at the other). Most of this heat is conducted by the lead-in to the thick glass press or disk which forms the base of the glass bulb. This can be considered as a "heat sink" so that the first-order junction temperature change is $\Delta\theta = TIS/K$, where T is the absolute temperature, I is the current, S is the Seebeck coefficient, and K is the thermal conductance of the lead-in. Widdis showed that this leads to an ac-dc difference term $\delta_{tp} = \alpha\Delta\theta/V_h$ where α is the Thomson coefficient and V_h is the heater voltage. There may, in addition, be a second-order term at the midpoint because the Peltier heat itself depends on the junction temperature. This can be calculated by carrying out the second-order approximation mentioned by Hermach in Appendix 2 of reference [4] to give, with reasonable accuracy, $\delta_p = +\Delta\theta^2/T_0\theta$, where T_0 is the heat-sink temperature. Of course, $\Delta\theta$ can be calculated only very roughly, but this is sufficient. For a typical 10 mA TE

it is less than 0.01°C, and the Peltier errors, δ_{tp} and δ_p (independent of frequency), are less than 1 ppm. This has been verified by comparisons with Evanohm-heater TEs which had copper lead-in wires butt-welded to the nickel alloy wires at the glass press. However, δ_p in particular could be significant in higher-range TEs.

VIII. Low- and High-Frequency Errors

As the frequency is lowered, the temperature of a TE begins to follow the cyclic fluctuations of the square of the heater current. If the TE is not a linear device, the average temperature rise may no longer be the same as at higher frequencies. Hermach's solution of the resulting nonlinear differential equation for the temperature rise has been verified experimentally [4], at least for high-range TEs having large heaters in which the heat abstracted by the thermocouple is negligible. However, for the low range TEs we are concerned with now, these formulas may not apply. The solutions for such cases would be even more difficult, and have not been attempted, particularly since the thermal mass of the bead should then also be considered. In the simpler case, Hermach showed that the ac-dc difference is $\delta_l = h\theta d^2/\omega^2 l^4$, where d is the diffusivity of the heater alloy, $2l$ is the heater length, $\omega = 2\pi f$, where f is the frequency, and h is a factor expressing the nonlinearities. The same relationship might be expected for the more complicated case, but with a different numerical factor. Thus, the agreement to better than 10 ppm among the TEs at 20 Hz, shown in Table I, with their varying lengths, gives strong verification to the absence of significant low-frequency errors down to this frequency.

These reference TEs have heaters less than 1 by 10^{-3} cm in diameter, with resistivities of 120 $\mu\Omega$ cm. The computed errors from skin effect are much less than 1 ppm even at 50 kHz. The ac and dc conductances and the capacitance between binding posts on the phenolic top of the box in which the TEs are mounted are much less than the limiting values of 0.01 μA/V and 100 pF, respectively, which might cause 1 ppm errors at audio frequencies.

Reactance and skin-effect errors in the resistor units of the TVCs, computed according to formulas developed by the authors [3], are also less than 1 ppm through 50 kHz up through the 100 volt range, and the comparisons verify this. They cannot easily be calculated for the higher ranges, which have several resistors and adjustable inner shields. Additional reactance errors can arise from the lumped capacitance C of the connector between the resistor and the TE. This shunts the heater, which at these frequencies can be considered as a lumped resistor R in series with an equivalent lumped inductance L. It can be shown that the resultant effect of this capacitance on the magnitude of the heater current approaches $\alpha^2/2 - \alpha\beta$ as the series resistance (voltage range) is increased, where $\alpha = \omega CR$ and $\beta = \omega L/R$ (α and $\beta \ll 1$). The computed error of less than 1 ppm at 50 kHz has been verified by deliberately doubling the capacitance.

IX. Other Errors

Peltier effects at the heater and lead-in junctions can also cause a second-order change in the effective dc resistance of a TE. The calculation is difficult and the results uncertain, but the change should be much less than one ppm for the 5 to 20 mA TEs in the NBS reference group. Thus, this cannot account for the somewhat larger changes in effective dc resistance implied by the voltage comparisons of the TEs alone (without series resistors) in the TVCs. Even larger and more puzzling changes have been observed in some other TEs. There is good evidence that they may be caused by rectification at oxide films, which may persist in spite of the welded joints, but there is as yet no direct proof of this.

Dc reversal errors ($\Delta I/I$ for the same EMF) provide a good clue in studying these secondary effects. As shown in Table IV, $\Delta I/I$ calculated by Widdis' formulas should not exceed, perhaps, 200 ppm with Evanohm or Karma, and 500 ppm with nickel-chromium heaters, even if the thermocouple is mounted off the midpoint by 5 percent of the length of the heater (which is easily noticeable). Larger differences are, thus, a sign of other difficulties.

As Hermach showed [4], the current from the heater to ground through the bead of an ungrounded TE can cause heating of the bead and, thus, an error. This is difficult to compute because power dissipated in the bead is somewhat more effective in raising the thermocouple temperature than that in the heater, and the currents in the two halves of the heater are no longer identical. However, rough calculations indicate that with one volt across the bead of TE_2 in the circuit of Fig. 3, the bead resistance of a 10 mA TE must be greater than 500 megohms if the error is to be less than 1 ppm. For the bead materials commonly used, the resistance is a sharp function of temperature and is much less at audio frequencies than with direct current. At NBS, bead resistances are normally measured with a 2 kHz ac bridge with rated direct current through the heater of a TE. The results have been verified (within a factor of 2) by ac-dc comparisons of pairs of TEs with added resistance between the two heaters to significantly increase the bead voltage.

X. Conclusions

A reference group of two very different kinds of TEs has been established. The authors believe that it is very unlikely that the average ac-dc difference of the group differs from zero by more than 2 ppm at audio frequencies. This is based on the agreement to better than 0.5 ppm of the averages of the two kinds of TEs, and on allowance of 1 ppm for the uncertainty of the average in the network of comparisons. The results are in excellent agreement with calculations, which show that the ac-dc differences should not exceed 1 ppm. With the precise techniques that have been developed, pairs of TEs of the group may be compared with a 3σ uncertainty of about 2 ppm without any evidence to date (in over three years of measurements) of significant

systematic errors. This is somewhat remarkable, since fluctuations in the best available wide-range ac and dc sources greatly exceed this, and most of these TEs have rather large residual thermal EMFs and have temperature coefficients of EMF exceeding 1000 ppm/°C.

Adjacent ranges of the TVCs may also be compared with the same precision to step up and down the voltage scale. Their ac-dc differences can be determined to better than 10 ppm when used with TEs of known ac-dc differences, again without evidence of systematic error. Alternating voltage measurements can be made to 20 ppm or better by using the TVCs or ac-dc transfer standards with appropriate dc standards.

This accuracy and precision in the ac-dc transfer, more than ten times better than heretofore available, are good indications of the virtue of simplicity in reference standards. Properly designed and constructed TEs are rather simple devices that correspond to the desired idealized mathematical models remarkably closely, thus providing the agreement between theory and experiment which is so desirable in a development such as this.

The agreement to better than 1 ppm between the conventional TEs and the new very different multijunction NPL TEs (which should theoretically have smaller errors), in addition to providing semi-independent verification of the accuracy of both, indicates that even higher accuracy may be possible in the future with these new designs. Conventional single-junction TEs could be improved by the use of bifilar heaters and closely spaced lead-in wires with good thermal conductance between the two halves of the heater and between the two lead-ins. In this way, other heater alloys could be used.

Well-designed and well-constructed ac-dc transfer standards can be remarkably stable over most of their frequency range. Most factors which may change the response, such as temperature and dimensional changes, have little or no effect on the ac-dc difference. There is already some evidence that long-time stabilities of a few ppm can be attained in properly designed and constructed TEs and TVCs. However, we have noted an apparently abrupt change of +5 ppm in one TE, accompanied by a change of over 100 ppm in its dc reversal difference. Thus, TEs should be compared frequently if the highest accuracy is desired.

Comparisons of adjacent ranges, with a step-up procedure such as the one described, can be used to guard against unexpected changes in TVCs. This has already been verified in the design and construction of two somewhat similar sets of TVCs by W. Scott, K. Ballard, and D. Bailey of the NBS Electronic Calibration Center, Boulder, Colo. These units incorporate large wire-wound resistors of controllable reactances and low temperature coefficients, so that they do not require troublesome forced-air cooling. They will be described elsewhere.

The step-up procedure is also feasible with simpler sets of TVCs incorporating fewer plug-in resistor units and two TEs of different current ranges. Two such sets have been built but have yet to be completely evaluated.

Appendix I

EMF Comparator

If the thermocouple resistance R_{t1} of TE_1 (Fig. 3) is much less than R_1+R_2, the EMF E_1 is substantially the same with alternating and direct currents applied during the test (the procedure involves holding the voltage at the output terminals of TE_1 constant). Then, from the definition of ac-dc difference, $(I_a-I_d)/I_d=\delta_1$. Similarly, for TE_2 $(I_a-I_d')/I_d'=\delta_2$, where I_d' is the direct current that would be required to produce the same EMF of TE_2 as I_a. The change D_a-D_d in detector D_1 which occurs when I is changed from I_a to I_d (I_d being adjusted to keep E_1 constant) results from the change in E_2. D_a-D_d may then be interpreted as a measure of the departure of I_d from the value I_d' which would have produced the same E_2 as would I_a. Thus, combining the above two equations and neglecting second-order terms, we have $(I_d'-I_d)/I_d=\delta_1-\delta_2$.

The sensitivity of the detector to small current differences in TE_2 can be determined by shunting its heater R_h with a resistor $R_s \gg R_h$ to cause a small change in its heater current ΔI, noting the change in deflection ΔD of D_1 and computing $s=\Delta I/I\Delta D$ ($\Delta I/I=R_h/R_s$ if the heater current of TE_1 is unchanged). Then, if s is constant over the range of deflections involved, we have $\delta_1-\delta_2=s(D_a-D_d)$, as in the text. Similarly, in the comparison of two voltage converters, a resistor $R_s \ll R_m$ can be added in series with TVC_2 to give proportional change in applied voltage $\Delta V/V=R_s/R_m$, where R_m is the TVC resistance. Then $s=\Delta V/V\Delta D$.

These two calibration methods must leave the current in TE_1 unchanged. The change ΔI can often be introduced and measured more conveniently in some way (as by changing the supply voltage) that changes the current in both TEs by a small known amount. We have found it convenient to disconnect E_1, set the voltage of P to the same value, short D_2, observe the resulting ΔD when I is changed, and compute s as before.

If only a few TEs are ordinarily used in the "standard" position (TE_2 in Fig. 3), it is convenient to make use of the approximate output-input relation (at a fixed frequency) for a TE, $\Delta E/E=n\Delta I/I$, where n is dependent on I but not ΔI if $\Delta I \ll I$, and is close to 2. For each such TE, n can be determined in advance at several values of E and plotted vs. E, since it is quite stable. Then the sensitivity of the detector in the circuit can be determined by inserting a small known voltage $\Delta E_p \ll E$ (with a Lindeck potentiometer, not shown in Fig. 3) in series with and opposing E_2, observing the change ΔD in D_1 and computing the factor $k=\Delta D/\Delta E_p$. Then, from this and the previous equations $\delta_1-\delta_2=(I_d'-I_d)/I_d=(E_d'-E_d)/n_2E_2=(D_a-D_d)/kn_2E_2$. E_2 is easily measured with potentiometer P.

If R_{t1} is not negligible, E_1 is not constant during the test, since the currents in R_1 and R_2 depend on both E_1 and E_2. The corresponding equations for determining $\delta_1-\delta_2$ by means of deflections of D_1 then contain additional correction terms involving the resistances of the several parts of the EMF comparator, and are too com-

plex to be useful for routine measurements. They show, however, that if $R_{t1} \leq (R_1+R_2)/100$, the simplified equations already derived are valid to a few percent of the computed $\delta_1-\delta_2$. They show that R_{t2} is not critical. For our comparator, $R_1+R_2=1100\ \Omega$ and $R_{t1} \leq 10\ \Omega$ for the usual TEs.

For each NPL converter, $R_t \approx 1000\ \Omega$. It is always placed in the TE_2 position, except when the two NPL converters are intercompared, requiring the use of the more complicated formula.

Appendix II

REs in Parallel

By using the definitions for n and δ of a TE (see Appendix I) we have, closely enough for small changes in E,

$$\frac{E_a - E_d}{nE_d} = \frac{I_a - I_d}{I_d} - \delta.$$

In the ac-dc test, nominally equal resistors are connected in series with TE_a and TE_b, and the two branches are connected in parallel. The sum of the two EMFs, E_a+E_b, is held constant. Then, with second subscripts to identity the two TEs, we have

$$E_{aa} + E_{ab} - E_{da} - E_{db} = 0$$

and

$$n_a E_{da}\left(\frac{I_{aa} - I_{da}}{I_{da}}\right) + n_b E_{db}\left(\frac{I_{ab} - I_{db}}{I_{db}}\right) = n_a E_a \delta_a + n_b E_b \delta_b$$

If the reactances of the two paths are equal

$$\frac{I_{aa} - I_{da}}{I_{da}} = \frac{I_{ab} - I_{db}}{I_{db}} = \frac{I_a - I_d}{I_d} = \delta_p$$

where I_a and I_d are the sums of the alternating and direct currents in the two branches.

If $E_a = mE$ and $E_b = (1-m)E$,

$$[n_a m + n_b(1-m)]\left[\frac{I_a - I_d}{I_d}\right] = n_a m \delta_a + n_b(1-m)\delta_b.$$

If the reactances of the two paths are not equal, additional terms will be introduced which are difficult to calculate. However, they are zero if $n_a m = n_b(1-m)$, i.e., if the TEs are matched in response. Then $\delta_p = (\delta_a+\delta_b)/2$. Even if the reactances are unequal, the added terms are essentially eliminated if a second test is made with the two resistors interchanged and the results averaged.

Acknowledgment

The authors express their appreciation and thanks to F. J. Wilkins for the two multijunction TEs, to L. Julie of the Julie Research Laboratories for suggesting the basic idea of the EMF comparator, and to the following for their cooperation in the manufacture of other TEs used in this group: the Levy brothers of the American Thermoelectric Company, L. R. Graham of Graham Associates, F. Gay of the Best Products Company, M. Rosenfield of the former Field Electrical Instrument Company, and L. W. Pignolet of Weston Instruments Incorporated.

The use of these particular TEs with heaters of Evanohm and Karma should not in any way be construed as constituting an exclusive endorsement by NBS of these products or alloys. Other TEs, made to the same specifications with the same or other alloys of equally low thermoelectric effects, should be equally suitable.

References

[1] "American standard requirements for electrical indicating instruments." New York: American Standards Association, C.39.1, 1964.

[2] F. J. Wilkins et al., "Multijunction thermal converter," *Proc. IEE (London)*, vol. 112, pp. 794–806, April 1965.

[3] F. L. Hermach and E. S. Williams, "Thermal voltage converters for accurate voltage measurements to 30 megacycles per second," *Trans. AIEE (Communication and Electronics)*, vol. 79, pt. I, pp. 200–206, July 1960.

[4] F. L. Hermach, "Thermal converters as ac-dc transfer standards for current and voltage measurements at audio frequencies," *J. Res. NBS*, vol. 48, pp. 121–138, February 1952.

[5] W. J. Youden, "Measurement agreement comparisons," *Proc. 1962 Standards Laboratories Conf.* Washington, D. C.: NBS, Misc. Pub. 248, August 16, 1963, pp. 147–152.

[6] F. C. Widdis, "The theory of Peltier and Thomson effects in thermal ac-dc transfer devices," *Proc. IEE (London)*, Monograph 497M, January 1962.

[7] Landolt-Bornstein, "*Zahlenwerte und Funktionen aus Physik, Chemie, Astronomie, Geophysik und Technik*," 6. Auf., Band II/6, (6th ed. vol. 2, pt. 6). Berlin: Springer-Verlag, 1959.

[8] D. Flach and L. A. Marzetta, "Calibration of peak a-c to d-c comparators," *Proc. 1965 ISA Conf.*, pt. 1, vol. 20, paper 14.

A System for Accurate Direct and Alternating Voltage Measurements

F. L. HERMACH, FELLOW, IEEE, J. E. GRIFFIN, MEMBER, IEEE, AND E. S. WILLIAMS

Abstract—A system for calibrating and using a group of dc and ac standards has been developed at NBS to meet increasing needs for greater accuracy in the measurement of direct and rms alternating voltages at audio frequencies. With a group of saturated cells, a universal ratio set as a potentiometer, a simplified self-calibrating volt box, and a new differential-thermocouple ac-dc comparator, an accuracy of 10 ppm can be obtained for direct voltage measurements and 40 ppm for rms alternating voltage measurements between 20 and 20 000 c/s, in terms of the direct volt and the ac-dc transfer standards maintained at NBS.

Introduction

THERE HAVE BEEN increasing needs for measuring direct voltages to about 20 ppm (parts per million) and rms alternating voltages at audio frequencies to perhaps 50 ppm. A system for calibrating and using a group of dc and ac standards has been developed at the National Bureau of Standards in an attempt to meet these needs. It consists of 1) a group of saturated standard cells; 2) a six-dial universal ratio set (URS) with a control box so that it may be used as an accurate potentiometer; 3) a simplified volt box of the Silsbee type and a new convenient method for calibrating it with the URS; 4) a new differential-thermocouple ac-dc comparator; and 5) an inductive voltage divider for low alternating voltage measurements and for calibrating the URS. A dc picoammeter for checking certain vital insulation resistances and suitable dc and ac detectors and other apparatus normally available in a standards laboratory are also required. With the system of calibrations, the sustained accuracy in use depends only on the standard cells, the very stable inductive divider, and the ac-dc difference of the comparator. As a result, the authors believe that after corrections based on these calibrations are applied, direct voltages from 0.5 to 1000 volts can be measured with an uncertainty (a "limit of error" which will only rarely be exceeded) of 10 ppm, and that alternating voltages from 0.5 to 500 volts at frequencies from 20 to 20 000 c/s can be measured with an uncertainty of 40 ppm in terms of the dc standards and the standards of ac-dc difference maintained at NBS.

Manuscript received May 3, 1965. This work was supported in part by the Metrology Engineering Center, Bureau of Naval Weapons, Pomona, Calif., and by the Army Metrology and Calibration Center, Frankford Arsenal, Philadelphia, Pa.

The authors are with the Electrical Instruments Section, National Bureau of Standards, Washington, D. C.

Universal Ratio Set as a Potentiometer

Potentiometers are normally calibrated with a URS, which is in essence a resistance divider[1] with a resolution of 0.5 ppm of the input for a six-dial instrument. Thus, its use as a potentiometer to obtain the highest accuracy has seemed natural, and has indeed been recommended.[2] However, a number of very important precautions must be observed before the accuracy realized begins to approach the precision. We have found it necessary to design and construct a control box to adapt the URS for voltage measurements with reasonable convenience and to minimize the various errors.

A URS can be used as a single range 0 to 2.1 volt potentiometer if it is supplied with an adjustable stable direct current, as shown in Fig. 1. To make the dials direct reading, the current I is adjusted by first setting the dials numerically equal to the EMF of the standard cell (SC) and then adjusting R_1 to null the galvanometer G with the cell connected. This eliminates a separate standard cell dial with its additional resistors and leads to greater accuracy. It is not as inconvenient as it may at first seem. The current drain of the usual 2100-Ω URS is only 1 mA with direct-reading dials, so that with six 14-ampere-hour mercury cells in series parallel, the drift is less than 3 ppm/hour. Thus, the standard cell balance need not be made very frequently.

The control box shown in Fig. 2 contains all of the components (except the standard cell) necessary for voltage measurements to 2.1 volts with the URS. In this way the URS is unchanged and is available for resistance ratio measurements by simply disconnecting a few wires. As shown in the figure, the potentiometer is ungrounded and two inputs are provided for voltage measurements, both of which may be reversed. This is a necessity (often overlooked) for many types of measurements, such as the reversed dc calibration of wattmeters and attenuators.

The control box is of metal and is lined with foamed plastic insulation for thermal stability. Each component is insulated with bushings or subpanels of tetrafluoroethylene (TFE), and all wire is similarly insulated. The insulation resistance must be greater than 2×10^9 Ω to

[1] J. L. Thomas, "Precision resistors and their measurement," NBS Circular 470, 1948.

[2] Proposed American Standard C39.6, "Automatic digital voltmeters and ratio meters," ASA, September 1963.

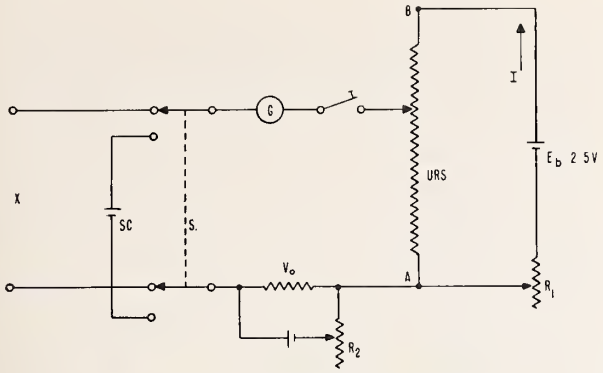

Fig. 1. URS as a single-range potentiometer.

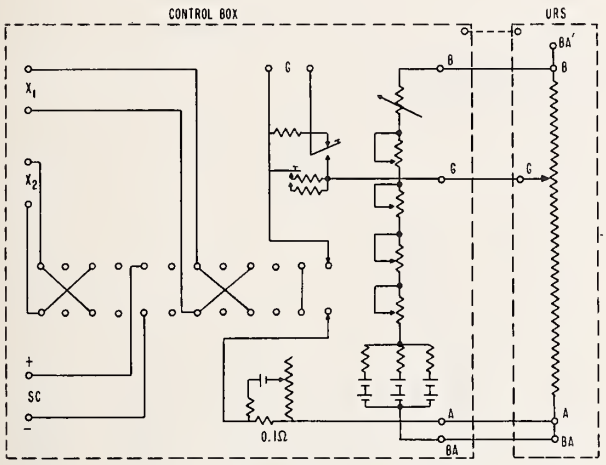

Fig. 2. Diagram of control box.

insure that leakage-current errors are less than 1 ppm. With TFE insulation this requirement is easily met and maintained in laboratory service. With all leads disconnected, the resistance of each circuit of the control box to the panel and between each pair of input posts has remained well above 10^{11} Ω even at 60 percent RH.

Resistor R_1 in the control circuit must be adjustable and stable to 0.001 Ω. Commercially available enclosed silver-alloy switches and a bifilar 0 to 0.1 Ω continuously adjustable resistor make this possible. Resistors with temperature coefficients less than 10 ppm/°C are used in the first four dials. The six-mercury cells are connected in three parallel groups of two cells each, with a 1-kΩ series resistor of low temperature coefficient to reduce circulating currents. Insulated copper wire (about 45 Ω) is wound around each cell and connected in series with it to compensate (at the cell current of 1/3 mA) for the temperature coefficient of EMF (about +60 μv/°C). The thermofree galvanometer key is provided with a resistor of low thermal EMF across the normally closed contact, as shown in Fig. 2, for proper damping and a stable zero reading. The saturated standard cells are housed in a separate temperature controlled air bath and may be intercompared by means of the URS or with a Lindeck potentiometer built into the standard cell box.[3]

The commercially available six-dial URS used with this control box is adjustable to 0.001 Ω (corresponding to 1 μV at 1 mA). For convenience, its dials have been marked in volts as well as ohms. Its principal resistors, which have temperature coeffcients matched to better than 5 ppm/°C, are mounted in a thermally shielded inner enclosure, and are connected to the circuit by enclosed silver-alloy switches of low thermal EMFs. A taught-band light-beam galvanometer, with a sensitivity of 500 mm/μA and a near-critical damping range of 500 to 2000 Ω, is used as a detector because of its excellent rejection of alternating currents at frequencies above a few c/s. It is supported on TFE resting on a metal plate, and is connected with a two-conductor shielded cable having TFE insulation. To eliminate external stray currents, this plate, the metal control box, the case of the URS, and the cable shield are all grounded. Because of the high insulation resistance, the potentiometer circuits may be grounded at the point of measurement rather than at the potentiometer terminals. It is undesirable to ground a potentiometer itself unless the circuit being measured is very well insulated because of small error-voltages which may result from ground currents in the potentiometer leads.

When the dials of the URS are set to zero, a residual voltage of a few μV normally remains because of switch and lead resistances. This is stable to better than 1μV, however, and is easily eliminated by the zero-adjust circuit shown in Figs. 1 and 2. Resistor R_2 is adjusted for a galvanometer null with the URS dials wet at 0 and the input switch in the "short" position.

The URS was calibrated by the Resistance and Reactance Section of NBS, with dc resistors and a direct reading ratio set. However, it is constructed with resistors of low electrical time constant. It can be checked conveniently at low audio frequencies by direct comparison with a suitable calibrated inductive voltage divider.[4] We have found the simple circuit of Fig. 3, described in Appendix I, satisfactory for this. The results of tests at 100 and 400 c/s agreed with the normal dc tests to 1 ppm of input.

As an additional overall check the URS with its control box was connected so that its output voltage could be measured with a Brooks-Harris wide-range potentiometer. After corrections to both potentiometers were applied, the residual differences at 25 dial settings of the

[3] A. W. Spinks and F. L. Hermach, "Portable potentiometer and thermostatted container for standard cells," *Rev. Sci. Instrum.*, vol. 26, p. 770, 1955.

[4] The possibility of comparing resistance ratio devices with inductive voltage dividers at low frequency (which was first suggested to us by F. K. Harris) has occurred to many people. The Resistance and Reactance Section of NBS has made such comparisons using different methods for injecting the necessary small quadrature voltage into the detector circuit. Their conclusions substantiate those reached in our investigation.

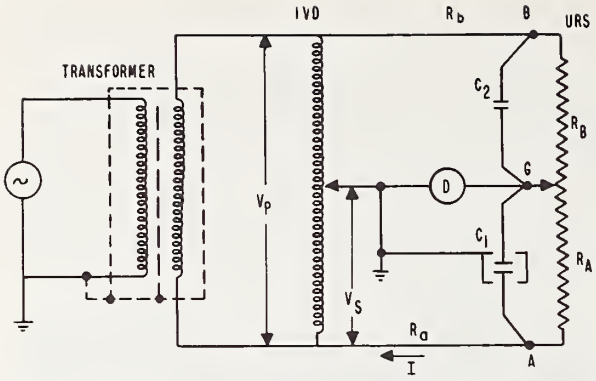

Fig. 3. Circuit for calibrating URS with inductive voltage divider (IVD). C_1—0 to 1100 pF, 3-terminal adjustable air capacitor; C_2—small low-loss capacitor connected directly to URS terminals; and D—tuned audio-frequency null detector. Note: Each dial of URS is set at midscale except decade under test.

URS did not exceed 2 μV, even though some time had elapsed since the calibration of the Brooks-Harris potentiometer.

A URS is normally calibrated by determining the increase in resistance (with A and G as the potential terminals) for each setting of each dial from the resistance at the zero setting in terms of an arbitrary unit. This can be expressed as $R-R_0=K(D+c)$, where $R-R_0$ is this increase for a setting D of the dials (in ohms or volts), c is the total correction, R_0 is the resistance with all of the dials at zero, and K is a constant. When the standard cell balance is made in the use of the URS as a potentiometer, we have, from Fig. 1, $E_s+V_0=IR_s=IK(D_s+c_s)+IR_0$, where R_s is the resistance between the branch points of A and G, at the combined dial setting D_s.[5] Similarly, when an unknown voltage V_x is measured, we have at balance $V_x+V_0=IK(D_x+c_x)+IR_0$. With V_x and all dials at zero, V_0 is adjusted to make $IR_0=V_0$. Then, since I is unchanged,

$$V_x = E_s \frac{(D_x + c_x)}{(D_s + c_s)}.$$

It is convenient to set D_s numerically equal to E_s-c_s. Then, very simply, $V_x=D_x+c_x$.

Voltage Divider

A guarded volt box designed by Silsbee is based on the principle that the resistance of any section is nominally equal to the sum of resistances of one or more adjacent lower sections. It can thus be calibrated with a direct-reading ratio-set and auxiliary resistors by a series of substitution measurements.[6] Silsbee's volt box (133 Ω/V) was originally designed for calibrating other volt boxes by direct comparison, so that it has more ranges than necessary for voltage measurements. In addition, with modern insulation, its guard circuit is no longer a necessity, and with stable, modern, high-resistivity alloys, higher-valued resistors can be used with less self-heating. A simpler, much smaller and lighter 12-range volt box embodying the same principle was designed and constructed for this system.[7] It is rated at 500 volts at 1 mA (1000 Ω/V) but it can be used with the 2 volts URS for measurements to 1000 volts with negligible self-heating errors. Its oil-filled sealed resistors are mounted directly on the binding posts, which are insulated from the top panel with TFE bushings. The measured temperature coefficients of the resistors are all less than 3 ppm/°C, and the computed temperature coefficient of each ratio is less than 2 ppm/°C. The wood box and an inner metal shield provide sufficient thermal and electrostatic shielding for laboratory environments. If the insulation resistance from the circuit to the metal shield (brought to a separate binding post) is greater than 2×10^{11} Ω, leakage current errors are less than 1 ppm even if all of the resistance is lumped at the worst possible place. In the three years that this divider has been in use, this resistance has been greater than 10^{14} Ω even at 60 percent RH.

Because of the relatively few ranges of this divider (2 to 500 volts in the series 2, 3, 5, 10, etc.), a direct "step-up" calibration may be made very accurately and conveniently with the URS, as shown in Fig. 4 and as described in Appendix II. Adjacent resistors of nominally equal value are intercompared with the URS connected as shown, and then with the leads at a and b interchanged. The average of the two URS readings is essentially independent of URS errors and lead resistance. The leads at g and b are each moved up 1 range on the volt box, posts 1 and 2 are short-circuited, and the procedure is repeated. This is continued in accordance with the schedule shown in Table I, until the top post is reached. A complete calibration including computations can be made rather quickly. As shown in the table, the results agreed with the more accurate and more versatile direct-reading-ratio-set method to 1 ppm.

In use, one pair of X posts of the URS control box is connected to the 0-1 posts of the volt box, and the unknown direct voltage V_{dc} is applied to the 0 and appropriate range posts. Then

$$V_{dc} = N'V_x(1 + n + w)$$

where, in addition to the terms already defined, N' is the nominal ratio of the volt box, $N'(1+n)$ is its actual ratio, and $w=R_2/R_v$, where R_2 is the resistance of the two leads from the volt box to the points at which voltage is to be measured, and R_v is the nominal resistance of the volt box.

[5] D and c are expressed in terms of the voltage markings ($m\Omega$) when the URS is used as a potentiometer.

[6] B. L. Dunfee, "Method for calibrating a standard volt box," *J. Res. NBS*, vol. 67c, p. 1, 1963.

[7] The layout, construction, and initial tests of this box were capably carried out by J. L. Yarne.

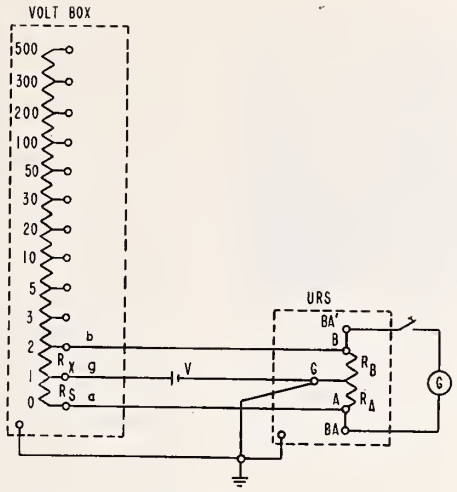

Fig. 4. Calibration of a volt box with the URS. Note: The values shown on the volt box are the voltage ratings and also the resistance in $k\Omega$ between the marked tap and the "0" post. Twice rated voltage may be applied without significant heating. Leads aA and bB are air-insulated.

TABLE I

Calibration of Volt Box with a URS

Section			N_k'	URS Reading		ΔR_A	s	x	Voltage Range	$N_k'x$	$\Sigma N_k'x$	Volt Box Correction	
S	X	Link		R_{A1}	R_{A2}	R_A			$N'=\Sigma N_k'$			URS	DRRS
				1055+	1055+								
0–1	1–2	—	1	.5510	.5600	+ 8.5	0	+ 8.5	2	+ 8.5	+ 8.5	+ 4.0	+ 3.4
0–1	2–3	1–2	1	.5540	.5570	+ 3.0	0	+ 3.0	3	+ 3.0	+ 11.5	+ 4.0	+ 3.9
0–2	3–5	2–3	2	.5680	.5430	−23.5	+ 4.0	−19.5	5	− 39.0	− 27.5	− 5.5	− 5.9
0–5	5–10	—	5	.5675	.5440	−22.5	− 5.5	−28.0	10	−140	−168	−17.0	−16.6
0–10	10–20	—	10	.5600	.5510	− 8.5	−17.0	−25.5	20	−255	−423	−21.0	−21.0
0–10	20–30	10–20	10	.5585	.5530	− 5.0	−17.0	−22	30	−220	−643	−21.5	−21.4
0–20	30–50	20–30	20	.5400	.5715	+30.0	−21.0	+ 9.0	50	+180	−460	− 9.0	− 9.0
0–50	50–100	—	50	.5490	.5630	+13.5	− 9.0	+ 4.5	100	+225	−235	− 2.5	− 2.4
0–100	100–200	—	100	.5545	.5570	+ 2.5	− 2.5	0	200	0	−235	− 1.0	− 1.1
0–100	200–300	100–200	100	.5560	.5560	0.0	− 2.5	− 2.5	300	−250	−485	− 1.5	− 1.4
0–200	300–500	200–300	200	.5540	.5575	+ 3.5	− 1.0	+ 2.5	500	+500	+ 15	0.0	− 0.6

URS readings were interpolated from galvanometer deflections to $\frac{1}{2}$ of last dial unit. All calculations are shown in ppm and are carried to nearest 0.5 ppm (where significant) for comparison with DRRS method. Corrections in URS column are calculated from $(\Sigma N_k'x)/N'$. Corrections in DRRS column were determined by method.[5]

Ac-Dc Comparator

A new type of transfer standard, a differential-thermocouple voltage comparator (DTVC), was designed, constructed, and calibrated for ac measurements. This contains two identical voltage converters, as shown in Fig. 5, each consisting of a chain of resistors (to obtain various ranges from 0.5 to 500 V) in series with the heater of a 10-mA thermoelement.[8] The two thermocouple outputs are permanently connected in opposition and to a galvanometer G. In use, the two voltage converters are first switched in parallel (by means of S_1) to a direct voltage source (not shown in the figure) which is nominally equal to the alternating voltage to be measured, and the outputs of the thermoelements are adjusted (with the shunt R_p) to obtain a null on the galvanometer. One converter is then switched to the ac source, and a null on the galvanometer is again obtained by adjusting the dc source. The alternating and direct voltages at the terminals of the instrument are then equal, and the direct voltage can be measured with the dc standards already described (volt box and URS potentiometer). To eliminate dc reversal errors in the thermoelements, the direct voltage is reversed, and the sequence of measurements is repeated. The results are then averaged. As shown in Appendix III, the unknown alternating voltage is simply $V_{ac}=V_{dc}(1+\delta)$ where V_{dc} is the corrected average direct voltage and δ is the ac-dc difference of the DTVC in proportional parts.

With the dual converters, errors from drifts and other uncertainties, which tend to limit the accuracy of the

[8] The hot junction of the thermocouple is electrically insulated from the heater wire by a small bead. The lower pole of switch S_1 makes contact before the upper one to keep the bead voltage low.

single thermoelement system, are greatly reduced. The dual principle also makes possible simultaneous comparisons of alternating and direct voltages with high precision. These factors contribute to high accuracy in measurements.

A dual hot-wire comparator was developed many years ago.[9] It consisted of two current-carrying parallel wires with a small mirror cemented as a bridge at their midpoints, to measure (with a reflected beam of light) the differential sag caused by the heating of the wires. However, transient unbalances because of temperature fluctuations made very precise measurements difficult. In any differential instrument, close matching of the dual channels is necessary to achieve a precision of 10 ppm. This might seem to be impractical with thermoelements because of their large temperature coefficients approaching 0.1 percent/°C. However, the temperature coefficients are nearly equal. Furthermore, the two thermoelements in the DTVC are mounted in two closely spaced holes in a thermally well-shielded copper block. Thus, the errors resulting from this source are considerably less than 5 ppm in a typical measurement under normal laboratory conditions.

Wire-wound audio-frequency resistance cards were used for the two identically arranged series-resistor chains to minimize self-heating errors. Repeated tests of the 5 and 500 volt ranges of the completed instrument with both voltage-converters in parallel have shown that after a 10-minute warmup net, self-heating changes do not exceed 10 ppm.[10]

A complete diagram of the DTVC is shown in Fig. 6. To reduce reactance errors, each voltage range has a separate resistor, and all unused resistors are connected to their respective shields through the range switch. The metal shields, which surround the components, prevent interaction between circuits. Simple L-C circuits with by-pass capacitors mounted on the thermocouple box provide considerable attenuation at radio frequencies. The difference in the lead resistance from the ac and dc input connectors to the common point at the ac-dc switch (S_1) on the instrument is less than 200 $\mu\Omega$. Enclosed silver alloy switches with contact resistances stable to better than 500 $\mu\Omega$ are used. Thus, the total error from unequal lead resistance is less than 15 ppm on the 0.5 volt range and correspondingly less on higher ranges.

The ac-dc differences of the alternating voltage converter of the DTVC were carefully measured with a newly developed set of coaxial thermal voltage converters at NBS. This set of coaxial converters has ranges from 0.5 to 500 volts in the sequence 0.5, 1, 2, 3, 5, 10, etc. By stepwise intercomparisons of adjacent ranges, the ac-dc difference of each range of this set has been determined relative to any one range to better than 10 ppm at audio frequencies. The 0.5 volt range has been compared repeatedly with a group of thermoelements, which at present serve as the NBS standard of ac-dc difference. From these intercomparisons, the ac-dc differences of the DTVC could be determined in terms of the average of the NBS group. The results at 20 000 c/s are shown in Table II. The measured differences were less than 10 ppm at lower frequencies.

Since there are two converters in the DTVC, there is considerable merit in comparing the ac-dc differences of each. Changes in the thermoelements or in the resistors which could slightly alter the ac-dc difference of one converter would be very unlikely indeed to affect both converters equally. It is easy to compare the ac-dc differences of the two converters by noting the changes in the galvanometer deflections with switch S_1 to the right and with direct, alternating, and reversed direct voltages successively applied to the dc input terminals of the instrument. The two thermoelements are matched well enough so that the applied voltages need be equal only to 0.05 percent. Calibrated ac and dc sources may be used or may be adjusted to give equal readings of a millivolt potentiometer connected to one of the thermocouple outputs. These checks can be made on each voltage range and provide precise and very valuable verifications of the constancy of the ac-dc differences.[11]

In using the DTVC, it is sometimes more convenient to adopt a deflection method rather than to obtain a null at each balance. In this technique the scale factor of the galvanometer is first determined, with the proper direct voltage applied, by momentarily shunting the heater circuit (switch S_2 in Fig. 5) and noting the change in deflection. Then, in a measurement at this voltage level, the galvanometer deflection is read with the double-pole selector switch S_1, in each position, with the nominal value of direct voltage applied. The direct voltage is reversed and the two deflections are again read, without resetting the dials of the URS or rebalancing the galvanometer. Then, as shown in Appendix III, the unknown alternating voltage is simply $V_{ac} = V_{dc}[1+s(D_{ac}-D_{dc})+\delta]$ where, in addition to the terms previously defined, D_{ac} and D_{dc} are the averages of the two galvanometer deflections with the selector switch in the ac and dc positions, respectively, and s is the scale factor in proportional parts per division of the detector.

A photograph of the complete system is shown in Fig. 7. Each of the components is used for other measurements in other areas, so that console mounting seemed impractical. The resistances of the two coaxial cables from the ac source (not shown) and the volt box to the DTVC must be equal to 10 ppm of the resistance of the DTVC range in use. Other leads are not critical.

[9] E. F. Northrup, "A new instrument for the measurement of alternating current," *Trans. AIEE*, vol. 24, pp. 741–757, 1905.

[10] After being energized, many thermoelements exhibit a drift up to 0.1 percent, with a 2- to 4-minute time constant. No effort was made to match these drifts in this instrument.

[11] Techniques for intercomparing the ac-dc differences of adjacent ranges to step up and down the alternating voltage scale are now being investigated.

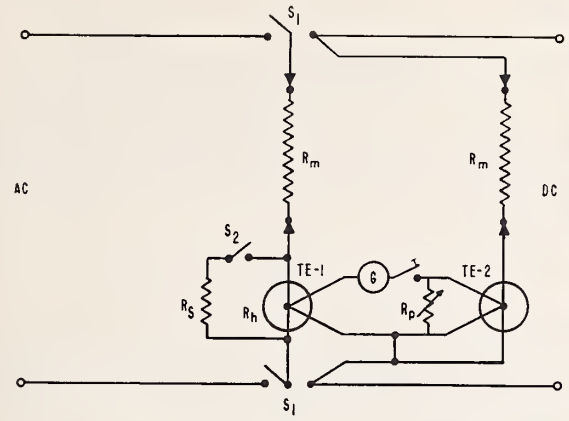

Fig. 5. Simplified diagram of the DTVC. Rm = series multiplier, 100 Ω/V, and R_h = resistance of TE heater 40 Ω ± plus additional resistance to make 50 Ω, 0.5 V range.

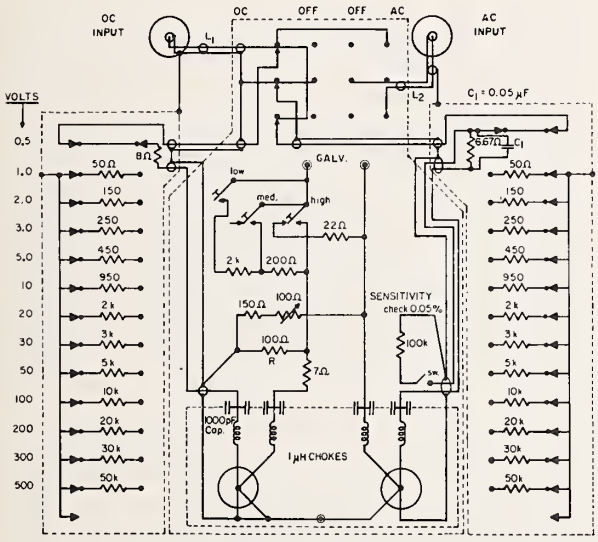

Fig. 6. Differential thermocouple voltage comparator. Note: All range resistors not in use are connected to the shields through additional switch contacts as shown. The shields are shown as dotted lines.

TABLE 11

Ac-Dc Differences of DTVC

Range V	Ac-Dc Difference ppm at 20 c/s
0.5	−30
1	−10
2	+10
3	+10
5	+10
10	0
20	0
30	+10
50	+10
100	0
200	0
300	+10
500	+30

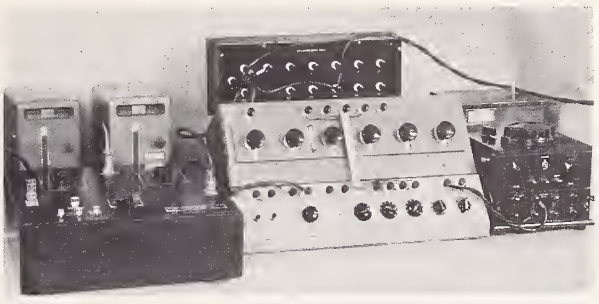

Fig. 7. Direct and alternating voltage measuring system. Note: The differential-thermocouple voltage comparator is at the left, the universal ratio set and control box at the center, the volt at the rear and the "standard cellar" at the right.

Accuracy

It is difficult to assess the accuracy of a complex measuring system such as this, in which several standards extend and subdivide the direct voltage scale and transfer to alternating voltage with high precision. Except near 1 direct volt, no voltage standards were available with stability and accuracy adequate to directly determine the precision and accuracy of the complete system.

As indicated in the text, the calibrations of the ratio standards were checked by more conventional techniques to verify that unknown systematic errors in the proposed new methods were not significant. For additional verification, direct voltages from 0.5 to 1.5 volts were measured simultaneously with the URS and the Brooks-Harris potentiometer. In several repeated tests the largest discrepancy (after calibration corrections were applied) was 3 ppm. Similarly alternating and direct voltages were compared at the same time by means of the DTVC and the coaxial thermal voltage converters. The DTVC was operated in its normal way, and a sequence of readings was used to greatly reduce errors from drifts in the coaxial converters. The largest discrepancy was 10 ppm. The observed agreements might lead one to believe that direct and alternating voltage measurements could be made to these accuracies if corrections were applied, but this is not necessarily so, since these are only partial tests with standards which are not completely independent. In the use of this system, it is indeed assumed that corrections for all known sources of errors, as determined from the calibrations of the several standards, will be applied, when significant, in accordance with thd formulas given. However, even after this has been done, there remain many residual errors, which cannot be evaluated precisely. The essential features of this system were developed in 1960, and some components have been in use over three years. In this time, enough experience in measuring direct and alternating voltages has been gained to estimate the upper limits of these residual errors (some of which are proportional to measured voltage in a given range and some of which are proportional to the range) and to ob-

tain the estimates of uncertainties given in the introduction.

Conclusions

The system described has met the desired goals in accuracy and in voltage and frequency ranges. Its continued accuracy in service can be based on a few highly stable standards by means of relatively direct and simple procedures of high precision. Many of the components of the system are readily available in a standards laboratory. Others can probably be constructed without too much difficulty. Most of them can be used for other measurements in addition to those described here.

The DTVC is much more stable than earlier single-unit ac-dc transfer standards, making more precise ac measurements possible. Its ac-dc differences were assigned with confidence only after several comparisons with the NBS ac-dc standards verified both the precision of the comparison process and the ac-dc stability of the comparator. It is not to be expected that the same certainty can be attached to the results of a single ac-dc test of a similar instrument. However, ac-dc intercomparisons of adjacent ranges in the user's laboratory may provide some of the additional assurance that would be needed in such cases.

Appendix 1

Ac Calibration of a URS

The circuit shown in Fig. 3 is easily set up in the laboratory if an ungrounded source or a shielded transformer is available. In this way a guarded detector is not required, and the shield of the 3-terminal capacitor may be grounded as shown. As is well-known, an inductive voltage divider can tolerate rather large shunt capacitances. The change in ratio with 5000 PF connected to one side of the divider used in these tests was undetectable ($<10^{-7}$ of input). At low frequencies (100 c/s is recommended), short unshielded leads are satisfactory; their resistances are not critical, since only changes in the effective resistance R_{AG} corresponding to changes in URS dial settings are measured. An input voltage of 10 volts is recommended. At this level, the resolution and noise level of the tuned detector should be less than 10 μV.

The capacitors C_1 and C_2 are necessary to achieve a sufficiently precise balance but need not be known accurately, since their effect on the magnitude of the URS ratio is small. This can be seen most easily by neglecting (for this evaluation only) the small lead resistances R_a and R_b. Then at balance $V_s = V_p Z_A/(Z_A+Z_B)$ where $Z_A = R_A/(1+j\alpha_1)$ and $Z_B = R_B/(1+j\alpha_2)$ and $\alpha_1 = \omega C_1 R_A$, $\alpha_2 = \omega C_2 R_B$. Then, if $V_s = M V_p(\cos\gamma - j\sin\gamma)$, where M is ratio of the magnitude of the output to the input voltage of the IVD, we have

$$\frac{V_p R_A(1+j\alpha_2)}{(R_A+R_B)(1+jc)} = MV_p(\cos\gamma - j\sin\gamma)$$

where

$$c = \alpha_2\left(\frac{R_A}{R_A+R_B}\right) + \alpha_1\left(\frac{R_B}{R_A+R_B}\right).$$

Equating real parts, using the series expansions of the trigonometric functions, and noting that γ, α_1, and α_2 are small compared to unity, gives to the desired approximation,

$$\frac{R_A}{R_A+R_B} \approx M\left(1 - \frac{\gamma^2}{2} + c\gamma\right).$$

Thus, if the phase defect angle of the inductive voltage divider (IVD) is less than 100 microradians, and α_1 and α_2 are each less than 0.01, the phase-defect-angle correction terms are less than 1 ppm.

The calibration consists of measuring the ratios for each setting of each dial of the URS. It is convenient to set all of the other dials at their midpoints so that the capacitance balance may be made with capacitors of reasonable size. For the first calibration, the measurements should be repeated after the frequency of the source has been doubled. If the results agree to 1 ppm of input, there is strong evidence that the residual reactances within the URS are negligible at both frequencies. If not, lower frequencies must be used.

The corrections to a URS are usually expressed in terms of the change in the resistance R_A (between the branch points at A and G) corresponding to changes in dial settings, with one hundredth of the average of the 20 resistors of the main ($\times 100$) dial as the unit of resistance. If the total resistance is constant, the correction for a given setting of any one dial is independent of other dial settings. This can be expressed as

$$\sum(R_{kn} - R_{k0}) = k\sum(D_{kn} + c_{kn})$$

where $R_{kn} - R_{k0}$ is the increase of the resistance R_A at the setting D_{kn} of the kth dial from the value R_{k0} at the zero setting D_{k0} of that dial, c_{kn} is the corresponding correction, and K is a constant. Similarly, $R_{1f} - R_{10} = KD_{1f}$, with zero correction by definition, where R_{1f} and R_{10} are the resistances at the 20 and 0 settings of the first ($\times 100$) dial.

From Fig. 3, at balance, and neglecting the reactances,

$$V_{AG} = V_s - IR_a = V_p M - IR_a = IR_A.$$

Combining these equations, if the kth dial is varied with the other dials fixed and if I is independent of dial setting, gives,

$$\frac{R_{kn} - R_{k0}}{R_{1f} - R_{10}} = \frac{D_{kn} + c_{kn}}{D_{1f}} = \frac{M_{kn} - M_{k0}}{M_{1f} - M_{10}}.$$

Thus,

$$c_{kn} = D_{1f}\left(\frac{M_{kn} - M_{k0}}{M_{1f} - M_{10}}\right) - D_{kn}.$$

TABLE III

Partial Calibration of a URS

Dial Settings			Frequency c/s	Corrected IVD Reading $=M_{kx}$	$M_{kx}-K_{ko}$	Correction, mΩ	
1st	2nd	Others				ac	dc‡
0	5	5.555	400	0263238	—	0.0	0
10				4999996	4736758	−0.6	−1
12				5947346	5684108	−1.2	−1
20				9736760	9473522*	0.0	0
9	0	5.555	400	4289492	—	0.0	0
	4			4478957	0189465	−1.2	−1
	10			4763156	0473664	−2.6	−2
0	5	5.555	100†	0263240	—	0.0	0
10				4999997	4736757	−0.6	−1
12				5947345	5684105	−1.6	−1
20				9736760	9473520*	0.0	0

* Equals $M_{1f}+M_{1o}$

† Tests at 100 c/s were made on another day.

‡ From dc tests.

In this way the correction for the setting of each dial can be determined in terms of the corresponding ratios (M) of the IVD.[12] Note that the lead resistances do not enter into the formula.

A portion of the data taken in one of several tests of the URS, and the computations to determine the corrections are given in Table III. These corrections in appropriate units apply to the URS when used for resistance as well as voltage measurements.

The constancy of the total resistance of the URS must also be checked to 1 ppm. This can be done easily by adding a stable 2000 Ω resistor in series with the B terminal of the URS, connecting the detector to the B terminal, and noting the changes required in the IVD as each dial of the URS except the first is varied through its range. The variation should not exceed 0.5 ppm of input of the IVD.[13]

Appendix II

Calibration of the Volt Box with the URS

Since the resistance of any section of the volt box is nominally equal to the total resistance of one or more lower voltage sections, the box can be calibrated by measuring these ratios systematically with the URS. Figure 4 shows the connections for the test of the first ratio. For the second ratio the leads to the volt box are connected to posts 0, 2 and 3 with a low resistance link (<1 mΩ) between 1 and 2. Connections for the other ratios are shown in Table I. Since quite a number of 1/1 ratios must be measured, an error in the true midpoint setting of the URS is compounded in the calculations. It can be essentially eliminated, however, by measusing each ratio a second time (before going on to the next), with the leads aA and bB interchanged at the volt box and taking the average of the two URS readings. Only the lower dials, which have negligible corrections in a reasonably good URS, will differ.

The voltage applied should produce rated current (1 mA) in the high-voltage sections of the voltbox. The power dissipation in the URS is only 2 mW, so that its heating is entirely negligible. To minimize errors from thermal EMFs, the dials of the URS are adjusted to give no change in galvanometer deflection when the supply voltage is reversed (thus balancing to a "false zero"). The galvanometer and URS control box are convenient for this test, with the A and G posts of the control box connected to the BA and BA′ posts of the URS, respectively, the control switch in the shorting position, and $V_0=0$.

From Fig. 4, at balance

$$\frac{R_x+R_b}{R_s+R_a}=\frac{R_{B1}}{R_{A1}}$$

where R_{A1} and R_{B1} are the values of R_A and R_B at balance, and the internal leads from the branch points of the volt box to its terminals are included in R_x and R_s. The resistances of the internal leads are negligible (less than 1 mΩ) for this box. R_a and R_b are the resistances of leads aA and bB.

With the outer leads interchanged at the volt box, at balance,

$$\frac{R_s+R_b}{R_x+R_a}=\frac{R_{B2}}{R_{A2}}.$$

Adding unity to each side of each equation and dividing the first equation by the second gives

$$\frac{R_x+R_a}{R_s+R_a}=\frac{(R_{B1}+R_{A1})R_{A2}}{R_{A1}(R_{B2}+R_{A2})}.$$

Subtracting unity from each side of the equation, noting that $R_{A1}+R_{B1}=R_{A2}+R_{B2}$, for a good URS, and

[12] For convenience, the "nominal" value of M can be computed in advance.

[13] Correction for larger changes can be applied when the URS is used but are too complicated to be useful.

solving for R_x gives

$$R_x = R_s\left[1 + \frac{R_{A2} - R_{A1}}{E_{A1}}\left(1 + \frac{R_a}{R_s}\right)\right].$$

The lead correction term is thus reduced to the second order of smallness, and only the difference in the readings of the URS is significant.

Let $R_x = R_x'(1+x)$ and $R_s = R_s'(1+s)$, where the primes refer to the nominal values and x and s are small compared with unity. Then, since $R_x' = R_s'$, we have, by neglecting second-order terms

$$x = s + \frac{R_{A2} - R_{A1}}{R_{A1}}.$$

In this volt box the potentiometer is always connected to the 0-1 section. If leakage currents are negligible, the voltage-ratio of a range of the volt box containing m sections is

$$N = \sum_{k=1}^{m} N_k$$

where N_k is the ratio of the resistance of the kth section of the box to the first section.

Let $N = N'(1+n)$ and $N_k = N_k'(1+x_k)$ where the primed quantities represent the nominal values and x_k is small compared with unity.

From this

$$n = \frac{\sum N_k' x_k}{N'}.$$

The calculations are carried out in accordance with the schedule of Table I.

The results are useful only if the same current passes through all of the resistors in use; i.e., if leakage and corona currents from the resistors to the metal shield of the box are negligible. The total leakage resistance is easily measured by connecting a 1-kV direct voltage source in series with a well-insulated dc picoammeter to the 500-V post and the shield of the volt box. The leakage and corona current indicated by the instrument should be less than 5 nA.

Appendix III

Formulas for Using the DTVC

The ac-dc difference of a thermal voltage converter such as the ac-dc converter of the DTVC (Fig. 5) is defined as $\delta = (V_{ac} - V_{dc})/V_{dc}$, where V_{ac} is the applied alternating voltage required to produce the same output EMF of the thermoelement (TE_1) as the average of the two directions of direct voltage V_{dc} applied to this same converter. In the null method of measuring an alternating voltage V_{ac}, the thermocouple shunt is adjusted with the switch S_1 to the right and the direct voltage is adjusted with S_1 to the left until a null of the detector is obtained in both switch positions without further adjustment. The direct voltage V_d is measured with external standards and then reversed. The procedure is repeated and a voltage V_r is measured. If V_{ac} is constant, the output EMF of TE_1 is the same when each null is obtained, so that, directly from the definition of δ,

$$V_{ac} = \frac{V_d + V_r}{2}(1 + \delta).$$

In the deflection method the deflections D_1 and D_2 are read with S_1 to the right and to the left, respectively. With the direct voltage reversed, deflections D_3 and D_4 are read in the same way. For each reading the direct voltage is held constant at the nominal value V_0. Then

$$\frac{V_d - V_o}{V_o} = s(D_2 - D_1) \quad \text{and} \quad \frac{V_r - V_o}{V_o} = s(D_4 - D_3)$$

where V_d and V_r are now the direct voltages in the direct and reversed position, respectively, that would have to be applied in place of the alternating voltage to produce the observed deflections D_2 and D_4, and s is the scale sensitivity factor.[14] Then

$$\frac{V_d + V_r}{2} = V_o(1 + s\Delta D)$$

where $2\Delta D = D_2 - D_1 + D_4 - D_3 = 2(D_{ac} - D_{dc})$.

The alternating voltage required to produce the same average deflection is, by the definition of ac-dc difference,

$$V_{ac} = \frac{V_d + V_r}{2}(1 + \delta) = V_o(1 + \delta + s\Delta D),$$

neglecting second-order terms.

The scale factor s is readily determined by momentarily shunting the 0.5 volt range, consisting of the heater of TE_1, with a resistor $R_s = 100$ KΩ as shown in Fig. 5. This decreases the current through TE_1 slightly and is equivalent to decreasing the input voltage to that converter by a proportional amount, $p = 5\times10^{-4}(V_r - 0.5)/V_r$, where V_r is the voltage range in use. From this, $s = p/D_s$, where D_s is the resulting change (considered positive) in galvanometer deflection.[15] The scale factor need not be known accurately, since only small differences between the nominal and actual applied voltages are involved. In practice it can be measured at several points and graphed as a function of V/V_r. It should, of course, be rechecked at one point occasionally.

More complete formulas for the deflection method of using the DTVC can be developed to take into account

[14] The change in voltage that is required to produce a 1 division deflection of the galvanometer.

[15] With the galvanometer now used, s is approximately 1×10^{-5}/mm (i.e., 10 ppm/mm) at rated voltage on all ranges. A more sensitive galvanometer can be used if necessary.

small errors arising because the detector has a linear instead of a quadratic scale, because the EMF vs. heater current characteristic of the two thermoelements may be different for the two directions of direct current, and because of other small aberrations. However, if the deflections and the dc reversal differences do not exceed 0.1 percent of the applied voltage, the resulting corrections are all less than 1 ppm.

For both the null and deflection methods, the direct voltage must be constant to perhaps 0.05 percent during each sequence of measurements, because the input output characteristics of the two thermoelements are not perfectly matched. Since the load on the dc source changes when the selector switch is operated, the internal resistance of this source must not exceed about 50 mΩ/V or the source must be readjusted. It would be desirable to add another set of resistors on the ac range switch and another pole on the selector switch to keep the load constant.

Author's Note: Other systems for accurately measuring dc voltages, with a different type of divider that is used also for the volt box calibration, have been disclosed. See for example:
DC Parameter Measurement by the Rationmetric Method, Loebe Julie, Data Systems Engineering March and June, 1964.
Making Measurements to standards Accuracy, Loebe Julie, Electronic Industries, September 1964.

Reprinted from IEEE TRANSACTIONS
ON *INSTRUMENTATION AND MEASUREMENT*
Volume IM-14, Number 4, December, 1965

PREPRINT INSTRUMENT SOCIETY of AMERICA
21st Annual ISA Conference and Exhibit • October 24-27, 1966, New York
Preprint Number 12.3-1-66

A COMPARATOR FOR THERMAL AC-DC TRANSFER STANDARDS

by Raymond S. Turgel, Physicist
National Bureau of Standards
Gaithersburg, Maryland

ABSTRACT

Thermal transfer standards play an important role in precision a-c measurements. They are calibrated by intercomparison with standards of known ac-dc difference. A comparator is described that simplifies such routine calibrations. A sequence of null balances in the measuring circuit operates a simple analog computer which indicates the result of the intercomparison directly in parts per million of ac-dc difference.

INTRODUCTION

Accurate a-c measurements in the audio frequency range depend on transfer standards which relate these measurements to the basic d-c units of current and voltage.

In recent years thermoelements and thermal voltage converters have been widely used as transfer standards especially at higher audio frequencies. They are convenient to use and are capable of accuracies of 100 ppm or better.[1,2,3]

A thermoelement generally consists of a heater in thermal contact with a thermocouple, but usually electrically insulated from it. The thermocouple output is a function of the heating effect of the heater current and to a first approximation is the same for direct current as for the equivalent rms alternating current. Actual characteristics deviate from those of the simplified model, and for certain geometric configurations limiting values for the departure from ideal conditions can be calculated, based on the thermoelectric properties of the materials used in construction.[1,4]

Since absolute calibration of transfer standards is not feasible, thermoelements must be intercompared to establish their inherent ac-dc difference. By selecting thermoelements of appropriate design and corroborating the calculated performance by experimental cross checks, NBS has established a group of thermoelements of known ac-dc difference with which other similar transfer standards can be compared.[5]

When high accuracy is required for the intercomparison a number of factors have to be taken into account. The output from the most commonly used thermoelements is obtained from a single thermocouple junction and is typically 10 mV. Multiple junction thermoelements with higher outputs have been constructed in England[6] and the USSR[7], but are not generally available. To achieve a resolution of a few ppm the system must be capable of sensing a voltage change of only a few nanovolts. This low voltage puts rather severe demands on the detector and associated circuitry which have to be designed to prevent noise and stray thermal emfs from masking the signal. A further complication is the temperature coefficient of the thermoelement itself, which often exceeds 0.1%/°C. Small changes in ambient conditions will therefore produce noticeable changes in output emf. The output is also affected by asymmetry in the construction with the result that the thermoelement response to d-c is dependent on the sign of the heater current. In some cases the observed change on reversal is considerably larger than can be explained from the geometry of the devices. Although manufacturers are making efforts to reduce this reversal effect it cannot be ignored when making precision measurements.

Fluctuations in the heater current will generally not produce identical changes in the outputs of two thermoelements being compared. This unequal response has to be considered in the circuit design since even with the stable power supplies now available some random fluctuations occur.

The measuring system therefore has to compensate for:

1. Ambient temperature drifts
2. D-C reversal effects
3. Power supply fluctuations

Since in a properly designed system the ambient temperature drifts are slow compared to the time it takes to make a measurement, the drift rate can be assumed to be constant. It is therefore possible to reduce the error from temperature changes by making a series of measurements arranged symmetrically in time. This same sequence can be used to average the output changes due to d-c reversal. Thus a sequence of comparison measurements using first a-c, then d-c forward, d-c reverse, and again a-c, made at uniformly spaced intervals will provide satisfactory compensation.[3]

The effect of power supply fluctuations can be reduced by a ratio circuit[5] which has proven

Superior numbers refer to similarly-numbered references at the end of this paper.

satisfactory in this respect. An adaptation of this circuit is discussed in detail in this paper.

THEORY

The ac-dc difference is defined as

$$D = (I_{ac} - I_{dc})/I_{dc} \text{ when } E_{ac} = E_{dc} \qquad (1)$$

where I denotes the heater current, and E the open circuit thermocouple emf. The subscripts indicate rms a-c or d-c excitation of the thermoelement heater. The relation

$$E = \text{constant} \times I^n \qquad (2)$$

is postulated for the thermoelements, where n is approximately equal to 2, but in practice may vary from 1.8 to 2.1.

Experimentally the comparator determines the quantity $D_T - D_S$ where D_T is the ac-dc difference of the "test" thermoelement, D_S the ac-dc difference of the "standard" thermoelement. (Similarly, other quantities are identified by the subscript T and S.)

As shown in the appendix

$$(D_T - D_S) = (1/n_S)\ (E_{Sac} - E_{Sdc})/E_{Sdc} \qquad (3)$$

This equation is valid only if the following conditions are maintained during actual measurements:

1. The output voltage of the "test" thermoelement must be the same when using alternating or direct current in the heater.

2. The heater currents in both "test" and "standard" thermoelements must be identical. For voltage transfer standards the equivalent condition requires that the voltages applied to the two thermal voltage converters (thermoelements in series with their range resistors) are equal to each other for both a-c and d-c heater currents.

The exponent n of equation (2) has to be determined separately for the operating range of the "standard" thermocouple. In practice n can be found using the relation $\Delta E/E = n(\Delta I/I)$, which is equivalent to equation (2), and measuring $\Delta E/E$ for a small change in current $\Delta I/I$. An accuracy of a few percent is sufficient for this measurement. Experience has shown that under normal condition n does not change with time.

From equation (3) it follows that the intercomparison is reduced to the experimental determination of the voltage ratio

$$(E_{Sac} - E_{Sdc})/E_{Sdc}$$

under the specified conditions. Because the difference of the two voltages in the numerator is small, considerably less accuracy is required if that difference can be measured directly instead of being calculated from the two values. It is therefore desirable to arrange the circuit so that this difference, or one equivalent to it, can be determined experimentally. In practice an intermediate step is required, because the "standard" thermoelement cannot simultaneously be excited with a-c and d-c to produce E_{Sac} and E_{Sdc}.

The basic circuit is shown in Figure 1. The outputs of the two thermoelements, E_T and E_S, are connected in series with polarities so that the sum of their emfs is connected across the voltage divider R. The divider can therefore always be adjusted to null the voltage across the detector, and proportional changes in E_T and E_S will not influence the null position.

If E_T remains constant and E_S varies the circuit will no longer be in balance. In a previous method[5] this unbalance was measured with a deflecting galvanometer. To calculate the ac-dc difference from the deflection measurements the sensitivity of the galvanometer had to be determined each time. In the present comparator a simpler procedure is followed. The detector is used only for null balance and therefore its sensitivity and linearity do not have to be taken into account. The ratio R is adjusted to an approximate balance and final null balance is achieved by injecting an emf E_A.

If a-c and d-c currents are applied to both thermoelement heaters in a time-symmetrical sequence as discussed before, then four values of E_A will be obtained, one for each null balance of the sequence. From these, using appropriate calibration factors, the ac-dc intercomparison value can be calculated.

$$\begin{aligned} E'_{Aac} &= E_{Sac} - E_{Tac} \\ E'_{Adc} &= E_{Sdc} - E_{Tdc} \end{aligned} \qquad (4)$$

where each of the E'_A values here are the averages of two readings.

With the condition given that $E_{Tac} = E_{Tdc}$ it follows that

$$E_{Sac} - E_{Sdc} = E'_{Aac} - E'_{Adc} \qquad (5)$$

combining equation (3) and (5) and noting that the denominator of (3) can be considered a calibration factor since it is independent of the ac-dc difference, we obtain the intercomparison value

$$D_T - D_S = (\text{calibration factor}) \times (E'_{Aac} - E'_{Adc}) \qquad (6)$$

DESIGN CONSIDERATIONS

The design objective set for this project was to produce a system that would reduce the effort involved in making routine intercomparisons of

thermoelements. An approach leading to full automation could economically not be justified, but preliminary studies showed that significant improvements over existing methods could be achieved without greatly increasing the complexity of the equipment. Within these limitations a set of specifications was formulated to incorporate the features deemed most desirable. These included:

1. A read-out giving the intercomparison value in parts per million of ac-dc difference without intermediate calculations;

2. The system to be self calibrating, with the built-in reference to require infrequent, if any, adjustment;

3. The system to be compatible with existing external a-c and d-c power supplies which may not be remotely programmable;

4. The system to be transportable in the sense that it can be moved easily within the laboratory.

To satisfy the first requirement a simple analog computer is incorporated into the system. Its function is to convert the ratio-circuit balancing adjustment into an electrical signal, store this signal, and then use it to compute the final result. The second requirement, the self calibrating feature, is part of the computer circuit. As described in the next section, by means of an internal comparison a calibration factor is obtained which is used to provide a readout in the desired units.

By using manual rather than servo adjustment of the power supplies, no particular difficulties arise with regard to compatibility. Since the time constants of different thermoelements vary, satisfactory servo control would in any case not be easily attainable.

To make the equipment movable within the laboratory no galvanometers or other devices needing firm supports are used. With minor modifications, in fact, all control circuits can operate from their own internal batteries, making the system independent of the power line, except for the power supplies to furnish the required test currents.

Battery operation has the additional advantage that circuits can be isolated to reduce spurious interaction with one another and with the thermoelements.

The preference for electronic detectors over galvanometers is prompted also by their faster response. To satisfy the requirement that the output of the "test" thermoelement remain constant throughout the set of measurements the emf has to be closely monitored. Thus essentially two measurements are necessary, the magnitude of the output E_T and the difference $E_S - E_T$. It seemed preferable to obtain the two null balances sequentially rather than simultaneously. Thus only one adjustment at a time is required and only a single detector is used. The detector, however, must then have a response time of not more than about 1 second, and must have a fast recovery from overload.

As shown in the appendix the error in the difference measurement due to power supply fluctuations is reduced by a factor of 10 in a typical case. Thus although the sequential system relies on the short term stability of the power supplies, many commercial power supplies are adequate.

PRINCIPLE OF OPERATION

Figure 2 is a block diagram of the comparator system showing the various functional components. In normal operation, either alternating or direct current is applied to the "test" and "standard" thermoelements in a prearranged sequence determined by the power selector switch. The outputs of the two thermoelements are fed into the ratio circuit which has been set initially to an approximate balance.

To satisfy the condition $E_{Tac} = E_{Tdc}$, the appropriate power supply is adjusted until the output of the "test" thermoelement is equal in magnitude to a reference voltage of opposite polarity. Equality of the two voltages is determined by connecting the null detector to the summing point. The magnitude of the reference voltage is approximately equal to the output of the thermoelement at the nominal operating point.

The null detector is then switched to the ratio circuit to measure the unbalance between the "test" and "standard" thermoelement outputs. To restore the ratio null balance a balancing voltage is added to the output of the "standard" thermoelement. This balancing voltage is generated by adjusting the analog computer. Four such voltage adjustments are made, one for each step of the AC, DC, DC-R, AC measuring sequence. The resulting four voltages are retained by the computing circuit and combined to give the final readout value. The power selector switch is linked mechanically to switching sections in the analog computer to coordinate the operation. The calibration network provided determines a proportionality constant relating the balancing voltage to the analog voltage. This constant is experimentally determined prior to the set of measurements using a self-calibration circuit not indicated on the block diagram.

The calibrating procedure compares a fixed known fraction of the output emf of the "standard" thermoelement with the balancing voltage generated when the analog computer is set to give a "full scale" reading. The calibrating network is adjusted until the balancing voltage equals this fraction of the output emf. By proper choice of the voltage divider, the output reading is then expressed in parts per million of I_{Sdc} in accordance with equations (1) and (6). The voltage divider which for this purpose has to be accurate only to

the order of a tenth of a percent is formed by two stable resistors and should not require periodic adjustments.

Thus the comparison measurement reduces to a calibration adjustment, followed by four successive ratio balances each preceded by a rapid emf check of the "test" thermoelement. After the last ratio balance, the analog computer provides a readout of the relative ac-dc difference of the thermoelements being compared.

CIRCUIT DESCRIPTION

The simplified circuit diagram, Figure 3, shows the main components in more detail. The outputs of the "test" and "standard" thermoelements are connected in series with the ratio resistor R_3 which is a 500-ohm Kelvin-Varley divider with three switched decades followed by a ten-turn voltage divider. This high resolution permits the initial ratio adjustment to be made easily so that the balancing voltages for the final null adjustment can be kept as small as possible. The range of the balancing adjustment is approximately 2 1/2 times the "full scale" indication in ppm, but precision of readings is improved if the balancing voltage is kept small.

The null detector is connected to the ratio circuit through a three-position low thermal emf switch with spring return to the center position. The third position of the switch is used to monitor the output of the "test" thermoelement with the null detector by comparing the reference voltage across R_4 with the thermocouple emf. The reference-voltage adjustment is also a Kelvin-Varley circuit with two switched decades and a ten-turn divider used as a current divider. Power is supplied from a mercury battery in an external battery compartment.

When calibrating the system, the "standard" thermocouple is disconnected from the ratio circuit so that its open circuit emf is applied across the voltage divider formed by R_2 and R_1. The small fraction of the emf across R_1 is nulled by the equal and opposite voltage drop produced across R_1 by a current derived from the analog and calibration circuits as described before.

Parts of the circuit enclosed by the dotted line on Figure 3 are contained in a carefully shielded and thermally lagged enclosure to minimize thermal emfs, leakage, and induced currents. Connection to the thermoelement outputs is made through gold-plated copper binding posts.

The power and control circuits are mounted on a separate panel. They are linked mechanically by the selector switch, but shielded from one another by a separate enclosure surrounding the power terminals and switch sections.

The analog computing section consists of four adjustable voltage dividers each connected across two mercury batteries providing a voltage output range from -1.35 volts to +1.35 volts. Each divider is associated with one of the four ratio balances required in the measurement sequence. In turn each adjustable voltage is connected to R_1 in series with the calibration and range selecting networks. To avoid confusion, the particular divider that is connected at the moment is identified by a pilot light controlled by the selector switch (not shown). After the measuring sequence has been completed, the four voltages that are now "stored" in the dividers are connected in series across the readout vacuum-tube voltmeter (VTVM), which has been calibrated to indicate parts per million of ac-dc difference by the calibration procedure. Switching circuits provide correct polarities of the "stored" voltages so that the sum of the d-c measurements is subtracted from the sum of a-c measurements.

Three full-scale ranges of ±50 ppm, +250 ppm, and +1250 ppm can be selected with a range switch. For routine intercomparisons, the 250 ppm range is generally appropriate. The "n_s" value (equation 3) is preset on a switch (see Figure 3) which modifies the sensitivity of the VTVM so that the relative meter indications are inversely proportional to n_s. Using the input impedance R_v of the VTVM as part of a voltage divider, the "n" switch adds resistance R_n, given by $R_n/R_v = (n_s/n') - 1$. In the particular design $n' = 1.80$ which represents therefore the lowest value that can be selected.

Since the calibration network resistors as well as the VTVM are used in essentially the same connection during calibration as during actual measurements, their long term stability does not influence the result. It is required only that they remain the same to 0.1 percent during the relatively short period of the measurement. As already mentioned the calibration essentially depends only on the ratio of R_1 to R_2 and on the ratio of the resistors in the range switch. Since these ratios have to be accurate to only 0.1 percent the long term stability requirement is easily satisfied.

PERFORMANCE

Intercomparisons of thermoelements were carried out on a number of voltage and current ranges. Table 1 shows the typical dispersion of readings using two thermal voltage converters (5 mA thermoelements and appropriate range resistors) at three frequencies in the audio spectrum. The term "reading" here refers to the result of a sequence of four measurements as described. The standard deviation for a reading is calculated from the data shown.

The particular converters used in this test agreed to 2 ppm or better, as established by previous calibrations. It will be seen that all readings except some at 50 kHz and 300 volts fall within the limit of ±10 ppm. The lower precision at 50 kHz is probably caused by greater fluctuations in the power supply.

Using two sets of high-current thermoelements which had not been intercompared before, readings

were obtained on 1, 3, 5, and 10 ampere ranges as shown in Table 2. With a few exceptions the readings fall into a ±10 ppm interval about the average. The scatter is slightly larger than with the voltage readings, which again is probably a consequence of the lower stability of the current source. All readings however are well within the present accuracy limits of 200 ppm set for the ac-dc difference determinations of thermal transfer standards at NBS.

CONCLUSIONS

A system has been designed for routine intercomparisons of thermal ac-dc transfer standards. The design aims of reducing the effort involved in making these measurements have been attained without greatly increasing the complexity of the equipment. Results obtained in tests agree with those of other methods[5] to within 10 ppm on most current and voltage ranges in the audio frequency range.

APPENDIX

The ac-dc difference D is defined as

$$D = \frac{I_{ac} - I_{dc}}{I_{dc}} \tag{1A}$$

when

$$E_{ac} = E_{dc} \tag{2A}$$

where I is the thermoelement heater current and E is the thermoelement output voltage generated by the thermocouple.

The following relations are postulated for thermoelements:

$$\begin{aligned} E_{dc} &= KI_{dc}^{n} \\ E_{ac} &= K'I_{ac}^{n} \end{aligned} \tag{3A}$$

where K and K′ are constants and the exponent n is the range of 1.8 to 2.1.

From equations (2A) and (3A) we have

$$KI_{dc}^{n} = K'I_{ac}^{n}$$

and thus

$$I_{ac} = (K/K')^{\frac{1}{n}} I_{dc} \tag{4A}$$

Substituting equation (4A) into (1A)

$$D = [(K/K')^{\frac{1}{n}} - 1] \tag{5A}$$

Since K and K′ are very nearly equal we can write $K' = K(1 - q)$ where $q \ll 1$.

Expanding $(K/K')^{\frac{1}{n}} = (1 + q/n + \ldots)$ neglecting higher terms and substituting in (5A) we have

$$D = \frac{q}{n} \tag{6A}$$

Designating the "test" thermoelement with the subscript "T" and the "standard" with "S", we have the following conditions for null balance for direct current:

$$\begin{aligned} I_{Tdc} &= I_{Sdc} \\ E_{Tdc} &= E_{ref} \\ \frac{E_{Sdc} - E_{Adc}}{E_{Tdc}} &= r \end{aligned} \tag{7A}$$

where E_A is the balancing voltage and r = ratio of voltage divider R (figure 1).

And similarly for alternating current:

$$\begin{aligned} I_{Tac} &= I_{Sac} \\ E_{Tac} &= E_{ref} \\ \frac{E_{Sac} - E_{Aac}}{E_{Tac}} &= r \end{aligned} \tag{8A}$$

Combining (7A) and (8A) and dividing by E_{Sdc}

$$\frac{E_{Sac} - E_{Sdc}}{E_{Sdc}} = \frac{E_{Aac} - E_{Adc}}{E_{Sdc}}$$

From (3A) and (6A)

$$\frac{E_{Aac} - E_{Adc}}{E_{Sdc}} = \frac{K_S I_{ac}^{n_S} (1 - n_S D_S) - K_S I_{dc}^{n_S}}{K_S I_{dc}^{n_S}} = \frac{I_{ac}^{n_S} (1 - n_S D_S) - I_{dc}^{n_S}}{I_{dc}^{n_S}} \tag{9A}$$

Since $E_{ref} = E_{Tac} = E_{Tdc}$ we obtain from (1A)

$$I_{ac} = I_{dc} (1 + D_T)$$

Raising the equation to the $n_S{}^{th}$ power, and neglecting higher terms in D_T of the expansion, since

$D_T \ll 1$, we have

$$I_{ac}^{n_S}(1 - n_S D_S) = I_{dc}^{n_S}(1 + n_S D_T - n_S D_S)$$

and therefore (9A) can be written as

$$D_T - D_S = \frac{1}{n_S}\left(\frac{E_{Aac} - E_{Adc}}{E_{Sdc}}\right) \qquad (10A)$$

In actual practice there is some error in adjusting E_T so that

$$E_{Tac} = E_{ref}(1 + y)$$

It can be shown that equation (10A) then becomes

$$D_T - D_S = \frac{1}{n_S}\left[\frac{E_{Aac} - E_{Adc}}{E_{Sdc}} + y\left(1 + \frac{E_{Adc}}{E_{Sdc}} - \frac{n_S}{n_T}\right)\right] \qquad (11A)$$

In a typical case the difference between n_S and n_T might be 10 percent. E_{Adc}/E_{Sdc} is designed to have a maximum of 700 ppm (250 ppm range). Even if one assumes a relatively large error in the adjustment of the output emf of the "test" thermoelement, that is

$$y = 100 \text{ nV}/5 \text{ mV} = 20 \text{ ppm}$$

the error term of (11A) will still be negligible.

$$\text{Error term} = 1/2 \times 20 \times 10^{-6}(1 + 700 \times 10^{-6} - 0.9)$$

$$= 1 \text{ ppm}$$

In the calibration procedure the balancing voltage E_A is adjusted to be equal to a fraction of the output voltage of the "standard" thermoelement (figure 3).

$$E_A' = \frac{R_1}{R_1 + R_2} E_{Sdc} \qquad (12A)$$

E_A' is obtained by setting the voltage in the analog computer to give a full scale reading on the VTVM (250 ppm) and adjusting the calibration network to obtain a null in the detector.

A particular value n_S' (= 1.8) is chosen in the calibration procedure for convenience in the circuit. An arbitrary choice does not influence the validity of the calibration obtained, because n_S is adjusted independently for the actual measurement. A different choice for n_S' would require a corresponding change in the ratio of R_1/R_2.

If D is the full scale indication of the readout, then, rearranging equation (10A) we have

$$2n_S' D_F = (E_{Aac} - E_{Adc})/E_{Sdc} \qquad (13A)$$

The factor of 2 is introduced because two pairs of E_A values are obtained in the measuring sequence. Combining (12A) and (13A)

$$2E_A'/E_{Sdc} = (E_{Aac} - E_{Adc})/E_{Sdc}$$

and therefore,

$$R_1/(R_1 + R_2) = 2n_S' D_F$$

Substituting numerical values

$$D_F = 250 \text{ ppm}, \quad n_S' = 1.8$$

then,

$$R_1/(R_1 + R_2) = 900 \text{ ppm}$$

and $R_1 = 18$ ohms, $R_2 = 20{,}000$ ohms.

ACKNOWLEDGEMENTS

The author thanks Mr. D. R. Flach of the Electrical Instruments Section of the National Bureau of Standards for assistance in testing the system and making the intercomparison measurements.

REFERENCES

1. Hermach, F. L., Thermal Converters as AC-DC Transfer Standards for Current and Voltage Measurements at Audio Frequencies, J. Res. NBS, Vol. 48, No. 2, pp. 121-138 (Feb. 1952).

2. Hermach, F. L., AC-DC Transfer Instruments for Current and Voltage Measurements, IRE Trans. on Instrumentation, Vol. I-7, No. 3 and 4, pp. 235-240 (December 1958).

3. Williams, E. S., Practical Aspects of the Use of AC-DC Transfer Instruments, NBS Technical Note 257.

4. Widdis, F. C., The Theory of Peltier and Thomson-Effect Errors in Thermal AC-DC Transfer Devices, Institution of Electrical Engineers (London), Monograph No. 497A (January 1962)

5. Hermach, F. L., and Williams, E. S., Thermal Converters for Audio Frequency Voltage Measurements, IEEE Trans. on Instrumentation and Measurement (to be published in 1966).

6. Wilkins, F. J., Multijunction Thermal Converters, The Institution of Electrical Engineers, Proceedings, Vol. 112, No. 4, pp. 794-805, (April 1965).

7. Rozhdestvenskaya, T. B., Electrical Comparators for Precise Measurements of Current, Voltage, and Power, p(111) Translation JPRS:29,373 (TT:65-30626), U. S. Dept. of Commerce, Clearinghouse for Federal Scientific and Technical Information.

Table 1

Relative AC-DC Difference of Pairs of Thermal Voltage Converters
(parts per million)

Frequency	50 Hz	10 kHz	50 kHz
Voltage Range	20V	100V	300V
$D_T - D_S$	-1	-2, +2, -1, +1	-10
	+3	+1, 0, -2, 0	-12
	0	0, -2, 0, +2	-12
	+3	+1, -2, -2, +2	- 4
	+2	-4, -1, 0, +4	- 6
Mean	1.4	-0.15	- 8.8
Standard Deviation	1.7	1.8	6.0
No. of Readings	5	20	5

Table 2

Relative AC-DC Difference of Pairs of High Current Thermoelements
(parts per million)

Frequency	10 kHz				50 kHz			
Current Range	1 A	3 A	5 A	10 A	1 A	3 A	5 A	10 A
$D_T - D_S$ (ppm)	0	-3	-15	+ 2	0	+ 8	- 7	-2
	-1	+1	-30	- 6	+6	+10	- 6	+4
	-4	-1	-12	+ 4	-3	+ 8	-11	0
	+8	+5	- 6	- 5	+2	+14	- 8	-1
	-4	-1	-17	-11	0	+20	- 4	-2
Mean	-3.2	0.2	-16	- 3.2	1.0	12	- 7.2	-0.2
Standard Deviation	9	3	9	7	3	5	3	2
No. of Readings	5	5	5	5	5	5	5	5

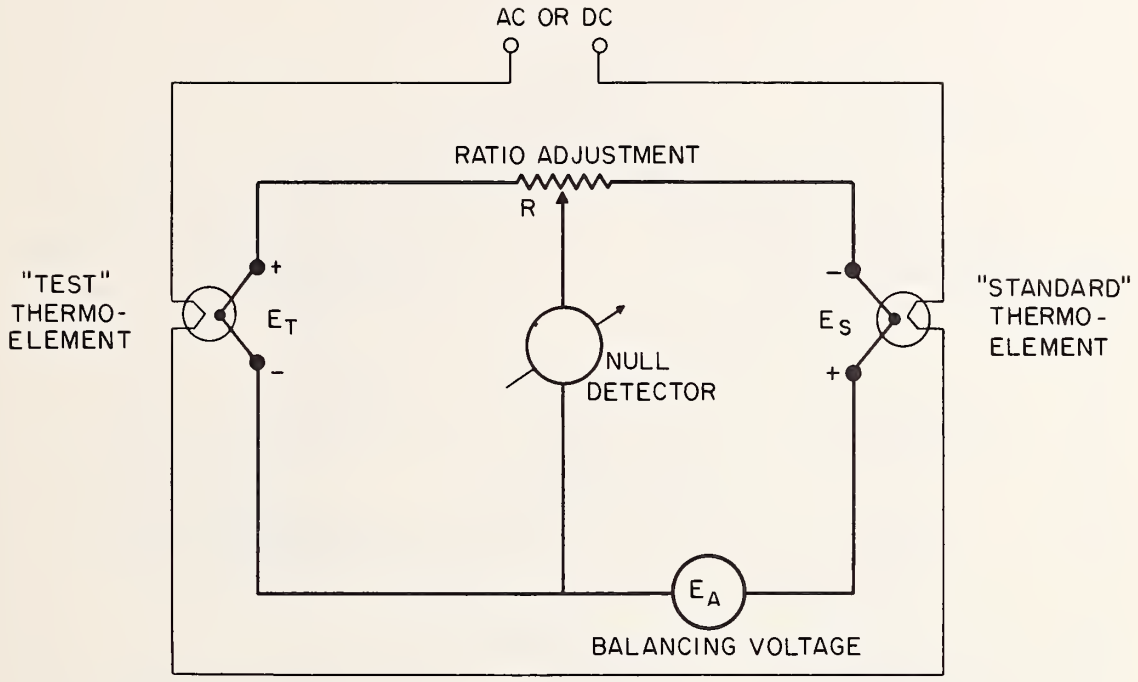

FIG. 1 BASIC CIRCUIT OF
THERMOELEMENT COMPARATOR

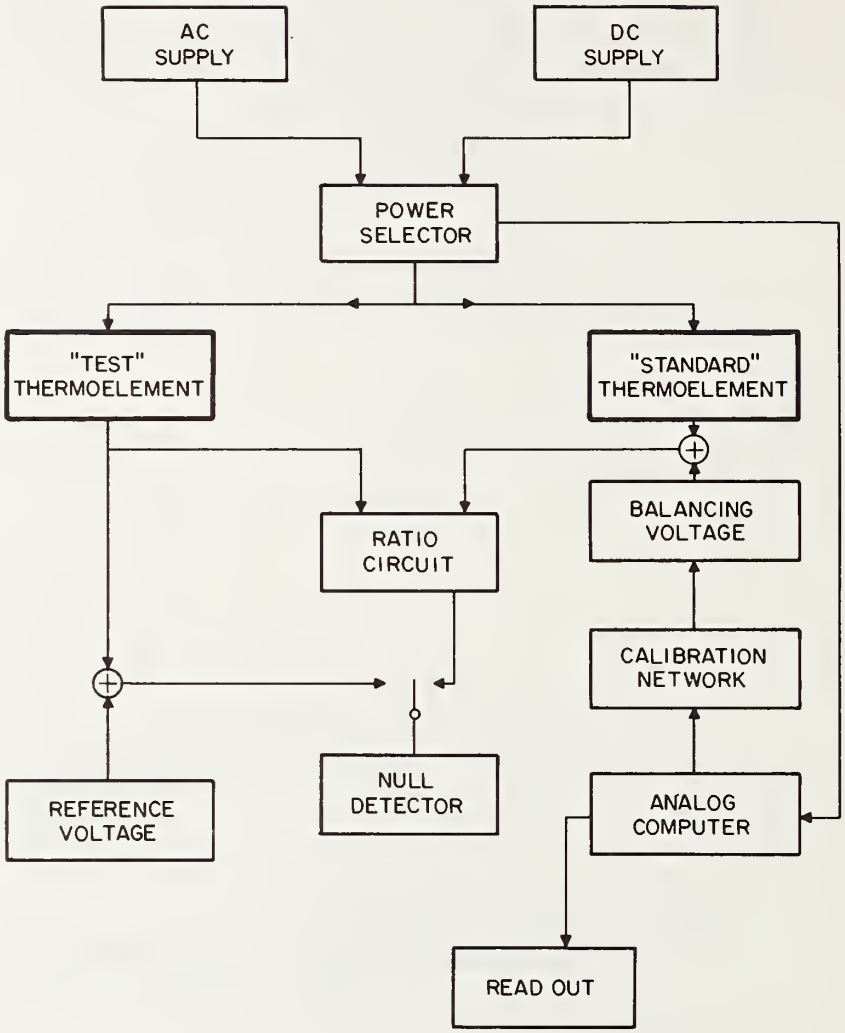

FIG. 2 THERMOELEMENT COMPARATOR

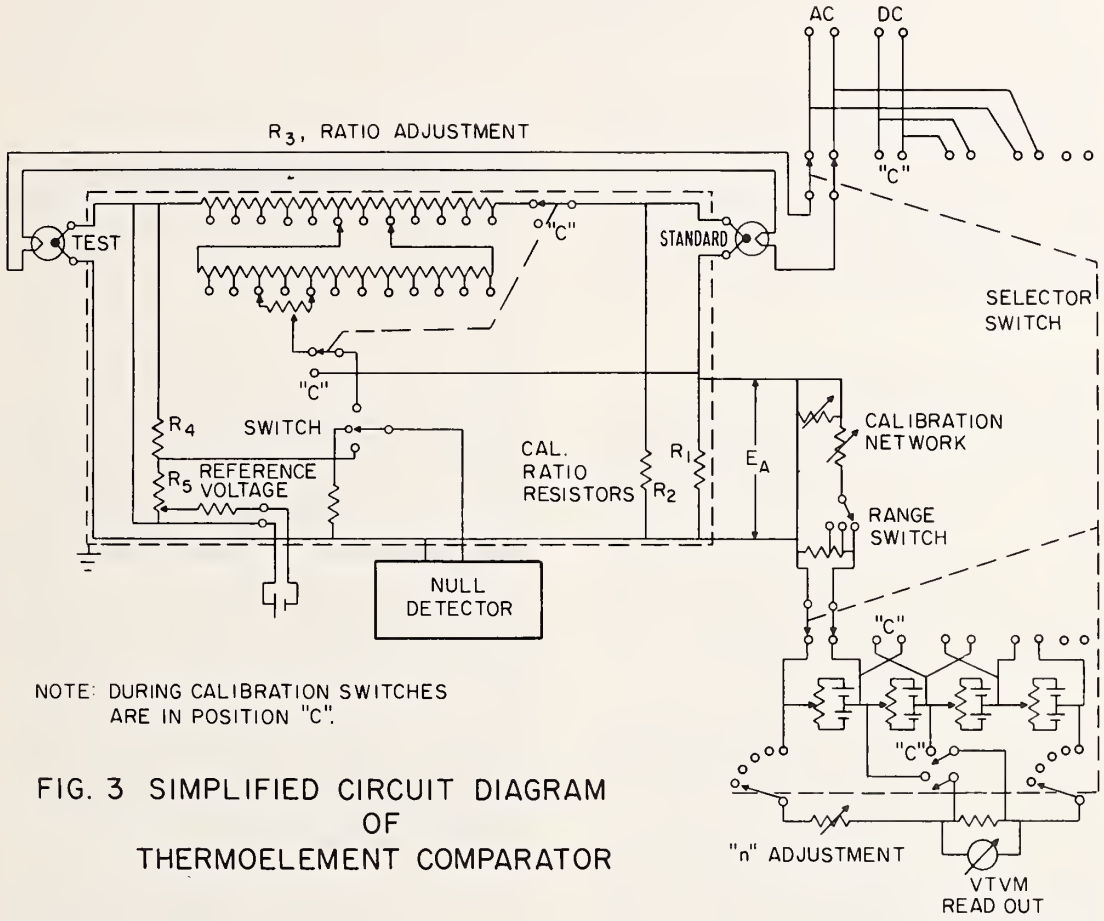

NOTE: DURING CALIBRATION SWITCHES ARE IN POSITION "C".

FIG. 3 SIMPLIFIED CIRCUIT DIAGRAM OF THERMOELEMENT COMPARATOR

PREPRINT INSTRUMENT SOCIETY of AMERICA
20th Annual ISA Conference and Exhibit • October 4-7, 1965, Los Angeles
Preprint Number 14.2-3-65

CALIBRATION OF PEAK A-C TO D-C COMPARATORS*

By: Donald Flach, Physicist
Louis A. Marzetta, Electronic Engineer
National Bureau of Standards
Washington, D. C.

ABSTRACT

Recent developments in commercial electronic power supplies have made practical the use of peak a-c to d-c comparison for measuring a-c voltage.[1,2] This paper describes two methods that have been developed at NBS for testing peak a-c to d-c comparators at the 10 and 20 volt level over a frequency range of 50 Hz to 4800 Hz. These two methods yield results which agree well within 50 parts per million (ppm).

PEAK A-C TO D-C COMPARATORS

A commercially available peak a-c to d-c comparator (see Fig. 1) uses a pair of precision summing resistors, one of which is connected to the a-c, the other to the d-c voltage, for the basic a-c to d-c comparison.[1,2] The summing resistors are followed by diodes which clip off all but a small portion of the composite wave. Following the diodes is a chopper which provides a ground reference, a X1, X10 amplifier, an output limiter, and an oscilloscope which is connected to the output as a null detector. This instrument has a frequency range of 0-20 kHz and is capable of measuring up to 20 volts peak.

Another type of peak a-c to d-c comparator, which operates on a time-gate principle[3], was constructed at NBS. This instrument was designed to operate over a frequency range from 50 to 2400 Hz, and with a 10 volt peak input. The basic idea in the development of a new peak comparator was to search for a circuit that would offer a simple, direct comparison of the peak of a sine wave with a precision d-c source, with a common ground connection for both sources. It was expected that the desired simplicity would place some restrictions on operational flexibility, but the purpose is a laboratory standard and not an instrument capable of operating under adverse conditions. In the design of the instrument, the use of precision summing resistors was avoided in order to obtain an independent method for calibrating the summing type comparators.

This system uses a pair of synchronized relays to slice out a section of the sine wave at its peak (see Fig. 2). Figure 3 shows the basic operating principle of the time-gate comparator. For the major portion of the sine wave, the relays are connected to the d-c voltage. The relays are connected to the a-c voltage for a brief interval as this a-c voltage passes through its peak value. They are then switched back to the d-c voltage for the remainder of the cycle. The comparator is balanced when the peak of the a-c signal is aligned with the d-c voltage line.

In operation, the input a-c voltage is clipped and is used to initiate a trigger circuit whose function is to generate synchronizing pulses occurring at the zero crossing of the sine wave. Since electro-mechanical relays cannot function at the higher speeds, six binary stages have been incorporated for the purpose of dividing the input frequency. A seven position switch allows the selection of a 1/1 to 1/64 frequency division, chosen to give a relay operating speed of about 50 operations per second. Thus, for example, a 2400 Hz input would be divided by a factor of 64 at the last binary. This lower frequency can be used to drive the relays. For this purpose a power amplifier is located after the dividers. By means of phase-delay adjusting resistors, the closing time of the relays can be set to provide a time gate situated at the peak of the sine wave. For the example stated above, the gate would be located at the peak of every 64th cycle of the 2400 Hz input potential. No information is lost by this procedure; however, the oscilloscope trace must have sufficient brilliance to present a usable expanded pattern in a low duty cycle.

The 10-volt d-c supply located between the relay output and amplifier input reduces the 10-volt average output from the relays to a level which will not overload the amplifier. The putpose of the amplifier is to provide the proper transfer circuit between the output of signal relays and the oscilloscope input. A first requirement in considering a choice of design is the degree of amplification itself. For oscilloscopes having a vertical deflection sensitivity between 0.01 and 0.1 volts per cm, the instrument amplifier should have an amplification factor between 10 and 100. An input impedance of at least 100,000 ohms was chosen to reduce loading errors to less than 10 ppm. The amplifier was designed with a bandwidth

Superior numbers refer to similarly-numbered references at the end of this paper.

in excess of 1 MHz so that the decrease in response at the highest signal frequency was less than 10 ppm.

All possible storage elements such as capacitors were deleted in the interest of quick recovery. Reactive feedback components were avoided in order to achieve an ideal flat frequency response with the desirable upper frequency roll-off characteristic. Amplification stability and quiescent d-c output level stability were compromised in order to achieve a flat frequency response. A simple control is provided for the adjustment of output d-c level.

CALIBRATION OF PEAK COMPARATORS WITH DIFFERENTIAL THERMOCOUPLE VOLTAGE COMPARATOR

The Differential Thermocouple Voltage Comparator[4] (DTVC) may be used for simultaneous comparison of rms a-c and d-c voltages. If the wave form is known, it is possible to use the instrument, in combination with a suitable transformer, for checking peak a-c to d-c comparators.

Figure 4 is a schematic of the DTVC. This instrument has two nearly identical voltage converters, as shown in Fig. 4 and in the simplified diagram in Fig. 5, each consisting of a chain of resistors in series with the heater of a thermoelement. The two thermoelement outputs are permanently connected in opposition and to a galvanometer, G. Voltage ranges from 0.5 to 500 volts are available with a frequency response of 20 Hz to 50 kHz. The use of separate resistors to reduce reactance errors for each range, shielding and isolation of a-c and d-c converters, and rf filters on the thermoelements, combine to reduce ac-dc transfer errors to 10 ppm or less for this instrument.

Figure 5 is a schematic diagram of the circuit used to test peak comparators with the DTVC. The ac-dc difference of a peak a-c to d-c comparator is evaluated by adjusting the d-c voltage to balance the peak comparator, and then measuring the difference between the rms a-c and d-c voltages with the DTVC.

A deflection method is used so that it is necessary to know the scale factor of the galvanometer. A built-in 0.05 percent sensitivity check enables the operator to calibrate the galvanometer scale on all but the lowest range. A galvanometer shunt is used to adjust the scale factor to a value convenient for computation.

With the applied voltages adjusted to balance the peak comparator under test, the AV converter (shown at the left in Fig. 5) is switched to the d-c and a-c voltages respectively, and the corresponding galvanometer deflections D_1 and D_2 are read. With the d-c voltage reversed, and the peak comparator again balanced, (to eliminate d-c reversal errors in the DTVC and to measure both the positive and negative peak) corresponding deflections D_3 and D_4 are read in the same way.* Then, as shown in appendix 3 of reference 3,

$$V_{ac} = V_0(1 + s\Delta D + \delta) \qquad (1)$$

where V_{ac} is the rms a-c voltage and V_0 is the nominal d-c voltage, s is the sensitivity factor (in proportional parts per division) and δ is the ac-dc difference of the AV converter of the DTVC, (defined as the proportional difference between the a-c and average d-c voltages required to produce the same output of this converter). ΔD is equal to $1/2(D_{ac} - D_{dc})$ where D_{ac} is the sum of the two galvanometer deflections with a-c voltage applied to the AV converter, and D_{dc} is the sum of the two galvanometer deflections with d-c voltage applied to both converters.

If the ratio of the peak to the rms values of the waveform is $\sqrt{2}$ (the same as for a sine wave), and the voltage ratio of the transformer in Fig. 5 is N, the peak value of the a-c voltage applied to the peak comparator is

$$V_p = \sqrt{2}NV_{ac} \qquad (2)$$

where V_{ac} is the output rms voltage of the a-c supply. Let $N = (1/\sqrt{2})(1 + n)$, where n is the small ratio correction factor, and define the ac-dc difference of the peak comparator as

$$\delta_p = \frac{V_p - V_o}{V_o}. \qquad (3)$$

Combining equations (2) and (3) results in:

$$\delta_p = \frac{V_{ac} - V_o}{V_o} + n\frac{V_{ac}}{V_o}. \qquad (4)$$

Then by changing eq (1) to the form of an ac-dc difference expression, substituting it in eq (4) and neglecting second order terms

$$\delta_p = \delta + n + s\Delta D. \qquad (5)$$

Distortion in the a-c source may introduce an error into the peak measurement. The harmonics in the output of the power-suppy-transformer combination were measured with a commercial wave

*A modification of the above procedure, which was used in most of the tests described in the report, is to follow the above procedure for the first two steps. On step (3) the peak comparator is not rebalanced. Step (4) remains the same. A second set of four readings is taken to measure the peak of the opposite polarity by reversing the d-c voltage. Thus eight readings are required to calibrate the test instrument, but this method is more convenient than the four-step procedure.

analyzer preceded by a twin-T network tuned to reduce the fundamental by at least 60 dB. The results are givn in table 2. Supplementary measurements with a Wien bridge constructed of wire-wound resistors and air capacitors of negligible voltage coefficient verified that the twin-T network did not introduce appreciable distortion. The effect of even harmonic distortion on the calibration is virtually eliminated by measuring both the positive and negative peaks and taking the average. Odd harmonics introduce an error which depends (among other things) on the phase relationship of the distorting harmonic to the fundamental. At the present time there is no known method of measuring this phase relationship; therefore, in the worst case there is an uncertainty in the results equal to the arithmetic sum of the odd harmonics.

A requirement for peak a-c to d-c comparison is the need for high cycle-to-cycle stability in the a-c source. Typically the a-c source used in these tests varied from cycle to cycle by less than 30 ppm, with occasional extremes of 100 ppm. With a little practice the operator could visually reduce the effect of cycle-to-cycle variations and ignore the occasional extremes.

By using the a-c supply to trigger the oscilloscope, a presentation of a single peak is obtained. With an oscilloscope sensitivity of 10mV/cm, changes as small as 10 ppm between the a-c and d-c voltages may be detected when the peak comparator has a voltage gain of 10, and is operating at 10 volts peak.

INTERCOMPARISON OF PEAK COMPARATORS

Figure 6 is a block diagram of the intercomparison circuit. For these tests the a-c supply was kept fixed at a value of 10 volts peak. This a-c amplitude was compared with a d-c voltage which was adjusted, in turn, to balance each comparator by means of an oscilloscope. The voltage settings of the precision d-c supply were recorded in each determination. This difference between the d-c voltage settings is equal to $\delta_{TG} - \delta_S$, where δ_{TG} is the ac-dc difference of the time-gate comparator, and δ_S is the ac-dc difference of the summing-type comparator. This may be shown as follows:

$$\delta_{TG} = \frac{V_{ac} - V_{o\,(TG)}}{V_o} \qquad (6)$$

$$\delta_S = \frac{V_{ac} - V_{o\,(S)}}{V_o} \qquad (7)$$

where V_{ac} is the a-c voltage when the comparator is balanced,

$V_{o(TG)}$ is the d-c voltage when the time-gate comparator is balanced,

$V_{o(S)}$ is the d-c voltage when the summing type comparator is balanced,

V_o is the nominal d-c voltage.

A rearrangement of the terms in equation (6) and (7) results in:

$$\frac{V_{o(TG)}}{V_o} = \frac{V_{ac}}{V_o} - \delta_{TG} \qquad \frac{V_{o(S)}}{V_o} = \frac{V_{ac}}{V_o} - \delta_S .$$

Assuming that the a-c voltages are equal, and subtracting the second equation from the first gives:

$$\frac{V_{o(S)} - V_{o(TG)}}{V_o} = \delta_{TG} - \delta_S . \qquad (8)$$

This type of test requires highly stable a-c and d-c supplies. The d-c supply stability has been measured and is 1 ppm/10 minutes, the a-c supply is stable to better than 20 ppm/10 minutes.

If the ac-dc difference of one peak comparator is measured with an rms standard, the comparator may then be used to calibrate another peak comparator without additional waveform error even if a different a-c source is used. However, a waveform error may, or course, result if the peak comparator is used for rms voltage measurements with a source of different harmonic content.

TEST RESULTS

Table 3 shows the results of the ac-dc difference tests on the two types of comparators using the circuits shown in Fig. 5. This table also shows the results of the direct intercomparison tests using the circuit shown in Fig. 6. The relative ac-dc differences, $\delta_S - \delta_{TG}$, compiled from the two methods agree to well within 20 ppm.

The positive sign in the $\delta_S - \delta_{TG}$ differences compiled from the direct intercomparison tests indicates a higher d-c voltage with the NBS comparator than with the summing comparator, for the same a-c source value. Note that all the differences are in one direction. This indicates a small but real offset in one of the comparators. Some portion of this offset would manifest itself as a systematic error in the case of other determinations involving the comparator.

The results are shown to the nearest ppm for the comparison of the different methods. It is not to be implied that the values of ac-dc differences are correct to one ppm.

The results given in table 3 are the average of a number of determinations made over a period of months. The standard deviations of the individual measurements on which the averages were based were less than 15 ppm. However, earlier measurements, (which were made while the calibration system was being investigated), and

other arrangements of connections showed occasional unexplained shifts of up to 30 ppm. The estimated overall uncertainty in the calibration of a peak comparator, including allowances for systematic errors and for three times the standard deviation of an average of four determinations, is less than 50 ppm with the time-gate comparator as the standard. It is less than 50 ppm from 400 through 2400 Hz with the DTVC as the standard, but must be increased to 100 ppm at 50 and 4800 Hz because of the waveform uncertainty already discussed. The agreement to 30 ppm or better between the two methods (lines 2 and 4 in table 3) indicates that the actual waveform error is very probably considerably less than this.

Because of the freedom from waveform errors, peak comparators are now tested by NBS with the time-gate comparator at 10 volts, at 50, 400, 1000, and 2400 Hz, with a conservatively stated accuracy of 100 ppm. Testing of peak comparators at 4800 Hz (outside the range of the time-gate comparator) will continue to be done with the DTVC.

ACKNOWLEDGMENTS

The authors gratefully acknowledge the help of J. E. Griffin who made the first calibrations of the commercial peak comparator with the DTVC, and C. J. Saunders who designed and evaluated the twin-T networks used with the wave analyzer.

REFERENCES

(1) Richman, Peter L., A New Absolute A-C Voltage Standard, Session IEEE Record of Convention, Paper 13, March 1963.

(2) Richman, Peter L., A New Peak-to-DC Comparator for Audio Frequencies, IRE Transactions on Instrumentation, Vol. I-11, p. 115, December 1962.

(3) Smith, W. E. and Clothier, W. K., Determination of the D.C./A.C. Transfer Error of an Electrostatic Voltmeter, Proceedings of the Institution of Electrical Engineers, Vol. 101-II, pp. 465-469, October 1954.

(4) Hermach, F. L., Griffin, J. E., and Williams, E. S., A System for Accurate D-C and A-C Voltage Measurements, Session 53 of IEEE Record of Convention, March 1965.

Table 1

AC-DC Difference of DTVC

Range V	AC-DC Difference ppm Frequency Hz 1 kHz	20 kHz
0.5		-30
1		-10
2		+10
3		+10
5		+10
10	0	0
20		0
30		+10
50		+10
100		0
200		0
300		+10
500		+30

Table 2

Waveform Distortion of Power Supply-Transformer Combination[1]

Harmonic	Distortion ppm Frequency Hz 50	400	1000	2400	4800
2	85	35	30	50	65
3	75	5	10	25	30
4	--	--	--	5	10
5	20	--	--	--	10
6	--	--	--	5	25
7	5	--	--	--	10
8	--	--	--	5	10
9	5	--	--	--	--
Sum of odd harmonics	100	5	10	25	50

Note 1. 1000 Ω across primary of transformer and 5000Ω load on secondary.

10 volts rms applied to transformer.

Note 2. Dashes indicate measured value less than 5 ppm.

Table 3

Intercomparison by Two Methods*

	50	400	1000	2400
δ_{TG} measured with DTVC	+32	- 4	- 8	+ 3
δ_S measured with DTVC**	+50	+14	+24	+42
Difference ($\delta_S - \delta_{TG}$)	+18	+18	+32	+39
$\delta_S - \delta_{TG}$ from direct intercomparison	+21	+11	+24	+31

*Measurements were made at 10 volts peak.

**δ_S measured at 4800 Hz was +41 ppm.

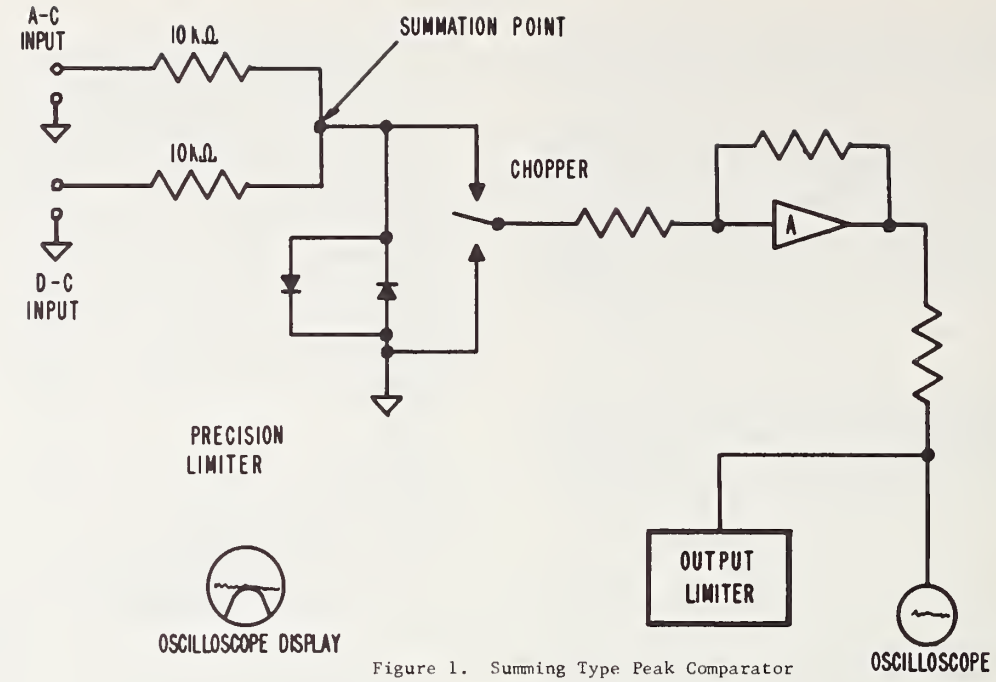

Figure 1. Summing Type Peak Comparator

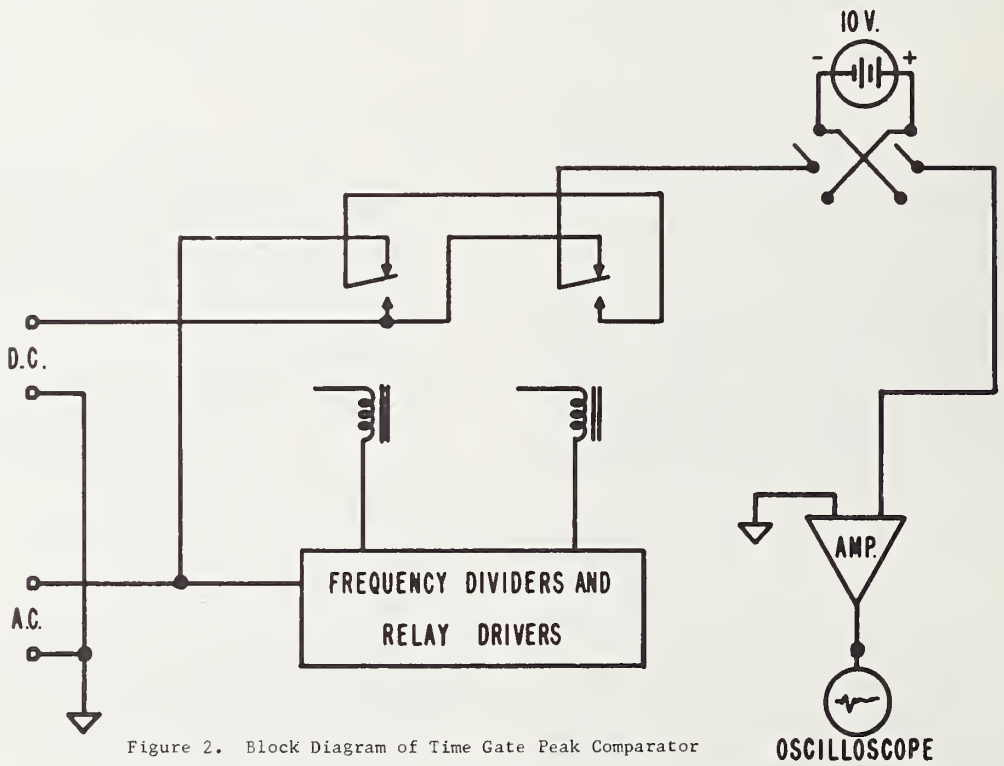

Figure 2. Block Diagram of Time Gate Peak Comparator

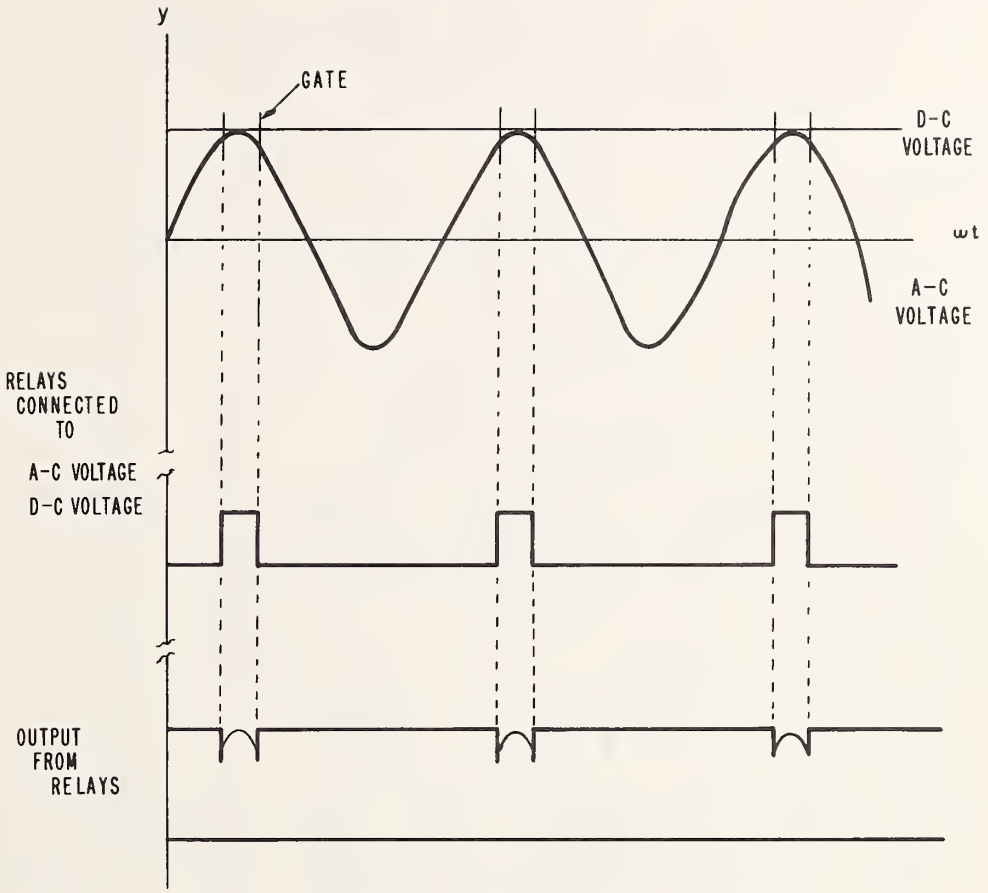

Figure 3. Time Gate Comparison of Peak A-C and D-C Voltages

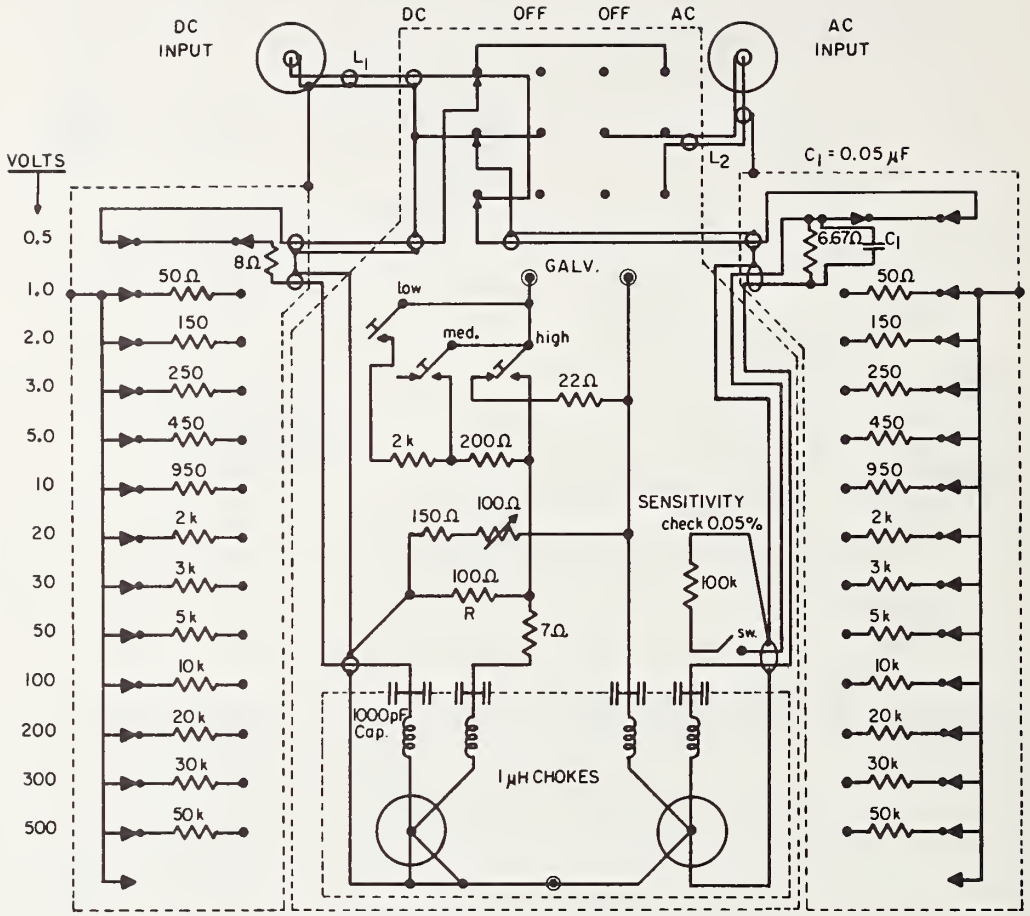

Figure 4. Differential Thermocouple Voltage Comparator

Note: All range resistors not in use are connected to the range shields through additional switch contacts as shown. The shields are shown as dotted lines.

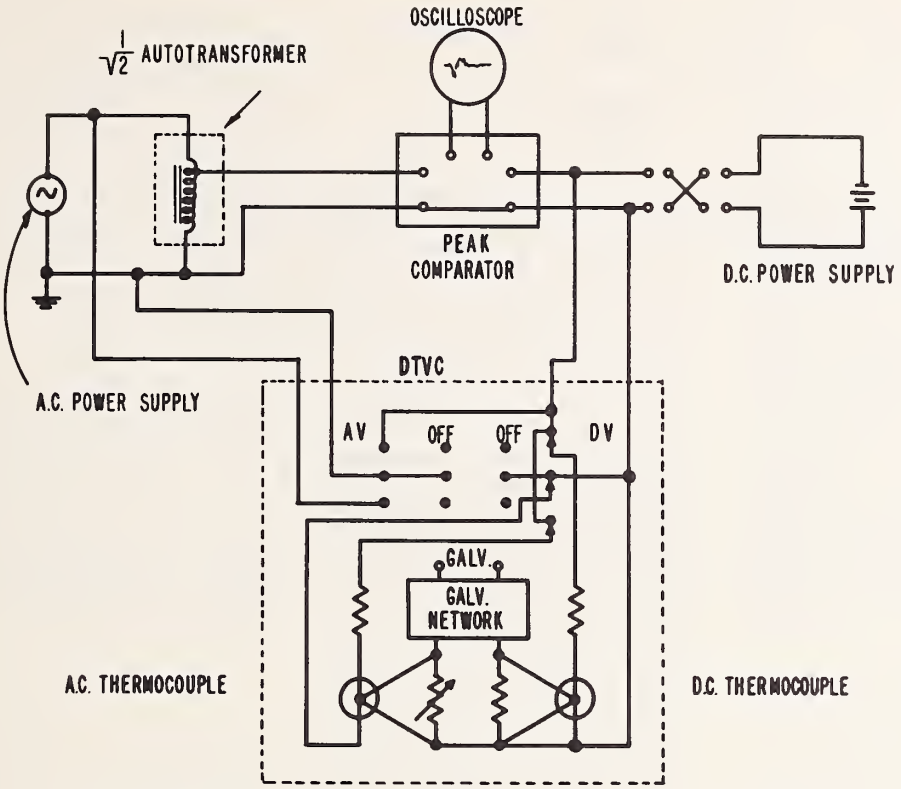

Figure 5. Test Setup for Calibrating Peak Comparators

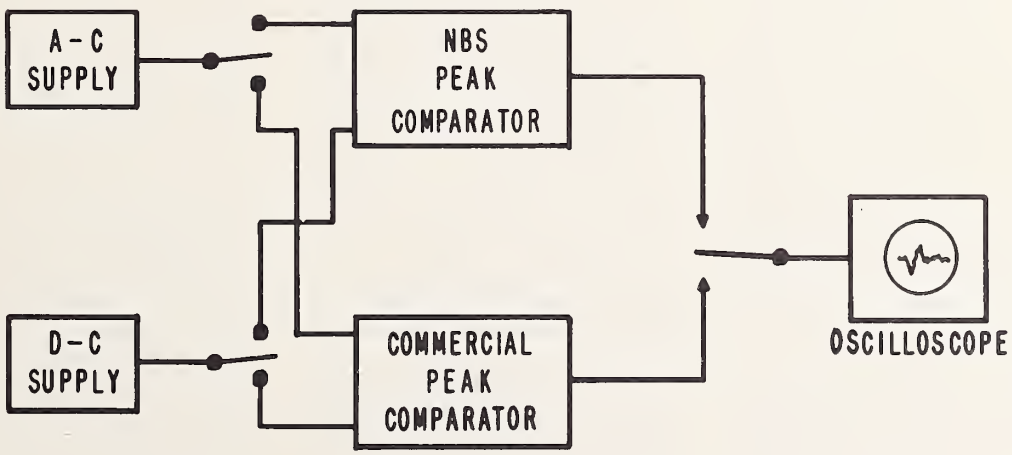

Figure 6. Direct Intercomparison Test

A Differential Thermocouple Voltmeter

J. E. GRIFFIN
ASSOCIATE MEMBER AIEE

F. L. HERMACH
MEMBER AIEE

Summary: An a-c voltmeter has been developed to indicate directly the percentage difference between an unknown voltage and the settings of the instrument dials. It is accurate to 0.05% from 5 cps (cycles per second) to 10 kc within the voltage range from 1 to 700 volts. Two 10-ma (milliampere) thermoelements are used; one in series with an a-c decade resistor, and the other energized from a constant-voltage d-c source, a Zener diode. A built-in galvanometer, calibrated in % of input voltage, indicates the difference between the two thermocouple-output emfs (electromotive forces), and has a resolution of more than 0.01%. The instrument was designed for rapidly calibrating other voltmeters, but it can be used also for a-c–d-c difference measurements—frequency response tests—to 0.02%.

HIGH ACCURACY in measurements is generally attained at the cost of increased time and effort, as with potentiometer techniques, or by means of rather complicated equipment such as electronic standards using feedback and similar techniques.

There is always the necessity for combining high accuracy with the simplicity which makes for reliability. This is particularly true in instrument calibrations in which many measurements of high accuracy are often required. Electrodynamic and electrostatic instruments of the higher accuracy classes suffer from limited frequency or voltage ranges, and thermocouple instruments from poor stability.[1]

The undesirable characteristics of thermocouple instruments are best overcome by a-c-d-c transfer techniques. With the thermoelement connected to the a-c source, the thermocouple-output emf is observed. The thermoelement is then connected to a d-c source, which is adjusted to give same thermocouple output. The d-c source is next measured with a d-c potentiometer of high accuracy. Ordinarily, this a-c to d-c transfer must

Paper 62-819, recommended by the AIEE Indicating and Integrating Instruments Committee and approved by the AIEE Technical Operations Department for presentation at the AIEE Middle Eastern District Meeting, Wilmington, Del., May 7–9, 1962. Manuscript submitted January 30, 1962; made available for printing March 6, 1962.

J. E. Griffin and F. L. Hermach are with the National Bureau of Standards, Washington, D. C.

The authors gratefully acknowledge the help of T. W. Cannon, who constructed the instrument, and J. Grant, who assisted with the test.

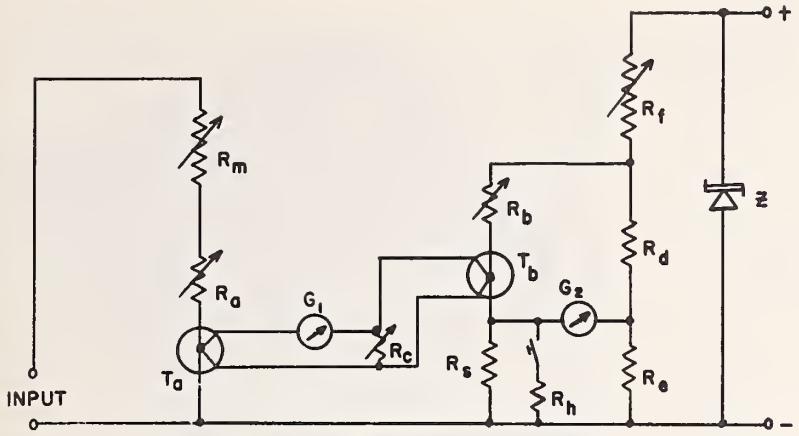

Fig. 1. Simplified circuit diagram of DTVM

be made for each measurement if better than 0.1% accuracy is required.[2]

This paper describes an audio-frequency a-c thermocouple voltmeter in which the transfer need be made only about twice a day to maintain a stability of 0.01%. As a result, a-c voltage measurements may be made rapidly, conveniently, and accurately.

Basic Principle

The basic principle of the differential thermocouple voltmeter (DTVM) may be seen in Fig. 1. A 10-ma thermoelement T_a of negligible a-c–d-c difference is connected in series with a decade resistor R_m. A second thermoelement T_b, having the same output emf at 10 ma, is connected to a stable d-c voltage source—Zener diode energized by a rectified and filtered a-c voltage. The outputs of the two thermoelements are connected together in opposition through a galvanometer G_1. Thus, when the galvanometer is balanced by adjusting the decade resistor R_m, the two heater currents are equal and the input voltage is a function of the setting of R_m, which is marked directly in volts. In addition, the scale of the galvanometer is marked to indicate directly the percentage difference between the actual input voltage and the voltage setting of R_m for slight differences between them. This is particularly convenient for calibrating other voltmeters.

Several preliminary calibration adjustments are necessary to insure that the resistances of the thermoelements are correct and that the thermocouple outputs are equal with equal heater currents. The resistances of the thermoelement heaters are checked in the internal bridge circuit with the galvanometer in position shown as G_2 in Fig. 1. First, with the bridge circuit as shown in Fig. 1, R_b is adjusted to balance the galvanometer. Then, with T_a and R_a switched in place of R_s, R_a is adjusted to balance the galvanometer. To check equality of the thermocouple-output emfs, the galvanometer is switched to position G_1—with T_a and R_a undisturbed. Also, R_c, which shunts the 12-ohm thermocouple of the thermoelement having the highest output emf, is adjusted to balance the galvanometer. These calibration adjustments do not require reference to external standards; are easily and rapidly carried out; and ordinarily need be made only twice a day to insure a stability of 0.01%.

An important but infrequent calibration adjustment is setting the reference current. This is done by connecting the input of the instrument to a known d-c 1-volt source, with the circuit as in Fig. 1, and adjusting R_f to balance the galvanometer. Because of the stability of the Zener diode which supplies the reference current, this 1-volt calibration need be made only semiannually or whenever the instrument receives a d-c calibration.

To improve stability, both thermoelements are mounted in a thermally lagged enclosure. They have closely matched temperature coefficients of output emf and have heaters of low-temperature coefficients of resistance. High-quality a-c resistors having low reactance are used. Thus, without applying corrections, measurements can be made to 0.05% or better from 1 to 700 volts at frequencies up to 10 kc. High accuracy is possible because of the a-c to d-c transfer, which reduces the effects of drifts and other changes in the thermoelements.

This DTVM is a modification of an instrument developed by W. Rump.[3] In Rump's instrument, a single-point potentiometer with a standard cell was used to adjust the d-c current through the second thermoelement. Zener diodes have now been developed with better than 0.01% stability, which greatly simplifies the standardizing circuits, and makes possible a lighter, more convenient, and much more compact instrument. The present instrument also differs from Rump's in a number of other respects, and is useful to much higher frequencies.

Today, differentially connected thermoelements are used in a commercially available 0.02% a-c–d-c transfer voltmeter but with uncalibrated resistors, so that a d-c volt box and potentiometer are required for the measurements. Recently, a calibrated 0.05% a-c voltage source, using differentially connected thermoelements in a feedback circuit with a Zener diode as the reference, was developed, independently of the present instrument.[4]

Description

Figs. 2 and 3 show a complete circuit diagram and a view of the DTVM. The heart of the instrument is, of course, the differential thermal converter, which consists of two 10-ma thermoelements, each having approximately 11-mv (millivolt) output, mounted in the thermally insulated enclosure shown in Fig. 4. Each thermoelement is contained in an evacuated glass bulb, and has an electrically insulating bead between its heater and the thermocouple hot junction. Each has a nickel-chromium heater, which, because of its low thermoelectric effects, has d-c reversal and a-c–d-c transfer errors less than 0.01%. The voltage thermoelement T_a, connected in series with the decade resistor, R_m in Fig. 1, is energized by the voltage to be measured. The reference thermoelement T_b is supplied by the internally mounted commercially available temperature-compensated Zener diode—energized from a 115-volt 60-cycle line—which has a 5.8-volt output with an 11-ma load.

The switch connecting the various calibration and operating circuits was selected because of its low contact resistance and low thermal emfs. Connections to the switch introduced negligible lead resistances into the circuits.

A resistor, part of R_f, in the Zener-diode circuit provides approximately 0.5% adjustment of the reference current. It is adjusted only in the external 1-volt check with the dials set in the 1-volt position. In addition to supplying a closely regulated current to the reference thermoelement T_b during voltage measurements, the Zener diode supplies the bridge circuit for checking and adjusting the resistance of the thermoelement heaters. One 100-ohm resistor R_s and two 1,000-ohm resistors, R_d and R_e, make up the

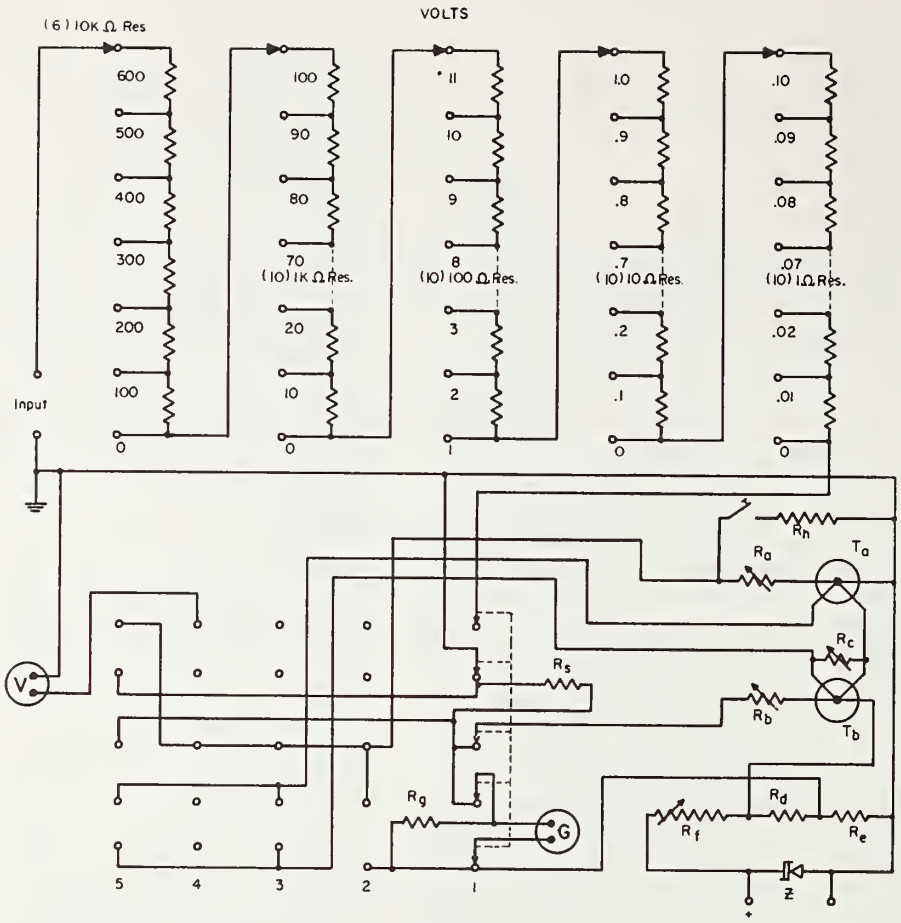

Fig. 2. Complete circuit diagram of DTVM

R_a&R_b—Manganin, 67.5 ohms; see text
R_c—25 ohms
R_d&R_e—Manganin, 1,000 ohms
R_f—Manganin, 320 ohms; see text
R_g—Manganin, 22 ohms
R_h—20 kilohms
R_s—Manganin, 100 ohms
T_a&T_b—Thermoelement, 10 ma, 11 mv
Z—Zener diode, 5.5 volts 11 ma
V—Rectifier voltmeter, 1 volt, 100 ohms

Switch Position
1. Adjust heater resistor R_b
2. Adjust heater resistor R_a
3. Adjust thermocouple output resistor R_c
4. Rectifier instruments
5. Volts

reference resistor and ratio arms of the bridge. These three resistors are adjusted to better than 0.01%.

The thermoelement heater circuit, consisting of T_a and R_a, provides the basic 1-volt range of the instrument. The heater resistance of each thermoelement is approximately 33 ohms. A 66-ohm a-c resistor and a 1.5-ohm adjustable bifilar resistor are connected in series with each heater to provide a total heater resistance of 100 ohms with a 1.5% adjustment. An a-c 5-dial decade resistor, connected in series with voltage thermoelement T_a, provides for voltage measurements from 1 volt to 700 volts in 0.01-volt steps. Resistors in the 0.01% accuracy class were used in the *X100*, *X10*, and *X1* dials, while resistors in the 0.05% accuracy class were used in the *X0.1* and *X0.01* dials. For preliminary setting of voltage, a 1-volt 100-ohm full-wave rectifier instrument, *V* in Fig. 2, is substituted for the thermoelement.

The *X1* dial is marked from 1 to 11 rather than 0 to 10, since the 1-volt heater of the voltage thermoelement is necessarily in series with the decade resistor. This requires that a voltage of 100 volts, for example, be set as the sum of 90 volts on the *X10* dial and 10 volts on the *X1* dial. Although this arrangement may seem awkward at first, the correct procedure for setting the dials is quickly grasped. A much more complicated circuit would have been necessary to provide for steps of 0 to 10 on the *X1* dial.

An adjustable resistor in the galvanometer circuit, Fig. 5, is used to set the galvanometer sensitivity. This adjustment is checked occasionally after the other checks are made, with T_a and R_a connected in place of R_s in Fig. 1. Connecting the 20-kilohm resistor R_h causes the two heater currents to differ by 0.50%, resulting in a 25-mm (millimeter) change in galvanometer deflection if the adjustment is correct.

A thermocouple instrument is a square-law device. However, to a first-order approximation, the galvanometer deflection is directly proportional to small changes in DTVM input voltage. This is possible since the voltage across the galvanometer is only a small part of the thermocouple output voltage. Let E_s and E_v be the outputs of the reference and voltage thermoelements, respectively, corresponding to input currents of I_s and I_v. Let ΔE be the change in thermocouple output caused by change ΔI in input current through the voltage thermocouple, corresponding to an input voltage change of ΔV. Let k be the proportionality constant, which, by calibration, is the same for both thermoelements,

Let

$$\Delta I = I_v - I_s$$

Then

$$\Delta E = E_v - E_s = kI_v^2 - kI_s^2 = 2kI_s\Delta I + k\Delta I^2$$
$$= 2E_s\Delta I(1+\Delta I/2I_s)/I_s$$

Since ΔI is never greater than 0.5% of I_s in the normal use of this instrument,

$$\Delta E \approx 2E_s\Delta I/I_s \approx 2E_s\Delta V/V$$

Maximum error from this approximation is less than 0.002% of the input voltage.

Sensitivity of the galvanometer is adjusted to cover a change in input voltage $\Delta V/V$ of $\pm 0.5\%$, or 0.02% per division for the full-scale deflection of ± 25 divisions of the center zero galva-

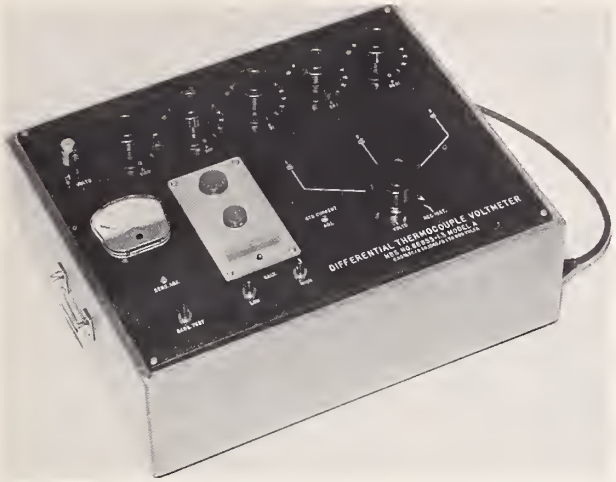

Fig. 3. Differential thermocouple voltmeter

nometer used in the instrument. Since the output emf E_s is 11 mv, the scale factor for the galvanometer, by the prior equation, must be 4.4 μv (microvolts) per division. Fig. 5 is a diagram of the galvanometer circuit, showing provisions for preliminary balances and the resistor for setting the sensitivity. The entire circuit of Fig. 5 is represented as G_1, G_2, and G in Figs. 1 and 2.

Temperature Compensation

The differential-thermocouple principle affords a means of temperature compensation. To accomplish this, the two thermoelements must have nearly equal temperature coefficients of emf and must be maintained at the same temperature. Several thermoelements were tested, grouped into pairs, and the combined temperature coefficient of each pair was measured. The net temperature coefficient of the pair used in the DTVM is 0.1 μv/C (microvolts per degrees centigrade), which causes an error in voltage measurement of only 0.0005%/C.

Temperature equality is maintained by means of a 1/8-in. copper temperature-lag box, approximately 2.5 by 3 by 4 in., shown in Fig. 4 The two thermoelements are mounted in holes in a small copper block and held in place with silicone grease. The block is placed inside a layer of foamed plastic approximately 1/2 in. thick. The foamed plastic, in turn, is placed in the copper box. The two thermoelement leads are shunted by 1,000-picofarad bypass capacitors. These capacitors, connected from each lead to the copper box, reduce any undesired r-f (radio-frequency) signals, such as television carrier waves, but offer high impedances to the audio-frequency signal being measured. Because the current through the capacitor is small and in quadrature with the current through the thermoelement heater, the error from this source is less than 0.001%, even at 10 kc.

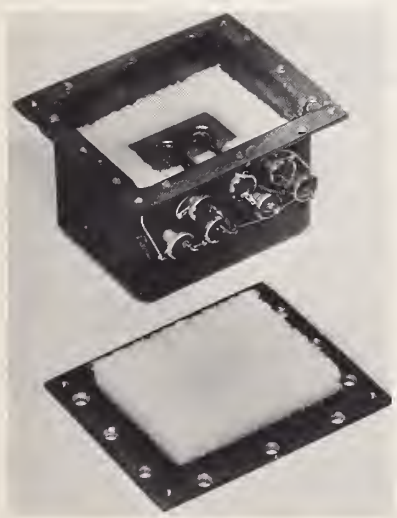

Fig. 4 (left). Thermoelements in temperature-equalization box

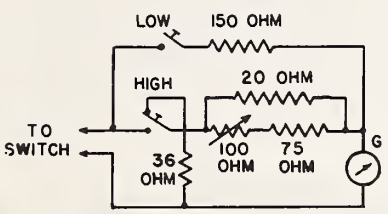

Fig. 5(above). Galvanometer circuit

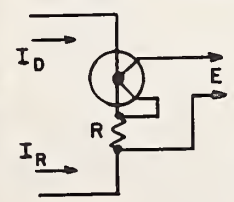

Fig. 6. Circuit for reducing d-c reversal errors

Errors and Compensation

The inside of the instrument is lined with copper, thus providing electrostatic shielding. The common input terminal is connected to this shield, and should be grounded when the instrument is in use. The switching circuit is arranged so that one side of both the Zener diode and the voltage thermoelement heater T_a are always grounded to this shield. Also, the thermocouple circuit is connected to the heater circuit to keep the voltage across the insulating bead of each thermoelement below 2 volts. For some thermoelements, errors may be caused by higher bead voltages.

An error in setting the heater resistance R_a of the voltage thermoelement will introduce an error of equal magnitude in the voltage measurement at the 1-volt level. However, this error is inversely proportional to the voltage. An error in setting the heater resistance R_b of the reference thermoelement will introduce only about 1/6 this error in the voltage measurements since it is in the 5.8-volt Zener-diode circuit. In the calibration checks, the voltage thermoelement is substituted directly for the 100-ohm reference resistor R_s, eliminating any errors in the bridge circuit except for this resistor.

During preliminary setting of voltage, using the rectifier instrument, both thermoelement heaters are connected in series in the Zener-diode circuit. Keeping the thermoelements energized reduces to a minimum the errors resulting from the small initial drift—up to 0.05%—which affects many thermoelements during the first few minutes after a large change in heater current.[2]

Galvanometer sensitivity is uniform within 1% of the end-scale deflection. The maximum error introduced into the measurement from this source is less than 0.005% of the input voltage.

Sensitivity control in the galvanometer circuit and current adjustment in the Zener-diode circuit are similar. Each consists of an adjustable resistor, shunted by a relatively low-resistance manganin resistor. This type of control is similar to a Waidner-Wolf element with the adjustment continuous rather than in steps. Such circuits minimize contact resistance and thermal emfs.

Copper-to-copper connections, thermal-free keys, and other precautions were taken to minimize residual thermal emfs in the galvanometer circuit. The Zener diode and filament transformer for the galvanometer light are mounted in a ventilated enclosure that is thermally insulated

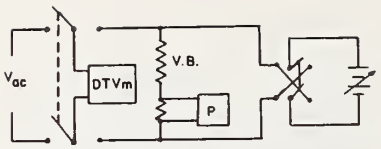

Fig. 7. Circuit for a-c–d-c transfer measurements

V_{ac}—A-c voltage to be measured
DTVM—Differential thermocouple voltmeter
VB—Volt box
P—D-c potentiometer

from the rest of the instrument. Temperature and residual thermal emfs inside the instrument, although greatly reduced, require approximately 6 hours to reach equilibrium after the Zener diode and lamp are energized. During this warm-up period, the total drift in calibration is approximately 0.05%. However, if the calibration procedure is carried out at half-hour intervals, the warm-up error is reduced to less than 0.005%. After the instrument reaches temperature equilibrium, it is stable within 0.01%, and a calibration twice daily should be sufficient. The Zener diode and lamp are expected to be continuously energized in periods of normal use of the instrument. The self-heating error from the voltage to be measured is less than 0.01% on all ranges.

The d-c reversal error of the DTVM is approximately 0.01%, primarily in the thermoelement. If the error were significantly larger, it could be reduced by the method shown in Fig. 6. The magnitude of the resistor R, needed to cancel the effect of reversal error, can be computed from the equation, $R = \Delta E/2I$, where ΔE is the difference in thermocouple output for $I_D = I_R = I$ in Fig. 6. The correction is so small that it need be only approximate. The polarity must be considered when connecting R into the thermocouple circuit. This procedure for reducing d-c reversal error also provides a convenient method of connecting the thermocouple and heater circuits.

Tests and Calibrations

Stability tests were made on the instrument extending over a 3-month period. During this time, the heater resistance R_a and R_b of the thermoelements did not vary by more than ±0.005%. Voltage measurements showed that the decade resistor and the bridge components were stable to ±0.01%. The Zener-diode voltage did not change by more than ±0.005%, with no evidence of drift. Supplementary tests verified the manufacturer's specifications that the temperature coefficient of the Zener diode was less than ±0.001%/C, and that its output was regulated to ±0.001% for a 10% line-voltage variation.

Table I. D-C Calibration of DTVM

Dial Settings of DTVM					Applied Volts	D-C Corrections, %
X100	*X10*	*X1*	*X0.1*	*X0.01*		
6	0	1	0	0	601	0.00
5	5	1	0	0	551	0.00
5	0	1	0	0	501	0.00
4	0	1	0	0	401	0.00
3	0	1	0	0	301	0.00
2	0	1	0	0	201	+0.01
1	0	1	0	0	101	+0.01
0	10	1	0	0	101	+0.01
0	5	1	0	0	51	0.00
0	2	1	0	0	21	+0.01
0	1	1	0	0	11	+0.01
0	0	11	0	0	11	+0.01
0	0	10	0	0	10	+0.01
0	0	5	0	0	5	+0.01
0	0	2	0	0	2	+0.01
0	0	1	10	0	2	+0.03
0	0	1	5	0	1.5	+0.02
0	0	1	1	0	1.1	+0.01
0	0	1	0	10	1.1	0.00
0	0	1	0	5	1.05	0.00
0	0	1	0	0	1.00	0.00

Table I shows results of a d-c calibration of the completed instrument, based on average values for the two directions of applied d-c voltage. The corrections listed are all well within ±0.05%, and agree within ±0.01% with those obtained from resistance measurements of the decade resistor.

Table II shows the a-c–d-c differences for several combinations of settings of the *X100* and *X10* dials, where capacitance effects are most likely to be appreciable, and at the top, middle, and low positions of the *X10* and *X1* dials. Additional difference measurements were made at several other dial settings including the *X0.1* and *X0.01* dials. In no instance was the a-c–d-c difference greater than 0.01% even at 20 kc. However, since capacitance effects, and consequently a-c-d-c differences, are dependent upon the dial-setting combination, and because tests at all possible dial settings are prohibitive, it was felt that the rated frequency should be conservatively set at 10 kc rather than 20 kc.

DTVM Uses

The instrument is particularly suited for calibrating a-c voltmeters. With voltage adjusted so that the pointer of the voltmeter under test is at a scale marking, and with dials of the DTVM set at the corresponding value, the percentage correction is read directly on the DTVM galvanometer. For highest accuracy, the d-c correction of the DTVM should be taken into account, so that $C_t = D + C_s$, where C_t and C_s are the percentage corrections of the test instrument and the DTVM, respectively; D is the percentage reading of the DTVM galvanometer.

For a-c measurements of the highest accuracy—0.02% or better—a direct a-c–d-c transfer method is usually required, and the circuit of Fig. 7 is used. Dials

Table II. A-C D-C Difference of DTVM

Dial Settings of DTVM*			Applied Volts	A-C-D-C Difference, %				
				Frequency				
X100	*X10*	*X1*		20 Cps	400 Cps	1 Kc	10 Kc	20 Kc
6	0	1	601	0.00	0.00	0.00	0.00	
5	10	1	601	0.00	0.00	0.00	+0.01	
5	0	1	501	0.00	0.00	0.00	0.00	
4	10	1	501				+0.01	
4	0	1	401				−0.01	
3	0	1	301				−0.01	
2	0	1	201				−0.01	
1	0	1	101			0.00	0.00	−0.01
0	10	1	101			0.00	0.00	0.00
0	5	1	51			0.00	0.00	0.00
0	1	1	11				0.00	
0	0	10	10				0.00	
0	0	5	5				0.00	
0	0	1	1	0.00	0.00	0.00	0.00	0.00

* The *X0.1* and *X0.01* dials were set at 0 for these tests.

of the DTVM are set to the nominal value of the voltage to be measured. With the DTVM switched to the a-c source, the galvanometer deflection is read. With the DTVM switched to the d-c source, the d-c voltage is set by reference to a volt box and potentiometer, and the galvanometer deflection is again read. The a-c voltage being measured is then $V_a = V_d [1+(D_a-D_d)/100]$, where V_a is the a-c voltage; V_d is the d-c voltage, corrected for potentiometer and volt box errors; and D_a and D_d are the galvanometer readings in per cent with the DTVM switched to a-c and d-c sources, respectively. An error will be introduced into this measurement if the lead resistances between the switch and the points of a-c and d-c measurement are not equal. Because of the low d-c reversal difference of this DTVM, the d-c source and potentiometer need not be reversed for this test.

The DTVM can be conveniently used for frequency influence tests or a-c-d-c difference tests of other voltmeters. Again, the circuit shown in Fig. 7 is used, with the voltmeter under test connected directly in parallel with the DTVM. The volt box and potentiometer are not required. Both instruments are switched in quick succession to: (1) the a-c source, (2) the d-c source, (3) the d-c source reversed, and (4) the a-c source again. In each case, voltages are adjusted to give the same readings of the voltmeter under test, and the deflection of the DTVM galvanometer is read. The a-c–d-c difference S_t of the voltmeter under test in per cent is simply $S_t=D_a-D_d$, where D_a and D_d are the average galvanometer readings with the instruments connected to a-c and d-c sources, respectively. A second a-c source can be used in place of the d-c source if an a-c reference frequency is desired. These procedures are highly useful because the frequency influence of a good instrument is small and relatively stable, so that subsequent tests of the instrument need be made only at the reference frequency—reversed direct voltage or alternating voltage.

Conclusions

This instrument is exceptionally convenient and is a time-saver. The modifications that have been incorporated make it much lighter and more compact than the instrument on which it was based.[3] Detailed descriptions of precautions taken in design should be particularly useful to others who may wish to construct a similar voltmeter. Equally important, these precautions illustrate once again that a careful study of sources of errors and of means of eliminating them cannot be neglected if the high accuracy inherent in a good basic method of measurement is to be realized in an actual instrument.

References

1. AC-DC Transfer Instruments for Current and Voltage Measurements, F. L. Hermach. *Transactions*, Professional Group on Instrumentation, Institute of Radio Engineers, New York N. Y., vol. I-8, 1958, p. 235.

2. A Wide-Range Volt-Ampere Converter for Current and Voltage Measurements, F. L. Hermach, E. S. Williams. *AIEE Transactions*, pt. I (*Communication and Electronics*), vol. 78, Sept. 1959, pp. 384–88.

3. Uber die genaue Absolutmessung von Wechselspannungen und einen Kompensator zur Prüfung von Wechselstrom Feinmessgeraten, W. Rump. *Elektrotechnik*, Berlin, Germany, vol. 5, Feb. 1951, p. 64–67.

4. Audio Voltage Calibratino Standard, K. J. Koep, G. B. Ruble. *AIEE Transactions*, pt. I (*Communication and Electronics*), vol. 81, July 1962, pp. 179–86.

A reprint from **COMMUNICATION AND ELECTRONICS**, published by American Institute of Electrical Engineers

November 1962 issue

NBS Technical Note 257
March 1965

PRACTICAL ASPECTS OF THE USE OF AC-DC TRANSFER INSTRUMENTS

E. S. Williams

Electrothermic transfer instruments may be used to make direct measurements of ac-dc difference or frequency influence. With a somewhat similar procedure an "unknown" a-c voltage or current may be accurately measured by determining the difference between it and a preset and accurately measured d-c equivalent. Test circuits and procedures are described and data taking and calculations are illustrated.

NBS Technical Note 188
April 1963

Calibration of Volt-Ampere Converters

E. S. Williams

These notes have been prepared to describe the National Bureau of Standards calibration services for volt-ampere converters (or transfer volt-ammeters), to suggest procedures for d-c standardization in the user's laboratory, and to describe a voltage comparator which can be used to make such calibrations quickly and easily.

U. S. Department of Commerce National Bureau of Standards

RESEARCH PAPER RP1344

Part of Journal of Research of the National Bureau of Standards, Volume 25, November 1940

STANDARD ELECTRODYNAMIC WATTMETER AND AC-DC TRANSFER INSTRUMENT

By John H. Park and Arthur B. Lewis

ABSTRACT

A description is given of the design and construction of the standard instrument used at the National Bureau of Standards in testing wattmeters and watthour meters.

The investigation to determine the accuracy of this instrument for alternating-current testing at frequencies up to 2,000 cycles per second is described and the results are given.

Journal of Research of the National Bureau of Standards Vol. 53, No. 2, August 1954 Research Paper 2521

Precise Comparison Method of Testing Alternating-Current Watthour Meters

A. W. Spinks and T. L. Zapf

A brief description of the basic method of testing alternating current watthour meters at the National Bureau of Standards is given, followed by a description of equipment for a faster and less laborious method.

Equipment with several novel features has been assembled for making precise tests of alternating-current watthour meters by a comparison method employing a group of carefully selected alternating-current watthour meters, which serve as a secondary standard group. One of this group, designated the "Standard Watthour Meter", is used with multirange instrument transformers as a reference standard to test other watthour meters with good precision. The testing procedure is explained, and the formulas used in computing the results of the tests are derived.

An analysis of the possible errors of measurement and data from numerous tests indicate that the measurement of energy applied to a watthour meter under test can be relied upon to better than 0.06 percent.

NBS Technical Note 266
December 1965

VOLTAGE RATIO DETECTOR FOR MILLIVOLT SIGNALS

by J. R. Houghton

ABSTRACT

A voltage ratio detector circuit for measuring ratios of a-c and d-c signals 5 millivolts or larger is described. The ratio is determined with a precision voltage divider which is accurate to within 0.001 percent of the indicated ratio when the ratio is near one. The detector has sufficient sensitivity and stability to indicate differences between two signals of 0.01 percent. Experimental results are presented to show the relative improvement in sensitivity of this voltage ratio detector over the previously used transfer admittance method for the calibration of vibration pickups.

Key words: Voltage ratio, vibration, calibration, thermal converter, electronic circuit, test method.

Instruments
Volume 23, Number 12, December 1950

Notes on the Care and Use of Electrical Instruments

F. D. Weaver

This article presents notes on precautions that should be observed by users of electrical instruments to enable them to achieve greater accuracy in measurements and to extend the useful life of their equipment.

Transformers and Inductive Voltage Dividers

Papers

Abstracts

315-411 O - 68 - 22

An International Comparison of Current-Ratio Standards at Audio Frequencies

BERNADINE L. DUNFEE, SENIOR MEMBER, IEEE, AND W. J. M. MOORE, SENIOR MEMBER, IEEE

Abstract—The results and analysis of an intercomparison between the National Research Council (NRC), Canada, and the National Bureau of Standards (NBS), Washington, D. C., of two contrasting types of current ratio standards (current comparator and current transformer) are presented. The agreement achieved between the two laboratories when their respective designs and methods of measurement were quite different is emphasized. To this end, the basic theories underlying the design and operation of the current comparator and current transformer are contrasted; the origin and significance of their respective errors are summarized; the $(N+1)$ method used at NBS to measure the errors of the multirange transformer standards up to 10 kHz is contrasted with the $(N+1)$ method (one of several) used at NRC in calibrating the comparator standards. The comparison circuit used at NRC to compare the respective standards of the two laboratories is described. The errors of the transformers as measured at NBS and NRC are presented and contrasted in both tabular and graphical forms.

Introduction

IN MANY INSTANCES the measurement of an ac electrical quantity is made possible or, at least, facilitated if accurately known ratio and phase relations can be established between two or more currents. This is particularly true when the measurements cover a broad frequency range or when the parameter being measured is relatively large (or small) in magnitude.

Anticipating future needs, the National Research Council (NRC), Canada, and the National Bureau of Standards (NBS), Washington, D. C., have been conducting independent programs in current-ratio measurements which include: 1) the design and construction of current-ratio standards for use at audio frequencies; 2) the development of methods for measuring the errors of the standards; and 3) the study of their use and application in the measurement of electrical quantities.

Contrasting approaches in both the design of the respective standards and in their calibration have been pursued. NRC has explored the current comparator [1]–[4] and extended its use up to 16 kHz; NBS, on the other hand, has focused on the current transformer, covering approximately the same frequency range. The respective work of each laboratory is described in two companion papers [5], [6].

The two different approaches have provided a more complete understanding of the behavior and limitations of current-ratio standards and their associated measuring systems, and an international comparison has provided an independent method for verifying results and estimated accuracies.

This paper incorporates information from the companion papers pertinent to the present discussion and describes in detail the results obtained when the NBS and NRC standards were compared at NRC.

Comparator and Transformer in Contrast

In its simplest version, the current comparator comprises a toroidal core of high permeability which carries a single-layer detection winding of many turns for sensing the flux condition of the core, and two windings, identified as primary and secondary, that carry the currents to be compared. It embodies the principle expressed by Ampere's Circuital Law $\oint H \cdot dl = \Sigma I$, with the added provision that when the line integral equals zero, the net electromotive force (EMF) induced in the detection winding, as measured at the terminals, is also zero. The significance of this equality is that the core operates under a condition of zero flux at the time of measurement so that errors that would arise from magnetizing and loss currents are avoided. Although this kind of magnetic error is eliminated and a greater inherent accuracy is assured, other errors of magnetic origin are present unless modifications are made in the basic design. As described by analysis and experiment [2], leakage flux assigned to either winding or to the external environment induces an EMF in the detection winding which is not a simple function of the currents being measured. Furthermore, the nonuniformity of permeability around the magnetic path produces an EMF even though the line integral may be zero. However, the inclusion of toroidal magnetic shields which surround and separate the critical windings can reduce the magnetic error to negligible proportions.

In contrast, the single-stage current transformer carries only two windings (primary and secondary) distributed around a toroidal core of high permeability. Since an EMF is required to establish and maintain a current through the total impedance of the secondary circuit, the operation of a current transformer requires a flux to be established in the magnetic core. Thus a small component of primary current must supply the working flux and the losses associated with the magnetic circuit so that, unlike the comparator, an error arises from this cause. Because it is of magnetic origin, this

Manuscript received June 28, 1965.

Bernadine L. Dunfee is with the Electricity Division, Electrical Instruments Section, National Bureau of Standards, Washington, D. C.

W. J. M. Moore is with the Division of Radio and Electrical Engineering, Electrical Engineering Section, National Research Council of Canada, Ottawa, Canada.

error can be identified as the magnetic error of the current transformer. Furthermore, since the flux is a nonlinear function of the magnetizing current, the error becomes a function of burden, frequency, nominal ratio, and secondary current. Some advantage is gained when the current transformer is to serve as a standard, since it need operate at only one burden which can be chosen with discretion. Thus at low frequencies, where the error is chiefly magnetic in origin, the current comparator is appreciably superior to the current transformer.

The only type of error considered thus far is the magnetic error, which, at frequencies not greatly exceeding 60 Hz, is the only one of concern. However, as the frequency increases another error of different origin is introduced. This error is associated with the windings and arises from the distributed capacitances that are present and acted upon by voltages that are either impressed or induced. These capacitances may exist within a winding, between windings, or between windings and shields. Thus, they are present in both types of ratio standards and their contribution to both the in-phase and quadrature components of the error increases with frequency. In contrast, the magnetic or low-frequency error of the current transformer decreases with increased frequency so that gradually its contribution to the total error becomes negligible and the capacitive or high-frequency component becomes dominant. Also, at higher frequencies the change of error with secondary current and the effects from residual magnetization become less significant. Thus, in the upper audio frequency range, the source of error is essentially the same in the two types of ratio standards and, except for differences in design that may alter the respective capacitance distributions, the marked advantage of the current comparator over the current transformer, as a ratio standard, diminishes.

Complete analysis of capacitance errors in comparator and transformer designs would be a formidable task and outside the scope of any one paper. However, general discussions and analyses pertinent to certain configurations appear in [7]–[11], and the two companion papers [5], [6]. It is sufficient here to state that, in general, the capacitive error is a complex function of several parameters with the ratio and phase angle components varying with the second and first power of the frequency, respectively. There does exist, however, an important concept that is necessary to the present discussion. A primary or a secondary current, as such, can no longer be assigned to the respective windings. In the presence of capacitance currents, the current entering one terminal of a winding will not be the same as that leaving the other terminal. Furthermore, the distribution of capacitance currents changes with any alteration in the voltage distribution or when a change is made in the "tie" connection between primary and secondary terminals.

Thus, several ratios for a given *nominal* ratio are available and a measurement can have meaning only by 1) specifying the potential of each winding, and 2) identifying the currents at the terminals where the measurement is made. The ratio discussed in this text, unless otherwise stated, refers to the currents at the terminals of like polarity when those terminals are at ground potential.

Calibration Prior to the International Comparison

The current comparators used in the intercomparison were part of the group described in one of the companion papers [5]. Each of the group was multirange and together covered a large number of selected ratios which permitted their calibration by three independent methods in a buildup or "boot-strap" process. In addition, ratios of the same nominal value were measured in a comparison circuit similar to that used in calibrating current transformers. Measurements were made at selected frequencies to a maximum of 16 kHz. The estimated uncertainty in the error ϵ assigned to the nominal ratios was 1 part per million (ppm), where the error ϵ is defined by the equation $I_s = I_p/n(1+\epsilon)$. [I_p and I_s refer to the primary and secondary currents at terminals of like polarity when those terminals are at ground potential and n is the nominal ratio.]

The two essentially identical NBS current transformers are discussed in the other companion paper [6]. They were multirange and carried the consecutive ratios of 1 to 1 to 6 to 1, inclusive. Measurements were made at NBS on all ratios at selected frequencies from 400 Hz to 10 kHz. A single "boot-strap" method was employed with verification of the results by an independent method provided by the intercomparison. The accuracy of the measured values was estimated at 10 ppm or better.

The "boot-strap" techniques employed at both laboratories required an initial calibration of the 1-to-1 ratios, which then served as the basis for the successive calibration of the higher ratios. The self-calibration circuits for measuring the 1-to-1 ratios and the balance equation (applicable to both the current transformer and current comparator) are indicated in Fig. 1.[1] In each case, the conductance G and capacitance C are adjusted for a null on detector D.

The higher ratios of the current transformers were measured in succession using the $(N+1)$ circuit of Fig. 2(a) [for the sake of clarity only the essential elements are included]. After each transformer was calibrated on its n ratio, it served as the standard S in calibrating the $(n+1)$ ratio of the other, identified as X. Thus, beginning with S connected for its 1-to-1 ratio with currents adding at A, calibration is made for the 2-to-1 ratio of X by measuring, in effect, the difference between their nearly equal secondary currents; the process is continued by comparing the 3-to-1 against the 2-to-1 etc., throughout the total range. The inserted voltage indicated by V_c, adjustable in magnitude and phase, com-

[1] The current comparator shown in this design is of the compensated type [3]. It has an additional winding (known as the compensation winding) with the same number of turns as the secondary winding located inside the magnetic shields.

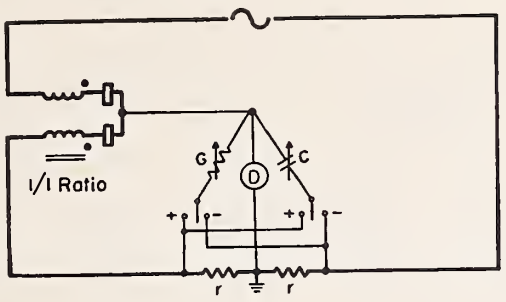

(a)

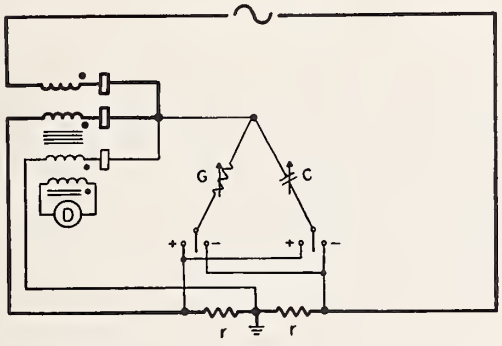

(b)

Fig. 1. Self-calibration circuit (1-to-1 ratio). (a) For current transformers. (b) For current comparators $\epsilon = r(G + j\omega C)$.

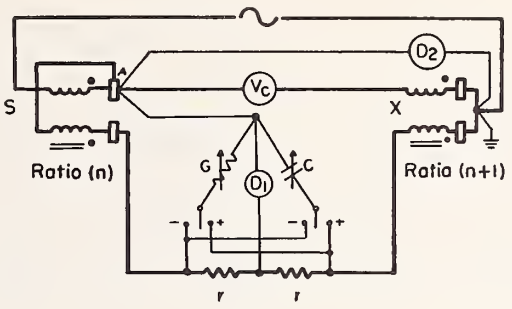

(a)

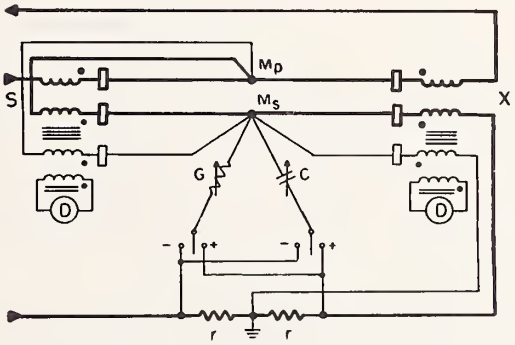

(b)

Fig. 2. $(N+1)$ calibration circuit for ratios >1. (a) For current transformers. (b) For current comparators.

pensates for the added burden impressed on X by its own primary winding.

The $(N+1)$ circuit of Fig. 2(b) represents one of three "boot-strap" methods used at NRC in the calibration of the comparators. Bearing the same identification as the one used at NBS, it serves to emphasize the similarities and differences between the two methods. Comparators S and X serve in the same capacity as that outlined for the transformer calibration and the successive buildup through the higher ratios is identical in the two cases. The secondary burden imposed on either S or X remains constant and, therefore, unlike the current transformer circuit, requires no compensation.

Insidious effects from capacitance currents occur in both circuits which could introduce errors in the measurements if not properly considered. The measuring branch in the network of Fig. 2(b) is confined solely to the secondary circuit so that the currents being compared are consistent with the definition; however, because of capacitance currents, the current that leaves one terminal of the secondary winding of S differs from that which enters the other terminal. Since this current enters the primary circuit at M_p a correction β_B, previously measured, appears in the balance equation. A similar but more complicated condition exists for the NBS circuit [Fig. 2(a)]. The measuring branch is not confined to the secondary circuit but bridges across primary and secondary. The "tie" between the windings of S differs from that used when it is calibrated as the unknown X; furthermore, measurements are made on X at the ends opposite to where the terminals are joined. The balance equation for this circuit contains two unknown parameters which must also be evaluated from a set of auxiliary measurements.

The Intercomparison

The intercomparison was accomplished by using the NRC current comparators to measure the errors of the NBS current transformers (identified as M-1 and M-2). The circuit is described in one of the companion papers [5] and is reproduced in Fig. 3, greatly simplified for the sake of clarity.

An over-simplified approach is perhaps useful here in understanding the circuit. Disregarding any capacitive or magnetic errors in the current comparator, assume first that the current transformer is free of error and that the G-C network is disconnected from point M_s. The primary and secondary windings of the comparator together with the magnetic shield constitute, in effect, a current transformer and hence the ampere-turns of the primary and secondary windings will nearly balance one another. However, complete ampere-turn balance must exist in the comparator as a whole. The residual ampere-turns must, therefore, be provided by the current in the compensation winding. This winding has the same number of turns as the secondary winding, hence the division

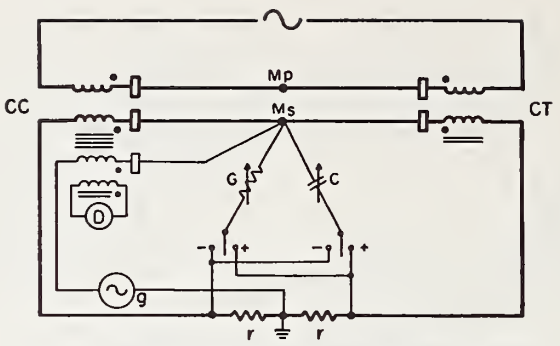

Fig. 3. Comparison circuit used in calibrating the current transformers $\epsilon_{CT}=r(G+j\omega C)+\epsilon_{CC}$.

of current between the two windings is immaterial. When the current transformer under test is not error-free, the procedure is to make it appear so to the current comparator by injecting current into the circuit through the G-C network. The values of G and C at balance are then a measure of the current transformer's error. Any error in the current comparator, of course, enters the balance equation.

It was imperative that the quantity measured and the conditions imposed on the current transformer be identical in the two laboratories to the extent that the desired accuracy is not impaired. In this respect, the burden imposed was the same in the two cases and the ratios measured refer to the same currents, conforming to the definition specified earlier. The latter can be clarified further by considering other aspects of the measuring process. The current transformer, equipped with shielded leads, is connected to the comparator at junctions M_p and M_s. The potential condition is satisfied by bringing points M_p and M_s to ground potential. This is achieved by 1) making a Wagner arm balance (not shown) and 2) injecting a small voltage at g to compensate for the impedance drop in the compensation winding.

The use of leads to connect the transformer to junctions M_p and M_s requires comment. Measurements at NBS were made *at* the terminals, i.e., the shielded leads (shields not shown) used in the NRC circuit and considered as part of the transformer were not present in the NBS circuit. Since the potentials of the windings, and therefore capacitance currents, are altered by the insertion of leads, the transformer errors as measured in the two laboratories would differ at the higher frequencies. It was necessary, therefore, to measure the "lead effect." This was done at both NRC and NBS with an agreement of 1 ppm. NBS values for the measured error ϵ were adjusted accordingly, the maximum adjustment of approximately 10 ppm in the real component occurring on the six-to-one ratio at 10 kHz.

Results (1 to 10 kHz)

To re-emphasize, the errors measured at NBS (adjusted for lead effect) and NRC refer to those currents that enter and leave terminals of like polarity through a pair of shielded leads when the ends of the leads are at ground potential; a noninductive burden of 0.10 ohm was imposed—lead resistance was small but was essentially the same in both calibrations.

Measured values and differences are shown in Table I for transformer M-1 where the errors are given in ppm (for phase angle this is the equivalent of microradians); the errors plotted against frequency for ratios 1 to 1 and 6 to 1, appear in Figs. 4 and 5. The measured errors for current transformer M-2 were identical to those shown in the table for M-1 to within 2 ppm;[2] the differences between the laboratories are essentially the same with a maximum again of 8 ppm. Although the values in Table I and the graphs refer to a secondary current of 5 amperes, measurements were made, also, at other secondary currents to a minimum 0.5 ampere. The largest change in going from 100 to 10 percent rated current occured at 1 kHz and amounted to 0.5 ppm in both the in-phase and quadrature components.

The errors as recorded in Table I are the total errors that include both the magnetic and capacitive components. The capacitive portion is the sum of all contributions from the winding impedances, lead impedances and any capacitance that shunts the primary. The first two can be determined experimentally [5] so that, with some reasonable estimate of the shunt capacitance, an artifice is established for computing the magnetic error. The magnetic error was estimated in this manner; its value for the six ratios at 10 kHz is given in Table II, using NRC values and assuming a shunt capacitance of 150 pF.[3] Since the contributions from capacitance to the real and quadrature components of error vary with the second and first power of the frequency, respectively, estimates of the magnetic error can be made for the remaining frequencies.

[2] This applied to both NRC and NBS values with one exception; at 1 kHz on the 3-to-1 ratio the NBS value for phase angle differed from the M-1 value by 6 ppm. It was believed that polarization, to be discussed later, accounted for this discrepancy.

[3] The estimate is based principally on the expected capacitances between the magnetic core (which is not grounded) and the windings; turn-to-turn capacitance or that resulting from terminal geometry would be much smaller for this design.

TABLE I

Errors of Transformer M-1 Measured at NRC and NBS at a Secondary Current of 5 Amperes
Parts Per Million

Nominal Ratio	1 kHz			5 kHz			10 kHz		
	NBS	NRC	Δ	NBS	NRC	Δ	NBS	NRC	Δ
1/1	$-5.1+j20.0$	$-5.4+j20.2$	$+0.3-j0.2$	$-3.8+j1.5$	$-4.0+j2.1$	$+0.2-j0.6$	$-1.8-j2.4$	$-2.1-j2.6$	$+0.3+j0.2$
2/1	$-5.0+j18.9$	$-5.3+j19.0$	$+0.3-j0.1$	$-2.4+j2.7$	$-2.8+j1.3$	$+0.4+j1.4$	$+4.1-j2.1$	$+2.1-j4.3$	$+2.0+j2.2$
3/1	$-5.1+j20.1$	$-5.3+j19.4$	$+0.2+j0.7$	$-2.0+j3.2$	$-2.5+j2.3$	$+0.5+j0.9$	$+6.4-j0.7$	$+3.1-j2.3$	$+3.3+j1.6$
4/1	$-5.6+j21.6$	$-5.3+j20.0$	$-0.3+j1.6$	$-1.9+j4.2$	$-2.3+j2.9$	$+0.4+j1.3$	$+8.4+j1.2$	$+3.9-j1.4$	$+4.5+j2.6$
5/1	$-5.8+j20.3$	$-5.4+j20.1$	$-0.4+j0.2$	$-1.5+j4.6$	$-2.0+j3.3$	$+0.5+j1.3$	$+11.7+j1.8$	$+5.2-j0.7$	$+6.5+j2.5$
6/1	$-6.3+j21.9$	$-5.5+j21.7$	$-0.8+j0.2$	$-0.9+j4.2$	$-1.8+j3.9$	$+0.9+j0.3$	$+14.7+j2.4$	$+6.3-j0.1$	$+8.4+j2.5$

Δ=the difference (NBS-NRC).

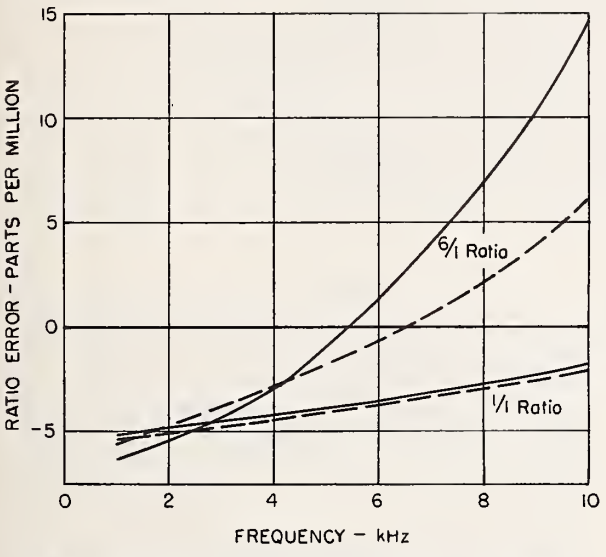

Fig. 4. Ratio error of current transformer M-1; NBS measurements ———, NRC measurements – – – – –.

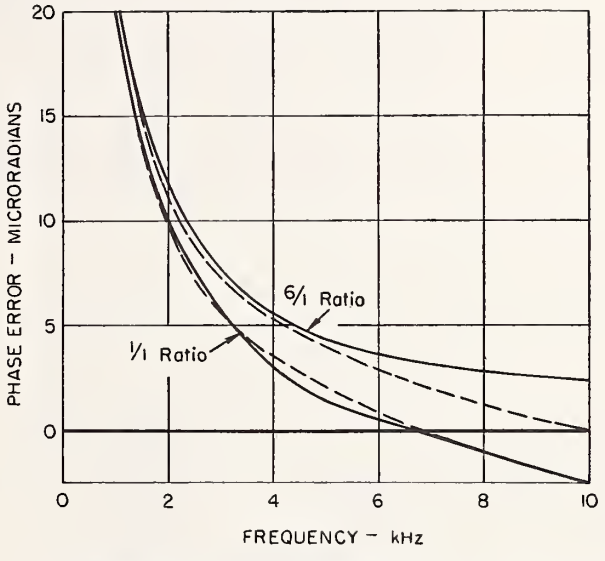

Fig. 5. Phase error of current transformer M-1; NBS measurements ———, NRC measurements – – – – –.

TABLE II

Estimate of Capacitive Errors for Transformers M-1 and M-2 at 10 kHz
Parts per Million

Nominal Ratio	NRC Calibration		Capacitive Error Components Due to			Residual Error	
	M-1	M-2	Winding Impedance	Lead Impedance	150 pf Primary Shunt Capacitance*	M-1	M-2
1/1	$-2.1-j2.6$	$-1.9-j2.7$	0	$0.0-j0.6$	$+2.2-j3.3$	$-4.3+j1.3$	$-4.1+j1.2$
2/1	$+2.1-j4.3$	$+2.3-j4.4$	$+3.1-j3.9$	$+2.9-j1.0$	$+0.5-j0.8$	$-4.4+j1.4$	$-4.2+j1.3$
3/1	$+3.1-j2.3$	$+3.2-j2.5$	$+2.4-j2.4$	$+4.6-j1.2$	$+0.2-j0.4$	$-4.1+j1.7$	$-4.0+j1.5$
4/1	$+3.9-j1.4$	$+4.1-j1.4$	$+1.7-j1.2$	$+6.5-j1.6$	$+0.2-j0.2$	$-4.5+j1.6$	$-4.3+j1.6$
5/1	$+5.2-j0.7$	$+5.4-j0.9$	$+1.1-j0.3$	$+8.1-j1.7$	$+0.1-j0.1$	$-4.1+j1.4$	$-3.9+j1.2$
6/1	$+6.3-j0.1$	$+6.6-j0.3$	$+0.7+j0.4$	$+9.5-j1.9$	$+0.1-j0.1$	$-4.0+j1.5$	$-3.7+j1.3$

* Assumed

Results (400 Hz)

The results at 400 Hz are examined separately in order to emphasize the effects of polarization observed at low frequencies. The values and differences for both M-1 and M-2 are given in Table III. The relatively poor agreement for phase angle is in startling contrast to that obtained at higher frequencies. This fact appears contrary to that expected, since the role of capacitance currents has essentially disappeared. However, polarization and its effect in current transformers become more critical at the lower frequencies and extreme care must be taken in demagnetizing the core and in avoiding sources of direct voltage in the measuring network. From evidence obtained at both NRC and NBS, it was concluded that the large differences evident at 400 Hz were caused by polarization, established periodically

TABLE III

Errors of Transformers M-1 and M-2 at a Frequency of 400 Hz and a Secondary Current of 5 Amperes
Parts Per Million

Nominal Ratio	M-1			M-2		
	NBS*	NRC	Δ (NBS-NRC)	NBS*	NRC	Δ (NBS-NRC)
1/1	$-6.9+j49.3$	$-6.9+j49.8$	$0.0-j0.5$	$-6.6+j54.0$	$-6.2+j48.6$	$-0.4+j5.4$
2/1	$-7.0+j46.9$	$-6.9+j46.1$	$-0.1+j0.8$	$-6.8+j59.2$	$-6.6+j47.8$	$-0.2+j11.4$
3/1	$-6.8+j49.9$	$-7.1+j46.4$	$+0.3+j3.5$	$-7.4+j65.1$	$-7.0+j50.5$	$-0.4+j14.6$
4/1	$-7.9+j61.4$	$-7.1+j47.7$	$-0.8+j13.7$	$-7.4+j66.4$	$-7.0+j51.9$	$-0.4+j14.5$
5/1	$-8.1+j59.6$	$-7.3+j47.5$	$-0.8+j12.1$	$-8.2+j72.0$	$-6.5+j46.9$	$-1.7+j25.1$
6/1	$-8.9+j65.4$	$-7.4+j52.4$	$-1.5+j13.0$	$-8.3+j68.2$	$-6.5+j47.7$	$-1.8+j20.5$

* NBS values are an average of maximum and minimum values when repeat measurements were made following a demagnetization process.

during the "boot-strap" measuring process at NBS. This evidence is discussed quite fully in Dunfee [6]; however, certain of its aspects should be noted here.

Small magnetizations can produce relatively large effects at 400 Hz. A maximum change of 20 ppm in the quadrature component of the error immediately following demagnetization was observed at NBS; essentially the same value was obtained at NRC when the transformers were calibrated on their 1-to-1 ratios "as received" and followed immediately by a calibration after demagnetization. In both laboratories, the maximum change was reduced to about 8 ppm at 1 kHz, and continued to decrease approximately with the first power of the frequency. The NBS values in Table III result from averages taken of the maximum and minimum measured values. Selection of the minimum values would improve the agreement between the laboratories; however, there is no justification for this choice because of the complex manner in which uncertainties are propagated through the "boot-strap" process. Strong evidence supports the fact that when the measuring circuit is devoid of direct voltage sources, careful demagnetization just prior to calibration assures a repeatability of results to 1 ppm.

Conclusions

The use of two or more distinct methods to measure the same quantity offers the best approach in establishing the accuracy limit of a measured value and verifying the methods employed. This arises principally because it is quite unlikely that the sources, magnitudes, and distribution of the errors of measurement are identical in the several methods. In this intercomparison, not only were the methods and circuits markedly different in the two laboratories but possible bias was reduced in having different personnel responsible for the measurements. The good agreement implies that the "boot-strap" method of NBS together with the auxiliary measurement give results accurate to 10 ppm and verifies further the validity of the methods used at NRC in evaluating the comparators. Experimental evidence indicates that careful demagnetization of the transformers must be observed at frequencies near and below 400 Hz.

References

[1] N. L. Kusters and W. J. M. Moore, "The current comparator and its application to the absolute calibration of current transformers," *Trans. AIEE (Power Apparatus and Systems)*, pt. III, vol. 80, pp. 94–104, April 1961.

[2] P. N. Miljanic, N. L. Kusters, and W. J. M. Moore, "The development of the current comparator, a high-accuracy a-c ratio measuring device," *Trans. AIEE (Communications and Electronics)*, pt. I, vol. 81, pp. 359–368, November 1962.

[3] N. L. Kusters and W. J. M. Moore, "The compensated current comparator; A new reference standard for current transformer calibration in industry," 1964 *IEEE Internat'l Conv. Rec.*, pt. 8, pp. 204–212.

[4] N. L. Kusters, "The precise measurement of current ratios," presented at the 1964 International Conference on Precision Electromagnetic Measurements, Boulder, Colo.

[5] N. L. Kusters and W. J. M. Moore, "The development and performance of current comparators for audio frequencies," this issue, page 178.

[6] B. L. Dunfee, "The design and performance of multirange current transformer standards for audio frequencies," this issue, page 190.

[7] P. N. Miljanic, "Capacitive error in current comparators," presented at the 1964 International Conference on Precision Electromagnetic measurements, Boulder, Colo.

[8] A. H. M. Arnold, "Dielectric admittances in current transformers," *Proc. IEE (London)*, pt. 2, vol. 99, pp. 727–734, 1950.

[9] —— "The effect of capacitance on the design of toroidal current transformers," *Proc. IEE (London)*, pt. 2, vol. 97, pp. 797–808, 1950.

[10] N. L. Kusters and W. J. M. Moore, "The effect of winding potentials on current transformer errors," *Trans. AIEE (Communications and Electronics)*, pt. I, vol. 81, pp. 186–191, July 1962.

[11] J. J. Hill, and A. P. Miller, "Design and performance of high precision audio-frequency current transformers," *Proc. IEE (London)*, pt. B, vol. 108, pp. 327–332, May 1961.

JOURNAL OF RESEARCH of the National Bureau of Standards—C. Engineering and Instrumentation
Vol. 69C, No. 4, October–December 1965

Comparators for Voltage Transformer Calibrations at NBS

Wilbur C. Sze

(July 28, 1965)

An inductive comparator is described for measuring ratio-correction-factor and phase-angle error of voltage transformers by comparison with reference transformers. The simple circuit utilizes a resistance-capacitance network and an inductive voltage divider. The relative magnitude of the ratio-correction-factors is obtained from the dial readings of the inductive voltage divider, and the phase angle between the voltage phasors is equal to $\pm\omega CR$. The accuracy of these measurements at 60 and 400 hertz is within 2 parts-per-million for ratio and within 10 microradians for phase angle at the limits of the phase-angle range of ± 38 milliradians. Only a few ranges of reference transformers are required since fractional ratios from 1/1 to 1/4 may be measured as readily as ratios near unity, without diminution in accuracy. A general discussion of a resistive comparator, which has been in continuous operation at NBS since 1939, is included.

Key Words: Voltage divider, inductive voltage divider, resistive voltage divider, voltage transformer calibration, ratio-correction-factor, phase-angle errors, voltage transformer comparator, voltage-transformer-test-set, comparator, test-set, calibration.

1. Introduction

The method most widely used by public utilities and standardizing laboratories to determine the ratio and phase angle of voltage transformers is by comparison with calibrated reference transformers. However, it is a relative rather than an absolute method, in that the accuracy of the results obtained depends upon the knowledge of accuracy of the reference transformers [1].[1]

At the NBS laboratories, a group of reference transformers is available by means of which test transformers having any ratio from 1:1 to 2000:1 can be calibrated. The accurate initial establishment of the voltage ratio and phase angle for these reference transformers has been discussed elsewhere and will not be repeated here [2, 3].

The purposes of this paper are (1) to describe the resistive comparator which has been in continuous operation since 1939; (2) to describe a new inductive comparator; and (3) to analyze various factors affecting the accuracy with which measurements can be made.

2. Resistive Comparator

This comparator was designed and constructed at NBS by F. K. Harris and has been in continuous operation since 1939, except for a very brief period during which new switches were installed to replace the worn out original ones [4, 5].

The schematic circuit of this comparator is shown in figure 1.[2] The in-phase voltage balance condition is achieved by adjusting the tap of the resistive divider, and the quadrature voltage, by varying the mutual inductor, M.

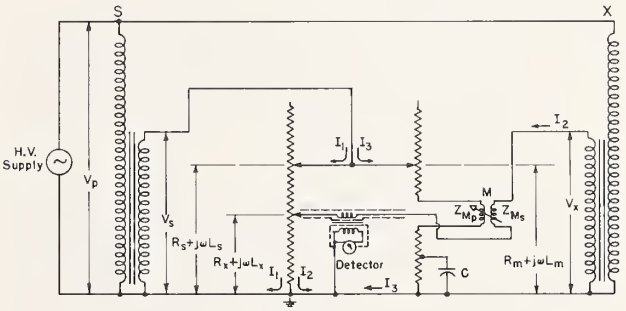

FIGURE 1.

2.1. Description of Components

The R_s and R_m circuits are supplied from the secondary of transformer S. Each can be varied from 2000 to 4000 Ω in increments of 100 Ω. The exact values are determined by the ratios of the test and reference transformers. The 100-Ω and 1000-Ω unit resistors of R_s are of woven wire and mounted on ceramic forms. Thus the residual, L_s, of R_s is reduced to a minimum [6]. The R_m circuit, nominally equal to R_s, include the primary circuit of M which has a d-c resistance of 200 Ω. The capacitor, C, shunting the lower portion of the resistance, serves to compensate for the self-inductance introduced by M [5]. Multiple taps are brought out from R_m to supply the shield potential of corresponding sections of R_s and of the detector circuit [7]. The shielding is shown in figure 4.

As shown in figure 2, the portion of the R_s circuit between 1800 and 2000 Ω carries a continuously adjustable tap, R_x, which is connected through the detector circuit and M to the secondary of the test transformer.

[1] Figures in brackets indicate the literature references at the end of this paper.

[2] Simplified by not showing the shielding arrangements around each segment of R_s.

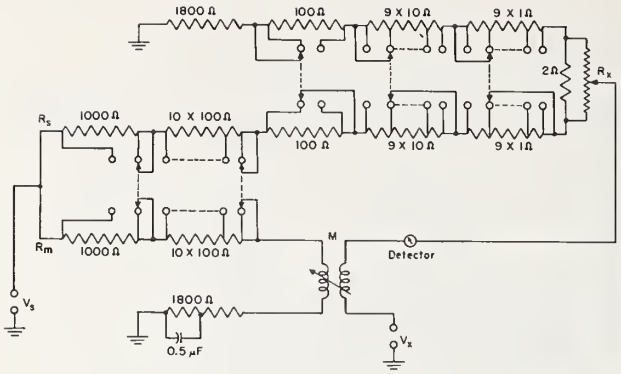

FIGURE 2.

The mutual inductor used in this circuit consists of a 10×20 mH per section unit (± 200 mH maximum) and a continuously adjustable inductometer (± 25 mH maximum) [8, 9].

Both the R_s/R_x ratio of the resistive divider and the mutual inductance, M, are periodically redetermined to insure that maximum accuracy is maintained for transformer testing. The residual reactances, L_s and L_x, were also accurately determined at the time the comparator was built.

The design is such that the resistors must dissipate considerable power. Therefore, the entire resistive divider, R_s and R_m, is immersed in oil to minimize the effect of temperature coefficient on the R_s/R_x ratio.

The detector circuit consists of a doubly shielded impedance-matching transformer (1000–4000 turns) and a wave-analyzer used as a tuned null detector.

2.2. Comparator Desk

Figure 3 shows the general layout of the desk. The resistive divider is located to the right with the R_s adjustment dials in the back and the R_x dials in front. The step mutual inductor and the inductometer are located in the left portion of the desk. The detector is in the rear right. Since this comparator is adaptable for calibrating voltage-transformer-test-sets, the panel shown at the lower left side of the desk is for arranging the connections for calibrating either transformers or test-sets. Figure 4 shows the internal wiring of the resistive divider and the individual shields around units of R_s.

2.3. Theoretical Relations

The equations for obtaining the ratio-correction-factor and phase-angle error are developed as follows. By definition, the voltage ratio of a transformer is the ratio of the primary terminal voltage to the secondary terminal voltage so that

FIGURE 3.

$$\frac{|V_{\text{Pri}}|}{|V_{\text{Sec}}|} = N' = Nf$$

where N' is the actual voltage ratio, N the nominal ratio, and f the ratio-correction-factor. If θ represents the angle between the primary and reversed secondary voltage phasors, then

$$V_s = \frac{|V_p|}{N'_s} (\cos \theta_s + j \sin \theta_s)$$

and [3]

$$V_x = \frac{|V_p|}{N'_x} (\cos \theta_x + j \sin \theta_x)$$

By inspection of figure 1, the following mesh current equations are obtained

$$V_s = I_1 Z_s + I_2 Z_x$$

$$V_x = I_1 Z_x + I_2 (Z_x + Z_{Ms}) + I_3 j\omega M$$

$$V_s = I_2 j\omega M + I_3 Z_m$$

[3] Subscripts s and x denote that the symbols refer to the reference or test transformers, respectively.

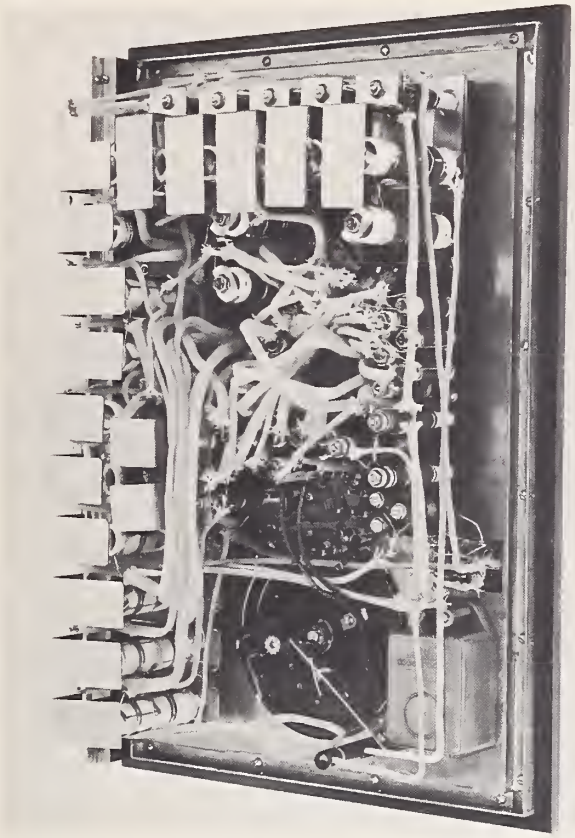

FIGURE 4.

$I_2 = 0$ when a null is indicated on the detector, then

$$V_s = I_1 Z_s = I_3 Z_m$$

and

$$V_x = V_s \left(\frac{Z_x}{Z_s} + \frac{j\omega M}{Z_m} \right)$$

Since $Z_m = R_m$ by the addition of C, and $R_m = R_s$ nominally, the balance equation becomes

$$\frac{(\cos \theta_x + j \sin \theta_x)}{N_x f_x} = \frac{(\cos \theta_s + j \sin \theta_s)}{N_s f_s} \left\{ \frac{R_x}{R_s} \left[1 + j\omega \left(\frac{L_x}{R_x} - \frac{L_s}{R_s} + \frac{M}{R_x} \right) \right] \right\}$$

and on separation

$$f_x = \frac{N_s R_s}{N_x R_x} \left(\frac{f_s \cos \theta_x}{\cos \theta_s - \sin \theta_s \omega \left(\frac{L_x}{R_x} - \frac{L_s}{R_s} + \frac{M}{R_x} \right)} \right)$$

$$\approx \frac{N_s R_s}{N_x R_x} + (f_s - 1) + \frac{1}{2}(\theta_s^2 - \theta_x^2)$$

and [4]

$$\theta_x = \theta_s + \omega \left(\frac{L_x}{R_x} - \frac{L_s}{R_s} + \frac{M}{R_x} \right) \text{ radians}$$

As previously indicated, R_s and R_m circuits constitute a burden on the reference transformer. Therefore, f_s and θ_s are determined with these burdens.

The design of the divider is such that the balance conditions require

$$\frac{N_x'}{N_s'} = \frac{R_s}{R_x} \geq 1,$$

this requirement is met by using reference transformers whose voltage ratios have been adjusted to values 2 percent less than the integral values usually encountered as nominal ratios in instrument transformers.

The minimum resolution of this setup is such that the precision for ratio measurements is 2 ppm and for phase angle, 15 μrad at 25 and 60 Hz. However, susceptibility of the mutual inductor to the gradients of stray magnetic fields, large residuals and uncertainty in ratio calibration of the resistive divider limit the accuracy of these measurements to 10 ppm and 60 μrad, respectively. These errors increase rapidly with frequency. Therefore, this comparator is not suitable for accurate calibrations beyond 60 Hz.

3. Inductive Comparator

This comparator avoids a number of the objectionable features of the resistive comparator. The shielding is simple and is easily accomplished; the method is capable of extension to cover the audio-frequency range; the apparatus is less bulky and requires very little power for operation; the components are inherently more accurate and stable and readily available commercially; the ratio difference is indicated directly on the decade dials; and the set (except the detector) is self-contained in one portable case.

The schematic diagram of the circuit is shown in figure 5, which indicates the positions of resistor, R, and detector when the voltage phasor of the test transformer, X, leads that of the reference transformer, S. For lagging angles, the positions of R and detector are

[4] The $(f_s - 1)$ and θ_s for the NBS reference transformers are very small. Therefore, the approximations made are justifiable.

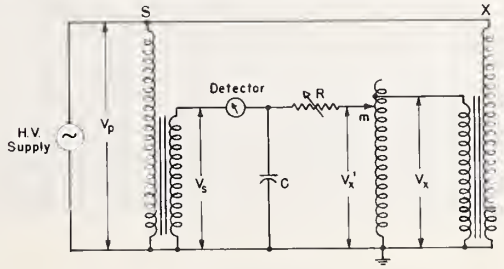

FIGURE 5.

simply interchanged. The in-phase voltage balance is obtained by adjusting the tap on the inductive voltage divider, and the quadrature voltage balance is obtained by adjusting either the resistor or the capacitor.

3.1. Theoretical Relations

As previously defined, the voltage ratio is

$$\frac{|V_{\text{Pri}}|}{|V_{\text{Sec}}|}=N'=Nf,$$

$$V_s=\frac{|V_p|}{N_s f_s}(\cos\theta_s+j\sin\theta_s),$$

and

$$V_x=\frac{|V_p|}{N_x f_x}(\cos\theta_x+j\sin\theta_x)=\frac{V'_x}{m},$$

m being the actual ratio of the inductive voltage divider. Corrections to the ratios and the phase angles of the inductive voltage divider used are insignificant and can be neglected. Then from figure 5,

$$\frac{V_s}{V'_x}=\frac{1-j\omega CR}{1+\omega^2C^2R^2}\approx 1-\omega^2C^2R^2-j\omega CR$$

The balance equation of the circuit becomes

$$\frac{N_x f_x(\cos\theta_s+j\sin\theta_s)}{mN_s f_s(\cos\theta_x+j\sin\theta_x)}=1-\omega^2C^2R^2-j\omega CR$$

and on separation and by neglecting second order terms

$$\theta_x=\frac{N_x f_x}{mN_s f_s}(\theta_s+\omega CR+\theta_s\omega^2C^2R^2)\approx\theta_s+\omega CR$$

radians, and

$$f_x=\frac{mN_s f_s}{N_x}\left(\frac{\cos\theta_x-\omega^2C^2R^2+\omega CR\sin\theta_x}{\cos\theta_s}\right)$$

$$\approx\frac{mN_s}{N_x}+(f_s-1)-\frac{1}{2}(\omega CR)^2$$

For relative lagging phase angle, with the detector and resistor, R, interchanged,

$$\theta_x\approx\theta_s-\omega CR \text{ radians, and}$$

$$f_x\approx\frac{mN_s}{N_x}+(f_s-1)+\frac{1}{2}(\omega CR)^2$$

3.2. Loading Effects

Since the input impedance of the inductive voltage divider at 60 Hz is in excess of 0.8 MΩ (nearly 1.00 power factor), the effect of loading of the f_x and θ_x of the test transformer can be expressed as

$$\left(\frac{\text{Equivalent Total Impedance Referred to Transformer Secondary}}{\text{(External Impedance)}}\right)$$

$$=(\text{Correction to } f_x \text{ and } \theta_x).$$

A transformer with an equivalent resistance of 1 Ω (which is easily measurable) will result in a correction of approximately 1 ppm [5].

The effect of loading by the quadrature balancing network on either the inductive voltage divider or the reference transformer is usually insignificant. At the limits of phase-angle range of ±37.8 mrad (130 min), the correction to ratio and phase angle of the inductive voltage divider is ~1 ppm and < 4 μrad, respectively; or, to the reference transformer, << 1 ppm and << 1 μrad.

3.3. Description of Components

All the components in this circuit are readily available commercially or accessible in most testing laboratories. In figure 5, R is a 0–10 kΩ, 10-turn, continuously adjustable resistor with small residual reactance. C is a 10 × 1 nF decade capacitor with a dissipation factor of < 0.0003. Both R and C were calibrated before and after assembly. The deviations from nominal values were found to be within 5 Ω and 5 pF, respectively.

The inductive voltage divider is a six-decade unit designed for optimum performance at 60 Hz.[5] For tests at higher frequencies (up to 1 kHz), it can easily be replaced by a unit of appropriate design, or by application of appropriate loading corrections to the ratio-correction-factor and phase angle. However, due to the simplicity of the circuitry and infrequent requests for calibrations at higher frequencies, a tem-

[5] Since maximum voltage on this divider is limited to 150 V at 60 Hz, it must be connected across the test transformer rather than the reference transformer whose secondary voltage may exceed this value in some instances.

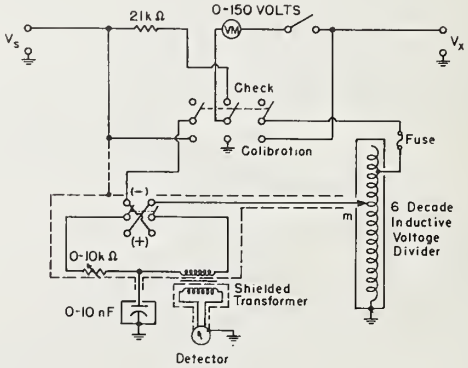

FIGURE 6.

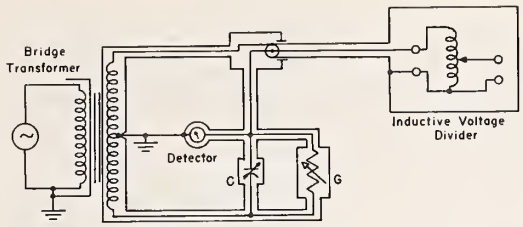

FIGURE 7.

porary setup is generally used at NBS. This consists of a high frequency divider, commercially available air capacitors, and an a-c decade resistor.

The input impedance of the inductive voltage divider was measured in a capacitive voltage divider setup; see figure 7 for circuit diagram [10]. The voltage-ratio corrections and phase-angle errors were obtained by a tracking method [11]. However, for a well designed inductive voltage divider, these corrections are usually < 0.2 ppm of input in ratio linearity deviation and < 8 μrad of input in phase deviation.

The detector circuit consists of a wave-analyzer used as a tuned null indicator and a specially constructed shielded transformer, shown in figure 6. This transformer is used to match impedances and to isolate the measuring circuit from the detector circuit electrostatically. It consists of a high permeability toroidal core, a 700-turn inner primary winding, two electrostatic shields, a 3500-turn outer secondary winding, and an overall Mu-metal case. The use of a toroid minimizes the magnetic pickup from stray fields in the laboratory.

The polarity checking voltmeter is a 0–150 V, 3-in. panel-type instrument of 3 percent accuracy. The 21 kΩ resistor matches its internal resistance. The voltmeter indicates the secondary voltage of the test transformer when the selector switch is in the "CALIBRATION" position.

Figures 8 and 9 show the exterior and interior of the comparator. The cylindrical shield shown in the interior view encloses the 10-kΩ resistor.

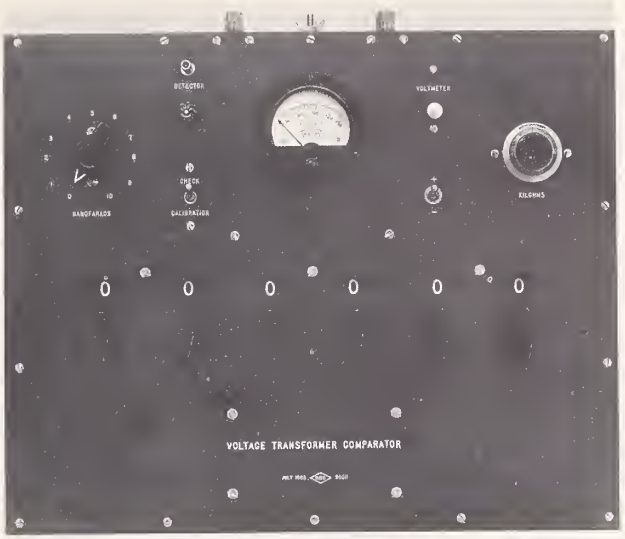

FIGURE 8.

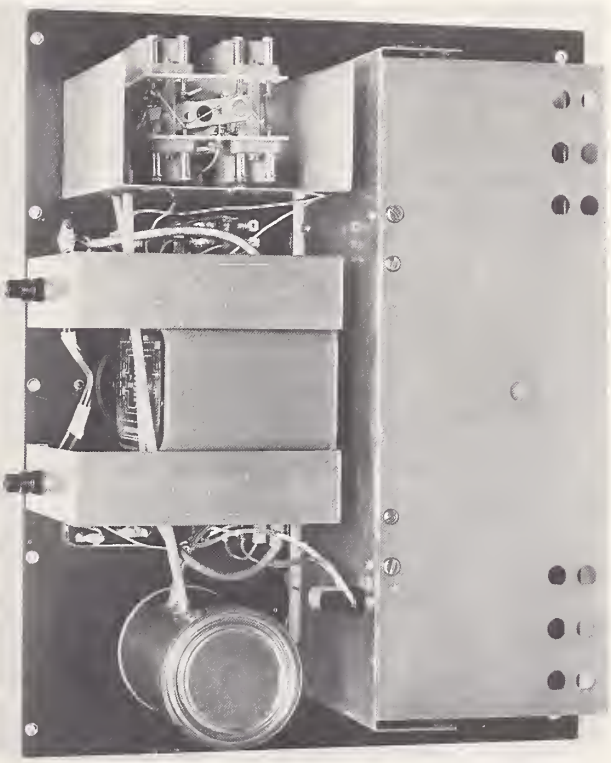

FIGURE 9.

3.4. Accuracy Determination

After the completion of the comparator, the calibration of each component was rechecked.

The accuracy of the completed comparator was verified by the following procedures: (1) connecting a single voltage source to both "V_s" and "V_x" terminals to obtain the zero corrections for C and R and the unity correction for dial settings of the inductive voltage divider; (2) calibrating several pairs of transformers of the same ratio to reference transformers of appropriate ratios, thus determining the relative ratio-correction-factors and phase-angle errors with several values of secondary burden for each pair of transform-

ers; (3) comparing each pair of these calibrated transformers to each other with the comparator alternately as reference and test units and with various combinations of previously used secondary burdens; and (4) connecting a single voltage source to "V_x" terminals and to the input of a calibrated inductive voltage divider, whose output is connected to "V_s" terminals in order to check the fractional ratio measurements.

3.5. Transformer Testing Procedure

A reference transformer is selected so that $N_s \geq N_x$. The selector switch is set to "CHECK" position; and the ratio, m, is set to equal N_x/N_s. The secondaries of the test and reference transformers are connected to "V_x" and "V_s" terminals respectively. With the transformers energized and the voltmeter switch depressed, the voltmeter indicates $(V_s - V_x)/2$ if the polarities of V_s and V_x are correctly connected to the comparator. [The polarity of V_x must be reversed if voltmeter indicates $(V_s + V_x)/2$.] The test proceeds with the selector switch turned to "CALIBRATION." V_x is now indicated on the voltmeter.

If $N_x > N_s$ by more than 10 percent, the test can still be made, but the reference transformer must be connected to "V_x" terminal and the test transformer to "V_s". At the balanced condition, the ratio, m, will indicate the reciprocal of the relative ratio-correction-factors, and the relative phase-angle switch will show the negative of the markings as shown in figures 6 and 8.

3.6. Consideration of Errors

An examination of errors requires a careful appraisal of all components of the measuring circuit as well as a justification of estimations, even though in this case one would expect most of the associated errors to be negligible.

The first to be considered are those possible errors concealed through approximation in developing the expressions for obtaining the ratio-correction-factor and phase-angle relations, where the effects of the residual of the 10-kΩ resistor and the dissipation factor of the decade capacitor are ignored. Approximate magnitudes of these errors can be obtained by adding the estimated equivalent residual reactance across R and estimated equivalent series resistance to C. These effects were found to be less than 0.5 ppm for ratio and 5 μrad for phase angle at the limits of the phase angle range (±38 mrad) at 60 Hz.

A second source of uncertainty is in the calibration of the inductive voltage dividers. However, past experience indicates that errors should not exceed 0.2 ppm of input in ratio linearity deviation and 2 μrad of input in phase deviation [12].

Errors caused by the leads, switch contacts, and imperfect shields are estimated to be < 0.5 ppm and < 2 μrad.

The last important uncertainty that should be considered is in obtaining the transformer secondary load corrections. Such errors are estimated to be 0.5 ppm and 3 μrad for each transformer.

Finally, one should add 3 times the standard deviations (0.3 ppm of ratio and 1 μrad) of the results obtained in repeated balances of the comparator to the combination of the systematic-error estimates.

Source of errors	Uncertainties to ratio-correction-factor		Uncertainties to phase angles	
	n	n^2	n	n^2
	ppm		μrad	
From assumptions made in equations	0.5	0.25	5	25
Calibration of the inductive voltage divider	.2	.04	2	4
Obtaining secondary load corrections (S)	.5	.25	3	9
Obtaining secondary load corrections (X)	.5	.25	3	9
Leads and contacts	.5	.25	2	4
Σn^2		1.04		51
$(\Sigma n^2)^{1/2}$	1.02		7.1	
3 × standard deviations	0.90		3.0	
Maximum error	1.9 ppm		10.1 μrad	

4. Conclusion

A high accuracy inductive comparator has been developed for measuring the relative voltage ratio and phase angle of voltage transformers and testing sets at power and audio frequencies. An overall accuracy of < 2 ppm in ratio measurements and < 10 μrad in phase angle at 60 and 400 Hz is achieved, with a slight reduction in the accuracy attainable at higher audio frequencies.

The simple circuit does not require any special equipment. Only a few ranges of reference transformers are required, since fractional ratios from 1/1 to 1/4 may be measured as readily as ratios near unity.

This inductive comparator could replace testing sets now in general use. It is compact and portable, has a broader useful frequency range, and exceeds the accuracy of many commercial sets presently available by one or two orders of magnitude.

The resistive comparator will continue to be used at NBS for calibration of voltage transformers at 25 Hz at which frequency the operating voltage is usually above the maximum operating voltage of the inductive comparator.

The author acknowledges the valuable help and advice received from Mr. F. L. Hermach, Chief, Electrical Instrument Section, NBS. Mr. R. J. Berry contributed skillfully in constructing the new comparator.

5. References

[1] F. B. Silsbee and F. M. Defandorf, A transformer method for measuring high alternating voltages and its comparison with an absolute electrometer, J. Res. NBS 20, 317–336 (1938) RP1079.

[2] W. K. Clothier and L. Medina, The absolute calibration of voltage transformers, Proc. Institution of Electrical Engineers, **104A**, 204–214 (1957).

[3] F. K. Harris, W. C. Sze, N. L. Kusters, O. Petersons, W. J. M. Moore, An international comparison of voltage transformer calibrations to 350 kV, IEEE Trans. on Communication & Electronics No. 70, pp. 13–19 (1964).

[4] Private communication from F. K. Harris, Chief, Absolute Electrical Measurements Section, NBS.

[5] F. K. Harris, Electrical Measurements (John Wiley and Sons, Inc., New York, N.Y.) pp. 410–411, 565–569 and 611–612 (1951).

[6] W. Duddell and T. Mather, Improvements in non-inductive resistance, British Patent No. 5171 (1901).

[7] F. B. Silsbee, A shielded resistor for voltage transformer testing, Bull. BS **20**, 489–514 (1926).

[8] Private communication from F. K. Harris and B. L. Dunfee, NBS.

[9] H. B. Brooks and A. B. Lewis, Improved continuously variable self and mutual inductor, J. Res. NBS **19**, 493 (1937) RP1040.

[10] M. C. McGregor, J. F. Hersh, R. D. Cutkosky, F. K. Harris and F. R. Kotter, New apparatus at NBS for absolute capacitance measurement, IRE Trans., Instr., **I-7**, 253–261 (1958).

[11] NBS Technical News Bulletin, **49**, 1 (1965).

[12] W. C. Sze, A. F. Dunn, and T. L. Zapf, An international comparison of inductive voltage divider calibrations at 400 and 1000 hertz, IEEE Trans. on Instr. and Meas. **IM-14**, No. 3, 124–131 (1965).

(Paper 69C4–206)

An International Comparison of Voltage-Transformer Calibrations to 350 Kv

F. K. HARRIS
FELLOW IEEE

W. C. SZE
SENIOR MEMBER IEEE

N. L. KUSTERS
MEMBER IEEE

O. PETERSONS
MEMBER IEEE

W. J. M. MOORE
SENIOR MEMBER IEEE

IN JUNE 1960, the Hydro-Electric Power Commission of Ontario inquired whether the United States National Bureau of Standards (NBS) in Washington could measure for them the ratio and phase-angle errors of a 350-kv voltage transformer then being built to their order. This request was also made at about the same time of the National Research Council of Canada (NRC) in Ottawa. Neither laboratory had, at that time, made calibration measurements on instrument transformers at this voltage level, but both had given the problem considerable thought; and it appeared that the request by Ontario Hydro afforded a unique opportunity not only to examine some of the problems involved in voltage-ratio measurements at 350 kv, but also to compare measurement results between the two national laboratories.

The transformer, as first built, developed troubles during shipment that required structural modifications; but finally, early in 1962, the completed transformer arrived in the High-Voltage Laboratory of NRC for calibration tests. From Ottawa it was carried by truck to Washington for further measurements in the High-Voltage Laboratory of NBS, and then returned to NRC for repeat measurements. In this way, it was believed that any changes resulting from its shipment could be detected, and perhaps separated out from the interlaboratory comparison.

The transformer is of unusual construction and, since this had considerable bearing on the test results, it will be described in some detail. Following this, the NRC and NBS tests will be separately discussed, and finally the results from the two laboratories will be compared.

Description of the Transformer

The transformer is a cascade type made by the Canadian General Electric Company.[1] It consists of three sections, each with a separate core and primary winding encased in a porcelain cylinder. The primary voltage is distributed equally among the series-connected primary windings of the three sections. To insure equal voltage distribution among the sections and to provide a low-impedance path for the load current, the cores are coupled by low-voltage windings. The secondary winding of the transformer is on the section nearest ground. Voltage ratios of 4,000:1, 3,000:1, and 2,000:1 are available at the rated primary voltage of 350 kv, by means of taps on the secondary winding. Additional ratios of 1,200:1 and 1,000:1 are obtained by connecting the primary voltage across the two lower sections of the transformer. The 1,200:1 ratio involves a nonintegral number of secondary turns, that is, one turn links only part of the core.

Shielding

Since the case of this transformer is made up of the porcelain cylinders that insulate its three sections, the windings are not electrically shielded; and the capacitive currents in the windings will depend on the location of nearby objects and the potential difference between them and the transformer section. The internal impedance of the transformer being high, appreciable voltage drops may result from these capacitive currents, so that the voltage ratio and phase angle of the transformer are dependent on its environment, and will change depending on the potential and distance of neighboring objects.

To reduce this proximity effect, shields were constructed and were connected to the ground and high-voltage terminal as shown in Fig. 1. Both shields were used for the three highest ratios, while only the lower shield was used for the 1,200:1 and 1,000:1 ratios. It will be seen from the result that these shields

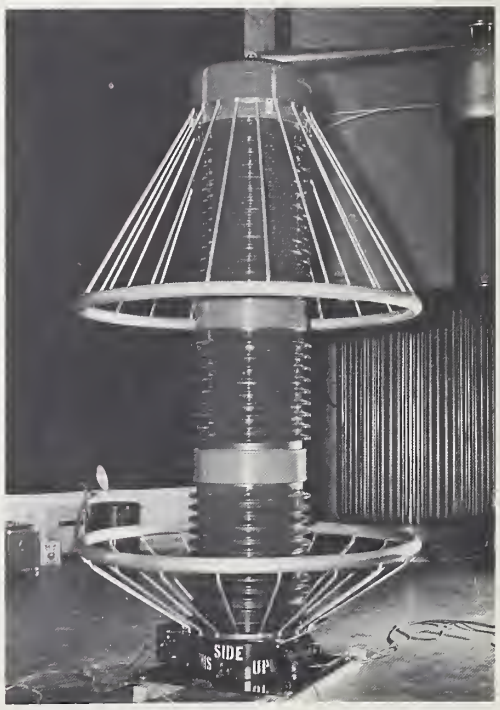

Fig. 1. Transformer equipped with shields

Paper 63-992, recommended by the IEEE Fundamental Electrical Standards Committee and approved by the IEEE Technical Operations Committee for presentation at the IEEE Summer General Meeting and Nuclear Radiation Effects Conference, Toronto, Ont., Canada, June 16–21, 1963. Manuscript submitted March 18, 1963; made available for printing May 7, 1963.

F. K. HARRIS and W. C. SZE are with the National Bureau of Standards, Washington, D. C.; and N. L. KUSTERS, O. PETERSONS, and W. J. M. MOORE are with the National Research Council of Canada, Ottawa, Ont., Canada.

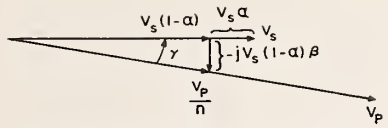

Fig. 2. Transformer errors as measured by high-voltage capacitance bridge

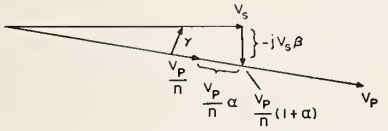

Fig. 3. Transformer errors as measured by capacitive voltage divider

make the transformer less sensitive to the location of external objects, but they do increase capacitance currents in the transformer windings, so that the ratio and phase angle of the transformer are substantially different in the shielded and unshielded condition.

NRC Tests

Calibration Methods

At NRC the transformer was calibrated with a new high-voltage capacitance-ratio bridge, based on the current-comparator principle, and two gas-dielectric capacitors.[2,3] The high-voltage capacitor was a commercial 50-pf (picofarad) compressed-gas unit rated at 500 kv, while the low-voltage capacitor was of parallel-plate construction with air dielectric. The capacitance ratio of the two capacitors is first determined with the same voltage applied to both, the current ratio, measured by a current comparator, being equal to the ratio of capacitances. The primary voltage is then applied to one capacitor and the secondary voltage to the other, and the ratio of currents is again measured. This ratio is the product of the voltage ratio and the capacitance ratio. The bridge is direct reading in transformer errors as defined by the vector diagram of Fig. 2 and the following equation:

$$\frac{V_p}{n} = V_s(1-\alpha)(1-j\beta) \qquad (1)$$

where V_p is primary voltage, V_s is secondary voltage, n is nominal ratio, α is in-phase error, and β is quadrature error.

The voltage applied to the capacitors during their ratio determination may be very different from that of the second measurement, and the stability of the capacitors with applied voltage must be known. An investigation covering this point has been reported previously.[4]

A capacitive voltage divider such as that used by Clothier and Medina was also available.[5] In this divider the ratio of capacitances is equal to the nominal ratio of the transformer. To permit the use of capacitors with gas dielectric, the capacitance of the low-voltage arm must be limited to a few thousand pf. For the high-voltage arm a 1-pf capacitor rated at 80 kv was available. Thus up to 80 kv, it was possible to calibrate the transformer by two methods. The balancing circuitry associated with the capacitive divider is direct reading in transformer errors; and the balance condition may be represented by the diagram of Fig. 3 and the following equation:

$$\frac{V_p}{n} = V_s(1-j\beta)/(1+\alpha) \qquad (2)$$

The stability of the capacitors with voltage is equally important in both methods.

Proximity Effect

While the influence of nearby objects on the transformer errors was reduced by the addition of the shields, these shields shifted the in-phase error in the negative direction by 1,500 ppm (parts per million) and the quadrature error in the positive direction by 730 ppm at the top three ratios. The calibration results tabulated later in this paper are applicable only when the shields are used, and with ample clearance around the transformer.

To illustrate the severity of the proximity effect, the changes in transformer errors corresponding to the introduction of certain objects in the vicinity of the transformer were recorded. One of these objects was a piece of tubing suspended from the high-voltage bus bar, approximately 4 feet from the transformer. The other was a high-voltage capacitor approximately 8 feet from the transformer. The outer part of the capacitor is a high-voltage electrode, and could either be grounded or excited from the high-voltage bus. These objects are shown in Fig. 4. The variations in transformer errors ($\Delta\alpha$, $\Delta\beta$) at a 2,000:1 ratio are recorded in Table I. The values given represent transformer error with the object present minus the error with the object removed. It will be noted that the largest variation occurs from proximity of an object at high voltage. The shields reduce this effect by a factor of three. The shift in transformer errors is much less when the object is grounded, and the shields are not as effective in reducing this shift.

Comparison of Test Methods and Transformer Stability

A limited number of calibration points were remeasured at NRC following the return of the transformer from NBS. These are summarized in Table II, together with data that are typical of the results obtained using the two methods of calibration described above.

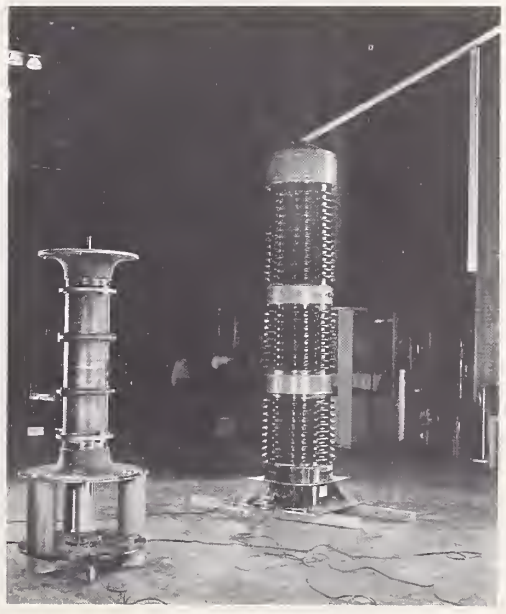

Fig. 4. Transformer and objects for which proximity effects were measured

A—Top right: tubing suspended from bus bar
B—Left: high-voltage capacitor

Table I

	Transformer Without Shields		Transformer With Shields	
	Δα (Ppm)	Δβ (Ppm)	Δα (Ppm)	Δβ (Ppm)
Tubing suspended from bus	−187	+ 95	−53	+29
Capacitor energized from bus	−273	+123	−86	+36
Capacitor grounded	+ 24	− 10	+14	− 9

Table II

Nominal Ratio	Secondary Volts	α (Ppm) Method 1 Before	Method 1 After	Method 1 Before − After	Method 2 (Before)	Method 1 − Method 2*
1,000:1	80	+1,202	+1,195	+ 7	+1,206	−4
1,200:1	66.7	−1,114	−1,289	+175	−1,111	−3
2,000:1	40	− 893	− 912	+ 19	− 894	+1
3,000:1	26.7	− 942	− 962	+ 20	− 944	+2
4,000:1	20	− 992	−1,010	+ 18	− 992	0
		β (Ppm)				
1,000:1	80	+ 340	+ 341	− 1	+ 344	−4
1,200:1	66.7	+ 231	+ 254	− 23	+ 235	−4
2,000:1	40	−1,177	−1,175	− 2	−1,177	0
3,000:1	26.7	−1,145	−1,141	− 4	−1,141	−4
4,000:1	20	−1,061	−1,056	− 5	−1,059	−2

* In using Method 2, the 1-pf capacitor (shown in Fig. 4) was connected to the high-voltage bus, and therefore contributed to the "proximity effect." Hence, to make a valid comparison between Method 1 and Method 2, it was necessary that voltage be impressed on this capacitor for the Method-1 measurements. Thus it will be noted that the data of Table II are not strictly equivalent to those of Table IV, for which the 1-pf capacitor was grounded.

It will be noted that the two test methods yield results that are in complete agreement, that is, their differences are random and well within the estimated accuracy (10 ppm) of the two methods. It will also be noted that there was a very marked shift in the 1,200:1 ratio values and a smaller but definite shift in the other ratios, after the transformer had travelled to Washington and back to Ottawa. Additional calibration points, not included in the table, indicated that differences between the measured values obtained before and after the NBS tests were constant over the whole voltage range of the transformer.

NBS Tests

At the National Bureau of Standards it was decided to use the method of Clothier and Medina, and a 1-pf free-air capacitor, rated at 350 kv, was constructed for use in the capacitive voltage divider. Its construction and characteristics are described in a companion paper.[6] The low side of the divider was made up of one to four 1,000-pf air capacitors of special construction, depending on the nominal ratio of the transformer. The circuit is shown schematically in Fig. 5, but simplified by not indicating the shielding in detail. Balance was achieved by adjusting the tap points on inductive voltage dividers connected across the secondary winding of the transformer. Commercial 6-decade inductive voltage dividers designed for 60-cycle operation were used. Positive or negative phase-angle errors could be compensated by moving the tap point to one side or the other of the indicated ground point of the divider, and so reversing the voltage of the branch with respect to the secondary voltage of the transformer.

Using the following expression for the relation between primary and secondary voltage of the transformer

$$\frac{V_p}{nV_s}=(1-\alpha-j\beta) \qquad (3)$$

and the balance equation of the network shown in Fig. 5,

$$i_1+i_3=i_2$$

we have

$$nV_s(1-\alpha-j\beta)\cdot j\omega C_1 = V_s\left[N_1 . j\omega C_2 - N_2\left(\frac{1}{R}+j\omega C_3\right)\right]$$

and on separation, this becomes

$$1-\alpha=\frac{1}{n}\cdot\frac{C_2}{C_1}\left[N_1-N_2\frac{C_3}{C_2}\right]\simeq\frac{N_1}{n}\cdot\frac{C_2}{C_1}$$

and

$$\beta=-N_2/(\omega nRC_1)$$

where N_1 and N_2 are the fractions of V_s impressed on C_2 and R, respectively, by the voltage dividers. Since this test network was not expected to become a permanent laboratory setup, it was not considered worthwhile to make it direct reading. It will be noted that the in-phase balance expression contains a term representing the equivalent shunt capacitance across the resistor R used for quadrature balance. In any practical case this would never be more than a few ppm and, with the resistance element and shielding used, it was found to be negligible. Thus the capacitance ratio becomes C_2/C_1 and, since C_1 is a free-air capacitor whose value is subject to ambient temperature, pressure, and humidity, this capacitance ratio was determined immediately before and after any series of transformer ratio measurements, and the mean of the ratio values was used in computing the transformer errors. If the two capacitance-ratio values were markedly different, indicating a considerable drift in the value of C_1, the run was discarded. The ratio C_2/C_1 was established in three steps with a 10:1 transformer-ratio-arm bridge, using equipment very similar to that described earlier by McGregor et al.[7]

As has already been pointed out in discussing the NRC test methods, the capacitance ratio is determined at a low voltage, whereas a very different voltage is impressed on one of the capacitors in voltage-divider operation. It is therefore important that any change of capacitance with voltage be known, so that an appro-

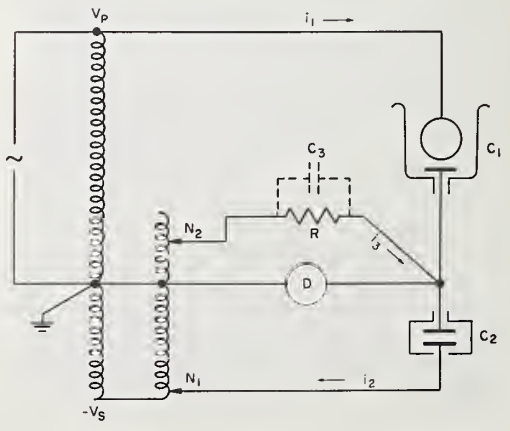

Fig. 5. NBS test circuit

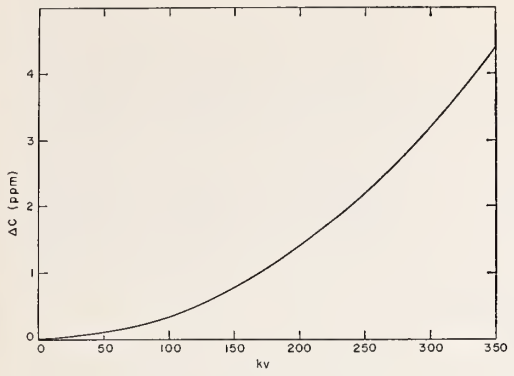

Fig. 6. Voltage corrections to NBS capacitor

priate correction to the ratio may be applied. This was investigated for the 1-pf 350-kv capacitor, and is separately reported.[6] The corrections arising from impressed voltage are shown in Fig. 6, capacitance increasing with increasing voltage. Measurements on the 1,000-pf low-voltage capacitors indicated that they change by not more than 1 part in 10^7 over the voltage range of interest.[7]

Another correction that must be taken into account results from the burden imposed on the transformer by the test-circuit elements connected across its secondary winding. This correction can be computed in terms of the impedance of the circuit elements, and the burden calibration of the transformer.

As to proximity effect, the shield system was used in the same way as at NRC and a cleared area with a radius of 11 feet was in all cases maintained around the transformer at ground level. In the space above the plane of ground shield, the clearance was nearly double this value, except for the high-voltage conductor between the transformer and the high-voltage capacitor. The test arrangement is shown in Fig. 7.

Results of the tests in the two national laboratories will be summarized below, using values which are generally the average of several determinations. First however, it will be instructive to look at the maximum spread in the NBS values used for these averages, to show the combined uncertainties and instabilities of the measuring method and equipment, and of the transformer. This is given in Table III. While most of this spread is believed to represent uncertainties of variations in balancing techniques, instabilities in measuring-circuit components, or errors in setting test burdens or voltages, there is some reason to suspect small variations in the transformer itself. Precautions were regularly taken to prevent core magnetization that could significantly affect ratio and phase-angle values at the lower test voltages; but on one occasion the transformer was inadvertently magnetized, and its subsequent stabilization was quite tedious. It is believed that day-to-day variations of a few ppm in transformer ratio were seen.

Comparison of NRC and NBS Test Results

In Table IV are listed the average ratio and phase-angle errors in ppm, observed for the transformer in the two national laboratories for various test conditions. All values were taken at a 60-cycle frequency. The NRC data tabulated are those taken before the NBS test.

As has been noted already, the transformer errors changed during the series of tests, and it is supposed that these shifts occurred as a result of road shocks during shipment of the transformer between the two laboratories. In Table V, the differences of Table II between the transformer errors before and after its trip to Washington are compared with the average differences from Table IV

Table III

Nominal Ratio	Number of Determinations	Maximum Spread (Ppm) $\Delta\alpha$	Maximum Spread (Ppm) $\Delta\beta$
1,000:1	5	6	4
1,200:1	7	13	6
2,000:1	12	17	6
3,000:1	13	23	8
4,000:1	10	18	10

between the initial NRC values and the NBS values.

Only for the 1,000:1 ratio are the differences between the in-phase errors found by the two laboratories greater than the observed differences in the NRC values before and after shipment to NBS. Since these measurements required that the upper shield ring of Fig. 1 be removed, with a consequent increase in the proximity effect, it may well be that this difference results in part from a minor difference in the arrangement of the high-voltage bus-bar and transformer connection in the two laboratories. The same statement concerning shield and lead arrangement could be made about the 1,200:1 ratio, but here any possible differences from this cause are masked by the very large "transportation" shift in the transformer itself. While it is rather suprising that such a large change in ratio would occur, it seems reasonable that the behavior of this ratio could be very different from the others since one turn of this secondary winding links only a portion of the core.

It may be noted from Table IV that the interlaboratory differences in quadrature errors appear to show a trend with changing voltage for the 1,000:1 and 1,200:1

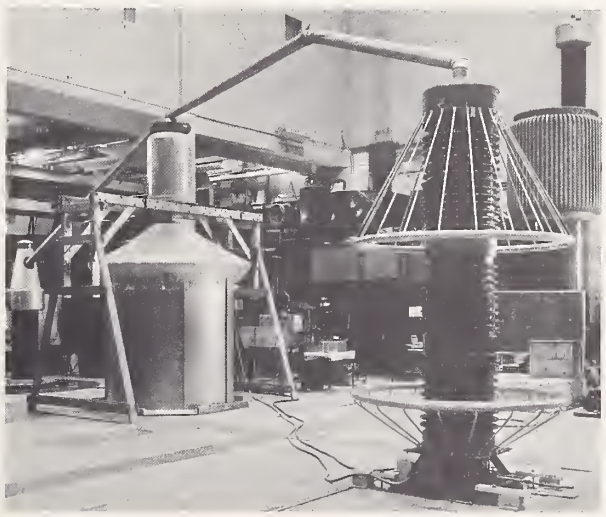

Fig. 7. NBS test arrangement

Table IV

Nominal Ratio	Secondary Volts	NRC α	NRC β	NBS α	NBS β	NRC−NBS Δα	NRC−NBS Δβ	Burden
1,000:1	50	1,208	373	1,227	386	− 19	−13	open circuit
	60	1,201	358	1,222	371	− 21	−13	
	69	1,196	349	1,218	360	− 22	−11	
	80	1,192	340	1,214	348	− 22	− 8	
	100	1,186	330	1,208	334	− 22	− 4	
	120	1,184	325	1,206	326	− 22	− 1	
	130	1,185	326	1,207	323	− 22	+ 3	
	50	1,110	55	1,131	67	− 21	−12	.882 ohms, unity power factor
	60	1,106	42	1,123	51	− 17	− 9	
	69	1,100	33	1,121	43	− 21	−10	
	80	1,098	23	1,115	29	− 17	− 6	
	100	1,091	13	1,109	18	− 18	− 5	
	120	1,089	8	1,107	8	− 18	0	
	130	1,088	9	1,109	5	− 21	+ 4	
					Ave.	− 20	− 6	
1,200:1	50	−1,108	241	−1,236	270	+128	−29	open circuit
	60	−1,118	235	−1,248	263	+130	−28	
	69	−1,124	231	−1,256	260	+132	−29	
	80	−1,130	229	−1,265	255	+135	−26	
	100	−1,138	231	−1,274	252	+136	−21	
	120	−1,140	241	−1,277	251	+137	−10	
	130	−1,140	249	−1,277	250	+137	− 1	
	50	−1,212	− 15	−1,338	+ 10	+126	−25	.882 ohms, unity power factor
	60	−1,224	− 20	−1,354	+ 2	+130	−22	
	69	−1,232	− 24	−1,365	0	+133	−24	
	80	−1,241	− 25	−1,374	− 3	+133	−22	
	100	−1,249	− 23	−1,385	− 7	+136	−16	
	120	−1,252	− 14	−1,389	− 10	+137	− 4	
	130	−1,252	− 9	−1,388	− 12	+136	+ 3	
					Ave.	+134	−18	
2,000:1	50	− 845	−1,174	− 848	−1,178	+ 3	+ 4	open circuit
	75	− 785	−1,170	− 786	−1,175	+ 1	+ 5	
	100	− 749	−1,164	− 751	−1,171	+ 2	+ 7	
	125	− 726	−1,160	− 727	−1,169	+ 1	+ 9	
	150	− 715	−1,158	− 718	−1,165	+ 3	+ 7	
	50	− 959	−1,495	− 968	−1,505	+ 9	+10	.882 ohms, unity power factor
	75	− 898	−1,492	− 907	−1,505	+ 9	+13	
	100	− 862	−1,488	− 871	−1,501	+ 9	+13	
	125	− 838	−1,484	− 848	−1,498	+ 10	+14	
	150	− 826	−1 482	− 836	−1,495	+ 10	+13	
					Ave.	+ 6	+10	
3,000:1	33.3	− 897	−1,142	− 906	−1,142	+ 9	0	open circuit
	50	− 840	−1,138	− 849	−1,142	+ 9	+ 4	
	66.7	− 805	−1,135	− 815	−1,135	+ 10	0	
	83.3	− 783	−1,130	− 794	−1,132	+ 11	+ 2	
	100	− 773	−1,128	− 783	−1,129	+ 10	+ 1	
	116.7	− 773	−1,128	− 782	−1,127	+ 9	− 1	
	33.3	− 948	−1,276	− 960	−1,276	+ 12	0	.882 ohms, unity power factor
	50	− 892	−1,272	− 901	−1,276	+ 9	+ 4	
	66.7	− 857	−1,268	− 866	−1,272	+ 9	+ 4	
	83.3	− 833	−1,264	− 846	−1,268	+ 13	+ 4	
	100	− 822	−1,262	− 833	−1,265	+ 11	+ 3	
	116.7	− 822	−1,262	− 832	−1,261	+ 10	− 1	
					Ave.	+ 10	+ 2	
4,000:1	25	− 955	−1,062	− 954	−1,060	− 1	− 2	open circuit
	37.5	− 910	−1,061	− 911	−1,060	+ 1	− 1	
	50	− 882	−1,058	− 882	−1,059	0	+ 1	
	62.5	− 863	−1,054	− 862	−1,057	− 1	+ 3	
	75	− 850	−1,056	− 852	−1,055	+ 2	− 1	
	87.5	− 850	−1,056	− 851	−1,051	+ 1	− 5	
	25	− 994	−1,157	− 993	−1,154	− 1	− 3	.882 ohms, unity power factor
	37.5	− 946	−1,155	− 951	−1,154	+ 5	− 1	
	50	− 920	−1,152	− 922	−1,154	+ 2	+ 2	
	62.5	− 898	−1,150	− 903	−1,151	+ 5	+ 1	
	75	− 889	−1,150	− 892	−1,148	+ 3	− 2	
	87.5	− 888	−1,149	− 890	−1,147	+ 2	− 2	
					Ave.	+ 2	− 1	

ratios. No such trend is observable in the in-phase error, nor is such a trend apparent in any of the three higher ratios. No explanation can be suggested for the quadrature peculiarity noted in the two lower ratios; but it may be concluded with considerable assurance that any voltage dependence of the capacitors was properly allowed for by both laboratories.

A slightly better internal consistency is to be noted in the NRC results of Table IV, which can probably be explained on the basis of better stability in the compressed-gas high-voltage capacitor (used by NRC) than in the free-air capacitor (used by NBS). The spread of NBS measurements given in Table III is further evidence toward this conclusion.

Conclusions

Within the past 3 years, this is the second international comparison of transformer calibrations in which these two national laboratories have participated. In the previous comparison, the agreement between NRC and NBS results at ratios of 1,000:1 and higher was between 100 and 300 ppm, based in both laboratories on resistive voltage dividers whose voltage coefficients of ratio could be evaluated only with difficulty and to a rough approximation.[5] In the present comparison the results agree between the laboratories within 20 ppm at ratios to 4,000:1 and voltages to 350 kv, except for the 1,200:1 ratio where the transformer instability made the measurements less meaningful. It may therefore be said that an improvement of an order of magnitude has been achieved, and that ratio and phase-angle measurements on voltage transformers are now reliable in either laboratory within 20 ppm and 10 microradians (2 arc seconds), at voltages to 350 kv.

Considering the ratio instability of the transformer and its sensitivity to neighboring objects, it appears that closer interlaboratory agreement would not be possible with a transformer of the type used.

References

1. Cascade-Type Potential Transformers, G. Camilli. *General Electric Review*, Schenectady, N. Y., vol. 39, Feb. 1936, pp. 95–99.

2. A Transformer-Ratio-Arm Bridge for High-Voltage Capacitance Measurements, N. L. Kusters, O. Petersons. *IEEE Transactions on Communication and Electronics* (*Paper 63-168*).

3. The Development of the Current Comparator, A High Accuracy A-C Ratio Measuring Device, P. N. Miljanic, N. L. Kusters, W. J. M. Moore. *AIEE Transactions*, pt. I (*Communication and Electronics*), vol. 81, Nov. 1962, pp. 359–68.

4. The Voltage Coefficients of Precision Capacitors, N. L. Kusters, O. Petersons. *IEEE Transactions on Communication and Electronics* (*Paper 63-169*).

5. The Absolute Calibration of Voltage Transformers, W. K. Clothier, L. Medina. *Proceedings*, Institution of Electrical Engineers, London, England, vol. 104A, June 1957, pp. 204–14.

6. An Experimental 350-Kv-1-Picofarad Air Capacitor, A. E. Peterson. *IEEE Trans-*

Table V

Nominal Ratio	NRC (Before) − NRC (After) Δα	NRC (Before) − NRC (After) Δβ	NRC (Before) − NBS Δα	NRC (Before) − NBS Δβ
1,000:1	+ 7	− 1	− 20	− 6
1,200:1	+175	−23	+134	−18
2,000:1	+ 19	− 2	+ 6	+10
3,000:1	+ 20	− 4	+ 10	+ 2
4,000:1	+ 18	− 5	+ 2	− 1

actions on Communication and Electronics (Paper 63-926).

7. New Apparatus at the National Bureau of Standards for Absolute Capacitance Measurement, M. C. McGregor, J. F. Hersh, R. D. Cutkosky, F. K. Harris, F. R. Kotter. *IRE Transactions on Instrumentation*, vol. I-7, Dec. 1958, pp. 253–61.

8. A Report on Canadian Participation in an International Comparison of Instrument Transformer Calibrations–1959, N. L. Kusters, W. J. M. Moore, O. Petersons, C. A. E. Uhlig. *Report ERB-571*, National Research Council of Canada, Radio and Electrical Engineering Division, Ottawa, Ont., Canada, 1960.

Discussion

K. M. Mitchell (The Hydro-Electric Power Commission of Ontario, Toronto, Ont., Canada): In this paper the authors have pointed out the limitations of this transformer with respect to its ratio stability and the influence of neighboring objects on its errors. With measuring techniques sensitive to a few ppm, these effects are clearly evident. This suggests the possibility that other influences on the errors of the transformer, such as temperature, frequency, and waveform, may also be significant in terms of these references. However, the paper does not discuss these influences. It would be appreciated if the authors could comment on their magnitude, and outline what precautions, if any, were necessary to minimize their effect on the intercomparison.

The proximity effect which the authors point out as a characteristic of any unshielded transformer has been shown in Table I to be an effect of practical significance, at least with respect to the cascade-transformer design used in this intercomparison. That such could be the case, I do not think has been generally appreciated. Considering the possible significance of the proximity effect and the growing numbers of potential transformers of the cascade type in service on electric utility systems, it would seem desirable that any revisions to national standards for instrument transformers should recognize this characteristic of unshielded or partially shielded transformers and possibly detail acceptable magnitudes for it. This infers the availability of a test method to establish compliance of a transformer with the requirement. Have the authors any suggestions for the formulation of a suitable test method?

With reference to the terms α and β which have been used to express the in-phase error and quadrature error, respectively, three different equations expressing the relationship between these terms and the primary and secondary voltage are given (see equations 1–3). Two of these are illustrated by the vector diagrams of Figs. 2 and 3. In the first of these expressions (Fig. 2), the in-phase error, α, is expressed as a fraction of the true secondary voltage and $\beta = \tan \gamma$, where γ is the phase-angle error. In the second expression (Fig. 3), although β may still be defined as $\tan \gamma$, α is expressed as a fraction of the nominal secondary voltage, that is, V_p/n. In the third expression (equation 3),

$$\frac{V_p}{nV_s} = (1 - \alpha - j\beta)$$

α is the in-phase error expressed as a fraction of the true secondary voltage, but β must be defined as $(1-\alpha)\tan\gamma$. It is appreciated that these differences in definition of α and β arise from the balance equations of the several test methods employed by the authors and that for small values of α and β they may not be significant. However, the errors of this transformer on the higher ratios are such that approximations of the order of 1 to $1^1/_2$ ppm are involved and differences of this magnitude are tabulated. I should like to ask whether in the preparation of Tables IV and V a common definition of α and β has been used or whether the differences in α and β tabulated here include differences in the definition of these quantities?

J. M. Vanderleck (The Hydro-Electric Power Commission of Ontario, Toronto, Ont., Canada): It is gratifying to know that the results agree between the two laboratories within 20 ppm. Phase-angle accuracy of 20 ppm is desired for corona-loss measurements of extra-high-voltage test lines in order to limit the phase-angle error owing to the voltage transformers to an acceptable value of 60 watts per 3-phase mile (60 watts is based on a charging kilovolt-ampere of 3,000 and phase angle of 20 ppm). The temperature influence on phase angle could be important since corona-loss measurements may be made from 0 to 95 degrees Fahrenheit ambient.

Other instances wherein instrument voltage-transformer accuracy is particularly significant are as follows:

1. Revenue metering of high-voltage circuits.

2. Acceptance tests on voltage transformers.

In the first case, it is desirable to know the error owing to the group of installed instrument transformers within 0.1% (1,000 ppm). To achieve this result, the errors of each of the five or six instrument transformers installed in service should be measured within 300 ppm. Thus, it is desirable that the errors of the reference-standard voltage transformer be known and certified by a national laboratory within 100 ppm.

A similar accuracy (100 ppm) is useful to minimize the doubt whether a voltage transformer conforms with purchase specifications during acceptance tests. An overall testing accuracy of 300 ppm can be achieved in practice if the accuracy of the reference-standard transformer is 100 ppm. An example will illustrate the extent of doubt using these data.

Suppose accuracy class 0.3 is specified for the voltage transformer and the rounding off method recommended by American Society for Testing and Materials[1] is stipulated, then true radio correction factor (RCF) of 1.0035 indicates nonconformance with the accuracy specification, and any lesser value indicates conformance. (In this example, a noncritical phase angle is assumed, for example, −7 minutes.) With a testing accuracy of 300 ppm, it is uncertain whether test data will indicate conformance or nonconformance when the true RCF ranges from 1.00320 to 1.00379.

The foregoing indicates that good use can be made of the accuracy provided by the national laboratories.

Reference

1. Designating Significant Places in Specified Limiting Values. *ASTM Designation E29-60T*, American Society for Testing and Materials, Philadelphia, Pa.

F. K. Harris, W. C. Sze, N. L. Kusters, O. Petersons, and **W. J. M. Moore:** As Mr. Mitchell has pointed out, the present report shows in a very striking fashion the degree to which capacitance currents to nearby objects can affect the ratio and phase-angle errors of a voltage transformer. We agree with him that such effects may be significantly larger in a cascade design than in a one-stage configuration. However, since cascade designs lead to economies of space and insulation at high voltages, it is probable that they will continue to find favor with instrument-transformer engineers. Thus it would certainly seem appropriate that proximity errors be considered in future revisions of the transformer standard. The data presented in Table I were intended simply to illustrate the performance changes that result from nearby objects at ground or high potential. A serious study of proximity effects on transformers of various designs should precede any attempt to describe a test method for inclusion in a transformer standard.

Mr. Mitchell is quite correct in assuming that temperature, frequency, and waveform could also influence our results, and we regret that we do not have very much information for him on the magnitude of these influences. In both laboratories tuned detectors with negligible harmonic response were used, and no anomalous behavior was observed in the presence of known waveform distortion in one of the laboratories at the highest voltage. Measurements were made on two ratios at frequencies that differed somewhat from 60 cps. In each instance the change in ratio error amounted to about 200 ppm and in quadrature error about 25 ppm for a frequency difference of 2 cps. Data on temperature effects are also meager. In each laboratory the temperature was controlled and the working area was shared with other groups, so that the determination of a temperature coefficient was not possible. The temperature difference between the two laboratories was approximately 2 C (degrees centigrade), the NRC laboratory being maintained at 21 C and the NBS laboratory at 23 C. On one occasion when laboratory temperature controls failed, measurements at the three highest ratios were made at a temperature that differed by approximately 2 degrees from the usual value. It was observed that the phase-angle error was changed in a negative direction by approximately 0.8% of its value (that is, about 8 ppm in the quadrature error), and no significant change was observed in the ratio error. One would of course anticipate that the largest temperature effect would be on the quadrature error, contributed by the product

of the quadrature component of the excitation current (capacitive for these ratios) and the change with temperature in the primary winding resistance. Neither laboratory is really prepared to determine the temperature coefficients of transformer errors, since the units we test are generally used as reference standards under normal laboratory conditions.

The in-phase (α) and quadrature (β) error terms tabulated are defined differently in the different methods; and approximations amounting to a part in a million are used, as Mr. Mitchell has stated. In view of the fact that uncertainties in our measurements and the observed transformer instability and proximity effects were all substantially larger than this figure, it did not seem important to reduce the approximations of our formulas to a common base, although we did report our data to the nearest ppm to give a complete picture of their statistical scatter.

The degradation of accuracy at successive echelons of measurement has been the subject of much discussion and some argument in recent years. We agree with Mr. Vanderleck that at present it is reasonable to require an accuracy of 100 ppm in the assignment of ratio and phase-angle values for reference transformers calibrated at a national laboratory, although there are already some instances in which better accuracy has been requested. It is indeed comforting to know our two laboratories have a substantial margin of accuracy in voltage-transformer calibration beyond this 100-ppm requirement. If, however, as Mr. Vanderleck suggests, the transformer is to be used over a 50 C temperature range for corona-loss measurements where quadrature errors of 20 ppm begin to be significant, there should certainly be a determination of temperature influence on its calibration.

A reprint from **COMMUNICATION AND ELECTRONICS**, published by The Institute of Electrical and Electronics Engineers, Inc.

January 1964 issue

The Precision Measurement of Transformer Ratios*

R. D. CUTKOSKY† AND J. Q. SHIELDS†

I. Introduction

A CONVENIENT and accurate method for calibrating a given capacitor in terms of another capacitor having a value ten times or one tenth the value of the first is by means of a precise, stable transformer with a ten-to-one ratio and low equivalent series impedances.[1,2] Such a measurement requires a knowledge of the open-circuit voltage ratio and equivalent series impedances of the transformer.

One method for measuring a nominally ten-to-one transformer ratio has been described by Thompson.[3] This method consists of determining the relative values of eleven nominally equal three-terminal capacitors by simple substitution and then setting up a bridge with the circuit of Fig. 1 with ten of the capacitors in parallel on the low voltage winding of the transformer and the eleventh capacitor on the high voltage winding. The bridge is balanced by means of a small variable admittance in parallel with one arm of the bridge.

This series of measurements, when suitable correc-

* Received by the PGI, June 24, 1960. Presented at the 1960 Conference on Standards and Electronic Measurements as paper 5-4.

† National Bureau of Standards, Washington, D. C.

[1] A. M. Thompson, "The precise measurement of small capacitances," IRE TRANS. ON INSTRUMENTATION, vol. PGI-7, pp. 245–253; December, 1958.

[2] M. C. McGregor, J. F. Hersh, R. D. Cutkosky, F. K. Harris, and F. R. Kotter, "New apparatus at the National Bureau of Standards for absolute capacitance measurement," IRE TRANS. ON INSTRUMENTATION, vol. PGI-7, pp. 253–261; December, 1958.

[3] A. M. Thompson, private communication; 1957.

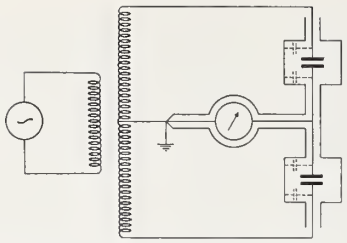

Fig. 1—Basic transformer bridge circuit.

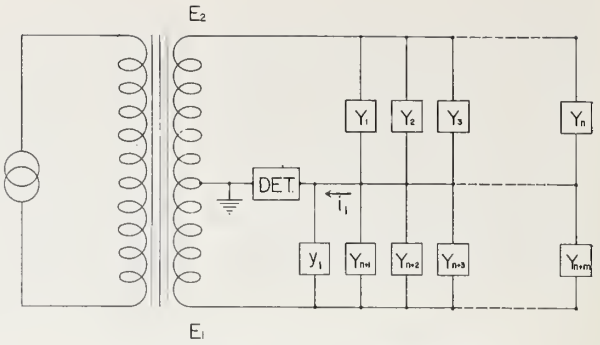

Fig. 2—Equivalent circuit of measuring system employing permutation method with $s = 1$.

tions are applied for the effect of finite lead impedances and load admittances, yields a value for the open-circuit transformer ratio.

If we are to obtain reliable ratio measurements, one requirement is that all of the capacitances involved drift at nearly the same rate. This can be achieved by constructing them to be identical and mounting them in good thermal contact with each other.

It can be shown that if eleven nominally equal three-terminal capacitors are mounted in this fashion with their detector leads connected together, and if eleven balances are made with the line lead of each capacitor in turn on the high-voltage side of a 10:1 transformer and the other ten line leads on the low-voltage side, one may obtain directly the voltage ratio at the points of interconnection independent of mutual coupling and ground impedances within the capacitor housing. The following section will show in detail how this is accomplished in the more general case of a transformer with a nominally $m:n$ ratio. The technique is similar to that used to establish known dc resistance ratios.

II. Theory of Permutation Method

Fig. 2 shows a transformer with open-circuit ratio

$$\frac{E_2}{E_1} \equiv -M \equiv -\frac{m}{n}(1 + \alpha + j\beta),$$

where m and n are integers and α and β are to be determined. Connecting $m+n$ admittances $Y_1, Y_2, \cdots, Y_k, \cdots, Y_{m+n}$ as shown, we have with the detector voltage zero,

$$i_1 = E_1 \sum_{k=n+1}^{n+m} Y_k + E_2 \sum_{k=1}^{n} Y_k.$$

If the admittances are permuted cyclically, each admittance Y_k is replaced by Y_{k+1}, and Y_{m+n} is replaced by Y_1. If this permutation is repeated $m+n$ times, each admittance appears with voltage E_2 n times, and with voltage E_1 m times. We then have, after adding the $m+n$ equations,

$$\sum_{s=1}^{m+n} i_s = mE_1 \sum_{k=1}^{m+n} Y_k + nE_2 \sum_{k=1}^{m+n} Y_k = (mE_1 + nE_2) \sum_{k=1}^{m+n} Y_k,$$

where i_s is the short-circuit detector current for the sth switch position. Balancing the bridge with a small admittance y_s, assumed for simplicity to be connected to the transformer winding of voltage E_1, we have

$$i_s = -E_1 y_s,$$

and

$$E_1 \sum_{s=1}^{m+n} y_s + (mE_1 + nE_2) \sum_{k=1}^{m+n} Y_k = 0.$$

Making use of the relationship

$$\frac{E_2}{E_1} = -\frac{m}{n}(1 + \alpha + j\beta),$$

we have

$$\alpha + j\beta = \frac{\sum_{s=1}^{m+n} y_s}{m \sum_{k=1}^{m+n} Y_k} = \frac{\overline{y_s}}{m\overline{Y_k}}, \tag{1}$$

where bars denote averages over the $m+n$ indices.

III. Lead Impedance Corrections

In the derivation of (1) in the previous section, it was assumed that the voltage ratio at the points of interconnection is constant and independent of the permuting switch position. Although this requirement can be satisfied, it is not necessary for the accuracy desired. Formulas will now be developed which relate the open circuit transformer parameters to the average balancing admittance and the average loading associated with the assembly of permutable capacitors called the "ratio device" in the sequel.

Let the voltages at the interconnection points after permuting s times be given by $E_1(1+e_s')$ and $E_2(1+e_s'')$, where E_1 and E_2 are the open-circuit voltages and e_s' and e_s'' are functions of the lead impedances and load admittances. Then the short-circuit detector current corresponding to this configuration is given for

the special case $m=10$ and $n=1$ by

$$i_s = E_1(1+e_s')\sum_{k\neq s} Y_k + E_2(1+e_s'')Y_s$$

$$= E_1(1+e_s')\left(\sum_k Y_k - Y_s\right)$$

$$- 10E_1(1+\alpha+j\beta)(1+e_s'')Y_s,$$

where k runs from one to eleven. Balancing with an admittance y_s assumed to have a voltage E_1, we have, after summing over all s from one to eleven,

$$\sum_s y_s + \sum_s (1+e_s')\left(\sum_k Y_k - Y_s\right) - 10\sum_s (1+e_s'')Y_s$$

$$- 10(\alpha+j\beta)\sum_s (1+e_s'')Y_s = 0.$$

Writing $Y_s=\overline{Y_s}+\Delta Y_s$, we have

$$\alpha+j\beta = \frac{\sum_s y_s + 10(\overline{e_s'}-\overline{e_s''})\sum_k Y_k - \sum_s \Delta Y_s(10e_s''+e_s')}{10\sum Y_s + 10\sum_s Y_s e_s''} = \frac{\overline{y_s}}{10\overline{Y_s}} + \overline{e_s'} - \overline{e_s''} + \epsilon_1,$$

where

$$\epsilon_1 = -\frac{1}{110}\sum_s \frac{\Delta Y_s}{\overline{Y_s}}(10e_s''+e_s')$$

$$- \frac{\sum_s Y_s e_s''}{\sum_s Y_s(1+e_s'')}\left[\frac{\overline{y_s}}{10\overline{Y_s}} + \overline{e_s'} - \overline{e_s''}\right.$$

$$\left. - \frac{1}{110}\sum_s \frac{\Delta Y_s}{\overline{Y_s}}(10e_s''+e_s')\right].$$

Writing $\overline{y_s}=j\omega\overline{c_s}+\overline{g_s}$ and $\overline{Y_s}=j\omega\overline{C_s}+\overline{G_s}$, and making the tacit assumption that $G_s \ll \omega C_s$, we have

$$\alpha+j\beta = \frac{\overline{c_s}}{10\overline{C_s}} - \frac{j\overline{g_s}}{10\omega\overline{C_s}} + \overline{e_s'} - \overline{e_s''} + \epsilon_1 + \epsilon_2,$$

where

$$\epsilon_2 = \frac{j\overline{G_s}}{\omega\overline{C_s}}\cdot\frac{\overline{y_s}}{10\overline{Y_s}}.$$

Fig. 3 represents the equivalent circuit of a three-winding transformer and the ratio device at the sth switch position. E_1 and $E_2=-ME_1=-10(1+\alpha+j\beta)E_1$ are the open-circuit voltages; Z_1 and Z_2 are the impedances of the transformer and leads; Y_s', Y_s'', and Y_s''' are the load admittances of the ratio device. A more accurate equivalent circuit would show a transmission line connecting the transformer to the ratio device, but for our purposes the transmission line is short enough to be considered as lumped at the interconnection points. Solving for e_s' and e_s'', we have

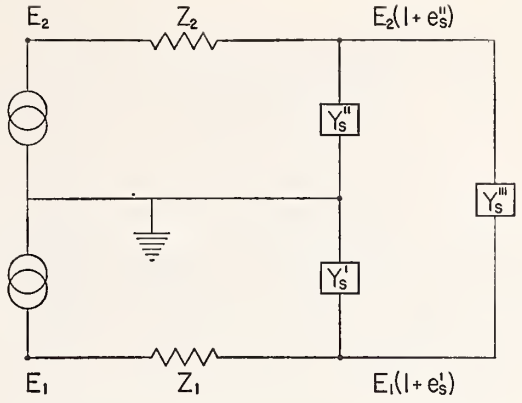

Fig. 3—Equivalent circuit of measuring system showing lead impedances and load admittances.

$$e_s' = -Z_1[Y_s' + (M+1)Y_s'''] + Z_1[Y_s' + (M+1)Y_s'''](\phi_s/(1+\phi_s))$$

$$- \frac{Z_1Z_2(Y_s'Y_s'' + Y_s'Y_s''' + Y_s''Y_s''')}{1+\phi_s}$$

$$e_s'' = -Z_2\left[Y_s'' + \left(1+\frac{1}{M}\right)Y_s'''\right] + Z_2\left[Y_s'' + \left(1+\frac{1}{M}\right)Y_s'''\right]\left(\frac{\phi_s}{1+\phi_s}\right)$$

$$- \frac{Z_1Z_2(Y_s'Y_s'' + Y_s'Y_s''' + Y_s''Y_s''')}{1+\phi_s},$$

where

$$\phi_s = Z_1(Y_s' + Y_s''') + Z_2(Y_s'' + Y_s''') + Z_1Z_2(Y_s'Y_s'' + Y_s'Y_s''' + Y_s''Y_s''').$$

Thus,

$$\alpha+j\beta = \frac{\overline{c_s}}{10\overline{C_s}} - j\frac{\overline{g_s}}{10\omega\overline{C_s}} + Z_2[\overline{Y_s''} + 1.1\overline{Y_s'''}] - Z_1[\overline{Y_s'} + 11\overline{Y_s'''}] + \epsilon_1 + \epsilon_2 + \epsilon_3,$$

where

$$\epsilon_3 = -\frac{1}{11}\sum_s\left(\frac{\phi_s}{1+\phi_s}\right)\cdot\left\{Z_2\left[Y_s'' + \left(1+\frac{1}{M}\right)Y_s'''\right] - Z_1[Y_s' + (M+1)Y_s'''\right\}$$

$$- (\alpha+j\beta)Y_s'''\left(10Z_1 + \frac{Z_2}{M}\right).$$

Writing

$$\overline{Y_s'} = j\omega\overline{C_s'} + \overline{G_s'}$$
$$\overline{Y_s''} = j\omega\overline{C_s''} + \overline{G_s''}$$
$$\overline{Y_s'''} = j\omega\overline{C_s'''} + \overline{G_s'''}$$
$$Z_1 = j\omega L_1 + R_1$$
$$Z_2 = j\omega L_2 + R_2,$$

we have, after separating real and imaginary parts,

$$\alpha = \frac{\overline{c_s}}{10\overline{C_s}} + \omega^2 L_1(\overline{C_s'} + 11\overline{C_s'''}) - \omega^2 L_2(\overline{C_s''} + 1.1\overline{C_s'''}) - R_1(\overline{G_s'} + 11\overline{G_s'''}) + R_2(\overline{G_s''} + 1.1\overline{G_s'''}) + \mathrm{Re}(\epsilon_0), \quad (2)$$

$$\beta = -\frac{\overline{g_s}}{10\omega\overline{C_s}} - \omega R_1(\overline{C_s'} + 11\overline{C_s'''}) + \omega R_2(\overline{C_s''} + 1.1\overline{C_s'''}) - \omega L_1(\overline{G_s'} + 11\overline{G_s'''}) + \omega L_2(\overline{G_s''} + 1.1\overline{G_s'''}) + \mathrm{Im}(\epsilon_0), \quad (3)$$

where

$$\epsilon_0 = \epsilon_1 + \epsilon_2 + \epsilon_3.$$

Making the assumptions that

$$|\alpha + j\beta| < 1 \times 10^{-4}$$
$$|Z_1|, |Z_2| < 0.1 \text{ ohm}$$
$$|Y_s'|, |Y_s''|, |Y_s'''| < 1 \times 10^{-3} \text{ mhos}$$
$$9 \times 10^{-8} \text{ mhos} < |Y_s| < 11 \times 10^{-8} \text{ mhos}$$
$$\left|\frac{\Delta Y_s}{\overline{Y_s}}\right| < 1 \times 10^{-4}$$
$$\left|\frac{\overline{G_s}}{\omega\overline{C_s}}\right| < 1 \times 10^{-4},$$

we can show that

$$|\epsilon_0| < 4.3 \times 10^{-5} |Y'|_{\max} + 8.1 \times 10^{-5} |Y''|_{\max} + 7.3 \times 10^{-4} |Y'''|_{\max} + 120 |\overline{y_s}|, \quad (4)$$

where $|Y'|_{\max}$ is the largest of the eleven values for $|Y_s'|$, and $|Y''|_{\max}$ and $|Y'''|_{\max}$ are defined similarly. It should be observed that ϵ_0 is the error caused by neglecting certain terms in mathematical expansions, and does not represent an inherent limitation of this method.

In general, it is desirable for the correction terms in (2) and (3) to be small. The impedances may be significantly reduced by careful attention to the methods of connection. For this reason, it is necessary to digress on the subject of transformer design.

IV. Transformer Design

Precision transformers with low series impedances are commonly constructed with heavy strap-copper secondaries having the turns of one side in close proximity to the turns of the other in order to reduce leakage inductance.[2] This construction produces a transformer with a large distributed capacitance between windings.

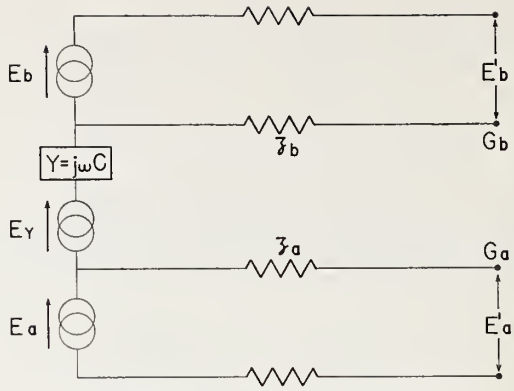

Fig. 4—Equivalent circuit of transformer showing impedances and interwinding capacitance.

Fig. 4 represents the two secondary windings of a transformer of voltages E_a and E_b. C represents the interwinding capacitance and E_Y is the open-circuit voltage between the two leads G_a and G_b. For use in a bridge circuit, the terminals G_a and G_b of the transformer are connected together and to the ground. We then have with

$$|YZ_a| \quad \text{and} \quad |YZ_b| \ll 1,$$

$$\frac{E_b'}{E_a'} \approx \frac{E_b + E_Y Z_b Y}{E_a + E_Y Z_a Y} \approx \frac{E_b}{E_a}\left[1 + \frac{E_Y}{E_b} Z_b Y - \frac{E_Y}{E_a} Z_a Y\right] \approx \frac{E_b}{E_a}\left[1 + j\omega C\left(\frac{E_Y}{E_b} Z_b - \frac{E_Y}{E_a} Z_a\right)\right].$$

E_Y is typically quite large and for a 10:1 transformer has a value between E_a and E_b. C is unavoidably large because of the close spacing between windings, and may be as great as 0.02 μf. From the above comments it can be seen that the stability of the transformer ratio depends upon the stability of Z_a and Z_b.

For this reason, it is necessary for Z_a and Z_b to be small and well defined. This can be accomplished by connecting the two secondary windings together permanently within the transformer housing with short low-resistance leads.

With the above connection made and a single lead brought out from this connection, the complete transformer with its primary can be represented by the equivalent circuit based on an ideal transformer as shown in Fig. 5(a). A, B, and G represent the terminals of a connection block to which the secondary leads are attached. The circuit of Fig. 5(a) is equivalent to that of Fig. 5(b). The accompanying formulas show that the common impedance ζ_4 enters into the series impedance terms, but not in a way basically different from ζ_1 and

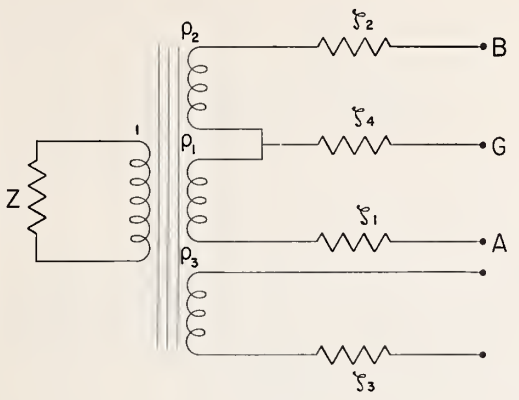

(a)

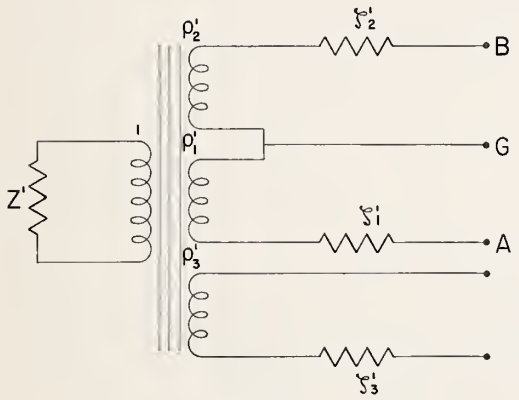

(b)

$$\zeta_1' = \zeta_1 + \zeta_4\left(1 + \frac{\rho_1}{\rho_2}\right) \qquad \zeta_2' = \zeta_2 + \zeta_4\left(1 + \frac{\rho_2}{\rho_1}\right)$$

$$\zeta_3' = \frac{\zeta_3 - \zeta_4\left(\frac{\zeta_3}{Z}\rho_3 - \rho_3^3\right)}{1 - \rho_3\frac{\zeta_4}{Z}}$$

$$(\rho_1')^3 = \rho_1^3\left(1 - \rho_3\frac{\zeta_4}{Z}\right) \qquad (\rho_2')^3 = \rho_2^3\left(1 - \rho_3\frac{\zeta_4}{Z}\right)$$

$$(\rho_3')^3 = \rho_3^3\,\frac{1}{\left(1 - \rho_3\frac{\zeta_4}{Z}\right)^2} \qquad (Z')^3 = Z^3\left(1 - \rho_3\frac{\zeta_4}{Z}\right)$$

$$\rho_1\rho_2\rho_3 = \rho_1'\rho_2'\rho_3' = 1.$$

Fig. 5—Ideal transformer representation for three-winding transformers, where the ρ's are ideal transformer ratios.

ζ_2. With reference to Fig. 5(b) and the associated formulas, the parameters of interest are

$$\frac{\rho_2'}{\rho_1'} = \frac{\rho_2}{\rho_1} \approx 10,\ \zeta_1' \approx \zeta_1 + 1.1\zeta_4,\ \text{and}\ \zeta_2' \approx \zeta_2 + 11\zeta_4.$$

It is usually best to make ζ_1' and ζ_2' as small as possible. Because of the factor 11 multiplying ζ_4 in the expression for ζ_2', it is particularly desirable to make ζ_4 as small as possible. This may be achieved in effect by bringing separate ground leads from the common connection point p within the transformer housing to the connection block terminal G, as in Fig. 6(a), and linking one of these leads with one of the high-voltage leads by means of a high-permeability core. This is electrically equivalent to breaking the connection at p. Fig. 6(b) shows the resulting equivalent circuit of the transformer whose terminals are A, B and G of the connection block. The terms Z_1+Z_3 and Z_2+Z_4 are the equivalent series impedances of the transformer, and E_B/E_A is the open-circuit voltage ratio we desire to measure. Since the value of E_B/E_A depends upon the loading admittances present in the transformer, and its leads to the connection block, these admittances must be well defined. This is generally accomplished by shielding all parts of the transformer and maintaining a fixed geometry by means of rigid construction.

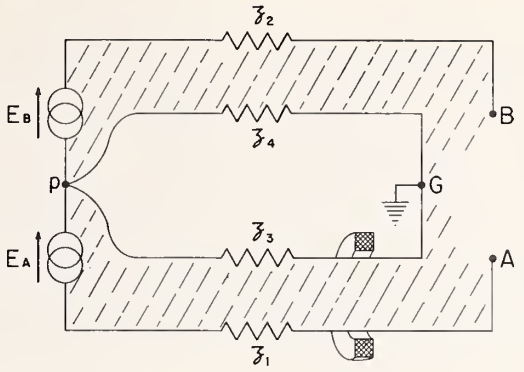

(a)

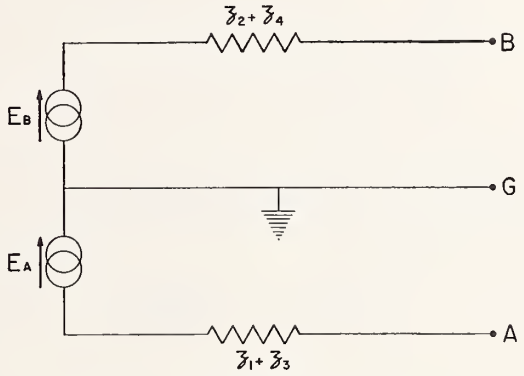

(b)

Fig. 6—Use of high-permeability core to reduce equivalent impedances.

It can be seen from the pictorial nature of Fig. 6(a) that the equivalent series inductances of the transformer can be reduced by reducing the shaded areas in the figure. In practice, each lead pair consists of a coaxial lead which, in addition to reducing the inductances as measured at the connection block, also minimizes the external fields produced by currents in these leads and hence interactions with other components of the measuring system.

The coaxial lead plus high-permeability core technique can also be profitably used to reduce effective

impedances from the connection block to the ratio device. The use of high-permeability cores in a related application has been discussed by Thompson.[1]

V. Lead Impedance and Load Admittance Measurement

Having discussed methods of obtaining small, well-defined impedances, we next turn our attention to the measurement of these impedances. One method of measurement may be developed by reference to (2) of Section III. If $\overline{C_s'''}$, for example, is increased by the addition of components within the ratio device (beyond the permuting switch), one obtains

$$\begin{aligned}\alpha = {} & \frac{\overline{c_s} + \overline{\Delta c_s}}{10\overline{C_s}} + \omega^2 L_1(\overline{C_s'} + 11\overline{C_s'''} + 11\overline{\Delta C_s'''}) \\ & - \omega^2 L_2(\overline{C_s''} + 1.1\overline{C_s'''} + 1.1\overline{\Delta C_s'''}) \\ & - R_1(\overline{G_s'} + 11\overline{G_s'''}) + R_2(\overline{G_s''} + 1.1\overline{G_s'''}) \\ & + \mathrm{Re}\,(\epsilon_0 + \Delta\epsilon_0), \end{aligned} \tag{5}$$

where $\overline{\Delta C_s'''}$, $\overline{\Delta c_s}$, and $\Delta\epsilon_0$ are the increases in $\overline{C_s'''}$, $\overline{c_s}$, and ϵ_0, respectively. Subtracting (2) from (5) and rearranging terms, we obtain

$$L_2 - 10L_1 = \frac{\overline{\Delta c_s}}{11\omega^2\overline{C_s}(\overline{\Delta C_s'''})} + \frac{\mathrm{Re}\,(\Delta\epsilon_0)}{1.1\omega^2(\overline{\Delta C_s'''})}. \tag{6}$$

Similarly, from (3),

$$R_2 - 10R_1 = \frac{\overline{\Delta g_s}}{11\omega^2\overline{C_s}(\overline{\Delta C_s'''})} - \frac{\mathrm{Im}\,(\Delta\epsilon_0)}{1.1\omega(\overline{\Delta C_s'''})}. \tag{7}$$

One might suppose that if similar measurements were made with components added beyond the permuting switch to increase C_s'', for example, the value of L_2 by itself might be obtained with comparable precision. However, since the permutation process places each added ground capacitance on the high-voltage side once and on the low-voltage side ten times, a change of $\overline{\Delta C_s''}$ in $\overline{C_s''}$ produces a corresponding change of 10 $\overline{\Delta C_s'}$ in $\overline{C_s'}$, so that one arrives again at values for $L_2 - 10L_1$ and $R_2 - 10R_1$. In fact, were it not for the loading admittances associated with the wiring between the permuting switch and the connection block, we would have $\overline{C_s'} \equiv 10\overline{C_s''}$ and $\overline{G_s'} \equiv 10\overline{G_s''}$, in which case knowledge of L_1, L_2, R_1, or R_2 alone would not be needed. This fact can best be seen if we let $\mathfrak{L} \equiv L_2 - 10L_1$ and $\mathfrak{R} \equiv R_2 - 10R_1$, and rewrite (2) and (3) in the following manner:

$$\begin{aligned}\alpha = {} & \frac{\overline{c_s}}{10\overline{C_s}} - \omega^2\mathfrak{L}\left(\frac{\overline{C_s'}}{10} + 1.1\overline{C_s'''}\right) \\ & - \omega^2 L_2\left(\overline{C_s''} - \frac{\overline{C_s'}}{10}\right) + \mathfrak{R}\left(\frac{\overline{G_s'}}{10} + 1.1\overline{G_s'''}\right) \\ & + R_2\left(\overline{G_s''} - \frac{\overline{G_s'}}{10}\right) + \mathrm{Re}\,(\epsilon_0), \end{aligned} \tag{8}$$

$$\begin{aligned}\beta = {} & -\frac{\overline{g_s}}{10\omega\overline{C_s}} + \omega\mathfrak{R}\left(\frac{\overline{C_s'}}{10} + 1.1\overline{C_s'''}\right) \\ & + \omega R_2\left(\overline{C_s''} - \frac{\overline{C_s'}}{10}\right) + \omega\mathfrak{L}\left(\frac{\overline{G_s'}}{10} + 1.1\overline{G_s'''}\right) \\ & + \omega L_2\left(\overline{G_s''} - \frac{\overline{G_s'}}{10}\right) + \mathrm{Im}\,(\epsilon_0). \end{aligned} \tag{9}$$

Since the loading admittances associated with the leads can be made very small, the quantities $\overline{C_s''} - \overline{C_s'}/10$ and $\overline{G_s''} - \overline{G_s'}/10$ in (8) and (9) will also be very small and, consequently, the accuracy to which L_2 and R_2 need be measured is greatly reduced.

The principal significance of this procedure for the measurement of $\mathfrak{L}$ and $\mathfrak{R}$ is that any component added past the interconnection points produces essentially no error by virtue of its mutual inductance with other portions of the circuit. Mutual inductance between the added component and other elements of the ratio device changes the effective values of the transfer admittances Y_k defined in Section II, but the derivation is still valid if these new values for the Y_k are used. In practice, since $\overline{Y_k}$ is needed only to an accuracy of a few per cent, the effect is insignificant.

Errors resulting from mutual inductances between the added component and the leads preceding the interconnection points also cancel to first order, since any change in the voltage at the interconnection points, caused by such mutual inductance, reverses sign when the component is switched from one side of the transformer to the other. It can be seen that the net effect is to leave the average voltage ratio at the interconnection points independent of such mutual inductance.

It can now be seen that the only mutual inductances which may produce errors in the measurement of α and β are those between the nonpermuted portions of the circuit. Since the nonpermuted circuit consists almost entirely of coaxial leads, we may expect all errors caused by mutual inductances to be negligible.

Since it is difficult to reduce the load admittances of the leads and switch to zero, values of L_2 and R_2 are still required in formulas (8) and (9), but relatively low accuracy is sufficient. One method of measurement may be developed by referring to (8). If components are added outside the ratio device so as to increase $\overline{C_s''}$ by an amount $\overline{\Delta C_s''}$ with corresponding increases $\overline{\Delta c_s}$ and $\Delta\epsilon_0$, one obtains

$$\begin{aligned}\alpha = {} & \frac{\overline{c_s} + \overline{\Delta c_s}}{10\overline{C_s}} - \omega^2\mathfrak{L}\left(\frac{\overline{C_s'}}{10} + 1.1\overline{C_s'''}\right) \\ & - \omega^2 L^2\left(\overline{C_s''} + \overline{\Delta C_s''} - \frac{\overline{C_s'}}{10}\right) \\ & + \mathfrak{R}\left(\frac{\overline{G_s'}}{10} + 1.1\overline{G_s'''}\right) + R_2\left(\overline{G_s''} - \frac{\overline{G_s'}}{10}\right) \\ & + \mathrm{Re}\,(\epsilon_0 + \Delta\epsilon_0). \end{aligned} \tag{10}$$

Subtracting (8) from (10) and rearranging terms, we obtain

$$L_2 = \frac{\overline{\Delta c_s}}{10\omega^2 \overline{C_s(\Delta C_s'')}} + \frac{R_e(\Delta\epsilon_0)}{\omega^2 \overline{(\Delta C_s'')}} \cdot \qquad (11)$$

Similarly, from (9), we have

$$R_2 = \frac{\overline{\Delta g_s}}{10\omega^2 \overline{C_s(\Delta C_s'')}} - \frac{\mathrm{Im}\,(\Delta\epsilon_0)}{\omega \overline{(\Delta C_s'')}} \cdot \qquad (12)$$

The capacitance coefficients C_s' and C_s'' in (2) and (3) represent principally the ground capacitances of the ratio device and are determined by the design of the component capacitors. Capacitors could be designed with ground capacitances significantly smaller than those incorporated in the ratio device, but this would probably be at the expense of their stability. C_s''' could be made zero by careful shielding, but it is normally very small and causes no particular trouble in measurement. We are faced then with the problem of measuring C_s', C_s'', and C_s'''.

In use, the ratio device is operated with the bridge balanced, meaning that the detector voltage is zero. Thus, a correct set of values for C_s', C_s'', and C_s''' may be obtained if the detector terminal is shorted to ground. The ratio device then has three remaining terminals to which are attached the leads from A, B, and G of the connection block. Representing this by Fig. 7, we see that C_s''' is the easiest coefficient to measure and is just the direct capacitance between points A and B. $\overline{C_s'''}$ is the average of the eleven measurements of C_s''' corresponding to the eleven switch positions. C_s' can be determined in practice by shorting B to G and measuring $C_s'+C_s'''$. This can be done with simple two-terminal capacitance measuring techniques. Since the transformer ratio is defined at the connection block, the desired value for $C_s'+C_s'''$ is the increase in ground capacitance of the connection block when the ratio device is connected to it.

Averaging the eleven measurements, we obtain $\overline{C_s'}+\overline{C_s'''}$, from which $\overline{C_s'}$ can be determined, and similarly, $\overline{C_s''}$. $\overline{G_s'}$, $\overline{G_s''}$, and $\overline{G_s'''}$ may be obtained simultaneously from the same type of measurement.

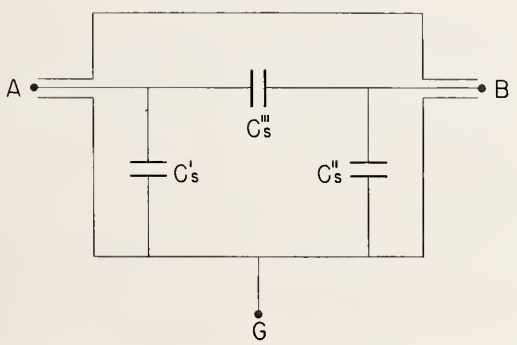

Fig. 7—Ratio device admittances with detector terminal shorted.

VI. Numerical Results

The procedures developed in the preceding sections of this paper have been applied to the measurement of a particular transformer, NBS 89785. This transformer was built according to the principles described at the 1958 Conference on Electrical Measurements[2] except that the thickness of the copper-strap secondary winding has been reduced to 0.030 inch to allow more room for insulation.

The ratio device and the transformer were placed in an oil bath with ± 0.01°C regulation. This decreased the drift rate of the capacitors in the ratio device, and hence improved the accuracy attainable with the measuring system. Since the transformer ratio is slightly temperature-sensitive, temperature control of the transformer was also required (see Fig. 8).

The work described below was all done at an angular frequency of 10^4 radians per second (about 1592 cps). The voltage level was monitored with an expanded-scale vacuum-tube voltmeter accurate to $\pm\frac{1}{4}$ per cent.

The small variable admittances, c_s and g_s, consisted of the low-range decade capacitor and the conductance balance control described by McGregor, *et al.*,[2] but almost any capacitor variable in steps of 10^{-6} pf and accurate to 10^{-7} pf would have been sufficient. The same applies to the conductance balance control, which must have steps of 10^{-8} μmhos accurate to 10^{-9} μmhos. Since only a small total range of the variable admittances is required, this is not difficult to achieve.

In Section II, it was assumed that the small variable admittances were connected to the low-voltage side of the transformer. It is necessary to reverse the signs of these admittances in order to balance the bridge at certain switch positions. We can accomplish this by connecting one or both of the variable admittances to the high-voltage side of the transformer, but this changes the apparent scale of the variable by a factor of ten as well as changing the sign. The transformer under investigation had a tap on the high-voltage side of the transformer at which the voltage was approximately equal to that of the low-voltage side, but 180° out of phase. Use of this tap for the balancing admittances, when required, greatly simplified the reduction of data.

Since the variable admittances have, in addition to their direct admittances, relatively high admittances to ground, it is necessary to measure these ground admittances as well as the effect on the ten-to-one transformer ratio of a ground admittance at each of the transformer terminals to which the variable admittances may be connected, and apply appropriate corrections. If it is borne in mind that the average voltage ratio is the quantity of interest (see Section III), the correction procedure is straightforward. It involves, in addition to the quantities mentioned above, a knowledge of how many times each of the variable admittances is on each low-voltage transformer tap.

The following parameters were determined for the

described system:

$\mathfrak{L} = -3.49 \times 10^{-6}$ henry $\quad \mathfrak{R} = -66.3 \times 10^{-3}$ ohms

$L_2 = 1.0 \times 10^{-6}$ henry $\quad R_2 = 50 \times 10^{-3}$ ohms

$\overline{C_s'} = 1101 \times 10^{-12}$ farads $\quad \overline{G_s'} = 44 \times 10^{-9}$ mhos

$\overline{C_s''} = 127.1 \times 10^{-12}$ farads $\quad \overline{G_s''} = 5 \times 10^{-9}$ mhos

$\overline{C_s'''} = 18.3 \times 10^{-12}$ farads $\quad \overline{G_s'''} = 1 \times 10^{-9}$ mhos.

Correction to α for loading of variable admittances $= -4 \times 10^{-9}$.

Correction to β for loading of variable admittances $= -19 \times 10^{-9}$.

Total correction to $\alpha = +39 \times 10^{-9}$.

Total correction to $\beta = -97 \times 10^{-9}$.

These corrections were determined several times at various temperatures and voltages. They were observed to be constant to $\pm 1 \times 10^{-9}$ over the range of conditions reported below.

$\overline{c_s}$ and $\overline{g_s}$ were determined from twenty-one separate bridge balances, with the ratio device switch running from one to eleven and back down to one. This procedure tends to eliminate the effect of a steady drift rate of any of the ratio device capacitors. The twenty-one balances could be made in a period of time ranging from twenty to thirty minutes, depending upon the experience of the operator.

Tables I and II represent the transformer ratio parameters as functions of temperature and voltage. Each number represents the mean of at least five ratio measurements. The probable error of each mean is 2×10^{-9} or less.

TABLE I

VARIATION OF α AND β WITH VOLTAGE—24.83°C

Voltage	α	β
90	-16×10^{-9}	-12×10^{-9}
100	$+26$	-16
110	$+62$	-14

TABLE II

VARIATION OF α AND β WITH TEMPERATURE—100 VOLTS

Temperature	α	β
24.62	$+12 \times 10^{-9}$	-4×10^{-9}
24.83	$+26$	-16
25.42	$+34$	-9

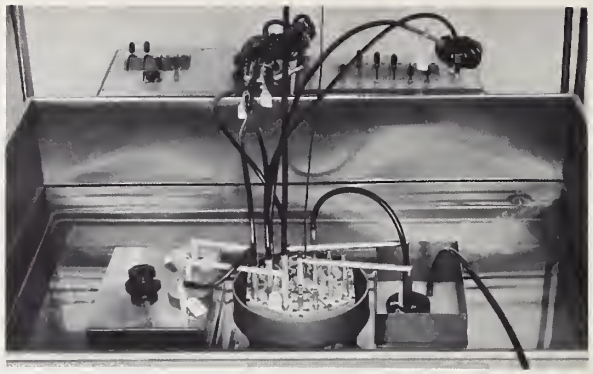

Fig. 8—Photograph of measuring system. From left to right in oil bath: ratio device, connection block, and transformer.

Attempts to repeat the numbers presented in Tables I and II were not completely satisfactory, the discrepancies occasionally being as large as 10×10^{-9}. Thorough investigation of the measurement equipment disclosed no sources of error large enough to account for discrepancies larger than 2×10^{-9}. It is believed that variations in the transformer ratio were being observed. Since it is necessary to wait at least a day after changing the oil bath temperature to obtain good temperature regulation, the apparent temperature dependence of the transformer ratio—in particular its phase defect angle—indicated by Table II, is probably at least partially due to random variations within the transformer.

Since the theoretical development of Section II assumes a linear volt-ampere relationship for the components of the ratio device, a method is needed to determine whether or not the capacitors have voltage coefficients large enough to produce an error. Sensitivity and drift problems make such a determination difficult, but comparisons with capacitors of radically different construction indicate that any voltage coefficient which may exist could not produce an error larger than 3×10^{-9} in α or β (50 per cent confidence interval). We conclude that with the equipment described above, ten-to-one transformer ratios may be determined to $\pm 4 \times 10^{-9}$ with a 50 per cent confidence interval. A more extensive investigation of voltage coefficients might reduce this figure.

ACKNOWLEDGMENT

The authors wish to thank Lai H. Lee for his assistance in obtaining the numerical results of this paper.

Reprinted from IRE TRANSACTIONS
ON INSTRUMENTATION
Volume I-9, Number 2, September, 1960

ISA TRANSACTIONS: 3 (238-242) 1964

Comparison Calibration of Inductive Voltage Dividers*

RAYMOND V. LISLE†
RCA Service Company
Missile Test Project
Patrick Air Force Base, Florida
and
THOMAS L. ZAPF‡
Radio Standards Laboratory
National Bureau of Standards
Boulder, Colorado

▶ Calibrated inductive voltage dividers serve as excellent standards of voltage ratio for use in the comparison calibration of other AC voltage dividers. Differences in phase angles in the dividers can be accommodated by the production of a voltage in the detector circuit in quadrature with the reference voltage. This paper discusses the comparison circuit, the handling of stray impedances, guarding, measurement procedures, quadrature voltage production, and errors. The comparison method described can be used in standardizing laboratories for the calibration of inductive voltage dividers and other voltage ratio equipment.

INTRODUCTION

Inductive voltage dividers may be described as tapped inductors wound on high-permeability cores. The relatively recent metallurgical development of ferromagnetic core material having extremely high magnetic permeability has made possible the construction of inductive voltage dividers having excellent stability and loading characteristics. The effects of internal loading are inherently small in such inductive voltage dividers, and errors in voltage ratios are frequently less than 1×10^{-6} in the low audio-frequency range. The absolute measurement of voltage ratios with uncertainties less than this is difficult. However, known voltage ratios embodied in an inductive voltage divider may be preserved as a standard and re-established again and again. The accurate initial establishment of voltage ratio for the calibration of inductive voltage dividers[1-4] is not discussed here, but a method of calibrating an inductive voltage divider by comparing it with a standard is presented. The comparison method, essentially as described herein, has been used at the National Bureau of Standards for several years and appears worthy of general use in standardizing laboratories. This method provides efficient, accurate calibration of inductive voltage dividers using common laboratory equipment with a standard inductive voltage divider. Comparison circuits have been mentioned in several publications[4-7] without detailed elaboration. This paper discusses in considerable detail a particularly successful type of comparison circuit.

*Presented at the 18th Annual ISA Conference and Exhibit, September 9-12, 1963, Chicago, Illinois.
†Standards Engineer.
‡Physicist, Radio Standards Engineering Division; Member—ISA Denver Section.

THE COMPARISON CIRCUIT

A simple bridge circuit for comparing inductive voltage dividers is shown in Figure 1. The standard inductive voltage divider is the divider for which the corrections are known. The unknown inductive voltage divider is the divider for which the corrections are to be obtained.

Other elements of the circuit are the guard divider and shielding circuit, flexible coaxial cables to the detector transformer, the detector, a resistor and capacitor for the introduction of a quadrature voltage in the detector circuit, and several fuses. The dashed lines indicate the connections of a capacitor that may be used to reduce loading.

The input terminals of the unknown and standard dividers are joined together by short, heavy leads having low impedance to reduce voltage drops between the

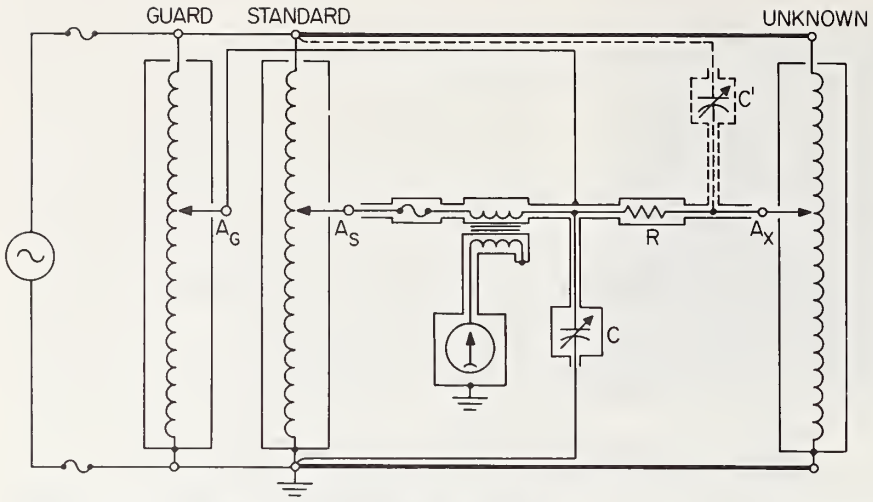

Figure 1. Bridge circuit for the calibration of an inductive voltage divider by comparison with a standard.

dividers. The electrical connection to the case of the standard divider should duplicate the connection used when the standard divider was calibrated. Similarly, the electrical connection to the case of the unknown divider should duplicate the connection to be used in subsequent work. In Figure 1 the cases are shown connected to the common terminals. These connections fix, in a reproducible manner, the stray capacitances from the windings to the case of each divider. Connecting the case to the output terminal is not recommended, as this would not fix the stray impedances from the case (and output terminal) to the surroundings, which are often quite uncertain and variable. The output of the guard divider is connected to the shield around the detector circuit. When comparing an unknown inductive divider with the standard, the guard divider is set at the same setting as the other dividers and drives the shield at nearly the same instantaneous potential as that of the conductors within. The guard divider may be either inductive or resistive because its only function is to maintain the proper potential on the shield. The guard circuit minimizes current leakage through the stray impedances of the detector circuit.

Usually there is a relatively large stray capacitance to ground from the detector transformer shield and the capacitor case. The current in this stray capacitance to ground must not be allowed in the shield of the flexible coaxial cables going to the output terminals of the dividers because a current in the shield can induce a voltage in the inner conductor. To minimize this error, the connection between the detector transformer shield and the capacitor case should be made as short as possible, and the output of the guard divider should be connected to the shield at some point in this vicinity. The major components of stray capacitive current then are conducted directly to the guard divider. The deleterious effect that is avoided by this procedure may be observed by increasing the length of the leads in the detector circuit and connecting the lead from the guard divider to a different point on the shield. If all leads are short the error may be insignificant.

It should be noted that, with the circuit shown in Figure 1, the guard circuit and the capacitor case are at a potential somewhat above ground, and care should be exercised in touching the shields to avoid hazardous shocks. Alternatively, the circuit may be grounded at the output of the guard divider, but the cases of the dividers will then be at a high potential. With this connection it may be necessary to use an isolation transformer between the power supply and the bridge circuit to avoid double grounding. Regardless of the grounding system selected, it is good practice to provide an outer covering of insulation for the shielding wherever needed to prevent accidental short circuits.

Many inductive dividers are provided with two "common" terminals connected together and to one extremity of the winding by a wire of low impedance so that one terminal may be used with the input circuit and the other may be used to make connections to the load. In the circuit shown in Figure 1 the inductive dividers are treated as three-terminal dividers, i.e., the common output terminal is ignored. A small voltage drop in the internal connection between the two common terminals would make the three-terminal measurements differ from four-terminal measurements in which both common terminals are used. However, the difference is usually small and often insignificant. Fuses are inserted in the circuit as shown in Figure 1 to prevent damage to components in the event of inadvertent short circuits. The fuse in the detector circuit prevents damage to the resistor, R, if a large unbalance of the bridge circuit is encountered.

VOLTAGE RATIO MEASUREMENT

Let $D + d$ represent the dial reading of an inductive voltage divider, where D is the reading of the decades to be calibrated (usually the highest three decades) and d is the reading of the lower decades. In most calibrations D will be a step setting of one of the highest three decades with the other two set to zero. The true ratio, A, can then be represented by $D + d + c$, where c is the

TABLE I

	Voltage ratio					Phase angle		
D_s	d_s	c_s	d_x	c_x	Ratio$_x$	γ_s, μrad	$\Delta\gamma$, μrad	γ_x, μrad
	$\times 10^{-6}$	$\times 10^{-6}$	$\times 10^{-6}$	$\times 10^{-6}$				
0.900	0.0	+0.4	+0.1	+0.3	0.900 000 3	−2	0	−2
0.500	0.0	0.0	+0.4	−0.4	0.499 999 6	+4	+1	+5
0.100	0.0	−0.1	+0.1	−0.2	0.099 999 8	+49	+3	+52
0.090	+0.1	−0.5	0.0	−0.4	0.089 999 6	+36	+4	+40
0.050	0.0	−0.3	0.0	−0.3	0.049 999 7	+42	+4	+46
0.010	0.0	0.0	0.0	0.0	0.010 000 0	+70	+20	+90
0.009	0.0	0.0	0.0	0.0	0.009 000 0	+60	+10	+70
0.005	+0.1	−0.1	0.0	0.0	0.005 000 0	+80	+30	+110
0.001	0.0	0.0	0.0	0.0	0.001 000 0	+330	+130	+460

correction to the setting D. For all practical purposes c is independent of d. At balance

$$D_x + d_x + c_x = D_s + d_s + c_s \tag{1}$$

where the subscripts x and s denote the unknown and the standard, respectively. Solving for the correction to the unknown divider and realizing that $D_x = D_s$, one obtains

$$c_x = c_s + d_s - d_x \tag{2}$$

Ordinarily, d_x would be set to zero. Under this condition

$$c_x = c_s + d_s \tag{3}$$

However, if $c_x < c_s$ and if the standard divider cannot be set to a negative d_s, the lower decades of the unknown divider, d_x, can be used to obtain the balance. If d_s is set to zero the ratio balance equation is

$$c_x = c_s - d_x \tag{4}$$

Typical data and results for a calibration at 100 V and 1000 cps are shown in Table I.

PHASE-ANGLE MEASUREMENT

A true voltage null at the detector can be obtained if a quadrature voltage is introduced into the circuit to compensate for the phase-angle difference between the unknown and the standard inductive voltage dividers. The RC combination in Figure 1 is used to develop and introduce a voltage in quadrature with the output of one of the dividers. If the capacitive reactance of C is made considerably larger than the resistance, R, the current in R will lead the voltage across the impedance $R - jX_c$ by nearly $\pi/2$ radians and will cause the quadrature voltage to appear across R. At balance the current in the detector is zero, and the voltage at the junction, of R and C is E_s, as indicated in Figure 2a. An expression for the current in R and C can be written

$$i = E_s/X_c \tag{5}$$

The quadrature voltage, e, is the product of i times R,

$$e = iR \tag{6}$$

and

$$e = E_s R/X_c = E_s \omega RC \tag{7}$$

From Figure 2a, γ_s and γ_x are the phase angles associated with the standard and the unknown inductive voltage dividers, respectively, and $\Delta\gamma$ is the phase-angle difference between the unknown and the standard dividers. An expression for $\Delta\gamma$ can be written from inspection of Figure 2a as

$$\tan\Delta\gamma = e/E_s \tag{8}$$

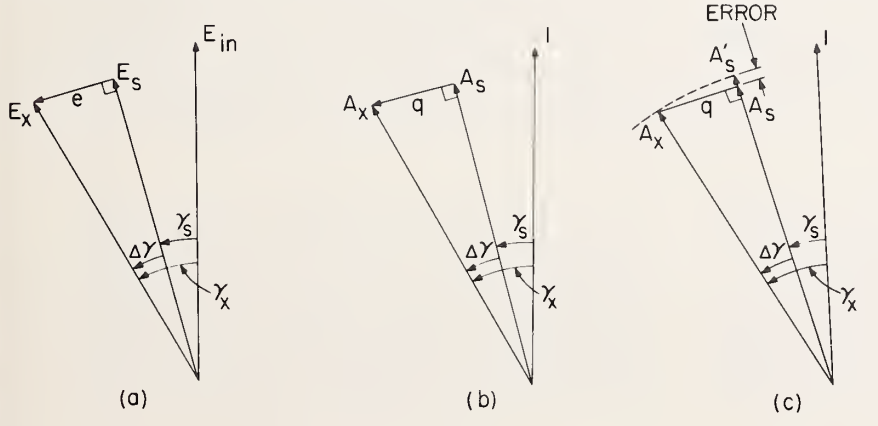

Figure 2. Phasor diagram: (a) voltage phasors; (b) voltage ratio phasors; (c) phasor diagram showing small error from quadrature circuit.

Combining the last two equations yields

$$\tan \Delta\gamma = \omega RC \tag{9}$$

For small angles $\tan \Delta\gamma \approx \Delta\gamma$, and

$$\Delta\gamma \approx \omega RC \tag{10}$$

This equation provides a design formula for the RC combination in the detector circuit. For any test frequency ω a variable capacitor can be chosen in combination with a resistor so that $\Delta\gamma$ in microradians is a multiple-of-ten times the reading of the variable capacitor in picofarads. Various multiplying factors can be obtained using resistors differing by multiples of ten. As an example, at a frequency of 1000 cps, resistors having values of 1592, 159.2, and 15.92 Ω, will produce multipliers of 10, 1, and 0.1, respectively. Thus a 0–100 pF variable air capacitor can be used to cover a wide range of phase-angle differences.

In the above discussion with reference to Figure 2a, it has been assumed that the phase angle of the unknown inductive voltage divider is larger than that of the standard inductive voltage divider. Under these conditions, $\Delta\gamma$ is positive, and the phase angle of the unknown inductive divider can be obtained from the equation

$$\gamma_x = \gamma_s + \Delta\gamma \tag{11}$$

If the difference $\gamma_x - \gamma_s$ is negative, the comparison circuit can be balanced by putting the RC combination on the other side of the detector with R connected to the standard divider. Under these conditions, the phase-angle balance equation would be

$$\gamma_x = \gamma_s - \Delta\gamma \tag{12}$$

Typical data and results from phase-angle measurements are shown in Table I.

DISCUSSION OF ERRORS

If errors from incorrect connections, incorrect frequency, or incorrect applied voltage (i.e., errors arising from conditions different from those under which the standard was measured) are precluded, the ponderable systematic errors, such as those arising from the assumptions made in the derivation of the equations, are of very small magnitude. These will now be investigated.

The error introduced by the approximation that $\tan \Delta\gamma \approx \Delta\gamma$ can be evaluated from the trigonometric expansion of the tangent, namely,

$$\tan \Delta\gamma = \Delta\gamma + \frac{\Delta\gamma^3}{3} + \frac{\Delta\gamma^5}{15} + \ldots \tag{13}$$

The second term, $\Delta\gamma^3/3$, evaluated for $\Delta\gamma = 300\ \mu$rad would be of the order of 1×10^{-11} rad, which is negligible, and higher order terms are smaller yet.

It is convenient to consider a phasor diagram of voltage-ratio phasors, as shown in Figure 2b, rather than one formed of voltage phasors, as in Figure 2a. The diagram in Figure 2b is formed by normalizing the voltage phasors by dividing the circuit voltages by the input voltage magnitude. The voltage ratio A of an inductive voltage divider is then $E_0/|E_{in}|$, and the quadrature component, $q = e/|E_{in}|$.

A small error in ratio from the voltage drop across R is illustrated in Figure 2c in which the angles have been grossly exaggerated to illustrate the error. In this diagram A_s is the apparent ratio at balance, smaller than the true ratio A'_s because the phasor q is added at right angles to the phasor A_s by means of the RC circuit. The error, $A'_s - A_s$, can be evaluated from the trigonometric series expansion for $\cos \Delta\gamma$, namely,

$$\cos \Delta\gamma = 1 - \frac{\Delta\gamma^2}{2!} + \frac{\Delta\gamma^4}{4!} - \ldots \tag{14}$$

From Figure 2c,

$$A_s = A_x \cos \Delta\gamma \approx A_x\left(1 - \frac{\Delta\gamma^2}{2!}\right) \tag{15}$$

The error in ratio is represented by the term $A_x(\Delta\gamma^2/2!)$. In comparing two good-quality inductive voltage dividers at a frequency of 1000 cps a $\Delta\gamma$ of 100 μrad would be experienced only at the lower values of ratio below about $A = 0.01$. The error in ratio would be approximately 5×10^{-11}. An error of this magnitude would be negligible in most cases.

Another source of error in both magnitude of voltage ratio and phase angle is the loading on the unknown divider by the capacitor C. To determine the magnitude of these errors in practical work, the difference in voltage ratio and phase angle can be observed when another capacitor having the same value as C is connected from the output terminal of the unknown divider to ground in the circuit in Figure 1 (i.e., across R and C). The observed differences may be subtracted from the original readings to yield the values of ratio and phase angle with no load. Alternatively, the loading may be eliminated by adding a capacitor as shown by the dashed lines in Figure 1: C' and C form a capacitive divider to reduce the loading of C on the output circuit of the inductive divider. The magnitude of C' must be adjusted depending on the ratio being measured and, in particular, must have a value equal to $CA_s/(1 - A_s)$.

The power source should have a reasonably low harmonic content, and the null detector should be tunable to suppress harmonics in the quadrature voltage, which would otherwise prevent the attainment of a precise null. To understand the need for a tunable null detector, consider that harmonic components exist in both E_s and E_x having a frequency $n\omega$, equal amplitude hE_s, and the same phase. The total voltage across R is

$$e = e_\omega + e_{n\omega}\ (\text{phasor sum}) \tag{16}$$

where e_ω is the fundamental component and $e_{n\omega}$ is the harmonic component as shown in Figure 3. The phasor $e_{n\omega}$ rotates n times faster than e_ω, and its magnitude can be expressed in terms of the phase-angle difference of the fundamental output voltages, $\Delta\gamma$. The expression is similar to that for equation (7), except the harmonic current is hE_s/X_c and the angular frequency is $n\omega$; thus

$$e_{n\omega} = hE_s n\omega RC = nhE_s\Delta\gamma \tag{17}$$

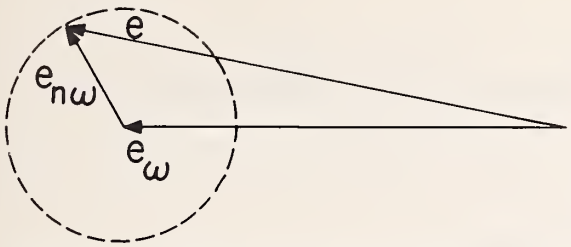

Figure 3. Phasor diagram showing effect of a harmonic in the quadrature voltage.

If this component is not suppressed by the detector, it would not by itself create a systematic error, but it would result in a limitation on the attainment of a null equivalent to a voltage-ratio uncertainty

$$u_A = \frac{e_{n\omega}}{|E_{\text{in}}|} = \frac{e_{n\omega}}{E_s/A} = A\frac{e_{n\omega}}{E_s} = Anh\Delta\gamma \qquad (18)$$

and a phase-angle uncertainty

$$u_\gamma = \frac{e_{n\omega}}{E_s} = nh\Delta\gamma \text{ [radians]} \qquad (19)$$

In a typical measurement at 1000 cps, where $A = 0.1$, $n = 3$, $h = 0.01$, and $\Delta\gamma = 20\ \mu$rad, it is found that $u_A = 0.06 \times 10^{-6}$ and $u_\gamma = 0.6\ \mu$rad. It is evident that a tuned indicating amplifier that suppresses the third harmonic by a factor of 10 would be sufficient to permit the discrimination of ratio to within $\pm\ 0.01 \times 10^{-6}$ in this case.

It should be noted that if a detector is used that has a linear response to small signals, it is possible to use it to interpolate between steps on the lowest decade of the divider.

MEASUREMENT VERIFICATION

A simple partial check on the bridge circuit and the calibration results can be performed by reversing the leads to the unknown divider and measuring the complement of the ratio.[4] Caution should be exercised because the case of the unknown divider will now be at a high potential if it has been connected to the common terminal. It can be seen that $1 - A_x$ is now to be compared with A_s. With this connection $c_x = -(c_s + d_s + d_x)$. The correction, c_x, obtained in this way may be compared with that obtained in the normal way.

The corrections to both inductive voltage dividers for the setting of $A = 0.5$ can be obtained from the complementary ratio measurements without prior knowledge of either of these corrections. If d_s is the reading of the standard for the normal circuit as shown in Figure 1, and d'_s is the reading of the standard with the unknown divider connections reversed, then

$$c_s = -(d_s + d'_s)/2 \quad \text{and} \quad c_x = (d_s - d'_s)/2 \qquad (20)$$

By a somewhat analogous method a check on the phase-angle measurements can be made. The formula for phase angle can be derived simply from the phasor diagrams of voltage ratio for the reversed connection. The phase angles of both inductive voltage dividers set at $A = 0.5$ can be obtained by the method of complementary measurements without prior knowledge of either of these phase angles.

CONCLUSION

If care is exercised in setting up the circuit, using good shielding practices, and a detector having adequate amplification and harmonic suppression is employed, the voltage ratios and phase angles of two good-quality inductive voltage dividers may be compared with negligible loss in accuracy. Several systematic errors in the circuit, for which corrections could be made, have been discussed and found to be negligible under the typical conditions described. The precision of the comparison is limited primarily by the resolution and stability of the standard and unknown dividers. The existence of a method for accurate comparison makes possible the use of calibrated inductive voltage dividers as standards for the calibration of other dividers and these, ultimately, for the very accurate measurement of voltage ratio and impedance ratio.

REFERENCES

1. Sze, W. C., *Trans. A.I.E.E., Part* I **76,** 444, 1957.
2. Harris, F. K., and W. C. Sze (NBS Washington), unpublished communications to the authors.
3. Zapf, T. L., *J. Res. NBS* **66C**, 25, 1962.
4. Engineering Bulletin No. 1 (Ratio Tran), Gertsch Products Inc., Los Angeles, California.
5. Engineering Bulletin No. 4 (Ratio Tran), Gertsch Products Inc., Los Angeles, California.
6. Morrison, N. E., Engineering Bulletin No. 20, Electro Scientific Industries, Portland, Oregon.
7. Morgan, M. L., Engineering Bulletin No. 29, Electro Scientific Industries, Portland, Oregon.

PREPRINT INSTRUMENT SOCIETY of AMERICA
21st Annual ISA Conference and Exhibit • October 24-27, 1966, New York
Preprint Number 12.3-2-66

COMPARATOR FOR CALIBRATION OF INDUCTIVE VOLTAGE DIVIDERS FROM 1 TO 10 kHz*

Wilbur C. Sze
Electrical Engineer
National Bureau of Standards
Washington, D.C. 20234

ABSTRACT

A high accuracy comparator is described for measuring the relative deviations in voltage ratios and phase angles of inductive voltage dividers. The new technique overcomes several inherent limitations of the existing comparison methods. The balance is accomplished by utilizing special shielded transformers and a resistance-capacitance network for in-phase and quadrature voltage injections. The measurements are accurate to within 1×10^{-7} of input in the frequency range from 1 to 10 kHz. Resolution is better than 2×10^{-10}

INTRODUCTION

The inductive voltage divider, since its first appearance about 15 years ago, has proven to be an increasingly valuable tool in the field of accurate electrical measurements as its striking characteristics become more widely known.

The development of material of extremely high magnetic permeability has made possible the construction of inductive voltage dividers with excellent stability and with deviations in ratio and phase angle of less than 5×10^{-7} of input.[1]** The accurate initial establishment of the voltage ratio and phase angle has been presented elsewhere and will not be repeated here.[2] These known voltage ratios and phase angles are preserved in the calibrated inductive voltage divider so that they may be used as a reference and re-established again by a satisfactory comparison circuit without significant degradation in accuracy.

At the National Bureau of Standards, a new comparison method, based on suggestions by Robert D. Cutkosky, has been developed for relative ratio and phase angle measurements from 1 to 10 kHz to an accuracy of better than one part in 10^7. This technique, which appears worthy of general use in standardizing laboratories, overcomes several inherent limitations of the existing comparison methods: (1) the dividers are treated as four-terminal networks as they were designed to be operated; (2) the test circuit imposes negligible burden on either the reference or the test divider; and (3) it is not necessary to use lower dials of either divider for in-phase voltage balancing.[3,4]

DESCRIPTION OF CIRCUIT

This technique uses a double toroidal transformer, one transformer for null detection and the other for injection of differential voltages. Figure 1-a shows the complete schematic circuit diagram simplified by omission of the shielding arrangements. D_1 and D_2 represent the reference and test dividers whose voltage ratios and phase angles are being compared. Their input and output terminals are connected together with short coaxial leads. The lead impedance between the input terminal of each divider and its junction point with the supply voltage should be very small and nearly equal. The detector circuit consists of a tuned null-indicator and a specially constructed shielded transformer, T_3, to match the impedances and to isolate the detector from the measuring circuit. The parallel pair of inductive voltage dividers, D_3 and D_4, inject, through the R-C network shown and transformer, T_2, in-phase and quadrature balance voltages into the lead connecting the output terminals of the dividers, D_1 and D_2. Transformer, T_1, is also specially constructed with an accurate 1/1 voltage ratio. The mid-point of the secondary winding is grounded so that both polarities of the injection voltages can be obtained from the outputs of D_3 and D_4 without the necessity of altering the circuit.

In order to realize an accuracy of better than one part in 10^7, coaxial chokes are required in the circuit to reduce the small but troublesome loop and ground currents to a minimum.[5,6] Each coaxial choke consists of an appropriate number of turns of a coaxial cable threaded through a high permeability core as indicated in Figure 1-a.

Photographs 1, 2, and 3 show the comparator and the circuit arrangement.

*This work was supported in part by the Metrology Engineering Center, Bureau of Naval Weapons, Pomona, California.

**However, in demonstrating the accuracy of the comparator, commercially available dividers were used.

Superior numbers refer to similarly numbered references at the end of this paper.

THEORETICAL RELATIONS

By definition, the voltage ratio of a divider is the ratio of the secondary or output terminal voltage, V_{OUT}, to the primary or input terminal voltage, V_{IN}, which can be expressed as

$$\frac{V_{OUT}}{V_{IN}} = d + \alpha d + j\beta d$$

where d is the nominal ratio or setting of the dials. αd is the in-phase deviation, and βd is the quadrature deviation. Both are expressed in parts-per-million (ppm) of input.

The equations for the relative in-phase deviation and quadrature deviation measurements can be derived from Figure 1-b as follows:

$$V_R = I_R R_1 + V_3$$

$$V_C = -I_C jX_C + V_3$$

$$V_3 = (I_C + I_R)\frac{R_2 Z}{R_2 + Z} \approx (I_C + I_R)R_2$$

where Z is the impedance of transformer T_2. Since in the circuit described here, $Z \gg R_2$, the above approximation is justified. V_C and V_R are the voltages between the output terminals of D_3 and D_4 and ground.

By solving for I_R and I_C from the first two equations and substituting in the third,

$$V_3 = \frac{V_C R_1^2 + V_R X_C^2 (1 + \frac{R_1}{R_2}) + jX_C R_1 [V_C (1 + \frac{R_1}{R_2}) - V_R]}{R_1^2 + X_C^2 (1 + \frac{R_1}{R_2})^2}$$

If r represents the turns ratio of T_2, then the voltage injected between output terminals of D_1 and D_2 is equal to V_3/r. However, V_C and V_R can also be expressed as decimal fractions of the supply voltage or by dial settings of D_3 and D_4 as d_C and d_R, respectively, and V_3 as d_3.

Again from Figure 1-a, when the detector indicates a null,

$$d_2(1 + \alpha_2 + j\beta_2) - d_1(1 + \alpha_1 + j\beta_1) = \frac{d_3}{r}$$

where d_1 and d_2 are the equal dial settings on the dividers D_1 and D_2, at the point being compared. α and β are expressed in parts-per-million of dial setting, d. By substituting the expression for d_3 in the previous equation and separating real and j terms,

$$\alpha_2 - \alpha_1 = \frac{d_C R_1^2 + d_R X_C^2 (1 + \frac{R_1}{R_2})}{r d_1 [R_1^2 + X_C^2 (1 + \frac{R_1}{R_2})^2]}$$

$$\beta_2 - \beta_1 = \frac{R_1 X_C [d_C (1 + \frac{R_1}{R_2}) - d_R]}{r d_1 [R_1^2 + X_C^2 (1 + \frac{R_1}{R_2})^2]}$$

If $X_C \approx R_1$ and $R_1 \gg R_2$, then the equations for the relative deviations can be approximated as

$$d_1(\alpha_2 - \alpha_1) \approx \frac{d_R}{r(\frac{R_1}{R_2})}$$

$$d_1(\beta_2 - \beta_1) \approx \frac{d_C R_2}{r X_C}$$

DESCRIPTION OF COMPONENTS

T_1, T_2, and T_3 are specially constructed shielded transformers using high magnetic permeability toroidal cores to insure close magnetic coupling and to conserve space in the circuit. The shields minimize the magnetic pick-up from stray fields in the laboratory.

Figure 3 shows the schematic circuit of T_1. It consists of a toroidal core, an inner primary winding, an electrostatic shield, an outer secondary winding, and an overall Mu-metal case. Each winding is wound on the core in a single, equally distributed layer from 0° to 360°, and the wire is brought from 360° back to 0° or the point of origin. Thus no loop is formed, and susceptibility to stray magnetic pickup is greatly reduced. (This same technique is used for winding T_2 and T_3.) The mid-point of the secondary winding is grounded. The size of the core and number of turns for 1 to 5 kHz and 5 to 10 kHz operations at 100 volts input are indicated in Figure 3.

Figure 2 shows the details of construction of T_2 and T_3 transformers as a single unit. T_2 and T_3 are identical and interchangeable. Each consists of a toroidal core and a 100-turn primary winding. The shielding arrangements are such that the cross capacitances at the gaps are reduced to a minimum.[7] The secondary winding consists of a single conductor connected between the outputs of the test dividers. The capacitance between this conductor and the shield is less than 4 pF. Therefore, it imposes no significant burden on either divider.

The inductive voltage dividers, D_3 and D_4, are commercially available units. Each consists of three decades and a continuously adjustable resistive divider. Their small voltage ratio and phase angle deviations were determined and found to be negligible, for the injection voltage, V_3, rarely exceeds 0.002 percent of the input voltage.

C is a three-terminal capacitor having a very small dissipation factor. R_1 and R_2 are three-terminal multi-decade resistors of very small residual reactance. For 1 kHz calibrations, C is generally set to equal 15.92 nF, R_1 = 10 kilohms, and R_2 = 10 ohms. (For 10 kHz calibrations, air capacitors of 1592 pF are used.) Thus one step on the top decade of D_3 and D_4 represents a difference of 1 ppm in in-phase or quadrature deviation.

The detector circuit consists of a preamplifier and a cathode-ray oscillograph. A narrow band-pass filter is used to discriminate against any noise before the first stage of amplification. A double elliptical pattern, suggested by Clothier, is shown on the cathode-ray oscillograph to indicate balance condition. The unbalance voltage from the comparison circuit is impressed on the vertical plates. On the horizontal plates is a signal of the same frequency whose phase can be adjusted so that angular departure of the major axis of the elliptical pattern represents in-phase unbalance and opening of the minor axis quadrature unbalance. At balance the figure appears to be a single line.[2,4,8] The resolution is such that an unbalance voltage of 0.1 nanovolt is easily observed.

TABLE OF RESULTS

The following table lists the in-phase deviations, $d_1\alpha_1$ and $d_2\alpha_2$, and quadrature deviations, $d_1\beta_1$ and $d_2\beta_2$, of two inductive voltage dividers at 10 kHz and with an input of 50 volts RMS. These values of $d\alpha$ and $d\beta$ for each divider were measured with this circuit using a third divider as a reference. Relative deviations were calculated from these results and listed in the table as "computed" $d_1(\alpha_2-\alpha_1)$ and $d_1(\beta_2-\beta_1)$ for comparison with those determined by a direct comparison of the two test dividers. The latter are listed as "measured" $d_1(\alpha_2-\alpha_1)$ and $d_1(\beta_2-\beta_1)$.

The computed and measured results listed in the table agreed to 0.02 ppm for $d_1(\alpha_2-\alpha_1)$ and 0.1 ppm for $d_1(\beta_2-\beta_1)$.

The voltage ratio is defined by the equation

$$\frac{V_{OUT}}{V_{IN}} = d(1+\alpha+j\beta),$$

and phase angle by

$$\tan\theta = \frac{\beta}{1+\alpha} \approx \beta$$

CONCLUSIONS

A high accuracy comparator has been developed for measuring the relative deviation in voltage ratio and phase angle of inductive voltage dividers from 1 to 10 kHz. An overall accuracy of better than one part in 10^7 is achieved.

The new technique overcomes several inherent limitations of the existing comparison methods and has a broader frequency range. It requires only a few pieces of special equipment, and these are easy to construct. This circuitry appears worthy of general use in standardizing laboratories.

ACKNOWLEDGMENT

The author acknowledges the valuable help and advice received from Mr. Robert D. Cutkosky. Mr. R. J. Berry contributed skillfully in constructing the components.

REFERENCES

(1) Hill, J. J., and Miller, A. P., "A Seven-Decade Adjustable-Ratio Inductively-Coupled Voltage Divider with 0.1 Part Per Million Accuracy," JIEE, Vol. 109, Part B, pp. 157-162, March 1962.

(2) Sze, W. C., Dunn, A. F., and Zapf, T. L., "An International Comparison of Inductive Voltage Divider Calibrations at 400 and 1000 Hertz," IEEE Trans. on Instr. and Meas., Vol. IM-14, No. 3, pp. 124-131, September 1965.

(3) Cutkosky, Robert D., is with the Absolute Electrical Measurements Section, NBS.

(4) "Electrical Calibration Service Extended--Inductive Voltage Dividers Calibrated up to 10 kHz," NBS Technical News Bulletin, Vol. 49, No. 1, January 1965.

(5) Thompson, A. M., "A.C. Bridge Methods for the Measurement of Three-Terminal Admittances," IEEE Trans. on Instr. and Meas. Vol. IM-13, No. 4, pp. 189-197, December 1964.

(6) Cutkosky, R. D., "Evaluation of the NBS Unit of Resistance Based on a Computable Capacitor," J. Res. NBS, Vol. 65A, No. 3, p. 147-158, May-June 1961.

(7) Guildner, L. A., and Edsinger, R. E., "The NBS Gas Thermometer II. Measurement of Capacitance to a Grounded Surface with a Transformer Ratio-Arm Bridge," J. Res. NBS, Engrg. and Instr., Vol. 69C, No. 1, pp. 13-18, January-March 1965.

(8) Clothier, W. K., National Standards Laboratory, Chippendale, N.W.W., Australia, private communications.

TABLE

d_1	PPM of Input $d_1\alpha_1$	$d_2\alpha_2$	Computed $d_1(\alpha_2-\alpha_1)$	Measured $d_1(\alpha_2-\alpha_1)$	PPM of Input $d_1\theta_1$	$d_2\theta_2$	Computed $d_1(\theta_2-\theta_1)$	Measured $d_1(\theta_2-\theta_1)$
.X	+0.15	+0.16	+0.01	+0.01	-0.4	-0.3	+0.1	0.0
.9	+1.27	-0.23	-1.50	-1.51	-0.4	-0.3	+0.1	+0.1
.8	+1.22	-0.31	-1.53	-1.53	-0.3	0.0	+0.3	+0.3
.7	+2.21	-0.33	-2.54	-2.53	+0.1	0.0	-0.1	-0.2
.6	+1.90	-0.42	-2.32	-2.32	-0.1	-0.2	-0.1	-0.2
.5	+1.63	-0.27	-1.90	-1.90	0.0	-0.4	-0.4	-0.4
.4	+1.17	+0.03	-1.14	-1.14	-0.1	-0.4	-0.3	-0.3
.3	+0.41	0.00	-0.41	-0.42	-0.4	-0.5	-0.1	-0.2
.2	+0.34	0.00	-0.34	-0.36	-0.3	-0.6	-0.3	-0.3
.1	+0.11	+0.04	-0.07	-0.08	-0.3	-0.5	-0.2	-0.2
.0X	-1.03	+0.21	+1.24	+1.25	-0.2	-0.4	-0.2	-0.2
.09	-0.96	+0.18	+1.14	+1.16	-0.2	-0.4	-0.2	-0.2
.08	-0.99	+0.15	+1.14	+1.15	-0.3	-0.4	-0.1	-0.1
.07	-0.88	+0.12	+1.00	+1.01	-0.2	-0.3	-0.1	-0.1
.06	-0.96	-0.16	+0.80	+0.81	-0.4	-0.4	0.0	-0.1
.05	-0.70	-0.01	+0.69	+0.71	-0.3	-0.3	0.0	0.0
.04	-0.43	-0.21	+0.22	+0.22	-0.2	-0.4	-0.2	-0.2
.03	-0.09	-0.01	+0.08	+0.08	-0.1	-0.2	-0.1	-0.1
.02	+0.02	+0.01	-0.01	-0.01	0.0	-0.1	-0.1	-0.1
.01	-0.01	0.00	+0.01	+0.01	-0.1	-0.1	0.0	0.0
.00X	-0.01	0.00	+0.01	+0.01	-0.1	-0.1	0.0	0.0
.009	-0.01	-0.01	0.00	0.00	-0.1	-0.1	0.0	0.0
.008	+0.01	0.00	-0.01	-0.01	-0.1	-0.1	0.0	0.0
.007	+0.03	0.00	-0.03	-0.02	-0.1	-0.1	0.0	0.0
.006	+0.04	+0.01	-0.03	-0.03	-0.1	-0.1	0.0	0.0
.005	+0.05	+0.01	-0.04	-0.04	-0.1	-0.1	0.0	0.0
.004	+0.06	+0.01	-0.05	-0.05	-0.1	-0.1	0.0	0.0
.003	+0.07	+0.01	-0.06	-0.06	-0.1	-0.1	0.0	0.0
.002	+0.09	+0.02	-0.07	-0.07	-0.1	-0.1	0.0	0.0
.001	+0.10	+0.02	-0.08	-0.08	-0.1	-0.1	0.0	0.0
.000X	+0.11	+0.02	-0.09	-0.09	-0.1	-0.1	0.0	0.0

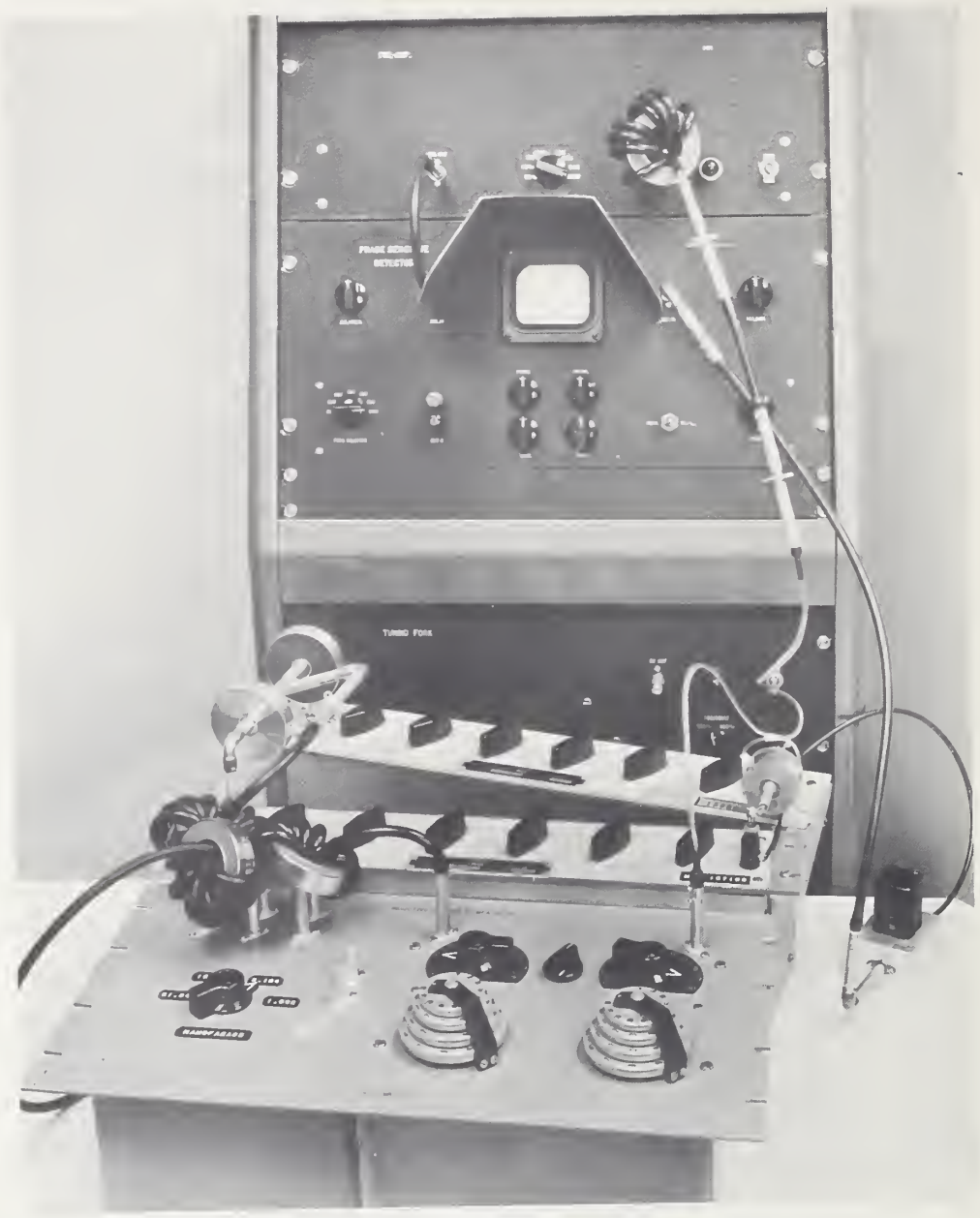

Photograph 1

Photograph 2

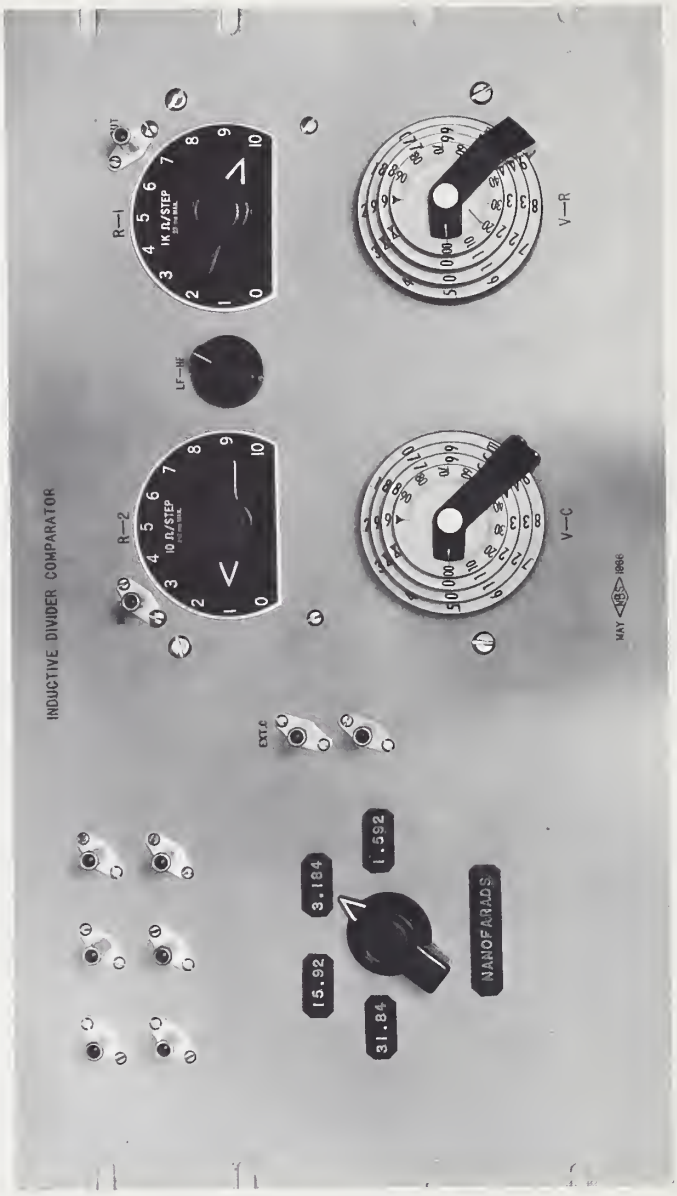

Photograph 3

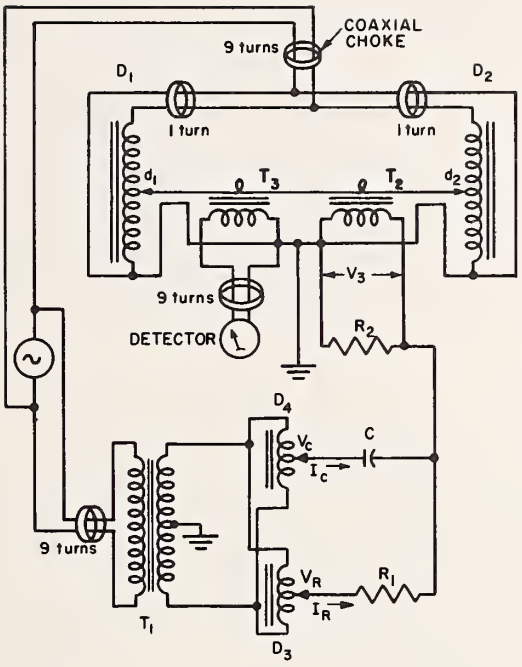

Fig. 1-a

Figure 1-a Schematic Circuit Diagram

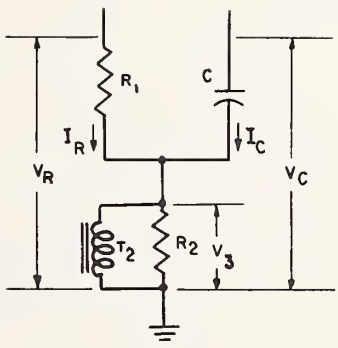

Fig. 1-b

Figure 1-b R-C Network

PIECE NO.	NOMENCLATURE	NO. REQ'D
NATIONAL BUREAU OF STANDARDS WASHINGTON, D.C. 20234		
COMPARISON CIRCUIT		
FOR VOLTAGE DIVIDER CALIBRATION		
MODEL	TYPE	SCALE
DIMENSIONS IN INCHES (Unless otherwise specified)	DRAFTSMAN H. P. K.	CHECKER
TOLERANCES (Unless otherwise specified)	PROJECT ENGR. SZE	PROJECT ENGR
DECIMALS ±.008 FRACTIONS ±.015 ANGLES ±½°	SUBMITTED BY CHIEF, SEC.	
DO NOT SCALE THIS PRINT	EXAMINED BY CHIEF ENGINEER	
DIV. SEC. 211.06	THIS PRINT ISSUED 4·16·66	APPROVED BY CHIEF, DIV. 66-04-16-548

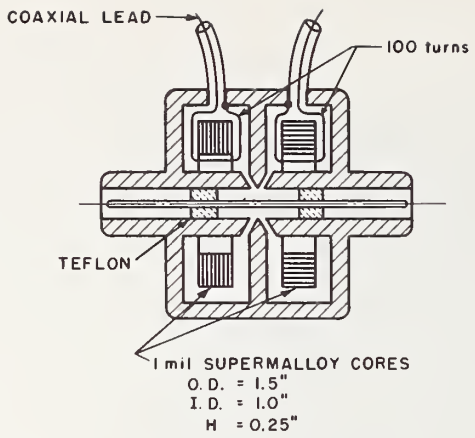

Fig. 2.

Figure 2 Injector-Detector Transformers

PIECE NO	NOMENCLATURE	NO REQ'D
NATIONAL BUREAU OF STANDARDS WASHINGTON, D.C. 20234		
INJECTOR-DETECTOR TRANSFORMER		
FOR VOLTAGE DIVIDER CALIBRATION		
MODEL	TYPE	SCALE
DIMENSIONS IN INCHES (Unless otherwise specified)	DRAFTSMAN H. P. K.	CHECKER
TOLERANCES (Unless otherwise specified)	PROJECT ENGR SZE	PROJECT ENGR
DECIMALS ±.005 FRACTIONS ±.015 ANGLES ±½°	SUBMITTED BY CHIEF, REC.	
DO NOT SCALE THIS PRINT	EXAMINED BY CHIEF ENGINEER	
DIV. SEC. 211.06	THIS PRINT ISSUED 4-16-66	APPROVED BY CHIEF, DIV. 66-04-16-549

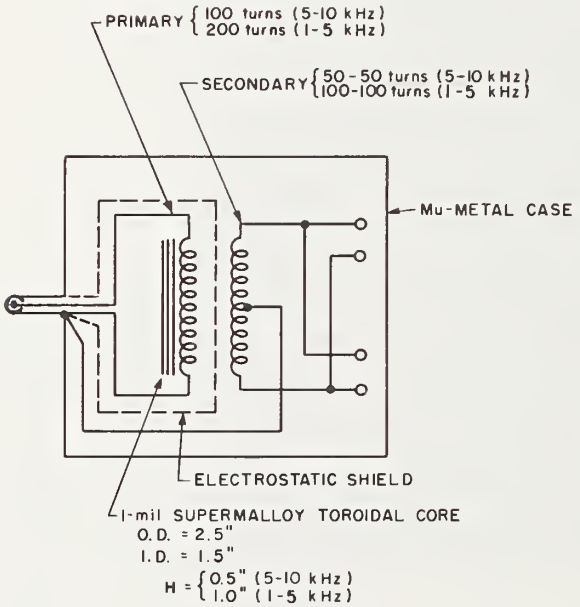

Fig. 3

Figure 3 Shielded Transformer

PIECE NO	NOMENCLATURE	NO REQ'D
NATIONAL BUREAU OF STANDARDS WASHINGTON, D.C. 20234		
SHIELDED TRANSFORMER		
FOR VOLTAGE DIVIDER CALIBRATION		
MODEL	TYPE	SCALE
DIMENSIONS IN INCHES (Unless otherwise specified)	DRAFTSMAN H. P. K.	CHECKER
TOLERANCES (Unless otherwise specified)	PROJECT ENGR SZE	PROJECT ENGR
DECIMALS ±.005 FRACTIONS ±.015 ANGLES ±½°	SUBMITTED BY CHIEF, SEC.	
DO NOT SCALE THIS PRINT	EXAMINED BY CHIEF ENGINEER	
DIV. SEC. 211.06	THIS PRINT ISSUED 4-16-66	APPROVED BY CHIEF, DIV. 66-04-16-547

Reprinted from IEEE TRANSACTIONS
ON *INSTRUMENTATION AND MEASUREMENT*
Volume IM-14, Number 3, September, 1965

An International Comparison of Inductive Voltage Divider Calibrations at 400 and 1000 Hz

W. C. SZE, SENIOR MEMBER, IEEE, A. F. DUNN, MEMBER, IEEE, AND T. L. ZAPF, SENIOR MEMBER, IEEE

Abstract—**The establishment and maintenance of the highest possible order of accuracy for the measurements of voltage ratio and phase angle are responsibilities of the national laboratories. This paper reports the results of an international comparison of a seven-decade inductive voltage divider by the United States National Bureau of Standards and the National Research Council of Canada. The calibration techniques used in each laboratory are discussed in detail, and the results of calibration at 400 and 1000 Hz are compared. The accuracies of measurements are within 0.1 ppm of input for voltage ratio and 1(setting of dials)$^{1/2}$ microradians for phase angle.**

Introduction

IN THE FALL OF 1954, inquiries were received about the calibration of voltage ratios and phase-angle errors of six-dial inductive voltage dividers at audio frequencies. An early test method, developed by Sze, in which the accuracy of voltage ratio determinations was dependent on the dc calibration of standard resistors and the ac-dc differences of the resistive divider, achieved a maximum accuracy of 0.005 per cent for voltage ratio and 60 microradians for phase-angle error measurements [1].

Since then, considerable progress has been made in measurement techniques by the United States National Bureau of Standards laboratories at Washington, D. C. (NBS-W), and Boulder, Colorado (NBS-B), and the National Research Council of Canada at Ottawa, Ontario (NRC). At present, each laboratory is capable of calibrating a voltage divider with uncertainty within $\pm 1 \times 10^{-7}$ of input for voltage ratio measurements and within 1/(setting of dials)$^{1/2}$ microradians for phase-angle errors at 400 and 1000 Hz.

The inductive voltage divider that was used for this international comparison had been used on several previous occasions for 1000 Hz interlaboratory comparison of calibrations between NBS-W and NBS-B. For the results reported in this paper, the divider was initially calibrated at NBS-W before it was shipped to NBS-B for calibration tests. From Boulder, it was returned to Washington for repeated measurements, sent to NRC for calibration, and then returned to Washington for final measurements. It was believed that in this way any changes resulting from its shipment could be detected and, perhaps, separated from the interlaboratory comparison.

The purposes of this paper are 1) to describe the instrument used for the international comparison of calibrations; 2) to discuss separately in some detail the calibration techniques of each laboratory; and 3) to compare the results of calibrations at the three laboratories at 400 and 1000 Hz.

Manuscript received January 12, 1965. This paper is National Research Council Rept. No. 8284.

W. C. Sze is with the High Voltage Sect., Electricity Div., National Bureau of Standards, Washington, D. C.

A. F. Dunn is with the National Research Council of Canada, Ottawa, Ontario.

T. L. Zapf is with the Electronic Calibration Center, National Bureau of Standards, Boulder, Colo.

Description of the Test Divider

The inductive voltage divider used for this comparison of calibrations is a seven-decade commercial device [2]. It consists of seven multitapped windings on four toroidal tape-wound cores of very high magnetic permeability. Each winding of the top two decades (10^{-1} and 10^{-2} per step of the input voltage) is wound on a separate core and encased in individual magnetic shields. The third and fourth decades share one core, and the last three decades share another magnetic core. The windings are connected in a modified Kelvin-Varley arrangement and provide a resolution of 1×10^{-7}. The useful frequency range claimed by the manufacturer is 50 to 10 000 Hz. The maximum input voltage is 0.35 (operating frequency) or 350 volts, whichever is smaller

NBS-W Test Method

At the National Bureau of Standards, Washington, D. C., the test inductive voltage divider was calibrated by direct comparison with a capacitance divider, made up of three-terminal capacitors whose relative values were obtained by intercomparison in a bridge having transformer-type ratio arms.

Bridge Circuits

With the test inductive voltage divider input connected across one arm of the bridge circuit (as shown schematically in Fig. 1, but simplified by not indicating the shielding arrangements), balance was achieved by adjusting the output taps (N_1 and N_2) of the inductive voltage dividers which were connected across the 10 percent taps (V_b and V_c) of the ratio arm transformer. $\sum_1^N C_2$ consisted of an appropriate number (N) of units of capacitors of the same nominal values. N depended on the setting of the dials (D) on the test divider. C_1 was larger than C_2 by a factor of one decade or more, depending on the ratio of the test divider. The in-phase voltage balance was achieved by insertion of a current

into the detector junction of the bridge through capacitor C_5. This current usually was less than 0.001 percent of the current through capacitor $\sum_1^N C_2$. The phase differences between the bridge arms were compensated by insertion of a quadrature current of appropriate magnitude into the detector junction of the bridge through resistor R and current divider $C_3/(C_3+C_4)$. These techniques had been fully described by McGregor, et al. [3].

Connection of C_1 was then moved from D to V_b, and the individual units C_2, making up $\sum_1^N C_2$ were compared to C_1 as shown in Fig. 2. Thus the capacitance divider ratio was determined accurately by a substitution method in which the exact values of C_1 and C_2 need not be known. However, these must be very stable capacitors of negligibly small voltage coefficient. As in the previous arrangement, the in-phase and quadrature differences between the bridge arms were compensated by insertion of currents of appropriate phase and magnitude.

All of the above steps were straightforward and could be done in a symmetrical fashion (comparison of capacitors, calibration of test divider, and recomparison) in less than one hour per decade by an experienced operator.

Although small three-terminal capacitors were much easier to calibrate than small two-terminal capacitors because of the virtual elimination of connection problems, a particularly troublesome source of error arose when the capacitance to ground was large. Cutkosky and Thompson have shown that if the capacitor is treated as a four-terminal network with a high permeability core or coaxial choke linking one ground lead with one active electrode lead, this small but significant error can be eliminated [4], [5].

This technique has been used throughout the NBS-W calibrations reported in this paper. Figure 3 shows the capacitor comparison circuit of Fig. 2 with high permeability cores inserted into each bridge arm and the detector leads.

Theoretical Relations

The equations for the voltage-ratio corrections and phase-angle errors were developed as follows: by definition, the voltage ratio of a transformer or divider is the ratio of the secondary or output terminal voltage V_{out} to the primary or input terminal voltage V_{in} so that

$$\frac{V_{out}}{V_{in}} = D(1 + \alpha + j\beta)$$

where D is the nominal ratio or setting of the dials and α is the zero-burden[1] ratio correction derived from the measured quantities. β is the difference in phase angle between the input and output voltage phasors of the divider.

[1] Zero-burden corrections were evaluated by observations with double the capacitance burden across the output terminals.

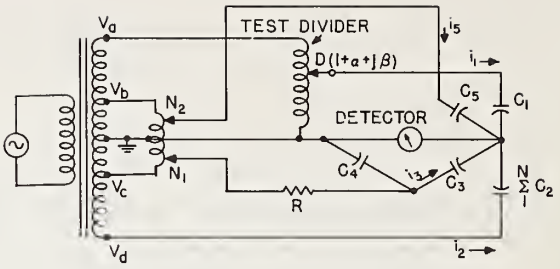

Fig. 1. Voltage divider calibration circuit.

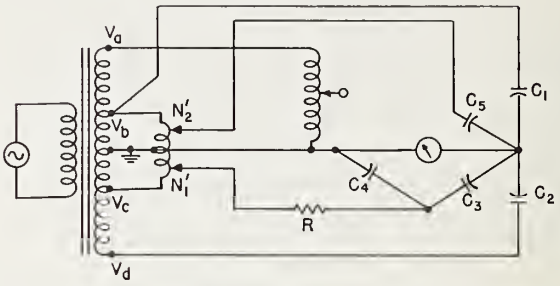

Fig. 2. Capacitance comparison circuit.

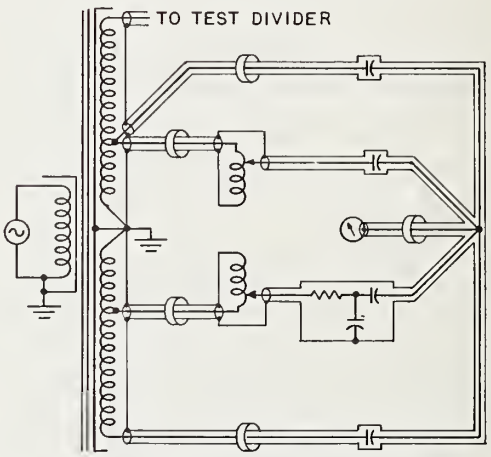

Fig. 3. Comparison circuit shown with high-permeability cores.

Figure 1 shows the general circuit for the calibration of a voltage divider. For the calibration of the first or 10^{-1} decade, we arrived at the following relations:

$$C_1 \approx 10C_2$$

$$V_a = V_a(1 + 0 + j0) \text{ or the reference voltage}$$

$$V_b = \frac{V_a}{10}(1 + \alpha_b + j\beta_b), \quad V_c = -\frac{V_a}{10}(1 + \alpha_c + j\beta_c),$$

$$V_d = -V_a(1 + \alpha_d + j\beta_d).$$

$D = N/10$ setting of dial on the 10^{-1} decade, N being an integral number from 1 to 10. The balance equation of the network is $i_1+i_5+i_2+i_3=0$. We have

$$V_a(j\omega C_1 + G_1)[D(1 + \alpha + j\beta)] + V_b N_2(j\omega C_5 + G_5)$$

$$+ V_d\left(j\omega \sum_1^N C_2 + \sum_1^N G_2\right) + V_c N_1\left(\frac{C_3}{C_3 + C_4}\right)$$

$$\cdot\left(j\omega C_R + \frac{1}{R}\right) = 0.$$

Since α_d, and $\beta_d < 1 \times 10^{-8}$ and α_b, β_b, α_c, and $\beta_c < 5 \times 10^{-6}$ and N_1 and N_2 readings are usually small, the terms involving the products of these figures are insignificant and, therefore, neglected. G's shown in the above equation are the conductances associated with the capacitors and C_R represents the equivalent shunt capacitance of resistor R. From the network of Fig. 2, a second balance equation is derived. By solving the two equations simultaneously, omitting insignificant terms, and separating j and real terms, we have

$$\alpha = \alpha_b + \frac{C_5}{NC_1}\left(\sum_1^N N_2' - N_2\right)$$

$$+ \frac{C_R C_3}{NC_1(C_3 + C_4)}\left(N_1 - \sum_1^N N_1'\right)$$

and

$$\beta = \beta_b + \frac{C_3}{\omega NRC_1(C_3 + C_3)}\left(\sum_1^N N_1' - N_1\right).$$

Similar equations could be developed for the calibration of the lower decades. It will be noted that the in-phase balance expression contained a term representing the effect of the equivalent shunt capacitance C_R across the resistor R, used for quadrature balance. In any practical case, this C_R would never be more than a few parts in 10^7; and, thus by careful selection of the resistance element and shielding used, it was easily made negligible.

Description of Apparatus

The usefulness of the bridges described in Figs. 1 and 2 depends to a great extent on the quality of the ratio-arm transformer, and particularly on the 10 to 10 and 10 to 1 ratios of the secondary windings. The method used at NBS-W for the precision measurement of these ratios has been fully described by Cutkosky [6]. The transformer used in the bridges was constructed in a similar manner to the ones described by McGregor, et al., and Dunn [3], [7].

The dividers, used to achieve the balance of the bridge by insertions of in-phase and quadrature currents into the detector junction, were high quality commercial seven-decade inductive voltage dividers. Their small voltage ratio and phase-angle errors could be neglected for the following reasons: 1) the dividers were connected to the 10 percent taps of the ratio-arm transformer; 2) the capacitance values of capacitors C_1 and C_2 would be adjusted so that the setting of N_2 would be very near zero; and 3) the loss angles of three-terminal capacitors were found to be so small that the use of a current divider $C_3/(C_3+C_4)$ was necessary in order that the setting of N_1 be made large enough to be useful.

The uniplanar-suspension capacitors (Fig. 4), a modification of a design by Clothier, were used for the capacitance divider [8]. They were of a coaxial cylindrical construction with dry air as dielectric between the active electrodes. Each one of the active electrodes was supported by three $\frac{1}{8}$ inch diameter sapphire balls placed 120° apart in a massive brass mounting block. The maximum adjustment of the threaded trimmer electrode could produce only a small change in total capacitance, and coarse trimming was accomplished by a lathe cut across the open end of one of the electrodes. Eleven capacitors were buried in the same mounting block, of which a decade was made up of ten capacitors that could be separately connected or summed. Each capacitor could be adjusted with a little care and brought to the same value to within a few ppm. The purpose of the block was to achieve a mounting that was relatively strain free and isothermal, and to achieve reasonable attenuation of ambient temperature and pressure changes. The individual units of this decade have not been readjusted since the initial adjustment which brought all ten very close to the eleventh in value. A ratio check has been made from time-to-time with this decade, and the usual day-to-day variations amounted to one part in 10^7. Since the temperature coefficient of capacitance of these units was approximately 20 ppm/°C, the small variations must mean that changes in ambient temperature were well attenuated and that the temperatures within the mounting block were nearly uniform on each measurement, in spite of the fact that room temperature moved through about 1°C range. It also must mean that the individual units were relatively stable dimensionally. Decades of 1 pF per unit and 100 pF per unit were also constructed on the same principle. Surfaces of all capacitor parts were gold plated before their final assembly.

The detector circuit consisted of a preamplifier and a cathode-ray oscillograph. An LC tuned circuit having a band-pass of about 7 Hz was used ahead of the preamplifier. In this way, sharp discrimination against noise was introduced before the first stage of amplification.

The cathode-ray oscillograph was used to indicate bridge balance; but the usual elliptical display pattern was modified as suggested by Clothier [9]. The amplified unbalance voltage from the detector arm of the bridge is impressed on the vertical plates of the CRO. On the horizontal plates is a synchronous signal whose phase can be adjusted so that angular departure of the major axis of the elliptical display pattern represents magnitude unbalance and opening of the minor axis quadrature unbalance. At balance the figure appears to

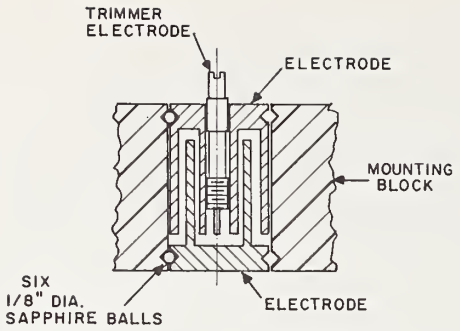

Fig. 4. 10 pF uniplanar-suspension capacitor.

be a single line which rocks about the horizontal as a result of random noise. In Clothier's modification a repetitive square-wave signal is superimposed on the horizontal plates, so that the elliptical pattern is doubled. The square-wave signal can be adjusted until the right tip of one ellipse just touches the left tip of the other, and at balance the adjacent ends appear to move past each other as a result of noise. An average horizontal position (i.e., balance) can now be estimated much more accurately than with a single ellipse, and an unbalance signal observed which is lower by almost an order of magnitude.

NRC Test Method

At the National Research Council, Ottawa, Canada, the test inductive voltage divider was also calibrated by direct comparison with a capacitance divider, using a transformer ratio bridge whose ratio, with the burden of the divider and measuring components, is established in the sequence of balances [7].

Ratio of Capacitance

The procedure begins by establishing known ratios of the capacitance divider. Eleven nominally equal three-terminal capacitors are assembled as a unit in a mounting block, of which a decade is made up of ten that can be individually connected or summed (the subscript m designates individual units and n, n units in parallel). The eleventh capacitor is represented by symbols G_F and C_F. In Fig. 5, the test divider is connected to the $F_S=1/1$ tap of the bridge transformer with a coaxial cable to establish a burden and to determine the zero reference balance (D_{Co}, D_{Go}) of the bridge with dials D_C and D_G. Then capacitors C_F and C_{nF} are connected to the bridge as shown and each C_{mF} is measured in terms of C_F. The balance equations are

$$G_{mF} = G_F(1 + \alpha_{X1} + \alpha_{S1}) + (D_{Gm} - D_{Go}) - \omega C_F(\beta_{X1} + \beta_{S1})$$

$$C_{mF} = C_F(1 + \alpha_{X1} + \alpha_{S1}) + (D_{Cm} - D_{Co}) + \frac{G_F}{\omega}(\beta_{X1} + \beta_{S1}),$$

and for n units in parallel (n being a running integer from 1 to 10).

$$G_{nF} = nG_F(1 + \alpha_{X1} + \alpha_{S1}) + \sum_1^n (D_{Gm} - D_{Go}) - n\omega C_F(\beta_{X1} + \beta_{S1})$$

$$C_{nF} = nC_F(1 + \alpha_{X1} + \alpha_{S1}) + \sum_1^n (D_{Cm} - D_{Co}) + \frac{nG_F}{\omega}(\beta_{X1} + \beta_{S1})$$

where α_{X1} and α_{S1} represent the in-phase ratio corrections of the $F_X=1/1$ and $F_S=1/1$ taps of the bridge transformer, while β_{X1} and β_{S1} are the respective quadrature corrections. Higher order terms of small quantities are neglected.

Capacitors with nominal values of a decade higher or lower can also be compared by selecting the appropriate ratio taps on the bridge transformer [7].

Calibration of the Test Divider

Figure 6 shows the general circuit diagram for the calibration of a voltage divider, whose true zero-burden voltage ratio is defined as before as

$$\frac{V_{out}}{V_{in}} = D(1 + \alpha + j\beta) = \frac{e - E_0}{E - E_0}.$$

The errors resulting from additional burdens imposed by the impedance of the coaxial cables and circuit components on the outputs of both the test divider and bridge transformer must be applied as correction terms to α and β of the bridge balance equation.

The following equations, $D\alpha$ and $D\beta$, with all the significant corrections added to the general bridge balance equation, represent the corrections to the nth tap of the first dial of the test divider:

$$D\alpha = \frac{n}{10}\alpha = \frac{n}{10}(\alpha_{S1} - \alpha_{S1}') + \frac{1}{10C_F}\left[\frac{n}{10}(D_{CS} - D_{Co}) + \left(\sum_1^n D_{Cm} - \frac{n}{10}\sum_1^{10} D_{Cm}\right) - (D_{Cn}' - D_{CEo}') - \frac{C_S + C_{GS}}{C_H}(D_{Cn}' - D_{Cn}'') + \frac{nC_F}{C_S^*} \cdot (D_{Cn}^* - D_{Co}^*) + \frac{nC_F}{C_S^*} \cdot \frac{C_S + C_{GS}}{C_H}(D_{Cn}^* - D_{Cn}^{**})\right]$$

and

$$D\beta = \frac{n}{10}\beta = \frac{n}{10}(\beta_{S1} - \beta_{S1}') - \frac{2}{10\omega C_F}\left[\frac{n}{10}(D_{GS} - D_{Go}) + \left(\sum_1^n D_{Gm} - \frac{n}{10}\sum_1^{10} D_{Gm}\right) - (D_{Gn}' - D_{GEo}') - \frac{C_S + C_{GS}}{C_H}(D_{Gn}' - D_{Gn}'') + \frac{nC_F}{C_S^*} \cdot (D_{Gn}^* - D_{Go}^*) + \frac{nC_F}{C_S^*} \cdot \frac{C_S + C_{GS}}{C_H}(D_{Gn}^* - D_{Gn}^{**})\right].$$

The term $n(D_{CS} - D_{Co})/10$ represents the correction to the nominal ratio of C_S to C_{nF}, when $n = 10$, as determined from the capacitance ratio measurement and

$$\left(\sum_1^n D_{Cm} - \frac{n}{10}\sum_1^{10} D_{Cm}\right)$$

is the correction to the nominal ratio of the capacitance divider determined previously.

D_{CEo}' is the dial setting for the reference zero balance of the calibration. This zero offset is caused by the impedance of the outer conductor of the coaxial cable connected from terminal E_0 of the test divider to the common ground point of the bridge as shown in Fig. 6. The term $(D_{Cn}' - D_{CEo}')$ represents the apparent or uncorrected α.

The presence of C_S from the output tap through the detector to the common ground point effectively shunts part of the test divider and changes the total impedance; in turn, depending on the dial setting D, it also changes the burden on the bridge transformer. The magnitude of this effect can be determined by connecting another capacitor $C_S^*(C_S^* \approx C_S)$ between terminal E and the detector junction point and by connecting C_S between the divider output terminal and the common ground point. The bridge is then balanced, with bridge dial-setting D_{Cn}^* for each setting D of the divider dials. When $D = 0$, there is no additional burden effect and this is selected as a subsidiary reference point D_{Co}^*.

In considering the measurement of the effect of the burdens due to the components generally associated with the bridge, the fact that the test divider has an equivalent output impedance (represented by $R_D + j\omega L_D$ in (Fig. 7) which varies with the dial setting D, must not be overlooked. The connections and measurements so far described represent the in-phase and quadrature corrections of the divider when burdened by $(C_S + C_{GS})$. The effect of this burden is given by

$$\text{Ratio (zero burden)} = \frac{e - E_0}{E - E_0} = \frac{n}{10}(1 + \alpha + j\beta)$$

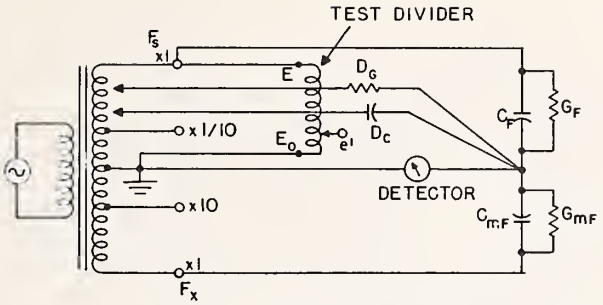

Fig. 5. Comparison of capacitors.

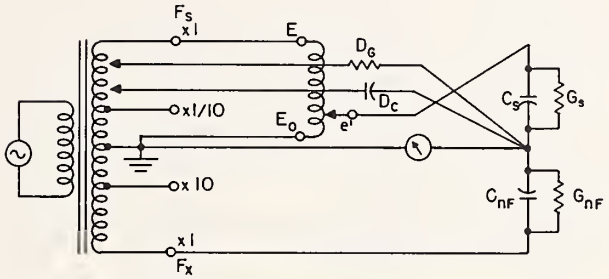

Fig. 6. Calibration of inductive voltage dividers.

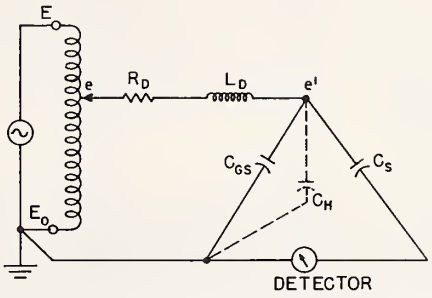

Fig. 7. Inductive voltage divider with external burden.

and

$$\text{Ratio (with burden)} = \frac{e' - E_0}{E - E_0} = \frac{n}{10}(1 + \alpha' + j\beta') = \frac{e - E_0}{E - E_0}[1 + (j\omega R_{Dn} - \omega^2 L_{Dn})(C_S + C_{GS})].$$

When an additional burden C_H is added to C_{GS}, the ratio becomes

$$\frac{e'' - E_0}{E - E_0} \equiv \frac{n}{10}(1 + \alpha'' + j\beta'').$$

These ratio expressions may be combined to give

$$\alpha = \alpha' + \frac{C_S + C_{GS}}{C_H}(\alpha' - \alpha'').$$

It is necessary to make the basic measurements D_{Cn}' and the subsidiary measurements D_{Cn}^* in order to deter-

mine the effective ratio of the bridge transformer at E, and the additional measurements D_{Cn}'' and D_{Cn}^{**} for each setting D, with C_H connected to take account of the residual output impedance of the test divider.

The coaxial cable between terminals F_S of the transformer and E of the divider will increase the effective leakage impedance of the transformer at E, which is chosen as one of the reference points of the calibration. The term $(\alpha_{S1}-\alpha_{S1}')$ represents the change of the bridge transformer ratio from $F_S=1(1+\alpha_{S1}+j\beta_{S1})$, effective at the transformer tap, to $F_S'=1(1+\alpha_{S1}'+j\beta_{S1}')$, effective at terminal E of the divider.

By combining the basic equation of balance with the subsidiary equations and the initial capacitance ratio calibrations, a pair of equations ($D\alpha$ and $D\beta$) are obtained relating the zero burden corrections to a series of observed bridge balances. All terms in these two equations are measurable quantities except for $(\alpha_{S1}-\alpha_{S1}')$ and $(\beta_{S1}-\beta_{S1}')$. Values are assumed for these terms in the final tabulation which make $\alpha_E=\beta_E=0$, as assumed for the test divider initially.

Similar equations can be developed for the calibration of the other dials of the divider.

NBS-B Test Method

At the National Bureau of Standards, Boulder, Colorado, the test inductive voltage divider was calibrated by direct comparison with a "standard" divider [10]. The voltage ratios and phase angle errors of the "standard" divider were determined, periodically, by the best method available.

Early Method

A transformer capacitance bridge method was used from 1959 until late 1963 for 1000 Hz measurements of the voltage ratios and phase-angle errors of the "standard" divider. This method was completely described by Zapf and played no part in this international intercomparison [11]. Therefore, there is no need to review it here. However, it did serve as the basis for all previous calibrations of the test divider, thereby providing an independent means of checking on the results reported in this paper. The overall uncertainty in voltage ratio calibration by this method was believed to be less than 2×10^{-7}.

Present Method

This method, under development since 1961, required the analysis of complex equivalent circuits and experimental verification of several basic assumptions before it was considered operational late in 1963. It provided the voltage ratio and phase-angle error data that were used in the NBS-B contribution to the international comparison. The method has been described, and it is necessary only to mention it briefly [14].

Internal loading is the cause of major systematic errors in inductive voltage dividers. The effects of internal loading can be controlled or predicted by a judicious choice of winding design [12]. Experimentation with several winding designs, and one in particular, demonstrated that a graph of errors (at the various taps of a divider) vs. the nominal voltage ratios fell on an S-shaped curve. As expected, it was found that a particular winding design used repeatedly, but with variations in wire size, number of turns, and core characteristics, yielded errors that fell on S curves of the same shape, but different amplitude. The task of predicting the shape of the S curve, with probable accuracy surpassing that which could be experimentally measured, was accomplished by solving the network equations for a carefully derived, complex, equivalent circuit representing the chosen design [13].

To measure the amplitudes of the S curves of various dividers, a method of complementary measurements was developed to accurately measure the true voltage ratios and phase angles at the nominal voltage ratio 0.25. (The complement of a voltage ratio is obtained by simply reversing the connections to the input of a divider.)

To summarize, the method is based on a particular design of inductive voltage divider for which the internal loading errors are calculable and measurable. Correction for these major systematic errors in particular dividers leaves residual errors of much smaller magnitude. There is both the expectation and experimental evidence that these residual errors are the result, primarily, of imperfections of random nature in the construction of each divider, and secondarily, of comparatively very small imperfections in the theoretical model on which the calculations are based. Therefore, by submitting the results from a large number of dividers to statistical processing, it is possible to improve upon the determination of the errors. The use of a group of dividers and statistical averaging reduces the effect of individual "particular errors" on the establishment of voltage ratios and phase angles.

The method outlined above was used at frequencies of 1000 and 400 Hz to calibrate a "standard" inductive voltage divider. At 1000 Hz ten 20-section dividers were used for establishing the corrections. At 400 Hz twelve 20-section dividers were used. The work at 1000 Hz produced results in agreement (a few parts in 10^8 of input) with results previously obtained by the capacitance bridge method, which is smaller than the differences between results from the NBS-B and either of the two other laboratories.

The mean of a group of ten or more was used for establishing the NBS-B values, and these were used in two ways, with input connections normal and reversed, thereby improving the results by a factor of four or more over individual dividers measured one way. A survey of the data taken at each ratio reveals that the standard deviation from the mean for the residual random errors at the taps of individual dividers in the group did not exceed, at any ratio, a voltage ratio of 3.4×10^{-8} for the 1000 Hz measurements, and 3.1×10^{-8} at 400 Hz.

TABLE I

1000 Hz

Dial Setting	NBS-W		NBS-B		NRC	
	$D\alpha(10^{-6})$	$D\beta(10^{-6})$	$D\alpha(10^{-6})$	$D\beta(10^{-6})$	$D\alpha(10^{-6})$	$D\beta\ 10^{-6})$
0.X00 000 0	+0.02	0.0	+0.01	−0.10	−0.04	−0.06
0.900 000 0	+0.14	−1.8	+0.06	−0.54	+0.07	−0.93
0.800 000 0	+0.19	−1.6	+0.10	−0.16	+0.11	−0.97
0.700 000 0	+0.08	−2.4	+0.05	+1.26	+0.08	+0.37
0.600 000 0	+0.03	+1.2	−0.01	+3.42	+0.03	+2.48
0.500 000 0	+0.00	+4.0	−0.06	+6.0	+0.02	+4.90
0.400 000 0	−0.10	+6.8	−0.13	+8.0	−0.03	+7.00
0.300 000 0	−0.26	+8.1	−0.32	+9.0	−0.19	+8.14
0.200 000 0	−0.18	+8.0	−0.20	+8.4	−0.10	+7.85
0.100 000 0	−0.13	+5.4	−0.18	+5.4	−0.11	+5.25
0.0X0 000 0	−0.15	+4.5	−0.20	+4.7	−0.12	+4.59
0.090 000 0	−0.20	+3.6	−0.17	+4.0	−0.12	+3.94
0.080 000 0	−0.18	+3.0	−0.15	+3.4	−0.11	+3.34
0.070 000 0	−0.18	+2.7	−0.14	+3.1	−0.12	+3.08
0.060 000 0	−0.14	+2.5	−0.11	+2.8	−0.10	+2.67
0.050 000 0	−0.12	+2.2	−0.11	+2.5	−0.09	+2.32
0.040 000 0	−0.11	+2.0	−0.09	+2.2	−0.08	+2.09
0.030 000 0	−0.08	+1.8	−0.08	+1.9	−0.07	+1.81
0.020 000 0	−0.06	+1.4	−0.07	+1.4	−0.05	+1.40
0.010 000 0	−0.02	+0.84	−0.04	+0.84	−0.03	+0.81
0.00X 000 0	−0.02	+0.78	−0.05	+0.76	−0.03	+0.74
0.009 000 0	−0.02	+0.72	−0.04	+0.67	−0.04	+0.63
0.008 000 0	−0.02	+0.53	−0.03	+0.59	−0.04	+0.55
0.007 000 0	−0.01	+0.43	−0.02	+0.55	−0.04	+0.50
0.006 000 0	−0.01	+0.37	−0.03	+0.51	−0.05	+0.45
0.005 000 0	−0.01	+0.37	−0.03	+0.47	−0.05	+0.42
0 004 000 0	−0.01	+0.35	−0.03	+0.44	−0.04	+0.38
0.003 000 0	−0.01	+0.33	−0.02	+0.37	−0.04	+0.33
0.002 000 0	−0.01	+0.27	−0.01	+0.30	−0.03	+0.26
0.001 000 0	−0.01	+0.16	−0.01	+0.20	−0.02	+0.15
			400 Hz			
0.X00 000 0	0.00	0.0	+0.03	0.00	+0.01	+0.02
0.900 000 0	+0.09	−0.9	+0.11	−0.54	+0.04	−0.59
0.800 000 0	+0.12	−1.6	+0.15	−0.48	+0.07	−0.63
0.700 000 0	0.00	−0.7	+0.12	+0.14	+0.05	+0.09
0.600 000 0	0.00	0.0	+0.11	+1.02	+0.09	+0.89
0.500 000 0	+0.08	+1.5	+0.12	+2.0	+0.14	+1.91
0.400 000 0	+0.04	+2.4	+0.08	+2.8	+0.16	+2.77
0.300 000 0	−0.07	+3.3	−0.06	+3.3	+0.06	+3.23
0.200 000 0	−0.05	+3.2	0.00	+3.2	+0.12	+3.16
0.100 000 0	−0.05	+2.1	−0.04	+2.2	+0.04	+2.10
0.0X0 000 0	−0.15	+2.0	−0.12	+2.1	0.00	+2.06
0.090 000 0	−0.08	+1.7	−0.11	+1.7	−0.01	+1.74
0.080 000 0	−0.08	+1.4	−0.07	+1.4	−0.02	+1.48
0.070 000 0	−0.07	+1.2	−0.08	+1.3	−0.02	+1.39
0.060 000 0	−0.06	+1.1	−0.06	+1.1	−0.01	+1.15
0.050 000 0	−0.05	+1.0	−0.05	+1.05	0.00	+1.03
0.040 000 0	−0.04	+0.88	−0.04	+0.96	+0.01	+0.92
0.030 000 0	−0.03	+0.75	−0.03	+0.84	+0.01	+0.79
0.020 000 0	−0.02	+0.60	−0.02	+0.64	+0.01	+0.60
0.010 000 0	−0.02	+0.34	0.00	+0.37	0.00	+0.35
0.00X000 0	−0.02	+0.34	−0.01	+0.37	0.00	+0.35
0.009 000 0	−0.04	+0.30	0.00	+0.32	0.00	+0.30
0.008 000 0	−0.02	+0.24	+0.01	+0.28	0.00	+0.25
0.007 000 0	0.00	+0.20	0.00	+0.25	0.00	+0.23
0.006 000 0	−0.02	+0.19	0.00	+0.23	0.00	+0.20
0.005 000 0	−0.02	+0.17	0.00	+0.21	0.00	+0.18
0.004 000 0	−0.02	+0.16	+0.01	+0.20	0.00	+0.15
0.003 000 0	−0.01	+0.14	+0.01	+0.17	0.00	+0.14
0.002 000 0	0.00	+0.11	0.00	+0.13	0.00	+0.10
0.001 000 0	0.00	+0.06	+0.01	+0.08	0.00	+0.06

Therefore, the standard error of the result was 0.8×10^{-8} or less at 1000 Hz, and 0.7×10^{-8} or less at 400 Hz.

In the establishment of voltage ratio, residual (i.e., uncorrected) systematic errors greater than $\pm2\times10^{-8}$ are believed to be very unlikely. These limits of systematic error are based on subjective considerations. Thus, the uncertainty in the establishment of voltage ratio is less than 5×10^{-8} computed by adding three times the standard deviation to the limits of systematic error.

The voltage ratios are preserved, or maintained, by means of a "standard" inductive voltage divider. The stability of this "standard" divider has been observed over a period of years. The divider used for the international comparison was calibrated by comparison with the "standard." It is believed that a proper allowance for systematic error in the maintenance of voltage ratio is $\pm2\times10^{-8}$, and for random variations a standard deviation of 2×10^{-8}. In the comparison with the "standard" divider an additional allowance of $\pm2\times10^{-8}$ for systematic error is warranted, and the standard deviation of the comparison method is about 0.7×10^{-8}.

The three sets of limits of independent systematic error mentioned above are ±2, ±2, and ±2 (all $\times10^{-8}$). A realistic combination of these limits might be taken as $\pm5\times10^{-8}$. The three standard deviations mentioned above are 0.8, 2, and 0.7 (all $\times10^{-8}$), and the square root of the sum of the squares is about 2.3×10^{-8}. These figures may be taken as a partially subjective estimate of the uncertainty in the calibration results at 1000 Hz on the top decade, describing errors that could be observed if the entire experiment were to be repeated by the same method, but with a different group of 20-section dividers constructed to the same specified design.

Adding the limits of systematic error and three times the standard deviation yields $\pm1.2\times10^{-7}$. These limits express concisely the uncertainty in voltage ratio associated with the results of the calibration at 1000 Hz at NBS-B and are strictly applicable only to the top decade. The uncertainties of results on the second and third decades are about the same as for the first decade; the expected improvement is offset by the necessity for additional comparison measurements.

Comparison of Calibration Results

Table I lists the voltage ratio corrections ($D\alpha$) and phase-angle errors ($D\beta$) observed for the test divider in the three national laboratories for 400 and 1000 Hz. All values were obtained with the case connected to the low voltage terminal of the input and with an input of 100 volts RMS (except 400 Hz data for NRC, which was performed at 40 volts input).

Values reported by NBS-W represent the average of three sets of measurements, which were taken before, between, and after the measurements taken by the other two laboratories. The maximum spread was 0.14×10^{-6} for the ratio correction at 0.5 setting and 1000 Hz. Spread on any other setting was much smaller than 1×10^{-7} and appeared at random. Therefore, it can be said that no apparent shift in either ratio or phase angle was noted after the divider was exposed to the hazards of travel and use.

The voltage ratio corrections for the lower four decades (10^{-4} to 10^{-7}) were less than 1×10^{-8}. Therefore, they are not included in this intercomparison of calibration report. The phase-angle errors associated with these lower decades are of secondary importance and perhaps of lesser general interest; thus, they are also omitted.

Conclusion

This is the first international comparison of inductive voltage divider calibration in which United States and Canadian national laboratories have participated. It is interesting to note the close agreement in the results obtained by three independent laboratories using completely different methods. The close agreement indicates that the voltage ratio and phase-angle measurements in each of the three laboratories are accurate to within ±0.1 ppm of input and $1/(\text{setting of dials})^{1/2}$ microradians at 400 and 1000 Hz.

Acknowledgment

Mr. Sze wishes to acknowledge the valuable guidance and help of Dr. F. K. Harris, Chief of the Absolute Electrical Measurements Section, Electricity Division, NBS, Washington, D. C.

References

[1] W. C. Sze, "Measurement of voltage ratios at audio frequencies, *Trans. AIEE (Communication and Electronics)*, vol. 76, pp. 444–449.

[2] Catalog Sheet C-25 (Voltage Divider), Electro Scientific Industries, Inc., Portland, Ore.

[3] M. C. McGregor, et al., "New apparatus at the National Bureau of Standards for absolute capacitance measurement," *IRE Trans. on Instrumentation*, vol. I-7, pp. 253–261, December 1958.

[4] R. D. Cutkosky, "Evaluation of the NBS unit of resistance based on a computable capacitor," *J. Res. NBS*, vol. 65A, pp. 147–158, May–June 1961.

[5] A. M. Thompson, "AC bridge methods for the measurement of three-terminal admittances," *IEEE Trans. on Instrumentation and Measurement*, vol. IM-13, pp. 189–196, December 1964.

[6] R. D. Cutkosky and J. Q. Shields, "The precision measurement of transformer ratios," *IRE Trans. on Instrumentation*, vol. I-9, pp. 243–250, September 1960.

[7] A. F. Dunn, "Determination of an absolute scale of capacitance," *Can. J. Phys.*, vol. 42, pp. 53–69, January 1964.

[8] W. K. Clothier, National Standards Lab., Chippendale, Australia, and F. K. Harris, National Bureau of Standards, Washington, D. C., private communications.

[9] W. K. Clothier, NSL, Chippendale, Australia, and R. D. Cutkosky, NBS, Washington, D. C., private communications.

[10] R. V. Lisle and T. L. Zapf, "Comparison calibration of inductive voltage dividers," *ISA Trans.*, vol. 3, no. 3, pp. 238–242, 1964.

[11] T. L. Zapf, "Voltage ratio measurements with a transformer capacitance bridge," *J. Res. NBS*, vol. 66C, pp. 25–32, January–March 1962.

[12] ——, "The calibration of inductive voltage dividers and analysis of their operational characteristics, *ISA Trans.*, vol. 2, no. 3, pp. 195–201, 1963.

[13] T. L. Zapf, C. H. Chinburg, and H. K. Wolf, "Inductive voltage dividers with calculable relative corrections," *IEEE Trans. on Instrumentation and Measurement*, vol. IM-12, pp. 80–85, September 1963.

[14] T. L. Zapf, "The accurate measurement of voltage ratios of inductive voltage dividers," *1964 Acta IMEKO*, Stockholm, Sweden, pp. 317–331.

U.S. Department of Commerce—Bureau of Standards
RESEARCH PAPER RP580
Part of Bureau of Standards Journal of Research, Vol. 11, July 1933

EQUIPMENT FOR TESTING CURRENT TRANSFORMERS

By Francis B. Silsbee, Ray L. Smith, Nyna L. Forman, and John H. Park

ABSTRACT

The equipment and test procedure developed at the Bureau of Standards for measuring the ratio and phase angle of current transformers up to currents of 12,000 amperes at power frequencies are described in detail. Data are given to show the accuracy of the standard current transformer used in the higher ranges, and the effectiveness of the shaping of the heavy-current circuit so as to minimize errors from stray magnetic fields.

IEEE Transactions on Instrumentation and Measurement
Volume IM-14, Number 4, December 1965

The Design and Performance of Multirange Current Transformer Standards for Audio Frequencies

BERNADINE L. DUNFEE, SENIOR MEMBER, IEEE

Abstract—The design, construction, and performance of two nearly identical, multirange current transformers for operation 400 Hz to 10 kHz and with errors of only a few ppm are discussed. A general discussion of the parameters that influence the performance of single-stage transformers and their consideration in effecting minimum errors throughout a wide frequency band is included. Construction of the two standards having consecutive ratios 1 to 1 to 6 to 1 and operating at a rated secondary current of 5 amperes is described. Circuit diagrams are used to describe 1) the self-calibration circuit for measuring the errors of the 1-to-1 ratios and 2) the $(N+1)$ circuit together with an auxiliary circuit for measuring the errors of ratios >1. Balance equations are derived in the Appendix. Measured values are presented; included are the results up to 16 kHz obtained at the National Research Council, Canada, during an international comparison and described in a companion paper [6]. The effects of polarization at low frequencies are emphasized by utilizing the 400 Hz data together with information obtained in supplementary experiments; also the role of winding and interwinding capacitances and the necessity for a more explicit definition of current ratio at the higher frequencies is highlighted.

IEEE Transactions on Instrumentation and Measurement
Volume IM-12, Number 2, September 1963

Inductive Voltage Dividers with Calculable Relative Corrections

THOMAS L. ZAPF , SENIOR MEMBER, IEEE, CARL H. CHINBURG , SENIOR MEMBER, IEEE, AND HARRY K. WOLF , SENIOR MEMBER, IEEE

Summary—Inductive voltage dividers are now used in measurement laboratories for the production of audio-frequency voltage ratios with errors (deviations from turns ratio) of a few parts in ten million of input. A major component of error arises from the interaction between distributed shunt impedances and leakage impedances in the windings. Correction for this systematic error in dividers of special design can result in an order-of-magnitude improvement in accuracy.

A solution using network equations has been obtained for the corrections to the relative errors of inductive voltage dividers of specific design. Earlier theoretical considerations, confirmed by measurements of limited accuracy, indicated an S-shaped curve of ratio error vs nominal ratio, and quadrature component vs nominal ratio. The results from recent calculations are in agreement with the earlier measurements and provide much better definition of the true shape of the S-curve. An algebraic equation has been derived for the limiting form of this S-shaped characteristic curve. A resistance analog of an inductive voltage divider was constructed to represent the lumped circuit parameters equivalent to the distributed shunt admittances and the winding impedances. Measurements of the gross errors in the analog have yielded experimental results in excellent agreement with those calculated from the network equations.

ISA Transactions
Volume 2, Number 3, July 1963

The Calibration of Inductive Voltage Dividers and Analysis of Their Operational Characteristics

THOMAS L. ZAPF
Radio Standards Laboratory
National Bureau of Standards
Boulder, Colorado

▶ A review of recent work in alternating-voltage ratio measurements at the National Bureau of Standards is followed by a discussion of equipment and methods of measurement now under investigation. Improvements in the accuracy of measurement of alternating-voltage ratio by capacitance bridge methods have reduced the overall limit of uncertainty in the calibration of voltage ratio of inductive voltage dividers to less than $\pm 2 \times 10^{-7}$. Calibrated inductive voltage dividers have been used as standards for the calibration of other dividers by a comparison method with relatively little degradation of accuracy. Recent investigations on the design and construction of inductive voltage dividers have demonstrated the feasibility of compensation of ratio errors arising from internal loading, and several inductive voltage dividers have been designed and constructed that have ratio errors less than $\pm 5 \times 10^{-8}$ at a frequency of 1000 cycles per second.

High Voltage and Surge Measurements

Papers

Abstracts

JOURNAL OF RESEARCH of the National Bureau of Standards—C. Engineering and Instrumentation
Vol. 66C, No. 1, January–March 1962

Special Shielded Resistor for High-Voltage D-C Measurements

J. H. Park

(September 26, 1961)

A new design for an accurate high-voltage d-c standard resistor has been devised. It is made up of a large number of individually shielded, one-megohm wire-wound resistors connected in series and arranged to form a vertical helix between a ground plate and a high-voltage electrode. The individual shields completely enclose each one-megohm resistor and prevent formation of corona at the surface of the resistance coil no matter how high the potential of the shield is above ground. The vertical helical configuration with a large "hat," or high-voltage electrode, on top serves to prevent concentration of electric field and corona formation at the high-potential end of the resistor. A 200-megohm unit, constructed during 1955 and tried out up to 100 kv in 1956, indicated the design to be free of corona errors but, for the particular one-megohm resistors used, the variation with temperature was quite large (0.01 percent per °C). A 100 megohm unit using low-temperature coefficient resistors has been recently constructed and tested up to 100 kv.

An experimental method of checking for corona or leakage errors at high values of voltage was developed. It consisted of accurately comparing the current "in" at the high voltage end of the resistor with the current "out" at the ground end for several different values of applied voltage. These measurements together with others performed to check temperature and leakage errors indicated that the value of resistance for the 100-megohm unit remains constant to within about 10 ppm for voltages up to 50 kv under ordinary laboratory conditions. At 100 kv the maximum error (caused by heating) was estimated to be about 40 ppm.

1. Introduction

Accurate measurements of d-c voltages at values above 10 v are nearly always dependent upon a resistive voltage divider which consists of a high resistance, R_1, in series with a low resistance, R_2. The voltage to be measured is connected across the series combination with R_2 at the ground end. The divider ratio, $(R_1+R_2)/R_2$, is chosen to give about a 1 v drop across R_2, which can then be measured with a null potentiometer. This is the well known "volt-box" method and tapped resistors or "volt boxes" are readily available for voltages up to at least 1,500 v. In extending this method to higher voltages the only additional difficulty is in designing a high-voltage resistor with an effective value which does not change with voltage.

A change in effective resistance with voltage may be due to any one or a combination of three factors: (1) heating of the resistance wire due to the I^2R loss—the magnitude of this change will depend upon the temperature coefficient of the entire resistor; (2) current leakage through the volume or over the surface of the insulation used to support the resistor—such leakage usually increases with voltage and in effect decreases the total resistance; (3) corona discharges which may appear at locations of high gradient along the resistor as the voltage is increased—in effect they "leak" part of the resistor current to ground. The heating effect, factor (1) can be quite bothersome unless the overall temperature coefficient is very low. However, a high-voltage resistor is most conveniently made up by connecting a large number of one-megohm units in series. Thus, temperature coefficient can be reduced to a negligible minimum by choosing some resistors with positive and others with negative temperature coefficients. This can readily be done if a large number of one-megohm units made up of either Karma [1] or Evanohm [1] wire are available and their temperature coefficients have been measured. Factors (2) and (3), above, cannot be measured and reduced to a low magnitude in any such simple manner. Thus, the primary design problem is to keep leakage and corona effects as low as possible. Also, some experimental method must be devised to check for these effects with full voltage applied to the complete resistor.

[1] Trade names for special alloys (NiCr+Al+Fe) having high resistivity and low temperature coefficient of resistance.

2. Helical Resistor Made in 1955

A special helical design to keep corona effects to a minimum when a large number of 1-megohm resistors are connected in series was first devised in January 1955. It was made up of 200 one-megohm wire-wound resistor units which had been obtained on surplus after World War II. Each unit consisted of wire wound on a cylindrical spool ¾ in. in diameter and 1¼ in. long and connected to screw terminals at each end of the cylinder. Overlapping brass caps with ribbon insulation between them were attached to the screw terminals as indicated in figure 1. These two brass caps form a complete potential shield around the unit and definitely fix the voltage gradient environment immediately surrounding the resistance wire. Such voltage gradients are determined only by the potential difference between the two caps which is equal to the *IR* drop across the resistor. Thus the possibility of corona appearing in the air immediately surrounding the resistance wire is eliminated no matter how high the potential of the resistor and its shields may be with respect to ground.

A jig was made to support the individually shielded units along a circular helical path. They were then soldered together in this position and mounted on a lucite tube 4 in. in diameter and 39 in. high as shown in figure 2. The circular helical shape keeps a uniform potential drop per turn along the lucite tube. The 24 inch diameter copper "hat" placed on top of the lucite tube serves to intercept electrostatic lines of force from objects at ground potential and prevents concentration of such lines of force at the top turns of the resistor helix. Thus the gradient at the outside surface of the individual resistor caps is very nearly the same for units near the top as those near the bottom, and the possibility of corona from these shield caps is greatly reduced or eliminated.

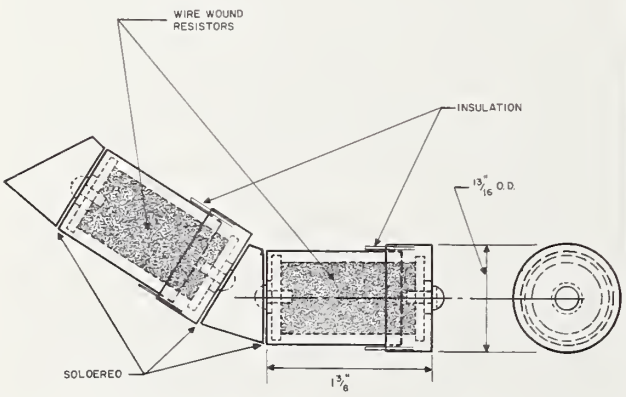

FIGURE 1. *Two one-megohm wire-wound resistors, mounted inside their shield caps, as used in first model of helical resistor.*

Indicates method of connecting resistors in series to form helix.

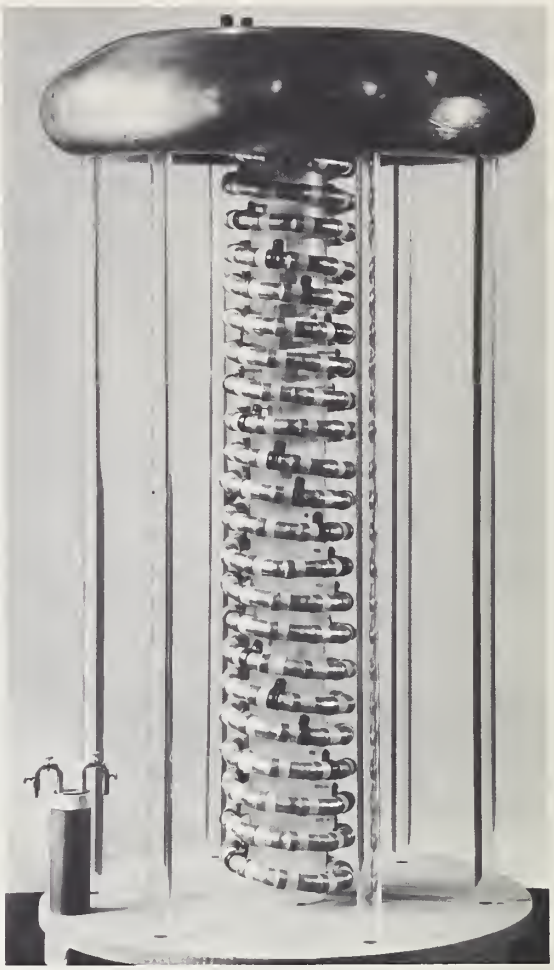

FIGURE 2. *The first model of helical resistor.*

Made during 1955.

If there were any corona discharge or even "dark current" from the resistor at some point between the high-voltage electrode and the low-voltage lead, it would cause the current "out" at the low-voltage lead to be less than the current "in" at the high-voltage electrode. This would introduce a change in the value of effective resistance which is used in voltage measurements. Current leakage through or over the surface of any insulating supports would cause a similar type of error. An experimental check for such errors can be obtained by getting a simultaneous measurement on the current "in" and "out" at various voltages up to the highest which can be used. This was done by adjusting the applied voltage to give a certain fixed value of current "in" under steady conditions and measuring the current "out".

The current "in" was set to a fixed known value by

passing it through a standard resistor and balancing the IR drop to that of a standard cell by use of a reflecting mirror galvanometer. The standard resistor, standard cell, and galvanometer were placed on top of the high-voltage electrode and covered with a 3-gal cylindrical can to prevent corona discharges from them. The resistance of the standard resistor used in this circuit was chosen to give the value of current desired. The current "out" was measured in the usual manner by passing it through a standard resistor and measuring the IR drop with a null potentiometer. The procedure then was to choose a value of standard resistor to give the required current "in" and adjust this current to give a balance on the reflecting galvanometer mounted inside the 3-gal can. When a balance was attained the current "out" was read on the potentiometer at the ground end. Any discrepancy between these two currents indicated either a leakage or corona effect.

Some special precautions taken during these measurements should be noted. The switch closing the galvanometer circuit inside the 3-gal can must not be closed until the current has been approximately adjusted to the correct value. This requires a remotely operated switch because the 3-gal can is at high voltage. A waxed cord was tried first for operating this switch but found to be unsatisfactory because it jarred the galvanometer off scale. A relay operated by a photoelectric cell circuit which could be closed by a beam of light was installed inside the 3-gal can and found to operate satisfactorily. It was also found desirable to place extra filter capacitors across the high-voltage supply, giving high RC time constants on both charge and discharge, thus serving to keep the current steady.

Current measurements were made using 5,000- and 2,000-ohm standard resistors in the 3-gal can giving voltage values of approximately 40 and 100 kv across the 200-megohm resistor. At 40 kv the current "in" and current "out" agreed to within about 20 ppm which was considered the limit of accuracy for this particular test. At 100 kv the agreement could be certain only to within about 70 ppm because of unsteadiness in the supply voltage. No further attempt to minimize these measurement errors was made at that time because the expected accuracy of the first model was about ± 0.01 percent.

Actually the largest error in this model was found to be due to the temperature coefficient of resistance of the 1-megohm resistors. Apparently Nichrome V wire had been used in winding these resistors. The measured change of resistance with room temperature as determined with low voltage applied was $+0.01$ percent per degree C increase in ambient temperature. The increase of resistance with applied voltage followed the square law as expected, and this total change from low to rated voltage of 100 kv was 0.09 percent. Correction curves were derived for changes in applied voltage and room temperature. It was concluded that, with care in applying these corrections, accuracies within 0.02 percent could be expected for applied voltage up to 50 kv.

3. Improved Helical Resistor Built in 1961

The first model has been used as a standard for calibrating other high-voltage resistors at the National Bureau of Standards for several years. In most cases the accuracy attainable was sufficient, but in several instances accuracy needs reached 0.01 percent or better. In view of the ever higher accuracy needs as time goes on, especially in experiments involving the accurate measurement of atomic and nuclear constants, it was decided to build another resistor of the same design using 1-megohm units with lower temperature coefficients.

In 1960 it was found that due to improvements in resistor winding techniques and to the development of special alloy wire of low temperature coefficient, it was possible to obtain 1-megohm units guaranteed to have a temperature coefficient less than 5 ppm per degree C. A large number were ordered, and on delivery their temperature coefficients were determined by measurements at three or more temperatures between 20 and 44 °C. They were all well within the 5 ppm per degree C limit—also some resistors increased and others decreased with rising temperature and in general the change was proportional to temperature. Thus it was possible to choose matched pairs of these resistors with nearly zero average temperature coefficient. By connecting such matched pairs in series, a high-voltage resistor with nearly zero change with temperature was made.

To keep corona and leakage errors as low as possible the same spiral type of construction as that in the first model was used. A new technique for making the shields and connecting them in a helix was devised. Each shielded unit contained two resistors and was assembled from brass parts, machined out of tubing, and a 45° brass elbow, as shown in figure 3. Polyethylene sheet insulation was used between the overlapping shields around each resistor as before. Eight of these units, fitted together, constitute a single turn of the helix with an outside diameter of 9½ in. They were fastened to a 7-in.-diam lucite tube (⅛ in. wall thickness) using one nylon clamp and screw for each unit. The pitch of the helix was chosen to prevent any possibility of corona between adjacent turns.

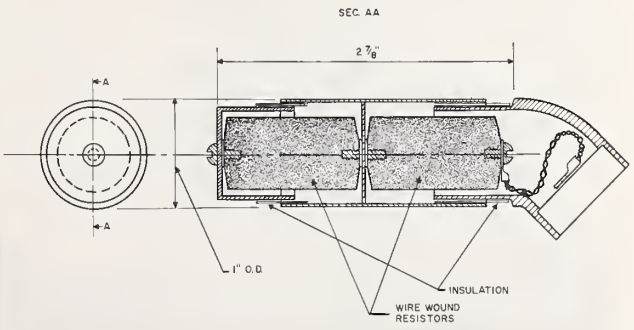

FIGURE 3. *A two-resistor shielded unit as used in the second model of helical resistor.*

First an estimate of required pitch was made based on a maximum rated voltage for each 1-megohm resistor of 1,000 v. This gave 16 kilovolts per turn. A pitch of 2⅜ in. per turn was taken, giving 1⅜ in. between adjacent brass shields from one turn to the next. A 1½-turn resistor (maximum rating 24 kv) was made up using this pitch and its resistance was measured at various voltages up to 27 kv. This was done using a wheatstone bridge with the 1955 model 200-megohm helical resistor as the other high-voltage arm. Only gradual uniform changes in resistance were noted as voltage was increased in steps from 5 to 27 kv, and they could be accounted for by heating effects. There was no evidence of corona effects even at 27 kv, which is 125 percent of the maximum to be used.

On the basis of these preliminary tests a 100-megohm resistor of 6¼ turns was made up with the same pitch. The lucite tube is 16½ in. long and mounted vertically between a brass ground plate and a high-voltage electrode as shown by the photograph in figure 4. The electrode on top of the lucite tube was designed so that another similar resistor could be placed on top of it. By stacking resistors and connecting them in series, voltage ranges in multiples of 100 kv could be obtained. At present only one 100-megohm resistor has been constructed because so far there has been no urgent requirement for very accurate measurements at voltages above 50 kv. However, corona tests on the high-voltage electrode were made up to 200 kv by using two 100 kv power supplies. The normally grounded brass plate was supported on ceramic insulators and connected to the minus 100 kv. The high-voltage electrode was connected to the plus 100 kv. For this test the 100 1-megohm resistors were removed but the same lucite tube was used to separate the electrode from the brass plate. Only a visual test could be made; thus the setup was put inside a completely enclosed dark box large enough to house an observer also. With a total voltage of 200 kv between brass plate and electrode there was no visible or audible evidence of corona. Since this was twice the maximum voltage ever to be used with the resistors in place, it was concluded that there would be no corona current off the middle shield electrode when two units are stacked in series. If more than two units are to be stacked, further corona tests should be made and possibly larger shield electrodes than the one shown in figure 4, which is 22 in. in diameter, would be required.

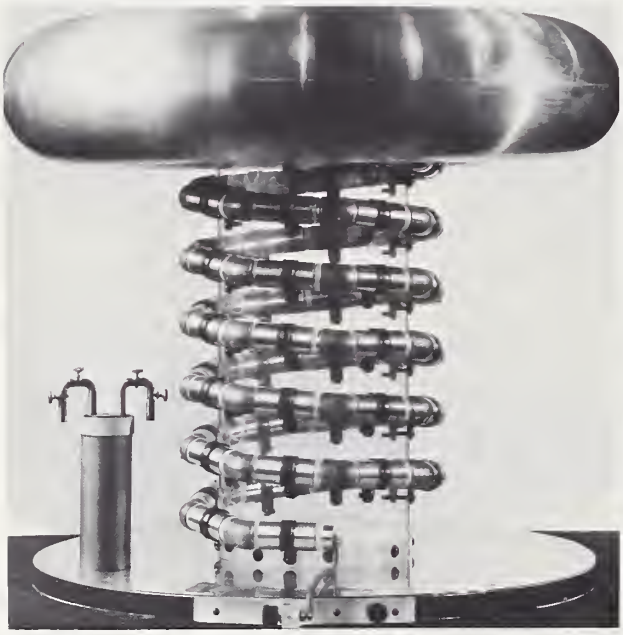

FIGURE 4. *100-megohm, 100 kv, helical resistor constructed in 1961.*

4. Accuracy Limits on 1961 Model

Throughout the design and construction of the 1961 model helical resistor, primary consideration was given to eliminating any possible corona or leakage errors. Corona tests were made using voltages much above the expected maximum rating. These precautions by themselves do not eliminate the possibility of corona and leakage errors. The crucial test for detecting such errors is to measure current "in" and current "out" by the method already described and used for the 1955 model.

The accuracy attained was considerably improved over that in the previous tests. In part the higher accuracy was obtained by using somewhat more sensitive galvanometers and reducing the effects of thermal emf's. However, the main improvement was obtained by stabalizing the d-c voltage supply, getting finer control, and using greater patience. Also, by a modified experimental procedure, any constant measurement errors such as might be introduced by the potentiometer, resistance standards, or standard cells were cancelled. This was done by taking current "in" and "out" measurements at low voltage with the 100-megohm resistor shorted, before and after each high-voltage check. Then if the potentiometer reading at balance is the same at high voltage as at low voltage with the resistor shorted, no leakage or corona effects are introduced by the high voltage.

Measurements were made with three different values of current (approximately 0.204, 0.509, and 1.019 ma) giving total voltages across the resistor of about 20.4, 50.9, and 101.9 kv. The odd values resulted from the use of 5,000-, 2,000-, and 1,000-ohm NBS-type resistance standards in conjunction with an unsaturated standard cell for setting current "in." A 5-dial null-type Wolff potentiometer was used to measure the voltage across a similar standard resistor connected between the resistor low-voltage lead and ground, yielding the current "out." The precision obtainable with stable current and fine control was considered to be within 10 ppm. The check of current "in" and "out" with the 100-megohm resistor shorted gave values agreeing within 10 ppm. With the 100-megohm resistor unshorted, requiring high voltage to balance current "in" and "out", settings on the Wolff potentiometer were the same within 10 ppm as with the 100-megohm resistor shorted.

The accuracy of setting the Wolff potentiometer with 20 and 50 kv across the resistor was within 10 ppm, i.e., the same as when the 100-megohm resistor was shorted. With 100 kv across the resistor this accuracy was estimated as within 20 ppm—the small increase being due to greater difficulty in holding current nearly constant at the required value.

Current "in" and "out" data were obtained on several different days over a period of 2 months. Room temperature varied only from 24 to 25 °C and relative humidity from 37 to 50 percent. Most of these data were taken with the brass ground plate connected to ground and tied to the resistor low-voltage terminal through the standard resistor used in measuring current "out" (because that is the way the resistor will normally be used). As a further check on possible leakage current errors when two or more complete units are connected in series, data were also taken with the brass ground plate connected to the resistor low-voltage lead and insulated from ground. On all of these tests the current "out" was found to be equal to the current "in" to within the accuracy of measurement. This shows that corona and leakage errors for this helical resistor are less than 10 ppm for voltages up to 50 kv and are not greater than 20 ppm for 100 kv.

The only other source of error is that due to the overall temperature coefficient of resistance of the 1-megohm wire-wound resistors. The temperature coefficient from 20 to 40 °C as measured for each 1-megohm resistor used in this resistor was less than 2 ppm per degree C. Also resistors with approximately equal positive and negative temperature coefficients were mounted as pairs. The overall temperature coefficient is estimated to be less than 0.4 ppm per degree C. Thus no correction for room temperature under normal laboratory conditions need be applied. Heating of the 1-megohm units due to current at the higher voltage values, however, might cause a slight error because the resistors are totally enclosed and attain higher temperature than they would in a free air space. An estimate of the magnitude of such heating errors was obtained as described in the following two paragraphs.

During the corona tests evidence of heating errors were detected (as already mentioned) when the resistance of the 1½-turn, 24-unit, test sample was measured at various voltages. These 24 units were all purposely chosen to have large temperature coefficients of the same sign so that temperature rise could be estimated from change in resistance. The average coefficient for the 24 units was −3 ppm per degree C. The total change in resistance, from a measurement at 9 kv taken immediately after putting voltage on, to a measurement at 12 kv after voltage had been on for about 70 min, was 70 ppm. This indicates a temperature rise of about 23 °C with 0.5 kv applied across each 1-megohm coil. Thus for the complete 100-megohm resistor it would take 50 kv to produce a 23 °C temperature rise; but since the complete resistor is made up of temperature compensated pairs, the 50 kv would cause a resistance change of less than 10 ppm.

Voltages above 12 kv were also applied to the 24-unit special test resistor in order to estimate possible heating errors at higher voltages. After 24 kv had been applied for 2 hrs the shields around the resistor units became noticeable hot to the touch and the total change in resistance was 270 ppm. Based on the −3 ppm temperature coefficient this would mean a 90 °C temperature rise for the resistance wire. Since the final 100-megohm resistor has an estimated temperature coefficient of 0.4 ppm, as compared to 3 ppm for the 24-unit special test resistor, its maximum change with 100 kv applied would be only 36 ppm. However, this voltage does cause considerable heating and should not be held continuously. It was arbitrarily decided that after applying voltages above 70 kv for 30 min a cooling period of 30 min should be allowed with no voltage applied.

5. Calibration of 100-Megohm Resistor

As explained in the preceding section, it has been experimentally demonstrated that corona and leakage errors for this 100-megohm resistor remain within certain limits up to 100 kv. Within these limits then it is permissible to calibrate or measure its resistance at low values of voltage and then use this measured resistance at much higher voltages to compute resistor IR drop.

One method of calibration was to measure each 1-megohm unit individually by placing it in the "unknown" arm of a Wheatstone bridge. All other arms of the bridge were made up of sealed NBS-type standard resistors except for a decade resistor box used for fine control by supplying from 0.00 to 10.00 ohms in 0.01-ohm steps. Values of all resistances used in the bridge, except the 1-megohm unit being tested, were carefully determined by the Resistance and Reactance Section of the National Bureau of Standards. Temperature corrections were applied when necessary. These measurements were made before the complete resistor was assembled. The total resistance was taken to be the sum of the measured values for the 100 units comprising the complete resistor.

A question now arises as to a possible change in effective resistance of an individual unit due to its being mounted inside its shield caps and their being mounted in turn on the lucite tube using nylon clamps and screws. Such a change could be caused by leakage current either via the lucite tube and nylon clamps or via the polyethelene between shield caps. Normally any leakage current via the lucite tube would have been detected during the current "in" and "out" tests but leakage via the polyethelene would not. To check for a possible error due to such leakage, the resistances of several matched pairs of the 1-megohm units were measured after they had been mounted inside their shields and on the lucite tube. In every case the resistance thus measured agreed to within 10 ppm with the sum of the resistance of the individual units as measured before assembly.

Another method of calibration was used with the complete resistor assembled. This was to make connections at every fifth brass elbow (every 10th resistor unit) so that the 100-megohm standard could be divided into 10 sections of 10-megohm units. These 10 sections were then connected in parallel and measured as a 1-megohm resistor. The resistances of all 10 sections in series could then be readily computed from the parallel resistance value, provided the resistance of each section is equal to 10 megohms (within 0.1 percent). Values were obtained in this manner on several different days and at room temperatures from 23 to 26 °C. All such values agreed with that obtained by summing individual resistor measurements to within 15 ppm.

6. Summary

A special design of high-voltage d-c resistor made up of a large number of individually shielded 1-megohm wire-wound resistors connected in series and arranged in helical form, was investigated and found to be suitable for voltages up to 100 kv.

Measurements on the first helical resistor built in 1955 indicated negligible leakage and corona errors to within the accuracy of the measurements made at that time. However the heating errors were considerable (0.01 percent per degree C) in this resistor because of the temperature coefficient of the wire-wound 1-megohm units.

A second helical resistor, of the same design, was constructed in 1961 using 100 one-megohm, low-temperature coefficient, wire-wound units. By using matched pairs of these units having temperature coefficients equal in magnitude and opposite in sign, the final 100-megohm resistor was estimated to have a temperature coefficient not greater than 0.4 ppm per degree C. Corona and leakage errors for this resistor as determined using improved measurement techniques were found to be less than 10 ppm at 50 kv and less than 20 ppm at 100 kv.

This 100-megohm resistor has a special "hat" or high-voltage electrode designed to give uniform gradients from it to ground. This would allow other similar resistors to be stacked on top of it and connected in series for higher voltages. Corona tests on the electrode indicated the feasibility of such "stacking". Exact limits of accuracy attainable at voltages above 100 kv have not yet been determined.

The construction of the two high-voltage resistors described above was carried out almost exclusively by John L. Mills. Harold N. Cones and John L. Mills performed most of the experimental measurements.

(Paper 66C1–83)

U. S. Department of Commerce
National Bureau of Standards

Research Paper RP1823
Volume 39, September 1947

Part of the Journal of Research of the National Bureau of Standards

Shunts and Inductors for Surge-Current Measurements

By John H. Park

The special requirements that must be fulfilled by a shunt intended to be used in surge-current measurements are explained. A tubular shunt with coaxial potential leads that meets these requirements is described, and factors affecting its design are discussed. A theoretical derivation of the "skin effect" in this type of shunt at high frequencies is given in one of the appendices.

The advantages of using a mutual inductor for obtaining oscillograms of the rate of change of current during a surge are outlined, and several types of mutual inductors developed especially for this purpose are described. Theoretical derivations, given in the appendices, indicate that the concentric-tube mutual inductors described in this paper can be used to measure the high-frequency components of a current surge up to 70 megacycles with less than 10 percent error.

Several shunts and mutual inductors of the designs described in this paper were constructed for use in the high voltage laboratory at the National Bureau of Standards. Their complete description and oscillograms showing results obtained with them are included.

I. Introduction

Surge-current generators are widely used in high-voltage laboratories to simulate the heavy current component of a lightning discharge. They are regularly employed in testing protective devices that are intended to withstand lightning discharges and in determining the effects of heavy-current discharges on various materials and apparatus. In order to correlate the test results obtained in various laboratories, it is necessary to know the magnitude and wave-form of the surge current used in each test.

A generally accepted method of measuring heavy-current surges is to insert a shunt in the discharge circuit and to apply the voltage drop across this shunt, through a suitable cable, to the deflecting plates of a cathode-ray-oscillograph capable of recording the variation of this voltage with time. The over-all accuracy of this method is dependent upon the three components used in the measurement: the cathode-ray-oscillograph, the cable, and the shunt.

The development of the cathode-ray-oscillograph to its present state of efficacy has involved years of work of a large number of experimenters and theorists. At the present time there are several types of oscillographs having recording speeds and response accuracies suitable for surge measurements. In general they may be classified as (1) the high-voltage cold-cathode type with the recording film inside the vacuum chamber, (2) the hot-cathode type with the film inside the vacuum chamber, and (3) the hot-cathode sealed-tube type using a fluorescent screen photographed by means of an external camera. Results reported in the present paper were obtained using an oscillograph of the first type; however, with slight modifications in design constants the apparatus to be described would be equally suitable for use with other types of oscillographs.

In order to facilitate safety precautions and to allow one cathode-ray-oscillograph (CRO) to be used with any one of several surge generators, the oscillograph is usually located at some distance from the surge generator and its potential divider and/or shunt and a cable (40 to 100 ft. long) is used to connect them to the deflecting plates of the oscillograph. The purpose of this cable is to reproduce the voltage drop across the shunt, at the deflecting plates of the oscillograph without distortion, and it must not introduce other voltages by induction from nearby currents. The use of coaxial-type cables reduces inductive effects to

a minimum, and when constructed with insulating material of low dielectric loss, such as polyethylene, coaxial cables are capable of transmitting all components of a surge up to at least 100 megacycles/sec over the distances required without significant attenuation. The terminations of the cable, at the shunt and at the oscillograph, are both important.

Various types of shunts have been used for measuring heavy-current surges [1,2,3],[1] and long before surge generators were in general use, the design of alternating current shunts to insure low residual inductance was given considerable attention [4,5]. Thus, the design of the shunts now in use at this laboratory for surge-current measurements is based on experience with shunts used for measuring large alternating currents as well as on subsequent experience in the field of surge-current measurement. The present paper will discuss the design of surge-current shunts, describe those constructed, and indicate the results obtained with them.

This paper will also describe a new design of mutual inductor for measuring rate of change of current. Because it tends to magnify the high frequency components in current waves it has been useful in their measurement.

II. Factors To Be Considered in the Design of a Shunt

1. Choice of the Best Type

In choosing the best type of design for a shunt to be used in measuring surge currents the three most important requirements are (1) the effective impedance considered as a 4-terminal network must be constant over as great a range in frequency as possible, (2) inductive effects of parts of the current circuit, other than the shunt, upon the potential-lead circuit of the shunt should be a minimum, and (3) it must be possible to connect the sheath of the cable from the shunt to the CRO, to ground at or near the shunt without introducing induced voltages in the shunt potential circuit (this is desirable to minimize the flow of ground currents in the sheath of the cable which might cause induced voltage at the CRO plates).

In order to determine compliance with requirement number one, the configuration of the shunt should preferably be such that its inductance and skin effect can be computed for as great a range in frequency as possible; otherwise the comparison of various types of shunts would require the actual construction of a large number with subsequent experimental comparisons. Two general types lend themselves to computations: (a) the concentric tubular and (b) the flat strip. Illustrations of these, giving the methods of attaching potential leads, are shown in figure 1. Another

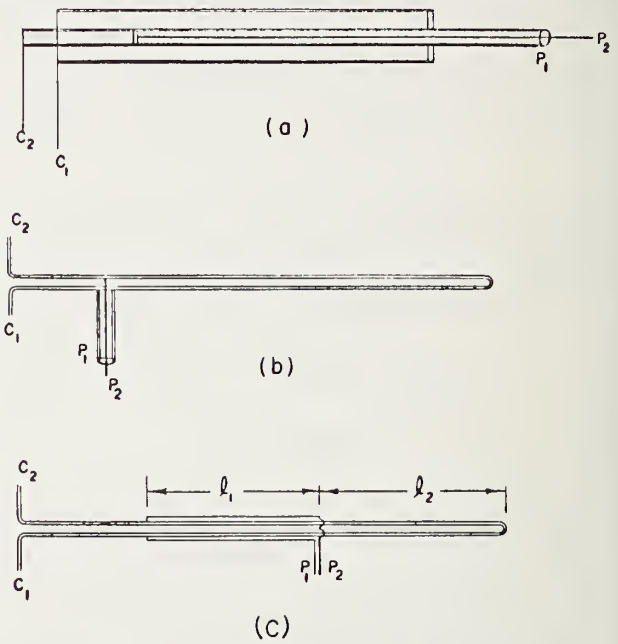

FIGURE 1.—*Three types of shunts whose inductance and skin effect can be computed.*

a, Concentric-tube shunt; *b*, flat-strip shunt; *c*, flat strip shunt with potential leads arranged to give minimum inductance.

type of shunt used by Bellaschi [1] in surge measurements consists of several twisted "hairpin" loops of resistance wire connected in parallel at the current terminals. This type of shunt has been found suitable for most surge-current measurements, but its inductance and skin effect cannot be accurately computed from theoretical formulas. An approximate theoretical computation by Brownlee [2] indicates that the twisted loop shunt would probably have a somewhat larger time constant than a flat strip shunt. Theoretical formulas for computing the inductance (assuming uniform distribution of current) and skin effect (for a limited frequency range) of the concentric tubular and flat strip shunts are

[1] Figures in brackets indicate the literature references at the end of this paper.

readily available.[2] [3] As suggested by Silsbee [4] a strip shunt with potential leads attached as shown in figure 1, c, could be designed so as to have zero effective inductance by a suitable choice of values of l_1 and l_2. However, this arrangement of potential leads prevents the shunt from complying with requirement (3) above, as will be explained later, so it is not considered in the following comparison of coaxial tubular vs. flat-strip shunts.

To compare the constancy of effective impedance as frequency changes, for the tubular and flat-strip shunts, two typical designs of shunt were assumed and their inductance and skin effect computed from the formulas referred to above. A concentric tubular shunt (fig. 1, a) in which the resistance material was a CuNi alloy ($\rho=22.9\text{x}10^{-6}$ ohm cm) tube whose outside diameter was 0.25 in. and wall thickness was 0.008 in. was chosen as one example because such a tube was readily available for use in constructing a shunt. For comparison purposes a strip shunt was chosen whose thickness was the same as the wall thickness of the tube, whose width was the same as the circumference of the tube, and whose separation between strips was taken to be 0.01 in. (The shunt length does not affect these computations provided it is several times the largest transverse dimension.) The time constants for the shunts as obtained using the theoretical formulas assuming uniform distribution of current were (1) for tubular shunt $L/R=-0.0365\text{x}10^{-6}$; and (2) for strip shunt $L/R=0.218\text{x}10^{-6}$. The skin effects at $f=1$ megacycle as obtained from formulas given by Silsbee were (1) for tubular shunt $R/R_{dc}=0.959$; and (2) for the strip shunt $R/R_{dc}=0.955$. It must be remembered that these results do not give an accurate evaluation of the constancy of effective impedance at frequencies over 1 megacycle, because at such frequencies the skin effect causes a nonuniform distribution of current density over the thickness of the tube or strip, for which the theoretical formulas used in the above computation do not hold—no published theoretical formulas good at these high frequencies were known to the author. However, the above results should serve their purpose as a comparison between the two types of shunts. The tubular shunt has a much lower time constant than the strip shunt, which means that its reactance will be negligible over a higher frequency range. The skin effect at 1 megacycle appears to be the same for both shunts, but the formula used in obtaining the skin effect for the strip shunt neglects edge effects that are known to considerably increase [5] the skin effect at higher frequencies. Thus it would appear that the tubular shunt, as it has no edge effects, would have less change in effective resistance at the higher frequencies than the strip shunt. A decrease in both inductance and skin effect could be obtained by using a thinner strip or a thinner walled tube, but this cannot be carried to extremes because of the heat capacity requirements of the shunt, which will be discussed later; any improvement made by this means in the strip shunt could probably also be made in the tubular shunt, though possibly not to the same extent. Thus, it would appear that either a coaxial tubular shunt or a flat strip shunt would satisfy requirement (1) (stated above), but that the tubular design would be preferable.

As indicated above, the readily available theoretical formulas are not capable of yielding the effective 4-terminal impedance of a strip or tubular shunt at frequencies of 1 megacycle or higher. Due to the axial symmetry of the tubular shunt, it is possible to develop a theoretical formula for calculating the impedance of such a shunt, taking into account the nonuniform distribution of current over the thickness of the tube (skin effect), which will hold for very high frequencies. The development of this theoretical formula (taken from hitherto unpublished notes of F. B. Silsbee) is given in appendix 1, and it permits the impedance of any tubular shunt to be computed for frequencies up to 10^9 or higher. The development of a similar formula for strip shunts would be much more difficult because of the lack of axial symmetry.

The inductive effects of current-carrying parts other than the shunt upon the potential lead circuit of the shunt (requirement 2), are dependent upon two factors: (a) the mutual inductance of the current carrying parts upon any loop in the potential circuit of the shunt, and (b) the maximum rate of change of current with time in the current-carrying part.

The maximum rate of change of current occurs on the front of the current wave, and it is some-

[2] See p. 400 of reference [4] for inductance of tubular shunt.

[3] See p. 81 of reference [5] for inductance of a flat-strip shunt; p. 86 for skin effect of flat strip, and p. 91 for skin effect of a tubular shunt.

[4] See p. 81 of reference [5].

[5] See reference [5], p. 86 and 87.

times taken to be the peak value of current divided by the time to peak. This is actually the average rate of change for the front of the wave, and any detailed study of the front of a current surge requires a more accurate basis for obtaining the maximum rate of change of current. Theoretically, the maximum rate of change of current for a capacitance discharging through an inductance and resistance occurs at the instant the circuit is closed and is equal to the voltage, E, to which the condenser was charged divided by the inductance, L, in the discharge circuit. The total inductance of the discharge circuit of a surge-current generator can be as low as 2 μh, and with a maximum voltage of 100 kv the maximum rate of change of current would be 5×10^{10} amp per second. Such a rate of change of current in the main current circuit would induce 50 v in the potential circuit of the shunt if the mutual inductance, M, between the two circuits were 0.001 μh. As a "pick-up loop" in the potential lead circuit of only 1 sq cm area, placed very close to a current-carrying part, may have a mutual inductance of 0.002 μh (giving a peak induced voltage of 100 v), the extreme importance of minimizing mutual inductance between the potential circuit of a shunt and all current-carrying parts becomes apparent. If the surge generator discharge circuit is fairly long so that its total inductance is more than 2 μh, the maximum rate of change of current will not be correspondingly reduced, because the stray capacitance across the discharge circuit will in effect short out the added inductance at the instant the surge is being initiated.

Referring to figure 1, a, the potential circuit of a tubular shunt may be considered as an extension of the coaxial cable from the CRO, ending in a direct short circuit from the central conductor to the sheath. Due to the axial symmetry of this arrangement the mutual inductance between the potential circuit and any current-carrying parts is the lowest obtainable. Even when the sheath of the cable is connected to ground and ground currents flow in the sheath of the cable and in the outer current return tube of the shunt itself, these ground currents will not induce voltage in the potential circuit of the shunt provided the density of such currents is symmetrical around the axis of the shunt. End effects or concentration of current along one side of the shunt axis can be largely eliminated by extending the two current-carrying tubes of the shunt several diameters beyond the end of the central conductor that serves as a potential lead.

To reduce mutual inductance in the potential circuit of a strip shunt the potential leads can be taken off the strip as a central conductor and coaxial tube as shown in figure 1, b. There still remains the small loop formed by the resistance ribbon itself which is in the potential circuit of the shunt and offers the possibility of inductive pick-up from such currents as might flow in the sheath of the cable and one of the current leads up to the potential circuit. There is no way of separating the potential circuit from end effects arising from such currents in a strip shunt. Although a strip shunt could be built with very low inductive pick-up between its potential circuit and current-carrying parts, the tubular shunt is the only design offering the possibility of entirely eliminating such inductive effects.

In order to understand the importance of being able to ground the sheath of the cable going from the shunt to the CRO at or near the shunt (requirement (3) above), it is necessary to consider the entire surge-current generator circuit. A schematic diagram of a surge-current generator is given in figure 2. The heavy lines show the path of the surge current from capacitor, C, through the tripping gap, test specimen, measuring shunt and the necessary connecting leads. No ground connections are necessary to complete the heavy-current discharge circuit, but this circuit is usually tied to the ground or the floor of the laboratory at some point between the low-voltage terminal of the capacitors and the test specimen in order to complete the charging circuit and to definitely fix the potentials of various parts of the discharge circuit with respect to ground. The self-inductance of the conductors forming the discharge circuit will depend upon their cross-section, length, and arrangement. Assuming the conductors to be of round cross section ½ in. in diameter, their inductance is 0.01 μ h per cm length for a return at a considerable distance. For the maximum rate of change of current 5×10^{10} amp per second, this means the maximum voltage difference between two points 1 cm apart on this discharge circuit is 500 v. Thus, if the discharge circuit were grounded at point g in figure 2, a shunt located only 10 cm from point g would be 5,000 v above ground as the discharge is initiated. This voltage will tend to

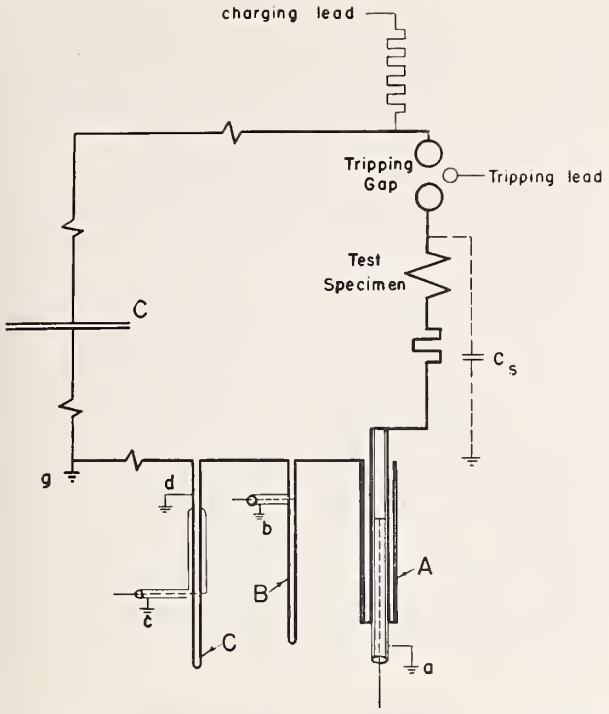

FIGURE 2. *Wiring diagram of surge-current generator showing method of connecting shunts, their potential lead arrangement, and several possible ground connections.*

make current flow in the sheath of the cable from the shunt to the CRO, through the ground connection at the CRO and back to point g through the laboratory grounding system. Due to the stray capacitance (C_s in fig. 2) from the lower ball of the tripping gap and parts of the discharge circuit to ground, this voltage will be of a high frequency oscillatory type occurring just as the main current discharge is initiated and any currents caused by it will induce voltages of the same character in any circuit coupled with them. In order to minimize such inductive effects at the CRO it is necessary that the cable from the shunt to the CRO have its sheath grounded at or near the shunt. In order to reduce the effect of stray capacitance (C_s in fig. 2) it may be desirable to ground other points in the discharge circuit, such as g, in addition to the sheath of the cable. Thus, the best type of shunt would be one which would allow any or all of these ground connections to be made and still have minimum pick-up due to induced voltages from ground currents.

In figure 2, all of the three types of shunts illustrated in figure 1 are represented as being connected in the discharge circuit of a surge generator in order to help explain the effect of ground currents on each. The ground currents most likely to cause inductive pick-up are those due to the high frequency oscillations arising from the stray capacitance, C_s, to ground. If a type C strip shunt were used, a consideration of the various possible ground connections in addition to the cable sheath ground at the CRO, leads to the following conclusions: (1) a single additional ground connection to the cable sheath at c would not be suitable, because then ground currents from C_s would flow in one potential lead of the shunt and induce high voltages in the loop formed by the potential leads; (2) a single additional ground connection at g would still permit cable-sheath currents, which flow to ground at the CRO end of the cable, to flow through one of the shunt potential leads (actually this is better than no ground at g); (3) two additional grounds, one at g and one at c would introduce a combination of the two above effects without eliminating either; (4) a single additional ground at d would reduce the inductive effects of ground currents but would not eliminate them entirely.

Thus the use of a shunt of this type would preclude the experimentally desirable flexibility in location of ground connections.

If a type B strip shunt were used, the same conclusions given for the type C would hold except all inductive effects would be much less because, as may be seen from the diagram, the arrangement of potential leads insures a lower mutual inductance between the potential circuit and current-carrying parts.

If a tubular, type A, shunt were used the ground current for any combination of ground connections would be symmetrically distributed around the axis of the coaxial potential circuit, thus, theoretically at least, eliminating any pick-up due to these ground currents.

The above considerations indicate that the coaxial tubular design is superior to other designs in surge-current measurement work because (1) it should be more constant in impedance over a wide range in frequency, (2) it can be constructed to insure minimum inductive pick-up from current-carrying parts of the surge generator, and (3) it offers the greatest freedom in location of ground connections at the surge generator. In view of these advantages it was decided to investigate

theoretically as well as experimentally the advantages and limitations of concentric tubular shunts for surge current measurements, realizing that some of the derived relations would be applicable to strip-type shunts.

2. Determination of Cross-Sectional Area and Length

The cross-sectional area and length of a shunt are related as follows:

$$V=lA$$
$$R=\rho l/A$$

where V is the volume of the resistance material, l its effective length, A the cross-sectional area, R the resistance, and ρ the volume resistivity.

Solving for A and l

$$A=\sqrt{\frac{V\rho}{R}} \tag{1}$$

$$l=\sqrt{\frac{VR}{\rho}} \tag{2}$$

The resistivity, ρ, is a constant of the shunt material, and it is well to choose a material having as high a resistivity as possible. The resistance of the shunt is determined by the maximum current to be measured and the maximum voltage that can be recorded at the CRO. The volume of the shunt resistance material is fixed by the largest amount of energy that must be absorbed by it during a single discharge of the surge generator. A reasonable temperature rise of say 100° C allows a thermal input of 100 times the specific heat times the mass of the shunt material. For most metals the specific heat is about 0.1 and density is 9, so in general the maximum allowable thermal input to the shunt would be 90 times V, in calories for V in cubic centimeters. The maximum energy fed into the shunt during a single discharge is equal to the energy initially stored in the surge generator capacitors ($1/2\ C\ E^2$), times the resistance of the shunt divided by the minimum effective resistance of the surge-generator circuit. As this minimum effective resistance is usually at least twice that of the shunt, the maximum shunt input energy may be taken as $1/4\ C\ E^2$. When the volume of shunt material computed from this energy input is inserted in the above equations, approximate values of l and A for the shunt are determined. It is best to choose the thinnest wall tubing available having approximately this cross-sectional area as the thinner the wall the slower the change in effective impedance as the frequency is increased (see appendix 1). The limit on wall thinness is set by magnetic stresses, to be discussed later.

If for practical reasons the values actually chosen for l and A differ markedly from the approximate values computed from eq 1 and 2 (this will necessarily be true if the preliminary value of l is too long for convenience or if tubing having approximately the estimated cross-sectional area is not available) the allowable energy input should be computed for the chosen values. This allowable energy input together with the resistance of the shunt and the maximum energy available from the surge generator ($\frac{1}{2}\ CE^2$) determine a minimum effective resistance for the surge-generator discharge circuit. Except in cases where an oscillatory discharge with extremely low damping is required, this minimum effective resistance will be exceeded.

3. Forces on a Tubular Shunt

When a heavy surge current is passed through a tube made of resistance material, it will be subjected to forces from two sources: (1) the action of the magnetic field produced by the current upon the current itself and (2) the thermal expansion of the tube arising from its sudden change in temperature when the current is applied. The magnetic force acts as a pressure from the outside tending to collapse the tube. A formula for computing this pressure is derived in appendix 2. It depends upon the square of the current through the tube and upon its cross-sectional dimensions. Except for extremely high currents most thin-wall tubes available for use in a shunt would probably withstand the pressure arising from the magnetic field; however, in the design of any shunt, and especially in the case of a shunt made with extra-thin-wall tubing, this pressure should be computed in order to make sure that the tube will not collapse.

The sudden change in shunt temperature when the discharge occurs introduces a stress in the tube whose approximate value can be computed. As the shunt tube itself is made of material having much higher resistivity than other current-carrying parts of the shunt and surge generator circuit, it will momentarily attain a higher temperature than its supporting parts during each current discharge. This sudden change in temperature

tends to increase the length of the tube, but it occurs so fast the tube does not have time to expand, and the tube is momentarily put in compression. The maximum compressive stress may be computed from the strain (total temperature change T, times coefficient of linear expansion, δ) and the stress-strain curve for the shunt material. The tube will then behave somewhat like a spring initially compressed and suddenly released; i. e., waves of stress will proceed along the tube, with the velocity of sound, being reflected at the ends and traveling back as tensile stress. The nature and magnitude of these stresses could be computed for any given tube if the exact masses connected to the two ends of the tube were known; however, the maximum stress would not be expected to greatly exceed the initial compressive stress that may easily be computed as noted above. Assuming the shunt material to be perfectly elastic and that it will not be stressed beyond its elastic limit, the maximum stress will be

$$S=ET\delta, \tag{3}$$

where E is the modulus of elasticity for the shunt material. If a value for S is taken equal to the maximum allowable stress (just below yield point) for the material being used, this equation gives an allowable temperature rise for the shunt. For most materials this allowable temperature rise is about 100° C. This value could probably be exceeded because of the high ductility of most resistance alloys; thus if a minimum resistance is desired in the surge generator discharge circuit (maximum energy in the shunt) it would be advisable to determine the maximum allowable temperature rise or energy input experimentally.

This could be done by placing a sample of tubing of the same material and cross-sectional dimensions as the shunt tube in the discharge circuit of a surge-current generator. The energy absorbed by the sample may be computed by multiplying the energy initially stored in the capacitors ($\frac{1}{2} C E^2$) by the ratio of the resistance of the sample to the total effective resistance of the complete surge generator discharge circuit including the sample tube. The total effective resistance of the surge generator can be deduced by using a shunt, whose resistance tube has a cross-sectional area at least five times that of the sample tube, in the discharge circuit and taking oscillograms of the discharge current. From measurements of frequency and logarithmic decrement on these oscillograms, the inductance and effective resistance of the complete surge-generator discharge circuit can be computed. Thus, by starting with the surge generator capacitors charged to a fairly low voltage, E, and taking repeated discharges through the sample tube at successively higher values of E the energy input at which the tube is broken or deformed may be determined. The safe allowable temperature rise for a tube of this particular material and size can then be stated.

The experimental procedure just described was carried out for a $\frac{5}{16}$-in. diameter CuNi alloy tube whose wall thickness was 0.039 cm and length 33 cm. No evidence of tube failure except discoloration due to the high temperature was noted for energy inputs below 160 joules/centimeter (instantaneous temperature rise of 400° C). However, after the first discharge at this energy input a slight bend in the tube was noted as though it were failing as a column in compression. After each discharge of successively higher energy input the bending was more pronounced and after a discharge at 268 j/cm (670° C temperature rise) in addition to the bending, decided crinkling and crushing were noted. The crushing was probably caused by magnetic forces acting at an instant when the tube was weakened because of its high temperature. These values of energy input exceed what might be considered a desirable design value.

The safe design value should be one that would not stress the tube beyond its elastic limit. This was determined in another experiment by measuring the length of the tube before and after each discharge. After two discharges, the energy input of each being equal to 60 j/cm (150° C temperature rise), no permanent change in length was noted. For energy inputs of 100 j/cm (260° C temperature rise) or greater an increase in length of about 0.2 mm (0.6 percent) was noted after each discharge. Thus, it was concluded that the maximum allowable temperature rise for a shunt made of this material should be about 150° C. This is only slightly above the maximum value (133° C) computed from the stress due to thermal expansion.

4. Inductance and Capacitance Between Current Terminals

Because of the method of attaching potential leads, the 4-terminal impedance of a tubular shunt

is constant over a wide range of frequency. However, at very high rates of change of current (high-frequency components of the surge), the distributed capacitance and inductance of the current circuit will cause variations in the root-mean-square values of these high-frequency components along the length of the shunt. That is, the instantaneous value of current along the length may differ from the value at the current terminals.

This variation in the instantaneous value of current along the length of the shunt is, of course, entirely negligible at lower frequencies, but in order to determine the frequency at which this effect becomes appreciable a solution for the current and voltage along the length of the tube, assuming uniformly distributed inductance and capacitance only, was obtained (in a manner similar to that used in appendices 3 and 4). The current at the potential lead end of the shunt, I_l, was found to be

$$I_l=\frac{I_c}{\cos \omega l\sqrt{LC}} \tag{4}$$

where

I_c=current at current terminals; L=distributed inductance per unit length of shunt; C=distributed capacitance per unit length of shunt; $\omega=2\pi f$ (f in cycles per second); l=length of current circuit in centimeters.

For concentric tubes whose wall thickness is small compared to their diameter, the inductance and capacitance per unit length are:

$$L=2 \log_e b/a\times10^{-9} \text{ henries} \tag{5}$$

and

$$C=\frac{0.555}{\log_e b/a}\times10^{-12} \text{ farads} \tag{6}$$

where a is the outer diameter of the inner tube, and b is the inner diameter of the outer tube. Multiplying eq 5 by eq 6 gives $LC=1.110\times10^{-21}$. Thus the quantity $\sqrt{LC}$ in eq 4 is a constant, and the variation in current along the length of the tubes depends only upon the length, l, of the tubes and the frequency of the current being measured. For shunts up to 100 cm long, the maximum variation in current is less than 10 percent for frequencies up to 21.5 megacycles.

The voltage between the current terminals was found to be

$$E_s=j\omega LlI\left(1+\frac{\omega^2LC}{3}l^2+\ldots\right) \tag{7}$$

The magnitude of this voltage does not affect the accuracy of the shunt, but it should be evaluated to indicate the insulation required between current terminals. For shunts up to 100 cm long the quantity in the bracket of eq 7 reduces to unity (within 5 percent) for frequencies up to 18 megacycles. Thus this voltage may be taken as equal to $j\omega LlI$ or $LldI/dt$. The total inductance of the current circuit for any tubular shunt, Ll, may be computed from its dimensions by use of eq 5, and the rate of change of current dI/dt depends upon the particular surge generator being used and its discharge circuit. For a typical shunt, 100 cm long, this inductance is about 0.14×10^{-6} henries, and for the maximum rate of change of current assumed above (5×10^{10} amp/sec) the voltage between current terminals is 7,000 v.

III. Description of Two Shunts

There are two surge generators being used in this laboratory at the present time. One is a 2,000 kv surge-voltage generator capable of giving 30,000 amp on short circuit. The other is a 100 kv 10μf surge-current generator capable of discharging a maximum of 200,000 amp. It was

TABLE 1.—*Constants of two tubular shunts*

	Shunt A	Shunt B
Four-terminal resistance	0.01 ohm	0.0018 ohm
Over-all length	39 in	38¼ in.
Length of resistance tube	26⅞₁₆ in	24⅞₁₆ in.
Diameter of outside tube	⅜ in	2 in.
Diameter of resistance tube	¼ in	1 in.
Wall thickness of resistance tube	0.008 in. (0.0203 cm).	0.0216 in. (0.06 cm).
Cross-sectional area of resistance tube	0.0392 sq cm	0.469 sq cm
Resistance tube material	German silver	80% Cu, 20% Ni
Resistivity of resistance tube (micro-ohm cm).	23.33	36.3
Ratio of a-c impedance to d-c resistance, at:		
f=0.25 megacycle	1.00	0.98
f=0.50 megacycle	1.00	0.92
f=1.0 megacycles	0.99	0.76
f=2.0 megacycles	0.96	0.48
f=5.0 megacycles	0.86	0.15
Allowable temperature rise—computed from stress due to thermal expansion	133°C	133°C
Allowable energy input	1320 joules	14,500 joules
Current limit due to magnetic force	87,600 amp	223,000 amp
Total inductance of current circuit	0.202 μh	0.106 μh
Maximum voltage drop at current terminals—L di/dt for di/dt=5x10 ¹⁰ amp/-sec	10,000 v	5,300 v

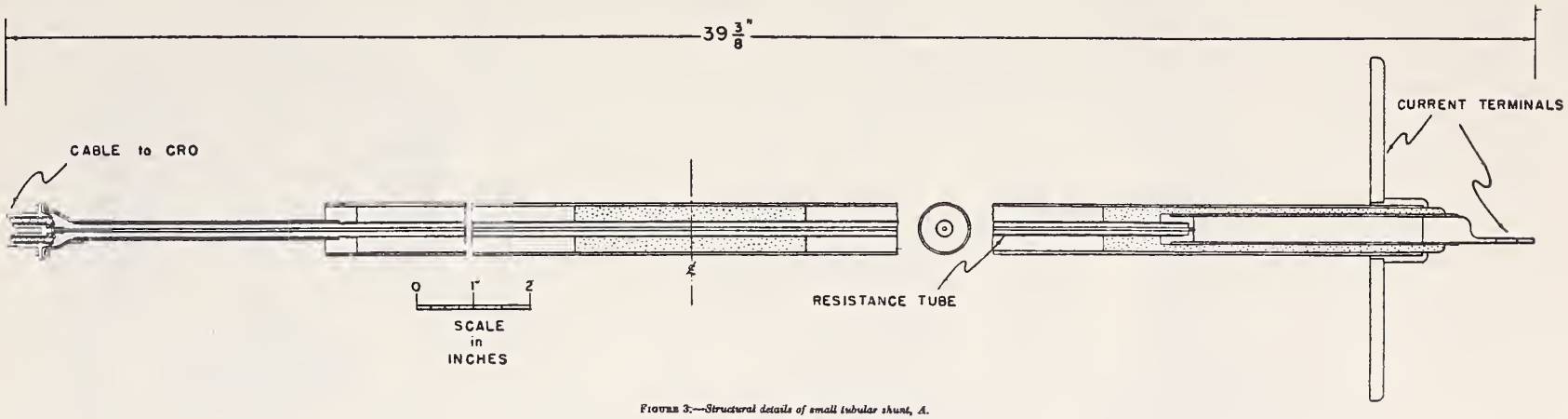

FIGURE 3.—*Structural details of small tubular shunt, A.*
See table 1 for additional dimensions and other constants.

FIGURE 4.—*Structural details of large tubular shunt, B.*
See table 1 for additional dimensions and other constants.

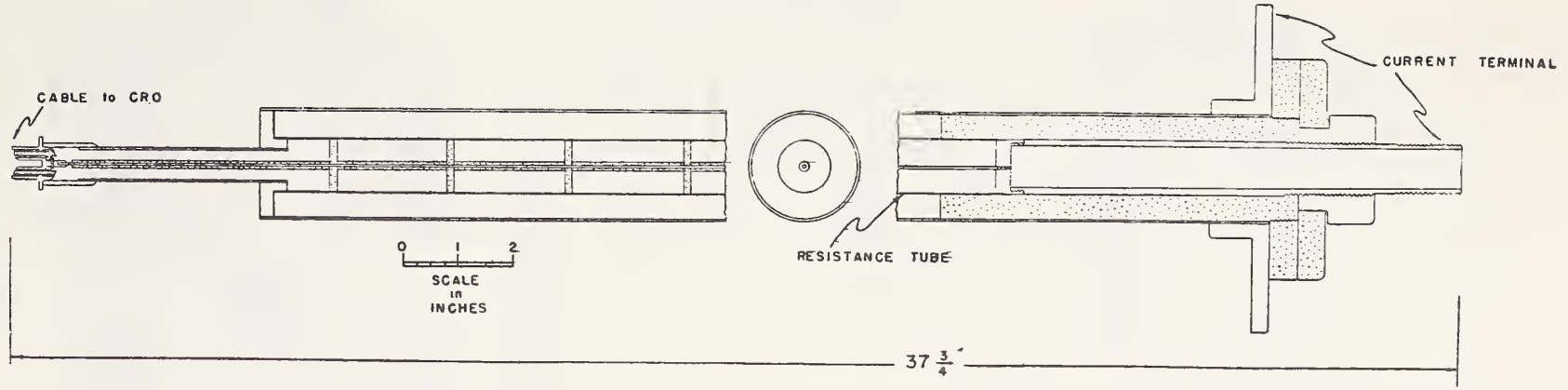

(Face p. 1m)

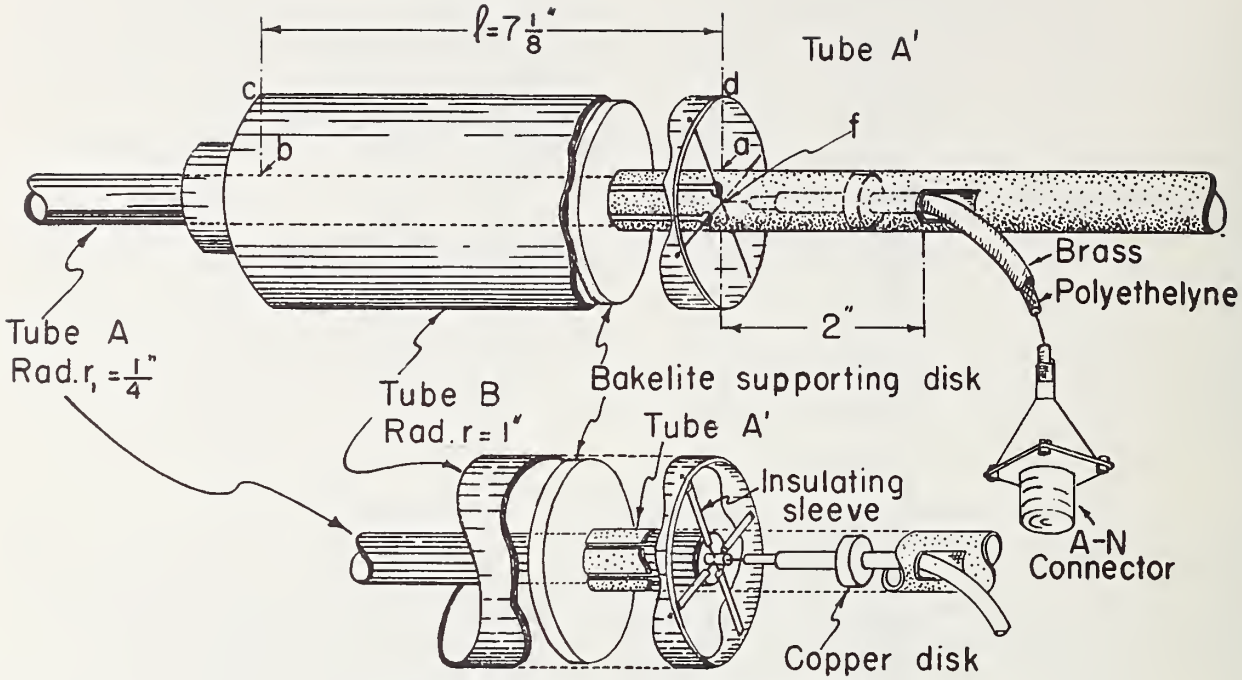

FIGURE 6.—*Type I concentric tube mutual inductor.*

$M = 0.05$ μh.

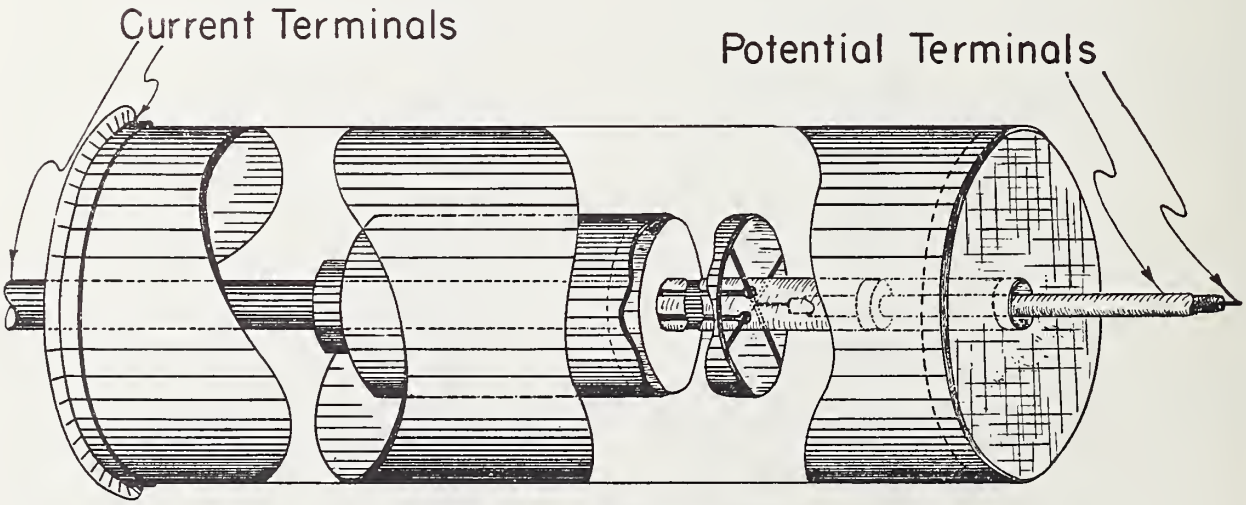

FIGURE 7.—*Type II concentric tube mutual inductor.*

thought that at least two shunts would be needed, one for currents from 10,000 to 50,000 amp and one for currents from 50,000 to 200,000 amp. As the CRO was capable of giving satisfactory records over the range from 200 to 2,000 v when used with a suitable potential divider at the deflecting plates, resistance values of 0.04 and 0.005 ohm were chosen for the two shunts that have been constructed. Cross-sectional drawings of the shunts are shown in figures 3 and 4. Their physical and computed constants are given in table 1. The resistance tubes were selected from a small stock of readily available thin-wall tubes, because at the time it was not feasible to wait for special tubes to be drawn.

The ratios of *a-c* impedance to *d-c* resistance given in table 1 were computed from the theoretical formulae derived in appendix 1. At frequencies above 5 megacycles for the 0.04 ohm and 1 megacycle for the 0.0048 ohm shunt, this ratio is considerably less than unity. This fact is of no great concern in the measurement of the present standard impulse-current test waves for which the fundamental-frequency component is of the order of 100 kc or less; but the fact should not be overlooked that the magnitude of higher-frequency components, probably present in such test waves, may be considerably reduced on a comparative basis. Other types of shunts, as they have some inductive coupling between their potential-lead circuit and current-carrying parts of the discharge circuit, may give an indication of these higher frequency superposed currents. However, this indication will depend, not upon the resistance of the shunt, but upon the unknown value of inductive coupling, and thus will give an erroneous idea of their magnitude. A method of accurately determining the magnitude of high-frequency components consists of using a mutual inductor, having a known value of coupling with the current circuit, in place of a shunt. Mutual inductors have been constructed and are used at this laboratory. They will be discussed in section IV.

The allowable energy input for these shunts was computed from the allowable temperature rise (obtained from the maximum stress due to thermal expansion) and the mass of each shunt (actual values are given in table 1). These values are useful in computing the minimum resistance that can be used in the discharge circuit of a surge generator without overheating these shunts. As an example: The surge voltage generator in this laboratory requires the dissipation of 33,300 j for each discharge when charged to full-rated voltage. Thus, when shunt A is used with this generator, the total resistance of the discharge circuit must be at least 33,300 divided by 1,320 times the shunt resistance (0.04 ohm) or 1.01 ohms. A similar computation for shunt B gives 0.107 ohm. As the minimum discharge resistance of this surge voltage generator is 6 ohms, either shunt may be used with any discharge circuit. The surge-current generator in this laboratory requires the dissipation of 50,000 joules when charged to full-rated voltage, thus the total resistance of the discharge circuit must be at least 1.52 ohms if shunt A is to be used or 0.0165 ohm if shunt B is to be used. As the minimum discharge resistance of this surge-current generator is 0.03 ohm, shunt B may be used with any discharge circuit, but shunt A should only be used when a resistance of at least 1.5 ohms is added (a resistance of about this value is needed to give a critically damped discharge).

The current limitations on these shunts due to magnetic forces were estimated by the formula given in appendix 2. These limitations are above the values of current expected to be used with these shunts. The inductances of the current circuits of these shunts were computed by using the formula given in eq. 5. The voltage drops computed from these inductances and the maximum expected rate of change of current indicate the desirability of having adequate insulation between the current terminals to prevent flashover.

IV. Mutual Inductors for Measuring Rates of Change of Current

1. General Considerations

For many experiments involving heavy-current surges, it is desirable to know the wave form of the rate of change of current, for example: (1) in studying the voltage induced in a circuit coupled with the heavy current discharge circuit and (2) in studying the voltage difference arising from inductance between two points on a conductor or a system of conductors carrying the heavy-surge current. The rate of change of current can be computed from an oscillogram of the current obtained by using a shunt, but this involves the inaccuracy of measuring the slope of the current wave at a number of points and plotting a curve

from these measured values of slope. In addition, the high-frequency components of the current wave form as they appear in the oscillogram obtained with a shunt may be highly distorted or attenuated and give an erroneous value of rate of change of current, especially at the point of maximum rate of change. A more accurate record of rate of change of current can be obtained with much less effort by inserting the primary of a mutual inductor in the heavy-current discharge circuit in place of the shunt and connecting the secondary of this inductor to the cable to the CRO. The record obtained on the CRO is then equal to $M\ di/dt$. If M (the mutual inductance of the inductor) is known, an actual oscillogram of the rate of change of current is obtained.

A mutual inductor, to be considered satisfactory for this purpose, must fulfill the following requirements: (1) Its mutual inductance must be of suitable value to give the proper voltage at the CRO (from 500 to 2,000 in this case). For the expected rates of change of current (from 1 to 5 times 10^{10} amp per second) this amounts to about 0.05 μh. This value of mutual inductance must be definite and should be computable from the physical dimensions of the inductor.

(2) The primary circuit of the inductor must be capable of carrying the heavy current discharge and should add a minimum impedance to the discharge circuit.

(3) The secondary circuit should have minimum coupling to all current carrying parts except the primary of the inductor.

(4) The method of connecting the secondary circuit to the cable going to the CRO should be such that the sheath of this cable can be connected to ground near the surge current generator without introducing coupling between ground currents in the sheath and the secondary circuit.

(5) The secondary circuit should have a minimum self-inductance. This may be explained as follows: The voltage to be measured at the CRO ($M\ dI/dt$) is impressed upon a circuit containing the self-inductance, L, of the secondary circuit and the surge impedance, R, of the cable to the CRO. It is the voltage across the surge impedance, R, that is recorded at the CRO and its value is

$$E_{\text{CRO}}=\frac{M\,dI/dt}{1+j\frac{\omega L}{R}}. \tag{8}$$

In order to have E_{CRO} equal to $M\ dI/dt$ for the high frequency components of I, it is apparent that the self-inductance, L, of the mutual inductor secondary circuit should be kept as low as possible. As L cannot be reduced to zero, the highest frequency components of I are subject to a phase displacement and attenuation, the magnitudes of which can be computed from the above equation for any assumed value of $\omega=(2\pi f)$.

A consideration of the various convention types of mutual inductors leads to the conclusion that none of them will fulfill the above requirements satisfactorily. The most promising type appeared to be one consisting of a straight single conductor primary insulated from, and running through, the central axis of a toroidal coil secondary of sufficient turns to provide adequate voltage at the CRO. It was thought that by introducing shields and connecting them to the primary circuit at an appropriate point with respect to the ground connection, an inductor of this type might fulfill most of the requirements listed above. A preliminary design of an inductor of this type was carried out, but the self-inductance of its secondary circuit had to be at least 2 μh in order to give the desired value of mutual inductance. When this value of inductance and 50 ohms for the CRO cable surge impedance, R, are inserted in eq. 8, it is found that the voltage at the CRO is only 0.9 of $M\frac{dI}{dt}$ for a frequency of 1.8 megacycles, for higher frequencies the attenuation would be much greater. The use of a mutual inductor of this type was, therefore, abandoned.

2. Mutual Inductors of Special Design

The first attempt to design a special mutual inductor to meet all of the requirements listed above resulted in the inductor shown in figure 5. The primary circuit is the straight length of No. 10 copper wire (with the return circuit at least 2 ft away, its effect can be neglected). The secondary circuit consists of the "D" formed by part of the No. 10 wire and the No. 16 wire. This arrangement permits the magnetic flux linking the secondary "D" to be computed as that due to an infinitely long, straight conductor, neglecting the effect of the return lead. The self-inductance of the secondary circuit is that due to the single "D" loop and can also be computed from its dimensions.

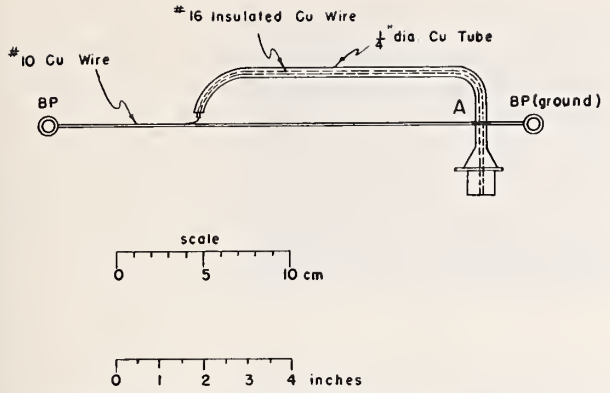

FIGURE 5.—*D-type mutual inductor used to obtain records of rate of change of surge currents.*

M=0.0986 μh

An inductor of this design, with dimensions corresponding to the scale in figure 5 was constructed. Its mutual inductance was computed to be 0.0986 μh and the self-inductance of its secondary circuit 0.25 μh. This value of self-inductance is considerably less than that of the toroidal secondary circuit mentioned earlier, and as a consequence frequencies up to 15 megacycles will be recorded with only 10 percent reduction in magnitude. The secondary circuit is connected to the CRO cable by coaxial leads, thus no voltage will be induced in it from ground currents flowing in the cable sheath. A mutual inductor of this type appears to fulfill the requirements of surge current testing fairly well. The one constructed in this laboratory has been of considerable value in obtaining records of the rate of change of surge currents. Its outstanding advantage lies in simplicity of construction.

The "D"-type mutual inductor has some drawbacks: (1) it is not completely unaffected by magnetic fields produced by other current-carrying parts of the surge generator circuit and (2) the self-inductance of its secondary circuit is about three times its mutual inductance (as a minimum it should be possible to make an inductor whose self-inductance is as low as its mutual inductance). Another mutual inductor has been designed in which the secondary circuit consists of a tube arranged coaxially with the primary conductor in order to overcome the small defects inherent in the "D"-type inductor.

A type I coaxial tube mutual inductor is shown in figure 6. Tube A constitutes the primary circuit of this inductor (the surge-current return lead is again assumed to be located at least 24 in. away so its effect can be neglected). The secondary circuit of this inductor consists of the following parts: (1) tube, A, from a to b, (2) a radial ring soldered on its inside to and around tube A at b and soldered on its outside to and around the inside of tube, B, at c, (3) tube B from c to d, and (4) the four-wire radial "spider" connection from d on tube B, going through but insulated from tube, A, and soldered to the central conductor of the potential leads at f. The secondary terminals are thus at a and f and are brought out through the concentric leads to the fitting for the CRO cable. How well this design of mutual inductor fulfills each of the requirements listed above may best be seen by considering each requirement, as follows: (1) The mutual inductance can be computed as that due to the magnetic flux produced by current in a long straight conductor (tube A) integrated over the region $a\ b\ c\ d\ a$ between the tubes. The mutual inductance thus derived in terms of the tube dimensions indicated on figure 6 is

$$M=2l\log_e\frac{r_2}{r_1}10^{-9}\text{ henry (for } l \text{ in cm)}.$$

There is a small correction to this value of inductance due to the thickness of tubes A and B, which can be computed by the method explained on page 397 of reference [4]. For $r_1=0.25$ in. and $r_2=1$ in., the length, l, of tube B should be about 7 in. to give a mutual inductance of 0.05 μh. (2) Because of the method of bringing out the secondary circuit leads used in this design, tube A must be at least 0.5 in. in diameter, and it should be made of a good conducting material such as copper. The wall thickness of this tube is relatively unimportant, and any ordinary thin wall copper tube can be used that is adequate to carry the heavy current discharge without damage. (3) The secondary circuit except for the ring and spider are coaxial conductors and thus have minimum coupling to all currents not flowing in the inductor. Likewise the radial ring and spider conductors are symmetrical about the axis which results in minimum coupling. (4) Also, because of the coaxial arrangement of the secondary circuit and leads to the CRO cable, any ground currents flowing in the cable sheath will have minimum

coupling with the secondary circuit and leads. (5) The self-inductance of the secondary circuit can be computed by the method explained on page 397 of reference [4], and it is found to be equal to the mutual inductance except for a small term arising from the finite thickness of tube, *B*. The self-inductance of the spider alone is less than 0.005 μh. Thus this design gives the minimum self-inductance that can be obtained in a straightforward manner.

An approximate value of the voltage impressed on the CRO cable can be obtained from eq. 8, but this equation neglects the capacitance between tube, *A*, and tube, *B*, and will not hold for the higher frequencies. A more accurate method for computing the value of this voltage is to consider the capacitance and inductance of the secondary circuit to be uniformly distributed along its length and solve for the voltage at the CRO end of this circuit by the methods normally used for circuits of uniformly distributed constants. This is done in appendix 3, and as shown there for a typical mutual inductor designed for surge-current measurements, the voltage impressed on the CRO cable will be equal to $M\ dI/dt$ (within 10 percent) for all frequencies up to 65 megacycles/sec.

The type I tubular mutual inductor appears to satisfy the requirements for surge-current measurement quite well. One was constructed in this laboratory having the approximate dimensions indicated in figure 6. This type of inductor is entirely satisfactory if the surge-generator discharge circuit is fairly long and can be arranged so that the inductor forms the final part of the return lead to ground. In case the minimum length of discharge circuit is required, the length of this inductor may add an appreciable inductance to the discharge circuit and it may also not be feasible to keep the return lead 24 in. away from the axis of the inductor. For such cases, a slightly different design of tubular inductor (type II) as indicated in figure 7 is suggested. It is the same as the type I inductor except that a return circuit is provided for the current by a larger tube, coaxial with the smaller tubes. This design brings the two current terminals close together and eliminates the problem of the location of the inductor with respect to other parts of the surge-generator circuit. It allows the inductor to be used in a discharge circuit of minimum length with the addition of the least possible inductance to the discharge circuit. The outer current return tube of the type II inductor also acts as an electrostatic shield for its secondary circuit. Because of the distributed capacitance between the outer-current return tube and the coaxial secondary circuit tube, currents and voltages in the secondary circuit will not be the same for the type II inductor as for the type I. Thus a computation of the voltage impressed on the CRO cable for a type II inductor must take into account the distributed capacitance and inductance of the circuit formed by the outer tube of the secondary circuit and the return current tube in addition to that of the secondary circuit itself. This is done in appendix 4, and while the results appear quite different from those obtained for the type I inductor in appendix 3, they indicate about the same upper limit in frequency (70 megacycles/sec).

Each of the three types of mutual inductors described above should prove useful for surge-current measurements. The "D" mutual inductor is very simple to construct and will measure superposed frequencies up to 15 megacycles/sec with less than 10 percent error. The tubular inductors are somewhat more complicated to construct but extend the frequency range to 70 megacycles/sec. The type I tubular inductor is suitable when the surge-generator discharge path is fairly long and the type II when a minimum length of discharge path is required. Inductors of both the "D"-type and the type I tubular have been constructed and proved very useful in this laboratory.

V. Experimental Results

The shunts and mutual inductors described above have been used in this laboratory for measuring current surges both from a surge-voltage generator and a surge-current generator and for various arrangements of discharge circuits. The oscillograms in figure 8 are typical of the results obtained. They are records of the discharge current and rate of change of current for a surge-current generator consisting of 40 1-μf, 50-kv, capacitors connected in series-parallel so as to give a total capacitance of 10 μf and a voltage rating of 100 kv. The discharge circuit consisted of a

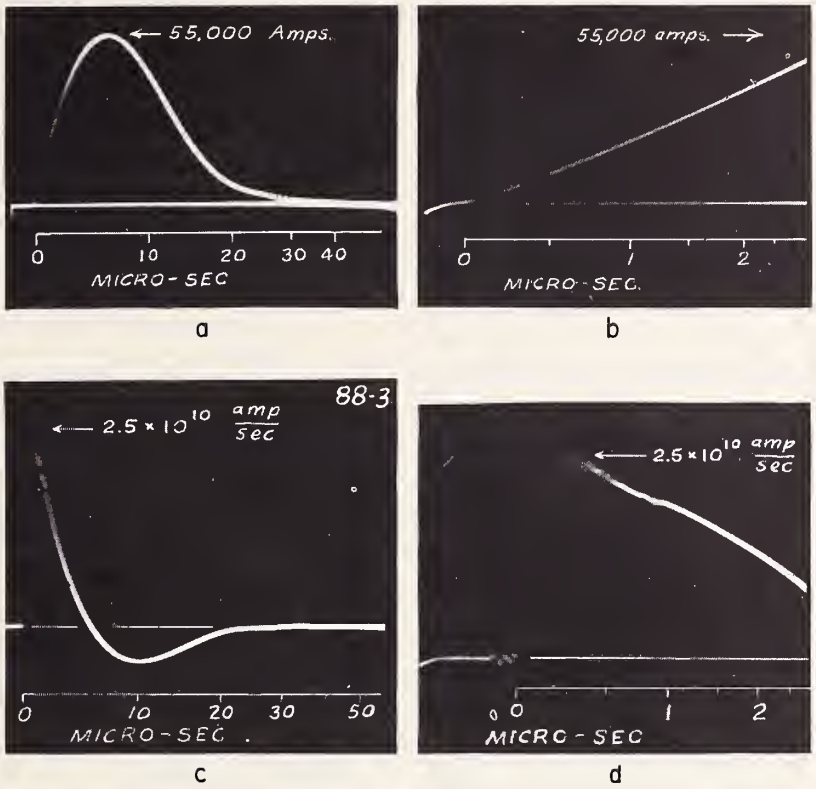

FIGURE 8.—CRO *records of a critically damped discharge from a surge-current generator.*

a, Current wave-form obtained by use of tubular shunt, *A*. *b*, early part of current wave-form on a faster CRO sweep. *c*, rate of change of current obtained by use of the mutual inductor shown in figure 6; *d*, early part of rate of change on a faster CRO sweep.

three-ball triggering gap; a 1-ohm resistor made up of 24 globar type B ceramic resistor units, assembled in the form of a cage (to minimize inductance) having sets of two 12-in. units in series, connected in parallel so that this assembly was 24 in. long; about 5 ft of copper busbar; and the shunt or mutual inductor. The total inductance of this generator and its discharge circuit is 2.5 μh and the 1-ohm resistor gives very close to critical damping. For the oscillograms shown in figure 8 the generator was charged to 75 kv and gave a maximum discharge current of 55,000 amp, the maximum rate of change of current being 2.5×10^{10} amp/sec.

The oscillogram in figure 8, a, shows the variation of current with time for the entire surge. Figure 8, b, shows the initial rise of the current on an expanded time scale (faster CRO sweep). Figure 8, c, shows the variation in the rate of change of current for the entire surge, and figure 8, d, shows the initial rate of change of current using a faster sweep The current records are quite smooth and just as anticipated from theory, as are the rate of change of current records except for the superposed high-frequency oscillations occurring just as the surge is initiated. These superposed oscillations have a frequency of about 40 megacycles and are probably caused by stray capacitance across parts of the discharge circuit, such as from one ball of the tripping gap to ground. If this stray capacitance is across a section of the discharge circuit having an inductance of 2 μh, it would require only about 10 $\mu\mu$f to produce the 40 megacycle oscillations. It is practically impossible to eliminate such stray capacitances. In the discharge circuit used in obtaining the oscillograms of figure 8, stray capacitances were reduced to as low a value as possible. For discharge circuits involving fairly large apparatus as a test specimen, stray capacitances will be larger, resulting in a superposed oscillation of lower frequency.

The slight upward curvature on the zero line

of oscillograms in figures 8, b and 8, d at the start of the sweep is introduced by the oscillograph and should not be considered as part of the surge record. The source of this "hook" in the CRO zero line is a small horizontal deflection given to the beam by the Norinder relay plates as voltage is initially applied to them. This deflection slightly alters the CRO sweep rate at its beginning but should, by itself, introduce no vertical deflection. However, since the focusing coil is located below the Norinder relay plates, this deflection puts the beam slightly off the axis of the focusing coil which then produces the small vertical deflection.

The oscillograms in figure 8 illustrate the advantages of using a mutual inductor in addition to a shunt when measurements of a current surge are being made. The superposed oscillations cannot be detected on the current record but can readily be seen and measured on the rate-of-change-of-current record. Their actual magnitudes in amperes can be computed from this record, and from measurements on the oscillogram of figure 8, d they were found to have a maximum amplitude of about 25 amp. Oscillations of this magnitude would be almost impossible to detect on a current record even though the attenuation of the shunt for these higher frequencies did not mask them out. The rate of change of current records are also of great value in studying the effects of induced voltages arising from the current surge. They further provide an accurate measurement for the time to maximum current (zero rate of change).

VI. References

[1] P. L. Bellaschi, Heavy surge currents—generation and measurement, Electrical Eng. **53,** 86 (Jan. 1934).

[2] T. Brownlee, Discussion of Bellaschi's paper, Heavy surge currents—generation and measurement, Electrical Eng. **53,** 481 (Mar. 1934).

[3] N. Rohats, A surge-current generator, General Electric Rev. **37,** 296 (June 1934).

[4] F. B. Silsbee, A study of the inductance of four-terminal resistance standards, Bul BS **13,** 375 (1916) S281.

[5] F. B. Silsbee, Notes on the design of four-terminal resistance standards for alternating current, BS J. Research **4, 73** (1930). RP133.

VII. Appendices

1. Effective Impedance of a Tubular Shunt as a Function of Frequency [6]

Let the radii of the inner and outer tubes be a, b, a', and b' as indicated in figure 9. Assuming the tubes to be coaxial and perfectly symmetrical about their axis the current density in either tube at a given radius, r, from the axis will be a constant for any given instant, so let

i_r = current density in inner tube at radius r, + if into paper

i_r' = current density in outer tube at radius r, + if into paper

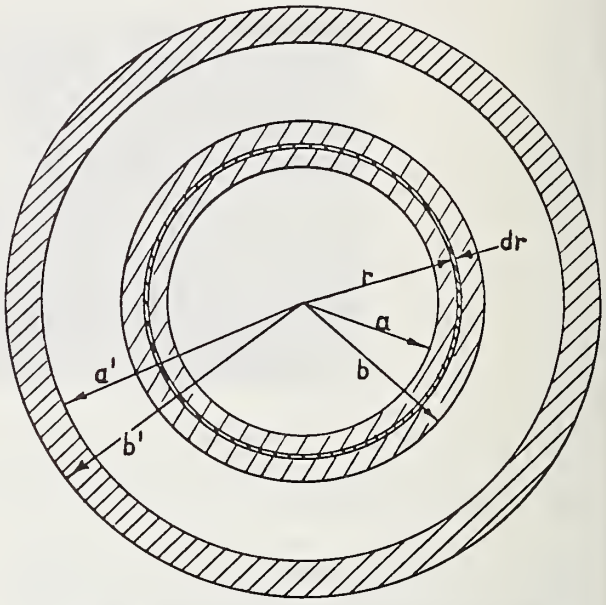

FIGURE 9.—*Cross-sectional view of a tubular shunt.*

Then

I = total instaneous current in inner tube

$$= \int_a^b 2\pi i_r r\,dr$$

I' = total instantaneous current in outer tube

$$= \int_{a'}^{b'} 2\pi i_r' r\,dr$$

Also, let:

e = emf drop per unit length of inner tube

e' = emf drop per unit length of outer tube

H_r = magnetic field at r taken + if clockwise

ρ = resistivity of inner tube material

ρ' = resistivity of outer tube material

Φ_r = total magnetic flux outside of radius r (all permeabilities assumed = 1).

NOTE.—The cgs magnetic system of units is used throughout this derivation and all dimensions are in centimeters.

[6] This derivation is taken from hitherto unpublished notes of F. B. Silsbee.

As all currents flow along lines parallel to the tube axis, e and e' are independent of r, so

$$e=\rho i_r+\frac{\partial \Phi_r}{\partial t} \tag{9}$$

$$e'=\rho' i_r'+\frac{\partial \Phi_r}{\partial t} \tag{10}$$

and

$$\frac{\partial e}{\partial r}=\rho \frac{\partial i_r}{\partial r}+\frac{\partial}{\partial t}\frac{\partial \Phi_r}{\partial r}=0 \tag{11}$$

$$\frac{\partial e'}{\partial r}=\rho' \frac{\partial i_r'}{\partial r}+\frac{\partial}{\partial t}\frac{\partial \Phi_r'}{\partial r}=0 \tag{12}$$

For the inner tube

$$\Phi_r=\int_r^b \frac{2I_z}{x}\,dx+2I\log\frac{a'}{b}+\int_{a'}^{b'}\frac{2(I+I_z')}{x}\,dx \tag{13}$$

where

$$I_z=\int_a^x 2\pi i_r r dr \text{ and } I_z'=\int_{a'}^x 2\pi i_r r dr$$

For $r>b'$, $\Phi_r=0$. Differentiating eq 13 with respect to r

$$\frac{\partial \Phi_r}{\partial r}=-\frac{2I_r}{r}=-\frac{2}{r}\int_a^r 2\pi i_r r dr \tag{14}$$

Similarly for the outer tube,

$$\Phi_r'=\int_r^{b'}\frac{2(I+I_z')}{x}\,dx \tag{15}$$

and

$$\frac{\partial \Phi_r'}{\partial r}=-\frac{2(I+I_z')}{r}=-\frac{2}{r}\left[I+\int_{a'}^r 2\pi i_r' r dr\right]=+\frac{2}{r}\int_r^{b'} 2\pi i_r' r dr \tag{16}$$

since $I=-\int_{a'}^{b'} 2\pi i_r' r dr$

Inserting eq 14 in eq 11 and eq 16 in eq 12,

$$r\frac{\partial i_r}{\partial r}=\frac{4\pi}{\rho}\frac{\partial}{\partial t}\int_a^r i_r r dr \tag{17}$$

$$r\frac{\partial i_r'}{\partial r}=-\frac{4\pi}{\rho'}\frac{\partial}{\partial t}\int_r^{b'} i_r' r dr \tag{18}$$

Differentiating again with respect to r

$$r\frac{\partial^2 i_r}{\partial r^2}+\frac{\partial i_r}{\partial r}-\frac{4\pi}{\rho} r\frac{\partial i_r}{\partial t}=0 \tag{19}$$

$$r\frac{\partial^2 i_r'}{\partial r^2}+\frac{\partial i_r'}{\partial r}-\frac{4\pi}{\rho'} r\frac{\partial i_r'}{\partial t}=0 \tag{20}$$

If $i_r=I_0 e^{j\omega t}$

$$\frac{\partial}{\partial t} i_r=+j\omega i_r$$

and eq 19 and 20 become

$$\frac{\partial^2 i_r}{\partial r^2}+\frac{1}{r}\frac{\partial i_r}{\partial r}+K^2 i_r=0 \tag{21}$$

$$\frac{\partial^2 i_r'}{\partial r^2}+\frac{1}{r}\frac{\partial i_r'}{\partial r}+K'^2 i_r'=0 \tag{22}$$

where $K^2=-j\omega\frac{4\pi}{\rho}$ and $K'^2=-j\omega\frac{4\pi}{\rho'}$, the solution of eq 21 is

$$i_r=Z_0(Kr)=C_1 J_0(Kr)+C_2 N_0(Kr) \tag{23}$$

where J_0 and N_0 are Bessel's functions of order 0 and of the first and second kind. C_1 and C_2 are constants of integration. Similarly the solution to eq 22 is

$$i_r'=Z_0'(K'r)=C_1' J_0(K'r)+C_2' N_0'(K'r) \tag{24}$$

The total current is

$$I=2\pi\int_a^b i_r r dr=2\pi\int_a^b r Z_0(Kr)\,dr \tag{25}$$

and from the general relation

$$\int x Z_0(\alpha x)dx=\frac{1}{\alpha} x Z_1(\alpha x) \tag{26}$$

it follows that

$$I=\frac{2\pi}{K}[bZ_1(Kb)-aZ_1(Ka)] \tag{27}$$

Similarly

$$I'=\frac{2\pi}{K'}[b'Z_1'(K'b')-a'Z_1'(K'a')] \tag{28}$$

Likewise

$$I_z=\frac{2\pi}{K}[xZ_1(Kx)-aZ_1(Ka)] \tag{29}$$

$$I_z'=\frac{2\pi}{K'}\left[xZ_1'(K'x)-a'Z_1'(K'a')\right] \tag{30}$$

To obtain values for the Φ_r's substitute eq 29 and 30 in eq 13 and 15. For the inner tube, after performing the integrations

$$\Phi_r=\frac{4\pi}{K^2}\left[-Z_0(Kx)\right]_r^b-\frac{4\pi aZ_1(Ka)}{K}\log\frac{b}{r}+2I\log\frac{b'}{b}+\frac{4\pi}{K'^2}\left[-Z_0'(K'x)\right]_{a'}^{b'}-\frac{4\pi a'Z_1'(K'a')}{K'}\log\frac{b'}{a'} \tag{31}$$

For the outer tube

$$\Phi_r'=2I\log\frac{b'}{r}+\frac{4\pi}{K'^2}\left[-Z_0'(K'x)\right]_r^{b'}-\frac{4\pi a'Z_1'(K'a')}{K'}\log\frac{b'}{r} \tag{32}$$

The voltage drop in the outer tube is

$$e'=\rho' i_r'+\frac{\partial\Phi_r'}{\partial t}$$

After substituting and simplifying

$$e'=\rho'\left\{\frac{2j\omega I}{\rho'}\log b'+K'a'Z_1'(K'a')\log b'+Z_0'(K'b')-\log r\left[\frac{2j\omega I}{\rho'}+K'a'Z_1'(K'a')\right]\right\} \tag{33}$$

Since e' is not a function of r, the coefficient of $\log r$ in eq 33 must vanish, this gives

$$Z_1'(K'a')=\frac{K'}{2\pi a'}I \tag{34}$$

This is one relation fixing the coefficients in Z_0'. The other relation is in eq 28. Substituting eq 34 in eq 28 gives

$$Z_1'(K'b')=0. \tag{35}$$

Voltage drop in inner tube is, similarly

$$e=\rho Z_0(Kb)+Ka\rho Z_1(Ka)\log b-Ka\rho Z_1(Ka)\log r+2Ij\omega\log\frac{b'}{b}+\rho'[Z_0'(K'b')-Z_0'(K'a')]+\rho'K'a'Z_1'(K'a')\log\frac{b'}{a'} \tag{36}$$

Coefficient of terms involving r must be zero, therefore

$$Z_1(Ka)=0 \tag{37}$$

Putting eq 37 in eq 27

$$Z_1(Kb)=\frac{KI}{2\pi b} \tag{38}$$

Inserting eq 37 and 34 in eq 36 gives

$$e=\rho Z_0(Kb)-2Ij\omega\log\frac{b}{a'}+\rho'[Z_0'(K'b')-Z_0'(K'a')] \tag{39}$$

The effective four-terminal impedance for a shunt with the potential lead inside the inner tube is

$$z=\frac{e-\frac{\partial}{\partial t}\Phi_a}{I}$$

From eq 31, 34 and 37

$$\frac{\partial \Phi_a}{\partial t} = \rho Z_0(Kb) - \rho Z_0(Ka) + \rho'[Z_0'(K'b') - Z_0'(K'a')] - 2j\omega I \log \frac{b}{a'} \tag{40}$$

Subtracting eq 40 from 39

$$e - \frac{\partial}{\partial t} \Phi_a = \rho Z_0(Ka) \text{ or } z = \frac{\rho Z_0(Ka)}{I} \tag{41}$$

From eq 24 and 34

$$Z_1'(K'a') = \frac{K'}{2\pi a'} I = C_1' J_1'(K'a') + C_2' N_1'(K'a') \tag{42}$$

From eq 24 and 35

$$Z_1'(K'b') = 0 = C_1' J_1'(K'b') + C_2' N_1(K'b') \tag{43}$$

From eq 23 and 37

$$Z_1(Ka) = 0 = C_1 J_1(Ka) + C_2 N_1(Ka) \tag{44}$$

From eq 23 and 38

$$Z_1(Kb) = \frac{KI}{2\pi b} = C_1 J_1(Kb) + C_2 N_1(Kb) \tag{45}$$

Solving eq 42, 43, 44, and 45 for the coefficients

$$C_1' = \frac{K'I}{2\pi a'} \frac{N_1(K'b')}{D'}$$

$$C_2' = \frac{K'I}{2\pi a'} \frac{J_1(K'b')}{D'},$$

where $D' = J_1(K'a') N_1(K'b') - J_1(K'b') N_1(K'a')$,

$$C_1 = -\frac{KI}{2\pi b} \frac{N_1(Ka)}{D} \tag{46}$$

$$C_2 = \frac{KI}{2\pi b} \frac{J_1(Ka)}{D}, \tag{47}$$

where $D = J_1(Ka) N_1(Kb) - J_1(Kb) N_1(ka)$.

From eq 23

$$Z_0(Ka) = C_1 J_0(Ka) + C_2 N_0(Ka)$$

Using this and putting in values of C_1 and C_2 from eq 46 and 47 eq 41 becomes

$$z = \frac{\rho K}{2\pi b} \left[\frac{N_0(Ka) J_1(Ka) - N_1(Ka) J_0(Ka)}{J_1(Ka) N_1(Kb) - J_1(Kb) N_1(Ka)} \right] \tag{48}$$

Using the general relation

$$N_0(Ka) J_1(Ka) - N_1(Ka) J_0(Ka) = \frac{2}{\pi Ka}$$

eq 48 becomes

$$\therefore z = \frac{\rho}{\pi^2 ab} \frac{1}{J_1(Ka) N_1(Kb) - J_1(Kb) N_1(Ka)} \tag{49}$$

Using the following general relations

$$J_1(Ka)=\sqrt{\frac{2}{\pi Ka}}\left[P_1(Ka)\sin\left(Ka-\frac{\pi}{4}\right)+Q_1(Ka)\cos\left(Ka-\frac{\pi}{4}\right)\right]$$

$$N_1(Kb)=\sqrt{\frac{2}{\pi Kb}}\left[-P_1(Kb)\cos\left(Kb-\frac{\pi}{4}\right)+Q_1(Kb)\sin\left(Kb-\frac{\pi}{4}\right)\right],$$

letting $b-a=d$, and putting in the following approximate values of P_1 and Q_1

$$P_1(Ka)=1+\frac{15}{128K^2a^2}$$

$$Q_1(Ka)=\frac{3}{8Ka}$$

the denominator of eq 49 becomes, for $K^2=-jm^2$

$$D_s=\frac{\sqrt{2ab}(1-j)\pi}{m}\left\{\left[\left(1+j\frac{15}{128m^2a^2}\right)\left(1+j\frac{15}{128m^2b^2}\right)+j\frac{9}{64abm^2}\right]\sin\frac{md}{\sqrt{2}}(1-j)+\right.$$

$$\left.\left[\left(1+j\frac{15}{128m^2a^2}\right)\left(\frac{3+3j}{8mb\sqrt{2}}\right)-\left(1+j\frac{15}{128m^2b^2}\right)\left(\frac{3+3j}{8ma\sqrt{2}}\right)\right]\cos\frac{md}{\sqrt{2}}(1-j)\right\} \tag{50}$$

Most of the terms inside the brackets in eq 50 are negligible if the frequency is much above 60 cycles per second. If $f=1{,}000$ c/s, $\rho\leqq 40{,}000$ (cgs units), $(b\text{-}a)\leqq 0.06$ cm, and $b=a=1$ (approximately), this equation simplifies to

$$D_s=\frac{\sqrt{2ab}(1-j)\pi}{m}\sin\frac{md}{\sqrt{2}}(1-j) \tag{51}$$

Letting $\frac{md}{\sqrt{2}}=\delta$ and putting eq 51 back in eq 49

$$z=\frac{\rho\delta}{2\pi d\sqrt{ab}}\left[\frac{(\sin\delta\cosh\delta+\cos\delta\sinh\delta)+j(\cos\delta\sinh\delta-\sin\delta\cosh\delta)}{(\sin\delta\cosh\delta)^2+(\cos\delta\sinh\delta)^2}\right] \tag{52}$$

where

ρ = resistivity of shunt material in cgs units
a = inner radius of shunt tube in cm
b = outer radius of spread tube in cm
d = thickness of shunt-tube wall in cm
$\omega=2\pi$ times the frequency of the current through the shunt.
z = vector impedance of shunt for values of above quantities used.
The d-c resistance of the tube in absohms, for $d<b$ is

$$R_{dc}=\frac{\rho}{2\pi d\sqrt{ab}} \tag{53}$$

and eq 52 becomes

$$z=R_{dc}\delta\left[\frac{(\sin\delta\cosh\delta+\cos\delta\sinh\delta)+j(\cos\delta\sinh\delta-\sin\delta\cosh\delta)}{(\sin\delta\cosh\delta)^2+(\cos\delta\sinh\delta)^2}\right] \tag{54}$$

Equation 54 is very nearly correct for any thin-wall tube when the frequency is above 1,000 cycles per second.

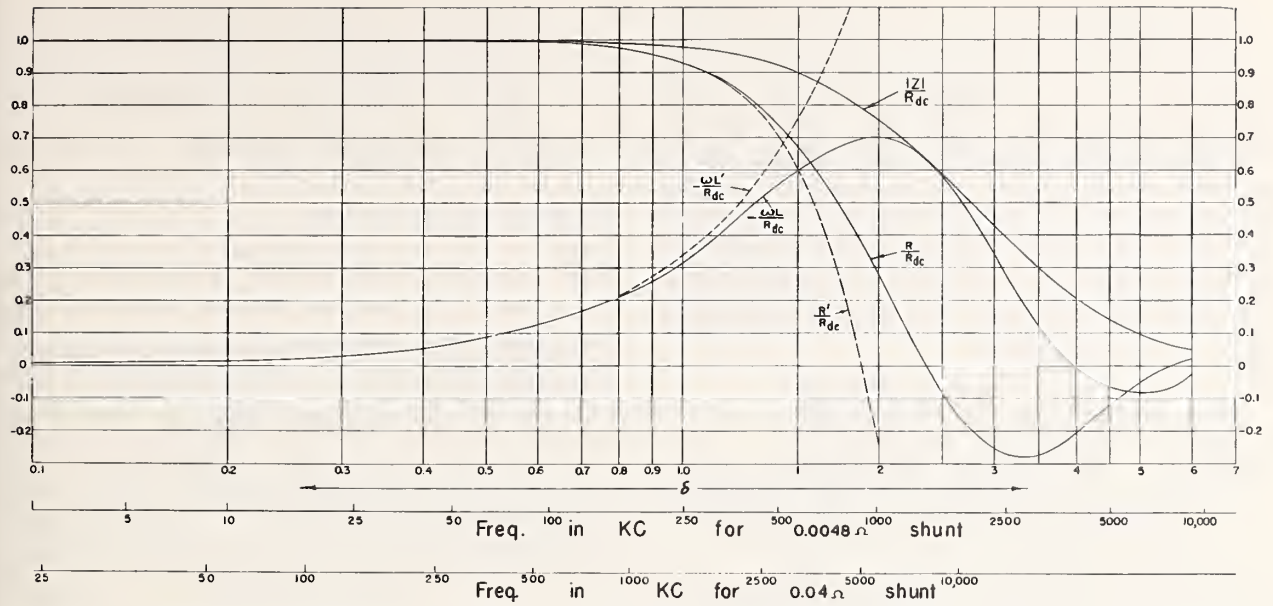

FIGURE 10.—*Curves showing ratios of a-c resistance R, reactance ωL, and impedance Z, to d-c resistance R_{dc}, plotted as ordinates against the parameter, δ, as abscissa.*

Abscissa scales in frequency are also shown for two tubular shunts. The solid-line curves were obtained from the formula derived in appendix 1. The dashed-line curves from formulas known to be applicable only at lower frequencies.

For lower frequencies, the skin effect formula as given on page 91 of Research Paper No. 133 (see reference 5) is

$$R=R_{dc}\left(1-\frac{7m^4d^4}{360}\right)=R_{dc}\left(1-\frac{7}{90}\,\delta^4\right) \qquad (55)$$

The inductance at lower frequencies, where the current is assumed to be uniformly distributed as given on p. 400 of Scientific Paper S281 (see reference 4) is, in abhenries per centimeter,

$$L=-\frac{d}{3a}.$$

For $d<<b$ this gives

$$\frac{\omega L}{R_{dc}}=-\frac{\delta^2}{3} \qquad (56)$$

Actual values of R/R_{dc}, $\omega L/R_{dc}$, and $|z|/R_{dc}$ as functions of δ are shown by the curves in figure 10. The solid lines represent values obtained from eq 54 and the broken lines values from eq 55 and 56. For $\delta<1$, the broken and solid curves coincide, but for $\delta>1$ the values obtained from eq 55 and 56 exhibit rapidly increasing errors as would be expected from the assumptions made in the derivation of these equations.

Frequency scales are also given on these curves for the two shunts in use at this laboratory.

2. Magnetic Force Due to Current in a Tube

Referring to figure 9, the magnetic field (H_r) at any point r distance from the axis of the tube, where $a<r>b$, for a total current, I, in abamperes uniformly distributed over the cross section of the tube, is

$$H_r=\frac{r^2-a^2}{b^2-a^2}\,\frac{2I}{r}.$$

The current density inside the metal of the tube is

$$i=\frac{I}{\pi(b^2-a^2)}.$$

The total current in the shell of thickness dr is

$$i_r=i2\pi r dr=\frac{2rI}{b^2-a^2}\,dr.$$

The total radial force (directed inward) on this shell of current, due to the magnetic field H_r is

$$F_r=i_rH_r$$

in dynes per centimeter length of tube. The total force on the entire tube per centimeter of length is

$$F=\int_a^b F_r=\int_a^b \frac{r^2-a^2}{(b^2-a^2)^2}\,4I^2dr$$

Performing the integration

$$F=\frac{4I^2}{(b^2-a^2)^2}\left(\frac{b^3}{3}-a^2b+\frac{2a^3}{3}\right)$$

This force expressed as a pressure per square centimeter is

$$P=\frac{F}{2\pi b}=\frac{2I^2}{\pi b(b^2-a^2)^2}\left(\frac{b^3}{3}-a^2b+\frac{2a^3}{3}\right),$$

which simplifies to

$$P=\frac{2I^2}{3\pi b}\left[\frac{1}{b+a}+\frac{a}{(b+a)^2}\right],$$

which is the pressure in dynes per square centimeter.

The collapsing pressure for thin-wall tubing as obtained from A. E. H. Dove's formula [7] is

$$P_c=\frac{2E}{1-m^2}\left(\frac{t}{D}\right)^3.$$

E is the modulus of elasticity and m is Poisson's ratio for the tube material; t is the wall thickness of the tube and D is its diameter. If E is expressed in dynes per square centimeter, the collapsing pressure P_c will also be in dynes per square centimeter. Equating this to the magnetically induced pressure due to current, I, as obtained above and solving for I, we obtain the current in abamperes at which the tube will collapse

$$I=1.085\sqrt{\frac{E}{1-m^2}\frac{(b-a)^3(b+a)^2}{b^2(b+2a)}}.$$

3. Effective Inductance of a Type I Concentric-Tube Mutual Inductor as a Function of Frequency

In a type I concentric-tube mutual inductor, shown schematically in figure 11, the current, I, whose rate of

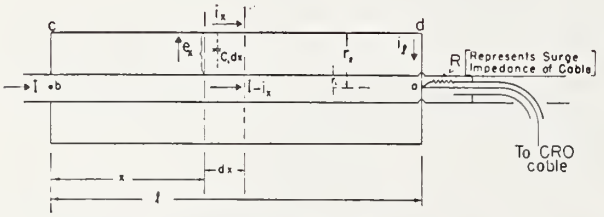

FIGURE 11.—*Schematic drawing of a type I concentric tube mutual inductor.*

change is to be measured, passes through the inner tube and the return circuit for this current is assumed to be far enough away (about 24 in.) so that its effect can be neglected. The secondary circuit of this mutual inductor consists of the length of the inner tube from a to b, the radial ring from b to c, the outer tube from c to d, and the four-wire "spider" from d to a. It is considered to be completed by the resistance, R, which represents the surge impedance of the cable to the CRO. Assuming that (1) all currents flowing in these tubes are uniformly distributed around the central axis, (2) end effects may be neglected, and (3) shunting capacitance from the outer tube to outside conductors may be neglected, differential equations can be written giving the relations of the currents in the tubes to the voltage difference between the tubes at any longitudinal distance, x, from the end of the outer tube. Using symbols defined as follows:

M_1 = mutual inductance per centimeter length of the inner tube, between it and the secondary circuit. Its value is very nearly the same as the self-inductance of the secondary circuit if the wall thickness of each tube is small.

[7] Taken from Marks' Handbook for Mechanical Engineers, Fourth Edition, p. 450

C_1 = capacitance per centimeter length between the inner and outer tubes,

e_x = the potential difference between the inner and outer tubes at the distance, x, from the end of the outer tube,

i_x = the current in the outer tube at the distance x from the end of the outer tube.

the differential equations are

$$di_x=j\omega C_1e_xdx \tag{57}$$

and

$$de_x=j\omega M_1(I-i_x)dx. \tag{58}$$

The solution of these differential equations gives equations for i_x and e_x containing two arbitrary constants:

$$e_x=K_1\sinh\left[\omega x\sqrt{C_1M_1}+K_2\right] \tag{59}$$

$$i_x=I+jK_1\sqrt{\frac{C_1}{M_1}}\cosh\left[\omega x\sqrt{C_1M_1}+K_2\right] \tag{60}$$

To obtain values for the arbitrary constants K_1 and K_2, use relations at $x=0$ and $x=l$. At $x=0$, $e_x=0$ and from eq 59

$$0=K_1\sinh\left[0+K_2\right].$$

As K_1 cannot be zero, $K_2=0$.
At $x=l$, $e_x=i_lR$, and from eq 59

$$K_1=\frac{i_lR}{\sinh\omega l\sqrt{C_1M_1}}.$$

Putting values of K_1 and K_2 in eq 60

$$i_x=I+j\frac{i_lR}{\sinh\omega l\sqrt{C_1M_1}}\sqrt{\frac{C_1}{M_1}}\cosh\omega x\sqrt{C_1M_1}$$

at $x=l$

$$i_l\left[1-jR\sqrt{\frac{C_1}{M_1}}\frac{1}{\tanh\omega l\sqrt{C_1M_1}}\right]=I \tag{61}$$

To get a relation between the voltage impressed on the CRO cable (i_lR) and the rate of change of the current being measured (dI/dt), multiply eq 61 by $j\omega M_1l$ and take R out of the brackets

$$i_lR\left[\frac{j\omega M_1l}{R}+\omega M_1l\sqrt{\frac{C_1}{M_1}}\frac{1}{\tanh\omega l\sqrt{C_1M_1}}\right]=j\omega M_1lI.$$

As $M_1l=M$, the total mutual inductance, the above equation becomes

$$\frac{i_lR}{M}\left[\frac{\omega l\sqrt{M_1C_1}}{\tanh\omega l\sqrt{M_1C_1}}+j\frac{\omega M}{R}\right]=j\omega I. \tag{62}$$

In this equation i_lR is the voltage impressed on the cable going to the CRO and thus is equal to the voltage recorded by the CRO. The value of M is constant and may be computed from the dimensions of the mutual inductor. The right-hand side of this equation is the rate of change of the current, I, being measured. The quantity in the brackets is unity for all but the higher frequencies. Thus, for most surge work the rate of change of the current being measured is obtained by dividing the voltage recorded at the CRO by the constant M. In order to determine the upper limit of frequency for which this relation holds, the magnitude of the vector quantity in the bracket must be

evaluated as a function of frequency. When the hyperbolic tangent is replaced by the first two terms in its series expansion the magnitude of this quantity becomes:

$$1+\omega^2\left(\frac{M_1C_1l^2}{3}+\frac{M^2}{2R^2}\right).$$

As shown by eq 5 and 6 in the main part of this paper, the product $M_1C_1=1.11\times10^{-21}$ and is the same for any pair of coaxial tubes provided they have thin walls. l is the length of the secondary circuit tube in centimeters. M is the total mutual inductance of the inductor in henries and can be computed from its dimensions as already shown in the main part of this paper. R is the surge impedance in ohms of the cable connected to the potential terminals of the inductor and going to the CRO where it is terminated by a resistance equal to R.

For the type I concentric-tube mutual inductor constructed and used at this laboratory $l=17.8$ cm and $M=0.05\mu$h. The surge impedance of the CRO cable, R, is 50 ohms. For these particular values, the magnitude of the quantity in the brackets of eq 62 varies with frequency as follows:

Frequency	
c/sec.	
30×10^6	1.02
40	1.03_8
50	1.06
60	1.08_6
70	1.11_7
80	1.15_5

For this example of a type I concentric-tube mutual inductor, the rate of change of current as measured at the CRO will be correct to within 10 percent for all frequencies up to about 65 megacycles.

4. Effective Inductance of a Type II Concentric-Tube Mutual Inductor as a Function of Frequency

In a type II concentric-tube mutual inductor as shown schematically in figure 12 the current, I, whose rate of change is to be measured passes through the inner tube (radius r_1) and returns through the outer tube (radius r_3). With this arrangement the current terminals are close together and the self-inductance of the primary current circuit is fixed and quite small. The secondary circuit of this mutual inductor is the same as that of the type I inductor. Making the same assumptions as stated in appendix 3, differential equations can be written giving the relations between currents in the three tubes and voltage differences between the tubes at any longitudinal distance, x, from the end of the middle tube (radius r_2). Using symbols defined as follows:

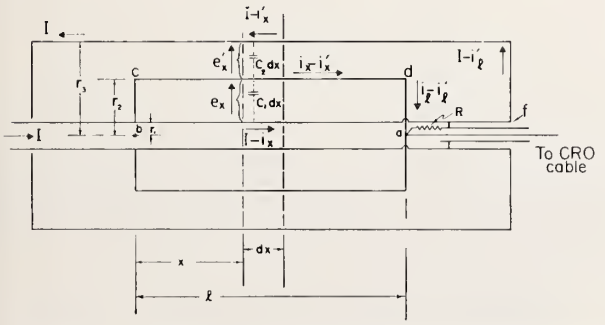

FIGURE 12.—*Schematic drawing of a type* II *concentric tube mutual inductor*

M_1 = mutual inductance per centimeter length of the inner tube, between it and the secondary circuit. This is the same as the self-inductance of the secondary circuit if the wall thickness of each tube is small,

L_2 = self-inductance per cm of the circuit formed by the middle and outer tubes,

C_1 = capacitance per cm between the inner and middle tubes,

C_2 = capacitance per cm between the middle and outer tubes,

e_x = the potential difference between the inner and middle tubes at distance, x, from the end of the middle tube,

e'_x = the potential difference between the middle and outer tubes at distance, x, from the end of the middle tube,

i_x = that part of the current flowing at x in the middle tube whose return path is in the inner tube,

i'_x = that part of the current flowing at x in the middle tube whose return path is in the outer tube,

L_0 = self-inductance of the circuit formed by the inner and outer tubes from a to f. The differential equations are

$$di_x=j\omega C_1e_xdx \tag{63}$$

$$di'_x=j\omega C_2e'_xdx \tag{64}$$

$$de_x=j\omega M_1(I-i_x)dx \tag{65}$$

$$de'_x=-j\omega L_2(I-i'_x)dx. \tag{66}$$

The solutions of eq 63 and 65 are

$$e_x=K_1\sinh\left[\omega x\sqrt{C_1M_1}+K_2\right] \tag{67}$$

and

$$i_x=I+jK_1\sqrt{\frac{C_1}{M_1}}\cosh\left[\omega x\sqrt{C_1M_1}+K_2\right] \tag{68}$$

The solutions of eq 64 and 66 are

$$e'_x=K_3\sin\left[\omega x\sqrt{L_2C_2}+K_4\right] \tag{69}$$

$$i'_x=I-jK_3\sqrt{\frac{C_2}{L_2}}\cos\left[\omega x\sqrt{L_2C_2}+K_4\right]. \tag{70}$$

The arbitrary constants K_1, K_2, K_3, and K_4 in the above equations can be determined by using the terminal conditions at $x=0$ and $x=l$.

At $x=0$, $e_x=0$, and $i_x'=0$. So from eq 67

$$0=K_1\sinh\left[0+K_2\right],$$

but K_1 cannot be zero, therefore $K_2=0$. Also, from eq 70

$$0=I-jK_3\sqrt{\frac{C_2}{L_2}}\cos K_4$$

giving

$$K_3=-j\sqrt{\frac{L_2}{C_2}}\frac{I}{\cos K_4}$$

At $x=l: e_x=R(i_l-i_l')$ and $e_x'=R(i_l-i_l')+j\omega L_0(I-i_l')$.

So from eq 67, after putting in value of K_2,

$$K_1=\frac{R(i_l-i_l')}{\sinh \omega l\sqrt{C_1M_1}}$$

Also, from eq 69, after putting in value of K_3

$$\tan K_4=-\tan \omega l\sqrt{L_2C_2}+\frac{j\sqrt{\frac{C_2}{L_2}}}{I\cos \omega l\sqrt{C_2L_2}}[R(i_l-i_l')+j\omega L_0(I-i_l')].$$

Using above values of K_1 and K_2 eq 68 at $x=l$ gives

$$i_l=I+jR(i_l-i_l'')\sqrt{\frac{C_1}{M_1}}\frac{1}{\tanh \omega l\sqrt{M_1C_1}} \tag{71}$$

Using above values of K_3 and K_4 eq 70 at $x=l$ gives

$$i_l''=I-\frac{I}{\cos \omega l\sqrt{C_2L_2}}+j\sqrt{\frac{C_2}{L_2}}\tan \omega l\sqrt{L_2C_2}\,[R(i_l-i_l'')+j\omega L_0(I-i_l'')] \tag{72}$$

Subtracting eq 72 from eq 71 and assuming i_l'' to be very small compared to I in the $j\omega L_0$ term, a value for R $(i-i\,)$, the voltage across the CRO cable, is obtained

$$(i_l-i_l'')R\left[\frac{\frac{\omega l\sqrt{M_1C_1}\cos \omega l\sqrt{L_2C_2}}{\tanh \omega l\sqrt{M_1C_1}}-\omega M_1l\sqrt{\frac{C_2}{L_2}}\sin \omega l\sqrt{L_2C_2}+j\frac{\omega M_1l}{R}\cos \omega l\sqrt{L_2C_2}}{1+\omega L_0\sqrt{\frac{C_2}{L_2}}\sin \omega l\sqrt{L_2C_2}}\right]=j\omega M_1lI$$

For concentric-tubular construction, if the wall thickness of the tubes is neglected the product of capacitance and inductance per cm is a constant for any two tubes. So let $\sqrt{M_1C_1}=\sqrt{L_2C_2}=a=3.33\times10^{-11}$. Also let $M_1l=M$, the total mutual inductance, then the above equation becomes

$$(i_1-i_l'')R\left[\frac{\frac{\omega al\cos \omega al}{\tanh \omega al}-\omega M\sqrt{\frac{C_2}{L_2}}\sin \omega al+j\frac{\omega M}{R}\cos \omega al}{1+\omega L_0\sqrt{\frac{C_2}{L_2}}\sin \omega al}\right]=j\omega MI$$

By expanding the first term in the numerator of the quantity in the brackets in series form and neglecting higher order terms, the equation becomes

$$\frac{(i_l-i_l'')R}{M}\left[\frac{1-\frac{(\omega al)^2}{6}-\omega M\sqrt{\frac{C_2}{L_2}}\sin \omega al+j\frac{\omega M}{R}\cos \omega al}{1+\omega L_0\sqrt{\frac{C_2}{L_2}}\sin \omega al}\right]=j\omega I \tag{73}$$

This equation is similar to eq 62 of appendix 3 for a type I mutual inductor. Thus, to determine the upper limit of frequency for which a type II inductor can be used, the magnitude of the vector quantity in the brackets of eq 73 must be evaluated as a function of frequency.

A type II mutual inductor having the following dimensions (see fig. 12):

$r_1=0.5$ in.
$r_2=1.0$ in.
$r_3=2$ in.
$l=7$ in.
distance from a to $f=2.5$ in.

is used as an example. By use of eq 5 and 6 in the main part of this paper values for M_1 L_2, C_2, and L_0 may be computed from these dimensions. Then, assuming the CRO cable surge impedance, R, to be 50 ohms, the magnitude of the quantity in the bracket of eq 73 varies with frequency as follows:

Frequency	
c/sec	
10×10^6	0. 998
30	. 982
50	. 952
60	. 932
70	. 908
80	. 885
90	. 861
100	. 835

For this example of a type II concentric-tube mutual inductor the rate of change of current as measured at the CRO will be correct to within 10 percent for all frequencies up to 70 megacycles.

WASHINGTON, March 28, 1947.

JOURNAL OF RESEARCH of the National Bureau of Standards—C. Engineering and Instrumentation
Vol. 66C, No. 3, July–September 1962

Spark-Gap Flashover Measurements for Steeply Rising Voltage Impulses

J. H. Park and H. N. Cones

(March 19, 1962)

Two designs of thin ribbon resistors have been devised which are suitable for high-voltage surges and have very low time constants (2×10^{-9} sec). They were used in making up dividers for measuring linearly rising chopped impulses with peak voltages up to 300 kilovolts and times to sparkover from 0.03 to 50 microseconds. Errors in divider ratio due to residual inductance were found by computation to be less than 1 percent. Stray capacitance errors were kept low by making total divider resistance 1,000 ohms or less. By a combination of computation and experimentation, capacitance errors were deduced to be not greater than 1 percent for times to sparkover 0.1 microsecond or greater.

A large number of oscillograph records were obtained of spark-gap flashover voltage with linearly rising voltage impulses at rates of rise up to 10,000 kilovolts per microsecond. From these oscillograms data were derived giving a relation between rate of rise (or rise time) and flashover voltage for (1) 12.5-cm-diameter spheres spaced 6 cm apart, (2) 25-cm-diameter spheres spaced 6 cm, and (3) 6.5-inch-diameter uniform field electrodes spaced 5 cm. Volt-time curves showing these relations were plotted. It is recommended that the curve for 25-cm-diameter spheres be used as a reference standard for interlaboratory comparison of measurement methods.

1. Introduction

The measurement of wave form and peak value of a steeply rising voltage impulse is of considerable importance in the testing of high-voltage equipment such as insulators, transformers, and lightning arresters. Such measurements are usually made by impressing the voltage impulse on the high-voltage terminal of a divider consisting of resistors, capacitors, or a combination of both, and connecting the low side of the divider through a coaxial cable to the deflecting system of a cathode ray oscillograph (CRO). For measuring the peak value of full-wave impulses or waves chopped on the tail, the accuracy of dividers is well established, and measurement methods can readily be checked using standardized sphere-gap breakdown tables [1, 2, 3].[1] However, the sphere-gap tables cannot be used for times to sparkover less than 2 μsec, because for such short times, the sparkover[2] voltage of sphere gaps increases as time to sparkover decreases giving a volt-time curve. This was noted in 1935 by Bellaschi and Teague [4]. Hagenguth [5] has shown that rod gaps and insulator strings also exhibit a volt-time effect.

Several years ago, in AIEE Conference Paper No. 57–215, the present authors suggested the use of sphere-gap volt-time curves as reference standards for checking measurement methods at times to sparkover less than 2 μsec. Since that time work reported from other laboratories [6, 7, 8, 9, 10] has indicated that such a standard could be useful. The purpose of the present paper is to serve as a permanent published record of the work done several years ago and to present results of later work in this field at the National Bureau of Standards.

[1] Figures in brackets indicate the literature references at the end of this paper.
[2] The terms sparkover and flashover are assumed to have the same meaning.

2. Requirements for Setting Up Volt-Time Standards

Before volt-time curves can be considered for adoption as part of a standard, experimental data must be obtained and published by various laboratories working in the high-voltage field. Conditions under which the data for such curves are obtained must be decided upon, and they should be such that they can be readily duplicated in all laboratories. Ordinary laboratory conditions of temperature, pressure, and humidity should be satisfactory, provided corrections for relative air density are applied. All comparisons can then be made at 760 mm of Hg pressure and either 20 or 25 °C temperature. No applicable corrections for humidity are available, but records should be kept to see if any correlation between humidity and flashover voltage can be detected.

Another condition which must be controlled is the location of the spheres with respect to floor, leads, divider, surge generator, and any other nearby objects. International Electrotechnical Commission Publication 52 entitled "Recommendations for Voltage Measurements by Means of Sphere-Gaps (One Sphere Earthed)" contains very definite specifications for clearance distances when spheres are used for 60-cycle or full-wave voltages. It would seem logical, at first, to adopt these same specifications for front-chopped wave measurements. Also, the effect of changes in such distances should be determined.

In addition to the above, it is necessary to specify wave shape of the applied voltage before chopping. In fact, in all steep-front testing it is extremely important to be able to define waveform exactly and in detail so that results obtained in different laboratories can be accurately compared. This is

true not only for checking measurement methods, but also for comparing test data on high-voltage equipment. Thus, even though other means are found for checking measurement methods in various laboratories, the task of obtaining an accurately definable wave front must be completed before any steep-front chopped-wave tests will give results which can be repeated in other laboratories.

The presently accepted methods of defining wave front and rate of rise use either the 10 and 90 or 30 and 90 percent voltage points together with some restriction on superposed oscillations. Such definitions pin down only two points on the wave front and give no possibility of fixing tolerances. However, if a *linearly rising wave front is defined as one which rises at a constant rate from 30 to 100 percent*[3] *of flashover (or breakdown) voltage, any departure from the defined waveform can be determined.* Although linearly rising waves, free from oscillations and curvature, are not always readily obtained in practice, they can in all cases be attained to within the required tolerance with a little patience in choosing and adjusting circuit parameters. Since they offer the only possibility of setting up a standard steep-front wave shape which can be accurately duplicated in various laboratories, it is suggested that linearly rising waves be adopted as the standard. This does require setting up an allowable tolerance from an exactly constant rate of rise and devising a practical method for measuring rate of rise at all points from 30 to 100 percent of flashover voltage. Both of these problems are discussed and a solution suggested in appendix I.

The remainder of this paper is devoted to (1) a description of the methods used at the NBS to obtain points on the volt-time curves, (2) an analysis of the accuracy obtained, and (3) a presentation of the results.

3. Impulse Generator Circuit Arrangements for Obtaining a Linearly Rising Voltage

The circuit arrangement and general precautions needed to obtain a linearly rising voltage will probably vary considerably for different laboratories. The impulse generator used in the present work has a nominal rating of 2,000 kv when its twenty ⅓-μf capacitor units are connected in series. A modified connection of the 20 units, putting two sections (10 units in series for each) in parallel on discharge, was used in the present work, giving a rated discharge voltage of 1,000 kv. The breakdown voltages of the gaps used varied approximately from 140 to 300 kv depending on the rate of voltage rise. Thus, breakdown could always be made to take place on the linearly rising portion of the applied voltage, i.e., much before the knee of the exponential curve.

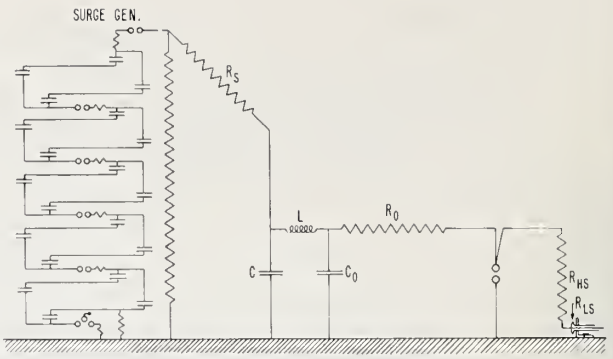

FIGURE 1. *Schematic diagram of impulse generator and discharge circuit used to obtain linearly rising voltages.*

A schematic diagram of the impulse generator and discharge circuit arrangement for obtaining various rates of voltage rise is shown in figure 1. Rate of voltage rise was controlled by (1) adjusting the generator charging voltage and/or (2) changing the time constant of the R-C circuit made up of "R_s" and "C." To keep rate of voltage rise linear up to breakdown, it was found that the charging voltage had to be maintained above about 50 percent of rated value. Thus large changes in rate of rise were made by using wide variation in R_s and C. Combinations of paper-oil capacitors connected in series were used to give fixed values of C as follows: 0.06, 0.006, 0.003, 0.002 μf (for steepest rates of rise $C=0$). R_s was made up of double wire-wound card resistors 2 in. wide and 12 in. long having values of 5, 15, 35, or 125 ohms each. They were used in series combinations giving values from 35 to 875 ohms. Because of residual inductance in the paper-oil capacitors, C resonates at about 1.3 Mc/s and produces oscillations on the rising front of the voltage across C. The lumped inductance "L" and capacitance "C_0" together with "R_0" act as a filter to give a smoothly rising voltage at the sphere gap. The inductor L consisted of 100 turns of polyethylene-insulated wire on a 2-in. diam bakelite tube, giving an inductance of 50 μh. The capacitor C_0 consisted of 3 aluminum hemispheres 1 m in diam, placed with their curved surfaces down and supported by porcelain-pedestal insulators so that the curved surfaces were kept about 8 in. above the conducting floor. The resistor R_0 consisted of the same type of cards as used for R_s, its value being held constant at 105 ohms (seven 15-ohm cards in series). Results were obtained with the test gaps at various distances from the aluminum hemispheres in order to study proximity effects.

4. Measurement-Methods and Dividers

Resistance dividers in conjunction with a cold-cathode CRO [11] were used for all measurements. Several different divider and gap arrangements (as indicated in figs. 2, 3, 4, 5, and 6) were tried to determine possible effects that the location of nearby conductors might have on either gap flashover or

[3] (Waveform below the 30 percent voltage point is not considered to be of importance in front-chopped testing because here the phenomenon being studied is dielectric failure for an applied voltage surge of short duration, and the mechanism probably is not initiated until the voltage magnitude approaches the full-wave breakdown value.)

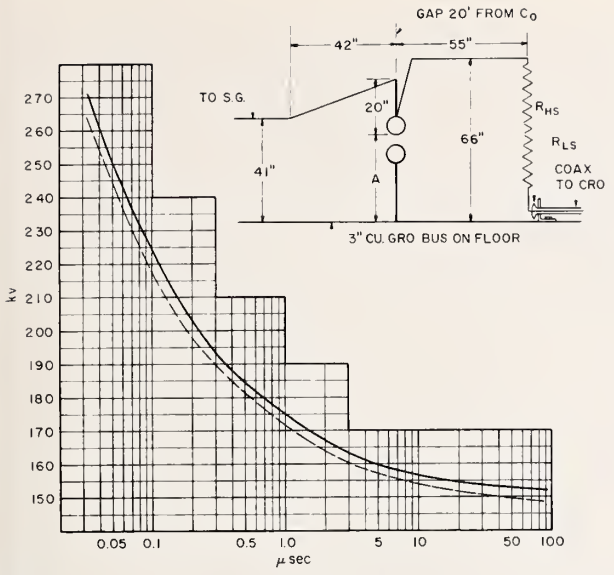

FIGURE 2. *Volt-time curve for 12.5-cm spheres spaced 6 cm, upper sphere negative.*

All voltages corrected to 760 mm of Hg and 25 °C. Solid curve obtained with A=34 in. Dashed curve with A=16 in. Insert shows sphere gap and divider arrangement. R_{HS}=1,000 ohms.

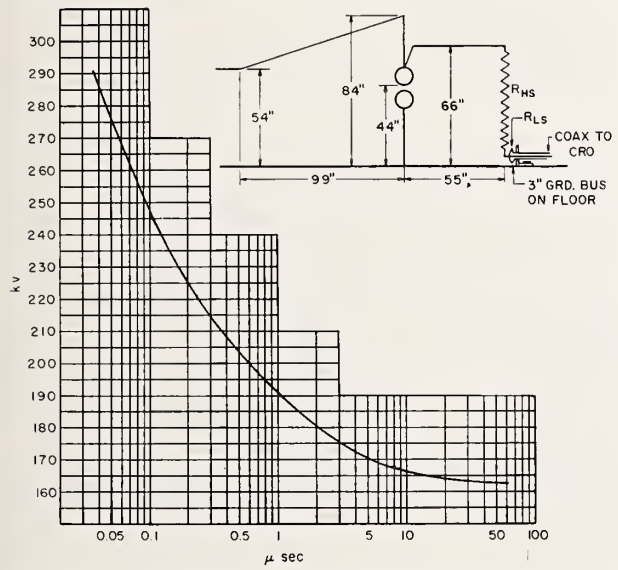

FIGURE 3. *Volt-time curve for 25-cm spheres spaced 6 cm, upper sphere negative.*

All voltages corrected to 760 mm of Hg and 25 °C. Insert shows sphere gap and divider arrangement. R_{HS}=1,000 ohms. Other sphere gap and divider arrangements also gave points falling on this curve.

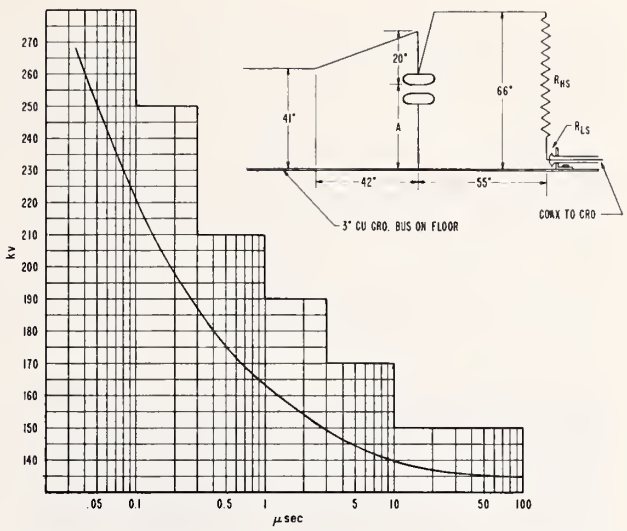

FIGURE 4. *Volt-time curve for uniform field gap, spacing 5 cm, upper electrode negative.*

All voltages corrected to 760 mm of Hg and 25 °C. Insert shows gap and divider arrangement. R_{HS}=1,000 ohms. Points obtained with A=20 in. and A=40 in. all fall on same curve.

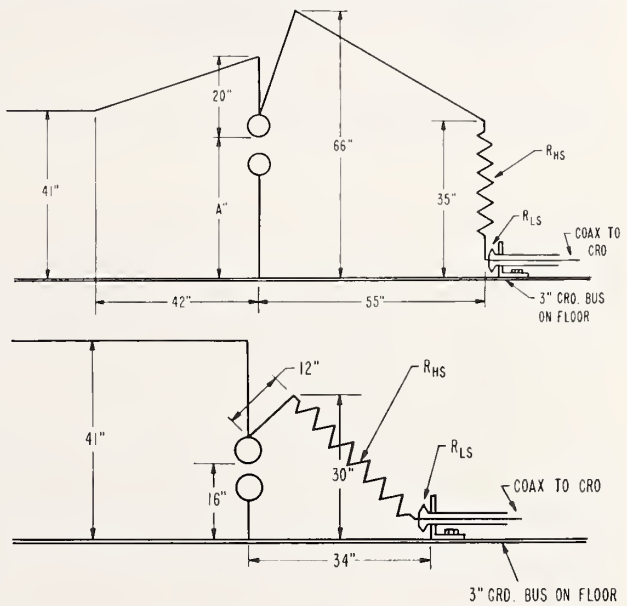

FIGURE 5. *Sphere gap and divider arrangements using* R_{HS} *=500 ohms (5–100 ohm ribbon-wound cards) with 12.5-cm spheres spaced 6 cm.*

(Upper) A. Similar to figure 2 except R_{HS}=500.

(Lower) B. With divider very close to spheres.

divider response. A 60-ft length of polyethylene coaxial cable (RG 8/U) was used for the connection from divider low side to the CRO. The method of terminating this cable at the oscillograph and determining its attenuation correction have been described in a previous publication [12]. A check for possible stray pickup voltage in the measuring circuit was made by using a special cable fitting between the divider low side and the cable to the oscillograph. This fitting offers no discontinuity or asymmetry in the cable sheath, but it disconnects the center conductor of the oscillograph cable from the divider low side and connects it to the cable sheath. With this fitting in place there should be no signal deflection recorded on the oscillograph when the generator is discharged and a voltage applied to the

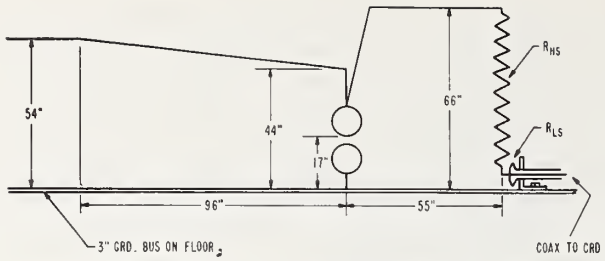

FIGURE 6. *Sphere gap and divider arrangement with 25-cm spheres spaced 6 cm.*

Spheres close to floor. R_{HS}=1,000 ohms.

FIGURE 7. *Double-wound card resistor cast in epoxy.*

Karma ribbon 1/16 inch wide and 0.001 inch thick with 0.001 inch Teflon between layers. Time constant, $L/R=0.002\times10^{-6}$.

divider. Any departures from a straight zero line would indicate pickup in the measuring circuits, probably due to ground currents in the cable sheath, CRO case, etc. Methods of connecting the cable to the oscillograph and arranging ground connections were devised and necessary changes made until this test indicated negligible pickup.

The divider high side (R_{Hs} of figs. 1 to 6) consisted of five or ten 100-ohm special Karma [4] ribbon resistor units. Each unit (see fig. 7) has an overall length of 6½ in. and consists of two oppositely wound layers of ribbon (1/16 in. wide and 0.001 in. thick) on a lucite card (1½ in. wide and 1/16 in. thick). Slots were milled in the edges of the lucite cards to keep the turns of ribbon uniformly spaced. The first layer of ribbon was enameled; but since the enamel did not completely cover the edges, a sheet of teflon (0.001 in. thick and 1½ in. wide) was laid over each side of the lucite card before starting to wind the second layer. A brass mold was specially constructed in which the double wound lucite cards were cast in epoxy resin (epon 815). All air bubbles were removed by placing the mold in a bell jar while the epoxy was still liquid and subjecting it alternately to low pressure (about 1 cm of Hg) and then room pressure (for at least three cycles). The resin was cured by baking overnight at about 55 °C.

[4] Karma is the trade name for an alloy (Ni 73 percent, Cr 20 percent+Al+Fe) having a high resistivity and low temperature coefficient.

The purpose of using this special construction was to get a resistor of minimum inductance which would withstand a high momentary voltage. Minimum inductance was obtained by using two oppositely wound layers connected in parallel and occupying as nearly as possible the same physical space. Sparking between turns and layers was prevented by (1) very uniform spacing and (2) casting in a high dielectric strength resin. The actual resistance and reactance of these units were measured at 0.5, 2.5, 10, and 30 Mc/s using a high-frequency bridge (at low voltage). Resistance did not change appreciably over this frequency range, and values of reactance were such that they could be represented by an inductance of 0.2 μh per unit. Thus, these ribbon-wound cards for the divider high side have a time constant (L/R) of 2×10^{-9} sec, which is much less than the minimum figure (10×10^{-9} sec) usually given for noninductive high-voltage wirewound resistors.

In order to determine how much voltage could be applied momentarily to these resistors, linearly rising chopped waves of increasing peak value were applied. For chopping times of about 0.7 μsec each resistor withstood a peak voltage of 60 kv, repeated at least 80 times with no apparent damage or change in resistance. For full waves or waves chopped on their tail such high values of peak voltage could not be applied because of the heating effects they might produce in the ribbon material. The instantaneous temperature of the ribbon is determined mainly by the energy [$\int i^2 r dt$] dissipated in the ribbon per shot. Full wave tests on the ribbon resistors indicated that each unit can withstand up to 300 joules on a single shot without damage provided sufficient cooling time is allowed between shots. The momentary resistance change due to this heating was estimated to be less than 0.5 percent because of the low temperature coefficient of Karma. If shots are repeated at 1-min intervals or less, the temperature buildup might cause failure. Whenever a series of shots is to be made, it is advisable to check resistor temperature occasionally between shots.

A set of seven resistors for use as the divider low side (R_{Ls} in figs. 1 to 6) was made with values from 2.60 to 15.8 ohms. This was done so that the CRO peak deflection could always be set, by choosing the proper R_{Ls}, at some value between 65 and 100 percent of full scale. A cable terminating resistor with taps could not be used at the CRO because of the special method used for cable termination [12].

Each low-side resistor consisted of elements made up of Karma ribbon (1/8 in. wide and 0.001 in. thick) bent back and forth on itself every 2 in. of its length. All bends were pressed flat in a vise. Small strips of mylar insulation (0.001 in. thick) were placed between adjacent 2-in. lengths of ribbon. All folds were then held tightly together between bakelite blocks and cast in epoxy for permanence. Each complete low-side resistor consisted of one, two, or three of these elements symmetrically placed as closely as possible around a coaxial chassis con-

nector mounted on a 3-in. wide copper busbar. All elements were connected in parallel and to the central coaxial terminal. The coaxial terminal provided the connection from the divider low side to the CRO cable. Measurements on these flat ribbon resistors, using a high frequency bridge and frequencies up to 30 Mc/s, indicated that their resistance remains essentially constant up to that frequency. Also their reactance can be represented by a fixed inductance. The time constant of each low-side resistor was measured and found to be about 2.5×10^{-9} sec.

5. Measurement Accuracy

The main sources of error after eliminating stray pickup, insuring proper cable termination, and correcting for cable attenuation are: (1) the oscillograph and (2) the divider. Repeated checks on the deflection sensitivity of the cold-cathode CRO used in the experimental work indicated that for deflections greater than 65 percent of full scale the accuracy of CRO voltage measurements was within ±1 percent. Sweep calibrations obtained by connecting the output of a signal generator (1.5 to 18 Mc/s) to the deflecting plates, indicated that time measurements could be made to within ±2 percent of total sweep time. Sweeps with total duration from 0.3 to 40 μsec were used. Their linearity was determined using the method described in appendix 8.1, and in measuring linearity of voltage rise only those sweep sections found to be linear to within 10 percent were used.

Divider errors, which ordinarily introduce the main source of uncertainty in steep-front measurements, depend mostly upon a combination of two effects: (1) stray capacitance from parts of the divider to nearby conducting surfaces and (2) residual inductance in the divider elements. If these two effects are considered separately, a computation can be made of the error introduced by each, based on measured or estimated values. Inductance errors were kept low in the present work by using special ribbon wound resistors as described in the preceding section. Actual values of time constant, as measured for these resistors, were inserted in the formula derived in appendix 8.2 to obtain computed values of error due to stray inductance. This gave an error of 0.5 percent for a rise time of 0.1 μsec and less error for longer rise times.

An exact computation of stray capacitance errors cannot be so easily deduced because stray capacitance depends on the location of the divider with respect to all nearby conductors. For the divider arrangements used (see figs. 2 to 6), all conductors except the laboratory floor and the high voltage lead to the divider were kept at sufficient distance to not affect divider capacitance. The error due to stray capacitance from a vertical divider to the grounded floor plane may be expressed as a time lag $t'=RC/6$, for a linearly rising voltage, as shown by Böckman and Hylten-Cavallius [13]. In this formula R is the total divider resistance and C is the total measured or estimated capacitance to ground. The percent error decreases as the time to measured value increases. Computed values are given in the following table for both the 1,000-ohm (see figs. 2, 3, 4, and 6) and 500-ohm (see fig. 5) divider used in the present work:

Total divider resistance	Estimated divider capacitance to ground	t'	Percent error for rise times		
			0.05 μsec	0.1 μsec	0.5 μsec
Ohms	*Picofarads*	μsec			
1,000	22	0.00367	−7.4	−3.7	−0.7
500	11	.000917	−1.8	−0.9	−0.2

The total stray capacitance error would include not only the component due to capacitance from divider to floor, as listed in the above table, but also a component of opposite sign due to capacitance from divider to its high voltage lead. Thus the total stray capacitance errors would be somewhat lower than those given in the above table.

A comparison of experimental results obtained with the 1,000 and 500-ohm dividers affords a basis for estimating the cancellation effect of the two stray capacitance components. As seen in the above table, flashover voltage measurements obtained with the 1,000-ohm divider would be expected to be several percent lower than those obtained with the 500-ohm divider unless the capacitance from the divider to its high voltage lead compensated for part of the capacitance from divider to ground. Measurements indicated that both dividers gave the same results for all rise times down to about 0.05 μsec. This indicated that, in the present work, errors due to stray capacitance for rise times greater than 0.1 μsec were probably not greater than 1 percent.

The above consideration of various possible errors indicates that the values of voltage here reported are accurate to within 1.5 percent for rise times greater than 0.1 μsec.

6. Experimental Results

Linearly rising voltages with various rates of rise obtained as explained in section 3 were used. Waveforms were considered to be linearly rising if the "true variation in rate of voltage rise" (δ'_{RR}) as defined and explained in appendix 8.1 was less than 20 percent. "Rates of voltage rise" were determined by the procedure described in appendix 8.1. Rise times or times to flashover were then obtained by dividing peak voltage at flashover by "rate of voltage rise." Typical examples of the impluse waveforms used are shown in figure 8. In all cases a negative polarity impluse was applied to the high-voltage electrode. Peak voltages were taken as those measured at the first sudden break in the smoothly rising trace. Other peaks occurring later were assumed to be due to reflection between sphere gap and divider. This is most clearly indicated in figure 8K for which the divider was very close to the spheres. Sufficient records, similar to those shown in figure 8, were taken so that complete volt-time curves could be plotted for three different electrodes: (1) 12.5-cm

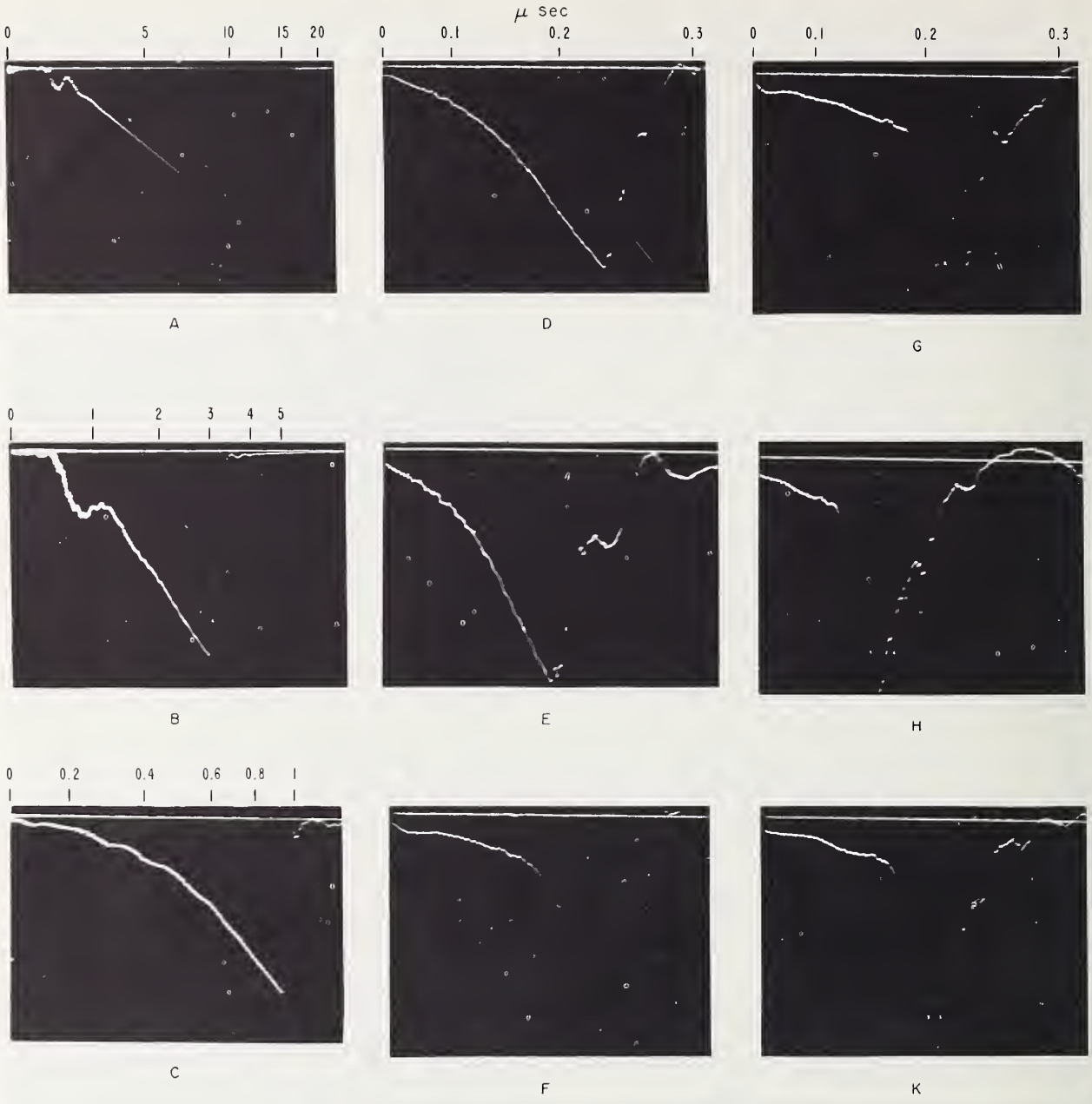

FIGURE 8. *Typical samples of oscillograms: linearly rising voltages.*

	Rise time	Peak	For divider setup see	R_{HS}	P″
	μsec	*kv*		*Ohms*	
A	27	135	Fig. 4	1,000	20″
B	2.7	164	Fig. 2	1,000	34″
C	0.86	171	Fig. 4	1,000	20″
D	.13	243	Fig. 3	1,000	42″
E	.093	230	Fig. 2	1,000	34″
F	.050	277	Fig. 6	1,000	17″
G	.037	266	Fig. 2	1,000	34″
H	.032	264	Fig. 5A	500	34″
K	.046	262	Fig. 5B	500	----------

diam spheres spaced 6 cm, (2) 25-cm diam spheres spaced 6 cm, and (3) 6.5-in. (16.5 cm) diam uniform field electrodes spaced 5 cm.

The solid line in figure 2 is the volt-time curve for 12.5-cm spheres spaced 6 cm apart obtained with the divider arrangement, also shown in figure 2, and A =34 in. The proximity of high voltage conductors of fairly large surface areas, such as parts of the generator or the 1 m hemispheres used as "C_0", were found to affect flashover voltage. To completely eliminate such effects, the gap was kept 20 ft from any generator or discharge circuit parts while obtaining this curve. It is an average drawn through about 200 plotted points. Each plotted point was obtained from four CRO records repeated at 30-sec intervals. The rates of voltage rise were always nearly identical for each of the four traces in a set. The four values of peak voltage usually agreed to within 1 percent. Plotted points were obtained for various rates of voltage rise over a period of several months and under various laboratory conditions: (1) ambient temperature 22 to 26 °C, (2) atmospheric pressure 748 to 762 mm of Hg, and (3) relative humidity 42 to 68 percent. All voltages were corrected for relative air density to 760 mm of Hg pressure and 25 °C. [1,2]. No correlation between humidity and flashover voltage at various rates of rise could be deduced, possibly because the actual range in humidity was not very great. Over 98 percent of the plotted points fell within ± 2 percent of the solid curve in figure 2.

Data were also obtained (1) with the horizontal distance between sphere gap and divider changed from 55 in., as shown in figure 2, to 20 in. and (2) using a 500-ohm divider arrangement as shown in figure 5A (A=34 in.). Points plotted from these data also fell along the solid curve.

When the distance from the floor to the sphere gap was changed, points did not fall along the same curve. A complete set of data for various rates of voltage rise was obtained for A=16 in. (see figs. 2 and 5). The dashed curve plotted using these data is 2 to 3 percent lower than the curve for A=34 in. as seen in figure 2.

Some data were also taken using the 500-ohm divider high side and the gap-divider arrangement of figure 5B. Here the lead from sphere to divider was kept as short as possible which accounts for the sharp break in the CRO record at flashover with no immediate oscillations (see fig. 8K). The oscillations occurring at flashover for some of the other divider arrangements (see figs. 8G and 8H) are probably due to reflection in the lead from sphere to divider. Flashover voltage was always taken as the first break in the linearly rising trace. For the divider arrangement of figure 5B the spheres are close to the floor which tends to make flashover voltage low, but the divider and its lead are high voltage conductors fairly close to the sparking point which tend to increase flashover voltage. The observed points fell fairly close to the soild curve in figure 2 showing that these effects tended to cancel each other.

For the purpose of finding a gap arrangement less dependent upon the location of the electrodes with respect to the floor and other nearby conducting surfaces, it was decided to also try 25-cm spheres spaced 6 cm apart. Using the divider arrangement shown by the insert in figure 3, the volt-time curve plotted in figure 3 was obtained. Procedures used were the same as those already described for 12.5-cm spheres. Proximity effects were studied by (1) changing to the sphere gap and divider arrangement shown in figure 6 (spheres much closer to floor); (2) moving the sphere gap and divider setup closer to the surge generator and the 1-m hemispheres used as C_0 (fig. 1), i.e., with the spheres 13 ft from the generator and 3 ft from the nearest hemisphere; and (3) going back to the sphere gap and divider setup shown in figure 3 but with sphere gap close to generator and hemispheres. Data obtained at various rates of voltage rise under all of the above conditions gave points falling along the volt-time curve plotted in figure 3. Thus, as was expected, 25-cm spheres spaced 6 cm apart afford a more satisfactory volt-time curve for use as a reference standard than 12.5-cm spheres spaced 6 cm.

For 60 c/s and full wave impulses, uniform-field gaps have been found to give more repeatable flashover voltages than sphere gaps [14, 15]. It was, therefore, considered advisable to try such gaps on front of wave flashover using linearly rising surges in the same manner as already described for sphere gaps. One pair of 6.5-in diam uniform field electrodes, rated at 140 kv peak, was constructed from solid brass according to the specification given by Bruce [14]. Values of flashover voltage were obtained at an electrode spacing of 5 cm with various rates of voltage rise. From plotted points using this data the volt-time curve in figure 4 was drawn. Proximity effects were determined by getting data with sparking point both 20 and 40 in. above the floor and with the gap near the generator and hemispheres (3 ft from nearest hemisphere) and at a much greater distance (15 ft from nearest hemisphere). All of these data gave points falling along the curve in figure 4, which indicated that proximity effects were much less than for 12.5-cm spheres spaced 6 cm but about the same as for 25-cm spheres spaced 6 cm. The scattering of the points about the curve was very nearly the same for uniform-field gaps as for 25 or 12.5-cm diameter spheres. The main disadvantage of uniform field gaps was found to be the difficulty encountered in getting the electrode axes sufficiently well alined.

All of the data used for plotting the curves in figures 2, 3, and 4 were obtained with a small needle of Co^{60} (equivalent to 0.5 mr per hour at 1m) placed inside the upper electrode. This was done because Bruce [8] found that full-wave surge breakdown data on spheres had the least scatter when a small amount of radium salt was placed inside one of the spheres. In order to find out if Bruce's conclusion held for breakdown on a linearly rising surge voltage, experimental data were obtained at several different rates of voltage rise with the Co^{60} removed. The points plotted from these data also fell along the curves, and the repeats from shot to shot were the same as with the Co^{60} inside the sphere except that

at slow rates of voltage rise (time to breakdown 8 to 10 μsec) repeats from shot to shot were not quite as good without the Co^{60}. The good repeats obtained without Co^{60} can be accounted for by radiation from other gaps in the surge generator circuit. When a 12-in. diam cardboard tube was placed around the measuring sphere gap, cutting off this radiation, the plotted points all fell to the right and above the curves; also repeat shots for a fixed rate of voltage rise yielded breakdown voltages differing as much as ±10 percent from an average value. These results indicate that a certain minimum ion density between the spheres is needed to obtain repeatable data, but probably radiation from other gaps in the surge generator circuit is sufficient if the measuring gap is not shielded from them. For very low rates of voltage rise (times to breakdown, say, greater than 5 μsec) the repeatability was definitely not as good as for the higher rates; and it was found advisable to use Co^{60}. An open carbon arc placed 3 ft from the sphere gap was also tried and found to give almost as good repeatability as the Co^{60} for low rates of voltage rise.

7. Conclusions

Special ribbon resistors with low and nearly matched time constants were used to make up the divider high and low sides. From a combination of experimental results and computations based on these resistors, it has been estimated that the results reported are accurate within 1.5 percent.

Data obtained using 12.5-cm spheres spaced 6 cm indicated a decrease in flashover voltage of 2 to 3 percent when the distance from laboratory floor to lowest point on upper sphere was decreased from 34 to 16 in. Variations were also noted when high voltage parts of the surge generator and discharge circuit, which have large surface areas, were placed within a radius of 20 ft from the sphere gap. Therefore, when volt-time curves for 12.5-cm spheres spaced 6 cm (from various laboratories) are being compared, the exact configuration of all conductors within a radius of 20 ft of the spheres should be considered.

For the uniform field gap, proximity effects were found to be negligible at distances greater than 4 ft from the sparking point. Also variations in distance of sparking point above the floor had little or no effect. The repeatability of results from shot to shot and day to day were found to be about the same for the uniform field gap as for sphere gaps. However, adjusting the mounting of the uniform field electrode so that the electrode axes were in accurate alinement was found to be a fairly time-consuming operation. Also uniform field electrodes are not readily obtainable but must be specially made. Because of these disadvantages and since uniform field gaps apparently give no marked decrease in scattering of flashover voltage for a linearly rising impulse, it was concluded that they should not be recommended for setting up a standard volt-time curve.

For 25-cm spheres spaced 6 cm, proximity effects were found to be negligible at distances greater than 4 ft from the sparking point, and the variation in distance of sparking point above the floor made no noticeable change in flashover voltage. Such spheres are probably available in most high voltage laboratories or they can easily be obtained. Therefore, the volt-time curve in figure 3, for 25-cm spheres spaced 6 cm, is considered best suited as a reference standard for use in checking the accuracy of steep-front impulse measurements at various laboratories.

8. Appendix

8.1. Definitions for Use in Measuring and Specifying Linearly Rising Impulses

A CRO with a linear sweep would be most convenient for accurate measurement and tolerance specification because a uniformly rising voltage would be recorded as a straight line, and any departure could be readily detected. If the sweep is not linear, to evaluate uniformity of rate of rise exactly, the voltage trace must be converted to its equivalent with a linear time base by a computing or graphical method. Although most oscillograph sweeps are not exactly linear over their entire range, this rather complicated conversion can be eliminated in most cases by devising a method for evaluating sweep linearity. Then practical limits in sweep nonlinearity can be specified, and particular sweeps or sections of sweeps which exceed these limits should not be used.

a. Determination of Sweep Nonlinearity

A sweep calibration is obtained by taking an oscillograph record with a suitable high-frequency signal applied to the deflecting system. Data obtained from measurements on this record can then be expressed as a plot of time in microseconds against sweep deflection in inches or centimeters, as illustrated in figure 9 for a typical CRO sweep. For a linear sweep this plot would, of course, be a straight line. Any departure from linearity is indicated by curvature of the plot. The degree of nonlinearity *between any two sweep deflections* d_1 *and* d_2, corresponding to time t_1 and t_2, is determined as follows: draw a straight line tangent to the plot at d_2 (see fig. 9) and call its intersection with the d_1 ordinate, t_1'. Sweep nonlinearity in percent, δ_{SL} is here defined as

$$\delta_{SL}=\frac{t_1-t_1'}{t_2-t_1'}\,100$$

for the sweep interval from t_1 to t_2. δ_{SL} is positive for $t_1 > t_1'$. In general, δ_{SL} may be either positive or negative; but usually the same sign is maintained throughout any one sweep, and its magnitude is less the shorter the interval t_2-t_1. This definition makes it possible to specify the degree of nonlinearity allowable for various types of measurements and in some cases to apply corrections for nonlinearity.

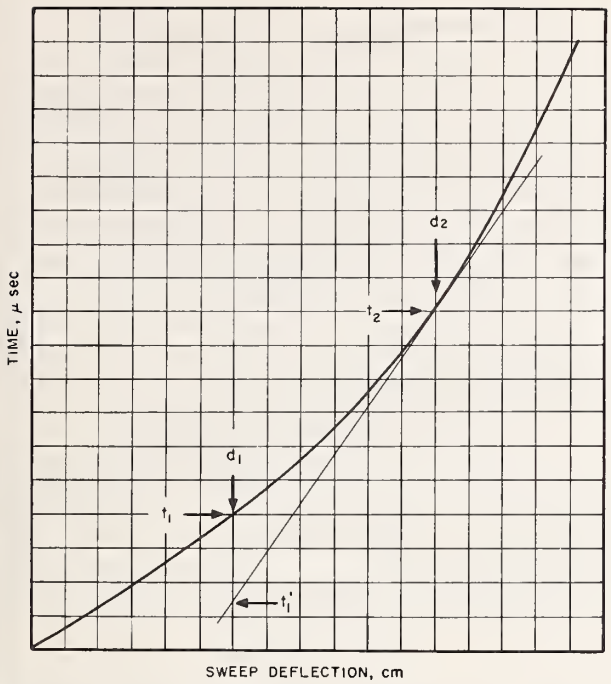

FIGURE 9. *Sweep calibration curve showing method for measuring sweep nonlinearity,* δ_{SL}

$$\delta_{SL}=\frac{t_1-t_1'}{t_2-t_1'}100$$

b. Definitions of Rate of Voltage Rise, Time to Flashover, and Specification of Tolerances

For a linearly rising waveform, the results of sphere gap sparkover data can be presented as a plot of sparkover voltage against either rate of voltage rise or time to sparkover. Since sparkover voltage depends mainly on rate of rise just prior to sparkover,[5] rate of voltage rise seems the more logical independent variable. However, volt-time curves are already a familiar concept in dielectric breakdown; and since measurement accuracy can best be expressed as a function of rise time, it is thought desirable to use time to sparkover as the independent variable. The definition of "time to sparkover" presents no problem if the voltage rise is exactly linear, but truly linear waveforms are hardly ever attained.

It becomes necessary, therefore, to consider exactly how "time to sparkover" should be determined.

For very short times to sparkover, in order to get repeatable results it is necessary that the rate of voltage rise be very nearly constant over the period of time "just prior to sparkover." It is this rate of rise that determines the magnitude of sparkover voltage. Thus, an equivalent or quasi *"time to sparkover" is defined as peak voltage divided by rate of voltage rise just prior to breakdown.* To measure this rate of rise, a straight edge is lined up with the section of voltage record from about 80 to 100 percent of the peak or sparkover voltage. For times to sparkover less than 1 μsec nearly all acceptable waveforms will fall along the straight edge in this section of the voltage record as indicated in figure 10A. If there is curvature in this section, which is more likely for times to sparkover greater than 1 μsec, the straight edge should be placed tangent to the curve at sparkover voltage as shown in figure 10B. The slope of the straight edge in terms of the

[5] The term "just prior to sparkover" is intended to mean that portion of the voltage rise between the voltage at which sparkover would occur for a 60-cycle voltage and the actual value of voltage at which sparkover occurs for the particular wave shape of the applied voltage. It would correspond to the section between e_{60} and e_m in figures 10A and 10B.

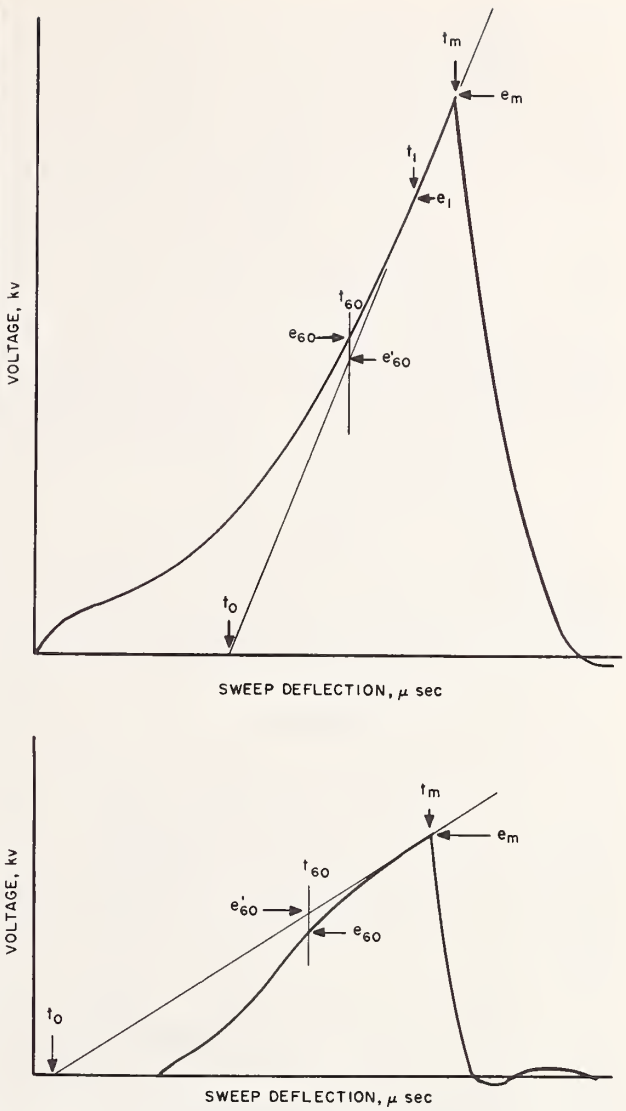

FIGURE 10. *Drawings of oscillograms showing method for measuring rate of voltage rise and variation in rate of rise,* δ_{RR}.

$$\delta_{RR}=\frac{e_{60}-e'_{60}}{e_m-e_{60}'}100$$

(Upper) A. Voltage impulse with very short time to flashover.

(Lower) B. Voltage impulse with longer time to flashover.

voltage and time coordinates of the trace is the rate of voltage rise. If the sweep is linear, this slope can be obtained by dividing peak voltage, e_m, by the time interval between the zero intercept of the straight edge and peak voltage point, $(t_m - t_0)$, as shown in figure 10A. Accuracy requirements are specified by saying that the sweep nonlinearity, δ_{SL}, must be less than 10 percent in the interval used to measure slope, $t_m - t_0$. Unless this interval is a fairly small fraction of the whole sweep, the 10 percent limit is quite likely to be exceeded. The slope can usually still be obtained to the required accuracy by using a shorter interval such as $(t_m - t_1)$ [see fig. 10A] and a smaller corresponding change in voltage, $(e_m - e_1)$. These measurements, of course, depend upon the particular sweep being used. It is probably easier to discard voltage traces occurring over sweep intervals with high values of δ_{SL} than to apply a correction to rate of rise which could be determined from sweep nonlinearity.

In addition to measuring rate of voltage rise just prior to sparkover by the method described, it is also necessary to determine whether rate of rise varies by a significant amount between 30 and 100 percent of sparkover voltage. Experimental data obtained with different wave shapes at the National Bureau of Standards have indicated that as long as the rate of voltage rise is constant from the 60-cycle peak sparkover value of voltage up to actual sparkover, it is not important that it also remain constant below the 60-cycle peak sparkover value. Thus, between the 30 percent voltage point and 60-cycle sparkover voltage it is only necessary to ascertain that the voltage rises approximately linearly and has no abrupt discontinuities. However, in the range between 60-cycle peak sparkover voltage and actual sparkover, it is necessary to define a "variation in rate of rise" and state tolerances. To do this, e_{60} (see fig. 10A) is taken as the point on the voltage trace corresponding to 60-cycle peak sparkover voltage. A vertical line through e_{60} intersects the sloping line drawn for measuring rate of rise just prior to flashover at e'_{60}. Then "variation in rate of voltage rise in percent," δ_{RR}, is defined as

$$\delta_{RR} = \frac{e_{60} - e'_{60}}{e_m - e'_{60}} 100.$$

This is a true measure of change in rate of rise from point (e_{60}, t_{60}) to point (e_m, t_m) provided the sweep is linear in this range. If the sweep is not linear, constancy of rate of rise would be indicated if $\delta_{RR} = \delta_{SL}$ where both δ_{RR} and δ_{SL} are determined for the same time interval $t_m - t_{60}$, and their signs are found using the definitions stated. Then the true variation in rate of rise, δ'_{RR}, can be defined as

$$\delta'_{RR} = \delta_{RR} - \delta_{SL}.$$

A tolerance is specified by saying that the true variation in rate of rise, δ'_{RR}, between the 60-cycle peak sparkover voltage and actual flashover voltage shall not be greater than 20 percent.

The voltage-time trace shown in figure 10A is typical of those obtained for times to sparkover up to about 1 μsec. For longer times, the curvature of the trace is more likely to be reversed in sign as shown in figure 10B. For very long times to flashover the actual voltage at sparkover approaches the 60-cycle (full-wave) value, and the tolerances as specified, by using $e_m - e_{60}$, allow considerable curvature just prior to flashover. This is not objectionable because flashover voltage changes very slowly with rise time for times greater than 10 μsec. To insure minimum spread of observed values in this range, it is necessary to irradiate the gap by using an ultraviolet lamp or some radioactive material placed inside one sphere.

c. Summary of Definitions and Tolerances

The following definitions and methods for expressing tolerances are proposed for use in obtaining sphere-gap volt-time curves from cathode ray oscillograph records.

Sweep nonlinearity between times t_1 and t_2 of an oscillograph record is defined in percentage as

$$\delta_{SL} = \frac{t_1 - t'_1}{t_2 - t'_1} 100$$

where t_1 is determined as indicated in figure 9.

Uncorrected variation in rate of voltage rise for a CRO chopped wave voltage trace is defined as the change in rate of rise from point (e_{60}, t_{60}) to point (e_m, t_m) and is given in percentage as

$$\delta_{RR} = \frac{e_{60} - e'_{60}}{e_m - e'_{60}} 100$$

where e'_{60} is determined as indicated in figure 10A or 10B.

True variation in rate of voltage rise is defined as

$$\delta'_{RR} = \delta_{RR} - \delta_{SL}$$

where δ_{RR} and δ_{SL} are determined using the same time interval.

Linearly rising wavefront is defined as one rising at a constant rate from 30 to 100 percent of flashover voltage.

Allowable tolerances can be fixed by requiring that $\delta'_{RR} \leqq 20$ percent, and that between the 30 percent voltage point and 60-cycle sparkover point the voltage shall rise approximately linearly with no abrupt discontinuities.

Rate of voltage rise is defined as the slope of the voltage rise trace just prior to flashover. It is obtained by measuring the slope of a straight edge which has been either (1) lined up with the section of voltage record from 80 to 100 percent of sparkover voltage as indicated in figure 10A or (2) placed tangent to the voltage trace at the sparkover point as indicated in figure 10B. The sweep time interval used in measuring this slope should be chosen so so that $\delta_{SL} \leqq 10$ percent.

Time to flashover is obtained by dividing peak voltage at flashover by rate of voltage rise as defined above.

8.2. Inductance Errors of a Resistance Divider—Stray Capacitance Neglected

Suppose a linearly rising voltage $e(t)=mt\ 1$, is applied across the divider, and

R_1=divider high side resistance
R_2=divider low side resistance
R=total divider resistance
L_1=divider high side inductance
L_2=divider low side inductance
L=total divider inductance
$R/L=\alpha$.

The divider low side resistance is assumed to be less than 10 ohms, thus the CRO cable connected in parallel with it can be neglected in a consideration of inductance errors.

The operational equation for finding current through the divider is

$$(R+pL)i=mt\ 1.$$

The Laplace transform of this equation is

$$(R+sL)I(s)=\frac{m}{s^2}$$

solving for $I(s)$

$$I(s)=\frac{m}{L}\frac{1}{s^2(s+\alpha)}. \tag{1}$$

To transform $I(s)$ to a function of time, let

$$\frac{L}{m}I(s)=f_1(s)=\frac{1}{s}f(s),\ \text{where}\ f(s)=\frac{1}{s(s+\alpha)}.$$

Also, the inverse transforms of $f_1(s)$ and $f(s)$ are $F_1(t)$ and $F(t)$ respectively, thus

$$F(t)=\frac{1-\epsilon^{-\alpha t}}{\alpha}$$

and by a well-known theorem in operational calculus

$$F_1(t)=\int_0^t F(\tau)d\tau$$

$$F_1(t)=\int_0^t \frac{1-\epsilon^{-\alpha\tau}}{\alpha}\,d\tau.$$

After performing the integration, this expression for $F_1(t)$ can be used with eq (1) to obtain

$$i(t)=\frac{m}{R}\left[t+\frac{L}{R}(\epsilon^{-\alpha t}-1)\right]. \tag{2}$$

Using this equation the divider low side voltage,

$$e_2=iR_2+L_2\frac{di}{dt}$$

can be computed as

$$e_2=\frac{R_2}{R}\,m\left[t+(\epsilon^{-\alpha t}-1)\left(\frac{L}{R}-\frac{L_2}{R_2}\right)\right].$$

The measured value of high side voltage is then

$$e_m=e_2\frac{R}{R_2}=m\left[t+(\epsilon^{-\alpha t}-1)\left(\frac{L}{R}-\frac{L_2}{R_2}\right)\right]. \tag{3}$$

The error in measured value due to inductance is

$$\delta=\frac{e(t)-e_m}{e(t)}$$

$$\delta=\frac{(1-\epsilon^{-\alpha t})\left(\frac{L}{R}-\frac{L_2}{R_2}\right)}{t}. \tag{4}$$

Since α can be easily be made equal to 10^8 or greater, the quantity $(1-\epsilon^{-\alpha t})$ is approximately equal to unity for all times greater than 0.05 μsec. Thus, the error becomes

$$\delta=\frac{\left(\frac{L}{R}-\frac{L_2}{R_2}\right)}{t}.$$

It approaches zero for $\frac{L}{R}=\frac{L_2}{R_2}$ which is true if $\frac{L_1}{R_1}=\frac{L_2}{R_2}$. Therefore, the error can be reduced to a negligible value by making the divider low side time constant nearly equal to that of the higher side.

9. References

[1] American standard for measurement of voltage in dielectric tests, AIEE Standard No. 4, ASA C68.1, (1953).
[2] Recommendations for voltage measurement by means of sphere-gaps (one sphere earthed), International Electrotechnical Commission Publication 53, (1960) (Obtainable from ASA Headquarters).
[3] Methods for measurement of voltage with sphere gaps, British Standards Institution—British Standard **358,** (1960) 24 pp.
[4] P. L. Bellaschi and W. L. Teague, Sphere-gap characteristics on very short impulses, Elec. J. **32,** 120 (1935).
[5] J. H. Hagenguth, Short-time sparkover of gaps, Elect. Engr. **56,** 67 (1937).
[6] C. J. Miller, Jr., and J. F. Wittibschlager, Measurements of steep-front waves with an isolated screen room installation, AIEE Communication and Electronics Paper 58–18, 262 (1958).
[7] F. C. Creed, The measurement of impulse waves chopped on the front CIGRE Paper 320 (1958).
[8] N. Hyltén-Cavallius, High voltage measuring devices and measuring errors, ASEA Technical Memorandum TM **9184** (1958).
[9] Unpublished report by P. R. Howard of the National Physical Laboratory at CIGRE Meetings in 1958.
[10] Informal results from D. L. Whitehead of Westinghouse Electric Corporation in Pittsburgh.
[11] John H. Park, A fifty-fold momentary beam intensification for a high-voltage cold-cathode oscillograph, J. Research NBS **47,** 87 (1951) RP2231.
[12] J. H. Park, Surge measurement errors introduced by coaxial cables, Communications and Electronics, **343,** (1958), AIEE Trans. Paper 58–110.
[13] Marius Böchman and Nils Hyltén-Cavallius, Errors in measuring surge voltage by oscillograph, ASEA Ludvika Sweden, (1946).
[14] F. M. Bruce, Calibration of uniform field spark gaps for high voltage measurements at power frequencies, J. IEE (London) **94,** pt II No. 38, 138 (1947).
[15] F. M. Bruce, High voltage spark discharges, Endeavour **XII,** No. 50, 61 (1954).

(Paper 66C3–96)

Journal of The Washington Academy of Sciences
Volume 38, Number 2, February 1948

The Measurement of High Voltage

F. M. Defandorf

This paper outlines the basic principles used in the precise measurement of direct-, alternating-, surge-, and pulse-voltages, 100 kilovolts and higher. The use of potential dividers, potential transformers, electrostatic instruments, generating voltmeters, air spark-gaps, and other devices in the measurement of high voltage is presented. A discussion of measuring high voltage by the deflection of free-moving charged particles and a description of the High Voltage Scale is also included.

Editors
August 28, 1967

Dielectric and Magnetic Measurements

Papers

Abstracts

SPE JOURNAL | STANDARDS FOR PLASTICS

■ **A comprehensive and useful review of various standards available in the field of polymer electrical testing.**

Standard Tests for Electrical Properties

About the Author

Dr. Arnold H. Scott was born in Sutherland, Iowa. He took his undergraduate work at the University of Mississippi and obtained his PhD degree from Johns-Hopkins University in 1928. He has been with the National Bureau of Standards since 1924 working in the field of dielectric measurements of electrical insulating materials. He is currently Chairman of ASTM Committee D-9 and ASA Committee C-59, both dealing with electrical insulating materials. He was the U.S. Delegate to various meetings of Technical Committee No. 15 of IEC from 1952 to 1960. He is a member of the Washington Academy of Sciences and the New York Academy of Sciences.

Arnold H. Scott,

Dielectrics Section, Electricity Division, National Bureau of Standards, Washington 25, D. C.

Electrical properties usually considered to be important when plastics are used for electrical insulation are:

1. Volume and Surface Resistivities
2. Permittivity (Dielectric Constant) and Dissipation Factor
3. Dielectric Strength
4. Arc Resistance or Tracking.

It is generally agreed that there is no such thing as "good" or "poor" electrical properties—only properties that indicate different degrees of suitability for specific applications. Therefore, before any electrical measurements are undertaken, the purpose of the testing and the end use or application for which the plastic is to be used should be known.

Electrical properties, particularly permittivity and dissipation factor, are often studied in relation to the chemical structure and physical characteristics of the material. There is an extensive literature on this subject but this is beyond the scope of the present paper which is primarily

concerned with the description and use of test methods.

Significance of Tests

Volume and Surface Resistivity—The exact values of volume and surface resistivity ordinarily are not very important because they are usually several orders of magnitude greater than required for properly insulating the electrical circuits involved. However in certain applications such as insulation for very low current measuring devices and for computer components, very high resistivities are required. Accurate values are then needed for the selection of the proper material and for design purposes. Also volume resistivity is often used in production control. Changes in composition or amounts of impurities are usually reflected in changes of volume resistivity before they are reflected in changes in other properties.

Permittivity and Dissipation Factor—Many plastics are used today in applications which require an accurate knowledge of their permittivity and loss. Various types of improvement in the composition and fabrication of plastics have tended to lower the dissipation factor, and have increased the need for more sensitivity in the measurement of this characteristic. Dissipation factor is often used as a check on the constancy of quality in the production of plastic materials.

Dielectric Strength — Dielectric strength can be used as a relative test for material inspection or quality control, or as a convenient preliminary test to determine whether a material merits further consideration. A comprehensive statement of significance appears as Appendix I of ASTM D 149.

Arc Resistance—Plastic materials are sometimes used under conditions where flashovers occasionally occur between metal parts attached to or supported by the plastic material. The flashovers and resulting arcs may eventually damage the insulating material by tracking or erosion to the extent that it is no longer useful as an insulation. The arc resistance test is an attempt to evaluate materials with regard to their ability to resist tracking or erosion.

Standards Activity

Much time has been spent in developing adequate test methods for determining these properties. Improved techniques of measurement have made it necessary to revise these methods from time to time. Several are under revision at the present time.

Standard methods for determining these properties have been prepared by Committee D-9 on Electrical Insulating Materials of ASTM. Internationally this work is performed by Technical Committee No. 15 on Insulating Materials of the International Electrotechnical Commission. ASTM Committee D 20 on Plastics looks to Committee D-9 for electrical test methods for plastics. Likewise Technical Committee No. 61 on Plastics of the International Standards Organization looks to IEC Technical Committee No. 15 for international electrical test methods for plastics.

Volume and Surface Resistivity

The basic methods of test for insulation resistance and volume and surface resistivities are given in ASTM D 257-61, Methods of Test for Electrical Resistance of Insulating Materials. The comparable international document is IEC Publication 93, Recommended Methods of Test for Volume and Surface Resistivities of Electrical Insulating Materials.* Publication 93 does not include the test method for insulation resistance but otherwise is essentially the same as ASTM D 257. A separate document for insulation resistance test methods is now being balloted in IEC. Except for a few variations in electrode systems, this document is essentially the same as that part of ASTM D 257 which deals with insulation resistance.

Electrodes Arrangements—For insulation resistance measurements almost any shape of electrode can be used provided it can be applied to or embedded in the specimen. However a value of insulation resistance has strict applicability only when the test specimen and electrodes have the same form as required in actual use because insulation resistance includes both volume and surface resistance.

To determine separately the volume and surface resistances (and thus resistivities) it is necessary to use a guard electrode system. When properly used this shunts the unwanted currents around the current measuring instrument or bridge detector. Precautions must be taken to see that the resistance between a measuring electrode and the guard electrode is high compared to that of the input of the current measuring instrument or the pertinent bridge element. Otherwise, part of the current which is to be measured by the voltmeter-ammeter method will be shunted past the instrument and will lead to erroneous results. In the bridge, the bridge ratio will be upset.

The most popular arrangement of electrodes for plate or sheet materials is the parallel guard-ring type, sometimes called the "bulls eye" pattern. W. G. Amey (1) has shown that the most practical dimensions for these electrodes includes a gap distance between the measuring and the guard electrodes equal to twice the thickness of the specimen. This permits the same electrodes to be used for volume and surface resistance measurements. The effective area for the measuring electrodes extends almost to the center of the gap and ASTM D 257 gives a correction for the difference between the area to the center of the gap and the effective area which can be applied if desired. However this correction is usually too small to be significant in view of the fact that duplicate measurements of resistance on dielectric specimens will seldom agree within 10% and the disagreement is usually 100% or more. Except in unusual cases the order of magnitude of the resistance is all that is required.

Electrode Materials—Various materials can be used for the contact electrodes which are applied to the specimens. Conductive silver paint is very popular because it permits moisture penetration to the specimen during conditioning. However the solvent in the paint may affect the specimen. This can be especially troublesome for plastic materials. A study is now being made of conductive rubber electrodes which can be pressed against the specimen. When these can be used it saves considerable time in sample preparation. Other materials such as evaporated gold or tinfoil are used for electrodes but they have the disadvantage of obstructing the movement of moisture into the specimen during conditioning.

Electrometers—Neither ASTM D 257 nor IEC Publication 93 include the use of electrometer type current measuring instruments although they do not exclude them. Neither do they discuss the problems which may be encountered in their use. Vacuum tube electrometers are now available which when used in the voltmeter-ammeter method will detect conductances (reciprocal resistances) as low as 10^{-17} mho and which are small, light weight and readily portable. The present purity of some plastics makes even greater sensitivity desirable if the conductances involved are to be measured with reasonable accuracy. Vibrating reed electrometers are somewhat more sensitive than vacuum tube electrometers but are heavier and are more cumbersome to

* Copies of IEC and ISO documents may be obtained from the American Standards Association.

use. All electrometers have high input resistances (up to 10^{12} ohms or more at highest sensitivities) and create problems of measurement if careful precautions are not taken. The leakage resistance between the measuring electrode and guard or ground in the voltmeter-ammeter method must be at least two orders of magnitude greater than the input resistance of the electrometer if the ground is connected to one side of the electrometer. Otherwise some of the current which it is desired to measure will be shunted past the electrometer and cause an erroneous measurement to be made. If the ground is attached to one side of the specimen the problem is greater because then the leakage to ground must be at least 2 orders of magnitude greater than the resistance being measured (2).

Gap Width—There is some tendency, when volume resistance measurements only are required, to make the gap between the measuring and guard electrodes small so that the effective area can be more accurately obtained. However a narrow gap may cause very large errors when electrometers are used in the voltmeter-ammeter method because the surface resistance between these electrodes may become less than the input resistance of the current measuring instrument and only a small fraction of the desired current is measured. This is especially apt to happen when measurements are made with the specimen in a high humidity. When the integration method is used with the vibrating reed electrometer to get maximum sensitivity, decaying currents in the insulating supports induce charges in the measuring circuit which may be an appreciable fraction of the charge flowing through the specimen. Thus measurements requiring long times of charge integration may and usually do give quite erroneous results.

Permittivity (Dielectric Constant) and Dissipation Factor

The general Standard for measurement of permittivity and loss in the U.S.A., is ASTM D 150, A-C Capacitance, Dielectric Constant, and Loss Characteristics of Electrical Insulating Materials, which is now under active revision. A comparable international document has been prepared by IEC TC/15 and this has been distributed as a Secretariat Document for comments from the various National Committees. Standards which have been prepared for special plastic materials and special techniques are: ASTM D 1673, Dielectric Constant and Dissipation Factor of Expanded Cellular Plastics used for Electrical Insulation; ASTM D 669, Dissipation Factor and Dielectric Constant parallel with Laminations of Laminated Sheet and Plate Insulating Materials; and ASTM D 1531, Dielectric Constant and Dissipation Factor of Polyethylene by Liquid Displacement Procedure.

Guard-ring Electrodes—The basic and classical method of accurately determining the permittivity of dielectric materials is the use of parallel guard-ring electrodes. Highly conducting contact (or specimen) electrodes (such as tinfoil, evaporated gold etc.) are applied to the opposite sides of a sheet or plate of the material. The electrodes on one side are arranged with a narrow gap between the guarded electrode and the guard electrode. Aside from an accurate measurement of the capacitance, accurate measurements of area and thickness must be made. Accurate area measurements require symmetrical guarded electrodes and very small and uniform gaps between the guarded and guard electrodes. These are often difficult to obtain with the uniformity required for the desired precision. Also accurate thickness measurements generally require that the faces be quite flat and that of the specimens be uniform in thickness requiring special preparation of the specimen either by precision molding or by grinding or machining the surfaces. A concept of the magnitude of the problem can be obtained by considering that if an accuracy of 0.1% in permittivity is desired, the thickness of a specimen which is 0.3 cm thick must be determined to 0.0003 cm (3 microns) or better. This is impossible with micrometers unless the surfaces are nearly optical flat and the material is hard. In addition, the effective diameter of a guarded electrode which has a diameter of 5 cm must be determined to 0.002 cm or better. It is difficult to cut a foil electrode with this uniformity and the optical problems of determining the exact edge of the electrode are great. However, an accuracy of 0.5% in permittivity can generally be obtained when reasonable care is taken in preparing the specimen and making the various measurements.

The guard-ring method has the disadvantage that measurements of capacitance and dissipation factor must be made on three terminal or guarded bridges. This usually means that cumbersome and time consuming bridge balancing is required and such bridges usually will not ordinarily operate accurately above 100 kc/s. This disadvantage is being partially overcome by the use of transformer bridges where the capacitances to ground cause negligible errors. However, commercial bridges of this type will not at present operate much above 10 kc/s with a sensitivity comparable to that of a Schering bridge with a Wagner earthing arm.

Micrometer-electrode Holder

A two-terminal technique which gives almost as good accuracy as the guarded-electrode technique is the use of the micrometer-electrode holder. This can be used at frequencies up to 100 Mc/s. This requires a specimen with a uniform diameter, with flat, parallel faces and with the side perpendicular to the faces. The edges must be sharp, with no rounding off. The specimen should have a diameter which is smaller than that of the holder electrodes by at least twice the thickness of the specimen. Measurements are often made with specimens the same size as the holder electrodes but the value obtained in this case is in error by 0.2% to 0.5% depending upon the permittivity and thickness of the specimen. Corrections to be applied in this case have not been determined. The precision with which the spacing between the holder electrodes can be measured enters into the accuracy of the method. The micrometer used to make this measurement should not be used to move the electrode to adjust the spacing, but only to sense its position. A disadvantage of this method is that the leakage over the side of the specimen enters into the dissipation factor measurement. The leakage distance is equal to the thickness of the specimen and the contribution of the leakage can be quite large especially if measurements are made in a humid atmosphere.

Edge Correction Method

To decrease the effect of surface leakage, contact electrodes can be applied to a specimen in such a way that the specimen extends beyond the electrodes. Instructions for computing the edge corrections required for specified electrode arrangements are given in both ASTM D 150 and the proposed IEC document. Another correction is required, that for the ground capacitance of the ungrounded electrode. This ground capacitance is a function of the area of the ungrounded electrode and its distance from the ground plane and surrounding objects. This capacitance has not been adequately determined although a formula for its computation is given in ASTM D 150. The best procedure is to mount the specimen so that it is as far from the ground plane and other objects as is practicable. Because of the uncertainties in the determination of the edge and ground

capacitances errors in the permittivity determination may range from one to five percent.

Liquid Displacement Method—A two-terminal method which is both accurate and rapid under limited conditions is the liquid displacement procedure (ASTM D 1531). This eliminates the need for contact electrodes on the specimen. If the specimen is in the form of a sheet or thin plate and if a liquid can be found whose permittivity is known and is close to that of the specimen, the thickness need not be known with great accuracy to obtain a very accurate measurement of the permittivity of the specimen. However the liquid must not absorb into the specimen or otherwise affect it appreciably during the measurement. Absorbed liquids even in minute (barely weighable) quantities can sometimes appreciably affect the electrical properties. With care this method can be used up to 100 Mc/s. If the permittivity is close to that of the specimen this method will yield values of permittivity which are in error by no more than 0.1%.

Air-Gap Method—Another method of determining the dielectric constant without the necessity of applying contact electrodes is the use of an air gap in series with the specimen. This method requires a cell with guard-ring type electrodes and thus 3 terminal measurements are necessary which limits the frequency range. Also the electrode spacing and the thickness of the specimen must be determined with greater accuracy because the error in the dielectric constant is greater than either the error in the spacing determination or the thickness of the specimen for this type of measurement.

Dissipation Factor—The determination of dissipation factor for plastics is important because the heat generated in the plastic per cubic centimeter is directly proportional to the loss index (formerly loss factor), which is the permittivity times the dissipation factor In many applications this heat loss and thus the loss index must be kept as low as possible. Some plastics have such low loss indexes that values as low as 0.00005 must be measured to characterize the material. Under these circumstances losses in the specimen holder or cell become important. Losses in the insulation supporting the insulated electrode of the holder and even oxide layers on the surfaces of the electrodes can produce serious errors in the measurement of the loss index of such a specimen. At high frequencies series resistance losses in the contact electrodes may become appreciable. To remedy this, the dissipation factor is often measured separately from the dielectric constant with no contact electrodes applied to the specimen. Otherwise special effort must be made to see that the contact electrode is thick (conductive) enough so that the resistance from any point of contact to any part of the area makes a negligible contribution to the loss measurement.

Dielectric Strength Test

Dielectric breakdown tests usually measure the breakdown voltage at weak spots in the dielectric caused by dielectric defects of various kinds. Solid commercial electrical insulating materials generally contain dielectric defects and therefore intrinsic dielectric strength cannot be determined from breakdown tests. Furthermore cumulative heating may develop in local paths within the material and breakdown may then occur because of thermal instability.

The general test for dielectric strength in the U. S. is ASTM D 149, Dielectric Breakdown Voltage and Dielectric Strength of Electrical Insulating Materials at Commercial Power Frequencies. A similar document is being prepared by IEC TC/15. However disagreement over the types of electrodes which should be used has not yet been resolved. There is a group which insists that for sheet and plate materials the electrode system should be a disk (2.5 or 5 cm in diameter) opposite a larger flat metal plate, rather than two opposing disks of the same diameter which is favored by the U. S. and others. The outcome of this argument will of necessity influence standards in the U. S. Although certain electrode systems are specified in ASTM D 149, special electrode systems are specified in some U. S. specifications for electrical insulating materials.

A study is being made of dielectric breakdown at higher frequencies. Breakdown at the higher frequencies may be more informative for plastics than that at 60 c/s. It is hoped that a standard method for higher frequencies will soon become available.

A standard which is useful in testing the quality of thin plastic materials is ASTM D 1389, Tentative Method for Dielectric Proof-Voltage Testing of Thin Solid Electrical Insulating Materials. Most thin plastic materials have occasional dielectric defects, such as fine pinholes and perhaps fibers. This test serves to indicate the frequency of occurrence of such defects.

Arc Resistance or Tracking

A method of test which has been devised to determine the relative ability of various insulating materials to withstand the deteriorating effects of low current arcs is ASTM D 495, Standard Method of Test for High-Voltage, Low-Current Arc Resistance of Solid Electrical Insulating Materials. This is a relative type of test and occasionally does not correlate with results from actual use. However, it is a very useful test in general for the limited range of conditions specified in the test. The test arcs are caused by overvoltage between the electrodes under dry conditions.

The International Electrotechnical Commission has issued a method of test for determining the relative ability of materials to resist the deteriorating effects of small arcs under specified moist conditions. It is published as IEC Publication 112, Recommended Method for Determining the Comparative Tracking Index of Solid Insulating Materials under Moist Conditions. This test can only make a relative comparison but it is generally felt that this test correlates with life service in the Scandinavian countries, Holland and in areas exposed to moisture. In this test a potential insufficient to cause arcing is applied between electrodes placed on the material under test. Drops of water having a specified salt content are allowed to fall on the material surface between the electrodes. Small arcs are formed between droplets on the surface and this leads to deterioration of the surface.

Various methods of testing tracking resistance under moist conditions are being studied and tested in the United States. A test called the Method of Test for Dust-and-Fog Tracking and Erosion Resistance of Electrical Insulating Materials is presently being balloted in ASTM Committee D-9. This could be useful in testing plastics for use under special conditions where surface contamination and moisture are problems.

Literature References

1. Amey, W. G., and Hamburger, Ferdinand, Jr., A Method of Evaluating the Surface and Volume Resistance of Solid Dielectric Materials, Proceedings of the American Society of Testing Materials. Vol. 49, 1949.
2. Scott, Arnold H., Insulation Resistance Measurements, Fourth Electrical Insulation Conference, The Shoreham Hotel, Washington, D. C., AIEE T-137-52, Page 115, Feb. 19-20, 1962.

THE END

Edited by
Dr. Charles F. Ferraro
FMC Corporation

JOURNAL OF RESEARCH of the National Bureau of Standards—C. Engineering and Instrumentation
Vol. 69C, No. 3, July–September 1965

Two-Terminal Dielectric Measurements Up to 6×10^8 Hz

Martin G. Broadhurst and Anthony J. Bur

(February 23, 1965)

A two-terminal dielectric specimen holder has been constructed and used to make dielectric constant and loss measurements on a single disk specimen at room temperature over a frequency range from 10^{-2} to 6×10^8 Hz. The measurement procedures are outlined and a detailed analysis of the working equations and measurement errors is presented.

1. Introduction

It is often important for the study of dielectric properties that measurements be made on a single specimen using a minimum amount of the material over as wide a range of temperatures and frequencies as possible. Low-frequency measurements can conveniently be made on a single disk-shaped specimen, but at higher frequencies conventional equipment requires the use of cylindrical or rectangular specimens of various sizes to fit different microwave guides and cavities. If the dielectric properties of a material are sensitive to differences in specimen preparation, then the use of different specimens to cover the desired frequency range could lead to results which seriously misrepresent the frequency dependence of the dielectric constant and loss even though the individual measurements may themselves be quite accurate.

The two-terminal parallel-plate dielectric specimen holder described in this paper was designed to make measurements on single disk-shaped specimens (about 1 to 2 g of material) over as wide a range of frequencies as possible. Minimum specimen and holder size together with simplicity of construction and operation have been emphasized in order that the cell could easily be fitted with an insulating jacket and operated at temperatures from −200 to +200 °C. The variable temperature operation of the holder will be reported in a later paper.

In this paper, we will discuss the construction of the holder currently in operation at room temperature, and develop the equations for its use with the low-frequency Scheiber bridge [1],[1] the General Radio Models 716C Schering Bridge and 1615A Transformer Bridge, and the Boonton Radio Corporation Models 260A, 280A, and 190A Q-meters. Dielectric constant and loss data obtained with the holder for a disk of commercial poly(methyl methacrylate) over a frequency range of 10^{-2} to 6×10^8 Hz will be presented to illustrate the use of the holder. The experimental errors will be analyzed and discussed in detail. Use of the holder to measure liquid specimens is described in a separate paper [2]. Some of the measurement techniques used here are related to techniques described in a previous publication from this laboratory [3].

[1] Figures in brackets indicate the literature references at the end of this paper.

2. Design and Construction of Specimen Holder

A schematic diagram of the specimen holder is shown in figure 1. The case, cap, and electrodes are made of brass, gold-plated to reduce surface losses at high frequency. The lower electrode, which is operated at high potential, is supported and insulated from the case by a fused silica ring, which in turn is supported by the bottom rim on the holder case. The lower electrode and silica ring are held fixed by small beads of epoxy cement. The upper electrode is connected securely to a brass pin, finely threaded on the upper end to accommodate the spacing nut.

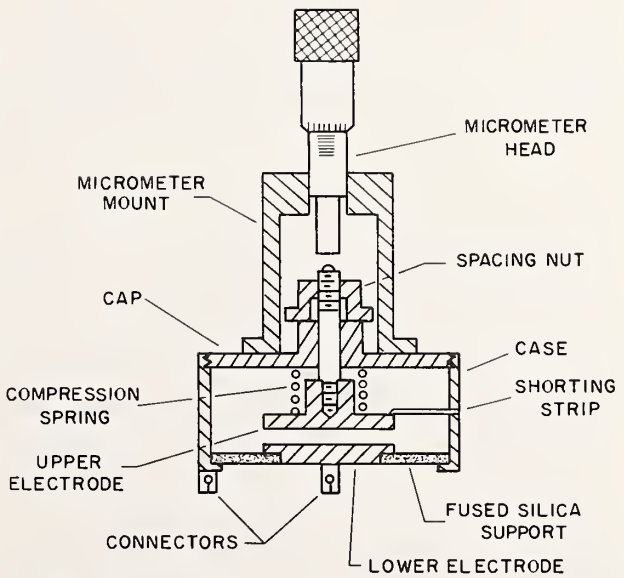

FIGURE 1. *A schematic diagram of the two-terminal dielectric specimen holder.*

The compression spring holds the spacing nut against the shoulder on the holder cap and rotation of the spacing nut raises or lowers the electrode and hence regulates the spacing. The spacing between the electrodes is determined by measuring the position of a steel ball, mounted at the top of the upper electrode assembly, with a micrometer barrel mounted rigidly to the holder cap. Electrical connection to the upper (ground potential) electrode is made by soldering four flexible gold foil strips between the upper electrode and case. Such an arrangement was preferred to conventional metal bellows mounting because of the former's shorter electrical path. Electrical connection to the holder is made through two connector caps soldered to the case and lower electrode, which fit snugly over pins suitably attached to the measuring equipment. The holder electrodes are 2.54 cm in diameter. The micrometer measures 10 μ per division and readings are estimated to 1 μ (1 $\mu = 10^{-6}$ m).

3. Theory of Measurements

Each dielectric constant and loss determination involves a specimen in and specimen out measurement of the holder impedance at the measurement frequency, and two calibration measurements of the empty holder capacitance at some convenient audio frequency. The calibration measurements can either be done separately and compiled in the form of a curve of measured capacitance versus electrode spacing which is then applicable to all measurement frequencies, or they can be performed at the time of each determination with increased accuracy.

Figure 2 shows a schematic diagram of the two-terminal holder for the two measurement frequency conditions, together with the assumed equivalent circuit and the effective series resistance and capacitance of the cell. The symbols used in figure 2 are explained in table 1. The two audio-frequency calibration measurements can be represented in a way similar to figure 2b except that the effects of lead inductance can be ignored. When the measurement frequency is itself in the audio range then the general measurement procedure outlined here can be simplified as is described in the following section.

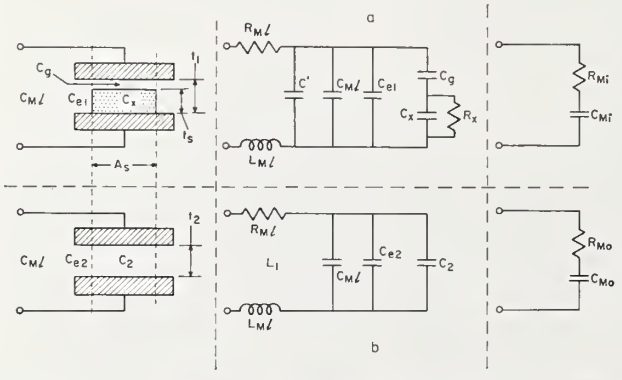

FIGURE 2. *A schematic representation of the two-terminal holder with (a) and without (b) a specimen and the corresponding assumed equivalent circuits.*

The symbols are defined in table 1.

TABLE 1. *Description of symbols used in text*

$C_x = \epsilon' \epsilon_0 \frac{A_s}{t_s}$ = equivalent parallel capacitance of the specimen.

$C_v = \epsilon_0 \frac{A_s}{t_s}$ = equivalent parallel vacuum capacitance of the specimen.

R_x = equivalent parallel resistance of the specimen.

$C_g = \epsilon_0 \frac{A_s}{t_1 - t_s}$ = capacitance of the airgap between the specimen and electrode.

$C_2 = \epsilon_0 \frac{A_s}{t_2}$ = capacitance berween adjacent areas A_s of the electrodes. C_1 corresponds to t_1.

C_c = the capacitance reading of the standard capacitor in a bridge when the cell is connected. C_{c1} corresponds to t_1 and C_{c_2} to t_2.

C_e = capacitance between the remainder of the electrodes including that portion outside the area A_s and the edges. C_{e_1} corresponds to spacing t_1 and C_{e_2} to t_2.

C_{Ml} = capacitance between the leads when the holder is in the measurement circuit.

C' = error capacitance due to distortion of the electric field (see discussion of errors).

R_{Ml}, L_{Ml} = equivalent resistance and inductance of holder leads when the holder is in the measurement circuit.

R_{Mi}, C_{Mi} = effective series resistance and capacitance of holder with specimen in.

C_{lc} = capacitance between the leads when the holder is in the calibration circuit.

Δf = the difference in frequency between the upper and lower half-power points of an L–C–R series resonant circuit.

R_{Mo}, C_{Mo} = effective series resistance and capacitance of holder with specimen out.

t_s, A_s = thickness and area of specimen.

t_1, t_2 = separation of electrodes at settings 1 and 2.

ϵ' = dielectric constant.

ϵ_0 = permittivity of free space.

ϵ'' = dielectric loss.

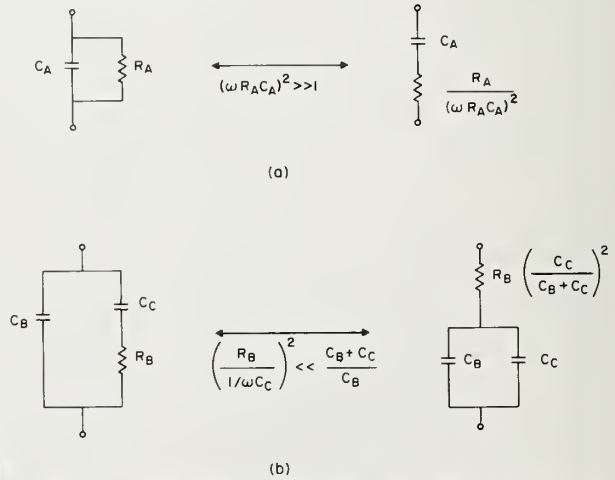

FIGURE 3. *Two simple transformations used to derive the working equations.*

In order to relate the equivalent circuits in figure 2 to their effective measured circuits, the approximate transformations shown in figure 3 were used. The approximations will be suitable for most low loss materials such as many polymers, glasses, and organic compounds. The validity criteria are shown in figure 3, and in general if $\epsilon''/\epsilon' < 0.1$ the transformation approximations will introduce less than 1 percent error in the results.

At the measurement frequency, the effective measured series capacitance and resistance of the holder with specimen in, C_{Mi} and R_{Mi}, and with specimen out, C_{Mo} and R_{Mo}, can be expressed as follows:

$$C_{Mi}=\frac{C_{Hi}}{1-\omega^2 L_{Ml} C_{Hi}} \tag{1}$$

$$R_{Ml}=R_{Ml}+\frac{R_x}{(\omega C_x R_x)^2}\left[\frac{C_x C_g}{C_{Hi}(C_x+C_g)}\right]^2 \tag{2}$$

$$C_{Mo}=\frac{C_{Ho}}{1-\omega^2 L_{Ml} C_{Ho}} \tag{3}$$

$$R_{Mo}=R_{Ml} \tag{4}$$

where

$$C_{Hi}=C'+C_{Ml}+C_{e_1}+\frac{C_x C_g}{C_x+C_g} \tag{5}$$

and

$$C_{Ho}=C_{Ml}+C_{e_2}+C_2. \tag{6}$$

One can write an expression for C_x which is independent of frequency or the type of electrical equipment used. If C_{Mo} is experimentally set equal to C_{Mi}, eqs (1) and (3) can be equated with the result,

$$C_x=\frac{C_g[C_2+(C_{e_2}-C_{e_1})-C']}{C_g-[C_2+(C_{e_2}-C_{e_1})-C']}. \tag{7}$$

From the calibration measurements (circuits correspond to that of figure 2b ignoring the lead inductance),

$$C_{c_1}=C_{lc}+C_{e_1}+C_1$$

$$C_{c_2}=C_{lc}+C_{e_2}+C_2, \tag{8}$$

one finds

$$C_2+(C_{e_2}-C_{e_1})=(C_{c_2}-C_{c_1}+C_1), \tag{9}$$

which can be substituted into eq (7) to give

$$C_x=\frac{C_g[(C_{c_2}-C_{c_1})+C_1-C']}{C_g-[(C_{c_2}-C_{c_1})+C_1-C']}. \tag{10}$$

Writing C_g and C_1 in the numerator in terms of measured quantities and applying the definition of ϵ' one finds

$$\epsilon'=\frac{C_x}{C_v}=\frac{1}{C_v}\left[(C_{c_2}-C_{c_1})+\frac{\epsilon_0 A_s}{t_1}-C'\right] \times\left[1-\frac{t_1-t_s}{t_1}-\frac{(C_{c_2}-C_{c_1})}{C_g}+\frac{C'}{C_g}\right]^{-1}. \tag{11}$$

The last term in brackets is the airgap correction term whose value is close to unity. It should be noted that this airgap term will be used in this form throughout the text. The effect of the error capacitance C' is also small (see discussion of errors) and hence the value of ϵ' is primarily dependent on the difference between two empty holder capacitances measured at audio frequencies and on the sample dimensions and initial holder spacing.

Since the holder is a part of the measurement circuit when the specimen is both in and out of the holder, the lead losses R_{Ml} can be eliminated by combining eqs (2) and (4), giving,

$$\Delta R_M=R_{Mi}-R_{Mo}=\frac{C_x D_x}{\omega}\left[\frac{C_g}{C_{Hi}(C_x+C_g)}\right]^2 \tag{12}$$

or

$$\epsilon''=\frac{C_x}{C_v}D_x=\frac{\omega}{C_v}\Delta R_M\left[\frac{C_{Hi}(C_x+C_g)}{C_g}\right]^2. \tag{13}$$

Unfortunately, there is not a convenient way to make resistance substitutions for the specimen loss so that the calculation of R_x will depend on the particular methods used at the measurement frequency.

4. Measurement Procedure

4.1. Q-Meter Procedure of Measurement

For Q-meter measurements in the frequency range 10^5 Hz to 2.5×10^8 Hz, two Q-meters were used, the Boonton Radio 260A Q-meter (100 kHz to 20 MHz) and the Boonton Radio 190A Q-meter (20 MHz to 250 MHz). The measurement procedure used is as follows: The holder is mounted on top of the Q-meter and connected in parallel with the Q-meter capacitor, C_s, with the shortest possible leads. With the specimen in the holder, the circuit is brought to resonance by tuning the Q-meter capacitor, C_s, to C_s'. The values of C_s', the electrode spacing t_1, and the Q of the circuit with the specimen in the holder, Q_i, are recorded. The specimen is then removed from the holder and the electrode spacing is decreased until resonance is achieved while holding C_s fixed at C_s'. The electrode spacing t_2 and the Q of the circuit with the specimen out, Q_o, are recorded.

The two resonant situations, with the specimen in and with the specimen out, occur at the same frequency and the total capacitance in the resonant circuits must be the same in both cases. The value of the total capacitance, C_T, is taken as the value of C_s when the Q-meter is tuned to resonance with the holder removed.

For the Q-meter measurement, the circuits of figure 2 may be viewed in parallel with the Q-meter capacitance C_s'. Considering figure 2a, one finds that if C_{Mi} and R_{Mi} are placed in parallel with C_s' then the transformation of figure 3b can be used to reduce the circuit to a simple L–C–R series circuit, for which the total series capacitance, the total series resistance and the Q of the resonant circuit with the specimen in the holder, C_T, R_{si}, and Q_i, are given as

$$C_T = C_{Mi} + C_s', \tag{14}$$

$$R_{si} = R_{Mi}\left(\frac{C_{Mi}}{C_T}\right)^2, \tag{15}$$

and

$$1/Q_i = \omega R_{si} C_T \tag{16}$$

where C_{Mi} and R_{Mi} are defined by eqs (1) and (2).

Likewise, with the specimen out and with the holder at spacing t_2, the resonant circuit can be represented by figure 2b in parallel with C_s'. The total capacitance, the total series resistance and the Q of the resonant circuit with the specimen out of the holder, C_T, R_{so}, and Q_o, are given as

$$C_T = C_{Mo} + C_s', \tag{17}$$

$$R_{so} = R_{Mo}\left(\frac{C_{Mo}}{C_T}\right)^2 \tag{18}$$

and

$$1/Q_o = \omega R_{so} C_T, \tag{19}$$

where C_{Mo} and R_{Mo} are given by eqs (3) and (4).

Equating the expression for C_T in eqs (14) and (17) will yield eq (11) of the previous section for the measured value of ϵ'.

An expression for ϵ'' is obtained from the difference, $Q_i^{-1} - Q_o^{-1}$, using eqs (16) and (19). Thus,

$$\Delta\left(\frac{1}{Q}\right) = Q_i^{-1} - Q_o^{-1} = \frac{\omega R_x}{(\omega R_x C_x)^2}\left[\frac{C_x C_g}{C_{Hi}(C_x + C_g)}\right]^2\left(\frac{C_{Mo}}{C_T}\right)^2 C_T. \tag{20}$$

Rearranging, dividing through by C_v, and using $C_{Hi} = C_{Ho}$, one obtains,

$$\epsilon'' = \frac{1}{\omega R_x C_v} = \left[\frac{C_T}{C_v}\Delta\left(\frac{1}{Q}\right)\right]\left(\frac{C_{Ho}}{C_{Mo}}\right)^2\left(\frac{C_x + C_g}{C_g}\right)^2. \tag{21}$$

In the above equation, the term in brackets is the dominant term and it alone would be present if there were no airgap or lead inductance. The term $(C_{Ho}/C_{Mo})^2$ results from the effect of lead inductance, which becomes significant above 30 MHz (see eq (3)). The third term, $[(C_x + C_g)/C_g]^2$, is the airgap correction.

Equation (21) can be reduced to following working equation:

$$\epsilon'' = \frac{C_T}{\epsilon_o A_s/t_s}\Delta\left(\frac{1}{Q}\right)\left(\frac{C_{Ho}}{C_T - C_s'}\right)^2\left[1 - \frac{t_1 - t_s}{t_1} - \frac{C_{c_2} - C_{c_1}}{C_g'} + \frac{C''}{C_g'}\right]^{-2} \tag{22}$$

In the above equation C_{Mo} has been replaced by $C_T - C_s'$ in accordance with eq (17). The capacitances, C_T and C_s', are obtained from the calibrated Q-meter capacitor. The capacitance C_{Ho} is obtained from the audio frequency calibration. Omitted from the above equations are the high-frequency corrections which must be applied to the values of Q and C_s as read from the 190A Q-meter. The manner in which these corrections are carried out is explicitly stated in the 190A Q-meter manual.

A more detailed description of Q-meter dielectric measurements may be obtained from a paper by Hazen [4] in which he shows how the Q-meter circuit may be adapted for the measurement of very low losses.

4.2. Two-Terminal Measurements at Audio Frequencies

The General Radio (GR) 716C Schering bridge was used for audio frequencies from 10^2 Hz to 10^5 Hz, and the GR 1615A transformer ratio arm bridge was used from 5×10^2 Hz to 2×10^4 Hz.

For audio frequencies the effects of the lead inductance can be ignored, and the circuits of figure 2 without the inductance are considered here. With these bridges one measures the dissipation factor and the effective series capacitance of the unknown. However, when $\epsilon''/\epsilon' < 0.1$ the series capacitance and the parallel capacitance of the unknown are equal (within 1 percent) and this case is treated here. For $\epsilon''/\epsilon' > 0.1$ the GR bridge manuals should be consulted.

If the holder and specimen are connected as a two-terminal device in an arm of the bridge and if the procedure of measurement which was used with the Q-meter is also used with the bridge, then the result for ϵ' is the same as eq (11) and

$$\epsilon'' = \frac{C_T}{C_v}(D_i - D_o)\left(\frac{C_x + C_g}{C_g}\right)^2, \tag{23}$$

where D_i and D_o are the dissipation factors with the specimen in and out of the holder, and C_T is the total capacitance in the arm of the bridge which contains the holder. Just as with the Q-meter measurement, C_T must be the same for the D_i and D_o measurements.

A variation on the above experimental procedure which utilizes the standard capacitor in the bridge is preferable when using a bridge circuit and null detector for a two-terminal measurement. First, a bridge balance is obtained with the specimen and holder in the bridge circuit. Then t_1, D_i, and the standard bridge capacitor reading C_{si} are recorded.

The sample is taken out of the holder. Keeping the spacing fixed at t_1, the capacitance of the standard capacitor, C_s, is varied to rebalance the bridge. The specimen-out values, C_{so} and D_o are recorded.

If a bridge measurement is made by changing the standard capacitor while holding the electrode spacing at t_1, then a distinction must be made between using the substitution method of measurement and using the bridge as a direct reading instrument. In the substitution method, the unknown is connected in parallel with the standard capacitor, whereas for the direct method the unknown is connected in the bridge arm electrically opposite the standard capacitor. The GR 1615A is most conveniently used to measure C and D directly. The substitution method is used with the GR 716C bridge by connecting a precision air ballast capacitor to the "unknown direct" terminals.

When the electrode spacing is t_1 for both "in" and "out" measurements and a direct measurement is made, the total capacitance in the unknown bridge arm will be different for the "in" and "out" balances. Let C_{Ti} and C_{To} be the total capacitance in the unknown bridge arm with the sample in and out of the holder respectively. For a direct measurement we have,

$$C_{Hi}=C_{Ml}+C_{e_1}+C'+\frac{C_xC_g}{C_x+C_g}, \tag{24}$$

$$C_{Ho}=C_{Ml}+C_{e_1}+C_1 \tag{25}$$

from which ϵ' can be calculated in terms of measurable quantities. Using $C_{Hi}-C_{Ho}=C_{si}-C_{so}$ we have for a direct measurement

$$\epsilon'=\frac{1}{\epsilon_0A_s/t_s}\left(C_{si}-C_{so}+\frac{\epsilon_0A_s}{t_1}-C'\right)\times\left[1-\frac{t_1-t_s}{t_1}-\frac{C_{si}-C_{so}}{C_g}+\frac{C'}{C_g}\right]^{-1} \tag{26}$$

and

$$\epsilon''=\frac{C_{Ti}}{\epsilon_0A_s/t_s}\left(D_i-\frac{C_{To}}{C_{Ti}}D_o\right)\left[1-\frac{t_1-t_s}{t_1}-\frac{C_{si}-C_{so}}{C_g}+\frac{C'}{C_g}\right]^{-2} \tag{27}$$

For a direct measurement with the GR 1615A transformer bridge it is conveniently true that $C_{To}=C_{so}$ and $C_{Ti}=C_{si}$.

On the other hand, for the substitution measurement, $C_{To}=C_{Ti}=C_T$ and $C_{si}<C_{so}$. For ϵ' and ϵ'' we have,

$$\epsilon'=\frac{1}{\epsilon_0A_s/t_s}\left(C_{so}-C_{si}+\frac{\epsilon_0A_s}{t_1}-C'\right)\times\left[1-\frac{t_1-t_s}{t_1}-\frac{C_{so}-C_{si}}{C_g}+\frac{C'}{C_g}\right]^{-1} \tag{28}$$

and

$$\epsilon''=\frac{C_T}{\epsilon_0A_s/t_s}(D_i-D_o)\left[1-\frac{t_1-t_s}{t_1}-\frac{C_{so}-C_{si}}{C_g}+\frac{C'}{C_g}\right]^{-2} \tag{29}$$

where the bracketed term in eqs (26) to (29) is the airgap correction term. To obtain the total capacitance, C_T, in the unknown arm of the GR 716C Schering bridge a separate bridge measurement is necessary. During the "in" and "out" measurement the ballast capacitance, C_B, remains fixed at C_T. After the specimen holder has been disconnected, C_B is measured by switching the bridge to "direct" and balancing the bridge by changing the standard capacitor. The dial reading of the standard capacitor is calibrated by measuring a known C_B. The calibration should also include the 1 pF capacitance of the bridge terminals.

4.3. Measurements at Ultra-Low Frequencies

The Scheiber ultra-low-frequency bridge was used in the frequency range 10^{-2}Hz to 2×10^{2}Hz [1]. Although the bridge was designed for use with a three-terminal dielectric cell, we have found that it may be easily adapted for measurements with a two-terminal cell. Ordinarily the leads from the bridge to the electrodes are shielded at ground potential and the shield encompasses the entire cell. For the two-terminal holder the electrode leads are shielded but the shield is abandoned at the base of the holder where the electrodes connect. A shield around the entire cell was improvised by lowering an aluminum box over the holder and connecting the the box to ground.

The substitution method of measurement with the electrode spacing fixed at t_1 for the "in" and "out" bridge balance is used. Equations (22) and (23) of Scheiber's paper [1] in conjunction with the airgap correction term of this paper were used to calculate the capacitance and conductance of the unknown.

For measurements below 10 Hz the surface conductivity of the sample can become a problem. It can be eliminated by wiping and cleaning the edges of the sample and thereafter handling the sample with tweezers and by introducing dry nitrogen through one of the ports of the cell.

4.4. Self-Resonant Measurements

The two-terminal holder can be used up to 600 MHz by shorting the terminals with an appropriate length conductor and exciting the resulting circuit at its self-resonant frequency. The Boonton model 280A UHF Q-meter was used as a combined oscillator and detector. The oscillator was coupled to the holder through a variable attenuator by means of a single-loop inductive probe. The signal was picked up with a capactive probe and rectified to give a d-c voltage which was applied to a voltemeter in the model 280A. The voltmeter is calibrated in

full and half-power levels which can be conveniently checked by switching 3 dB into the inductive probe. The oscillator frequency was measured with a Hewlett Packard model 524C frequency meter and 540A transfer oscillator.

Measurements were made by placing the specimen in the holder and tuning the circuit by adjusting the oscillator frequency. The frequency corresponding to the half-power points is then determined and recorded along with the electrode spacing. The specimen is then removed and the circuit retuned by adjusting the holder electrode spacing. The frequencies corresponding to the half-power points are again measured and recorded. One or more additional measurements of electrode spacing and corresponding resonance frequency must be made in order to determine the change in capacitance with resonance frequency.

Calculations are based on eqs (1) through (6), where the terminals in figures 2a and 2b are shorted. Thus we treat the problem as a simple series $L_T C_T R_T$ circuit for which the dissipation factor D_T and total capacitance C_T are

$$D_T=\omega C_T R_T, \tag{30}$$

$$C_T=\frac{1}{\omega^2 L_T}. \tag{31}$$

One may obtain ϵ' from eq (11) and ϵ'' from eq (13) remembering that here $C_{Hi}=C_T$ and

$$\Delta D_M=D_{Mi}-D_{Mo}=\omega C_T(R_{Mi}-R_{Mo}). \tag{32}$$

Substituting (32) into eq (13) gives

$$\epsilon''=\frac{C_T}{C_v}\Delta D_M\left(\frac{C_x+C_g}{C_g}\right)^2. \tag{33}$$

The ratio of the frequency separation of the half-power points to the resonance frequency is measured to obtain the dissipation factor. The total capacitance which cannot be measured directly can be obtained by differentiating eq (31) to obtain

$$\frac{dC_T}{df_M}=-\frac{2}{f_M}C_T. \tag{34}$$

Hence we can write

$$\epsilon''=-\frac{dC_T}{df_M}\cdot\frac{\Delta f_i-\Delta f_0}{2C_v}\left(\frac{C_x+C_g}{C_g}\right)^2. \tag{35}$$

Since the only part of C_T which changes with spacing, t, is the calibration capacitance C_c of the holder one can write

$$\epsilon''=-\frac{dt}{df_M}\cdot\frac{dC_c}{dt}\cdot\frac{\Delta f_i-\Delta f_0}{2C_v}\left(\frac{C_x+C_g}{C_g}\right)^2. \tag{36}$$

Finally

$$\epsilon''=-\frac{dt}{df_M}\cdot\frac{dC_c}{dt}\cdot\frac{\Delta f_i-\Delta f_0}{2\epsilon_0 A_s/t_s}\times\left[1-\frac{t_1-t_s}{t_1}-\frac{C_{c2}-C_{c1}}{C_g}+\frac{C'}{C_g}\right]^{-2}. \tag{37}$$

5. Sample Data

In order to illustrate the results which can be obtained with the dielectric specimen holder described in this paper, room temperature measurements were made on two specimens machined from the same 2.54-cm-diam poly(methyl methacrylate) rod into disks of average thicknesses 0.3150 cm and 0.1577 cm. The disk faces were made flat and parallel to better than 10 μ and no contact electrodes were applied. Both specimens were kept at about 23 °C at a relative humidity of 50 percent for several months before being measured. The measuring techniques used are those described in detail in the previous sections, and the measurements on the two specimens over the whole frequency range took about 10 hr. Calculations of ϵ' and ϵ'' were done by hand. The results of the measurements are shown in figure 4 which is a plot of the values of ϵ' and ϵ'' versus log frequency for the 0.3150-cm-thick specimen of poly(methyl methacrylate).

The data for the two specimens measured were found to agree to within 1 percent for ϵ' and 5 percent for ϵ'' at all frequencies, and with just a few exceptions, the agreement was within 0.3 percent for ϵ' and 2 percent for ϵ'' over the frequency range covered. In addition, the highest frequency values, which are the most crucial as far as the magnitude of the circuit correction is concerned, agree with each other and with measurements made using a reentrant cavity [3] within 0.3 percent in ϵ' and 2 percent in ϵ''. Additional measurements made on specimens of polychlorotrifluoroethylene and fused silica gave results which were also accurate to within the limits claimed in this paper except for the loss in fused silica which could not be detected at high frequency.

6. Discussion of Measurement Errors

The two-terminal method described in this paper was intended to provide values of ϵ' and ϵ'' over the entire range of applicable frequencies without imposing rigid requirements on specimen preparation and cell construction. In addition to uncertainties in the quantities explicitly appearing in the working equations of the previous section, attention must be given to the assumptions and approximations upon which these equations are based, the errors due to which will appear in an error capacitance term C'.

The error capacitance (in fig. 2 and eq (5)) includes corrections to the ideal assumed capacitance

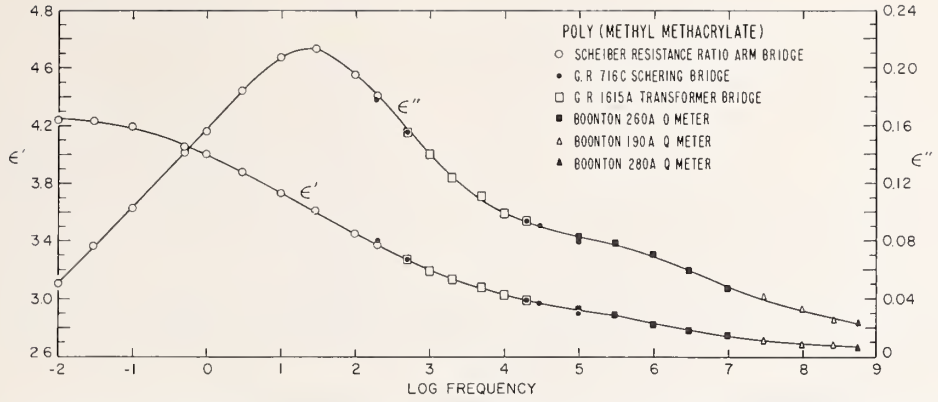

FIGURE 4. *The dielectric constant (ϵ') and loss index (ϵ'') of a 0.3150-cm-thick disk of commercial poly(methyl methacrylate) as a function of frequency as measured with the two-terminal dielectric specimen holder using various measuring equipment.*

resulting from distortions of the electric field between the measuring electrodes because of (a) tilted, misalined or nonflat electrode surfaces, (b) the presence of an airgap, (c) departure of the specimen geometry from an ideal right circular cylinder, (d) electrode edge effects, and (e) the presence of air between the electrodes.

(a) The errors due to nonideal electrodes are all second order effects with the actual capacitance given by

$$C=\epsilon'\epsilon_0\frac{A}{t}\left[1+0\left(\frac{\Delta}{t}\right)^2\right]$$

where A and t are the electrode area and separation and Δ represents the variation in t in the case of tilted or uneven electrodes or the distance between axes of the electrodes in the case of misalined electrodes. It is not difficult to keep mechanical errors to within 25 μ (25 μ=0.001 in.). With typical separations, t, of 1000 μ these errors amount to roughly $<$0.1 percent. In addition, the tilt error increases the capacitance whereas the misalinement error decreases it. Also since each determination of C involves a difference between two measurements, the effects tend to cancel. Thus the mechanical construction need not require special attention.

(b) The airgap causes some distortion of the field at the edge of the specimen (which increases with gap width and dielectric constant) and makes the actual capacitance higher than its uncorrected value. This in turn leads to a high value for the specimen capacitance C_x. An upper limit to this error ($\epsilon'=\infty$) for a typical measurement was calculated to be 0.2 percent [6], and one can reasonably conclude that in most cases the error from this source is $<$0.1 percent.

(c) Geometric imperfections in the specimen also lead to distortions. Rounded corners would cause an error similar to the airgap error. Uneven or nonparallel specimen surfaces lead to an actual capacitance greater than that assumed. The airgap capacitance is particularly affected by nonideal specimen surfaces. The specimen surface may well be tilted with respect to the adjacent electrode surface so that the airgap is a wedge of average thickness t=15 μ and variation Δ=10 μ. In this case the assumed airgap capacitance may be in error by 20 percent. (This calculation is based on the worst case—the capacitance of two concentric but mutually tilted circular disks in the limit of minimum separation.) Fortunately, the airgap capacitance enters the calculations in a very insensitive way so that an error of 20 percent in C_g would result in an error of perhaps 0.5 percent in C_x, and the error would be such as to increase the value of C_x above its true value. The geometry of the specimen does not appear to be particularly critical and special molding and machining techniques are not required.

(d) Electrode edge effects have been studied extensively [5]. With the specimen in place the edge capacitance is higher than one assumes and hence the calculated value of C_x is too high. In general, this error increases with ϵ' and also with the proximity of the specimen to the edge of the electrode. If the distance between the specimen and the electrode edges is twice the separation of the electrodes then this error is $<$0.1 percent [5]. Thus it is advisable to design the holder accordingly keeping in mind that measurement sensitivity decreases as the ratio of electrode area to specimen area increases, i.e., as C_x becomes a smaller part of the total capacitance.

(e) Since ϵ' for air is about 0.06 percent higher than assumed, then the actual capacitance with specimen removed is higher than calculated, thus lowering ϵ' by $<$0.1 percent. The effect on the airgap is negligible.

A final approximation of the accuracy of the measurements can be obtained from an estimate of the accuracy of the measured quantities in the working equations. Generally, the calibration capacitances can be measured to the nearest 0.1 percent, the linear dimensions to the nearest micron and the area of the sample using a traveling microscope to 0.02 percent. Considering eq (11) for ϵ' the factors and

their percent uncertainty are C_v, ±0.3 percent; $[(C_{c_2}-C_{c_1}+\epsilon_0 A_s/t_s-C']$, ±0.3 percent; the airgap correction term, ±0.5 percent. In eqs (22), (23), (27), and (29) for ϵ'', the factors and their percent uncertainty are C_T, ±0.2 percent; $\epsilon_0 A_s/t_s$, ±0.3 percent; $\Delta\left(\frac{1}{Q}\right)$, ±3 percent; $C_{Ho}/(C_T-C_s')$, ±0.3 percent; (D_i-D_o), ±(0.5% +0.00005) for GR 1615A; (D_i-D_o), ±(2% +0.0005) for GR 716C; and the airgap correction ±1 percent. For eq (37) the percent uncertainty of the terms are dt/df_M, ±0.5 percent; dC_c/dt, ±1 percent; and Δf_i and Δf_o, ±(0.2%+10kHz).

The total percent uncertainty for ϵ' and ϵ'' is obtained from the square root of the sum of the squares of the uncertainties in the working equations. For ϵ' the percent uncertainty is ±0.7 percent over the entire frequency range 10^{-2} to 6×10^8 Hz. For ϵ'' we have ±(1.5%+0.0005) for the ultra low frequency bridge, ±(1.8%+0.0005) for the GR 716C bridge, ±(0.6%+0.0001) for the GR 1615A bridge, ±(4%+0.0005) for the 260A and 190A *Q*-meters, and ±(1.6%+0.0005) for the self-resonant measurements.

7. References

[1] D. J. Scheiber, J. Res. NBS **65C** (Eng. and Instr.), No. 1, 23(1961).

[2] A. J. Bur, 1964 Annual Report of the Conference on Electrical Insulation, National Academy of Sciences-National Research Council Publication 1238, p. 70.

[3] A. H. Scott, D. J. Scheiber, A. J. Curtis, J. I. Lauritzen, Jr., and J. D. Hoffman, J. Res. NBS **66A** (Phys. and Chem.), No. 4, 269(1962).

[4] T. Hazen, Presented to the 13th Annual Wire and Cable Symposium, Atlantic City, New Jersey, December 2–4, 1964.

[5] A. H. Scott and H. L. Curtis, J. Res NBS **22,** 747(1939) RP 1217.

[6] J. I. Lauritzen, Jr., unpublished results.

(Paper 69C3–195)

UNITED STATES DEPARTMENT OF COMMERCE • Luther H. Hodges, *Secretary*
NATIONAL BUREAU OF STANDARDS • A. V. Astin, *Director*

Basic Magnetic Quantities and the Measurement of the Magnetic Properties of Materials

Raymond L. Sanford and Irvin L. Cooter

National Bureau of Standards Monograph 47

Issued May 21, 1962

315-411 O - 68 - 29

439-I

Preface

Since 1909 when the first NBS Circular on Magnetic Testing was issued, successive revisions have been prepared in order to keep up to date with the development of new magnetic materials and methods of testing. Since the last circular, C 456, Magnetic Testing, was issued in 1946 the importance of magnetic materials and testing methods has greatly increased. In view of the many requests for information regarding magnetic quantities, materials, and testing methods, the present revision and extension of the previous circular has been prepared. It supersedes Circular C 456, Magnetic Testing.

Contents

Basic Magnetic Quantities and the Measurement of the Magnetic Properties of Materials

R. L. Sanford and I. L. Cooter

This paper gives general information regarding the two basic quantities, magnetic induction, B, and magnetizing force, H, and also the magnetic constant Γ_m (often designated by the symbols μ_v and μ_0). Information is also given regarding the magnetic properties of various materials and methods and apparatus commonly used in the Magnetic Measurements Section for measuring these properties by means of reversed direct current or alternating currents of low frequency. Magnetic measurements peculiar to high frequencies are not discussed. In view of the gradual adoption of the rationalized mksa system of units, this system is included as well as the classical cgs electromagnetic system.

1. Introduction

The work of the Magnetic Measurements Section of the National Bureau of Standards includes (1) testing of specially prepared test specimens intended for use as standards for checking magnetic testing apparatus (2) investigation and development of magnetic testing apparatus (3) calibration of mutual inductors, test coils, and instruments for measuring magnetic fields, and (4) investigations in the field of magnetics such as studies of phenomena associated with nuclear magnetic resonance or the selection and testing of materials suitable to be used as standards of magnetic susceptibility.

This monograph gives general information regarding magnetic quantities and units, the magnetic characteristics of various materials, and methods and apparatus commonly used in the Magnetic Measurements Section for magnetic testing.

2. Magnetic Quantities and Units

2.1. Systems of Units—Dimensions

For many years magnetic quantities have been expressed in the cgs electromagnetic [1] system of units. In this system the centimeter, gram, and second are taken to be the basic units in which the concepts length, mass, and time respectively are expressed. A three-dimensional system lacks the "resolving power" necessary to distinguish between the magnetic quantities denoted by the symbols B and H. The ratio between these two quantities in empty space, μ_v or μ_0, is arbitrarily assigned the value unity in this system and therefore μ_v or μ_0 is usually omitted from the equations without affecting the *numerical* values.

Another system based on the meter, kilogram, and second as the units of length, mass, and time respectively has been adopted by the International Electrotechnical Commission (IEC) and is rapidly gaining favor. It seems likely that this system eventually will replace the cgs system. In this system the ratio of B to H in empty space is not unity and consequently it cannot be ignored. A fourth dimension in addition to length, mass, and time is required to characterize magnetic and electrical quantities in this system. It must be electric or magnetic in nature. The IEC has chosen electric current, I, as the fourth dimension. When the four dimensions $LMTI$ are applied to magnetic quantities the distinction between B and H is clearly evident.

At the same time that the IEC adopted the mksa (Giorgi) system of units a further step was taken, namely, "rationalization." The object of rationalization is to transfer the factor 4π from linear equations to those having circular symmetry. In the rationalized system, the ratio of B to H in empty space,[2] Γ_m is $4\pi \times 10^{-7}$ h/m. By applying four dimensions to quantities in the cgs electromagnetic system (which is not inherently three-dimensional, as is ordinarily assumed) additional "resolving power" can be gained, the distinction between B and H then becomes clearly evident and mutual consistency between the two systems of units is brought about. The symbols L, M, T, and I denoting length, mass, time, and current respectively may be applied to either system.[3]

[1] There are two other cgs systems, namely the electrostatic system and the gaussian system, but in this monograph cgs means cgs electromagnetic unless otherwise specified.

[2] Since this is a true definitional constant, whereas the symbol μ denotes relationships usually not constant, the symbol Γ_m is used instead of μ_v or μ_0 to avoid confusion.

[3] Many writers consider Q (quantity of electricity) to be a more simple concept than current and use it as the fourth dimension. The dimensions then are $LMTQ$.

2.2. Basic Quantities

There are two basic magnetic quantities and a constant from which all other magnetic quantities are derived. They are magnetic induction, B (often called flux density), magnetizing force or magnetizing field, H (also called magnetic field strength or magnetic intensity), and the magnetic constant Γ_m.

a. Magnetic Induction, B

A current-carrying conductor in a magnetic field experiences a mechanical force, the magnitude of which depends upon the magnitude of the current and the field, the length of the conductor and its orientation in the field. This dependence on direction and magnitude identifies the field as a vector field. Its direction is considered to be the direction of the conductor for which the mechanical force is zero. The quantity measured by the mechanical force experienced by a current-carrying conductor in a magnetic field is called *magnetic induction*, B.

If a linear conductor is perpendicular to the direction of the field and the field is uniform along its length

$$B=F/Il$$

where B=magnetic induction
F=mechanical force
I=current
and
l=length of the conductor.

There is another phenomenon by which the presence of a magnetic field can be detected and its magnitude determined. If a conducting loop or coil is placed in a magnetic field and the strength of the field is varied, the orientation of the coil in the field is changed or the coil is removed from the field, an electromotive force will be induced in the coil during the change. At any instant while a change is taking place

$$e=Na\ dB/dt$$

where e=instantaneous induced emf
N=number of turns in the coil
a=average area of the turns
B=magnetic induction
t=time.

Provided that B is uniform over the area a, the total change in induction, ΔB, in a given time is

$$\Delta B=\frac{1}{Na}\int_{t_1}^{t_2} e\,dt.$$

The units for the cgs and mksa (Giorgi) systems are as follows:

Symbol	cgs	mksa (Giorgi)
B	gauss	tesla
F	dyne	newton
I	abampere	ampere
l	centimeter	meter
e	volt	volt
a	square centimeter	square meter
t	second	second

The dimension [4] of magnetic induction is

$$[B]=MT^{-2}I^{-1}.$$

b. Magnetizing Force, H

In view of the general acceptance of the concept that the magnetic behavior of materials is due to the presence within them of electrons in motion (spins or rotations) it is reasonable to conclude that magnetism is simply one of the manifestations of an electric current. Magnetic induction at a given point must therefore be due to the influence of electric currents. The magnetizing influence of an electric current is proportional to its magnitude and depends upon its geometrical configuration. The measure of the ability of an electric current to produce magnetic induction at a given point is called the magnetizing force (magnetic field strength or magnetic intensity), H.

At the middle of a very long uniformly wound solenoid

$$H=KNI/l$$

where H=magnetizing force
K=a constant depending on the system of units
N=number of turns
I=current
l=axial length of the solenoid.

The units for the two systems are as follows:

Symbol	cgs	mksa (Giorgi)
H	oersted	Ampere-turn per meter
K	4π	1
N	turn	turn
I	abampere	ampere
l	centimeter	meter

The dimension of magnetizing force is

$$[H]=L^{-1}I.$$

2.3. Magnetic Constant, Γ_m

The magnetic constant for any system of units is the proportionality factor in the expression relating the mechanical force between two currents

[4] The square brackets in a dimensional equation denote "the dimension of."

to their intensities and geometrical configurations. In differential form this may be written

$$d\mathbf{F}=\Gamma_m I_1 I_2 d\mathbf{l}_1\times(d\mathbf{l}_2\times\mathbf{r}_1)/nr^2$$

where

Γ_m is the magnetic constant

$d\boldsymbol{F}$ is the element of force of a current element

$I_1 d\boldsymbol{l}_1$ on another current element

$I_2 d\boldsymbol{l}_2$ at a distance r.

$\boldsymbol{r}_1$ is a unit vector in the direction from l_1 to l_2

n is a dimensionless factor which is unity in unrationalized systems and 4π in rationalized systems.

The magnetic constant is also equal to the ratio of the magnetic induction, B, to the corresponding magnetizing force, H, in a vacuum. For this reason it is often called the permeability of space (or vacuum) and denoted by the symbol μ_v or μ_0. Since the symbol μ, with or without subscripts is used to denote several different relationships between B and H which in general are not constant, the symbol Γ_m is used to denote the magnetic constant. The value of Γ_m determines the system of units employed. In the classical cgs system the value of Γ_m is unity and it is a numeric. In the rationalized mksa (Giorgi) system its value is $4\pi\times10^{-7}$ and the dimension is $LMT^{-2}I^{-2}$ (henries per meter).

2.4. Derived Quantities

The principal derived quantities are associated with the idea of a *magnetic circuit*, somewhat, but not exactly, analogous to an electric circuit. It is a magnetic structure which may contain one or more airgaps or other "nonmagnetic" materials and designed to contain certain continuous lines of magnetic induction. Ideally, none of the induction would escape from the circuit. However, since there is no insulator for magnetism, this ideal condition is rarely if ever realized. The magnetic flux which escapes from a magnetic circuit is called *leakage flux* or simply *magnetic leakage*.

a. Magnetic Flux, ϕ

Given a plane surface or cross section within the boundaries of which there is a uniformly distributed field of magnetic induction, B everywhere having a direction normal to the plane of the surface, the product of the induction, B, by the area, A, is the magnetic flux.

$$\phi=BA$$

where

ϕ=magnetic flux

B=magnetic induction uniformly distributed and normal to the plane of the surface of which

A=area.

If the induction is not uniformly distributed over the area, the surface integral of the normal component of B over the area is the magnetic flux

$$\phi=\iint\mathbf{B}\cdot\mathbf{dA}$$

where

ϕ=magnetic flux

B=Magnetic induction

and

dA=an element of area.

It is important to note that although both B and A are vectors, ϕ is a scalar and cannot have direction.

The units in the cgs and rationalized mksa systems are

Symbol	cgs	mksa
ϕ	maxwell	weber
B	gauss	tesla
A	cm^2	m^2

The dimension of magnetic flux is

$$[\phi]=L^2MT^{-2}I^{-1}.$$

b. Magnetomotive Force, $\mathcal{F}$

In a magnetic circuit, the line integral of the magnetizing force around the circuit is called the magnetomotive force. It is proportional to the total ampere-turns linked with the circuit.

$$\mathcal{F}=KNI$$

where

$\mathcal{F}$=magnetomotive force

N=number of turns

I=current

and

K=a constant depending on the system of units.

The units for the two systems are

Symbol	cgs	mksa
$\mathcal{F}$	gilbert	ampere-turn
N	turn	turn
I	abampere	ampere
K	4π	1

The dimension of magnetomotive force is $[\mathcal{F}]=I$.

c. Magnetic Reluctance, $\mathcal{R}$

The magnetic flux resulting from a given magnetomotive force acting on a magnetic circuit is determined by the magnetic reluctance $\mathcal{R}$, of the circuit. Thus

$$\phi=\mathcal{F}/\mathcal{R}$$

where

ϕ=flux

$\mathcal{F}$=magnetomotive force.

and

$\mathcal{R}$=magnetic reluctance.

The units are

Symbol	cgs	mksa
ϕ	maxwell	weber
$\mathcal{F}$	gilbert	ampere-turn
$\mathcal{R}$	(5)	

The dimension of reluctance is $[R]=L^{-2}M^{-1}T^2I^2$.

Table 1. *Magnetic quantities and units*

Quantity and dimension (mksa)	Symbol	cgs Unit [a] Name	cgs Unit [a] Equation	Name of rationalized mksa unit	To convert cgsem value to rationalized mksa values, multiply by
Induction $MT^{-2}I^{-1}$	B	gauss	$B=\frac{F}{Il}$ (I in abamperes)	tesla (weber/m^2)	10^{-4}
Magnetizing force $L^{-1}I$	H	oersted	$H=\frac{4\pi NI}{10l}$ (I in amperes)	ampere-turn per meter	$\frac{10^3}{4\pi}=79.58$
Magnetic Constant $LMT^{-2}I^{-2}$	Γ_m		$\Gamma_m=\frac{B}{H}$ (in vacuum)		$4\pi\times10^{-7}=12.57\times10^{-7}$
Flux $L^2MT^{-2}I^{-1}$	ϕ	maxwell	$\phi=\iint_A BdA$	weber	10^{-8}
Magnetomotive Force I	$\mathcal{F}$	gilbert	$\mathcal{F}=\int Hdl$	ampere-turn	$10/4\pi=0.7958$
Reluctance $L^{-2}M^{-1}T^2I^2$	$\mathcal{R}$		$\mathcal{R}=\frac{\mathcal{F}}{\phi}$		$10^9/4\pi=79.58\times10^6$
Normal permeability $LMT^{-2}I^{-2}$	μ		$\mu=\frac{B}{H}$		$4\pi\times10^{-7}=12.57\times10^{-7}$
Relative Permeability (dimensionless)	μ_r		$\mu_r=\frac{\mu}{\Gamma_m}$		(a)
Susceptibility (dimensionless)	k		$k=\frac{\mu_r-1}{4\pi}$		$4\pi=12.57$

[a] In this table, "cgs unit" refers to the unrationalized cgs electromagnetic system.

3. Magnetic Characteristics of Materials

3.1. Magnetic Permeability

Magnetic permeability, denoted by a symbol μ, with or without certain subscripts, is a term used to express various relationships between magnetic induction, B, and magnetizing force, H, in a material under specified conditions. The simplest relationship is the ratio of induction to the corresponding magnetizing force.

$$\mu=B/H.$$

This is usually called absolute permeability or simply the permeability. The term has a specific significance, however, only under certain definite conditions. For certain types of material the ratio is constant, not depending upon the degree of magnetization. For other materials the ratio depends upon the induction. If the corresponding values of B and H are determined by a standardized normal procedure (to be described later) the ratio of B to H is called the normal permeability. This is generally denoted by the symbol μ, without subscripts. It relates only to points on the normal induction curve. The symbol μ with various subscripts denotes either the normal permeability at specified values of B or H or the ratio of certain changes in B to the corresponding changes in H. In this discussion, the term permeability (symbol μ) denotes normal permeability.

Permeability has the dimension

$$[\mu]=LMT^{-2}I^{-2}$$

in the rationalized mksa system.

The symbol μ_r denotes the quantity called relative permeability. It is the ratio of the permeability of a material to that of space (or vacuum). Or it may be defined as the ratio of the permeability of a material to the magnetic constant.

$$\mu_r=\mu/\Gamma_m$$

Since this is the ratio of two quantities having the same dimensions, μ_r is seen to be a dimension-

[5] Previous to 1930 the cgs unit of reluctance was called the oersted, but the International Electrotechnical Commission, in 1930 adopted the name oersted for the cgs unit of magnetizing force, leaving the unit of reluctance without a name.

less ratio and its value is independent of the system of units. The absolute permeability is the relative permeability multiplied by the value of Γ_m pertinent to the system of units employed. In the cgs system, the valuc of Γ_m is unity so that the numerical value of the absolute permeability in this system is the same as that of the relative permeability. It is for this reason that in the cgs system the normal permeability is considered also to be a dimensionless ratio which leads to the conclusion that B and H are quantities of the same kind.

3.2. Magnetic Susceptibility

The magnetic induction, B, in a material due to a magnetizing force, H, is made up of two components, that induced in the space alone, $\Gamma_m H$, and that due to the magnetization[6] of the specimen, B_i. That is

$$B=\Gamma_m H+B_i.$$

The ratio of these two components is called the magnetic susceptibility, k

$$k=B_i/\Gamma_m H$$

since

$$B_i=B-\Gamma_m H$$

$$k=B_i/\Gamma_m H=(B/\Gamma_m H)-1=\mu_r-1.$$

This differs from susceptibility in the classical cgsem system by the factor 4π because in the cgsem system in which $\Gamma_m=1$, the equations are customarily written

$$B=H+4\pi J$$

$$J=(B-H)/4\pi$$

and

$$k=J/H=(B-H)/4\pi H=(\mu-1)/4\pi.$$

J is called intensity of magnetization and has the dimensions of magnetic induction. The ratio of J to H, therefore, has the dimensions of permeability although susceptibility is actually a dimensionless constant. However, in the cgsem system only three dimensions are employed, B and H are considered to be quantities of the same kind, and μ is a dimensionless ratio. In the mksa system as has been previously noted Γ_m is not unity and therefore in vacuum B is not equal to H, their ratio is not unity and so neither the values nor the dimension of Γ_m can be ignored as they are in the classical cgsem system.

Susceptibility is used to characterize materials whose permeability differs from unity by only a very small amount. The susceptibility of a material divided by its density, ρ, is called its mass susceptibility, χ.

[6] The component due to the magnetization of the specimen is called the intrinsic induction, B_i

$$\chi=k/\rho$$

The mass susceptibility multiplied by the atomic weight A is called atomic susceptibility, χ_A.

$$\chi_A=\chi A$$

3.3. Classification of Materials [32]

The magnetic properties of materials result from the motions of electric charges within them. The motions are either rotation in orbits or spins about the axis of the charges. These motions constitute equivalent electric currents and therefore produce magnetic fields. The field-producing effect of an orbit or spin is called its *magnetic moment.* It is a vector whose direction is that of the axis of spin or of the normal to the plane of the orbit and whose magnitude is the product of the equivalent current and the area enclosed by its path. The magnetic moment of a magnetized body is the vector sum of its internal moments. Dimensionally, $[m]=L^2I$ where m is the magnetic moment.

In the past, materials have been classified as diamagnetic, paramagnetic, or ferromagnetic. However, two other classes are now recognized, namely, antiferromagnetic and ferrimagnetic. The magnetic properties of a single atom depend upon the relative locations and directions of spins of its electrons. The spin of the nucleus and orbital motion of the electrons constitute such small parts of the magnetic moment that they can generally be neglected. The moments of two electrons in the same orbit or shell whose spins are in opposite directions mutually cancel. An atom has a permanent magnetic moment if there is an excess of spins in one direction.

The magnetic properties of materials composed of associated atoms depend upon the arrangement of the atoms with respect to each other. This determines the kind of interactions between their magnetic moments. The forces of interaction (also called exchange forces) are functions of the ratio of the distance between atoms to the diameter of the orbit or shell in which the uncompensated spins are located.

Diamagnetic materials have no permanent magnetic moment. However, moments are induced by the influence of a magnetic field. The induced moments have a direction opposite to that of the inducing field. Consequently the relative permeability is less than unity. The diamagnetic susceptibility is negative. The diamagnetic susceptibility is very small, not more than a few parts in a million, and usually independent of temperature and applied magnetic field. It is probably present in all materials but usually masked by other larger effects.

Paramagnetic materials have a permanent magnetic moment but the interatomic spacing is so great that there is negligible atomic interaction. The relative permeability is greater than unity so the susceptibility is positive. Although the effect is greater than the diamagnetic effect, it is still

very small, not more than a few parts in a hundred thousand. There are two kinds of paramagnetism called strong and weak. Except for high fields of the order of 10^4 gausses (1 tesla) or higher the strong paramagnetic susceptibility is constant with field at a given temperature but varies inversely with temperature at a given field. Weak paramagnetism is due to the effect of conduction electrons in conducting metals and is practically independent of temperature.

Ferromagnetic materials have a relative permeability greater than unity and generally very high. The permeability is not constant but depends upon the degree of magnetization. Ferromagnetic materials exhibit hysteresis, that is, the induction corresponding to a given magnetizing force depends upon previous magnetic history. Furthermore, the intrinsic induction approaches a limiting or saturation value as the magnetizing force is increased indefinitely. Ferromagnetism has sometimes been called a special case of paramagnetism but in view of the differences in the processes involved, it should not be so classified.

Ferromagnetic materials are temperature-sensitive and when the material is heated, the temperature at which it is transformed from the ferromagnetic condition to the paramagnetic condition is called the Curie temperature.

In ferromagnetic materials, the interatomic distances compared to the diameter of the orbit or shell in which the uncompensated spins are located are such that neighboring atoms have their magnetic moments alined parallel and in the same direction. This is called positive interaction. Not all of the moments in a body are oriented in the same direction. Instead, they are lined up in groups called domains which act as magnetic entities. Each domain is spontaneously magnetized to saturation but because they are oriented in various directions the resultant magnetization in any direction may be anything from zero to the saturation value at which all domains would be oriented in the direction of the applied field.

Antiferromagnetic materials are those whose interatomic distances are less than the critical value so that the magnetic moments of neighboring atoms line up parallel to each other but in opposite directions, that is, antiparallel. The susceptibility of these materials is so low that they might easily be mistaken for paramagnetic materials. The experimentally distinguishable characteristic is that the susceptibility increases instead of decreasing as the temperature is raised until the thermal agitation destroys the interaction. Above this temperature the material becomes paramagnetic. This is analogous to the Curie point in ferromagnetic materials but is called the Neèl point for this class of materials.

Ferrimagnetic materials are those in which unequal magnetic moments are lined up antiparallel to each other leaving a net permanent moment. Permeabilities are of the same order of magnitude as those of ferromagnetic materials but are lower than they would be if all the atomic moments were parallel and in the same direction.[7] Under ordinary conditions the magnetic characteristics of ferrimagnetic materials are quite similar to those of ferromagnetic materials.

3.4. Magnetic Hysteresis and Normal Induction

One of the important characteristics of ferromagnetic materials is the phenomenon of magnetic hysteresis. This phenomenon is illustrated in figure 1. If a demagnetized specimen is subjected to the influence of a magnetizing force, H, which is increased from zero to higher and higher values, the magnetic induction, B, also increases but not linearly with H. This is shown by a curve *oabcd*. This nonlinearity is another of the characteristics of ferromagnetic material.

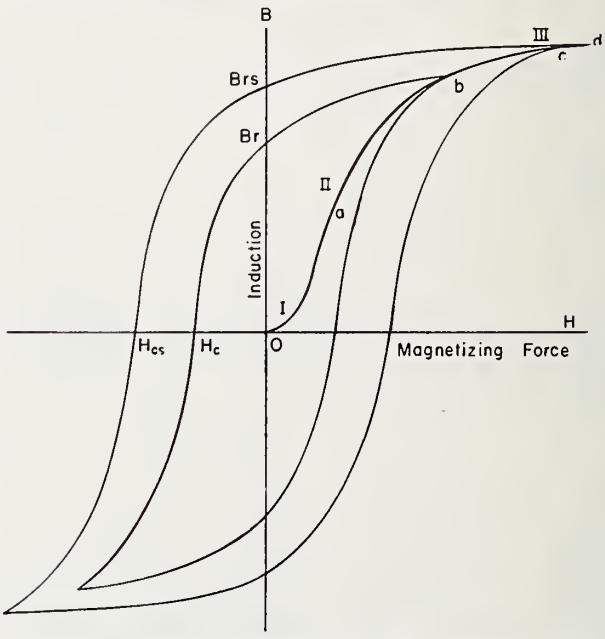

FIGURE 1. *Normal induction curve and hysteresis loops.*

If the increase in H is stopped at a point such as b and then decreased, the induction does not retrace the original curve in reverse order but lags behind it as indicated by the curve b, B_r, H_c, etc. This lag is called *magnetic hysteresis.* The point where the magnetizing force is zero is called the *residual induction*, B_r. The negative magnetizing force at which the induction becomes zero is called the *coercive force*, H_c. The closed curve starting from b through B_r, H_c, etc. back again to b is called a *hysteresis loop.* The loop does not always close at the first reversal of the magnetizing force but will close after enough reversals have been made.

[7] There is a technically important class of material called ferrites. The atomic interactions in these materials is mainly antiferromagnetic but there is a net magnetic moment which gives them ferromagnetic characteristics. The ferrites are ceramic bodies having extremely high electrical resistivity which makes them particularly valuable for use at high frequencies.

If the limits of H in each direction are equal, the limits of B in the two directions will also be equal and the material is said to be in a *symmetrically cyclic condition*. The induction at the tip of such a loop is called the normal induction. The ratio of B to H at this point is called the *normal permeability* $\mu = B/H$.

It is easy to see that the size of a hysteresis loop for a given material depends upon the value of induction at its tip. The *normal induction curve, oabcd,* is the locus of the tips of a family of cyclically symmetrical hysteresis loops.

The normal induction curve usually consists of three distinct stages. In stage I the rate of increase of B as H is increased is comparatively small. The steep part of the curve represents stage II of the magnetization. In this stage, a small increase in H produces a relatively large increase in B. In stage III the rate of increase of B is again small. In this stage the intrinsic induction, B_i, asymptotically approaches a limiting value which is called the *saturation induction*, B_s. For this reason, stage III is sometimes called the saturation range. Magnetic saturation is another of the distinguishing characteristics of ferromagnetic materials.

The magnetizing force and induction at the tip of a hysteresis loop are denoted by the symbols H_m and B_m, respectively. As B_m is carried higher and higher in the saturation range there comes a time when further increase does not produce any further increase in B_r and H_c. The maximum values of these quantities are called *retentivity*, B_{rs}, and *coercivity*, H_{cs}, respectively.

For permanent-magnet materials, the important part of the hysteresis loop is that portion in the second quadrant between the residual induction point, B_r, and the coercive force point, H_c. This is called the *demagnetization curve*. Points on this curve are designated by the coordinates B_d and H_d. The product of B_d and H_d for any point on the demagnetization curve represents the energy external to the magnet which could be maintained under ideal conditions. A curve obtained by plotting the products of the corresponding coordinates B_d and H_d as abscissas against the induction B_d as ordinates is called the *energy-product curve*. The maximum value of the energy-product, $(B_dH_d)_m$ is a good criterion of the relative quality of permanent magnet materials.

3.5. Core Loss

When materials are subjected to alternating magnetic fields, as in the cores of transformers, a certain amount of energy is expended which cannot be recovered but is dissipated in the form of heat. This loss of energy is called core loss. Core loss is made up of two major components, hysteresis and eddy currents.[8] The hysteresis loss depends upon the area of the hysteresis loop and the frequency of alternations. The eddy currents are induced in the core by the alternating magnetic flux and depend not only upon the frequency and maximum induction but also upon the electrical resistivity of the material, the thickness of the laminations, and the insulation between them.

4. Measurement of Static Magnetic Fields

4.1. General Principles

There are two aspects of a basic phenomenon by which magnetic fields can be measured. They are (1) the mechanical force experienced by a current-carrying conductor in a magnetic field or (2) the electromotive force induced in a conducting loop (test coil) when the magnetic induction encircled by or linked with the loop is changing, either because the induction is varying or because the loop is moving with respect to the induction. It is important to note that the quantity measured by either method is by definition magnetic induction, B. Magnetizing force, H, is calculated in terms of either electric current and its geometry or a measured value of B divided by the magnetic constant, Γ_m. In the cgs system, Γ_m is unity so there is no numerical difference between B and H. Consequently, it is general practice in certain cases to measure B and call it H. In the mksa system, Γ_m is not unity so it must be taken into account in determining the value of H in a magnetic field.

There are several additional methods by which magnetic fields can be measured. These are (1) change in electrical resistance due to a magnetic field, (2) the Hall effect, (3) behavior of saturable magnetic cores in a magnetic field, (4) optical effects, and (5) nuclear magnetic resonance.[9] The measurement of a magnetic field in terms of the mechanical force experienced by a current-carrying conductor is, of course, basic. However, accurate measurements by this method, although simple in principle, require somewhat elaborate apparatus and very careful experimental procedure. Such apparatus is not commonly available. A pivoted-coil arrangement is similar in principle and often used on account of its convenience if high accuracy is not required.

4.2. Pivoted Coil

A pivoted (or suspended) coil is essentially an inversion of the well-known d'Arsonval type of instrument. In the d'Arsonval instrument the coil is located in the constant field of a permanent magnet and its deflection against the restoring force of a spring or suspension is a measure of the current in the coil. The inversion consists

[8] A third component may be observed at high frequencies, but at lower frequencies it is usually negligible compared with the total loss.

[9] The methods commonly used in the field of terrestrial magnetism are not described in detail but only such methods as find application primarily in connection with the testing of materials are considered.

in substituting the field to be measured for the field of the permanent magnet. The coil, preferably without the usual iron cylinder within it, is mounted in a fixture so that it can be placed in proper position in the field to be measured. There are three different methods of making the measurements. The most convenient is employed in a commercially available instrument. By this method, the current necessary to produce a certain standard deflection is observed by means of a milliammeter connected in series with the coil and the adjusting resistors. Since the current is inversely proportional to the field, the milliammeter is calibrated in terms of the field strength in gausses. It would also be possible to observe the deflection of the coil due to a standard current or to measure the torque required to bring the deflection back to zero. The first mentioned method is most convenient. The presence of an iron core inside the moving coil is objectionable because it distorts the field being measured. One limitation of this type of instrument is that for accurate results the field must be uniform throughout the volume occupied by the coil so that fields of small extent cannot be accurately measured.

4.3. Pivoted Magnet

The pivoted coil has two disadvantages. It is too large to go into small spaces such as the gap in the magnetic circuit of a d'Arsonval instrument. Also it requires connections to a source of current. The development of permanent magnet materials having extremely high coercivity has made it possible to produce an instrument by which magnetic fields can be measured in terms of the torque on a very small magnet. This instrument, called a gaussmeter, consists of a light-weight shaft pivoted at each end and supported between jewels. A small cylindrical Silmanal magnet is mounted on the shaft near its lower end. At the other end is a hair spring for measuring the torque and a pointer which moves over a scale, calibrated in gausses. The magnet is about an eighth of an inch long in the direction of the shaft. It is magnetized in a direction perpendicular to the axis of the shaft. The moving system is enclosed in a thin-walled protective tube which extends perpendicularly from the back of a case which houses the scale and pointer. The pointer is mounted on the shaft in a direction parallel to the magnetic axis of the magnet so that when the pointer reads zero on the scale it also indicates the direction of the field in which the magnet is located. To measure the strength of the field, the instrument is rotated about the axis of the probe until the scale reading is a maximum. The axis of the magnet is then at right angles to the direction of the field and the scale reading shows its value in gausses. It is important to avoid exposing the magnet to a field greater than 5,000 gausses as the magnets cannot be stabilized for higher fields and therefore the calibration would be affected.

Alternating fields and fields greater than 5,000 gausses can be measured by a modified form of the instrument in which the Silmanal magnet is replaced by a cobalt-plated surface on soft iron. By this system, the general direction of the field can be determined, but not its polarity.

The gaussmeter is regularly furnished with probes either 1¼ in. or 5 in. long and diameters of 0.052 in. or 0.090 in.

4.4. Ballistic Methods

Ballistic methods are so called because they employ a ballistic galvanometer. In making a measurement, a test coil connected to a ballistic galvanometer is placed in the field with its axis in the direction of the field and the deflection of the galvanometer is noted when the test coil is either suddenly removed from the field or rotated 180° about its diameter.[10] This produces an impulsive current in the galvanometer circuit which is proportional to the total change in linkage between the field and the test coil.

a. Ballistic Galvanometer

The ballistic galvanometer commonly used for magnetic measurements is a moving-coil instrument of the d'Arsonval type.[11] It is an instrument for integrating electrical impulses of short duration. The coil is usually suspended but some pivoted-coil instruments are also in use. The moment of inertia of the coil is high and the restoring force due to the suspension or spring is low so that the natural period on open circuit is long, usually of the order of 20 sec or more. The behavior of the galvanometer is controlled mainly by the amount of resistance in its circuit. This determines the amount of electromagnetic damping due to the current induced in the coil as it moves in the field of the permanent magnet. The damping due to air friction is usually negligible compared to the electromagnetic damping.

If the external resistance has a certain critical value, the return of the coil to its zero position after a deflection occurs in a minimum of time without oscillation. This is called critical damping. The external resistance for critical damping is an important characteristic of a ballistic galvanometer.

If the external resistance is greater than the critical value, the return to zero after an impulse is by a series of oscillations of continually decreasing amplitude. The galvanometer is then said to be underdamped.

If the external resistance is less than the critical value, the galvanometer is overdamped. The maximum deflection for a sudden impulse comes sooner than when critically damped but

[10] If the field arises from an electromagnet the field may be reversed by reversing the current in the magnetizing coil.

[11] For an excellent detailed discussion of the theory and operation of the ballistic galvanometer see Harris, Electrical Measurements, pp. 301–341, Wiley, 1952.

the return to zero is slow. For magnetic measurements, the ballistic galvanometer is usually used in the overdamped condition. Some operators, however, like to have the galvanometer critically damped or very slightly underdamped. Under this condition it is necessary that the impulse be complete before the coil has moved appreciably from its zero position. Otherwise, if the impulse is prolonged, the integration will not be complete and the reading will be low.

For measurements of magnetic fields it is usually possible to produce sudden brief impulses but in the testing of ferromagnetic materials, the impulses are likely to be of such long duration that it is necessary to use a very heavily overdamped galvanometer if good accuracy is to be obtained. As a rule, the intrinsic sensitivity of a ballistic galvanometer is sufficiently high to permit an increase in damping by shunting the galvanometer as shown in figure 2. The figure shows alternative methods of connecting a ballistic galvanometer to a test coil. The choice of methods is a matter of taste. In both diagrams *TC* is the test coil, *RS* is a series resistor for adjusting the sensitivity, and *RP* is a resistor connected in parallel with the galvanometer when the key *K* is closed on the lower contact. In diagram *A* the galvanometer can be short-circuited by closing *K* on the upper contact. This will stop the motion of the coil almost instantly if it is swinging. In diagram *B* the resistor *RC* is permanently connected to the galvanometer and so adjusted that when key *K* is open the galvanometer is critically damped. This allows the galvanometer coil to return to its zero position after a deflection in minimum time without oscillation.[12] Some operators omit *RP* when this connection is used.

If the restoring force could be made zero, the only control of the galvanometer deflection would be the electromagnetic damping.[13] The motion of the galvanometer coil would then follow the change in flux linkage in the test coil exactly and the final deflection would not be influenced by the time taken by the change. An instrument whose torsional restraint is so small that this condition is closely approximated is called a fluxmeter. As a rule, however, it is more convenient to have a suspension or spring stiff enough to give a fairly stable zero. A galvanometer which is sufficiently overdamped to approach the performance of a true fluxmeter is said to have fluxmeter characteristics.

If the circuit of a galvanometer with a weak suspension or spring is not free of temperature gradients or contacts between dissimilar metals, thermal electromotive forces may be very troublesome by causing an unsteady zero and spurious deflections. Also, it is desirable to have a method for setting the galvanometer exactly on zero quickly and easily. Figure 3 is a diagram of a

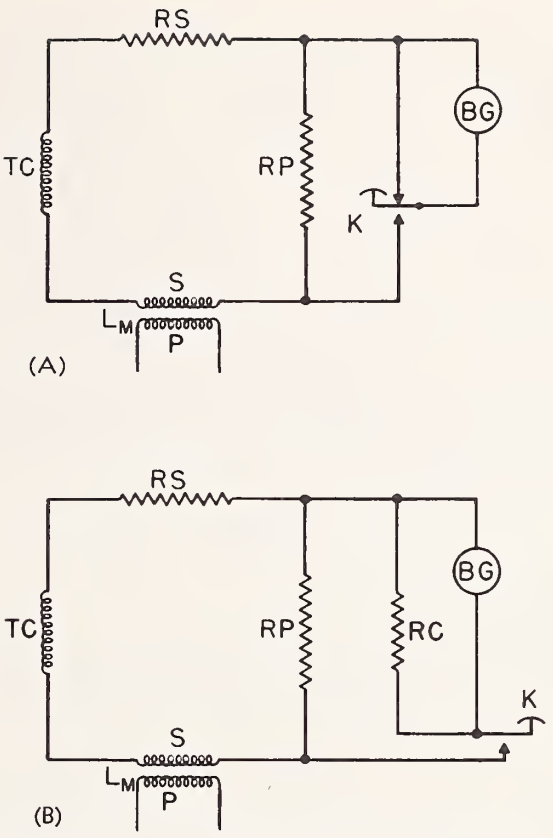

FIGURE 2. *Connections for ballistic galvanometer.*

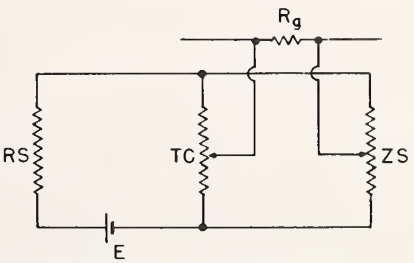

FIGURE 3. *Zero adjuster and thermal emf compensator.*

device which has been found to be very useful. Two slide-wire resistors are connected in parallel to a small dry cell through a high resistance. The two sliders are connected to opposite ends of a resistor of low value which is inserted in the galvanometer circuit. Contact *ZS* has a detent so that it can always be set at the same position. To compensate for thermal emfs, the slider *TC* is set so that the galvanometer does not drift when contact *ZS* is on the detent. To set the zero, contact *ZS* is moved one way or the other till the galvanometer reads zero. It is then quickly returned to its neutral position. The galvanometer is calibrated by means of a mutual inductor of known value whose secondary winding (in fig. 4) is connected permanently in series with the test coil.[14] It is often convenient to adjust the sensi-

[12] In practice the resistance is often adjusted so that the galvanometer is slightly underdamped and will pass beyond zero once before coming to rest. This makes it possible to be sure that the coil is swinging freely between the pole pieces without friction.

[13] Except for a slight amount of air damping which usually is negligible.

[14] If necessary, to avoid the possible effects of stray fields, a noninductive resistance equal to that of the secondary coil may be substituted for the coil after calibration.

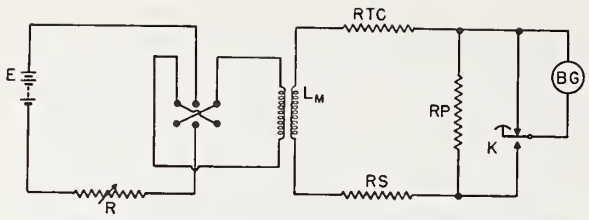

FIGURE 4. *Calibration circuit for ballistic galvanometer.*

tivity so that the scale is direct reading in terms of induction thus avoiding the necessity of multiplying the reading by an odd-valued scale constant to obtain the value of the field in specified units. The calibrating current which must be switched in the primary of the mutual inductor is calculated by the formula

$$I_c=\frac{KBaN}{L_m}$$

where

I_c=current

K=a constant dependent upon the system of units

B=induction

aN=area-turns of the test coil

L_m=mutual inductance.

In the cgs system I_c is in amperes, B is in gausses, aN is in cm^2-turns, L_m is in henries, and K is 10^{-8}. In the mksa system I_c is in amperes, B is in teslas, aN is in m^2-turns, L_m is in henries, and K is unity.

If the field is to be measured by withdrawing the test coil, the resistance in the galvanometer circuit is adjusted so that when I_c is suddenly reduced to zero the deflection is 10 cm. If the field is to be measured by flipping the coil through 180° or by reversing the field, the galvanometer is adjusted to read 10 cm when I_c is reversed. If the value of H is desired, it is only necessary to divide the observed value of B by Γ_m. In the cgs system Γ_m is unity so that H is numerically the same as B. In the mksa system Γ_m is $4\pi\times10^{-7}$ so that it is not possible as it is in the cgs system simply to measure B and call it H.

b. Intercomparison of Mutual Inductors and Calibration of Test Coils

At the National Bureau of Standards the standard of mutual inductance is one built with considerable care for use in determining the unit of resistance. The value of mutual inductance has been computed in terms of the dimensions of the inductor and is known to a few parts in a million. Since ballistic magnetic measurements are carried out with direct currents, the working standards of mutual inductance are calibrated by comparison with the primary standard using a direct-

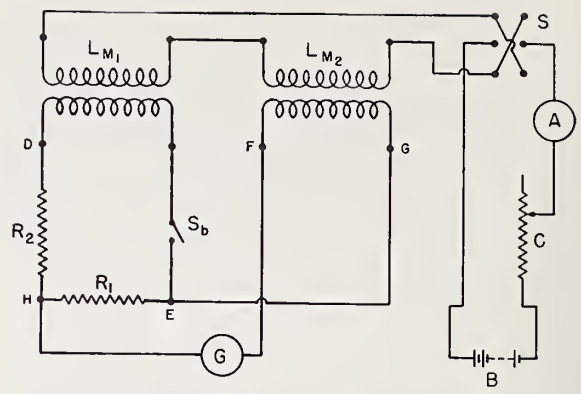

FIGURE 5. *Diagram of connections.*

current method somewhat similar to one proposed by Maxwell [1].[15] A diagram of connections is shown in figure 5. L_{m1} and L_{m2} are the mutual inductors to be compared. L_{m1} must have the greater value. The primary windings are connected in series to the battery, B, through the reversing switch, S, the rheostat, C, and the ammeter, A. The secondary windings are connected so as to oppose each other. R_1 and R_2 are adjustable precision resistors. It is important that the ballistic galvanometer, Ⓖ, be connected as indicated because if it is connected between points E and G leakage currents might give trouble unless the insulation between coils in the inductors is practically perfect. A measurement is carried out as follows. With switch S_b closed R_1 is set at some convenient value and the primary current is set at a value not exceeding the current-carrying capacity of the primary windings of the inductors. R_2 is then adjusted so that upon reversal of the primary current by switch S there is no residual deflection of the galvanometer. If the self-inductances of the secondary windings of the two inductors are not equal there may be a small double kick but this is generally not troublesome. When balance is obtained, the value of L_{m2} is

$$L_{m2}=L_{m1}\frac{R_1}{\Sigma R}.$$

ΣR is the total resistance of the secondary circuit of L_{m1} including R_1, R_2, the secondary winding of L_{m1}, and all the leads. The excess over R_1+R_2 is determined by setting R_1 and R_2 to zero, opening switch S_b, and measuring the resistance of the rest of the circuit by means of a Wheatstone bridge connected across S_b. Correction for the resistance of the leads to the bridge can be made by measuring their resistance with switch S_b closed. The usual precautions should be taken against the effect of stray fields. Leads should be twisted and the two inductors should be located at some distance from each other and so oriented that no interaction between the primary of one inductor and the secondary of

[15] Figures in brackets indicate the literature references on page 33.

the other can be observed. Some errors may result from capacitance between the primary and secondary circuits. This can be minimized by repeating the observations after reversing the connections of the primary of one inductor and the secondary of the other and averaging the results.

It is usually not feasible to calculate the value of area-turns of a test coil with a satisfactory degree of accuracy, especially if it has more than one layer. It is much better to determine the value experimentally. If a test coil is placed at the middle of a long slender solenoid whose pitch of winding is uniform and accurately known, its area-turns can be calculated from the mutual inductance between the solenoid and test coil and the induction per unit current in the solenoid. The mutual inductance can be determined by the method described above. It is important that the axis of the test coil be alined with that of the solenoid. The error due to lack of alinement is proportional to $1-\cos\theta$ where θ is the angle between the two axes. If the angle is less than 2.5°, the error from this source will not exceed 0.1 percent.

The value of area-turns is calculated from the equation

$$(aN)=KL_m/C$$

where

aN=area-turns

K=a constant depending on the system of units

L_m=the mutual inductance

C=the value of induction per ampere in the solenoid.

In the cgs system, K is 10^8, L_m is in henries, and C is in gausses per ampere. Area is then in square centimeters. In the mksa system K is unity, L_m is in henries, C is in teslas per ampere, and area is in square meters.

If a coil whose area-turns value is to be determined is too large to insert in an available solenoid or has a handle which cannot be detached, the calibration field may be obtained by means of a Helmholtz arrangement. This consists of two identical very short coaxial coils, the axial distance between them being equal to their radius. This produces a very uniform field along about the middle third of the axis between the coils. If a is the radius in centimeters, N is the number of turns in each coil, and i is the current in amperes, the magnetizing force at the midpoint between the two coils is

$$H=\frac{0.4\pi Na^2i}{\left(\frac{5a^2}{4}\right)^{3/2}} \text{ oersteds.}$$

This reduces to

$$H=\frac{0.8991Ni}{a} \text{ oersteds.}$$

To convert to ampere turns per meter (mksa units) multiply by $10^3/4\pi=79.58$. If coils having very small values of area-turns are to be tested this can be done in the field between the poles of an electromagnet. The field must be uniform over the area of the test coil and measured by a standard method. Since it is generally not feasible to reverse the current in the electromagnet, the reading must be made either upon suddenly removing the coil from the field or preferably by rotating it through 180° about an axis which is perpendicular to the direction of the field.

4.5. Rotating Test Coil

A continuously rotating test coil can be used to measure magnetic fields. The coil is rotated at constant speed about a diameter. It is connected through a commutator or cam-operated reversing switch to a d-c instrument which indicates the average voltage induced in the coil. If the reversal comes at the time when the a-c voltage induced in the coil is zero, the reading on the instrument will be a maximum and will be proportional to the magnetic field. Commercial instruments operating on this principle have the rotating coil at the end of a long shaft which has at its other end a synchronous motor. The shaft has to be long enough to avoid errors due to stray fields from the motor. The accuracy of the measurement depends directly upon the accuracy with which the frequency of the power source is controlled. The apparatus is generally calibrated by observations in known fields.

4.6. Bismuth Spiral [2]

One of the so-called secondary effects which is utilized to measure magnetic fields is the change in electrical resistance of a conductor when it is subjected to the influence of a transverse magnetic field. Most metals show this effect, but only in bismuth is it sufficiently large to be of practical value for the measurement of magnetic fields.

The bismuth spiral is made of small insulated bismuth wire wound bifilarly in a flat spiral, all the turns being in one plane. The ends are usually soldered to heavy copper leads. The spiral is held in place and protected from mechanical damage by thin discs of mica which are fastened to the copper leads. The diameters of the spirals range from 0.5 to 2.0 cm and they are ordinarily about a millimeter thick overall. It is essential that the bismuth be of very high purity. Otherwise, anomalous and uncertain results will be obtained. The major difficulty encountered in the use of a bismuth spiral is that it has two temperature coefficients; not only does bismuth have the ordinary temperature coefficient in the absence of a magnetic field but also the change in resistance due to a magnetic field depends upon the temperature. If proportional change in resistance is plotted against the value of magnetic field, the curve is not linear below about 5,000 gausses. Above this value the curve is practically

linear but the projection of the linear part does not pass through zero.

Bismuth spirals are not much used at present but the principle might be useful for some applications.

4.7. Hall Effect

The Hall effect furnishes a very convenient means for the measurement of magnetic fields. Instruments are available which utilize this principle. It can be very simply stated as follows. If a thin strip or film of metal, usually bismuth, indium antimonide, or indium arsenide, has a current in it, two points can be found at opposite ends of a line approximately at right angles to the current which will be at the same electrical potential if no magnetic field is acting. If a magnetic field is applied at right angles to the plane of the strip a difference of potential appears between the two points. This difference of potential is proportional to the intensity of the magnetic field. In practical instruments a-c is used so that the emf produced by the action of a magnetic field can be amplified and thus provide increased sensitivity. Calibration is carried out in magnetic fields of known value.

4.8. Saturable Core

A saturable core[16] is one which reaches practical saturation under the influence of a relatively low magnetic field. Thus a very small change in the effective magnetizing force will produce a large change in the inductance of a coil containing a saturable core. This principle is used for the measurement of magnetic fields. This is done by energizing a coil containing a saturable core with alternating current. The frequency is usually a few kilocycles per second. If a steady magnetizing field such as that of the earth is also present, there will be induced in the circuit a second harmonic component. This second harmonic voltage is proportional to the intensity of the superposed steady field. The steady field is determined in either of two ways. The amplified second harmonic voltage may be filtered out and measured or the steady field may be neutralized by means of direct current in a coil surrounding the core. When this is done, the second harmonic voltage disappears. The value of the field is then calculated in terms of the direct current, and the turns and dimensions of the coil. This is the more precise method because variations in the amplifier only change the sensitivity with which the balance can be made. If the second harmonic voltage is measured directly, the apparatus must be calibrated in fields of known values.

4.9. Nuclear Magnetic Resonance

Nuclear magnetic resonance is another phenomenon by which it is possible to measure homogeneous magnetic fields with very high accuracy. The measurement is based on the equation

$$2\pi\nu=\gamma_p B$$

or transposing,

$$B=\frac{2\pi\nu}{\gamma_p}.$$

In this equation B is the field in gausses, ν is the resonance frequency in cycles per second and γ_p is a quantity called the gyromagnetic ratio. The gyromagnetic ratio γ_p is the ratio of the magnetic moment of a nucleus to its angular momentum.

The measurement is made by immersing a sample of material containing nuclei, whose gyromagnetic ratio is known, in the steady field to be measured. The sample is then subjected by means of a surrounding coil to an alternating magnetic field at right angles to the steady field. The frequency of the alternating field is adjusted to be equal to the resonance frequency of the nuclei in the sample. At this frequency which is directly proportional to the intensity of the steady field there is an absorption of energy from the exciting circuit. This is generally observed by means of a cathode ray oscilloscope. B is then calculated, using the equation

$$B=\frac{2\pi\nu}{\gamma_p} \text{ gausses}^{17}$$

where ν is the resonance frequency and γ_p is the gyromagnetic ratio.

5. Tests With Direct Currents

5.1. Testing of Materials

General Principles. The principal object of testing ferromagnetic materials by d-c methods is to obtain data from which normal induction curves and hysteresis loops can be plotted. This is done either by using suitably shaped specimens such as rings which constitute the entire metallic part of the magnetic circuit or by means of permeameters. A permeameter is a magnetic circuit provided with magnetizing and test windings in which a test specimen can be inserted so as to compose a part of the circuit. Since there is no material which acts as an insulator with respect to magnetism, the magnetic circuit must be arranged so as to produce the greatest possible uniformity in the distribution of magnetic induction across the section and along the length of that part of the specimen directly involved in the test. Several permeameters have been developed which differ

[16] Several devices using this principle are described in the book, Saturating Core Devices, by L. R. Crow, The Scientific Publishing Company, Vincennes, Indiana.

[17] To convert from gausses (cgs) to teslas (mksa) multiply by 1×10^{-4}.

from each other in form of magnetic circuit and method of determining corresponding values of H and B. In the Koepsel [3] and Esterline [4] permeameters. the ends of the specimen are clamped between iron pole pieces resembling those of a d'Arsonval instrument but much larger. The magnetizing winding surrounds the specimen. Compensating coils in series with the main magnetizing winding are mounted on the pole pieces. Their function is to compensate for the magnetic reluctance of the pole pieces. In the Koepsel apparatus there is a regular d'Arsonval moving coil whose pointer gives an indication of the value and direction of B in the specimen when there is a current of fixed value in the coil. Values of H are estimated in terms of the current in the magnetizing winding. In the Esterline apparatus, the d'Arsonval coil is replaced by a rotating armature. When this armature is driven at a constant speed the induced voltage is taken to be a measure of B in the specimen. Neither of these permeameters is capable of very high accuracy and neither is at present in common use.

Other permeameters have been developed by DuBois [5], Hughes [6], Picou [7], Iliovici [8], Niwa [9], and Burrows [10]. The Burrows permeameter is based on the principle of so distributing the magnetomotive force around the magnetic circuit that there is negligible magnetic leakage, at least from the specimen under test. It was for many years accepted as the standard apparatus for d-c magnetic testing. However, the operation of this apparatus is tedious and time-consuming and is unduly sensitive to nonuniformity in magnetic properties along the length of the specimen. Also, it requires two similar specimens. The MH permeameter [11] was developed with the object of eliminating or minimizing these drawbacks and has been adopted by the Magnetic Measurements Section as the standard method for d–c magnetic testing in the range of magnetizing force up to 300 oersteds (approximately 24×10^3 amp-turns/m). The Fahy Simplex permeameter [12] has been in general use for many years for tests in the same range of magnetizing force and for this reason is used for testing when so requested. The advent of very hard magnetic materials requiring the use of very high magnetizing forces for testing led to the development and adoption of the High-H permeameter [13] for magnetizing forces up to 5,000 oersteds (approximately 40×10^4 amp-turns/m).

These three methods, the MH, High-H, and Fahy Simplex permeameters, are called ballistic methods because a ballistic galvanometer is employed in the measurements.

In ballistic tests, values of B are obtained in terms of the deflection of a ballistic galvanometer connected to a test coil (B-coil) surrounding the specimen. The deflection is proportional to the change in the induction linked with the test coil. If the change is simply a reversal in direction, then the induction is one half of the observed change. There are two ways in which values of H may be determined. One way is to calculate it in terms of the current-turns per unit length at a given section of the magnetic circuit. This is the method employed in the testing of ring specimens and in the Burrows permeameter. The other way is to determine B in the air at a suitable location and calculate the value of H from the equation

$$H=B/\Gamma_m.$$

Since $\Gamma_m=1$ in the cgsem system, it has become general practice to determine B[18] and call it H. This does not lead to a *numerical* error in the cgsem system. It has also become general practice to call the coils by which this determination is made H-coils. If H is calculated in terms of current the magnetic circuit and magnetizing windings must be so arranged that there is no magnetic leakage from the part of the specimen over which the B-coil extends and the magnetizing winding must be uniformly distributed over the same portion of the specimen. This is the principle involved in the Burrows permeameter and approximated in the ring test.

If H is determined ballistically, it is not necessary that the magnetizing winding surround the section of the specimen surrounded by the B-coil but the magnetic circuit must be so arranged that the field of induction in the region adjacent to the specimen occupied by the H-coil is uniform or if not it must be possible to extrapolate to the surface of the specimen. This is the underlying principle of the MH and High-H permeameters.[19]

In ballistic tests, as described earlier, the galvanometer is calibrated by means of a mutual inductor whose secondary winding is part of the galvanometer circuit. Excepting during calibration, the secondary winding may be replaced by a noninductive resistor having the same resistance. This is to avoid errors which might be caused by pickup from other parts of the circuit.

It is customary to adjust the sensitivity of the galvanometer so that the scale is direct-reading in terms of induction or magnetizing force. Thus, in the cgs system, the magnetic induction on reversal may be 1,000 gausses/cm of deflection or the magnetizing force may be 1, 10, or 100 oersteds/cm. By this procedure the necessity of multiplying the scale reading by an odd-valued factor is avoided. If H is measured in terms of current in the magnetizing winding, only the calibration for B needs to be made.

The calibrating current for a selected value of B is given by the equation

$$I_c=\frac{KBAN}{L_m}$$

[18] Any quantity determined in terms of an induced emf in a test coil is *by definition* B and not H.

[19] The Fahy Simplex permeameter operates on a somewhat different principle and is described later.

where

I_c=calibrating current in amperes
K=a constant depending upon the system of units.
B=the selected value of induction
A=the cross sectional area of the specimen
N=number of turns in the test coil
L_m=mutual inductance in henries.

In the cgs system K is 10^{-8}, B is in gausses, and A is in square centimeters.

In the mksa system, K is unity, B is in teslas, and A is in square meters.

In calibrating for a selected value of H the equation becomes

$$I_c=\frac{K\Gamma_m HaN}{L_m}$$

where

I_c=calibrating current in amperes
K=a constant depending upon the system of units.
Γ_m=the magnetic constant
H=the selected value of magnetizing force
aN=area-turns of the test coil
L_m=mutual inductance in henries.

In the cgs system K is 10^{-8}, Γ_m is unity, H is the selected value of magnetizing force in oersteds, and aN is the area-turns of the test coil in cm^2-turns.

In the mksa system, K is unity, Γ_m is $4\pi\times10^{-7}$, H is the selected value of magnetizing force in ampere-turns per meter, and aN is area-turns in m^2-turns.

Since the calibration is usually made by reversal of the calibrating current, care must be taken when measuring changes in induction or magnetizing force as in the determination of points on the hysteresis loop to multiply the readings by 2.

Because the area of the B-coil is larger than that of the specimen, a correction must be made to the observed value of B to account for the "air" flux existing in the space between the coil and the specimen. Thus the induction, B, is

$$B=B_{obs}-k\Gamma_m H$$

where

B_{obs}=observed value of B (for specimen of area A)
$k=\frac{a-A}{A}$
a=area of the test coil
A=area of the specimen
Γ_m=the magnetic constant
H=the magnetizing force.

In the cgs system, B is in gausses, Γ_m is unity and H is in oersteds. In the mksa system, B is in teslas, Γ_m is $4\pi\times10^{-7}$ and H is in ampere-turns per meter.

k is a numeric and has the same value in either system.

In making observations of normal induction, the specimen should first be demagnetized to eliminate latent polarization due to previous magnetization. This is done by subjecting it to the influence of reversals of magnetizing force of gradually decreasing magnitude starting from a peak value well into the third stage of magnetization. The frequency of reversal should be low enough so that induced eddy currents will not interfere with the demagnetizing process. About 1c/s has been found satisfactory for the average case. If the specimen does not compose the entire magnetic circuit and has a small cross section compared with the rest, it may be necessary to demagnetize the rest of the magnetic circuit using a larger specimen and then to repeat the process with the smaller specimen in place. After demagnetization, the magnetizing current is set at the value corresponding to the lowest-point desired and reversed several times until successive readings of the induction are the same. The specimen is then in a symmetrically cyclic condition and the observed induction is the normal induction. The corresponding magnetizing force is then determined either by taking a ballistic deflection or by observing the magnetizing current according to the type of apparatus being used. Additional points on the normal induction curve are determined in the same way. Demagnetization need not be repeated if each point so determined is higher than any preceding one. It is the practice of some observers to start with the highest point and then to demagnetize from each point to the next lower one. This is sometimes preferable, especially if the specimen is likely to be heated unduly.

If points on a hysteresis loop are to be determined, cyclic condition is first obtained by several reversals of the magnetizing current corresponding to the tip of the loop and the resulting values of B and H observed. The current is then suddenly reduced in value by inserting additional resistance in the magnetizing circuit. For points on the negative side of the H-axis, the current is simultaneously reversed and reduced. The observed changes in B and H are subtracted from the values at the tip and the results thus obtained are taken to be the coordinates of the required point on the hysteresis loop.

The process is repeated for other points, care being taken to reestablish cyclic condition at the tip before each observation.

In setting up apparatus for ballistic testing, it is important to twist the conductors in both primary and secondary circuits and so to locate the mutual inductor with reference to the rest of the apparatus as to prevent errors due to stray fields.

5.2. Ring Method

Although a ring would appear to be the ideal form of specimen for magnetic testing, it has certain disadvantages which should always be

taken into account. The principal advantage is the absence of airgaps and end effects.

In the cgs system, H is calculated using the equation

$$H=\frac{0.4\,N\,I}{D}$$

where

H=magnetizing force in oersteds
N=number of turns in winding
I=current in amperes
D=mean diameter of the ring in cm.

To convert to rationalized mksa units (ampere-turns per meter) multiply by $1000/4\pi=79.58$. This calculation is sufficiently accurate for most purposes provided that the mean diameter of the ring is large compared to its radial width. Since the outer circumference of the ring is greater than the inner circumference, the turns per unit length are less on the outside than on the inside and consequently the magnetizing force is not uniform across the section. Table 2 shows the ratio of the average value of H to that at the mean radius in rings of either circular or rectangular cross section. For difference no greater than 1 percent, a ratio of at least 10 of mean diameter to radial width is usually recommended.

TABLE 2. *Ratio of average value of* H *to value at mean radius in rings of rectangular and circular sections* [*13*]

Ratio of diameter to radial thickness	H_a/H_r	
	Rectangular	Circular
2	1.0986	1.0718
3	1.0397	1.0294
4	1.0216	1.0163
5	1.0137	1.0102
6	1.0094	1.0070
7	1.0069	1.0052
8	1.0052	1.0040
10	1.0033	1.0025
19	1.0009	1.0007

It is not safe to assume, however, that simply making the ratio 10 or more assures accurate results. Errors may also result from irregularity in winding or from nonuniform magnetic properties along the circumference of the ring. Irregularity in winding can be minimized by the exercise of extreme care in winding or by the use of a winding machine. However, errors due to nonuniformity in the specimen which can neither be calculated nor conveniently determined experimentally may be large and therefore, the use of ring specimens as reference standards for checking the accuracy of other methods is not recommended. The method is also limited to low magnetizing forces which can be applied without producing excessive heating.

In spite of the disadvantages of the ring specimen for measurements of high accuracy or for standardizing purposes, this form of specimen is widely used in production testing for quality control or the development of new materials, notably the ferrites. Its use has been greatly facilitated in recent years by the development of a machine by which extremely uniform windings can be rapidly applied. The secondary winding is applied first so as to minimize the effect of air-flux between coil and specimen.

A diagram of connections for the ring test is shown in figure 6. Current is derived from the battery, B, controlled by the resistors R and R', and measured by the ammeter A or some more precise method for measuring current. The current can be reversed by switch C or reduced by opening switch C', or reversed and reduced by operating both switches simultaneously. If switch D is closed upward the current is in the magnetizing coil M. If D is closed downwards, the current will be in the primary winding, P, of the calibrating inductor.

The secondary or test winding, T, is connected in series with the secondary winding of the inductor and the series resistor, RS, and the parallel resistor, RP, as shown. The ballistic galvanometer is connected through the key k across the resistor RP.

The procedure for making a test is described on p. 13 et seq.

5.3. Straight Bar and Solenoid

It is possible to make ballistic tests with a straight specimen of uniform cross section magnetized in a solenoid. In this case, the determination of the magnetic induction at the midsection of the bar offers no particular difficulty. The principal problem lies in the determination of the magnetizing force. This arises from the fact that the magnetic circuit comprises not only the bar but also the air-space in which the lines of

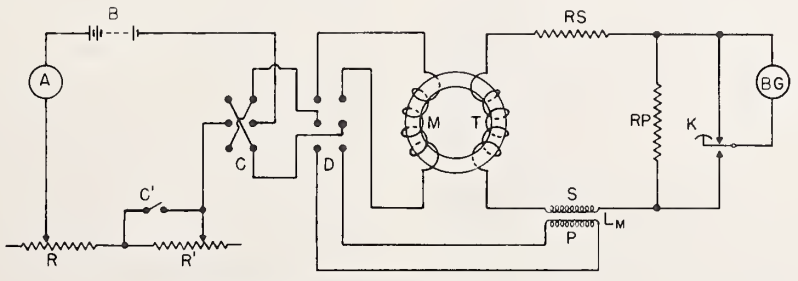

FIGURE 6. *Connections for the ring test.*

TABLE 3. *Demagnetizing coefficient and factor*

D=ratio of length to diameter	$H=H'-\frac{NI}{\Gamma_m}$			$II=H'-\frac{D_B B_i}{\Gamma_m}$				Equation [a]	
	Ellipsoid	Mann [14]		Du Bois [15]		Shuddemagen [16]			
	N	N	D_B	N	D_B	N	D_B	N	D_B
10	0.2549	0.2550	0.0203	0.2160	0.0172	0.2000	0.0159	0.2512	0.0200
15	.1350	.1400	.0111	.1206	.0096	.1040	.0083	.1235	.0098
20	.0848	.0898	.00714	.0775	.0062	.0655	.0052	.0747	.0059
30	.0432	.0460	.00366	.0393	.00313	.0335	.00267	.0367	.00292
40	.0266	.0274	.00218	.0238	.00189	.0206	.00164	.0222	.00176
50	.0181	.0183	.00146	.0162	.00129	.0139	.00110	.0150	.00119
60	.0132	.0131	.00104	.0118	.00094	.0101	.00080	.0109	.00087
70	.0101	.0099	.00080	.0089	.00071	.0077	.00061	.0083	.00066
80	.0080	.0078	.00062	.0069	.00055	.0061	.00049	.0066	.00052
100	.0054	.0052	.00041	.0045	.00036	.0041	.00033	.0045	.00035
150	.0026	.0025	.00020	.0020	.00016	.0020	.00016	.0022	.00017
200	.0016	.0015	.00012	.0011	.00009	.0012	.00009	.0013	.00011

[a] $\log_{10}N=1.15-1.75\log_{10}D$
$\log_{10}D_B=0.05-1.75\log_{10}D$

NOTE: The above values of N and D_B are calculated for cgsem system of units.

induction extend from one end of the bar to the other. Thus the total magnetomotive force is not confined to the space within the solenoid and consequently the magnetizing force available for the bar is less than would be calculated in terms of the ampere-turns per unit length in the solenoid. Classical theory attributes this diminution to the effect of fictitious poles near the ends of the specimen and therefore the effect has been called a "demagnetizing" effect. The effect is expressed by the equation

$$H=\mathrm{H}'-\frac{D_B B_i}{\Gamma_m}$$

where

H=the effective magnetizing force

H'=the apparent magnetizing force

D_B=the demagnetizing coefficient

B_i=intrinsic induction

Γ_m=the magnetic constant.

In the cgs system, Γ_m is 1. In the rationalized mksa system, Γ_m is $4\pi\times10^{-7}$.

Except for ellipsoids of revolution, D_B cannot be calculated but must be determined experimentally. It has been found that the demagnetizing coefficient is practically constant up to about the top of the second stage of magnetization. Above this the value decreases with increased induction. Within the linear range, the value for bars of circular section is a function of the ratio of the length to diameter of the specimen [20] but published tables by different experimenters are not in perfect agreement.

According to Bozorth [32], the demagnetizing factor depends not only upon the dimensional ratio but also upon the permeability. He also gives graphs by which apparent permeability can be converted to true permeability or vice versa. Most of the tables available at the present writing are given in terms of "intensity of magnetization" rather than in terms of B_i. The equation commonly given is

$$H=H'-NI$$

where H and H' are the true and applied magnetizing force respectively, N is the demagnetizing factor, and I is the "intensity of magnetization." The intensity of magnetization as understood here is $B_i/4\pi$ so that

$$N=4\pi D_B.$$

Table 3 shows some published values of the demagnetizing factors together with equations which practically average the values given by Mann [14], DuBois [15], and Shuddemagen [16]. These equations provide a means for estimating the demagnetizing factor for intermediate values of the dimensional ratio.

The diagram of connections shown in figure 6 for the ring test is substantially right for the solenoid test. The only changes required are to take M to be the solenoid winding and T to represent the test coil at the middle of the test bar. In calculating the applied magnetizing force H', if the solenoid is very long compared to its mean diameter and if the cgs system of units is used, the equation is

$$H'=0.4\pi\ n\ I$$

where

H'=applied magnetizing force in oersteds

n=number of turns per cm

I=current in amperes.

If the solenoid is relatively short, a more nearly accurate value can be obtained by using the

[20] For sections other than circular, the diameter is taken to be the diameter of the circle which has the same area as that of the bar.

equation

$$H' = \frac{0.4\pi n I l}{\sqrt{l^2+d^2}}$$

where

l=length of the solenoid in cm

and

d=mean diameter of the winding in cm.

A more accurate value for multilayer coils can be obtained by calculating each layer separately and adding the results. To convert from oersteds to rationalized mksa units, multiply by $1000/4\pi = 79.58$.

Unless the test coil is wound directly upon the specimen its area should be determined and the standard air-flux correction should be applied to the observed value of B. (See p. 14.)

On account of the difficulty of obtaining accurate values of the demagnetizing factor this method is not capable of high accuracy but for some purposes it may be the most convenient for straight specimens if approximate results are good enough.

5.4. Permeameters

a. MH Permeameter

The MH [21] permeameter [11] was designed with the purpose of producing an instrument which would not have the disadvantages inherent in the Burrows permeameter but would have comparable accuracy. It should also be an absolute instrument in the sense that its constants can be determined from its own dimensions and therefore do not have to be calibrated by reference to any other permeameter. The MH permeameter fulfils these essential requirements. In addition, it has the advantages that it requires only a single specimen and is more simple and rapid to operate than the Burrows permeameter. Furthermore, it is much less sensitive to the effect of nonuniform magnetic properties along the length of the specimen. It is also used for ordinary magnetic testing within its proper range; that is, up to 300 oersteds or 24×10^3 amp-turns per meter. The permeameter is shown in figure 7. The magnetic circuit is made of laminated electrical sheet of armature grade. The laminated structure reduces the effect of eddy currents induced in the circuit by the changes in flux incident to the testing procedure. The specimen and the symmetrical U-shaped yokes which span it rest on two end pieces supported by Bakelite blocks. The yokes are recessed so as to make good contact with the end pieces and the ends of the specimen in such a way that no clamping is required. This eliminates mechanical strain in the specimen. The symmetrical yokes promote a uniform distribution of magnetic induction across the section of the specimen and along its length. The distribution is also improved by auxiliary windings around the ends of the yokes and the end pieces. These are connected in series with the main magnetizing coil which surrounds the specimen. The proper number of turns in these auxiliary coils depends upon the magnetic properties of the yokes and end pieces and is determined experimentally for each instrument. The preferred length of test specimen is 28 cm but specimens as short as 24 cm can be used if necessary.

[21] MH is a designation for "medium H."

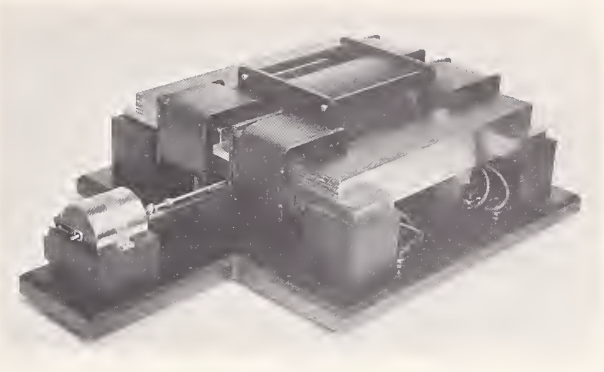

FIGURE 7. *MH permeameter.*

FIGURE 8. *Test coil assembly for MH permeameter.*

The test-coil assembly is shown in figure 8. This assembly is held in place within the magnetizing coil by two Bakelite rings. A platform extending between these rings serves to hold the B-coil in place and to support flexible specimens such as strips of electrical sheet so as to prevent errors due to mechanical strain.

A 100-turn B-coil extends over the middle 3 cm of the specimen. Just above it, but not surrounding the specimen, is a compensating coil adjusted to have the same value of area-turns as the B-coil. This coil is connected in series opposing the B-coil so that the reading of the galvanometer upon reversal of the magnetizing current is proportional to the intrinsic induction, B_i. Thus the usual air-flux correction is not required. If desired, the total induction, B, can be obtained simply by adding to the observed value of B_i the value of $\Gamma_m H$. In the cgs system $\Gamma_m=1$. In the mksa system, $\Gamma_m=4\pi\times10^{-7}$. The B-coil is able to accommodate specimens as large as 1×3 cm in cross section.

The H-coil system is also shown in the figure 8. It consists of two rectangular coils with nearly identical values of area-turns mounted on a turntable below the specimen. The upper coil extends into a recess in the supporting platform so as to

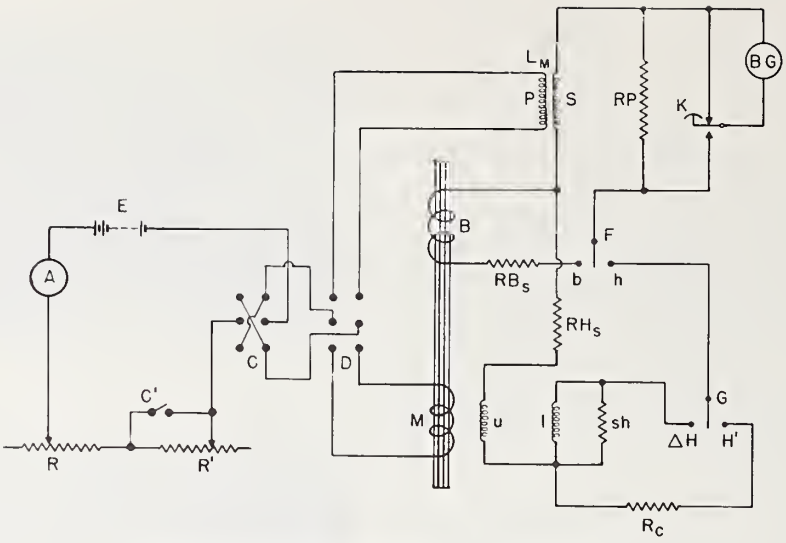

FIGURE 9. *Connections for the MH permeameter.*

come close to the surface of the specimen. The turntable can be rotated through 180° about a vertical axis by means of a rack and pinion arrangement operated by an iron-clad solenoid and plunger located far enough away from the magnetic circuit to avoid interference. The lower coil has the larger value of area-turns and is adjusted to equality of effective value of area-turns by means of a noninductive shunting resistor. If the two coils are connected in series opposing and rotated the reading of the galvanometer will be proportional to the gradient of the magnetic field. A reading taken by means of the upper coil alone together with the gradient permits extrapolation to the surface of the specimen and thus the determination of the magnetizing force acting on the specimen.

The use of rotating coils (flip coils) has some advantages over a fixed-coil system, especially when determining points on a hysteresis loop. With fixed H-coils, it is necessary to calculate values of H_d for a point on the loop in terms of the difference between two large quantities. With the flip coils the value of H_d is determined directly with suitable sensitivity and observations can be repeated without the necessity of reestablishing a symmetrically magnetized condition. The Burrows criterion for perfect demagnetization is that the induction for a given low magnetizing force shall be a maximum. This is not feasible to apply experimentally. With the flip coils, it is only necessary to observe whether or not the magnetizing force corresponding to a given low magnetizing current has the same absolute value regardless of the direction of the current. If there is a difference, the presence of residual magnetization is indicated. The demagnetizing procedure should then be repeated.

Taking into consideration all the possible sources of error inherent in the apparatus, it is estimated that by the exercise of great care in taking the readings and averaging several readings for each point, values of induction are accurate to within about 0.5 percent. Values of magnetizing force will come within the same accuracy or 0.05 oersted, whichever is larger. For routine tests, values of either induction or magnetizing force accurate to within 1 percent should be obtained without difficulty.

Figure 9 is a diagram of connections for the MH permeameter.

Battery E furnishes the magnetizing current which is controlled by resistors R and R' and measured by ammeter A or by a standard shunt and potentiometer. With switch D closed upward the current is in the primary winding P of the calibrating inductor L_m. If it is closed downward, the magnetizing winding is energized. With selector switch F closed on b, the B-coil B is connected to the galvanometer circuit through the calibrating resistor RB_s. If F is closed on h, the H-coils are in the galvanometer circuit through the calibrating resistor RH_s. The selector switch, G, determines whether the upper coil, u, alone is in the circuit or the coils u and l are connected in series opposing. Resistor sh is for adjusting the effective area turns of coil l to be equal to the area-turns of coil u. R_c, noninductive resistor, is to compensate for the resistance of coil l so that the resistance of the galvanometer circuit will be the same whether one or two coils are connected.

It should be noted that for a specimen which is magnetically nonuniform along its length, the values of B and H obtained by the MH permeameter relate only to the part of the specimen linked with the B-coil.

b. High-H Permeameter

The High-H permeameter [13] shown in figure 10 is used for testing "hard" magnetic materials at magnetizing forces up to 5,000 oersteds

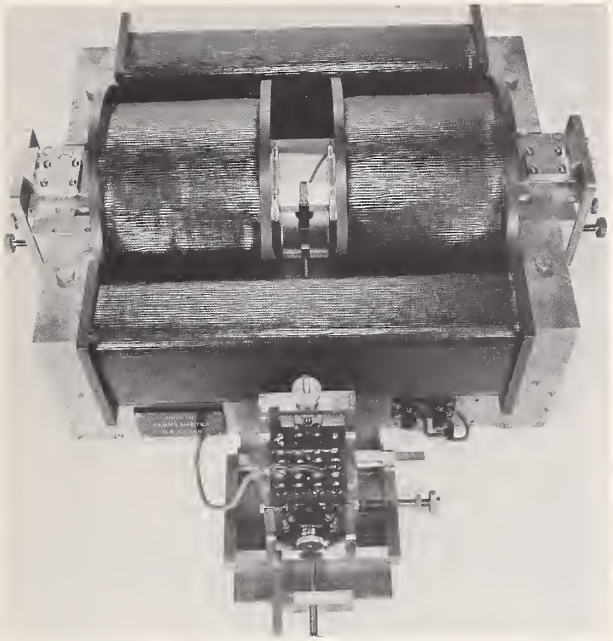

FIGURE 10. *High-H permeameter.*

(40×10^4 amp. turns/meter). Since only a short length of the specimen is included in the test, it is possible to apply the high magnetizing forces without appreciable heating. The magnetic circuit is made of laminated electrical sheet of armature grade. The specimen, of rectangular cross section, is held in pole pieces extending between two U-shaped yokes. The construction of the pole pieces is indicated in the sketch of figure 11. They have longitudinal channels into which filler pieces are fitted as shown. The specimen is located in the space between the bottom of the channel and the filler. The distance between pole pieces, or gap length, is adjustable; and scales are provided to indicate the gap length up to 10 cm, which is the maximum generally used. The filler pieces are fastened at their outer ends to heavy brass plates which are clamped to the ends of the pole pieces so as to keep the fillers parallel with the bottom of the channels. The main magnetizing coils surround the pole pieces and auxiliary coils are wound on the yokes.

Two similar *H*-coils are mounted one above the other on a vertical shaft below the specimen. They can be rotated 180° by means of a small motor through beveled gears and a long horizontal shaft. The lower coil has a slightly greater value of area-turns than the upper coil and is adjusted to have the same effective value by a noninductive shunt. If the two coils are connected to the galvanometer in series, opposing, and rotated through 180° from a position such that their axes are parallel to the direction of the field, the deflection is proportional to the radial gradient of the field. If the axis of the upper coil is set to be the same distance below the surface of the specimen as the distance between the axes of the coils this gradient can be used directly to extrapolate the value obtained by the upper coil alone to the surface of the specimen.

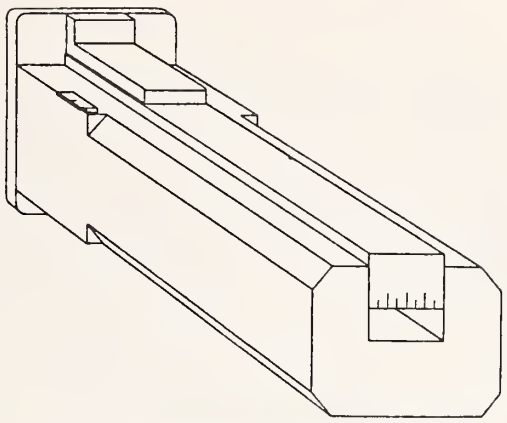

FIGURE 11. *Pole pieces of the high-H permeameter.*

In order to keep the air correction small, individual *B*-coils are wound on thin brass forms to fit specimens of various sizes. The coils are 5 mm long and usually have 25 turns.

Relatively short specimens can be used but for specimens 5 cm or less in length, it is better to butt the ends against the pole pieces rather than to attempt to insert them in the regular way.

It is estimated that for magnetizing forces from 100 to 5,000 oersteds (8×10^3 to 40×10^4 amp-turns/meter) it is possible under favorable conditions to obtain values of either induction or magnetizing force which will be accurate within 0.5 percent. Under ordinary conditions of routine testing, the errors probably do not exceed 1 percent.

The wiring diagram shown in figure 9 applies also to the High-H permeameter if it is understood that the magnetizing coil, *M*, is on the pole pieces instead of over the specimen.

c. Fahy Simplex Permeameter

For several years, the Fahy Simplex permeameter [12] has been in use in many laboratories for routine magnetic testing. Since this permeameter tends to give average values of the properties of a nonuniform specimen, agreement with another permeameter which includes only a relatively short section in the test should be expected only for a uniform specimen. Unless a specimen has been checked for uniformity, it is safer to assume that it is nonuniform, and lack of agreement should not be interpreted as an error of either permeameter.

For checking other Fahy Simplex permeameters, the Magnetic Measurements Section has calibrated one by reference to a standard permeameter using uniform bars as standards. This instrument is used as a working standard and constitutes a practical means of making the check.

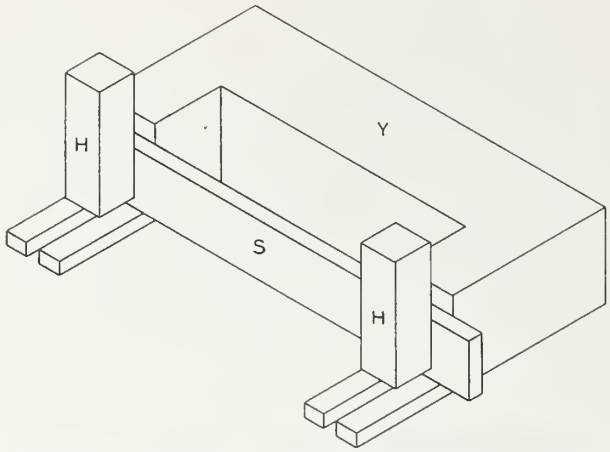

FIGURE 12. *Magnetic circuit of Fahy Simplex permeameter.*

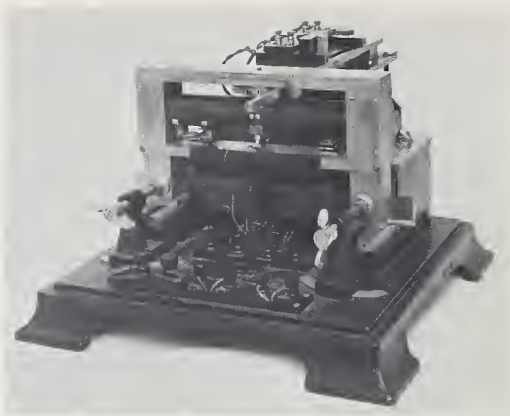

FIGURE 13. *Modified Fahy Simplex permeameter.*

The magnetic circuit of the Fahy Simplex permeameter is indicated in the sketch of figure 12. The yoke, Y, is made of laminated silicon sheet. Two soft iron blocks, H, make contact with the ends of the specimen. Clamps hold these blocks and the specimen in place against the pole pieces of the yoke as shown. The magnetizing winding is wound on the yoke. The B-coil for measuring the magnetic induction has 100 turns uniformly wound on a brass form which surrounds the specimen and extends over its whole length between the pole pieces. For determining the magnetizing force, a uniformly wound H-coil of many turns on a straight nonmagnetic form extends horizontally between the upper ends of the H-blocks.

In order to gain the advantages of "flip coils" for the determination of magnetizing force, especially for points on the hysteresis loop, the NBS instrument was modified by providing a means of rotating the H-coils through 180° about a vertical axis. The modified instrument is shown in figure 13. The H-blocks had to be lengthened slightly so that the H-coil could clear the magnetizing coil but experiment showed that this did not affect the accuracy of the results. As previously stated, the flip coil arrangement makes it possible to determine values of H_d on the hysteresis loop with adequate sensitivity and to repeat the observation without the necessity of repeating the process of producing a symmetrically cyclic condition for each repetition of the observation. It also provides a convenient and positive indication of proper demagnetization. Demagnetization has been complete if for a very small magnetizing force, the values of H are equal for reversals with the magnetizing current in either direction.

The Fahy Simplex permeameter is not an absolute instrument. It requires calibration by reference to an absolute instrument which is taken to be a standard; if it were not for the inevitable magnetic leakage, the theory of the instrument would be comparatively simple. The H-coil is assumed to indicate the difference of magnetic potential between the ends of the H-blocks. These blocks then in effect transfer the ends of the coil to the ends of the specimen. On account of leakage, however, the actual situation is not quite so simple. Experiment has shown that if the actual value of area-turns in the H-coil is used in calculating H, the value thus obtained is not correct.

The single-yoke arrangement leads to a nonuniform distribution of induction both along the length and across the section of the specimen. Also, since the magnetizing coil is on the yoke rather than on the specimen, some of the leakage flux is linked with the H-coil. The reluctance of the H-blocks should also be taken into consideration. In view of all of the potential sources of error inherent in the design, it was somewhat surprising to find that a simple correction proportional to the observed magnetizing force would bring the results practically in line with the results obtained with an absolute instrument if uniform specimens are used in the intercomparison. This correction is most conveniently applied by assigning to the H-coil a value of what might be called the "effective" area-turns which is somewhat different from the measured value. It has been found that if the specimen is laminated, the maximum number of strips for which reasonable accuracy can be obtained is ten. The error is apparently a function of the number of air gaps between the pole pieces and the H-blocks.

With so many factors involved, it is not feasible to give a precise estimate of the accuracy obtained but in general, under normal conditions, values of either B or H for normal induction may reasonably be expected to be accurate within 2 percent. For the determination of coercive force, another phenomenon must be taken into consideration. It has been found that when the average induction as indicated by the B-coil is zero, the B in the part of the specimen next to the pole pieces has already reached a negative value while the outer part next to the H-blocks is

still positive. Since the H-blocks are in contact with this outer part, the value of H_c will be low. The error depends upon the slope of the hysteresis loop at the H_c point. If it were vertical, there would be no error. As a rule, the slope is less and consequently the error is greater the higher the value of H_c.

The Fahy Simplex permeameter has found favor primarily on account of its easy manipulation and the requirement of only a single specimen. Its accuracy is probably within the range of uniformity of most magnetic materials.

The wiring diagram is like that of figure 9 except that coil l and resistor sh are omitted and the magnetizing coil M is on the yoke instead of over the specimen.

5.5. Tests of Low-Permeability Materials

Materials having a permeability only slightly in excess of unity are generally tested in a straight solenoid. Since the intrinsic induction for such materials is very low, the correction for self-demagnetization is small and can be neglected without appreciable error in the value of magnetizing force calculated in terms of the current. In order to obtain a satisfactory degree of precision in the determination of the intrinsic induction it is necessary to balance out the direct effect of the magnetizing field. This can be done by connecting the secondary of a mutual inductor of variable value in series-opposition with the test coil which usually has several hundred turns The primary of the inductor is connected in series with the solenoid. The mutual inductor is adjusted so that, with no specimen in the test-coil, there is no deflection of the ballistic galvanometer upon reversal of the magnetizing current The galvanometer can then be used at its maximum sensitivity. When a specimen is inserted within the test coil and the magnetizing current is reversed, the galvanometer deflection is proportional to the intrinsic induction. The galvanometer is calibrated by means of a standard mutual inductor in the usual way.

In the Fahy Low-Mu permeameter [17] a somewhat different arrangement is employed. Two similar test coils are used. The specimen is inserted in one coil and the other constitutes a compensating coil to balance out the effect of the magnetizing force on the main test coil. The compensating coil has a value of area-turns somewhat greater than that of the other coil. In order to balance the system with no specimen present, the compensating coil is shunted with a resistor whose value is adjusted so that, with no specimen in the test coil, no deflection of the galvanometer results from a reversal of the magnetizing current. Then when a specimen is inserted in the test coil and the magnetizing current is reversed, the resulting deflection is proportional to the intrinsic induction. The galvanometer is calibrated in the usual way by means of a standard mutual inductor.

5.6. Magnetic Susceptibility

The measurement of magnetic susceptibility requires the use of much more sensitive apparatus than is needed for the measurement of ferromagnetic properties. Just as in the measurement of magnetic fields, there are only two basic methods for the determination of magnetic susceptibility. One is the measurement of the minute mechanical forces experienced by a body in a nonuniform magnetic field. The other is by means of induction methods. For precise measurements, the force methods are more commonly used.

The principal methods in use by the Magnetic Measurements Section are known as the Gouy method [18], the Faraday method [19], and the Thorpe and Senftle method [20].

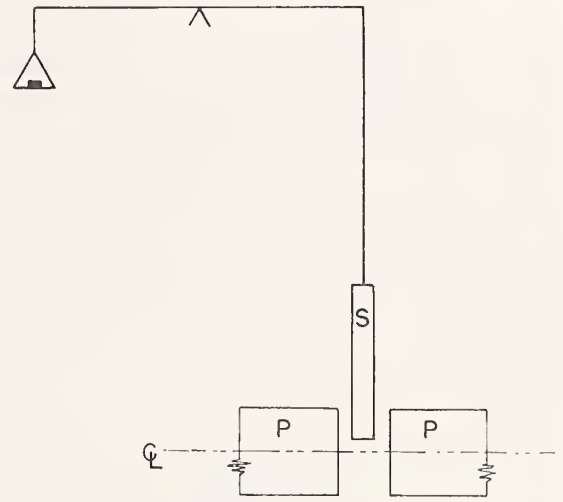

FIGURE 14. *Gouy apparatus.*

The Gouy apparatus is illustrated by the diagram of figure 14. A cylindrical specimen, s, of uniform cross section, A, is hung from a sensitive balance with its axis vertical. The lower end is located in the uniform part of the magnetic field between the poles, P, of a powerful electromagnet, and usually above the center line of the pole pieces. The specimen should be long enough to bring its upper end into a much weaker field. The force due to the application of the magnetic field is measured by the balance. The magnetic susceptibility is then calculated by using the equation

$$f=kA(B_1^2-B_2^2)/2\Gamma_m \text{ [22]}$$

Transposing,

$$k=\frac{2\Gamma_m f}{A(B_1^2-B_2^2)}$$

[22] Note: In the classical egsem system of units, the equation is usually given as $f=kA(H_1^2-H_2^2)/2$. This equation is dimensionally inhomogeneous but gives the same numerical results as the other because in this system Γ_m is unity and there is no numerical distinction between B and H.

	cgsem	mksa (rationalized)
k=volume susceptibility	------	------
f=force	dynes	newtons
Γ_m=magnetic constant	1	$4\pi\times10^{-7}$
A=area of specimen	cm^2	m^2
B_1=field at lower end	gausses	teslas
B_2=field at upper end	gausses	teslas.

The use of rationalized units yields values of magnetic susceptibility which are 4π times the values obtained by the use of unrationalized units. (See pp. 4–5). The Magnetic Measurements Section generally uses the nuclear magnetic resonance method (see pp. 12–13) for measuring B_1 and a pivoted magnet instrument for measuring B_2. (In the classical cgsem system, it is customary to measure B and call it H.) The Gouy apparatus at NBS is equipped for measurements at temperatures as low as that of liquid hydrogen.

The Faraday method is adapted to measurements of magnetic susceptibility of specimens too small for the Gouy method. A small sample of magnetically isotropic material experiences no mechanical force when placed in a uniform magnetic field. However, if there is a gradient in the field, a force will be experienced. In this case

$$f=\frac{m\chi BdB/dy}{\Gamma_m}.^{23}$$

Transposing,

$$\chi=\frac{\Gamma_m f}{mBdB/dy}$$

where

	cgsem	mksa (rationalized)
χ=mass susceptibility	(see pp. 5–6)	
Γ_m=magnetic constant	1	$4\pi\times10^{-7}$
f=mechanical force	dynes	newtons
m=mass	grams	kilograms
B=magnetic field	gausses	teslas
y=distance	cm	m.

Here as with the Gouy method, the values in a rationalized system are 4π times those in an unrationalized system.

Measurements with this method on an absolute basis are attended with some difficulty. The apparatus is generally calibrated by the use of standard samples of known susceptibility. The standard must be of the same size and shape as the specimen to be tested and located in the same position in the nonuniform field.

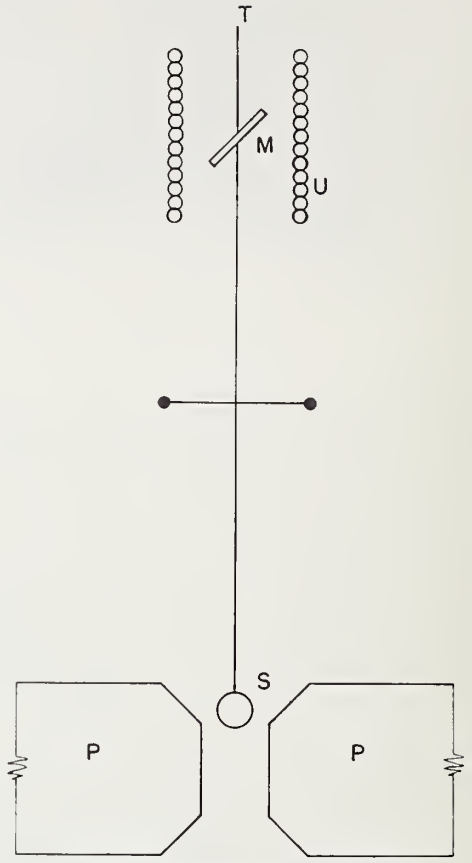

FIGURE 15. *Vertical beam Faraday apparatus.*

The apparatus is shown diagrammatically in figure 15. The specimen, S, is mounted at the lower end of a quartz beam, and a permanent magnet, M, is mounted near the upper end. The beam is supported by a horizontal beryllium-copper wire near the midpoint; the specimen is carefully positioned between the pole pieces in the region where the product of the field by the field gradient is constant over the volume of the specimen. Measurements are made by applying a field and then restoring the beam to its original position by means of a torque exerted on the permanent magnet by a current in the solenoid, u. The position of the beam is indicated by observing the tip, T, with a telescope and scale.

The Thorpe and Senftle method, described by Thorpe and Senftle [20], is generally used for measuring small samples of material. The method is illustrated in the diagram of figure 16. A quartz spring supports the specimen initially in a position between the poles of the magnet and slightly below the center of the pole faces. After the deflection of the spring, due to the application

[23] The force is given as $f=m\chi HdH/dy$ when the classical cgsem system of units is used. This equation is dimensionally inhomogeneous but gives rise to no numerical error because Γ_m is unity and no distinction is made between B and H in the classical cgsem system.

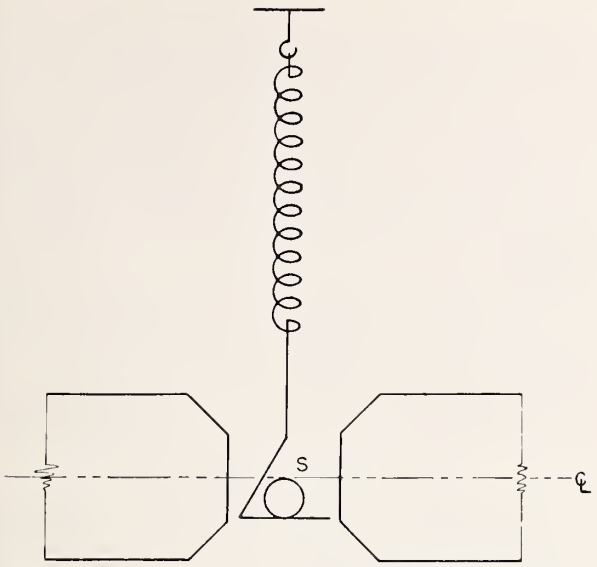

FIGURE 16. *Quartz Helix magnetic susceptibility balance.*

of the field, has been observed for this position, the magnet is lowered to a new position and another observation of the deflection is made. This procedure is repeated for several selected positions of the magnet until there is no observable change in deflection when the magnet is moved to a lower position. From the proper integration of the curve of displacement of the sample versus the distance of the magnet from the sample, the maximum value of the magnetic field between the poles of the magnet, the mass of the sample, and the elastic constant of the quartz spring, it is possible to calculate the magnetic mass susceptibility of the sample by the equation

$$\chi=\frac{2AK\Gamma_m}{mB^2_{\max}}$$

where

χ=mass susceptibility

A=area under the curve

K=elastic constant of the quartz spring

Γ_m=magnetic constant

m=mass of the sample

B=the maximum field of the magnet.

Since

$$m=\mathrm{Kh/g}$$

where

h=measured static deflection of the quartz spring

and

g =acceleration due to gravity,

$$\chi=\frac{2gA\Gamma_m}{hB^2_{\max}}.$$

The induction methods most generally used are a-c bridge or balance methods [24] and the vibration magnetometer.[25] These methods involve the inducing of voltage in a coil as a result of changing flux linkages due to the applied field or a position change of the coil or sample. These methods have the advantages that they use uniform magnetic fields and cover a larger range of susceptibilities than the force methods; however they usually require a standard material for calibration purposes.

5.7. Magnetic Standards

In view of the nature of the magnetic units, it is obviously not feasible to realize them in concrete form. The calibration of magnetic testing apparatus is carried out in terms of the electrical units by the use of standard shunts, potentiometers (or ammeters), and mutual inductors. The basic standards are (1) a mutual inductor so designed that its value can be calculated from its dimensions (2) a standard resistor, and (3) a standard cell. These basic standards are used to calibrate working standards and these working standards in turn are used for the calibration of the measuring circuits. For the intercomparison and standardization of permeameters it is necessary to make use of carefully selected and prepared test specimens whose magnetic properties are accurately determined by some standard method. It may perhaps be proper to refer to such test specimens as magnetic standards.

The preparation and maintenance of standards of magnetic susceptibility present some difficult problems. The material must be of high purity (ferromagnetic impurities are particularly troublesome) and means must be provided to prevent contamination during handling or storage. Questions of stability and temperature effects are also important. Standards of susceptibility are required for the calibration of apparatus with which it is difficult or impossible to obtain absolute results. The Magnetic Measurements Section has a continuing program for the investigation of standard materials such as water, benzene, nickel chloride, and hydrated ferrous ammonium sulfate (Mohr's salt) and the improvement of methods of preparations and measurement of standards specimens.

5.8. Limits of Accuracy

The problem of magnetic testing consists in determining simultaneous values of magnetic

[24] Magnetochemistry—P. W. Selwood Interscience Publishers.
[25] A Vibrating Sample Magnetometer by N. V. Frederick—IRE Transaction on Instrumentation I-9, No. 2 (Sept. 1960).

induction and magnetizing force. It is relatively easy to obtain fairly accurate values of induction, but the accurate determination of the corresponding magnetizing force is more difficult. It is only by the exercise of great care in the selection of test specimens and manipulation of the testing apparatus that an accuracy of 1 percent can be attained. The influence of the quality and condition of the test specimen is of great importance, especially in the standardization of permeameters because inaccuracies really arising from the condition of the specimen itself should not be charged to the testing apparatus.

5.9. Requirements of Standard Specimens for D-C Permeameters

Specimens to be used as standards for the calibration or intercomparison of permeameters should be chosen and prepared with the following points in view: (1) magnetic uniformity along the length, (2) metallurgical stability, and (3) uniformity of section.

If the specimen varies in permeability along its length, errors are introduced in the measurements which cannot be calculated or eliminated by compensation, and which may be of considerable magnitude. It is possible to have errors due to this cause alone which amount to 25 percent or more. Moreover, various methods are sensitive to this influence in varying degrees. It is obvious, therefore, that such specimens should not be used for the intercomparison or standardization of testing apparatus. Various methods for the determination of the degree of uniformity of magnetic-test specimens have been proposed [21], but probably the most satisfactory one is to prepare a specimen much longer than is required for the final form and to make measurements at suitable intervals along its length. If the results of these measurements are in agreement, then the specimen is, from this point of view, satisfactory to use as a standard.

It is well known that specimens of steel freshly heat-treated are not metallurgically stable; that is, changes in internal structure or condition may go on for some time. These changes are accompanied by corresponding changes in magnetic properties. It is necessary, therefore, to make sure that specimens to be used as magnetic standards are metallurgically stable. This can be accomplished by either natural or artificial aging.

It is quite obvious that irregularity in cross section along the length of a specimen would have an effect similar to that of a variation in magnetic permeability. For this reason, it is important that care should be used in preparing the specimen to maintain a uniform cross section.

5.10. General Precautions

In the calibration and use of magnetic standards, it is necessary to avoid (1) mechanical strain, (2) variations in temperature, and (3) mechanical vibration.

Mechanical strain influences the magnetic properties of materials to a marked degree. It is important, therefore, in the calibration and use of magnetic standards that they be clamped without bending. The effect of bending is particularly noticeable in materials of high permeability and in the steep part of the magnetization curve.

The effect of variations in temperature is not negligible [22], and care should be taken that standards be not heated during the course of a test. The temperature coefficient is not constant and varies for different materials or even for the same material with different heat treatments.

Mechanical vibration should be avoided in magnetic testing. It has a tendency to increase the apparent permeability and to decrease the hysteresis. This is generally not a serious factor, but for work of high accuracy, it should be considered and the specimens protected from excessive vibration.

6. Tests With Alternating Currents

6.1. Core Loss and A–C Permeability at Power Frequencies

Magnetic tests with alternating currents are extensively employed by producers and users of magnetic core materials in connection with quality control and for obtaining design data. These tests are generally made by methods specified by the American Society for Testing Materials. Since magnetic materials are continually being improved and new and better methods of testing are being developed, the specifications require frequent revision in which the Magnetic Measurements Section cooperates. For this reason, it is neither necessary nor desirable to give detailed descriptions of the current standard methods. The general principles are presented here but for specific details, the reader is referred to the latest Standards on Magnetic Materials issued by the ASTM [23].

The principal objects of testing with alternating currents are to determine core loss, a-c permeability, and incremental permeability of laminated magnetic core materials. The test specimens usually consist of strips of flat-rolled material assembled in the form of a square magnetic circuit inserted in four solenoids which are permanently mounted on a suitable base. Each of the solenoids has two uniformly distributed windings. The corresponding windings of the four coils are connected in series to form primary and second windings having an equal number of

turns. The primary winding carries the magnetizing current. The secondary winding is used to energize voltmeters and the voltage coil of a wattmeter (if used). A third winding may be required in certain types of tests. The set of coils mounted on a base is generally called an Epstein frame.

Since flat-rolled core material has directional properties, half of the specimen strips are generally cut with their long dimension in the direction of rolling and half in a direction at right angles to the direction of rolling. Certain materials with oriented grain structure may have the strips all cut in the direction of rolling. When the strips are cut "half and half" they are so assembled that strips on opposite sides of the square are cut in the same direction.

There are two principal types of testing methods in which the Epstein frame is used, voltmeter-wattmeter methods, and bridge methods.

a. Voltmeter-Wattmeter Methods

The basic diagram of connections for these methods is shown in figure 17. The a–c source should deliver as nearly a sinusoidal voltage as possible with a minimum amount of distortion when fully loaded. The current is controlled preferably by means of a suitable autotransformer rather than by series reactance. Excessive resistance or inductance in the circuit causes an undesirable amount of distortion in the wave form. Connected in series with the primary winding, P, of the test frame are: an ammeter, A, of low internal impedance, the primary winding of a calibrated mutual inductor, L_m, the current coils of a wattmeter, W, designed specially for measurements at very low power factors and the primary winding of a compensating mutual inductor, L_{mc} (if used).

The secondary winding of the compensating inductor, L_{mc} (when used) is connected in series—opposition to the secondary winding, S, of the test frame. When the selector switch Sw is closed downward, the rms-reading voltmeter, rms Vm, the average-reading voltmeter,[26] Av Vm, and the potential coil of the wattmeter, W, are connected in parallel to the secondary winding S of the test frame through the secondary winding of the compensating inductor, L_{mc}. The 50-cm Epstein test requires a specimen consisting of 10 kg (22 lb) of material cut into strips 50 cm (19 1/16 in) long and 3 cm (1 3/16 in.) wide. This relatively large sample previously was required in order to obtain a fair average result for material which was not very uniform even throughout a single sheet. The strips are assembled in the test frame with butt joints at the corners, which are clamped to maintain a low magnetic reluctance at the joints. Improved manufacturing techniques now permit the use of much smaller samples and the 25-cm Epstein test[27] requiring only 2 kg (4.4 lb) is now standard.

[26] This is an instrument whose moving system responds to the average value of the rectified alternating current.

[27] Tests are often made on smaller specimens but the 2 kg sample is standard at present.

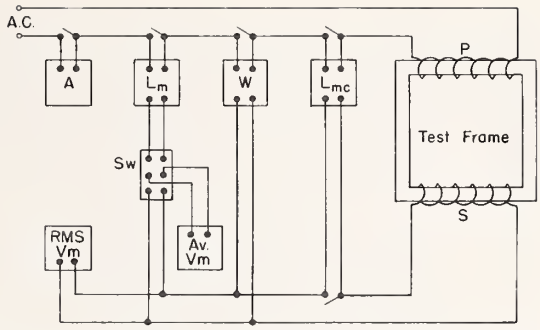

FIGURE 17. *Diagram of connections for Epstein tests by the voltmeter-wattmeter methods at power frequencies.*

In carrying out tests using the 25-cm Epstein frame, a better joint at the corners than the butt joint used in the 50-cm apparatus is required on account of the shorter magnetic circuit. A double-lap joint has been adopted. This requires strips at least 28 cm (11 3/32 in.) long. Strips up to 50 cm (19 1/16 in.) long can be used if necessary. The width of the strips is the same as in the 50-cm test, i.e., 3 cm (1 3/16 in.).

The sample is first weighed and then inserted in the test frame in four equal groups in such a way that at each corner the strips of adjacent groups successively overlap and groups at opposite sides of the square are cut in the same direction. No insulation other than the natural oxide is used between strips except in the case of oxide-free material. The corners may be clamped to reduce the magnetic reluctance but it must be done carefully so as not to introduce excessive mechanical strain in the strips.

The apparatus is then connected to the a–c source and the current is adjusted so that the voltage of the secondary coil of the test frame as indicated by the average-reading voltmeter corresponds to the desired maximum induction in the specimen. This voltage is given by the equation

$$E_{ave}=\frac{4B_mANf}{10^8}$$

where

E_{ave} = average voltage
B_m = maximum induction in gausses
A = cross-sectional area of the specimen, cm^2
N = number of turns in secondary coil
f = frequency in cycles per second

(If B is in teslas and a is in m^2, the factor 10^8 is not needed.)

The cross-sectional area of the specimen is determined from the mass, density, and length of the strips

$$A=\frac{m}{4l\delta}$$

where

A = area in cm^2
m = the mass in grams
l = length of a strip in cm
δ = density in g/cm^3.

The density for most of the conventional materials is assumed from their chemical composition. For other materials, the density must be determined experimentally. For silicon-iron alloys the values range from 7.55 to 7.85 depending upon the silicon content. (See table 4.) Densities of nickel-iron alloys vary from 7.85 to 8.90. (See table 5.)

TABLE 4. *Silicon-iron alloys*

Silicon content range	Assumed density
Percent	*g/cm³*
0 to 0.5	7.85
0.5 to 2.0	7.75
2.0 to 3.5	7.65
3.5 to 5.0	7.55

TABLE 5. *Iron-nickel alloys*

Density determined from straight lines joining points given below.

Nickel	Density
Percent	*g/cm³*
0	7.85
30	8.00
50	8.26
80	8.64
100	8.90

After the frequency and voltage have been properly adjusted, the wattmeter is read. The value obtained includes not only the total loss in the core but also the losses in the instruments connected to the secondary winding of the test frame. The loss in each instrument is E^2/R where E is the rms voltage and R is the ohmic resistance of the instrument.

If the wave-form distortion as indicated by the form factor, ff, differs from 1.111 (form factor of a sine wave) by more than 1 percent, it is necessary to make a correction to the observed value of the core loss to account for the fact that whereas the hysteresis component of the total loss is a function of the average voltage, the eddy-current component is a function of the rms voltage [24].

If the cross-sectional area of the specimen is much less than that of the secondary coil of the test frame, a correction must be made for the extra induced voltage due to the air flux. This correction can be calculated from the equation

$$E_a=\frac{4Nf\Gamma_m H_p(a-A)}{10^8}$$

where

E_a=average voltage due to air flux
N=number of turns in secondary coil
f=frequency in cycles per second
Γ_m=magnetic constant=1
a=area of secondary coil in cm²
A=area of specimen in cm²
H_p=peak magnetizing force in oersteds.

If the mksa system of units is employed, the equation becomes

$$E_a=4Nf\Gamma_m H_p(a-A)$$

in which

E_a=average voltage due to air flux
$\Gamma_m=4\pi\times10^{-7}$
H_p=peak magnetizing force in amp-turns/m and areas are in m².

In the cgs system, the peak magnetizing force is calculated by using the equation

$$H_p=\frac{0.4\pi NI_p}{l_a}$$

where

H_p=peak value of magnetizing force in oersteds
N=number of turns in primary winding
I_p=peak current, amperes
l_a=assumed length of the magnetic circuit=94 cm.

In the mksa system, H_p is in ampere-turns/meter and l_a is in meters (0.94 meter) and the equation is

$$H_p=\frac{NI_p}{l_a}.$$

The peak value of the magnetizing force, H_p, is determined in terms of the peak current and the number of turns per unit length in the magnetizing winding, P. The peak current is proportional to the average voltage induced in the secondary winding of the mutual inductor, L_m

$$I_p=KE_{ave}.$$

The factor K is determined by observing the average voltage induced by a sinusoidal current of known value.

The a-c permeability is taken to be the ratio of the maximum induction to the peak value of magnetizing force.

It is convenient to compensate for the extra voltage due to air flux by means of the compensating mutual inductor (L_{mc} in the diagram). The mutual inductance is adjusted to be equal to that between the primary and secondary windings of the test frame (no specimen inserted). If this is done, the indicated induction is the intrinsic induction, B_i, in the specimen.

The specific core loss is calculated by dividing the corrected value of total watts by the "active weight" of the specimen. The active weight is

$$m_1=\frac{ml_1}{4l}$$

where

m_1=active weight in kg
m=weight in kg
l_1=assumed length of magnetic circuit=94 cm
l=length of strips.

b. Bridge Methods

Generally, core loss and a-c permeability are determined by the voltmeter-wattmeter method. In many cases, however, there are certain advantages, such as increased sensitivity and greater frequency range, in making these measurements by a bridge method. For measurements at low inductions (not over 1,000 gausses or 0.10 tesla) and at high frequencies, the bridge methods have been used successfully for several years. More recently, however, bridge circuits have been developed by which measurements may be made at higher inductions. The ASTM [23] has approved as standard a modified Hay bridge for use in measurements at inductions up to 10 or 12 kilogausses in nonoriented steels or 16 to 18 kilogausses in oriented silicon steels. For measurement at higher inductions, the distortion in the wave form of the exciting currents is considerable and it has been found necessary to use special techniques [25] in order to obtain accurate results with bridge methods.

Figure 18 is a diagram of a modified Hay bridge currently approved as standard by the ASTM [23]. The assumed equivalent impedance of the coil containing the test specimen is shown in the diagram at the right. The inductance of the coil alone without the specimen, L_w, and its resistance, R_w, are considered to be in series as shown. They are balanced by the capacitance C'_w and the resistance R'_w respectively. Ordinarily the inductance of the coil alone is so small that it is negligible and C'_w need not be used.

The apparent additional resistance, R_1, due to the core loss and the inductance, L_1, due to the permeability of the test material are considered to be in parallel. They are balanced by the resistance, R_b, and the capacitance C_b. R_a and R_c are fixed resistors whose product is equal to the product of the impedances of the other two arms of the bridge. Since R_c carries the total exciting current it must have such current-carrying capacity that it will not be heated excessively.

D is a detector, tuned to the fundamental frequency of the voltage supply. This detector should have a high impedance and high sensitivity to the fundamental frequency. Previously, vibration galvanometers have been employed for this purpose, but they have been almost entirely replaced by electronic devices of various kinds.

The a-c source is connected to the bridge through an isolating transformer. In the arrangement recommended by the ASTM, this transformer has a tapped secondary for convenience in selecting the proper range of voltage to be applied. The primary is fed from an autotransformer connected to the generator. This provides the fine control of the applied voltage. Other arrangements may be employed provided that there is isolation between the source and the bridge and the series resistance is not used to control the current. Resistance tends to distort the wave form of the induced voltage and may lead to excessive errors. [25]

For incremental values, the d-c magnetizing current may be supplied to the secondary winding, N_2. The average a-c voltage is then read across the primary winding, N_1. The IR drop in this winding causes a slight error but this is usually negligible. The d-c source must furnish a steady current. A storage battery is ordinarily the best

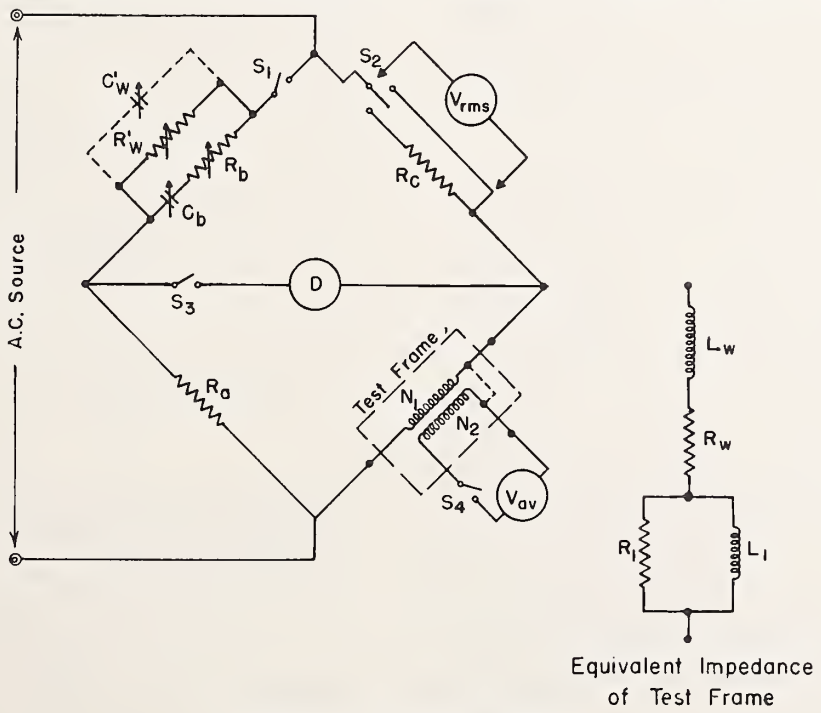

FIGURE 18. *Modified Hay Bridge.*

source as rectified a-c requires a great deal of filtering. The d-c circuit contains a series inductor of at least 10 h when carrying maximum current. This is to limit the a-c current in the d-c circuit to a negligible value.

The maximum induction in the specimen is indicated by a voltmeter connected to the secondary winding N_2 of the test frame. The voltmeter, V_{ave}, indicates the average voltage.[28] The maximum induction in terms of average voltage in cgs units is

$$E_{ave}=4\ BANf\times 10^{-8}$$

where

E_{ave}=average volts

B=maximum induction, gausses (if the air-flux compensating inductor is used, B is the intrinsic induction, B_i)

A=area of specimen, cm^2

N=number of turns in winding

f=frequency, cycles per second.

In mksa units,

B=induction in teslas

A=area in m^2

and the factor 10^{-8} is omitted. The other factors remain the same.

The rms value of the exciting current can be determined by connecting the rms-reading voltmeter across the resistor R_c as indicated.

As in d-c testing, the first step, especially if measurements are to be made at low values of induction, is to demagnetize the specimen. This is accomplished by first setting switch S_2 so as to take R_c out of the circuit and opening switch S_3 and then with switch S_4 closed, setting the a-c source to zero and connecting it to the bridge. The voltage is then raised until the average voltmeter indicates that a maximum induction of the order of 14 kilogausses has been reached. The current is then gradually and steadily decreased until the indicated induction is somewhat lower than the lowest at which a measurement is to be made. If this point is below about 1,000 gausses (0.100 teslas) it will be necessary to take into account the drift in values which takes place immediately after demagnetization. This drift is rapid during the first few seconds but the rate of change decreases as time goes on. For this reason, if reproducible results are to be obtained, a standard procedure must be followed. For the best reproducibility, it is necessary to wait several hours after demagnetization before making the test. This would be very inconvenient in most cases. Fortunately, it has been found that a satisfactory degree of agreement can be obtained if balance is reached about 3 min after demagnetization. If the test induction is higher than 1,000 gausses (0.100 teslas) the drift is not observed.

R'_W and C'_W (if used) are preset according to the equations

$$R'_W=\frac{R_aR_c}{R_W}$$

and

$$C'_W=\frac{L_W}{R_aR_c}\quad (C \text{ in farads}).$$

These balance the resistance, R_W, and the inductance, L_W, of the test winding, N (specimen not inserted), thus avoiding the necessity of calculating the effect of R_W and L_W.

Since R_c must carry the total exciting current and the voltage drop across it must be less than 10 percent of that across the test winding to avoid excessive distortion of the wave form, its proper value will depend upon the range of inductions at which measurements are to be made. Ordinarily, 1,000 ohms is used for the lowest range (10 to 50 gausses), 100 ohms is used for the medium range (50 to 500 gausses) and 10 ohms for the higher range (500 to 10,000 gausses). The resistor R_a may be set so as to make permeability direct-reading in terms of C_b or core loss may be direct-reading in terms of R_b. Directions for setting may be found in the ASTM specifications.

Readings are made as follows. With switch S_2 set to connect R_c into the circuit and switches S_1, S_3, and S_4 closed, the applied voltage is raised to the point at which the desired induction as indicated by the average-reading voltmeter is reached. Balance is then obtained by successively adjusting R_b and C_b until the detector shows a minimum reading. The balance equations are as follows

$$L_1=R_aR_cC_b$$

and

$$R_1=\frac{R_aR_c}{R_b}$$

where

L_1=inductance due to the permeability of the test material, henries;

and

R_1=increased apparent resistance due to core loss in the test material, ohms.

In the cgs system

$$L_1=\frac{0.4\pi N_1{}^2A}{10^8 l_1}\times\mu_L$$

and since

$$L_1=R_aR_cC_b$$

[28] According to ASTM specifications, the scale of this instrument is calibrated in terms of average volts multiplied by 1.111, the form factor of a pure sine wave. This may be confusing in some instances, especially when an rms-reading voltmeter and average-reading voltmeter are used together to determine the form factor.

it follows that

$$\mu_L = \frac{R_a R_c C_b l_1 \times 10^8}{0.4\pi N_1^2 A}.$$

In these equations

μ_L = effective a-c permeability of the test material

l_1 = assumed effective length of the magnetic circuit = 94 cm

N_1 = number of turns in the primary winding.

In the mksa system, the equation is

$$\mu_L = \frac{R_a R_c C_b l_1}{N_1^2 A}$$

where

l_1 = assumed effective length in meters = 0.94

and

A = area in square meters.

Areas are determined from the length, mass, and density of the strips.

Core loss, P_c, is calculated from the observed values of R_1 and E_1

$$P_c = \frac{E_1^2}{R_1} = \frac{E_1^2 R_b}{R_a R_c}$$

The specific core loss $P_{B:f}$ is

$$P_{B:f} = \frac{P_c}{m_1}$$

where m_1 is the active mass as indicated above.

Reactive or quadrature power is

$$P_q = \frac{E_1^2}{\omega L_1} = \frac{E_1^2}{\omega C_b R_a R_c}$$

the unit is called the var. The specific value is P_q/m_1 where m_1 is the effective mass, determined as shown above.

Incremental values of permeability and core loss are determined in the order of increasing values of biasing magnetizing force. Direct current is supplied to the secondary winding and adjusted to the required value and reversed several times to establish a cyclic condition in the specimen. The a-c is then applied and the bridge is adjusted and readings taken as described above.

The d-c magnetizing force is calculated as follows:

In the cgs system, the biasing or d-c magnetizing force is

$$H_b = \frac{0.4\pi N_2 I_{d\text{-}c}}{l_1}$$

where

H_b = biasing magnetizing force, oersteds

$I_{d\text{-}c}$ = d-c current, amperes

l_1 = assumed length of the magnetic circuit, cm.

In the mksa system

$$H_b = \frac{N_2 I_{d\text{-}c}}{l_1}$$

where

$I_{d\text{-}c}$ = d-c current, amperes

and

l_1 is in meters

H_b is then ampere-turns per meter.

For incremental tests, the average-reading voltmeter is connected to the primary winding N_1. For this test values of incremental induction, B_Δ are limited to not more than 1,000 gausses (0.1000 tesla).

6.2. A-C Measurements at Higher Than Power Frequencies

Magnetic materials have been developed which are particularly useful at high frequencies on account of their extremely high electrical resistance. They are ceramic materials called ferrites. Magnetic tests of these materials are usually made on specimens in the form of small rings. Although the Hay bridge can be adapted to make measurements at the higher frequencies, it has the disadvantage that each ring must be wound individually. In order to obviate this difficulty, Haas [26] has developed a radiofrequency permeameter similar in principle to an instrument developed earlier for power frequencies by Kelsall [27]. It is shown diagrammatically in figure 19.

The radiofrequency permeameter consists essentially of a transformer. The primary is wound on a powdered ring core. The secondary consists of a central conducting tube over which the ring specimen can be placed. The one-turn secondary is completed by a coaxial outside cylinder and end plates which form a single short-circuited turn which is linked with both the primary core and the specimen as shown in the equivalent circuit. The top plate is removable for insertion of the test specimen. Measurements are made of the input

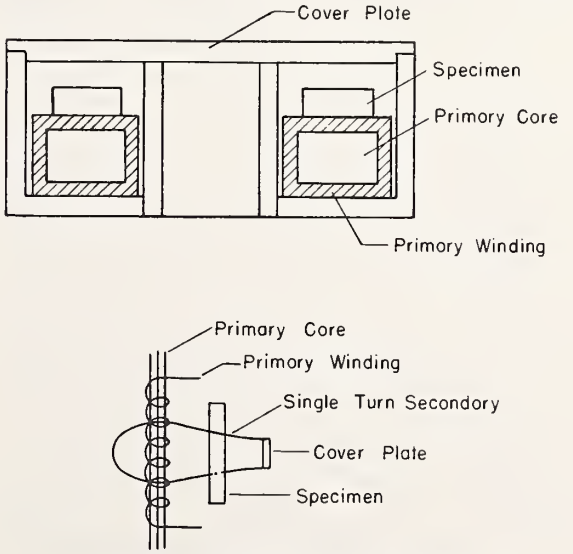

FIGURE 19. *Radio frequency permeameter.*

impedance of the primary winding with no specimen and the secondary open-circuited, with the secondary circuit closed but no specimen, and with the secondary circuit closed and a specimen in place. These measurements can be made with a Q-meter or an impedance bridge. From the values thus obtained, initial values of complex permeability and losses can be computed. Details of the measurements and computations can be obtained from the original paper [26].

7. Typical Magnetic Properties of Materials

Magnetic materials are used under a great variety of conditions both for cores and for permanent magnets. In order to meet many of these special requirements, it is frequently necessary to "tailor make" the material. This may require "special" alloying elements, heat-treating temperatures and procedure, and special mechanical working. In general, however, the metallic magnetic materials employed in practice are alloys mainly composed of one or more of the ferromagnetic metals, iron, nickel, and cobalt. Other elements are always present, either as undesired impurities or as alloying elements added for the purpose of producing certain desired characteristics. In figure 20 are shown typical normal induction curves of annealed samples of iron, nickel, and cobalt of comparatively high purity. These curves are given only for the purpose of general comparison and should not be considered as representing critical values. Small variations in the degree of purity or in the annealing procedure lead to substantial differences in normal induction.

Magnetic materials employed in commercial practice may be considered under the following six classifications: (1) solid core materials; (2) electrical sheet or strip; (3) special alloys; (4) ferrites; (5) permanent-magnet materials; and (6) feebly magnetic materials. In view of the rapid and continued progress in the development of magnetic materials, it is only feasible to give data characteristic of several of the materials commercially available at present. These data indicate merely the range of properties obtainable in the various classes of material and should not be considered as critical, since considerable variation from these values will be found in practice.

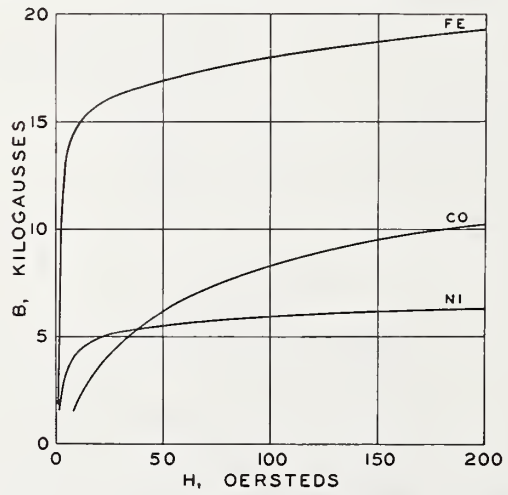

FIGURE 20. *Typical norml induction curves of annealed samples of iron, nickel and cobalt.*

7.1. Solid Core Materials

These materials are used for the cores of direct-current electromagnets, relays, field frames of d-c machines, etc. The principal requirement is high permeability particularly at relatively high inductions. For the majority of uses, it is desirable that the coercive force and hysteresis be low. The principal materials employed are soft iron, low-carbon steel, cast iron, and an alloy of approximately 49 percent of cobalt, 49 percent of iron, and 2 percent of vanadium known as Permendur or Supermendur. Permendur is characterized by very high permeability in the upper part of the normal induction curve and a saturation induction approximately 10 percent greater than that of pure iron. Its cost is relatively high, however, and its use is limited in general to pole tips in which a very high induction is required. Several varieties of soft iron are available, such as Armco iron, Norway iron, and Swedish charcoal iron. These irons are especially refined to reduce impurities and to make as pure iron as is commercially feasible. A typical composition is 99.91 percent of iron, 0.02 percent of carbon, with small percentages of manganese, phosphorous, and sulfur. Low-carbon steel should not have more than 0.0 to 0.2 percent carbon and should contain only the usual small amounts of the ordinary impurities. Cast iron has a relatively low permeability and is used principally in field frames when cost is of primary importance and extra weight is not objectionable. Cast iron is high in carbon (about 3%) and also contains about 3 percent of silicon and varying percentages of phosphorous, manganese, and sulfur.

The best magnetic properties for these materials are obtained by a suitable annealing treatment after machining and fabrication processes have been completed. The properties of cast iron can be greatly improved by malleabilizing, a process that converts a large part of the carbon to the amorphous form.

Typical normal induction curves for solid core materials are given in figure 21.

7.2. Electrical Sheet and Strip

The term electrical sheet (or strip) is commercially used to designate iron-silicon alloys produced in sheet or strip form and used as core

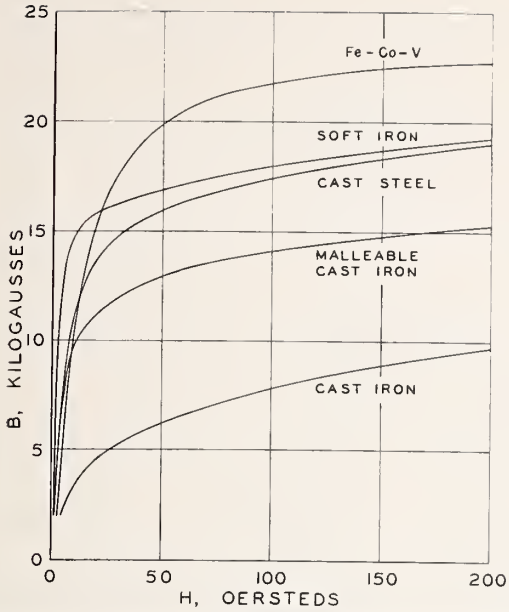

FIGURE 21. *Typical normal induction curves for solid core materials.*

materials in alternating-current apparatus such as transformers, motors, electromagnets, or relays. The principal requirements are high permeability, low hysteresis, and high electrical resistivity. The several grades differ mainly with respect to their silicon content, which ranges from 0.5 percent to approximately 5 percent. Alloys containing the higher percentages of silicon are practically nonaging; that is, the permeability and losses do not change appreciably with time. The required magnetic properties are produced by annealing.

By a suitable combination of cold-rolling and heat treatment, electrical sheet may be produced in which the majority of the crystals are given a favorable orientation. Such material has considerably better magnetic properties in the preferred direction than ordinary grades. their maximum permeability is approximately twice as high and they have much lower core losses combined with higher permeability at high induction than ordinary grades. Figure 22 shows typical normal induction curves for two grades of electrical sheet and oriented-grain material. The improvement in the oriented-grain material is particularly conspicuous in the upper part of the normal induction curve.

The different grades of electrical sheet and strip are usually sold on the basis of guaranteed maximum values of total core loss, as determined in accordance with the specifications of the American Society for Testing Materials [23]. The common designations of the various grades are armature, electrical, motor, dynamo, and transformer. The transformer grades are further subdivided into classes denoted by numerals corresponding to the core loss under standard conditions. Armature, electrical, and motor grades are used principally in small motors, a-c magnets and starting trans-

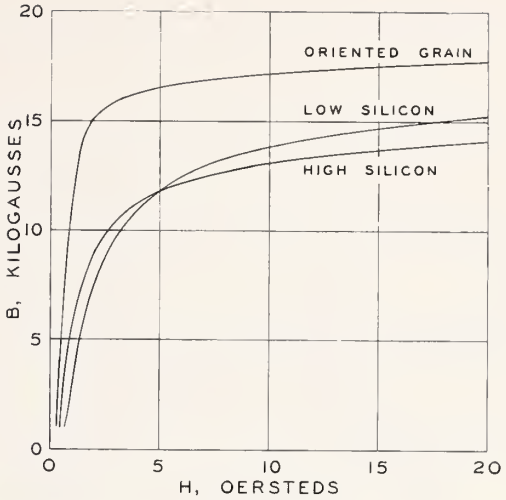

FIGURE 22. *Typical normal induction curves for electrical sheet.*

formers. The dynamo grade is used in high-efficiency rotating machines and small transformers. The transformer grades are used in power and radio transformers.

7.3. Special-Purpose Materials

For certain applications, special alloys and other materials have been developed which, after proper fabrication and heat treatment, have superior properties in certain ranges of magnetization. For instance, alloys of nickel and iron with possible small percentages of molybdenum or chromium have very high values of initial and maximum permeability. Alloys of this class which may have from 70 to 80 percent of nickel are called Permalloys. Special attention to the purity of the constituents, the manufacture, fabrication, and heat treatment has resulted in an alloy of nickel, iron, molybdenum, and manganese that has a maximum permeability greater than one million. This alloy when commercially prepared and rolled into thin tapes (0.001 to 0.004 in. thick) has a maximum d-c permeability between 300,000 and 900,000. An alloy of 50 percent nickel and 50 percent iron is called Hipernik. Another alloy having a small percentage of copper in its composition is called Mumetal. The characteristics of these alloys differ in detail but in general they have high initial and maximum permeability, low hysteresis, and low saturation values. The alloy, Supermendur, of 49 percent of iron, 49 percent of cobalt and 2 percent of vanadium has high permeability which persists at higher values of induction than the nickel-iron alloys.

Typical permeability curves for several special-purpose alloys are given in figure 23 and figure 24.

A certain alloy of nickel, cobalt, and iron after suitable heat treatment has very nearly constant permeability for inductions below 1,000 gausses and is called Perminvar. The 50–50- nickel- iron

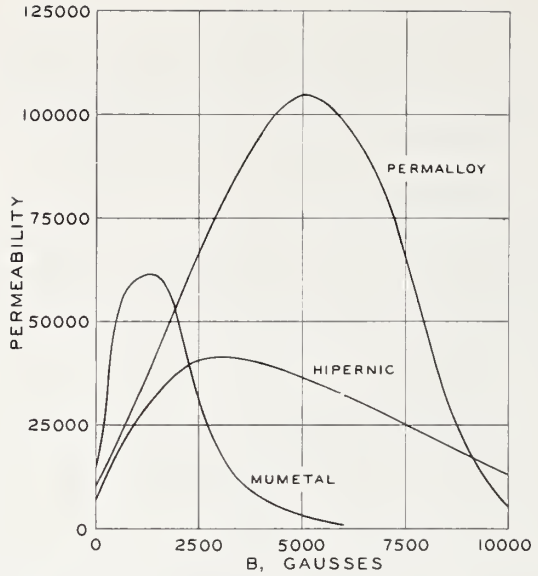

FIGURE 23. *Typical permeability curves for special purpose alloys I.*

alloy can also be heat-treated so as to have similar characteristics.

Many of the above described alloys are rolled into thin tape (as thin as 0.0001 in.) and spirally wound cores are prepared from the tape. This permits the designer to make use of their directional properties as well as to use them at much higher frequencies by decreasing eddy-current effects.

Another series of magnetic alloys of copper, nickel, and iron is temperature-sensitive having an approximately linear relation between permeability and temperature. These are called Thermalloys. The principal use is in the compensation of watt-hour meters for temperature variations. They are also used in certain types of thermal relays.

Although chemical composition and impurities are very important in the preparation of a magnetic alloy, experience has shown that with the same chemical composition a wide variety of magnetic properties can be obtained by varying the mechanical working and type of heat treatment. This is very striking in the nickel-iron and iron-silicon alloys and has led to the development of materials having a practically rectangular hysteresis loop. These are of great importance in the field of electronics.

7.4. Ferrites

Ferrites are nonmetallic ceramic materials whose extraordinarily high electrical resistivity is especially useful for high-frequency applications. They are finding increasing use in applications such as electronic computers, antenna rods, isolators, and magneto-strictive devices. They are made of iron oxide combined with certain bi-

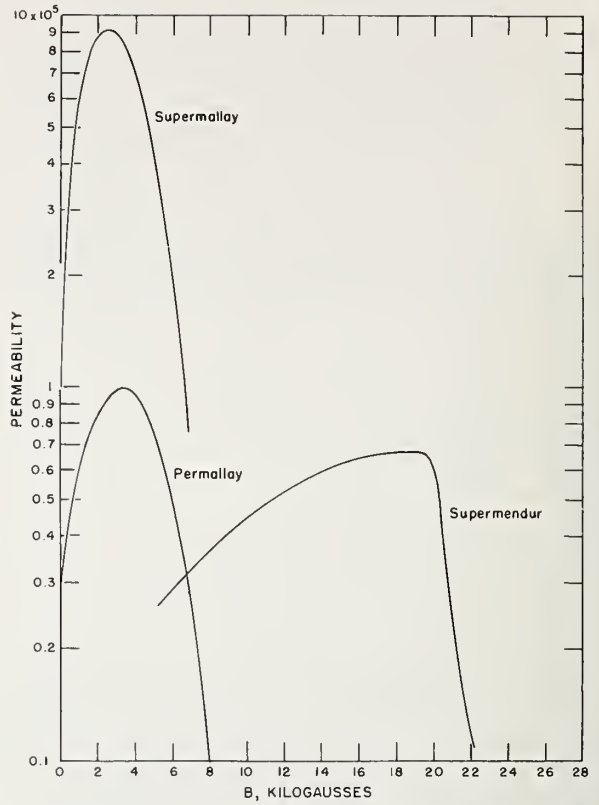

FIGURE 24. *Typical permeability curves for special purpose alloys II.*

valent oxides, hydroxides, or carbonates of metals such as manganese, cobalt, nickel, copper, zinc, or magnesium. The process of manufacture is similar to that of other high-grade ceramic materials. The powdered materials, which must be of high purity and proper particle size, are mixed in suitable proportions, pressed or extruded to the desired shapes, and fired. This procedure produces chemical compounds of the metallic oxides.

These materials are often called "soft" ferrites to distinguish them from certain ceramic materials used for the manufacture of permanent magnets. In common with other ceramics, they are mechanically hard and brittle and require special tools for cutting or grinding. Also, since they require no critical materials, they are relatively low in cost.

Although the saturation induction of the soft ferrites is not high, this is not important because they are generally used at low inductions. Their relative initial permeabilities (100 to 1,500) are very good for the high frequencies involved. The principal disadvantage of the ferrites is their low Curie points which range from 100 to 500 °C. This is important if they are to operate at temperatures much higher than room temperature. Typical magnetic properties of some ferrites at room temperature are shown in figure 25. In figure 26 is shown the temperature dependence of magnesium-manganese ferrite.

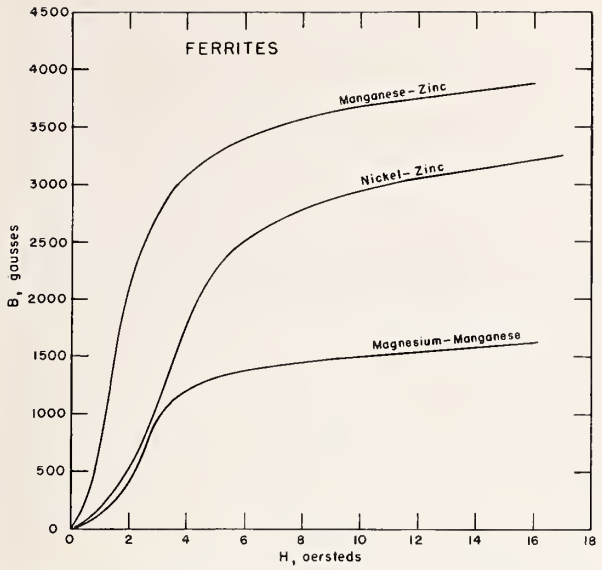

FIGURE 25. *Typical normal induction curves for "soft" ferrites.*

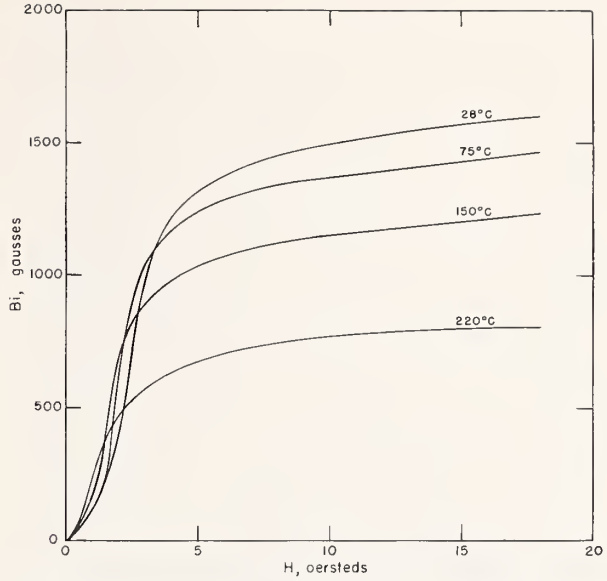

FIGURE 26. *Temperature dependence of a magnesium-manganese ferrite.*

7.5. Permanent-Magnet Materials

Although it is possible to make permanent magnets of almost any kind of steel that is capable of being hardened by heat treatment, it is best to use materials especially produced for the purpose. Magnets made from other types of material are likely to be inferior in quality or unnecessarily expensive. Before the development of the special magnet steels, magnets were generally made of plain high-carbon tool steel. This type of steel is relatively inexpensive, but its magnetic properties are so greatly inferior to those of the special steels that now it is practically never used for making permanent magnets.

Permanent-magnet materials may be grouped in five classes as follows: (a) Quench-hardened alloys; (b) precipitation-hardened alloys; (c) work-hardened materials; (d) ceramics; and (e) iron-powder compacts. Figure 27 shows typical demagnetization curves for several permanent-magnet materials.

a. Quench-Hardened Alloys

Tungsten, chromium, and cobalt magnet steels have been in use for many years. Prior to the first world war, tungsten steel was the standard high-grade permanent-magnet material. The optimum tungsten content is between 5 and 6 percent, with about 0.6 percent of carbon. During World War I, when tungsten was scarce, chromium magnet steel was developed and extensively used in this country. There are two principal grades, one containing about 1 percent of chromium and 0.6 percent of carbon, and the other containing about 3.5 percent of chromium and 0.9 percent of carbon. The 3.5-percent chromium steel is used in many applications. Shortly after World War I, the Japanese metallurgist Honda announced the development of a new permanent-magnet steel having cobalt as the principal alloying element, which he named KS magnet steel. This steel also contained substantial percentages of tungsten, chromium, and molybdenum. The coercive force of this material is about four times as great as that of the tungsten or chromium magnet steels. This development stimulated further investigations which led to the commercial production of several types of cobalt magnet steel having various percentages of cobalt. High-cobalt magnet steels have from 35 to 41 percent of cobalt, and low-cobalt steels have from 8 to 9 percent. These steels also have tungsten and chromium in addition to the cobalt. An intermediate cobalt steel has 17 percent of cobalt and about 9 percent of chromium. Tungsten is sometimes substituted for part of the chromium.

The quench-hardened alloys can be forged and machined from the ingot.

b. Precipitation-Hardening Alloys

The most important permanent-magnet materials are of the precipitation-hardening variety. This group includes the Alnico, Cunife, Cunico, and Vicalloy. The process of hardening in these alloys is related to the change from a single phase at high temperature into two new phases when the temperature is lowered beyond a certain value. The fact that high values of coercive force can be obtained with alloys containing no carbon was anounced in 1932 by Seljesater and Rogers [28] in the United States, Köster [29] in Germany, and Mishima [30] in Japan. These precipitation-hardening permanent-magnet alloys contained aluminum, nickel, and iron. Although the residual induction was relatively low, the coercive forec

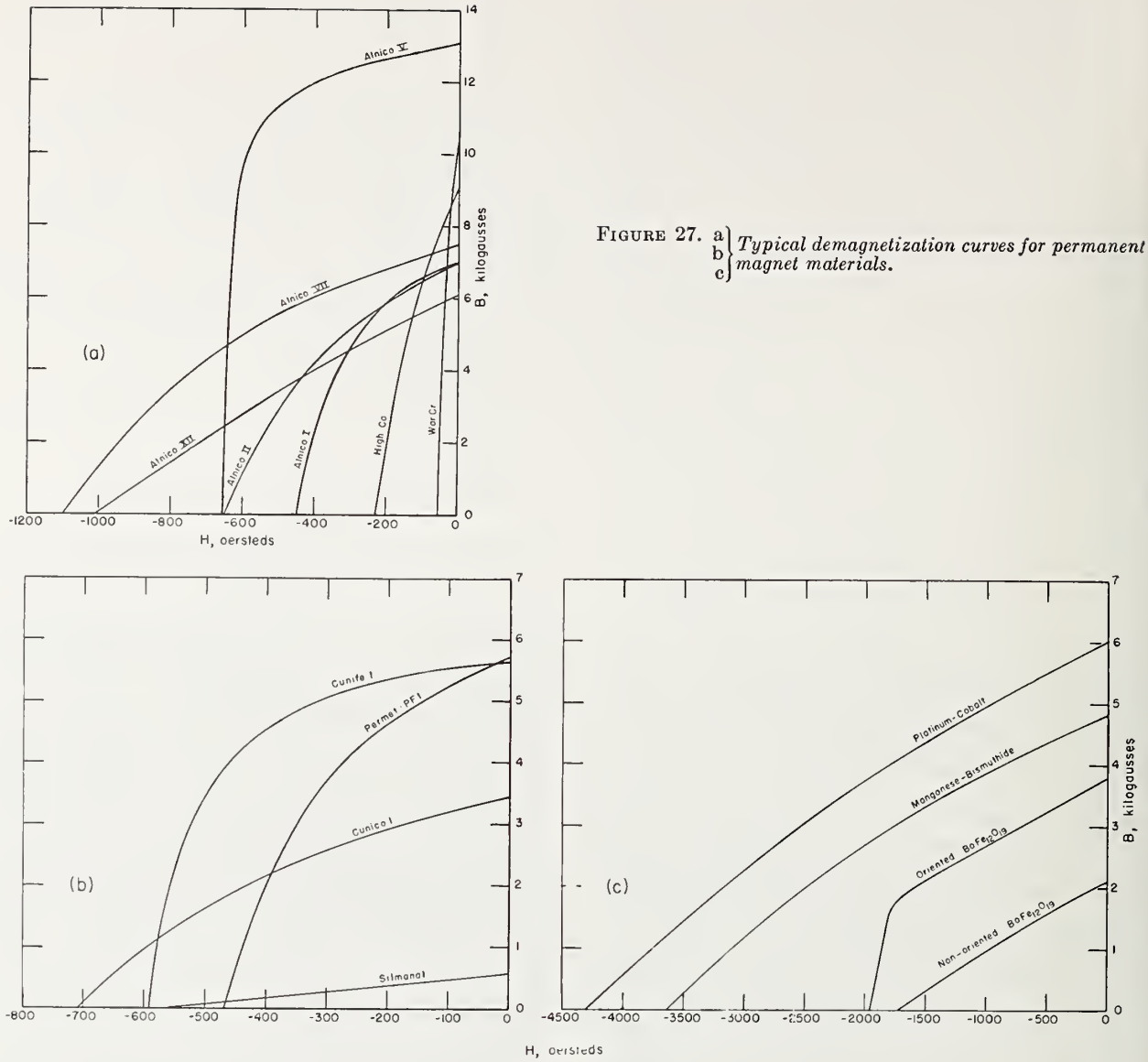

FIGURE 27. a, b, c } *Typical demagnetization curves for permanent magnet materials.*

was so high, about 475 oersteds, that new applications of permanent magnets were made possible. Further investigation showed that the addition of cobalt to the aluminum, nickel, and iron could increase both the residual induction and coercive force. There are more than twenty different commercial varieties called Alnico having coercive force values ranging from 400 to 1,100 oersteds and maximum energy products from 1.2×10^6 to approximately 7×10^6 gauss-oersteds. The Al-Ni-Co-Fe alloys are very hard and brittle, so that they cannot be formed by the usual methods of forging and machining but must be either cast or molded in powder form and then sintered. Final finishing is done by grinding.

Other alloys that belong to the precipitation-hardening group, however, are unusual for high coercive force permanent-magnet material in that they are so ductile that they can be formed readily by rolling or drawing and can be drawn to fine wires before the final heat treatment [31]. Cunife, Cunico, Silmanal, and Vicalloy are alloys of this type.

The platinum alloys have very high values of coercive force but their low residual induction and high cost limit their usefulness.

c. Work-Hardened Alloys

Several ordinarily "nonmagnetic" alloys of iron may become ferromagnetic after cold working due to a phase change in the material. Stainless steel (18% chromium, 8% nickel) is "nonmagnetic" at room temperature after being rapidly cooled from 1,200 °C in the usual process of manufacture. However, if it is hardened by cold working such as

drawing through a reducing die it may develop properties such that it makes an acceptable permanent-magnet material at room temperature. If this work-hardened alloy is then reheated to a high temperature and cooled slowly it regains its original nonmagnetic condition at room temperature. Another alloy that shows this property contains 45 percent iron, 15 percent Ni, and 40 percent Cu. Nesbitt [32] has measured a coercive force of 240 oersteds and a residual induction of 4,400 gausses in wire of this composition which after quenching from 1,000 °C, was then cold drawn from 0.026 to 0.006 in. Increasing the percentage of iron to 60 percent, decreasing the percentage of copper to 25 percent, with 15 percent nickel produced an alloy that after similar treatment as above resulted in a coercive force of 170 oersteds and residual induction of 11,000 gausses.

d. Ceramic Magnet Materials

A commercial development in permanent-magnet materials which is increasing in importance each year is the barium ferrite or ceramic permanent-magnet material. This is a chemical compound and has mechanical characteristics similar to other ceramics. They are hard, brittle, have a lower density than metals, and extremely high electrical resistivity. The basic ingredients are barium carbonate and iron oxide. These materials in powdered form are compressed in dies under high pressure to the required shape. This compacted material is then sintered at a high temperature. This process produces a material which has an H_c of approximately 2,000 oersteds, a B_r of approximately 2,000 gausses, and a demagnetization curve which is practically a straight line. Further improvements in ceramic materials have resulted in a highly-oriented barium-iron oxide whose magnetic properties, on a weight basis, are almost equal to those of Alnico V. The coercive force is approximately 2,000 oersteds, the residual induction 4,000 gausses, and the energy product is 3.5 times that of the unoriented variety. At right angles to the direction of grain orientation, however, this material exhibits negligible permanent-magnet properties and has a permeability of only approximately 1.0.

e. Powder Magnets

Although pure iron is usually regarded as a high-permeability or "magnetically soft" material yet theory has predicted and experiments have proved that compacts of pure iron powders may produce very good permanent magnets. Powder magnets have been produced of iron and iron alloys (such as 70% iron and 30% cobalt) (Permet) with particle size of about 10^{-5} cm diameter with H_c up to 500 oersteds and energy product of 1.5×10^6 gauss-oersteds. The permanent-magnet properties result from the discrete small particles of a single phase instead of from the presence of two or more phases as in most other metallic permanent-magnet material. Further experimental work with particle size and shape and processes of manufacture have produced, in the laboratory, magnets with energy products comparable to those of Alnico V and theoretical considerations predict even higher values.

Manganese-bismuth permanent magnets also belong to this group. This material is an anisotropic aggregate of crystals of the intermetallic compound manganese bismuthide (Mn Bi) and is a product of powder metallurgy. Manganese bismuthide is prepared from the chemical action between molten bismuth and powdered manganese when heated to approximately 700 °C in an inert atmosphere of argon or helium. Cooling is accomplished in such a manner as to produce crystallization of the compound. Laboratory-produced material may have a residual induction of approximately 4,800 gausses and a coercive force of 3,600 oersteds with energy product values as high as 5×10^6 gauss-oersteds.

Powder metallurgy has also produced sintered Alnico magnets. These magnets have greater mechanical strength and more uniform magnetic properties than the cast variety at the expense of a slight decrease in the magnetic properties.

Magnet materials prepared from metal oxides such as cobalt ferrites and Vectolite have been made and used for many years; however, they have been practically superseded by the barium ferrites.

7.6. Feebly Magnetic Materials

It is occasionally desirable to use metallic materials for tools or parts of equipment which require practically nonmagnetic materials. Oxygen-free, high-conductivity copper, copper-beryllium alloy, and pure aluminum are often used where mechanical strength is not required. Aluminum-bronze, nickel-copper, stainless steels, and manganese steels can be used if a permeability not exceeding 1.10 is permissible. In using such a material, it should be kept in mind that even when the bulk material is sufficiently nonmagnetic, mechanical working, surface contamination or temperature effects may make it unsatisfactory.

8. References

[1] Gray, Absolute measurements in electricity and magnetism, 2d Ed. p. 535, MacMillan Co., London (1921).

[2] George S. Smith, Use of bismuth bridge magnetic fluxmeter for ac fields, Trans AIEE **58,** p. 52 (1939).
George S. Smith, A new magnetic fluxmeter, Trans AIEE **56,** p. 441 (1937).

[3] A. Koepsel, Apparat zur bestimmung der magnetischen eigenschaften des eisens in absoluten mass und directer ablesung, ETZ. **15,** p. 214 (Apr. 12, 1894).
C. W. Burrows, An experimental study of the koepsel permeameter, BS Sci. Pap. **11,** 101 (1914) S228.

4] R. B. Treat and J. W. Esterline, A new magnetic testing apparatus, Elec. World **30,** 696 (1897).
[5] H. E. J. G. Du Bois, Magnetic circuits and their measurements, Electrician **27,** 634 (1891).
[6] E. Hughes, A magnetic bridge for testing straight specimens, Proc. Phys. Soc. (London) **37,** 233 (1925).
[7] R. V. Picou, Permeametre universal, Bul. Soc. Int. des Elec. [2] **2,** 828, (1902).
[8] A Iliovici, Sur un nouveau permeametre universal, Bul. Soc. Int. des. Elec. [3] **3,** 581 (1913).
[9] Y. Niwa, A null method for testing magnetic properties of materials, Researches Electrotech. Lab. (Tokyo) No. 142 (1924).
[10] C. W. Burrows, The determination of the magnetic induction in straight bars, Bul. BS **6,** 31 (1909) S117.
[11] R. L. Sanford and P. H. Winter, A permeameter for magnetic testing at magnetizing forces up to 300 cersteds, J. Research NBS, **45,** (July, 1950) RP2109.
[12] F. P. Fahy, A permeameter for general magnetic analysis, Chem. and Met. Eng., **19,** 339 (1918).
R. L. Sanford, Performance of the Fahy simplex permeameter, BS J. Research **4,** 703 (1930) RP174.
[13] R. L. Sanford and E. G. Bennett, An apparatus for magnetic testing at magnetizing forces up to 5,000 oersteds, J. Research NBS **23,** 415 (1939) RP1242.
[14] C. R. Mann, Phys. Rev. **3,** 359 (1896).
[15] H. Du Bois, Wied Ann. **7,** 942 (1902).
[16] C. L. B. Shuddemagen, Proc. Am. Acad. Arts Sci. **43,** 185, (1907).
[17] The Fahy low-mu permeameter for measuring low permeability, Iron Age **130,** 330 (1932).
[18] L. G. Gouy, Compt. rend. **109,** 935 (1889).
[19] M. Faraday, Experimental researches Vol. III, Taylor and Francis, London, pp. 27 and 497 (1855).
[20] Arthur Thorpe and Frank E. Senftle, Absolute method of measuring magnetic susceptibility, Rev. Sci. Inst. **30,** No. 11, 1006–1008, (Nov. 1959).
[21] R. L. Sanford, Determination of the degree of uniformity of bars for magnetic standards, Bul. BS **14,** 1 (1916) S295.
[22] R. L. Sanford, Temperature coefficient of magnetic permeability within the working range, Bul. BS **12,** 1 (1915) S245.
[23] See latest edition ASTM Standards—Metals—Test Methods.
[24] G. Camilli, A flux voltmeter for magnetic tests, Transactions AIEE **XLV,** pp. 721–728 (1926).
[25] I. L. Cooter and W. P. Harris, Investigation of an alternating-current bridge for the measurement of core losses in ferromagnetic materials at high flux densities, J. Research NBS **57,** No. 2, (Aug. 1956) RP 2699.
W. P. Harris and I. L. Cooter, Improved bridge method for the measurement of core losses in ferromagnetic materials at high flux densities, J. Research NBS **60,** No. 5, (May, 1958) RP2865.
[26] Peter H. Haas, a radio-frequency permeameter, J. Research NBS **51,** No. 5, (Nov. 1953) RP2454.
[27] G. A. Kelsall, Permeameter for alternating-current measurements at small magnetizing forces:, J. Opt. Soc. Am. and Rev. Sci. Instr. **8** (Feb., 1924).
[28] K. S. Seljesater and B. A. Rogers, Magnetic and mechanical hardness of dispersion-hardened iron alloys, Trans. Am. Soc. Steel Treating **19,** 553 (1932).
[29] W. Köster, Dauermagnetwerkstoffe auf der grundlage der auscheidungs hartung, Stahl U. Eisen **53,** 849 (1933).
[30] Mishima, Magnetic properties of iron-nickel-aluminum alloys, Ohm (July, 1932) abstracted in Iron Age **130,** 346 (1932).
[31] I. L. Cooter and R. E. Mundy, Cunife wire magnets of small size, J. Research NBS **59,** No. 6, (Dec. 1957) RP2808.
[32] Richard M. Bozorth, Ferromagnetism, D. Van Nostrand Co., Inc. p. 401 (1951).

PREPRINT INSTRUMENT SOCIETY of AMERICA
20th Annual ISA Conference and Exhibit • October 4-7, 1965, Los Angeles
Preprint Number 14.1-3-65

THE CALIBRATION OF PERMANENT MAGNET STANDARDS*

by Irvin L. Cooter
Chief, Magnetic Measurements Section
Electricity Division
National Bureau of Standards
Washington, D.C. 20234

ABSTRACT

The increased demand for the calibration of permanent magnets used as reference standards has required a new magnet calibration facility at the National Bureau of Standards, Washington, D.C. The method procedure and apparatus used in the calibration of reference magnets are described.

INTRODUCTION

Magnetic fields are essential to the operation of many devices used for defense, research and industrial applications. Many of these applications require that the flux density in the gap of a magnetic structure be known to an accuracy of 0.1 to 5 percent. Modern materials and design have increased the efficiency of these magnetic structures and have improved the stability of the magnetic field in the gap. Improvements and innovations in the measurement techniques have permitted these magnetic field measurements to be more easily and generally made with increased accuracy. The measuring system employed usually consists of two parts; a probe head that is inserted in the gap of the magnetic structure and an indicating or measuring instrument. Since the probe head and measuring instrument system are usually calibrated to read flux density, they are often called gaussmeters or magnetometers. (Perhaps later the name will be changed to teslameters).

The more sensitive gaussmeters use electronic amplification with adjustable gain for calibration purposes. The gaussmeters are usually calibrated by inserting the probe head in a reference field and adjusting the gain of the amplifier so the measuring instrument indicates the correct flux density. The reference field in many cases is the flux density in the gap of a permanent magnet. Therefore, it is very essential that the permanent magnets used as standards be calibrated and maintained as reference standards in the laboratory.

The Magnetic Measurements Section, Institute for Basic Standards, of the National Bureau of Standards, Washington, D.C., has a service of calibrating these reference standards for the many users. The calibration procedure is based on the accurate measurement of the flux density in the gap of an electromagnet or at the center of a set of Helmholtz coils. This accurately known flux density is compared with the flux density in the gap of the permanent magnet standard through the use of a suitable transfer instrument.

THE MEASUREMENT OF MAGNETIC FIELDS

There are many methods of measuring magnetic field. Several of these methods may be called absolute methods. Included among these methods are:

1. The test coil method. This requires a known value of area turns of a test coil for flipping, vibrating or rotating purposes.
2. Nuclear Magnetic Resonance Magnetometer.
3. Electron Paramagnetic Resonance Magnetometer
4. Rubidium Magnetometer
5. Helium Magnetometer

Several other methods by which magnetic fields are commonly measured use devices dependent on other effects such as:

a. The Hall Effect
b. Magnetoresistance
c. Saturable magnetic cores
d. Optical effects
e. Torque
f. Susceptibility - paramagnetic and diamagnetic

There are many other effects that can be but are infrequently used such as:

g. Deflection of electron beam
h. Magnetostriction
i. Ettingshausen effect
j. Thermal effects

ABSOLUTE METHODS FOR MEASURING MAGNETIC FIELDS

At the present time in the Magnetic Measurements Section there are two methods used for the absolute measurements of magnetic fields.

*Contribution of the National Bureau of Standards, not subject to copyright.

1. The Test Coil Method

2. Nuclear Magnetic Resonance Method

The Test Coil Method is used when it is desired to measure field less than 0.02 tesla (200 gausses) in the gap of the electromagnet and for the smaller fields produced at the center of the Helmholtz Coils. The Nuclear Magnetic Resonance Method is used for measuring the magnetic field in the gap of the electromagnet where the field is approximately 0.02 tesla or more.

1. The Test Coil Method

This method requires that the area turns of a test coil be determined by basic consideration. Referring to figure 1 - S is a long, single layered solenoid; the magnetic field at the central region of this solenoid may be computed from the geometry of the solenoid and winding, and the current in the winding; C is a search coil placed concentric with the solenoid in the central region. L_m is a mutual inductor whose mutual inductance has been calculated from its dimensions and this value is known to a few parts in a million. A potential divider circuit is connected across the secondary of the mutual inductor and R_1 is connected in series with the coil C through the ballistic galvanometer BG. The primary of the mutual inductor is connected in series with the winding of the long solenoid and provision is made to reverse and to measure the current in these windings. It is easily shown

that at balance

$$AN = \frac{R_1 L_m}{(R_1 + R_2)k}$$

Where AN is the area turns of the coil in m^2-turn, L_m is the mutual inductance of the inductor in henries, and k is the solenoid constant in teslas/ampere. The values of k and L_m are determined from mechanical measurement.

2. Nuclear Magnetic Resonance Method

The phenomenon of nuclear magnetic resonance makes it possible to measure homogeneous fields with very high accuracy. Under the best conditions it is possible with this method to measure magnetic fields within a few ppm. The measurement is based on the equation

$$2\pi\nu = \gamma_p B$$

or by transposing

$$B = \left(\frac{2\pi\nu}{\gamma_p}\right) = \frac{\nu}{\gamma_p/2\pi}$$

In this equation B is the flux density in teslas, ν is the resonance frequency in hertz (c/s) and γ_p is a quantity called the gyromagnetic ratio. The gyromagnetic ratio, γ_p, is the ratio of the magnetic moment of a nucleus to its angular momentum. Usually the proton resonance of a water sample is observed. The accepted value at present for $\gamma_p/2\pi$ for water is 4.25759×10^7 hertz/tesla.

The measurement is made by immersing a sample of material containing nuclei whose gyromagnetic ratio is known, in the steady homogeneous magnetic field to be measured. The field must be uniform within 0.1 percent over the volume of the sample in order to obtain a good resonance curve. The water sample in the probe is subjected by means of a surrounding coil to an alternating magnetic field at right angle to the steady field. The frequency of the alternating field is adjusted to be equal to the resonance frequency of the nuclei in the sample. At this frequency which is directly proportional to the intensity of the steady field, there is an absorption of energy from the exciting current. This is observed by means of a cathode-ray oscilloscope and the resonance frequency is read from a digital counter. B is then calculated using the equation

$$B = \frac{\nu \times 10^{-7}}{4.25759} \text{ teslas}$$

Where ν is the resonance frequency in hertz.

TRANSFER DEVICES

A few of the permanent magnet standards are designed to be directly measured with a NMR gaussmeter; however, most of these standards are designed to be used with the Hall effect, rotating coil, search coil or torque devices. Measuring instruments based on these principles are thus used as transfer devices between the permanent magnet standards and the reference fields.

1. The Hall Effect

This effect furnishes a very convenient means for the measurement of magnetic fields where probes having very small dimensions are needed. As a result of extensive development work many commercial instruments are available using this basic principle. The principle can be stated very simply using figure 2. If a thin strip or film of metal, usually bismuth, indium, antimonide or indium arsenide has a current, I, in it, two points (a and b) can be found at opposite ends of a line approximately at right angles to the current which will be at the same electrical potential, if no magnetic field, B, is acting. If a magnetic field is applied at right angles to the plane of the strip, a difference of electrical potential appears between these two points. This difference of electrical potential is proportional to the intensity of the magnetic field. The effect is large enough that for a fairly large field, the

voltage may be measured directly without amplification. For small fields and for increased sensitivity alternating current is used or produced so that the emf generated by the action of the magnetic field could be amplified. Instruments using this principle are generally nonlinear and require calibration in the range in which they are to be used.

2. Search Coils

These coils are frequently used in conjunction with integrating devices such as ballistic galvanometers, flux-meters, and electronic integrators. In making the measurement a test coil connected to the integrating device is placed in the magnetic field with its axis in the direction of the field and the deflection or reading observed when the test coil is either removed from the field or rotated 180° about its diameter. The signal produced is proportional to the total change in flux linkage between the field and the test coil.

A continuously rotating test coil is also often used to measure magnetic fields. The coil is rotated at constant speed about a diameter. It is connected through a commutator or cam operated reversing switch to a d-c instrument which indicates the average voltage induced in the coil. If the reversal comes at the time when the a-c voltage induced in the coil is zero, the reading on the instrument will be a maximum and will be proportional to the field. Commercial instruments operating on this principle have the rotating coil at the end of a long shaft which has at its other end a reversing commutator and synchronous motor. The shaft has to be long enough to avoid errors due to stray fields from the motor on the probe and to prevent the effect of the field being measured on the motor itself. The accuracy of the measurement depends directly upon the accuracy with which the frequency of the power source is controlled and variations in the resistance and spurious voltages at the reversing commutator are minimized. The voltage output of this instrument is linear with respect to the magnetic flux density being measured except at small fields where effects due to commutation may become significant. This instrument is usually calibrated through the use of two or more fields.

3. Pivoted Magnets

These are usually torque devices also used with permanent magnet standards. As a result of the development of permanent magnet materials having extremely high coercivity, it has been possible to produce an instrument by which magnetic fields can be measured in terms of torque on a small magnet. This instrument consists of a light weight shaft pivoted at each end and supported between jewels. A small cylindrical, high H_c magnet is mounted on a shaft near its lower end. At the other end is a hair spring for measuring the torque and a pointer which moves over the scale. For fields higher than 0.5 tesla a modified form of the instrument is used, in which the permanent magnet is replaced by a material which becomes magnetized by induction.

PERMANENT MAGNET STANDARDS AND THEIR CALIBRATION

As may be deduced from the description of the various types of probe heads and measuring devices used for transfer instruments in the above section, there are large variations in permanent magnet standards. Among these variations are field strength, the physical size and shape, air gap and access opening dimensions, guide and stop arrangements for the probe head, temperature control, designed accuracy and other characteristics. Therefore, calibration of these standards requires a considerable range of reference magnetic fields and several types of probes and measuring instruments. This may be seen from figure 3. The Magnetic Measurements Section in the Electricity Division of the Institute for Basic Standards, National Bureau of Standards, Washington, D.C., is equipped for and has calibrated permanent magnet standards having fields in the range of 0.0001 to 1.6 teslas. This range will be extended to 2 tesla in the near future. The facilities used for setting up the reference fields are a Helmholtz coil, a 7" symmetrical yoke electromagnet, and a 12" symmetrical yoke electromagnet

The reference field to be used when calibrating permanent magnet standards having gap fields of 0.02 tesla or less are produced using a set of Helmholtz coils or the 7" electromagnet. These reference fields are measured using search coils whose area-turns have been measured using the method 1 described in the section entitled ABSOLUTE METHODS FOR MEASURING MAGNETIC FIELDS. The gap field of the permanent magnet standard is compared with the reference field through a suitable transfer instrument.

Reference fields greater than 0.02 tesla are produced using the 7" or 12" electromagnet. These reference fields are usually measured by the nuclear magnetic resonance technique. For these fields, the probe head of the transfer instrument most generally used are the search coil, rotating coil and Hall effect. Since the permanent magnet standards requiring calibration are not uniform with respect to gap dimensions or in other respects, it is usually required that the same type or preferably the same probe head be used in the calibration procedure as will be used in the field measurement when the magnet is used as the standard. This is particularly true when search coils are used as probes since frequently they are custom-made and it is unlikely that we would have a search coil having the same geometry. Also in many cases the flux-density in the magnet

submitted for test is not uniform over the volume of the active portion of the probe head.

In the calibration procedure, the probe head and measuring instruments are used as transfer devices only between the reference field of an electromagnet and the field of the permanent magnet standard. The reference field is supplied in the gap of the 7" or 12" electromagnet. This field is constant and homogeneous over a volume larger than the measurement probe head of a nuclear magnetic resonance (NMR) magnetometer. Figure 4 is a photograph of the calibration setup for permanent magnets using the 7" electromagnet. Location and identification of the various components may be seen from figure 5. The NMR probe head is placed near the center of this highly uniform magnetic field. The transfer probe head in the case shown, is a Hall effect device that is inserted in the gap of the permanent magnet and a reading is obtained on the Hall effect measuring device. In our case we use a sensitive digital voltmeter as a readout device of the gaussmeter. The Hall effect probe is placed in the gap of the electromagnet adjacent to the NMR probe and the current from the power supply of the electromagnet is adjusted until the same reading is obtained on the digital voltmeter as when the Hall probe was in the gap of the permanent magnet standard. The frequency of the radio frequency field applied in NMR magnetometer is then varied until the resonance curve appears on the cathode ray oscillograph. This resonance frequency is then measured by means of the electronic counter. The flux-density existing in the gap may then be calculated from the equation

$$B = \frac{\nu \times 10^{-7}}{4.25759}$$

where B is this flux density in teslas and ν is the resonance frequency in hertz. This calculated flux density in the gap of the reference is equal to the flux density that exists in the gap of the permanent magnet standard. The transfer probe is always positioned as closely as possible to the NMR probe when in the electromagnet and is positioned for a maximum reading near the center of the air gap of the permanent magnet standard, if any degrees of freedom are possible. However, it is highly desirable and is usually required that appropriate guides and stops be supplied to the permanent magnet standard if accuracy of 1 percent or better is desired. Usually the value of the magnetic field in the permanent magnet is reported to an accuracy of 0.1 to 5 percent depending on the individual need. Permanent magnet standards having flux density from 0.0001 to 1.6 teslas have been calibrated.

ACKNOWLEDGMENTS

The new calibration setup using the 7" electromagnet was made possible through the financial support of the Bureau of Naval Weapons. Robert E. Mundy had the major responsibility for the supervision of the setup and its use in the calibration program of the section.

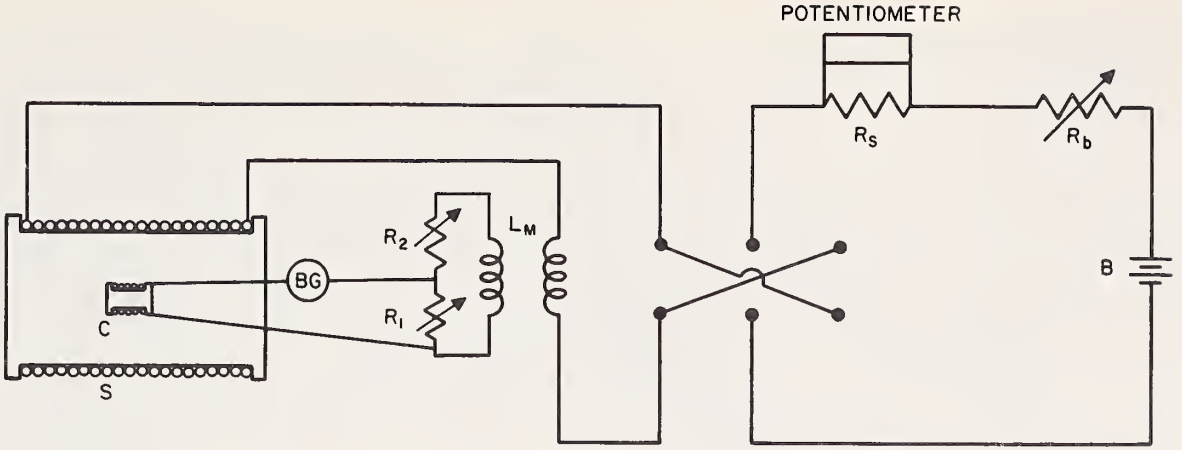

Figure 1 - Circuit for the Calibration of Test Coils

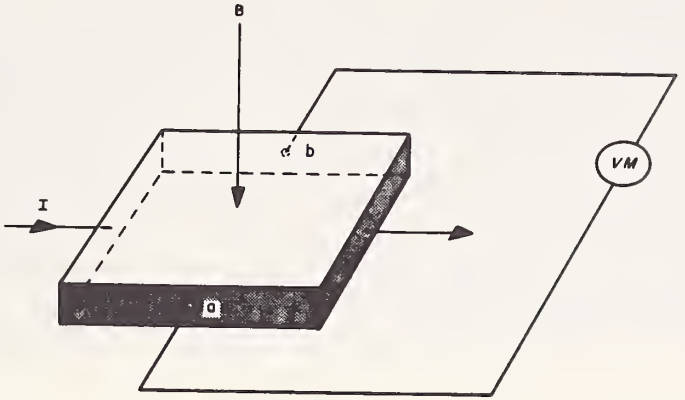

Figure 2 - The Hall Effect

Figure 3 - Permanent Magnet Standards and Test Probes

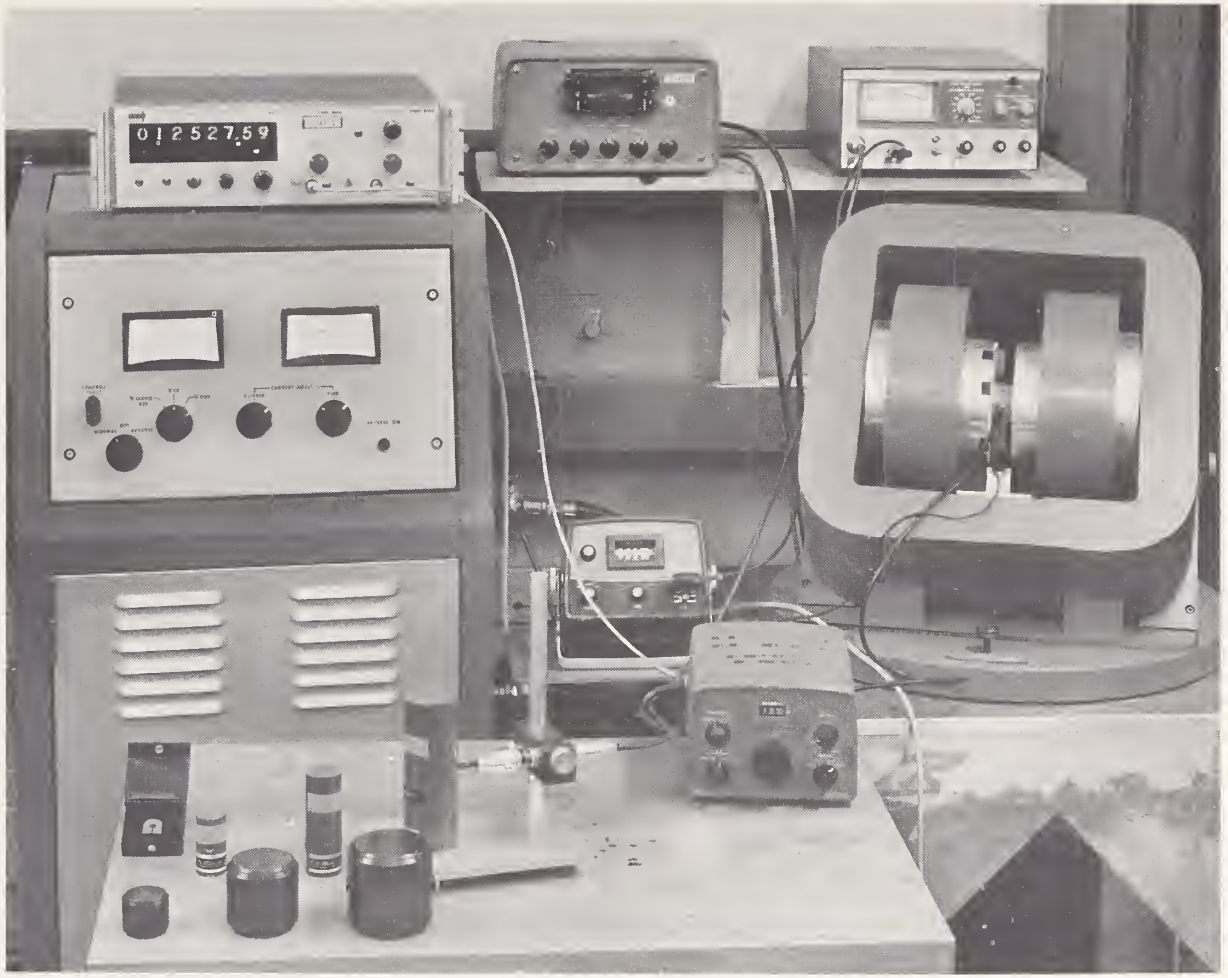

Figure 4 - Set-Up for the Calibration of Permanent Magnet Standards

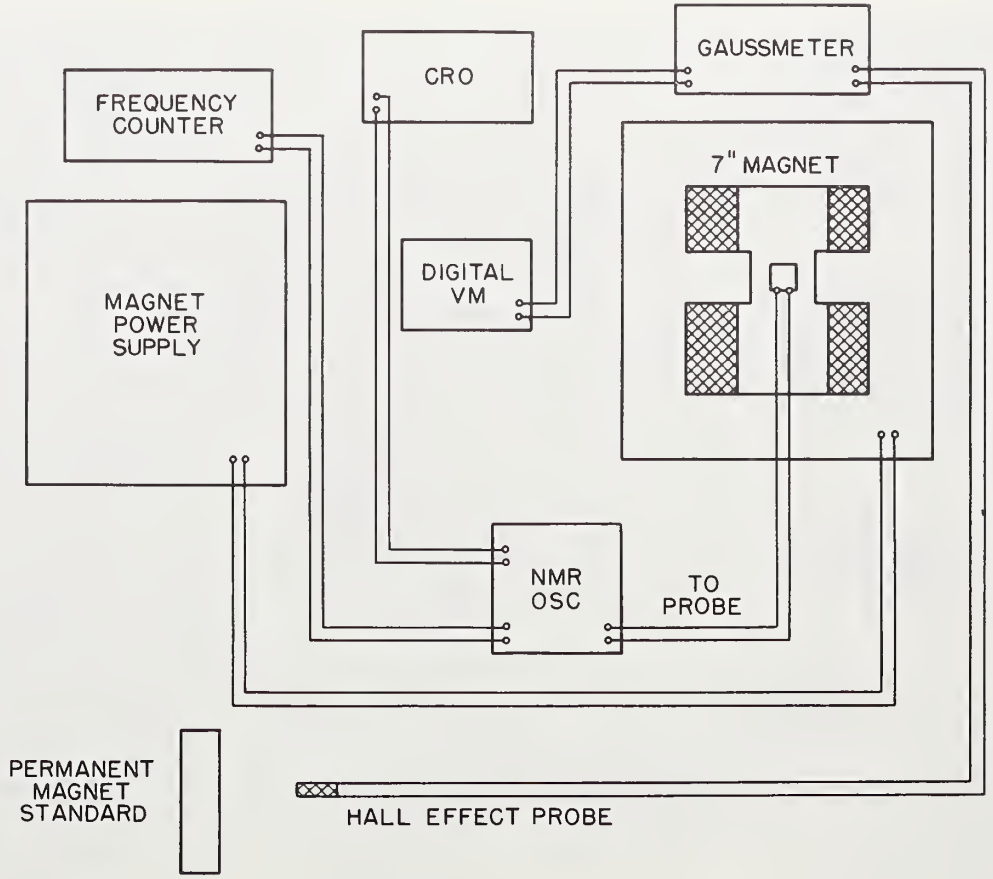

Figure 5 - Block Diagrams of Figure 4

Encyclopedia of Chemical Technology
Volume 7, 1965

Electrical Testing

Arnold H. Scott

Methods of testing for resistivity, dc dielectric conductivity, dielectric constant and ac loss, dielectric strength, arc resistance, and tracking and erosion under moist conditions are described to give a person working in chemical technology an understanding of the types of electrical tests that can be made and some idea of their usefulness.

JOURNAL OF RESEARCH of the National Bureau of Standards—C. Engineering and Instrumentation
Vol. 65C, No. 1, January–March 1961

An Ultra Low Frequency Bridge for Dielectric Measurements

Donald J. Scheiber

(October 11, 1960)

The bridge described is capable of measuring the parallel capacitance and resistance of dielectric specimens in the frequency range of 0.008 to 200 cps. It employs no earthing device and is directly connected to a three terminal oscillator. The substitution method is employed. The capabilities of the bridge are experimentally tested by measurements upon known capacitors and resistors and by comparison with results obtained using a Schering bridge near 100 cps. The apparatus is capable of accuracies previously unattained at these low frequencies. Capacitances between zero and 100 pf may be measured to an accuracy of $\pm(0.05\%+0.002$ pf) at frequencies above 5 cps. Below 5 eps the accuracy becomes $\pm[0.05\%+(0.002+2\times10^5/fR_D)$pf], where f is the frequency in eps and R_D is the equivalent resistance in ohms across the detector terminals. Conductances between 10^{-9} and 10^{-15} mhos may be measured to an accuracy of about $\pm(1\%+3f\times10^{-15}$ mhos) when $f\geq0.1$ cps. When $f<0.1$ cps the accuracy is about $\pm(1\%+2\times10^{-16}$ mhos). The dielectric constant (ϵ') of a specimen may be determined to an accuracy proportional to that of capacitance measurements. The loss index (ϵ'') may be determined to an accuracy of about $\pm(1\%+5\times10^{-4}/C_v)$ when $f\geq0.1$ cps and $\pm(1\%+3\times10^{-5}/fC_v)$ when $f<0.1$ cps. Here C_v is the vacuum capacitance of the specimen expressed in picofarads. The effects of stray impedances shunting the bridge ratio arms, are investigated. Useful modifications of the bridge are discussed.

Proceedings from the Electrical Insulation Conference
IEEE-NEMA, 1967

Low Frequency Dielectric Behavior

William P. Harris

Electrical engineers, as well as polymer physicists and materials researchers, can gain useful information from a study of the behavior of dielectrics, and of high-megohm resistors at very low frequencies. This is illustrated by examples.

There are two main methods of obtaining ultra-low-frequency data. One is to apply a dc voltage producing a time-dependent current which corresponds to an inverse frequency plot. The other is to use an alternating voltage, usually sinusoidal, and apply this to a bridge circuit including the material under study. Recent developments in the latter methods are presented, along with some typical results.

Key Words - Bridge, Dielectrics, Dielectric Measurements, Dielectric Phenomena, Electrical Measurements, Low Frequency, Measurements, Operational Amplifiers, Ultra Low Frequency.

Subject Index[1]

[Reference is to volume number, boldface, followed by page number of this volume]

[1] The letter "A" following the page number indicates an abstract only.

Author Index[1]

[1] The letter "A" following the page number indicates an abstract only.

NATIONAL BUREAU OF STANDARDS

The National Bureau of Standards[1] was established by an act of Congress March 3, 1901. Today, in addition to serving as the Nation's central measurement laboratory, the Bureau is a principal focal point in the Federal Government for assuring maximum application of the physical and engineering sciences to the advancement of technology in industry and commerce. To this end the Bureau conducts research and provides central national services in three broad program areas and provides central national services in a fourth. These are: (1) basic measurements and standards, (2) materials measurements and standards, (3) technological measurements and standards, and (4) transfer of technology.

The Bureau comprises the Institute for Basic Standards, the Institute for Materials Research, the Institute for Applied Technology, and the Center for Radiation Research.

THE INSTITUTE FOR BASIC STANDARDS provides the central basis within the United States of a complete and consistent system of physical measurement, coordinates that system with the measurement systems of other nations, and furnishes essential services leading to accurate and uniform physical measurements throughout the Nation's scientific community, industry, and commerce. The Institute consists of an Office of Standard Reference Data and a group of divisions organized by the following areas of science and engineering:

Applied Mathematics—Electricity—Metrology—Mechanics—Heat—Atomic Physics—Cryogenics[2]—Radio Physics[2]—Radio Engineering[2]—Astrophysics[2]—Time and Frequency.[2]

THE INSTITUTE FOR MATERIALS RESEARCH conducts materials research leading to methods, standards of measurement, and data needed by industry, commerce, educational institutions, and government. The Institute also provides advisory and research services to other government agencies. The Institute consists of an Office of Standard Reference Materials and a group of divisions organized by the following areas of materials research:

Analytical Chemistry—Polymers—Metallurgy — Inorganic Materials — Physical Chemistry.

THE INSTITUTE FOR APPLIED TECHNOLOGY provides for the creation of appropriate opportunities for the use and application of technology within the Federal Government and within the civilian sector of American industry. The primary functions of the Institute may be broadly classified as programs relating to technological measurements and standards and techniques for the transfer of technology. The Institute consists of a Clearinghouse for Scientific and Technical Information,[3] a Center for Computer Sciences and Technology, and a group of technical divisions and offices organized by the following fields of technology:

Building Research—Electronic Instrumentation — Technical Analysis — Product Evaluation—Invention and Innovation— Weights and Measures — Engineering Standards—Vehicle Systems Research.

THE CENTER FOR RADIATION RESEARCH engages in research, measurement, and application of radiation to the solution of Bureau mission problems and the problems of other agencies and institutions. The Center for Radiation Research consists of the following divisions:

Reactor Radiation—Linac Radiation—Applied Radiation—Nuclear Radiation.

---

[1] Headquarters and Laboratories at Gaithersburg, Maryland, unless otherwise noted; mailing address Washington, D. C. 20234.
[2] Located at Boulder, Colorado 80302.
[3] Located at 5285 Port Royal Road, Springfield, Virginia 22151.

NBS TECHNICAL PUBLICATIONS

PERIODICALS

JOURNAL OF RESEARCH reports National Bureau of Standards research and development in physics, mathematics, chemistry, and engineering. Comprehensive scientific papers give complete details of the work, including laboratory data, experimental procedures, and theoretical and mathematical analyses. Illustrated with photographs, drawings, and charts.

Published in three sections, available separately:

• Physics and Chemistry

Papers of interest primarily to scientists working in these fields. This section covers a broad range of physical and chemical research, with major emphasis on standards of physical measurement, fundamental constants, and properties of matter. Issued six times a year. Annual subscription: Domestic, $6.00; foreign, $7.25*.

• Mathematical Sciences

Studies and compilations designed mainly for the mathematician and theoretical physicist. Topics in mathematical statistics, theory of experiment design, numerical analysis, theoretical physics and chemistry, logical design and programming of computers and computer systems. Short numerical tables. Issued quarterly. Annual subscription: Domestic, $2.25; foreign, $2.75*.

• Engineering and Instrumentation

Reporting results of interest chiefly to the engineer and the applied scientist. This section includes many of the new developments in instrumentation resulting from the Bureau's work in physical measurement, data processing, and development of test methods. It will also cover some of the work in acoustics, applied mechanics, building research, and cryogenic engineering. Issued quarterly. Annual subscription: Domestic, $2.75; foreign, $3.50*.

TECHNICAL NEWS BULLETIN

The best single source of information concerning the Bureau's research, developmental, cooperative and publication activities, this monthly publication is designed for the industry-oriented individual whose daily work involves intimate contact with science and technology—*for engineers, chemists, physicists, research managers, product-development managers, and company executives.* Annual subscription: Domestic, $3.00; foreign, $4.00*.

*Difference in price is due to extra cost of foreign mailing.

NONPERIODICALS

Applied Mathematics Series. Mathematical tables, manuals, and studies.

Building Science Series. Research results, test methods, and performance criteria of building materials, components, systems, and structures.

Handbooks. Recommended codes of engineering and industrial practice (including safety codes) developed in cooperation with interested industries, professional organizations, and regulatory bodies.

Special Publications. Proceedings of NBS conferences, bibliographies, annual reports, wall charts, pamphlets, etc.

Monographs. Major contributions to the technical literature on various subjects related to the Bureau's scientific and technical activities.

National Standard Reference Data Series. NSRDS provides quantitative data on the physical and chemical properties of materials, compiled from the world's literature and critically evaluated.

Product Standards. Provide requirements for sizes, types, quality and methods for testing various industrial products. These standards are developed cooperatively with interested Government and industry groups and provide the basis for common understanding of product characteristics for both buyers and sellers. Their use is voluntary.

Technical Notes. This series consists of communications and reports (covering both other agency and NBS-sponsored work) of limited or transitory interest.

CLEARINGHOUSE

The Clearinghouse for Federal Scientific and Technical Information, operated by NBS, supplies unclassified information related to Government-generated science and technology in defense, space, atomic energy, and other national programs. For further information on Clearinghouse services, write:

Clearinghouse
U.S. Department of Commerce
Springfield, Virginia 22151

Order NBS publications from:
Superintendent of Documents
Government Printing Office
Washington, D.C. 20402

U.S. GOVERNMENT PRINTING OFFICE : 1968 O - 315-411

Announcement of New Volumes in the NBS Special Publication 300 Series Precision Measurement and Calibration

Superintendent of Documents
Government Printing Office
Washington, D.C. 20402

Dear Sir:

Please add my name to the announcement list of new volumes to be issued in the series: National Bureau of Standards Special Publication 300, Precision Measurement and Calibration.

Name_____

Company_____

Address_____

City_____ State_____ Zip Code_____

(Notification key—N: 353)

(cut here)

Official SI Unit Names and Symbols

[For a complete statement of NBS practice, see NBS Tech. News Bull. Vol. 52, No. 6, June 1968.]

Name	Symbol	Name	Symbol
meter	m	newton	N
kilogram	kg	joule	J
second	s	watt	W
ampere	A	coulomb	C
kelvin [1]	K	volt	V
candela	cd	ohm	Ω
radian	rad	farad	F
steradian	sr	weber	Wb
hertz	Hz	henry	H
lumen	lm	tesla	T
lux	lx		

Additional Names and Symbols approved for NBS use

curie [2]	Ci	mho	mho
degree Celsius [3]	°C	mole	mol
gram	g	siemens [4]	S

[1] The same name and symbol are used for thermodynamic temperature and temperature interval. (Adopted by the 13th General Conference on Weights & Measures, 1967.)

[2] Accepted by the General Conference on Weights & Measures for use with the SI.

[3] For expressing "Celsius temperature"; may also be used for a temperature interval.

[4] Adopted by IEC and ISO.

Table for converting U.S. Customary Units to those of the International System (SI)[5]

To relate various units customarily used in the United States to those of the International System, the National Bureau of Standards uses the conversion factors listed in the "ASTM Metric Practice Guide", NBS Handbook 102. These are based on international agreements effective July 1, 1959, between the national standards laboratories of Australia, Canada, New Zealand, South Africa, the United Kingdom, and the United States.

To convert from:

(1) inches to meters, multiply by 0.0254 exactly.
(2) feet to meters, multiply by 0.3048 exactly.
(3) feet (U.S. survey) to meters, multiply by 1200/3937 exactly.
(4) yards to meters, multiply by 0.9144 exactly.
(5) miles (U.S. statute) to meters, multiply by 1609.344 exactly.
(6) miles (international nautical) to meters, multiply by 1852 exactly.
(7) grains (1/7000 lbm avoirdupois) to grams, multiply by 0.064 798 91 exactly.
(8) troy or apothecary ounces mass to grams, multiply by 31.103 48 . . .
(9) pounds-force (lbf avoirdupois) to newtons, multiply by 4.448 222 . . .
(10) pounds-mass (lbm avoirdupois) to kilograms, multiply by 0.453 592 . . .
(11) fluid ounces (U.S.) to cubic centimeters, multiply by 29.57 . . .
(12) gallons (U.S. liquid) to cubic meters, multiply by 0.003 785 . . .
(13) torr (mm Hg at 0 °C) to newtons per square meter, multiply by 133.322 exactly.
(14) millibars to newtons per square meter, multiply by 100 exactly.
(15) psi to newtons per square meter, multiply by 6894.757 exactly.
(16) poise to newton-seconds per square meter, multiply by 0.1 exactly.
(17) stokes to square meters per second, multiply by 0.0001 exactly.
(18) degrees Fahrenheit to Kelvins, use the relation $t_K = (t_F + 459.67)/1.8$.
(19) degrees Fahrenheit to degrees Celsius, use the relation $t_C = (t_F - 32)/1.8$.
(20) curies to disintegrations per second, multiply by 3.7×10^{10} exactly.
(21) roentgens to coulombs per kilogram, multiply by $2.579\ 760 \times 10^{-4}$ exactly.

[5] Système International d'Unités (designated SI in all languages).